TRANSACTIONS
OF THE
AMERICAN INSTITUTE
OF
ELECTRICAL ENGINEERS

VOLUME 72
1953

PART II. APPLICATIONS AND INDUSTRY

PUBLISHED BY THE
AMERICAN INSTITUTE OF ELECTRICAL ENGINEERS
33 WEST 39TH STREET
NEW YORK 18. N. Y., U. S. A.

Copyright 1953 by the American Institute of Electrical Engineers
Printed in U. S. A. by The Mack Printing Company, Easton, Pa.

Applications and Industry Index for 1953

1. Technical Subject Index

Abnormal Conditions on Aircraft Parallel A-C Power Systems, The Effects of. Caldwell, Wood........379–84; disc. 385
Adjustable Speed D-C Drives for Deep-Draw Presses. Robinson, DiVincenzo........9–16
Air-Break Contactors at Low Currents, Arcing Time of High-Voltage. Lister........145–9; disc. 149
(Air Transportation) Control of Metal Build-up in Minimum Pressure Sensitive Contact Systems. Dallas, Stuelpnagel........398–403
(Air Transportation) Differential Reactive Current Protection Relay. Stineman....407–11; disc. 411
(Air Transportation) Methods for Prediction of Steady-State Performance for Unbalanced Regulated 3-Phase Generators. Wilson......413–21; disc. 421
(Air Transportation) New Developments in Differential-Type Hydraulic Transmissions and Controls. Eisengrein........423–9
Aircraft A-C Generators, Parallel Operation of. Larson........403–07
Aircraft A-C Systems, Co-ordination of Overvoltage and Short-Circuit Protection for. Trbovich, Kidwell, Tucker........369–73; disc. 373
Aircraft Alternators, Directional Detection for Parallel. Mamett, Granath........374–9
Aircraft Alternators, Power Equalizer Systems for. Granath, Hawkes........209–14; disc. 214
Aircraft, Continuous Current Capacity of Bundled Cables for. Schach, Schroeder........386–97; disc. 397
Aircraft Current Limiters and its Effect on Current Division in Networks, Change in Resistance of. Oman........231–7; disc. 237
Aircraft Generators, Commutation of Low-Voltage D-C. Franklin........254–62
Aircraft, Parallel A-C Power Systems, The Effects of Abnormal Conditions on. Caldwell, Wood........379–84; disc. 385
Aircraft Protection from Thunderstorm Discharges to Antennas. Bryant, Newman, Robb........248–52; disc. 253
Aircraft-Type Generator-Regulator System, The Use of an Analogue Computer to Optimize the Transient Response of an. James........363–8
A-C Generators, Parallel Operation of Aircraft. Larson........403–07
A-C Power Systems, The Effects of Abnormal Conditions on Aircraft Parallel. Caldwell, Wood........379–84; disc. 385
A-C Systems, Co-ordination of Overvoltage and Short-Circuit Protection for Aircraft. Trbovich, Kidwell, Tucker........369–73; disc. 373
A-C Tachometer with Constant-Current Excitation, Drag-Cup. Frazier........150–2; disc. 152
A-C Versus D-C Power for Underground Mines. Linsenmeyer, Owen........217–22
Alternator-Rectifier System for Caboose Power Supply, An Axle-Driven. Hoffer, Weber..133–7; disc. 137
Alternators, Directional Detection for Parallel Aircraft. Mamett, Granath........374–9
Alternators, Power Equalizer Systems for Aircraft. Granath, Hawkes........209–14; disc. 214
Amplifier Actuated Valve, Hydraulic Servos Incorporating a High-Speed Hydraulic-. Scrafford........175–9; disc. 180
Analogue Computer to Optimize the Transient Response of an Aircraft-Type Generator-Regulator System, The Use of an. James........363–8
Analysis Applied to Most Commonly Encountered Nonlinearities, Describing Function Method of Servomechanism. Grief........243–8
Analytical Solution of Heat Flow Versus Wire Temperature for Electric Cables Buried in Plaster, An. Goff........160–4; disc. 164
Analyzer Study of Certain Nonlinearly Damped Servomechanisms, A Differential-. Caldwell, Rideout........165–9; disc. 169
Antennas, Aircraft Protection from Thunderstorm Discharges to. Bryant, Newman, Robb........248–52; disc. 253
Application and Operation of D-C Drives on Rubber Calenders. Sellers, Wheeler, Halter........194–201; disc. 201
Application and Standardization of High Rupturing Capacity Current-Limiting Fuses, The. Gibson........126–31; disc. 131
Application of Electric Equipment in Coal Preparation Plants, Technical Aspects of. Morton.....349–55
Approximation of Transient Response from Frequency Response Data. Dawson........289–91
Arc in Argon and Helium, The Electric. Jones, Skolnik, Kouwenhoven........16–21
Arcing Time of High-Voltage Air-Break Contactors at Low Currents. Lister........145–9; disc. 149
Arcs, Controlling D-C. Hurtle......225–30; disc. 230
Argon and Helium, The Electric Arc in. Jones, Skolnik, Kouwenhoven........16–21
Automatic Control of Gas Turbines for Natural Gas Pipeline Pumping. Ingemanson, Loft, Wilt........295–300
Axle-Driven Alternator Rectifier System for Caboose Power Supply, An. Hoffer, Weber........133–7; disc. 137

B

Backlash in a Velocity Lag Servomechanism. Nichols........462–6
Bibliography on Feedback Control. (Committee Reports)........430–62
Braking on Diesel-Electric Locomotives, Dynamic. Johansson, Stiger........105–10; disc. 110
Build-up in Minimum Pressure Sensitive Contact Systems, Control of Metal. Dallas, Stuelpnagel........398–403
Bundled Cables for Aircraft, Continuous Current Capacity of. Schach, Schroeder......386–97; disc. 397

C

Cables Buried in Plaster, An Analytical Solution of Heat Flow Versus Wire Temperature for Electric. Goff........160–4; disc. 164
Cables for Aircraft, Continuous Current Capacity of Bundled. Schach, Schroeder....386–97; disc. 397
Caboose Power Supply, An Axle-Driven Alternator-Rectifier System for. Hoffer, Weber........133–7; disc. 137
Calenders, Application and Operation of D-C Drives on Rubber. Sellers, Wheeler, Halter........194–201; disc. 201
Canada, Diesel-Electric Locomotives in. Sylvester, Haney........152–5; disc. 155
Capacity of Bundled Cables for Aircraft, Continuous Current. Schach, Schroeder....386–97; disc. 397
Car, A Track-Laying Shuttle. Brauns..360–2; disc. 362
Carriage Drive and the Basic Duty Cycle of Carriage Performance, The Magnetic Amplifier Controlled Log-. Rose........305–13; disc. 313
Cars, A New Control for Heavyweight Rapid-Transit. Lichtenfels........49–53
Change in Resistance of Aircraft Current Limiters and Its Effect on Current Division in Networks. Oman........231–7; disc. 237
Characteristic Power Requirements for Performing Various Functions in Underground Coal Mines. Musser........336–40
Circuits, The Effect of Reactive Components in the Measurement of Grounding. Harrison........340–3; disc. 343
Closed-Loop Poles of Feedback Control Systems, Quick Methods for Evaluating the. Biernson........53–68; disc. 68
Closed-Loop Systems, Relative Stability of. Kirby, Beaumariage........22–43
Coal Mines, Characteristic Power Requirements for Performing Various Functions in Underground. Musser........336–40
Coal Preparation Plants, Technical Aspects of Application of Electric Equipment in. Morton...349–55
(Committee Reports) Bibliography on Feedback Control. (53–250), (53–251), and (53–393)........430–62
Commutation of Low-Voltage D-C Aircraft Generators. Franklin........254–62
Complex-Variable Differentiation, Determination of the Maximum Modulus or of the Specified Gain of a Servomechanism by. Higgins, Siegel........467–8; disc. 468
Components in the Measurement of Grounding Circuits, The Effect of Reactive. Harrison........340–3; disc. 343
Computer to Optimize the Transient Response of an Aircraft-Type Generator-Regulator System, The Use of an Analogue. James........363–8
Constant-Current Excitation, Drag-Cup A-C Tachometer with. Frazier........150–2; disc. 152
Contact Systems, Control of Metal Build-up in Minimum Pressure Sensitive. Dallas, Stuelpnagel...398–403
Contactors at Low Currents, Arcing Time of High-Voltage Air-Break. Lister.......145–9; disc. 149
Contacts, The Spreading and Interface Resistances of Electric. Little, Kouwenhoven........314–23
Continuous Current Capacity of Bundled Cables for Aircraft. Schach, Schroeder....386–97; disc. 397
Control for Heavyweight Rapid-Transit Cars, A New. Lichtenfels........49–53
Control for Lighting Systems, Electric Distribution and. Kahler, Bell........92–8; disc. 98
Control of Metal Build-up in Minimum Pressure Sensitive Contact Systems. Dallas, Stuelpnagel........398–403
Control Systems by Means of Nonlinear Feedbacks, Optimization of Nonlinear. Neiswander, MacNeal........262–70; disc. 270
Controlling D-C Arcs. Hurtle......225–30; disc. 230
Controls, New Developments in Differential-Type Hydraulic Transmissions and. Eisengrein.....423–9
Co-ordination of Overvoltage and Short-Circuit Protection for Aircraft A-C Systems. Trbovich, Kidwell, Tucker........369–73; disc. 373
Correlation Between Frequency and Transient Responses of Feedback Control Systems. Chu........81–92
Coulomb Friction in Feedback Control Systems. Haas........119–23; disc. 123
Criteria and Standard Forms, The Synthesis of "Optimum" Transient Response. Graham, Lathrop........273–86; disc. 286
Criterion for Linear Systems, A Relative Damping. Koenig........291–4; disc. 294
Current Capacity of Bundled Cables for Aircraft, Continuous. Schach, Schroeder.....386–97; disc. 397
Current Limiters and its Effect on Current Division in Networks, Change in Resistance of Aircraft. Oman........231–7; disc. 237
Current-Limiting Fuses, The Application and Standardization of High Rupturing Capacity. Gibson........126–31; disc. 131
Current Protection Relay, Differential Reactive. Stineman........407–11; disc. 411

D

Damping Criterion for Linear Systems, A Relative. Koenig........291–4; disc. 294
Deep-Draw Presses, Adjustable Speed D-C Drives for. Robinson, DiVincenzo........9–16
Describing Function Method of Servomechanism Analysis Applied to Most Commonly Encountered Nonlinearities. Grief........243–8
Design Factors Favoring Diesel-Locomotive Electrical Maintenance. Stair........155–6; disc. 156
Design of Transformers for Resistance Welding Machines. Knight........238–43
Detection for Parallel Aircraft Alternators, Directional. Mamett, Granath........374–9
Determination of the Maximum Modulus, or of the Specified Gain, of a Servomechanism by Complex-Variable Differentiation. Higgins, Siegel........467–8; disc. 468
Detroit Committee on Electrolysis, A Discussion of the. Rayner........469–71
Developments in Differential-Type Hydraulic Transmissions and Controls, New. Eisengrein....423–9
Diesel-Electric Locomotive Ground Relays. McDonald........170–4; disc. 174
Diesel-Electric Locomotive Maintenance Personnel, Education and Training of. Teker, Ainsworth........115–19
Diesel-Electric Locomotives, Dynamic Braking on. Johansson, Stiger........105–10; disc. 110
Diesel-Electric Locomotives in Canada. Sylvester, Haney........152–5; disc. 155
Disel-Electric Locomotives, Split-Pole Exciters: Their Design and Application on. Stiger........357–60

Diesel-Electric Rail Car, Wanted: A Modern. Anderson..........345–8; disc. 348
Diesel-Locomotive Electrical Maintenance, Design Factors Favoring. Stair..........155–6; disc. 156
Diesel Locomotive Heavy Electric Repair Shop, Equipment and Functions of a Modern. Thomas..........157–9; disc. 159
Diesel Locomotives, Electric Transmission with. McGee..........138–44; disc. 144
Differential Analyzer Study of Certain Nonlinearly Damped Servomechanisms, A. Caldwell, Rideout..........165–9; disc. 169
Differential Reactive Current Protection Relay. Stineman..........407–11; disc. 411
Differential-Type Hydraulic Transmission and Controls, New Developments in. Eisengrein..........423–9
Differentiation, Determination of the Maximum Modulus or of the Specified Gain of a Servomechanism by Complex-Variable. Higgins, Siegel..........467–8; disc. 468
D-C Aircraft Generators, Commutation of Low-Voltage. Franklin..........254–62
D-C Arcs, Controlling. Hurtle......225–30; disc. 230
D-C Drives for Deep-Draw Presses, Adjustable Speed. Robinson, DiVincenzo..........9–16
D-C Drives on Rubber Calenders, Application and Operation of. Sellers, Wheeler, Halter..........194–201; disc. 201
D-C Generator, Flashover Torque of a. Coho....43–8
D-C Power for Underground Mines, A-C Versus. Linsenmeyer, Owen..........217–22
Directional Detection for Parallel Aircraft Alternators. Mamett, Granath..........374–9
Discharges to Antennas, Aircraft Protection from Thunderstorm. Bryant, Newman, Robb..........248–52; disc. 253
Discussion of the Detroit Committee on Electrolysis, A. Rayner..........469–71
Distribution and Control for Lighting Systems, Electric. Kahler, Bell..........92–8; disc. 98
Distribution Systems in Strip Mines, Review of Grounding Practices on 480-Volt Portable. Bennett..........300–04
Drag-Cup A-C Tachometer with Constant-Current Excitation. Frazier..........150–2; disc. 152
Drive and the Basic Duty Cycle of Carriage Performance, The Magnetic Amplifier Controlled Log-Carriage. Rose..........305–13; disc. 313
Drives for Deep-Draw Presses, Adjustable-Speed D-C. Robinson, DiVincenzo..........9–16
Drives on Rubber Calenders, Application and Operation of D-C. Sellers, Wheeler, Halter..........194–201; disc. 201
Duty Cycle of Carriage Performance, The Magnet Amplifier Controlled Log-Carriage Drive and the Basic. Rose..........305–13; disc. 313
Dynamic Braking on Diesel-Electric Locomotives. Johansson, Stiger..........105–10; disc. 110

E

Education and Training of Diesel-Electric Locomotive Maintenance Personnel. Taker, Ainsworth..........115–19
Effect of Reactive Components in the Measurement of Grounding Circuits, The. Harrison..........340–3; disc. 343
Effects of Abnormal Conditions on Aircraft Parallel A-C Power Systems, The. Caldwell, Wood..........379–84; disc. 385
Effects of Friction in an Optimum Relay Servomechanism. Stout..........329–35; disc. 335
Electric Arc in Argon and Helium, The. Jones, Skolnik, Kouwenhoven..........16–21
Electric Contacts, The Spreading and Interface Resistances of. Little, Kouwenhoven..........314–23
Electric Distribution and Control for Lighting Systems. Kahler, Bell..........92–8; disc. 98
Electric Equipment in Coal Preparation Plants, Technical Aspects of Application of. Morton..........349–55
Electric Transmission and Diesel Locomotives. McGee..........138–44; disc. 144
Electrolysis, A Discussion of the Detroit Committee on. Rayner..........469–71
Equalizer Systems for Aircraft Alternators, Power. Granath, Hawkes..........290–14; disc. 214
Equipment and Functions of a Modern Diesel Locomotive Heavy Electric Repair Shop. Thomas..........157–9; disc. 159
Equipment in Coal Preparation Plants, Technical Aspects of Application of Electric. Morton..........349–55
Errors in Relay Servo Systems. Kazda..........323–8; disc. 238
Excitation, Drag-Cup A-C Tachometer with Constant-Current. Frazier..........150–2; disc. 152
Exciters: Their Design and Application on Diesel-Electric Locomotives, Split-Pole. Stiger...357–60

F

(Feedback Control) A Relative Damping Criterion for Linear Systems. Koenig......291–4; disc. 294
(Feedback Control) Approximation of Transient Response from Frequency Response Data. Dawson..........289–91
(Feedback Control) Backlash in a Velocity Lag Servomechanism. Nichols..........462–6
Feedback Control, Bibliography on. (Committee Reports)..........430–62
(Feedback Control) Determination of the Maximum Modulus, or of the Specified Gain, of a Servomechanism by Complex-Variable Differentiation. Higgins, Siegel..........467–8; disc. 468
(Feedback Control) Errors in Relay Servo Systems. Kazda..........323–8; disc. 328
(Feedback Control) Relative Stability of Close-Loop Systems. Kirby, Beaumariage..........22–43
Feedback Control Systems, Correlation Between Frequency and Transient Responses of. Chu.. 81–92
Feedback Control Systems, Coulomb Friction in. Haas..........119–23; disc. 123
Feedback Control Systems, Limiting in. Kochenburger..........180–92; disc. 192
Feedback Control Systems, Quick Methods for Evaluating the Closed-Loop Poles of. Biernson..........53–68; disc. 68
Feedback Control Systems, Transient Measurement of. Ferguson, Looney..........110–14
Feedbacks, Optimization of Nonlinear Control System by Means of Nonlinear. Neiswander, MacNeal..........262–70; disc. 270
Flashover Torque of a D-C Generator. Coho.....43–8
Frequency and Transient Responses of Feedback Control Systems, Correlation Between. Chu..........81–92
Frequency Response Data, Approximation of Transient Response from. Dawson..........289–91
Frequency Response Method for Nonlinear Servomechanisms, Open-Loop. Cosgriff..........222–5
Friction in an Optimum Relay Servomechanism, Effects of. Stout..........329–35; disc. 335
Friction in Feedback Control Systems, Coulomb. Haas..........119–23; disc. 123
Function Method of Servomechanism Analysis Applied to Most Commonly Encountered Nonlinearities, Describing. Grief..........243–8
Fuses, The Application and Standardization of High Rupturing Capacity Current-Limiting. Gibson..........126–31; disc. 131

G

Gain of a Servomechanism by Complex-Variable Differentiation, Determination of the Maximum Modulus or of the Specified. Higgins, Siegel..........467–8; disc. 468
Gas Turbines for Natural Gas Pipeline Pumping, Automatic Control of. Ingemanson, Loft, Wilt..........295–300
Generator, Flashover Torque of a D-C. Coho....43–8
Generator-Regulator System, The Use of an Analogue Computer to Optimize the Transient Response of an Aircraft-Type. James..........363–8
Generators, Commutation of Low-Voltage D-C Aircraft. Franklin..........254–62
Generators, Methods for Prediction of Steady-State Performance for Unbalanced Regulated 3-Phase. Wilson..........413–21; disc. 421
Generators, Parallel Operation of Aircraft A-C. Larson..........403–07
Grounding Circuits, The Effect of Reactive Components in the Measurement of. Harrison..........340–3; disc. 343
Grounding Practices on 480-Volt Portable Distribution Systems in Strip Mines, Review of. Bennett..........300–04

H

Heat Flow Versus Wire Temperature for Electric Cables Buried in Plaster, An Analytical Solution of. Goff..........160–4; disc. 164
Helium, The Electric Arc in Argon and. Jones, Skolnik, Kouwenhoven..........16–21
High-Voltage Air-Break Contactors at Low Currents, Arcing Time of. Lister..........145–9; disc. 149
Hydraulic Servos Incorporating a High Speed Hydraulic-Amplifier Actuated Valve. Scrafford..........175–9; disc. 180
Hydraulic Transmissions and Controls, New Developments in Differential-Type. Eisengrein.....423–9

I

(Industrial Control) Bibliography on Feedback Control. (Committee Reports)..........430–62
Industrial Plants, 240/416-Volt 3-Phase 4-Wire Power and Lighting Supply for Modern. Shuler..........71–7; disc. 77
Interface Resistances of Electric Contacts, The Spreading and. Little, Kouwenhoven..........314–23
Interurban Becomes a Railroad, An. Jones....99–105

L

Lag Servomechanism, Backlash in a Velocity. Nichols..........462–6
(Land Transportation) A New Control for Heavyweight Rapid-Transit Cars. Lichtenfels..........49–53
(Land Transportation) A Track-Laying Shuttle Car. Brauns..........360–2; disc. 362
(Land Transportation) An Interurban Becomes a Railroad. Jones..........99–105
(Land Transportation) Controlling D-C Arcs. Hurtle..........225–30; disc. 230
(Land Transportation) Design Factors Favoring Diesel-Locomotive Electrical Maintenance. Stair..........155–6; disc. 156
(Land Transporation) Diesel-Electric Locomotive Ground Relays. McDonald......170–4; disc. 174
(Land Transportation) Diesel-Electric Locomotives in Canada. Sylvester, Haney......152–5; disc. 155
(Land Transportation) Dynamic Braking on Diesel-Electric Locomotives. Johansson, Stiger..........105–10; disc. 110
(Land Transportation) Education and Training of Diesel-Electric Locomotive Maintenance Personnel. Teker, Ainsworth..........115–19
(Land Transportation) Electric Transmission with Diesel Locomotives. McGee....138–44; disc. 144
(Land Transportation) Equipment and Functions of a Modern Diesel Locomotive Heavy Electric Repair Shop. Thomas..........157–9; disc. 159
(Land Transportation) Flashover Torque of a D-C Generator. Coho..........43–8
(Land Transporation) Wanted: A Modern Diesel-Electric Rail Car. Anderson.....345–8; disc. 348
Lighting Supply for Modern Industrial Plants, 240/416-Volt 3-Phase 4-Wire Power and. Shuler..........71–7; disc. 77
Lighting Systems, Electric Distribution and Control for. Kahler, Bell..........92–8; disc. 98
Limiters and Its Effect on Current Division in Networks, Change in Resistance of Aircraft Current. Oman..........231–7; disc. 237
Limiting Fuses, The Application and Standardization of High Rupturing Capacity Current. Gibson..........126–31; disc. 131
Limiting in Feedback Control Systems. Kochenburger..........180–92; disc. 192
Linear Systems, A Relative Damping Criterion for. Koenig..........291–4; disc. 294
Locomotive Electrical Maintenance, Design Factors Favoring Diesel-. Stair..........155–6; disc. 156
Locomotive for Low Vein Haulage, A Low Height 15-Ton Mine. Brauns..........355–7
Locomotive Ground Relays, Diesel-Electric. McDonald..........170–4; disc. 174
Locomotive Heavy Electric Repair Shop, Equipment and Functions of a Modern Diesel. Thomas..........157–9; disc. 159
Locomotive Maintenance Personnel, Education and Training of Diesel-Electric. Teker, Ainsworth..........115–19
Locomotives, Dynamic Braking on Diesel-Electric. Johansson, Stiger..........105–10; disc. 110
Locomotives, Electric Transmission with Diesel. McGee..........138–44; disc. 144
Locomotives in Canada, Diesel-Electric. Sylvester, Haney..........152–5; disc. 155
Locomotives, Split-Pole Exciters: Their Design and Application on Diesel-Electric. Stiger.....357–60
Log-Carriage Drive and the Basic Duty Cycle of Carriage Performance, The Magnetic Amplifier Controlled. Rose..........305–13; disc. 313
Loop Frequency Response Method for Nonlinear Servomechanisms, Open-. Cosgriff..........222–5
Loop Systems, Relative Stability of Closed-. Kirby, Beaumariage..........22–43
Low-Height 15-Ton Mine Locomotive for Low Vein Haulage, A. Brauns..........355–7
Low-Voltage D-C Aircraft Generators, Commutation of. Franklin..........254–62

M

Machines, Design of Transformers for Resistance Welding. Knight..........238–43
Magnetic Amplifier Controlled Log-Carriage Drive and the Basic Duty Cycle of Carriage Performance, The. Rose..........305–13; disc. 313
Maintenance, Design Factors Favoring Diesel-Locomotive Electrical. Stair..........155–6; disc. 156

Measurement of Feedback Control Systems, Transient. Ferguson, Looney....110–14
Metal Build-up in Minimum Pressure Sensitive Contact Systems, Control of. Dallas, Stuelpnagel....398–403
Methods for Evaluating the Closed-Loop Poles of Feedback Control Systems, Quick. Biernson....53–68; disc. 68
Methods for Prediction of Steady-State Performance for Unbalanced Regulated 3-Phase Generators. Wilson....413–21; disc. 421
Mine Locomotive for Low Vein Haulage, A Low Height 15-Ton. Brauns....355–7
Mines, A-C Versus D-C Power for Underground. Linsenmeyer, Owen....217–22
Mines, Characteristic Power Requirements for Performing Various Functions in Underground Coal. Musser....336–40
Mines, Review of Grounding Practices on 480-Volt Portable Distribution Systems in Strip. Bennett....300–04
(Mining) Technical Aspects of Application of Electric Equipment in Coal Preparation Plants. Morton....349–55
(Mining) The Effect of Reactive Components in the Measurement of Grounding Circuits. Harrison....340–3; disc. 343
Modulus or of the Specified Gain of a Servomechanism by Complex-Variable Differentiation, Determination of the Maximum. Higgins, Siegel....467–8; disc. 468
Multitransformer Welding Presses. Ogden....202–08

N

Networks, Change in Resistance of Aircraft Current Limiters and Its Effect on Current Division in. Oman....231–7; disc. 237
New Developments in Differential-Type Hydraulic Transmissions and Controls. Eisengrein....423–9
Nonlinear Control Systems by Means of Nonlinear Feedbacks, Optimization of. Neiswander, MacNeal....262–70; disc. 270
Nonlinear Servomechanisms, Open-Loop Frequency Response Method for. Cosgriff....222–5
Nonlinearities, Describing Function Method of Servomechanism Analysis Applied to Most Commonly Encountered. Grief....243–8

O

Open-Loop Frequency Response Method for Nonlinear Servomechanisms. Cosgriff....222–5
Operation of Aircraft A-C Generators, Parallel. Larson....403–07
Optimization of Nonlinear Control Systems by Means of Nonlinear Feedbacks. Neiswander, MacNeal....262–70; disc. 270
Optimum Relay Servomechanism, Effect of Friction in an. Stout....329–35; disc. 335
"Optimum" Transient Response: Criteria and Standard Forms, The Synthesis of. Graham, Lathrop....273–86; disc. 286
Overvoltage and Short-Circuit Protection for Aircraft A-C Systems, Co-ordination of. Trbovich, Kidwell, Tucker....369–73; disc. 373

P

Parallel Aircraft Alternators, Directional Detection for Mamett, Granath....274–9
Parallel A-C Power Systems, The Effects of Abnormal Conditions on Aircraft. Caldwell, Wood....379–84; disc. 385
Parallel Operation of Aircraft A-C Generators. Larson....403–07
Performance for Unbalanced Regulated 3-Phase Generators, Methods for Prediction of Steady-State. Wilson....413–21; disc. 421
Personnel, Education and Training of Diesel-Electric Locomotive Maintenance. Teker, Ainsworth....115–19
Phenomena in Servomechanisms with Emphasis on the Tachometer Stabilized System, Some Saturation. Levinson....1–9
Pipeline Pumping, Automatic Control of Gas Turbines for Natural Gas. Ingemanson, Loft, Wilt....295–300
Plants, 240/416-Volt 3-Phase 4-Wire Power and Lighting Supply for Modern Industrial. Shuler....71–7; disc. 77
Plaster, An Analytical Solution of Heat Flow Versus Wire Temperature for Electric Cables Buried in. Goff....160–4; disc. 164
Poles of Feedback Control Systems, Quick Methods for Evaluating the Closed-Loop. Biernson....53–68; disc. 68
Portable Distribution Systems in Strip Mines, Review of Grounding Practices on 480-Volt. Bennett....300–04
Power and Lighting Supply for Modern Industrial Plants, 240/416-Volt 3-Phase 4-Wire. Shuler....71–7; disc. 77
Power Equalizer Systems for Aircraft Alternators. Granath, Hawkes....209–14; disc. 214
Power for Underground Mines, A-C Versus D-C. Linsenmeyer, Owen....217–22
Power Requirements for Performing Various Functions in Underground Coal Mines, Characteristic. Musser....336–40
Power Systems, The Effects of Abnormal Conditions on Aircraft Parallel A-C. Caldwell, Wood....379–84; disc. 385
Presses, Adjustable Speed D-C Drives for Deep-Draw. Robinson, DiVincenzo....9–16
Presses, Multitransformer Welding. Ogden....202–08
Pressure Sensitive Contact Systems, Control of Metal Build-up in Minimum. Dallas, Stuelpnagel....398–403
Protection for Aircraft A-C Systems, Co-ordination of Overvoltage and Short-Circuit. Trbovich, Kidwell, Tucker....369–73; disc. 373
Protection from Thunderstorm Discharges to Antennas, Aircraft. Bryant, Newman, Robb....248–52; disc. 253
Protection Relay, Differential Reactive Current. Stineman....407–11; disc. 411
Pumping, Automatic Control of Gas Turbines for Natural Gas Pipeline. Ingemanson, Loft, Wilt....295–300

Q

Quick Methods for Evaluating the Closed-Loop Poles of Feedback Control Systems. Biernson....53–68; disc. 68

R

Rail Car, Wanted: A Modern Diesel-Electric. Anderson....345–8; disc. 348
Railroad, An Interurban Becomes a. Jones....99–105
Rapid-Transit Cars, A New Control for Heavyweight. Lichtenfels....49–53
Reactive Components in the Measurement of Grounding Circuits, The Effect of. Harrison....340–3; disc. 343
Reactive Current Protection Relay, Differential. Stineman....407–11; disc. 411
Rectifier System for Caboose Power Supply, An Axle-Driven Alternator. Hoffer, Weber....133–7; disc. 137
Regulated 3-Phase Generators, Methods for Prediction of Steady-State Performance for Unbalanced. Wilson....413–21; disc. 421
Relative Damping Criterion for Linear Systems, A. Koenig....291–4; disc. 294
Relative Stability of Closed-Loop Systems. Kirby, Beaumariage....22–43
Relay, Differential Reactive Current Protection. Stineman....407–11; disc. 411
Relay Servo Systems, Errors in. Kazda....323–8; disc. 328
Relay Servomechanism, Effects of Friction in an Optimum. Stout....329–35; disc. 335
Relays, Diesel-Electric Locomotive Ground. McDonald....170–4; disc. 174
Repair Shop, Equipment and Functions of a Modern Diesel Locomotive Heavy Electric. Thomas....157–9; disc. 159
Resistance of Aircraft Current Limiters and Its Effects on Current Division in Networks, Change in. Oman....231–7; disc. 237
Resistance Welding Machines, Design of Transformers for. Knight....238–43
Resistances of Electric Contacts, The Spreading and Interface. Little, Kouwenhoven....314–23
Response from Frequency Response Data, Approximation of Transient. Dawson....289–91
Response Method for Nonlinear Servomechanisms, Open-Loop Frequency. Cosgriff....222–5
Response of an Aircraft-Type Generator-Regulator System, The Use of an Analogue Computer to Optimize the Transient. James....363–8
Responses of Feedback Control Systems, Correlation Between Frequency and Transient. Chu....81–92
Review of Grounding Practices on 480-Volt Portable Distribution Systems in Strip Mines. Bennett....300–04
Rubber Calenders, Application and Operation of D-C Drives on. Sellers, Wheeler, Halter....194–201; disc. 201
Rupturing Capacity Current-Limiting Fuses, The Application and Standardization of High. Gibson....126–31; disc. 131

S

Saturation Phenomena in Servomechanisms with Emphasis on the Tachometer Stabilized System, Some. Levinson....1–9
Sensitive Contact Systems, Control of Metal Build-up in Minimum Pressure. Dallas, Stuelpnagel..398–403
Servo Systems, Errors in Relay. Kazda....323–8; disc. 328
Servomechanism Analysis Applied to Most Commonly Encountered Nonlinearities, Describing Function Method of. Grief....243–8
Servomechanism, Backlash in a Velocity Lag. Nichols....462–6
Servomechanism by Complex-Variable Differentiation, Determination of the Maximum Modulus or of the Specified Gain of a. Higgins, Siegel....467–8; disc. 468
Servomechanism, Effects of Friction in an Optimum Relay. Stout....329–35; disc. 335
Servomechanisms, A Differential-Analyzer Study of Certain Nonlinearly Damped. Caldwell, Rideout....165–9; disc. 169
Servomechanisms, Open-Loop Frequency Response Method for Nonlinear. Cosgriff....222–5
Servomechanisms with Emphasis on the Tachometer Stabilized System, Some Saturation Phenomena in. Levinson....1–9
Servos Incorporating a High-Speed Hydraulic-Amplifier Actuated Valve, Hydraulic. Scrafford....175–9; disc. 180
Short-Circuit Protection for Aircraft A-C Systems, Co-ordination of Overvoltage and. Trbovich, Kidwell Tucker....369–73; disc. 373
Shuttle Car, A Track-Laying. Brauns.360–2; disc. 362
Solution of Heat Flow Versus Wire Temperature for Electric Cables Buried in Plaster, An Analytical. Goff....160–4; disc. 164
Specified Gain of a Servomechanism by Complex-Variable Differentiation, Determination of the Maximum Modulus or of the. Higgins, Siegel....467–8; disc. 468
Speed D-C Drives for Deep-Draw Presses, Adjustable. Robinson, DiVincenzo....9–16
Split Pole Exciters: Their Design and Application on Diesel-Electric Locomotives. Stiger....357–60
Spreading and Interface Resistances of Electric Contacts, The. Little, Kouwenhoven....314–23
Stability of Closed-Loop Systems, Relative. Kirby, Beaumariage....22–43
Standardization of High Rupturing Capacity Current-Limiting Fuses, The Application and. Gibson....126–31; disc. 131
Steady-State Performance for Unbalanced Regulated 3-Phase Generators, Methods for Prediction of. Wilson....413–21; disc. 421
Strip Mines, Review of Grounding Practices on 480-Volt Portable Distribution Systems in. Bennett..300–04
Study of Certain Nonlinearly Damped Servomechanisms, A Differential-Analyzer. Caldwell, Rideout....165–9; disc. 169
(Subways) A New Control for Heavyweight Rapid-Transit Cars. Lichtenfels....49–53
Synthesis of "Optimum" Transient Response: Criteria and Standard Forms. Graham, Lathrop....273–86; disc. 286

T

Tachometer Stabilized System, Some Saturation Phenomena in Servomechanisms with Emphasis on the. Levinson....1–9
Tachometer with Constant-Current Excitation, Drag-Cup A-C. Frazier....150–2; disc. 152
Technical Aspects of Application of Electric Equipment in Coal Preparation Plants. Morton....349–55
Temperature for Electric Cables Buried in Plaster, An Analytical Solution of Heat Flow Versus Wire. Goff....160–4; disc. 164
Three-Phase Generators, Methods for Prediction of Steady-State Performance for Unbalanced Regulated. Wilson....413–21; disc. 421
Thunderstorm Discharges to Antennas, Aircraft Protection from. Bryant, Newman, Robb....248–52; disc. 253
Time of High-Voltage Air-Break Contactors at Low Currents, Arcing. Lister....145–9; disc. 149
Torque of a D-C Generator, Flashover. Coho....43–8
Track-Laying Shuttle Car, A. Brauns....360–2; disc. 362
Training of Diesel-Electric Locomotive Maintenance Personnel, Education and. Teker, Ainsworth....115–19
Transformers for Resistance Welding Machines, Design of. Knight....238–43
Transient Measurement of Feedback Control Systems. Ferguson, Looney....110–14
Transient Response: Criteria and Standard Forms, The Synthesis of "Optimum". Graham, Lathrop....273–86; disc. 286

Transient Response from Frequency Response Data, Approximation of. Dawson..............289–91
Transient Response of an Aircraft-Type Generator-Regulator System, The Use of an Analogue Computer to Optimize the. James..............363–8
Transient Responses of Feedback Control Systems, Correlation Between Frequency aud. Chu.....81–92
Transmission with Diesel Locomotives, Electric. McGee..............138–44; disc. 144
Transmissions and Controls, New Developments in Differential-Type Hydraulic. Eisengrein...423–9
(Transportation, Air) Aircraft Protection from Thunderstorm Discharges to Antennas. Bryant, Newman, Robb..............248–52; disc. 253
(Transportation, Air) Change in Resistance of Aircraft Current Limiters and Its Effect on Current Division in Networks. Oman..............231–7; disc. 237
(Transportation, Air) Commutation of Low-Voltage D-C Aircraft Generators. Franklin..........254–62
(Transportation, Air) Methods for Prediction of Steady-State Performance for Unbalanced Regulated 3-Phase Generators. Wilson......413–21; disc. 421
(Transportation, Air) New Developments in Differential-Type Hydraulic Transmissions and Controls. Eisengrein..............423–9
(Transportation, Air) Power Equalizer Systems for Aircraft Alternators. Granath, Hawkes..............209–14; disc. 214
(Transportation, Land) A Low Height 15-Ton Mine Locomotive for Low Vein Haulage. Brauns..............355–7
(Transportation, Land). A Track-Laying Shuttle Car. Brauns..............360–2; disc. 362
(Transportation, Land) An Axle-Driven Alternator-Rectifier System for Caboose Power Supply. Hoffer, Weber..............133–7; disc. 137
(Transportation, Land) An Interurban Becomes a Railroad. Jones..............99–105
(Transportation, Land) Design Factors Favoring Diesel-Locomotive Electrical Maintenance. Stair..............155–6; disc. 156
(Transportation, Land) Diesel-Electric Locomotive Ground Relays. McDonald......170–4; disc. 174
(Transportation, Land) Diesel-Electric Locomotives in Canada. Sylvester, Haney.......152–5; disc. 155
(Transportation, Land) Dynamic Braking on Diesel-Electric Locomotives. Johansson, Stiger..............105–10; disc. 110
(Transportation, Land) Education and Training of Diesel-Electric Locomotive Maintenance Personnel. Teker, Ainsworth..............115–19
(Transportation, Land) Electric Transmission with Diesel Locomotives. McGee....138–44; disc. 144
(Transportation, Land) Equipment and Functions of a Modern Diesel Locomotive Heavy Electric Repair Shop. Thomas..............157–9; disc. 159
(Transportation, Land) Split-Pole Exciters: Their Design and Application on Diesel-Electric Locomotives. Stiger..............357–60
(Transportation, Land) Wanted: A Modern Diesel-Electric Rail Car. Anderson.....345–8; disc. 348
Turbines for Natural Gas Pipeline Pumping, Automatic Control of Gas. Ingemanson, Loft, Wilt...295–300
240/416-Volt 3-Phase 4-Wire Power and Lighting Supply for Modern Industrial Plants. Shuler..............71–7; disc. 77

U

Unbalanced Regulated 3-Phase Generators, Methods for Preduction of Steady-State Performance for. Wilson..............413–21; disc. 421
Underground Coal Mines, Characteristic Power Requirements for Performing Various Functions in. Musser..............336–40
Underground Mines, A-C Versus D-C Power for. Linsenmeyer, Owen..............217–22

V

Valve, Hydraulic Servos Incorporating a High-Speed Hydraulic-Amplifier Actuated. Scrafford..............175–9; disc. 180
Variable Differentiation, Determination of the Maximum Modulus or of the Specified Gain of a Servomechanism by Complex-. Higgins, Siegel..............467–8; disc. 468
Velocity Lag Servomechanism, Backlash in a. Nichols..............462–6

W

Wanted: A Modern Diesel-Electric Rail Car, Anderson..............345–8; disc. 348
Welding Machines, Design of Transformers for Resistance. Knight..............238–43
Welding Presses, Multitransformer. Ogden....202–08
(Welding) The Spreading and Interface Resistances of Electric Contacts. Little, Kouwenhoven...314–23
Wire Temperature for Electric Cables Buried in Plaster, An Analytical Solution of Heat Flow Versus. Goff..............160–4; disc. 164

2. Author Index

Aaron, M. R. Disc..............123
Ainsworth, E. R.; J. W. Teker. Education and Training of Diesel-Electric Locomotive Maintenance Personnel. (53–70)..............115–19
Anderson, K. O. Wanted: A Modern Diesel-Electric Rail Car. (53–361)..............345–8; disc. 349
Atwell, C. A. Disc..............156
Axelby, George S. Disc..............335
Aydelott, J. C. Disc..............144

B

Barlow, E. P. Disc..............397
Beaumariage, D. C.; M. J. Kirby. Relative Stability of Closed-Loop Systems. (53–102)..........22–43
Beaumariage, D. C.; M. J. Kirby. Disc..............68
Bell, R. N.; W. H. Kahler. Electric Distribution and Control for Lighting Systems. (53–73)..............92–8; disc. 99
Bennett, R. B. Review of Grounding Practices on 480-Volt Portable Distribution Systems in Strip Mines. (53–329)..............300–04
Biernson, George. Quick Methods for Evaluating the Closed-Loop Poles of Feedback Control Systems. (53–42)..............53–68; disc. 70
Boggess, Paul F. Disc..............385
Brauns, J. W. A Low Height 15-Ton Mine Locomotive for Low Vein Haulage. (53–365)..........355–7
Brauns, J. W. A Track-Laying Shuttle Car. (53–366)..............360–2
Brehaus, W. O.; W. F. Milliken, C. L. Muzzey, I. C. Statler. Disc..............287
Brereton, D. S.; S. C. Cooke. Disc..............77
Brown, H. F. Disc..............348
Bryant, J. M.; M. M. Newman, J. D. Robb. Aircraft Protection from Thunderstorm Discharges to Antennas. (53–196)..........248–52; disc. 253

C

Caldwell, R. R.; V. C. Rideout. A Differential Analyzer Study of Certain Nonlinearly Damped Servomechanisms. (53–107).....165–9; disc. 170
Caldwell, S. C. Disc..............214
Caldwell, S. C.; A. J. Wood. The Effects of Abnormal Conditions on Aircraft, Parallel A-C Power Systems. (53–371)..............379–84; disc. 385
Chapman, R. L. Disc..............156
Chu, Yaohan. Correlation Between Frequency and Transient Responses of Feedback Control Systems. (53–100)..............81–92
Coho, O. C. Flashover Torque of a D-C Generator. (53–83)..............43–8
Collier, D. M. Disc..............270
Cooke, S. C.; D. S. Brereton. Disc..............77
Cosgriff, R. L. Open-Loop Frequency Response Method for Nonlinear Servomechanisms. (53–253)..............222–5
Curdts, E. B. Disc..............343

D

Dallas, J. P.; T. R. Stuelpnagel. Control of Metal Build-up in Minimum Pressure Sensitive Contact Systems. (53–376)..............398–403
Dawson, Charles H. Approximation of Transient Response from Frequency Response Data. (53–248)..............289–91
DiVincenzo, A. P.; C. E. Robinson. Adjustable Speed D-C Drives for Deep-Draw Presses. (53–4)..9–16
Dolkart, Leo. Disc..............79

E

Edwards, Charles M. Disc..............152
Eisengrein, R. H. New Developments in Differential-Type Hydraulic Transmissions and Controls. (53–369)..............423–9

F

Ferguson, F. H.; C. H. Looney. Transient Measurement of Feedback Control Systems. (53–101)..............110–14
Fett, G. H. Disc..............287
Franklin, Paul W. Commutation of Low-Voltage D-C Aircraft Generators. (53–305)..........254–62
Frazier, R. H. Drag-Cup A-C Tachometer with Constant Current Excitation. (53–17)..............150–2; disc. 152

G

Geohegan, K. P. Disc..............294
Geohegan, K. P.; K. Kinnen. Disc..............286
Gibson, J. W. The Application and Standardization of High Rupturing Capacity Current-Limiting Fuses. (53–129)..............126–31; disc. 132
Goff, J. E. An Analytical Solution of Heat Flow Versus Wire Temperature for Electric Cables Buried in Plaster. (53–71)..............160–4; disc. 164
Goldberg, Leon J. Disc..............149
Graham, Dunstan; R. C. Lathrop. The Synthesis of "Optimum" Transient Response: Criteria and Standard Forms. (53–249).....273–86; disc. 288
Granath, John A.; A. K. Hawkes. Power Equalizer Systems for Aircraft Alternators. (53–179)..............209–14; disc. 216
Granath, J. A.; F. Mamett. Directional Detection for Parallel Aircraft Alternators. (53–363)......374–9
Green, Francis A. Disc..............201
Grief, H. D. Describing Funetion Method of Servomechanism Analysis Applied to Most Commonly Encountered Nonlinearities. (53–254)......243–8

H

Haas, Vinton B., Jr. Coulomb Friction in Feedback Control Systems. (53–108).....119–23; disc. 123
Hagenguth, J. D. Disc..............253
Halter, A. C.; J. F. Sellers, B. G. Wheeler. Application and Operation of D-C Drives on Rubber Calenders. (53–145)..............194–201; disc. 201
Hamer, Howard. Disc..............192
Hamilton, W. S. H. Disc..............137
Hammond, S. B. Disc..............164
Haney, D. F.; J. D. Sylvester. Diesel-Electric Locomotives in Canada. (53–68)..............152–5
Harrison, L. H. The Effect of Reactive Components in the Measurement of Grounding Circuits. (53–359)..............340–3; disc. 345
Hatch, P. H. Disc..............155, 348
Hawkes, Albert K.; J. A. Granath. Power Equalizer Systems for Aircraft Alternators. (53–179)..............209–14; disc. 216
Higgins, Thomas J.; C. M. Siegel. Determination of the Maximum Modulus, or of the Specified Gain, of a Servomechanism by Complex-Variable Differentiation. (53–392)..........467–8; disc. 468
Hoffer, A. H.; G. W. Weber. An Axle-Driven Alternator-Rectifier System for Caboose Power Supply. (53–78)..............137–7; disc. 137
Hopkin, Arthur M. Disc..............271
Hugus, F. R. Disc..............362
Hurtle, R. L. Controlling D-C Arcs. (53–305)..............225–30; disc. 230
Hutchison, W. M. Disc..............174

I

Ingemanson, C. R.; A. Loft, H. J. Wilt. Automatic Control of Gas Turbines for Natural Gas Pipeline Pumping. (53–323)..............295–300
Inman, Richard W. Disc..............344

J

James, H. B. The Use of an Analogue Computer to Optimize the Transient Response of an Aircraft-Type Generator-Regulator System. (53–368)..............363–8
Jatras, S. J.; D. G. O'Brien. Disc..............180
Johansson, A. V.; H. R. Stiger. Dynamic Braking on Diesel-Electric Locomotives. (53–48)..............105–10; disc. 110
Jones, C. H. An Interurban Becomes a Railroad. (53–35)..............99–105
Jones, T. B.; M. Skolnik, W. B. Kouwenhoven. The Electric Arc in Argon and Helium. (53–87)..............16–21

K

Kahler, W. H.; R. N. Bell. Electric Distribution and Control for Lighting Systems. (53–73)..............92–8; disc. 99

Karda, Louis F. Errors in Relay Servo Systems. (53-354)..........323–8; disc. 328
Kidwell, R. E., Jr.; M. Trbovich, W. M. Tucker. Coordination of Overvoltage and Short-Circuit Protection for Aircraft A-C Systems. (53-364)..........369–73; disc. 373
Kinnen, K.; K. P. Geohegan. Disc..........286
Kirby, M. J.; D. C. Beaumariage. Relative Stability of Closed-Loop Systems. (53-102)..........22–43
Kirby, M. J.; D. C. Beaumariage. Disc..........68
Knight, D. L. Design of Transformers for Resistance Welding Machines. (53-296)..........238–43
Kochenburger, Ralph J. Limiting in Feedback Control Systems. (53-109)..........180–92; disc. 193
Koenig, J. Frank. A Relative Damping Criterion for Linear Systems. (53-247)..........291–4; disc. 294
Kouwenhoven, W. B.; T. B. Jones, M. Skolnik. The Electric Arc in Argon and Helium. (53-87)..........16–21
Kouwenhoven, William B.; C. W. Little, Jr. The Spreading and Interface Resistances of Electric Contacts. (53-353)..........314–23
Kusters, N. L.; W. J. M. Moore. Disc..........69

L

Larson, L. R. Parallel Operation of Aircraft A-C Generators. (53-372)..........403–07
Lathrop, R. C.; D. Graham. The Synthesis of "Optimum" Transient Response: Criteria and Standard Forms. (53-249)..........273–86; disc. 288
Lebens, J. C. Disc..........131, 237
Levinson, E. Some Saturation Phenomena in Servomechanisms with Emphasis on the Tachometer Stabilized System. (53-110)..........1–9
Lichtenfels, I. W. A New Control for Heavyweight Rapid-Transit Cars. (53-51)..........49–53
Linsenmeyer, J. Z.; A. G. Owen. A-C Versus D-C Power for Underground Mines. (53-185)..........217–22
Lister, C. A. Arcing Time of High-Voltage Air-Break Contactors at Low Currents. (53-19)..........145–9; disc. 150
Little, Clarence W., Jr.; W. B. Kouwenhoven. The Spreading and Interface Resistances of Electric Contacts. (53-353)..........314–23
Loft, Arne; C. R. Ingemanson, H. J. Wilt. Automatic Control of Gas Turbines for Natural Gas Pipeline Pumping. (53-323)..........295–300
Looney, C. H.; F. H. Ferguson. Transient Measurement of Feedback Control Systems. (53-101)..........110–14

M

MacNeal, R. H.; R. S. Neiswander. Optimization of Nonlinear Control Systems by Means of Nonlinear Feedbacks. (53-252)..........262–70; disc. 272
Mamett, F.; J. A. Granath. Directional Detection for Parallel Aircraft Alternators. (53-363)..........374–9
Matthysse, I. Disc..........237
McDonald, Donald C. Disc..........286
McDonald, G. R. Diesel-Electric Locomotive Ground Relays. (53-77)..........170–4; disc. 174
McGee, P. A. Electric Transmission with Diesel Locomotives. (53-69)..........138–44; disc. 144
Milliken, W. F.; W. O. Brehaus, C. L. Muzzey, I. C. Statler. Disc..........287
Moore, W. J. M.; N. L. Kusters. Disc..........69
Morton, W. R. Technical Aspects of Application of Electric Equipment in Coal Preparation Plants. (53-358)..........349–55
Musser, H. P. Characteristic Power Requirements for Performing Various Functions in Underground Coal Mines. (53-360)..........336–40
Muzzey, C. L.; W. F. Milliken, W. O. Brehaus, I. C Statler. Disc..........287

N

Neiswander, R. S.; R. H. MacNeal. Optimization of Nonlinear Control Systems by Means of Nonlinear Feedbacks. (53-252)..........262–70; disc. 272
Newman, N. N.; J. M. Bryant, J. D. Robb. Aircraft Protection from Thunderstorm Discharges to Antennas. (53-196)..........248–52; disc. 253
Nichols, Nathaniel B. Backlash in a Velocity Lag Servomechanism. (53-394)..........462–6

O

O'Brien, D. G.; S. J. Jatras. Disc..........180
Ogden, Jack. Multitransformer Welding Presses. (53-180)..........202–08
Oman, Henry. Change in Resistance of Aircraft Current Limiters and Its Effect on Current Division in Networks. (53-272)..........231–7; disc. 238
Owen, A. G.; J. Z. Linsenmeyer. A-C Versus D-C Power for Underground Mines. (53-185)..........217–22
Owen, T. B. Disc..........421

P

Peterman, L. C. Disc..........79, 98
Povejsil, D. J. Disc..........286

R

Rapp, Philip C. Disc..........288
Rayner, R. L. A Discussion of the Detroit Committee on Electrolysis. (53-413)..........469–71
Rideout, V. C.; R. R. Caldwell. A Differential Analyzer Study of Certain Nonlinearly Damped Servomechanisms. (53-107)..........165–9; disc. 170
Robb, J. D.; J. M. Bryant, M. M. Newman. Aircraft Protection from Thunderstorm Discharges to Antennas. (53-196)..........248–52; disc. 253
Robinson, C. E.; A. P. DiVincenzo. Adjustable Speed D-C Drives for Deep-Draw Presses. (53-4)..........9–16
Rose, H. A. The Magnetic-Amplifier Controlled Log-Carriage Drive and the Basic Duty Cycle of Carriage Performance. (53-316)..........305–13; disc. 314
Rubinoff, Morris. Disc..........125

S

Schach, M.; L. D. Schroeder. Continuous Current Capacity of Bundled Cables for Aircraft. (53-375)..........386–97; disc. 397
Scholl, R. A. Disc..........79
Schroeder, L. D.; M. Schach. Continuous Current Capacity of Bundled Cables for Aircraft. (53-375)..........386–97; disc. 397
Scrafford, Robert L. Hydraulic Servos Incorporating a High-Speed Hydraulic-Amplifier Actuated Valve. (53-103)..........175–9; disc. 180
Sellers, J. F.; B. G. Wheeler, A. C. Halter. Application and Operation of D-C Drives on Rubber Calenders. (53-145)..........194–201; disc. 201
Sherrard, Emil S. Disc..........192, 215
Sherrard, E. S.; W. M. Tucker. Disc..........411
Shuler, William. 240/416-Volt 3-Phase 4-Wire Power and Lighting Supply for Modern Industrial Plants. (53-72)..........71–7; disc. 80
Siegel, Clifford M.; T. J. Higgins. Determination of the Maximum Modulus, or of the Specified Gain, of a Servomechanism by Complex-Variable Differentiation. (53-392)..........467–8; disc. 468
Sklansky, Jack. Disc..........468
Skolnik, M.; T. B. Jones, W. B. Kouwenhoven. The Electric Arc in Argon and Helium. (53-87)..........16–21
Smith, D. S. Disc..........314
Spink, Paul G. Disc..........328
Stair, J., Jr. Design Factors Favoring Diesel-Locomotive Electrical Maintenance. (53-50)..........155–6; disc. 157
Statler, I. C.; W. O. Brehaus, W. F. Milliken, C. L. Muzzey. Disc..........287
Stiger, H. R. Split-Role Exciters: Their Design and Application on Diesel-Electric Locomotives. (53-372)..........357–60
Stiger, H. R.; A. V. Johansson. Dynamic Braking on Diesel-Electric Locomotives. (53-48)..........105–10; disc. 110
Stineman, Russell W. Differential Reactive Current Protection Relay. (53-373)..........407–11; disc. 412
Stineman, Russel W. Disc..........215, 373, 421
Stout, T. M. Effects of Friction in an Optimum Relay Servomechanism. (53-355)..........329–35; disc. 336
Stout, Thomas M. Disc..........169
Stuelpnagel, T. R.; J. P. Dallas. Control of Metal Build-up in Minimum Pressure Sensitive Contact Systems. (53-376)..........398–403
Sylvester, J. D. Disc..........110
Sylvester, J. D.; D. F. Haney. Diesel-Electric Locomotives in Canada. (53-68)..........152–5

T

Teker, J. W. Disc..........159
Teker, J. W.; E. R. Ainsworth. Education and Training of Diesel-Electric Locomotive Maintenance Personnel. (53-70)..........115–19
Thomas, F. Equipment and Functions of a Modern Diesel Locomotive Heavy Electric Repair Shop. (53-76)..........157–9; disc. 160
Trbovich, M.; R. E. Kidwell, Jr., W. M. Tucker. Coordination of Overvoltage and Short-Circuit Protection for Aircraft A-C Systems. (53-364)..........369–73; disc. 373
Tucker, W. M.; E. S. Sherrad. Disc..........411
Tucker, W. M.; M. Trbovich, R. E. Kidwell, Jr. Coordination of Overvoltage and Short-Circuit Protection for Aircraft A-C Systems. (53-364)..........369–73; disc. 373

V

Vincent, W. D. Disc..........313

W

Weber, G. W.; A. H. Hoffer. An Axle-Driven Alternator-Rectifier System for Caboose Power Supply. (53-78)..........133–7; disc. 137
Wheeler, B. G.; J. F. Sellers, A. C. Halter. Application and Operation of D-C Drives on Rubber Calenders. (53-145)..........194–201; disc. 201
Whittaker, C. C. Disc..........230
Wilson, B. J. Methods for Prediction of Steady-State Performance for Unbalanced Regulated 3-Phase Generators. (53-374)..........413–21; disc. 421
Wilt, H. J.; C. R. Ingemanson, A. Loft. Automatic Control of Gas Turbines for Natural Gas Pipeline Pumping. (53-323)..........295–300
Wood, A. J.; S. C. Caldwell. The Effects of Abnormal Conditions on Aircraft Parallel A-C Power Systems. (53-371)..........379–84; disc. 385
Woodson, Herbert H. Disc..........152

Preface

The AIEE *Transactions* for 1953 (volume 72) is published in three parts: Part I. Communication and Electronics; Part II. Applications and Industry; and Part III. Power Apparatus and Systems. The papers in each of the three parts are classified according to subject matter as follows:

Part I. Communication and Electronics

- Communication Switching Systems
- Radio Communications Systems
- Special Communications Applications
- Telegraph Systems
- Television and Aural Broadcasting Systems
- Wire Communications Systems
- Basic Sciences
- Computing Devices
- Electrical Techniques in Medicine and Biology
- Electronic Power Converters
- Electronics
- Instruments and Measurements
- Magnetic Amplifiers
- Metallic Rectifiers
- Nucleonics

Part II. Applications and Industry

- Air Transportation
- Domestic and Commercial Applications
- Land Transportation
- Marine Transportation
- Production and Application of Light
- Chemical, Electrochemical and Electrothermal Applications
- Electric Heating
- Electric Welding
- Feedback Control Systems
- General Industry Applications
- Industrial Control
- Industrial Power Systems
- Mining and Metal Industry

Part III. Power Apparatus and Systems

- Carrier Current
- Insulated Conductors
- Power Generation
- Protective Devices
- Relays
- Rotating Machinery
- Substations
- Switchgear
- System Engineering
- Transformers
- Transmission and Distribution

- Education
- Safety
- Research

Each part has been indexed separately in the back of that particular part. The three parts are not cross-referenced; hence the user should determine first whether the subject matter of the paper desired is in the field of communication and electronics, applications and industry, or power apparatus and systems. Papers are listed in the subject index under several key words in the titles. The original numbers assigned to the papers are given in the author index.

Volume 72 contains the technical papers and related discussions presented at these meetings:

1. Winter General Meeting, New York, N. Y., January 19–23, 1953.
2. Southern District Meeting, Louisville, Ky., April 22–24, 1953.
3. North Eastern District Meeting, Boston, Mass., April 29–May 1, 1953.
4. Summer General Meeting, Atlantic City, N. J., June 15–19, 1953.
5. Pacific General Meeting, Vancouver, B. C., Canada, September 1–4, 1953.
6. Middle Eastern District Meeting, Charleston, W. Va., September 29–October 1, 1953.
7. Aircraft Electric Equipment Conference, Seattle, Wash., September 30–October 2, 1953.
8. Fall General Meeting, Kansas City, Mo., November 2–6, 1953.

Statements and opinions given in the papers and discussions published in *Transactions* are the expressions of the contributors for which the American Institute of Electrical Engineers assumes no responsibility.

Some Saturation Phenomena in Servomechanisms with Emphasis on the Tachometer Stabilized System

E. LEVINSON
ASSOCIATE MEMBER AIEE

Synopsis: This paper describes some experimentally observed servomechanism saturation phenomena and introduces principles and techniques useful in the explanation of these phenomena and in the analysis of saturating servomechanisms. Typical tachometer servomechanism frequency responses with varying input magnitude, including the "jump" resonance phenomenon, are described. The simple principle "that the effect of saturation is to lower the average gain value of the path in which saturation takes place" is applied to the linear transfer function plot to explain the frequency responses. An analytical graphical technique for obtaining the steady-state frequency response of a saturating servomechanism is presented and is used to explain the phenomenon of jump resonance. Techniques for obtaining the transient response of simple saturating servomechanisms are also presented.

THE USE of tachometric feedback through a high-pass filter for the stabilization of servomechanisms is a fairly well-known[1] and frequently used technique. The great advantage of this method over a simple lead network is that a high K_v (low velocity lag) system can be obtained with a small bandwidth (less transmission of noise). Figure 1 is a block diagram of a typical servomechanism system stabilized by means of tachometric feedback through a high-pass filter.

In checking the performance of servomechanisms of this type by obtaining the closed-loop frequency response with varying input signal magnitude, one often encounters some very peculiar phenomena. A typical set of responses is displayed in Figure 2. For small signals the servomechanism performs as expected, with peaking and crossover frequency comparing favorably with linear theory. As the signal size increases, higher peaking at the higher frequencies begins to take place and in some instances, the phenomenon of "jump" or "bending" resonance such as that described in Figure 3 may occur. However, at still larger signal inputs, this high-frequency peaking disappears and the crossover frequencies become lower and lower.

It is the main purpose of this paper to offer a workable explanation of this set of responses. In developing this explanation, certain principles and techniques will be expounded that may be very useful in the analysis of any servomechanism exhibiting saturation effects. In addition, the transfer function of the tachometer feedback through high-pass filter servomechanism will be developed into an extremely useful form where each breakpoint is easily related to the parameters of the system. This same transfer junction form is obtained in a slightly different manner by Dowker.[2]

Mechanics of Explanation

The first basic principle to be employed is that the effect of saturation is to lower the average gain value of the path in which saturation takes place (a typical saturation curve and saturation gain function are shown in Figure 6). These changes in gain parameters are reflected on the decibel-log ω transfer function plot and used to explain the closed-loop responses encountered. What is obtained is a different decibel-log ω plot for each condition of saturation with linear analysis still being applied. The frequency response is then related to the decibel-log ω plot by the considerations that response crossover frequency is close to decibel-log ω crossover and that a −12-decibel-per-octave crossover slope of the decibel-log ω plot means high peaking in the frequency response.

A second analytical graphical technique which may be used to obtain the steady-state frequency response of any saturating servomechanism, will be employed to explain the phenomenon of jump resonance. This phenomenon is shown to take place in a simple servomechanism loop with a saturating forward path by means of this analytical graphical technique. The same equations are then shown to exist for the tachometer stabilized case in special circumstances.

Explanation of Frequency Response Curves by Use of "Gain" Principle

As developed in Appendix I, and referring to Figure 1, an approximate expression for the open-loop transfer function of a tachometer through high-pass filter stabilized servomechanism system is

$$H(p)=\frac{\theta_0}{E}(p)=\frac{K_v(1+\tau_2 p)}{p(1+\alpha\tau_2 p)\left[1+\frac{\tau_m}{\alpha}p\right]};\qquad \begin{array}{c}\alpha\tau_2>>\tau_m\\ \alpha>>1\end{array}\quad(1)$$

where

$$K_v=\frac{K_eK_1K_2K_m}{N}$$

is the open-loop forward gain around the outer loop.

$$\alpha=\frac{K_TK_3K_2K_m}{N_T}$$

is the open-loop gain around inner tachometer feedback loop. τ_2 is the time constant of the high-pass filter. τ_m is the time constant of the motor and load.

It is observed that the system breakpoints are readily related to the system parameters and this fact is displayed in the transfer function plot in Figure 4. Working with this plot, the effects of saturation will now be studied.

If, as the signal size increases, saturation takes place in the tachometer feedback path (such as block K_3, for instance) first while the forward path is still linear, then the system will behave as though it has a smaller α with the same K_v. A decrease in α moves the first breakpoint out and the third breakpoint in as shown in dotted lines in Figure 4. This leads to a new crossover frequency ω_c' which is higher than ω_c and in a −12-decibel-per-octave slope. This means high peaking at high frequencies with high-frequency crossover such as obtained in the curves of Figure 2.

As the signal size increases further, the forward path begins to saturate also and the servomechanism acts as though K_v has decreased. The effect of this is to move the 0 decibel line up as shown by the dashed lines in Figure 4.

Paper 53-110, recommended by the AIEE Feedback Control Systems Committee and approved by the AIEE Committee on Technical Operations for presentation at the AIEE Winter General Meeting, New York, N. Y., January 19–23, 1953. Manuscript submitted October 10, 1952; made available for printing December 15, 1952.

E. Levinson is with the Sperry Gyroscope Company, Great Neck, N. Y.

The author wishes to express his thanks to E. F. vonArx of the Sperry Gyroscope Company for his valuable comments and inspirational guidance which proved very helpful in the preparation of this paper.

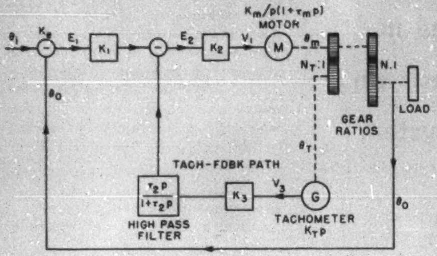

$$H(p) \cong \frac{K_V(1+\tau_2 p)}{p(1+a\tau_2 p)(1+\tau_{m/a} p)}, \quad K_V = \frac{K_e K_1 K_2 K_m}{N}; \quad a = \frac{K_T K_3 K_2 K_m}{N_T}$$

Figure 1 (left). Block diagram of tachometer-through-high-pass-filter stabilized servomechanism

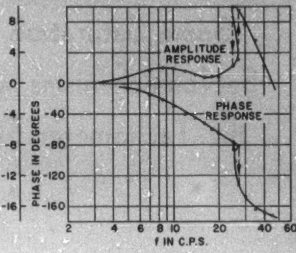

Figure 3 (right). Jump resonance phenomenon in frequency response

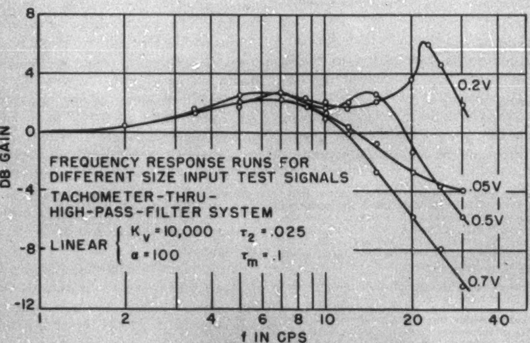

Figure 2. Typical set of saturation frequency responses for tachometer system

This leads to another new crossover frequency ω_c'' which is lower than ω_c' and possibly in a -6-decibel-per-octave slope. The high peaking effect should, therefore, disappear and frequency crossover should occur at lower and lower frequencies. This was precisely the behavior obtained in the curves of Figure 2.

At still larger signal magnitudes, the crossover frequency will fall in the first -12-decibel-per-octave slope and high peaking at low frequencies with low-frequency crossover will begin to take place.

If, as the signal size increases, saturation takes place in the forward path first, then the system would probably not exhibit the initial high peaking at high frequencies effect, since by the time the α path begins to saturate, the system would be in the ω_c'' type of region. Therefore, if it is desired to minimize the high-frequency peaking type of nonlinearity, K_v should be made to saturate simultaneously or sooner than α.

The effects of saturation on transient responses to step displacement inputs of different magnitudes can be explained or predicted from the frequency response plots. Thus, in the signal size region of high peaking at high frequencies, a quicker rise time, more oscillatory response should be obtained than in the linear signal region. At still higher signal magnitudes, the rise time should increase and the response should be less oscillatory. These expectations are borne out in the set of transient responses shown in Figure 5.

This basic principle of gain change with saturation can be extended to the study of saturation effects in any servomechanism system with special application in multiple-loop systems where the effect of each loop can be investigated one by one.

"Gain" Principle Applied to Single-Loop System

A simple single-loop lead network stabilized servomechanism system will be treated as another example. The transfer function of this type of servomechanism system is

$$H(p) = \frac{\theta_0}{E}(p) = \frac{K_v(1+\tau_1 p)}{p(1+\tau_m p)(1+\tau_2 p)} \qquad (2)$$

This is plotted in Figure 7 along with a typical block diagram. A typical set of frequency responses of this system with varying signal magnitude is shown in Figure 8. It is observed that as the signal magnitude increases, the peaking initially decreases and the crossover frequency decreases. With further increase in signal magnitude, the peaking begins to increase and the crossover frequency gets lower and lower. These effects are explained with reference to the decibel-log ω plot of Figure 7.

The only gain parameter in a single-loop system is K_v and the effect of a decrease in K_v is to move up the zero decibel line. As the signal magnitude increases, the effective K_v decreases and crossover takes place at a new and lower ω_c'. The initial change in peaking depends on the original K_v in the system and the relative proximity of the crossover frequency to a -12-decibel-per-octave slope. If crossover is originally at a point like *B*, then we would initially expect less peaking with increased signal size. If crossover were originally at a point like *A*, more peaking with increased signal size would be expected. With a further increase in signal magnitude, K_v decreases further and eventually the crossover frequency ω_c'' occurs in the first -12-decibel-per-octave slope. Therefore, the peaking begins to increase and the crossover frequency gets lower and lower.

Explanation of "Jump" Resonance and Frequency Response Analysis of Saturating Servomechanisms

The transfer function of a simple uncompensated single loop with forward path saturation is

$$\frac{\theta_0}{E} = \frac{K_v(|E|)}{p(1+\tau_m p)} \qquad (3)$$

where $K_v(|E|)$ is a function of the magnitude of the error signal such as that in Figure 6. This type of saturation may

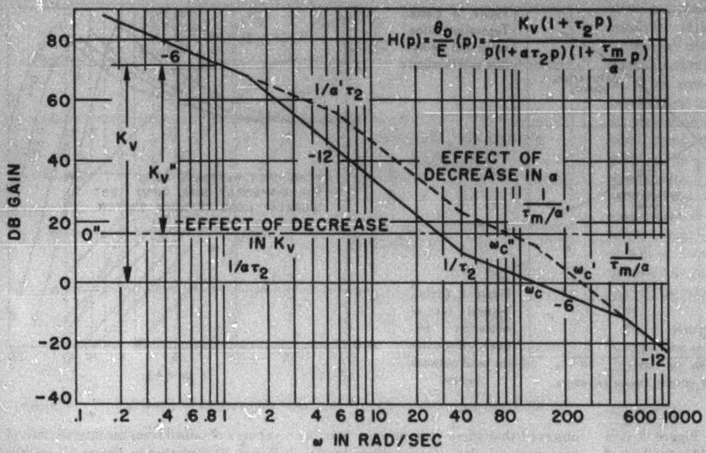

Figure 4. Linear transfer function plot for tachometer stabilized system

be caused by torque saturation of the motor or amplifier saturation or any combination of the two. Now

$$\frac{\theta_i}{E}=1+\frac{\theta_0}{E}=\frac{p(1+\tau_m p)+K_v(|E|)}{p(1+\tau_m p)} \quad (4)$$

The differential equation relating E to θ_i is therefore

$$\tau_m\frac{d^2E}{dt^2}+\frac{dE}{dt}+K_v(|E|)E=\tau_m\frac{d^2\theta_i}{dt^2}+\frac{d\theta_i}{dt} \quad (5)$$

For $\theta_i = \theta_{im} \sin \omega t$, this equation is similar to the Duffing equation.[3] The left-hand side of this equation has the identical form of a "soft spring" mechanical system with damping. Various iterative and perturbation techniques have been employed[3,4] to solve the Duffing equation under special circumstances and a graphical solution for the system without damping has been made by Den Hartog.[5] In every solution, bending resonance is shown to take place.

When equation 5 is integrated on both sides, the left-hand side of the resultant equation has the identical form of a resistance-inductance-capacitance series circuit with a nonlinear capacitance. It may be expected that such a circuit will also exhibit jump resonance.

The technique employed here not only takes damping into account but has the advantage of easily being extended to higher order systems, as will be shown.

Inverting equation 4

$$\frac{E}{\theta_i}(p)=\frac{p(1+\tau_m p)}{p(1+\tau_m p)+K_v(|E|)} \quad (6)$$

It is desired to obtain the steady-state frequency response of E or θ_0 to sinusoidal input

$$\theta_i=\theta_{im}e^{j\omega t}$$

Assuming that the distortion in the resultant signal is negligible (distortion will always exist in a nonlinear system), so that

$$E=|E|\,e^{j(\omega t+\phi_E)}$$

$j\omega$ then can be substituted for p as in a linear analysis and obtain as the frequency response

$$\frac{E}{\theta_i}(j\omega)=\frac{j\omega(1+j\omega\tau_m)}{j\omega(1+j\omega\tau_m)+K_v(|E|)} \quad (7)$$

or

$$|E|=\frac{\omega\sqrt{1+\omega^2\tau_m^2}\,|\theta_i|}{\sqrt{[K_v(|E|)-\omega^2\tau_m]^2+\omega^2}} \quad (8)$$

and

$$\phi_E=90°+\tan^{-1}\omega\tau_m-\tan^{-1}\frac{\omega}{[K_v(|E|)-\omega^2\tau_m]} \quad (9)$$

Since $K_v(|E|)$ is a function of $|E|$, it is not possible to solve for $|E|$ or ϕ_E directly. However, the following graphical procedure will enable a solution for $|E|$ and therefore, ϕ_E, θ_0, and ϕ_0.

Squaring equation 8 and transposing

$$[K_v(|E|)-\omega^2\tau_m]^2|E|^2=\omega^2(1+\omega^2\tau_m^2)|\theta_i|^2-\omega^2|E|^2 \quad (10)$$

Now taking the square root

$$[K_v(|E|)-\omega^2\tau_m]|E|=\pm\omega\sqrt{(1+\omega^2\tau_m^2)|\theta_i|^2-|E|^2}$$

or

$$K_v(|E|)|E|=\omega^2\tau_m|E|\pm\omega\sqrt{(1+\omega^2\tau_m^2)|\theta_i|^2-|E|^2} \quad (11)$$

Figure 5 (below). Experimental set of transient responses for saturating tachometer stabilized system

A. 0.07-volt step
B. 0.2-volt step
C. 0.5-volt step
D. 2-volt step

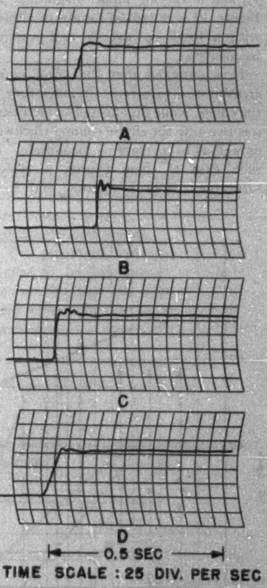

The left-hand side of equation 11 is the saturation curve of the forward path. The right-hand side is a family of ellipses. The intersections of these ellipses with the saturation curve is the magnitude of $|E|$ at the particular ω and $|\theta_i|$. Each of the parameters, K_v, τ_m, ω, and $|\theta_i|$ can be varied and its effect on the magnitude of

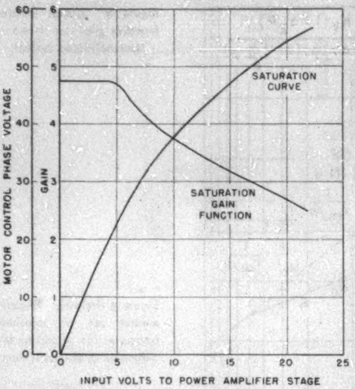

Figure 6 (left). Typical saturation curve and saturation gain function

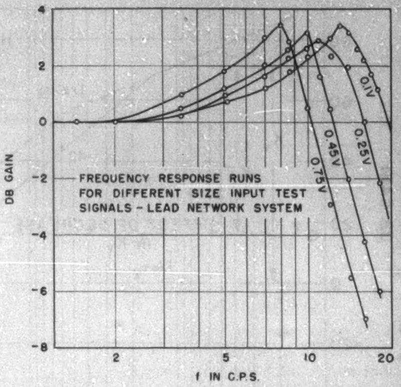

Figure 8 (right). Typical set of saturation frequency responses for lead network system

$|E|$ can be determined. Figure 9 is a typical family of ellipses with a fixed ω and τ_m and a varying input magnitude $|\theta_i|$. Figure 10 is a typical family of ellipses with a fixed τ_m and $|\theta_i|$ and varying frequency ω.

It is observed that the effect of increasing $|\theta_i|$ is to increase the magnitude of the ellipse, while the effect of an increasing ω is to rotate the ellipse counter clockwise as well as to increase its magnitude. In each case of these figures, a typical saturation curve is plotted and it is observed that there may be one, two (a tangency), or three intersections in the first quadrant. Because of origin symmetry, the same intersections will take place in the third quadrant and will therefore give the same values of $|E|$. Therefore, only the first quadrant need be considered. It is this possibility of three intersections that leads to the phenomenon of bending resonance. This possibility can not take place in a linear system as shown by the linear K_s plots.

An amplitude frequency response of $|E|$ versus ω obtained from the intersections of Figure 10 is plotted in Figure 11 and the bending resonance phenomenon is observed. The three values of $|E|$ do not occur simultaneously in a physical system. What does occur can be observed from the movement of the ellipses as ω increases or decreases.

As ω increases the intersection with the $K_s(|E|)|E|$ curve increases and $|E|$ takes on values along *CA* of Figure 11. Although for ω values that give rise to $|E|$ values along *EA*, there also exist other *E*

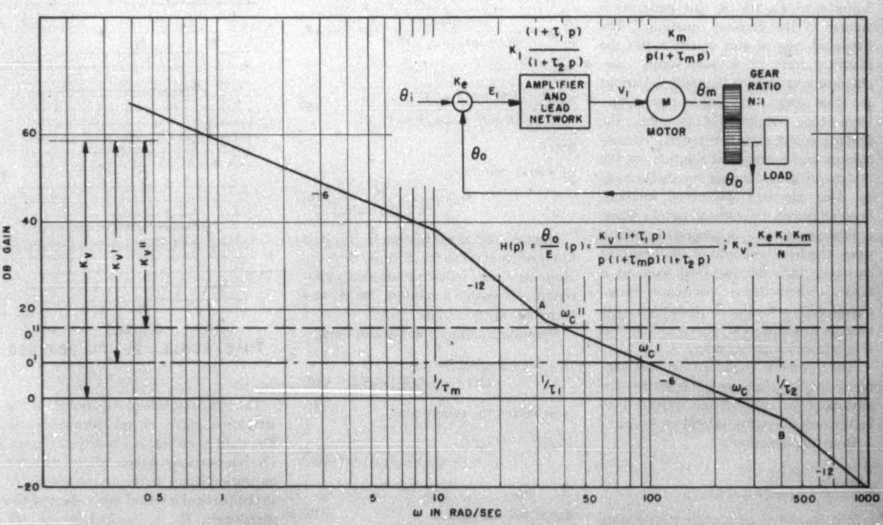
$K_1 \frac{(1+\tau_1 p)}{(1+\tau_2 p)}$
$\frac{K_m}{p(1+\tau_m p)}$
θ_i
K_e
E_1
AMPLIFIER AND LEAD NETWORK
V_1
M
MOTOR
θ_m
GEAR RATIO N:1
LOAD
θ_o
θ_o
$H(p) = \frac{\theta_o}{E}(p) = \frac{K_v(1+\tau_1 p)}{p(1+\tau_m p)(1+\tau_2 p)}$; $K_v = \frac{K_e K_1 K_m}{N}$
DB GAIN
K_v
K_v'
K_v''
-6
-12
A
ω_c''
ω_c'
-6
ω_c
B
-12
$1/\tau_m$
$1/\tau_1$
$1/\tau_2$
60
40
20
0''
0'
0
-20
0.5
1
5
10
50
100
500
1000
ω IN RAD/SEC

Figure 7. Transfer function plot and block diagram of lead network single-loop system

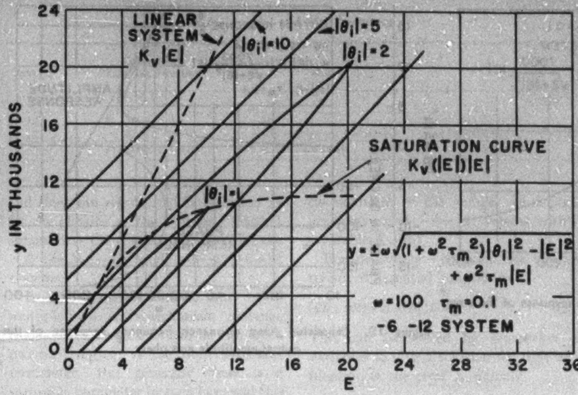

Figure 9. Typical family of ellipses with fixed ω and τ_m and variable input magnitude $\theta_i|$

solutions, these do not occur because the $|E|$ values along EA are stable solutions. At point A, the ω ellipse is tangent to the $K_v(|E|)|E|$ curve. At a value of ω slightly above the tangency value, there is only one intersection and this is at a much larger value of $|E|$. Thus, there is a discontinuous jump in the value of $|E|$ from point A to point D. Further increases in ω still lead to one intersection but with decreasing values of $|E|$ as shown in arc DF.

If the response is measured with decreasing frequency, however, a different set of magnitudes is obtained. As ω decreases, the $|E|$ values increase along arc FB, and although more than one intersection exists from D to B, the $|E|$ values remain along DB because these values are stable solutions. At point B, the ω ellipse is tangent to the $K_v(|E|)|E|$ again, but this time at a smaller value of ω and a larger value of $|E|$. At a value of ω slightly below the tangency, there is only one intersection and this is at a much lower value of $|E|$. Thus, there is again a discontinuity, this time a drop in the value of $|E|$ from point B to point E. Further decreases in ω still lead to one intersection and decreasing values of $|E|$ as shown in arc EC.

Thus, the region AB does not take place physically and is therefore, in a certain sense, unstable. Proof of this instability using a Mathieu equation technique is performed in Stoker.[3]

From equation 3 the magnitude and phase of the output position can be obtained

$$|\theta_0|=\frac{K_v(|E|)|E|}{\omega\sqrt{1+\omega^2\tau_m^2}} \tag{12}$$

$$\phi_0=\phi_E-90^\circ-\tan^{-1}\omega\tau_m \tag{13}$$

Substituting equation 9 in equation 13 gives

$$\phi_0=-\tan^{-1}\frac{\omega}{(K_v(|E|)-\omega^2\tau_m)} \tag{14}$$

The amplitude and phase of the output response for the $|E|$ response of Figure 11 are plotted in Figure 12. It is observed that the general nature of these responses is identical to the experimental responses of Figure 3.

From equation 29 of Appendix I, it is observed that for α equal zero (no tachometer feedback), the tachometer stabilized transfer function reduces to equation 3. In a highly saturated tachometer feedback path, α approaches zero, the transfer function approaches equation 3, and the possibility of jump resonance will occur.

One may wonder why this phenomenon occurs so rarely in servomechanism studies. One reason, of course, is that few development engineers bother to examine servomechanism performance to very large input signals. But perhaps the greatest reason is that most servomechanisms are lead network or otherwise compensated so that the open-loop transfer function of the system looks generally like a straight −6-decibel-per-octave slope. It will be shown that bending resonance can not take place for systems of this ideal type if the saturation curve is of the usual form.

In a straight −6-decibel-per-octave system, the −12-decibel break point is pushed out to infinity or τ_m approaches zero. For $\tau_m = 0$, equation 3 reduces to

$$\frac{\theta_0}{E}=\frac{K_v(|E|)}{p}$$

and equation 11 reduces to

$$K_v(|E|)|E=\pm\omega\sqrt{|\theta_i|^2-|E|^2} \tag{15}$$

The family of ellipses in this case are rectangular ellipses as plotted in Figure 13. Increasing $|\theta_i|$ blows up the ellipses, while increasing ω elongates the y axis of the ellipses. The important point to note from Figure 13 is that for any positive-sloped single-valued $K_v(|E|)|E|$ function, there is always only one intersection in the first quadrant. Bending resonance, therefore, cannot occur in this ideal type of servomechanism system.

The preceding technique can be extended to the lead network compensated servomechanism, the tachometer stabilized servomechanism, or any other servomechanism, and although the expressions

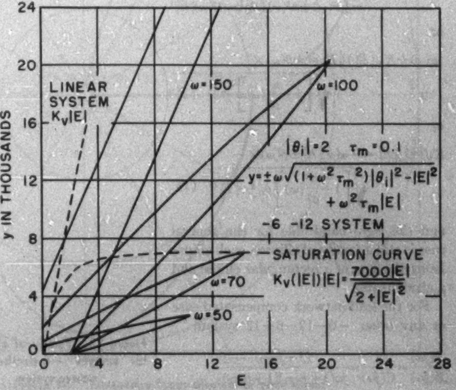

Figure 10. Typical family of ellipses with fixed $|\theta_i|$ and τ_m and variable frequency ω

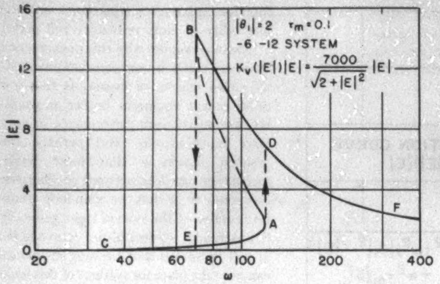

Figure 11. Calculated jump resonance frequency response of the error magnitude

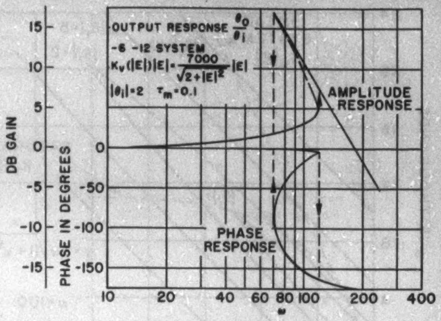

Figure 12. Calculated jump resonance frequency response of the output amplitude and phase

get more and more complicated, the application of the technique does not become too unwieldy.

A generalized expression can be obtained for any servomechanism system where $K_v(|E|)|E|$ is the only saturable parameter. For the general servomechanism system

$$\frac{\theta_0}{E}(j\omega)=K_v(|E|)\frac{A(j\omega)}{B(j\omega)}=\frac{K_v(|E|)}{C(j\omega)} \tag{16}$$

$$\frac{E}{\theta_i}(j\omega)=\frac{1}{1+\dfrac{\theta_0}{E}(j\omega)}=\frac{C(j\omega)}{C(j\omega)+K_v(|E|)} \tag{17}$$

where

$$C(j\omega)=\frac{B(j\omega)}{A(j\omega)}=\alpha(\omega)+j\beta(\omega)$$

then

$$|E|^2=\frac{[\alpha^2(\omega)+\beta^2(\omega)]|\theta_i|^2}{[\alpha(\omega)+K_v(|E|)]^2+\beta^2(\omega)}$$

or

$$[\alpha(\omega)+K_v(|E|)]^2|E|^2 = [\alpha^2(\omega)+\beta^2(\omega)]|\theta_i|^2-\beta^2(\omega)|E|^2$$

or

$$[\alpha(\omega)+K_v(|E|)]|E| = \pm\beta(\omega)\times\sqrt{\left[1+\frac{\alpha^2}{\beta^2}(\omega)\right]|\theta_i|^2-|E|^2}$$

or

$$K_v(|E|)|E| = -\alpha(\omega)|E|\pm\beta(\omega)\times\sqrt{\left[1+\frac{\alpha^2}{\beta^2}(\omega)\right]|\theta_i|^2-|E|^2} \tag{18}$$

and the right-hand side for the general case is still a family of ellipses, each ellipse being the sum of a rectangular ellipse and a straight line.

For the lead network compensated case or any other −6−12−6−12 system

$$\frac{A(j\omega)}{B(j\omega)}=\frac{1}{C(j\omega)}=\frac{(1+j\omega\tau_2)}{j\omega(1+j\omega\tau_1)(1+j\omega\tau_3)}$$

Therefore

$$C(j\omega)=\frac{j\omega(1+j\omega\tau_1)(1+j\omega\tau_3)}{(1+j\omega\tau_2)}=\alpha(\omega)+j\beta(\omega)$$

This is expanded in Appendix II to give

$$\alpha(\omega)=-\omega^2\frac{[(\tau_1+\tau_3-\tau_2)+\omega^2\tau_1\tau_2\tau_3]}{1+\omega^2\tau_2^2} \tag{19}$$

$$\beta(\omega)=\frac{\omega[1-\omega^2[\tau_1\tau_3-\tau_2(\tau_1+\tau_3)]]}{1+\omega^2\tau_2^2} \tag{20}$$

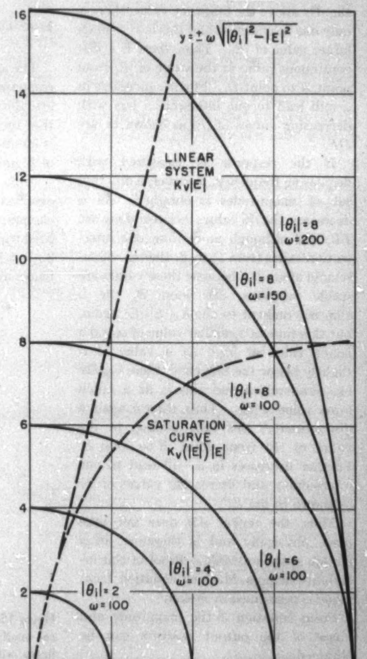

Figure 13. Family of ellipses for straight −6-decibel-per-octave system

Table I. $\alpha(\omega)$ and $\beta(\omega)$ Functions

System	Open-Loop Transfer Function	$\alpha(\omega)$	$\beta(\omega)$
6	K_v/p	0	ω
6−12	$K_v/p(1+\tau_1 p)$	$-\omega^2\tau_1$	ω
6−12−6−12	$\dfrac{K_v(1+\tau_2 p)}{p(1+\tau_1 p)(1+\tau_3 p)}$	$\dfrac{-\omega^2[(\tau_1+\tau_3-\tau_2)+\omega^2\tau_1\tau_2\tau_3]}{1+\omega^2\tau_2^2}$	$\dfrac{\omega\{1-\omega^2[\tau_1\tau_3-\tau_2(\tau_1+\tau_3)]\}}{1+\omega^2\tau_2^2}$

and these are substituted in equation 18 for the plotting of the ellipses. Table I summarizes the α and β functions for the −6, the −6−12, and −6−12−6−12 systems.

In tachometer stabilized and other multiple-loop servomechanism systems, the same expression 18 can be employed provided $K_v(|E|)$ is the only saturable parameter. But generally there is a saturable parameter in each loop and this parameter is a function of a different quantity in each loop. Thus, in a tachometer stabilized system the tachometer feedback loop gain α is a function of the output speed $|d\theta_0/dt|$ while the forward loop K_v is a function of the error signal $|E|$. It can be appreciated that a general analytical solution for this case would be extremely complicated. This indicates an advantage of the gain change with saturation principle used to explain the responses of Figure 2.

However, if it is assumed that saturation to increasing $|\theta_i|$ takes place in one path, while the other paths are linear, then the technique can be extended to multiple-loop systems. A frequency expression relating the saturable quantity to θ_i must be obtained, for example $j\omega\theta_0/\theta_i$ in the tachometer feedback path case, and then expanded into an expression analogous to equation 18 for graphical plotting.

It should be remembered that throughout the preceding analysis it was assumed that the distortion in the E response could be neglected. This may not be possible in some applications.

Transient Response Analysis of Simple Saturating Servomechanisms

Some insight into the transient response of a saturating servomechanism might be gained from observation or manipulation of the frequency responses obtained by the preceding methods. This procedure is questionable, however, because of the fact that the superposition principle does not hold in nonlinear systems. Although it is beyond the objectives of this paper to obtain the transient responses of saturating servomechanisms, it may prove useful to indicate some possible techniques for the solutions of the simple −6-decibel-per-octave and −6−12 systems with a saturable $K_v(|E|)$.

For the simple −6 system, the characteristic differential equation is

$$(dE)/(dt)+K_v(|E|)E=0 \qquad (21)$$

This can be solved by separation of variables to give a solution for time as a function of the error E, namely

$$t=-\int\frac{dE}{K_v(|E|)E}+C \qquad (22)$$

This integration can be performed graphically on a reciprocal plot of the saturation curve.

For the normal saturation curve, the time constant of the saturation case is greater than that of the linear case and furthermore is a function of the initial error magnitude E_0. This latter fact is true of all nonlinear systems. The output response $\theta_0(t)$ can be obtained from the error response as in the linear case: $\theta_0(t)=\theta_i(t)-E(t)$. This will, of course, apply in every system.

For the −6 −12 system, the characteristic differential equation is

$$\tau_m\frac{d^2E}{dt^2}+\frac{dE}{dt}+K_v(|E|)E=0 \qquad (23)$$

This can be solved by the technique of isoclines in the phase plane.[6,7] The family of isoclines is given by

$$\frac{dE}{dt}=v=-\frac{1}{\tau_m S+1}K_v(|E|)E \qquad (24)$$

and they are observed to be *multiples of the saturation curve.* Thus, given a saturation curve, the isoclines can be plotted; the phase plane trajectory can then be obtained using the isoclines[7]; and finally the time response plot can be obtained from the trajectory using the relationship $t=|\int dE/v|$.

For the normal saturation curve, the phase plane trajectories are stable spirals as in the linear case. The normalized transient response is a function of the initial magnitude of E_0 as in all nonlinear systems.

Some Further Points Concerning Saturation in Frequency Response

In several instances, saturation is a frequency as well as a magnitude effect.

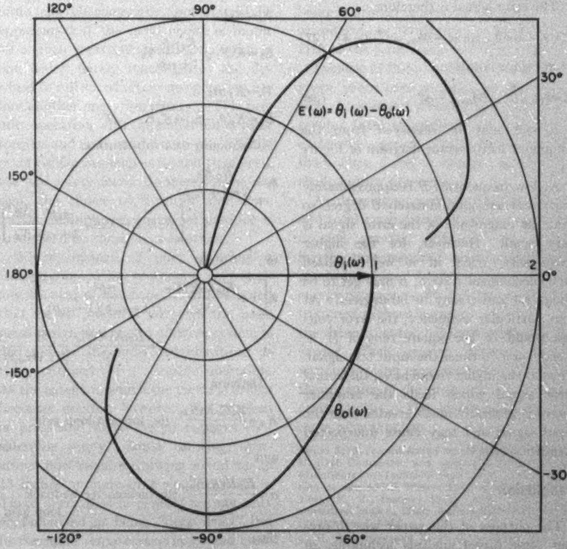

Figure 14. Frequency locus diagram of error signal

Two such instances are discussed in the following.

TACHOMETER PATH SATURATION

The following analysis will show that it is a fairly simple matter to saturate the tachometer feedback path. If the input test function is a sinusoidal wave, then the motor or output position can be assumed to be $\theta_m = \theta_{mm} \sin \omega t$. The tachometer output voltage is $K_T/N_T d\theta_m/dt$ so that

$$V_T = \frac{K_T}{N_T}\omega\theta_{mm}\cos\omega t \tag{25}$$

or

$$V_{T_{rms}} = \frac{K_T}{\sqrt{2}N_T}\omega\theta_{mm} \tag{26}$$

Thus, at large signals (large θ_{mm}) and high frequencies (large ω), the tachometer output voltage becomes very large and saturation in the tach feedback path will likely take place.

FORWARD PATH SATURATION

The following analysis will show that frequency effects are also a large factor in forward path saturation. If the input test function is a sinusoidal wave $\theta_i = \theta_{im} \sin \omega t$ then the output signal will be some magnitude and phase multiplication of the input signal. $\theta_0 = B\theta_{im}\sin(\omega t - \phi)$ where B and ϕ are functions of ω (the gain and phase frequency response of the servomechanism).

The error signal is therefore

$$E = \theta_i - \theta_0 = \theta_{im}\sin\omega t - B\theta_{im}\sin(\omega t - \phi) \tag{27}$$

or in vector notation

$$E = \theta_{im}\angle 0^\circ - B\theta_{im}\angle -\phi^\circ \tag{28}$$

E can now be observed from the frequency locus vector diagram of Figure 14.

At low frequencies B is approximately unity and ϕ is approximately 0 degree so that the magnitude of the error signal is very small. However, for the higher frequencies, even in a well-stabilized servomechanism system, B may get to be about 1.4 and ϕ may be 90 degrees. At that particular frequency, the error voltage would be the square root of $[1 + (1.4)^2]$, or 1.72 times the input test signal. Thus at the higher frequencies, the actual error signal which feeds the amplifier stages is generally much greater than the input signal and may cause unexpected saturation effects.

Conclusion

The purpose of this paper was to present some useful analysis techniques in dealing with saturation effects in servomechanisms. No devices for compensating or minimizing these effects were advanced although suggestions towards these can be derived from the analysis. Whether the saturation effects are harmful or not depends on the application of the particular servomechanism system being studied.

The principles expounded here should by no means be treated as natural laws. All that can be said is that they work in a few simple cases and can, therefore, be placed alongside the other nonlinear analytical tools in the servomechanism engineer's bag of tricks.

Lastly, the transfer function form for a tachometer stabilized servomechanism presented here is an extremely useful one in the design and analysis of such servomechanisms and is not limited to studies of saturation.

Appendix I. Transfer Function for Tachometer Through High-Pass Filter Stabilized Servomechanism System

Referring to the block diagram of Figure 1

$$\theta_0 = \frac{\theta_m}{N}, \quad \theta_T = \frac{\theta_m}{N_T}$$

$$\frac{\theta_m}{V_1} = \frac{K_m}{p(1+\tau_m p)}$$

$$V_1 = K_2 E_2$$

$$E_2 = K_1 E_1 - \frac{K_3\tau_2 p}{1+\tau_2 p}V_3$$

$$V_3 = K_T p\theta_T$$

$$E_1 = K_e(\theta_i - \theta_0) = K_e E$$

Combining and substituting

$$\theta_0 = \frac{K_m K_2}{Np(1+\tau_m p)} \times \left[K_1 K_e E - K_3 K_T \frac{\tau_2 p^2}{1+\tau_2 p}\frac{N\theta_0}{N_T}\right]$$

or

$$\theta_0\left[1 + \frac{K_m K_2 K_3 K_T}{N_T}\frac{\tau_2 p^2}{p(1+\tau_m p)(1+\tau_2 p)}\right] = \frac{K_m K_2 K_1 K_e}{N}\frac{E}{p(1+\tau_m p)}$$

Defining

$K_v = \dfrac{K_e K_1 K_2 K_m}{N}$, the forward-loop gain

and

$\alpha = \dfrac{K_T K_3 K_2 K_m}{N_T}$, the tachometer feedback loop gain

then

$$\theta_0[p(1+\tau_m p)(1+\tau_2 \mathrm{p}) + \alpha\tau_2 p^2] = K_v E(1+\tau_2 p)$$

and

$$\frac{\theta_0}{E} = \frac{K_v(1+\tau_2 p)}{p(\tau_m\tau_2 p^2 + [\tau_m + (1+\alpha)\tau_2]p + 1)} \tag{29}$$

The quadratic in the denominator can be factored into

$$(1+\tau_1 p)(1+\tau_3 p)$$

where

$$\tau_1\tau_3 = \tau_m\tau_2$$

$$\tau_1 + \tau_3 = \tau_m + (1+\alpha)\tau_2$$

or

$$\frac{\tau_1}{\tau_2} \times \frac{\tau_3}{\tau_2} = \frac{\tau_m}{\tau_2} \tag{30}$$

and

$$\frac{\tau_1}{\tau_2} + \frac{\tau_3}{\tau_2} = \frac{\tau_m}{\tau_2} + 1 + \alpha \tag{31}$$

Now in almost all practical systems τ_2 is generally of the same order of τ_m, while $\alpha >> 1$. Therefore, $1+\tau_m/\tau_2$ is usually negligible compared to α. Also, for stability it is generally desired that τ_3 be at most $1/8\tau_2$, while for high K_v systems τ_1 is always large compared to τ_2. Therefore, τ_3/τ_2 is usually negligible compared to τ_1/τ_2.

Then in equation 31

$$\frac{\tau_1}{\tau_2} \cong \alpha$$

or

$$\tau_1 = \alpha\tau_2$$

and substituting this in equation 30

$$\frac{\tau_3}{\tau_2} = \frac{\tau_m/\tau_2}{\alpha}$$

or

$$\tau_3 = \tau_m/\alpha$$

Therefore

$$\frac{\theta_0}{E} \cong \frac{K_v(1+\tau_2 p)}{p(1+\alpha\tau_2 p)\left(1+\dfrac{\tau_m}{\alpha}p\right)} \tag{32}$$

Appendix II. $\alpha(\omega)$ and $\beta(\omega)$ for 6−12−6−12 System

$$C(j\omega) = \frac{B(j\omega)}{A(j\omega)} = j\omega\frac{(1+j\omega\tau_1)(1+j\omega\tau_3)}{(1+j\omega\tau_2)}$$

$$C(j\omega) = j\omega\frac{[1-\omega^2\tau_1\tau_3 + j\omega(\tau_1+\tau_3)]}{(1+j\omega\tau_2)} \times \frac{(1-j\omega\tau_2)}{(1-j\omega\tau_2)}$$

$$C(j\omega) = j\omega\frac{[1-\omega^2[\tau_1\tau_3 - \tau_2(\tau_1+\tau_3)] + j\omega[(\tau_1+\tau_3-\tau_2) + \omega^2\tau_1\tau_2\tau_3]]}{1+\omega^2\tau_2^2}$$

$$C(j\omega) = -\omega^2\frac{[(\tau_1+\tau_3-\tau_2)+\omega^2\tau_1\tau_2\tau_3]}{1+\omega^2\tau_2^2} + j\omega\frac{[1-\omega^2[\tau_1\tau_3 - \tau_2(\tau_1+\tau_3)]]}{1+\omega^2\tau_2^2} \tag{33}$$

Therefore

$$\alpha(\omega) = -\omega^2\frac{[(\tau_1+\tau_3-\tau_2)+\omega^2\tau_1\tau_2\tau_3]}{1+\omega^2\tau_2^2} \tag{34}$$

and

$$\beta(\omega)=\omega\frac{[1-\omega^2[\tau_1\tau_2-\tau_3(\tau_1+\tau_2)]]}{1+\omega^2\tau_3^2} \qquad (35)$$

References

1. A Comparison of Two Basic Servomechanism Types, **Herbert Harris**. *AIEE Transactions*, volume 66, 1947, pages 83–93.

2. Theory of Servomechanisms (book), **H. M. James, N. B. Nichols, R. S. Phillips, C. H. Dowker**. *Radiation Laboratory Series*, volume 25, McGraw-Hill Book Company, Inc., New York, N. Y., 1947, page 356.

3. Non-Linear Vibration in Mechanical and Electrical Systems (book), **J. J. Stoker**. Interscience Publishers, New York, N. Y., 1950.

4. Steady Oscillations of Systems with Non-Linear and Unsymmetrical Elasticity, **M. Rauscher**. *Journal of Applied Mechanics* (New York, N. Y.), volume 5, 1938, pages A-169–A-177.

5. Mechanical Vibrations (book), **J. P. Den Hartog**. McGraw-Hill Book Company, Inc., New York, N. Y., second edition, 1940, page 403.

6. Non-Linear Mechanics (book), **N. Minorsky**, J. W. Edwards, Ann Arbor, Mich., 1947.

7. Non-Linear Techniques for Improving Servo Performance, **D. McDonald**. *Bulletin S-2*, Cook Research Laboratories, (Chicago, Ill.), 1950.

No Discussion

Adjustable Speed D-C Drives for Deep-Draw Presses

C. E. ROBINSON
NONMEMBER AIEE

A. P. DiVINCENZO
ASSOCIATE MEMBER AIEE

Synopsis: The trend in the automobile industry toward larger and more complex stamped parts for fabricating automobile bodies has necessitated radical changes in the design of stamping presses and their associated drives. The drive problems presented by these more complex machines and operations have led to the development of new drive systems. This paper deals with the application of d-c adjustable-speed drives to deep-drawing presses. Basic drive considerations and description of a typical drive are discussed.

Press Development

In the simpler types of presses, such as those required to perform blanking operations where the metal is sheared only and no drawing action takes place, the moving die is driven by a crank which gives it a simple harmonic motion. Since all the work is done in the brief interval immediately after the die engages the metal, the press is so arranged that this contact occurs at a point very near to dead center of the crank. With the great mechanical advantage thus afforded, only a comparatively small torque applied at the crank shaft produces a tremendous force on the moving die where the shearing of the metal is in progress.

The conventional press of this character is driven by a squirrel-cage motor through a clutch mechanism. A flywheel is built into the transmission on the power side of the clutch, and a brake is provided on the load side.

The energy for performing the actual shearing of the metal is provided by the flywheel which loses approximately 8 per cent of its speed in the transfer of energy, all of which occurs in as little as 10 degrees of travel of the press crank. The flywheel is reaccelerated to full speed during the remaining 350 degrees of travel or some portion of this remainder. The motor is provided with a high-resistance squirrel-cage winding which gives it a high slip with load characteristic. The energy required by the particular stamping operation, and inertia of the flywheel, and the frequency of operation all go into the determination of motor rating and optimum slip characteristic, but it will be apparent that the ideal choice of motor for a given press and shearing operation is one which barely reaccelerates the flywheel to full speed after one operation before another operation ensues. This permits operation with the minimum of peak torques and peak motor currents. While practical factors such as flexibility of press use and safety factor do compromise design, the choice of flywheel and drive motor combinations in actual practice is predicated on these considerations.

Where, instead of pure shearing, a stamping operation requires a very shallow drawing of the metal, it will be noted that for all practical purposes the basic press design and choice of drive system is dictated by the same considerations as those outlined for a shearing operation. As the extent to which the metal is drawn becomes greater, however, the problem of press and drive design requires considerable study. Some drawing operations now require drawing metal up to 13 inches or more in a single operation. These operations in general are not only characterized as being "deep draw" but furthermore require very large and complex dies. This, in turn, means vast stressing forces in the press and great torque requirements of the drive system.

Where a deep-draw operation such as forming an automobile top is involved, the total stroke of the moving die or "ram" must be at least twice as great as the depth of draw in order that sufficient separation of the dies occurs to permit removal of the formed piece. In actual practice a press with a stroke of 36 inches would probably not have a useful working or forming stroke of more than 13 inches. Even so, it will be apparent that if a simple crank action press is used for such an operation, engagement of moving die and metal will occur not at a point near dead center or 180 degrees of crank travel but at a point more nearly 100 degrees of crank travel, and deforming of the metal will continue until 180 degrees of crank travel is reached. Energy is, therefore, being expended in forming the metal over an interval of 80 degrees or almost one-fifth of the total crank travel per cycle.

Because of this long drawing interval, a given press can, without exceeding its stress limitations, do work requiring much greater total expenditure of energy per cycle when doing a deep-draw operation than when doing a simple blanking or shallow-draw operation.

As drawing operations became deeper and total expenditure of energy per cycle became greater, flywheels or greater inertia were required until a point was reached where flywheels of sufficient energy storage could not be accelerated from rest without burning out the rotor of the driving motor. Such operations also caused much greater stresses in the various moving press members because of the engaging of the work further up on the crank stroke. The clutch also became more of a problem.

Paper 53-4, recommended by the AIEE Industrial Control Committee and approved by the AIEE Committee on Technical Operations for presentation at the AIEE Winter General Meeting, New York, N. Y., January 19–23, 1953. Manuscript submitted May 1, 1952; made available for printing October 7, 1952.

C. E. Robinson and A. P. DiVincenzo are both with the Reliance Electric and Engineering Company, Cleveland, Ohio.

Figure 1. Motor speed versus time for one press cycle

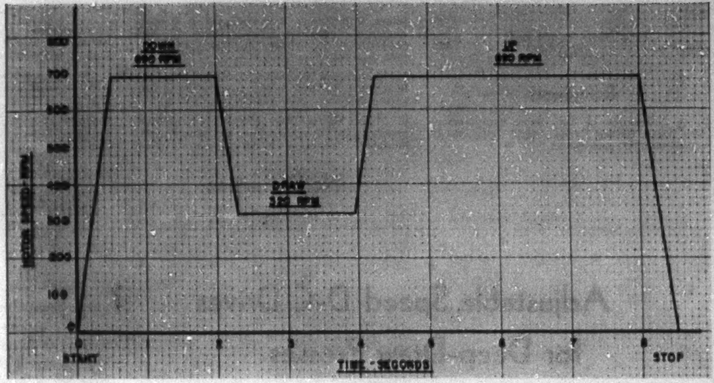

Consequently, presses for deep-draw work had to be so designed that, instead of a simple crank motion, a double toggle action was used to move the die. The flywheel and clutch were eliminated and a much larger motor of high torque characteristic was used instead. In this system, since a comparatively small amount of energy is stored in all the moving parts the motor is actually required to provide sufficient torque to force the die through its work stroke. The motor, furthermore, starts and stops each time the press starts and stops. While such a duty cycle presents great problems of motor design, such motors, along with suitable control equipment, have been developed and a considerable number of such drives have been in successful operation for over 12 years.

While such presses and drive systems successfully solved the problems of torque, energy per stroke, stress, and clutch maintenance, another problem peculiar to deep-draw operations, still existed. This has to do with the speed at which the metal is drawn. As explained earlier, in the case of the simple crank action press performing a deep-draw operation, the die engages the metal when the crank has traveled approximately 100 degrees from top dead center. With the crank turning at uniform angular velocity, the velocity of the die is, therefore, nearly at the maximum value attained in its simple harmonic cycle when the drawing of the metal begins. In drawing metal it has long been recognized that it requires greater effort to start the metal flowing than it dies to continue the operation. Because of this effect, if the initial speed of drawing is too high, the metal tears instead of flowing. An ideal drawing cycle would, therefore, begin at a slow speed with the speed increasing as the work progresses. The crank action press provides exactly the opposite speed condition.

The double toggle presses provide a considerably improved speed condition but still have a higher rate of drawing at the initiation of the cycle. It is conceivable that a system of mechanical linkages could be devised whereby with a constant speed prime mover the die could

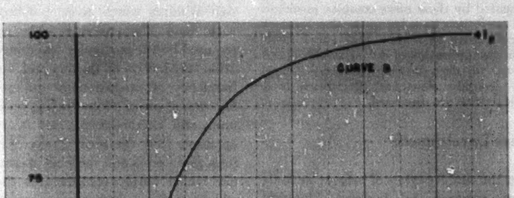

Figure 2. Field forcing principle

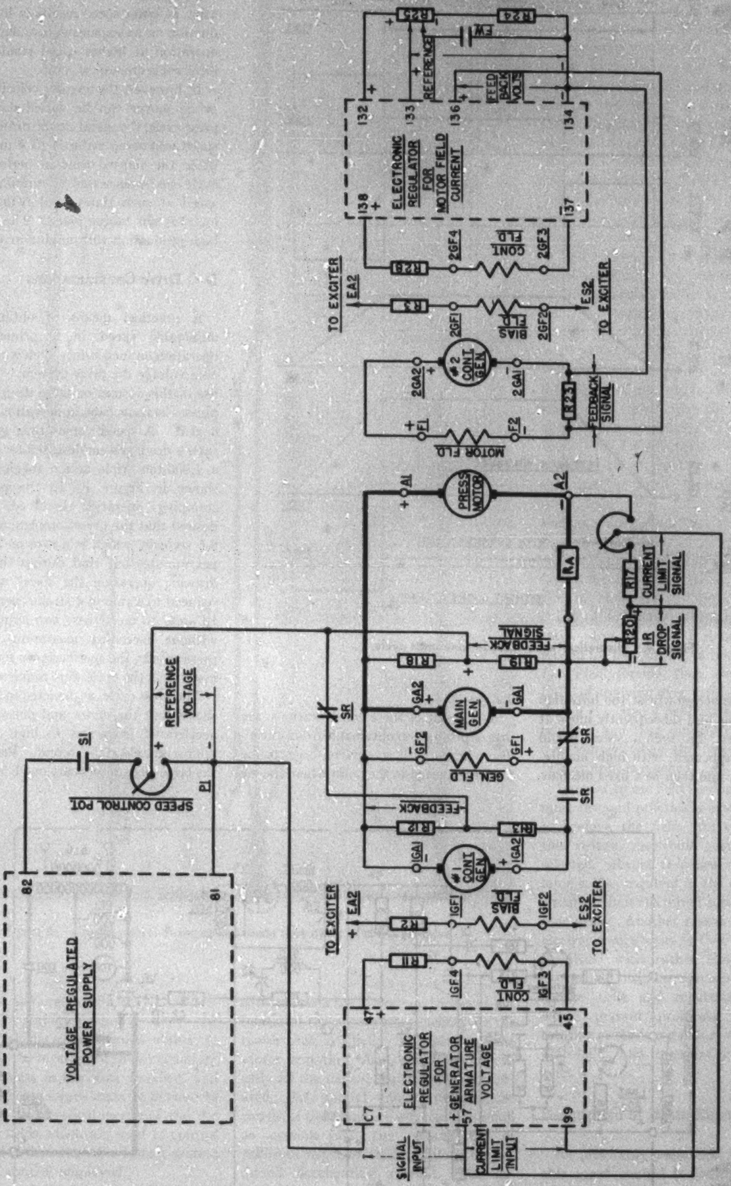
VOLTAGE REGULATED POWER SUPPLY
82
81
SPEED CONTROL POT.
S1
P1
REFERENCE VOLTAGE
+
-
ELECTRONIC REGULATOR FOR GENERATOR ARMATURE VOLTAGE
47
45
C7
57
99
SIGNAL INPUT
CURRENT LIMIT INPUT
CONT FLD
1GF4
1GF3
R11
R2
BIAS FLD
1GF1
1GF2
EA2
ES2
TO EXCITER
TO EXCITER
#1 CONT GEN
1GA1
1GA2
R12
R13
FEEDBACK
SR
GEN FLD
GF2
GF1
MAIN GEN
GA2
GA1
R18
R19
FEEDBACK SIGNAL
R20
IR DROP SIGNAL
R17
CURRENT LIMIT SIGNAL
RA
PRESS MOTOR
A1
A2
MOTOR FLD
F1
F2
R23
FEEDBACK SIGNAL
#2 CONT GEN
2GA2
2GA1
R3
BIAS FLD
2GF1
2GF2
EA2
ES2
TO EXCITER
TO EXCITER
R28
CONT FLD
2GF4
2GF3
ELECTRONIC REGULATOR FOR MOTOR FIELD CURRENT
138
137
132
133
136
134
R25
FW
R24
REFERENCE
FEED BACK VOLTS

Figure 3. Basic circuit of drive

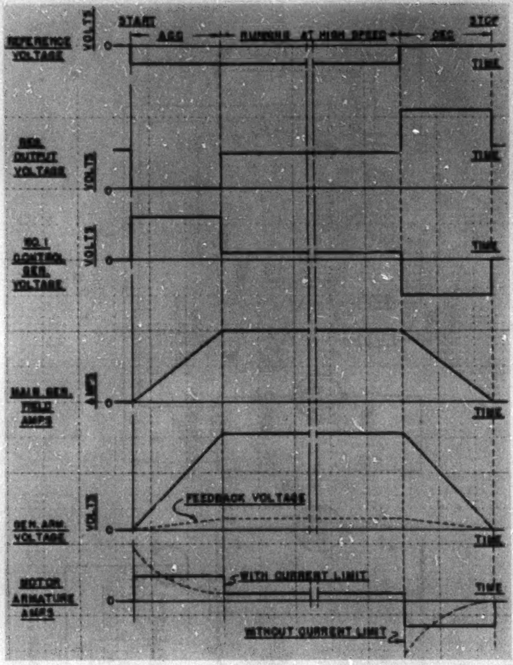

Figure 4. Theoretical wave forms for one press cycle

be made to move slowly at the initiation of the drawing and subsequently move at a higher speed; but such a system would be very complicated, with high maintenance, and would then be a fixed mechanical design.

As a result of these considerations, the rate of production obtainable from a deep-draw press with a squirrel-cage prime mover is limited to the point where the die speed at the initiation of actual drawing is not so great as to tear the metal. Operation at lower speed results in lower production on an expensive installation, and operation at higher speed results in an intolerable amount of scrap.

If, however, the angular velocity of the prime mover can be varied during the press cycle, the metal can be drawn at low speed and scrap reduced to a minimum, while the elapsed time in performing a cycle can be decreased by running at high speed at such times as drawing of the metal is not taking place. The result is high production with minimum scrap.

D-C Drive Considerations

A practical means of obtaining an adjustable speed in a prime mover operation on such a duty cycle is an adjustable voltage d-c drive system. The first use of this system on large deep-drawing presses has now been in operation for over a year. A speed versus time graph for such a drive system designed for use with a 1,000-ton triple action toggle press is shown in Figure 1. In the particular stamping operation involved, it was desired that the press complete a cycle in 8.5 seconds, which is a rate of 7 strokes per minute, but that during the actual drawing operation the speed would be reduced to a rate of 4 strokes per minute. In order to meet these two requirements without exceeding maximum practical press speeds, the speeds shown for various instants in the cycle were required.

The press cycle, as depicted in Figure 1, shows that the motor and press must be accelerated from rest to high speed in approximately 0.5 second. Because of the large-size motors employed, 500 horse-

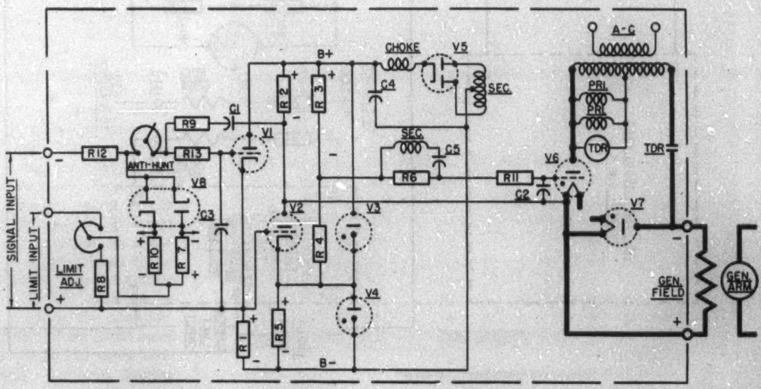

Figure 5. Diagram of electronic regulator

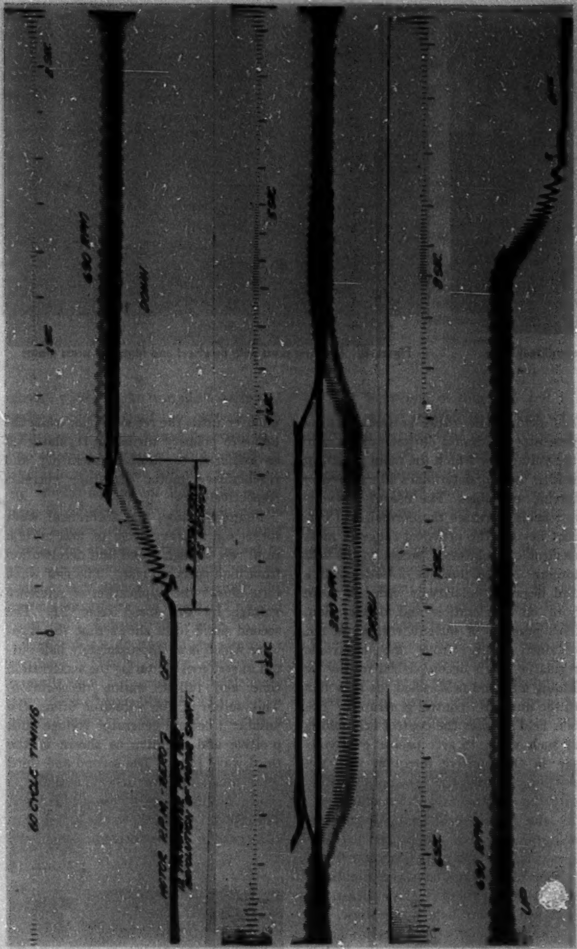

Figure 6. Oscillogram showing speed versus time cycle of d-c press drive

power for the press of Figure 1, this presents two major problems. First, the motor must have the torque ability to accelerate the mass of the motor armature and the press in the time specified, and secondly, some means must be devised to overcome the electrical inertia of the d-c machine fields which are used to control the speed in the adjustable voltage system of speed control employed.

Because of the large step-down gear ratio between the motor and the press, the inertia of the press parts reflected to the motor shaft is small. The inertia of the motor armature, then, comprises practically all the inertia that must be accelerated. By special motor design, the inertia of the armature was made as small as possible and the commutator of sufficient capacity to commutate the required accelerating current. The accelerating current was considered as held at a constant value instead of the steep rise and exponential decay normally experienced. This, of course, precluded that the control would use some form of current limit acceleration.

For the 500-horsepower drive, the time constant of the motor and generator fields is approximately 2 to 3 seconds. This means that any field current change will require an elapsed time of 2 to 3 seconds to make 63.2 per cent of the change and 6 to 9 seconds to make 98 per cent of the change. This follows from the fact that any current change in the highly inductive fields occurs exponentially. The elapsed time of 6 to 9 seconds is much larger than can be tolerated if the speed of the motor is to be changed in a fraction of a second. In order to overcome the electrical inertia of the generator and motor fields, the drive employs field forcing.

Figure 2 shows the exponential rise of field current for a field having a time constant of 2 seconds, with the field voltage applied instantaneously at time t zero. Curve A is for an applied voltage which will give the required value of I_F. Note that this takes approximately 9 seconds to reach final value. If the applied field voltage is four times that of Curve A, so that the final value of I_F would be $4I_F$, then the current rise is shown by curve B. Note that the time required to reach 63.2 per cent of $4I_F$ is still 2 seconds, since this is the time constant defined by the L/R ratio. But on curve B it now takes 0.6 second for the current to reach the value I_F. Field forcing, then, consists essentially of applying over-voltage to the field during the time a field current change is required and then quickly removing the over-voltage when the desired value of field current is reached.

In order to use field forcing, the control must respond practically instantaneously to remove the field over-voltage. For this reason, electronic regulators were selected. Rapid response of the regulator is also required in the current limit circuit to limit the initial accelerating current peak. Another reason for selecting electronic regulators is that they can be stabilized with rather simple and inexpensive antihunt circuits. Both response time and regulator instability would present problems with either rotating or static regulators which require both bulky and expensive stabilizing circuits.

Description of Basic Circuit

As previously mentioned, the adjustable speed control is obtained with the adjustable voltage system of speed control

Figure 7. Simple crank action press and conventional drive

Figure 8. Drawing press with flywheel and high-slip press motor

in which the press motor speed is controlled by varying the motor armature voltage. A small amount of the speed range is covered by weakening the shunt field of the motor. This was done in order to reduce the main generator size. Thus the drive has two regulating systems. One regulator controls the generator or motor armature voltage, and the other regulates the motor shunt field current.

Figure 3 is the basic circuit of the drive. The generator voltage regulator system consists essentially of a d-c reference voltage supply, an electronic regulator, and a d-c control generator which supplies excitation to the main generator field. The speed at which the drive is to run is adjusted by the speed potentiometer which adjusts the magnitude of the d-c reference voltage. The reference voltage is opposed by a feedback voltage which is a portion of the generator voltage which is being regulated. The difference between the reference voltage and the feedback voltage—that is, the error—is applied to the input of the electronic regulator, where it is greatly amplified. The electronic regulator in turn supplies sufficient excitation to the main generator field, through the number 1 control generator, so that the feedback voltage practically equals the reference voltage.

A voltage drop proportional to armature loop circuit current is used as a voltage drop signal. This signal voltage is added to the reference voltage so that the motor armature voltage increases with load, thus compensating for the inherent motor speed drop with load due to the armature loop circuit resistance.

Number 1 control generator is employed for two reasons. First, the use of field forcing requires that the main generator field become a low-voltage field. The ratio between control generator maximum output voltage and the voltage for which the main generator field is wound determines the degree of forcing available. The use of low-voltage fields increases the normal field current beyond the practical range of most electronic regulators. Secondly, the field forcing voltage must be of both positive and negative polarity in order to force both on acceleration and deceleration. This reversal of output voltage is not obtained easily from the electronic regulator but is accomplished readily by adding a second field called the bias field to the number 1 control generator. The bias field opposes the control field and is of such value to give proper over-voltage in the positive direction with the electronic regulator at zero output, while with the electronic regulator at full output the control field supplies sufficient excitation to give the proper negative over-voltage to the main generator field.

Figure 3 shows only one speed potentiometer. Actually there are three potentiometers which control the down, draw, and up speed of the die. Each potentiometer is selected by a relay, such as *S1*, which is energized by a cam switch which denotes die position. Thus the three die speeds may be preset for press operation.

The electronic regulator has a current limit circuit to limit accelerating and decelerating motor currents. A current limit signal of a few volts is obtained from a resistor in the armature loop circuit and applied to the limit circuit input of the regulator. When the voltage drop across the armature signal resistor exceeds a set value, the limit signal overrides the regulator signal to control the regulator. The limit circuit is responsive to the polarity of the limit signal so that one polarity turns the regulator on, while the opposite polarity turns the regulator off as required to limit accelerating and regenerative motor armature currents respectively.

Figure 4 shows the theoretical wave forms for a press cycle of acceleration from rest to high speed and deceleration from high speed to rest. The first wave form shows the application of reference voltage by the speed relay *S1*. The second wave form shows that the regulator which is at approximately half output at rest goes off during the acceleration time and full-on during deceleration. This action of the regulator drives the number 1 control generator voltage both positive and negative as shown in the third wave form. The second and third wave forms are not actually square as shown, but have slightly rounded corners. The last wave form shows the motor armature current. The dotted line shows the

Figure 9. Direct connected a-c drive and drawing press

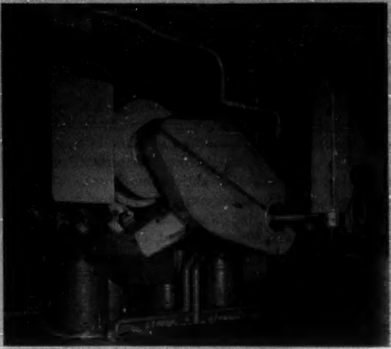

Figure 10 (left). 500-horsepower d-c drive motor in press pit

Figure 12 (right). Control cabinet for 500-horsepower press drive. Electronic regulators and control generators on left side, press auxiliary control on right panel

current wave form that would be obtained without current limit. A current with such a wave shape would be practically impossible to commutate both because of its initial rate of rise and its magnitude. By employing current limit, the initial peak is reduced to a value that can be safely commutated and held at this value during the entire accelerating period to give the maximum torque and shortest possible accelerating time. Actually the current wave form has a rounded leading front and a slightly trailing edge.

Figure 5 is a diagram of the electronic regulator. This regulator consists essentially of a 2-stage d-c amplifier comprised of the two tubes *V1* and *V2*, and a power amplifier consisting of a thyratron rectifier comprised of tubes *V6* and *V7*. The thyratron rectifier is the half wave with back rectifier type used with highly inductive loads. The regulator has a very high steady-state voltage gain and a much larger power gain. From the wave forms of Figure 4, it can be seen that the regulator has sufficient gain and rapid response to act practically as an on-off device during acceleration periods.

The current limit circuit of the electronic regulator consists of two diodes biased so that they do not conduct. When the current limit signal reaches a magnitude which overcomes the diode bias, the diode conducts and applies the current limit signal voltage to the input grid of the first regulator tube. There are two diodes, one for both positive and negative limit.

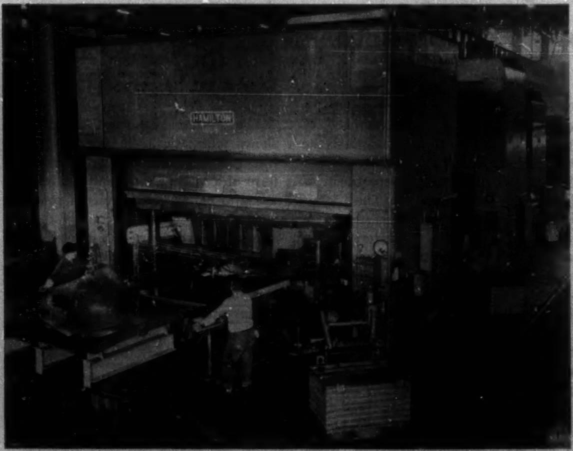

Figure 11. Floor view of 1,000-ton triple action press

Figure 3 also shows the basic circuit of the motor field regulator. The regulating system is similar to the armature voltage regulator. In this case, the motor field current is regulated so speed changes due to motor field heating are overcome. A voltage proportional to motor field current is used as the negative feedback signal and made to oppose the reference voltage, which in this case is supplied by the electronic regulator. The difference or error voltage is applied to the input of the electronic regulator and amplified. The regulator, in turn, supplies the control field of the number 2 control generator which, in turn, supplies the motor field. Again, field forcing is employed to overcome the time constant of the motor field. Because of field forcing, the number 2 control generator must be employed to supply the large motor field current and reversing voltage necessary.

Field weakened speeds are only required during the down and up motions of the die, the draw portion of the cycle requiring full field for maximum torque. In order to select the field weakened speeds, the cam switch which denotes die position operates relay *FW* whose contact selects the reference voltage to give either full or weak motor field current as required.

Note that the armature loop circuit does not use a main line contactor, but is connected in solid. This was done to eliminate a large, expensive main line contactor which would have a severe duty cycle in this application. When stopped, then, the main generator voltage must be reduced to practically zero volts to prevent the motor from creeping. This is accomplished by "suiciding" the main generator with its own shunt field.

Suiciding consists of connecting the shunt field across the motor armature in reverse so that it cannot "build up" as a self-excited machine. Thus, any voltage appearing across the generator armature is applied to the field with such a polarity that it tends to reduce the armature voltage. Since the generator field is a low-voltage field, it is very effective in reducing the armature voltage to less than a volt.

Suiciding is applied by a normally closed contact of relay *SR*. When running, the normally open contact of relay *SR* connects the generator shunt field to the number 1 control generator. When suicided, it is also necessary to keep the electronic regulator in range. This is accomplished by a second normally closed contact on *SR* which picks up a feedback signal from the number 1 control generator to about zero volts. The fact that the electronic regulator is operating in this standby condition is used effectively to prevent drive start-up in case of regulator or control failures.

Referring again to Figure 3, it can be seen that the relays which are really essential to run the drive are *SR*, *FW*, *S1*, and *S2* and *S3*. *S2* and *S3* are speed relays, similar to *S1*, which select the up and down speed potentiometers. Only five relays, then, are required to start the drive, run it through its cycle, and stop it.

Furthermore, the relays are all small standard control relays which are essentially in signal circuits. *SR* is the largest of the relays because it must carry the generator field current. A total of nine contacts on these relays are all that are required. Thus, through the use of electronic control the number of relays to run the drive through its cycle has been kept at a minimum, the relays that operate during a press cycle are small, and the relay contacts are not required to break circuits carrying large current considering the size of the drive.

Figure 6 is a speed oscillogram of the press speed for a press cycle of the 500-horsepower drive. The press cycle is the same as that shown in Figure 1, and from Figure 6 it is seen that it is completed in 8.5 seconds as was originally specified.

One interesting point shown by the oscillogram, as determined from tachometer commutator ripple, is that starting from rest the motor shaft attains a speed of approximately 700 rpm in three revolutions of the shaft. On stopping, the motor comes from a speed of 700 rpm to rest in three revolutions of the shaft. When expressed in this manner, it can be seen that the drive is functioning rapidly in order to accomplish the requirements of Figure 1.

Conclusions

Five drives of the type described are in operation, with one drive having over 1 year's service. Results obtained have been satisfactory, with production records exceeding anticipated figures. The facility for jogging at any desired low speed in setting dies and the ability to adjust press speed as desired offer additional production advantages which are being exploited to increase production above contemplated rates.

"Automation" (mechanical loading and unloading of the press) is now being used extensively and is constantly being improved and perfected. By having adjustable speed, regardless of die used, the chances of being able to operate the press "on the hop" are excellent. A press operated on the hop can produce as many as 25 per cent more pieces. Running on the hop also reduces wear and tear from a mechanical standpoint on the press and greatly reduces the demands of the electrical system. For example: a 10-stroke press run on the hop will produce ten pieces; if motor is stopped and started, it will produce $7^1/_2$ pieces.

No Discussion

The Electric Arc in Argon and Helium

T. B. JONES
MEMBER AIEE

MERRILL SKOLNIK
NONMEMBER AIEE

W. B. KOUWENHOVEN
FELLOW AIEE

MEASUREMENTS of the electrical characteristics of arcs, such as the variation of voltage with current and with arc length, have been carried out by Ayrton,[1] Nottingham,[2] and Suits,[3] and others for currents below 20 amperes and by Finkelnburg[4] for carbon arcs for currents above 20 amperes. Most of the work has been done at atmospheric pressure. The great increase in the use of inert gases for arc welding has resulted in the publication of much valuable data on the behavior of arcs in these atmospheres under typical welding conditions. It appears, however, that there is a need for more quantitative information on the characteristics of the inert gas arc under controlled laboratory test conditions. In particular, this information is needed for arc currents in excess of 20 amperes and for gas pressures in the neighborhood of atmospheric such as pertain when the inert gas arc is used for welding.

With this in view the Department of Electrical Engineering of The Johns Hopkins University has undertaken an investigation of the characteristics of inert gas arcs as a portion of its program of fundamental arc studies being sponsored by the Office of Naval Research. This paper presents the electrical characteristics of the d-c tungsten arc for the current range 10 to 100 amperes in an atmosphere of argon. Voltage-current curves, voltage-arc length curves, and plasma gradients data are presented. In addition, the qualitative behavior of this arc is described in detail. Some data is also given for the tungsten arc in helium. It is felt that information of this type will be useful not only for the theoretical study of the arc mechanism but also in the design and development of equipment and processes.

Experimental Apparatus

The vacuum-tight test chamber is shown schematically in Figure 1. It is constructed of 6-inch brass pipe in the form of a maltese cross and can be evacuated to better than 1-micron pressure. Two arms of the cross contain the rod electrodes, which were mounted horizontally along the same axis, while the other two arms contain the observation port and the gas inlets and outlets. Means are provided for projecting the

---

Paper 53-87, recommended by the AIEE Electric Welding Committee and approved by the AIEE Committee on Technical Operations for presentation at the AIEE Winter General Meeting, New York, N. Y., January 19–23, 1953. Manuscript submitted November 28, 1950; made available for printing December 4, 1952.

T. B. JONES, MERRILL SKOLNIK, and W. B. KOUWENHOVEN are with The Johns Hopkins University, Baltimore, Md.

arc image onto a screen adjusting the electrode separation, and controlling the gas pressure. The arc is started with a high-frequency arc starter. The pressure in the chamber was maintained at 3 pounds per square inch (± 1 pound per square inch) above atmospheric by means of a blow-off valve. Water cooling tubes and air blowers were used to keep the chamber walls cool. A high capacity storage battery was used as the power supply for all tests.

Test Conditions

The final test conditions and procedures were arrived at only after a great amount of exploratory work consisting of numerous tests under a variety of conditions repeated again and again. In one instance identical electrical measurements were made on the argon arc each day for 8 consecutive days to test the reproducibility of data. These exploratory tests brought out quite clearly the absolute necessity of adopting definite, precise test conditions and procedures and rigid adherence thereto if the data is to have meaning and reproducibility. It is evident then that the data to be presented in this paper pertains to arc under the specific test conditions reported here. The necessity therefore of describing the test conditions in detail cannot be over emphasized.

Tungsten was chosen as the electrode material for the following reasons:

1. It has a high melting point thus permitting higher currents without loss of material and creation of instability due to droplet formation.
2. It has high electric conductivity, virtually eliminating consideration of voltage drops in the resistor and I^2R effects within the electrode itself.
3. Comparative tests on tungsten and carbon arcs showed the former to possess greater stability and better reproducibility of data.
4. Tungsten electrodes are widely used for inert arc welding.

It was decided to use tungsten electrodes for the anode as well as cathode since it was felt that the introduction of another metal into the picture would only serve to complicate the results. The study of the effect of electrode combinations on the behavior of inert arcs is contemplated as another phase of this arc research program.

It was further decided to use electrodes of the same diameter for both anode and cathode. It is recognized that this does not conform to welding practices generally. It was felt, however, that so little is known about the effect of relative electrode diameters, for example between anode and cathode, on the behavior of inert gas arcs that the most logical choice would be to have both electrodes of the same diameter.

With this reasoning as a basis, electrodes of 1/4-inch diameter were selected for the tests. In the case of the cathode this diameter is considerably larger than that employed for straight polarity welding over the current range of 20–100 amperes. It was recognized that this might contribute to instability of the cathode spot, making measurements more difficult than if a smaller cathode were used. The larger diameter however permitted a much wider current

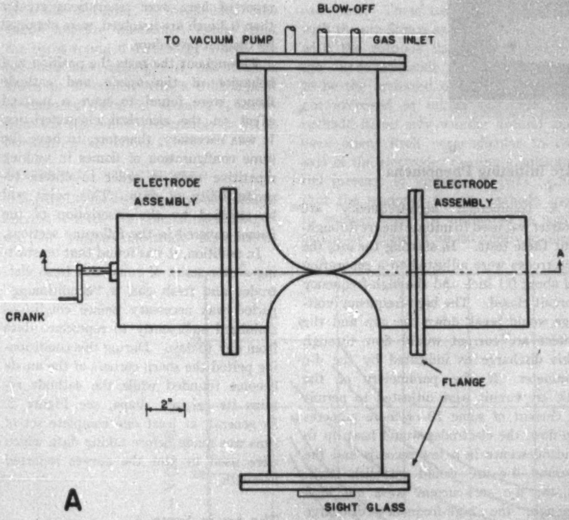

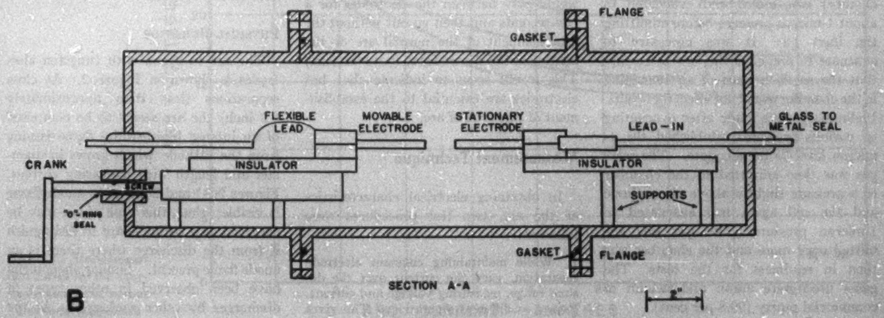

Figure 1. Test chamber

A. Top view B. Cross section

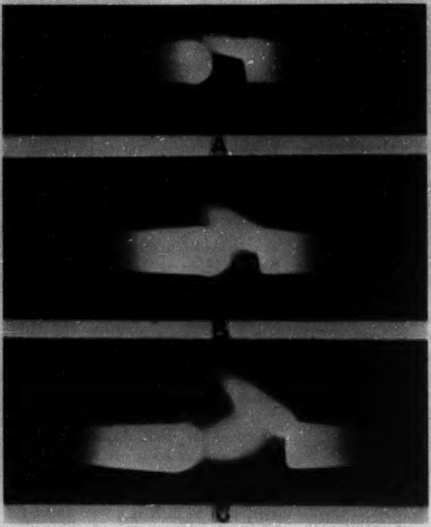

Figure 2. Argon-tungsten arc at 1/500-second exposure with red filter

A. Electrode separation 0.2 inch, current 20 amperes
B. Electrode separation 0.2 inch, current 70 amperes
C. Electrode separation 0.4 inch, current 70 amperes

range to be covered without sufficient melting of either electrode (in particular, the anode) to cause detachment of a droplet or enough distortion of the shape of the electrode tips to affect the test results. It was found in the exploratory tests that if a mobile droplet were formed on either electrode, the distortion of the shape of the tips produced thereby had such a marked effect on the behavior of the arcs that accurate data could not be obtained.

The electrodes were of the type employed for commercial inert arc welding except that they were dipped in hot KOH to remove the surface oxides. If this were not done, random voltage oscillations would occur.

After mounting the electrodes, the chamber was sealed and evacuated to about 1-micron pressure before admitting the inert gas. It was necessary to evacuate to pressures this low to be sure that the small amount of air remaining in the chamber would not affect the results. Preliminary tests made after evacuating to various pressures established the 1-micron level to be adequate. The inert gas was then admitted to the chamber to a pressure slightly above atmospheric and the cell again was evacuated to 1-micron pressure. The gas was admitted once more and the chamber was then in readiness for the tests. The gases used were argon and helium of commercial purity (99.8 per cent).

Arc Initiating Phenomena

A commercial high-frequency arc starter was used to initiate the arc throughout these tests. In starting the arc, the electrodes were adjusted to a separation of about 0.1 inch and the high-frequency circuit closed. The high-frequency voltage would break down the gap and the direct arc current would flow through this discharge as indicated by the d-c ammeter. If the parameters of the d-c arc circuit were adjusted to permit a current of some 70 or more amperes to flow, the electrodes would heat up to incandescence in a few seconds and the normal d-c arc would establish itself. If the d-c arc current were not high enough, the high-frequency discharge would play between the electrodes for a few seconds and then go out without the establishment of the normal arc or the heating of the electrodes to incandescence. This would seem to indicate that hot electrodes are essential to the establishment of this type of arc.

Measurement Technique

In obtaining electrical characteristics of the arc, two test procedures were followed:

1. While maintaining constant electrode separation, vary the current over the desired range, measuring voltage and current. Repeat at different separations. This gives a family of voltage-current curves at various separations. From these curves the voltage-electrode separation curves may be obtained for any desired current.
2. While maintaining constant current, vary the electrode separation measuring the voltage and separation. Repeat at different currents. This gives a family of voltage-electrode separation curves at various currents from which the voltage-current curves can be derived.

It was found that test procedure number 1, gave the better results. With test procedure number 2 for separations between 0.05 inch and about 0.3 inch, the results were uniform, reproducible, and checked closely results obtained by the first procedure. At separations greater then 0.3 inch, the behavior of the cathode and anode flames tended to become erratic, making it difficult to obtain good data. Consequently, all curves reported here were separations greater than 0.3 inch are involved, were obtained by the first procedure.

Throughout the tests the position and behavior of the anode and cathode flames were found to have a marked effect on the electrical characteristics. It was necessary, therefore, to have the same configuration of flames in making repetitive tests in order to obtain reproducibility of data. This point will be clarified by the description of the flames covered in the following sections.

In addition, it was found that on starting a new series of runs with fresh electrodes and fresh gas, a "conditioning" period was necessary before conditions stabilized sufficiently to reproduce data from day to day. During this conditioning period the sharp corners of the anode become rounded while the cathode retains its original shape, see Figure 2. In general, at least one complete set of runs was made before taking data which were used to plot the curves reported herewith.

The Arc in Argon

PHYSICAL BEHAVIOR

The arc in argon with tungsten electrodes is shown in Figure 2. At close separations (less than approximately 0.3 inch) the arc seems to be composed of an intense bluish-white flame issuing from the cathode which grows in diameter and length with increasing current, Figures 2(A) and 2(B). No anode flame is visible; thus, this type of arc may be classified as a cathodic arc to distinguish it from the discharge where there is an anode flame present. Similar phenomena have been observed in other types of discharges by other workers.[5,6] At the longer separations (greater than 0.3 inch) the anode flame begins to appear. At low currents this flame is shorter, wider, and less intense than the cathode flame, and a dark space of approximately 0.04 inch separates the anode from the anode flame. As the current increases, the anode flame grows larger and brighter, Figure 2(C) but is never as intense as the cathode flame over the current range reported here. These observations were substantiated by high-speed motion pictures.

While the arc is burning, the anode electrode becomes white hot for a length of approximately 1 inch and the tip appears to be molten; however, no droplets are formed. The cathode electrode is dark except for the bright cathode spot. Examination of the electrodes after the test show that the loss of electrode material is negligible. The anode appears unaffected except that the tip is rounded and shiny where the tungsten has melted, but the cathode seems to be coated with a thin deposit of tungsten metal for about $2^1/_2$ inches from the tip, which presumably is transferred from the anode.

Electrical Characteristics

Figure 3 shows a family of voltage-current curves for the tungsten-argon arc for various electrode separations. These curves were taken by procedure number 1 previously discussed with both increasing and decreasing current. There was no significant difference between the curves taken by decreasing the current and obtained by increasing the current. The voltage as read on the voltmeter is actually the sum of the arc voltage plus the voltage drop in the electrodes. However, both calculations and measurements indicate that the latter drop is negligible even at the high temperatures that are encountered. The voltage read by the voltmeter was taken as the true arc voltage. These curves represent the average of many tests and are believed to be precise to ±0.5 volt. The word precise is used rather than accurate because the voltage values obtained are reproducible only if the arc has the same flame configuration for each test. These tests were conducted with the arc flames as shown in Figure 2, with the cathode flame slightly above the anode electrode, since this seemed to be the preferred position. If care is not exercised in taking the data, the cathode flame may wander around and even orient itself perpendicular to the axis of the electrodes causing a substantial increase in voltage. It was found that the tendency for the cathode spot to wander could be mitigated to some extent by means of an externally applied magnetic field of small magnitude in a direction along the axis of the electrodes. A field of about 200 gausses was obtained by winding 180 turns of wire around the outside of the test chamber and passing a direct current of 5 amperes through the wire. The application of this field had negligible effect on the arc voltage as tests conducted with and without the field were closely reproducible.

The voltage-current curves of Figure 3 show the usual hyperbolic shape typical of V-I curves for d-c arcs. Over the current range reported here, the curves do not assume a positive slope such as characterizes the high current arc in air; so this arc, even for currents up to 100 amperes does not seem to fall into the classification of the high current arc of Finkelnburg.[7] The decrease in voltage with current increase is quite rapid for currents below 40 amperes. At currents above this the curves tend to level off, and it is possible that at higher currents than those reported here, the slope may become positive. The decrease in voltage with current seems to be associated with the growth of the cathode and anode flames and the intense degree of ionization produced thereby. Whether the charge carriers associated with these flames originate predominately from the electrode material or the gas cannot be stated with certainty at this

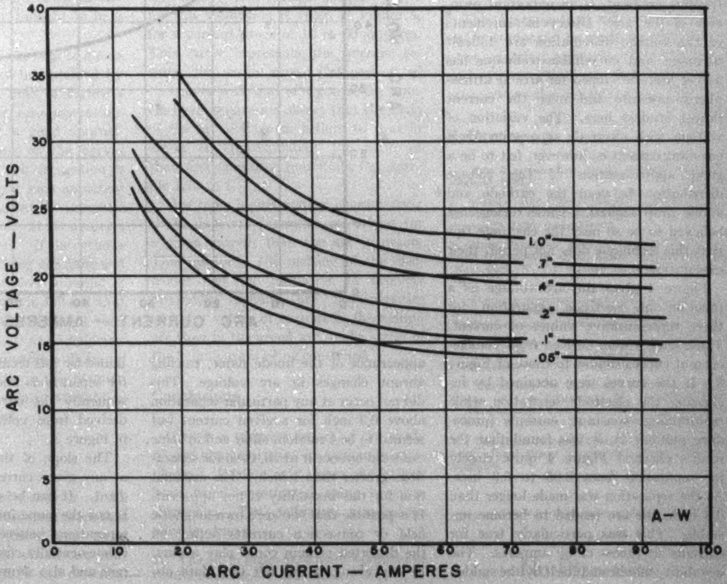

Figure 3. Voltage-current curves for the tungsten-argon arc at various electrode separations

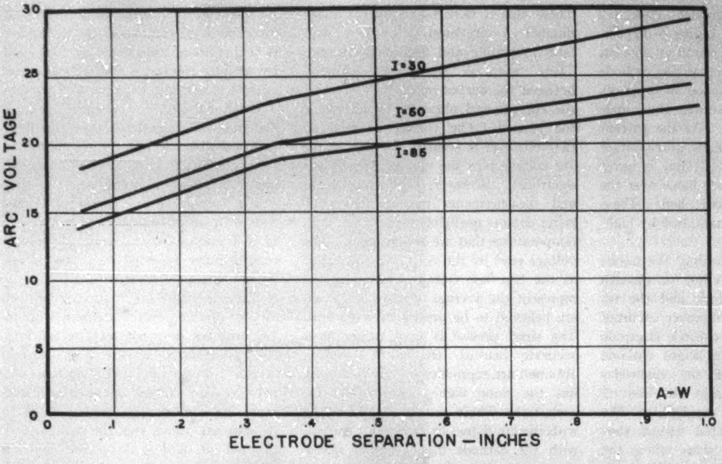

Figure 4. Voltage-electrode separation curves for the tungsten-argon arc at various currents

Figure 5 (below). Voltage-current curve for the tungsten-helium arc at 0.2-inch electrode separation

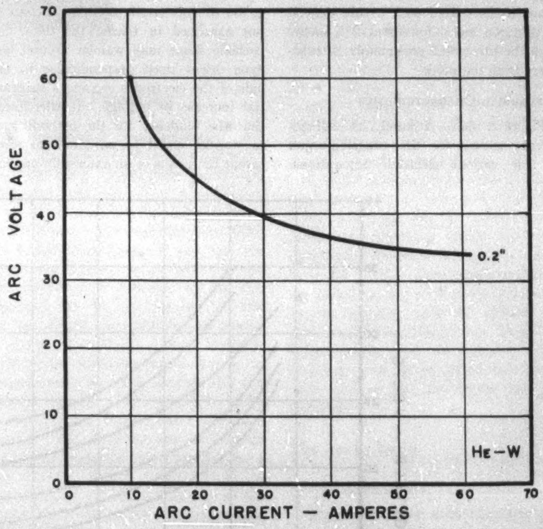

time. It is likely that spectrographic studies of the entire plasma region would help in clarifying the processes. It can only be stated that on the basis of the visible light emitted, the arc column does not appear to contract in cross section as does the high current carbon arc in air.[7]

The distribution of voltage between the electrodes along the arc column (plasma gradient) is an important property of the arc. Direct measurements of the voltage distribution are difficult to make, and no reliable technique has as yet been developed for arcs at atmospheric pressure and over the current ranges studied here. The variation of voltage with electrode separation for a constant current is, however, felt to be a good approximation of the voltage distribution between the cathode and anode drop regions. These regions are believed to be so near the electrode tips that this technique does not permit their exploration.

Figure 4 gives the arc voltage as a function of electrode separation for three representative values of current. These curves were derived from voltage-current curves similar to those of Figure 3. If the curves were obtained by increasing the electrode separation while maintaining constant current (procedure number 2), it was found that the results checked Figure 4 quite closely for separation from 0.05 to 0.3 inch. As the separation was made longer than 0.3 inch, the arc tended to become unstable. This was particularly true for currents in excess of 30 amperes. The instability manifested itself by the sudden appearance of the anode flame, causing abrupt changes in arc voltage. This did not occur at any particular separation above 0.3 inch for a given current but seemed to be a random affair and in some cases did not occur at all, even for separations greater than 1 inch. The explanation for this instability is not apparent. It is possible that the arc's own magnetic field or convection currents acting on the distorted column could play a part. In any event, it was felt that data obtained by this technique were not reliable for separations above 0.3 inch and consequently the curves of Figure 4 were derived from voltage-current curves as in Figure 3.

The slope of the curves of Figure 4 at any given current is the plasma gradient. It can be seen that the gradient is not the same for all separations. For separations between 0.05 and 0.3 inch, it is essentially constant for a given current and also shows only slight variation

Table I. Plasma Voltage Gradients for the A-W Arc

	Gradient, Volts per Inch	
Current	Below 0.3 Inch	0.3—1.0 Inch
30	16.8	9.5
50	16.5	7.0
85	16.9	6.5

for different currents. It has an average value of about 16.7 volts per inch. At longer separations, the arc has two plasma regions, see Figure 2 (C), hence, two gradients, one corresponding to the cathode flame and the other corresponding to the anode flame. The anode flame gradient is roughly one-half the cathode flame gradient and decreases with increasing current. The values of the gradients are shown in Table I.

These curves seem to give evidence that at close separations over the current range covered the arc is maintained by a cathodic discharge as mentioned previously. It should, of course, be borne in mind that computations of plasma gradient by this method assume that with the current constant, the sum of the anode and cathode drops remains constant as the separation is varied. Thus, any changes of arc voltage with separation are due to voltage changes associated with maintenance of the plasma only. This is generally thought to be a valid assumption.

An approximation of the sum of anode and cathode drops may be obtained by extending the straight lines of Figure 4 to the vertical axis for zero separation. This is obviously not a good approximation since the shape of the curves between 0- and 0.05-inch separation is not known. However, if such an extension is made, it is seen that the intercept decreases from 17.5 volts at 30 amperes to 13 volts at 85 amperes. If the cathode drop is considered as being constant and equal to the first excitation potential of argon (11.5 volts), then it follows that the anode drop decreases from 5.9 volts at 30 amperes to 1.4 volts at 85 amperes. In view of the questionable validity of obtaining the anode drop in this manner, it would seem undesirable to attempt to draw further conclusions.

The Arc in Helium

The appearance and behavior of the arc in helium is quite different from that in argon. Although these two gases possess similar chemical properties, both being inert, their physical and electrical properties are quite different as shown in Table II.

At low currents in helium (below 30 amperes) a reddish-purple flame issues from the cathode which is smaller and less intense than the cathode flame of argon shown in Figure 2. With a current of 40 to 50 amperes, the region between the electrodes begins to show a blue color, symmetrical in appearance with respect to the electrodes. At a still higher current, the reddish-purple cathode flame is no longer visible. This disappearance of the cathode flame occurs suddenly and apparently at no particular value of current. Its disappearance is accompanied by a sharp drop in voltage of about 5 volts. Thus, it seems that there are at least two forms of the helium arc. It should be emphasized that this drop of voltage may occur over a relatively large range of current and usually does not occur at the same value twice. In general, the visible light from the helium arc appears less intense than from argon and the behavior of the flames is much more difficult to observe.

To date it has been impossible to develop a measurement technique yielding consistent, reproducible measurements and therefore complete data for the helium arc cannot be presented. The most consistent results have been obtained at an electrode separation of 0.2 inch. The voltage current curve for this separation is given in Figure 5, for a current range of 10 to 60 amperes. This curve represents the average results for seven runs. Comparison of this curve with that of argon at the same electrode separation shows that the ratio of the arc voltage in helium to that in argon is approximately the ratio of their first excitation potentials, for example 1.72 to 1.

Due to its higher voltage characteristic the helium arc generates more heat for a given current than the arc in argon. This results in the melting of the electrodes and the formation of droplets producing unstable arc characteristics at lower values of current in the helium arc than in the argon arc. The study of the helium arc is being continued.

Conclusions

This is a progress report of the study of arc characteristics in various atmospheres. To date only argon and helium have been investigated using tungsten electrodes. The following conclusions may be drawn:

1. The arc in argon gave more reproducible results than the arc in helium.

Table II. Comparison of the Properties of Argon and Helium

	Argon	Helium
Atomic number	18	2
Atomic weight	39.94	4.00
First ionization potential	15.68	24.46
First excitation potential, metastable state	11.49	19.77
Heat conductivity, centimeter-gram-seconds	38.9×10^{-6}	339×10^{-6}
Specific heat, centimeter-gram-seconds (at −180 degrees centigrade)	0.133	1.25
Viscosity, micropoises at 20 degrees centigrade	221.7	194.1
Density, centimeter-gram-seconds	1.7837	0.17847

2. The arc in argon was stable and consistent results could be obtained as long as there was no appreciable melting of the anode.

3. The slope of the voltage-current characteristic in argon is considerably smaller for currents in excess of 50 amperes than for lower values of current. This means that wide current variations can occur in this region with small changes in arc voltage.

4. The plasma gradient in argon is essentially constant and independent of the current for electrode separations between 0.05 inch and 0.3 inch. For greater electrode separations the gradient is lower and decreases with increasing current. This is of importance from the standpoint of automatic welding control.

This investigation will be continued and it is planned to study arc characteristics in other atmospheres than argon and helium. Not only pure gases but gas mixtures also will be investigated.

References

1. The Electric Arc (book), **Ayrton.** London, England, 1902.

2. Normal Arc Characteristic Curves, **W. B. Nottingham.** *Physical Review* (New York, N. Y.), volume 28, 1926, pages 764–68.

3. High Pressure Arcs in Common Gases in Free Convection, **C. G. Suits.** *Physical Review* (New York, N. Y.), volume 55, March 15, 1939, pages 561–67.

4. Untersuchungen Uber Hochstromkohlebogen I, **W. Finkelnburg.** *Zeitschrift fuer Physik* (Berlin, Germany), volume 112, 1939, pages 305–25.

5. Fundamental Phenomena in Sodium-Vapor Lamps, **C. G. Found.** *General Electric Review* (Schenectady, N. Y.), volume 37, 1934, page 269.

6. Mechanism of Electrical Discharges in Gases of Low Pressure, **M. J. Druyvesteyn, F. M. Penning.** *Reviews of Modern Physics* (New York, N. Y.), volume 12, April, 1940, pages 170–73.

7. The High Current Carbon Arc, **W. Finkelnburg.** *Final Report Number 1052*, FIAT (London, England).

No Discussion

Relative Stability of Closed-Loop Systems

M. J. KIRBY
MEMBER AIEE

D. C. BEAUMARIAGE
ASSOCIATE MEMBER AIEE

Synopsis: Frequency response plots have long been used to predict transient as well as steady-state responses of closed loop linear systems, avoiding the exact and laborious solution of differential equations. This paper considers the relations between specific properties of frequency response plots and the corresponding properties of the early portions of the time responses. It is shown that the common output/input transfer function plots are in reality plots of the Laplace transform of the impulse (transient) response. The Laplace transform of a time function is a real integral in which an exponential kernal is multiplied by the time function, and the product summed from time zero to infinity. This process amounts to a mechanism by which the kernal scans the time function as the frequency is varied. This paper gives a method for interpreting Laplace transform plots and extending their use, and presents a method for estimating the size, frequency, damping, and phase of oscillations in the corresponding time response. "Standard" plots are included to aid in estimating particular properties. The method is relatively quick in application, and makes use of functions and techniques already familiar in Laplace transform analysis. In addition, it is not limited to the responses of systems having rational transforms, or to responses to impulses or step inputs, but can be used to estimate the response to almost any desired input, and is applicable to systems having time-varying elements.

PLOTS of transfer functions are widely used in the analysis and design of linear systems, particularly servomechanisms.[1–3] A plot of a fairly simple function indicates the properties of the time response without the labor of solving the differential equation relating output to input and time. Frequency is the independent variable, and the quantity plotted is the output/input ratio for sinusoidal inputs, or a closely related operational expression.

When the system has lumped parameters, such a plot gives three kinds of information concerning the response. As a transfer function it indicates the steady-state response to periodic inputs and the performance of the system as a building block in larger systems. In addition it indicates, by encirclement or nonencirclement of a critical point, the absolute stability or the ultimate growth or decay of the final part of the transient. Finally, the shape of the plot is related to the early portion of the transient, and transfer function plots are employed to predict what is loosely called "relative stability."

The steady-state transfer function concept and the indication of absolute stability are widely understood; the techniques have also been extended beyond the realm of lumped-parameter systems.[4–6] The measurement of relative stability, however, has not been developed to the state where comparable definite techniques are available. The quantities which are involved are usually not clearly defined, and the interpretations of plots differ among individuals. It is often believed, for example, that the indication of relative stability is accomplished by some generalization of the principle by which absolute stability is measured. Unless thoroughly understood and justified, such generalizations and extensions can result in errors. An example of this is given later, wherein usual techniques are applied to a multiloop servo system.

This paper shows how the common output/input transfer function plots indicate relative stability because they are at the same time plots of the Laplace transform of the time response of the system to a unit impulse input. The Laplace transformation measures the time response by comparing it to the kernal of the transform ϵ^{-st}, which is an exponential whose properties can be varied at will by varying s.

The transform is formed by a real integration in the time domain; its formation is easily visualized as a physical process involving products, areas, and other quantities closely related to the time response of the system. Although the Laplace transform of a particular system response is usually obtained by operational means rather than by integration, the plot of the transform can always be interpreted in terms of this process of integration, comparison, and measurement. This allows the various properties of the plot of the transform to be related directly to properties of the time response, which are of interest, without intermediate steps and concepts such as the complex frequency plane, location of poles and zeros, phase, and others usually associated with steady-state transfer function analysis.

Of equal importance is the fact that the use of the Laplace transform as a measuring device can be extended beyond the limits of the usual transfer function plots:

1. Most practical problems involve inputs other than an impulse; the responses of a system to different inputs can easily be investigated and compared.
2. The responses of linear systems for which the output/input ratio concept breaks down can be investigated, for example, those having time-varying elements.
3. Unconventional methods of plotting the transform can be used to obtain more information about a system's response.

The General Method

The method of estimating relative stability which has the widest application and the greatest possibility of generalization is given below. Although it is in common use, the process is not usually thought of as stated here:

1. Choose a suitable input function and write the differential equation relating system output θ_0 to input θ_i and time t.
2. Take the Laplace transform of each term. Collect the transformed terms into an equation in which the Laplace transform $y(s)$ of the output $\theta_0(t)$ is the unknown function of the Laplace variable s.
3. Solve this equation for $y(s)$ as a function of s.
4. Choose a manner of varying s which will make the resulting plot of $y(s)$ sensitive to the properties which are of interest in $\theta_0(t)$ and plot $y(s)$ as a function of s. The usual method is to let the real part (damping) of s be zero and vary the imaginary part (frequency).
5. Note the pertinent properties of the plot of $y(s)$.
6. Estimate the properties of the time function $\theta_0(t)$ corresponding to the properties of $y(s)$, either on the basis of experience or by direct comparison with plots of transforms of familiar functions.

Relations between particular properties of the transform plots and the time responses are discussed later.

The usefulness of the method lies in the fact that the transform $y(s)$, although it gives only an estimate of the time response $\theta_0(t)$, is usually much easier to obtain and plot than $\theta_0(t)$ itself. Two restrictions must be observed, however.

Paper 53-102, recommended by the AIEE Feedback Control Systems Committee and approved by the AIEE Committee on Technical Operations for presentation at the AIEE Winter General Meeting, New York, N. Y., January 19–23, 1953. Manuscript submitted October 20, 1952; made available for printing January 7, 1953.

M. J. KIRBY and D. C. BEAUMARIAGE are with the Sperry Gyroscope Company, Greak Neck, N. Y.

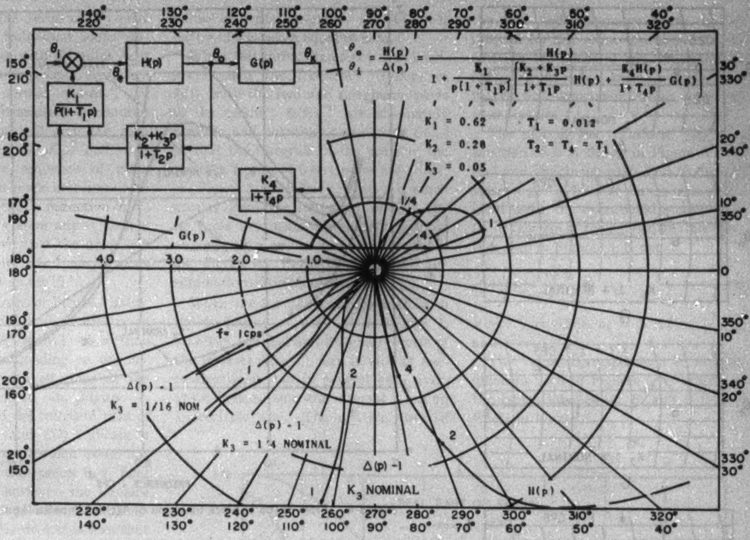

Figure 1. Frequency plots for a multiloop servo system

First the quantity plotted as the Laplace transform $y(s)$ must be equal to the integral

$$y(s)=\int_{t=0}^{t=\infty}e^{-st}\theta_o(t)dt \qquad (1)$$

although it is usually obtained by other means (for example, operationally or experimentally). In addition, this integral must converge, that is, the system under consideration must be absolutely stable; this can usually be determined quite easily.

This 6-step procedure is followed whenever the relative stability of a constant-coefficient system is estimated by plotting the steady-state output/input transfer function as a function of frequency. The first four steps are not then separated as

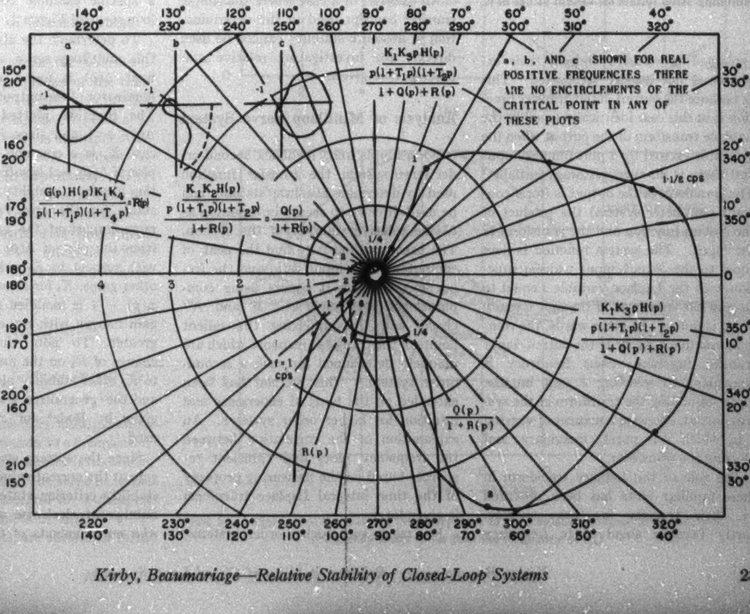

Figure 2. Stability plots of multiloop servo system to determine margins with respect to K_3

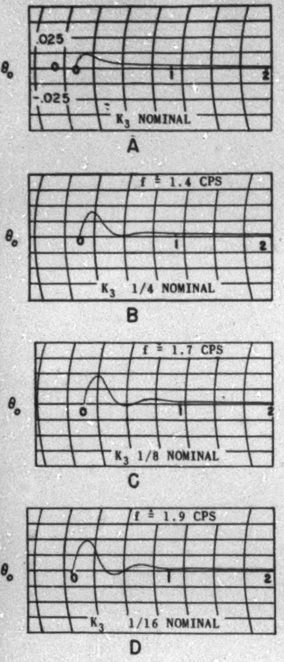

Figure 3. Transient responses of $\theta_o(t)$ of multiloop servo system for various values of K_3

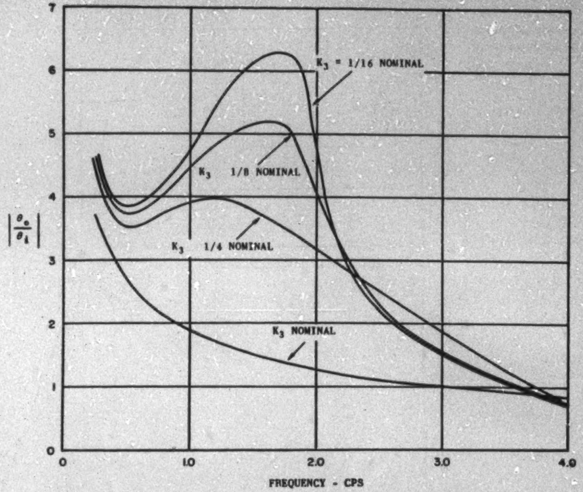

Figure 4. Plots of the Laplace transform of $\theta_o(t)$ for impulse inputs of $\theta i(t)$

explained previously; indeed, their existence is not usually recognized. This is because the output/input transfer function is in this case identically equal to the Laplace transform of the output when the system is excited by a unit impulse input and there is no energy storage initially.[1] The transform of the output is (for a constant parameter system) the product of the system function and the transform of the input. The system function is here equal to the output/input transfer function with the Laplace variable s equal to $j\omega$, and the transform of the unit impulse input is unity. In other words, the common practice of plotting the output/input transfer function versus frequency is equivalent to selecting a unit impulse input, obtaining the transform of the system output, choosing a manner of varying s in which s is purely imaginary, and plotting the transform.

The role of the Laplace transform in these familiar plots has been obscured by their transfer function concepts, partly because steady-state frequency responses are usually more easily measured in the laboratory than transient responses. In addition, much control system stability theory has been derived from communication engineering which dealt primarily with steady-state rather than transient concepts.

An example of a case where the simple transfer concept used in the determination of absolute stability cannot be used directly for investigating relative stability is now given.

Analysis of Multiloop Servo System

For a simple unity feedback second-order servo system the transfer function used to determine absolute stability can be used directly to secure information as to the relative stability of the system. The usual method is to find the peak of the output over input ratio and the frequency at which it occurs using computational aids such as "M and N" charts and then inferring the salient points of the transient response which are uniquely determined for such a second-order system.[1] This method has been extended on the basis of experience and intuition for higher order systems. An explanation of the correlation between the frequency plots and transient responses based on the measuring property of the time integral Laplace transform is given later.

For many such higher order systems, particularly multiloop servos and combination open-cycle closed-cycle systems such as discussed in a recent paper,[7] the plots made for the determination of absolute stability cannot, of course, be used directly to secure information as to the relative stability of the system. As a specific example consider the multiloop servo of Figure 1.

To determine the absolute stability of this multiloop servo a system determinant $\Delta(p)$ is found which is the denominator of the output over input ratio.[8] The function plotted for stability is $\Delta(p) - 1$ and since for this particular case K_1 is a common factor this single plot of $\Delta(p) - 1$ is sufficient to determine the absolute stability. The system is stable for the gain values chosen, but more important the gain margin found from the plot of $\Delta(p) - 1$ is a margin with respect to K_1 only. If one of the other gains, K_3 for example, is decreased, $\Delta(p) - 1$ is modified as shown but the gain margin with respect to K_1 is made greater. To note the effect of this change of K_3 on the margin with respect to K_3 other stability plots must be made and the generalized stability criterion as given by Bode[8] for multiloop system used.

Since the system was stable with the gain at the normal values, the generalized stability criterion states that "the total number of clockwise and counterclockwise encirclements of the critical points must be equal in the series of Nyquist diagrams for the individual loops obtained by beginning with all gains zero and restoring the gains successively in any order to their normal values." In particular, if K_3 is considered as restored last, this final plot will give the gain margin with respect to K_3. Following this procedure the sequence of plots shown in Figure 2 is made and it appears from the final plot that a reduction of K_3 will not make the system any relatively less stable. Observe that the $\Delta(p) - 1$ plot in Figure 1 for K_3 reduced does "approach the -1 point".)

As the transient runs of Figure 3 show, the response becomes more oscillatory as K_3 is reduced. Figure 3(A) is a time response of θ_0 corresponding to an impulse input of θ_i with all gains at the nominal values noted in Figure 1. When K_3 is reduced the transient runs of Figure 3(B), (C), and (D) indicate a more oscillatory system which would not be indicated by the preceeding final stability plot. If, however, the Laplace transform of θ_0 is plotted for various values of K_3 as in Figure 4, it is seen that this Laplace transform plot does indicate accurately a more oscillatory response as K_3 is decreased. Since the interpretation and extension of transform plots such as Figure 4 are based upon the mechanism by which the transform integral of equation 1 is formed, this will be discussed next.

The Mechanism of Measurement

The process by which the transform $y(s)$ measures the properties of the time function $\theta_0(t)$ rises directly from the definition of the transform, equation 1. The time function $\theta_0(t)$ is multiplied by the kernal, ϵ^{-st}, and the product is summed from time to zero infinity. The Laplace variable s is in general complex and has a real part, σ, and an imaginary part, $j\omega$. The integral 1 is thus equal to the sum of two real integrals which are the real and imaginary parts of $y(s)$

$$y(s) = \int_{t=0}^{t=\infty} \epsilon^{-\sigma t} \cos \omega t \theta_0(t) dt - j \int_{t=0}^{t=\infty} \epsilon^{-\sigma t} \sin \omega t \theta_0(t) dt \quad (2)$$

The way in which this multiplication and summation amounts to a comparison between $\theta_0(t)$ and the kernal is shown in Figures 5 through 8. The steps in forming the transform integral for a damped oscillatory time function, $\theta_0(t) = \epsilon^{-0.2t} \cos (t - 30 \text{ degrees})$, are shown for three values of kernel frequency $j\omega$. The real part σ of s is taken equal to zero.

When the kernal frequency ω is much lower than the frequency (unity) of $\theta_0(t)$, both the real and imaginary parts of the product $\theta_0(t)\epsilon^{-st}$ are alternately positive and negative at successive times so that the integrals of the parts of the product from $t = 0$ to $t = \infty$ are small; see Figure 5. Similarly, when ω is much greater than the frequency of $\theta_0(t)$ the products are again alternately positive and negative and each integral is small; see Figure 6. Here the integral is the summation of the shaded areas.

When the kernal frequency is close to the frequency of $\theta_0(t)$, as in Figure 7, however, the real and imaginary parts of the product $\theta_0(t)\epsilon^{-st}$ vary in size at successive times, but in general have average values, so that the integral 2 has an appreciable size. The relative sizes of the real and imaginary parts of this integral for any value of ω depend upon whether the phase of the component in $\theta_0(t)$, which is at kernal-frequency ω, makes this component closer to cosine ωt or sine ωt.

The plot of the transform $y(s)$ as a function of ω is shown in Figure 8; the real and imaginary parts and the vector sum are plotted. The curves were calculated using the operational equation for the transform of the particular time function used in Figures 5, 6, and 7.

$$y(s) = \gamma \frac{s + a_0}{(s + a_1)^2 + \beta^2} \quad (3)$$

where $\gamma = 0.866$, $a_0 = 0.777$, $a_1 = 0.2$, and $\beta = 1$.

The values corresponding to the frequencies used in Figures 5, 6, and 7 are the points labelled A, B, and C respectively in Figure 8.

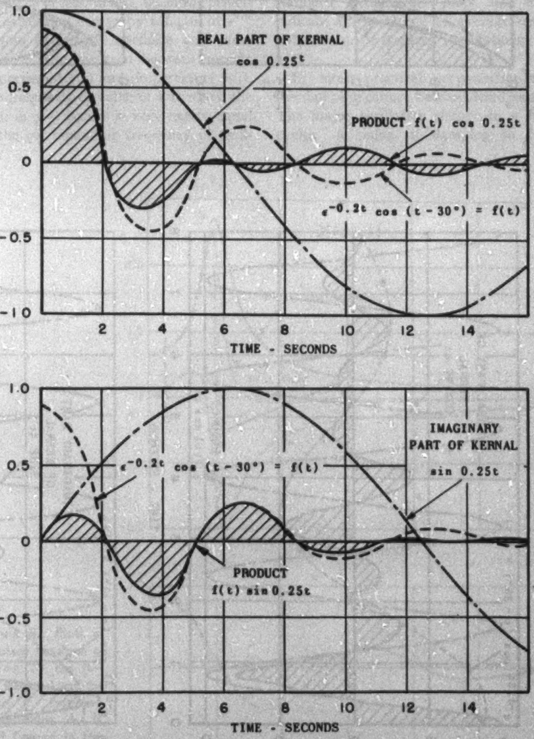

Figure 5. Formation of the real and imaginary parts of the Laplace transform of f(t) for a kernal frequency much lower than the frequency of f(t)

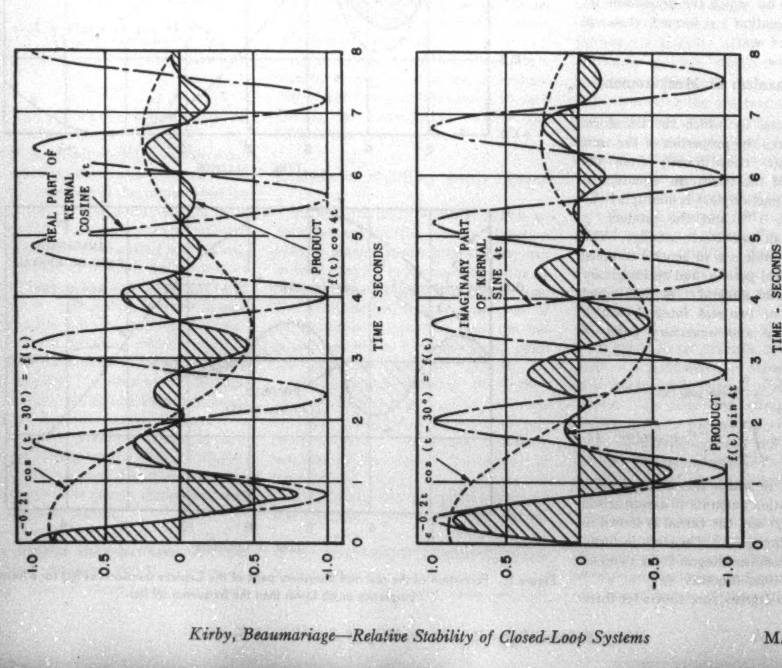

Figure 6. Formation of the real and imaginary parts of the Laplace transform of *K*(*t*) for a kernal frequency much higher than the frequency of *K*(*t*)

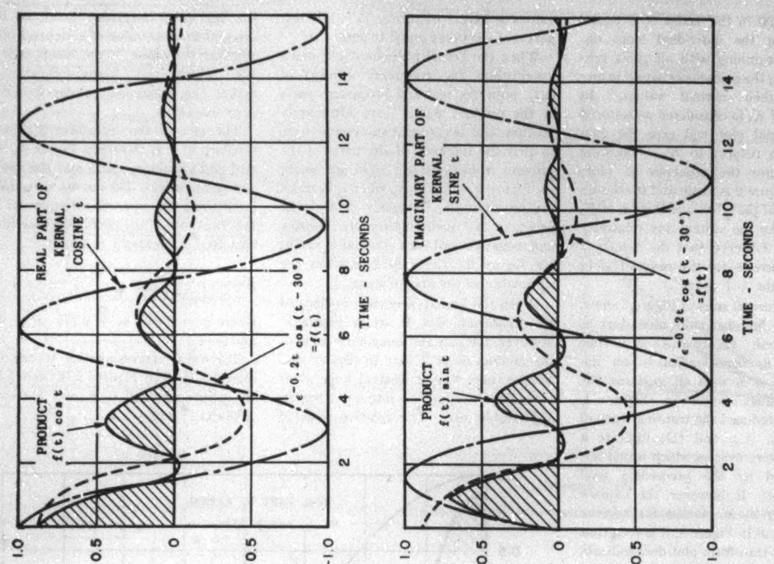

Figure 7. Formation of the real and imaginary parts of the Laplace transform of *K*(*t*) for a kernal frequency equal to the frequency of *K*(*t*)

The process of plotting the transform in Figure 8, whether from an equation such as 3 or from experimental data or otherwise, is equivalent to choosing values of kernal frequency ω, forming the products, and summing them for each value of ω, as in Figures 5, 6, and 7. The kernal ϵ^{-st} can be thought of as a test function and the process of varying its frequency and plotting the transform can be thought of as a process of scanning the time function. When a value of ω is chosen which corresponds to a frequency which is present in considerable quantity in the time function $\theta_0(t)$, the transform plot will have a large value at this frequency, indicating the presence of that component in $\theta_0(t)$. The shape of the plot of $y(s)$, and particularly the shapes of the peaks and the relative sizes of the real and imaginary component of $y(s)$, are important in determining the type of time response.

Interpretation of Transform Plots

The sixth and final step in the general method of interpretation amounts to noting the significant properties of $y(s)$, estimating the corresponding properties of $\theta_0(t)$, and constructing either on paper or in the imagination a time function having these properties. In the following paragraphs, relationships between specific properties of transform plots and time responses are defined, and procedures for approximating $\theta_0(t)$ are illustrated.

The important properties of the transient responses of servo-mechanisms are usually those associated with oscillations; the basic problem is to determine the frequency, damping, and other properties of each significant oscillation. The corresponding properties of the transforms are associated with peaks in the plots of $y(s)$ versus s.

The first step in interpreting a transform plot should be an estimate of the ratio of damping to frequency α/β of the major oscillation. The remaining steps in the analysis will depend upon the value of this ratio.

The damping of the oscillation in $\theta_0(t)$ depends upon the sharpness of the corresponding peak in $y(s)$. A general numerical equation relating the width of the peak to the rate of decay of $\theta_0(t)$ is not obtained easily. Figures 9 through 17 are nine standard plots of responses of second-order systems having damping/frequency ratios of 0.2, 0.5, and 0.8 and three values of phase angle. The sharpness can be estimated from the height of the peak at points near its maximum, not more than 20 per cent above or below. When the damping/frequency ratio is 0.2, the value of $y(s)$ at points 20 per cent above and below its maximum is from 60 to 80 per cent of the peak value (Figures 9, 10, and 11). When α/β is 0.5, (Figures 12, 13, and 14) the value of $y(s)$ at these points is 90 to 95 per cent of its peak value, and when α/β is 0.8, $y(s)$ is 98 or 99 per cent of its peak value at frequencies 20 per cent above and below the peak (Figures 15, 16, and 17).

If points farther than 20 per cent from the peak frequency are used, the estimate will be unduly influenced by the shape of the plot near zero frequency, and by secondary peaks at higher frequencies, when present. Although these latter properties contribute to the over-all impression of sharpness or lack of it in the plot of $y(s)$, they are not related to the rate of decay of the principal oscillation.

When the damping/frequency ratio α/β is 0.5 or less, that is, when the principal oscillation decays by a factor of $\epsilon^{-\pi}$ or less each cycle, definite and independent relations exist between specific properties of $y(s)$ and properties of $\theta_0(t)$. The frequency or value of s at which the peak in $y(s)$ occurs is very nearly equal to the corresponding frequency of oscillation in $\theta_0(t)$. The magnitude of $y(s)$ at its peak indicates the size of the oscillation; size here means the product of the initial amplitude of the envelope and the time constant $(1/\alpha)$; see equation 8. The relative magnitudes of the real and imaginary components of $y(s)$ at its peak indicate quite accurately the relative closeness of $\theta_0(t)$ to a cosine or to a sine wave, in other words, the phase. Therefore, when it has been determined that the damping/frequency ratio is small, the size of the oscillation, its frequency, and phase can be estimated one by one and in any order. It will always be useful to compare the transform plot being investigated with the standard plots of Figures 9 through 17 in order to strengthen the estimate of $\theta_0(t)$. After the properties of the principal oscillation have been estimated, the shape of the transform plot at frequencies near zero and well above the peak should be considered. Differences between the plot in question and standard second-order plots here can indicate the existence of average components or secondary oscillations in $\theta_0(t)$.

In most practical servomechanisms the damping cannot be considered small. The major oscillation decays in a few cycles. A value of damping to fre-

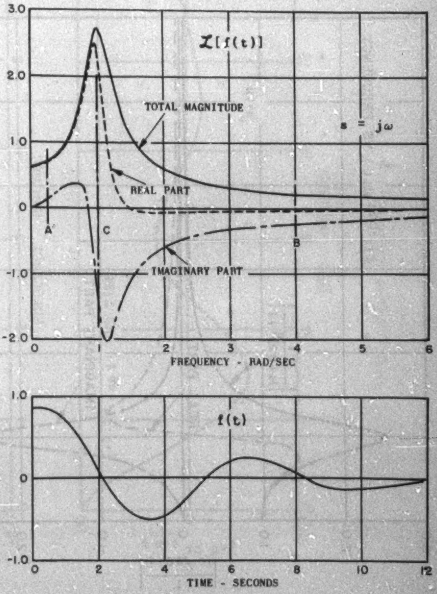

Figure 8. Plots of Laplace transform of $f(t)=\epsilon^{-0.2t}$ cos $(t-30$ degrees) and the time response. Frequencies A, B, and C used in Figures 5, 6, and 7 respectively

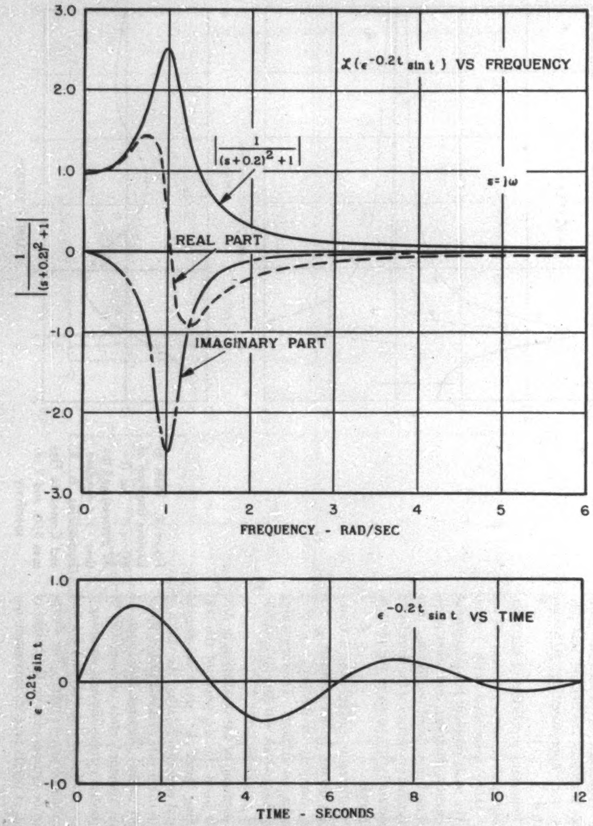

Figure 9. Laplace transform and time response of $\epsilon^{-0.2t}\sin t$

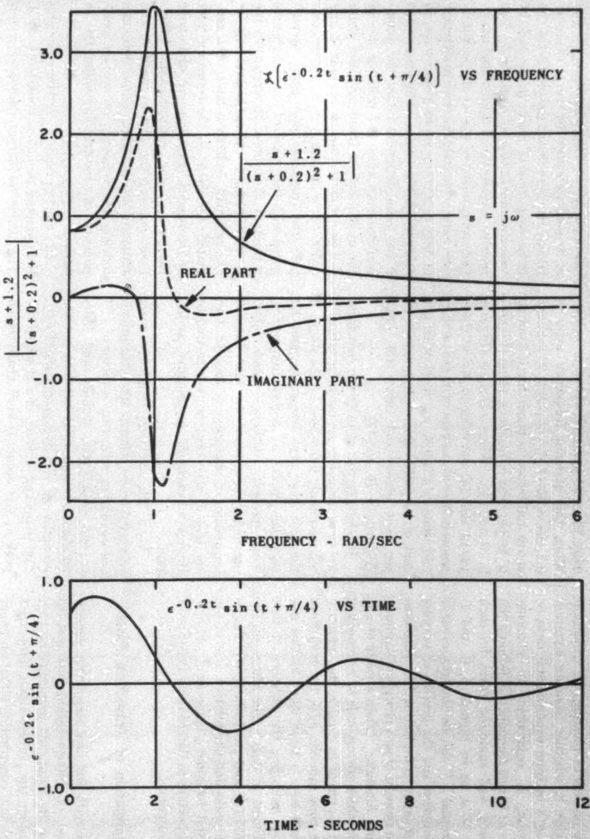

Figure 10. Laplace transform and time response of $\epsilon^{-0.2t}\sin(t+\pi/4)$

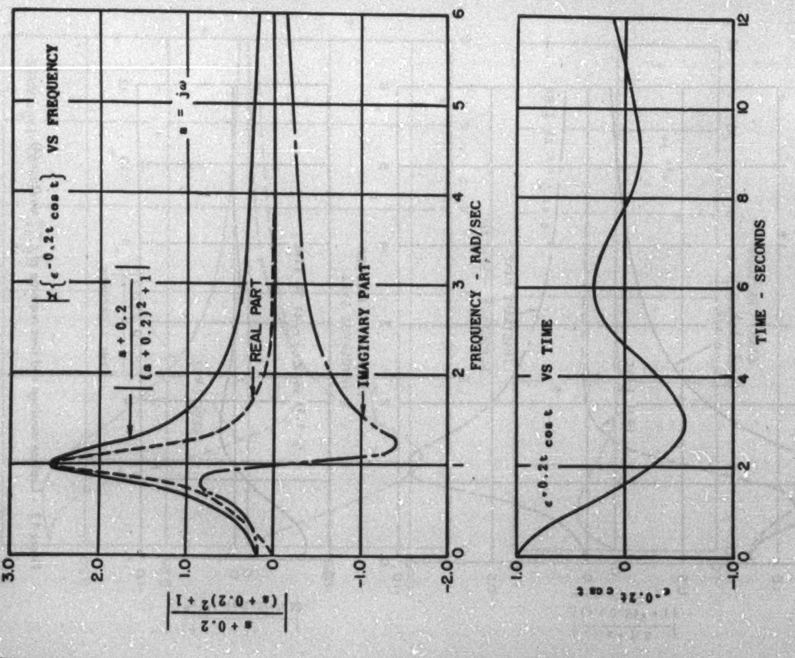

Figure 11. Laplace transform and time response of $\epsilon^{-0.2t} \cos t$

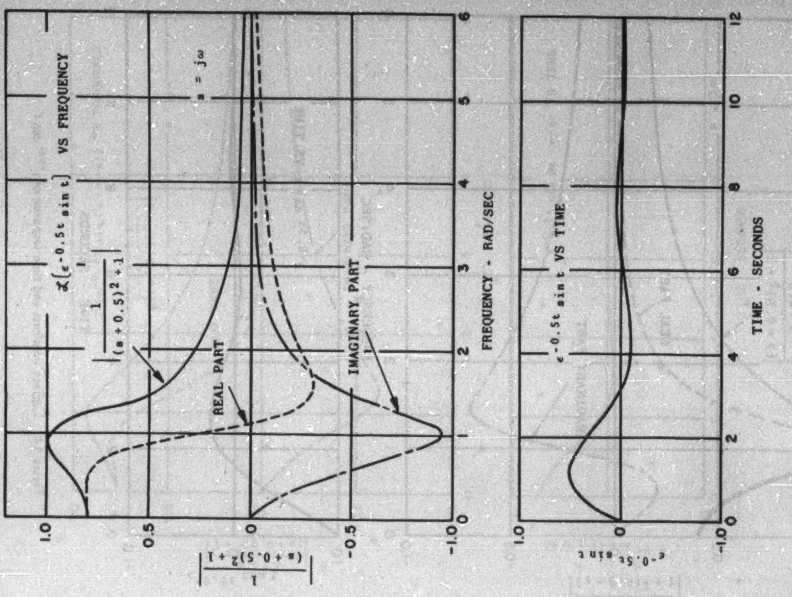

Figure 12. Laplace transform and time response of $\epsilon^{-0.5t} \sin t$

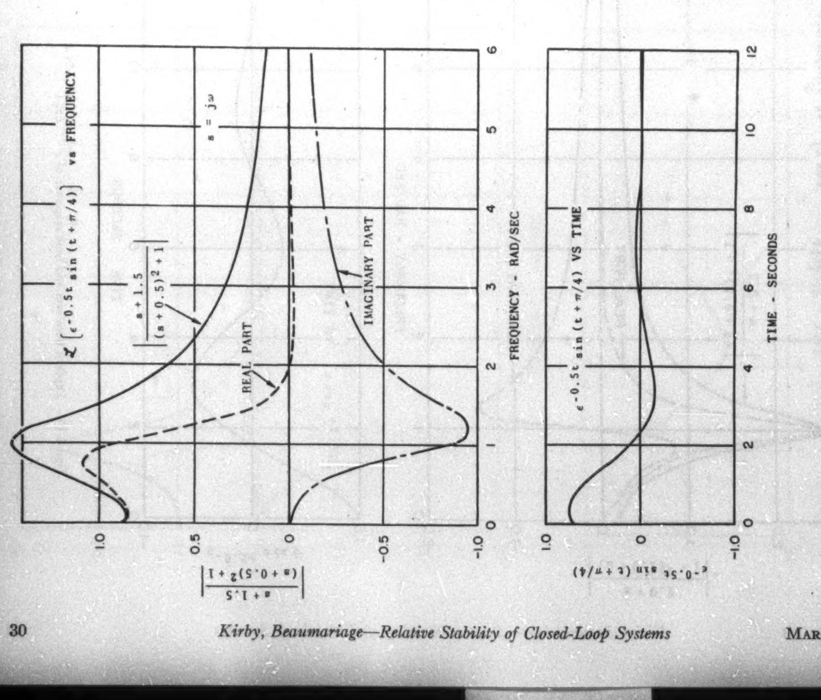

Figure 13. Laplace transform and time response of $\epsilon^{-0.5t}\sin(t+\pi/4)$

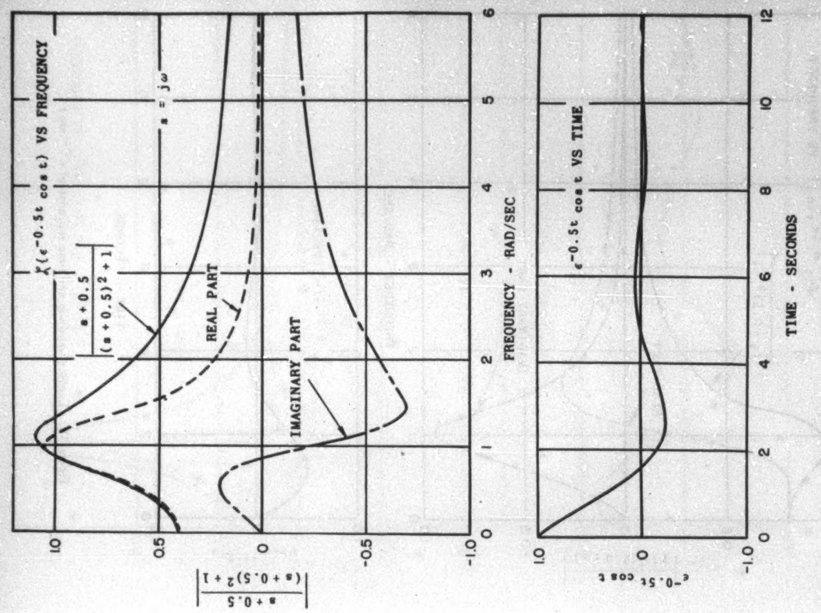

Figure 14. Laplace transform and time response of $\epsilon^{-0.5t}\cos t$

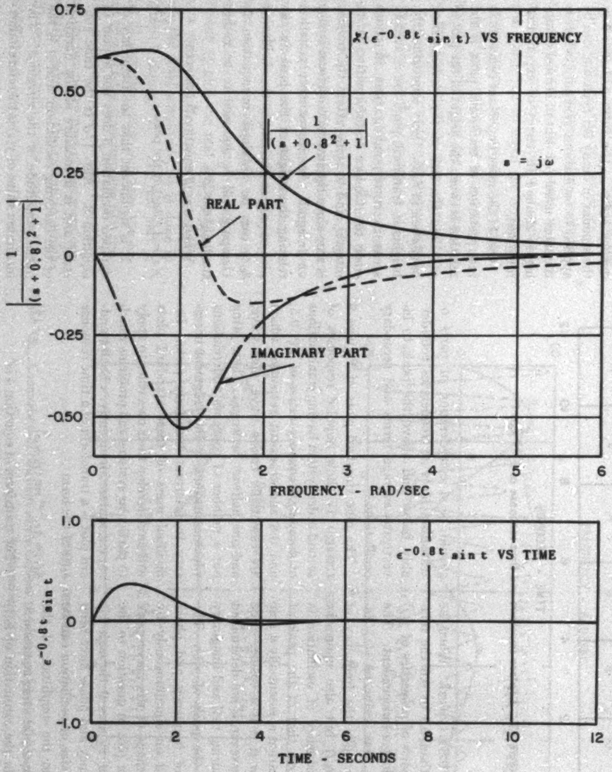

Figure 15. Laplace transform and time response of $\epsilon^{-0.8} \sin t$

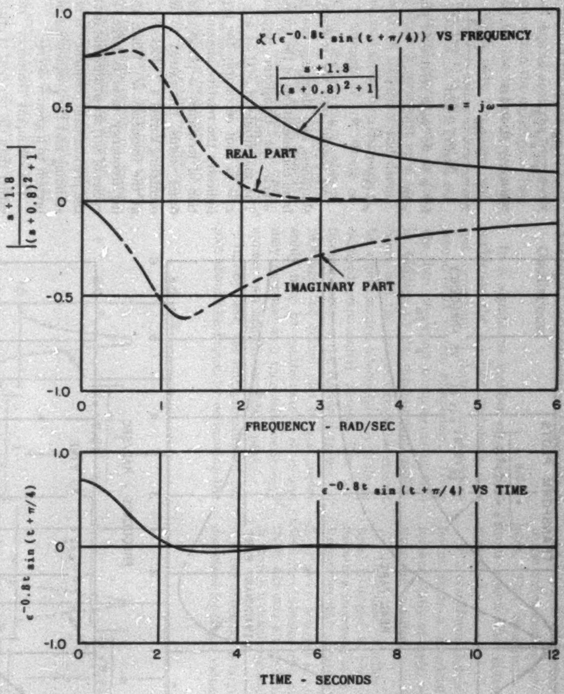

Figure 16. Laplace transform and time response of $\epsilon^{-0.8t} \sin(t+\pi/4)$

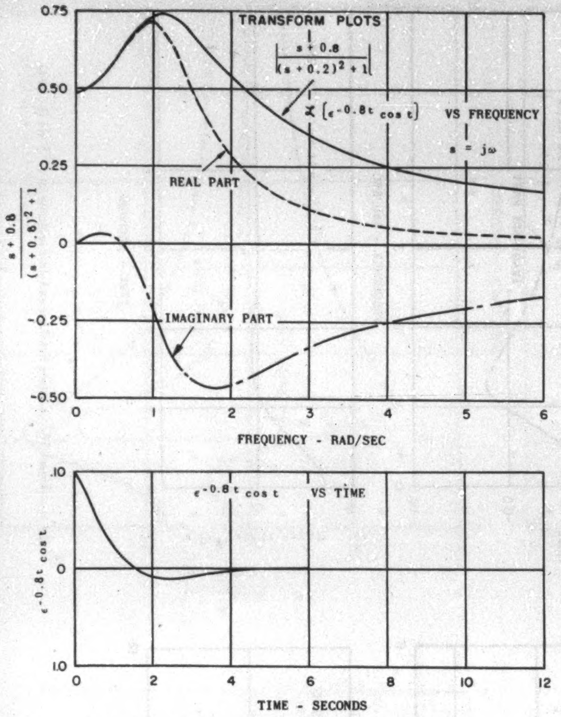

Figure 17. Laplace transform and time response of $\epsilon^{-0.8t}$ cos t

quency (α/β) of 0.8 is typical. When the ratio is larger than 0.5 or 0.6 the relations between pairs of properties of $y(s)$ and $\theta_0(t)$ are no longer independent. The location of the peak value of $y(s)$ depends not only upon the frequency of oscillation of $\theta_0(t)$ but also upon the phase. The frequency of oscillation is appreciably above that of the peak of $y(s)$ if the oscillation is essentially a sine wave and below if it is a cosine. The phase of $\theta_0(t)$, however, is not determined simply by measuring real and imaginary components at the peak of $y(s)$. The determination of frequency and phase must be carried on simultaneously by comparing the shape of the major peak in the transform plot in question to the standard plot of Figures 9 through 17. Once the frequency and phase have been established the size of oscillation can be determined from the amplitude of the peak of the value of $y(s)$ using equation 8. The final step in the estimation of $\theta_0(t)$ should be a consideration of parts o transform plots at frequencies considerably below and above the peak to investigate average terms and secondary oscillations.

The nine standard plots of Figures 9 through 17 show impulse responses of second-order system having combinations of damping/frequency ratios of 0.2, 0.5, and 0.8 and transient responses which are essentially cosine wave, sine wave, and one halfway between. These bring out a number of concepts and relations which contribute to the judgment necessary to interpret transform plots. Individual users of these standard plots will soon develop their own rules to apply to particular systems and problems which are encountered frequently. Each standard plot is a transform of a time response $\theta_0(t)$ of the form

$$\theta_0(t) = A\epsilon^{-\alpha t} \sin (\beta t + \varphi) \tag{4}$$

The transform of equation 4 is[9]

$$y(s) = \frac{A\beta}{(s+\alpha)^2+\beta^2} \tag{5}$$

when $\varphi = 0$, and is

$$y(s) = \frac{A\beta}{\sqrt{(a_0-\alpha)^2+\beta^2}} \frac{s+a_0}{(s+\alpha)^2+\beta^2} \tag{6}$$

for $\varphi \neq 0$. a_0 is related to phase angle φ by

$$\varphi = \tan^{-1} \frac{\beta}{a_0-\alpha} \tag{7}$$

An insight into the relation between sharpness and damping can be gained from considerations of the mechanism by which the transform measures $\theta_0(t)$. The magnitude of $y(s)$ at any value of $s = j\omega$ (not necessarily the peak value) indicates the relative amount of oscillation of frequency ω present in $\theta_0(t)$, in other words, the extent to which the oscillating kernel ϵ^{-st} "locks in" with $\theta_0(t)$ at the frequency ω. When the damping/frequency ratio is large, successive cycles of $\theta_0(t)$ are so different in shape that the predominant frequency is not as outstanding and the frequencies near it are present to a greater degree.

The damping/frequency ratio α/β, rather than the per cent of critical damping, is used to describe the amount of damping and the curves of $y(s)$ are plotted on linear rather than log-frequency scales. The ratio α/β indicates the amount of decay per cycle and can be applied to oscillations generally, whereas the more usual per cent of critical damping is defined in terms of exponential functions.

One of the more important concepts in interpretation of transform plots is the relation between the height of the plot of $y(s)$ and the size of the corresponding oscillation in $\theta_0(t)$. Very approximately, heights in transform plots are related to areas in corresponding time functions since the Laplace transformation is an integral, and to some extent the reverse is true since the inverse transform is also an integral. An approximate equation relating the height of the peak in the plot of $y(s)$ to the size of the oscillation $\theta_0(t)$ can be obtained in equation 5. Damping will be assumed to be rather small ($\alpha^2 << \beta^2$).

When $s = j\beta$ equation 5 becomes

$$y(s) = A/(2\alpha j) \text{ at the peak} \tag{8}$$

It is significant that the frequency of damped oscillation β does not appear in equation 8. Also $1/\alpha$ is the time constant and is a measure of the duration of the decaying oscillation, and A is the initial amplitude of the envelope. The maximum value of $y(s)$ is therefore indicative of the area of the envelope of $\theta_0(t)$, and does not depend upon the frequency of oscillation within the envelope. This is illustrated by the transform plots of Figure 18, which have the same peak value of $y(s)$ for two values of β differing by 8 to 1, when A, α, and φ remain the same. The height of the peak in the plot of $y(s)$ depends somewhat upon the phase for a given frequency and damping, however, as is shown by a comparison of Figures 9 through 17. It should be emphasized that the maximum value of $y(s)$ is a measure of the size of the entire time response, $\theta_0(t)$, and is not basically an indication of the response at some particular instant, for example, the maximum overshoot or first reversal of the transient oscillation.

Both linear and log-frequency plots of $y(s)$ are useful but emphasize different information. If, for example, two peaks at different frequencies have the same heights and the same width on linear scale, the corresponding oscillations in the time functions have the same initial amplitude and duration of their envelopes but different frequencies of oscillation within these similar envelopes, Figure 18. If two peaks at different frequencies have the same height and shape on log-frequency plots, they have the same α/β, that is, they decay in the same number of cycles but the initial amplitude of the higher frequency peak will be larger.

The relative closeness of an oscillation to a sine wave or to a cosine is conveniently described in terms of a phase angle which is zero when the oscillation is a sine wave. In a steady-state transfer function analysis the phase angle is plotted together with the magnitude of the transfer function, since the latter alone usually cannot give all the available information about the system.

Since the output/input transfer function is also the Laplace transform of the impulse response, the tangent of the phase angle is the ratio of the imaginary to the real part of the transform. When the transform is plotted to measure transient response, the concept of an angle introduces an unnecessary step on the interpretation of the plot. It is more efficient to plot the real and imaginary parts of the transform directly, together with the total amplitude, as is done in Figures 9 through 17. The real part of $y(s)$ at any frequency indicates the extent to which the time response $\theta_0(t)$ contains a cosine wave of that frequency, and the imaginary part of the transform similarly indicates the extent to which $\theta_0(t)$ locks in with a sine wave of that frequency.

Average Components and Secondary Oscillations

In a significant number of practical problems, the Laplace transform does not correspond to that of any standard second-order system completely. There are then important components in $\theta_0(t)$ in addition to the predominant oscillations, and the system's response cannot be approximated adequately by a single damped exponential alone. The difference between the standard transform plot and the actual plot of $y(s)$ under study may be greatest at $s = 0$ and may decrease as s increases, or it may appear as a definite secondary peak.

In any case, the interpretation of the plot should be begun by estimating the predominant oscillation and sketching in the corresponding part of the transform plot. This constitutes the base line from which the difference, $\Delta y(s)$, is measured.

If a transform plot is sufficiently different from a standard plot to make further study of $\Delta y(s)$ worth while, two steps are in order:

1. Determine whether the difference $\Delta y(s)$ is largest at $s=0$ and decreases as frequency increases, or is larger at higher frequencies than at zero.
2. If $\Delta y(s)$ is larger at higher frequencies, determine whether the maximum is relatively flat over a wide band of frequencies, or there is a definite secondary peak.

If the difference is largest at $s = 0$ and decreases for larger values of s, there is a

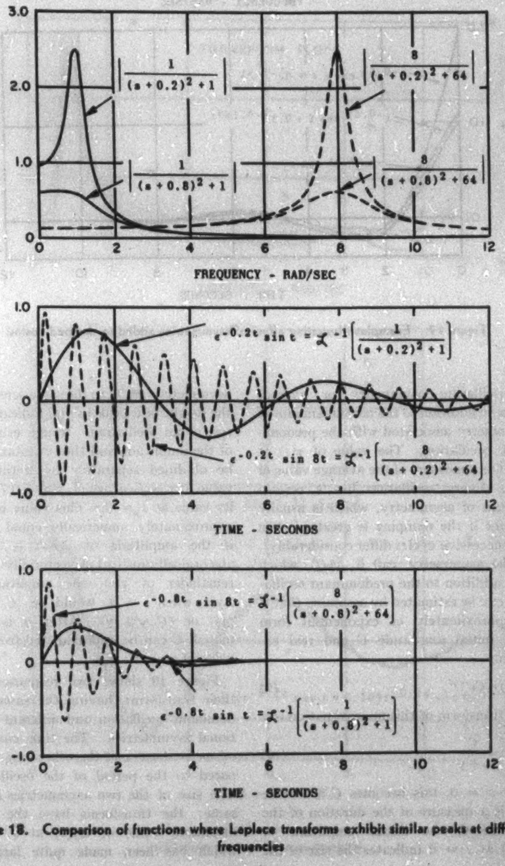

Figure 18. Comparison of functions where Laplace transforms exhibit similar peaks at different frequencies

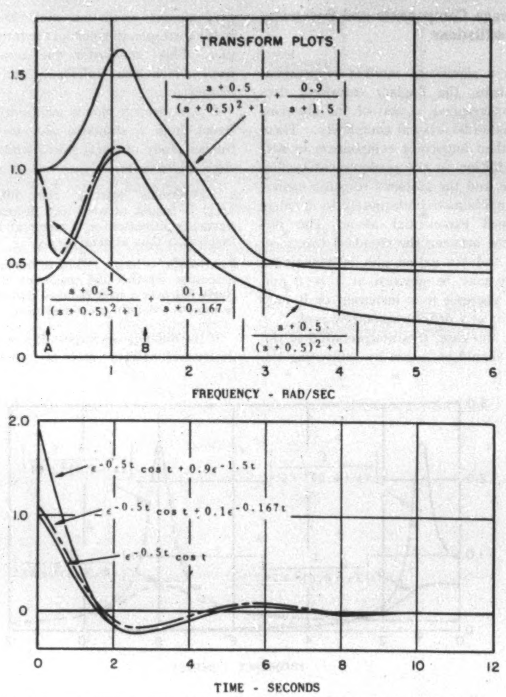

Figure 19. Examples illustrating effect of asymmetries added to damped cosine

nonoscillating asymmetry or average value in addition to the normal amount of asymmetry associated with the predominant oscillation. The value of $y(s)$ at $s = 0$ is a measure of the average value of $\theta_0(t)$. Every oscillation has a certain amount of asymmetry, which is usually greater if the damping is greater (when the successive cycles differ considerably).

The asymmetry, call it $\Delta\theta_0(t)$, which is in addition to the predominant oscillation can be estimated by assuming that it is approximately of exponential form with initial amplitude C and real exponent

$$\Delta\theta_0(t) = C\epsilon^{-\gamma t} \tag{9}$$

The transform of this approximation is

$$\Delta y(s) = \frac{C}{s+\gamma} \tag{10}$$

At $s = 0$, this becomes C/γ. Since $1/\gamma$ is a measure of the duration of the asymmetry, the initial amplitude of $\Delta y(s)$ at $s = 0$ indicates the size of the asymmetry, $\Delta\theta_0(t)$, in the same sense that the height of a peak in $y(s)$ indicates the size of an oscillation. Rough estimates of the amplitude and time constant may be obtained separately by noting the value of $s = j\omega$ at which $y(s)$ is 0.7 times its value at $s = 0$. This value is very approximately numerically equal to γ; if the amplitude of $\Delta y(s)$ is added algebraically instead of vectorially to the remainder of $y(s)$, the amplitude of $\Delta y(s)$ when $s = j\omega$ would be $|C/(\gamma + j\gamma)|$ or $(C/\sqrt{2}\ \gamma)$. After γ is estimated, C can be approximated from the value of $y(s)$ at $s = 0$.

Figure 19 shows two responses and their transforms, having the same predominant oscillation and different additional asymmetries. The time constant of one is short, and the other long, compared to the period of the oscillation. The size of the two asymmetries is the same; the transforms have the same maximum value of $\Delta y(s)$ at $s = 0$, which has been made quite large to illustrate the preceding statements. The values of ω at which $\Delta y(s)$ in each case is 0.7 times its value at $s = 0$ are shown at points A and B for the $\Delta\theta_0(t)$ with the short- and long-time constants respectively. It is seen that these values of ω do approximate γ quite closely.

If the maximum difference $\Delta y(s)$ occurs at a frequency higher than zero but is flat and without a well-defined peak, the time response is essentially a pulse with a duration corresponding to a half-cycle of a frequency near the center of the broad maximum in $\Delta y(s)$. The size, or roughly, the product of peak value times duration of the impulse, is indicated by the height of the maximum in $\Delta y(s)$; see Figures 20 through 25.

When the transform plot contains a distinct secondary peak there is a corresponding distinct secondary oscillation. The problem of interpretation is not to estimate the oscillation's properties to an accuracy of a few per cent. It is rather to establish whether such an oscillation exists at all, and if so at what frequency, about how large the amplitude, and roughly how long it will persist. This is sufficient information to determine, for example, how much control energy may be expended in the oscillation. This is an important question, for instance, in some air-borne installation where the reservoir of control energy is of limited size.

The principles of interpreting secondary peaks are basically the same as for the larger peaks which denote primary oscillations. The size and duration, however, are easier to obtain and are more useful expressed as a fraction of the size and duration of the major oscillation rather than as absolute numbers. Also, the process of estimating the size of $\Delta y(s)$ above a base line amounts to using arithmetic instead of complex algebra. This is not extremely accurate but is usually sufficient. If the secondary peak appears distinct, there will normally be several cycles of the secondary oscillation, so that the frequency, size, and damping can be estimated separately. The phase is not usually of interest.

Figures 20 through 25 show transform plots and time responses in which small secondary oscillations are present in addition to primary oscillations. The secondary peaks have amplitudes amounting to 10 per cent of the predominant peak, and are three octaves above it in frequency. It is not generally feasible to interpret secondary peaks which are smaller in relative amplitude or much closer to the predominant peak than this.

Four kinds of primary oscillations are

illustrated; both sine and cosine waves, having relatively large damping ($\alpha/\beta = 0.8$) and small damping ($\alpha/\beta = 0.2$). To each of these, in Figures 20 through 23, three secondary oscillations having different amounts of damping are added. The three secondary peaks are the same height above the base line of the transform plot.

As expected, the areas of the envelopes of the secondary oscillations are about 10 per cent of the areas of the primary oscillations. The flattest of the secondary peaks in the transfer plots, having no distinct maximum, indicates single half-cycles or pulses in the corresponding time responses. As the secondary peaks become more distinct in the transform plots, a greater number of cycles appear in the time responses; the amplitude of the envelope decreases and the duration lengthens.

The secondary oscillations of Figures 20 through 23 are all sine waves. In Figures 24 and 25, secondary cosine waves are added to the same primary oscillations as in Figures 20 and 22 to show that the phase of the secondary oscillation does not greatly affect the transform plot.

Responses to Different Inputs

Perhaps the most difficult element in the interpretation of Laplace transform plots is the adjustment to the fact that the transfer function plot corresponds to the time response to a unit impulse, whereas almost all individual experience and discussions in the literature have tended to relate a frequency response plot to the time response to a unit step input. There is no harm in the transfer-function–step-input relationship; however, a system's impulse response is usually a much more convenient base line for comparing and estimating its response to different practical inputs. All of the transform plots discussed thus far in this paper, therefore, have been transforms of impulse responses. When the system under investigation is one of the large class having linear, lumped elements, the transform of the response to any input is found simply by multiplying the transform of the impulse response by the transform of that input. The plot of the product can be analyzed by the techniques given herein to estimate the response to the input which is of interest.

The effects of an input or driving force on a linear system are, first, to produce a steady-state or particular integral term in the response, and second, to redistribute the magnitudes of the various transient terms or complimentary functions. Both of these effects are of interest when a transform plot is analyzed.

Most practical inputs fall into one of four groups:

1. Steps of displacement, velocity, acceleration, and so forth.

2. Exponential impulses ϵ^{-at} where a is a constant.

3. Oscillation which can be approximated by sinusoids with or without damping.

4. Pulses of various shapes (rectangular, peaked, and so forth) whose length is appreciable compared to the system time constants.

The transforms of the first group are of the form ($1/s^n$), where n is unity for a step of displacement, two for a step of velocity, and so on. These transforms are infinite at $s = 0$, but severely attenuate any higher natural frequencies in a system's impulse response. The transforms of the second group are of the form $[1/(s + a)]$. Such functions are sometimes useful for approximating pulses or gradual rises (when combined with a step).

The third group of inputs have transforms of a form such as $[1/(s^2 + a^2)]$ where a is the frequency of oscillation. They generally add another oscillation of frequency a to the system's impulse response and attenuate the oscillations already present.

The transforms of pulses of appreciable length generally contain transcendental terms such as ϵ^{-sT}, where T is a time

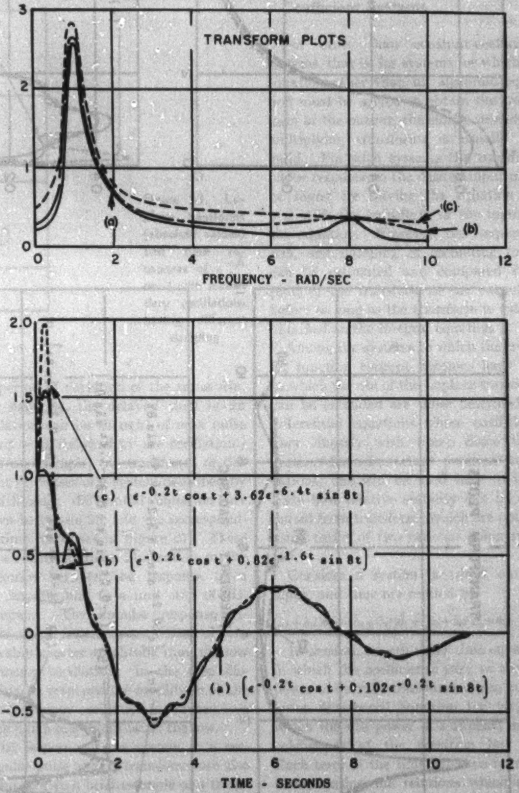

Figure 20. Laplace transforms (absolute values) and time responses of $\epsilon^{-0.2t}\cos t$ with secondary oscillations having different damping

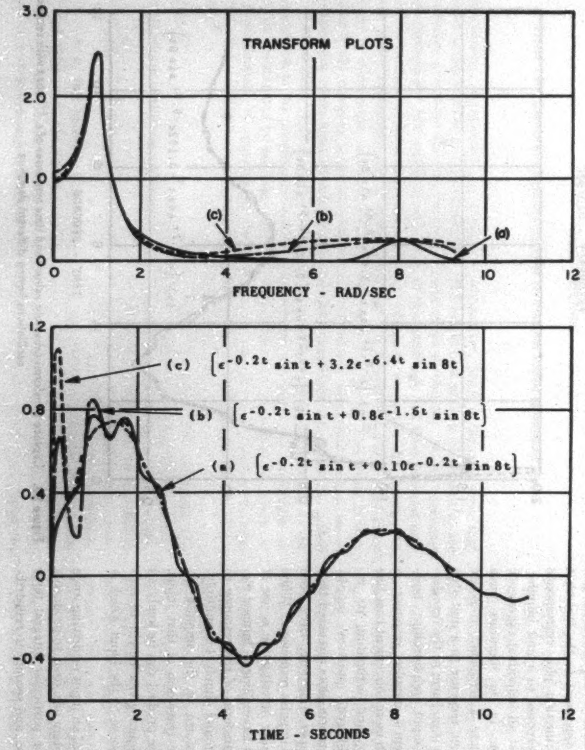

Figure 21. Laplace transforms (absolute values) and time responses of $\epsilon^{-0.2t}$ sin t with secondary oscillations having different damping

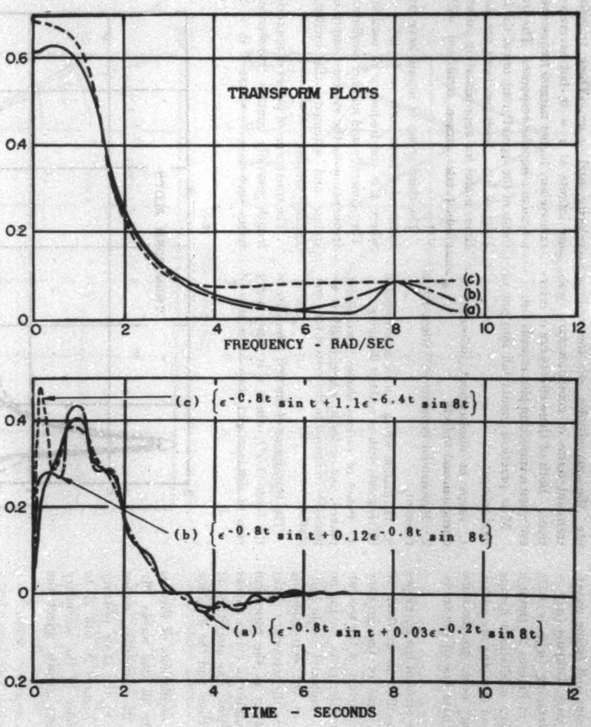

Figure 22. Laplace transforms (absolute values) and time responses of $\epsilon^{-0.8t}$ sin t with secondary oscillations having different damping

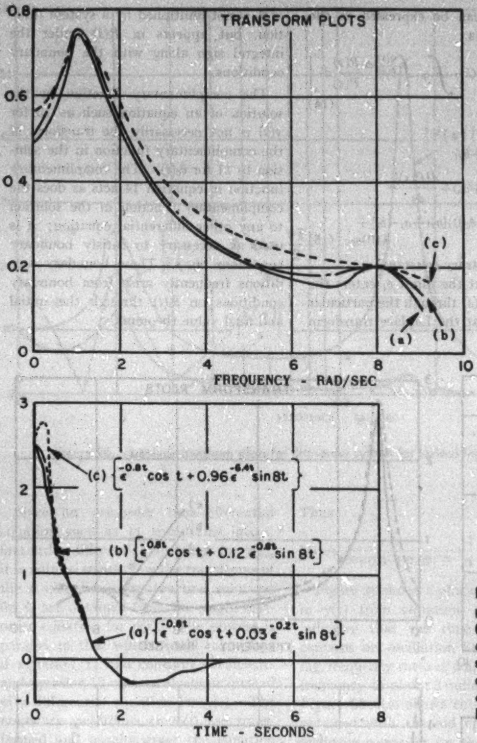

Figure 23. Laplace transforms (absolute values) and time responses of $\epsilon^{-0.8t}$ cos t with secondary oscillations having different damping

constant related to the length of the pulse. There are also algebraic terms determined by the shape of the pulse.

The plot of the transform of the response of a system to a practical input can usually be interpreted by first investigating the steady-state response, sketching its transform, and estimating the sizes and shapes of the peaks in the total transform from this as a base line. Sometimes the steady-state term is known from boundary values or other considerations. In any case, if the transform of the response is infinite at $s = 0$, there is a constant displacement, velocity, or acceleration which persists indefinitely. If the transform is infinite at some frequency other than zero, there is a steady oscillation of that frequency present in the response. If the transform has a transcendental term, with periodic maxima and minima as frequency increases, the time response generally contains a pulse or a series of pulses whose length is simply related to the period of variation of the transform. (For example, the delayed start of an oscillation can be thought of as a pulse from $t = 0$, followed by the oscillation.)

As an example, the transforms of different responses of a system described by a fifth-order differential equation are shown in Figure 26, and the corresponding time responses in Figure 27. These are a rather extreme illustration of the difference between the response to a unit impulse and to a unit step of displacement. The impulse response exhibits a high frequency oscillation of considerably greater amplitude than the low frequency oscillation; in the step displacement response the amplitude of the high frequency oscillation is reduced to a value much less than that of the low.

The response of the system to a rectangular pulse and its transforms are also shown to give a brief example of a transcendental transform.

The same general rules of interpretation apply as before. Large peaks in the Laplace transform indicate the presence of an oscillation of considerable size in the time response, the size being the magnitude of the product summed over all time. The sharpness of the plot indicates the rate of decay. Smaller periodic peaks in the Laplace transform plot are characteristic of pulse responses and the spacing of the periodic maxima and minima in a transform plot indicate the time constant or length of the impulse. An excellent discussion of the frequency components of a pulse is given by Goldman.[10]

The interpretation of Laplace transform plots of this nature may not give the exact shape of each oscillation near $t = 0$ but will give much useful information about the time response.

Extension of Method to Variable Coefficient Systems

For other than constant-coefficient systems, that is, for systems for which an equation other than an algebraic equation must be solved to obtain the transform of the output, the simple process of multiplying transforms is usually not valid. For such systems the transform of the response to the desired input must be found by solving the equation for $y(s)$ with the transform of the input in the equation. However, the frequency, size, and damping of oscillating terms can be estimated and compared from plots of the transform of the output as before so long as the transform is validly obtained as the integral equation 1.

Among the systems to which the transfer function concept becomes hazy but to which the use of the Laplace transform can be extended are those described by differential equations whose coefficients vary linearly with time. Since these systems have important practical applications, one will be used here to illustrate how relative stability can be estimated from transforms which are not the usual ratios of two rational polynomials in s.

Consider a system in which output, input, and time are related by

$$(a_2+b_2t)\ddot{\theta}_0+(a_1+b_1t)\dot{\theta}_0+(a_0+b_0t)\theta_0=\theta_i \quad (11)$$

In general, an nth-order time equation in which the coefficients vary as the rth power of t can be transformed into an rth order differential equation for $y(s)$, in which the nth power of s appears in the coefficients of the equation for $y(s)$. Each term of the time equation is transformed using the relations which state that multiplication by t in the time domain corresponds to differentiation with respect to s. In practice the differential equation for s can usually be solved only when $r = 1$, so the use of the Laplace transformation is restricted to equations such as 11 in which the coefficients vary as $(a + bt)$.

Using standard equations[9,11,12] equation 11 transforms term by term into

$$a_2s^2y(s)-a_2s\theta_0(0)-a_2\dot{\theta}_0(0)-2b_2sy(s)-b_2s^2y'(s)+b_2\theta_0(0)-a_1\theta_0(0)+a_1sy(s)-b_1y(s)-b_1sy'(s)+a_0y(s)-b_0y'(s)=\mathfrak{L}\{\theta_i(t)\} \quad (12)$$

or

$$-y'(s)[b_2s^2+b_1s+b_0]+y(s)[a_2s^2+a_1s+a_0-2b_2s-b_1]=\mathfrak{L}\{\theta_i(t)\}+\theta_0(0)[a_2s+a_1-b_2]+\dot{\theta}_0(0)a_2 \quad (13)$$

The solution for $y(s)$, the Laplace transform of $\theta_0(t)$, can be expressed in the standard form as

$$y(s)=\epsilon^{+\int\frac{Q(s)}{P(s)}ds}\left[C-\int\epsilon^{-\int\frac{Q(s)}{P(s)}ds}\frac{R(s)}{P(s)}ds\right] \quad (14)$$

where

$$P(s)=(b_2s^2+b_1s+b_0)$$

$$Q(s)=(a_2s^2+a_1s+a_0)-\frac{d[P(s)]}{ds}$$

$$R(s)=\mathfrak{L}\{\theta_i(t)\}+\theta_0(0)[a_2s+a_1-b_2]+\dot{\theta}_0(0)a_2 \quad (15)$$

and C is an arbitrary constant.

It is seen that the input θ_i enters the expression for $y(s)$ through the particular integral and that the Laplace transform of θ_i is not multiplied by a system function, but appears in $R(s)$ under the integral sign along with the boundary conditions.

The complimentary function in the solution of an equation such as 13 for $y(s)$ is not necessarily the transform of the complimentary function in the solution to 11 for $\theta_0(t)$. The complimentary function in equation 14 acts as does the complimentary function in the solution to any other differential equation; it is used as necessary to satisfy boundary conditions on y. These boundary conditions frequently arise from boundary conditions on $\theta_0(t)$ through the initial and final value theorems.

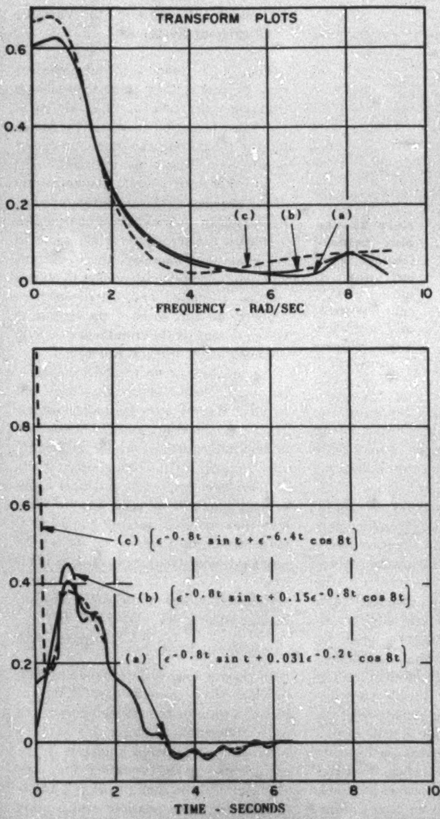

Figure 24. Laplace transforms (absolute values) and time responses of $\epsilon^{-0.8t}$ sin t with secondary oscillations; phase of secondary oscillation different from Figures 20 through 23

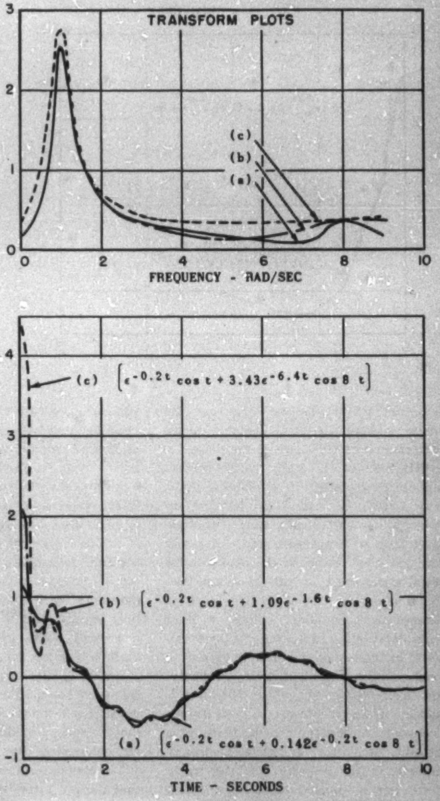

Figure 25. Laplace transforms (absolute values) and time responses of $\epsilon^{-0.2t}$ cos t with secondary oscillations; phases of secondary oscillations different from Figures 20 through 23

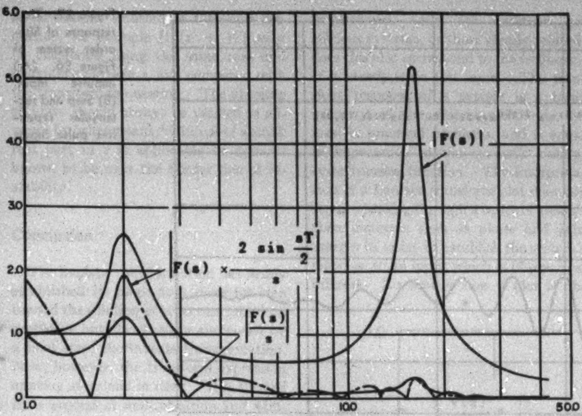

Figure 26. Laplace transform plots for fifth-order system for various inputs

Since an *n*th-order time-differential equation such as 11 transforms into a first-order differential equations for $y(s)$, it is natural to ask how the transforms of the n complimentary function solutions for θ_0 are obtained from the single first-order equation for $y(s)$. The process is parallel to that which would take place if equation 11 had constant coefficients and equation 13 were an algebraic instead of a differential equation for $y(s)$. The boundary conditions on $\theta_0(t)$ are transformed and usually enter the equation for $y(s)$ as n separate driving forces, each producing a particular integral solution for $y(s)$ which is the transform of a different $\theta_0(t)$ solution. When some of the boundary conditions are lost in the process of transformation, as occurs in the following example, it is necessary to make use of the complimentary function in the solution for y.

As a specific example consider for equation 14 the case where

$$a_2=0,\ b_2=1,\ a_1=1,\ b_1=0.6,\ a_0=0.3,\ b_0=9.09$$

The input is taken as $\theta_i(t) = a_0 + b_0t$ with no initial energy storage. For these conditions, the steady-state portion of the output is then constant and unity. When $Q(s)/P(s)$ is expanded in partial fractions and substituted into the integrals in equation 4 the expression for $y(s)$ becomes

$$y(s)=\frac{1}{[s^2+0.6s+9.09]^{1/2}}\times \left[C-\int\frac{9.09+0.3s}{[s^2+0.6s+9.09]^{1/2}}\frac{10}{s^2}ds\right] \quad (16)$$

Thus

$$y(s)=\frac{C}{[s^2+0.6s+9.09]^{1/2}}+\frac{1}{s} \quad (17)$$

Figure 28 shows a plot of the first term in $y(s)$ from equation 17. The peak indicates that the time response $\theta_0(t)$ contains an oscillation having a damping/frequency ratio α/β about 0.5, and a frequency of about 3 radians per second. Figure 28 also shows the time response obtained with the aid of an electronic analogue computer for the same system using equation 11. The shape of the envelope and the oscillation within it in the time response agree with the estimate based on the transform plot. For convenience in the computer setup, the input θ_i used in obtaining the time response in Figure 28 is a simple ramp function rather than $(a_0 + b_0t)$; this does not affect the oscillation.

To illustrate further how the rules for interpreting transform plots apply to time-varying as well as constant-coefficient systems, the value of b_0 in the system of the previous example was multiplied by 4. The plot of $y(s)$ from equation 17 with the increased value of b_0 is plotted in Figure 29. The shape of the peak is not changed, but the peak is shifted to a frequency which is double the previous value. It would be estimated from a comparison of the transform plots that the effect of multiplying by 4 is to leave the shape of the envelope of the time response unchanged but double the frequency within it. This is verified by plots of the time responses, in Figure 29, which is quite parallel to Figure 18.

Constant-coefficient approximations are often used in studying time-varying systems. In the present examples, it might seem reasonable to divide the equation by t and let t become very large. The resulting approximation to the transform is, instead of equation 17

$$y(s)=\frac{C}{s^2+0.6s+9.09} \quad (18)$$

This transform and also the approximation with b_0 multiplied by 4 are also plotted for comparison with the exact transforms in Figure 29. The constant coefficient approximation to the time response would in each case be estimated to decay less quickly than the exact response, because of the sharper peak in the plot obtained from equation 18. Time responses obtained on the analogue computer for the constant-coefficient approximation show that this estimate is correct. This illustrates the limitations of constant-coefficient approximations; a plot of the actual Laplace transform of the time function in question gives the desired information about the time response.

The numerical values in the example of equation 13 and Figures 28 and 29 were chosen in order to get a fairly simple solution for $y(s)$ in closed form. In more complicated cases a series of solutions may be necessary, or some other device such as applying the input at a time other than $t = 0$ may be of help in solving the differential equation for $y(s)$. Furthermore, differential equations are by no means the only way to obtain transforms of the responses of systems whose parameters are not lumped and constant. The differential equation method of finding $y(s)$ is illustrated briefly here because it has not been discussed extensively elsewhere. However, a number of excellent books show other methods of obtaining Laplace transforms.[11-13] So long as the transform is equal to the integral of equation 1, and so long as it is convergent, the properties of the system response will be indicated by a plot of the transform.

Irrational terms such as appear in equation 17 are typical elements of the transforms of the responses of systems having time-varying components. Transforms of functions such as Bessel functions, having no damping term under the radical present important special cases. If $(1/\sqrt{s^2 + 1})$, the transform of the Bessel function of zero order, is plotted using pure imaginary values of s the plot becomes infinite at $s = 1$, apparently

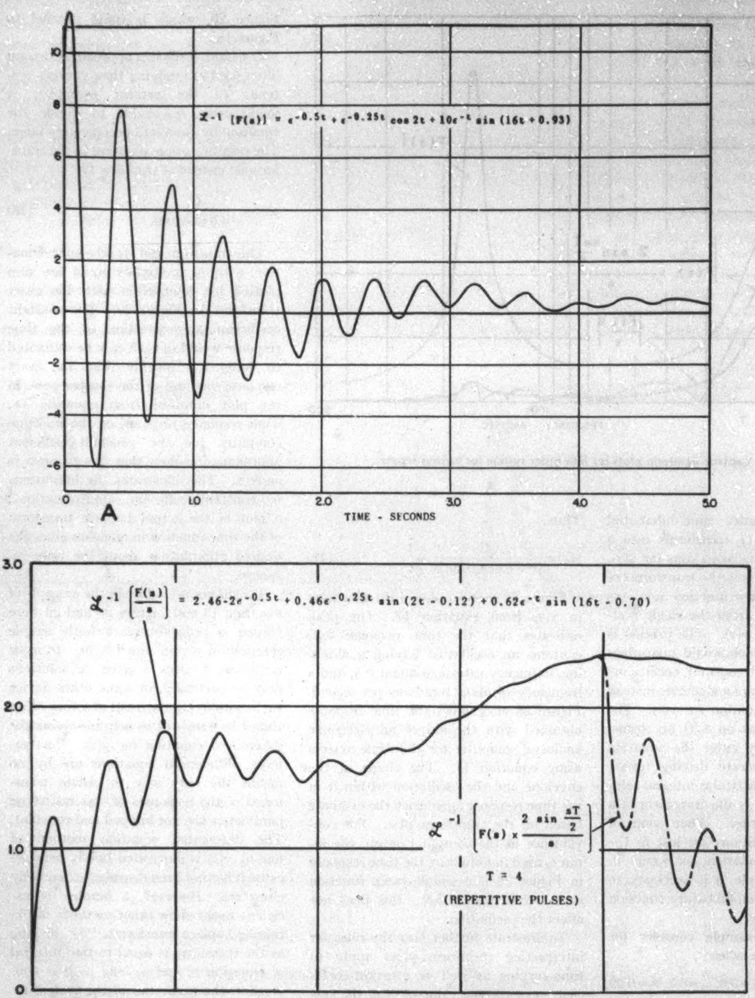

Figure 27. Time response of fifth-order system of Figure 26. (A) Impulse input. (B) Step and rectangular repetitive pulse inputs

indicating a sustained oscillation and an unstable system. Yet the Bessel function $J_0(t)$ is known to be stable, being finite at the origin and decaying approximately as $(1/\sqrt{t})$ times a sinusoid, after a few cycles. The envelope of the Bessel function decays so slowly, however, that the integral from time zero to infinity is infinite unless a convergence factor (that is, a real part) is included in the exponent of the kernel of the transform. This is understood when it is remembered that the integral from time zero to infinity of $(1/(t + a))$ is infinite, while the integral of ϵ^{-bt} is finite, regardless of the values of a and b (excluding zero values). (The a is included to keep the $1/t$ function finite at the origin.)

To interpret a transform such as that of a Bessel function, the transform can be plotted with a small, fixed real part, σ, in s in addition to the usual varying imaginary part. The plot will have a maximum value at the frequency of the oscillation. To estimate the size of the oscillation, the value of the transform of an undamped sinusoid of the same frequency, for example $[1/(s^2 + 1)]$, may be calculated using the same real and imaginary parts in s, and compared with the transform in question. The absolute stability should always be verified in advance by other means;[4,5] the use of a small real part in s is applicable to systems known to be near the border line of instability.

Conclusion

The Laplace transformation has firmly established its place as a powerful step toward the solution of otherwise laborious problems, but always to be succeeded by a final step, the inverse transformation. Now, however, the transform expression appears as an end in itself. It is formed by a process of multiplication and summation which has a physical analogue and which can be easily visualized. The kernal of the transform can be thought of as a standard or test function whose frequency can be varied at will to scan the unknown responses and investigate the existence of a similar frequency in it. A simple plot of the transform is usually all that is necessary to estimate the important features of the time response. This is of considerable practical importance, since it is usually easier to plot the transform than to obtain the inverse transformation and subsequently plot this.

Furthermore, the application of transform plots can be extended considerably to the analysis of systems for which it is possible to find a transform of the system response in a valid manner, but for which the inverse transform expression for the time function cannot be easily obtained.

In development work, where a great many trial solutions must be used to obtain an increasingly closer approach to a desired result, these are frequently worked out by a computer or simulator. The chief function of analysis by simple plots is then to guide the simulator work by exploring areas of possible interest, and as a check to verify the reasonableness of the simulator results. The use of Laplace transform plots amounts to an extension of the use of relatively cheap mathematical models to reduce the amount of more expensive physical simulation.

It must be borne continually in mind that the frequency in a frequency response plot is not necessarily the frequency of a steady-state sinusoidal input; it is the frequency of the oscillating kernal of the Laplace transformation which scans the function $\theta_0(t)$ which is transformed. Only for constant coefficient systems, or those closely related, does this also correspond to the frequency of a steady-state test input. The transient response of a system is a basic property of the system which can be used in practical problems, and is equal in importance to the system's steady-state transfer function. The interpretation of a Laplace transform plot does not require passing through a series of steady-state concepts such as phase and gain margin in order to establish the system's response to an input which is of practical interest. No matter how a plot is obtained, so long as the quantity plotted is equal to the integral of equation 1, the techniques explained herein can be used to estimate the time response.

This offers possibilities for increased practical application, for example, in the testing of complex electromechanical systems. Transient responses are generally easier to obtain than frequency responses, particularly when a system contains heavy mechanical or aerodynamic elements. When a transient response is available, the Laplace transform as a function of frequency can be estimated by a process akin to the inverse

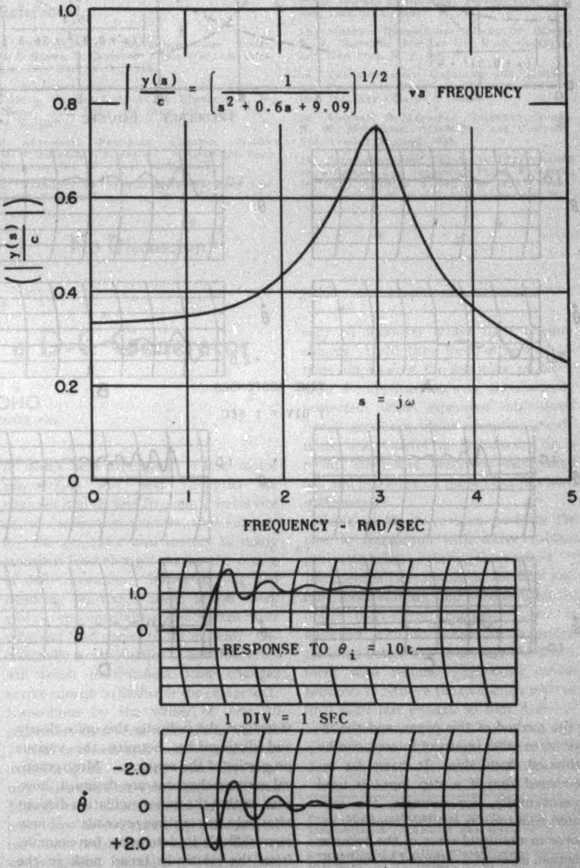

Figure 28. Transform plot and time response of equation 11 for $a_2=0$, $b_2=1$, $a_1=1$, $b_1=0.6$, $a_0=0.3$, $b_0=9.09$, and $\theta_i(t)=10t$

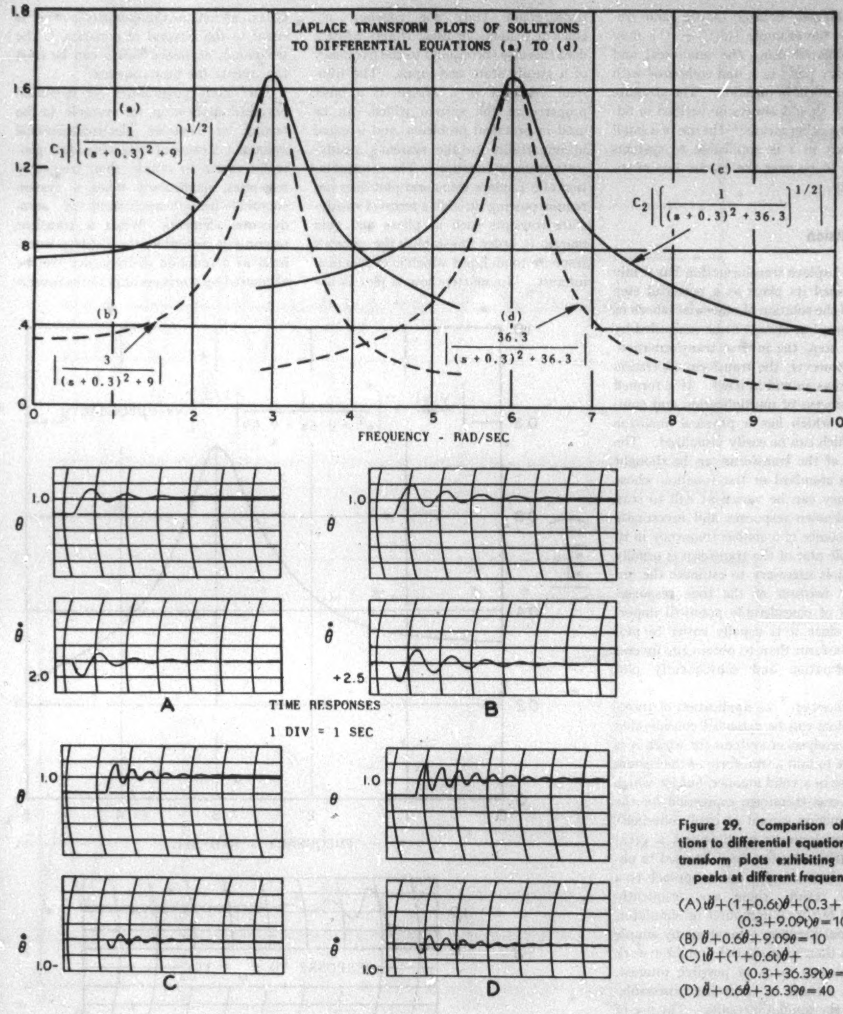

Figure 29. Comparison of solutions to differential equations with transform plots exhibiting similar peaks at different frequencies

(A) $t\ddot{\theta}+(1+0.6t)\dot{\theta}+(0.3+$ $(0.3+9.09t)\theta=10t$

(B) $\ddot{\theta}+0.6\dot{\theta}+9.09\theta=10$

(C) $t\ddot{\theta}+(1+0.6t)\dot{\theta}+$ $(0.3+36.39t)\theta=40t$

(D) $\ddot{\theta}+0.6\dot{\theta}+36.39\theta=40$

of the method of this paper, and the responses to other inputs of interest can be estimated from this. It must be remembered that if a step input is used experimentally, for example, the estimated transform is not the frequency response in the usual sense of the transfer function, unless it is adjusted by multiplication by *s*.

When several cycles of an oscillation are present in a transient response, the transform plot indicates this quite clearly and distinguishes between the various properties of the response. Most practical servomechanisms are designed, however, so that the major oscillation dies out after only two or three reversals. It may seem difficult to determine, for example, from the relatively broad peak in the transform plot, whether the response is a damped oscillation or the sum of a number of exponential functions. This is not a basic limitation on accuracy but rather an indication that the time response can be described adequately in more than one way. A method[14] for approximating the responses of well-damped servomechanisms makes use of the fact that an oscillation which consists of only a few reversals can be represented by two or three alternately positive and negative exponential terms having negative exponents, almost as well as by a damped sinusoid of the type $\epsilon^{-\alpha t}\cos(\omega t+\varphi)$. This extends to Laplace transform plots also. The important principle is that a given shape of a peak in a transform plot is associated with a particular shape of transient response, regardless of the formal mathematical expression which describes the transient.

Although not strictly within the scope of the method given in this paper, one additional field of possible extension of frequency plots deserves notice. Nyquist and many subsequent writers have considered plots using a complex frequency, or a real part σ, as well as the imaginary part ω of the operator s. Many such extensions of the usual frequency plots are possible and seem to have advantages in particular cases. For example, the degree of damping of a particular oscillation can be determined quite accurately by holding the imaginary part of s constant at the frequency of oscillation and plotting the transform expression as a function of the real part σ. Positive values of σ do not appear fruitful. Use of negative values will indicate a peak at the value of σ corresponding to the value of damping of the oscillation. This procedure amounts to exploring the locations of the poles of the frequency response of the system in the left half of the complex frequency plane. The quantity plotted is not the complete integral as given in equation 1, but rather only the lower limit, for negative values of σ greater than any pole of the frequency response. This lower limit, or system frequency response function, is related to the time response through the inverse transformation rather than through the transform integral of equation 1.

References

1. Principles of Servomechanisms (book), **G. S. Brown, D. Campbell.** John Wiley and Sons, Inc., New York, N. Y., 1948.

2. Servomechanisms and Regulating Systems Design, Volume I (book), **H. Chestnut, R. W. Mayer.** John Wiley and Sons, Inc., New York, N. Y., 1951.

3. Automatic Feedback Control (book), **W. R. Ahrendt, J. F. Taplin.** McGraw-Hill Book Company, Inc., New York, N. Y., 1951.

4. Stability of Servomechanisms with Linearly Varying Elements, **M. J. Kirby.** *AIEE Transactions*, volume 69, part II, 1950, pages 1662–68.

5. Stability of Varying-Element Servomechanisms with Polynomial Coefficients, **M. J. Kirby, R. M. Giulianelli.** *AIEE Transactions*, Volume 70, part II, 1951, pages 1447–51.

6. Frequency Analysis of Variable Networks, **L. A. Zadeh.** *Proceedings*, Institute of Radio Engineers (New York, N. Y.), March 1950, page 291.

7. Combination Open Cycle-Closed Cycle Servomechanisms, **J. R. Moore.** *Proceedings*, Institute of Radio Engineers (New York, N. Y.), March 1951.

8. Network Analyses and Feed-Back Amplifier Design (book), **H. W. Bode.** D. Van Nostrand and Company, Inc., New York, N. Y., 1945.

9. Transients in Linear Systems (book), **M. F. Gardner, J. L. Barnes.** John Wiley and Sons, Inc., New York, N. Y., 1942.

10. Frequency Analysis, Modulation and Noise (book), **S. Goldman.** Prentice-Hall, Inc., New York, N. Y., 1948.

11. Modern Operational Calculus (book), **R. V. Churchill.** McGraw-Hill Book Company, Inc., New York, N. Y., 1941.

12. Transformation Calculus and Electrical Transients (book), **S. Goldman.** Prentice-Hall, Inc., New York, N. Y., 1949.

13. Modern Operational Calculus (book), **N. W. McLachlan.** MacMillan and Company, Ltd., London, England, 1948.

14. Servomechanism Transient Performance from Decibel-Log Frequency Plots, **H. Harris, Jr., M. J. Kirby, E. F. von Arx.** *AIEE Transactions*, volume 70, part II, 1951, pages 1452–59.

No Discussion

Flashover Torque of a D-C Generator

O. C. COHO
ASSOCIATE MEMBER AIEE

LITTLE information has been presented in the past regarding the behavior of d-c machines during flashover particularly as regards the torque developed during this abnormal operation condition. This paper presents the results of a series of torque measurements made during flashover tests on a d-c generator. The time variation of torque during flashover and the significance of speed, excitation, and fault resistance are discussed.

General

The past several years have witnessed a very rapid rise in the use of diesel-electric locomotives. D-c electric drives are employed, consisting of diesel-driven shunt or compound generators and a number of series-type traction motors, depending upon the specific locomotive design. The traction motors may be operated in various combinations of series-parallel and with various amounts of series field strengths. These motor connections and field strengths are changed rapidly and frequently in service as the locomotive operates, thus subjecting the generator and motors to many transient load changes during the course of daily operation. Wheel slipping and bouncing on rough track or on track cross-overs contribute still more repetitive transient load surges to the system. Occasionally a combination of circumstances will result in transient load changes severe enough to flashover the equipment. Inspections by the writer of over 50 generators on several railroads in service 1 year or more and built by different manufacturers revealed that the traction generators on every unit had been flashed over at some time or other at least once as evidenced by commutator bar and brushholder melting due to severe arcing. It thus is evident that the generators must be built to resist arcing damage, to withstand short-circuit torques, and to minimize the tendency to flashover under these circumstances. Until these locomotive applications emphasized the flashover problem, most d-c applications were satisfactorily protected with expensive high-speed circuit breakers, clean operating conditions, and careful maintenance. As a result, studies of flashovers have been few and literature on the subject has been quite meager.

Some studies have been made in the past in connection with direct current generator behavior during short circuit.[1–4] Information is available on the load current, field current, and torque behavior under short-circuit conditions prior to flashover with the objective of understanding better how to protect the equipment with suitable high-speed circuit breakers to remove the excitation and the load fault fast enough so that flashover and ensuing damage will not occur. In a locomotive application, however, it does not prove economically sound to

---

Paper 53-83, recommended by the AIEE Land Transportation Committee and approved by the AIEE Committee on Technical Operations for presentation at the AIEE Winter General Meeting, New York, N. Y., January 19–23, 1953. Manuscript submitted October 20, 1952; made available for printing December 2, 1952.

O. C. Coho is with the General Electric Company, Erie, Pa.

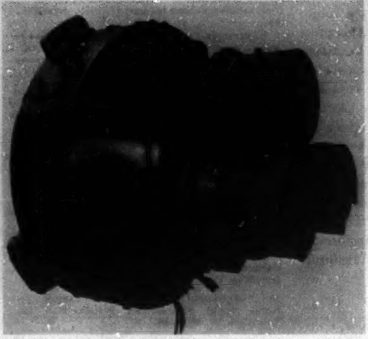

Figure 1 (left). Type of traction generator used in investigation

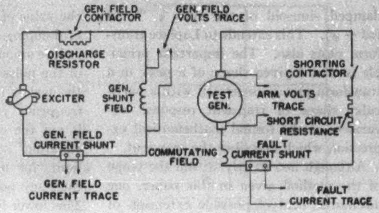

Figure 3 (right). Circuit diagram

provide each of four or more traction motors plus the generator with the necessary high-speed breaker equipment to handle fault currents, flowing in either direction with the rapidity necessary to reduce flashovers. In addition to the added cost, the frequency of the previously mentioned load surges is such that the circuit breakers would be tripping out unnecessarily on many transients so that the crew would be engaged in the resetting operation entirely too frequently. Finally, such a high-speed breaker application does not offer protection against another common cause of flashover, that produced by the accumulation of dirt, dust, oil, and moisture so often prevalent in locomotive operation. The necessary availability for service simply precludes any daily cleaning maintenance programs. Rather it has been the practice of the trade to design the equipment to handle these load surges and to expect adverse atmospheres with the expectation that occasional flashovers will happen. Under present practice, a flashover severe enough to arc to ground will initiate action to remove generator excitation by means of a ground relay. When the crew notices that a ground relay has been tripped, they reset and reload at once without maintenance to the equipment. If the equipment accepts load without tripping again, the locomotive unit continues in operation until the scheduled maintenance period, usually monthly. At that time, steps are taken to repair the accrued damage of flashovers, if necessary.

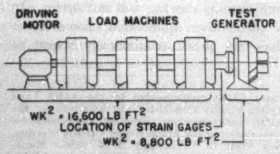

Figure 2. Test generator coupled to multiunit load machine

It is thus seen that the motors, generators, and control equipment must be built to withstand a relatively large degree of abuse. The motors and generators must be capable of accepting occasional flashing and the control equipment must be able quickly and reliably to remove excitation to minimize the damage.

The General Electric (GE) Company has been engaged in a study of the various flashover phenomena associated with their locomotive electric drives. These studies are being directed toward minimizing the flashover damage, reducing the tendency to flash over by improved motor and generator design and by higher speed control action, and evaluating the forces, torques, and stresses involved during such abnormal operation. This last subject has been studied least of all in the past. This paper is a summary of some of the accumulated data on flashover torques. This, of course, is of significant value in connection with coupling, crankshaft, bearing, and gear design.

Equipment

The machine used in this investigation was a GE model *GT-581* traction generator used on Alco-GE 1,600-horsepower locomotives. It is nominally rated at 1,000 rpm, 850/580 volts, 1,320/1,900 amperes continuous. It has ten poles and is of the noncompensated type, that is, pole face windings are not used. The outside dimensions are 59-inch diameter by 39 inches long over coupling and bearing. The armature is 43-inch diameter by $10^1/_4$-inch core length. The commutator has 405 segments and is 24 inches in diameter. The machine weighs 9,900 pounds. Figure 1 shows the generator assembled with the gear-driven auxiliaries.

The following data are presented in both conventional units and, for the purposes of comparison with other machines, on a per-unit (percentage) basis. The bases for the per-unit (p.u.) values are as follows:

1. Volts, maximum continuous rating = 850
2. Load current, maximum continuous rating = 1,900 amperes
3. Resistance, 850 volts/1,900 amperes = 0.447 ohm
4. Speed, maximum rated = 1,000 rpm
5. Torque, (7.04×850 volts×1,900 amperes)/1,000 rpm = 11,370 pound feet
6. Field current (full field) = 46 amperes
7. Excitation, 850 volts/1,000 rpm = 0.85 volts/rpm equivalent to 6,300 armature kilolines per pole

Method of Test

Since the generator is a single-bearing machine with the rotor partly supported by the diesel-engine crankshaft, the generator was most readily tested by coupling to a flange of an available multiunit load machine designed expressly for general testing of large traction generators. The physical arrangement is shown in Figure 2. The load machines were not energized during this series of tests since the test generator was short-circuited by external resistance. The tests were conducted by raising the speed to slightly above the desired test speed by means of the driving motor. The driving motor was then de-energized and the set allowed to coast. When the desired speed was reached the generator was short-circuited.

A circuit diagram of connections is shown in Figure 3. The machine was excited by its own amplidyne exciter

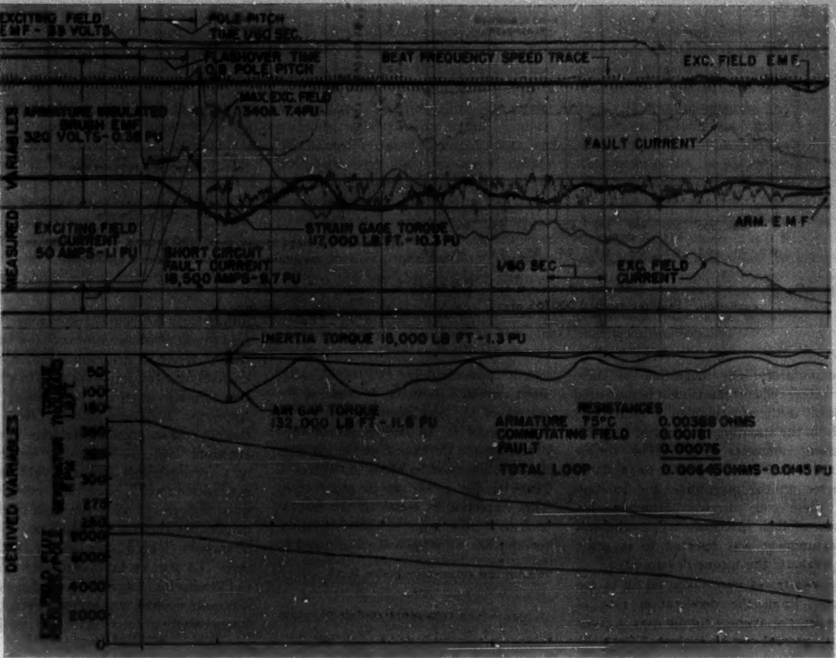

Figure 4. Record of short-circuit flashover. Speed 360 rpm. Full field excitation. Fault resistance 0.000765 ohm

on all except very low speed tests where the amplidyne was not capable of developing sufficient output because of the low speed. In such cases, excitation was furnished by a supplementary test exciter. As indicated on the diagram, oscillograph traces were taken of armature insulated brush voltage, fault current, and exciting field volts and current. Strain gauge records were also made on some later tests. These gauges were used as a measure of the shear strain on the surface of the shaft between the test generator and the first load machine. The gauges were actuylly arranged to indicate tensile strain at a 45-degree angle from which the shear stress and thence the shaft torque is readily derived. The gages were arranged on the shaft and so connected that weight strains were balanced out for any rotational orientation.

Speed was indicated by a magnetic pickup located adjacent to the small auxiliary equipment gear on the commutator end of the generator. The a-c output of this pickup was added to the output of an external a-c generator of constant frequency. By proper choice of this beat frequency, an output with a series of nodes is obtained. Analysis of this output reveals a simple relation between change of speed and the time between nodes. Thus small changes of speed between discrete time intervals can be readily obtained with fair accuracy. The rate of change of speed is of use in evaluating the inertia torque of the test generator and the average torque decelerating the entire setup.

Variation of Torque During Flashover

The history of a typical flashover is shown by Figure 4. The machine was flashed over at 360 rpm full excitation by a practically dead short circuit. The external resistance of the fault consisted only of the leads to the short-circuiting contactor. The fault resistance, 0.00076 ohm (0.0017 p.u.), is slightly more than one-tenth the machine resistance. Immediately after application of the fault, the armature voltage drops abruptly from 320 volts open circuit to 86 volts. This initial value to which the voltage falls is proportional to the ratio of the fault inductance, including commutating field inductance, to the total circuit inductance. The voltage will then eventually level off to a value proportional to the ratio of fault resistance to total resistance provided flashover does not occur. However, after the armature has rotated approximately 80 per cent of a pole pitch, both voltage and fault current change abruptly. Apparently, the flashover is consummated at this time, as the subsequent voltage and current traces are very irregular indicating presence of arcing. At this point of defined flashover, the fault current has reached 17,200 amperes (9.05 p.u.). From this time on, the generator armature current is composed of the fault current plus the many components in the various coils irregularly short-circuited by the arc around the

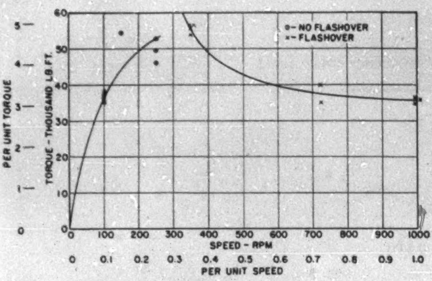

Figure 5. Average torque over 7/60 second versus speed. Full field excitation. Fault resistance 0.000765 ohm

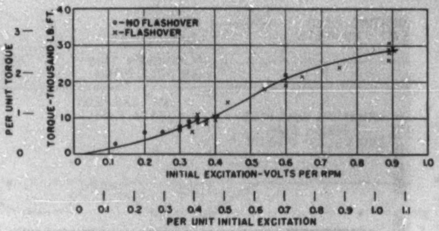

Figure 6. Average torque over 7/60 second versus excitation. Fault resistance 0.048 ohm. Speed 1,000 rpm

commutator. The magnitude of these armature coil currents cannot be measured readily as they are completely "locked up" within the armature exclusive of the fault current ammeter shunt. The torque during flashover depends to a large degree on the magnitude and location of these coil currents. However, because of their inaccessibility, mechanical measurement was resorted to in order to evaluate the torque developed.

Speed traces were taken on all of the tests. From the deceleration rate of the set, the average torque over a given time interval can be evaluated from the WK^2. Much of the testing was done in this manner. However, since the assembly of the test generator, load machines, and driving motor armatures on a common shaft is a lightly damped mass elastic system subject to torsional oscillation, the average torque can be evaluated accurately only over a long enough time interval to average out oscillatory speed variations in the generator. It was found that a time of 7 cycles (7/60 second), embracing 3 cycles of the major natural frequency, was sufficient to average out this oscillation effect and considerable testing was done on this basis.

It soon became evident however, that the average torque over a period of 7 cycles did not tell the complete story. Inspection of the fault current and exciting field current traces during the cycles immediately after flashover show these currents at a maximum value considerably higher than their average over 7 cycles. Thus, it is not inconceivable that the air-gap torque might be subject to wide variation with peaks significantly greater than average. Accordingly, shaft torque measurements by strain gauge were included on later tests of which Figure 4 is representative. A maximum value of 117,000 pound-feet or 10.3 p.u. is indicated approximately $1^1/_2$ cycles after short circuit. However, because of the inertia of the test generator itself, the shaft torque is not truly representative of the torque developed at the air gap. A correction must be added to the strain-gauge torque to obtain air-gap torque. This correction is equal to the instantaneous inertia torque of the test generator and has a foot-pound value equal to

$$\frac{WK^2 \text{ of test generator} - \text{pound feet}^2}{308} \times$$
$$\text{rpm per second deceleration}$$

The inertia torque, as approximately derived from deceleration data, is shown together with the air-gap torque as a derived variable in the lower part of Figure 4.

A most interesting observation in regard to the air-gap torque is its surprisingly wide variation. Although the derived inertia torque component is approximate, since it is computed for discrete time intervals, it is a small correction compared to the wide air-gap torque variation and any error therein cannot explain these wide swings in torque.

A clue to this phenomena is suggested by the behavior of the exciting field current. Since the field excitation is furnished by a low impedance exciter, the field circuit resistance is of such low value that it tends to maintain constant flux linkages over the periods of time in which the torque variations take place, see Appendix I. Consequently, any demagnetizing magnetomotive force due to armature currents is readily reflected by a corresponding opposing field magnetomotive force. Since the oscillogram trace indicates a wide variation in field magnetomotive force from an initial 50 amperes (1.1 p.u.) to a peak of 340 amperes (7.4 p.u. at 1.6 cycles) then down to 150 amperes (3.3 per unit at 3.3 cycles), it is quite evident that armature reaction magnetomotive force must be subject to similar wide variations.

A plausible hypothesis can be offered for this armature reaction variation. During the flashover, many of the armature coils are linking considerable exciting flux. However, when they become short-circuited by the arc, they are free to produce individual short-circuit currents which will tend to maintain constant flux linkages. As these coils proceed toward the poles of the opposite polarity, less coil current will be required to maintain these linkages. Finally, as they continue on toward the next pole of same polarity as that when they were short-circuited, conditions will again exist as at flashover and currents will

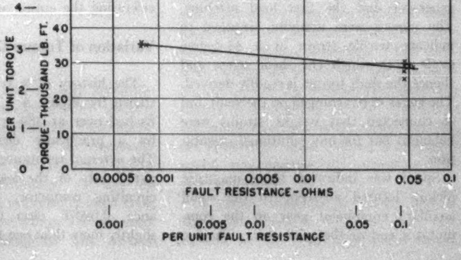

Figure 7. Average torque over 7/60 second versus fault resistance. Speed 1,000 rpm

again approach the initial conditions. Thus, a complete cycle is undergone over a distance of two pole pitches. If allowance is made for the speed reduction during the flashover, it is seen on Figure 4 that variations take place in both field current and external fault current of this approximate frequency. Although the flashover pictured by Figure 4 was removed before steady-state conditions were established, there is evidence that the wide current variations are attenuating rapidly. This is to be expected since the time constant of the armature coils, particularly when short-circuited by an arc, is quite small on the order of several cycles as compared with the relatively long time constant of the exciting field. Thus, the current variations and accompanying torque variations die out rapidly.

It is to be noticed that the maximum air-gap torque, 132,000 pound feet, is very close to twice the average torque, 65,000 pound feet, over a period of 7 cycles. An independent check of the latter figure is available by computing the torque required to decelerate the entire set over the same period of time. This value is

$$\frac{25{,}400}{308}\times\frac{360\text{ rpm}-278\text{ rpm}}{7/60\text{ second}}=58{,}000\text{ pound feet}$$

which checks fairly well with the preceding. Since much of the data presented in the following are based on average torque over 7/60 seconds, oscillograms at various speeds with available strain gauge measurements were checked and it was found that in all cases the ratio between maximum torque and average was very near 2 to 1 as in this case. Accordingly, the peak torques for this particular generator and test setup are very close to twice the average values indicated on the charts.

Variation of Torque with Speed

After the commutator is short-circuited by an arc, it becomes helpful to adopt a-c theory to explain certain aspects of the behavior, for the rotating armature is similar in some respects to a rotating squirrel-cage winding of an induction motor. It is true, of course, that the exciting flux is stationary in the d-c machine, whereas the flux of an induction motor is rotating at synchronous speed. However, since induction motor behavior is most simply described as a function of the slip or speed differential between exciting flux and rotor, then the actual speed or a short-circuited commutator of a d-c machine adopts a new significance, for it corresponds to the aforementioned slip.

It is well known that in an induction motor at very low slips, the torque is proportional to the slip. The rotor currents, which produce torque by reacting with the constant exciting flux, are in phase with the slip speed voltage generating them and limited only by rotor resistance. Because of the latter, these currents are also so located spacewise with respect to the exciting flux as to produce the maximum torque interaction. As the slip increases the currents rise in proportion thus producing a corresponding increase in torque. However, as the slip continues to rise, the reactance of the rotor becomes of such significance that although the rotor currents rise, they become gradually reoriented with respect to the exciting flux to the extent that the torque no longer increases directly proportional to slip. At a slip where the reactance equals the resistance of the rotor, the maximum torque is developed. Finally, at higher slips the torque falls off since the rotor currents, although extremely high, are so located with respect to the flux as to minimize the torque reaction.

If such reasoning is applied to a d-c machine with a short-circuited commutator, it would be expected that the flashover torques would be a maximum at relatively low speeds. This proved to be the case as illustrated by Figure 5. Data are presented for a series of full field flashovers produced by the 0.000765 ohm (0.0017 p.u.) fault. Flashover torques at 350 rpm are significantly greater than at higher speeds and the shape is somewhat suggestive of the familiar torque slip curve of an induction motor or an eddy-current clutch.

At speeds below 350 rpm, the machine commutated the fault current successfully and did not flash over. However, the torque data in this speed range indicate the short-circuit torque curve approximately blends into the flashover torque curve.

Variation of Torque with Excitation

Since the armature currents are generated by the exciting flux and the torque is proportional to the product of current and flux, it would be expected that the torque would vary as the square of the excitation for a given speed. However, it is readily realized that saturation and arc behavior also probably affect the phenomena materially. The results of a series of tests taken at rated speed 1,000 rpm with 0.048 ohm (0.107 p.u.) fault resistance are shown on Figure 6. The fault resistance is the maximum or marginal value which produces flashover. The torque is plotted versus initial excitation. It is quite apparent that, for the higher excitations, approaching saturation, the torque is decidedly less than that prorated by the square relationship. For instance, at one-half normal excitation, 0.4 volt per rpm, the flashover torque is approximately full-load torque, 1.0 p.u. By the square law, $(0.85)^2/(0.40)$ or 4.5 times normal would be expected at full excitation. However, the tests show only about 2.5 to three times normal, indicating these other effects to be of significant importance.

It is interesting to note that the tests below 0.4 p.u. full excitation did not produce flashover, yet the torque-excitation relation is essentially in line with the torques at higher excitations where flashover occurred.

Variation of Torque with Fault Resistance

Some of the flashovers in this testing program were initiated with a near dead short circuit to simulate the worst condition of rates of rise of current that might be expected from violent current surges in operation. Other tests were conducted with a much higher fault resistance of just sufficient value to induce flashover in order to minimize external loading and approximate conditions which might exist in case of a flashover caused by excessive dirt or other external contamination. Examination of the results of these tests, as charted by Figure 7, discloses that the torques are about 25 per cent greater for the dead short-circuit condition. The total loop circuit resistance, including generator and fault, is nearly ten times more for the marginal fault than for the near dead short circuit. This indicates that the arc current of the flashover is by far the dominant component of armature current, as might be expected.

Another interesting fact in regard to the arc current, not depicted on Figure 7, resulted from tests wherein the generator was slightly modified to provide an easier access to ground by reducing the distance between the brushholders and the armature bead ring. The resulting arc path is correspondingly reduced. Flashover torque measurements, with the flashover induced with the marginal resistance, were slightly increased approaching the values shown for the dead short-circuit fault. This indicates that the mechanical layout of the design has a minor but nevertheless definite effect.

Summary

The tests indicate that a maximum flashover air-gap torque of nearly 12 times normal can be expected at full excitation on direct short circuit at low operating speed. This somewhat confirms rough estimates, based on considerably simplified circuit assumptions, of between 10 and 15 times normal often quoted as a rule of thumb for noncompensated machines. Although the tests were all made on one particular design of d-c generator, it is felt that with due allowance for the number of poles, peripheral speed, armature resistance and permeance, core and gap dimensions, arc lengths and so forth, these results can be safely prorated to similar noncompensated machines.

The operating speed at which flashover occurs deserves primary consideration, and torques appear to be a maximum at the lowest speed at which flashovers can be initiated. As expected, the flashover torques increased with initial excitation, with saturation being of importance at high excitation levels. Finally, the initiating fault resistance has but a minor effect, with a dead short circuit resulting in slightly more torque than would a flashover resulting from marginal fault resistances.

Appendix I. Constant Exciting Field Linkages

This is illustrated by the lower graph of Figure 4, showing the exciting field flux per pole. The curve is derived from the field current and field voltage behavior by step-by-step integration in accordance with the following relation

$$\phi=\frac{V_{fo}}{NP}\left(\frac{V_f}{V_{fo}}-\frac{I_f}{I_{fo}}\right)t\times10^{-5}\text{ kilolines}$$

where

ϕ = incremental change in flux
N = turns per pole
P = number of poles
V_f = field voltage during time increment
V_{fo} = initial field voltage, volts
I_f = field current during time increment
I_o = initial field current
t = time increment, seconds

Notice that irregularities are minor and that the flux gradually decays with a long time constant until the field circuit contactor opens near the end of the trace after which the flux decays at a more rapid but still gradual rate.

References

1. Current and Torque of D-C Machines on Short Circuit, T. M. Linville. *AIEE Transactions*, volume 65, 1946, pages 956–65.

2. Protection of Large D-C Machines by Means of High-Speed Circuit Breakers, J. Elmer Housley, Otto Jensen. *AIEE Transactions (Electrical Engineering)*, volume 63, September 1944, pages 637–40.

3. D-C Machine Flashover and Bus Short-Circuit Protection, T. B. Montgomery, J. F. Sellers. *AIEE Transactions*, volume 60, 1941, pages 1168–73.

4. The Short-Circuit Characteristics of D-C Generators, G. E. Frost. *AIEE Transactions (Electrical Engineering)*, volume 65, June 1946, pages 394–402.

No Discussion

A New Control for Heavyweight Rapid-Transit Cars

I. W. LICHTENFELS
MEMBER AIEE

AN ADVANCE over the original combination of electric-operated cam controller with pneumatic circuit contactors, this new system utilizes two motor-operated controllers; one to establish main circuits, and the other to commutate resistance. Refinements, introduced as the result of operating experience with equipment of the previous type, give smoother operation and improved dynamic braking characteristics. Compactness and ease of maintenance have been achieved to a marked degree.

Development

Seven hundred and fifty car equipments of the previous type[1] have been operating for the past 3 years on the subway system of the New York Board of Transportation. Along with higher accelerating and braking rates for improved scheduled speeds, dynamic braking was incorporated into the propulsion control for the first time on a large scale. This form of braking has been successful in providing both smoothness of operation for rider approval and uniform characteristics for operator approval. Reduction in brake shoe and wheel wear has resulted in lower operating and maintenance costs and cleaner subways. General Electric pioneered the extensive use of all-electric motor-operated cam-type control for 375 of these equipments. A motor-operated controller in conjunction with electropneumatic contactors comprise the control system. The success of this first all-electric controller prompted further development of a complete cam-control system. This system has two motor-operated controllers. One changes resistance in a manner similar to the system previously described. The other establishes the main circuits and replaces the electropneumatic contactors which were formerly used for this purpose.

Components

The components of a car propulsion control are shown in Figures 1, 4, and 5. Except for the line circuit breakers, which are mounted separately for safety reasons, all apparatus is mounted in one group. The equipment comprises the following:

1. A motor-operated circuit controller which, by cam action, establishes main circuit for reversing, braking, coasting, series power, parallel power, and field shunting.
2. A motor-operated resistance controller which changes the main resistance values for smooth operation in series power, parallel power, coasting, and braking.
3. A control panel, comprising control devices which receive the train line signals originating at the motorman's master controller and translate them into local car circuit changes by operating the circuit and resistance controllers.
4. A regulating relay, the nerve center of the control system. This relay receives a signal of the amount of power or brake desired and allows the controllers to progress accordingly.
5. Two line circuit breakers, the protective devices which not only complete the normal power feed and dynamic braking circuit but also quickly open these circuits when trouble appears.
6. A main resistor assembly, comprising all the main resistors, and consisting of nine honeycomb units arranged for forced cooling and easy unit replacement.

The purpose of these control devices is to translate the wishes of the operator into train movement and to so do this that people will be rapidly and smoothly transported. Since 2,500 or more people are handled in a single train, the human element is of primary importance; and it has been so considered in the design of this system.

System Operation

The schematic diagram, Figure 2, together with the following description, will illustrate the operation of the system.

The motorman initiates train line signals at his operating position by manipulating brake or power levers. These signals are transmitted to all the cars of a train which may consist of 1 to 11 cars. The first power position, "switching," energizes train wires *1* or *2*, *GS*, and *6*. Train wire *1* energizes the main line circuit breaker *LB1*. Train wire *6* energizes *LB2*, and *GS* picks up *KC* relay to run the circuit controller to a power position, closing cam-operated switches *M1* and *SA*. The four traction motors are now in series with all resistance in the circuit. Note that the main resistance is in three groups: *R1-R6*, *R7-R12*, and *R13-R22*. This is a low tractive effort position used for coupling cars.

The second power position, "series," energizes train wire *4* to pick up *KR* relay, which advances the resistance controller *KMR* under control of the regulating relay.

The third power position, "parallel," initiates transition from series to parallel at end of series cycle. It then advances the control to cut out resistance with the motors in parallel. When all parallel resistance is out, the traction motor fields are shunted for increased train speed.

Shutting off the power de-energizes all power train wires and energizes wire *5*. This keeps the control in coasting which is same motor connection as braking but at a very low motor current. During coasting or braking, switches *LB2*, *P1*, *P2*, *B1*, and *B2* are closed, placing the main resistors across the motors which are not generating. Calling for brake de-energizes train wire *5*. The control then regulates for braking instead of coasting current. The complete sequence of operation of the main switches is shown in the table in Figure 2.

The amount of motor current and hence the "feel" of the car, is automatically controlled by the current regulating relay *CL*. This relay is the heart of the system. This relay has three main coils, making it responsive to accelerating current, braking current, and a rate signal. The combined effect of these coils causes the relay to drop out or pick up. When the relay picks up, its contacts stop the progression of the main controller by short-circuiting the pilot motor armature. When it drops out, the main controller advances to build up current until it is again arrested by the relay picking up. Actually, this process happens very rapidly so that it produces a regulating action. Since the same relay controls both circuit and resistance controllers, the *HO* or transfer relay is provided.

Paper 53-51, recommended by the AIEE Land Transportation Committee and approved by the AIEE Committee on Technical Operations for presentation at the AIEE Winter General Meeting, New York, N. Y., January 19–23, 1953. Manuscript submitted October 20, 1952; made available for printing November 19, 1952.

I. W. LICHTENFELS is with the Locomotive and Car Equipment Department, General Electric Company, Erie, Pa.

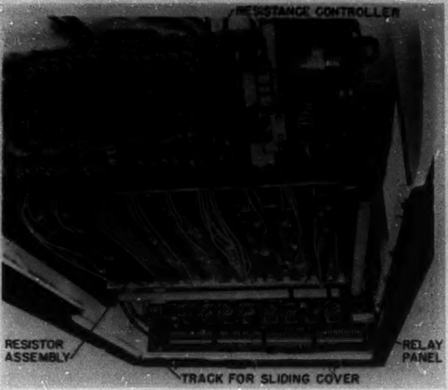

Figure 1. View of control package from under side, with sliding cover removed

Smooth Operation

The jerks and jolts ordinarily associated with high accelerating and braking rates have been eliminated to provide a fast but smooth operating car. This has been accomplished by the following design improvements:

1. More accelerating and braking steps Twenty accelerating and 22 braking positions provide small increments of tractive and braking effort. This is made possible by using the same contact units in both motoring and braking.
2. The use of a new technique in resistor proportioning based on energy change rather than current change per notch.
3. Uniform change in rate, which is accomplished by a combination of controller driving motor speed and cam development rather than by air line restrictions and time delay relays as on previous equipments.

Skip-Bridge Transition

The basically sound bridge, or closed-circuit, series-to-parallel transition as used in this new control system has been further improved until this operation is just another accelerating step. Two major improvements have been applied:

1. Skip feature. Referring to the notching curve, Figure 3, it will be seen that some change in transition between low and high rates is desirable. In systems previously tried this was provided by a floating feature which merely omitted the end of the series and the start of the parallel steps. Besides being complicated, this system did not use all the series steps at high rate, hence some power savings of series operation were lost. The new skip system uses all available series steps merely omitting the first parallel step or steps to provide the ultimate in smoothness of operation.
2. Cam-operated switching. The use of cam-operated switches allows a rapid change in circuits without timing troubles arising as was the case in the unit-switch systems.

Dynamic Brake Reliability

Dynamic brake reliability has been greatly increased by a simple change in control. The previous system required that two low-voltage (38 volt) control train line circuits be energized to secure dynamic braking. The new system does not require any train wires to be energized. At a speed where dynamic brake is effective (about 10 mils per hour) a coasting circuit is established by merely releasing power. De-energizing train wires causes dynamic braking to build up.

A bad-order relay *BO* protects the motors and control on a disabled car in a train and also gives a visual indication of the bad-order car. When the operator calls for power, the bad-order relay is closed by voltage appearing at the main motor circuit. This energizes *BO* coil in the *A2* motor circuit. If no motor voltage appears, the relay stays out, the control does not progress beyond switching, and the dynamic brake motor circuit stays open. Thus an electrically disabled car in a train become a trail car. Of course, as a single car it would not even start.

Traction Motor Protection

Prevention of motor damage is always a primary consideration. It becomes even more desirable when dynamic braking is the principal braking system. In this case motor protection has been designed into the control system itself rather than obtained by adding protective devices which complicate the system.

The main line circuit breakers, *LB1* and *LB2*, are of the direct-acting magnetic type for fast opening on overload. The term, direct-acting means that the fault current is made to assist in opening the circuit by having the overload strike the contactor armature. Previous devices provided for an overload to operate a set of contacts to de-energize a magnet valve, which in turn drops out the line contactor. The direct-acting type clears a fault in approximately half the time, thus greatly reducing motor damage. Full fault protection is provided both in motoring and dynamic braking.

Grounding protection, similar to that obtained with differential relays, is provided by proper location of the bad-order relay pick-up circuit. In this way the bad-order relay is made to serve the dual purpose of preventing control progression with a ground fault, and indicating a bad-order car.

Traction Motor Field Forcing

Dynamic brake control at high train speed is achieved by means of field control of the traction motors. This system enables dynamic braking to be used at high speeds without developing excessive motor voltage. A serious control problem, however, is that of attaining fast brake response without roughness resulting from brake overshoot. This problem, arising from the inherent slow response of the traction motors to a change in field shunting, has been overcome by a simple field-forcing scheme. Referring to the cam development of the circuit controller, Figure 2, it is seen that the controller progresses during coasting or braking from position *8* to *2*. At the same time, field shunting main fingers *S1* to *S6* inclusive operate to change the amount of shunting. Field forcing is obtained by momentarily subjecting the motor to a pulse of full field between notches. For example, in going from *6* to *5*, finger *S2* opens before *S1* closes. In the time between the opening of *S2* and closing of *S1*, motors *1* and *2* get a pulse of full field to accelerate their response. By this simple means, which requires no extra parts, a fast and positive braking response is obtained even in the shunted field range of the control.

Blown Resistors

Forced ventilation greatly reduces the size of the main resistors required for dissipation of accelerating and braking

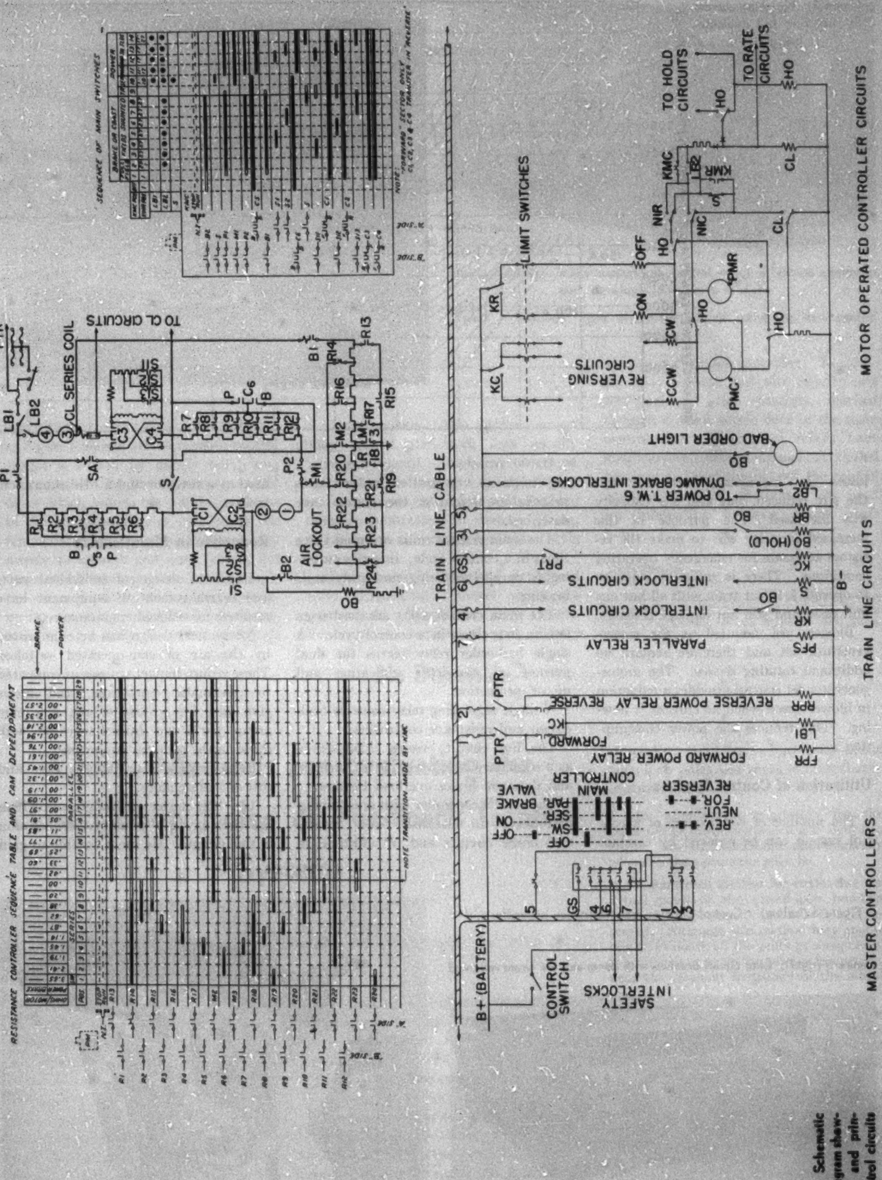
RESISTANCE CONTROLLER SEQUENCE TABLE AND CAM DEVELOPMENT
SERIES
PARALLEL
NOTE TRANSITION MADE BY KMC
SEQUENCE OF MAIN SWITCHES
BRAKE OR COAST
POWER
NOTE "FORWARD" SECTOR ONLY CL, C2, C3 & C4 TRANSFER IN "REVERSE"
PTR
LB1
LB2
P1
SA
CL SERIES COIL
TO CL CIRCUITS
C3
C4
C1
C2
R1
R2
R3
R4
R5
R6
R7
R8
R9
R10
R11
R12
R13
R14
R15
R16
R17
R18
R19
R20
R21
R22
R23
R24
M1
M2
P2
B1
B2
BO
AIR LOCKOUT
S1
TRAIN LINE CABLE
LIMIT SWITCHES
KR
KC
REVERSING CIRCUITS
BAD ORDER LIGHT
DYNAMIC BRAKE INTERLOCKS
TO POWER T.W. 6
BO (HOLD)
INTERLOCK CIRCUITS
PARALLEL RELAY
REVERSE POWER RELAY
FORWARD POWER RELAY
REVERSE
FORWARD
FPR
RPR
PFS
PRT
B+ (BATTERY)
B−
CONTROL SWITCH
SAFETY INTERLOCKS
REVERSER
FOR.
NEUT.
REV.
MAIN CONTROLLER
OFF
SW.
SER.
PAR.
BRAKE VALVE
ON
MASTER CONTROLLERS
TRAIN LINE CIRCUITS
MOTOR OPERATED CONTROLLER CIRCUITS
TO HOLD CIRCUITS
TO RATE CIRCUITS
HO
KMC
KMR
NIR
NIC
CL
PMR
PMC
CW
CCW

Figure 2. Schematic wiring diagram showing main and principal control circuits

Figure 3. Notching curves for motoring and dynamic braking

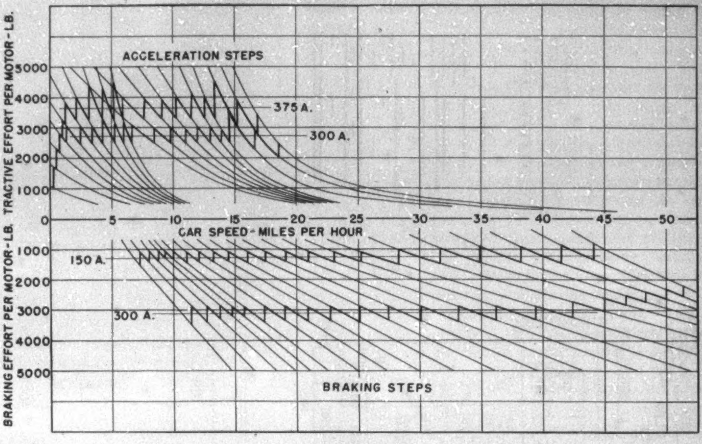

losses. In this instance not only was the size reduced, but also the capacity was increased. The purpose of this increased capacity was to make the resistors adequate for emergency operating conditions. There is sufficient capacity to operate a 10-car train with all but one unit dead and still not damage resistors.

Blowers are mounted on the motor-generator set and therefore require no additional rotating device. The motor-generator set control provides a reduction in blower speed when no current is flowing. This reduces the power consumption.

Utilization of Control Devices

The number of components of a control system can be reduced by combining functions. Several examples of this practice are found in the system here described.

The main resistor units are used three times in a control cycle; in series motoring, in parallel motoring, and in dynamic braking.

The main contact units are used from two to four times in a control cycle. A single bad-order relay serves the dual purpose of bad-order indication and motor protection.

A single regulating relay controls both circuit and resistance controllers.

The line circuit breaker *LB2* serves as a secondary line power circuit breaker and dynamic brake overload breaker.

The circuit controller with one driving unit serves to establish power, coast, and brake circuits and in addition, is used as a reverser and a field-shunt controller.

Reduction in Maintenance

Improved design of individual parts and rearrangement of equipment have resulted in reduced maintenance.

Mechanical design has been improved by the use of cam-operated switches. These reduce impact stresses as compared to pneumatic contactors, and hence give long life. Most of the new cam group parts are interchangeable with those on the previous equipment.

Better accessibility reduces time and cost of maintenance.

The long-neglected maintenance man has been given a primary consideration in this design. He must be able to gain

Figure 4 (below). Control package from resistance controller end

Figure 5 (right). Line circuit breaker, with cover and arc chute removed

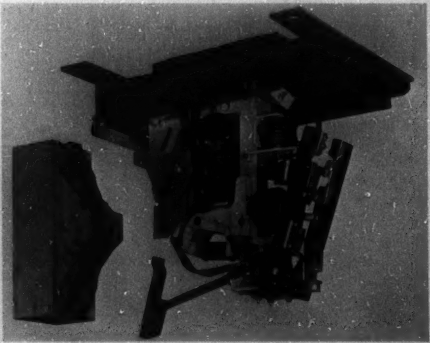

RESISTANCE CONTROLLER
RESISTOR ASSEMBLY

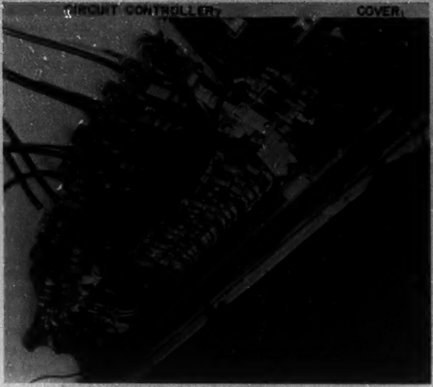

Figure 6 (left). View underneath control group at circuit controller end, showing sliding cover in place

Figure 7 (above). Type of rapid-transit car using this new control system

ready access to apparatus. For instance, as Figure 6 shows, access to main control groups is gained by merely unlatching two covers. The first is a wrap-around cover which swings back allowing access to the circuit controller. To reach the remainder of the apparatus it is necessary merely to unlatch and push back a flat cover which runs on rollers. This simple procedure contrasts with older arrangements requiring unlatching, removing, and finding a place to stack a multitude of loose covers. Also, these covers lying around the work area usually become a hazard. Replacing covers on the new control requires merely moving the two covers into place and latching them as contrasted to finding, lifting, replacing, and latching the older style covers.

Maintenance is facilitated in several ways. Expendable control parts are prominently placed for easy access. For instance, contactor tips are directly in front of the main controller. Regulating relay settings and rate adjustments are made by dial rheostats, reached through a small access door in the main control box. All control relays have identical mechanical components. Sealed bearings are used throughout the control equipment. This eliminates all need for lubricating between major overhauls.

Reference

1. A New Lightweight Rapid Transit Control Equipment, I. W. Lichtenfels, H. G. Moore. *AIEE Transactions*, volume 70, part I, 1951, pages 224–26.

No Discussion

Quick Methods for Evaluating the Closed-Loop Poles of Feedback Control Systems

GEORGE BIERNSON
ASSOCIATE MEMBER AIEE

AN EVALUATION of the closed-loop poles of a feedback control system is almost necessary if one desires an accurate knowledge of its time response. If these poles are known, the response of the system to any kind of input can be determined fairly simply. However, evaluation of the closed-loop poles has long been a stumbling block in feedback control design, because it often requires finding the roots of a polynomial of high order. In 1947 Evans[1] presented the root-locus method which facilitates this evaluation, but yet is still quite cumbersome. In 1951 Kusters and Moore[2] simplified Evans' approach by utilizing generalized frequency-response plots. This paper extends this method of Kusters and Moore, and supplements it with a method for estimating by inspection approximate values of the closed-loop poles from the open-loop transfer function, and a numerical method for evaluating the closed-loop poles exactly.

Thus, this paper presents three approaches to the problem of finding the closed-loop poles from a knowledge of the open-loop poles and zeros of a feedback-control system.

1. An approximate expression for the poles will be developed which is designed to enable one to understand approximately where on the s-plane the poles lie.

2. A numerical method for evaluating the actual poles of the closed-loop function from the approximate poles will be presented. Although this method may enable one to evaluate all the poles in some cases, it is difficult to apply for poles at frequencies near the resonant frequency of the closed loop.

3. Finally, a graphical method will be developed which will present a simple means of plotting the function along various radial axes throughout the s-plane. Al-

---

Paper 53-42, recommended by the AIEE Feedback Control Systems Committee and approved by the AIEE Committee on Technical Operations for presentation at the AIEE Winter General Meeting, New York, N. Y., January 19–23, 1953. Manuscript submitted April 7, 1952; made available for printing November 19, 1952.

George Biernson is with the Massachusetts Institute of Technology, Cambridge, Mass.

This work was sponsored by the United States Air Force under contract number *W-33-038ac-13969*.

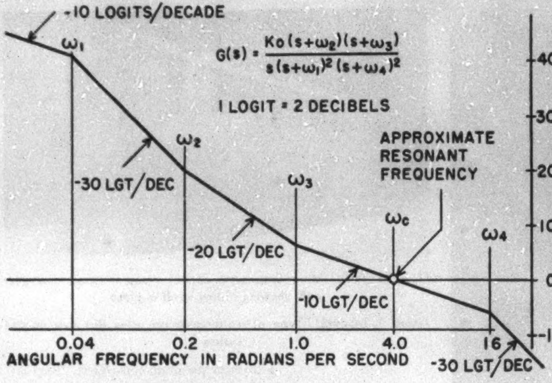

(a) ASYMPTOTIC MAGNITUDE PLOT

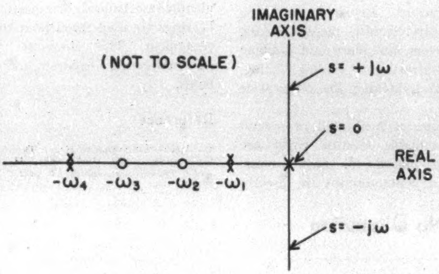

(b) S-PLANE PLOT OF OPEN-LOOP POLES AND ZEROS

Figure 1. Graphical representations of function of equation 20

A. Asymptotic magnitude plot
B. S-plane plot of open-loop poles and zeros

though this method is sufficiently general to enable one to evaluate all of the closed-loop poles, it is not so convenient as the numerical method for evaluating poles distant from the resonant frequency. This graphical method is an extension of the method presented by Kusters and Moore.

Thus, when applying this procedure to evaluate the closed-loop poles of a system, one would:

1. Determine an approximate expression for the closed-loop poles.
2. Then determine exact expressions for the poles distant from the resonant frequency, by the numerical method.
3. Finally, determine the poles near the resonant frequency by the graphical method.

The term resonant frequency has been used only to designate a general area of frequencies. Consequently, it may be replaced by the more convenient term crossover frequency (denoted as ω_c), which is defined as the frequency at which the magnitude asymptote of the open-loop function is equal to unity. If the closed-loop magnitude peak is near to $M_p=1.3$, the crossover frequency ω_c will be fairly close to the resonant frequency.

The transfer functions of the control system that are to be studied in this paper are expressed in general form in equations 1, 2, and 3. The symbols used are the new symbols proposed by the AIEE Feedback Control Systems Committee.[3] The open-loop transfer function designated as $G(s)$ is defined as the ratio of the transform of the controlled variable C, often termed output θ_o, to the transform of the actuating signal E, often termed error signal ϵ. This transfer function, which is often termed $KG(s)$, is equal to

$$\frac{C}{E}=G(s)=\frac{KA(s)}{B(s)} \tag{1}$$

where $A(s)$ and $B(s)$ are polynomials in s. A root of $A(s)$ is defined as a zero of C/E because at that value of s, $A(s)$, and hence C/E, becomes zero. A root of $B(s)$ is defined as a pole of C/E because at that value of s, C/E becomes infinite.

There are two closed-loop functions that will be considered: the ratio of the transform of the controlled variable C (output θ_o) to the transform of the reference input R (input θ_i); and the ratio of the transform of the actuating signal E (error ϵ) to the transform of the input R (input θ_i)

$$\frac{C}{R}=\frac{G(s)}{1+G(s)}=\frac{KA(s)}{KA(s)+B(s)} \tag{2}$$

$$\frac{E}{R}=\frac{1}{1+G(s)}=\frac{B(s)}{KA(s)+B(s)} \tag{3}$$

These relations can be derived easily from the relation

$$E=R-C \tag{4}$$

It is the purpose of this paper to evaluate from the roots of $A(s)$ and $B(s)$ (which are usually known) the roots of $[KA(s)+B(s)]$, which are the poles of the closed-loop functions.

The variable s, which has been mentioned, is the Laplace transform complex variable.[4] Sometimes it is replaced by the symbol p or λ. In a naive sense it may be considered to denote the operation d/dt.

The new term logit (abbreviated lgt.) recently defined[5] shall be used in place of the decibel. The value of an amplitude ratio A expressed in logits is

$$\text{lgt } A = 10 \log_{10} A$$

Hence the logit is related to the decibel by the relation

2 decibels = 1 logit

Since the decibel is basically a power-ratio unit, the author agrees with the Institute of Radio Engineers Standards Committee that it is not an adequate signal-ratio unit for feedback control use.

Approximate Values of Poles

ANALYSIS

A method for obtaining the approximate values of the closed-loop poles will now be presented. This method is intentionally nonrigorous because its purpose is one of orientation: to show the reader approximately where on the s-plane the closed-loop poles lie, so that he may know where to direct his attention when evaluating them. The approximate values of the poles will be quite close to the exact values of the poles for poles distant in magnitude from the crossover frequency—that is, for poles of magnitude much greater than, or much less than, the crossover frequency ω_c. For poles near the crossover frequency in magnitude, the approximate values are quite inaccurate; but they are still important because they indicate the number of poles that lie in this region.

In Figure 1(A) is an asymptotic plot of the magnitude (in logits) versus the frequency ω (on a log scale) for a typical open-loop function $G(j\omega)$, which will be used as an illustration. Note that at the crossover frequency ω_c, the asymptote slope is -10 logits per decade (-20 decibels per decade). In general ω_c must occur either in the region of -10 logits per decade asymptote slope, or quite close to that region. If it does not, the phase lag will generally be so great that the system will be unstable.

Figure 1(A) shows that for frequencies near ω_c the magnitude of $G(s)$ is approximately unity

$$|G(s)| \approx 1, \text{ for } s = j\omega \approx j\omega_c \qquad (5)$$

while for low frequencies it is quite large

$$|G(s)| \gg 1, \text{ for } s = j\omega \ll j\omega_c \qquad (6)$$

and for high frequencies it is quite small

$$|G(s)| \ll 1, \text{ for } s = j\omega \gg j\omega_c \qquad (7)$$

It will be shown later that the magnitude of a function $G(s)$ is approximately the same for all values of s equidistant from the origin of the s-plane, except for values of s near a pole or zero of $G(s)$. Hence

$$|G(s)| \approx |G(j\omega)|, \text{ for } |s| = \omega \qquad (8)$$
$$\text{except near poles and zeros of } G(s)$$

By means of equation 8, equations 5, 6, and 7 may be generalized to the form

$$|G(s)| \approx 1, \text{ for } |s| \approx \omega_c \qquad (9)$$
$$\text{except near poles and zeros of } G(s)$$

$$|G(s)| \gg 1, \text{ for } |s| \ll \omega_c \qquad (10)$$
$$\text{except near zeros of } G(s)$$

$$|G(s)| \ll 1, \text{ for } |s| \gg \omega_c \qquad (11)$$
$$\text{except near poles of } G(s)$$

Equation 10 holds for values of s near a pole of $G(s)$, because $|G(s)|$ is very large in that region due to the pole; while equation 11 holds for values of s near a zero of $G(s)$, because $|G(s)|$ is very small in that region due to the zero.

Near a zero of $G(s)$, equation 10 still holds if the factor containing that zero is divided out from $G(s)$. Thus, near an nth-order zero of G, at $s = s_a$

$$\left|\frac{G}{\left(\frac{s}{s_a}-1\right)^n}\right| \gg 1, \text{ for } |s| \ll \omega_c \text{ and } s \approx s_a \qquad (12)$$

Similarly, equation 11 holds near a pole of $G(s)$ if the factor containing that pole is multiplied out. Thus, near an nth-order pole at $s = s_b$

$$\left|\left(\frac{s}{s_b}-1\right)^n G\right| \ll 1, \text{ for } |s| \gg \omega_c \text{ and } s \approx s_b \qquad (13)$$

Note that s_a, being a zero of G, is a root of $A(s)$; while s_b, being a pole of $G(s)$, is a root of $B(s)$.

Equations 9, 10, and 11 indicate that the complex-frequency plane may be divided into three regions

$|s| \approx \omega_c$

$|s| \ll \omega_c$

$|s| \gg \omega_c$

For low complex frequencies, $|s| \ll \omega_c$, equation 10 shows that the expression for E/R, given in equation 3 becomes approximately

$$\frac{E}{R} = \frac{1}{G+1} \approx \frac{1}{G} = \frac{B(s)}{KA(s)} \qquad (14)$$
$$\text{except near the zeros of } G(s)$$

because $|G| \gg 1$, except near the zeros of G. Thus for $|s| \ll \omega_c$, E/R closely approximates $1/G$ except for small regions around the zeros of G. Consequently, at low complex frequencies, E/R and $1/G$ have approximately the same poles and zeros, the zeros of G being approximately equal to the poles of E/R. The large difference between E/R and $1/G$ near the zeros of G (poles of $1/G$) merely indicates that the poles of E/R are shifted slightly from the poles of $1/G$.

For high complex frequencies, $|s| \gg \omega_c$, equation 11 shows that the expression for C/R, given in equation 2, becomes approximately

$$\frac{C}{R} = \frac{G}{G+1} = \frac{1}{(1/G)+1} \approx G = \frac{KA(s)}{B(s)} \qquad (15)$$
$$\text{except near the poles of } G(s)$$

because $|1/G| \gg 1$, except near the poles of G. Thus, for $|s| \gg \omega_c$, C/R closely approximates G except for small regions around the poles of G. Consequently, C/R and G have approximately the same zeros and poles at high complex frequencies.

For frequencies near $s = j\omega_c$, the magnitude of $G(s)$ may be approximated by

$$|G(s)| \approx \left|\frac{\omega_c}{s}\right|, \text{ for } s \approx j\omega_c \qquad (16)$$

since the magnitude slope is approximately -10 logit per decade and the magnitude is approximately unity at the crossover frequency. If, in Figure 1(A), the break frequency ω_4 were increased and the break frequency ω_3 were decreased, causing the -10 logit-per-decade asymptote to widen about ω_c, the phase of $G(s)$ would approach -90 degrees at the crossover frequency $s = j\omega_c$. The complete function $G(s)$ then would be approximated in the region near the crossover frequency by

$$G(s) \approx \frac{\omega_c}{s}, \text{ for } s \approx j\omega_c \qquad (17)$$

If this region of -10 logit per decade is sufficiently wide about the frequency ω_c, equation 17 can be shown to hold for all values of s a distance ω_c from the origin

$$G(s) \approx \frac{\omega_c}{s}, \text{ for } |s| \approx \omega_c \qquad (18)$$

Equations 2 and 3 show that the closed-loop functions have poles when $G(s) = -1$. Substitution of this value of $G(s)$ into equation 18 yields the approximate closed-loop pole

$$s \approx -\omega_c \qquad (19)$$

This approximation is quite good if the -10 logit-per-decade asymptote is quite wide about ω_c. As the width of this section decreases, the pole becomes shifted from the value of equation 19 by an increasing amount. The amount of this shift will be discussed in detail later.

Both closed-loop functions must have the same poles, these poles being the roots of the denominator expression of equations 2 and 3, $[KA(s) + B(s)]$. Equation 14 shows that the "low-frequency" zeros of $A(s)$ must be approximately equal to the low-frequency poles of E/R, and hence they must be approximately equal to the low-frequency roots of this denominator expression. Similarly, equation 15 shows that the "high-frequency" zeros of $B(s)$ must be approximately equal to the high-frequency roots of the denominator expression. Equation 19 shows that the denominator expression must also contain a root approximately equal to $-\omega_c$. Thus the approximate roots of the denominator expression $[KA(s) + B(s)]$ are:

1. The zeros of $A(s)$ of magnitude less than ω_c (low-frequency zeros).
2. The zeros of $B(s)$ of magnitude greater than ω_c (high-frequency zeros).
3. The root $-\omega_c$.

(Note that the magnitute of a pole or zero means $|s|$—that is the magnitude of s—at the pole or zero; to state that a pole is near a frequency ω_2 in magnitude means that $|s|$ at the pole is approximately equal to ω_2. The term magnitude in this sense does not refer to the magnitude of a function of s, such as $|G(s)|$.)

EXAMPLE OF FIGURE 1

As an example, the approximate closed-loop poles of the example of Figure 1(A) will be evaluated. The open-loop function is

$$\frac{C}{E}=G=\frac{K_0(s+\omega_2)(s+\omega_3)}{s(s+\omega_1)^2(s+\omega_4)^2} \tag{20}$$

where

$$\omega_1=0.04$$
$$\omega_2=0.2$$
$$\omega_3=1$$
$$\omega_4=16 \tag{21}$$

A plot of the open-loop poles and zeros of equation 20, on the s-plane, is shown in Figure 1(B). Each zero is represented by ○ and each pole by +. As is shown, equation 20 has a single-order zero at $(s=-\omega_2)$ and $(s=-\omega_3)$, a single-order pole at $(s=0)$, and double-order poles at $(s=-\omega_1)$ and $(s=-\omega_4)$.

Near the crossover frequency, ω_c, the magnitude asymptote of equation 20 is equal to

$$\text{Asymp}|G=\left|\frac{K_0}{s\omega_4^2}\right| \tag{22}$$

If the asymptote is unity at the crossover frequency $(s=j\omega_c)$, and ω_c is equal to 4, K_0 is equal to

$$K_0=\omega_c\omega_4^2=4\omega_4^2 \tag{23}$$

Note that ω_c is the geometric mean between ω_3 and ω_4, and hence is equidistant between them on a logarithmic scale. As a rough approximation, such a gain setting yields the lowest resonance peak of the closed-loop function C/R, for a great many systems.

Substitution of equation 23 into equation 20 yields as the denominator expression for the closed-loop functions

$$[KA(s)+B(s)]=\omega_c\omega_4^2(s+\omega_2)(s+\omega_3)+s(s+\omega_1)^2(s+\omega_4)^2 \tag{24}$$

Since ω_2, $\omega_3<\omega_c$ and $\omega_4>\omega_c$, the method developed in the previous section entitled "Analysis" yields for the approximate factors of this expression

$$\underbrace{(s+\omega_2)(s+\omega_3)}_{\substack{\text{zeros of } A(s)\\ \text{below } \omega_c}}(s+\omega_c)\underbrace{(s+\omega_4)^2}_{\substack{\text{zeros of } B(s)\\ \text{above } \omega_c}} \tag{25}$$

That the number of approximate roots has to be equal to the number of roots obtained from factoring the denominator factor exactly, can be proved by the following reasoning. In order that the open-loop function go to zero at infinite frequency, the order of the polynomial $B(s)$ must be greater than that of the polynomial $A(s)$. Consequently, the order of the denominator expression must be equal to the order of $B(s)$. This is illustrated in equation 24. Hence the number of exact zeros of the denominator expression must be equal to the number of zeros of $B(s)$. Equation 25 shows that the number of approximate roots is equal to

(1) the number of zeros of $B(s)$ above ω_c (that is, greater than ω_c in magnitude),

(2) plus the number of zeros of $A(s)$ below ω_c (less than ω_c in magnitude),

(3) plus one.

Hence it must be equal to the number of zeros of B(s), because for frequencies below ω_c, $A(s)$ must have one less zero than $B(s)$ in order that the function approximate the expression of equation 17 near the resonant frequency.

Substitution of equation 25 into the closed-loop transfer functions, equations 2 and 3, yields the following approximate expressions

$$\frac{C}{R}\approx\frac{\omega_c\omega_4^2}{(s+\omega_c)(s+\omega_4)^2}=\frac{K_0}{(s+\omega_c)}\frac{(\text{zeros of } A(s) \text{ above } \omega_c)}{(\text{zeros of } B(s) \text{ above } \omega_c)} \tag{26}$$

$$\frac{E}{R}\approx\frac{s(s+\omega_1)^2}{(s+\omega_c)(s+\omega_2)(s+\omega_3)}=\frac{(\text{zeros of } B(s) \text{ below } \omega_c)}{(s+\omega_c)(\text{zeros of } A(s) \text{ below } \omega_c)} \tag{27}$$

SHIFTING OF POLES

An exact evaluation of the zeros of the denominator of the closed-loop functions shows that each zero of the approximate expression has become shifted, either positively or negatively, or has combined with another zero to form a conjugate-complex pair. The denominator expression given in equation 24 for the example of Figure 1 will be shown later to have the factors

$$(s+0.198)(s+1.51)(s^2+8.7s+30)(s+22.6) \tag{28}$$

Compare this with the numerical evaluation of the approximate factors given in equation 25.

$$(s+0.2)(s+1)(s+4)(s+16)^2 \tag{29}$$

The approximate zero at $-\omega_2=-0.2$ is shifted to -0.198 in the exact expression of equation 28; the approximate zero at $-\omega_3=-1$ is shifted to -1.51. One of the zeros at $-\omega_4=-16$ is shifted to -22.6; while the other is shifted toward the zero at $-\omega_c=-4$, combining with it to form the underdamped quadratic $(s^2+2\zeta\omega_n s+\omega_n^2)$ with $\omega_n=\sqrt{30}=5.5$ and damping ratio $\zeta=8.7/2\ \omega_n=0.79$. Numerical and graphical methods for evaluating the amount of shift will be presented in the two following sections entitled "Numerical Method" and "Graphical Method of Evaluating Poles."

Numerical Method

ANALYSIS

The exact value of a closed-loop pole can often be found by a numerical reiteration process which employs as its starting value the approximate value of the pole obtained by the method given in the preceding section. This reiteration process converges very rapidly for poles quite distant in magnitude from the crossover frequency, but it does not converge for poles very close in magnitude to the crossover frequency. This process will now be described.

Equations 2 and 3 show that the closed-loop functions have poles when $(1+G)=0$, or

$$1=-(1/G),\ 1=-G \tag{30}$$

Multiply both sides of these equations by equal factors

$$\left.\begin{aligned}\left(\frac{s}{s_a}-1\right)^n&=-\left(\frac{s}{s_a}-1\right)^n\left(\frac{1}{G}\right) && (31)\\ \left(\frac{s}{s_b}-1\right)^n&=-\left(\frac{s}{s_b}-1\right)^n G && (32)\end{aligned}\right\}\ \text{at poles of closed loop}$$

By equation 12 it is seen that for low values of $|s|$ (low complex frequencies), the magnitude of the right-hand expression of equation 31 is much less than unity near an nth-order zero of G at s_a

$$\left|\left(\frac{s}{s_a}-1\right)^n\left(\frac{1}{G}\right)\right|\ll 1, \text{ for } |s|\ll\omega_c,\ s\approx s_a \tag{12A}$$

By equation 13 it is seen that for high complex frequencies the magnitude of the right-hand expression of equation 32 is much less than unity near an nth-order pole of G at s_b

$$\left|\left(\frac{s}{s_b}-1\right)^n G\right|\ll 1, \text{ for } |s|\gg\omega_c,\ s\approx s_b \tag{13}$$

Since the right-hand expressions of equations 31 and 32 are almost zero near the corresponding G-function zero or pole, the equations may be approximated by

$$\left(\frac{s}{s_a}-1\right)^n\approx 0 \tag{33}$$

$$\left(\frac{s}{s_b}-1\right)^n\approx 0 \tag{34}$$

These approximate expressions yield

for poles of the closed-loop function the low-frequency zeros of $A(s)$ and the high-frequency zeros of $B(s)$. That these are the approximate poles has also been demonstrated in the preceding section. The approximations of equations 33 and 34 becomes increasingly exact as $|s_a|$ becomes much less than ω_c and as $|s_b|$ becomes much greater than ω_c. However, even when $|s_a|$ and $|s_b|$ are close to ω_c, the right-hand expressions of equations 31 and 32 are approximately constant for values of s close to s_a and s_b respectively, while the left-hand expression varies greatly. Hence equations 31 and 32 can be approximated quite closely by

$$\left.\begin{aligned}(s-s_a)^n &\approx -[(s-s_a)^n/G]s=s_a \quad (35)\\ (s-s_b)^n &\approx -[(s-s_b)^nG]s=s_b \quad (36)\end{aligned}\right\}\text{at poles of closed loop}$$

for values of s close to the corresponding zero of $A(s)$ or $B(s)$. Solving these equations for s will yield a closer approximation to the poles of the closed-loop functions. If the right-hand expressions of equations 35 and 36 are then evaluated at these new values of s, the equations can be re-evaluated and a still closer approximation of the poles obtained. Unless the value $|s_a|$ or $|s_b|$ is close to the crossover frequency, this process will generally converge quite rapidly, and may be employed even with complex roots.

It is more convenient to evaluate the deviation of the closed-loop pole from the corresponding zero of $A(s)$ or $B(s)$, rather the value of the pole itself. If we define these deviations as δ_a and δ_b, we have as the values of the exact closed-loop poles

$$s=s_a+\delta_a$$

$$s=s_b+\delta_b \qquad (37)$$

Note that for real open-loop poles and zeros the values s_a and s_b are negative real numbers, and hence $(-s_a)$ and $(-s_b)$ are positive. Express equations 35 and 36 in terms of δ

$$(\delta_a)^n \approx -[(s-s_a)^n/G]_{s=s_a}, \quad \text{for } |s_a|<\omega_c, \text{ and } s\approx s_a \qquad (38)$$

$$(\delta_b)^n \approx -[(s-s_b)^nG]_{s=s_b}, \quad \text{for } |s_b|>\omega_c, \text{ and } s\approx s_b \qquad (39)$$

EXAMPLE OF FIGURE 1

The best way to describe this numerical method is to consider a specific example. Let us evaluate the exact closed-loop poles of the transfer function of Figure 1. A numerical expression for the open-loop function of Figure 1 may be obtained from equations 20, 21, and 23.

$$G=\frac{4(s+0.2)(s+1)}{s(s+0.04)^2[(s/16)+1]^2} \qquad (40)$$

The approximate factors for the denominator expression have been given in equation 29.

First consider the shift of the approximate zero of the closed-loop denominator expression that occurs at $s=-\omega_2=-0.2$. As shown in equation 31, the closed-loop functions will have a pole when

$$(s+0.2)=\frac{-(s+0.2)}{G} = -\frac{s(s+0.04)^2[(s/16)+1]^2}{4(s+1)} \qquad (41)$$

Employ the approximation of equation 38 by setting in equation 41

$s=-0.2+\delta_2$ in left-hand expression (42)

$s=-0.2$ in right-hand expression (43)

This yields

$$[(-0.2+\delta_2)+0.2]\approx -\left[\frac{s(s+0.04)^2[(s/16)+1]^2}{4(s+1)}\right]_{s=-0.2} \qquad (44)$$

$$\delta_2\approx -\frac{(-0.2)(-0.2+0.04)^2[(-0.2/16)+1]^2}{4(-0.2+1)} = 0.0016 \qquad (45)$$

Since this is a small percentage change, the approximate equations 44 and 45 may be considered exact. By evaluating equation 42 we get as the "exact" value of the closed-loop pole $s=(-0.2+0.0016)=-0.1984$.

Consider the shift of the approximate closed-loop pole at $s=-\omega_3=-1$. The closed-loop functions will have a pole when (by equation 31)

$$(s+1)=\frac{-(s+1)}{G} = \frac{-s(s+0.04)^2[(s/16)+1]^2}{4(s+0.2)} \qquad (46)$$

Set

$s=(-1+\delta_3)$ in the left-hand expression (47)

$s=-1$ in the right-hand expression (48)

This yields

$$\delta_3\approx -\frac{(-1)(-1+0.04)^2[(-1/16)+1]^2}{4(-1+0.2)} = -0.253 \qquad (49)$$

The second approximation of the closed-loop pole obtained by substituting equation 49 into equation 47 is $s=(-1-0.253)=-1.253$. Since this is a fairly large change from the first approximation $s=-1$, the process must be repeated. Set in equation 46

$s=(-1+\delta_3)$ in the left-hand expression (47)

$s=-1.253$ in the right-hand expression (50)

This yields $\delta_3\approx -0.373$. The third approximation to the pole is $s=(-1-0.373)=-1.373$. Since this value is still quite different from the value in equation 50, a fourth approximation must be made, in which $s=-1.373$ is set in the right-hand expression of equation 46. If this process is repeated, it yields with each successive try the following approximate poles: −1.435, −1.468, −1.485, −1.496, −1.503, −1.507, −1.509, and finally −1.51.

For this particular pole the process converged fairly slowly, because the closed-loop pole was so close to the crossover frequency. The graphical method presented in the next section will prove much easier for evaluating the poles near the crossover frequency in magnitude.

Consider the shifts of the approximate double-order pole at $s=-\omega_4=-16$. As shown in equation 32, the closed-loop functions will have poles when

$$(s+16)^2=-(s+16)^2G = \frac{-4(s+0.2)(s+1)(16)^2}{s(s+0.04)^2} \qquad (51)$$

Employ the approximation of equation 39 by setting in equation 51

$s=(-16+\delta_4)$ in left-hand expression (52)

$s=-16$ in right-hand expression (53)

This yields

$$(\delta_4)^2\approx\frac{-4(-16+0.2)(-16+1)(16)^2}{(-16)(-16+0.04)^2} = (0.232)(16)^2 \qquad (54)$$

Hence δ_4 has two approximate roots

$$\delta_4\approx\pm\sqrt{0.232}(16)=\pm 7.7 \qquad (55)$$

This shows that the approximate double-order pole has split in two, one pole moving away from zero frequency and the other pole moving toward zero frequency. Since the pole moving toward zero frequency combines with the pole at the crossover frequency to form a pair of complex roots, it cannot be evaluated exactly by this method, but must be evaluated by the graphical method. However, the pole moving away from the crossover frequency can be evaluated quite easily. The second approximation for this pole is

$$s=(-16-7.7)=-23.7 \qquad (56)$$

To obtain the third approximation, set s equal to −23.7 in the right-hand expression of equation 51. This yields as the negative value of δ, −6.4. Hence the third approximation of the pole is $(-16-6.4)=-22.4$. A fourth approximation yields as the pole, −22.6; and a fifth yields −22.56.

The exact values of three of the five closed-loop poles have been evaluated. The remaining two cannot be evaluated by this method because they are so close

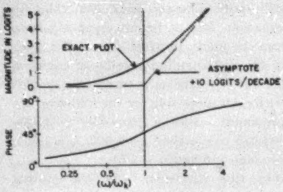

Figure 2. Log plots of $(s+\omega_k)/\omega_k$ along imaginary axis

to the crossover frequency. However, if the complete closed-loop denominator expression is divided by the expanded expression for the three roots that have been evaluated, the quotient (a quadratic) can then be factored to obtain the two remaining roots. This is illustrated in the following. From equation 40 the closed-loop denominator expression is

$$[KA(s)+B(s)]=4(16)^2(s+0.2)(s+1)+s(s+0.04)^2(s+16)^2 \quad (57)$$

$$=s^5+32.0s^4+257s^3+1024s^2+1229s+205 \quad (58)$$

The expression for the three roots that have been evaluated exactly is

$$(s+0.198)(s+1.51)(s+22.6)=s^3+23.3s^2+38.9s+6.77 \quad (59)$$

Dividing equation 59 into equation 58 by long division yields as the quotient

$$(s^2+8.7s+30)=(s+4.35-j3.3)(s+4.35+j3.3) \quad (60)$$

with a remainder of $(-15s^3+10s^2)$. Since this remainder is quite small with respect to equation 59, it can be assumed that the roots have been evaluated quite accurately. The quadratic of equation 60, comprising the two remaining roots, has for ω_n and ζ

$$\omega_n=\sqrt{30}=5.5$$

and

$$\zeta=8.7/2(5.5)=0.79$$

We have thus shown that the closed-loop poles of a function which are not too close to the crossover frequency may be evaluated quite simply by the numerical method. Once these poles have been evaluated they may be removed from the closed-loop denominator expression by long division. The resultant quotient then may be of sufficiently low order to be factored directly. On the other hand, these poles close to the crossover frequency can always be evaluated fairly easily by the graphical method which will be presented in the next main section.

SHIFTS OF COMPLEX POLES

So far, the numerical method has been employed to determine only the shifts of poles on the negative real axis. This method may also be employed to determine the shift of any pole, whether real or complex, provided that the pole does not lie too close to the crossover frequency. For example, consider an open-loop function which is the same as that of Figure 1, except that it has an additional high-frequency denominator quadratic with $\omega_n=14.1$ and $\zeta=0.71$. The function is

$$G=\frac{4(s+0.2)(s+1)(16)^2}{s(s+0.04)^2(s+16)^2(s+10-j10)\times(s+10+j10)} \quad (61)$$

The underdamped quadratic is shown in factored form. Let us consider the complex pole of this quadratic in the upper half plane. By equation 32 the closed-loop has a pole when

$$(s+10-j10)=-\frac{4(s+0.2)(s+1)(16)^2}{s(s+0.04)^2(s+16)^2(s+10+j10)} \quad (62)$$

Employ the approximation of equation 39 by setting in equation 62

$s=(-10+j10+\delta)$ in the left-hand expression (63)

$s=(-10+j10)$ in the right-hand expression (64)

This yields

$$\delta\approx-0.0271\,\underline{/-25.9^\circ}=-0.0244+j0.0118 \quad (65)$$

Since δ is very small, equation 65 can be considered exact. Substitution of equation 65 in equation 63 yields as the value of the upper-half-plane pole to four significant figures $s=(-10.02+j10.01)$. The lower-half-plane pole is the conjugate of this: $s=(-10.02-j10.01)$.

Graphical Method of Evaluating Poles

When analyzing a feedback control system, one usually plots the magnitude and phase of the open-loop function, $G(s)=G(j\omega)$, as a function of the frequency ω, for positive values of ω. These magnitude and phase plots may also be considered as plots of $G(s)$ along the positive imaginary axis of the s-plane. However, it will be shown that the function may be plotted almost as readily along any other radial axis. It will also be shown that these plots along other radial axes, especially along the negative real axis, will prove quite useful for evaluating the closed-loop poles.

In order to simplify the description of this method, we shall assume that the function has no poles or zeros in the right-half plane and that we shall not want to plot the function in the right-half plane. These restrictions are not basic, however, and could be removed merely by generalizing the rules for obtaining the phase plots. An understanding of the method presented in this paper will make these generalizations apparent.

PLOTS OF $G(s)$ ALONG POSITIVE IMAGINARY AXIS

When a frequency plot of a function of s is made, one usually substitutes $(j\omega)$ for s and plots the magnitude and phase of the resultant function versus the frequency ω. This is a plot of the function along the positive imaginary axis of the s-plane.

For example, the open-loop transfer function of Figure 1, expressed as a function of s, is

$$G(s)=\frac{K_0(s+\omega_2)(s+\omega_3)}{s(s+\omega_1)^2(s+\omega_4)^2} \quad (20)$$

The value of this function on the positive imaginary axis of the s-plane, that is, for $s=j\omega$ is

$$G(j\omega)=\frac{K_0(j\omega+\omega_2)(j\omega+\omega_3)}{j\omega(j\omega+\omega_1)^2(j\omega+\omega_4)^2} \quad (66)$$

The simplest method of plotting the function of equation 66 is to consider each zero and pole separately, forming its plots of magnitude in logits (decibels) and phase as functions of log ω, by means of templates. The plots of the complete function are then obtained by adding graphically the magnitude plots and the phase plots of the individual factors.[6] Expressions for the magnitude and phase (for $s=j\omega$) of the normalized factor $[(s+\omega_k)/\omega_k]$, which has a zero at $-\omega_k$, are

$$\left|\frac{s+\omega_k}{\omega_k}\right|_{s=j\omega}=\left|1+j\left(\frac{\omega}{\omega_k}\right)\right|=\sqrt{1+\left(\frac{\omega}{\omega_k}\right)^2} \quad (67)$$

$$\text{Ang}\left[\frac{s+\omega_k}{\omega_k}\right]_{s=}=\text{Ang}\left[1+j\left(\frac{\omega}{\omega_k}\right)\right]=\tan^{-1}\left(\frac{\omega}{\omega_k}\right) \quad (68)$$

Plots of the magnitude in logits and phase, versus log ω, are shown in Figure 2. Similarly, it can be shown that plots of the magnitude in logits and phase versus log ω, of the factor $[\omega_k/(s+\omega_k)]$, which has a pole at $-\omega_k$, can be obtained merely by inverting the curves of Figure 2.

Note that the magnitude plot of Figure 2 may be approximated by two asymptotes, one at zero logits and the other rising +10 logits per decade (or +20 decibels per decade). When the complete magnitude plot of a function is drawn, one first plots the asymptotes and then adds to these the deviation of the exact plot of each factor from the asymptotic plot. It will be shown that when a function is plotted along other radial axes in the s-plane, the same asymptotic plot will be used, except that the horizontal-axis variable will be generalized from ω to $|s|$, and the deviation of the actual function from the asymptotic approximation will be different.

PLOTS OF FUNCTIONS ALONG OTHER RADIAL AXES OF THE s-PLANE

We shall form the plots of a function of s along a general radial axis of the s-plane designated as O-X. Define the angle of this axis as ψ_x, and the angle between this axis and the negative real axis as $-\theta_x$, as shown in Figure 3. (Thus, $\psi_x + \theta_x = 180°$). Rather than designate the axis by the angles θ_x or ψ_x, however, consider another criterion. Suppose a zero existed on this axis with the value $(-\alpha + j\beta)$, as shown in the figure. Since complex zeros of a realizable transfer function must exist in conjugate pairs, the transfer function having this zero must have the factors:

$$(s+\alpha-j\beta)(s+\alpha+j\beta)=[s^2+2\alpha s+(\alpha^2+\beta^2)] \tag{69}$$

This is a quadratic factor with $\omega_n = \sqrt{\alpha^2+\beta^2}$ and $\zeta=\alpha/\sqrt{\alpha^2+\beta^2}$. By Figure 3 it is seen that this value of ζ for a zero on the O-X axis, which we shall designate as ζ_x, is equal to

$$\zeta_x = \cos\theta_x = -\cos\psi_x \tag{70}$$

Thus, each axis on the s-plane may be designated by ζ_x. It is preferable to employ ζ_x rather than ψ_x because ζ_x gives directly the damping ratio associated with a zero or pole which lies on that axis. However, it should be noted that there are two axes corresponding to each value of ζ_x one at the angle $+\psi_x$ (that is, in the upper half of the s-plane) and the other at the angle $-\psi_x$ (in the lower half of the s-plane).

It should also be noted that ω_n is equal to the distance from the origin to the zero, and hence is equal to the magnitude of s at that zero. Hence the undamped natural frequency ω_n of a pole or zero is equal to the magnitude of s (that is $|s|$) at the pole or zero.

We shall determine the value of the function $(s+\omega_k)$ at the point x on the O-X axis. This function has a zero at $s=-\omega_k$, which is designated as the point k in Figure 4. Define the vector drawn from the point k to the point x as $\mathbf{G}_{kx}$. The value of s at the point x then is

$$s_x = -\omega_k + \mathbf{G}_{kx} \tag{71}$$

Hence, the value of $(s+\omega_k)$ evaluated at the point x is

$$[(s+\omega_k)]_{s=s_x} = (-\omega_k+\mathbf{G}_{kx})+\omega_k = \mathbf{G}_{kx} \tag{72}$$

This result may be generalized by the following statement: If a function consists of a single zero (either real or complex), the value of that function at any point x on the s-plane is equal to the vector drawn from the zero of the function to the point x, times a constant. The value of any function, evaluated at a point x on the s-plane, is equal to the product of the vectors drawn from the zeros of that function to the point x, divided by the product of the vectors drawn from the poles of that function to the point x, times a constant.

Hence, our problem becomes one of finding an expression for the vector $\mathbf{G}_{kx}$ as a function of the point x on the O-X axis. Since the value of s at the point x is defined as s_x, the length O-X is equal to $|s_x|$. Now in Figure 4, O-a-x is a right triangle; hence,

$$\text{Length}\,(O-a) = |s_x|\cos\theta_x = |s_x\ \zeta_x \tag{73}$$

$$\text{Length}\,(a-x) = |s_x|\sin\theta_x = |s_x|\sqrt{1-\zeta_x^2} \tag{74}$$

Now, the length $(O$-$k)$ is equal to ω_k; hence

$$\text{Length}\,(a-k) = \text{Length}\,(O-k) - \text{Length}\,(O-a)$$

$$= \omega_k - |s_x|\zeta_x \tag{75}$$

The vector $\mathbf{G}_{kx}$ then, is

$$\mathbf{G}_{kx} = [\text{Length}\,(a-k)] + j[\text{Length}\,(a-x)]$$

$$= \omega_k - |s_x|\zeta_x + j|s_x|\sqrt{1-\zeta_x^2} \tag{76}$$

Normalize by dividing through by ω_k

$$(\mathbf{G}_{kx}/\omega_k) = 1 - |s_x/\omega_k|\zeta_x + j|s_x/\omega_k|\sqrt{1-\zeta_x^2} \tag{77}$$

The magnitude and phase of the normalized $\mathbf{G}_{kx}$ are

$$G_{kx}/\omega_k| = \sqrt{1+|s_x/\omega_k|^2 - 2\zeta_x|s_x/\omega_k|} \tag{78}$$

$$\text{Ang}\,[\mathbf{G}_{kx}] = \tan^{-1}\left\{\frac{|s_x/\omega_k|\sqrt{1-\zeta_x^2}}{1-|s_x/\omega_k|\zeta_x}\right\} \tag{79}$$

Plots of equations 78 and 79 for various values of ζ_x are shown in Figure 5. If there is a pole at $-\omega_x$ rather than a zero, plots of the function can be obtained merely by inverting these curves—just as for plots along the imaginary axis.

It is more convenient, however, to plot first asymptotic approximations of the magnitude and phase functions, and then graphically add to them the deviations of the exact plots from the approximations. The function $(s+\omega_k)$ evaluated at $s=s_x$ may be approximated as follows

$$\mathbf{G}_{kx} = (s_x+\omega_k) \approx \begin{cases} \omega_k, \text{ for } |s_x| < \omega_k & (80) \\ s_x, \text{ for } |s_x| > \omega_k & (81) \end{cases}$$

Hence the magnitude asymptotes are

$$G_{kx}| = |s_x+\omega_k| \approx \begin{cases} \omega_k, \text{ for } |s_x| < \omega_k & (82) \\ |s_x|, \text{ for } |s_x| > \omega_k & (83) \end{cases}$$

This is the same as the usual magnitude asymptotic approximation made when the function is plotted along the imaginary axis, illustrated in Figure 2, except that the frequency variable is $|s_x|$ rather than ω. Therefore, one can say: The asymptotic approximations of the magnitude of a function of s versus $|s|$ along all radial axes on the s-plane are the same.

Define $|d_{kx}|$ as the deviation of $|G_{kx}|$ from its asymptotic approximations in equations 82 and 83. For $|s_x| < \omega_k$

$$|d_{kx}| = \left|\frac{G_{kx}}{\omega_k}\right| = \sqrt{1+\left|\frac{s_x}{\omega_k}\right|^2 - 2\zeta_x\left|\frac{s_x}{\omega_k}\right|} \tag{84}$$

For $|s_x| > \omega_k$

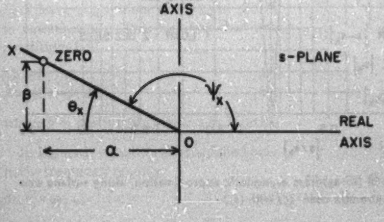

Figure 3 (left). Radial axis on s-plane

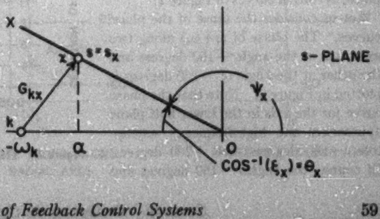

Figure 4 (right). Evaluation of $(s+\omega_k)$ at the point x on the s-plane

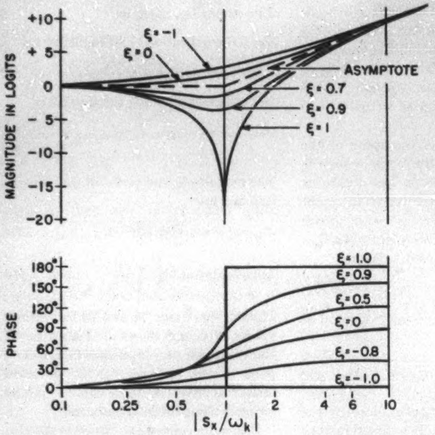

Figure 5. Plot of $(G_{kz}/\omega_k)=(s+\omega_k)/\omega_k$ along upper-half-plane axis at angle $\cos^{-1}(\zeta)$ with negative real axis

$$d_{kz}| = \left|\frac{G_{kz}}{s_z}\right| = \sqrt{1+\left|\frac{\omega_k}{s_z}\right|^2 - 2\zeta_z\left|\frac{\omega_k}{s_z}\right|} \qquad (85)$$

Comparing equations 78 and 84 with equation 85 shows that the function $|d_{kz}|$ is symmetric about the frequency $|s_z| = \omega_k$ if the frequency is plotted on a log scale. For example, the function will have the same value at $|s_z| = 2\omega_k$ that it has at $|s_z| = \omega_k/2$. Plots of this function for various values of ζ_z are shown in Figure 6. For a factor having a pole at $-\omega_k$, these curves should be inverted.

From equations 80 and 81, it is seen that the phase may be approximated by

$$\text{Ang}\,[\mathbf{G}_{kz}] = \text{Ang}\,(s_z+\omega_k) \approx$$

$$\begin{cases} 0, \text{ for } |s_z| < \omega_k & (86) \\ \text{Ang}\,(s_z) = \psi_z, \text{ for } |s_z| > \omega_k & (87) \end{cases}$$

Plots of deviation of exact phase, given in equation 79, from this approximation are shown in Figure 7 for various values of ζ_z. These plots of deviation are also symmetric about $|s_z| = \omega_k$ when the frequency is plotted on a logarithmic scale, as may be proved by geometric reasoning. To obtain the phase plots for a factor with a pole at $-\omega_k$, one should employ $-\psi_z$ as the value for the high-frequency phase asymptote in equation 87, and invert the phase deviation curves of Figure 7.

Let us consider the sense of the phase curves. The phase of $(s+\omega_k)$ along two axes, one at the angle +160 degrees and the other at the angle of −160 degrees is plotted in Figure 8. Note that the phase curve for the axis in the lower half plane approaches the high-frequency asymptote, −160 degrees, not +200 degrees. Of course, the angles −160 degrees and +200 degrees coincide on a polar plot, but they do not coincide on a plot of phase-versus-frequency. Consequently, the following convention will be employed when choosing the value of ψ_z for the angle asymptote of equation 87.

Measure ψ_z, for the phase asymptote, in a positive direction when the axis on which the function is to be plotted lies above the zero; measure ψ_z in a negative direction when the axis lies below the zero.

For the phase deviations, a similar rule applies. If the axis on which the function is to be plotted lies above the zero the phase deviation is positive for the low-frequency portion and negative for the high-frequency portion; the reverse holds if the axis lies below the zero. In any case, the deviations will add to the asymptotes so that there is no discontinuity of the phase plot along a radial axis, except right at a zero or pole.

For a pole, the situation is exactly reversed. For example, if there were a pole at $-\omega_k$ instead of a zero in Figure 8, the phase plot labeled OX^- would be the phase plot along the upper-half-plane axis OX^+, while the other plot would be the plot along OX^-.

These conventions guarantee that the phase curves along any radial axis will be continuous except right at a pole or zero. On the other hand, if one plots the phase curve along another path in the s-plane, 360-degree discontinuities will occur wherever the path intersects a radial axis on which a pole or zero lies, provided that the intersection is outside the pole or zero. For example, in Figure 8 the phase curve along the A-B axis is seen to have a 360-degree discontinuity at the point where the A-B axis intersects the O-K axis. These 360-degree discontinuities, however, do not present any basic difficulty because they are only apparent discontinuities; they do not represent discontinuities in the actual value of the function but only in the particular phase plot that is employed. If the function were plotted on a polar plot, no discontinuities of phase would occur.

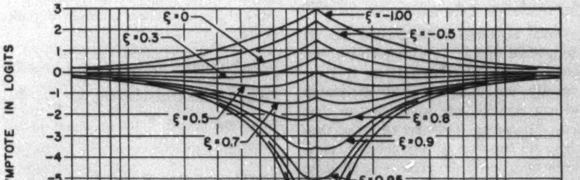

Figure 6. Deviation of magnitude of $(s-s_k)$ from asymptotic approximation, along s-plane axis at angle $\cos^{-1}(\zeta)$ with (s_k)

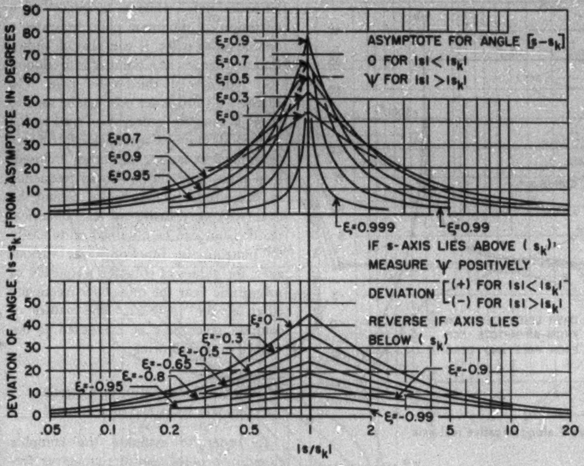

Figure 7. Deviation of angle of $(s-s_k)$ from asymptotic approximation, along s-plane axis at angle $\cos^{-1}(\zeta)$ with (s_k)

PLOT OF EXAMPLE OF FIGURE 1 ALONG NEGATIVE REAL AXIS

As an illustration, the transfer function of Figure 1 is plotted along the negative real axis in Figure 9. The broken line represents the magnitude asymptote and hence is the same as the asymptotic curve of Figure 1. The dashed curves represent the deviations from the asymptotes corresponding to the individual zeros and poles. Note that the deviations are negative (in logits) for zeros, and positive (in logits) for poles. These dashed curves are added to the broken-line magnitude asymptote to form the complete magnitude plot shown by the solid curve. The dashed curves representing the deviations corresponding to the poles at $-\omega_1$, and $-\omega_4$ are added twice, because these are double-order poles. The curve of phase that is drawn is the same as the phase asymptote, since the deviation of phase from the asymptote (shown in Figure 7) is zero for the negative real axis.

The closed-loop functions C/R and E/R have poles when $G=-1$, as shown in equation 30. This requires that two conditions hold

$$|G|=1 \tag{88}$$

$$\text{Ang}\,(G)=p(180°) \tag{89}$$

where p = odd integer, positive or negative

In Figure 9, equation 89 is satisfied only in the frequency regions

$$0<|s|<\omega_2;\quad \omega_3<|s|<\infty \tag{90}$$

Within the frequency regions of equation 90, equation 88 shows that there is a closed-loop pole in Figure 9 wherever the magnitude of G is unity—that is, wherever the magnitude plot crosses the zero logit line. Consequently, there are three closed-loop poles on the negative real axis, which are indicated in Figure 9 by the points 1, 2, and 3. These poles, occurring at $|s|=0.20$, 1.50, and 22.6 were calculated previously by the numerical method.

At point 1 the slope of $|G|$ is very steep, which explains why our calculations showed a very small shift of the exact closed-loop pole from the approximate closed-loop pole at $-\omega_2$. This shift is toward zero frequency, because near ω_2 the phase condition of equation 89 is satisfied only for $|s|<\omega_2$. The open-loop pole at $-\omega_4$ is second order, and hence the phase condition of equation 89 is satisfied both for $|s|<\omega_4$ and $|s|>\omega_4$. Hence this open-loop pole divides to form two closed-loop poles: one shifted away from zero frequency to point 3; and the other shifted toward zero frequency to form, with the pole at $-\omega_c$, a conjugate-complex pair of poles, which, however, cannot be evaluated by the plot of Figure 9, because this pair does not appear on the negative real axis. The pole at 2 was shifted from the open-loop zero at $-\omega_3$ away from zero frequency, because, near ω_3, the phase condition of equation 89 is satisfied only for $|s|>\omega_3$. Since the slope of $|G|$ for frequencies above point 2 is very small, a very slight decrease in gain would cause a large shift of this pole away from zero frequency, which explains why it was difficult to evaluate this pole by the numerical method.

If the value of ω_4 in G were increased somewhat, while the other poles and zeros were kept constant, this plot would take the form of the curve shown in Figure 10.

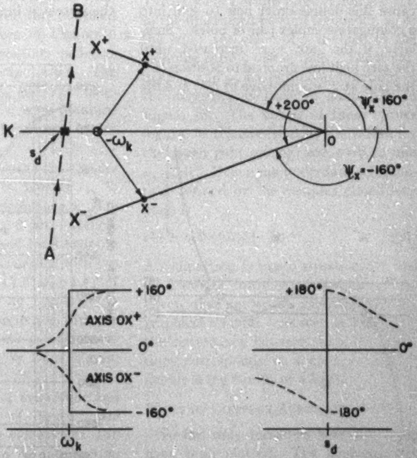

Figure 8. Proper direction for measuring ψ_z

PHASE PLOTS ALONG RADIAL AXES

PHASE PLOT ALONG A-B

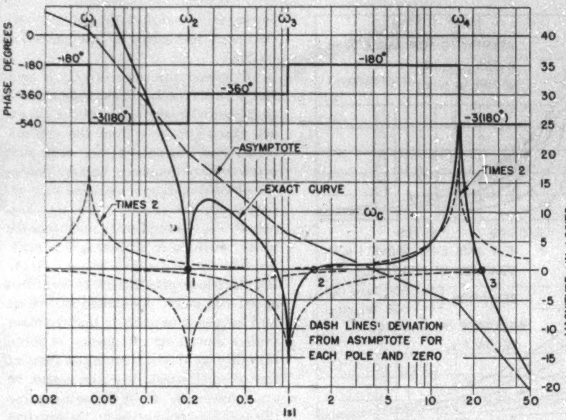

Figure 9. Plot of function of Figure 1 along negative real axis

Then if the gain were set so that the zero logit line were at position (A), as shown in Figure 10, in the frequency interval $\omega_3<|s|<\omega_4$ the plot of $|G|$ would intersect the zero logit line at three points, labeled $2'$, $4'$, and $5'$, rather than at one point, as in Figure 9. Thus, all five closed-loop poles would occur on the negative real axis. However, if the gain were decreased until the zero logit line rose to position (B), the pole at $5'$ would move to $5''$ and the poles at $2'$ and $4'$ would move together to form a double order pole at $2''$. A further decrease in gain would cause this double-order pole to split into a conjugate-complex pair of poles. Similarly, if the gain were increased until the zero logit line dropped to position (C), the pole at $2'$ would move to $2'''$, and the poles at $4'$ and $5'$ would move together to form a double-order pole at $5'''$. This double-order pole would split into a pair of conjugate-complex poles if the gain were increased still further. Thus, in the frequency region $\omega_3<|s|<\omega_4$ there are three poles, one which is real, and the other two which may be real or conjugate-complex, depending upon the value of gain and the width of the interval between ω_3 and ω_4.

We may therefore postulate the following: Where the phase is 180 degrees on the negative real axis, an intersection of the zero logit line by $|G|$ indicates a single-order pole, while a tangency at a maximum or minimum point indicates a double-order pole; it can also be shown that a tangency at a point of inflection of $|G|$ indicates a third-order pole. (In Figure 9 a third-order pole can be seen to occur if the gain is decreased by 1 logit.) Almost all practical feedback-control systems have at least 2 and often 3 closed-loop poles near the crossover frequency in magnitude. These poles cannot be evaluated very easily by the numerical method but can be obtained quite easily by plotting the function along various axes, for values of complex frequency of magnitude near the cross-over frequency (that is, for $|s|\approx\omega_c$). The values of complex poles may be evaluated as described in the following.

GRAPHICAL EVALUATION OF COMPLEX POLES FOR EXAMPLE OF FIGURE 1

In order to evaluate the complex closed-loop poles near the crossover frequency, plots of the open-loop function G along various axes of the s-plane will be employed to obtain a locus of possible closed-loop poles for varying values of gain, which is similar to the root locus employed by Evans.[1]

A plot of G for the example of Figure 1 along the upper-half-plane axis corresponding to $\zeta=0.5$ is developed in Figure 11. The broken lines represent the magnitude and phase asymptotes. Notice that the phase asymptote near the crossover frequency (that is, the phase asymptote in the region in which we are interested) is at the angle $[180°-\cos^{-1}\zeta]$.

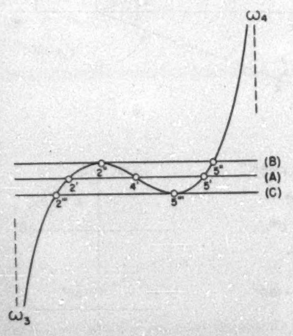

Figure 10. Magnitude plot of G(s) along negative real axis near $-\omega_c$

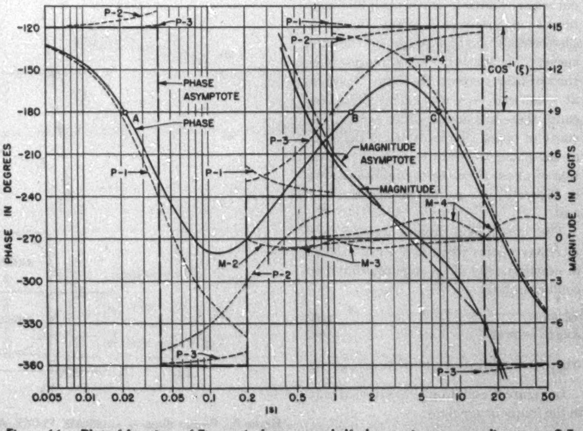

Figure 11. Plot of function of Figure 1 along upper-half-plane axis corresponding to $\zeta=0.5$

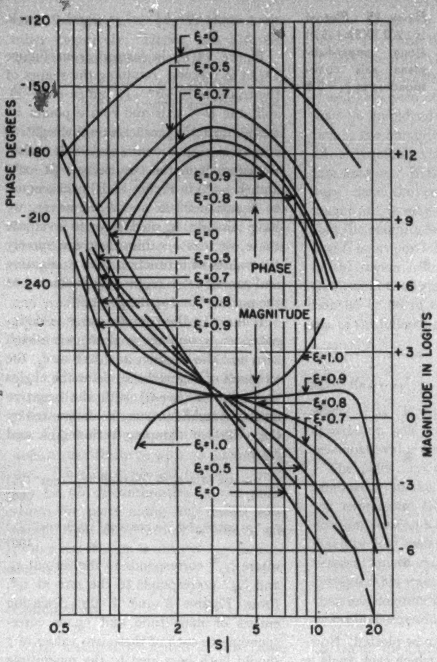

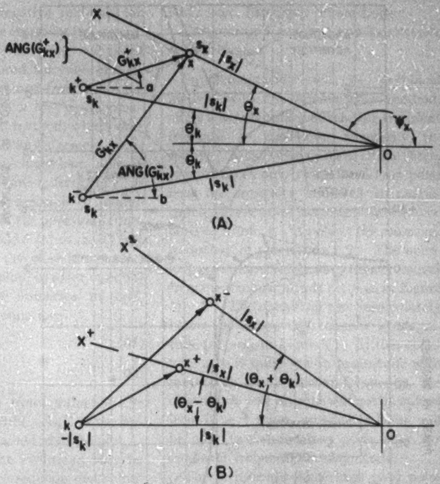

Figure 12 (left). Plots of function of Figure 1 along various axes

Figure 14 (above). Development of method for plotting complex factors

A. Original configuration
B. Rotated axes

The dashed curves labeled *P-1*, *P-2*, *P-3*, and *P-4* represent the deviations from the phase asymptotes corresponding to the poles and zeros at $-\omega_1$, $-\omega_2$, $-\omega_3$, and $-\omega_4$ respectively. Similarly, the dashed curves labeled *M-2*, *M-3*, and *M-4* represent the deviations from the magnitude asymptotes corresponding to the poles and zeros at $-\omega_2$, $-\omega_3$, and $-\omega_4$ respectively. Curves *P-2*, *P-3*, *M-2*, and *M-3* were obtained directly from Figures 6 and 7 for the curves corresponding to $\zeta=0.5$. Curves *P-1*, *P-4*, and *M-4* were obtained by doubling these curves of Figures 6 and 7, because the open-loop poles at $-\omega_1$ and $-\omega_4$ are of double order. The solid curves, representing the exact magnitude and phase curves, were obtained by adding graphically the dashed curves to the asymptotes.

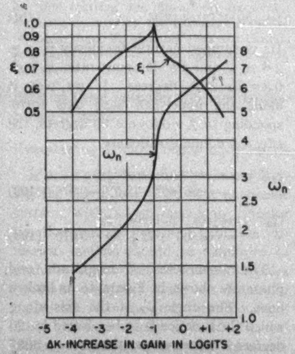

Figure 13. Plots of ζ and ω_n of the complex closed-loop poles for function of Figure 1, versus system gain

The phase curve intersects the 180-degree line at three points, labeled *A*, *B* and *C*. The value of magnitude at *B* is 4 logits and at *C* is -1.25 logits. Hence, if the gain were decreased by 4 logits, a closed-loop pole would occur at *B* with $\zeta=0.5$ and (since $|s|$ at *B* is 1.4) $\omega_n=1.4$; if the gain were increased by 1.25 logits, a closed-loop pole would occur at *C* with $\zeta=0.5$ and $\omega_n=7.2$. Since the point *A* corresponds to an extremely low value of gain, it is of no interest to us.

In Figure 12 curves of magnitude and phase for the example of Figure 1 are drawn for the following values of ζ: 1.0, 0.9, .8, 0.7, 0.5, and 0. An intersection of a phase curve for a given ζ with the 180-degree line determines a possible closed-loop pole (for the proper value of gain). The reciprocal of the value of magnitude corresponding to this intersection is equal to the increase in gain necessary to produce this closed-loop pole. The frequency of this intersection is equal to the undamped natural frequency ω_n of the pole; the value of ζ is equal to the damping ratio ζ of the pole. These values of ζ and ω_n are plotted as functions of the necessary increase in gain, ΔK, in Figure 13. The values of these curves for $\Delta K = 0$ logits (that is, the values for the given gain setting) are $\zeta=0.72$ and $\omega_n=5.6$. Hence the underdamped quadratic formed by the complex closed-loop poles is

$$s^2+2(0.72)(5.6)s+(5.6)^2 \qquad (91)$$

A comparison between equations 91 and 60 shows a fairly good agreement between the numerical method and the graphical method. As seen in Figure 13, the discrepancy between these two equations corresponds to a change in *K* of merely a few tenths of a logit.

Plots of Complex Zeros and Poles

So far, only functions with real roots have been plotted. The approach will now be generalized to enable us to plot functions with complex zeros and poles.

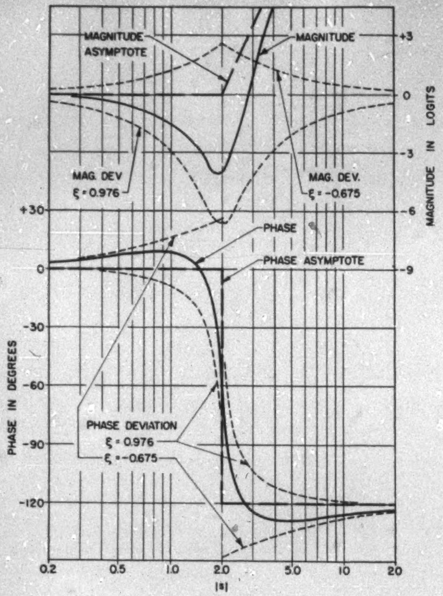

Figure 15. Plot of $[s+2(0.3)(2)s+(2)^2]$ along upper-half-plane axis corresponding to $\zeta_x=0.5$

Since complex zeros or poles must exist in conjugate pairs, we shall consider each pair together. Consider a function with zeros at $s=s_k$ and $s=s_k^*$ (where s_k^* represents the conjugate of s_k) evaluated at $s=s_x$

$$(s_x-s_k)(s_x-s_k^*)=s_x^2-s_x(s_k+s_k^*)+s_k s_k^* \qquad (92)$$

Expressions for the magnitude and phase asymptotes are as follows (note that $|s_k|=\omega_n$, the undamped natural frequency)

$$|(s_x-s_k)(s_x-s_k^*)| \approx \begin{cases} |s_k|^2=\omega_n^2, \text{ for } |s_x|<\omega_n & (93) \\ |s_x|^2, \text{ for } |s_x|>\omega_n & (94) \end{cases}$$

$$\text{Ang}\,[(s_x-s_k)(s_x-s_k^*)] \approx \begin{cases} \text{Ang}\,(s_k s_k^*)=0, \text{ for } |s_x|<\omega_n & (95) \\ \text{Ang}\,(s_x^2)=\psi_x^+ +\psi_x^-, \text{ for } |s_x|>\omega_n & (96) \end{cases}$$

These asymptotic approximations are merely generalizations of the approximations that were made previously for zeros on the negative real axis. Note that the asymptotes do not depend (explicitly) upon the damping ratio ζ of the zeros, but only upon s_x and the undamped natural frequency $\omega_n=|s_k|$.

In equation 96 the angles ψ_x^+ and ψ_x^- both represent the angle of the axis along which the function is to be plotted. However, the direction in which each angle is to be measured, depends, as before, upon whether the axis lies above the corresponding zero or below it. Since there are two zeros, there are two values of ψ_x: one ψ_x^+ corresponding to the zero in the upper half plane, and the other ψ_x^- corresponding to the zero in the lower half plane. Consequently, if the axis lies above both zeros, both angles are measured positively; if it lies between the zeros, ψ_x^+ is measured negatively and ψ_x^- is measured positively; if it lies below both zeros both ψ_x^+ and ψ_x^- are measured negatively.

A method for evaluating the exact magnitude and phase curves is developed in Figure 14(a). The product of two vectors $\mathbf{G}_{kx}^+$ and $\mathbf{G}_{kx}^-$ in Figure 14(A) drawn from the points k^+ and k^- (which lie at the two zeroes s_k and s_k^*) to the point x, is equal to the value of equation 92 at $s=s_x$. The magnitude of this product is equal to

$$|G_{kx}^+||G_{kx}^-|=[\text{Length}\,(k^+-x)]\times[\text{Length}\,(k^- -x)] \qquad (97)$$

The phase of this product is equal to

$$\text{Ang}\,(\mathbf{G}_{kx}^+)+\text{Ang}\,(G_{kx}^-) = \text{Ang}\,(0-k^+-x)+\text{Ang}\,(0-k^- -x) \qquad (98)$$

since angle $(0-k^+-a)$ is equal to angle $(0-k^- -b)$.

Figure 14(B) is formed from Figure 14(A) as follows: retaining the shapes of the triangles $(0-k^+-x)$ and $(0-k^- -x)$, split the O-X axis and rotate points k^+ and k^- until they coincide on the negative real axis. Equations 97 and 98 show that the product of the two vectors $(\mathbf{k}-\mathbf{x}^-)$ and $(\mathbf{k}-\mathbf{x}^+)$ in Figure 14(B) is also equal to equation 92 at $s=s_x$. However, we have already learned how to evaluate these vectors because they are merely the values of a function with a negative real zero at $s=-|s_k|=-\omega_n$ evaluated at the point x^+ and at the point x^-.

If the ζ of the complex zeros is designated as ζ_k, and the angle between each zero and the negative real axis as θ_k, the two axes of Figure 14(B) lie at the angles $(\theta_x-\theta_k)$ and $(\theta_x+\theta_k)$ with the negative real axis, and hence may be designated by the effective damping ratios ζ_{kx}^+ and ζ_{kx}^-

$$\zeta_{kx}^+=\cos(\theta_x-\theta_k)=\cos(\cos^{-1}\zeta_x-\cos^{-1}\zeta_k) \qquad (99)$$

$$\zeta_{kx}^-=\cos(\theta_x+\theta_k)=\cos(\cos^{-1}\zeta_x+\cos^{-1}\zeta_k) \qquad (100)$$

where ζ_{kx}^+ corresponds to the zero at s_k, and ζ_{kx}^- corresponds to the zero at s_k^*. From Figures 6 and 7 the deviation curves of magnitude and phase corresponding to each of these two values of ζ should both be added to the magnitude and phase asymptotes to obtain the exact plots of equation 92. When plotting the phase deviation for a given zero, the low-frequency portion is plotted positively, as before, if the axis lies above the zero, and negatively if the axis lies below the zero.

This procedure is illustrated in the following example. Let us plot the underdamped quadratic

$$[s^2+2(0.3)(2)s+(2)^2] \qquad (101)$$

Its undamped natural frequency is $\omega_n=2=|s_k|$, and its damping ratio is $\zeta_k=0.3=\cos 72.5$ degrees. If we plot it along the upper-half-plane axis corresponding to $\zeta_x=0.5=\cos 60$ degrees, the effective damping ratios are

$$\zeta_{kx}^+=\cos(\cos^{-1}\zeta_x-\cos^{-1}\zeta_k) = \cos(60°-72.5°)=0.976 \qquad (102)$$

$$\zeta_{kx}^-=\cos(\cos^{-1}\zeta_x+\cos^{-1}\zeta_k) = \cos(60°+72.5°)=-0.675 \qquad (103)$$

The asymptotes of magnitude and phase are shown in Figure 15 as broken lines. The angle ψ_x of the axis along which the function is to be plotted is 120 degrees if measured positively or $(-360°+120°)$ if measured negatively. Since the axis lies between the zeros of the quadratic of equation 101, one value of ψ_x

must be measured positively and the other negatively. Hence, the high-frequency phase asymptote is

$$\psi_x^{+}+\psi_x^{-}=(-360°+120°)+(120°)$$
$$=2(120°)-360°=-120° \qquad (104)$$

The deviations of magnitude and phase from the asymptotes corresponding to the two effective damping ratios are shown in Figure 15 as dashed curves. These are added to the asymptotes to form the complete magnitude and phase plots shown as solid curves. Note that the phase deviation corresponding to $\zeta=0.976$ is plotted negatively for $|s_x|<\omega_n$ and positively for $|s_x|>\omega_n$, because the axis lies below the upper-half-plane zero; while the phase deviation corresponding to $\zeta=-0.675$ is plotted positively for $|s_x|<\omega_n$ and negatively for $|s_x|>\omega_n$, because the axis lies above the lower-half-plane zero. When the phase deviations are added to the asymptotes, they produce a smooth curve with no discontinuities. This must always happen; there can be no discontinuities in the phase curve for plots along any radial axis, except right at a zero or a pole, if the proper convention is observed in measuring ψ_x.

Conclusions

The methods presented in this paper may be used for three different purposes:

1. For quick evaluation of the closed-loop poles of a particular system, which has set values of gain and other system parameters.
2. For indicating the change in the values of the closed-loop poles with variations in the settings of gain and open-loop poles and zeros, in order to show what the optimum settings are and how critical these settings are.
3. For relating the open-loop frequency response directly to the transient response of the system, by showing that the closed-loop poles are derived from open-loop poles and zeros.

Each of these purposes will now be discussed in detail.

EVALUATION OF THE CLOSED-LOOP POLES

If one's purpose is merely that of finding the closed-loop poles of a particular system, with a set open-loop transfer function and set values of gain, the numerical method should be employed to evaluate as accurately as desired the poles (real and complex) which are distant in magnitude from the crossover frequency. Since there is usually at least one real closed-loop pole so near the crossover frequency in magnitude that it cannot be evaluated readily by the numerical method, the open-loop function should be plotted along the negative real-axis for values of $|s|$ near the crossover frequency. If very accurate values of the real poles in this region are desired, the value of each closed-loop pole obtained from this plot may be employed as a first approximation in the numerical method, which usually will quickly yield an extremely accurate answer. If the closed-loop pole is very near the crossover frequency in magnitute, it may be desirable to assume that the magnitude of the open-loop function G is proportional to $|s|$ or to $|(1/s)|$ in the region near the closed-loop pole. One would then employ, in place of equation 35 or 36 in the numerical method, one of the following equations

$$\omega_k'\approx|(s/G)|_{s=-\omega_k''} \qquad (105)$$

$$\omega_k'\approx|sG|_{s=-\omega_k''} \qquad (106)$$

where $-\omega_k'$ is the exact value of the closed-loop pole; while $-\omega_k''$ is the approximate value obtained from the plot.

The poles that are evaluated may be removed from the closed-loop denominator expression $[KA(s)+B(s)]$ by long division, leaving a quotient that is of sufficiently low order to be factorable by classical methods. For practically all systems, this quotient will be no higher than second order if all the poles that may be evaluated readily are removed.

CHANGES OF CLOSED-LOOP POLES WITH VARIATIONS IN GAIN AND OPEN-LOOP POLES AND ZEROS

Evaluation of the closed-loop poles for a specific open-loop function G by means of plots of G along various axes in the s-plane is somewhat more cumbersome than the above described method. However, even for the most complicated open-loop function, these plots are very easy to construct in comparison to other methods now employed for evaluating the closed-loop poles of high-order systems.

On the other hand, it usually is necessary for one to know the value of the major closed-loop poles (that is, those near the crossover frequency in magnitude) for a number of values of gain, and probably for a number of values of the open-loop poles and zeros, in order that one can determine the optimum settings of these parameters, and whether these settings are critical. This information can be obtained quite readily from the plots of the open-loop function along various axes of the s-plane for values of $|s|$ near the crossover frequency. These plots are a very powerful tool for explaining the basic principles of the operation of the closed-loop system, and can give the designer a great deal of insight into methods for improving the system's performance.

RELATION BETWEEN OPEN-LOOP FREQUENCY RESPONSE AND TRANSIENT RESPONSE

Supplementation of the graphical method with the approximate method, offers a simple means of relating transient response to open-loop frequency response. Most systems have either three, or sometimes only two, closed-loop poles near the crossover frequency in magnitude. These poles have been shown to be derived from: 1. A pole at the crossover frequency in magnitude. 2. The open-loop pole immediately above the crossover frequency in magnitude (at $-\omega_4$ in Figure 1). 3. The open-loop zero immediately below the crossover frequency in magnitude (at $-\omega_3$ in Figure 1). If this open-loop zero is quite low in magnitude with respect to the crossover frequency, the closed-loop pole it forms will not be shifted from it very much, and hence there will be only two closed-loop poles near the crossover frequency in magnitude.

These three (or sometimes two) poles near the crossover frequency in magnitude determine the major form of the transient response of the system to a step input of position. For systems with a fairly good degree of stability (not much greater than 30 per cent peak overshoot of the transient), the main characteristics of this response are the build-up time, and the amount of peak overshoot. Closed-loop poles at reasonable intervals below the crossover frequency in magnitude, effect only the low-frequency response of the system. They reduce the amount of error due to constant velocities, constant accelerations, and so forth, but also add long tails to the transient response. Closed-loop poles at reasonable intervals above the crossover frequeny in magnitude generally have little effect upon the transient response. They primarily determine the high-frequency filter action of the system by minimizing the transmission of high-frequency noise signals. However, if a pair of high-frequency closed-loop poles is quite underdamped, it may introduce an undesirable secondary oscillation into the transient response.

The graphical method is very useful for evaluating the three (or sometimes two) poles near the crossover frequency in magnitude. For the other closed-loop poles, the values given by the approximate method generally are sufficiently accurate for determining their effect on the transient response, because the shift of the exact values of these poles from the approximate values is usually quite small.

However, the calculation of the coefficients of the partial-fraction ex-

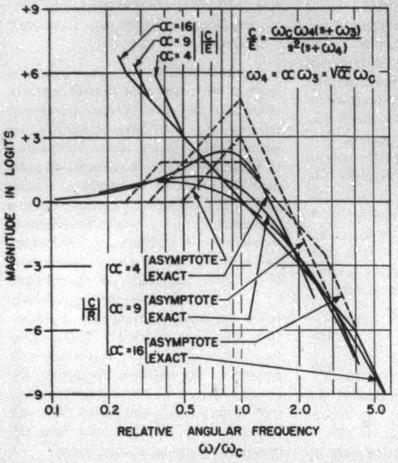

Figure 16. Plots of $|C/R|$ and $|C/E|$ for function of equation 109 with varying α

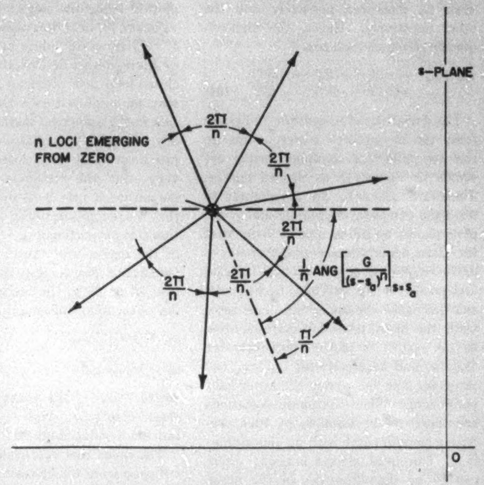

Figure 18. Loci of shift of closed-loop poles from an nth-order open-loop zero

pansions of C or E associated with these other poles presents a problem because the approximate poles are not exact factors of the closed-loop denominator expression $[KA(s) + B(s)]$. This may be overcome by assuming when calculating these coefficients, that for poles below ω_c in magnitude

$$\frac{E}{R}=\frac{E}{C}=\frac{1}{G} \tag{107}$$

and for poles above ω_c in magnitude

$$\frac{C}{R}=\frac{C}{E}=G \tag{108}$$

These approximations are very good as long as the shift of the exact pole from the approximate pole is quite small.

In conclusion, the methods presented in this paper are not only very useful for evaluating the closed-loop poles of a system; but even more important they offer a simple means of relating transient response directly to the open-loop frequency response.

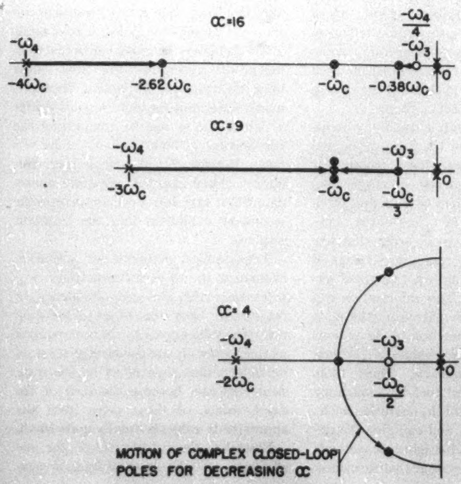

Figure 17. Shift of exact closed-loop poles from approximate closed-loop poles for function of equation 109

Appendix I. The Basic Third-Order System

The following example is presented because it illustrates the basic third-order system, which a great many systems approximate in the region near the crossover frequency. Its transfer function, plotted in Figure 16, is

$$G=\frac{\omega_c(s+\omega_3)\omega_4}{s^2(s+\omega_4)} \tag{109}$$

For convenience, set the crossover frequency ω_c midway between ω_3 and ω_4 on a logarithmic plot: $\omega_c=\sqrt{\omega_3\omega_4}$; and define the frequency ration (ω_4/ω_3) as α, so that

$$\omega_c=\sqrt{\alpha}\omega_3=\omega_4/\sqrt{\alpha} \tag{110}$$

The ratio α corresponds to the attenuation ratio of a lead network.

The approximate factors of the closed-loop denominator expression are

$$(s+\omega_3)(s+\omega_c)(s+\omega_4) = [s+(\omega_c/\sqrt{\alpha})][s+\omega_c][s+\sqrt{\alpha}\omega_c] \tag{111}$$

The exact closed-loop denominator expression is

$$KA(s)+B(s)=s^3+\omega_c\sqrt{\alpha}s^2+\omega_c^2\sqrt{\alpha}s+\omega_c^3 \tag{112}$$

This may be factored into

$$(s+\omega_c)(s^2+(\sqrt{\alpha}-1)\omega_c s+\omega_c^2) \tag{113}$$

For large values of α, the quadratic factor of equation 113 can be factored into two real single-order factors; for lower values of α it becomes an underdamped quadratic with $\omega_n=\omega_c$ and $\zeta=(\sqrt{\alpha}-1)/2$. Let us consider three different values of α. For $\alpha=16$; $\omega_3=0.25\omega_c$, $\omega_4=4\omega_c$, and equation 113 becomes

$$(s+0.38\omega_c)(s+\omega_c)(s+2.62\omega_c) \tag{114}$$

For $\alpha=9$; $\omega_3=0.33\omega_c$, $\omega_4=3\omega_c$, and equation 113 becomes

$$(s+\omega_c)^3 \tag{115}$$

For $\alpha=4$; $\omega_3=0.5\omega_c$, $\omega_4=2\omega_c$, and equation 113 becomes

$$(s+\omega_c)(s^2+2\zeta\omega_c s+\omega_c^2),\text{ where }\zeta=0.5 \tag{116}$$

Asymptotic plots of $|C/E|$ and $|C/R|$ for the three values of α are shown in Figure 16. Exact plots of the magnitude of the closed-loop function, C/R are also shown. These exact plots illustrate the increase in M_p (peak value of $|C/R|$) with the decrease of α.

Plots of the shifts of the exact closed-loop poles from the approximate closed-loop poles are shown in Figure 17. The symbol ⊗ represents a closed-loop pole while (X) and (O) represent open-loop poles and zeros respectively. At this setting of gain there is no shift of the approximate pole at $-\omega_c$. For decreasing α, the other two poles shift by increasing amounts toward $-\omega_c$ from the approximate values at $-\omega_3$ and $-\omega_4$. At $\alpha=9$, both of these poles reach $-\omega_c$ at the same time, forming a triple-order pole. A further decrease in α causes two poles to separate from this triple-order pole and form a conjugate-complex pair of poles, which travel along a circle with the origin as its center, so that the distance of all the poles from the origin remains constant at ω_c.

It should be noted that for $\alpha=9$, the resonant peak of the closed-loop function is $M_p=1.3=1.14$ lgt., and yet all of the closed-loop poles are real. This system is quite different in this respect from the basic second-order system

$$\frac{C}{R}=\frac{\omega_n^2}{s^2+2\zeta\omega_n s+\omega_n^2} \tag{117}$$

which has a ζ of 0.43 for an M_p of 1.3. For a given M_p the damping ratio ζ of the complex closed-loop pair of poles of the third-order system of Figure 16 must be significantly greater than that of the second-order system of equation 117, and yet the peak overshoot of the transient responses for both systems are essentially the same. Consequently, it is not safe to assume (as is often done) that the value of damping ratio of the two major complex closed-loop poles of a system is by itself a good indication of stability. Although the low-frequency and high-frequency closed-loop poles generally have little effect upon stability (unless they are quite underdamped), all of the poles of magnitude near the crossover frequency have an important effect upon the system stability.

Appendix II. Direction of Shift of Closed-Loop Poles From Open-Loop Poles and Zeros

Let us examine in more detail the direction of shifts of closed-loop poles from open-loop poles and zeros. These shifts occur along the s-plane loci for which the phase is an odd multiple of 180 degrees. A single-order open-loop pole or zero has one such locus emerging from it and hence tends to form a single closed-loop pole; a double-order open-loop pole or zero has two such loci emerging, and hence tends to form two closed-loop poles, which are shifted along each locus; and so forth, for higher-order open-loop poles and zeros.

In order to evaluate the direction of these loci at the open-loop poles and zeros, consider the following identity

$$G=[(s-s_a)^n][G/(s-s_a)^n] \tag{118}$$

In the vicinity of an nth-order zero at $s=s_a$, the second factor of equation 118 is quite constant. The angle of G is equal to

$$\text{Ang}\,(G)=n[\text{Ang}\,(s-s_a)]+\text{Ang}\,[G/(s-s_a)^n] \tag{119}$$

Equation 89 stated that closed-loop poles can occur only when the angle of G is an odd multiple of 180 degrees

$$\text{Ang}\,(G)=p(180°) \tag{89}$$

Substitution of equation 89 into equation 119 yields

$$\text{Ang}\,(s-s_a)=\frac{p}{n}(180°)-\frac{1}{n}\text{Ang}\,[G/(s-s_a)^n] \tag{120}$$

Equation 120 gives the angle of vectors drawn from the nth-order zero at s_a to points on the loci along which the closed-loop poles move. Consequently, if Ang $[G/(s-s_a)^n]$ is evaluated at $s=s_a$, equation 120 gives the angles of the loci emerging from the nth-order zero at s_a, there being one locus angle for a single-order zero ($n=1$), two loci angles for a double-order zero ($n=2$), and so forth. Since Ang $[G/(s-s_a)^n]$ is quite constant in the region about the zero at s_a, the angles of the loci will be quite constant in this region, and hence they will emerge from the zero in approximately straight lines.

By means of equation 120, a general plot can be made of the loci emerging from an nth-order zero at s_a, for which the phase of G is an odd multiple of 180 degrees. Such a plot is shown in Figure 18. Notice that the relative angles between the loci are equal.

In a similar fashion it can be shown that the angles of the loci emerging from an nth-order pole at $s=s_b$ are equal to

$$\text{Ang}\,(s-s_b)=\frac{p}{n}(180°)+\frac{1}{n}\text{Ang}\,[(s-s_b)^nG] \tag{121}$$

evaluated at $s=s_b$.

Let us apply equations 120 and 121 to a type of G-function that is quite frequently met in practice. Consider an open-loop function G with a negative real zero at $-\omega_3$ of order n and a negative real pole at $-\omega_4$ of order n', where $-\omega_3$ is the first singularity below ω_c (the crossover frequency) in magnitude, and $-\omega_4$ is the first singularity above ω_c in magnitude.

On the negative real axis, at $s=-\omega_c$, the following relations hold

$$\text{Ang}\,(s+\omega_4)=0,\text{ since }\omega_4>\omega_c \tag{122}$$

$$\text{Ang}\,(s+\omega_3)=180°,\text{ since }\omega_3<\omega_c \tag{123}$$

$$\text{Ang}\,(G)=-180°,\text{ for reason of stability} \tag{124}$$

Consequently, at $s=-\omega_c$

$$\text{Ang}\,[(s+\omega_3)^n/G]=n[\text{Ang}\,(s+\omega_3)]-\text{Ang}(G)=(n+1)180° \tag{125}$$

$$\text{Ang}\,[(s+\omega_4)^{n'}G]=n'[\text{Ang}\,(s+\omega_4)]+\text{Ang}\,(G)=-180° \tag{126}$$

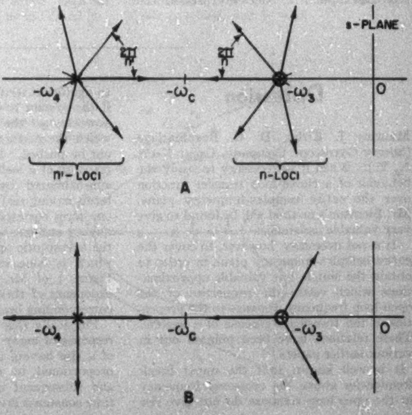

Figure 19. Loci of shift of closed-loop poles, near the crossover frequency, for a common type of transfer function

A. nth-order pole at ω_4; nth-order zero at $-\omega_3$

B. Fourth-order pole at $-\omega_4$; third-order zero at $-\omega_3$

The angle $[(s+\omega_3)^n/G]$ has the same value at $s=-\omega_3$ that it has at $s=-\omega_c$ because the function does not contain any singularity at $-\omega_c$, nor does it contain any singularity between ω_c and ω_3 in magnitude. Consequently, equation 125 also holds at $s=-\omega_3$. Similarly, it can be shown that equation 126 also holds at $-\omega_4$.

Substitution of equations 125 and 126 into equations 120 and 121 respectively yields as the angles of the loci emerging from the nth-order zero at $-\omega_3$ and the n'th-order pole at $-\omega_4$

$$\text{Ang}\,(s+\omega_3)=\left(\frac{p+1}{n}\right)(180°)+180°, \quad \text{for } s=-\omega_3 \qquad (127)$$

$$\text{Ang}\,(s+\omega_4)=\frac{p-1}{n'}(180°), \text{ for } s=-\omega_4 \qquad (128)$$

These loci are plotted in Figure 19(A). In Figure 19(B) the loci for specific values of n and n' are shown ($n=3$, $n'=4$). Notice that each open-loop pole and zero produces one closed-loop pole which moves along the negative real axis toward $-\omega_c$. If the order of the open-loop or zero is no greater than 4, the other closed-loop poles tend to move away from $-\omega_c$, and consequently, there are only three closed-loop poles in the region near the cross-over frequency in magnitude.

Appendix III. Graphical Evaluation of Coefficients of Partial-Fraction Expansion

Once the poles of a function have been evaluated, it is necessary to evaluate the coefficients associated with these poles in order to determine the transient response. Although these coefficients may be evaluated fairly readily by ordinary numerical methods, it is useful to consider a method for evaluating them graphically. (The following analysis is essentially a restatement of Appendix A of the paper by Kusters and Moore.[2])

The controlled variable $C(s)$ for a given reference input $R(s)$ may be expressed as[4]

$$C=\left(\frac{G}{1+G}\right)R=\sum_{j=1}^{J}\frac{K_j}{(s-s_j)}+\sum_{L=1}^{L}\frac{K_l'}{(s-s_l')} \qquad (129)$$

where the first summation contains all of the (J) poles of the transfer function $(C/R)=G/(1+G)$; while the second summation contains all of the (L) poles of the transform R. We shall limit ourselves in this discussion to the evaluation of the J coefficients K_j of the poles of (C/R), and shall not consider the evaluation of the coefficients K_l' of the poles of R.

For single-order poles K_j is equal to

$$K_j=(s-s_j)\left(\frac{G}{1+G}\right)R\bigg|_{s=s_j} \qquad (130)$$

Since $G=-1$ at the pole $s=s_j$, we may apply L'Hospital's rule to obtain

$$K_j=-(dG/ds)^{-1}R\big|_{s=s_j} \qquad (131)$$

We would like to evaluate K_j from plots of G along the radial axis in the s-plane passing through the pole at $s=s_j$. Express G and s in polar form

$$G=|G|\epsilon^{j\phi},\ \phi=\text{Ang}\,G \qquad (132)$$

$$s=|s|\epsilon^{j\psi},\ \psi=\text{Ang}\,s \qquad (133)$$

On a radial axis in the s-plane, ψ is constant and equal to the angle of the axis, while $|G|$, ϕ, and $|s|$ are variables. Differentiation of equations 132 and 133 yields for (dG/ds) along a radial axis

$$\frac{dG}{ds}=\left[\frac{\partial|G|}{\partial|s|}+j|G|\frac{\partial\phi}{\partial|s|}\right](\epsilon^{j\phi}/\epsilon^{\phi}) \qquad (134)$$

Substitute equation 134 into equation 131, noting that at a pole of (C/R): $G=-1$, and hence $|G|=1$, $\epsilon^{\phi}=-1$

$$K_j=\left[\frac{\partial|G|}{\partial|s|}+j\frac{\partial\phi}{\partial|s|}\right]^{-1}\epsilon^{j\psi}R\bigg|_{s=sj} \qquad (135)$$

Since the plots of G are usually drawn to a log-log scale, a more convenient expression for K_j is

$$K_j=\frac{sR}{\dfrac{(\partial y/\partial x)}{10}+j\dfrac{(\partial\phi/\partial x)}{2.30}}\Bigg|_{s=sj} \qquad (136)$$

where

$\partial y/\partial x$ = slope of $|G|$ plot in logits/decade

$\partial\phi/\partial x$ = slope of Ang G plot in radians/decade

If the pole is real, then $(\partial\phi/\partial x)=0$; and if the reference input is a unit step, then $R=(1/s)$. Equation 136 simplifies to

$$K_j=10(\partial y/\partial x)^{-1}\big|_{s=sj} \qquad (137)$$

Thus, for a step input, the coefficient K_j at a real pole is proportional to the reciprocal of the slope of the magnitude plot of G along the negative real axis at that pole. At a maximum or minimum point on the $|G|$ plot along the negative real axis, K_j becomes infinite, and hence such a point must yield a higher-order pole, as was stated previously. This graphical method may be extended to allow evaluation of the coefficients at higher-order poles, but the evaluation procedure becomes quite cumbersome.

References

1. CONTROL-SYSTEM SYNTHESIS BY ROOT LOCUS METHOD, **W. R. Evans.** *AIEE Transactions*, volume 69, part I, 1950, pages 66–69.
2. AUTOMATIC AND MANUAL CONTROL (book) **A. Tustin**, "A Generalization of the Frequency Response Method for Study of Feedback Control Systems," **N. L. Kusters, W. J. M. Moore.** Butterworth Scientific Publications, London, England, 1952.
3. PROPOSED SYMBOLS AND TERMS FOR FEEDBACK CONTROL SYSTEMS, **AIEE Committee Report.** *Electrical Engineering*, volume 70, October 1951, pages 905–09.
4. TRANSIENTS IN LINEAR SYSTEMS (book), **M. F. Gardiner, J. L. Barnes.** John Wiley and Sons, Inc., New York, N. Y., volume I, 1945.
5. FUNDAMENTAL CONSIDERATIONS REGARDING THE USE OF RELATIVE MAGNITUDES, **J. W. Horton.** *Proceedings*, Institute of Radio Engineers (New York, N. Y.), April 1952.
6. PRINCIPLES OF SERVOMECHANISMS (book), **G. S. Brown, D. P. Campbell.** John Wiley and Sons, Inc., New York, N. Y., chapter 8, 1948.

◆

Discussion

Maurice J. Kirby, D. C. Beaumariage (Sperry Gyroscope Company, Great Neck, N. Y.): When it is necessary to study the behavior of a closed-loop transfer function over the entire complex-frequency plane, Mr. Biernson's method will be found to give very valuable assistance.

It is not necessary, however, to cover the entire complex-frequency plane in order to obtain the simple but valuable approximations which relate the properties of the open-loop frequency response to the properties of the transient response of a system. These relations have been pointed out in various earlier papers.[1,2]

It is well known that the upper break frequencies above the crossover frequency in the open-loop response do not give rise to significant terms in the transient response if the system is well stabilized. They do, however, set the limit of stability beyond which the performance of the system cannot be pushed. Furthermore the transient response of a well stabilized system can be approximated by a sum of exponential terms having real exponents.[2] In this sum, one term corresponds to the crossover frequency and one to each break frequency in the asymptotic open-loop transfer function which is concave upward (ω_c, ω_2, ω_3 in Figure 1 of Mr. Biernson's paper). The exponents of these terms are equal to the corresponding break frequencies.

Physically this means that the transient response of many common systems consists of a rise having a time constant inversely proportional to the crossover frequency, and subsequent decays or "tails" having time constants inversely proportional to the breaks such as ω_2 and ω_3 below the crossover frequency. The amplitudes of these terms, and hence the degree of overshoot in the response to a step of input displacement, or the peak error in the response to a step of velocity, can be approximated rather simply. From this it is obvious that integral networks or others which add low-frequency breaks to the open-loop transfer function add corresponding tails to the transient response; these decay with time constants $1/\omega_2$, and $1/\omega_3$, in the example of the paper.

REFERENCES

1. LINEAR SERVO THEORY, **Robert E. Graham.** *Bell System Technical Journal* (New York, N. Y.), October 1946, page 616.
2. SERVOMECHANISM TRANSIENT PERFORMANCE FROM DECIBEL-LOG FREQUENCY PLOTS, **H. Harris, Jr., M. J. Kirby, E. F. Von Arx.** *AIEE Transactions*, volume 70, part II, 1951, pages 1452–59.

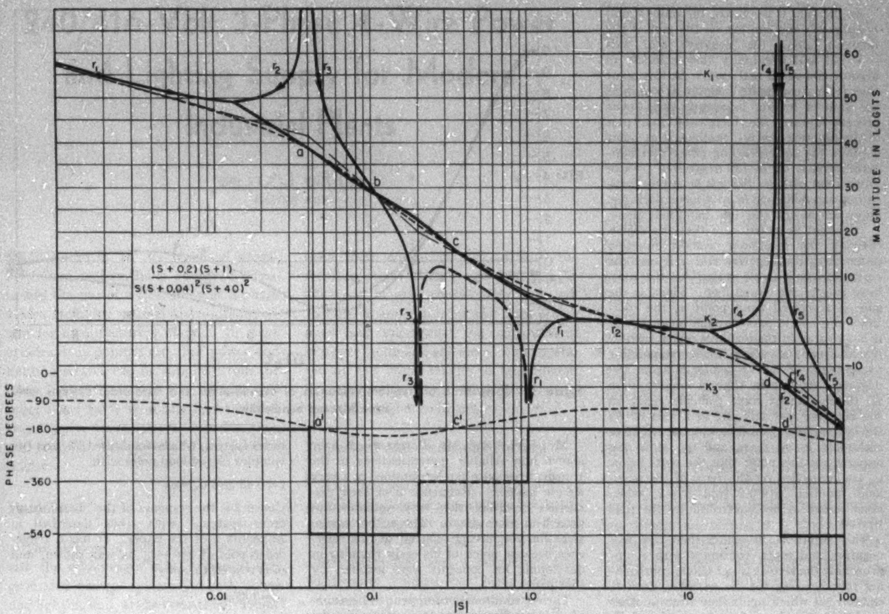

Figure 1. Plot of open-loop transfer functions and closed-loop locus

▬ Open-loop transfer function along negative real axis
- - - Open-loop transfer function along positive imaginary axis
—— Closed-loop locus

N. L. Kusters, W. J. M. Moore (National Research Council, Ottawa, Ontario, Canada): Mr. Biernson is to be complimented on the work that he has done on methods of evaluating the poles of the closed-loop transfer function from the poles and zeros of its open-loop counterpart, and especially with regard to the detailed analysis he has presented in their support. There is no doubt that a knowledge of the location of the poles of the closed-loop transfer function is of considerable importance in assessing the performance of a feedback-control system.

It is our opinion, however, that a clearer understanding of the factors affecting the location of the poles of the closed-loop function and their exact determination can best be obtained by studying the root locus as gain is increased from zero to infinity.

The root locus can be obtained by considering a plot of the log-magnitude and the phase curves of the open-loop transfer function against log $|s|$ along both the negative real and positive imaginary axis of the s-plane. These curves are quite easily drawn, since:

1. along the negative real axis, the phase curves are straight lines.
2. along the positive imaginary axis, the log-magnitude curves can be approximated by straight line asymptotes.

From these open-loop curves, a root-locus plot of the closed loop can easily be drawn on the same diagram.

A plot of these curves for the open-loop transfer function is shown in Figure 1 of the discussion. This function is similar to that discussed by the author except that it includes the variation which he indicated in Figure 10 of the paper.

$$\frac{(s+0.2)(s+1)}{s(s+0.04)^2(s+40)^2}$$

At very low values of gain, such as K_1, there are five negative real roots r_1, r_2, r_3, r_4, and r_5 since at these points on the plot of the open-loop function along the negative real axis, the value of the function is unity and the phase is −180 degrees or an odd multiple thereof. It is apparent that the location of these roots at this low gain is largely determined by the poles of the open-loop transfer function which occur at $|s|=0$, $|s|=0.04$, and $|s|=40$.

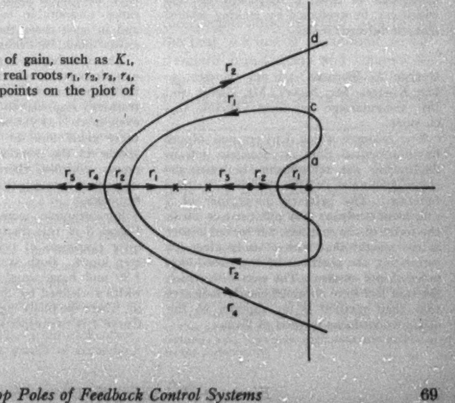

Figure 2. Root-locus plot in S-plane (not to scale)

As the gain is increased, the roots r_1 and r_2 approach one another on the plot of the function along the negative real axis ($s=-\omega$) and eventually they coincide to become two equal real roots. At this point they form a conjugate complex pair and, as the gain is further increased, their locus proceed toward the imaginary axis plot of the function ($s=j\omega$), reaching it at point a where the corresponding phase plot indicates a phase lag of 180 degrees (a'). The locus then crosses the $s=j\omega$ curve, indicating instability or in root-locus parlance, an excursion into the right-hand half plane.

It should be noted here that the region between the open-loop transfer function plots along the negative real axis and the $s=j\omega$ axis is a stable region for the root-locus plot of the closed loop. Thus, as the gain is increased from point a, the root-locus plot has to pass through point b since it has to stay in the unstable region until it reaches point c, where the corresponding phase curve of the $s=j\omega$ plot is again 180 degrees. At a gain slightly smaller than K_2 these complex roots coincide again on the negative real axis and at a gain of K_2 the system has again five separate negative real roots, r_3, r_1, r_2, r_4, and r_5. It is also apparent at this point that the roots below ω_c are controlled by the zeros of the open-loop function $|s|=0.2$ and $|s|=1$, while those above ω_c are controlled by the pole $|s|=40$.

This situation, in which there are five negative real roots, continues with r_1 approaching the zero at $|s|=1$ and r_2 approaching root r_4 along the $s=-\omega$ plot, until r_2 equals r_4 at which point they form another conjugate complex pair. At a gain of K_3 then, the system has two stable conjugate complex roots r_2 and r_4 and three negative real roots r_3, r_1, and r_5. The system finally becomes unstable at a gain corresponding to point d, at which the phase lag of the $s=j\omega$ plot is again 180 degrees (d'), and the complex roots r_2, and r_4 assume positive real parts.

The foregoing could also have been explained by using the root-locus method of Evans, which would give a plot similar to Figure 2 of the discussion. However any attempt to plot this figure accurately for the function described is practically impossible, due to the large separation of its poles and zeros. This is an inherent disadvantage in Evan's root-locus method which can be overcome by making several plots of different scales.

George A. Biernson: I am thankful to Mr. Kusters, Mr. Moore, Mr. Kirby, and Mr. Beaumariage for their valuable discussions.

The example which Kusters and Moore have presented does an excellent job in illustrating the relationship between the closed-loop poles and the open-loop transfer function. The primary importance of a root-locus study, as they point out, is not in the forms of the root loci, per se, but rather in the insight that such a study gives for estimating the positions of the closed-loop poles of any system. The ease with which the root loci were obtained clearly indicates that their method is far superior to the original root-locus method of Evans.

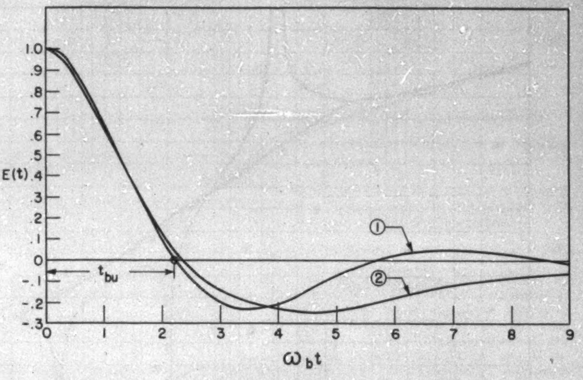

Figure 3. Comparison of transient responses of second-order and third-order systems with same Mp and bandwidth

Mr. Kirby and Mr. Beaumariage have shown how reliable approximations to the transient response can be obtained in a very simple manner. Reference 2 of their discussion describes this very valuable approach in more detail. The author apologizes for not having referred to this reference because much of his early thinking in developing his concepts were inspired by that paper.

These two discussions appear to be somewhat in conflict in that one emphasizes the advantages of the rigorous graphical method; and the other, the simplicity and adequacy of the approximation method. Let us consider the relative practical merits of the two and also how they compare with the standard frequency-response method of analysis.

If one desires to obtain a good approximation to a transient response, without excessive labor, it is best to divide the complex-frequency plane into three regions: high frequency, mid frequency, and low frequency.

High-frequency poles ($|s|>>\omega_c$) generally have little effect upon the transient response and can usually be neglected. However, if they are quite underdamped, they may cause undesirable secondary oscillations; and in such cases their values and coefficients should be evaluated exactly.

The mid-frequency poles ($|s|\approx\omega_c$) are the most important because they determine the build-up time and peak overshoot of the transient response to a step input. However, there is as yet no simple way to relate these characteristics of the transient response to the positions of the closed-loop poles; whereas, there is a simple correspondence between them and the frequency response.

For example, consider the curves in Figure 3 of this discussion, which are the error responses of two systems to a unit step input. Both systems have an M_p of 1.30 and have equal bandwidths. Bandwidth is defined by the frequency, denoted ω_b, where the phase lag of C/R is 90 degrees. Curve *1* is the response of a simple second-order system, which (for $M_p=1.30$) has two complex closed-loop poles with

$$\zeta=0.43 \text{ and } \omega_n=\omega_b$$

Curve *2* is the response of the "basic third-order system," with $\alpha=9$, described in Appendix I of the paper. It has a triple-order pole at $s=-\omega_c$, as was shown, and ω_c is related to ω_b by

$$\omega_b=1.47\omega_c$$

The equations for these two transient curves are

$$E(t)=1.107\epsilon^{-0.43\omega_b t}\sin(0.904\omega_b t+64.6°)$$

and

$$E(t)=\epsilon^{-\omega_c t}(1+\omega_c t-\omega_c^2 t^2)$$

Despite the differences in the positions of the closed-loop poles and in the forms of the transient equations, the values of peak overshoot (P_{ov}) and build-up time (shown in the figure as t_{bu}) are practically the same for the two systems. They are

$$\left.\begin{array}{l}\text{System 1 } P_{ov}=0.23,\ t_{bu}\omega_b=2.22\\ \text{System 2 } P_{ov}=0.25,\ t_{bu}\omega_b=2.38\end{array}\right\}\ \begin{array}{c}\text{For}\\ M_p=1.30\end{array}$$

Thus, the standard frequency-response approach appears to be the best simple method for analyzing the effect of the mid-frequency poles upon the transient response.

It is in the low-frequency region ($|s|<<\omega_c$) where the methods of this paper are most valuable. The author has found that a combination of the approximation method and the graphical method is usually adequate for determining such things as tails in the transients, the error response for constant velocity inputs, and so forth. However, in certain complex multiloop control systems, secondary feedback paths can produce unusual pole-zero configurations in the low-frequency portion of the transfer function of a particular loop; and the author has found the graphical approach invaluable in determining their effect. Besides, a firm understanding of the graphical method is extremely useful for enabling one to make intelligent use of the approximation method.

240/416-Volt 3-Phase 4-Wire Power and Lighting Supply for Modern Industrial Plants

WILLIAM SHULER
FELLOW AIEE

RECENTLY, in the technical magazines, articles have appeared advocating the use of a 277/480-volt 3-phase 4-wire grounded neutral distribution system for manufacturing plants. In these articles, it is pointed out that power and lighting service can be supplied from the same feeders by connecting motors, and other large loads requiring 3-phase electric supply, to the 3-phase conductors, and lamps to the phase and neutral conductors.

Purpose

The purpose of this paper is to emphasize the advantages of a 3-phase 4-wire grounded neutral system for both power and lighting and, at the same time, demonstrate the superiority of a 240/416-volt system over the 277/480-volt system. The 240/416-volt system is preferable for at least four reasons.

Advantages

First, it will permit the use of fluorescent lamps which have already been designed and catalogued and will not necessitate the development of another completely new line of accessories.

Second, the Underwriters' Laboratories have placed a 250-volt limit on general purpose switches for lighting circuits. The phase-to-neutral voltage of the 240/416-volt system is below this limit. The 277/480-volt system necessitates remote control for all lighting circuits, and hence, adds more expense, as well as complication, to the distribution system.

Third, it will permit the use, in 3-phase banks, of single-phase transformers having a low-voltage winding rated at 240 volts.

The fourth, and principal, reason for favoring a lower voltage system arises from the fact that manufacturing plants in America are now equipped with individually motor-driven machine tools operating at an average load that is far below their rating. When these motors are operated at 480 volts, 460 volts, or even their design voltage of 440, the resulting power factor is very low, and the efficiency is also considerably reduced. In fact, it appears from test data which have been taken that the improvement in power factor and efficiency, when operated at 416 volts, results in less current in the secondary feeders than when operated at the higher voltages.

Important and Pertinent Factors

The suggestion that machine tool motors be operated at a voltage below the nominal rating may appear to be a radical idea in view of the fact that for many years there has been a conviction that inadequate voltage was being supplied to most 3-phase induction motors.

However, considering the tremendous success which has attended the introduction of the 3-phase 4-wire low-voltage network system which operates at 120/208 volts, a 240/416-volt system can scarcely be called revolutionary. The number of complaints which our industry is receiving due to low voltage on network systems have become negligible. If, therefore, this system has proved to be so satisfactory, it is obvious, from the motor curves and test reports shown in Figures 1 to 11 and Tables I to VII inclusive, that a 240/416-volt system should be equally satisfactory in the modern manufacturing plant.

In discussing this subject, three factors must be taken into consideration.

1. The jack-shaft, which was almost universally used in the early part of this century when electric power began to compete with other forms of power in manufacturing plants, has been supplanted by the individually motor-driven machine tool.
2. Machine tools have become so complicated and so expensive that the additional cost of a motor twice the size of the required motor is an insignificant item. As a result, it seems probable that the machine tool designer has specified an oversized motor in order to be sure of ample torque.
3. Most large manufacturing plants now have distribution substations located at relatively short distances from each other. This has reduced the length of secondary feeders, and the voltage drop has been reduced not only by the shortening of the feeders but also by the introduction of low-impedance distribution arrangements.

Effect of Recent Voltage Standardization

Recently, the Transmission and Distribution and the Electrical Equipment Committees of the Edison Electric Institute agreed with the manufacturers on a voltage standardization which should result, ultimately, in considerable savings in money to the operating companies, as well as in simplification of manufacturing for the equipment suppliers. The standard voltages for power and lighting are now 480, 240, and 120.

Inasmuch as The Dayton Power and Light Company has a very large residential load supplied at 12 kv from the substation busses, the voltage is in excess of 12 kv, because it is the plan to deliver 124 volts at the terminals of the first transformer nearest the substation supplying residential customers. Where such busses and/or feeders also supply manufacturing plants, it is obvious that instead of delivering 480 volts to the power customers, we deliver something in excess of that. In one case, the voltage went up above 490 volts at the transformer bank supplying one of the large customers. It is probable that many systems having adequate distribution facilities are receiving similar complaints.

Our company has been purchasing transformers rated 12,000-480/240 or 240/120. There have been many high-voltage complaints from power customers. It is apparent that instead of confining our purchases to standard transformers having this rating, it will be necessary for us to purchase either transformers having taps above normal voltage or in the next voltage class, namely, the 13.2-kv class, in order to eliminate these complaints. A third, and by far the best, solution is to continue to buy standard transformers and connect the 120-volt or 240-volt secondaries in wye to give either 120/208 or 240/416 volts.

Paper 53-72, recommended by the AIEE Industrial Power Systems and Transmission and Distribution Committees and approved by the AIEE Committee on Technical Operations for presentation at the AIEE Winter General Meeting, New York, N. Y., January 19–23, 1953. Manuscript submitted October 20, 1952; made available for printing December 4, 1952.

WILLIAM SHULER is with The Dayton Power and Light Company, Dayton, Ohio.

The author wishes to acknowledge the contributions of D. D. Colker, The Dayton Power and Light Company, who contributed to the test data and offered helpful suggestions on the preparation of this paper, and also the assistance of the manufacturers who have submitted data and curves on motor performance.

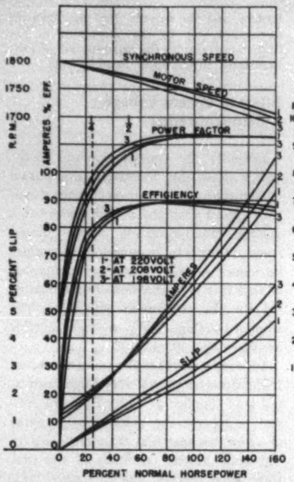

Figure 1 (left). Typical characteristics of standard 3-phase induction motor, 220 volts, 1,800-rpm synchronous speed

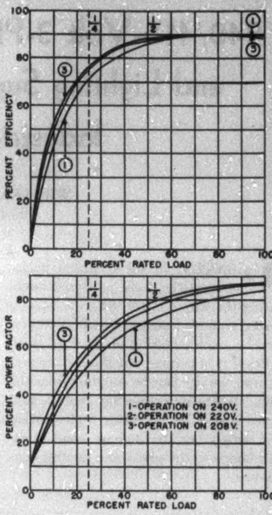

Figure 3 (right). Efficiency and power-factor curves for 25-horsepower 3-phase induction motor, 220 volts, 1,800-rpm synchronous speed, 40-degree-centigrade rise

Test Data Interpreted by Reference to Motor Performance Curves

For many years, tests conducted by our test department on customers' premises have indicated that their motors are operating at a very low power factor.

Although all of the motor performance curves and much of the test data presented in this paper are based on 220-volt operation, it must be borne in mind that in every case the performance would be the same for both the 120/208-volt and the 240/416-volt systems.

The typical standard 3-phase induction motor operates at a fairly high power factor at full load. In Figure 1 are curves showing the characteristics of a standard 25-horsepower 3-phase squirrel-cage induction motor of the 220-volt class and in the 1,800-rpm synchronous speed range, which is considered typical of 3-phase motors rated 50 horsepower and under. These curves, as well as all others shown, will be the same for motors rated 440 volts, since the volts per phase per turn are the same in both ratings. These characteristics will vary with the different types of motors, but the curves shown are considered typical of the average motor encountered in a modern factory. The curves shown in Figure 1 are based on three voltages. The number 1, 2, and 3 curves represent applied voltages at the motor terminals of 220, 208, and 198 volts respectively. These curves show the effect of normal and undervoltage on the operation of the motors.

Refer to the curves and note that if the average power factor of a customer's load when uncorrected is as low as 70 per cent and the voltage at the motor terminals is 220 or 440 volts, it indicates that the motors are operating at less than 25 per cent of full load. The efficiency of a motor, when operating at 220 volts at one-fourth load, is 6 per cent less than it would be if it were operating at 198 volts, and the power factor is about 8 per cent less.

These curves indicate that the efficiency of the motors, when operating at 198 volts, is as good or better than when operating at 220 volts until they are loaded up to 70 per cent of their full-load rating. Even at 100 per cent of rating, the efficiency is not more than 2 per cent less at 198 volts than it is at 220 volts. Furthermore, the power factor, when operating at 198 volts, is higher than when operating at 220 volts until the motor is loaded above 130 per cent of full load.

The ampere curves are also interesting. The current in the customer's secondary feeders is no more when operating at 198 volts than when operating at 220 volts until the motors are loaded to approximately 45 per cent of full load. Below that rating the amperes are less.

Effect on slip is shown by curves *1* and *2*. Representing operation at 220 and 208 volts respectively, they indicate a change in slip of approximately .3 of 1 per cent at full load. This would correspond to a speed change of approximately 5 rpm on 1,800-rpm motors which, obviously, would not be noticeable. However, since a normal average load of approximately 25 per cent is indicated, the change in slip, as shown by curves *1* and *2*, is negligible.

Curves shown in Figure 1 are for motors manufactured prior to 1939, and while it

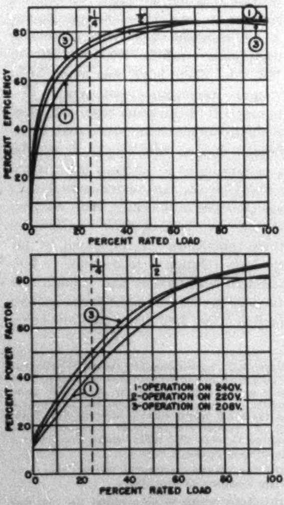

Figure 2. Efficiency and power-factor curves for 5-horsepower 3-phase induction motor, 220 volts, 1,800-rpm synchronous speed, 40-degree-centigrade rise

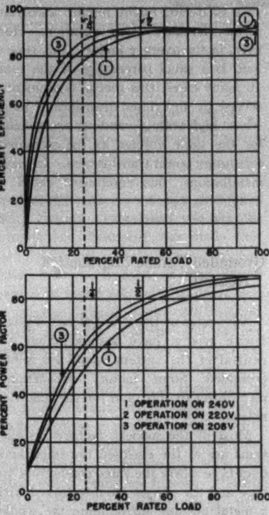

Figure 4. Efficiency and power-factor curves for 50-horsepower 3-phase induction motor, 220 volts, 1,800-rpm synchronous speed, 40-degree-centigrade rise

Table I. Load and Power Factor Tests. Small Plant with Delta-Connected Secondaries

Time	Kilowatts	Kilovars	Per Cent Power Factor	Volts
AM				
8:00	48	79.2	51.8	244
9:00	50.4	81.2	52.7	240
10:00	46.8	74.4	53.1	240
11:00	50.4	87.6	49.8	244
PM				
1:00	50.4	87	50.0	
2:00	52.8	93.6	49.0	
2:15	50.4	91.2	48.3	

The above readings were taken during a 6¼-hour production run under normal plant operation.

Table II. Load and Power Factor Tests. Small Plant with Wye-Connected Secondaries

Time	Kilowatts	Kilovars	Per Cent Power Factor	Volts
AM				
8:00	48	62.5	60.8	216
9:00	67	91.2	59.2	212
10:00	64.8	86.5	59.9	212
11:00	57.6	81.5	57.7	212
PM				
1:00	52.8	72	59.2	
2:00	48	69.5	56.7	
2:15	52.8	64.8	63.0	

The above readings were taken during a 6¼-hour production run under normal plant operation.

is probable that most of the motors in service on our system are of the vintage corresponding to these curves, additional information on motors designed from 1945 to 1948 is presented in Figures 2 to 4 inclusive.

In Figure 2 are performance curves, showing efficiency and power factor only, based on operation at 240, 220, and 208 volts for a 5-horsepower 1,800-rpm motor. At 25-per-cent load, the efficiency of this motor is 7 per cent less when operating at 240 volts than it is when operating at 208 volts, and the power factor is 8 per cent less. However, if we assume operation at 50-per-cent load, the efficiency is 3 per cent less when operating at 240 volts than when operating at 208 volts, and the power factor is 7 per cent less.

In Figure 3 is a similar set of curves for a 25-horsepower 1,800-rpm motor. Referring again to the operation at 25-per-cent load, the efficiency, when operating at 240 volts, is 6 per cent less than when operating at 208 volts, and the power factor is over 8 per cent less. At 50-per-cent load, the difference in efficiency is 2 per cent; in power factor 7 per cent.

Figure 4 shows a similar set of curves for a 50-horsepower 1,800-rpm motor. In this case, the improvement in efficiency is 7 per cent and in power factor 10 per cent when operated at 208 volts instead of 240 volts. At 50-per-cent load, the gain in efficiency is 3 per cent and in power factor 7 per cent.

In all cases, these curves show that even at 100-per-cent load the increase in efficiency, when operating at 240 volts, is only 2 per cent more than when operating at 208 volts, although the power factor is still 4 per cent less.

Test Data

Tables I and II show data which were taken at a small plant and which indicate the change in power factor when the secondaries of the transformers serving this customer were changed from delta to wye. This resulted in a change in their power service entrance voltage from approximately 240 volts to approximately 208 volts. The manager stated that the operating conditions prevailing at the time of these two tests were similar. The data prove there is a considerable improvement in power factor when operating at the lower voltage. In fact, it is about 9 per cent higher. This factory has continued to operate on 208 volts 3 years after the transformer bank was connected in wye.

Data in Table III were secured at the largest plant supplied by our company. For the purpose of the test, the feeder was stripped of all capacitors which had been installed for power-factor correction. The voltage drop along the feeder was very slight. It is interesting to note that the voltage at one time was 444 and the power factor 70.7 per cent and at another time, when the voltage dropped to 434, the power factor was 75.0 per cent. Throughout the table, there are similar variations in load, power factor, and voltage.

Table IV shows a tabulation of results obtained from tests at the plant of another large customer. The 3-phase transformer on which the tests were made carries all the lighting load in the area fed by it as well as the power load. Part A shows that during periods of heavy loading, the power factor varies from 70.7 per cent to 77.2 per cent. Part B represents part A corrected to eliminate the effect of lighting load. It indicates that the motors were operating at a power factor ranging from 45.0 per cent to 51.0 per cent. This customer is located near one of our substations, and the voltage at the transformer bank varies from 480 to over 490 volts.

Present low-voltage a-c network systems are adequately supplying the power load, as well as the lighting circuits, at the nominal voltage of 120/208 without autotransformers. Furthermore, the data here presented indicate that the lower voltage is beneficial not only to the power company supplying the load but also to the customer because of the increase in efficiency and power factor. Lower voltage is also of considerable benefit to those customers operating on a

Table III. Load and Power Factor Tests. Large Plant with Delta-Connected Secondaries

Time	Kilowatts	Kilovars	Per Cent Power Factor	Volts
7-26-49				
AM				
8:00	736	720	73.5	442
9:00	608	608	70.7	456
10:00	688	720	69.1	440
11:00	752	752	70.7	444
PM				
1:00	752	720	75.1	434
2:00	720	720	70.7	436
3:00	688	680	71.7	432
4:00	640	592	73.5	440
5:00	640	560	75.3	440
7-27-49				
AM				
8:00	768	720	72.9	440
9:00	640	640	70.7	452
10:00	760	736	71.8	436
11:00	688	720	69.1	440
PM				
1:00	680	656	72.0	428
2:00	720	656	73.9	436
3:00	680	624	73.7	436
4:00	672	576	76.0	436
5:00	672	608	74.1	436

Table IV. Load and Power Factor Tests. Large Plant with Delta-Connected Secondaries

*	Time	Kilowatts	Kilovars	Per Cent Power Factor	Volts
Part A					
8-15-49					
AM					
	8:00	496	424	76.0	
	9:00	504	456	74.1	From
	10:00	488	472	71.8	
	11:00	480	456	72.5	480
PM					
	1:00	496	408	77.2	
	2:00	504	440	75.3	to
	3:00	480	432	74.3	
	4:00	376	240	84.3	492
	5:00	312	240	79.2	
8-16-49					
AM					
	8:00	472	408	75.7	
	9:00	456	400	75.2	From
	10:00	472	440	73.1	
	11:00	464	464	70.7	480
PM					
	1:00	456	420	73.5	
	2:00	456	416	73.8	to
	3:00	464	416	74.4	
	4:00	360	264	80.6	492
	5:00	304	240	78.4	
Part B					
8-16-49					
AM					
	8:00	242	408	51.0	
	9:00	226	400	49.0	From
	10:00	242	440	48.0	
	11:00	234	464	45.0	480
PM					
	1:00	226	420	47.0	
	2:00	226	416	48.0	to
	3:00	234	416	49.0	
	4:00	130	264	44.0	492
	5:00	74	240	59.0	

* One of several 750-kva transformers.

schedule carrying a power-factor clause, inasmuch as the lower voltage reduces by a very considerable amount the kilovolt-ampere of corrective capacitors required to reduce their kilovolt-ampere demand.

The Reactive Kilovolt-Ampere Input to an Induction Motor Varies as the Square of the Applied Voltage and, in Some Cases, by an Even Greater Power

As stated early in this article, customers are benefited by a lower service voltage for their motor load because in a modern factory with machine tools individually driven, there has been a tremendous amount of over-motoring resulting in an average load far below the rating of the machine tool motors. This statement does not apply to a few applications such as fully and continuously loaded air compressors, ventilating fans, pumps, and motors of that type. However, many motors in this class have been found to be underloaded.

Table V. Load and Power Factor Tests. Large and Small Plants

Kind of Business	Kilowatts	Kilovars	Per Cent Power Factor	Volts
Machine shop	321	624	45.7	250
Foundry	457	546	64.1	236
Laundry	104	96	73.5	234
Aircraft parts	112	104	73.3	230
Concrete building products	115	163	57.7	226
Die casting	66	60	73.7	226
Machine and tool	190	204	68.2	220
Airplane propellers	110	139	62.1	231
Blowers and fans	144	204	57.6	248
Putty	102	132	61.3	229

Probably the principal objection to less than normal voltage for plant distribution systems is the fear that some motors may be loaded beyond the point of stability where a further increase in load would result in a reduction of torque developed. The pull-out torque of an induction motor varies as the square of the voltage. It is, therefore, reduced by 19 per cent when the voltage is reduced by 10 per cent. In the case of a 416-volt system, the reduction in voltage is less than $5\frac{1}{2}$ per cent. The reduction in pull-out torque would, therefore, be only 10 per cent. It has been obvious on all tests made that this reduction is insignificant, since in almost all cases, the pull-out torque at normal voltage varies from 210 per cent to 250 per cent of full-load torque.

Some objections might be raised on the basis that the pull-out torque is still further reduced when disturbances occur on the system. This argument, it would appear, is not valid because if it were, trouble would have been experienced on our low-voltage network systems. The experience of the operating companies with the low-voltage network system refutes this argument. These disturbances do not cause trouble because the modern transmission and distribution system is protected by relays and other protective devices which relieve the system of disturbances in such a short period of time that no appreciable effect is observed on the performance of motors.

Special Considerations

There are a few items that require special attention in any plan which may be proposed to change a distribution system from 480-volt delta to 240/416 volt, 3 phase, 4 wire.

First, all protective devices should be studied to determine whether the protection is adequate. This may depend on whether the neutral is grounded through a resistance or solidly grounded.

Second, any welders or ovens which could not be reconnected so as to operate at 240 volts single phase, in the case of welders, or 240/416 volts wye, in the case of ovens, might require autotransformers for satisfactory operation. However, in the average factory, this type of load is a small percentage of the total. In many cases, this special equipment is served by individual transformer banks whose high-voltage windings are specified for the same voltage as the step-down substation power transformers. In future installations, this equipment could be bought to operate on the 120/208- or 240/416-volt systems.

Grounded Versus Ungrounded Neutral

Advocates of the 277/480-volt 3-phase 4-wire system have assumed that the neutral of the system would be solidly grounded. Some factory maintenance men object to this plan for the following reason.

Most of the modern factory installations are of the enclosed low-impedance duct type where the three conductors are bare and the phases are interleaved with a metal housing surrounding the whole. Factory maintenance men do make contact with their tools between this housing and one of the phases. In the case of a delta system having no ground, the current flowing is of a limited value, and the worst results have been occasional shocks. The opinion of these men is that this type of trouble is much less hazardous to personnel than a solidly grounded neutral would be because in that case, the phase-to-ground current would produce a heavy short-circuit current, and the damage to personnel might be very great.

Where this objection exists, it could be met by grounding the neutral through a relatively high resistance. This would eliminate the high voltages which might be set up due to resonance between the capacitance and the inductance of the circuits, and at the same time would reduce the fault current flowing from phase conductor to duct sheath to a very small value. However, if this resistance were kept at a figure considerably below the resistance of the human body, it would still limit the voltage to which personnel would be subjected to a value represented by the phase-to-neutral voltage. In the case of a neutral grounded through resistance, it would, of course, be necessary to insulate the neutral conductor in the duct system.

It is believed that the objections previously mentioned do not offset the advantages of the solidly grounded neutral. For many years in England they have been using a 3-phase 4-wire 240/416-volt system. In a recent letter from one of

Table VI. Individual Motor Tests

Machine	Average Kilowatts	Maximum Kilowatts	Kilovars	Average Per Cent Power Factor	Volts
Punch press, 3-phase, 30 horsepower, 1,760 rpm	13	20	9	82.6	444
Planer, 3-phase, 40 horsepower, 880 rpm	4	5.2	17.2	22.6	436
Milling machine, 3-phase, 10 horsepower, 1,750 rpm	2	3	3	55.3	432

the members of the United Kingdom Electricity Supply Team which visited this country, the statement was made that after consideration of the various voltages which have been used, it was finally decided to make 240 volts standard and to use the 3-phase 4-wire 240/416-volt system for both domestic and factory purposes. It was further stated that they have had very few accidents, and only a small proportion of these can be said to have been avoidable had the voltage from phase to ground been limited to 120 volts. To complete their story, however, consider a paragraph from the letter which reads as follows: "Fairly stringent Factory Regulations apply with regard to the use of portable apparatus or lights which require, except in the case of earth free situations, that such apparatus should be supplied through transformers from the general 240 volt system at 110 volts with the mid-point of the winding on the low voltage side earthed so as to limit the voltage to earth on the output side to 55 volts."

Miscellaneous Additional Test Data

Table V shows data secured from tests made on many other customers both large and small. In each case, the data taken have been based on the maximum power factor which, incidentally, almost always occurred during periods of maximum load and at either 10:00 am or 11:00 am. These data are indicative of four considerable advantages resulting from the operation of motors at less than nameplate rating.

1. Increased efficiency of operation for the motors.
2. Improved power factor on the utility's system.
3. Reduced transformer capacity required for serving existing loads.
4. Improved regulation on transformer banks and secondaries.

Special Tests

Table VI shows some special tests which were made on individual machine tools at the largest plant served by our company. These three machines were chosen by the operating superintendent as representing machines which he felt were fully loaded and were doing the job for which they were designed. It should be noted that these motors are operating at practically design voltage—the punch press at 444 volts, the planer at 446 volts, the milling machine at 432 volts. The punch press had an average power factor which was fairly high, namely, 82.0 per cent. However, the graphic chart in Figure 5, indicates that even at the peak swing, the maximum input was less than full load, since the motor was a 30-horsepower motor. The planer, Figure 6, operating at a power factor of 22.6 per cent, is ridiculously underloaded. The milling machine, Figure 7, operating at a power factor of 55.0 per cent, was

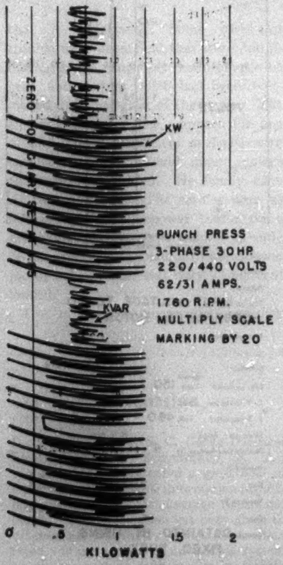

Figure 5. Kilowatt-kilovar input to 30-horsepower 3-phase induction motor driving punch press

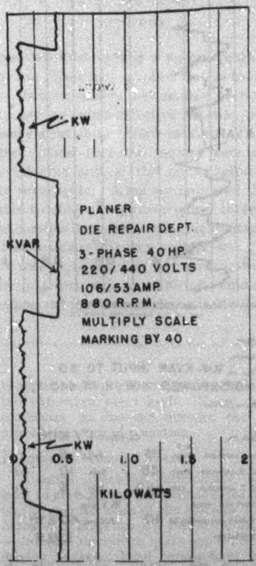

Figure 6. Kilowatt-kilovar input to 40-horsepower 3-phase induction motor driving planer

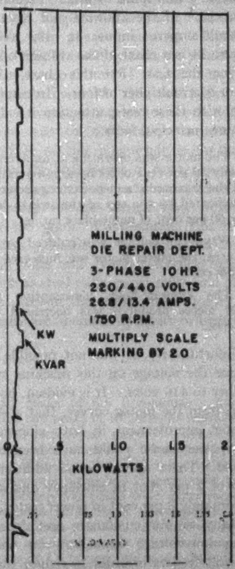

Figure 7. Kilowatt-kilovar input to 10-horsepower 3-phase induction motor driving milling machine

Table VII. Motor Test Using Normal and Reduced Terminal Voltage

Voltage	Kilowatts	Kilovars	Per Cent Power Factor	Kilowatt-hour per 1,000 Pieces
492	8.90	13.0	56.2	103
440	8.60	9.2	64.9	99.5

Test results on a percentage comparison are as follows:

440	normal	normal	normal	normal
492	3.5% Inc.	41.3% Inc.	8.7% Dec.	3.5% Inc.

operating at less than 40 per cent of rating.

In addition to these special tests, a similar test was made at another large plant on an automatic screw machine for the purpose of determining the percent load carried and the improvement in power factor and efficiency when operating at 10 per cent below the normal voltage. In this case, a watthour meter was installed to secure the energy consumption per 1,000 pieces produced with the voltage at 492 and again with the voltage at 440. The data are shown in Table VII. Figure 8 is a chart of the kilowatt and reactive kilovolt-ampere input at 440 volts. Figure 9 is a chart of the voltage taken during the test. For this chart there is a multiplier of four. Figure 10 is a chart of the kilowatt and reactive kilovolt-ampere input at 492 volts. Figure 11 is a chart of the voltage taken during the test. For this chart, also, there is a multiplier of four. In connection with these tests, attention is called to three principal facts.

1. The motor was operating at an average of only 30 per cent of its horsepower rating and the maximum horsepower requirement, as indicated by the top of the swings, was only 50 per cent of name-plate rating.
2. When the voltage was reduced by 10 per cent, the power factor was increased by 8.7 per cent.
3. The kilowatt-hour consumption per 1,000 pieces produced was decreased 3.5 per cent.

Unfortunately, it was not possible to reduce the voltage on this machine still further to 416 volts. It is evident, however, from the motor curves, that a still greater improvement in both efficiency and power factor could have been obtained. There should be an additional gain of 2 per cent in efficiency and approximately 3 per cent in power factor.

Many of our customers are already using low-voltage capacitors on their 440-volt feeders in order to reduce their kilovolt-ampere demand charges and, at the same time, reduce the losses on their secondary feeders. A change of these existing systems from 480-volt delta to 240/416-volt wye would, therefore, result in a reduction in the leading reactive kilovolt-ampere input to these capacitors. This, however, would be offset by an equal, or possibly greater, reduction in the lagging reactive kilovolt-ampere input to their motors so that no penalty would be imposed upon them because of the operation at the lower voltage.

Emphasis should be placed on the fact that in all of the tests made, the current carried by the secondary feeders would have been less at the lower voltage than at the higher voltage, because the improvement in efficiency and power factor more than offset the effect of the lower voltage.

Better Motor Application

It is inevitable that the reaction of many engineers to this report will be to demand that factory equipment manufacturers make better application of motors to machine tools. It is doubted that much could be accomplished in this way, since the cost of the motor is such an insignificant part of the total cost of the machine tool. Furthermore, a problem which already exists must be faced, namely, a tremendous number of underloaded motors. Even though machine tool manufacturers started today making suitable application of motors to their machine tools, it would be many years before this change could materially affect the over-all performance in a given factory. In addition to these points, it should be emphasized again that even though the motors are carrying full load, the loss in efficiency at the lower voltage is very slight, and there continues to be an improvement in power factor.

Attitude of Factory Maintenance Engineers

In duscussing the subject of reduced voltage for motor operation with many of our customers, factory men have been found who are opposed on the grounds that they already have too many motors that are overloaded and are having too many failures on that account. So far none of our customers' maintenance men have been able to give us a single machine

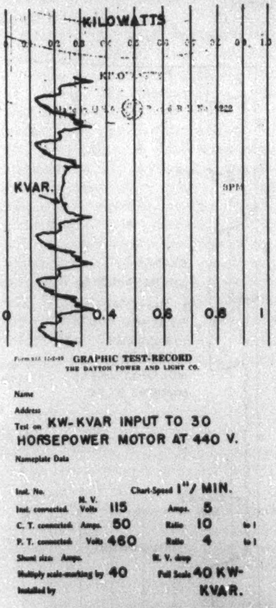

GRAPHIC TEST-RECORD
THE DAYTON POWER AND LIGHT CO.

Name
Address
Test on KW-KVAR INPUT TO 30 HORSEPOWER MOTOR AT 440 V.
Nameplate Data
Inst. No. Chart-Speed 1"/ MIN.
Inst. connected. M. V. Volts 115 Amps. 5
C. T. connected. Amps. 50 Ratio 10 to 1
P. T. connected. Volts 460 Ratio 4 to 1
Shunt size. Amps. M. V. drop
Multiply scale-marking by 40 Full Scale 40 KW-KVAR.
Installed by

Figure 8. Kilowatt-kilovar input, at 440 volts, to 30-horsepower 3-phase induction motor driving screw machine

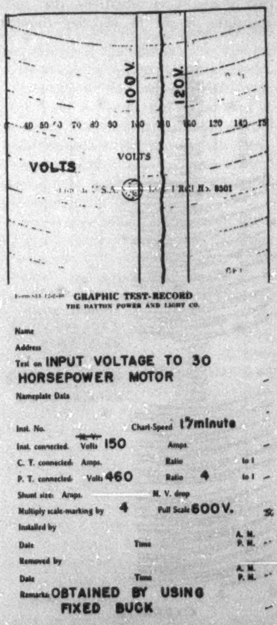

GRAPHIC TEST-RECORD
THE DAYTON POWER AND LIGHT CO.

Name
Address
Test on INPUT VOLTAGE TO 30 HORSEPOWER MOTOR
Nameplate Data
Inst. No. Chart-Speed 1"/minute
Inst. connected. ~~M. V.~~ Volts 150 Amps.
C. T. connected. Amps. Ratio to 1
P. T. connected. Volts 460 Ratio 4 to 1
Shunt size. Amps. M. V. drop
Multiply scale-marking by 4 Full Scale 600 V.
Installed by
Date Time A. M. P. M.
Removed by
Date Time A. M. P. M.
Remarks OBTAINED BY USING FIXED BUCK

Figure 9. Terminal voltage of 30-horsepower 3-phase induction motor on screw machine (fixed buck)

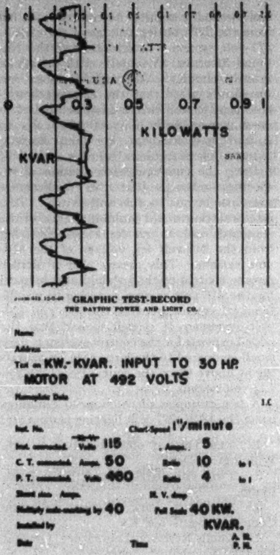

GRAPHIC TEST-RECORD
THE DAYTON POWER AND LIGHT CO.

Name
Address
Test on KW.-KVAR. INPUT TO 30 HP. MOTOR AT 492 VOLTS
Nameplate Data
Inst. No. Chart-Speed 1"/minute
Inst. connected. Volts 115 Amps. 5
C. T. connected. Amps. 50 Ratio 10 to 1
P. T. connected. Volts 480 Ratio 4 to 1
Shunt size Amps. M. V. drop
Multiply scale-marking by 40 Full Scale 40 KW.
Installed by KVAR.
Date Time A. M. P. M.

Figure 10. Kilowatt-kilovar input, at 492 volts, to 30-horsepower 3-phase induction motor on screw machine

that is overloaded. Some cases of trouble were unearthed that were due to bad bearings, improper maintenance of gear, and motors which had been overloaded due to neglect of that type. The electrical maintenance engineer for one of our largest customers declared with emphasis that they had many motors that were overloaded. He finally gave us two to check. The results were as follows: A 40-horsepower motor on a broaching machine was loaded to only 56 per cent of rating, and a 15-horsepower motor on a grinder was only 73-per-cent loaded.

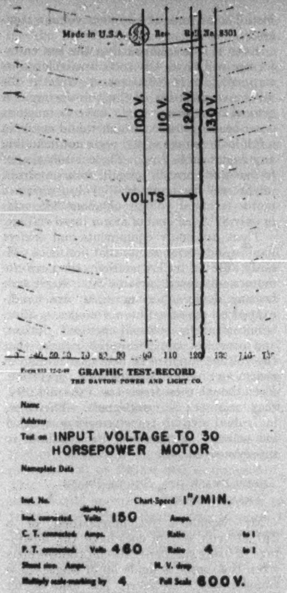

GRAPHIC TEST-RECORD
THE DAYTON POWER AND LIGHT CO.

Name
Address
Test on INPUT VOLTAGE TO 30 HORSEPOWER MOTOR
Nameplate Data
Inst. No. Chart-Speed 1"/MIN.
Inst. connected. Volts 150 Amps.
C. T. connected. Amps. Ratio to 1
P. T. connected. Volts 460 Ratio 4 to 1
Shunt size Amps. M. V. drop
Multiply scale-marking by 4 Full Scale 600 V.

Figure 11. Terminal voltage of 30-horsepower 3-phase induction motor on screw machine

One of our customers who manufactures motors referred a special problem to us. They had supplied motors to one of their customers and six had been returned as being defective because they had burnt out. After making a test, they found that the motors were not overloaded and, at this point, asked us to investigate. A survey indicated that this trouble was probably due to resonance with its accompanying high voltages. The customer's service voltage was 220. It was suggested that a grounding bank be installed with the 220-volt windings connected in wye and the neutral solidly grounded and the 2400-volt windings connected in delta. In this case, naturally, the phase leads of the 220-volt windings were connected to the power supply bank, and the 2400-volt leads were insulated and isolated. This, in effect, gave the 220-volt system a grounded neutral and eliminated the high voltages and the motor failures.

It is evident that many factory maintenance men attribute failures to overloading that are due to either high-voltage surges or to neglected maintenance on bearings, gears, and so forth.

Conclusion

The data given in this report are only a part of what have been collected over a period of almost 4 years. During this time, the data and subject matter have been discussed with many utility engineers. It is amazing to find so many in the industry who are either apathetic or convinced that the data are not typical. So far, utility engineers appear reluctant to make similar tests in their customers' factories.

Finally, it should be pointed out that whereas in this report reference has been made to the 120/208- and the 240/416-volt systems, we are dealing with nominal values. On our low-voltage network system, we plan to carry from 122 to 124 volts from phase to neutral. Likewise, on a 240/416-volt system, we would plan to maintain from 244 to 248 volts from phase to neutral. This would give a 3-phase voltage for motor operation of from 423 to 430 volts. Certainly, a voltage of this magnitude is far better from the standpoint of both the utility company and the customer than the existing voltages which vary from 470 to 490 volts. Furthermore, this report refers primarily to motors rated 220 or 440 volts and avoids reference to loads such as steel mills, paper mills, and heavy industry of that type where motors normally are operated at 2.4 kv or higher.

◆

Discussion

D. S. Brereton and **S. C. Cooke** (General Electric Company, Schenectady, N. Y.): Mr. Schuler has presented a great deal of interesting and valuable information regarding average loads in average industrial plants. The information has been given to substantiate the theory that a lower than rated voltage applied to an electric system supplying machine tools results in slightly improved performance from a power factor and efficiency standpoint. This theory is based on data showing that the motors being supplied are operating at considerably less than their rated loads. Under these conditions, no one can question the improved efficiency of operation.

Loading of Machine Tools

It seems somewhat questionable, however, to draw general conclusions based only on the average loads of the machine tools. Many such loads are of a duty-cycle nature with higher than rated peaks applied to the driving motors. Load curves have been taken of different machine tool loads, some of which are outlined here. A certain press with a 5-horsepower motor had extended load peaks of 6.5 horsepower. Another press had peaks of 10 horsepower applied to a 7.5-horsepower motor. 7.5-horsepower peaks were found on a 5-horsepower motor on still another press. A reamer with a 15-horsepower rating had 19-horsepower peaks; 7.0-horsepower peaks were experienced for extended times on a 5-horsepower worm gear milling machine. An interval grinder with a 3.5-horsepower drive had maximum loads of 7.5 horsepower, and a 24-inch drill equipped with a 3-horsepower motor had momentary peaks of 11 horsepower. The nature of machine tool operations is such that there is always a certain amount of machine idle time. Putting work in and taking it out and performing other operations such as inspection results in idle time. Such times of no load have a great effect on reducing the average load of the machine with the result that the average load appears to be considerably under the machine rating. Also, machine tools are designed to handle a certain range of types of work. Therefore, a good portion of the time the work being done may not represent the design capability of the machine. Based on average loads, a lower than normal voltage would be satisfactory, but based on full load and peaks of 130 per cent, 150 per cent, or even 200 per cent and more, as indicated by the examples just given, normal voltage (or even higher than normal) is essential to prevent motor stalling. As pointed out by the author, the torque of an induction motor is proportional to the square of the voltage. Even though motor rated maximum torques might be 200 or 250 per cent, the voltage would not have to be very low to cause stalling under the preceding example conditions. It should be realized that the power distribution system should be designed not only for the average load condition but also to accommodate the maximum load condition.

The paper presents as one of the basic factors the fact that machine tools are overpowered because of the relative cost of the motor to the complete tool. In dealing with machine tool manufacturers it has been found that they are desirous of using the proper motor for the job to be done. However, the motor must be capable of handling the maximum load to which the machine tool might be subjected. Therefore, when comparing the motor size to the average load, which will be low as mentioned previously, the machine appears to be overmotored even though it actually is not.

A major point which apparently has been overlooked is the problem associated with the control equipment on modern complex machine tools. Even if the driving motor could withstand the application of below rated voltage, the machine control might well fail to operate properly. This is particularly true of machines with electronic controls which contain devices that are very sensitive to voltage. The adoption of a 240/416-volt system would mean that special controls would be required on all such machines. This would necessitate two similar standard lines which would increase the cost to the consumer without any additional features or advantages.

Voltage Level

It is worth emphasis that regardless of voltage level there will still be voltage spread between the first and last transformer on the utility lines. Even though the voltage is high on the first transformer, it will more than likely be low on the last transformer with the resulting reductions in maximum torque on the motors supplied.

It is well known that the voltage supplied by the utility to the industrial plant is subject to variation as utility loads increase and decrease. The amount of this voltage spread varies considerably among various power companies, but in many cases has been found to be excessive for satisfactory industrial plant operation. In such cases it has been necessary for the industrial to install some form of a system voltage regulator.

Even if it is assumed that the last transformer will have 416 volts available as its terminals, it is necessary to consider the inherent regulation of the transformer. A typical transformer might have as much as 4-per-cent regulation which would result in a full load voltage of 400 volts not including any feeder cable drop. The combination of feeder and branch circuit voltage drops might well be another 15 volts, giving a motor terminal voltage of about 385 volts or only $87^{1}/_{2}$ per cent of motor rated voltage.

There are many equipments and devices used in industrial plants that are more seriously affected by low voltages than are the motors discussed previously. Resistance heating devices, for example, are handicapped by excessively low voltages. Electronic devices, solenoid-operated devices, and capacitor equipments all require that the voltage supplied be held near normal in order to assure satisfactory operation. Even though these items are in the minority, they cannot be neglected. Therefore, individual step-up transformers or another low-voltage system will be required to supply such loads.

Three-Phase or Single-Phase Transformers?

Mr. Schuler's recommendation of a 240/416-volt system does have the advantage of using standard 240-volt transformers when the source is made up of single-phase transformers. However, the load center type of system, using a medium voltage for distribution to the load centers for conversion to the utilization low voltage, has greatly increased in the last 10 years for both factory and commercial building applications. All major manufacturers have met the engineering soundness and economic advantage of the load center system by making available unit-type substation equipment. This type of substation incorporates the 3-phase transformer and has found much favor in industrial plants. The adoption of the 240/416-volt system would require the development of new 416Y/240-volt rated 3-phase transformers. This would mean two standard ratings of transformers which are not a great deal different in voltage rating and which would result in higher costs to the user, with no increase in consumer benefits.

480Y/277-Volt System for Commercial Buildings

The use of the 480Y/277-volt system has long been popular in the industrial field. The savings available due to the higher voltage, in place of the conventional 208Y/-120-volt system, are available to commercial buildings by using the 24-volt control system. The author noted that the remote control system "adds more expense, as well as complication, to the distribution system." This control method permits the power system to meet simply and conveniently the increasing demands of flexibility placed on the modern commercial building. The group switching of many different lighting fixtures and the controlling of fixtures from several locations is readily accomplished. This permits the higher current-carrying lighting circuits to be kept to a simplified minimum. It is true that the 24-volt control method is required to control loads fed from the 277-volt leg voltage of the 480Y/-277-volt system. Article *2113* of the National Electrical Code deals with voltage of branch circuits. Although it does not specifically state that the 250-volt household type of wall switch must be applied to meet a maximum limit of 150 volts to ground (as it does state for lamp holders, fixtures, or receptacles below a height of 8 feet), the common interpretation of inspectors indicates that this requirement must also be met by this wall switch. This interpretation would prohibit the use of the standard wall switch for loads operating from the 240-volt leg voltage of the 416-volt system. This means that a similar remote control method should also be used for the 416-volt system resulting in no differential expense between the 480- and 416-volt systems. It is well to add that the added expense for the control system is very small compared to the large gain by operating at above twice the conventional 208Y/-120-volt system.

A few examples of commercial buildings using the 480Y/277-volt lighting system are:

1. New Dupont office building outside Wilmington, Del.
2. Twin Falls High School, Twin Falls, Idaho.[1]
3. Appliance Park, General Electric Company, Louisville, Ky.
4. Knolls Research Laboratory, General Electric Company, Schenectady, N. Y. (Used 480Y/277-volt lighting with control but contactors instead of 24-volt remote control).
5. Tobyhanna Signal Depot, Tobyhanna, Pa. (Administration Building includes cafeteria, dispensary, and post exchange).
6. Marietta Signal Depot, Marietta, N. Y. (The lighting for this depot is principally for the warehouse area, but also includes the office area).
7. New York Telephone Company Office Building, Menands, N. Y.

System Neutral Grounding

The author tells of his experiences with factory maintenance men concerning the relative hazard of the grounded and ungrounded system. There is no doubt that a greater "splash" during a fault will occur from the solidly grounded system with its several thousand amperes fault current than from the ampere or two when an ungrounded industrial system is faulted to ground. The assumption is made that the ungrounded system is less hazardous to personnel. It is well to mention that only approximately 25 milliamperes are required to kill an average person. It will require about 10 milliamperes to be "frozen" to an energized conductor. From this the conclusion seems to be that there is no advantage in being shocked by an ungrounded over a grounded system since an ungrounded system will deliver a great deal more current than that required to kill a person. In fact, if a ground already exists on the ungrounded system and a person comes in contact with one of the other phase conductors, the driving voltage would be approximately 73 per cent greater than the grounded system. Along with the advantage of (1) greater safety, system neutral grounding provides (2) reduced operating and maintenance expense, (3) improved service reliability, (4) better system and equipment overcurrent protection, and (5) improved transient overvoltage protection.

Mr. Schuler should be commended for noting the effect of possible overvoltages on the ungrounded system. Reference is made here to an unpublished 1951 AIEE paper by R. H. Kaufmann, in which he points out the effect of overvoltages caused from (1) lightning, (2) static, (3) physical contact with a higher voltage system, (4) resonant effect in the series inductive-capacitive circuits, (5) repetitive restrike, (6) switching surges, (7) forced current zero interruption, and (8) autotransformer connections.

CONCLUSION

It is not our purpose to disagree with the philosophy of combined light and power systems because their many advantages are apparent. The popular 480Y/277-volt system has been used in a great number of industrial plants and commercial buildings. The paper indicates that the 277-volt system will require the development of a complete new line of fluorescent lamps and accessories. The only design change required is that of the ballast and that has already been done. Such ballasts have been available for about 10 years. The market offers, as standard equipment, all the equipment necessary for the 480Y/277-volt combined light and power system. The 480Y/277-volt system has all the advantages of combining light and power in a 3-phase 4-wire solidly grounded system with no sacrifice in voltage at any of the utilization equipments.

REFERENCE

1. VOLTAGE UP—WIRING COSTS DOWN, A. I. **Sawyer.** *Electrical West*, San Francisco, Calif., volume 109, number 6, December 1952, pages 82–84.

L. C. Peterman (Ford, Bacon and Davis, Inc., New York, N. Y.): Mr. Schuler's report on the advantages of a 240/416-volt combined light and power system for industrial plants is one approach, and perhaps a logical one, to the problem of too-high utilization voltage which plagues many industrial plants today. The arguments in favor of this system are a repetition of those advanced 30 years ago in favor of the 3-phase 120/208-volt system, and the objections raised likewise repeat the objections 30 years ago of those who felt that the latter system had serious defects or even that it would not work. The successful operation of the 120/208-volt networks in every major city of the country (except one) has silenced the objectors.

The prevalence of the 120/208-volt network hastened the adoption of the 120-volt lamp standard and lamps were made available for that voltage. Much other equipment was boosted from 110-volt rating to 115 or 117 volts. But industrial plant engineers complain, and rightly so, that utilities give them 480-volt systems (and sometimes it is 500 volts) while the manufacturers sell them 440-volt motors and controls to operate on those systems.

There is no logic to a 277/480-volt system because the motor voltage is too high, and standardization work to date has not helped the industrial plant engineer to meet this problem adequately. Further, there is today no recognized standard of 277 volts for the supply transformer, but utilities over the country have thousands of 240-volt transformers that can be used for supplying Mr. Shuler's system. We hear of the great advantage of repetitive manufacture, quantity production, and minimum number of types and voltages. Why promote a new transformer style to confuse still further the problem of effective and real standardization, which in spite of years of effort by outstanding individuals and committees has not been achieved?

R. A. Scholl (Public Service Company of Indiana, Inc., Kokomo, Ind.): Mr. Shuler has presented a lot of factual data on induction motor performance due to operating at voltages above as well as below name-plate rating. The tests that he made in the industrial plants verify his analysis of motor performance curves. Even with the author's findings, it is believed that the adoption of a 240/416-volt 3-phase 4-wire system is a step in the wrong direction and should not be advocated.

The author's comment on standardization of voltages by manufacturers of equipment as 120 or 240 or 480 is questioned. This does not mean that all utilization equipment should operate at those voltages or at points above those figures due to normal regulation. Those designated voltages mean that the equipment is designed for normal excitation at a given voltage and will have certain characteristics at that value. A transformer with a voltage rating of 7200–480/240 or 240/120 is of the same ratio as an older transformer rated 6600–220/110. The utility should establish the voltage level for its customers to give proper voltage at terminals of utilization equipment and not on the basis of transformer name-plate rating. The main problem becomes one of regulation from substation bus to using equipment. Voltage levels have been creeping higher over a period of years. This can be attributed largely to the widespread use of 120/208-volt 3-phase 4-wire systems. The congested areas of cities have 120/208-volt systems operating on a network. This is entirely proper where a high percentage of the load is 120 volts single phase. The system has good regulation and there are very few motors requiring high starting torque. Large factories having heavy lighting loads and also large numbers of soldering irons and hand tools can use this 120/208-volt system to advantage for these particular loads. Most industrial plants require a higher voltage to properly supply 220-volt motors; therefore, the 3-phase power could best be supplied at 240 or 480 volts.

The electric supply for 120-volt incandescent lamps, office machines, and convenience outlets will require further transformation when using a 240/416-volt system, the same as when using a 277/480-volt system. Standard voltages for fluorescent lamp ballasts are 110–125, 199–216, 220–250, and 240–280. Unfortunately when fluorescent lamp fixtures first came into use the trade did not adopt ballasts that fall in the range of 199–250 volts. For new installations, it would be no more of a problem to use 240–280 volt ballasts than ones rated 199–216. For large installations the switching of lamps in large groups by magnetic contactors or with the newer low-voltage remove control devices will usually save money regardless of the voltage of the system used. Therefore, for lighting loads there is little difference in using the 240/416- or 277/480-volt system.

The major disadvantage to the 240/416-volt system is the reduced torque and overload capacity of the motor. Motor performance varies as the square of the voltage for each of the characteristics just mentioned. Even in machine shops there are compressors, hoists, and other devices whose capacity is seriously effected by too low a voltage. Unless the single-phase voltage remains above 120 volts at the service entrance, many motors will operate from 400 to 410 volts. Most substation feeders supply several classes of service, such as; single-phase 3-wire for residential and commercial customers; 240- or 480-volt 3-phase delta system for power to commercial and industrial customers; and in some cases 120/208-volt Y systems. If either 120/208- or 240/416-volt systems supply industrial loads from this multiple-purpose feeder, it becomes practically impossible to establish a satisfactory voltage level for all customers. Supplying the first customers from the substation at 122 volts would be desirable. This would result in an unsatisfactory arrangement for 3-phase motors to be supplied from a 120/208-volt system. Using a 277/-480-volt system or the 480-volt delta connection would result in voltage no higher than 10 per cent above the 440-volt motor rating. Ballasts rated at 240–280 should be used on the wye system. The ballasts and lighting fixtures are a more permanent part of the building and do not need interchangeability with other plants. On the other hand, the industrial plant motors are items of much higher investment and may be moved to other plants; therefore, the rating should continue to be 220/440 volts.

Machine tool manufacturers do over-motor the machines. This is partly because the motor must be capable of making the heaviest cut continuously, yet much of the time the work tool is making light cuts or spinning idle. Mr. Shuler's recommendation of adopting the 240/416-volt system might be advisable in a few installations; however, it is believed that the problems resulting from overpowering of tools and the resulting low power factor can best be handled by other means, and not by adopting voltages that are not full multiples of 120.

Leo Dolkart (Commerical Light Company, Chicago, Ill.): The paper by Mr. Shuler is very interesting. My experience covering a period of many years bears out the advantages derived from a network distribution system. Where the utility power supply is limited to a 120/208 4-wire grounded neutral system, it will be found very suitable for the average industrial plant where the motors do not exceed 50–60 horsepower in size. The system is flexible enough to be very economical for light and power distribution off one set of service mains. Where larger motors are in use and where motors are scattered and far from distribution centers, a 240/416 3-phase system is to be preferred. During World War II I was instrumental in introducing the 416 3-phase 4-wire grounded neutral system for a large naval project.

A few years ago, I found that many

manufacturers of machines had a tendency to underrate their machines rather than to overrate them. In this, therefore, I differ from the author. One often hears of machine salesmen claiming that their machines take less horsepower to operate and consequently are more economical in the long run. On the other hand, I also agree with Mr. Shuler that in many cases an apparent overload on a motor is actually due to faults in bearings, gears, or undue friction as well as to high voltage surges. The latter are, of course, very hard to determine and to isolate.

On the whole the paper is very meritorious.

William Shuler: The author thanks the discussers for their comments.

As a prelude to his closing discussion, he wishes to point out that this system is suggested for modern industrial plants, as indicated by the title of the paper.

Mr. Brereton and Mr. Cooke state that the paper presented information regarding average loads in average industrial plants. The paper does not deal only with average loads; it also deals with maximum loads and shows high speed charts which indicate that even in the case of maximum loads, such as are experienced on punch presses and other tools having high peak loads, the input to the motor is less than full load. Furthermore, the data presented were obtained by tests in many diversified industrial plants and not in average plants. Some of them were small, having demands as low as 50 kw, and others were large, having demands ranging from 10,000 to 25,000 kw.

They also state that the reduction in voltage suggested "results in slightly improved performance from a power factor and efficiency standpoint." The data we have obtained indicate that the change from 480 volts to 416 volts for a supply voltage will result in considerable improvement in power factor. For example, in the case of an induction motor load having a power factor of 50 per cent, it will be increased to 60 per cent, and in the case of a power factor of 60 per cent, it will be increased to 70 per cent. In the case of the former, this means a reduction of reactive kilovolt-ampere input of approximately 23 per cent. In the latter case, the reduction is almost 24 per cent. The author maintains that this is much more than a slight improvement. Also, attention is called to the fact that a reduction of from 480 to 440 volts on a special machine tool, designed for the particular job it is now doing, resulted in an improvement in efficiency of $3^{1}/_{2}$ per cent and that a voltage reduction of 13.3 per cent, which is equivalent to reducing the voltage from 480 to 416 volts, would result in an improvement in efficiency of about 5 per cent. This would hardly be considered slight by the customers whom we serve.

Brereton and Cooke make reference to tests which they have made on some small motors, namely 5, $7^{1}/_{2}$, 15, and $3^{1}/_{2}$ horsepower. Unfortunately, they did not state what percentage of the total load these motors represented.

Under the heading "Loading of Machine Tools," they refer to controls. Certainly no difficulty would be found in operating controls on a phase-to-neutral basis which would permit the use of standard 240-volt equipment. The problem here cannot be any different from that involved in factories operating with a 120/208-volt supply.

Under the section entitled "Voltage Level," their discussion refers to the question of regulation. This is very clearly covered in the paper, and I regret to note that, apparently, neither Mr. Brereton nor Mr. Cooke took the trouble to make some very simple calculations. The highest regulation found was 5.25 per cent, the lowest was 1.7 per cent, and the average was about 2.5 per cent. The 5.25-per-cent regulation occurred at a plant having a demand of 25,000 kw. At the time of the test, this load was supplied by four 4/0 overhead lines for a distance of approximately $2^{1}/_{2}$ miles from the bus. This regulation has been reduced, since this load has been transferred to our transmission system. It is inconceivable that a modern public utility would tolerate the regulation mentioned in this part of their discussion. Furthermore, the modern manufacturing plants with the low impedance busses and the employment of secondary capacitors are maintaining very close regulation on their supply transformers and secondary feeders. The author is familiar with voltage drops such as are mentioned in their discussion only in the case of the investigations which we make in connection with the small municipal properties and the co-operatives in our company's territory.

The author is very much in favor of 3-phase transformers. However, both the Engineering Department and the Operating Department of our company prefer the single-phase transformers, because the price, as catalogued by the principal manufacturers, is less for three single-phase transformers than for one 3-phase transformer of the same capacity. In fact, the price is so much less that the cost of the high-tension busses is more than offset by the difference in the cost of the transformers themselves. For instance, in the 12-kv class the cost of a 3-phase 500-kva transformer is approximately 14 per cent more than the cost of three single-phase transformers having the same capacity, and a 3-phase 300-kva transformer costs 8 per cent more than three single-phase transformers. Furthermore, should the transformer manufacturers eliminate this price differential, it would be a very simple thing to connect the 240-volt windings in wye, thereby securing a 416Y/-240-volt rated 3-phase transformer. The author believes there would not be as much difficulty in having such a transformer accepted as standard as must have been encountered in securing the acceptance of a 480Y/277-volt rated 3-phase transformer.

In their discussion, Mr. Brereton and Mr. Cooke state, "Article *2113* of the National Electrical Code deals with voltage of branch circuits. Although it does not specifically state that the 250-volt household type of wall switch must be applied to meet a maximum limit of 150 volts to ground (as it does state for lamp holders, fixtures, or receptacles below a height of 8 feet), the common interpretation of inspectors indicates that this requirement must also be met by this wall switch." This statement is untrue. Mr. Swan of the National Board has stated that standard wall switches rated 250 volts can be used on 240-volt grounded circuits as outlined in section *2113*. This practice must meet the requirements of section *3812* which in effect imposes the use of conduit or armored cable to secure grounded enclosure for the switch. The inspectors in our territory interpret section *2113* in the same way and will accept the use of 250-volt switches for the control for 240-volt grounded branch circuits. Therefore, no remote control system would be necessary for branch lighting circuits operating 240 volts from phase to ground.

Under the heading "System Neutral Grounding," Brereton and Cooke say, "The assumption is made that the ungrounded system is less hazardous to personnel." The author did not make any such assumption. He stated that some of the factory engineers are opposed to a ground on their distribution system. In the author's opinion, as stated in the paper, a solidly grounded neutral is recommended.

In conclusion their discussion states, "The popular 480Y/277-volt system has been used in a great number of industrial plants and commercial buildings." In the author's opinion, this popularity will wane. Motors are coming into the market manufactured with oriented iron. The no load or magnetizing currents of these motors at 480 volts is so high that it represents more than 50 per cent of the full load current rating of a 440-volt motor.

L. C. Peterman's concise discussion and irrefutable comments are appreciated. He has unquestionably met with the problems that are presented by a 480-volt supply system and is convinced that the 240/416-volt system would be just as advantageous as the 120/208-volt network has proved to be over many years.

The author has no comments to make on the statement of R. A. Scholl regarding the standardization of voltages with respect to the voltage rating of transformers. However, he does take exception to the statement regarding the adequacy of a 120/208-volt system for serving power loads. The Western Electric Company has a very large plant in Allentown, Pa., which, 2 or 3 years ago, had a peak load of approximately 6,000 kw. This plant is operating on the basis of 120/208 volts for both power and lighting.

Also, the author differs with him regarding the ballast for fluorescent lamps. Before submitting the paper for publication, the author checked with two of the principal fluorescent lamp manufacturers, and they definitely were opposed to the adoption of 277 volts because it would merely add to the number of accessories required and add another voltage to their catalogues.

Mr. Scholl's remarks regarding the inadequacy at 416 volts because of the reduction in torque does not meet the facts which I have given. A reduction in voltage from 440 to 416 would result in a reduction of the pull-out torque of only 12 per cent. Reference to the torque curve of the motor is sufficient to indicate that such a reduction is of no importance. The author is not recommending any change in the rating of motors. Certainly it would be very unwise to do so after all of the standardization work that has been accomplished to date. In fact, the principal point of the paper is that motors designed for 440-volt operation and applied to machine tools in accordance with present practice are ideally suited for operation at 416 volts.

Mr. Dolkart's comments were of considerable interest to the author, since he had no knowledge that there was a 240/416-volt 3-phase 4-wire system in use in this country. Mr. Dolkart says there are some machines in this country that are loaded beyond the capacity of their motors. With this I agree. However, if those cases are relatively rare, and all indications point to the fact that they must be, then manufacturing plants could not possibly be justified in designing their supply systems to take care of these rare instances instead of the great majority.

In conclusion, the author wishes to state that there is one very important additional advantage which has not been mentioned to date and that is the ease with which a 120/-208-volt 3-phase 4-wire auxiliary system could be secured by the installation of highly efficient and inexpensive single-phase autotransformers. The low-voltage system could be used for the supply of office machines, desk fans, portable tools, and so forth, and, in addition, could be used for lighting in those cases where a customer did not desire to employ the higher voltage lamps.

The author hopes that the data presented will be checked by the engineers of other utility companies and manufacturing plants. The 240/416-volt 3-phase 4-wire system offers very substantial benefits to both the utilities and their customers.

Correlation Between Frequency and Transient Responses of Feedback Control Systems

YAOHAN CHU
STUDENT MEMBER AIEE

THE performance of a feedback control system is often evaluated on the basis of the transient response, for which the step function is used as the input. The abrupt change of input or disturbance may represent important actual operating conditions that the system may be subjected to. However, synthesis or design on this basis is mathematically difficult to carry out when the system has a characteristic equation of high order. As a result, synthesis on the sinusoidal or frequency basis has been developed and widely used. It is obviously most desirable to know the correlation between the frequency and transient responses so that a criterion for the frequency response method may be properly established.

Mathematically, such a correlation can be established by Fourier transformation. Nevertheless, it does not give physical insight and thus is not of much use to the designer of a feedback-control system. In general, it is indeed difficult to formulate the correlation generally and quantitatively with easily understood results. Through the use of the root-locus method developed by Evans,[1] it is possible to demonstrate the nature of the correlation between the frequency and transient responses by knowing the correlation between the frequency locus and the root locus. The exact nature of the correlation for a system will depend on their particular shapes. Thus, although no general quantitative relation is established, yet the correlation of each system may be examined individually.

The purpose of this paper is:

1. To show that the frequency and transient responses are correlated by conformal transformation by establishing the correlation between the frequency locus and the root locus.
2. To indicate, as illustrations, several published methods[2–4,8,11] of evaluating the transient response from the frequency response by conformal transformation.
3. To interpret the transient behavior from the existing M_p criterion for synthesis by frequency response method by investigating the pole-zero configuration of the closed-loop transfer function, which is related by the root locus to the open-loop transfer function.
4. To compare the frequency and root loci of several conditionally stable systems.
5. To demonstrate the analogous procedure of synthesis in frequency and in time domains.

Correlation Between Root Locus and Frequency Locus

Figure 1 shows a simplified block diagram of a feedback control system, where $G(s)$ is the open-loop transfer function and s is the complex variable. By means of the frequency-response method a frequency locus may be constructed on the G-plane, as shown in Figure 2. This locus is the conformal transformation of the complete imaginary axis of the s-plane onto the G-plane. These two corresponding curves of Figures 2 and 3 are drawn in thin curves. The thin solid curve represents the transformation from the positive imaginary axis of the s-plane, while the thin dotted curve represents that from the negative imaginary axis. The frequency locus is symmetrical with respect to the real axis of the G-plane.

For the same open-loop transfer function $G(s)$, a root locus may be constructed on the s-plane by the root-locus method, as shown in Figure 3. Since the root locus is the locus of all points of s which gives the function $G(s)$ a phase angle of ±180 degrees, it is the conformal transformation of the negative real axis of the G-plane onto the s-plane. These two corresponding curves of Figures 2 and 3 are drawn in thick solid curves. Unlike the frequency locus, the conformal transformation of the positive real axis of the G-plane on the s-plane is not the root locus. (It is the locus, however, if the system is a regenerative-feedback one.) This is shown by the thick dotted curves. The root locus is symmetrical with respect to the real axis of the s-plane.

In brief, the frequency locus and the root locus are conformal transformations from the s- to the G-plane or from the G- to the s-plane, respectively, by the complex function $G(s)$. This transformation concept is regarded as the correlation between the frequency locus and the root locus.

The loci of Figures 2 and 3 are drawn with the following open-loop transfer function $G(s)$

$$G(s)=\frac{K_g}{s(\tau_1 s+1)(\tau_2 s+1)}$$

It is to be noted that for a given value of K_g only one frequency locus may be drawn; however, the corresponding root locus gives an infinite number of values of K_g. In order to distinguish this fact,

---

Paper 53-100, recommended by the AIEE Feedback Control Systems Committee and approved by the AIEE Committee on Technical Operations for presentation at the AIEE Winter General Meeting, New York, N. Y., January 19–23, 1953. Manuscript submitted September 3, 1952; made available for printing December 24, 1952.

YAOHAN CHU is with Massachusetts Institute of Technology, Cambridge, Mass.

The author wishes to express his appreciation to Prof. Walter McKay for his encouragement in the course of the work, and to Dr. Victor C. M. Yeh from whose work[7] was obtained the majority of the shapes of the root loci in Figure 5.

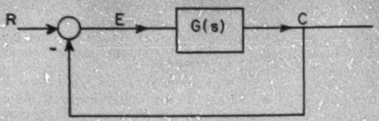

Figure 1 (left). Simplified block diagram of a feedback control system

Figure 2 (right). Frequency locus for

$$G(s)=\frac{K_v}{s(\tau_1 s+1)(\tau_2 s+1)}$$

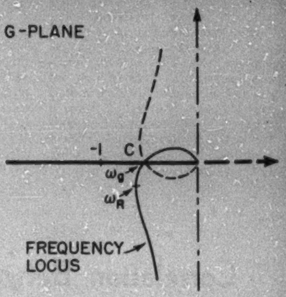

the symbol K instead of K_v, is employed for plotting the root locus. The relation between K and K_v is illustrated in Figure 4, wherein K is a parameter, while the indicated values of K_v are certain selected values.

The point C on the G-plane of Figure 2 corresponds to the point D (and also the point D') on the s-plane of Figure 3. This results from the fact that it is the only point of intersection between these two pairs of curves (thick solid and thin solid). Therefore, the frequency ω_g at point C of the frequency locus is also the value of s at point D on the root locus. This pair of points is significant; it is known from the root-locus method that the value of K at the point D is its maximum value of the system, beyond which the system will be unstable. This value of K may be called the gain limit or stability limit. It is known from the theory of frequency response method that the reciprocal of the absolute value of $G(jw)$ at the point C along the negative real axis of the G-plane is the gain margin.[6] It can be shown easily that the gain margin is related to the gain limit by

$$\frac{\text{Gain limit}}{\text{Gain margin}}=K_v$$

Since K_v and the gain margin are known when synthesized in the frequency domain the gain limit of the system is thus readily obtainable. It will be noted from the preceding relation that the gain margin is inversely proportional to K_v (gain limit is constant for a given system). The system will become less oscillatory as the gain margin increases, Figure 4(B), because the increase corresponds to choosing the predominate pair of roots from a root locus with an increasingly larger damping ratio, as indicated by the points on the root locus in Figure 4(A) with the corresponding value of K as that of the frequency locus. It will be noted that the system is at its stability limit when K is equal to K_4.

A second point of interest resulting from the correspondence between point D on the G-plane of Figure 2 and point C on the s-plane of Figure 3, is that the value of the frequency ω_g on the root locus of Figure 3 indicates the maximum possible bandwidth, which is obtained if the system is synthesized in the frequency domain. This is because the resonant frequency ω_R, Figure 2, of the frequency locus is always smaller than the frequency ω_g (at point C of Figure 2), if the system components are of minimum-phase type. Therefore, once the root locus is drawn when the system is synthesized by the root-locus method, the maximum possible bandwidth is immediately known without going into the frequency domain.

A collection[7,8] of root loci with corresponding frequency loci is shown in Figure 5. These demonstrate the correlation between the root locus and the frequency locus. All the root loci (except the cases o and q) are of simple geometrical curves: straight lines, circles, hyperbolas (cases l, m, and n), and a parabola (case r). Note that the systems of cases g and n are always unstable.

It may now be concluded that since the frequency locus is the conformal transformation of the imaginary axis of the s-plane onto the G-plane by the transfer function $G(s)$ and the root locus is the transformation of the negative real axis of the G-plane onto the s-plane by the same transfer function, and since transient response can be worked out when the roots are selected from the root locus, it can be stated that the frequency response and the transient response are correlated by conformal transformation, as they ought to be in view of the known existence of the correlation provided by the Fourier transformation.

Correspondence Between s-Plane and G-Plane for a Given $G(s)$

The frequency locus may be generalized by putting $s=\sigma+j\omega$ into the transfer function $G(s)$. Thus, by using σ as a parameter a family of constant-σ loci is obtained. The frequency locus is the constant-σ locus with σ equal to zero. This family, as shown in Figure 6, is the conformal transformation of all lines parallel to the imaginary axis of the s-plane, onto the G-plane. If the lines parallel to the real axis of the s-plane are conformally transformed on the G-plane, a family of constant-ω loci is obtained, as is also shown in Figure 6. By means of these two families of loci, 1-to-1 correspondence between the s and G-planes is established.

Similarly, the root locus may be generalized by the relation Ang $G(s)=\varphi$. For various values of φ, a family of constant-φ loci (or phase-angle loci[10]) may be constructed. The root locus is the constant-φ locus with φ equal to ±180 degrees. This family is shown in Figure 7. It is the conformal transformation of all radial lines from the origin of the G-plane onto the s-plane. If all concentric circles with the origin of the G-plane as the center are conformally transformed onto the s-plane a family of constant-r loci (or gain loci) is obtained, as shown in Figure 7. By means of these two families of loci, 1-to-1 correspondence between the s- and G-planes is also established.

The 1-to-1 correspondence between the s- and G-planes means that for every point on the G-plane there is corresponding point on the s-plane, and vice versa. Then, any information encompassed on the G-plane may be obtained from the s-plane by means of the transformation and vice versa. Since the loci on the G-plane give information on the frequency response and since the loci on the s-plane give that on the transient response, it follows that either of these two ways of correspondence, one with the two families of constant-σ and constant-ω loci and the other with the two families of gain and phase-angle loci, may be used in finding the actual correlation. Several methods[2–5,11] have been advanced which make use of this correspondence to evaluate the transient response from the frequency response, as indicated in the next section.

Obviously, if the two families of gain and phase-angle loci, Figure 7(B), are plotted on the s-plane, the frequency locus is the plot on the G-plane of the values of r and φ of all the points of the imaginary axis on the s-plane. Similarly, if the two families of constant-σ

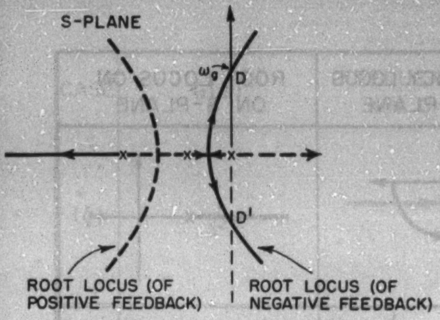
S-PLANE
ω_g
D
D'
ROOT LOCUS (OF POSITIVE FEEDBACK)
ROOT LOCUS (OF NEGATIVE FEEDBACK)

Figure 3 (above). Root locus for $G(s)=\dfrac{K}{s(\tau_1 s+1)(\tau_2 s+1)}$

and constant-ω loci, Figure 6(B), are plotted on the *G*-plane, the root locus is the plot on the *s*-plane of the values of σ and ω of all the points of the negative real axis of the *G*-plane.

Evaluation of Transient Response from Frequency Response

The frequency locus, which is the plot of the open-loop transfer function with $s=j\omega$ on the polar co-ordinates of the *G*-plane, is the open-loop frequency response. The frequency response of a system is the plot of the closed-loop transfer function with $s=j\omega$. Both of these two frequency responses may be plotted in either polar co-ordinates or as attenuation and phase-diagrams.[9]

Methods have been developed to evaluate the transient response from either the frequency locus (or open-loop frequency response) or from the closed-loop frequency response. Since the desired roots are to be selected on the left half of the *s*-plane and since the frequency locus is the conformal transformation along the imaginary axis of the *s*-plane, the frequency locus itself cannot give the value of the desired roots. Thus, any attempt to find the roots (and then to evaluate the transient response) by means of the correspondence between the *s*- and *G*-planes requires some transformation not along the imaginary axis of the *s*-plane but along some line or curve on the left half of the *s*-plane where the desirable roots are located. Profos,[2] and recently Russell and Weaver,[3] have utilized the correspondence shown in Figure 6. Kusters and Moore,[4] Bierson,[5] and Leonhard[11] have developed the conformal transformation of the open-loop transfer function $G(s)$ along a constant damping-ratio line on the *s*-plane onto the *G*-plane. Both transformations employ lines on the left half of the *s*-plane in order to find the roots directly from their corresponding frequency loci. The desirability of a particular curve on the left half of the *s*-plane will greatly depend on the convenience for plotting its corresponding frequency locus on the *G*-plane. They do not differ in principle.

The above-mentioned methods make use of the frequency locus (or open-loop frequency response). Although the open-loop frequency response itself does not give the possible values of the roots directly, yet the closed-loop frequency response does, because the closed-loop frequency response can be obtained from the closed-loop transfer function and the transient solution can be worked out if the closed-loop transfer function is known. An excellent example of using the closed-loop frequency response is Floyd's method.[6] This enables one to find the impulse response of a system from the real part of the closed-loop frequency response (although this can be done directly from the frequency locus on an over-lay chart). It would rather be expected that some other methods might be developed along this approach of using the closed-loop frequency response. An obvious way along this approach is to find out the first-order factors (such as $\tau s+1$ or $1/(\tau s+1)$) and second-order factors (such as $\tau^2s^2+2\xi\tau s+1$ or $1/(\tau^2s^2+2\xi\tau s+1)$) from the closed-loop frequency response by trial-and-error procedure. When these factors are found, the closed-loop transfer function is then determined, and the transient solution may be worked out from the closed-loop transfer function. Although the practicability of this suggested method will depend on the amount of work required to find out the factors for a given closed-loop frequency response, yet such a relation between the closed-loop frequency response and the

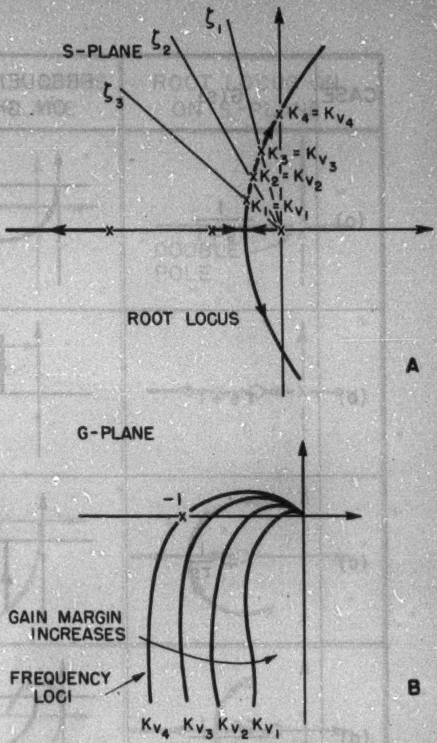

Figure 4 (right). Relation between K's of frequency locus and K's of root locus

A—Root locus on s-plane
$K_1<K_2<K_3<K_4$
K_4 is the gain limit
B—Frequency loci on G-plane

CASE	G(s)	FREQUENCY LOCUS ON G-PLANE	ROOT LOCUS ON ON S-PLANE
(a)	$\frac{1}{\tau s+1}$	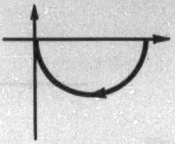	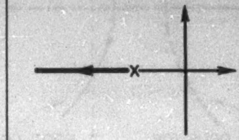
(b)	$\tau s+1$	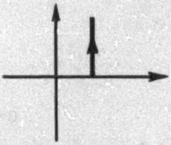	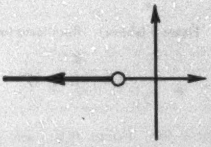
(c)	$1+\frac{1}{\tau s}$	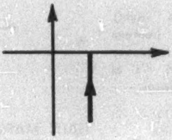	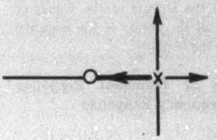
(d)	$\frac{\tau s+1}{\alpha\tau s+1}$	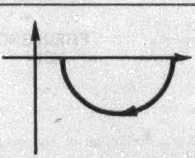	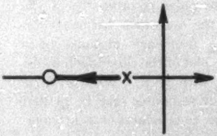
(e)	$\frac{1}{s(\tau s+1)}$	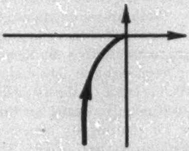	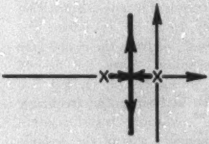
(f)	$\frac{1}{\tau^2 s^2+2\zeta\tau s+1}$	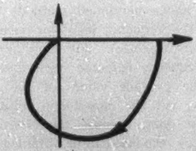	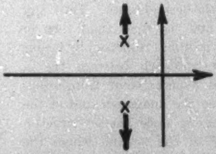

Figure 5. A collection of root loci and their corresponding frequency loci

CASE	G(s)	FREQUENCY LOCUS ON G-PLANE	ROOT LOCUS ON ON S-PLANE
(g)	$\frac{1}{s^2}$	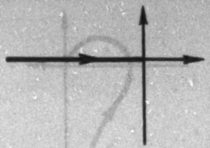	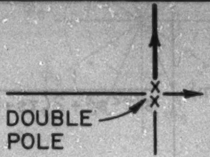
(h)	$\frac{\tau_1 s+1}{s(\tau_2 s+1)}$	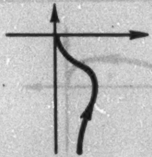	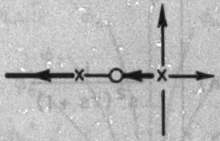
(i)	$\frac{\tau_1 s+1}{\tau_2^2 s^2+2\zeta\tau_2 s+1}$ $\tau_2>\zeta\tau_1$	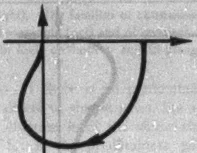	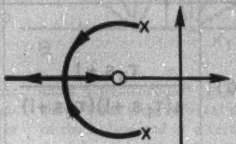
(j)	$\frac{\tau_1 s+1}{\tau_2^2 s^2+2\zeta\tau_2 s+1}$ $\tau_2<\zeta\tau_1$	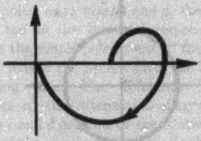	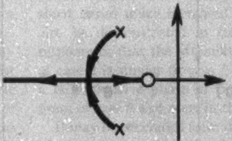
(k)	$\frac{\tau s+1}{s^2}$	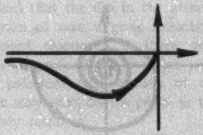	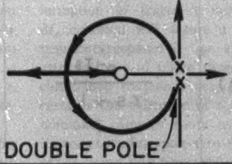
(l)	$\frac{1}{S(\tau_1 s+1)(\tau_2 s+1)}$	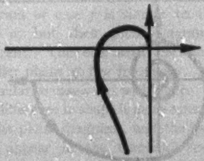	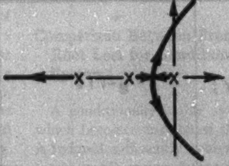

Figure 5 (continued)

CASE	G(s)	FREQUENCY LOCUS ON G-PLANE	ROOT LOCUS ON S-PLANE
(m)	$\frac{1}{s(\tau^2 s^2+2\zeta\tau s+1)}$	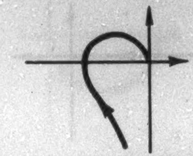	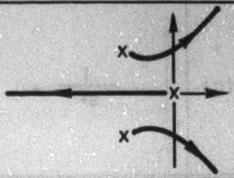
(n)	$\frac{1}{s^2(\tau s+1)}$	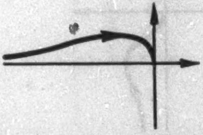	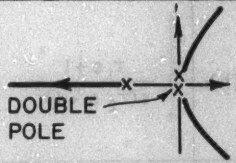
(o)	$\frac{\tau_3 s+1}{s(\tau_1 s+1)(\tau_2 s+1)}$	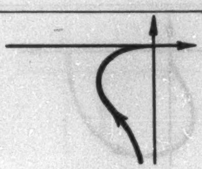	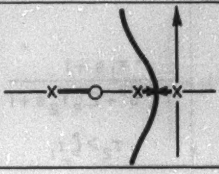
(p)*	e^{-Ts}	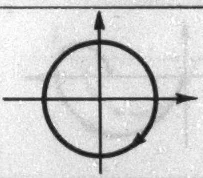	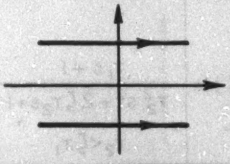
(q)*	$\frac{e^{-Ts}}{\tau s+1}$	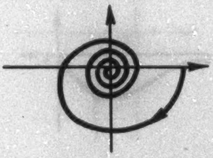	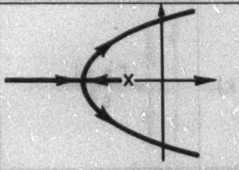
(r)*	$e^{-\sqrt{Ts}}$	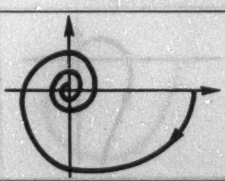	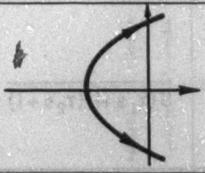

Figure 5 (continued). * Fundamental branch only

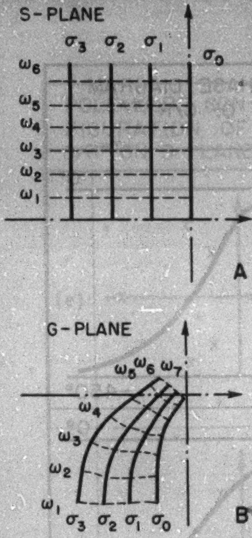

Figure 6 (left). The families of constant-σ locus and of constant-ω locus on both *s*- and G-plane

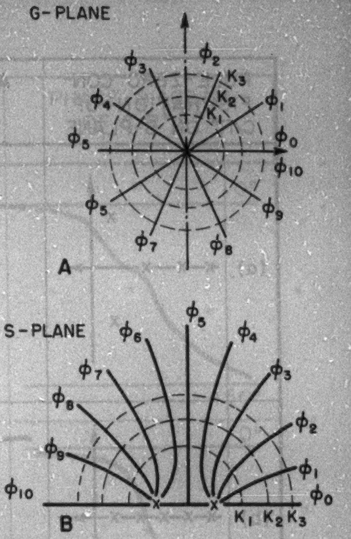

Figure 7 (right). The families of constant-φ locus (or phase-angle loci) and of constant-r loci (or gain loci) on both *s*- and G-plane

pole-zero configuration of the closed-loop transfer function reveals the nature of correlation between the frequency response and the transient response, and thus provides a better interpretation of the closed-loop frequency response. It is recalled that the closed-loop transfer function is related to the open-loop transfer function by the root locus.

Examination of M_p Criterion in Frequency-Response Method

If the poles and zeros of the closed-loop transfer function are known, as is the case when synthesized by the root-locus method, the frequency response of the system may be readily obtained if plotted as attenuation and phase diagrams.[12] Figure 8 is a collection of several closed-loop frequency responses as attenuation and phase diagrams with their corresponding pole-zero configurations on the *s*-plane.

An examination of the cases of Figure 8 reveals the relation between the M_p criterion of the frequency-response method and the pole-zero configuration, which gives the transient response. The first five cases of Figure 8 show closed-loop frequency responses with no zero. The attenuation diagram of case *a* has a resonant peak. This is regarded as the desirable type of frequency response and is characterized in the pole-zero configuration by a pair of predominate complex poles. If there is no predominate pair and all are of simple poles, the attenuation diagram is of the shape shown in case *b*. If the predominate pole is a simple pole in addition to a pair of complex poles, as in cases *c* and *d*, there is a long tail in the transient response, because the simple pole closest to the imaginary axis of the *s*-plane gives the longest settling time. The difference in the shapes of the attenuation diagrams of cases *c* and *d* depends on the relative location of the simple and complex poles. It is known in the frequency response method that the dip in the attenuation diagram of case *c* gives unsatisfactory transient response. If there are two pairs of predominate complex poles, as the pole-zero configuration of case *e*, there may exist double peaks in the frequency response.

The last three cases of Figure 8 show the presence of a zero. The attenuation diagram of case *f* is similar to that of case *a*, but their phase-diagrams are different. The one with the zero has smaller phase at low frequency. Case *g* is similar to case *c* but with a zero; again, the difference in shape is more conspicuous in the phase diagrams, and the long tail will appear in the transient response. If the zero is very close to the origin of the *s*-plane, the peak in the attenuation diagram becomes huge. This is consistent with the deduction that when the zero is near the origin of the *s*-plane, the overshoot is tremendous.[10] It has also been shown[10] that if the zero is at the right half of the *s*-plane and at a certain distance from the origin, the peak time in the transient response is reduced, yet the overshoot is not much increased. This may also be demonstrated in the frequency response in that the attenuation diagram of case *h* is similar to case *f*, but there is a large positive phase in the phase diagram of case *h* and none in that of case *f*.

It may be concluded from the discussion of these cases that the frequency response does give considerable useful information in transient behavior. The M_p criterion will assure a satisfactory transient response if one examines the attenuation and phase diagrams of the closed-loop frequency response and ascertains the existence of a pair of predominate complex roots by visualizing its corresponding pole-zero configuration of the closed-loop transfer function.

Comparison Between Frequency and Root Loci for Conditionally Stable Systems

A conditionally stable system is one which becomes unstable if the loop gain is reduced sufficiently, whereas an absolutely stable system is one in which instability does not result on decreasing the loop gain. A position servo with tachometer, in cascade with a resistance-capacitance high-pass network as the

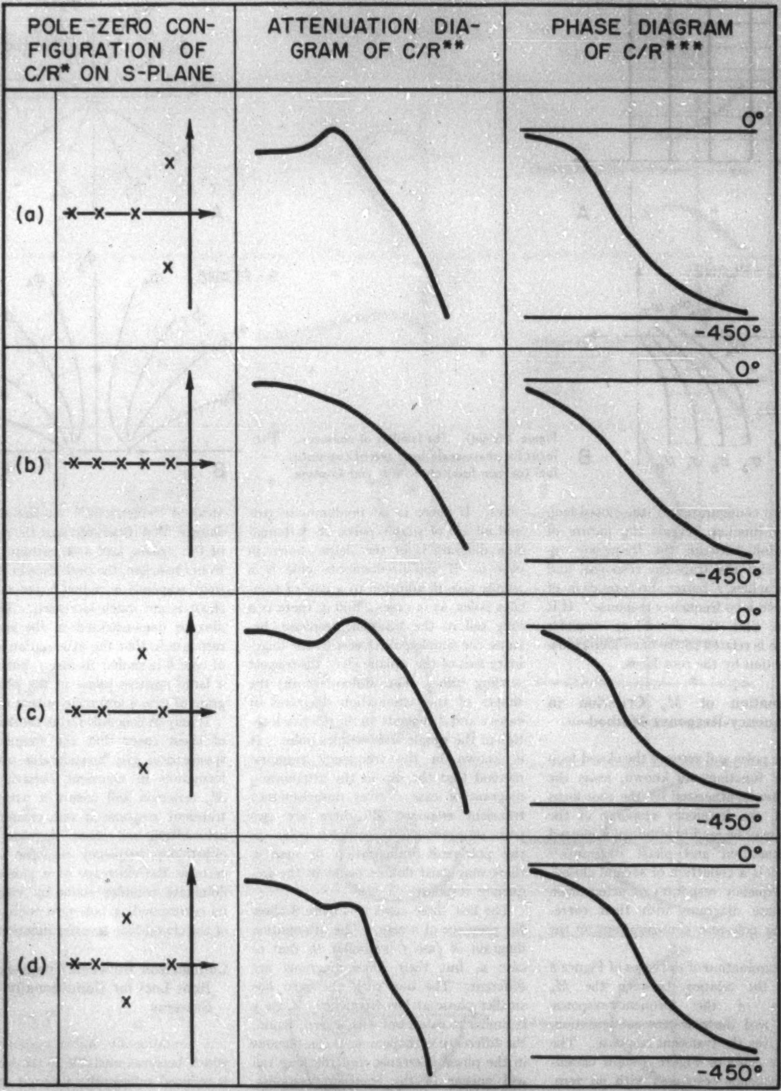
POLE-ZERO CONFIGURATION OF C/R* ON S-PLANE
ATTENUATION DIAGRAM OF C/R**
PHASE DIAGRAM OF C/R***
(a)
(b)
(c)
(d)
0°
-450°

Figure 8. A collection of pole-zero configuration of C/R and its corresponding attenuation and phase diagrams

*C/R is the closed-loop transfer function
** diagram of log (C/R) versus log ω
***diagram of phase angle versus log ω

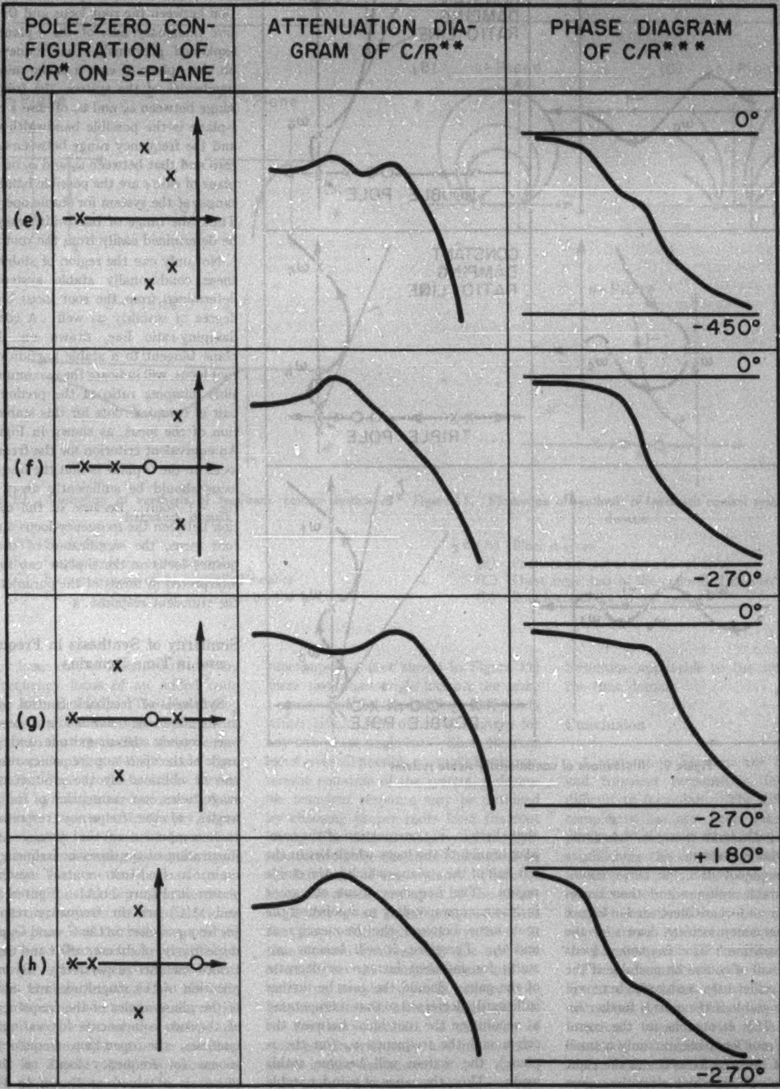
POLE-ZERO CONFIGURATION OF C/R* ON S-PLANE
ATTENUATION DIAGRAM OF C/R**
PHASE DIAGRAM OF C/R***
(e)
0°
-450°
(f)
0°
-270°
(g)
0°
-270°
(h)
+180°
-270°

Figure 8 (continued)

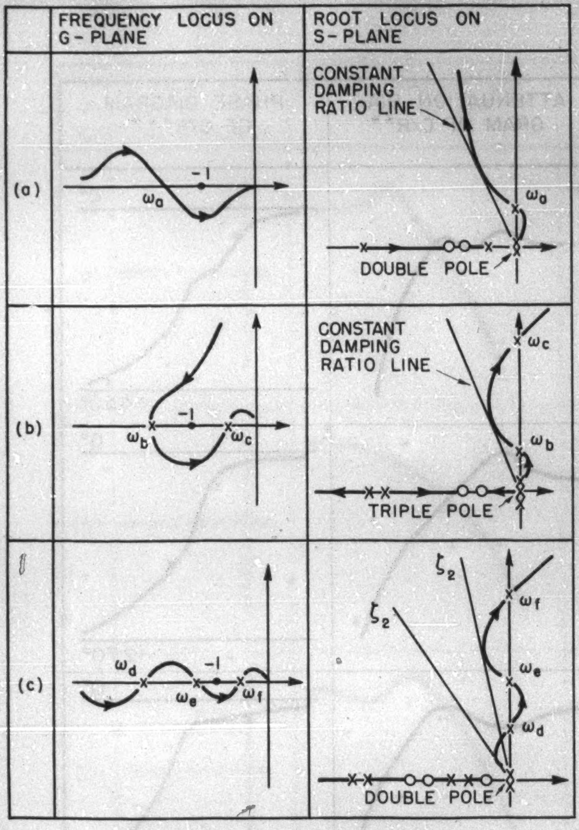

Figure 9. Illustrations of conditionally stable systems

feedback path, is an example of a conditionally stable system.

The frequency loci for three conditionally stable systems and their corresponding root loci are illustrated in Figure 9. All frequency loci are drawn for the stable condition. The frequency locus of case *a* will of course be unstable if the gain is sufficiently reduced, but will always be stable if the gain is further increased. This is obvious on the corresponding root locus because only a small portion of the root locus lies in the right half of the *s*-plane, which gives the region of instability at low value of gain. The frequency locus of case *b* will be unstable for sufficient increase or decrease of the gain. The corresponding root locus shows that there is only one portion of the complex branch of the locus which lies in the left half of the *s*-plane, which is the stable region. The frequency locus of case *c* is drawn, corresponding to a point on the root locus between the frequencies ω_e and ω_f. Therefore, it will become unstable for sufficient increase or decrease of the gain. Should the gain be further sufficiently decreased so that it is operated at a point on the root locus between the origin and the frequency ω_d (on the *s*-plane), the system will become stable again. Thus, the range of gain for stable operation can be determined easily from the root locus.

The frequencies ω_a to ω_f are those on the frequency loci at the points of intersection of the frequency locus with the negative real axis of the *G*-plane. These are also the values on the imaginary axis of the *s*-plane at the points of intersection between the root locus and the positive imaginary axis of the *s*-plane. As explained previously, the frequency ω_a on the *s*-plane of case *a* is the minimum bandwidth of the system, the frequency range between ω_b and ω_c of case *b* on the *s*-plane is the possible bandwidth range, and the frequency range between ω_d and zero and that between ω_e and ω_f on the *s*-plane of case *c* are the possible bandwidth ranges of the system for stable operation. Thus, the range of bandwidth may also be determined easily from the root locus.

Not only can the region of stability of these conditionally stable systems be determined from the root locus but the degree of stability as well. A constant damping-ratio line, drawn on the *s*-plane tangent to a stable portion of the root locus, will indicate the maximum possible damping ratio of the predominate pair of complex roots for this stable portion of the locus, as shown in Figure 9. An equivalent criterion for the frequency locus on the *G*-plane is that the frequency locus should be sufficiently away from the −1 point. Because of the correlation between the frequency locus and the root locus, the significance of the frequency locus on the *G*-plane can thus be interpreted in terms of the parameters of the transient response.

Similarity of Synthesis in Frequency and in Time Domains

Synthesis of feedback control system in the frequency domain is a powerful one, because the magnitude and phase angle of the open-loop frequency response can be obtained by the product of the magnitudes, and summation of the phase angles, of the frequency responses of each component of the system. As an illustration of synthesis in frequency domain, a feedback control system is shown in Figure 11(A). Figures 11(B) and 11(C) are the frequency responses (or frequency loci on the G_1- and G_2-planes respectively) of the controller and the controlled member respectively. By multiplication of the magnitude and addition of the phase angles of the frequency loci of the two components for various frequencies, the open-loop frequency response (or frequency locus on the *G*-plane) is obtained as shown in Figure 10(D). The shape of the frequency locus with respect to the −1 point on the *G*-plane determines the absolute stability and the degree of stability. The fre-

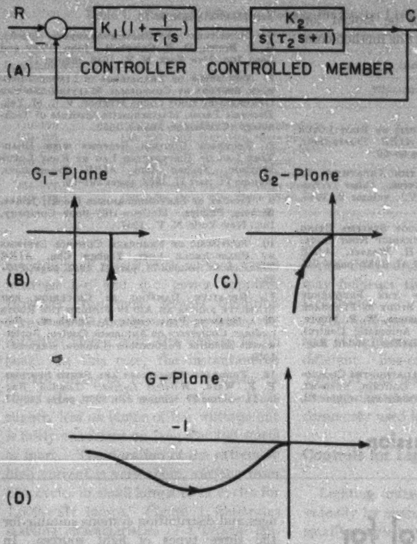

Figure 10. Illustration of synthesis of feedback control system in frequency domain

(A) Block diagram
(B) Frequency locus of the controller
(C) Frequency locus of the controlled member
(D) Frequency locus of the open-loop transfer function

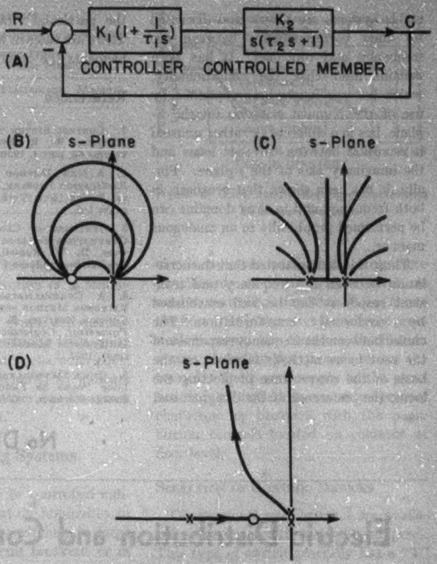

Figure 11. Illustration of synthesis of feedback control system in time domain

(A) Block diagram
(B) Phase-angle loci of the controller
(C) Phase-angle loci of the controlled member
(D) Root locus of the control system

quency locus can be reshaped readily by the frequency locus of an added component into the loop. The closed-loop responses can be read off the *G*-plane with reference to the two families of contours—not shown in Figure 10(D)—and then replotted. Such synthesis will be further simplified by using attenuation and phase diagrams.[9] The polar-frequency locus has been used in Figure 10 because of clarity in demonstrating the similarity.

The root-locus method is one for synthesis in the time domain. Furthermore, a correlation between the frequency locus on the *G*-plane and the root locus on the *s*-plane has been previously established. A way of synthesis by the root-locus method similar to that by the frequency-locus method has been developed by the introduction of the phase-angle loci.[10] The same system as the one illustrated in Figure 10(A) is shown in Figure 11(A). Figures 11(B) and (C) show the phase-angle loci of the controller and the controlled member respectively. The root locus of the system, Figure 11(D), can be readily obtained by superimposing (not shown in Figure 11) these two phase-angle loci on the same *s*-plane, and by identifying the points which give a sum of ±180 degrees for any two phase-angle loci. Since the root locus gives all possible roots of the characteristic equation of the system, a desirable transient response may be obtained by choosing proper roots from the root locus. The desired stability of the system restricts the choice to those roots on the left half of the *s*-plane. The root locus can also be reshaped by the phase-angle loci of an added component into the loop. Although this synthesis in time domain involves only the addition of angles on the complex plane and requires no templates, yet in general more graphical work is involved than that in the frequency domain. A similarity of synthesis in frequency and in time domains is thus demonstrated.

It is an advantage of the frequency-response method that the frequency function is a complex one, and conformal transformation may be applied. The root-locus method makes conformal transformation applicable to the synthesis in the time domain.

Conclusion

A correlation between the frequency and transient response is, in general, difficult to formulate. The difficulty or complexity has now been linked to the particular shape of the root locus. By establishing the correlation between the frequency locus on the *G*-plane and the root locus on the *s*-plane through conformal transformation, the frequency response may be interpreted in terms of the parameters of the transient response.

The performance of a feedback control system can be evaluated when the poles and zeros of its closed-loop transfer function, together with a multiplying constant, are specified. These poles and zeros, which give closed-loop frequency response on the one hand and the transient response on the other hand, may be used as a guide to interpret the frequency response in terms of transient response and vice versa. Several conditionally stable systems are shown and discussed for their correspondence between the frequency and root loci. It has been demonstrated that the conditionality, which has previously been explained by use of the Nyquist criterion on the G-plane, lies in a different or rather unusual intersection between the root locus and the imaginary axis of the s-plane. Finally, it has been shown that synthesis in both frequency and in time domains can be performed graphically in an analogous manner.

Thus, it is demonstrated that the correlation between the frequency and transient responses can be well established by conformal transformation. The choice between the frequency response and the root locus methods is made on the basis of the convenience in plotting the locus, the preference of the designer, and the particular result to be looked for. There are cases in which one method complements the other.

References

1. Control System Synthesis by Root Locus Method, **W. R. Evans.** *AIEE Transactions,* volume 69, part I, 1950, pages 66–69.

2. A New Method for the Treatment of Regulation Problem, **P. Profos.** *Sulser Technical Review* (New York, N. Y.), volume 2, 1945, pages 1–5.

3. Synthesis of Closed-Loop Systems Using Curvilinear Squares to Predict Root Location, **D. W. Russell, C. H. Weaver.** *AIEE Transactions,* volume 71, part II, 1952, pages 95–105.

4. A Generalization of the Frequency Response Method for the Study of Feedback Control Systems, **N. L. Kusters, W. F. Moore.** *Proceedings,* Conference on Automatic Control, Butterworths Scientific Publications(London, England), 1952.

5. Quick Methods for Evaluating the Closed-Loop Poles of Feedback Control Systems, **George Biernson.** *AIEE Transactions,* volume 72, part II, 1953, pages 53-70.

6. Principles of Servomechanisms (book), **G. S. Brown, D. P. Campbell.** John Wiley and Sons, Inc., New York, N. Y., 1948, chapter 11.

7. The Study of Transients in Linear Feedback Systems by Conformal Mapping and the Generalized Root Locus Method, **V. C. M. Yeh.** *Doctorate Thesis,* Massachusetts Institute of Technology (Cambridge, Mass.), 1952.

8. Feedback Control Systems with Dead-Time Lag or Distributed Lag by Root Locus Method, **Yaohan Chu.** *AIEE Transactions,* volume 71, part II, 1952, pages 291–96.

9. Theory of Servomechanisms (book), **James, Nichols, Phillips.** McGraw-Hill Book Company, Inc., New York, N. Y., 1947.

10. Synthesis of Feedback Control Systems by Phase-Angle Loci, **Yaohan Chu.** *AIEE Transactions,* volume 71, part II, 1952, pages 330–39.

11. Relative Damping as Criterion for Stability and as an Aid in Finding the Roots of a Hurwitz Polynomial, **A. Leonhard.** *Proceedings,* Conference on Automatic Control, Butterworths Scientific Publications (London, England), 1952.

12. Feedback Amplifiers and Servo Systems, **E. E. Ward.** *Wireless Engineer* (London, England), volume 27, number 320, 1950, pages 146–53.

No Discussion

Electric Distribution and Control for Lighting Systems

W. H. KAHLER
NONMEMBER AIEE

R. N. BELL
ASSOCIATE MEMBER AIEE

HIGHER illumination levels and new lighting sources make it necessary to re-examine possible methods of power distribution and control for lighting loads. As a result of the higher lighting load densities and versatile lighting sources, the designer must now exercise a considerable amount of engineering judgment in planning the distribution system. New design techniques make it possible to provide maximum convenience and reliability at minimum cost and with a minimum use of critical materials. The purpose of this paper is to discuss some of the requirements of the different lighting sources and analyze the modern trends in power distribution and control for lighting loads.

Lighting Sources

The principal lighting sources used for interior illumination today are filament, fluorescent, and mercury vapor lamps. Under certain conditions all of these sources are suitable for industrial lighting, and the filament and fluorescent lamps are used extensively for commercial interiors such as stores, schools, and office buildings. Filament lamps are operated directly from the supply voltage provided for lighting, while fluorescent and mercury lamps require an auxiliary device called a ballast to provide the correct lamp-starting voltage and to limit the operating current.

CIRCUIT VOLTAGES FOR LIGHTING

Filament lamps for lighting are generally supplied for 120-volt circuits. Lamps for 240-volt circuits are also available but are not generally recommended because efficiency is lower, filaments are more fragile, and cost is higher.

Flourescent and mercury lamp ballasts could be designed for any distribution voltage, but the controlling factors are the common distribution voltages and economics. Many vapor lamps require high voltage for starting and a line voltage higher than 120 volts often permits a lower cost ballast which requires less critical material. These higher line voltage ballasts may also have lower wattage loss.

Table I indicates the utilization voltages and distribution systems suitable for the three types of light sources. In general, branch circuits for lighting should not exceed 150 volts to ground according to the National Electrical Code. However, a maximum of 300 volts to ground is allowed in industrial plants and commercial areas for lighting fixtures that are equipped with mogul lampholders or lampholders approved for the application. In such installations, switch control cannot be an integral part of the fixture. Also, the equipment must be mounted not less than 8 feet above the floor.

LIGHTING LOAD CHARACTERISTICS

The design of a lighting circuit and the selection of circuit protective devices necessitates a knowledge of not only normal line current but also an understanding of the abnormal currents that occur when the circuit is closed or opened.

FILAMENT LAMPS

The filament lamp, when cold, has a resistance of about one fourteenth of that when it is hot. This characteristic results in a very high in-rush of current when the circuit is first closed. The

---

Paper 53-73, recommended by the AIEE Industrial Power Systems Committee and approved by the AIEE Committee on Technical Operations for presentation at the AIEE Winter General Meeting, New York, N. Y., January 19–23, 1953. Manuscript submitted April 16, 1952; made available for printing December 3, 1952.

W. H. Kahler is with the Westinghouse Electric Corporation, Cleveland, Ohio. R. N. Bell is with E. I. duPont de Nemours and Company, Inc., Wilmington, Del.

Table I. Practical Utilization Voltage for Interior Lighting Systems

Approximate Equipment Rating	Distribution System	Lamp Type (Asterisk Where Practical)		
		Filament	Fluorescent	Mercury
110–125	120/240 volts, three wire, single phase	*	*	*
110–125	120/208 volts, four wire, three phase	*	*	*
199–216	120/208 volts, three wire, three phase		*	*
220–250	240 volts, two wire, single phase		*	*
220–250	240 volts, three wire, three phase		*	*
254–277	265–460 volts, four wire, three phase		*	*
440–480	460 volts, three wire, three phase		*	*

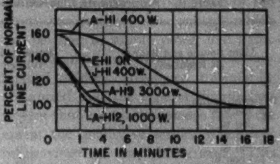

Figure 2. Line current starting characteristics of mercury lamps

magnitude of this in-rush current varies between a-c and d-c power supplies. However, the most serious condition occurs on alternating current when the circuit is closed with the voltage at its peak. In this case, the instantaneous current taken by the lamp is about 14 times the normal peak values. It is slightly less on lamps of low wattage but is fairly consistent on lamps of 100 watts or more. The duration of the extremely high current is very short, varying from $2^1/_2$ cycles in small lamps to 12 cycles for 1,000-watt lamps. Figure 1 illustrates starting characteristics of a typical filament lamp.

Fluorescent Lamps

The starting characteristics of fluorescent luminaires are quite different from filament lamps. When the circuit is closed, the line current is only about twice normal current and endures for only 2 or 3 cycles.

When a lamp reaches end of life, however, certain fluorescent ballasts will draw higher-than-normal line current due to the low power-factor condition created. This fact should be recognized when selecting the rating of the circuit protective and control devices.

The fluorescent lamp with its associated ballast is actually an inductive load. This factor must be considered when determining the rating of the control devices to be used with fluorescent lamps.

Mercury Vapor Lamps

The starting and operating characteristics of the mercury vapor lamps are also quite different from those of the filament lamp. The line-starting current for each type of lamp varies in peak value as well as in duration. Figure 3 illustrates the starting characteristics of several typical mercury vapor lamps. It should be noted that the high-starting current endures over a considerable period of time in comparison to the filament lamp.

As with some fluorescent circuits, a mercury lamp outage may also create a higher-than-normal line current which may influence the selection of a protective device.

The different sizes, types, and auxiliaries of light sources actually have quite different line-current characteristics; Table II has been prepared to indicate the specific characteristics for the more commonly used lamps.

Controls for Lighting Systems

Lighting units may be controlled individually by switches at the luminaires, in small groups by wall switches, in large groups by branch circuit breakers, or in very large groups by contactors or circuit breakers controlling one or more panelboards. Generally it is more economical to control groups of lighting units, but the best method for a particular application depends upon the type of areas illuminated.

Individual luminaire control is not used extensively because very few work areas can be lighted with one unit. Small groups of luminaires as in a private office are best controlled by one or more wall switches. Large groups as found in store areas or general offices may be controlled by wall switches on the columns or directly from the panelboard, using the circuit breakers as switches.

Industrial lighting involving medium and large areas is generally controlled from panelboards mounted on columns or on the wall. For the higher mounting heights, however, the length of the branch circuit becomes particularly long since panelboards mounted at floor level are used to control lighting 30 to 50 feet above the floor. It is therefore sometimes practical to mount the complete distribution system including panelboards above the trusses. The power supply to the panel boards is controlled by remotely operated contactors or breakers with the pushbutton controls located on columns at floor level.

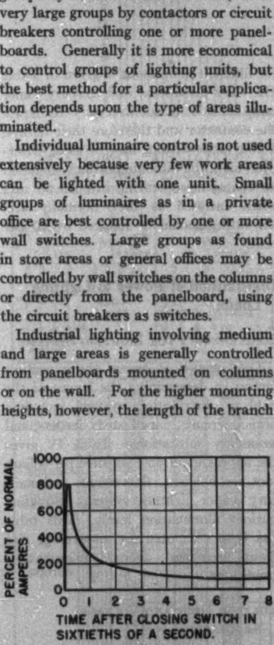

Figure 1. Starting characteristics of incandescent lamps

Selection of Control Devices

Conventional wall switches are available with ratings of 10, 20, and 30 amperes. This type of switch generally has a "T" rating which indicates that the switch may be operated at full-load current on filament lamp loads. However, where the switch controls an inductive load such as fluorescent or mercury lighting, the ampere rating should be twice the normal line current of the load.

Circuit breakers in panelboards may be used to control as well as protect lighting circuits. It is not necessary to derate the circuit breaker for controlling filament lamp or inductive loads beyond the derat-

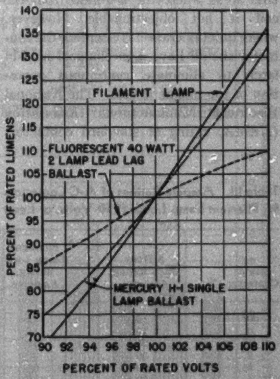

Figure 3. Influence of variations in voltage on light output

Table II. Approximate Line-Current Characteristics of Typical Light Sources

Light Source and Ballast (If Required)	Rated Line Voltage	Starting Current	Normal Line Current	Maximum Line Current With One Lamp Out
Filament Lamps				
1–200 W*	120		1.66	
1–300 W	120		2.50	
1–500 W	120		4.20	
1–750 W	120		6.25	
1–1,000 W	120		8.30	
Fluorescent Lamps				
Preheat type				
2–40 W lead-lag	118		0.85	1.2
2–40 W lead-lag	236		0.43	0.6
2–90 W lead-lag	118		2.05	*
2–90 W lead-lag	236		1.02	*
2–90 W lead-lag sequence	265		1.55	*
Slimline (instant start) type				
2–38 W, 48-inch T-12 lead-lag	118		0.95	1.8
2–38 W, 48-inch T-12 series	118		0.90	1.4
2–58 W, 72-inch T-12 lead-lag	118		1.4	2.2
2–58 W, 72-inch T-12 series	118		1.4	1.9
2–72 W, 72-inch T-12 lead-lag	118		1.65	3.15
2–75 W, 96-inch T-12 lead-lag	118		1.7	2.7
2–75 W, 96-inch T-12 series	118		1.7	1.9
2–96 W, 96-inch T-12 lead-lag	118		2.2	3.5
Mercury Lamps				
1–400 W single lamp	115	6.8	4.2	4.3
1–400 W single lamp	230	3.4	2.1	2.2
2–400 W lead-lag	115	4.5	7.6	†
2–400 W lead-lag	230	2.3	3.8	†
1–1,000 W single lamp	115	14.2	10.4	10.6
1–1,000 W single lamp	230	7.2	5.2	5.3
1–1,000 W single lamp	460	3.6	2.8	2.9
1–3,000 W single lamp	230	21.0	15.0	15.4
1–3,000 W single lamp	460	10.5	7.5	7.7
2–3,000 W two lamp	230	42.0	30.0	†
2–3,000 W two lamp	460	21.0	15.0	†

* W = watts.

† Less than normal line current.

ing normally applied because of an enclosure.

Remotely operated contactors or breakers in the panelboard feeders may be used to control general lighting in high-bay industrial areas, auditoriums, or other locations where a single or remote control is required for a large group of lighting units. Contactors with magnetic hold-in coils may be used in most industrial areas where the a-c hum from the coil is not objectionable. However, where quiet operation is essential, the contactor should have a mechanical hold-in latch to eliminate continuous operation of the magnetic coil. The National Electrical Manufacturers Association (NEMA) rating of standard contactors for filament lamp loads is given in Table III. For fluorescent and mercury vapor lamp loads it is not necessary to derate the contactor and therefore their normal 8-hour ampere rating may be used. However, all of the tabulated ratings are based on contactors operating in open air and when enclosed as they normally are, the rating should be reduced by 10 per cent.

Table III. Ampere Ratings of A-C Contactors for Filament Lamp Loads (250 Volts, or Less)

Size of Contactor	8-Hour Open Rating, Amperes	Filament Lamp Load Rating, Amperes
00	10	5
0	15	8
1	25	12
2	50	30
3	100	60
4	150	120
5	300	240
6	600	480

Distribution of Power to Lighting Loads

Load Density for Lighting Systems

Load density is one of the important factors in determining the layout of the lighting distribution system including branch circuits, panelboards, feeders, and secondary substations. Table IV gives the approximate volt-amperes per square foot for filament, fluorescent, and mercury vapor lighting systems providing various illumination levels. This table has been computed for an average size plant area and average maintenance conditions.

Voltage Drop and Voltage Regulation

It is usually considered good design practice to limit the voltage drop in lighting feeders to no more than 1 per cent and in the branch circuits to no more than 2 per cent.

The rated life and light output values of light sources are based upon the lamps operating at rated design voltage. Therefore, the distribution system should be designed to provide line voltage as close as practical to the rated voltage of the lamp.

The curves in Figure 3 show how light output varies with voltage for typical filament, fluorescent, and mercury equipment.

Branch Circuits for Lighting

The National Electrical Code classifies branch circuits as 15, 20, 30, and 50 amperes. According to the code it is the rating of the circuit protective device which actually determines the rating of the circuit. Fluorescent equipment and medium base screw shell lampholders are permitted on 15- and 20-ampere circuits. Heavy duty lampholders are permitted on all four sizes of branch circuits.

Circuits are normally protected by circuit breakers or fuses. The primary function of an over-current protective device is to guard against over-heating of the circuit conductor and to isolate a circuit fault. The operation of a thermal protective device (circuit breaker or fuse) is affected by the ambient temperature around the device. Circuit breakers are calibrated in open air and therefore when enclosed should be derated. The NEMA recommends derating factors for circuit breakers of 30 per cent when used in panelboards and 20 per cent when individually enclosed.

The selection of a circuit breaker size must therefore be based upon its derated value plus consideration of starting, operating, and possible lamp outage conditions of the lighting load. With mercury vapor lighting in particular, it is necessary to co-ordinate the time-current curve of the breaker with the time-current characteristic of the mercury vapor load. This is a rather tedious procedure, and therefore Table V has been prepared for all common lamps used with consideration given to all factors that influence the breaker selection.

Lighting Panelboards

The cost and amount of critical material in branch circuit wiring will depend to some extent upon the location of panelboards and the number of circuits per panel. Panelboards are generally available with from 4 to 42 circuits per panel. By using only a few circuits per panel, the length of branch circuits may be

Table IV. Load Density—Approximate Volt-Amperes per Square Foot for Typical Lighting Systems

Approximate Foot-candle Average Size Room	Industrial Areas, Direct Lighting			Office Areas		
	Fluorescent	Mercury	Filament	Direct-Indirect Fluorescent	Semi-Indirect Fluorescent	Indirect Filament
10	0.6	0.7	1.5			
20	1.2	1.5	3.0	1.5	2.7	7.0
30	1.8	2.0	4.5	2.0	4.0	11.0
50	3.0	3.5	7.5	3.5	6.5	18.0
75	4.5	5.0	11.0	5.0	10.0	
100	6.0	7.0	15.0	7.0	13.0	

minimized. Also, voltage drop may be reduced and it may be possible to prevent the necessity of increasing wire size on long circuits to limit voltage drop. With only a few circuits per panel however, the panel cost per circuit is increased and feeder cost is generally greater. It is, therefore, a designer's responsibility to analyze this relationship of panelboard size versus the length of branch circuits to determine an economical and practical panelboard layout.

FUNDAMENTAL DISTRIBUTION SYSTEM DESIGN

One of the first decisions to be made is whether to use a combined lighting and power system or separate systems for each. In a combined system the power and lighting loads are supplied from the same secondary substations, whereas in a separate system separate substations are provided for the lighting load.

The advantages of the combined system for power and lighting are simplicity and lower cost. The principal advantage of the separate power and lighting arrangement is its ability to limit the magnitude of voltage fluctuations resulting from suddenly applied loads. In some industrial plants the magnitude and frequency of the suddenly applied loads such as motor starting and load fluctuations produced by welders may produce an objectionable light flicker condition on a combined system. In installations where severe power-load fluctuations are encountered, the additional cost of a separate supply for lighting may be justified.

The ability of the separate system to limit voltage flicker is the result of using separate secondary substations for the power and lighting loads. With this arrangement the voltage drop in the secondary substation transformer, which is produced by a suddenly applied power load, has no effect on the supply to the lighting load. In most power distribuiton systems, the voltage drop in the substation transformer will be a substantial part of any voltage dip to which the lighting load may be subjected. For this reason the magnitude of the voltage fluctuations are appreciably smaller when a separate lighting supply is installed.

TYPES OF ELECTRICAL DISTRIBUTION SYSTEMS

It is not within the scope of this paper to present a detailed discussion of the characteristics and relative merits of the eleven basic system arrangements which can be used to supply power and lighting loads in an industrial plant or a commercial building. However, it should be recognized that the type of distribution system that is used determines to a large extent the quality of service which will be provided for the lighting load. This is one of the reasons that the selection of the distribution system for a plant or building deserves a lot of careful consideration and planning.

The two characteristics of a distribution system which are most significant in connection with the power supply to lighting loads are service continuity and voltage regulation. Service continuity is measured in terms of the amount of load dropped and the probable duration of any power outages for faults at different locations in the system. Voltage

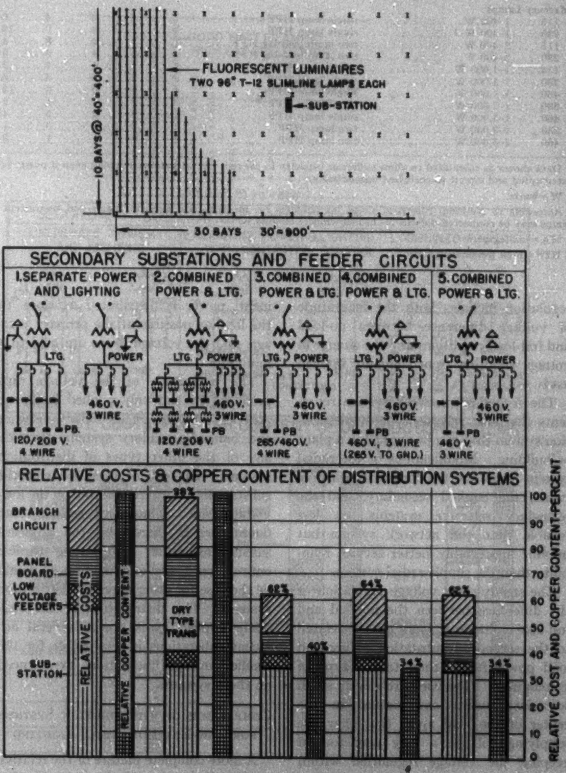
10 BAYS @ 40'=400'
FLUORESCENT LUMINAIRES
TWO 96" T-12 SLIMLINE LAMPS EACH
SUB-STATION
30 BAYS 30'=900'
SECONDARY SUBSTATIONS AND FEEDER CIRCUITS
1. SEPARATE POWER AND LIGHTING
LTG.
POWER
PB.
120/208 V. 4 WIRE
460 V. 3 WIRE
2. COMBINED POWER & LTG.
LTG.
POWER
PB
120/208 V. 4 WIRE
460 V. 3 WIRE
3. COMBINED POWER & LTG.
LTG.
POWER
PB
265/460 V. 4 WIRE
460 V. 3 WIRE
4. COMBINED POWER & LTG.
LTG.
POWER
PB
460 V., 3 WIRE (265 V. TO GND.)
460 V. 3 WIRE
5. COMBINED POWER & LTG.
LTG.
POWER
PB
460 V. 3 WIRE
460 V. 3 WIRE
RELATIVE COSTS & COPPER CONTENT OF DISTRIBUTION SYSTEMS
BRANCH CIRCUIT
PANEL BOARD
LOW VOLTAGE FEEDERS
SUB-STATION
RELATIVE COSTS
RELATIVE COPPER CONTENT
98%
DRY TYPE TRANS.
62%
40%
64%
34%
62%
34%
0
10
20
30
40
50
60
70
80
90
100
RELATIVE COST AND COPPER CONTENT-PERCENT

Figure 4. Distribution study with fluorescent lighting

Table V. Number of Lighting Units per Circuit Calculated for Thermal-Magnetic Type Breaker

Line Voltage	Lamps per Unit	Type of Ballast	Breaker Ratings 15	20	25	35	50
			Derated Value (70%) for Continuous Operation of Panel Breakers* 10.5	14.0	17.5	24.5	35
Filament Lamps							
120	1–100 W†		12	16	‡	‡	‡
120	1–200 W		6	8	‡	‡	‡
120	1–300 W		4	5	7	10	14
120	1–500 W		2	3	4	6	8
120	1–750 W		1	2	2	4	5
120	1–1,000 W		1	1	2	3	4
Fluorescent Lamps							
Preheat type							
118	2–40 W, 48-inch T-12	lead-lag	12	16	‡	‡	‡
236	2–40 W, 48-inch T-12	lead-lag	24	32	‡	‡	‡
118	2–90 W, 60-inch T-17	lead-lag	5	7	‡	‡	‡
236	2–90 W, 60-inch T-17	lead-lag	10	14	‡	‡	‡
265	4–90 W, 60-inch T-17	lead-lag sequence start	7	9	‡	‡	‡
Slimline type							
118	2–38 W, 48-inch T-12	lead-lag, 425 MA§	11	14	‡	‡	‡
118	2–38 W, 48-inch T-12	series, 425 MA	11	15	‡	‡	‡
118	2–58 W, 72-inch T-12	lead lag, 425 MA	7	10	‡	‡	‡
118	2–58 W, 72-inch T-12	series, 425 MA	7	10	‡	‡	‡
118	2–72 W, 72-inch T-12	lead-lag, 600 MA	5	7	‡	‡	‡
118	2–75 W, 96-inch T-12	lead-lag, 425 MA	6	8	‡	‡	‡
118	2–75 W, 96-inch T-12	series, 425 MA	6	8	‡	‡	‡
118	2–96 W, 96-inch T-12	lead-lag, 600 MA	4	6	‡	‡	‡
Mercury Lamps							
115	1–400 W	single lamp HPF ‖	1	2	3	4	6
230	1–400 W	single lamp HPF	3	5	6	9	12
115	2–400 W	two lamp lead-lag HPF	1	1	2	3	4
230	2–400 W	two lamp lead-lag HPF	2	3	4	6	9
115	1–1,000 W	single lamp HPF	1	1	1	2	3
230	1–1,000 W	single lamp HPF	2	2	3	4	6
460	1–1,000 W	single lamp HPF	4	5	6	9	13
230	1–3,000 W	single lamp HPF	0	0	1	1	2
460	1–3,000 W	single lamp HPF	1	1	2	3	4
230	2–3,000 W	two lamp HPF	0	0	0	0	1
460	2–3,000 W	two lamp HPF	0	0	1	1	2

* Data shown as calculated to allow sufficient capacity to prevent circuit breaker tripping even if power is interrupted and circuit re-energized immediately.

† W = watts.

‡ According to National Electrical Code, lampholders for medium-base filament lamps and fluorescent lamps may be connected only to 15- and 20-ampere circuits.

§ MA = milliamperes

‖ HPF = high power factor.

regulation includes both the magnitude of voltage difference between no-load and full-load conditions and the change in voltage resulting from suddenly applied loads.

The secondary network system represents the most reliable type of distribution system that can be applied in a plant or building. Modifications of the radial system such as the primary selective radial, the banked secondary, and the secondary selective systems are less reliable than the network system but provide appreciably better service reliability than the simple radial system.

The steady-state voltage regulation or the difference between the no-load and full-load voltages is more closely related to the secondary substation rating and load power factor than to the type of system used. The use of relatively small secondary substations located in the center of the load areas that they are supplying will go a long way toward keeping the voltage regulation within reasonable limits. With this arrangement, power is distributed as close to the load as possible at the primary voltage, and the voltage drops are held to a minimum.

The magnitude of the voltage dips produced by suddenly applied loads are generally smaller on secondary network and banked-secondary systems than on any of the other types of distribution systems. In both of these systems the substations are interconnected on the low-voltage side. Thus any sudden load fluctuation is shared by the adjacent substations rather than being thrown entirely on a single substation as would be the case for other types of distribution systems. The distribution of the suddenly applied loads among several adjacent substations is responsible for the smaller voltage fluctuations experienced on these systems.

COMPARISON OF DISTRIBUTION SYSTEMS FOR LOW-BAY INDUSTRIAL LIGHTING

A more complete picture of the relative merits of several methods of distributing power to lighting loads can be obtained from the results of comparison of supplying the lighting in a typical low bay industrial plant installation. A brief description of the basis for this comparison and also the results obtained are shown in Figure 4. Both system investment and copper content were considered in this comparison.

The comparison was based on an industrial plant which was 900 by 400 feet with bays 30 by 40 feet. The total of power and lighting loads was assumed to be 12.5 volt-amperes per square foot. The lighting layout consisting of 2-unit 96-inch slimline fluorescent luminaires mounted in continuous rows spaced 8 feet apart. Fluorescent lighting was selected on the basis of it being the most practical and economical source for this type of installation. The lighting layout provides approximately 50 foot-candles of light and the lighting load amounts to approximately 3.3 volt-amperes per square foot.

The five system arrangements which were investigated in our comparison are listed in the following text. These five systems were selected because they appeared to offer the greatest possibility of providing a satisfactory solution to the problem of supplying the lighting load n this plant.

1. Separate power and lighting. Lighting 120/208 volts, power 460-volt wye system.
2. Combined power and lighting. Lighting 120/208 volts by small dry-type transformers, power 460-volt wye system.
3. Combined power and lighting. Lighting 265 volts from 460/265 volt system, power 460-volt wye system.
4. Combined power and lighting. Lighting 460 volts, power 460-volt wye system.
5. Combined power and lighting. Lighting 460 volts, power 460-volt delta system.

The economic comparison included the installed cost of all of the distribution system required for the lighting loads from the secondary substations to the branch circuits to the luminaires. The cost of the luminaires and lamps were not included in the comparison. In this particular case the cost of the luminaires and lamps would be essentially the same for the five arrangements being considered. The substation cost for the combined systems was obtained by dividing up the total cost of the substation in relation to the amounts of power and lighting load which the substation supplied.

The copper comparisons were based on the copper content of the secondary substations, low-voltage feeders, and branch circuits in the distribution systems supplying the lighting load.

In the combined systems, separate low-voltage feeders were provided for supplying the lighting load. Each of the five arrangements was designed so that the sum of the voltage drop in the low-voltage feeders and the branch circuits was limited to 3 per cent or less. Twenty-ampere branch circuits were used in each of the five systems.

The economic comparison shows that the two systems which employ a 120/208-volt supply to the lighting load required the largest investment. The separate power and lighting arrangement was actually the most expensive. The combined system using small dry-type transformers to step down to 120/208-volts for lighting required just slightly less investment than the separate power and lighting arrangement. The relatively high cost of the small dry-type transformers in this combined system was primarily responsible for its cost being almost comparable to that of the separate arrangement.

The relative cost of all three of the arrangements in which the lights were supplied directly from a 460-volt system was appreciably less than the separate power and lighting system. These three arrangements were approximately equal in cost being about 60 per cent of the investment in the separate power and lighting arrangement.

The relative copper contents varied in approximately the same fashion as the system investments. The copper content of the arrangement in which 265-volt fluorescent lamps were connected from line to neutral on the 460-volt wye system was 40 per cent of the separate power and lighting arrangement. The two schemes in which the luminaires were connected line to line on the 460-volt system required 35 per cent of copper in the separate power and lighting scheme.

Comparison of Distribution System for High-Bay Industrial Lighting

To further investigate the different distribution system arrangements which can be used to supply the lighting load in an industrial plant, a comparison of the power distribution to high-bay lighting was made. This comparison was based on supplying the lighting load in two adjacent high-bay areas which were 80 by 860 feet. Both 1,000-watt filament high-bay lights and 1,000-watt mercury vapor units were considered for lighting in this installation. The lighting layout for both filament and mercury vapor sources was designed to provide approximately 50 foot-candles of illumination. The power and lighting loads were supplied from secondary substations at three locations in the plant area.

A comparison of three distribution system arrangements for supplying the 1,000-watt filament lighting is illustrated in Figure 5. The three systems that were considered for supplying the 1,000-watt incandescent units are the following:

1. Separate power and lighting system with lighting supplied at 120/208 volts from panelboards installed at the floor level.

2. Separate power and lighting system with lighting supplied at 120/208 volts from panelboards installed overhead. Remotely controlled contactors installed overhead for control of lights.

3. Combined power and lighting system with small dry-type transformers stepping down to 120/208 volts for lighting. Panelboards and dry-type transformers overhead. Lighting controlled by circuit breakers at floor level.

The economic comparison of these three schemes shows that the separate system with panelboards at the floor level and the combined system using small dry-type transformers for lighting require approximately the same amount of investment. The cost of separate power and lighting system employing remote contactor control was about 8 per cent higher than the other two schemes. The difference in copper content among these three arrangements was so small that for practical purposes they can be considered negligible.

The comparison which was made on the basis of 1,000-watt mercury vapor lighting for the high-bay installation is outlined in Figure 6. The distribution system arrangements which were considered for supplying this mercury vapor installation are the same five arrangements that were investigated in the low-bay fluorescent lighting comparison. As

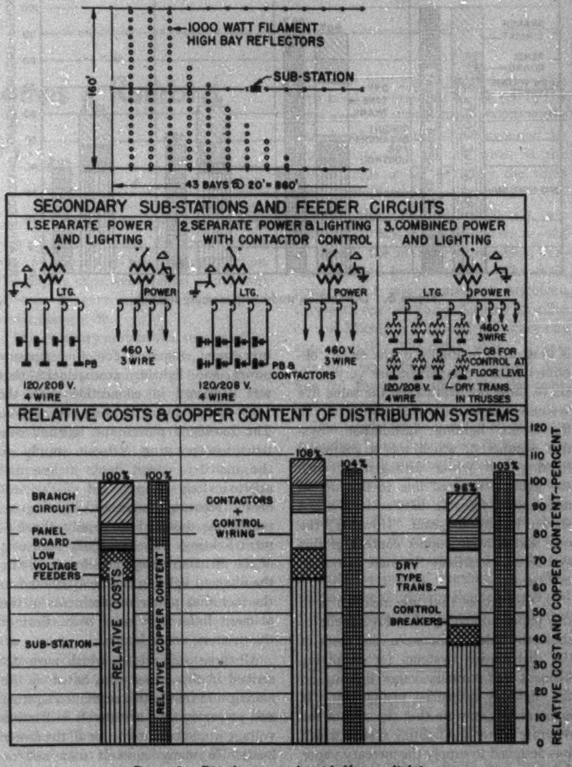

Figure 5. Distribution study with filament lighting

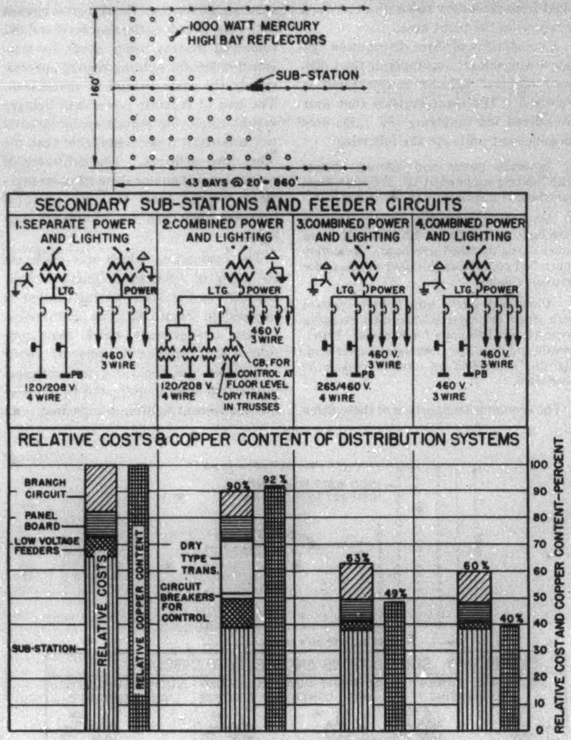

Figure 6. Distribution study with mercury lighting

is illustrated in Figure 6, the results obtained in this comparison are very similar to those obtained when the same five systems were considered for supplying the fluorescent lighting installation. System number 5, which was a combined lighting and power arrangement with the lights connected line to line on an ungrounded 460-volt delta system, is not shown in the diagram. However, the cost and relative copper content of this system are essentially the same as system number 4.

In the figures that are included with this paper no attempt has been made to show the relation between the costs of the distribution systems for supplying filament and mercury vapor lighting on the high-bay industrial installation. It is interesting to note that the cost of the separate power and lighting system which was designed to supply the mercury vapor lighting was roughly 67 per cent of the investment required for the separate power and lighting arrangement that was discussed in connection with the 1,000-watt filament lighting comparison. The combined power and lighting systems incorporating 460-volt supply to the mercury vapor lights represented approximately 43 per cent of the cost of the separate power and lighting arrangement designed to supply the filament lighting. The relatively high cost of the distribution systems for supplying the filament lighting can be attributed to the fact that power requirements of the filament lighting is over twice that of the mercury vapor lamps.

All three comparisons which were described in this paper were based on the assumption that with a combined lighting and power system, a 460-volt utilization voltage would be suitable for all the power loads. In many cases it may not be practical to supply all of the power loads from the 460-volt system. This factor will tend to reduce the advantages which are shown for a 460-volt supply to the lights. However, in most instances the amount of power load which it is desirable to supply at a somewhat lower voltage will be relatively small and introducing this consideration into the comparisons should not have any appreciable effect on the over-all results.

Conclusions

The results of the comparisons indicate that the investment in the distribution system for supplying lighting loads can be considerably reduced by installing a combined power and lighting arrangement in which the lights are supplied directly from the 460-volt supply to the lighting load. The reluctance of many individuals to go to voltages higher than 120 volts for lighting plus the failure of most distribution engineers to recognize the inherently lower cost and copper savings in this type of system is apparently responsible for the fact that 460-volt supply to lighting loads has not become more widely used.

The line-to-neutral connection of the lights on the 460-volt system appears to be the most practical method at the present time. Connecting the lights line to line on either a 460-volt delta or a 460-volt grounded wye system is feasible and offers the advantage of slightly lower cost branch circuits from the panelboards. However, line-to-line connection of lights makes it necessary to use either 2- or 3-pole circuit breakers in the lighting panelboards. Panelboards consisting of 2- or 3-pole breakers which can be applied on a 460-volt system are somewhat more expensive than the panelboards containing single-pole breakers which are used when the lights are connected from line to neutral.

◆

Discussion

L. C. Peterman (Ford, Bacon and Davis, Inc., New York, N. Y.): If we accept the economy of distribution of the 265-volt system for lighting, we limit ourselves to fluorescent or mercury lighting units. And in numerous industrial applications filament lighting is eminently satisfactory and has the lowest over-all cost for fixtures and lamps. This sometimes is overlooked in what seems to be almost a mania for taking up the new and casting aside the old.

We cannot agree that the cost of supplying incidental 120-volt service from 265-volt circuits will not seriously affect the economic comparison in favor of 265-volt circuits. Our experience indicates that office areas, trouble lamps, and portable tools require widespread convenience outlets 33 per cent to 100 per cent as numerous as lighting outlets. If panel-boards and small transformers are added to the 265-volt system, the latter is increased considerably in cost. And when the small 1-, 2-, or 3-kva transformers are added will they be tapped to a 265-volt circuit (requiring a special transformer) or will a special 460-volt circuit be run just for these transformers?

The 265/460-volt system, as presented, is not a universal system applicable to all types of lighting units as are some of the other systems presented. For a true comparison, all systems estimated should be able to supply all types of lighting units, or the estimates should include the cost of fixtures and lamps to give at least approximately equivalent illumination results.

We see no advantage in using 3-phase transformation for the 460/120-208-volt lighting circuits. Unless 3-phase 208-volt service is required for special purposes, single-phase transformers are lower in cost and usually can be balanced acceptably across phases on the 3-phase 460-volt circuit. Using single-phase transformers and with certain other refinements, we have been able to reduce costs for the 460-volt combined power and light system from 10 per cent to 25 per cent below the cost of other acceptable system(s).

Strangely enough, in considering the 265-volt system, we have been advised at times that to specify such voltage (or 277 volts) for transformer secondaries will entail delayed delivery because the voltage is nonstandard.

We commend Mr. Kahler and Mr. Bell for the use of 460 as a circuit voltage, which recognizes the obvious but sometimes overlooked fact that 480 on a transformer name plate does not necessarily, in fact seldom, represent the proper utilization voltage.

W. H. Kahler and **R. N. Bell:** It certainly was not the intent of this paper to encourage high-voltage distribution systems for all types of lighting layouts. It is true that 120 volts is best for incandescent lighting and, where incandescent lamps predominate in the over-all lighting load, a 120-volt distribution voltage is best. However, where all or a high percentage of the lighting load is fluorescent or mercury, the higher voltage distributions will prove to be more economical.

Where small dry-type transformers are required for incandescent lamps and receptacle circuits, these transformers are generally connected to 460 volts line to line rather than to 265 volts line to neutral. The use of single-phase versus 3-phase dry-type transformers is determined by the amount and type of load to be served and also the particular engineering preference.

In the past most 460-volt 3-phase distribution systems have been supplied by delta-connected transformers because industry has preferred the ungrounded secondary for power equipment. In recent years some industrial plants have seen advantages to grounded power systems and also have seen the advantages to 265 volts for lighting. Therefore, the 265/460-volt 4-wire Y-connected transformers have become universally available from the major manufacturers of transformers and unit substations. If the demand for 265 volts for lighting increases, we would expect the Y-connected transformer to become standard apparatus for all suppliers.

An Interurban Becomes a Railroad

C. H. JONES
ASSOCIATE MEMBER AIEE

ONE OF the most important advances in rail transportation after the turn of the century was the introduction of electric traction motors for passenger train service. This boom started a crisscross of short interurban electric lines throughout the country with the idea in mind of reaching out and covering more territory. At the time of this boom there were two trends of thought in the traction field—alternating current and direct current.

In May 1906 the Chicago Lake Shore and South Bend Railway Syndicate was formed to acquire the securities of the Chicago Lake Shore and South Bend Railway Company, a successor to the Indiana Air Line Railway Company. This syndicate, favoring a-c propulsion power, started construction on an interurban line from South Bend, Ind. to Chicago, Ill.

The original electrification of the railroad in 1908 was a 6,600-volt single-phase a-c contact system. The construction consisted of one 1/2-inch Siemens-Martin steel cable as the main messenger, one 4/0 copper intermediate wire and one 3/0 grooved iron contact wire. The intermediate wire was suspended from the main messenger by means of rigid hangers. The steel contact wire was in turn suspended from the intermediate wire by means of bronze duplex clips. The duplex clips were spaced equidistant between hangers and provided a good feeder connection.

This catenary system was supported by a wooden pole line which, upon its completion, was considered by many as the finest pole line in the country. The poles were 45-feet long-leaf yellow pine, creosoted and set with a concrete collar at the bottom about 3 feet in outside diameter and 1 foot thick and another similar collar just below the surface of the ground. The pole spacing was 167 feet on tangent track with shorter spacings on curves varying with the degree of the curve. On single track between Gary and South Bend, Ind., the poles were located on the south side of the track approximately 9 feet from the center of the track. In double-track territory between Gary and the Illinois-Indiana state line, the poles were located between the tracks. From the state line to Kensington, Ill., the poles were placed on the outsides of both main tracks.

Attached to these poles were 9-foot tee section, bare steel mast arms. The main messenger wire was supported by a pin-type insulator attached to the top of the mast arm. A 5-foot wood steady strain was placed between the mast arm and the intermediate and contact wires at the proper angle so as to steady the wires from wind effect.

With this 25-cycle 6,600-volt a-c system only two substations were needed to furnish the necessary propulsion current required by the trains. The main power plant was located at Michigan City with one substation located 22 miles east of Michigan City and the other one approximately 33 miles west. Transmission lines attached to the wood pole line fed the substations from the main power station.

The single track portion of the line, extending from Gary to South Bend, was equipped with automatic semaphore-type block signals. These signals were two position and used the left-hand upper quadrant. The track circuits for these signals were 60 cycles, alternating current, so as not to be interfered with by the 25-cycle propulsion current. A 2,200-volt a-c signal primary line fed the signal system with a pole-mounted transformer

---

Paper 53-35, recommended by the AIEE Land Transportation Committee and approved by the AIEE Committee on Technical Operations for presentation at the AIEE Winter General Meeting, New York, N. Y., January 19–23, 1953. Manuscript submitted October 23, 1952; made available for printing November 28, 1952.

C. H. JONES is with the Chicago South Shore and South Bend Railroad, Michigan City, Ind.

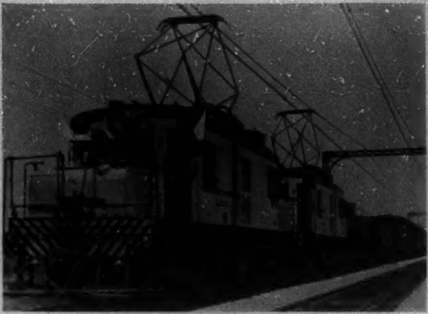

Figure 1. A pair of 900-class 100-ton locomotives, equipped with 2-way space radio, operating in multiple unit

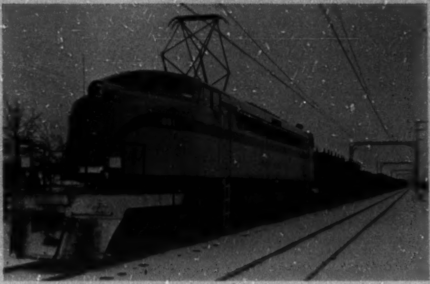

Figure 2. One of the 800-class 275-ton locomotives pulling freight train through "ideal section" near Gary, Ind.

at each signal location to step the 2,200 volts down to 110 volts for motor operation and another tap further reduced it to 12 volts for the track circuit.

The railroad had two full metallic circuit telephone lines extending from Kensington to South Bend with the main switchboard located in the general offices at Michigan City. One circuit was used exclusively for dispatching and the other for the general business of the railroad.

The original track consisted mainly of 70# ASCE Bessemer steel rail on 8-foot creosoted red oak cross ties ballasted to a depth of 6 inches with bank run gravel.

In March 1908 five interurban coaches were delivered, but it was not until July of that year that time table number 1 was issued inaugurating regular service between South Bend, Ind. and Michigan City, Ind. with a running time of 1 hour and 30 minutes. In September of the same year regular service was extended to Gary. In April 1909 scheduled trains were put in service between South Bend, Ind., and Kensington, Ill., where passengers transferred to Illinois Central suburban trains for downtown Chicago.

In May 1912 an agreement was made with the Illinois Central whereby Lake Shore Line coaches would be handled by Illinois Central suburban steam engines to the Chicago terminal at Randolph Street. By switching the cars to the Illinois Central at Kensington, it was possible to ride from South Bend to Randolph Street without necessitating a change.

The passenger equipment included 11 passenger motor cars and eight combination motor and baggage cars weighing 55 tons each and attaining a speed of 69 miles per hour. There were also ten 50-foot trailers weighing $27^1/_2$ tons and four 60-foot trailers of about the same weight.

The electric equipment on the motor cars included four Westinghouse number 148 single-phase motors rated at 125 horsepower equipped with multiple-unit controllers with five points for acceleration. The controller was not equipped with a dead-man control, although the controller would move to off position if released. A 6,600-volt autotransformer was used to reduce the incoming voltage for use on the car. Two traction motors were permanently hooked in series, and the maximum voltage tap on transformer was 800 volts. The control voltage, which operated only the contactors, was furnished from a 18-volt 9-cell battery, charged on the floor and changed each time the car was shopped for inspection. Lighting on the motor cars was taken from the 110-volt tap on the transformer. The headlights were originally carbon arc operating from 110 volts, but were later changed to 6 volts using a 110 to 6-volt transformer.

All of the cars were equipped with one pantagraph and at least one trolley pole. It was necessary for the trains to stop at each end of the cities and operate a changeover switch under the cars, which permitted the operation of equipment on 800 volts through the city streets and 6,600 volts outside of the cities.

After about 15 years of operating, freight service was started and two 70-ton Westinghouse freight locomotives and a few freight cars were purchased.

In the summer of 1925 the railway's value had depreciated to only a percentage of the original outlay. Track, equipment, signals, and stations were virtually ready to fall apart. The Chicago Lake Shore and South Bend Railway had collapsed financially under the heavy pressure of high costs during World War I. Parallel hard-surfaced roads and growing motor transportation threatened to strip it of possibilities for the future. It was forced into receivership. The Midland Utilities Company, operating a number of gas, electric, and transportation companies, realizing the strategic location, became interested in the insolvent Chicago Lake Shore and South Bend Railway. They could foresee a region destined to become a summer vacation area with great industrial cities.

After a survey was made by a group of Midland Utilities transportation engineers, this property was purchased and the Chicago Lake Shore and South Bend Railway became the Chicago South Shore and South Bend Railroad.

Up until this time the Illinois Central suburban service was steam operation. Due to the growth and frequency of service, the Illinois Central deemed it necessary to abandon steam engines in favor of electric traction using 1,500 volts direct current. Because of the close association of the Illinois Central commuter service and the South Shore interurban service, the Midland Utilities immediately converted to 1,500 volts direct current for propulsion power in order to establish a terminal in downtown Chicago, by running on the Illinois Central tracks from Kensington to Randolph Street, a distance of 14 miles.

When the rebuilding problem arose, the management at that time had to choose between a light overhead collection system with separate feeder for conductivity or a system whereby all the conductivity is placed in the contact and supporting wires. After much consideration the latter-type construction was selected.

In converting to the new system, the management decided on using the same pole line as the old poles were considered adequate for the new type of construction. Having been previously set in concrete, they were secure enough to withstand the increased loads imposed by the new catenary; therefore, only a minimum amount of straightening was required and the pole line was ready for the conversion operation. On the Kensington and Eastern section, Bates expanded steel trusses were attached between the poles to support the catenary over the double track main line. Suspension insulators were clamped to these trusses and the main catenary messenger attached to them. On the center pole and single pole overhead construction an adjustable type of galvanized bracket arm was installed. The main messenger was attached to an insulator on top of the mast arm similar to previously mentioned 6,600-volt construction. This new-type arm eliminated the heavy rusting condition experienced with the earlier-type construction. All pole spacing on tangent track remained at 167 feet except on a portion of track paralleling the New York Central Railroad immediately east of Gary.

The new construction of the catenary, carried out between Gary and Kensington consisted of one 0.728 inch diameter copperweld main messenger cable, one 250,000-circular-mil intermediate cable, and one 4/0 grooved copper contact wire, which had 65-per-cent conductivity. The new catenary construction between Gary and Michigan City was of the same type except that the main messenger consisted of one 0.81-inch diameter copperweld cable and the intermediate messenger was 300,000-circular-mil cable. This larger design was necessary to increase the current-carrying capacity in this single track territory where only one catenary was involved. This construction used the rigid hanger between the main messenger and the intermediate cable for a good electrical connection. The contact wire was supported from the intermediate cable by means of flexible hangers.

This changing of the overhead catenary system as far east as Michigan City was completed about 1930. During this same period a 500,000-circular-mil feeder cable was installed on the pole line from Michigan City to South Bend. The old steel main messenger was still used. A 4/0 grooved contact wire was suspended from the old contact wire by means of duplex clips. This was to add sufficient carrying capacity over this stretch of single track line. A feed tap tied the feeder cable and the catenary system together about every fifth pole. Through all cities where the South Shore operates in city streets, it was necessary to install a 750,000-circular-mil cable on the pole line. This larger feeder cable was necessary to furnish sufficient capacity through these locations due to the direct suspension type of construction. In this construction, the poles are located in the parkway between the curbing and sidewalk on both sides of each street with a 3/8 inch messenger wire cross spanning the distance between opposite poles. The contact wire is attached to the span wire by means of a trolley steady device. A feed tap also connected the feeder cable on the pole line with the contact wire about every sixth span.

A section of track immediately east of Gary was rebuilt with Bates built-up galvanized overhead bridges. These towers were spaced at 300-foot intervals over the mile and a half section of double track. The 0.72 main messenger was supported by means of a pin-type insulator attached to the top of the bridge. The intermediate is suspended from the main messenger by means of hangers of various lengths the longest of which were 58 inches and located nearest the bridges. On the south side of these bridges, a riser section was located to support the 33,000-volt transmission line. This section became known as the "ideal section."

With the change to the 1500-volt d-c system, eight new substations were built along the right-of-way. These consisted of four rotary converter stations and four mercury-arc rectifier stations. These stations were spaced approximately 10 miles apart along the line. The overhead system was separated into eight sections with the section insulators being located at the substations. In addition to these eight substations, a 1,500-volt feed was obtained from the Illinois Central substation at Kensington to help feed the Hammond to Kensington section.

The eight substations are owned and maintained by the Northern Indiana Public Service Company. The South Shore purchases the current at the various substation locations and is reponsible for all of the maintenance outside of the substations. The Public Service Company feeds the substations with a 33,000-volt 3-phase primary line which is attached to crossarms located on rented pole space at the top of the railroad's mast arm pole lead.

The substations vary in output capacity. One station has a 750-kw output, while six other stations have 1500-kw output. The largest substation is a Brown-Boveri mercury-arc rectifier located at Michigan City and it has an output capacity of 3,000 kw.

The substations are controlled by a carrier current supervisory superimposed on one land wire. This supervisory control permits the automatic opening and closing of any substation feeder by remote control from the railroad's dispatcher's office. The Public Service Company has the automatic supervisory control over the substation rectifiers and rotary converters in the same manner.

Under this program, the old semaphore signals were replaced with automatic block position color light signals. Use of impedance bonds at the insulated joints which separated track circuits was necessary to permit the negative return of the propulsion current to flow unobstructed to the substations. These bonds halted

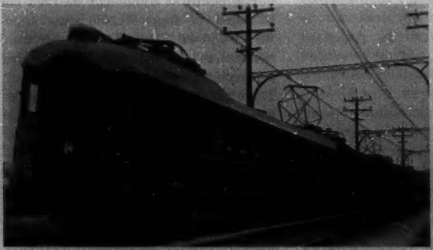

Figure 3. Three-car passenger train composed of three modernized air-conditioned cars near Michigan City, showing typical curve catenary construction

Figure 4. One of the original 6,600-volt a-c passenger cars which became obsolete with the rehabilitation program

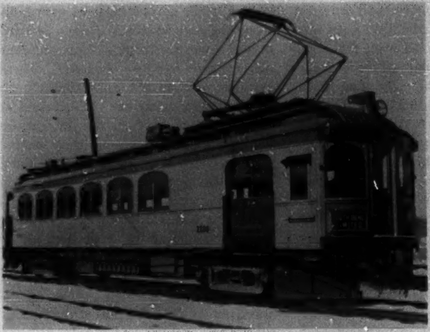

Figure 5 (above). "Old 1126," a 6,600-volt a-c passenger car after conversion to 1,500-volt d-c operation

Figure 7 (right). Original Hegewisch, Ill., passenger station, showing overhead construction and semaphore-type signal employed during 6,600-volt a-c operation

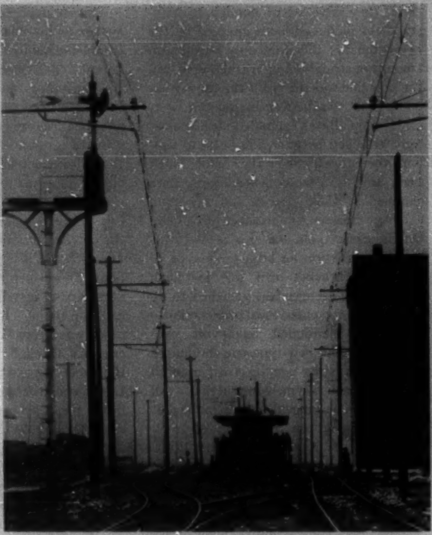

the flow of the alternating track current at that location for the signal system and permitted the passage of the direct negative current. On double track main, the signals were 3-position color lights and on single track, 2-position lights were used. The signals were spaced approximately 1 mile apart. With the changeover, the majority of the centrifugal track relays were replaced with vane track relays.

Another circuit was added to the telephone system between Michigan City and Illinois State Line. This was a message circuit used for company business. Since the trains were operating over the Illinois Central Railroad into Chicago, it was necessary to extend the telephone circuit to Randolph Street. The dispatch wire and one company message circuit were extended.

The major portion of the light original 70# rail on the main line was replaced with 100# rail.

The first d-c equipment was delivered in June 1926. These cars were put in service between South Bend and Michigan City without suspending operations. D-c operation was moved west as substations were finished.

Originally, 10 combination baggage and coach cars, 15 coaches, 2 parlor cars, 2 dining cars, and 10 trail cars were purchased. Hourly service between Chicago and South Bend, and half-hourly between Chicago and Gary was instituted. This improved service between Chicago and Gary resulted in an increase of 45 per cent of travel in the first 2 months of operation. The rehabilitation brought astonishing results and it was necessary to place an order for more equipment. In all, 69 pieces of passenger equipment were purchased. This equipment consisted of 50 motor cars, weighing 130,000 pounds and seating 56 passengers; 13 trail cars, weighing 99,000 pounds and seating 50 passengers; 4 parlor cars, and 2 diners. The cars were 60 feet long with all steel body and underframe and an insulated roof.

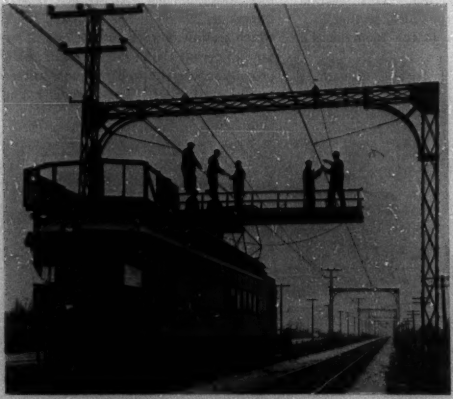

Figure 6. Overhead maintenance crew working from insulated deck of line car on typical catenary construction

The electrical equipment on each car consisted of four Westinghouse type-*567-C9* 750-volt d-c 210-horsepower traction motors with 24 to 59 gear ratio giving a maximum speed of 72 miles per hour. These motors were controlled by Westinghouse type-*HBF* electropneumatic unit switch control working on a 32-volt auxiliary circuit. A type-*XM-160* controller was used, equipped with reverser handle and dead-man control. The control was nonautomatic and the controllers were located at each end of every car in order to obtain a maximum of flexibility in train assembly. The controller had ten notches, five series, and five series-parallel positions, the last series-parallel

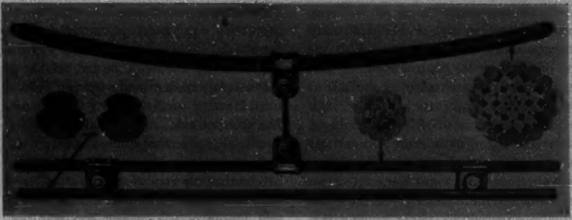

Figure 8. Section of present catenary system consisting of one 0.81-composite 191-strand primary messenger cable, one 250,000-circular-mil 19-strand copper secondary messenger cable, and two 4/0 grooved bronze trolley wire, 80-per-cent conductivity

position giving short field connection for additional speed.

The switch group was comprised of 11 Westinghouse *UP-602* switches for acceleration, transition, and field shunting, plus two *UP-602* switches connected in series for line switches. The line switches opened simultaneously in case of overload, as well as when the master controller was returned to off position.

Current collection was provided by a spring-raised air-lowered double-shoe pantagraph and a trolley pole for auxiliary or emergency use; however, due to speed and 2-direction operation, the trolley pole was impractical and another pantagraph was installed. Lightning protection was obtained by a type *IC* capacitor lightning arrester located on the car roof.

All the control circuits necessary for multiple operation were train lined through all the cars in two separate jumpers in order to keep the size to a minimum for easy handling. A 1,500-volt bus line from the motor cars furnished power for auxiliary circuits on all trail cars. The 1,500-volt bus line receptacles were protected by contactors which were opened by switches on the angle cock of the air brake lines. The drum-type reverser was operated by an electropneumatically controlled air engine.

Each motor and trail car was equipped with a Westinghouse *YX-11* $2\frac{1}{2}$-kw 1,500–32-volt motor-generator set designed to give close regulation without external regulating devices. The generator was a compound machine with series field connected to carry battery current. If the generator voltage would decrease, the battery discharged to the load through the series field, which, in turn, increased the generator excitation. This series field also acted differentially to prevent the battery from charging at too high a rate.

Air was furnished by a Westinghouse *D3F* 35-cubic-foot-per-minute compressor. The motor was a 10 horsepower 1,500-volt series type controlled by a type *J* Westinghouse air brake, electric compressor governor.

Headlights consisted of a 32-volt 250-watt lamp mounted in front of a circular reflector. All interior lighting and ventilating fans were taken from the 32-volt battery.

Heat was furnished by a Peter Smith hard coal stove circulating hot water. Auxiliary electric heat was furnished from strip heaters operating on 1,500 volts and controlled from a thermostat mounted inside the car.

In October 1929, the South Shore Line won the Charles A. Coffin prize and the Electric Traction Speed Trophy. This was the first time in the history of the industry that the same railroad had won both honors at the same time. The Coffin award was presented for distinguished contribution to the development of electric railway transportation for the convenience of the public and benefit of the industry. The Electric Traction Speed contest, won by this railroad in a field of 22 fast interurbans, classed the South Shore Line as the fastest electric railway in America. A goal was set to eventually make all through trains on at least a 2-hour schedule. Westinghouse Engineers made an intensive study of the traction motor speed characteristics and recommended increasing the air gap on the traction motor to give a higher balancing speed. By increasing the air gap and improving physical properties, the speed was increased about 6 miles per hour.

Along with the rehabilitation of equipment for improved passenger service came the desire for increased freight service. Immediately new interchange connections were built with steam railroads, and by 1929 the South Shore Line had connections with 13 railroads.

In June 1926, four Westinghouse locomotives were purchased to give rapid overnight freight service which had been inaugurated. These locomotives weighed 80 tons and were powered by four Westinghouse number *358*, 750-volt 360-horsepower series motors, two connected permanently in series. A type-*HBF-MU* double-end control was used, employing a type number *337* Westinghouse controller with nine steps in series and seven steps in series-parallel. The 1-hour rating is 30,400# tractive effort in full field with a speed of 17 miles per hour. The over-all length of the engine is 39 feet 8 inches. A Westinghouse *YX-11-A* motor-generator set is used to charge a 32-volt battery. A type-*YB-4* 1,500-volt blower unit is used for cooling the traction motors. Air brakes are of the Westinghouse *14 EL* type.

In 1927 to meet the demands of rapidly increasing freight business, two Westinghouse 53-ton switcher locomotives, available for immediate shipment, were purchased to give additional motive power until heavier locomotives were delivered. These locomotives were powered by four 125-horsepower 750-volt number *562* Westinghouse series motors. A type-*HBF* double-end control and *UP-602* unit switches were used. The gear ratio was 60 to 17 with a 1-hour rating of 15,200# full field, and speed of 12.5 miles per hour. The trucks were of Baldwin 4-wheel type equipped with 36-inch wheels. There were two type-*Y4D* Westinghouse blowers used for cooling traction motors. Brakes were furnished by Westinghouse air brake, type *14 EL*.

Because of a further substantial increase in freight business and the necessity of fast overnight service, four more 80-ton Westinghouse-Baldwin locomotives were purchased in 1928. In 1930 one more 80-ton Westinghouse locomotive and three General Electric locomotives of the same design and size were purchased. The electrical design was similar so that multiple-unit operation was possible between all 80-ton Westinghouse and General Electric locomotives.

After the panic of 1929, improvements were curtailed except where a substantial saving in maintenance was realized. In 1931 all parlor and diners were taken out of service. No major changes were made on the railroad until 1937.

When the railroad began its modernization program in 1937, a second contact wire was installed along side of the first one. This was also a 4/0 grooved copper wire. In 1942 the job of replacing the old steel main messenger east of Michigan City was begun. Again, due to single track main line, 0.81-copperweld cable was used as the main messenger, 300,000-circular-mil cable was used as the intermediate messenger, and two 4/0 grooved copper contact wires were installed.

In 1947 the railroad began replacing poles in the telephone signal lead, located on the opposite side of the track from the mast arm poles in single tract territory, with poles of sufficient height to permit the attaching of a Bates expanded steel truss between the mast arm pole and the telephone-signal pole. This type of construction has been installed on alternate poles extending east from the Ideal Section to Michigan City, a distance of 15 miles. The trusses not only provided a more flexible method of aligning and adjusting the catenary system, as the catenary is suspended from an insulator which is attached by means of a beam clamp to the bottom side of the beam, but it strengthens both the mast arm pole lead and the telephone-signal pole lead during high wind and heavy sleet and ice conditions.

In 1940 a portable substation was built to supplement the eight existing ones already in use. This was a rotary converter-type station and was mounted on two railroad cars. One car supported the converter and its auxiliaries and the other was the transformer car. It was normally located on a siding just west of Gary, which placed it in the middle of the heavy traffic and switching area. This station was also moved at various times to the site of one of the fixed stations and was put on the line at the required location so that the fixed station could be removed from service for an indefinite period to permit extensive overhauling and checking to be carried out.

The majority of the work on the catenary system is performed from the top deck of a multiple-unit line car especially built in the company shops for this work. This car has a completely insulated top deck and a portable deck, with a hydraulic hoist mounted atop the insulated deck. This movable deck facilitates the maneuverability that is required in maintaining an overhead catenary system and a wooden pole line.

In 1945 the railroad began eliminating the 2-position color light signals that were in use on single track main, and replaced them with the 3-position color light signals, thus making the signal system the same over the entire line.

With the rapid increase of automotive traffic, a strong effort was made to eliminate or adequately protect all dangerous highway grade crossings. This was accomplished by installing either automatic crossing gates or automatic flashing lights or both.

The installation of a 2-way space radio system was started in 1947. This system consisted of one main station in Michigan City and two repeater relay stations, one located 22 miles east of Michigan City and the other 32 miles west. With the use of dual remote control stations—one in the Chief Dispatcher's office and one at the switchboard operator's position, both located in the general offices at Michigan City—and the repeater relay stations any mobile unit on the railroad right-of-way between South Bend and Kensington can be contacted immediately. Present installations include 11 freight locomotives, 12 motor vehicles, including supervisory automobiles, and signal and line maintenance trucks. Fourteen portable handie-talkie radios have been installed in the railroad's cabooses so that end-to-end communication between engine and caboose can be maintained.

During this modernization period, the 100# rail is gradually being replaced by 115# rail. Pressure welded rail has replaced the conventional jointed rail on some sections of the railroad. The main line has been entirely reballasted with crushed limestone.

The first trend toward modernization of cars was the installation of new seats in ten coaches and painting the interior of the cars with light colored paints to help attract passenger business. In 1939 mechanical-type water coolers were installed in the passenger cars using a reciprocating compressor driven by a 32-volt motor from the battery.

All traction motor bearings and journal bearings were of the sleeve type. As a result, a great number of the road failures were due to hot bearings. One of the big improvements toward reduced maintenance was the changeover to roller bearings. In 1940, this program was started which eliminated all hot bearings on the traction motors and journals.

In 1941 passenger business had increased tremendously and it became necessary to obtain more seating capacity. It was impossible to purchase new equipment because of the war effort, so it became necessary to concentrate on increasing the seating capacity of the equipment on hand. A proposition was submitted to the Pullman Company for lengthening the cars. A design was worked out to cut the cars at approximately the center and add a 17-foot 6-inch section which would increase the length of the cars to 77 feet 6 inches and increase the seating capacity from 56 to 80 passengers. Because the Pullman Company could do the job only in 10-car lots, this program of modernization was undertaken in the South Shore shops, as this number of cars could not be removed from service at one time.

Several improvements were made to bring this equipment up to present-day standards. Fluorescent lighting was installed using a 32-volt motor driving a 110-volt alternator made by the Safety Car Heating and Lighting Company. Forced ventilation was installed using an overhead blower for pulling in outside air and recirculating the air in the car. Mechanical air conditioning was to have been installed but at that time a 1,500-volt motor of the proper size was not available. Keep pace with modern trends of passenger comfort, the subject of air conditioning was again considered in 1945. Because a 1,500-volt motor of the proper size still was not available, Waukesha equipment was selected. This equipment consisted of a 20-horsepower 4-cylinder propane engine driving a 7-ton reciprocating-type compressor. The evaporator and ventilating fan consisted of a Trane upright unit located in a compartment at one end of the car. To give better heat regulation in air-conditioned cars, an automatic-fired thermostatically controlled oil heater was installed. Hot water was circulated by a pump through finned radiation located the full length of each side of the car. Other improvements made in these cars were the installation of double-glazed picture-type windows and partitions for smoking and no-smoking compartments.

Due to the additional 32-volt load on the lengthened cars, larger motor-generator sets are now being installed. These sets are a General Electric *GMG-150* rated at 5 kw. Also, sealed-beam headlights are being installed on all of the passenger equipment using two, 200-watt sealed-beam lamps enclosed in a Mars-type case.

By 1950 30 coaches and six trail cars had been lengthened. Eighteen of these 30 coaches were equipped with mechanical air conditioning and oil heat and the seating capacity increased by 36 per cent.

In 1941 when freight business was on the upswing, additional freight motive power, geared for speed, was found necessary. As a result, the two 50-ton locomotives were sold in favor of the four 100-ton Westinghouse-Baldwin locomotives purchased from the Illinois Central Railroad. These locomotives are powered by four number *360*-type 750-volt 365-horsepower series motors. A type-*HBF-MU* double-end control is used with 11 steps in each position; inductive shunting is used for higher speed. The 1-hour rating is 31,000 tractive effort in full field at a speed of 17.7 miles per hour. The over-all length of the engine is 40 feet, 1 inch.

Two type-*YX-9A3* blowers are used for cooling traction motors, each driving a 32-volt generator for battery charging. As the blowers are in continuous operation when the locomotive is in service, a voltage regulator prevents the battery from becoming overcharged. Air brakes are of the New York Air Brake Company type *ESWL-LT*.

Additional freight motive power was discussed in 1947, but to have a company build only a couple of locomotives was very expensive. Some preliminary study and designs were made for building a locomotive in the shops on the property; however, this idea was cast aside in 1949 when 20 General Electric locomotives became available. These locomotives were built for Russia on a lend-lease order but before the completion of the order, the United States State Department stopped shipment. The South Shore purchased three of these locomotives. As the locomotives were designed for 3,300-volt d-c operation, it became necessary to convert the electrical phase for 1,500 volts direct current. With some assistance from General Electric engineers, this conversion was made in the railroad company's shops.

These locomotives employ eight General Electric 750–1,500-volt motors. The 1-hour rating is 5,500 horsepower with a tractive effort of 85,500# in full field at 25 miles per hour. Acceleration is nonautomatic with electropneumatic contactors, series-parallel switch; and electropneumatic operation is arranged to give 16 steps in series, 10 steps in series-parallel, and 11 steps in parallel plus two reduced field steps in each motor combination.

There are two motor-generator blower sets consisting of a 1,500-volt motor, 50-volt generator and blower mounted on a common shaft. The generator is under regulator control for lighting, control, and battery charging. Two 150-cubic-foot-per-minute 2-stage air compressors furnish air for air brakes and electropneumatic control operating at 50 volts, one compressor operating from each of the two motor-generator sets. The locomotives were originally equipped with regenerative braking, but because the South Shore had no use for electric braking and because it furnished several contactors necessary for conversion, this feature was not used.

The locomotives are 88 feet 10 inches long with a total weight of 545,600 pounds and a weight of 405,600 pounds on the drivers. The locomotives, being of road-type construction, are designed to negotiate a curve of 360 foot radius or 16-degree minimum.

The modernization program on the South Shore is still in full swing. The railroad, by employing the latest available equipment in the electrical and communications fields, has endeavored to present to the public a rapid and efficient means of public transportation service.

The transformation from an interurban to a railroad has been a successful one and the South Shore's future intent is to keep abreast with the trend of time, always keeping public safety and convenience as the prime goal.

No Discussion

Dynamic Braking on Diesel-Electric Locomotives

A. V. JOHANSSON
MEMBER AIEE

H. R. STIGER
ASSOCIATE MEMBER AIEE

Synopsis: The increasing prominence of the diesel-electric locomotive on American railroads has given new impetus to the use of dynamic braking. Originally intended as a means of controlling both passenger and freight train speed on mountain grades, it has been refined to the point where it is increasingly used for controlling freight train speed in relatively level territory. A recent refinement of braking control takes advantage of additional traction motor capacity available at lower speeds. Extensive service tests have demonstrated the operational and economic value of this form of braking.

ONE OF the great advantages of the diesel-electric locomotive over steam motive power is its ability to provide dynamic braking. When operating in dynamic braking, the traction generator is used to excite the fields of the traction motors, see Figure 2. The motors then act as separately excited generators, driven by the motion of the train, and produce a voltage. When resistors are connected across the motor armatures, this voltage causes current to flow and load the motors. As a result they produce a torque which opposes the torque produced by the wheels.

The advantages of dynamic braking are greatest in mountainous territory, but it has also been found valuable on railroads not having heavy grades. In such cases the dynamic brake provides a quick, easy means of applying retarding force to the train when its speed must be restricted, and for bringing it almost to a halt when a stop must be made. The latter is of particular advantage for freight trains. As a rule the reduction of braking effort as the speed decreases makes the braking rate too low for passenger trains.

There is nothing particularly new about the basic idea of dynamic braking. It is a simpler form of the regenerative braking used on electrified roads years before the diesel-electric locomotive came into being. The prime difference between dynamic and regenerative braking lies in the method used to dissipate the power produced. Dynamic braking uses a resistor built into the locomotive for this purpose. Regenerative braking employs the railroad power system to take the energy from the train and use it elsewhere or dissipate it in resistors at the substation.

Dynamic Braking Limitations

During dynamic braking the diesel engine is normally operating at idle speed. This reduces the ventilation to the traction motors, and consequently their rating. Therefore, it often becomes necessary to increase the motor ventilation over what it is with the engine idling. Various methods are used, depending on whether the traction blowers are mechanically or electrically driven. The amount of ventilation required depends

---

Paper 53-48, recommended by the AIEE Land Transportation Committee and approved by the AIEE Committee on Technical Operations for presentation at the AIEE Winter General Meeting, New York, N. Y., January 19–23, 1953. Manuscript submitted October 20, 1952; made available for printing November 19, 1952.

A. V. JOHANSSON and H. R. STIGER are with the General Electric Company, Erie, Pa.

Courtesy of the Denver and Rio Grande Western Railroad

Figure 1. Dynamic braking is of particular advantage in handling trains on mountain grades

on the braking requirements which, in turn, depend on the locomotive application. On special locomotives this requirement is cared for in the design. On standard locomotives the braking provided is naturally that which can be most economically obtained, consistent with high quality. Operating experience indicates that it meets average requirements.

Normally the requirements on the traction generator are not limiting during dynamic braking. Rather, the traction motors are the limiting part of the system in the following ways:

1. Field current I_f, which is limited by heating.
2. Armature current I_a, which is limited by heating.
3. Peak volts per bar V/B, which is limited by motor design.

The way in which these affect a braking effort curve is shown in Figure 3. In the past, armature current during braking had to be limited to a maximum value that would not exceed the safe heating limit of the motors at high speed where the core loss is greatest. This meant that the braking effort followed the constant I_a curve in Figure 3, and the maximum possible braking effort available at lower speeds could not be utilized. The latest American Locomotive Company–General Electric Company (Alco–GE) system provides automatic control of the traction motor current to hold it within safe heating limits at all speeds. The result, as shown in Figure 3, is that greater braking effort is available at lower speeds. At higher speeds the peak volts per bar limit still exists. This requires a manual reduction in motor armature current as indicated at the right-hand end of the curves in Figure 3.

Operating Advantages of Dynamic Braking

Years of operating experience, first with regenerative braking and later with dynamic braking also, have served to demonstrate certain advantages inherent in these systems. With the increasing popularity of the diesel-electric locomotive during the last decade these advantages assumed new importance, and railroads tried to evaluate them more accurately. In a report on a series of extensive tests conducted by a large western railroad[1] the economic advantages of the dynamic brake are listed as follows:

1. Reduction in the number of overheated wheels in both freight and passenger equipment.
2. Elimination of long, costly stops for wheel cooling in heavy grade territories.
3. Reduction in number of thermal cracked wheels.
4. Reduction in wheel wear as a result of reducing the use of air brakes to a minimum.
5. Reduction in wearing of parts of brake rigging and attachments.
6. Reduction in brake beam and brake beam attachment failures.
7. Reduction in number of derailments caused by failures of brake beams and brake beam attachments.
8. The ability to reduce train speed with the dynamic brake in conjunction with the air brake without attendant brake shoe and wheel damage.
9. Better train handling in regard to slack action where dynamic brake is properly used.

Braking Resistors

A suitable resistor, see Figure 4, must be provided to control the amount of energy produced by the traction motors and, therefore, the braking effort of the locomotive. The design and construction of a locomotive-mounted resistor for dissipating such large amounts of power is not simple. Yet it appears safe to say that the problem is simpler with a fixed resistor load than it is with regenerative braking where the power system is the load. In that case the voltage level of the power system is constantly changing, often very sharply, over a wide range.

The design and construction of the braking resistor is a study of its own, and it can be touched upon only briefly here. Practically all dynamic braking resistors are forced ventilated. This is necessary because space is at a premium. In nearly every case, the blower is driven by a series motor that receives its power from connections across a portion of the braking resistor itself. This provides a dependable source of power and eliminates the need for control devices. It has the advantage that the blower motor runs at a speed roughly proportional to the load on the grids which it must cool. Therefore, maximum cooling is provided when the resistor load is greatest. This connection also provides a system characteristic such that when the greatest braking effort is required the blower load is a maximum and helps supply some of the braking effort. Since the power developed by the traction motors in dynamic braking must be thrown away through the resistor, the power to run the blower motor costs nothing.

Control of Dynamic Braking

The value of dynamic braking would be largely lost if an effective method of controlling it did not exist. An impor-

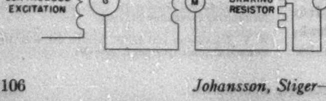

Figure 2 (left). Fundamental circuits for dynamic braking

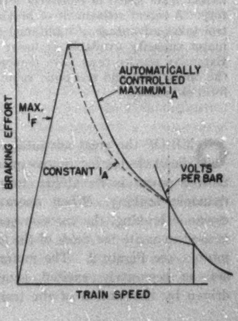

Figure 3 (right). Braking effort curves, showing the effect of automatic control of armature current

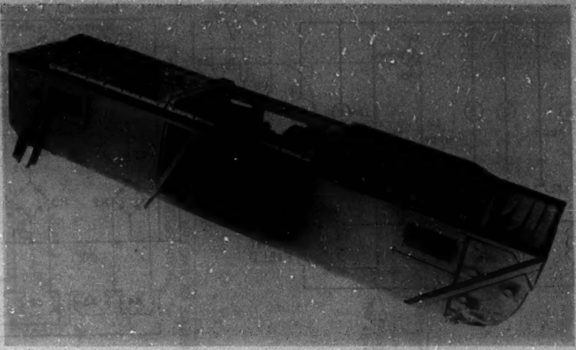

Figure 4. Forced ventilated dynamic braking resistor assembly

tant part of such control lies in the selection of the value of resistance for the braking resistor. How this resistance determines the braking curve is illustrated in Figure 5. This shows two curves of braking effort, *ABC* and *ADE*. Curve *ABC* has a braking resistor twice that of *ADE* in ohms. Lines *AB* and *AD* represent maximum field current which may be applied to the traction motor without excessive heating. This is the same for both curves. Figure 5 shows that, other things remaining the same, half the resistance allows maximum braking effort to be obtained at half the train speed. The armature current is the same for both curves, so the braking horsepower depends on the resistance and will be in proportion to the resistance value selected. These curves also show that maximum braking effort is independent of resistance; but braking effort for any particular speed—above that for maximum braking—is directly proportional to resistance and, of course, to horsepower. Since the horsepower is a function of the resistance selected—assuming traction motor field and armature current ratings to be fixed—the train speed for maximum braking effort will rise in proportion to the horsepower.

Control of Dynamic Braking by the Engineman

Most diesel-electric locomotives are equipped for multiple-unit operation. In such use the engineman must be able to control all units by operating a braking handle in the lead unit. With this handle he ultimately controls field current, from a separately excited source, for the traction motors. By watching the traction motor ammeter, he controls the run-in of slack on the train when he first applies dynamic braking and later avoids exceeding the operating limits imposed upon him. A brake warning relay in each unit, connected across a portion of the braking resistor, detects overvoltage and provides an indication on a warning light trainlined into the leading cab.

The Alco-GE System of Dynamic Braking

The dynamic braking control equipment on a modern Alco-GE locomotive includes the braking resistors and a pneumatically operated, 2-position braking switch which sets up motoring or braking connections. In addition, two braking relays set up control and excitation circuits for dynamic braking, and a third relay provides the brake warning as already described. In the engineman's control stand there is a commutator rheostat geared to the braking handle. The brush arm is connected potentiometer style to provide a source of voltage which may be sent back over a train wire to the other coupled units. This voltage determines the amount of traction motor field current provided—up to the limit of traction motor armature current. When this point is reached the armature current provides a signal which overrides the manual control and automatically regulates the field current to maintain a predetermined armature current. On some types of Alco-GE locomotives the armature current is modulated by train speed. Additional dynamic braking equipment consists of certain reactor windings used only in dynamic braking, a small rectifier, and certain small resistor tubes.

Figure 6 shows a schematic diagram of the system with most contacts and adjustments omitted for simplicity. At the left of the figure are four traction motors (numbered 4, 2, 3, and 1) and their braking resistors. Across a portion of the resistor for motor 3 is the blower motor *K1* and the brake warning relay *BWR*. Across another portion of the same resistor is the current measuring coil on the reactor *X3*. This coil and its associated resistor are used to measure braking current in terms of voltage across a portion of the resistor.

The traction generator *G* is shown connected to supply current to the four traction motor fields in series. The common connection of the generator and the four traction motor armatures simplifies the switching required to go from motoring to braking. It also provides ground relay protection during braking through the relay coil *GR*. The generator starting winding, a series winding used in cranking the engine, is connected in the generator circuit during braking. It provides a differential effect which requires the exciter to work at a higher level of excitation. The voltage drop across the generator commutating field is used to measure motor field excitation by means of coil *D1-D2* on reactor *X1*.

An amplidyne exciter *E* feeds the generator shunt field *GS-GSS*. The generator field current flows through coil *D3-D4* on reactor *X3*, which measures generator field current. To permit a simple adjustment of the effect of the current in this reactor coil, proportional current from the exciter is fed into the *D2-D1* coil on the *X3* reactor.

The exciter shunt field *F1-F2* is fed from the transformer *T1* through the rectifier *R1*. The exciter field current is controlled by having the rectifier feed

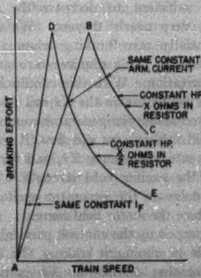

Figure 5. Typical braking effort curves, showing effect of varying ohmic value of braking resistor

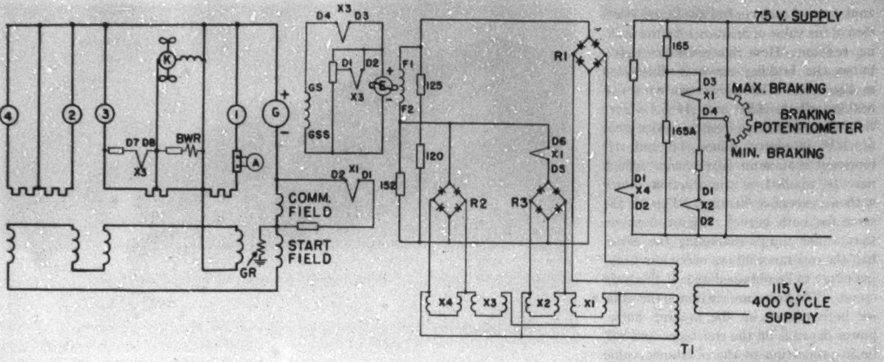

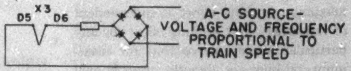

Figure 6. Simplified schematic diagram of dynamic braking circuits on Alco-GE road locomotives

into resistance *152* whose voltage may range from a few volts below that supplied by the rectifier to a few volts above it. The difference is available to control current flow through the exciter field in one direction or the other. At the right is the braking potentiometer with its brush arm in the minimum braking position, that is, as it is immediately after setting up the braking circuits. This allows maximum current to flow through the *165* resistor and the *D3-D4* coil on *X1* to the other side of the 75-volt d-c supply. This gives maximum battery bias on *X1* and no bias on *X2*, which is short-circuited. Reactor pairs *X1-X2* and *X3-X4*, arranged as voltage pairs, are connected across another secondary of transformer *T1*. With constant voltage applied to each pair, saturation of either reactor in the pair by means of direct current will increase the voltage across its mate. Saturation of *X1* will increase the voltage across *X2*. This voltage, rectified by *R3*, appears as a higher voltage on resistance *152*, reducing the current in the exciter field. In minimum braking, the d-c bias on *X1* fed by resistor *165* is sufficient to decrease the field current very nearly to zero. We want substantially zero braking when going into braking. This requires zero motor field excitation. With this condition no current would flow in the *X1* coil *D1-D2*, connected across the generator commutating field. If current did flow, it would further saturate reactor *X1*, and further reduce the exciter field strength. This would decrease the generator excitation and reduce the motor field current.

To sharpen up the control, particularly desirable in minimum braking, the boot strap winding *D5-D6* on *X1* is used. This winding, shown immediately above rectifier *R3*, takes the output of reactor pair *X1-X2* and uses it to further excite *X1*. Up to this point the effect of the three windings on the saturation of *X1* has been additive. The terminal symbols *D1-D2*, et cetera are established for each winding so that current flowing from *D1* to *D2* will be additive with current flowing from *D*-odd to *D*-even, in any other coil on the same reactor and, of course, subtractive for reverse polarity.

After the slack has been run in, more braking is desired. The engineman moves the braking handle so that the potentiometer brush arm turns toward the maximum braking position, and provides a voltage of increasing value. This increases excitation on *X2* reactor, which has only one d-c coil. Thus more excitation is required on *X1* to return to the same value of voltage across *X2*. At the same time the range is still further extended by decreasing the additive current in the *D3-D4* winding, and finally reversing it as the brush arm reaches a potential above that of the mid point of the *165-165A* voltage divider.

The incremental transient decrease of the voltage across the *152* resistance allows more exciter field current to flow. This in turn causes more motor field current to flow, producing more drop across the generator commutating field. As a result more current flows through the *D1-D2* winding of *X1*. This winding thus controls the exciter field current at points above minimum braking, with the values controlled being preset by the braking potentiometer brush arm voltage. The current in this winding is determined by generator excitation and is controlling the exciter field current. Hence, for a given braking handle position, a balance point is reached where the current in the commutating field allows just enough exciter field current to flow to maintain the generator current. Any decrease in generator current allows more exciter field current to flow, and any increase reduces the exciter field strength.

In this way the *X1-X2* reactor pair provides the engineman with control of braking current as long as he does not try to exceed a preset limit. He controls the leading unit directly and, with the same potentiometer, the other units through a train wire.

Automatic Current Limit

Until recently, the preceding description covered the entire system of dynamic braking control on Alco-GE locomotives. Now, however, a current limit based on traction motor armature current has been introduced. This provides an overriding control of braking, preset and automatically regulated. With it the engineman can control dynamic braking with much greater ease, since he need not watch his ammeter or brake warning light so closely. It protects the equipment by preventing accidental or deliberate overloads. It provides a better balance of braking between coupled units because it goes deeper into the system to take a measurement of output. Instead of motor field current, it measures motor line current. This substantially eliminates the effects of varying motor characteristics and wheel sizes between units. Of course, it does not eliminate these factors between motors of the same unit. As applied to Alco-GE road locomotives, this refinement allows greater braking at low train speeds than at high speeds. It does this by taking advantage of the lower core loss at low speeds, allowing more copper loss for the same motor heating. To do this with ordinary engineman control of dynamic braking would be very difficult. It would require complex operating instructions which would probably prove most confusing to the engineman.

Figure 6 shows a winding *D8-D7* of reactor *X3* connected across part of the braking resistor for motor 3. This winding measures the braking current in motor 3, and controls the voltage across resistor *152* whenever the voltage across *X4* exceeds that across *X2*. The generator field current in braking also flows through the *D3-D4* coil on *X3*. The *D8-D7* winding is connected subtractively to obtain a close regulation of motor current throughout the speed range for full braking. Figure 7 shows how the proper characteristic is obtained. The flat section *AB* is produced by maximum braking handle position controlling a fixed motor field current. It is obtained at train speeds below that at which motor 3 generates enough voltage to sufficiently excite *X3* so that the voltage across *X4* will exceed *X2*, as previously described. Beyond *B* the curve turns down to zero excitation at *C*. This is marked natural characteristic and shows the slope of response which must be followed by net ampere turns in *X3* to produce the values of exciter field current shown by the ordinate. All parts of the curve are intended to show the excitation on *X3* given by winding *D8-D7* only. The curve marked unstable shop characteristic shows the effect of having the *D3-D4* winding on *X3* subtractive to *D8-D7*. Thus it shows the excitation provided *X3* by the *D8-D7* winding which must be diminished by that from the *D3-D4* winding to return to the natural characteristic. The excitation on *D3-D4* is large at high exciter field currents and disappears at low exciter field currents.

The curve just discussed is unstable on the road because less output of motor 3 would result in more excitation on the exciter and vice versa. So an additional winding on *X3*, properly adjusted and connected across the exciter armature, is used to decrease the effect of the *D3-D4* winding without working with heavy-current low-voltage windings of a fixed number of turns. This restores the characteristic to that marked stable shop characteristic. It is the curve sought in standstill adjustment of the system where battery voltage, through a suitable rheostat and instrument, is used to simulate motor 3 voltage.

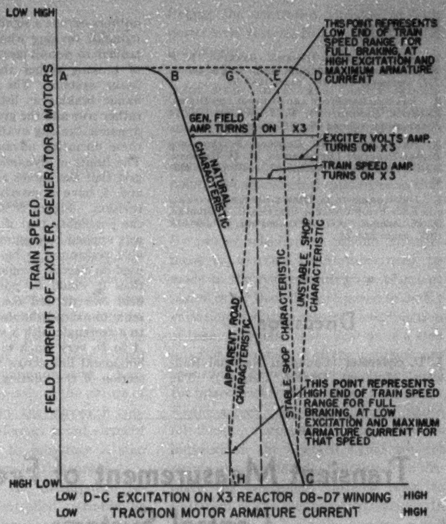

Figure 7. Controlled braking characteristics. Entire characteristic may be shifted to the left or right by changing X4 D1-D2 ampere-turns

All recent Alco-GE road-type locomotives with dynamic braking have been equipped with a recalibrating winding on *X3*. Since this is fed from the locomotive axle generator through a rectifier, it receives a d-c signal proportional to train speed. This provides excitation additive to that provided by the *D8-D7* winding. The result is to recalibrate the system so that less motor current will flow at high speeds than at low speeds. Thus advantage is taken of the reduced core loss at low speeds. This produces the curve marked apparent road characteristic. Although it has a negative slope it is not unstable because an outside element—train speed—controls the slope. Actually this curve is simply the stable shop characteristic cut back varying amounts at various train speeds. Any transient changes follow the slope of the stable shop characteristic.

This method of automatically controlling maximum braking current provides regulation without using any moving parts except the setup devices. The unstable shop characteristic, Figure 4, is actually stable in the shop if a separate source of power is used for the *D8-D7* winding on *X3* is used, but would be unstable on the road. If an incorrect adjustment or other defect produces this sort of characteristic on the road, the effect of the connection of the *D7-D8* winding across a portion of braking resistor which is in series with the blower motor results in minimum hunting. The motor tends to hold the voltage constant across its section of resistance. This makes any transient change in voltage appear almost wholly across the section of resistance adjacent, thereby giving a leading signal to the *D8-D7* coil on reactor *X3*.

Conclusion

The popularity of dynamic braking on diesel-electric locomotives indicates its desirability and acceptance by the railroads. This is based upon its economic advantages, proved by years of operating experience. Furthermore, these advantages are obtained by the addition of very little equipment not required for traction purposes, so the capital investment is relatively insignificant. Progress in the design of dynamic braking systems has further enhanced the advantages. The refined system described in this paper automatically provides maximum permissible braking capacity throughout the locomotive operating range. It permits this brake to be used advantageously on almost any railroad profile and makes additional braking power available at lower speeds where it is of particular advantage in freight service.

References

1. Advantages of Dynamic Braking, J. P. Morris. *Railway Age* (New York, N. Y.), volume 127, December 17, 1949, pages 1087–89.

2. Braking Resistors and Control for Diesel-Electric Locomotives, E. F. Weiser. *AIEE Transactions*, volume 66, 1947, pages 229–32.

3. Developments in Control Systems for Diesel-Electric Locomotives, M. D. Henshaw. *AIEE Transactions*, volume 66, 1947, pages 233–41.

4. Developments in Diesel-Electric-Generator Excitation Control Systems, C. A. Brancke, G. M. Adams. *AIEE Transactions*, volume 66, 1947, pages 223–28.

◆

Discussion

J. D. Sylvester (Canadian National Railways, Montreal, Quebec, Canada): The authors outline a significant development in dynamic braking wherein the range is extended to permit greater use of this form of braking rather than the straight air-brake system. The advantages for dynamic braking as listed in the paper are rather true and the greater the range of the dynamic braking available, the greater are these operating advantages in magnitude. The limits of dynamic braking listed suggest that the curves as shown in Figures 3 and 5 have a possibility of still greater revision. Figure 5 in particular suggests the possibility that if a variable resistance was applied to dynamic braking, the variable resistance to be something like that used on electric locomotives in acceleration, then it would be possible, with constant field current and constant armature current, to extend the dynamic braking curve to a rectangle with a very steep slope from A to D_1 very much to the left of D, and a horizontal line across the top to an intersection of the limiting volts per bar curve as shown in Figure 3. In other words, head-end power would be just as responsible in stopping a train as it is in accelerating a train, and the conventional air-brake system would be a standby only.

The economics of this would be far reaching to railway operators.

A. V. Johansson and **H. R. Stiger**: Varying the dynamic brake resistor in several steps, as suggested by Mr. Sylvester, would increase the speed range over which maximum braking effort could be obtained. This would, however, be effective for use only with relatively short trains. With long trains, the rate of deceleration would necessarily be quite low compared to that obtainable with air brakes. The additional equipment required would tend to increase both first cost and maintenance expense. These considerations appear to seriously limit the application of such a scheme from both practical and economic standpoints.

Transient Measurement of Feedback Control Systems

F. H. FERGUSON
MEMBER AIEE

C. H. LOONEY
NONMEMBER AIEE

Synopsis: Transient measurement techniques permit rapid determination and comparison of the operational characteristics of feedback control systems. Instrumentation is described which introduces a repetitive step function to a system and visually displays its dynamic response. Provision is made for precisely measuring response magnitude as a function of time and obtaining permanent records for future reference. Refinements necessary for accurate determination of the response of carrier systems is discussed. Examples of system response patterns are given.

APPLICATION of feedback control systems has become so extensive that much engineering effort is spent in their evaluation and maintenance. Application involves introduction of a step function to a system and determination of system response with respect to time. Transient analysis gives information concerning speed of response and tendency of a system towards oscillation.

Transient measurement can save valuable time when tests on a production basis or routine maintenance checks are necessary. The design engineer, aware of both system limitations and specified operational requirements, can make critical adjustment of parameters of a system prototype to obtain excellent overall performance. The transient response of the prototype then can be recorded and other systems of the same design considered in proper adjustment when their transient response to an equivalent step function corresponds to that of the prototype.

Requirement of Transient Measurement

Requirements of the measuring means are necessarily determined by characteristics of the feedback control system to be studied. Present systems have error detectors, amplifiers, and power converters of widely varying form so that even those systems which have the same functional application are not necessarily composed of the same mechanical, hydraulic, or electrical components. In addition to this physical diversity, there exists a large variation in output power level and response time scale. Instrumentation to examine transient response should be adaptable to all such systems without bothersome alteration either to the system or the measuring means.

Consideration of various applications indicates that response duration may be expected to lie within a range from 15 milliseconds to 3 seconds. Here, response duration is defined as the interval elapsing between initiation of the step function and the time the system obtains a condition of steady-state minimum error. It is desirable that the measuring instrument introduce a repetitive train of step function inputs to the system to provide the operator with a continuous flow of information. In effect, this requires a constant frequency square wave input with a half-period continuously adjustable within the range of expected transient duration.

Further requirements are imposed by carrier feedback control systems. In order that the response be repetitive it is necessary that initiation occur at a fixed magnitude of carrier phase. This implies that the response duration for carrier systems must contain an integral number of cycles of the carrier. Interpretation of the response wave form of carrier systems is difficult because the information on which the system acts is dependent upon the time phase relationship inherent between system signal and fixed phase reference voltages and is not necessarily defined by the envelope of the response. For this reason, a method of phase sensitive detection should be included to assist in the interpretation of the response wave form of carrier systems.

The instrument should permit some method of providing a permanent record so that the response of a system in optimum

---

Paper 53-101, recommended by the AIEE Feedback Control Systems Committee and approved by the AIEE Committee on Technical Operations for presentation at the AIEE Winter General Meeting, New York, N. Y., January 19–23, 1953. Manuscript submitted October 21, 1952; made available for printing December 23, 1952.

F. H. Ferguson and C. H. Looney are both with the Naval Research Laboratory, Washington, D. C.

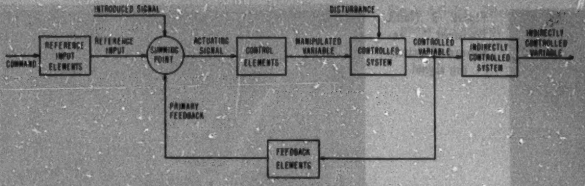
INTRODUCED SIGNAL
DISTURBANCE
COMMAND
REFERENCE INPUT ELEMENTS
REFERENCE INPUT
SUMMING POINT
ACTUATING SIGNAL
CONTROL ELEMENTS
MANIPULATED VARIABLE
CONTROLLED SYSTEM
CONTROLLED VARIABLE
INDIRECTLY CONTROLLED SYSTEM
INDIRECTLY CONTROLLED VARIABLE
PRIMARY FEEDBACK
FEEDBACK ELEMENTS

Figure 1. Block diagram of basic feedback control system

adjustment may be used at a later time as a guide for adjustment of similar systems. Provision should be included to obtain accurately the numerical magnitude of the transient response as a function of time.

Consideration of Step Functions

There are three methods of introducing a step function to the basic feedback control system shown in Figure 1. These are:

1. Manipulation of the command.
2. Manipulation of the disturbance.
3. Introduction of a signal to the summing point.

Manipulation of the command requires that it be changed suddenly from quiescence to a new fixed value. This effects a difference between reference input and primary feedback to actuate the control elements. Thereupon, the control functions to cause the magnitude of the controlled variable to correspond to the new command value and obtain a final static condition of minimum error. Various systems differ greatly in the nature of their command and the physical construction of their reference input element making it difficult to introduce a step function to the system by this means.

Manipulation of the disturbance requires that the controlled variable be coerced from synchronization with the reference input. A transient condition is initiated at the instant the constraint is removed. The physical difficulty of forcing the controlled variable of high power level systems from synchronization is apparent.

Addition of a signal to the summing point from an external source accomplishes the desired offset of synchronization and sudden removal of this signal initiates a transient condition. In the majority of installations the signals at the summing point exist as electrical quantities so that any of these can be conveniently manipulated by means of fast-acting contacts. By proper selection of contact arrangement no external connections need be made to the system during the transient period other than those required to detect variation of system response as a function of time. Repetitive application of a step function is obtained if the contacts are opened and closed in a cyclic manner and the introduced signal is a fixed magnitude. Requirements on wave form phase relationship, impedance, or other factors imposed on the injected signal are not stringent since its only function is to displace the controlled variable prior to initiation of the measured transient. In the majority of cases the injected signal can be obtained directly from one of the fixed reference potentials of the feedback control system under investigation.

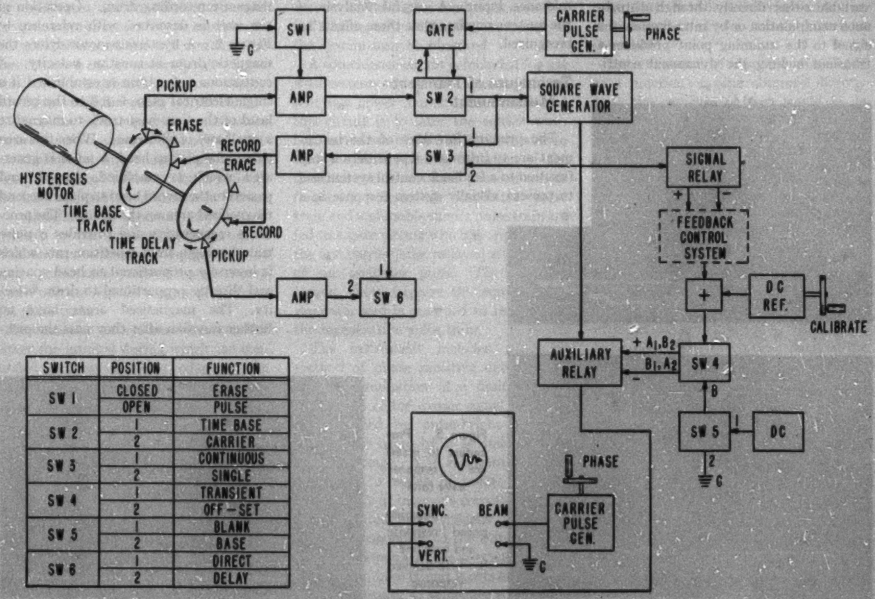
SW1
G
GATE
CARRIER PULSE GEN.
PHASE
PICKUP
AMP
SW 2
2
1
SQUARE WAVE GENERATOR
ERASE
RECORD
ERACE
AMP
SW 3
1
2
SIGNAL RELAY
+
−
FEEDBACK CONTROL SYSTEM
HYSTERESIS MOTOR
TIME BASE TRACK
TIME DELAY TRACK
RECORD
PICKUP
AMP
2
1
SW 6
+
DC REF.
CALIBRATE
+ A1,B2
B1,A2
−
AUXILIARY RELAY
SW 4
B
SW 5
1
DC
2
G
PHASE
SYNC.
BEAM
VERT.
CARRIER PULSE GEN.
G

SWITCH	POSITION	FUNCTION
SW 1	CLOSED	ERASE
	OPEN	PULSE
SW 2	1	TIME BASE
	2	CARRIER
SW 3	1	CONTINUOUS
	2	SINGLE
SW 4	1	TRANSIENT
	2	OFF-SET
SW 5	1	BLANK
	2	BASE
SW 6	1	DIRECT
	2	DELAY

Figure 2. Block diagram of instrument

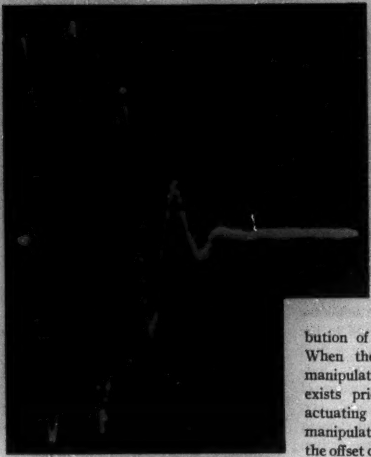

Figure 3 (left). Transient response of actuating signal

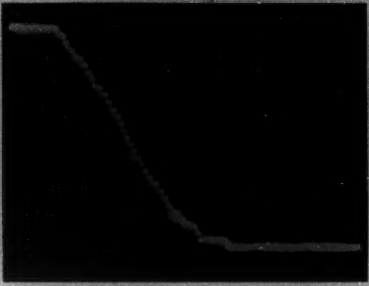

Figure 4 (right). Transient response of controlled variable

The difference between these methods of introducing a step function to the system must be considered. Transient response following application of a step change in command includes the transfer characteristics of the reference input element. Displacement of the controlled variable either directly through disturbance manipulation or by introduction of a signal to the summing point produces a transient lacking the dynamical contribution of this reference input element. When the transient is introduced by manipulation of the disturbance there exists prior to transient initiation an actuating signal magnitude such that the manipulated variable is proportional to the offset controlled variable in magnitude. Thus, at the instant of transient initiation the dynamical effect of the control element also is absent. Introduction of a signal to the summing point differs in that the actuating signal is a minimum prior to transient initiation and removal of the introduced signal corresponds closely to a step function change in magnitude of the reference input. A careful analysis of the system requires that these effects be recognized.

Techniques of Transient Measurement

The primary functions of the instrument are to introduce repetitively a step function to a feedback control system and to present visually system response in a form amenable to measurement. The instrument is composed of two basic parts: a time base unit and a control unit. The time base unit includes an adjustable period, electromechanical square wave generator, and the mechanism for continuous time measurements while the control unit contains the electronic circuits and selector switches required for the various displays.

Generation of a square wave having a half-period continuously adjustable within the range of expected transient duration is obtained from an oscillator in which the necessary feedback is furnished by a magnetic recording drum. Operation of the unit is described with reference to Figure 2. A hysteresis motor drives the magnetic drum at constant velocity. A continuous pulse train is established if a single electrical pulse is fed to the record head of the time base track to magnetize a small area of the drum. When this area passes the pickup head, a pulse is generated which is amplified, shaped, and passed to the record head to place a second magnetized area on the drum. The process is regenerative and provides a pulse train having a fixed repetition rate which is inversely proportional to head spacing and directly proportional to drum velocity. The magnetized areas have no further function after they pass the pick-

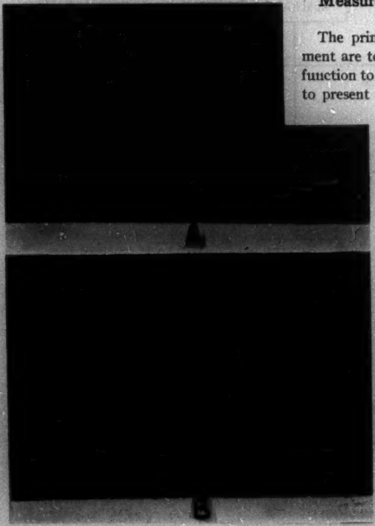

Figure 5. Procedure to measure response wave form

A. Superimposed response and base line
B. Time-delayed response
C. Null of response magnitude

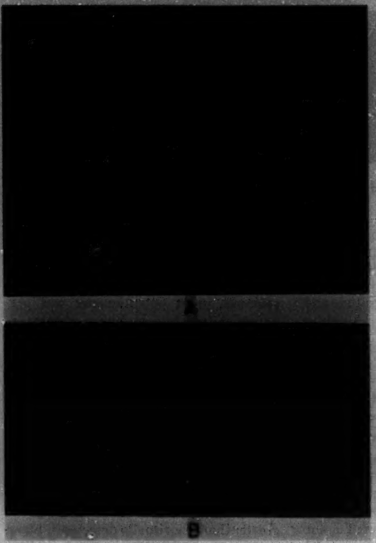

Figure 6 (left). Effect of carrier phase at transient initiation

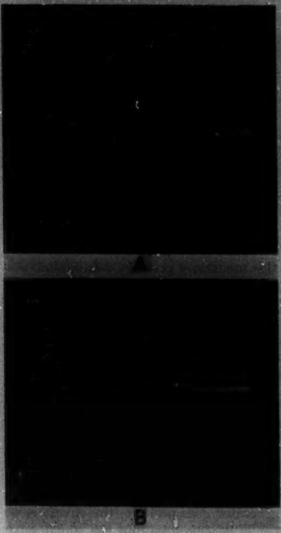

Figure 7 (right). Visual detection of in-phase component

A. In-phase actuating signal

B. Quadrature component actuating signal

up head, and, therefore, are erased by a permanent magnet. Normal manufacturing tolerances on machine parts and excitation of the motor by the commercial 60-cycle-per-second line will establish the time interval to an accuracy of 0.5 per cent; with a regulated frequency supply this figure could be held to 0.1 per cent.

The pulse train triggers a square wave generator which drives a fast-acting relay to alternately inject and remove the signal introduced to the summing point of the feedback control system. A voltage corresponding to system response is applied to the vertical amplifier of a cathode-ray oscilloscope equipped with long persistance screen, and sweep synchronizing signals are supplied from the pulse train.

Examination of system variations for either the interval during which the controlled variable is being offset or the transient response interval is provided by an auxiliary relay acting in synchronism with the square wave. A direct potential supplied to this relay is introduced to the vertical amplifier of the oscilloscope to displace the trace offscreen during the alternate half-cycle. Examination of system variation during the offsetting period permits adjustment of the square wave half-period to a value which assures that the system has reached quiescence before the transient is initiated and also allows adjustment of the magnitude of the step function input to a value below the saturation level of the system. When these conditions are satisfied the repetitive transient response of the system may be observed.

A coincidence circuit is included for use with systems which have alternating current as a power source. The function of this circuit is to alter the square wave half-period established by the oscillator so that the time point of initiation of the transient occurs at a fixed phase of carrier frequency. Both the oscillator pulse train and a phasable carrier pulse train are fed to a gate circuit which is triggered by the first carrier pulse received after arrival of an oscillator pulse. The resultant output pulse triggers the square wave generator and is recorded to re-establish the regenerative pulse train.

The instrument includes a visual method of phase sensitive detection to permit examination of a desired phase component of the carrier signal. This is accomplished by pulse-brightening the oscilloscope beam by a second phasable carrier voltage. The resultant response pattern is a series of points disposed horizontally at intervals corresponding to carrier period and vertically at magnitudes corresponding to the instantaneous values of response at the selected phase.

The time base circuit meets all requirements necessary to introduce a repetitive step function to the feedback control system and provide a synchronized sweep for examination of system response. The control unit which permits measurement and recording of the transient is now described.

Determination of response magnitude as a function of time obtained directly from the response pattern would be in error, proportional to sweep nonlinearity or vertical amplifier drift and distortion. To obtain greater accuracy a null method of comparing complex response wave forms with a calibrated direct potential is used. Time measurement is accomplished through the use of the time delay track on the magnetic drum. Its record head is paralleled electrically with the time base record head so that the spacing between consecutive magnetized areas on each track is equal. As the angular position of the pickup head of the time delay track is varied, each generated pulse is proportionately shifted in time with respect to the time base pulse train. The pulses are amplified and shaped to provide a synchronizing signal for the sweep. In this manner the response pattern is displaced horizontally. A desired point on the transient curve may be made to coincide with sweep initiation. The magnitude of response at this point is measured with respect to a zero magnitude reference line. A ground connection is supplied to the auxiliary relay to short-circuit the input to the vertical amplifier on alternate half-cycles thus establishing the base line. A calibrated direct reference voltage from a precision potentiometer is added to the response signal to displace the trace vertically until the initial portion, which corresponds to the measured point in time, is in correspondence with the zero magnitude base line. The setting of the calibrated potentiometer then is a measure of response magnitude at the desired time. Increasing the gain of the vertical amplifier increases the resolution with which the null point is determined. In this manner, a point-by-point tabulation of response magnitude as a function of time is obtained which is independent of sweep nonlinearity or amplifier drift and distortion.

Permanent records for future reference are obtained by photographic reproduction. To facilitate use of the camera, a sequence circuit limits presentation to a single excursion of the response pattern. To achieve this the square wave generator is included in the time base circuit. When the output of the square wave generator goes positive, the circuit is no longer regenerative and the signal relay holds the control system in the offset position while the auxiliary relay introduces the fixed direct current potential to position the spot vertically off-screen. The camera shutter is opened and a pulse is manually introduced to the oscillator circuit by means of switch *1*. The pulse triggers the square wave generator which drives negative. This signal is recorded on the time base track, the relays operate and the sweep is synchronized to display the transient. At the end of the transient interval the recorded signal is reproduced to cause the square wave generator to go positive, thus breaking the pulse train with the spot positioned off-screen.

Application of the Instrument

To illustrate application of the transient response indicator, a carrier-type instrument servomechanism was constructed. The system employed potentiometers as the error detecting means and an induction generator as a minor feedback element. A potentiometer energized from a d-c source was included as a measure of the controlled variable.

The response of the servomechanism is given in Figures 3 through 8. The curve of Figure 3 is the modulated carrier transient response of the actuating signal. Figure 4 gives the response of the controlled variable as measured by the d-c excited potentiometer for corresponding conditions of step function magnitude and system adjustment. (The discontinuities of the trace result from slide-wire resolution.)

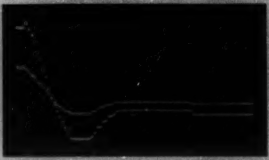

Figure 8. Display of in-phase and quadrature components

Figure 5 shows the successive steps in determination of the values of time and magnitude for a point on the response curve with the system adjusted for one overshoot of the controlled variable. The zero magnitude base line is superimposed on the response pattern of Figure 5(A). In Figure 5(B), the sweep has been time-delayed so that the selected point (in this case the peak magnitude of the overshoot) occurs at sweep initiation. The pattern has been shifted vertically in the trace of Figure 5(C) so that the initial and final points of the time-delayed response curve lie on the base line. The magnitude of the response at this point is read from the calibrated d-c potentiometer.

The variation which occurs in actuating signal response when the time of transient initiation coincides with different phase angles of the carrier frequency is illustrated in Figure 6(A). One trace shows response when the transient initiation occurs at the peak magnitude of the actuating signal carrier voltage and the second trace shows response when transient initiation is delayed by a time corresponding to 50 degrees of the carrier (2.3 milliseconds). It is noted that the transient duration is shorter when step function initiation corresponds to the peak magnitude of the carrier frequency. The curves of Figure 6(B) show response of the controlled variable for these same conditions. The change in carrier phase at the instant of transient initiation is reflected in response as a time delay with response wave shape essentially unaltered, but shifted in time by approximately 4 milliseconds. Examination of a family of response curves shows that this delay becomes progressively larger as transient initiation approaches 0 degree phase of the carrier frequency.

The error response curves of Figures 7 and 8 were obtained by adding inertia to the system and adjusting gain and damping to give an underdamped pattern. In Figure 7(A) the transient response of the actuating signal is shown for correct phase matching of reference input and primary feedback. Beam brightening pulses at carrier frequency have been adjusted to occur in-phase with this signal to give a visual detection of signal envelope. In Figure 7(B) the phase of the reference input potentiometer was purposely shifted to introduce a quadrature component to the actuating signal. Under these circumstances the true measure of response is not determined by the envelope of the curve. In Figure 7(B) the carrier frequency beam brightening pulses again occur in-phase with system reference voltage. It is seen that the envelope and the detected in-phase component of the signal differ. The initial magnitude of the envelope is greater than the visually detected in-phase component. The first cross-over point has a broad envelope due to the quadrature component; however, measurement of response magnitude in the vicinity of cross-over by means of visual detection is possible. Subsequent cross-over points are not indicated from examination of the envelope but are shown by the beam brightened portion of the trace. Figure 8 illustrates the selectivity of this technique. The two curves represent detection of the in-phase and quadrature components for the same conditions as in Figure 7. Intensity has been adjusted so that the trace of the amplitude modulated carrier is not visible.

Conclusions

The instrument developed is sufficiently versatile to allow determination of transient response of a large number of feedback control systems with a minimum of alternation to either the instrument or the system. Transient characteristics may be examined for repeated application of a step function and the effect of system adjustments observed. The instrument is self-contained; it provides the necessary step-function inputs and permits either photography or quantitative determination of response magnitude as a function of time.

No Discussion

Education and Training of Diesel-Electric Locomotive Maintenance Personnel

J. W. TEKER
ASSOCIATE MEMBER AIEE

E. R. AINSWORTH
NONMEMBER AIEE

WIDESPREAD use of diesel-electric locomotives on American Railroads has created an unprecedented demand for personnel trained in the operation, inspection, and maintenance of many types of electric equipment. The locomotive builders and the railroads, working together, have developed successful programs for training such personnel. Contributing vendors and the trade press have ably seconded these efforts. The application of basic principles of education has served to develop teaching techniques which are producing personnel capable of coping with the problems of this new era in railroading.

A New Task in Education

Since the turn of the century electricity has played a steadily increasing role as a servant of the railroads. In the beginning this growth was so gradual that the recruiting and training of the relatively small electrical maintenance force was not a major problem. But the coming of the diesel-electric locomotive swiftly changed this picture. The last 10 years have seen the electric horsepower installed by the railroads increase from 2,000,000 to 25,000,000. This phenomenal growth has caused a revolution in this 100-year old industry. Personnel, shops, and facilities geared to the maintenance of steam locomotives were suddenly faced with diesel-electric operation. In the early stages of such a drastic change some confusion was inevitable.

From the lessons of those pioneer days, often learned through delays and breakdowns, there emerged a pattern of maintenance knowledge for both the builder and the operator of diesel-electric locomotives. The next step was the dissemination of this knowledge at working levels. Part of this task proved to be relatively easy. The mechanical aspect of this new motive power was readily accepted by personnel already mechanically minded. While new standards of precision and cleanliness had to be established, the workmen's background of experience was reasonably close to the essentials necessary to understand his new job. Even the maintenance of motor and generator brushes, bearings, gears, and belts involved primarily mechanical functions. Hence these duties were assumed with understanding and comparative ease. But the same could not be said in cases where electrical faults occurred. Here was an element new to the railroad mechanic—one about which he had only vague notions and many fears. The builders and railroads together had to muster enough expert people to diagnose and direct the correction of these electrical troubles.

The advantages of the diesel-electric locomotive were so outstanding that American railroads eagerly embarked on a program of wholesale dieselization. The growing fleets of these locomotives emphasized the need for educating and training electrical personnel to man the required maintenance programs. In many cases experienced railroad supervisors found themselves in the same position as the men they were supposed to direct or teach. Both lacked background and experience in electric equipment. A further complication was introduced by the rapid evolution of the diesel-electric locomotive. This resulted in a diversity of sizes and types, of varying complexity.

Such circumstances demanded a training program of a character and scope far exceeding anything then being carried on. The challenge was met and steps taken to implement such a program. Yet even while it was being set up trains moved and the equipment was kept in repair—a truly phenomenal job—again demonstrating ability of American railroads to rise to the occasion.

Early Method of Instruction

The service engineer, trained by the locomotive builder, was usually the first on the scene to put the locomotive into service. The assigned railroad personnel, both operators and maintainers, were subject to his direct instruction in handling and servicing the equipment. He rode the trains and worked with the men at service points until a self-sufficient maintenance nucleus was trained and functioning. Locomotive riding was discontinued as soon as crews were capable and outlying maintenance people learned routine duties. More time could then be spent with the maintainers, especially on diagnosis and correction of the electric control difficulties. Of necessity, much of this instruction was "how to do," rather than "why." The primary objectives were to get the unit going quickly, keep it going, and make miles without delays.

Instruction Books

Instruction books, covering the operation and maintenance of the equipment, have been used since the earliest days. They incorporate the best information available to the builder at the time of publication. Usually these books are written for each locomotive design and for each piece of new equipment. In the course of time a railroad with a diversity of locomotives accumulates a considerable library of builders' manuals and instructions. These are extremely valuable in the continued operation and proper maintenance of the motive power, serving as reference sources for information on limits, adjustment data, and so forth.

Field experience, as reported by service technicians and investigated by factory engineers, dictates periodic revisions of the instructions. Hence the distribution of instruction books must be known so that they can be kept up to date.

There are two schools of thought regarding the use of instruction books on railroads. The first favors wide distribution to get the instructions directly down to the level where work is done. This practice has the advantage of putting a maximum amount of information at the disposal of the workmen. A possible drawback is that, in the pressure of work, the men will not find time to study the instructions. Moreover, specific instructions for a given type of equipment may become general practice, even though not applicable to other equipment. A wide distribution makes it difficult to keep the instruction books up to date.

The other school of thought advocates the distribution of a minimum number of books to key people only. These persons

---

Paper 53-70, recommended by the AIEE Land Transportation Committee and approved by the AIEE Committee on Technical Operations for presentation at the AIEE Winter General Meeting, New York, N. Y., January 19–23, 1953. Manuscript submitted October 20, 1952; made available for printing December 5, 1952.

J. W. Teker and E. R. Ainsworth are with the General Electric Company, Erie, Pa.

then have the responsibility of extracting and interpreting the instructions in terms suitable to govern their local conditions. This method gives local supervisors close control of maintenance practices. Of course there is the possibility that the instructions will remain on the office shelf and the men at working level be left to their own devices. This may result in a variety of maintenance practices at different points on the same railroad system.

Instruction books are most valuable for the maintenance of motive power, but they are not well adapted for use in the education and training of personnel new to diesel-electric locomotives. Of necessity, the information these books contain is largely specific, so that a background of basic knowledge and training is desirable for their proper understanding and use. To meet this need other media of instruction have been developed.

Schools

Schools conducted at the plants of locomotive builders are a natural outgrowth of the factory training of service engineers. Expert instructors, with a factory background and familiarity with operating problems, conduct these classes on an organized basis. Such schools are located at the factory and have teaching facilities, such as classroom slide and moving picture projectors, models, and other demonstration material. Conducted tours through the factory permit inspection of the equipment to be maintained. Seeing operations performed is a valuable aid in effectively clinching the knowledge gained in the classrooms.

While this orderly education is extremely valuable, it cannot be used for reaching the mass of men engaged in maintenance work. The fact that the students must be away from their jobs and homes makes it expensive. Time limitations require a concentrated presentation so that only men who are naturally students can absorb the material. A very effective use of such schools is for the education of key railroad personnel who have teaching ability. They, in turn, then act as instructors for the men on their own properties.

Schools conducted by the railroads themselves are a means of reaching more men, particularly those who actually do the maintenance work on the locomotives. Since such schools are held locally, the time element is not as important as when they are away from home. The classes are shorter, usually not over 2 hours, instead of 8 hours. They are spread over a longer period and only one item is handled at a time. The classes are usually conducted by a railroad man who may have attended a factory school, or arrangements may be made to have the builder's instructor do the teaching. Such schools bring the teachers to the students rather than have the students go to the teacher.

Instruction cars are another effort to bring the school to the men. These are patterned after the well-known air brake instruction cars, which served so well to instruct railroad personnel in the specialized equipment of the air brake. The advent of the diesel-electric locomotive introduced the widespread use of other types of specialized equipments, and the railroads were quick to adopt the instruction car method here also. These cars, owned either by the locomotive builders or the railroads, all follow a general pattern. About half the car is devoted to mechanical equipment. The other half is fitted up for electrical instruction. Cut-away sections, typical control setups, and other visual aids are provided.

Arrangements are made in advance at the various maintenance points to utilize this facility effectively. Generally, three sessions are held to reach all three working shifts, for example: 9 to 11 a.m., 1 to 3 p.m., and 7 to 9 p.m.

A number of railroads find it advantageous to own their own instruction cars. Education and training is a continuing effort. It must keep pace with labor turnover, with the modernization of equipment, and with improvements in methods. Such a car serves to educate personnel, at all the service points on a widespread railroad system, in the best available maintenance practices.

Diesel Clubs

Diesel clubs are a powerful and timely influence for the advancement of education. They combine the natural inclination toward social gatherings with shop talk. The power of such motivations is amazing. It brings men to meetings on their own time after a day's work, regardless of weather to listen to and talk shop. Such clubs afford opportunities to learn and to exchange experience, and are quick to bring results. Points picked up at these sessions are soon put into practice on the job.

These clubs enjoy the active co-operation of the railroads, the builders, and the vendors, both in supplying speakers and furnishing subject material. This is beneficial to all concerned. Active membership in these clubs tends to be divided between workmen and supervisors but allows typical American mingling. Programs, however, are slanted to suit the respective memberships.

This type of activity is formalized in a national body through the Locomotive Maintenance Officers Association. The electrical aspects of locomotive operation are occupying an ever-increasing part of this association's program time and committee work. This tends toward a better understanding and spreading of electrical know-how on a nationwide basis.

In addition to the general exchange of information by railroad maintenance officers, the Association of American Railroads, through its electrical section, studies and records on its proceedings accepted electrical practices. These records are an authoritative source of valuable information for educational programs, and constitute excellent reference material.

Magazines and Vendors' Bulletins

Trade magazine articles are an important educational tool. Publications formerly devoted to mechanical subjects have definitely recognized the demand for electrical subject matter. Some have established electrical sections and added electrical editors to their staffs. Even titles have been changed to better describe this broadened scope. Published material includes abstracts of meetings, "how to do" articles, and valuable hints in the form of question and answer columns. Staff editors make trips into the field to survey trends, problems, and needs. They then seek material from authoritative sources along these lines.

The value of this effort must not be underestimated. Interest in such subjects runs high, and each issue of the publication is read with interest by subscribers. Also, there are nonsubscribers who read office copies, so that the circulation figures for any magazine are not a true index of its effectiveness. These periodicals, because of the factual and authoritative character of their material, influence thinking and mold viewpoints on current problems. Certain articles become available for distribution to interested parties in reprint form. These accumulate as reference material in notebooks or scrapbooks of many individuals.

Presently the demand is for articles dealing with fundamentals and reasons for the "how" of electric equipment maintenance and operation. The popularity and effectiveness of these articles is governed by the simplicity of their approach. Unfamiliar terminology must be avoided and the language kept at newspaper level. For example, a technical paper with its theoretical and mathematical treatment of a subject is worthless for this purpose. Its message will be lost regardless of its value.

Bulletins issued by vendors of various parts, such as bearings, oil products, carbon brushes, and instruments must not be overlooked. Their contribution to the education of personnel is important, and such information should be passed on to the men. Some of these publications are broad in their scope, and others are specific. For example, carbon products bulletins may explain brush terminology and show the relationship between brushes and factors affecting commutation. An instrument vendor's publication may not only explain a meter but may also show its value for checking insulation or for measuring the output of a locomotive power plant. Another may dwell only on checking viscosity of insulating varnishes or measuring temperatures of ovens. Collectively, these publications make a vast fund of specialized knowledge available to electrical personnel for application to their everyday problems.

Personal contacts between railroad employees and builders' or vendors' engineers and service people is a specialized kind of education. This is often a 2-way relationship of mutual benefit, especially in the study and solution of difficulties that may arise. The railroad learns about some of the design considerations and thereby gains an intimate understanding of the mechanism. The builder in turn, learns about the exacting requirements set up by a given duty. Hence, intelligent maintenance and good product design are both aided.

Self-Help

Self-help means are available to all. Libraries have books ranging from texts on elementary electricity to engineering treatises. Larger communities offer night classes. Wherever the mail goes, there is opportunity for correspondence courses. Many a supervisor and master mechanic worked up through the ranks in days of the steam locomotive by burning midnight oil. The same can be done today in the study of electricity.

Apprentice Programs

Apprentice systems have long been a principal means of training the electrician, machinist, boilermaker, and others in the related skills of the huge railroad industry. In all probability the emphasis in this system will be altered to provide for the training of the electrical personnel now required in such numbers for maintenance of diesel-electric locomotives. In the meantime however, the sudden swing of the railroads to this new motive power has created a demand for men far beyond the capacity of the existing electrical apprenticeship programs. The problem today is one of retraining men experienced along other lines directly for these duties, while suitable and adequate programs are being developed.

Generally, it is the younger men who transfer, those who have not yet formed attachment to steam. Those among the older personnel who transfer are usually the ones who were able to foresee the new trend or who, because of their key positions, were urged by management to change over and prepare themselves for the coming of the new motive power. With the decline of steam power, however, more older men began to strive for these new jobs on the basis of their seniority. Depending on local circumstances, they sometimes displaced the younger men already doing effective work. There is the possibility that the full use of apprentice system training in electrical maintenance may be delayed until this situation is stabilized.

Service Technicians' Training

Locomotive builders anticipated the need for trained men in their electrical shop crafts. To furnish these, especially for their own service shops, they instituted factory training programs. Likely young men who wish to qualify for such jobs are enrolled. This is a long-term training, with emphasis on developing manual skills in all the phases of motor, generator, and control construction by actually doing the work. In addition there is regular class work, homework, and a series of inspection tours conducted by qualified instructors from both factory and engineering departments. Upon completing his training the graduate is ready to take a position in the builder's repair or service shop. While developed primarily for training builder's personnel, such a program could be adopted by the railroads if it appeared desirable.

Junior Engineers' Training

College graduates are being offered opportunities in railroading as never before. The technical complexity of modern transportation tools demands the analytical training and fundamental grounding provided by college curriculums for the management of these facilities. The problem here is one of training an individual, having the necessary qualifications, in the ways of railroading, as contrasted with the training of a railroad man in the fundamentals of the equipment. A typical long-range plan brings the college man through the various departments of the railroad, including roadway and track, shops and office, on various assignments. This permits the man to get the feel of railroading and also allows the railroad to measure the man.

Teaching Techniques and Problems

Certain circumstances characteristic of this field strongly influence the teaching techniques. Education and training must be considered separately. Under education are grouped those techniques having to do with learning by instruction and study. They include lectures and demonstrations by the instructor. In training, the student practices what he has learned in order to gain the required skill.

One problem common to both forms of teaching is the matter of interest. Any presentation or training program—whether it be in class, at a club meeting, through casual contact, or by the written word—becomes ineffective unless it holds interest. Any technique should be examined and considered in the light of its ability to motivate interest. One of the sources of interest is the natural, inherent curiosity about a subject connected with one's work. Another is ambition; looking ahead and preparing for the future. Still another is the very practical one of holding a job right now. The instructor's enthusiasm is another stimulus to the interest of the class. Indeed, a certain amount of showmanship, not too unrestrained, with surprises that are are later explained, will add to the enthusiasm displayed by the students. Different types of men will show widely varying degrees of interest. Young men, or older ones, who see the going of steam and are intrigued with the mechanism of the diesel-electric accept the change and seek every opportunity to perfect themselves in the understanding of the new motive power. But there are those who through time, have gained position and formed attachments to steam power.

They have preference for steam, so that they are not eager to change. They must start all over, so they have fears. With no understanding of electricity they doubt their ability to learn. They may mask these fears with an attitude of indifference. The instructor should tactfully let them know that he understands their position. All these factors need to be considered in setting up an educational program.

Where classes are set up on the man's own time, they compete with fishing, lodge meetings, gardening, and other diversions for a share of his interest. For these reasons summer classes are more difficult than those held in winter. To keep a man's attendance for 2 hours a day 5 days a week, for a month is a real challenge. The literature and subject material is issued in small parcels at each class session rather than as a complete text at the first class. This tends to keep the men coming and also confines attention to the subject at hand. An attendance record of 75 per cent or better justifies issuing a diploma.

An important point is to have no comparative examinations or tests. This avoids fear on the part of the students of being embarrassed by a revelation of what they don't know. It is an important consideration, especially where men and supervisors sit in the same classes. The same fear curtails the asking of questions and tends to stifle the spontaneous conduct of a class. It must be remembered that many of the men and supervisors are already working at the very job they are studying. Self-checking and self-scoring systems are accepted methods of testing their knowledge. These list the questions on the subject and the student goes through them. Then the instructor gives the correct answers and each student checks, corrects, and scores his own paper. No attempt is made to record or disclose the result. Each man is on his own. Wherever possible, separate classes should be held for workmen and for supervisors in order to promote ease and freedom of action.

The Instructor's Approach

The class sessions should be kept short and only one topic should be studied at a time. The level of understanding must be considered in the teaching approach. The instructor must begin where the students are. He must be certain that his class understands him and that they are following him as he goes. One quick unfamiliar term or phrase, and the class is lost. The explanations must fit the student's thinking and provoke his thought process. A feeling of confidence must prevail between instructor and student. This should be based, not on what the instructor knows, but rather on the ability of the student to understand and accept facts on his own as right and reasonable.

Words are the means by which thought flows from instructor to student. Hence they should be chosen with the utmost care. The words used must suit the audience for which they are intended. This is true for the spoken[1] as well as the written[2] message. For example, there is the everyday street level, newspaper kind of language generally understood by all. Next is shop talk, which is complicated only by the names of parts, tools, materials, or processes peculiar to a certain trade, and easily understood by those familiar with that activity. Finally there is the professional language based on terms and laws of highly developed and specialized activities, such as medicine, chemistry, and engineering. A background of specialized training is necessary to follow the thought and absorb the ideas expressed in such terms, and even then it often can be done only by careful study and reference. A practical recognition of these three language levels is most important. Articles, instruction books, and talks must be worded for the level at which they will be used if their message is to be understood.

Subject Matter and Procedure

Differences in the character of the subject matter are also important. There is a distinction between "how" and "why." It is one thing to show a man how to do something and another to tell him why it is done. Both are necessary; but in teaching electricity, emphasis should be on the why. This is the same in any given instance, whereas the how can be varied to suit the situation. Knowing the reason for a procedure fixes it more firmly in mind and makes it easy to devise methods to suit a given situation. A man who knows the why acts logically and intelligently when confronted with a new problem. He can figure it out himself.

In teaching the approach to any complex problem, circuit analysis, or chain of events, the instructor should show how it can be reduced to simple, easily understood parts. He should compare unfamiliar phenomena to something the students understand by using analogies. Many electrical concepts have an equivalent physical analogy which should be drawn upon. For instance the flow of current in the electric circuit can be likened to the flow of water in a closed hydraulic system. The idea of no flow without a circuit must be driven home. Show that what goes out into a circuit must also come back before the machines will start. Flow in various types of circuits—series, parallel, and their combinations—should be studied. The object of such instruction is to build familiarity with the tracing of circuits. Once this is established wiring diagrams with their terminology can be considered.

After the preliminary steps have been completed, emphasis should be laid on control. Both control circuits and control mechanisms should be studied, since practically all trouble shooting is done through these channels. One training method is to introduce faults in a circuit and have class members locate and correct them. The subject of electric rotating machinery should come last. Motors and generators may be shown to be identical machines. Emphasizing their similarity and the purely mechanical nature of much of their maintenance will dispel many misgivings in the minds of students.

Electrical terms can also be correlated with familiar concepts; volts as equivalent to water pressure, amperes as volume of water flow, and resistance as the opposition to flow resulting from the size of a pipe and the condition of its interior surface. Insulation may be pictured as confining electricity to a circuit as pipes confine water or steam.

An important factor to take into account at the outset is the natural fear of electricity. A student may master all the fundamentals in the classroom, and yet hesitate to apply them when confronted with the equipment. This caution should be respected and can even be used to advantage in teaching good safety practices. The students should be taught precautions against establishing circuits through the body, such as working with one hand, the use of insulated rods, and the wearing of gloves. They should also be taught to make an electric circuit harmless by removing fuses, opening switches, or shutting down equipment whenever possible. But the final step will be taken only when confidence is established within the man himself. The quickest way to bring this about is by practice. Show him how, and then have him practice until all uncertainty leaves. Training in classes must be watched to insure that all members benefit as much as possible. In almost every group there will be those who know and have confidence and are eager to demonstrate. They will push forward while the others seek the rear and look on. This situation can be remedied by calling on all individuals to participate.

Phases of Education

The education and training of these men goes through three distinct phases. The first is operation: how to start, stop, and control the locomotive; and the simple theory of its operation. The second is running maintenance: what to do to keep the equipment in running order; how to locate, trace, and correct trouble. Here the reasons behind maintenance procedures can be given in as much detail as seems desirable. The third phase is overhaul, reconditioning, and repair: how to rebuild the equipment. Again, reasons for recommended procedures may be discussed.

Generally, electrical personnel comes either from the mechanical ranks or from among men who have acquired a good mechanical understanding in the process of their work. Such a familiarity with the mechanical end of the locomotive is essential for a proper performance of the electrical work. Jobs of this type call for men of high ability with a wide scope of understanding and analytical powers. Because of this the instructor finds the majority of the students more than ready to meet him half way.

A Sound Investment

Many railroads already have become aware that providing able instructors, good teaching and training aids, and suitable classrooms is a wise policy. Trained men bring results in terms of lower maintenance costs and improved reliability of equipment. This, in turn, is reflected in the better service so essential to the railroads in their tremendous task of furnishing transportation on a competitive basis.

No business is better than the men who give it life; their abilities and attitudes make it what it is. Track can be laid; locomotives can be built; but men must be trained if this multibillion dollar railroad investment is to continue to produce the life blood of our economy—efficient transportation.

References

1. The Art of Plain Talk (book), **Rudolf F. Flesch.** Harper Brothers, New York, N. Y., 1946.

2. The Art of Readable Writing (book), **Rudolf F. Flesch.** Harper Brothers, New York, N. Y., 1949.

No Discussion

Coulomb Friction in Feedback Control Systems

VINTON B. HAAS, JR.
ASSOCIATE MEMBER AIEE

Synopsis: The presence of coulomb friction in servomechanisms often results in undesirable effects, such as an operating deadzone, low-frequency wander, and poor dynamic performance for low level signals. Methods of compensation for these adverse effects are discussed and a specific example is presented. Also, a general procedure, using frequency-response techniques, is outlined for the synthesis of compensation in systems affected by coulomb friction. The methods employed are based on the recognition that coulomb friction in a control device has a describing function which reduces gain and introduces phase lag. The describing function is determined by both the amplitude and the frequency of the input signal to the device.

THE technique of extending the conventional frequency response method to control systems containing nonlinear elements is described in the literature.[1-3] This paper discusses a procedure for applying the technique to systems affected by the presence of coulomb friction. The validity of the procedure is confirmed by analogue computer studies. The simplicity of the procedure is illustrated by its application to an analysis of the effect of coulomb friction on the performance of the Massachusetts Institute of Technology (MIT) numerically controlled milling machine.[4]

The effect of coulomb friction is observed as a force opposing motion of a controlled member. With the member at rest the stiction coulomb friction force is equal in magnitude and in opposition to the driving force. With the member in motion the sliding coulomb friction force is constant in magnitude, but its direction is dependent on the sense of the velocity, since the force always opposes motion. The coulomb friction force is

$$\mathbf{F}_F(t)=C\frac{\dot{\mathbf{X}}(t)}{|\dot{\mathbf{X}}(t)|}\text{ for }\dot{\mathbf{X}}(t)\neq 0 \qquad \text{(1A)}$$

$$-\alpha C<F_F(t)<\alpha C\quad\text{for }\dot{\mathbf{X}}(t)=0 \qquad \text{(1B)}$$

where

α = ratio of stiction to sliding coulomb friction force
C = magnitude of sliding coulomb force
$\dot{\mathbf{X}}(t)$ = relative velocity of the engaged members

The general approach to nonlinear systems by the frequency response method is to divide the components of the system into those components which are linear and frequency-variant and those which are nonlinear and amplitude-variant. The describing function of a nonlinear component is the ratio of the output signal to the input signal where a sinusoidal input signal is considered and where only the fundamental harmonic component of the output is taken into account. The describing function thus obtained will depend upon the input signal amplitude.

Nomenclature

$\mathbf{a}$ = dimensionless coulomb friction force = $\mathbf{F}_F/C$
$\mathbf{B}$ = dimensionless vector position of engaged member = $(\mathbf{X}K)/C$
$|\mathbf{B}|$ = magnitude of the vector $\mathbf{B}$
$\dot{\mathbf{B}}$ = vector velocity = $j\omega\mathbf{B}$
$|\dot{\mathbf{B}}|$ = magnitude of the vector $j\omega\mathbf{B}$
C = magnitude of the sliding coulomb friction force
D = viscous damping
$\mathbf{F}_F(t)$ = coulomb friction force as a function of time

---

Paper 53-108, recommended by the AIEE Feedback Control Systems Committee and approved by the AIEE Committee on Technical Operations for presentation at the AIEE Winter General Meeting, New York, N. Y., January 19–23, 1953. Manuscript submitted October 21, 1952; made available for printing December 5, 1952.

Vinton B. Haas, Jr., is with the University of Connecticut, Storrs, Conn.

The author wishes to acknowledge the valuable assistance of J. O. McDonough and Prof. W. M. Pease of Massachusetts Institute of Technology. Most of the material contained in this paper was prepared in partial fulfillment of the requirements of the Electrical Engineer degree at Massachusetts Institute of Technology. Dr. R. J. Kochenburger, University of Connecticut, gave valuable assistance during the computer studies.

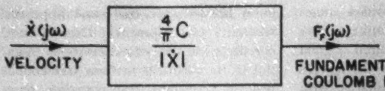
$\dot{X}(j\omega)$
VELOCITY
$\frac{\frac{4}{\pi}C}{|\dot{X}|}$
$F_F(j\omega)$
FUNDAMENTAL OF COULOMB FORCE

Figure 1 (above). Describing function of an element subjected to coulomb friction

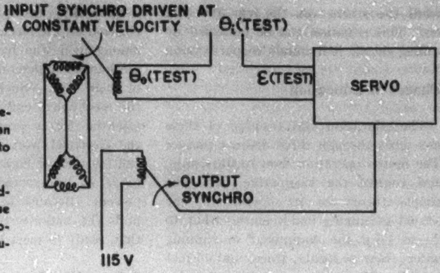

Figure 2 (right). Closed-loop frequency response testing of a servomechanism with coulomb friction

$\mathbf{F}_F$ = coulomb friction force vector
K = system gain or stiffness
$j=\sqrt{-1}$
M = mass
u = dimensionless angular frequency $=\omega/\omega_n$
$\mathbf{X}(t)$ = relative position as a function of time
$\dot{\mathbf{X}}(t)$ = relative velocity as a function of time
$\mathbf{X}$ = relative position vector
$|\mathbf{X}|$ = magnitude of the vector $\mathbf{X}$
$\dot{\mathbf{X}}$ = relative velocity vector
$|\dot{\mathbf{X}}|$ = magnitude of the vector $\dot{\mathbf{X}}$
α = ratio of stiction to sliding coulomb friction force
τ = time constant associated with MIT milling machine
ω = angular frequency $=2\pi f$
ω_n = undamped natural angular frequency $=\sqrt{K/M}$
ζ = damping ratio $=D/(2\sqrt{KM})$

According to equation 1 the nonlinear coulomb friction force is a function of the velocity $\dot{\mathbf{X}}$. When a sinusoidal variation of velocity is assumed, the form of the coulomb friction force function, plotted against time, is a square wave of amplitude C. The fundamental harmonic component of this force function is a sinusoidal wave of amplitude $4C/\pi$. The fundamental harmonic component of the coulomb friction force output is in phase with the velocity. The describing function obtained by considering only the fundamental component of the output is shown in Figure 1.

The conventional experimental tests for obtaining linear frequency response are modified for systems affected by coulomb friction. In contrast to conventional tests the input synchro is driven at a constant velocity as shown in Figure 2. The advantage of this method is that the output is constantly in motion, the coulomb force is constant, and the nonlinearity does not affect the sinusoidal response.

Comparison of Results for Idealized Control System

A control system is studied which is characterized by the relation

$$(\mathbf{X}_{in}-\mathbf{X}_{out})K=(Ms^2+Ds)\mathbf{X}_{out}+\mathbf{F}_F \qquad (2)$$

in which the mass M and the viscous damping D are negligible and the only significant parameters are the gain K and the coulomb force $\mathbf{F}_F$. The mechanical analogue of such a system is shown in Figure 3. For a sinusoidal input variation the wave form of the output is determined by the input amplitude. Figure 4 illustrates the wave forms of $\mathbf{X}_{in}$, $\mathbf{X}_{out}$, and $\mathbf{F}_F$ for two different amplitudes of $\mathbf{X}_{in}$, and for an assumed ratio of stiction to sliding coulomb friction force of 1.3 ($\alpha=1.3$). If the peak amplitude of $\mathbf{X}_{in}$ is less than 1.15 C/K, the output does not move and the coulomb friction force varies sinusoidally. If the peak amplitude of $\mathbf{X}_{in}$ is greater than 1.15 C/K, the output remains stationary until $(\mathbf{X}_{in}-\mathbf{X}_{out})=1.3\ C/K$; then the output suddenly moves a distance 0.3 C/K and continues to follow, but lags the input until $(\mathbf{X}_{in}-\mathbf{X}_{out})<C/K$.

A describing function, $\mathbf{X}_{out}/\mathbf{X}_{in}$, is obtained as a function of the amplitude of $\mathbf{X}_{in}$ (considering only the fundamental component of $\mathbf{X}_{out}$ in Figure 4) by conventional Fourier series analysis. Polar plots of this describing function are presented in Figure 5 for ratios of stiction to coulomb-friction force of 1.3 and 2.0. The plots are given as a function of $\mathbf{X}_{out}K/C$ for convenience.

An approximate describing function $\mathbf{X}_{out}/\mathbf{X}_{in}$ can be obtained more simply by making the approximations outlined previously; these resulted in the describing function shown in Figure 1.

From Figure 1 and equation 2, with $M=0$ and $D=0$

$$(\mathbf{X}_{in}-\mathbf{X}_{out})=\mathbf{F}_F/K=\frac{4C\dot{\mathbf{X}}_{out}}{\pi K|\dot{\mathbf{X}}_{out}|} \qquad (3)$$

Equation 3 in phasor-form is

$$\frac{\mathbf{X}_{out}}{\mathbf{X}_{in}}(\mathbf{X}_{out})=\frac{1}{1+\dfrac{j4C}{\pi K|\mathbf{X}_{out}|}} \qquad (4)$$

A polar plot of this describing function also presented in Figure 5. The locus of the describing function of equation 4 is a semicircle.

The approximation of considering only the fundamental component of a nonlinear output is valid, if this output is subject to low-pass filtering. In equation 3, however, the signal $\mathbf{X}_{out}$ is differentiated to form $\dot{\mathbf{X}}_{out}$, which, in turn, generates the coulomb force. Despite the lack of low-pass filtering, the approximate curve of Figure 5 agrees qualitatively with the more exact curves. When physical systems are used in which mass and damping are not negligible, the higher harmonics of coulomb force are attenuated and the approximation of considering only the fundamental attains greater validity.

The determination of the describing function from equation 2 when the mass and damping are not negligible is greatly facilitated by using an analogue computer.

Analogue Computer Studies

To investigate further the validity of the approximation of Figure 1, an analogue computer was constructed to represent equation 2 when mass and viscous damping are not negligible. Equation 2 may be made dimensionless for computer representation.

$$(\mathbf{B}_{in}-\mathbf{B}_{out})=(-u^2+2j\zeta u)\mathbf{B}_{out}+\mathbf{a} \qquad (5)$$

where

$\mathbf{B}_{in}=K\mathbf{X}_{in}/C$
$\mathbf{B}_{out}=K\mathbf{X}_{out}/C$
$u=\omega/\omega_n$
$\omega_n=\sqrt{K/M}$
$\zeta=D/2\sqrt{KM}$

and for a stiction to sliding coulomb force ratio of 1.3

$-1.3<a<1.3$ for $\dot{\mathbf{B}}_{out}=0$

($\mathbf{a}$ will have whatever value within this range is necessary to maintain $\dot{\mathbf{B}}_{out}=0$)

$\mathbf{a}=\dot{\mathbf{B}}_{out}/|\dot{\mathbf{B}}_{out}|$ for $\dot{\mathbf{B}}_{out}\neq 0$

A block diagram layout of the computer is shown in Figure 6.

The nonlinear function is generated

Figure 3. Mechanical analogue of a basic servomechanism with coulomb friction

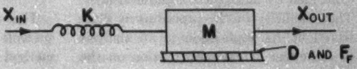

by feeding the velocity signal through a high gain amplifier and limiting the amplifier output with an ordinary neon tube. The neon tube simulates the stiction to sliding friction effect, since the firing voltage is greater than the conducting voltage. The tube used in the analogue has a ratio of firing voltage to conducting voltage of 1.3. The describing function $\mathbf{B}_{out}/\mathbf{B}_{in}$ for a sinusoidal input is obtained by considering only the fundamental harmonic component of $\mathbf{B}_{out}$.

The calculated transfer function $\mathbf{B}_{out}/\mathbf{B}_{in}$, using the approximation of Figure 1, is

$$\mathbf{B}_{out}/\mathbf{B}_{in}=\frac{1}{1-u^2+2j\zeta u+j\dfrac{\frac{4}{\pi}}{|\mathbf{B}_{out}|}} \qquad (6)$$

The describing function of equation 6 is a function of the frequency and amplitude of signal. A plot of this function in the complex plane requires a family of loci. The describing function is conveniently calculated for various values of $\mathbf{B}_{out}$, ζ, and u. These values of $\mathbf{B}_{out}$, ζ, and u were also represented by means of the computer, and a comparison of calculated and measured transfer functions was made. Comparisons were made for $u=0.05$, 0.1, 0.5, and 1.0 at $\zeta=0.25$ and $\zeta=1.0$, for several values of $\mathbf{B}_{out}$. The results obtained from this comparison validates the approximation, shown in Figure 1, of considering only the fundamental harmonic component of the nonlinear output. In general, the computed and observed phase angles of the transfer function agreed within 10 degrees and the magnitudes of the transfer function within 15 per cent. Some of the error in comparison must also be attributed to experimental deviations and not to the approximation of Figure 1.

Table I. Comparison of Observed and Calculated Wander on the Milling Machine

Orifice Size, Diameter in Inches	Amplifier Gain	Frequency of Wander in Radians Per Second		Peak-to-Peak Amplitude of Wander in 0.0001 Inch	
		Observed	Calculated	Observed	Calculated
		Original Thrust-Bearing Plate			
0.030	6.85	12.5	12.5	35.0	35.0
0.030	2.75	5.5	8.0	42.0	45.0
0.016	7.00	5.5	7.0	15.0	15.0
0.016	4.50	1.7	5.5	17.0	20.0
		Modified Thrust-Bearing Plate			
0.016	7.00	5.0	7.0	3.0	4.0

Application of Procedure to Analysis of Effect of Coulomb Friction on Performance of MIT Numerically Controlled Milling Machine

The machine-drive system of the MIT numerically controlled milling machine[4] consists of three separate servomechanisms, one for each degree of motion of the machine. All three motions of the machine are similarly driven, hence a description of the cross-slide servomechanism will suffice to illustrate the procedure. The principal element of the servomechanism is an electrically controlled variable-speed hydraulic transmission which drives the cross slide through a lead screw and an antibacklash nut. To obtain cross-slide position feedback, a standard synchro receiver is coupled to the cross slide through a precision rack and gear train, which cause one degree of rotation of the synchro shaft for each 0.0005 inch of cross-slide travel. The error signal obtained by comparing the synchro receiver and transmitter signals is amplified and drives an a-c torque motor. The torque motor strokes a hydraulic amplifier which in turn strokes the hydraulic transmission. Compensation is introduced in the control system by a spring-dashpot feedback on the hydraulic amplifier.

The cross slide was observed to wander at a low frequency with no command signal; this was attributed to coulomb friction. The frequency of the wander could be varied from 1 to 12 radians per second and the amplitude from 0.001 to 0.004 inch peak-to-peak by adjusting the amplifier gain and the orifice size of the dashpot feedback of the hydraulic amplifier. Using the procedure outlined in this paper, it is possible to predict quantitatively the amplitude and frequency of the wander for variations in the conditions listed here.

Referring to Figure 3, it is possible to explain qualitatively the wander caused by coulomb friction. The spring shown represents the effect of the torsional and compressional resilience of the lead screw, the deflection of the lead-screw thrust-bearing plate, and the torsional deflection of the power-drive gears. A positional error causes the hydraulic motor to rotate, compressing the spring until the level of coulomb force is attained; the cross slide will then move and overshoot the desired position. The spring is then released and put in tension in order to move the cross slide in the

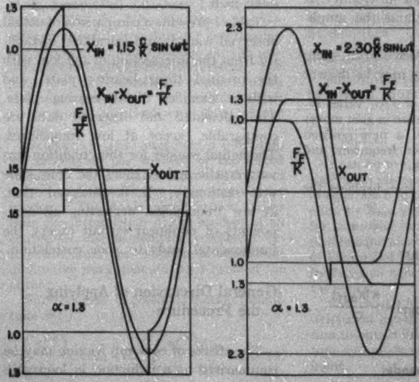

Figure 4 (left). Wave forms of input, output, and coulomb force

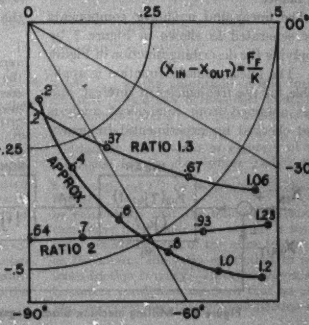

Figure 5 (right). Polar locus of $\frac{X_{out}}{X_{in}}$ as a function of $X_{out}K/C$

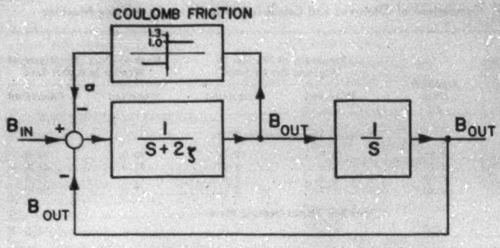

Figure 6 (above). Block diagram of analogue computer representing equation 5

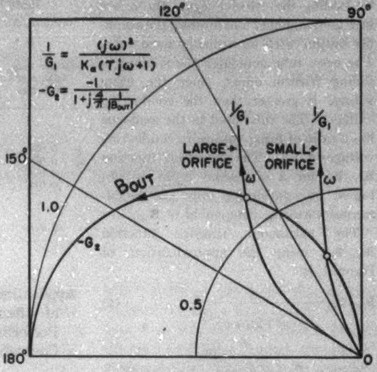

Figure 8 (right). Determining points of milling machine instability from intersection of $1/G_1$ and $-G_2$

opposite direction. This process is repeated as a periodic function of time.

The motion of the cross slide is described by

$$(\mathbf{X}_a-\mathbf{X}_{out})K=(M\,s^2+D\,s)\mathbf{X}_{out}+\mathbf{F}_F \qquad (7)$$

where

$\mathbf{X}_a$ = the angular position of the hydraulic motor referred to the cross slide
$\mathbf{X}_{out}$ = the cross-slide position
K = the spring effect
M = the mass of the cross slide
D = the viscous damping
$\mathbf{F}$ = the coulomb force

Dividing the equation by K results in

$$(\mathbf{X}_a-\mathbf{X}_{out})=(M/K\,s^2+D/K\,s)\mathbf{X}_{out}+\mathbf{F}_F/K \qquad (8)$$

where M/K and D/K are neglected since the spring is extremely stiff, and the frequencies of interest in the analysis are low. In addition, the feedback effect of $\mathbf{F}_F$ on leakage and compression in the hydraulic transmission is neglected since the transmission is designed for forces well in excess of the coulomb friction level. However, the application of the procedure outlined in this paper for analyzing the effects of coulomb friction is not limited to systems where these assumptions may be made.

The linear and nonlinear components are separated as shown in Figure 7 by applying the describing function of Figure 1. The linear transfer function is applicable for the frequencies of interest and was obtained from component analysis and checked by experimental frequency response. The gain K_a varies directly with the amplifier gain, and directly with the area of the orifice in the feedback dashpot of the hydraulic amplifier. The time constant τ varies inversely with the area of the orifice. The response function

$$\frac{\mathbf{X}_{out}}{\mathbf{X}_{in}}=\frac{G_1G_2}{1+G_1G_2} \qquad (9)$$

where

$$G_1(j\omega)=\frac{K_a j\omega\tau+1}{(j\omega)^2}$$

$$G_2|\mathbf{B}_{out}|=\frac{1}{1+\frac{j4}{\pi|\mathbf{B}_{out}|}}$$

$$\mathbf{X}_{out}=\frac{C}{K\mathbf{B}_{out}}$$

The system is unstable when $G_1G_2=-1$ or when $-G_2=1/G_1$. The locus of $1/G_1$ is plotted as a function of $(j\omega)$ and $-G_2$ as a function of $|\mathbf{B}_{out}|$. The intersection of these two loci indicate instability at the frequency of $1/G_1$ and the amplitude of $-G_2$.

Figure 8 shows these loci. From them the following conclusions may be drawn:

1. Since the amplitude of $1/G_1$ varies inversely with gain, an increase in gain moves the intersection point to a new position corresponding to a higher frequency and lower amplitude of wander.

2. Increasing the orifice size displaces the $-1/G_1$ locus to the left, resulting in a new intersection point corresponding to a higher frequency and greater amplitude of wander.

3. The intersection point is expressed in terms of the dimensionless displacement $\mathbf{B}_{out}$. The frequency of wander is thus independent of the magnitude of friction force and spring stiffness; however, the dimensional amplitude of wander varies directly with friction force and inversely with spring stiffness.

Quantitative data are obtained by assigning appropriate values of K_a and τ for the linear transfer function. It was determined experimentally that the most effective spring action in cross-slide motion was the deflection of the lead-screw thrust-bearing plate. This plate was 2 inches thick over a short span, and was bolted to the frame of the milling machine with four 1-inch bolts. Despite its construction, the deflection of this plate was 0.005 inch peak-to-peak as the cross slide wandered. The value of C/K used in the calculations was 0.005 inch.

Table I presents a comparison of actual observed wander and calculated instability from the intersection of the loci with the original thrust-bearing plate, and with a modified thrust-bearing plate. The calculated and observed data are comparable except at low frequencies. The actual wander for this condition was very erratic and at times the cross slide was stationary. It is observed that, at low frequencies, neglecting all components of nonlinear output except the fundamental leads to poor correlation.

General Discussion of Applying the Procedure

The effects of coulomb friction may be summarized as a reduction in loop gain

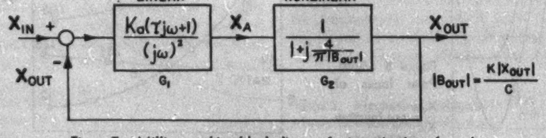
LINEAR
NONLINEAR
X_{IN}
+
-
X_{OUT}
$\frac{K_a(\tau j\omega+1)}{(j\omega)^2}$
G_1
X_A
$\frac{1}{1+j\frac{4}{\pi|B_{OUT}|}}$
G_2
X_{OUT}
$|B_{OUT}| = \frac{K|X_{OUT}|}{C}$

Figure 7. Milling machine block diagram for investigation of wander

and the introduction of phase lag for low amplitude signals. The result of these effects upon the over-all performance depends upon the linear elements of the system. Coulomb friction causes an operational dead band in systems where torque is generated by error. This dead band may be narrowed by increasing the over-all stiffnessof the system. For example, in a systen in which error generates rate of change of torque there will be no dead band due to coulomb friction; however, in other systems, such as the milling machine, an undesirable wander may result. Increasing the stiffness of the system short of an infinite torque constant may lead to wander at the low frequencies of the lag network. The phase lag of the network, cascaded with that due to coulomb friction, may result in low-amplitude low-frequency wander.

Dynamically, the effects of coulomb friction will be more pronounced for low-level signals. The resulting reduction of gain and phase lag at these signal levels results in slower response and less dynamic stability. These results may be partially offset by appropriately adding phase lead.

There is no general panacea for coulomb friction; however, the procedure of this paper does permit investigation of compensation and design modifications to improve the performance of a specific system. The algebraic form of the nonlinear-describing function makes it possible to manipulate with ordinary block-diagram algebra.

The mode of applying the procedure will depend upon the system to be analyzed. However, the most general synthesis problem this author can conceive of is the synthesis of a nonlinear compensation for a system adversely affected by the presence of coulomb friction. It is felt that the ideal manner of compensating for nonlinearity is the employing of nonlinear compensation.

A general procedure for synthesizing nonlinear compensation is as follows:

1. The linear block diagram for the system to be investigated is derived either experimentally or analytically.

2. The block to represent coulomb friction force, shown in Figure 1, is inserted in the appropriate manner.

3. The system transfer function C/E is obtained by block diagram algebra, or by solution of simultaneous equations. This transfer function is a function of amplitude of signal and frequency. (See, for example, equation 6.)

4. The describing function of the nonlinear compensation to be synthesized is G_2. The modified transfer function of the system is now G_1 (the original transfer function) times G_2 (the describing function of the nonlinear compensation).

5. The function $1/G_1$ is plotted in the complex plane as a family of loci. Each locus is plotted as a function of frequency for a constant magnitude of error signal. It may be necessary to initially prepare a family of loci in which each locus is plotted as a function of amplitude of error for a constant frequency.

6. A specific point on the $-G_2$ locus represents a specific amplitude of error signal. This point will also be the $(-1+j0)$ point for the $1/G_1$ locus plotted for the same amplitude of error. This $-G_2$ locus should be shaped to obtain the desired peak value of magnitude $|M|$, the system response function, for all operating amplitudes of error signal by the conventional method. In other words, the $-G_2$ locus should act to make the family of $1/G_1$ loci a single locus of desired shape by shifting the $(-1+j0)$ point for various amplitudes of signal. The analytical process of shaping the desired $-G_2$ locus is straightforward and not particularly laborious. Synthesizing a nonlinear-compensation system which will approximate this locus may be fairly difficult.

Conclusions

The procedure outlined may be used to synthesize or analyze systems subjected to coulomb friction effects. The use of an algebraic nonlinear-describing function provides an expedient means for investigating such nonlinear phenomena.

References

1. A Frequency Response Method for Analyzing and Synthesizing Contactor Servomechanisms, R. J. **Kochenburger.** *AIEE Transactions*, volume 69, part I, 1950, pages 270–84.

2. Sinusoidal Analysis of Feedback-Control Systems Containing Nonlinear Elements, E. Calvin **Johnson.** *AIEE Transactions*, volume 71, part II, July 1952, pages 169–81.

3. Locus Curve Method for Regulators with Friction, W. **Oppelt.** *Zeitschrift fuer Deutscher Ingenieure* (Berlin, Germany), volume 90, 1948, pages 179–83. Translated in *Report 1691*, National Bureau of Standards (Washington, D. C.), 1952.

4. A Numerically Controlled Milling Machine, Final Report to the U. S. Air Force on Construction and Initial Operation, **Servomechanisms Laboratory.** *Massachusetts Institute of Technology* (Cambridge, Mass.).

◆

Discussion

M. R. Aaron (Bell Telephone Laboratories, Murray Hill, N. J.): Mr. Haas has developed a useful procedure for determining the effects of coulomb friction on the performance of feedback-control systems. The purpose of this discussion is to point out an alternate approach to the problem which yields results identical with those of the author.

Jacobsen[1] in 1930 suggested a procedure for simplifying the analysis of the forced vibration of a single degree-of-freedom system subject to friction other than viscous friction. The basic simplification arises from the introduction of the concept of an equivalent viscous-damping coefficient determined from the criterion of equivalent dissipative work done during 1 cycle of the output.

For the case of coulomb friction (amplitude ±C)

$$\int_{x(o)}^{x\left(\frac{\pi}{\omega}\right)} C\,dx_{\text{out}} = C_e \int_{x(o)}^{x\left(\frac{\pi}{\omega}\right)} \frac{dx_{\text{out}}}{dx}\,dx_{\text{out}} \qquad (1)$$

where C_e is the equivalent viscous damping coefficient. If it is further assumed that the output wave form remains essentially sinusoidal, and of the same frequency as the input despite the existence of coulomb friction, then

$$X_{\text{out}} = |\mathbf{X}_{\text{out}}| \cos \omega t \qquad (2)$$

Substituting equation 2 in equation 1 and integrating yields

$$C_e = \frac{4C}{\pi\omega|\mathbf{X}_{\text{out}}|} \qquad (3)$$

It can be seen that the expression for the equivalent viscous-damping coefficient given in equation 3 of my discussion, when multiplied by $\dot{\mathbf{X}}_{\text{out}}$, yields the author's symbol $\mathbf{F}_f$ for sinusoidal inputs. In addition, the use of this equivalent coefficient for the system of Figure 3 of the paper results in the transfer function which is given by equation 6 of the paper.

The transfer function just referred to is rewritten in equations 4 and 5 of my discussion to obtain information about the amplitude and phase of the output relative to the input

$$\frac{|\mathbf{B}_{\text{out}}|}{|\mathbf{B}_{\text{in}}|} = \frac{\left\{\left[1-\left(\frac{4C}{\pi K|\mathbf{X}_{\text{in}}|}\right)^2\right](1-u^2)^2+4\zeta^2u^2\right\}^{1/2} - 2\zeta\left(\frac{4Cu}{\pi K X_{\text{in}}}\right)}{(1-u^2)^2+4\zeta^2u^2} \qquad (4)$$

$$\varphi = -\tan^{-1}\frac{2\zeta u+\frac{4C}{\pi K|\mathbf{X}_{\text{in}}|}\,\frac{|\mathbf{B}_{\text{in}}|}{|\mathbf{B}_{\text{out}}|}}{(1-u^2)} \qquad (5)$$

where $\mathbf{X}_{\text{in}}$ is the amplitude of the input sinusoid (which can be assumed units, for convenience), and φ is the phase angle of the output relative to the input.

Equation 4 is plotted in Figure 1 of the discussion for the case where $\zeta = 0.5$, and $\frac{C}{K|\mathbf{X}_{\text{in}}|} = 0$ and 0.4 respectively. It should be emphasized that the following assumptions have been made: the output is essentially sinusoidal, and of the same frequency as the input; the ratio of stiction to coulomb friction is unity. In other words, the boundary conditions are such that no stop motion occurs, and the coulomb friction is a

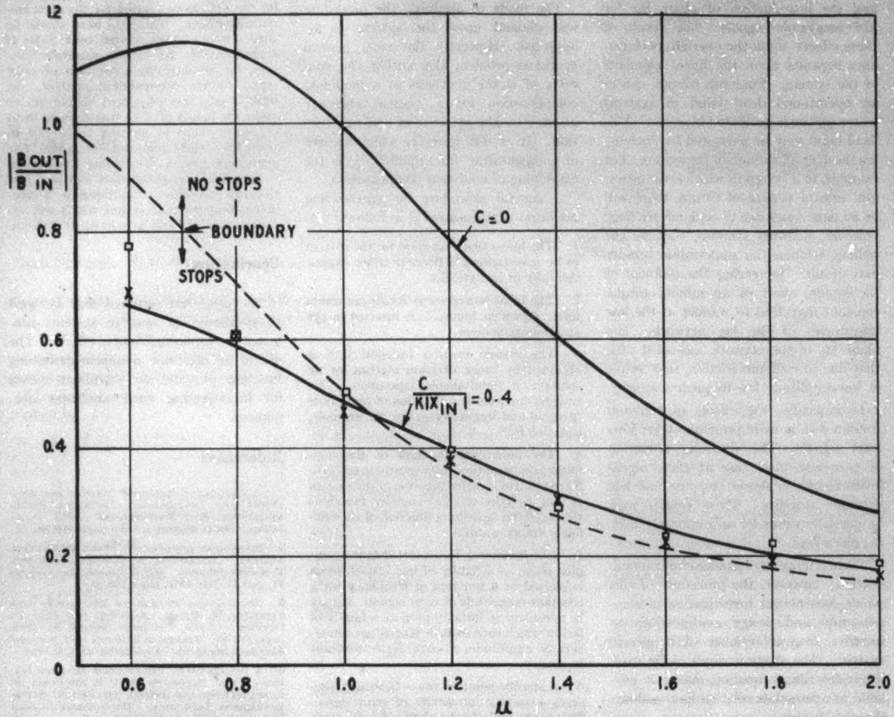

Figure 1. Amplitude ratio with coulomb and viscous damping

□ Measured on analogue computer × Computed, Den Hartog — Computed, Jacobsen

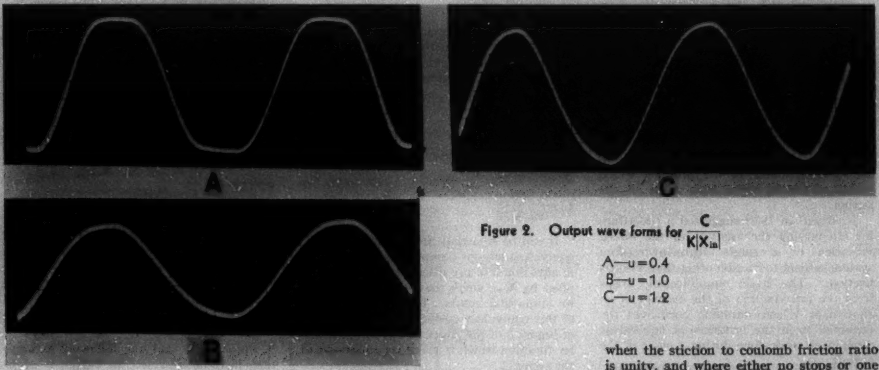

Figure 2. Output wave forms for $\frac{C}{K|X_{in}|}$

A—u=0.4
B—u=1.0
C—u=1.2

square wave. Stop motion occurs when the mass comes to a dead stop over a portion of each half cycle of the output. During the stop interval, the coulomb friction force may have any value between ±C.

Den Hartog[2,3] has solved the problem of the forced vibrations of the system of Figure 3 of the paper exactly for the case when the stiction to coulomb friction ratio is unity, and where either no stops or one stop occurs per half cycle. The equations that result from this analysis are quite complicated and are not reproduced here; however, points computed from Den Hartog's equation for output amplitude over

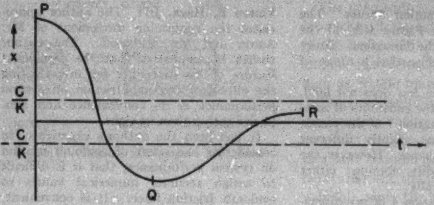

Figure 3. Motion for $M\ddot{\mathbf{x}}+D\dot{\mathbf{x}}+K\mathbf{x}=\mathbf{F}_F$

input amplitude, for sinusoidal motion with no stops, and $\zeta=0.5$, $C/(K|\mathbf{X}_{\text{in}}|)=0.4$ are plotted in Figure 1 of the discussion. In addition, Den Hartog has determined conditions for the occurrence of stops. This analysis results in the boundary curve of Figure 1 of the discussion, which defines the region of validity for the use of the equation mentioned.

Approximately 2 years ago, I was interested in investigating the effects of coulomb friction on feedback-control systems by using the methods described in the foregoing. At that time an analogue computer of the Philbrick type was used to obtain experimental data to verify the approximate analysis of Jacobsen. A configuration similar to that of Figure 6 of the paper was used where the peak amplitude of the output, input, and voltage representing coulomb friction were measured for several input frequencies and damping coefficients.

Measured points for the case where $\zeta=0.5$, and $C/(K|\mathbf{X}_{\text{in}}|)=0.4$ are plotted in Figure 1 of the discussion. The agreement between the measured characteristic and the calculation based on the approximation of Jacobsen and the work of Den Hartog agree within better than 10 per cent over the region $u=0.8$ to $u=1.8$. The output wave forms for three different values of u are shown in Figure 2 of the discussion. For $u=1.0$ and 1.2 the outputs are essentially sinusoidal as expected, while for $u=0.4$ the phenomenon of stop motion is depicted.

It can be concluded for the system of Figure 3 of the paper and its equivalents that for the region where no stop motion occurs, the effect of coulomb friction is to reduce the output-to-input-amplitude ratio as in equation 4 of the discussion, with an attendant increase in phase shift below $u=1.0$ and an attendant decrease in phase shift above $u=1.0$. In addition to the points emphasized in this discussion, other useful information about the effects of coulomb friction, damping proportional to the nth power of velocity, and mixed damping in feedback control systems can be obtained from a study of the papers of Den Hartog, Jacobsen, and others listed in the references.

REFERENCES

1. STEADY FORCED VIBRATIONS AS INFLUENCED BY DAMPING, L. S. Jacobsen. *Paper AMP-53-9, Transactions*, The American Society of Mechanical Engineers (New York, N. Y.), 1930.
2. FORCED VIBRATIONS WITH COMBINED VISCOUS AND COULOMB DAMPING, J. P. Den Hartog. *Philosophical Magazine* (London, England), May 1930.
3. FORCED VIBRATIONS WITH COMBINED COULOMB AND VISCOUS DAMPING, J. P. Den Hartog. *Paper AMP-53-9, Transactions*, The American Society of Mechanical Engineers (New York, N. Y.), 1931.
4. THE EFFECT OF COULOMB FRICTION ON THE PERFORMANCE OF SERVOMECHANISMS, G. D. McCann, F. C. Lindvall, C. H. Wilts. *AIEE Transactions*, volume 67, part I, 1948, pages 540–46.
5. MEASURING THE COULOMB AND VISCOUS COMPONENTS OF FRICTION, C. Kennedy. *Instruments* (Pittsburgh, Pa.), volume 15, October 1942.
6. VIBRATIONS DAMPED BY SOLID FRICTION, S. Thomas. *Philosophical Magazine* (London, England), March 1930.
7. THE EFFECTS OF BACKLASH AND SPEED DEPENDENT FRICTION ON THE STABILITY OF CLOSED CYCLE CONTROL SYSTEMS, A. Tustin. *Journal*, Institution of Electrical Engineers (London, England), 94, part IIA, number 1, pages 143–51.

Morris Rubinoff (University of Pennsylvania, Philadelphia, Pa.): It may be interesting to consider the effect of coulomb friction directly from the differential equation. As a simple preliminary example consider damped oscillatory motion in the presence of coulomb friction, but ignoring stiction

$$M\ddot{\mathbf{x}}+D\dot{\mathbf{x}}+K\mathbf{x}=\mathbf{F}_F \tag{1}$$

where

$$\mathbf{F}_F=C\frac{\dot{\mathbf{x}}}{|\dot{\mathbf{x}}|} \quad \text{for } \dot{\mathbf{x}}\neq 0$$

$$-C<F_F<C \quad \text{for } \dot{x}=0$$

Then as long as $\dot{\mathbf{x}}$ and hence $\mathbf{F}_F$ do not change sign, equation 1 of my discussion may be modified to

$$M\ddot{\mathbf{z}}+D\dot{\mathbf{z}}+K\mathbf{z}=0 \tag{2}$$

where

$$\mathbf{z}\equiv\mathbf{x}-\mathbf{F}_F/K$$

Equation 2 of my discussion has the familiar solution

$$\mathbf{z}=\mathbf{z}(0)\epsilon^{-\alpha t}\cos\omega t \tag{3}$$

where we assume, without loss of generality, that initially the mass M is at rest and maximally displaced upward. In this case $F_F=+C$ and $z=x-C/K$. Clearly M will move down for almost a half cycle ($\omega t\approx\pi$) to an amplitude of approximately $z(0)\epsilon^{-\alpha\pi/\omega}$ below $z=0$, that is, below $x=C/K$. The path is shown as PQ in Figure 3 of the discussion.

At Q, the motion and $\mathbf{F}_F$ reverse direction. Nevertheless equation 3 of my discussion still holds. M moves up for almost a half cycle with approximately the same fractional loss in amplitude when it reaches R. But in this case the amplitude R is measured from $x=-C/K$; in other words, there is a frictional amplitude loss of $\Delta x=4C/K$ per cycle.

Since R in Figure 3 of the discussion lies between $\pm C/K$, M stops at R. The frequency spectrum of the motion may be obtained by Fourier transform, the integral being evaluated piecewise. However, it is clear that there will be a large component of angular frequency ω, where

$$\omega^2=\frac{K}{M}-\frac{D^2}{4M^2}$$

The method is easily extended to the control system characterized by equation 2 of the paper. The equation may be rewritten, ignoring only damping (not mass, as in the paper) and using $\mathbf{x}$ for $\mathbf{X}_{\text{out}}$, $\mathbf{y}$ for $\mathbf{X}_{\text{in}}$

$$M\ddot{\mathbf{x}}+K\mathbf{x}=K\mathbf{y}+\mathbf{F}_F \tag{4}$$

where stiction is included through the author's relation

$$-\alpha C<F_F<\alpha C \quad \text{for } \dot{x}=0 \tag{5}$$

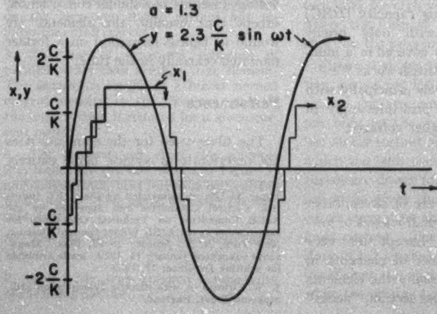

Figure 4 (left). Motions for $M\ddot{\mathbf{x}}+K\mathbf{x}=2.3C\sin\omega t+\mathbf{F}_F$; $M\omega^2\ll K$

Figure 5 (below). Motion for $M\ddot{\mathbf{x}}+K\mathbf{x}=\mathbf{y}+\mathbf{F}_F$

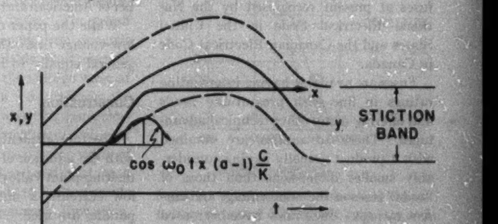

As before the substitution $\mathbf{z}\equiv\mathbf{x}-\mathbf{F}_F/K$ yields the single equation

$$M\ddot{\mathbf{z}}+K\mathbf{x}=K\mathbf{y} \quad \text{for } \dot{\mathbf{z}}\neq 0$$

$$\ddot{z}=0 \quad \text{for } \dot{z}=0 \text{ as long as } K|\mathbf{y}-\mathbf{x}|<\alpha C \qquad (6)$$

If we assume the sinusoidal driving force $\mathbf{y}=A \sin \omega t$, the solution of equation 6 of my discussion when $\dot{\mathbf{z}}\neq 0$ is

$$z=a \sin \omega_0 t+b \cos \omega_0 t+\frac{A \sin \omega t}{1-(\omega/\omega_0)^2} \qquad (7)$$

where $K\equiv M\omega_0^2$ defines ω_0. For $\omega_0\gg\omega$, as assumed by the author, the coefficients a and b obey the following initial conditions at each change of direction of motion

$$a \cos \omega_0 T-b \sin \omega_0 T\approx 0$$

$$a \sin \omega_0 T+b \cos \omega_0 T+A \sin \omega T\approx z(T) \qquad (8)$$

and hence

$$z=[z(T)-A \sin \omega T] \cos \omega_0(t-T)+A \sin \omega t \qquad (7\mathbf{A})$$

Equation 6 of my discussion specifies that no motion occurs until the net force overcomes stiction, at which time $K|A \sin \omega t-x|=\alpha C$ and, in fact $K[A \sin \omega T-x(T)]=-\alpha F_F$. Then equation 7($A$) becomes

$$z=(1-\alpha)(F_F/K) \cos \omega_0(t-T)+A \sin \omega t; \quad t>T \qquad (7\mathbf{B})$$

Since $\omega_0\gg\omega$, equation 7(B) discloses that there is a jump $\Delta\mathbf{z}=\Delta\mathbf{x}=2(1-\alpha)\frac{\mathbf{F}_F}{K}$ in time $\Delta t=\pi/\omega_0$ whenever motion occurs. The effect is illustrated in Figure 4(A) of the paper and Figure 4 of the discussion. Study of the latter will disclose that a range of motions is possible.

When the relation $\omega_0\gg\omega$ does not hold, the only change is in the constants of integration, a and b of equation 7 of the paper, which obey conditions slightly different than equation 8 of the paper. However, the solution may be readily obtained either analytically or graphically.

The solution of equation 4 of my discussion for arbitrary slowly varying input $\mathbf{y}$ may now be obtained simply by observing the following facts:

1. The bounding lines $\pm C/K$ in Figure 3 of the discussion define a stiction band. For equation 4 of my discussion, these lines are parallel to $\mathbf{y}$ at a distance $\pm\alpha C/K$ from $\mathbf{y}$.
2. Motion is induced whenever $|\mathbf{y}-\mathbf{x}$ increases to $\alpha C/K$.
3. The resultant motion is of the form $\left[\mathbf{x}-\mathbf{y}=(1-\alpha)\frac{\mathbf{F}_F}{K} \cos \omega_0 t\right]$ with $t=0$ initially. (Note that this assumes that the Fourier transform of $\mathbf{y}$ has only components with $\omega\ll\omega_0$ (see equation 7 of the discussion).
4. The motion ceases when $\dot{x}=0$, that is, when $\dot{\mathbf{y}}=(\alpha-1)\frac{\mathbf{F}_F}{K}\omega_0 \sin \omega_0 t$.

A sample graphical solution is indicated in Figure 5 of the discussion. The extension to more rapidly varying $\mathbf{y}$ may be obtained from equation 7 of my discussion.

Vinton B. Haas, Jr.: The author appreciates the confirming discussions of Mr. Aaron and Mr. Rubinoff. The author wishes to emphasize that the significant feature of his procedure for investigating the effects of coulomb friction on system performance is its convenience and simplicity rather than its rigor.

It has been the author's experience, in considering the effect of coulomb friction on system performance, that it is difficult to assign accurate numerical values to coulomb friction force. It is convenient, therefore, to have a quick engineering tool to appraise the effect of coulomb friction, since the accuracy of the data available would not in most cases justify a detailed calculation. It is most desirable to appraise the effect of coulomb friction on system performance for a range of friction coefficients.

The analysis of the effect of coulomb friction may indicate, in some instances, that its presence has a desirable effect on system performance. If the opposite is true, that is, if the effect proves undesirable, the analysis may indicate methods of system modification which will compensate for these undesirable effects, such as, using a more rigid thrust-bearing plate as in the case of the MIT milling machine.

The author feels that the procedure outlined in the paper would be improved if the describing function of coulomb friction force were modified to include the effect of the ratio of stiction to sliding coulomb friction force, and he is presently investigating this possibility.

The Application and Standardization of High Rupturing Capacity Current-Limiting Fuses

J. W. GIBSON
NONMEMBER AIEE

IT HAS become widely realised that fault values on low-voltage systems often greatly exceed the interrupting rating (10,000 amperes) of the cartridge fuses at present recognised by the National Electrical Code in the United States and the Canadian Electrical Code in Canada.

Fuses are available having interrupting ratings in line with present-day needs and offering many other technical advantages. These advantages are obtained with a product actually having considerably smaller dimensions than those of "code" fuses of the same voltage and current ratings. Such fuses have been used for about 20 years in Great Britain.

The design and performance of the modern high rupturing capacity (HRC) fuse will be dealt with only briefly here, since it has been covered in a number of American and British works.[1-4]

While the paper deals principally with low-voltage fuses, the principles apply in general equally to higher voltages.

Construction

The fuse elements are of silver, often with the addition of small masses of low-melting-point alloy. Except for very low currents, a number of elements in parallel are used. Usually the elements are not of uniform cross section, "necks" being formed at points where it is desired to initiate the arc; the method of forming the necks depends on whether wire or strip elements are used. The filler is a granular inert material, usually a very pure silica. It does not evolve gas and the fuse is of the sealed type, simplifying the construction and obviating the risk of external flashover. A close control is held on the materials and manufacturing processes with the result that the fuse is a precision article with a highly consistent performance. A typical 200-ampere low-voltage fuse is shown in Figure 1. High-voltage fuses are of a similar construction, except that usually, the elements are wound in helical formation on a former mounted centrally in the tube.

Performance

The silver used for the elements does not deteriorate in service, being entirely

---

Paper 53-129, recommended by the AIEE Industrial Control Committee and approved by the AIEE Committee on Technical Operations for presentation at the AIEE Winter General Meeting, New York, N. Y., January 19–23, 1953. Manuscript submitted January 14, 1952; made available for printing December 17, 1952.

J. W. Gibson is with Electric Transmission Ltd., Stoke-on-Trent, England.

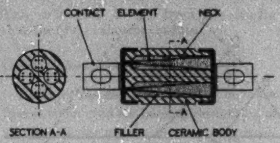

Figure 1. Typical 200-ampere HRC fuse

free from the oxidation trouble to which copper is subject and from crystallization such as occurs in zinc at the normal working temperature.

The neck or necks are made sufficiently long for the arc voltage developed during operation to be high enough, compared with the system voltage, to force the current down to zero without waiting for the normal zero pause, as do a-c interrupters other than fuses. On the other hand, the length is not made great enough to develop objectionably high overvoltages. The use of a filler of pure granular quartz allows the necessary arc voltage to be developed over a fairly short length, and this largely accounts for the shortness of the HRC fuse, compared with the "code" fuse.

A primary objective in the design of the fuse is to restrict the total element cross section. This reduces the amount of metallic vapour to be deionised when the fuse blows. Further, by lowering the thermal capacity of the element, the "cutoff" current is reduced and therefore the inductive energy to be handled by the fuse is reduced. Both factors help in the attainment of high interrupting capacity in a fuse of small volume. The reduction in cutoff current (that is, the considerable current-limting effect) is obtained in the following ways:

1. Silver, through its high conductivity, inherently has a small cross section for a given current rating.
2. The specific heat of silver is low—not much more than half that of copper. A low specific heat naturally has no influence on the long-time fusing current but reduces the cutoff current.
3. The use of separated elements in parallel rather than a single large element. The separation results in a higher normal current density in the elements, that is the cross section is reduced for a given current rating.
4. The elements are short (for example $2^1/_2$ inches for the fuse shown in Figure 1) and consequently heat is readily transmitted to the ends. This again increases the current density.
5. The use of the necks previously mentioned.
6. The fairly high thermal conductivity of the filling powder.

The net result is that the cross section is very small, the full-load current density in the necks of the elements in the 200-ampere fuse already mentioned being as high as 88,000 amperes per square inch.

The small-section requirement for high interrupting rating would normally tend to result in high watt loss. To reduce this watt loss and so avoid excessive temperature rises, the use of the neck is very valuable, since the high-resistance part of the elements is confined to a fraction of their length. The shortness of the fuse also helps in this connection. In addition, the positive temperature coefficient of resistance of silver ensures that the elements have a much lower resistance at rated current than they have when on the point of melting.

A further reduction in watt loss is assured by the low melting point alloy inserts, now generally used for all except very low current ratings. When the temperature of the element reaches the melting point of the alloy, diffusion of the alloy into the silver occurs. The amalgam has a higher resistivity than pure silver and heating is increased. The action continues progressively until fusion occurs. In effect, therefore, the melting point of the silver element is reduced from 960 degrees centigrade to little more than 200 degrees centigrade. A considerably cooler running fuse is the result. In addition, the time-lag on moderate overloads is increased.

The time-current characteristic for the 200-ampere HRC fuse compared with that of a typical 200-ampere code fuse is shown in Figure 2. The quick operation of the HRC fuse under heavy fault conditions is shown by the greater steepness of its curve. The shape of the time-current characteristic can to some extent be controlled by varying the proportions of the element (length of neck and ratio of cross section at the neck to that of the rest of the element), but the possibilities are restricted compared, for example, with fuse links for high-voltage expulsion fuses where the form of the element has less effect on the interrupting ability.

Figure 3 shows typical current-limitation curves for HRC fuses. The cutoff current for any particular fuse depends not only on the available fault current but on the instant on the voltage wave at which the fault occurs. Accordingly the curves are drawn for whatever fault closing angle gives the maximum value of cutoff current at any particular value of fault current. The left-hand part at a slope of 1/1 corresponds to fault currents insufficient to give current limitation, while the closing angle is such as to give asymmetrical conditions: the current actually passed by the fuse is greater than the numerical value of the available current, since this value is expressed in rms amperes. The extreme right-hand part of the curves is for symmetrical faults and has a slope of 1/3, since for extreme conditions of current limitation, the cutoff current is proportional to the cube root of available fault current. Intermediate parts of the curve relate to partially asymmetrical faults. The curves are based on an assumed ratio of rms asymmetrical current to rms symmetrical current of 1.25, and are for 60 cycles per second.

Another important characteristic of a fuse is the value of $\int i^2dt$, that is, the square of the current actually passed by the fuse, integrated over either the melting time, the arcing time, or the total interrupting time. These "let-through" values will be designated in what follows as $(i^2t)_m$, $(i^2t)_a$ and $(i^2t)_t$ respectively. The last determines the heating by the fault current of any apparatus in series with the fuse, whether equipment being protected or the elements of a "protected" fuse. Provided the times under consideration are short (of the order of 0.1 second and less) heat dissipation from the elements during the melting period is negligible, and $(i^2t)_m$ is independent of actual values of current. In other words, every fuse has a characteristic value of $(i^2t)_m$. On the other hand, $(i^2t)_a$, and also $(i^2t)_t$, vary not only with fault cur-

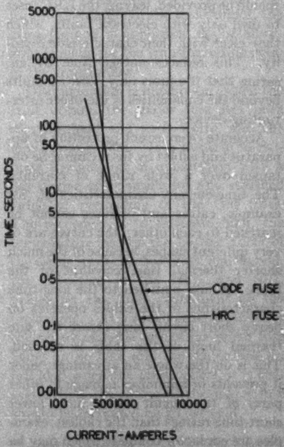

Figure 2. Comparison of time-current characteristics of typical 200-ampere code fuse and 200-ampere HRC fuse

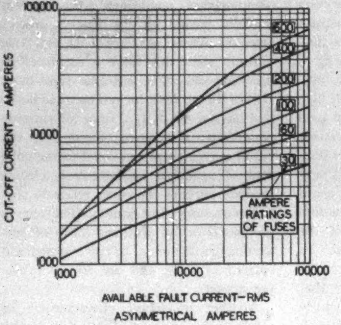

Figure 3 (left). Current-limitation curves

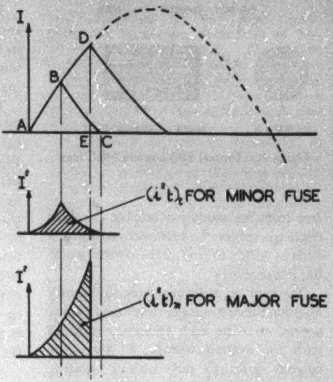

Figure 5 (right). Fuse discrimination

rent, but also with circuit voltage, power factor or time constant, and (for a-c circuits) fault-closing angle.

Principles Governing Fuse Application

Short-Circuit Protection and Overcurrent Protection

In general, the application of HRC fuses (as with most other fuses) is for short-circuit protection rather than overcurrent protection. Electrical systems and circuits should, wherever possible, be so laid out that outages need not occur as a result of overloading. Where this cannot be avoided, as in motor circuits where mechanical overloading is always liable to occur, suitable overcurrent relays should be provided, leaving the HRC fuses to deal only with electrical faults, which they clear with their characteristic rapidity. This reduces outage time by ensuring that the fuses only blow on faults beyond the capabilities of the other interrupting device.

Accurate overcurrent protection of apparatus and cables by fuses cannot be obtained over a wide range of currents. The time-current characteristics of, for example, cables and of fuses cannot be matched to each other; the curves are of very different shapes, because of the much shorter thermal time constant of the fuses. A fuse matched to the long-time characteristics of the cables operates on heavy short circuit long before the safe thermal limit of the cable is reached. This is on the whole an advantage, since it prevents or minimizes damage to other parts of the circuit which have lower short-time ratings than the cables; examples are contactor contacts which may be subject to welding, and current transformers which may be damaged by electromagnetic forces.

Choice of Current Rating

The current rating of fuse to be used depends on four principal factors as follows.

Full-Load Current of Circuit

This factor, taking into account any anticipated overcurrents, may be the only one to be considered for general distribution systems for public supply. For factory distribution and, in particular the protection of individual pieces of equipment, the factors enumerated in the following text may necessitate an increased size of fuse.

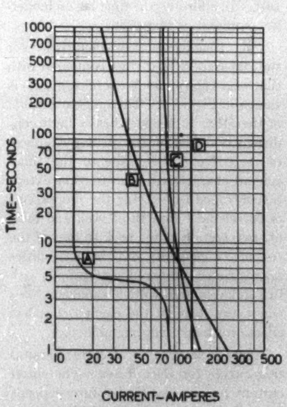

Figure 4. Co-ordination of HRC fuse and relay

A. Starting current of motor. Full-load current 14 amperes, locked rotor current 84 amperes

B. Characteristic of overcurrent relay, minimum setting 115 per cent of motor full-load current

C. Characteristic of 40-ampere HRC fuse

D. Interrupting capacity of controller

Ability to Withstand Initial Overcurrents

In many practical cases, these transient overcurrents necessitate a larger fuse than if only steady full-load current had to be considered. In such cases, the fuses are to be regarded as giving short-circuit protection rather than overcurrent protection.

Equipment taking overcurrents when switched in may be divided into two classes:

1. Motors, where the overcurrent persists for a time from about 1/2 second to 1 minute or more. In the case of direct started induction motors, the current, after the rapid dying away of the initial d-c component, remains at nearly the full locked-rotor value until the motor is almost up to speed. The fuse is therefore selected on a basis of locked-rotor current and starting time. For ordinary starting duty, for example, individual machine tool drives, it is generally satisfactory to choose a fuse which, from its time-current characteristic, will carry 110 per cent of locked-rotor current for 12 seconds.

Where reduced voltage starting is used, a fuse of lower current rating is suitable. It is necessary to bear in mind that with some methods of transition, transient currents when changing to the run position of the controller may for the first cycle or so be considerably higher than if the full voltage were switched direct on to the stationary motor. It is therefore inadvisable to use a fuse of less rating than about 70 per cent of that used for direct starting.

2. Apparatus with which the transient is complete in a very few cycles (for example capacitors and tungsten lamps) or reduced to a low value in a few cycles (for example transformers). Since during the short periods of time in question, loss of heat from the fuse elements is very small, selection may be made on the basis of the maximum i^2t value of the current inrush for the apparatus.

This value must be less by a safe margin than the $(i^2t)_m$ value for the fuse.

Co-ordination with Other Interrupters

Fuses for Backup Protection. Where the fuse is to be used for backup protection of another device of less interrupting capacity, it is necessary that the time-current characteristics shall intersect at the required take-over value. Two important cases will be considered.

The first case is motor controllers. Here the take-over point is well defined, since the controller is designed to take care of the maximum current which can occur in normal service, namely the locked-rotor current. The fuse should have such a rating that it operates only on currents higher than this; it thus serves solely to protect the cables and apparatus against electric faults.

Figure 4 shows typical time-current characteristics of a fuse and of a thermal overload relay in the controller, A being the take-over point. Ideally, the overcurrent relay should be matched to the whole of the motor heating characteristic from currents slightly more than full load up to locked-rotor current, in order that the motor may have adequate thermal protection. It is difficult in practice to achieve sufficiently long time lag in the relay, particularly if of the ordinary inexpensive type and it is frequently considered sufficient if the minimum setting is say 115 to 125 per cent of full-load current and if there is sufficient delay with locked-rotor current to avoid risk of a trip when starting.

If the relay is matched to the motor in the way just given and if the fuse is matched to the motor as recommended in item 1 under the section entitled "Ability to Withstand Initial Overcurrents," then correct co-ordination between fuse and relay will be obtained, as shown in Figure 4. It will be seen that the controller is relieved of interrupting currents greater than its rating. For this optimum protection to be obtained, it is necessary that each motor should have its own set of fuses.

The HRC fuse has an advantage in the steepness of its time-current characteristic in the neighborhood of the take-over point; accurate co-ordination is obtained because the curves do not intersect at a very acute angle.

This method of using fuses has the important advantage that since overloads on the motor can be dealt with only by the overcurrent relays, the risk of these overloads causing single-phasing by blowing one fuse of a 3-phase group is avoided.

The second case is backing-up of circuit breakers of inadequate interrupting capacity. This use of HRC fuses is chiefly for cases where the growth of system fault kilovolt-amperes has rendered existing circuit breakers inadequate. It may also be applied in new installations where for economic reasons, it is desired to avoid the cost of a full-rated breaker.

The requirements are similar to those for protection of controllers, except that usually selection is not based on transient overcurrents, such as occur in individual motor circuits. If, however, there is any particular value of overcurrent expected to occur frequently in normal working, a check should be made with the time-current characteristic of the fuse to ensure that there is no risk of its being blown under these conditions. On the whole, the choice of fuse is dictated by the necessity for the take-over point to be within the interrupting rating of the circuit breaker. The take-over point is usually higher in proportion to normal load than with controllers on account of the higher interrupting capacity of circuit breakers.

Discrimination Between Fuses. Where discrimination is required between HRC fuses in series such that faults on the load side of branch circuit fuses shall not blow main fuses, conditions are quite different. In factory distribution, the use of HRC fuses, not only in the circuits of individual motors, but also in main feeders, presents considerable advantages, since a fault on a motor does not shut down any healthy circuits. Unless an elaborate "unit" system of protection is used, similar discrimination cannot be obtained with series-connected circuit breakers having instantaneous trips; graded time lags are necessary and have the disadvantage that the fault is left on the system for an excessive time.

The conditions governing the grading of HRC fuses will now be considered.

It is first necessary that the time-current characteristic of any fuse A must lie throughout its length to the left of that of any fuse B nearer to the point of supply. Discrimination can be predicted in this way only when the arcing time of fuse A is small compared with its total interrupting time. On heavy faults the arcing time (though much shorter than with noncurrent-limiting fuses) becomes a considerable proportion of the total interrupting time and a comparison of melting time curves is no longer of value. For discrimination to be obtained under these conditions, the current must reach its peak value and be reduced to zero by the "minor" fuse before the melting point of the elements of the "major" fuse is attained. This does not mean that the melting time for the major fuse need exceed the total interrupting time of the minor fuse. Referring to Figure 5, the fault is initiated at A and the minor fuse cuts off at B, the current than falling during the arcing period till it reaches zero at C. If the minor fuse had not been in the circuit, the current in the major fuse would have increased until cutoff occurred at D. The time AE for this to take place is seen to be less than the total interrupting time AC of the minor fuse. Nevertheless, discrimination does occur. The criterion is that the $(i^2t)_m$ value for the major fuse shall exceed the $(i^2t)_t$ value for the minor fuse. Comparison of the shaded areas in Figure 5 shows that this condition was satisfied in the case considered.

Discrimination can thus be predicted if the various i^2t values are known, and a method of presenting this information is given in the last section of this paper. Arcing times depend not only on available fault current, but also on voltage, power factor or time constant, and for a-c circuits on the fault closing angle. It is impracticable to test fuses for a complete range of all these varying conditions and consequently information regarding $(i^2t)_a$ cannot have very high accuracy. Nevertheless, the method already outlined gives much better results than a comparison merely of times.

Where discrimination is required between fuses on the high-voltage and low-voltage sides of a transformer, whereby the high-voltage fuse must operate only for internal faults in the transformer, the same method is applicable if due allowance is made for the transformation ratio of the transformer.

Discrimination is impaired if, when the fault occurs, the major fuse has been carrying load and so is warm, and the minor fuse is cold. It is possible to estimate the amount of impairment with a fair degree of accuracy for any specified value of preloading of the two fuses. The procedure is to calculate, first, the temperature rise of the hottest parts of the elements of the two fuses, and second, the reduction in the $(i^2t)_m$ and $(i^2t)_a$ values for the fuses consequent on the preloading. As a rough general guide for the nearly extreme case of the minor fuse being on no load and the major fuse on full load when the fault occurs, it is suggested that the rating of the major fuse should be increased by 25 per cent.

Current Limitation

The current-limiting property of the uses gives very valuable protection to

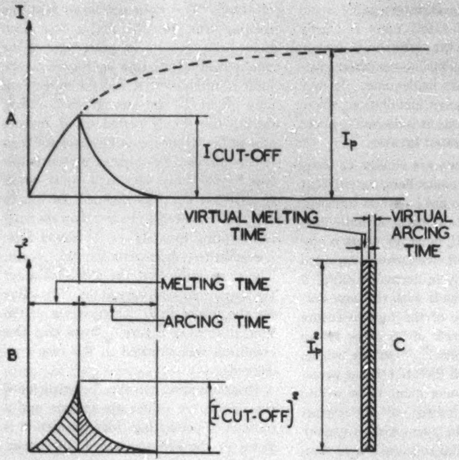

Figure 6. Virtual time

A. Current-time relationships
B and C. (Current)^2-time relationships

all the components of the circuit against the destructive effects of short circuits. As seen in Figure 3, HRC fuses, particularly if of small or medium current rating, limit the current to a small fraction of the available value. Since the electromagnetic forces and the rate of heating are proportional to the square of the current, stresses are usually reduced to values which all equipment can readily withstand. This can be checked by comparing values, as supplied by the fuse manufacturer, of $(i^2t)_t$ and of cutoff current with corresponding withstand values for the equipment. Current limitation also greatly reduces both damage at the point where the short circuit takes place, and general disturbance to the system.

The mechanical stress set up in equipment as a result of a single pulse of current fed through a fuse is in general not the same as that set up by a steady current equal to the cutoff current. The two values would only be the same if the equipment were completely rigid mechanically. In practice, stress does not appear until deflection has occurred, and the maximum stress with a fuse in circuit is considerably reduced when there is appreciable "give" in the parts of the equipment. There is thus a margin of safety in comparing cutoff currents with known maximum withstand currents for equipment.

In motor circuits, components which are particularly vulnerable to short circuits are contactor contacts, overcurrent relays (whether thermal or magnetic) and multiturn current transformers. Also cables, if of small section, may be melted or have their insulation damaged or may suffer severe damage from electromagnetic effects. Investigations in high-power testing stations have confirmed that when the appropriate HRC fuses for direct-starting motor duty are included in the circuit, normal types of contactor and switch can safely be closed on a fault of very high kilovolt-amperage provided that the contacts are ordinarily robust. In the preceding, it is assumed that each motor circuit is separately protected by fuses.

For back-up protection of circuit breakers, the fuses will be so selected (see the section entitled "Fuses for Backup Protection") that the breaker will not have to interrupt faults above its rating. In order to check its ability also to make on faults, it is well to compare the cutoff current of the proposed fuse with the value of current which the breaker is known to be able to make, bearing in mind the safety margin mentioned.

Summary of Advantages of HRC Low-Voltage Fuses Compared with "Code" Fuses

1. High interrupting capacity. Code fuses are tested at only 10,000 amperes and this only with direct current; it is known that the interrupting capacity of some of these is considerably less with alternating current. It should be noted that large fault current is frequently associated with small values of normal current.
2. Very high speed on heavy faults.
3. Very pronounced current limitation.
4. Low voltage-surge on circuit interruption.
5. Accurate and consistent performance.
6. Freedom from deterioration. Correctly selected fuses thus only blow when required, to do so, the renewals are therefore few.
7. Accurate co-ordination with overcurrent trips and with other HRC fuses.

These advantages are such as to allow fuses to be used in many situations where circuit breakers were previously considered necessary.

A Comparison of HRC Fuses with Circuit Breakers

1. In low current ratings, the fuses have a higher interrupting capacity than is commercially practicable with circuit breakers.
2. With fuses, small current rating implies correspondingly small interrupting times and let-through values, so that the conductors of the circuit are adequately protected. With circuit breakers, there is no appreciable current limitation, nor (in general) are they faster in the smaller sizes. Consequently, in the smaller current circuits, there is great risk of conductors being burnt out before interruption of heavy faults is completed.
3. Where the fuses are used as backup for motor controllers, it is usually easier to obtain precise "take-over" from the overcurrent relays on heavy short circuit, than when circuit breakers are used as backup.
4. Lower cost of fuses.

Standardization

The Trend of Standardization

The earlier standards in the various countries usually specified the following:

1. Voltage rating(s).
2. Current ratings.
3. Temperature rise.
4. Fusing current at long times and (some standards only) at shorter times of the order of minutes or seconds.
5. Interrupting tests with direct current of a specified, fairly low, value. No time constant was specified.
6. Dimensions (some standards only).

Various national standards have now extended their requirements in some of the following ways:

1. With the recognition that d-c and a-c performances may be widely different, interrupting tests on alternating current, usually at fairly high values, have been introduced.
2. Methods of preparing time-current characteristics are specified, the basis being either prospective (available) current or the rms value of the actual current.
3. Current-limiting characteristics are called for.

4. For specialised applications, requirements regarding discrimination between fuses have been introduced.

PROPOSED METHOD OF PREPARING TIME-CURRENT CHARACTERISTICS

The quantities mentioned in the preceding section are those which are necessary in applying the fuses, with the exception that no existing standard, so far as the author knows, yet covers the presentation of information regarding the let-through characteristics of the fuse, that is, i^2t values. In addition, present methods of preparing time-current characteristics involved ambiguity for times less than about 0.1 second. Shorter values of melting time depend not only on current but also on rate of rise of current, and this fact must be taken into account in interpreting the characteristics.

The first method of plotting the characteristics (time-available current) has the drawback that the shape of the curve varies with the degree of asymmetry of the short circuit, and the user naturally does not know the phase instant at which a fault will occur. Melting and arcing times can both be shown, but the curves can give no direct indication of i^2t values.

The second method (time-actual rms current) has the drawback that the user does not know the value of the rms actual current, but only the available current. The value of $(i^2t)_m$ can be taken easily from any point on that part of the melting characteristic which has a slope of 2/1. Although arcing times can be shown, this involves ambiguity and these times cannot be used to determine $(i^2t)_a$ since for any particular operation of a fuse the rms value of current in the arcing period can differ considerably, up or down, from the current in the melting period.

These difficulties are overcome by a method proposed by Dr. I. Herlitz, which has now been endorsed by the International Electrotechnical Commission. The proposal is to plot "virtual time" against prospective, that is, available current. Virtual time is equal to $(i^2t)/I_p^2$, where I_p is the prospective current and i^2t can be applied to the melting, arcing, or total interrupting periods. Consider for example the total interrupting period. The virtual total interrupting time (much shorter than the true time if there is considerable current limitation) is the time for which a steady current numerically equal to the full I_p value would have to flow to produce the same heating effect in the circuit as is actually produced. This is illustrated in Figure 6, showing conditions in a d-c circuit. The cross-hatched areas in (C) are equal to the correspondingly cross-hatched areas in (B).

Melting time-actual rms current characteristics are, for all practical purposes, coincident with virtual melting time-prospective current curves drawn to the same scale of amperes and seconds and may be used as such. Both coincide with those which would be obtained by plotting actual current against actual time if the fuse operated in a d-c circuit of zero inductance.

Values of $(i^2t)_t$ can easily be read from the curves for calculation of the heating effect of the let-through current on the circuit components. If virtual time curves for two fuses in series are plotted on the same sheet, comparison of the curve of total interrupting time for the minor fuse with the melting time curve for the major fuse will show immediately whether discrimination between the two fuses is likely.

References

1. THE HIGH-RUPTURING-CAPACITY CARTRIDGE FUSE, WITH SPECIAL REFERENCE TO SHORT-CIRCUIT PERFORMANCE, J. W. Gibson. *Journal*, Institution of Electrical Engineers (London, England), volume 88, part II, February 1941, pages 2–40.

2. PERFORMANCE CRITERIA FOR CURRENT LIMITING POWER FUSES—I AND II, C. L. Schuck, E. W. Boehne. *AIEE Transactions*, volume 65, 1946, pages 1028–45; discussion, pages 1191–94.

3. ELECTRIC FUSES (book), H. W. Baxter. Edward Arnold and Company, London, England, 1950.

4. A NEW HIGH INTERRUPTING CAPACITY LOW-VOLTAGE POWER FUSE, C. L. Schuck. *AIEE Transactions*, volume 69, 1950, pages 770–76.

◆

Discussion

J. C. Lebens (Bussmann Manufacturing Company, St. Louis, Mo.): Mr. Gibson's paper was most interesting and presented a viewpoint slightly different from that of the protection engineers in the United States.

I think the author's proposed method of preparing time-current characteristics using prospective current and virtual time is most excellent and deserves serious consideration. In fact, our company already has adopted its use and finds that it greatly clarifies the picture. It not only has been of help in making co-ordination studies but it has given the user, not thoroughly versed in the mechanics of circuit interruption, a better conception of what he can expect under fault conditions in his circuit.

To our way of thinking the concept of prospective current and virtual time is necessary to represent the time-current characteristics over the entire range of fuse operation from the low overloads to heavy short circuits. If the concept is not used, instantaneous values of peak current must be employed at times less than .01 second and rms values of current for the longer times. Hence, a single curve cannot be used to show the relationship between time and current over the entire range without using virtual time and prospective current.

In discussing the principles governing fuse application, the author is thinking in terms of obtaining only short circuit protection with the fuse. This is in agreement with the English practice. However, in the United States, where dual element fuses are used extensively, over-load as well as short-circuit protection is considered a function of the fuse.

Since the author recommends reducing the physical size of the fuse giving only short-circuit protection to something less than the dimensions specified by the National Electrical Code the results are the same. In the author's system he recommends protecting the cables and apparatus against short circuit with a smaller fuse having high rupturing capacity and using separate thermal overload relays to protect against overloads.

Dual-element fuses combine the short-circuiting fuse and the thermal overload device in a standard fuse enclosure as specified in the National Electrical Code. This permits the use of standard equipment and still gives the fast clearing and current-limiting action under short circuit as well as protection at the lower overloads. Hence, from a fundamental consideration, the results are the same but the relative costs of the two approaches heavily favors the use of the dual-element fuse.

P. C. Jacobs, Jr. (The Chase-Shawmut Company, Newburyport, Mass.): Mr. Gibson's paper is an excellent presentation of the advantages and the principle of application of current-limiting fuses.

This paper is of particular interest, since the Chase-Shawmut Company has for the past 10 years been engaged in the development of high-interrupting-capacity current-limiting-type fuses known as the Amp-trap.

Our development has followed a more or less parallel course to that in England. However, since the current limiting fuses developed here are designed to meet the conditions of American practice, there are some significant differences in characteristics between the American and the English current limiting fuses described by Mr. Gibson.

In the first place, our National Electric Code provides a workable system for overcurrent protection and standards for the the characteristics of current protective devices in the overload range. These operating characteristics are quite different from the British standards.

Many of us believe that the National Electric Code could be expanded to provide workable rules for effective short-circuit protection. However, experience over a period of many years has shown that the existing code is valuable, and devices developed for application on American systems should be consistent with the provisions of the code and should be capable of being applied using the application rules given in the code.

As a result, the American current-limiting fuses have low overcurrent characteristics, such that an operating time of approximately 10 minutes is obtained at a current of 1.5 times rating. The English current limiting type fuses have an operating time of approximately 10 minutes at currents of about 2 times rating.

The difference in the low overcurrent operating characteristic of the American and British high-interrupting-capacity fuses is not great and could be adjusted by a change in the current ratings. There is a much larger and much more important difference in the current-limiting characteristics of the two types. Since the reason for a large difference in the current limiting characteristics of American and English fuses may not be obvious, we would like to explain the method by which these characteristics have been established.

Mr. Gibson has carefully explained the reasons for obtaining current-limiting action and the manner in which the cutoff or let-through current of the device controls the magnetic and thermal stress that is imposed on the electrical equipment protected by current-limiting fuses.

In general, the American Amp-trap has been developed by starting with low current or overload characteristics that conform to the National Electric Code and adjusting the current-limiting or cutoff characteristics to meet the capabilities of the equipment that the high-interrupting capacity fuses would be required to protect when installed according to the Code rules. This has resulted in three classes of Amp-traps with differing degrees of current-limiting action.

As Mr. Gibson has explained, current limiting is obtained only at high available current and there is a minimum available current at which current limiting starts. At available currents higher than this minimum the actual cutoff or let-through current of the fuse varies as approximately the cube root of the instantaneous peak available current. The minimum available current at which the current-limiting action starts is a convenient measure of high current performance of current-limiting fuses.

The British fuses described by Mr. Gibson start to limit at currents of approximately 38 times rating. The corresponding class of Amp-trap, which is furnished in ratings up to 600 amperes inclusive, becomes current limiting at about 18 to 20 times rating.

It is believed that the necessity for having American current-limiting-type fuses with a lower cutoff current than the British equivalent is caused by the very high load density encountered in American distribution systems. This has brought about extremely low system reactances and as a result it is becoming quite common to find that where it is desirable and convenient to connect a load distribution panel or a motor control center into a system there will be an available short-circuit current that will range from 50,000 to 100,000 rms amperes. The greater part of the load distribution equipment and the motor control equipment is for small ampere loads which requires a high degree of current limiting in the backup protective device.

We also have the tendency on American distribution systems to lump or group together load distribution circuits and control, so that the backup protective device on the feeder has to have a relatively large continuous current rating and a still higher degree of current limiting.

To meet the requirements of industrial distribution systems at 480 and 240 volts, a second class of Amp-traps has been developed. This development covers current ratings ranging from 800 amperes to 3,000 amperes with current limiting starting at approximately 12 times the current rating.

The problem of 208-volt distribution systems in large downtown buildings is similar but even more severe. This has brought about the development of a third class of Amp-trap having continuous current ratings up to 5,000 amperes, with current-limiting action starting at approximately five times rating.

Mr. Gibson has brought out that the HRC current-limiting fuses are nondeteriorating. It is obvious that it is meant that the fuses are constructed of materials that will not deteriorate in strength during service and the fusible elements will not be damaged by surge loading. This is important as it is well known that some of our National Electric Code fuses will deteriorate in strength when subjected to adverse conditions in service. Likewise, it was a recognized fault of some of the earlier high-capacity fuses that the fusible elements could be damaged by surge loading. In many cases damage characteristics showing the safe limits of surge loading have been published for such fuses.

In the American development of high-interrupting-capacity low-voltage fuses it was possible to benefit by this known experience. The strongest insulating materials known are used to make the strength of the structure far greater than the minimum requirements. Not only will the structure not deteriorate under adverse service conditions but will not be damaged by accidental mishandling. It was found that damage characteristics could be eliminated by proper design and nondeteriorating fusible elements have been used from the start.

J. W. Gibson: Mr. Lebens is to be congratulated on combining extreme values of time lag on overload with high interrupting capacity in one fuse. Whether or not this results in a cheaper solution to the motor protection problem than a combination of fuses for short-circuit protection with relays for overload protection surely depends largely on the frequency with which overloads occur. If such frequency is appreciable, the cost of replacements of the necessarily somewhat expensive dual-element fuse more than outweighs the first cost of the relay equipment, bearing in mind that in either case contactors are required; further, with the fuse/relay combination, supply can be restored immediately after operation on overload. In addition, the fuse/relay combination greatly reduces the risk of damage by single phasing, particularly if the fuses are fitted with striker pins for opening the contactor when any one of the three blows.

Mr. Jacobs makes a plea for obtaining close overload protection by using a fuse having low "fusing-factor" (ratio of asymptotic fusing current to rated current). British experience over the years has on the whole been that more fuses blow when not required than do not blow when preferably they should; this is in spite of the use of fuses with a somewhat higher fusing-factor (usually about 1.6) than is permitted in the United States. In addition, the use of such values of fusing-factor minimizes trouble by long-time overheating of fuse contacts and the like.

Mr. Jacobs urges the use of fuses with extremely low cut-off values. My own view is that even normally low cut-offs result in i^2t values so greatly less than with circuit breakers as to be perfectly acceptable. British practice is to take frequent advantage of the discriminative properties and low cost of HRC fuses by using them both in main and branch circuits of a system. I do not quite understand Mr. Jacobs' references to the ratio of current at which limitation begins to current rating, for which he quotes a figure of 38 for British fuses. An analysis shows that this ratio is not constant but for any particular type of fuse construction is approximately proportional to the cube root of the fuse rating. This is borne out by Figure 3 of the paper, where for example a 200-ampere fuse has a ratio of approximately 13.

An Axle-Driven Alternator-Rectifier System for Caboose Power Supply

A. H. HOFFER
ASSOCIATE MEMBER AIEE

G. W. WEBER
NONMEMBER AIEE

Synopsis: The application of 2-way telephone communication to moving railroad trains has created a need for a dependable power supply for railway cabooses. A study of the system requirements indicated an axle-driven alternator-rectifier equipment to be better suited to this application than the conventional d-c generator. A 3–5-kw alternator system has been developed, paying particular attention to the requirements of this service and to the fact that the equipment must operate over long periods without attention.

System Requirements and Limitations

THE PRIME requisite of a caboose power supply is reliability with a bare minimum of maintenance. Unlike the railway passenger car, the caboose receives a minimum of electrical attention and the periodic overhaul may not occur at stated intervals. For this reason the maintenance requirements of its electric system must be extremely low. This stipulation strongly discourages the use of a small engine-generator set with its need for regular fuel, lubrication, and coolant servicing. The alternative type of power supply system is the axle-driven generator with a large storage battery.

The system must provide full output over a very wide speed range. While it is expected that a large part of the operation will be at low speeds, as in drag freight service, one operator has specified a range from 10 to 90 miles per hour.

A third requirement is that the control be fully automatic. The generator must be self-excited and must build up at a speed below 8 miles per hour. The system must include both current limit and voltage control features to protect the battery and the charging equipment. At standstill the parasitic power drain from the battery must be very small to prevent discharging during long layovers.

General Description

The axle-driven alternator-rectifier system shown in Figure 1, with its schematic wiring diagram shown in Figure 2, includes the following components:

1. Axle-driven alternator (Figure 3).
2. Gear drive and centrifugal clutch (Figure 4).
3. Selenium rectifiers—power and control (Figure 5).
4. Rectifier fan.
5. Voltage control relay (Figure 6).
6. Current limit relay (Figure 6).
7. Line contactor (Figure 6).
8. 300-ampere-hour 32-volt battery.

The equipment, when applied to a caboose, is rated to produce a d-c output of 80 amperes. The voltage may be preset between 36 and 45 volts, over a speed range from 10 to 90 miles per hour. It may also be applied to other equipment on which a small power supply may be required, such as work-train, baggage, express, and railway postal cars. Depending on the speed range, the output may be as high as 125 amperes, still regulated at a preset value between 36 and 45 volts, shown in Table I.

Reliability is the keynote of the design. This is evidenced by the choice of a totally enclosed alternator with a gear-type drive and a relatively large 300-ampere-hour, 32-volt battery.

Operation

The alternator is mounted under the caboose, see Figure 4, and driven from the axle by an outboard-type double-reduction gear unit with a 5.28-to-1 gear ratio. A splined propeller shaft with universal joints provides for the movement of the truck relative to the car body. When the axle drive reaches a predetermined speed, somewhat below the voltage cut-in speed of the alternator, the centrifugal clutch engages and connects the gear drive to the alternator.

With the small residual flux in the alternator fixed by design, the system constants are such that the alternator voltage will build up at some speed below 430 rpm (8 miles per hour with 5.28 gear ratio and 33-inch wheels). A selenium rectifier in series with the rectifier fan isolates the fan from the field circuit during build-up. This permits the use of a common field and fan rectifier with no appreciable decrease in the build-up speed. As the voltage builds up, the rectifier fan starts and the line contactor closes, actuated by the fan motor current. When the rectified voltage exceeds the voltage of the battery, direct current begins to flow to the battery and its connected load. When the rectified voltage tends to exceed the desired charging voltage, the voltage control relay begins reducing the alternator field current by opening its normally closed contact intermittently, thus inserting resistance in the field circuit. A further reduction of field current to essentially zero is possible when the normally open contacts begin short-circuiting the field intermittently. The current relay acts in an exactly similar manner when the desired maximum load current is exceeded, reducing voltage to hold constant current. Note that when the current limit relay reduces the voltage to a value less than the setting of the voltage control relay, the latter is inactive and the former has complete control. Capacitors *C1* and *C2*, and resistor *R4* form an arc-suppression circuit for the contacts of both relays. Voltage adjustment over the range required by 32 volt-lead acid or nickel alkaline batteries is done by means of adjustable resistor *R3*.

When the train slows down and the alternator speed falls, a point is reached where the alternator can no longer hold full voltage. The load current falls to zero when the rectified voltage falls below the battery voltage, and reverse current is blocked by the rectifiers. When the voltage of the control rectifier reaches a very low value, the line contactor will disconnect the battery and its load from the system. The rectifier fan will also stop. The primary function of the line contactor is to remove the rectifier leakage and the voltage relay coil loads from the battery while the equipment is idle. In case of fan failure resulting from a locked rotor, the fan fuse will blow, de-energizing the line contactor coil. Similarly, any failure that opens this circuit will also deenergize the line contactor coil. Thus the rectifiers are protected against damage by fan failure for any cause.

A 3-phase full-wave bridge of selenium rectifiers is used to provide high efficiency and a low a-c ripple in the d-c output. Six 40-ampere time-delay fuses protect the individual branches of the bridge. This provides closer, faster protection for both

---

Paper 53-78, recommended by the AIEE Land Transportation Committee and approved by the AIEE Committee on Technical Operations for presentation at the AIEE Winter General Meeting, New York, N. Y., January 19–23, 1953. Manuscript submitted October 20, 1952; made available for printing December 8, 1952.

A. H. Hoffer and G. W. Weber are with the General Electric Company, Erie, Pa.

PENNSYLVANIA
478110

Figure 1. Sample axle-driven alternator mounted under a caboose

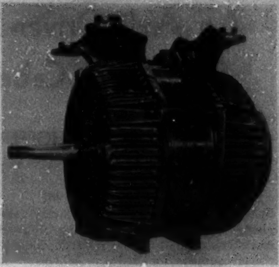

Figure 3. Exterior of alternator

the a-c and d-c circuits than would be possible with a single fuse of larger size. The selenium rectifier stacks have a special vapor-resistant coating to reduce damage from moisture and corrosive vapors.

Comparison of the Alternator-Rectifier and D-C Generator Systems

For the purpose of evaluating these two systems, the alternator-rectifier system will be compared to a typical d-c machine, also totally enclosed and capable of performing the same service.

The fundamental difference between the alternator and the d-c generator lies in the location of the power windings and rectifying devices. From this stems many of the advantages that the alternator enjoys.

BRUSHES

The d-c machine has its power windings located in the rotating armature, necessitating a commutator and a high-current-collecting brush rigging with a multiplicity of brushes. These introduce high friction and contact losses as well as high brush maintenance. The a-c machine has its power windings located in the stator, and only a small exciting current need be carried to slip rings by the brushes. The brush drop loss at full load is reduced from 176 to 3 watts, and the brush friction loss at maximum speed is reduced from 350 to 16 watts.

POWER CONVERSION

The d-c machine rectifies its power from alternating to direct current by its commutator. The ability of a machine to commutate well depends, to a great measure, on the reactance voltage per bar. This voltage varies directly with the speed, the load current, the number of poles, and the number of commutator bars. It also varies with the square of the number of turns per armature coil. As the full output speed range of a d-c machine is widened, it becomes increasingly more difficult to obtain good commutation and long brush life at the high-speed end of the range.

The a-c machine has its power rectified externally, and hence has no commutator. Therefore, it requires no space for a commutator and no extra surface area to dissipate comutator losses. Also, since it has no speed limitation imposed by difficulties in obtaining good commutation, the a-c machine can be made considerably smaller and lighter than its d-c counterpart.

COMPARTMENTATION

In a totally enclosed d-c machine, air from the main body of the machine must be blown over the commutator to keep it cool. This air becomes contaminated with carbon dust, some of which is deposited on the insulating surfaces of the machine. This results in reduced creepage resistance and the danger of dielectric breakdown.

In the alternator the slip-ring losses are low, allowing the rings and brushes to be isolated in a separate chamber. Thus the carbon dust, which, incidentally, is far less with slip rings than with commutators, can be kept away from all the windings.

FIELD WINDINGS

The alternator is simple in construction and operation. It has only one field coil which excites all of the pairs of poles in parallel. It requires no series, differential or commutating field windings, such as may be required by the d-c machine.

STABILITY

A d-c machine is considered unstable if at any speed its excitation requirements decrease for an increase in load. As the speed range increases, it becomes pro-

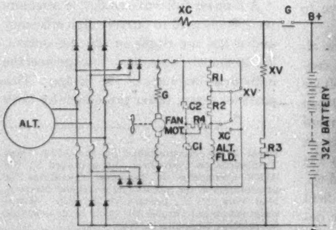

Figure 2. Schematic diagram

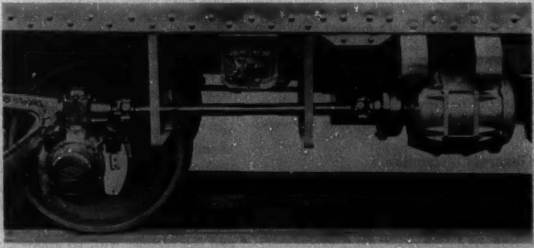

Figure 4. Closeup of caboose installation showing gear drive, centrifugal clutch, and sample alternator

Figure 5. Selenium rectifier group

gressively more difficult to design a stable d-c machine.

The alternator-rectifier system, on the other hand, is inherently stable at all speeds and can produce full output over an extreme range of load and speed without the need of stabilizing windings.

CONTROL FEATURES

The control for an alternator-rectifier system is inherently simpler than that for a d-c generator. Since the alternator output is alternating current, no polarity reversing switch is required. Furthermore, the valve action of the rectifiers prevents the flow of reverse current, thus eliminating the usual reverse current relay.

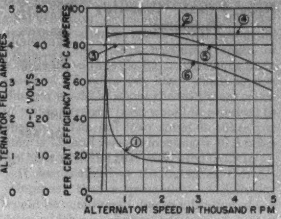

Figure 7. System performance curves

1. Field amperes
2. Direct voltage
3. D-C load amperes
4. Rectifier efficiency
5. Alternator efficiency
6. System efficiency

Another potential advantage of the a-c system lies in the fact that the presence of an a-c power supply makes possible the development of a completely static regulator and the elimination of all contact-making devices. However, the system now in use, as shown in Figures 2 and 6, employs the vibrating-type voltage and current relays.

INITIAL COST

The maximum speed-range at full load establishes the size and cost of the system. The combination of the a-c machine with its external rectifier is comparable in cost to the d-c machine alone. Moreover, since the field current requirements of an a-c machine are less than that of its d-c counterpart, a less expensive regulator can be used.

SYSTEM EFFICIENCY

The over-all efficiency of the alternator-rectifier system at the low speeds which generally characterize freight service is greater than that of the d-c generator system. Table II compares the losses in the two systems, and Figure 7 shows how the a-c system efficiency varies with speed. In the middle of the speed range the efficiencies of the two systems are almost identical. At extremely high speeds the efficiency of the a-c system is slightly less than that of the d-c system. However, operation at these high speeds is rare.

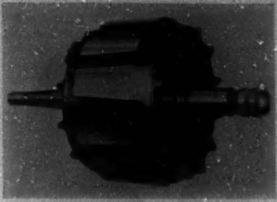

Figure 8. Rotor assembled on shaft

Alternator Design

This alternator is a 12-pole 3.2-kw machine with a speed range of 537 to 5,070 rpm and a frequency range of 53.7 to 507 cycles. Its simplicity stems from the design of its rotor, shown in Figure 8. This is assembled by pressing two similar 6-legged castings onto the ends of a prewound rotor sleeve which, in turn, is pressed onto a shaft. The twelve tapered field poles are essentially fixed cantilevers, very sturdy in construction and offering high resistance to centrifugal forces. The rotor magnetic circuit was especially designed to require very little exciting power. This minimized the size and cost of the regulator. Since all the pairs of poles are excited in parallel by a single field coil, the alternator requires much less field power than does the d-c machine. As previously indicated, care was taken in choosing the magnetic materials for the rotor, to provide just the right amount of residual flux to make the machine build up at low speeds, and yet not provide an overvoltage at no-load and high speed.

The leads of the single field coil are brought out through shallow slots in the shaft to the slip ring assembly which is housed in a separate brush-holder compartment. The slip ring assembly consists of two brass rings molded in open resin. The rings are presprayed with molten copper to increase their surface

Table I. Alternator-Rectifier System Performance*

	Gear Ratio			
	2.54	3.09	3.44	5.28
Rated d-c output, amperes	125	125	125	80
Rated d-c output, volts	40	40	40	40
Maximum regulated d-c output, volts	45	45	45	45
Wheel diameter, inches (maximum)	36	36	36	33
Wheel diameter, inches (minimum)	33	33	33	31.5
Maximum permissible speed, miles per hour	135	111	100	90
Minimum continuous speed, miles per hour	30	25	22	10
Minimum full-load cut-in speed, miles per hour, 25 degrees centigrade	25	21	18	9.5
Minimum voltage cut-in speed, miles per hour, 32 volts d-c, no load	18	15	14	8

* These ratings are obtained from a single alternator. Rectifier size and capacity increase with the full-load current rating.

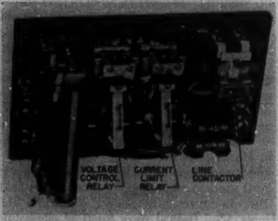

Figure 6. Control panel

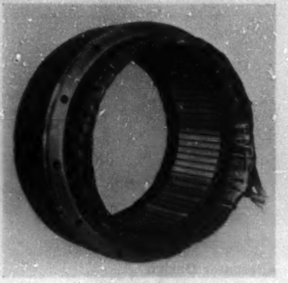

Figure 9 (left). Completely wound stator

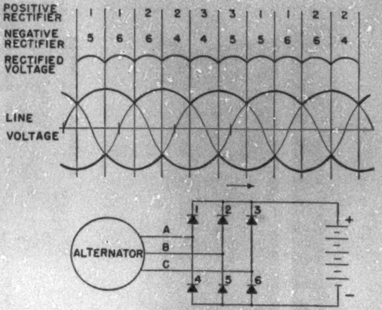

Figure 10 (right). Sequence diagram for 3-phase full-wave bridge rectifier

hardness and decrease their friction and contact drop. Two brushes, at right angles, ride each ring to provide positive current collection and prevent arcing at the rings. Each brush is 2 inches long, and the wear rate is extremely low. Each of the four brush holders is securely bolted to integrally cast framehead studs to prevent misalignment. Field tests indicate that a set of rings and brushes may last for many years so that need for brush maintenance is reduced almost to the vanishing point.

In designing the stator, Figure 9, for this machine, 72 slots were chosen since this yields a large number of voltage and current combinations should it be desired to rewind the machine to supply a different voltage system. The high number of slots also minimizes the stator leakage reactance and the load loss. The stator windings are wye-connected to give the lowest cut-in speed for the alternator and to prevent circulating currents. Class *B* insulation is used throughout.

This machine was designed with a large air gap to minimize the load loss in the solid pole faces which varies inversely as the square of the air-gap length.

The line current wave form of an alternator loading into rectifiers is not the same as that for one loading into a balanced resistive load. When a sine wave alternator loads into a balanced resistive load, the current wave form is identical with and in phase with the impressed voltage wave form. In an alternator loading into a 3-phase full-wave bridge of rectifiers, the current at any instant flows only in the phase which is most positive and the phase which is most negative while no current flows in the third phase, see Figure 10. Every 60 electrical degrees, or six times every cycle, one rectifier stops conducting and another starts. Every time a rectifier cuts in, a transient oscillation appears in the line current (Figure 11) whose time constant is determined by the inductance, capacitance, and resistance of the circuit. The amplitude of these transients increases directly with load and speed. The rectifiers can handle them easily, but the air gap of the alternator must be made large to limit the load loss introduced. The solid poles act as amortisseur windings to damp out these transients and minimize their effect.

The over-all dimensions of the alternator are: height $20^{7}/_{16}$ inches, width 21 inches, and length 24 inches. The complete machine weighs 408 pounds.

Long experience in the design of railway equipment has proved the totally enclosed design to be the most satisfactory, hence it was used on this equipment. The machine is completely sealed with neoprene gaskets to keep out dirt and moisture. For better cooling, its nonmagnetic aluminum frameheads are ribbed inside and out, as shown in Figure 3. Fan blades, cast integral with each end of the rotor, see Figure 8, circulate air through the stator and windings and return it to be cooled against the framehead ribs.

The machine is fitted with two similar heavy-duty prelubricated ball bearings. Here again, ease of assembly and disassembly was kept in mind. The slip-ring end bearing pulls off over the slip rings without disturbing them. The outer race of the drive end bearing is securely clamped, while a special anticreep device prevents the outer race of the slipring end bearing from rotating, yet allows it axial freedom to compensate for thermal expansion of the rotor.

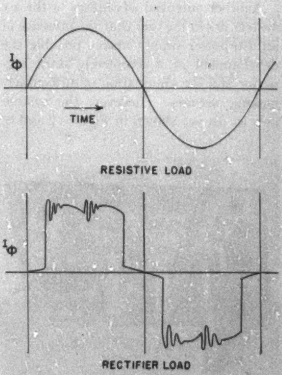

Figure 11. Typical wave forms of alternator phase current with resistive and rectifier loads

Table II. Comparison of Typical A-C and D-C System Losses

Based on Net Output of 80 Amperes at 40 Volts D-C at 10 Miles Per Hour

Item	Alternating Current, Watts	Direct Current, Watts
Brush contact drop loss	3	176
Brush friction loss	2	40
Windage loss	4	3
Armature copper loss	350	356
Field copper loss	48	442
Commutating pole copper loss	0	146
No-load core loss	101	21
Load loss	40	18
Rectifier and fan loss	720	0
Reverse current relay loss	0	15
Regulator loss	64	360
Total	1,332	1,577
Efficiency	70.6 per cent	67.0 per cent

The alternator is hung under the side of the caboose and is isolated from body vibration by four rubber mounts.

Conclusion

A sample equipment of similar design has been operating successfully on a major railroad for over a year. Additional equipments are currently being supplied. Some of the outstanding features of this new system are high reliability, over-all simplicity, low maintenance, low initial cost, small size, light weight, extreme speed range and versatility.

References

1. Selenium Rectifiers in Motor Vehicle Power Systems, **Glen Ramsey.** *AIEE Transactions*, volume 68, part I, pages 149–53.

2. Very High Frequency Radio Communications in Train Operation, **F. H. Menagh, A. E. Jones.** *Electrical Engineering* (New York, N. Y.), volume 71, April 1952, pages 312–17.

3. An A-C Vehicle Generating System, **Albert D. Gilchrist.** *Electrical Engineering* (New York, N. Y.), volume 66, August 1947, pages 779–80.

Discussion

W. S. H. Hamilton (New York Central Railroad, New York, N. Y.): This paper is very interesting in that it shows one solution of a very difficult problem. It is noted that the authors passed over the mechanical drive for the generator attached to the end of the axle very quickly. I wish to comment on that first, as it has been one of the most difficult developmental projects which I have participated in, over many years of experience with rolling stock equipment.

During World War II, the New York Central made a survey of possible postwar needs and determined that an axle-driven generator for supplying power for radios and cabooses would probably be one of the requirements of the post-war period.

After studying the various problems involved, including operation around sharp curves, we came to the conclusion that a drive mounted on the end of the axle and through a vertical propeller shaft driving a vertical generator mounted inside the car approximately above the axle would be the simplest method of solving the problem, particularly as operation around 100-foot-radius curves is involved. Accordingly in March 1945, the development of such a drive and the designing of a 2-kw 40-volt d-c vertical generator to go with it was undertaken.

While drives taken from the end of the axle are fairly common in Europe, they had not been used in the United States up until that time; neither so far as I know has a vertical drive and a vertical generator been used elsewhere to date.

At that time (1945) the requirements of the manufacturers of radio equipment were that all radio equipment must operate from 117 volts, 60 cycles, alternating current. When the necessary conversion losses were included, this meant that a 2-kw generator was necessary. This proved to be a very good generator, developing 2 kw at 650 rpm and having a cut-in speed of 500 rpm at 32 volts. It also has a maximum speed of 4,200 rpm to provide for a maximum train speed of 75 miles per hour which it was thought would be about the maximum speed at which a freight train would be required to operate. The full load speed in miles per hour is 12, and the cut-in speed is 10.5 miles per hour with the gear ratio used (5.28 to 1).

It was realized at the outset of this development that a great deal of difficulty would be enountered due to vibration of the drive which on cabooses has to be mounted on the truck side frame. Also the problem was complicated by it being necessary to open up the drive in order to have access to the waste for repacking and oiling. Accordingly, the drive was arranged with two handles with cams and springs to hold it in place and still allow it to be swung open to provide access to the waste without disconnecting the propeller shaft. A short horizontal drive shaft having square rounded ends was provided between the end of the axle and the drive proper (a construction which is quite commonly used in driving speed recorders, especially in Europe).

One of these drives was installed on a caboose on January 8, 1947, and has operated on the same caboose most of the time since then. This particular division is a relatively slow speed division with a maximum speed limit on freight trains of 35 miles per hour.

Difficulties were encountered with breakage of the horizontal drive shaft due apparently to torsional shocks; also a great deal of difficulty was encountered in keeping the handles closed and they finally had to be replaced by bolts.

The vertical generator behaved very well and is still in service. Trial applications of this drive were made also to two passenger baggage cars in 1947, one of them being equipped with the same safety vertical generator and the other with a 2-kw inductor alternator, further mention of which will be made later.

The results of all these test applications indicated to us by the middle of 1948 that for successful operation in service of this nature on nonroller bearing boxes, a drive of this type must be:

1. Rigidly bolted to the truck side frame or journal box.
2. Have access doors for packing and oiling the waste.

Accordingly the development of this drive with these features in mind was continued, and in April 1950, a wooden model of the proposed drive with access doors was made up for for the pupose of showing to those responsible on the railroad for the maintenance of journal boxes, the space provided for working on the waste. These access doors are shown clearly in Figure 4 of the paper.

The cabooses were equipped with this drive in August 1951 for service in the western part of New York State but were not actually used for about a year.

By this time (1951) the requirements of the radio equipment manufacturers had changed and they were willing to design radio equipments which would operate from 12 volts, d-c, instead of 110 volts, a-c. This in turn reduced the power necessary so that a 1-kw generator was large enough for the purpose.

Accordingly a Leece-Neville type *5184G6* a-c generator with rectifiers, which rates 75 amperes at 14 volts was selected. On account of the small size of the armature, no clutch was provided between the generator and the propeller shaft. The rectifiers are installed in a locker above the generator which has ventilating holes from the inside of the caboose near the bottom of the locker, the whole locker being ventilated by a $3^{1}/_{2}$-inch globe ventilator installed above the roof of the caboose. In this way, it was possible to avoid using a fan for forced cooling of the rectifiers. The Leece-Neville equipment also includes their type of vibrating voltage regulator actuated by the direct voltage, which maintains constant voltage above a certain speed and also has a current limit relay to limit the output of the generator.

These two cabooses have been in active service since August 1952 and have run approximately 18,000 miles each to January 1, 1953.

The only difficulty encountered has been wear of the spline teeth in the spline bushing in the axle and on the end of the horizontal driving shaft which connects to the drive proper. It has been necessary to use a hardened steel bushing in the axle and to provide a lubricating fitting for introducing lubricant at the inner end of the shaft spline teeth in order to reduce the wear. This lubricating fitting looks as though it were successful and had overcome the last major obstacle in the application of these drives.

We are also trying out for the effect of an accelerated life test, one of these drives with 3.70-to-1 gear ratio on a passenger baggage car driving the same safety vertical generator that was originally installed on the car in 1947. This has been running now since November 1952 and has run approximately 6,000 miles to January 1, 1953. With the lubricating fitting for the spline teeth previously mentioned, the operation seems to be satisfactory.

We also have in service 5 baggage cars with 1.5-kw safety d-c generators hung under the car body at the outside, very similar to Figure 4 of the paper except that the drive shaft comes up at an angle directly from the drive housing itself, instead of from a supplementary gearbox mounted on top of the drive proper. These drives are mounted on roller bearings so that the problems have been very much easier than on nonroller bearings, and very good success has been obtained with them since their installation in 1950 and 1951.

During the tests in 1947–1948, a 2-kw, 3-phase inductor alternator with rectifiers, arranged to give a d-c output of 50 amperes at 40 volts was tested. This was much the same as the generator shown in the authors' paper, except that it was vertically mounted, and being of the inductor type, had no slip rings. The frequency varied from 125 cycles per second at 750 rpm to 761 cycles per second at 4,600 rpm, the maximum speed. A blower was used for cooling the rectifiers.

It was in service for about a year but had to be abandoned due to dirt causing the rectifier plates to arc over. It was, however, a very interesting application.

The idea of an inductor alternator for small size generators such as 1 kw or 2 kw, is attractive in eliminating even the collector rings which are present in the design shown in the authors' paper. While the efficiency is lower than that of a machine with a revolving field, the absence of all connections to the rotor makes it attractive under the conditions present on baggage cars and cabooses, and it is hoped that some day this development will be taken up again. It is necessary with such a generator to supply a small amount of current from the battery when the car is at rest in order to insure building up of the generator voltage as the car begins to move; but in order to prevent undue battery discharge, this circuit can be interrupted by a pressure-operated switch connected to the brake pipe on the car, so that when the car is standing, with no air pressure or air pressure below that required to properly operate the brakes on the train, this small field current drain is cut off.

It would be interesting also if some one would explore the possibilities of building a generator of larger capacity than 5 kw, utilizing the alternator principle, either of the inductor or field-excited type, with rectifiers, to see how it would compare in cost and weight with the conventional 20- and 30-kw motor-generator sets now used on main line passenger cars. Such an alternator would immediately have the advantage of eliminating the induction motor now required for stand-by operation, as the stand-by power could be fed into the rectifiers direct. Also the rectifiers could be mounted underneath the car and blown with relatively clean air obtained from within the car body, as it is necessary to remove a certain amount of air from the car interior anyway for proper operation of the air conditioning system.

Such a generator would also eliminate the commutator and pole changer of the present d-c generator, do away with their maintenance and other troubles experienced in service due to dirt.

A. H. Hoffer and G. W. Weber: The authors wish to thank W. S. H. Hamilton for his interesting history of the development of the gear drive. Also of interest was his review of the various types of machines—especially the inductor-type alternator—which have been investigated in the field as sources of power supply to cabooses.

Before designing the rotating-field alternator, the inductor-type alternator was carefully considered and finally rejected. Although it had no slip rings, it was heavier, larger, and more expensive than the rotating-field-type machine. Moreover, it was estimated that the maintenance costs associated with a successful brush-and-slip-ring combination would be so low that the inductor-type construction could not be justified. Reports from field tests to date have supported this prediction.

Larger capacity alternator-rectifier systems are presently being studied. The high cost of rectifiers limits the ability of these larger systems to compete with conventional d-c machines. The advantage of eliminating the induction motor is questionable since it introduces the need for a step-down transformer, for some means of regulating the widely variable wayside-power voltage, and for providing a current limit. The downward trend in rectifier cost and size per kilowatt may, however, soon tip the economic balance in favor of the alternator-rectifier system.

Electric Transmission with Diesel Locomotives

P. A. McGEE
MEMBER AIEE

THE FIRST diesel locomotive, I understand, employed direct side rod drive, somewhat similar to steam power. As might be expected, this transmission of diesel power was not found satisfactory.

The Transmission Problem

A simple analysis of the problems involved in transmitting the torque of a diesel engine to the rims of a locomotive wheel will show the necessity of employing some type of torque converter between the diesel engine and the driving wheels.

As a simple specification, it may be stated that an efficient locomotive unit should be capable of accelerating its train, using tractive forces up to the limit of its adhesion. Throughout its operating speed range, the locomotive should deliver its rated horsepower.

Such a locomotive unit gives a constant horsepower characteristic which will be referred to later.

Since a diesel engine develops practically a constant torque over its operating speed range, it must operate at its maximum rated speed to develop its rated output. In order, therefore, to obtain the full available rated horsepower for accelerating purposes and over the operating speed range of the train, it becomes necessary to have a torque converter between the diesel power plant and the driving wheels.

The commercially developed torque converters available are as follows:

1. Electric power transmission considered in this paper.
2. Straight mechanical gear shift drive as commonly employed with relatively small power units in highway and to a lesser extent in rail transportation.
3. Hydraulic torque converter as extensively employed in certain highway and earth working services. This drive is also employed to a limited extent in rail service in this country and is employed and proposed for extensive rail services in Europe and other countries.
4. Combination of hydraulic and straight mechanical converters used in services outlined in items 2 and 3.

Diesel locomotives for class one railroads in this country normally employ minimum axle loads of 55,000 pounds. Under favorable rail conditions, starting tractive efforts of 16,000 pounds per axle may be developed with this load.

With a 4-driving-axle unit this gives a total tractive effort of 64,000 pounds and with a 6-driving-axle unit a total tractive effort of 96,000 pounds, which power is generally delivered from one power plant.

When units are operated in multiple, to obtain say a 4,500-horsepower passenger locomotive with eight driving axles or a 6,000-horsepower freight locomotive with sixteen driving axles, starting tractive efforts of the order of 128,000 pounds and 256,000 pounds respectively are encountered.

The mechanical problems in transmitting this large tractive power from a limited number of power plants is not simple. The efficient control of these forces is actually the design problem of a diesel locomotive.

Early History of Diesel Power Transmission

The first practical application of internal combustion power to revenue traffic in this country was probably the McKeen

---

Paper 53-69, recommended by the AIEE Land Transportation Committee and approved by the AIEE Committee on Technical Operations for presentation at the AIEE Winter General Meeting, New York, N. Y., January 19–23, 1953. Manuscript submitted October 24, 1952; made available for printing December 3, 1952.

P. A. McGee is a consulting engineer in New York, N. Y.

The following manufacturers have my sincere thanks for the typical wiring diagrams and locomotive charactesistic curves supplied and employed in this paper: The American Locomotive Company of The General Electric Company, Baldwin-Lima-Hamilton Corporation, Westinghouse Electric Corporation, The Electro-Motive Division of General Motors Corporation, and Fairbanks, Morse and Company. Unfortunately, it was not possible to include all the data and curves submitted.

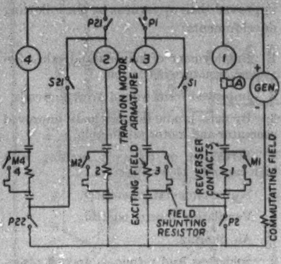
P21
P1
4
2
3
1
GEN
S21
S1
A
TRACTION MOTOR ARMATURE
M4
M2
M1
EXCITING FIELD
REVERSER CONTACTS
FIELD SHUNTING RESISTOR
COMMUTATING FIELD
P22
P2

CONNECTIONS	CONTACTORS CLOSED S1	P1	P2	S21	P21	P22	M1	M2	M3	M4
SER. PAR. FS1	●			●						
SER. PAR. FS2	●			●			●	●	●	●
PARALLEL FS1		●	●		●	●				
PARALLEL FS2		●	●		●	●	●	●	●	●

Figure 1. Schematic diagram 4-motor power and exciter circuits

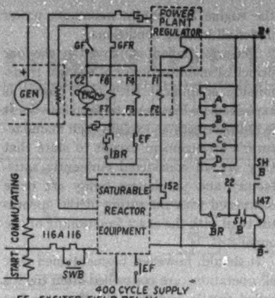
POWER PLANT REGULATOR
B+
GF
GFR
GEN
F6
F4
F1
F7
F3
F2
C2
IBR
EF
A
B
C
D
SH B
22
147
SATURABLE REACTOR EQUIPMENT
152
COMMUTATING
START
116A 116
SWB
BR
B-
EF
400 CYCLE SUPPLY

EF EXCITER FIELD RELAY
GF GENERATOR FIELD CONTACTOR
GFR FIELD DISCHARGE RESISTOR
BR BRAKING RELAY
SWB BRAKING SWITCH
A,B,C,D SEQUENCE RELAYS
147 BRAKING POTENTIOMETER
116 TEMPERATURE COMPENSATING RESISTOR
SH} CONTACT ON CONTROLLER, CLOSED WHEN
B} SELECTOR HANDLE IS IN BRAKING ZONE

car employed around 1910. This car employed a gas engine with straight mechanical gear shift clutch drive and possessed many advantages over a steam locomotive or steam propelled rail car for branch line services. The gear shift and clutch, however, were not found satisfactory and an electric transmission with a manually controlled generator field switch, which apparently was beyond the understanding of the available steam trained crews was developed.

As a result of these difficulties, the development of internal combustion rail motive power languished until after World War I.

With the general increase in crew wages and materials at the end of World War I, railroad management became branch line conscious and a receptive market became available for simple motor car units. In 1924 the classic transmission control which, in one form or another, is now employed in practically all types of diesel-electric transmissions was developed.

Needless to say, many refinements have been added since 1924 and today we can choose the product of many manufacturers for diesel-electric control which automatically develops the diesel power available for traction purposes without any hazard of overloading or stalling the diesel engine.

Modern Diesel-Electric Transmission

The basic elements of an electric transmission consist of the following:

1. A d-c normal 600-volt electric generator generally direct coupled to the diesel engine.
2. Series-wound d-c traction motors generally axle-hung, similar to street car motor suspension, with a simple gear connection to the driving axles.
3. An auxiliary generator set or sets employed to excite the main generator and supply battery charging or other auxiliaries. These are generally direct or belt driven.
4. Blowers for engine water cooling, motor cooling either direct driven or driven from auxiliary generator.
5. Compressors for air brake and control supply either direct or belt or auxiliary generator driven.
6. Main control switches for traction motor control, reverser, field taps, and motor combinations.
7. Starter control from battery to main generator.

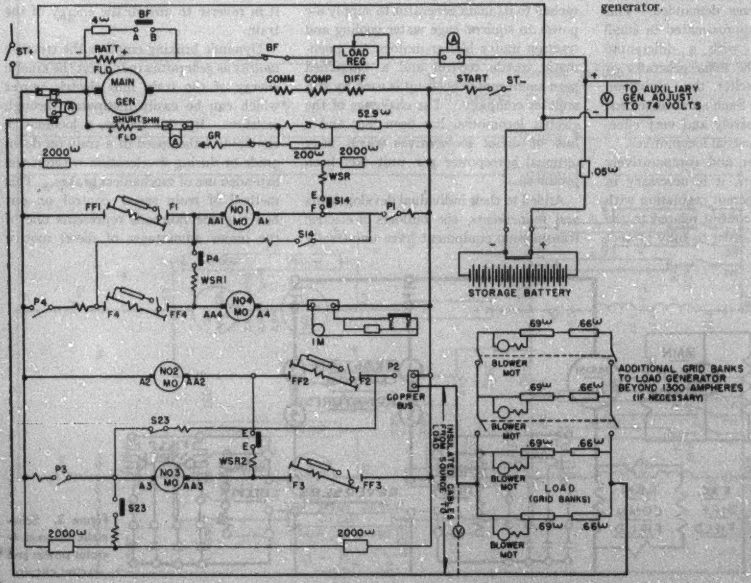
ST+
4ω
BF
A
B
BATT
FLD
BF
LOAD REG
A
MAIN GEN
COMM
COMP
DIFF
START
ST-
TO AUXILIARY GEN ADJUST TO 74 VOLTS
V
SHUNT FLD
SHN
A
GR
52.9ω
2000ω
200ω
2000ω
WSR
E
F
S14
.05ω
FF1
F1
NO1 MO
AA1
A1
P1
S14
P4
WSR1
P4
F4
FF4
AA4
NO4 MO
A4
STORAGE BATTERY
IM
.69ω
.66ω
BLOWER MOT
NO2 MO
A2
AA2
FF2
F2
P2
COPPER BUS
ADDITIONAL GRID BANKS TO LOAD GENERATOR BEYOND 1300 AMPHERES (IF NECESSARY)
S23
E
E
WSR2
INSULATED CABLES FROM LOAD SOURCE TO
P3
NO3 MO
A3
AA3
F3
FF3
LOAD (GRID BANKS)
S23
2000ω
2000ω
V

Figure 2. Schematic diagram 4-motor power and exciter circuits arranged for load test

8. Load regulator generally receiving its impulse from the engine governor and controlling generator field or exciter field, to regulate the generator output.

9. Control switches operated from throttle control to engine governor, generally giving eight engine speed positions.

10. Control switches to fuel pumps, air compressors, blowers, and auxiliary generators and control and lighting circuits.

11. Relays controlling automatic functions of motor transitions, field taps. Reverse current and ground relays, and relays controlling dynamic brake when employed.

12. Temperature and speed indicators with warning signals.

13. Reverser, master control, and throttle control at operator's position.

14. Necessary load indicators, speed indicators, and air gauges with auxiliary control switches located conveniently at operator's position.

Many articles have been written decribing in detail the functioning of various manufacturers' diesel-electric transmission. They all contain the basic elements just outlined with certain variations.[1–10]

The objective of all these transmissions is to give automatically a generator output up to the normal rating of the diesel engine, at all engine speeds and under all train loading conditions.

This characteristic of the generator may be expressed as a constant volt-ampere output or a voltage in inverse ratio to the amperes demanded. This condition can be approximated in small output generators with a differential field winding on the main generator or on the auxiliary exciter, thus giving inherent regulation. Such an arrangement is employed extensively and very effectively on small industrial locomotives.

With road power and comparatively large size generators, it is necessary to supplement this inherent regulation with some type of load control related to the engine governor, in order to fully protect the engine and obtain maximum power under all loading conditions.

The arrangement employed by the four principal manufacturers of electric transmission equipment with road power, is explained in Figures 1 to 4 inclusive. It is not necessary to explain each manufacturer's arrangement except to state that they are all considered eminently satisfactory and purchasers today are more concerned with the rating of the apparatus than with the exact functioning of the apparatus.

It should, however, be mentioned that all operations are controlled from the so-called trottle and that the operator has simply to notch out from notch 1 to notch 8 at a rate depending upon his load meter to put his train in motion up to its maximum speed. All motor transitions, field taps, and engine regulation may be completely automatic and from his load meter the operator knows the heating load on his motors and the extent to which his transmission load exceeds or is below the continuous rating of the motors and generator.

Many interesting refinements have been incorporated in the most recent equipments. One company now employs an amplidyne exciter scheme which, with tuned frequency relays for forward and reverse transition, supplies the optimum in power output control. Another company employs an a-c alternator attached to its main generator to supply a-c power to squirrel-cage water cooling and traction motor blower motors. A pneumatic trottle control and a simplified permanent motor hook-up is used by still another company. The challenge of the electric locomotive has been met and a line of diesel locomotives which have optional horsepower per unit has been produced.

Added to their individual developments and refinements, the builders of electric transmission equipment have universally improved their apparatus by the following developments:

1. Employment of silicone and other improved armature insulation.

2. Improved form wound armature coils.

3. By mass production methods, improved generator and motor production.

4. Perfection of dynamic braking with high-capacity blown resistors.

5. Water temperature control.

6. Ventilating shutter control.

7. Air filtering.

8. Solderless lead terminals and oil resisting rubber cable.

9. Locomotive slip relays and control.

10. Apparatus subassembly for convenience in replacement and maintenance.

11. Development of maintenance procedure, to obtain maximum economy and availability.

12. Maintenance kit packages and unit exchange with factory-conditioned parts and units.

It may be definitely stated that electric transmission in its present high degree of development is ideal in its functioning for road, yard, and industrial locomotive services.

Dynamic Braking

One of the unique features of electric transmission is the possibility of working it in reverse to absorb the energy of the train.

Dynamic braking employs the traction motors as generators to convert the kinetic energy of the train into electric power which can be easily dissipated through resistors. By this means, a locomotive can control the speed of a train on down grade or during deceleration without the extended use of mechanical brakes. This method of train speed control on our heavy grade railroads represents one of the major advantages of diesel motive

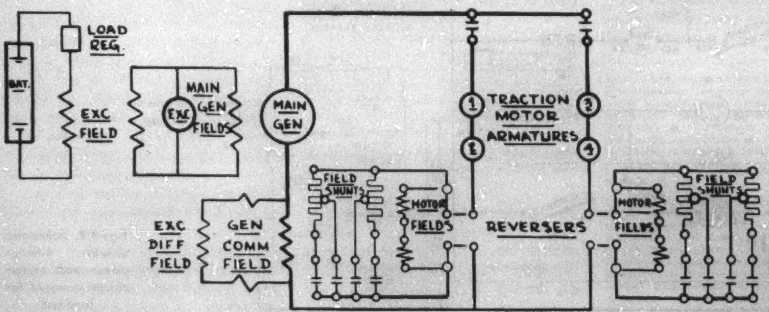

Figure 3. Schematic diagram 4-motor power and exciter circuits

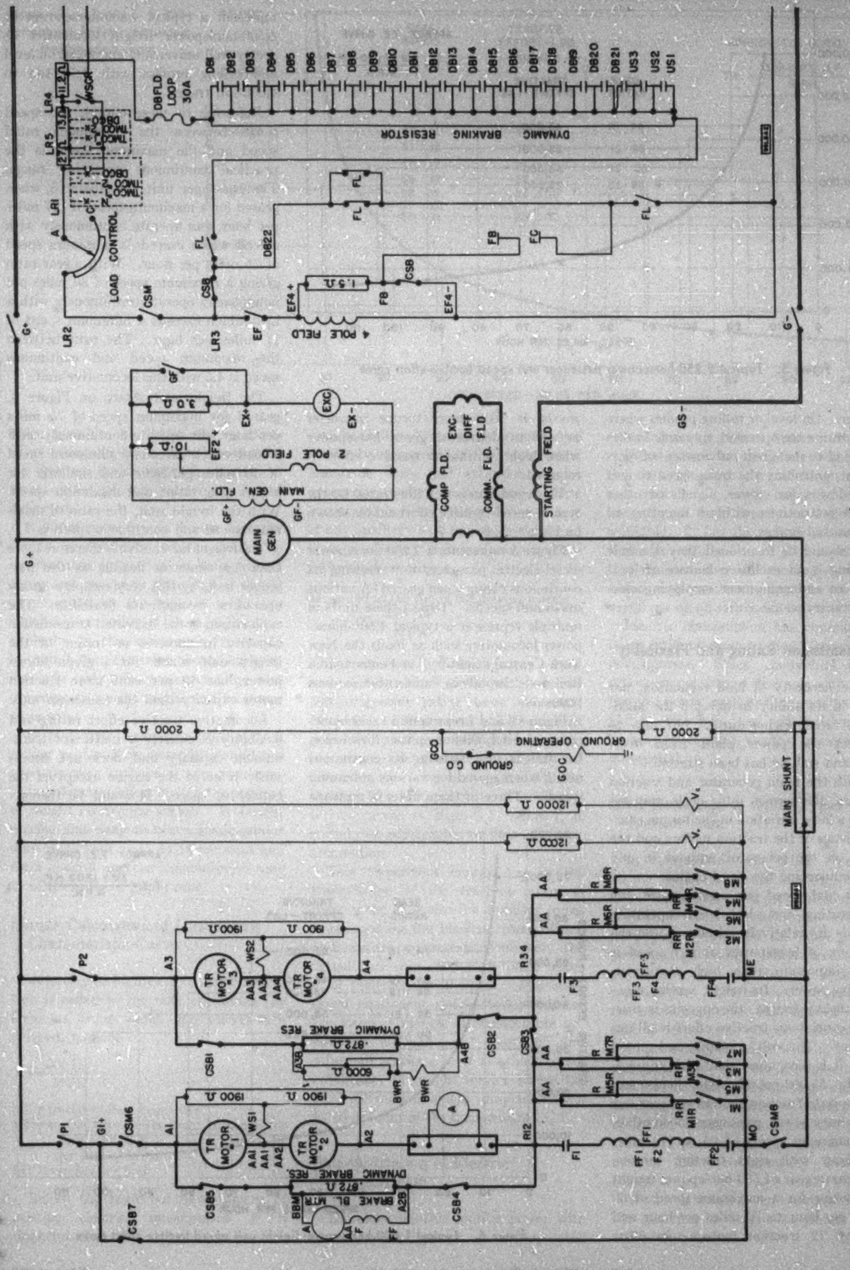
LOAD CONTROL
DBFLD LOOP 30A
DYNAMIC BRAKING RESISTOR
DB1
DB2
DB3
DB4
DB5
DB6
DB7
DB8
DB9
DB10
DB11
DB12
DB13
DB14
DB15
DB16
DB17
DB18
DB19
DB20
DB21
DB22
US1
US2
US3
LR1
LR2
LR3
LR4
LR5
WSCR
TMCO
DBCO
FL
CSB
CSM
EF
G+
G-
GS-
4 POLE FIELD
EF4+
EF4-
FB
FC
1.5 Ω
3.0 Ω
10 Ω
GF
EXC
EX+
EX-
EF2+
2 POLE FIELD
MAIN GEN. FLD.
GF+
GF-
MAIN GEN
COMP FLD.
EXC-DIFF FLD
COMM. FLD.
STARTING FIELD
2000 Ω
GROUND OPERATING
GROUND C.O
GCO
GOC
12000 Ω
MAIN SHUNT
P1
P2
G1+
CSM6
CSM8
TR MOTOR #1
TR MOTOR #2
TR MOTOR #3
TR MOTOR #4
WS1
WS2
A1
A2
A3
A4
AA1
AA2
AA3
AA4
1900 Ω
DYNAMIC BRAKE RES
.872 Ω
6000 Ω
A3B
A4B
BWR
CSB1
CSB2
CSB3
CSB4
CSB5
CSB7
A
R12
R34
F1
F2
F3
F4
FF1
FF2
FF3
FF4
MO
ME
AA
R
RR
M1
M2
M3
M4
M5
M6
M7
M8
M1R
M2R
M3R
M4R
M5R
M6R
M7R
M8R
BRAKE BL. MTR
BBM
A2B
F
FF
V

Figure 4. Schematic diagram 4-motor power and exciter circuits

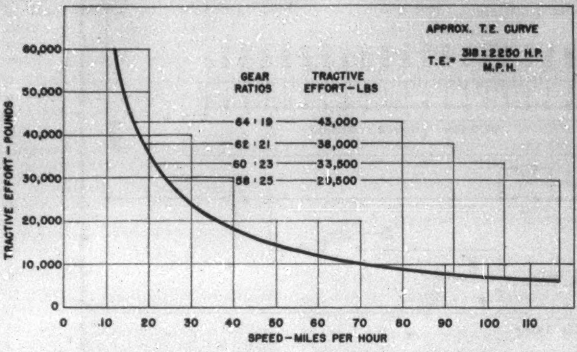

Figure 5. Typical 2,250-horsepower passenger unit speed tractive-effort curve

power. On level or rolling profiles where long trains are operated, dynamic brakes have also the great advantage of normally controlling the train speed to suit slow-downs for curves, signals or other speed restrictions without resorting to mechanical brakes.

It should be mentioned that dynamic braking is an exclusive feature of locomotives and equipment employing electric transmission.

Transmission Rating and Flexibility

The necessity of load regulation, not only in its ability to develop the maximum rated engine output but also to protect the power plant from overload and stalling has been stressed.

With the main generator and traction motors, the service duty cycle may require a large variation in the torque characteristics of the traction motors and the duty on the generator without in any way influencing the diesel engine.

For high-speed passenger service, the accelerating and slow speed operating periods are relatively infrequent and the question of horsepower at high speed is more important than high continuous tractive power. In freight service, especially heavy freight, the opposite is true. High continuous tractive effort is all important. This will be readily understood when it is recognized that with approximately 55,000-pound axle loads and appropriate traction motors we gear our 4,500-horsepower passenger locomotives for maximum speeds of 95 to 110 miles per hour with eight traction motors, whereas we gear a 4,500-horsepower freight locomotive for a maximum speed of 60 miles per hour to 70 miles per hour and employ 12 traction motors. In other words, it takes more torque converter motors to deliver a given horsepower when high continuous tractive effort is required.

This condition is well illustrated by the typical speed-tractive effort curves shown on Figures 5, 6, and 7.

Figure 5 represents a 2,250-horsepower diesel-electric passenger unit showing its continuous rating when geared for various maximum speeds. Two of these units in multiple represent a typical 4,500-horsepower locomotive such as hauls the New York Central "Century" or Pennsylvania Railroad "Broadway" and other famous trains.

Figures 6 and 7 represent a 1,600-horsepower and a 1,500-horsepower diesel-electric freight unit showing its continuous rating when geared for various maximum speeds. Three of these units in multiple represent a typical 4,800-horsepower or 4,500-horsepower freight locomotive as pretty well universally employed on level and rolling profiles with 3,000-ton to 4,000-ton trains.

Referring to these curves, the speed range between the continuous rated speed and the maximum speed is the practical continuous operating range. The passenger unit, see Figure 5, when geared for a maximum speed of 117 miles per hour, can operate continuously with a load which exceeds a minimum speed of 25 miles per hour. With a gear ratio giving a maximum speed of 80 miles per hour, it can operate continuously with a load which exceeds a minimum speed of 17 miles per hour. The ratio between the maximum speed and continuous speed is 4.5 with this locomotive unit.

The freight unit shown on Figure 6, geared for maximum speed of 75 miles per hour, can operate continuously with a load which exceeds a minimum speed of 10 miles per hour and similarly for higher gear ratios and maximum speed. With the freight unit, the ratio of maximum speed and continuous speed is 7.0.

The freight locomotive is therefore more than 1.5 times as flexible as the passenger unit, by this very complete measure of a locomotive's flexibility. The explanation is the increased transmission capacity in amperes or torque of the freight unit which, for a given horsepower, has 40 per cent more traction motor capacity than the passenger unit.

Locomotive tractive effort rating and flexibility is entirely a matter of transmission capacity and does not necessarily refer to the engine except in the matter of speed. It would be theoret-

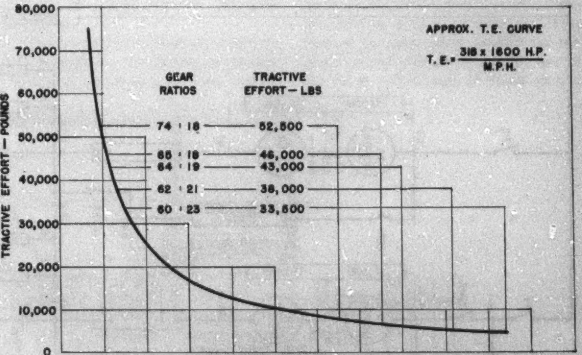

Figure 6. Typical 1,600-horsepower freight unit speed tractive-effort curve

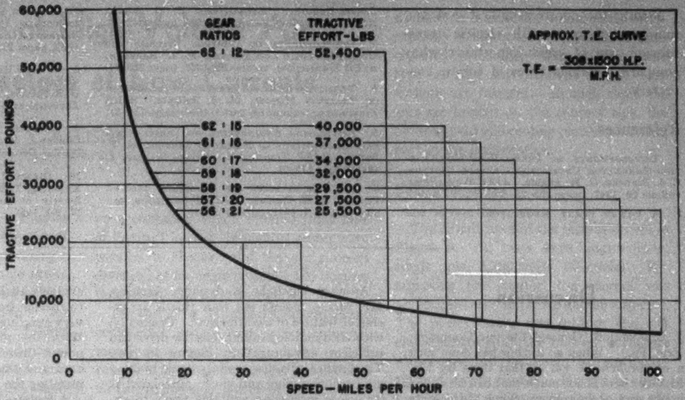

Figure 7. Typical 1,500-horsepower freight unit speed tractive-effort curve

ically possible to obtain the tractive effort rating shown on these curves with one-quarter the horsepower stated on these curves at one-quarter the speed indicated.

It is not necessary to discuss here the degree of flexibility which should be incorporated in any given transmission equipment except to state that it should be governed by the type of service to which a locomotive or car equipment is applied. In this connection, it should be noted that excessive motor capacity not only adds unnecessary cost but also unnecessary weight to the motive power equipment.

In passenger service, operating on a rolling profile, it is generally considered good practice to have a minimum continuous tractive effort of 10 to 12 per cent of weight on driving wheels. In freight service, this value in heavy grade service may be as high as 17 to 18 per cent and for a general purpose locomotive, it may be of the order of 15 per cent.

Simple Calculation of Locomotive Characteristic Curve

Referring to Figures 5, 6, and 7, attention is called to the note explaining the formulas from which the curves are derived, namely

$$TE = \frac{308\,HP}{MPH}$$

TE = tractive effort in pounds
HP = engine horsepower input to generator shaft and 308 is approximately 82 per cent of factor 375
MPH = miles per hour

Before the perfected development of existing electric transmissions, it is doubtful that this approximation with such a perfect continuous output curve would be accepted at its face value. Numerous tests and extensive service experience confirm the accuracy of these curves and indicate that with the release of any auxiliary load for which the diesel plant is adjusted, it immediately appears n the traction output.

Measured at the rim of the driving wheels

$$TE = \frac{375\,HP}{MPH}$$

Generators of 1,500-horsepower output and traction motors of 400-horsepower to 500-horsepower rating have maximum efficiencies of 96 per cent and 92 per cent respectively and over their normal operating range the combined efficiency of generator, motors, and gears will be between 82 and 85 per cent. The characteristic curves in Figures 5, 6, and 7, as stated, are constructed on this efficiency assumption.

This 18-per-cent energy loss in the transmission of the traction power is regrettable, as is also the auxiliary losses occasioned by the blowers, compressors, and control apparatus. However, the actual fuel consumed with these losses is of relatively small value. The additional equipment weight to provide for the losses, although of considerable importance in high-speed passenger and suburban services, is of relatively small importance in freight service where the total locomotive weight may be only 6 to 10 per cent of the train weight.

Standardization of Electric Transmission

Diesel locomotive motive power with electric transmission is now the accepted standard in our United States railroads.

Diesel power has an inherent thermal economy which is far reaching in all countries which must import fuel or have liquid fuel directly or indirectly available. It has the further advantage that when standardized it gives a production, maintenance, and operating economy which may eventually lead to its universal use on all railroads.

Electric transmission has contributed in no small measure to diesel locomotive development. When individual axle drives are considered desirable with large tractive power such as that employed on U.S.A. railroads and when dynamic braking is required, electric transmission is essential.

Brief Reference to Other Types of Transmission

In comparison with other types of torque converters, the electric transmission efficiency of 82 per cent compares favorably with the hydraulic systems developed today. In the small horsepower output range, where mechanical gear shift transmission or hydraulic combinations thereof can be applied, the mechanical drive may have a 5-per-cent to 15-per-cent efficiency advantage.

In the matter of weight with high-speed passenger and rail car equipments, it becomes increasingly necessary with the development of straight mechanical and hydraulic drives to consider the possibility of obtaining lighter electric transmission than commercially available today.

With freight and general purpose power, the question of weight as stated is of small importance.

Finally the question of first cost and maintenance cost, with electric transmission, are of great importance when comparing various types of torque converters.

References

1. Developments in Diesel-Electric Traction-Generator Excitation Control Systems, **C. A. Brancke, G. M. Adams.** *AIEE Transactions,* volume 66, 1947, pages 223–28.

2. A Power Plant Regulating System for Diesel-Electric Locomotives, **C. B. Lewis.** *AIEE Transactions,* volume 66, 1947, pages 242–46.

3. Developments in Control Systems for Diesel-Electric Locomotives, **M. D. Henshaw.** *AIEE Transactions,* volume 66, 1947, pages 233–41.

4. Twenty-Five Years Progress in the Design of Traction Motors, **M. J. Baldwin.** *AIEE Transactions,* volume 68, part I, 1949, pages 132–37.

5. Application Engineering on Diesel-Electric Locomotives in Railroad Service, **G. T. Bevan.** *AIEE Transactions,* volume 68, part I, 1949, pages 125–31.

6. The Renaissance of Electric Motive Power. **A. H. Candee.** *AIEE Transactions,* volume 68, part I, 1949, pages 138–44.

7. Fifteen Years' Progress in the Design of Industrial Diesel-Electric Switchers, **R. W. Barrell.** *AIEE Transactions,* volume 71, part II, 1952, pages 215–19.

8. A 3,000 Horsepower Diesel-Electric Locomotive for the Seaboard Air Line Railway, **D. R. Staples, T. L. Weybrew, C. A. Atwell.** *AIEE Transactions,* volume 66, 1947, pages 215–19.

9. Electric Drives for Locomotives, **A. H. Candee.** *Mechanical Engineering* (New York, N. Y.), December 1950.

10. Diesel Locomotive Bug—Hunters, **E. W. Kettering, T. B. Dilworth, J. M. Norris.** *Journal,* Society of Automotive Engineers (New York, N. Y.), 1952.

Discussion

J. C. Aydelott (General Electric Company, Erie, Pa.): When an author has done such a comprehensive job as that done by Mr. McGee there is not much that can be added in the way of discussion. Some of the facts which the author has mentioned, however, may be highlighted.

The broad problem is to connect something which is moving (the crankshaft of the diesel engine) with something which is standing still (the locomotive and train) to cause the latter to move. This problem is solved beautifully by using an electric generator on the diesel engine and electric traction motors on the locomotive axles. Mr. McGee has touched on the many good points of this system and has done a good job of bringing out the distinctive features offered by the various builders. The fundamental similarities of these locomotive drives, however, far outweigh any differences in detail. It is worth remarking that the locomotive builders in this country are practically unanimous in the selection of electric drive for their locomotives.

About two-thirds of the way through his paper Mr. McGee discusses the ratio of the maximum speed of a locomotive to its continuous speed and illustrates his discussion with a passenger locomotive in which this ratio is 4.5 to 1 and a freight locomotive having the ratio of 7 to 1. Mr. McGee points out that the freight locomotive must have more traction motors to provide this additional "flexibility" in the use of the diesel engine horsepower. This is looking at the picture from the prime mover point of view. The converse statement is also interesting and instructive. The proper amount of electrical material to be used on a locomotive is determined by its weight which limits the tractive effort which it can develop and by the top speed at which the locomotive must run. If the horsepower of such a locomotive is low it will have great flexibility, using Mr. McGee's words. However, it should be noted that as horsepower is increased, the same trains can be handled faster and that this higher horsepower can be accommodated with practically no change in the amount of electrical material required. This is the direction which improvement in future locomotives may be expected to take.

Another highlight is dynamic braking. Mr. McGee points out that this is an exclusive feature of electric drive. Originally, without dynamic braking, electric drive had sufficient advantages to dictate its use. The further advantages of dynamic braking are becoming more and more appreciated as its use is increasing and this tends to entrench electric drive all the more firmly in locomotive application.

One more feature of electric drive which Mr. McGee did not mention is worth noting. Much of the tremendous investment which the railroads have in diesel-electric locomotives can be salvaged if it some day becomes economical to put a trolley wire up over the track. Studies indicate that it is entirely feasible to install conversion apparatus in the cab in place of the diesel engine and its accessories and run the locomotive under a wire. Much of the cab and all the running gear including the traction motors will still be useful.

Mr. McGee has not exaggerated in pointing out the many advantages of electric drive on diesel-electric locomotives.

P. A. McGee: I thank J. C. Aydelott for his remarks and further comments on the advantages of electric transmission.

As stated in my paper, I feel that the manufacturers of electric transmission equipment in the United States are to be congratulated on the developments which give us, from the operating standpoint, an ideal transmission.

In this country with our relatively high axle loads and large tractive effort per locomotive unit, the electric transmission has many advantages and is recognized as our standard transmission.

With light-weight cars and for some special applications, it seems to me that electric transmission will require some weight reduction to compete with recent mechanical drive developments.

Mr. Aydelott refers to my discussion on the ratio between maximum speed and continuous speed. This is of course a vital ratio, more particularly since railroads are now I feel rather overstressing universal or general purpose diesel units.

It is a fact that straight electric locomotives, in their limited and restricted applications to date, have ridiculously small maximum and continuous speed ratios. This explains their inflexibility and assignment to specific freight and passenger duties with very exacting rules on their tonnage ratings. With the universal application of diesel power, these limitations could not be tolerated and the railroads are constantly demanding the so-called foolproof locomotive.

A foolproof locomotive is one with sufficient transmission capacity to permit continuous operation up to the slipping point of the wheels. If speeds in excess of 100 miles per hour are required, the transmission would, with this continuous rating, be unduly heavy and expensive. My paper states the generally accepted continuous ratings with various types of service.

I cannot agree with Mr. Aydelott that by keeping the horsepower low you obtain greater flexibility and that the modern tendency is to increase horsepower with a sacrifice of flexibility.

Railroad operators and even design engineers are very apt to confuse ability to pull and horsepower.

A simple case of such confusion is well illustrated by an incident that occurred a few years ago with a very capable operating vice-president of one of our large systems. The particular railroad had a number of diesel units, the power plants of which were under-rated. By very simple modifications, it was possible to increase the engine horsepower rating by approximately 12 per cent.

With this increase in power, the operating vice-president requested a 12-per-cent tonnage rating increase with these units. It took a lot of explaining to convince this practical railroader that his transmission equipment had not been increased and the additional power could be used only to obtain higher speed.

There is a very large difference between horsepower obtained with increase in speed and horsepower secured through increase in tractive effort. The former is cheaply obtained, the latter is costly and requires larger and better transmission apparatus. Not just a few more engine rpm or an increase in brake mean effective power but an actual increase in thermal rating of the whole transmission apparatus is effected.

This reasoning applies to mechanical and hydraulic just as with electric transmission. The criterion in any comparison of the various types of transmissions must be the relative flexibility or the ratio of maximum to permissible continuous speed.

Arcing Time of High-Voltage Air-Break Contactors at Low Currents

C. A. LISTER
MEMBER AIEE

A HIGH-voltage air-break contactor must be able to interrupt the circuit to motor loads or static loads covering a wide current range. Considerable attention has been given to the ability of contactors to interrupt fault currents, but little has been published on the problem of obtaining satisfactory performance at low currents. The difficulty at low currents is one of getting acceptably short arcing time.

It has been pointed out previously that for low power-factor static loads the arcing time at low currents is relatively long.[1,2] Some tests on motor loads have shown very short arcing time for low currents, and it may be that there is no danger of excessively long times with such loads.[1] However, to make application simple, it is desirable to design a contactor with acceptably short arcing time at low currents, regardless of the type of load, provided, of course, that fault interrupting ability is not sacrificed. This paper considers some of the factors which affect the low current arcing time of high-voltage air-break contactors.

Examination of the interruption process employed in high-voltage air-break contactors will show the reason for the relatively long arcing times at low currents. Figure 1 shows those parts of a typical contactor which are involved in the interruption process. In operation an arc is drawn between contact tips and is forced onto and up arc runners by a transverse magnetic field set up by a series excited blowout. As the arc is forced into contact with cooling plates, it is deionized and extinguished. At low current, the blowout field is weak so that the arc travels at a relatively low velocity and consequently the arcing time is long.

Two factors which affect the arcing times of contactors are evident, the strength of the blowout and the position of the cooling plates. In order to determine the relative importance of these factors, an experimental study was undertaken in which low-current arcing times of static loads were measured using blowout coils having 1 to 32 turns and with the cooling plates placed successively in the five positions shown in Figure 1. A less extensive set of tests was also made on a contactor which differed from that of Figure 1 in that the cooling plates were parallel to the arc and the arc runners diverged at an angle of about 120 degrees throughout the interruption region.

For the 10 to 40 amperes current range considered, arcing time varied approximately as a small negative power, −0.25 to −0.35, of the blowout flux density and as the minus one power of distance between contact tips and cooling plates. Arc velocity measured along the shortest line between tips and cooling plates was constant for a given value of the product "blowout flux density times current" and varied nearly as a small power of this product. Arc velocity along parallel arc runners was higher than along runners which diverged.

When the current to be interrupted was made sufficiently small, a large percentage of interruptions occurred without the arc transferring to the arc runners and with an arcing time of less than 1 cycle. This effect appeared more pronounced at higher tip opening velocity.

While the character of load handled by a contactor is not subject to control by the contactor designer, it is useful to know the effect of the type of load on arcing time. Tests on static loads in which the power factor was varied showed that as the power factor was increased for a fixed and sufficiently small current, the percentage of interruptions which occurred without arc transfer increased; but for those interruptions in which arc transfer did occur the arcing time was independent of the power factor. No motor loads were used in the tests, but it has been pointed out by others that with motor loads, counter electromotive force reduces the recovery voltage across the tips thereby making interruption simpler. It is believed that the fast interruptions of motor loads which have been reported previously[1] were of the same type as the interruptions noted here without arc transfer. In such cases the arcs are broken on the contact tips, the blowout field and cooling plates not taking part in the interruption.

Test Procedure

The circuit used in the tests is shown in Figure 2. All tests were single phase, single pole, 2,300 volts, 60 cycles. By adjusting the reactor, the current was set successively at 11, 20, and 39 amperes. The power factor was 0.15 or less. A coil separate from the blowout structure was connected between the stationary tip and its arc runner. During an interruption, this coil was energized when the arc transferred to the arc runner so that oscillograms of the voltage across this coil and the blowout coil revealed the arc transfer instant as well as the instant of interruption. A simple circuit employing another pole of the contactor was used to indicate the instant of tip separation. Figure 3 is an oscillogram of a typical interruption.

Supplementary tests were made to determine the variation of flux density throughout the region of arcing. As the constant flux density lines of Figure 4 show, the flux density was nearly uniform throughout the interruption region. This uniformity was found to hold over the entire range of blowout strengths used.

Effects of Changes in Blowout Strength and Position of Cooling Plates

In analyzing the interruption tests it is convenient to divide the total arc time into the time for arc transfer and the time to interrupt after transfer. This is desirable because it separates the transfer problem from the interruption problem.

Figure 5 shows a typical set of arcing-time characteristics for the contactor of Figure 1. The "time to interrupt after arc transfer" is plotted against "current" for various numbers of blowout turns and for a single position of the cooling plates. The points shown are average values based on three or more tests taken under identical conditions. These characteristics show plainly the rapid increase of arcing time as the current is decreased. The results of other tests taken at currents below 10 amperes are not plotted. In such tests the arcs were extinguished without transferring to the arc runners and in a total arcing

---

Paper 53-19, recommended by the AIEE Industrial Control Committee and approved by the AIEE Committee on Technical Operations for presentation at the AIEE Winter General Meeting, New York, N. Y., January 19–23, 1953. Manuscript submitted December 5, 1951; made available for printing November 6, 1952.

C. A. Lister is with the Electric Controller and Manufacturing Company, Cleveland, Ohio.

Portions of the experimental data included in this paper were taken from a thesis submitted to Case Institute of Technology in partial fulfillment of the requirements for the degree of Master of Science in Electrical Engineering.

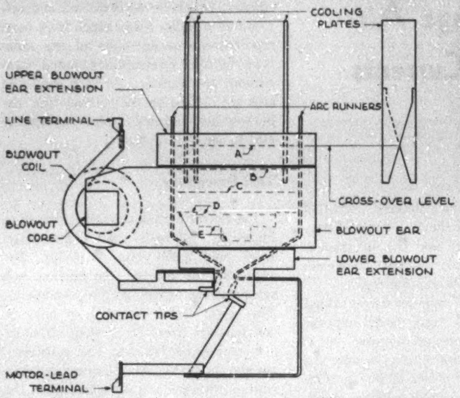
COOLING PLATES
UPPER BLOWOUT EAR EXTENSION
LINE TERMINAL
ARC RUNNERS
BLOWOUT COIL
A
B
C
D
E
CROSS-OVER LEVEL
BLOWOUT CORE
BLOWOUT EAR
LOWER BLOWOUT EAR EXTENSION
CONTACT TIPS
MOTOR-LEAD TERMINAL

Figure 1 (left). Schematic diagram of high-voltage air-break contactor. Dashed lines A-E show cross-over levels for various positions of cooling plates

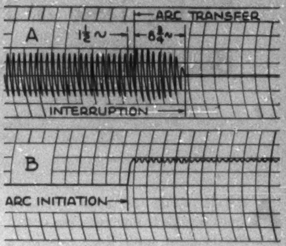

Figure 3. Typical oscillogram of current interruption. Cooling plates position C, 20 amperes rms, 8 blowout turns

A—Voltage across blowout coil and transfer indication coil

B—Voltage across tips of adjacent pole in contact separation circuit

time of less than 1 cycle. This phenomenon will be discussed later.

If the arcing times of Figure 5 are plotted on log-log scales and flux density is used as a parameter instead of the number of blowout turns, the resulting curves are nearly straight parallel lines. Likewise a log-log plot of "arcing time after transfer versus flux density" for several constant values of current yields similar straight parallel times. The lines of these two sets of characteristics have nearly the same slope which shows that the arcing time after transfer varies approximately as the same power of both flux density and current. Therefore, it appears that a single curve "arcing time after transfer versus the product 'blowout flux density times current' " should give with fair accuracy the same essential information as given in the several curves of Figure 5. This was found to be true and in Figure 6 the single curve for cooling plate position *C* gives in different form, the information of the three curves of Figure 5. The other curves of Figure 6 show "arcing-time after transfer versus blowout flux density times current" for two more of the five cooling plate positions used and the time required for the arcs to transfer to the arc runners. The transfer time curve, like the others, is a straight line for practical purposes.

One result observed on certain oscillograms deserves special mention. In the tests where the maximum number of blowout turns was used, the current decreased markedly during the arcing time, the effect being particularly noticeable for the tests at 11 amperes. A current decrease was also noticeable for many of the other tests, but the decrease appeared small enough to neglect. A current decrease would be expected to increase the arcing time for those tests in which it was pronounced and, for the more remote plate positions, the experimental results were in general agreement. A possible explanation for the current attenuation is that velocities were high enough to cause more than normal heat transfer from the arc to the air.

Plainly the time-after-transfer curves of Figure 6 can be expressed very nearly by the equation

$$t_2=K(BI)^{-k} \tag{1}$$

where

t_2 = time between arc transfer and interruption in cycles

B = blowout flux density in lines per square inch taken at a reference point in the arc chute

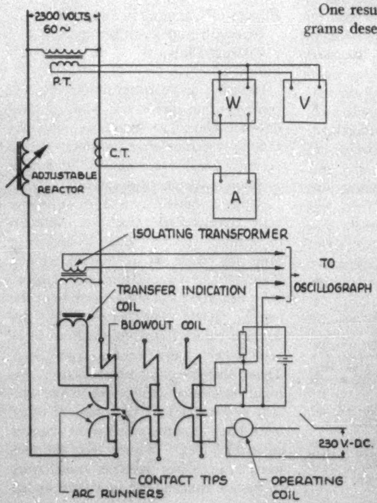
2300 VOLTS 60 ~
P.T.
W
V
C.T.
ADJUSTABLE REACTOR
A
ISOLATING TRANSFORMER
TO OSCILLOGRAPH
TRANSFER INDICATION COIL
BLOWOUT COIL
230 V-DC.
CONTACT TIPS
OPERATING COIL
ARC RUNNERS

Figure 2 (left). Test circuit for interruption tests

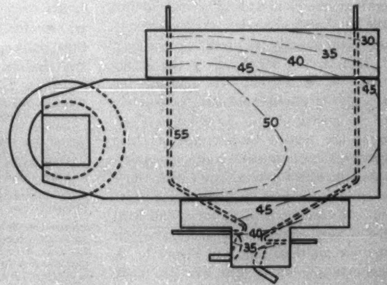
30
35
40
45
45
50
55
45
40
35

Figure 4 (right). Flux distribution midway between blowout ears. Lines of constant flux density are shown. Numbers give peak lines per square inch for 60 rms ampere-turns excitation

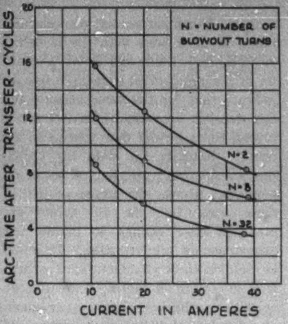

Figure 5. Arc-time after transfer versus current for various numbers of blowout turns

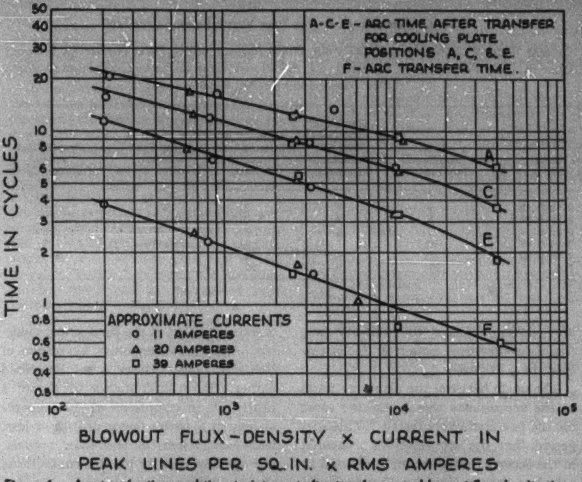

Figure 6. Arc transfer time and time to interrupt after transfer versus blowout flux density times current for various cooling plate positions

I = current in rms amperes
k, K = constants for a fixed position of the cooling plates. k varied in the range 0.24 to 0.32 for different plate positions.

The transfer time curve can be expressed similarly by

$$t_1 = K(BI)^{-k} \qquad (2)$$

where

t_1 = time between the initiation of the arc and its transfer to the arc runner above the stationary contact tip
K = constant
k = 0.37
B and I have the same meaning as in equation (1)

The previous results are useful in estimating average arc velocities. In Figure 7 the arc times after transfer, of Figure 6, are plotted against the distance from the contact tips to the cooling plates for several values of *BI*. Assuming that for a given current and flux density an arc must be driven the same distance into the cooling plate stack for extinction regardless of the location of the stack, the distances between cooling plate locations correspond directly to differences in arc travel, and therefore the inverse slope of the curves of Figure 7 is arc velocity. It is evident from the curves that when the arc is moving between the parallel parts of the arc runners the velocity is constant. If the velocity is plotted against *BI* on log-log scales, a straight line with slope 0.18 results, showing that the velocity varies as *BI* to the 0.18 power, see Figure 8. The average upward velocity of the arc was somewhat lower in the region where the arc runners diverge than in the region where the arc runners are parallel.

When the results for the contactor with arc runners which diverged throughout the interruption region were examined, it was found that they too could be expressed by equation 1. k for this contactor was 0.40 for the transfer time and from 0.33 to 0.36 for the time after transfer depending upon the position of the cooling plates. Again arc velocity was found to be constant for a given value of *BI* and in this case the "time-versus-distance" curves converged to a point near zero distance from the tips, indicating that velocity was constant all along the

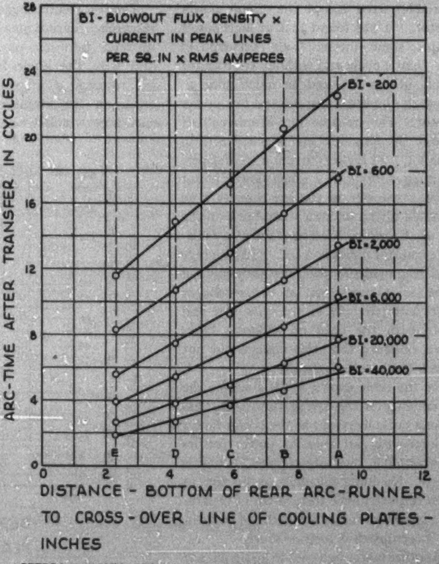

Figure 7. Arc time after transfer versus distance above rear arc runner for various values of blowout flux density times current

LETTERS INDICATE CROSS-LEVEL FOR COOLING PLATE POSITIONS A-E

Table I. Summary of Arcing Time Versus Power-Factor Tests

Current 19.6—21.1 Amperes, 2,300 Volts, Single Phase, Cooling Plates Position C, Blowout Coil—5 Turns Permanently Connected, 24 Additional Turns on Same Core Inserted When Arc Transfers to Rear Arc Runner

Power Factor	Total Number of Interruptions	Number of Interruptions with Arc Transfer to Runners	Number of Interruptions without Arc Transfer	Arcing Time with Arc Transfer, Cycles	Arcing Time without Transfer, Cycles
0.12–0.13	9	7	2	$8-8\frac{1}{4}$	$\frac{3}{4}-1$
0.19–0.20	3	3	0	$7\frac{3}{4}-8$	
0.42–0.44	7	4	3	$7\frac{1}{4}-8\frac{1}{4}$	$\frac{1}{2}-\frac{3}{4}$
0.66–0.67	10	7	3	$7\frac{1}{2}-7\frac{3}{4}$	$\frac{1}{2}-1$
0.88–0.89	30	6	24	$7\frac{3}{4}-8$	$\frac{1}{2}-1$
1.0	27	0	27		$\frac{1}{2}-1$

arc runners. Again the velocity was found to vary as a power of *BI*, in this case the 0.31 power.

The angle between the diverging parts of the arc runners was nearly the same for the two contactors tested. This suggested that the arc velocities measured in the second contactor might be used to calculate the arc time for that region of the Figure 1 contactor in which the arc runners diverged. When such calculations were made, they agreed fairly well with the measured times.

Effect of Power Factor

A group of tests, similar to those previously described, were made with all variables fixed except the circuit power factor. It was found that at high power factor, some interruptions occurred in less than a cycle and without arc transfer while others required as much time as those at the same current and low power factor. The results for a current of about 20 amperes are summarized in Table I. At higher current a greater percentage of tests at a given power factor show a transfer to the arc runners. As is noted in the table, a second coil on the blowout core was used in place of a separate transfer indication coil. This change had been made for other tests not covered here, and comparison of the results of tests with two coils on the same core and tests with the coils on separate cores gave evidence that this change did not affect the results basically.

As the table shows, at 20 amperes the probability of the arcing time being less than a cycle increases as the power factor is increased, but even at power factors of about 0.9, one interruption in five is long. No doubt the phase of the current with respect to the instant tip of separation is a major factor in whether a particular interruption is long or short.

Another factor believed to be significant in determining whether an interruption is long or short, is the tip opening velocity. This was suggested by results of the low power factor tests described earlier. For the contactor of Figure 1 nearly all interruptions at 10 amperes or less, at a power factor of 0.15 or less, had arcing times of less than 1 cycle. Tip opening velocity for this contactor is about 40 inches per second. For the second contactor with a tip opening velocity of about 20 inches per second the current had to be reduced to about 6 amperes at a power factor of 0.15 in order to have nearly all interruptions occur in less than 1 cycle.

Areas for Research

The test results suggest areas for future research. Variations in arc velocity with distance between parallel arc runners and with the angle between diverging arc runners, if known, are not found easily in the literature. Knowledge of such factors might be useful in contactor design. A comparison of arc velocities found in these tests with the velocities given by L. J. Linde and B. W. Wyman[2] for arcs along parallel runners in free air indicate that for the same current and flux density, arc velocity in free air is several times greater than that in an arc chute. Actually the data for velocities in free air[2] are for values of *BI* somewhat above the range of *BI* of these tests, but the *BI* values approached close enough to permit fair comparison of arc velocities. It would be useful to know what factors are particularly important in causing decreased arc velocities within arc chutes. For example, spacing of the cooling plates and width of the arc chute might be significant factors.

Factors which determine whether an arc is extinguished before reaching the arc runners have been investigated to a limited extent but much more remains to be done. It would be useful to know the motor size, particularly at 4,160 volts, for which arcs of rated current fail to be extinguished on the contact tips and must be driven into the cooling plates. This will be investigated by using reactors to simulate the primary leakage reactance of each phase of an induction motor and adjusting the applied voltage to a value approximating the difference between line voltage and the counter electromotive force.

Conclusions

The following conclusions have been reached.

1. For two high-voltage air-break contactors, the time for arc transfer to the arc

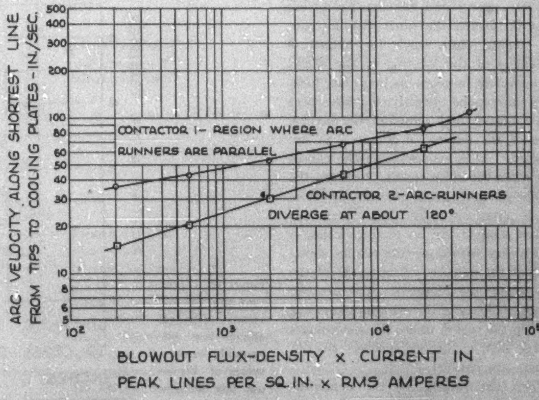

Figure 8. Arc velocity versus blowout flux density times current for two contactors

runners and the time to interrupt the arc after transfer varied as a small negative power of blowout flux density × current. The exponent for time after transfer was between −0.24 and −0.32 for one contactor and between −0.33 and −0.36 for the second depending upon the distance of the cooling plates from the tips. The exponent for transfer time was −0.37 for the first contactor and −0.40 for the second. In the first contactor the arc runners diverged initially and then ran parallel while in the second contactor the arc runners diverged throughout the interruption region.

2. In the first contactor the arc velocity along parallel parts of the arc runners was found to be constant for a given value of flux density × current. In the second the arc velocity along the continually diverging arc runners was similarly found to be constant. In each case arc velocity varied as a small power of flux density × current. When the velocities found for the second contactor were used to calculate arc times in that portion of the first contactor in which the arc runners diverged, the results were in close agreement with those found experimentally.

3. The distance of the cooling plates from the contact tips is a very important factor in the arcing time of a contactor since the arc velocity is a constant when all other variables are fixed. Although changes in the direction of the arc runners result in discontinuities in the slope of the "time versus distance" curve, the variation of time with distance is essentially a first-power relationship.

4. The blowout strength is not nearly so important a factor in arc time as distance of the cooling plates from the contact tips since arc time varies as only a relatively small power, about 0.25 to 0.35, of the blowout flux density.

It should be pointed out that in applying the conclusions about the position of cooling plates and the blowout strength to contactor design, the effect of these variables at high currents must also be considered. For example, in choosing the position of the cooling plates it is desirable for fast, low-current interruptions to bring the plates as close to the tips as possible, but it is also necessary that sufficient clearance be made between the plates and the arc runners so that the largest arcs to be interrupted will be able to move freely. Otherwise, the maximum current which can be interrupted satisfactorily will be lowered.

Since arcing time varies as only a small power of flux density, and since at high currents the blowout is certain to be saturated, it would appear that a relatively small amount of blowout iron and copper should be specified in an economically balanced design. However, an increase in the amount of blowout iron would raise the saturated value of flux density and should thereby improve the high-current interrupting ability of a contactor. Furthermore, increased blowout flux density should permit a slight lowering of the cooling plates as stronger forces are available for driving the arcs into the confined spaces. It is also possible that the greater forces on the arcs and the higher arc velocities might permit the use of more economical material for the cooling plates.

5. When the current to be interrupted was made sufficiently small, a large percentage of arcing times were less than a cycle and arc transfer did not occur. It appeared that higher tip opening velocities increased the maximum current value at which this effect was pronounced.

6. As the circuit power factor was increased for a fixed and sufficiently small current, the percentage of interruptions which occurred without arc transfer increased, but for those interruptions in which arc transfer did occur, the arcing time was independent of the power factor.

References

1. High-Voltage Motor Controllers Coordinated with Distribution Switchgear, **T. B. Montgomery, T. H. Bloodworth.** *AIEE Transactions*, volume 70, part II, 1951, pages 1354–60.

2. The Development, Design, and Performance of Magnetic-Type Power Circuit Breakers, **L. J. Linde, B. W. Wyman.** *AIEE Transactions (Electrical Engineering)*, volume 65, June 1946, pages 386–93.

3. Fundamentals of A.C. Circuit Interruption (book), **E. Salzer.** Allis-Chalmers Manufacturing Company, Milwaukee, Wis., 1950, pages 19–25.

4. Gaseous Conductors (book), **J. D. Cobine.** McGraw-Hill Book Company, Inc., New York, N. Y., 1941.

5. Heat Transfer Methods in Arc Interruption, **C. G. Suits.** *General Electric Review* (Schenectady, N. Y.), volume 42, 1939, pages 432–35.

6. Luftschutze zum Steuren von Hochspannungsmotoren Grosser Leistung, **F. Kassau.** *Fachberichte des Verbandes Deutscher Electrotechniker* (Berlin, Germany), volume 10, 1938, pages 42–46.

7. The Physical Mechanism of Low- and High-Current Arcs, and Their Relation to the Welding Arc, **Wolfgang Finkelnburg.** *AIEE Transactions*, volume 70, part I, 1951, pages 800–08.

◆

Discussion

Leon J. Goldberg (General Electric Company, Schenectady, N. Y.): This paper is an important contribution to design information on air-break contactors in revealing the effects of certain design variables on speed of interruption of low currents. It happens to be a fortunate circumstance that these effects do not dictate design features in conflict with those required for high current interruption.

A contactor must interrupt all currents from very small values to the maximum for which it is rated. It is very important that the high and maximum values be interrupted in short times because of the wear on the arcing parts, the need in many cases to stop a running motor promptly, and in some cases to limit the damage done by fault current. Furthermore a long arc duration at high current interruption may be indicative of a dangerously close approach to maximum interrupting ability. On the contrary, a low current interruption need not necessarily be of very short-time duration. All that is required is reliability and surety of interruption. Low currents may be caused by light running motors. In this case the counterelectromotive force of the motor assures short arc duration and reliable interruption. The most difficult interruption is on low power factor static reactor loads. In this case surety of interruption is indicated, notwithstanding several cycles of arc duration, if the arc voltage in succeeding half-cycles is successively greater for each half-cycle and without intermediate decreases. This has always occurred in those low current interruptions for which this author has seen oscillograms, even in development models that had less than expected maximum current interrupting ability.

Figure 1 of the discussion summarizes some interesting data tending to support the idea that for a general type of air-break contactor critical features of the arc interrupting structure importantly affect maximum interrupting ability, but do not greatly affect the pattern of the arc duration–current relation. In making this figure 64 points were plotted from test data taken with four different models of contactors, in which the blowout turns and the voltage were also varied. Some of the chutes had arc barriers transverse to the plane of the arc, some parallel to the plane of the arc. Variations in arc duration due to these variables of design and test were not sufficiently distinct to establish different trends with precision. Furthermore, the curves presented in reference 1 of Mr. Lister's paper replotted on the figure in this discussion fall approximately on the lower edge of the 80-per-cent band. The data of Mr. Lister's Figure 5 (showing arc time after transfer)

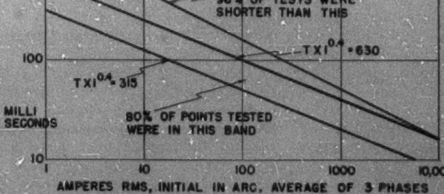

Figure 1. Arc duration on 5,000-volt contactors, 8-per-cent power factor, air-core reactor loads

fall on and slightly overlap the 80-per-cent band. Thus, several contactor variations, including the differences inherent to three different manufacturers' designs, show surprisingly close agreement in time-current characteristics.

C. A. Lister: The author wishes to thank Mr. Goldberg for the additional information he has contributed on the subject of arcing time of high-voltage air-break contactors The middle curve of Figure 1 of the discussion represents arcing times which are twice the arcing times of the lower curve for the same currents. For each contactor tested by the author, an average arcing time, for interruptions with arc transfer, was found at each current, and variations from this time were seldom more than 10 per cent. Differences between the arcing times of contactors of different designs were distinct and were as great as 2 to 1.

Mr. Goldberg claims that with motor loads the counterelectromotive force assures short arc duration, and some tests on 2,300-volt motors reported in reference 1 of the paper support this theory. The author feels that the question of arcing times with motor loads is important enough to warrant further study.

Short arc times are particularly necessary for contactors used in reversing motor starters. If the arcs on the contactor used for one motor direction are not extinguished by the time the contactor for the reverse direction closes, a direct short circuit is placed on the power supply. While potential interlocking[1] is used to prevent this possibility, such protection does not fail safe, and it would be desirable to have contactor arcing time short enough to preclude this possibility of short-circuiting the power supply. Thus, it would be useful to know whether, for all sizes and makes of motors and for all degrees of speed and loading, the arcs on a contactor would be extinguished before a reversing contactor could close.

The boundary between the rapid interruptions which occur without the arcs leaving the contact tips and the much longer interruptions in which the arcs are driven into the cooling plates has not, to the author's knowledge, been found, and it appears that extensive testing on a large number of motors would be required to define this boundary. At the limiting condition of stalled rotor one would certainly expect the longer type interruption.

Since recovery voltage appears to be the key to the problem, it was felt worth while to make some interruption tests at voltages well below rated contactor voltage. Such tests may give some indication of what would occur with motor loads.

Tests were made at voltages of 230, 465, 575, 670, 770, and 950. These, like most of the previous tests, were made with currents in the range of 10 to 50 amperes and at power factors of between 0.1 and 0.2. In these tests no arc transfers were observed at 230 volts. At 465 volts some arc transfers were found, but arc times were always less than one-half the arc time at the same current and 2,200 volts. At 575 and 670 volts some tests in which arc transfer occurred had arc times less than half the time for the same current and 2,200 volts while others had arc times nearly the same as those at 2,200 volts. At 770 and 950 volts arc times were only slightly less than those for the same currents and 2,200 volts.

At a given voltage, in the range 465 to 950 volts, some groups of interruptions failed to show a single transfer to the arc runners while other groups at nearly the same current and power factor showed a very high percentage of transfers. It was observed that when certain reactors were used in the circuit high percentages of arc transfers were likely. This is to be expected as different reactors would give different transient recovery voltages across the open tips and those tending to give high transient recovery voltages would be expected to cause the arc to be maintained longer.

While the results of the tests do not prove that long arcing times will be obtained with motor loads, they show that long arc times may occur with normal frequency recovery voltage well below rated voltage and, therefore, they indicate a possibility of long arcing times with motor loads. In the absence of proof that motor loads will always assure low enough transient recovery voltage across the contactor tips so that arcing time will be short, it seems good practice to assume that the contactor arcing time will be that which is found when the arc is extinguished by being driven into the cooling plates.

REFERENCE

1. A-C MINE-HOIST CONTROL, **James W. Cooke, G. W. Heumann**, *General Electric Review* (Schenectady, N. Y.), vol. 50, no. 12, December 1947, pages 26–32.

Drag-Cup A-C Tachometer with Constant-Current Excitation

R. H. FRAZIER
FELLOW AIEE

AS A consequence of recent publication of a general analysis of the drag-cup a-c tachometer,[1] numerous inquiries have been received relative to the desirability of operating such a device from a current source. Hence, a brief examination of the possibilities of such operation seems worth while. In these communications the ideas expressed about constant-current operation have been to the effect that with fixed exciting flux extreme linearity of output voltage with respect to speed should be achieved, and that troubles caused by change of winding resistance with change of temperature should be eliminated. Mathematical examination shows that extreme linearity indeed is theoretically possible. However, design difficulties in the tachometer itself, temperature effects other than change in winding resistance, and the difficulties of designing and constructing an adequate current source make doubtful the practical realization of the theoretical advantages of operation from a current source to a sufficient extent to show superiority over operation from a voltage source.

Steady-State Operation

The investigation is limited to the simple case of the output winding unloaded, which suffices to illustrate the principal points. The steady-state equivalent circuit shown in Figure 1 (which is adapted from Figure 4 of reference 1) then can be used. The winding resistance and any external series impedance have no influence on the operation of the tachometer and hence are omitted from the diagram. If core loss resistance r_c is absent, the primary leakage reactance x_{1m}' also has no influence on the operation of the tachometer. The voltage output then is

$$\mathbf{V}_L = j\alpha\mathbf{I}_m(\mathbf{Z}_f-\mathbf{Z}_b)/2 = \alpha\mathbf{I}_m r_2 x_\phi^2 n/ [2r_2x_{22}-j(r_2^2-x_{22}^2)-jx_{22}^2n^2] \qquad (1)$$

or

$$\rho' = V_L/\mathbf{I}_m = \alpha n/b[2a-j(1-a^2)-ja^2n^2] \qquad (2)$$

in which the forward impedance $\mathbf{Z}_f$ and the backward impedance $\mathbf{Z}_b$ are

$$\mathbf{Z}_f \equiv jx_\phi[r_2+j(1-n)x_2]/[r_2+j(1-n)x_{22}] \qquad (3)$$

$$\mathbf{Z}_b \equiv jx_\phi[r_2+j(1+n)x_2]/[r_2+j(1+n)x_{22}] \qquad (4)$$

Other defined quantities and ratios are

Paper 53-17, recommended by the AIEE Feedback Control Systems Committee and approved by the AIEE Committee on Technical Operations for presentation at the AIEE Winter General Meeting, New York, N. Y., January 19–23, 1953. Manuscript submitted July 28, 1952; made available for printing November 5, 1952.

R. H. FRAZIER is with the Massachusetts Institute of Technology, Cambridge, Mass.

The writer expresses appreciation to Miss Constance D. Boyd for editorial assistance in preparation of the manuscript.

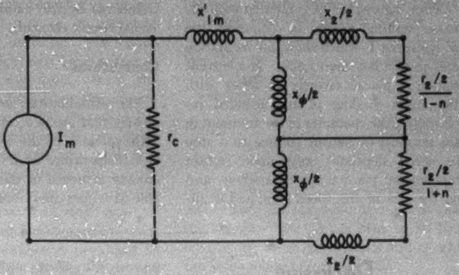

Figure 1. Equivalent circuit for induction tachometer supplied from current source

$$x_{22} \equiv x_\phi + x_2 \tag{5}$$

$$a \equiv x_{22}/r_2 \tag{6}$$

$$b \equiv r_2/x_\phi^2 \tag{7}$$

where

x_ϕ = magnetizing reactance
x_2 = leakage reactance of the rotor with respect to the main winding
r_2 = rotor resistance
α = turns ratio, auxiliary to main winding
n = per-unit speed based on synchronous speed

All parameters are referred to the main winding. The angle by which $\mathbf{I}_m$ leads $\mathbf{V}_L$ can be computed from

$$\tan \phi' \approx (1-a^2)/2a \tag{8}$$

The full-speed ratio and phase errors are

$$|\Delta\rho'/\rho'| \approx a^2(1-a^2)n_f^2/(1+a^2)^2 \tag{9}$$

$$|\Delta\phi'| \approx 2a^3 n_f^2/(1+a^2)^2 \tag{10}$$

If calibration is made at speed $n_f/\sqrt{2}$, the extreme errors are half the errors indicated by equations 4 and 5.

Here ratio and phase of the output voltage are based on $\mathbf{I}_m$, and maximizing the ratio and reducing the phase angle to zero depend on tachometer design and not on external circuitry. With the tachometer phased (if the speed error is neglected)

$$a = 1 \tag{11}$$

$$\rho' = \alpha n/2ab = \alpha x_\phi^2 n/2x_{22} = \alpha x_\phi^2 n/(x_\phi + x_2) \tag{12}$$

and large αx_ϕ and small x_2 are needed to achieve large ρ'. The condition of equation 11 also greatly reduces ratio error, which must be computed from an exact equation rather than from equation 9 when ϕ' is of the order of $\Delta\phi'$. If calibration is made at speed $n_f/\sqrt{2}$

$$|\Delta\rho'/\rho'| \approx n_f^4/32 \approx 0.00012 \tag{13}$$

$$|\Delta\phi'| \approx n_f^2/4 \approx 0.016 \text{ radian, or } 0.88 \text{ degree} \tag{14}$$

for n_f of 0.25 per unit.

The ratio error indicated is smaller and the phase-angle error is larger than computed for the idealized cases in reference 1 with use of a voltage source. Since close design for the condition of equation 11 is difficult, the ratio error inevitably must exceed the figure of equation 13, and a phasing network following the output terminals is unavoidable if zero phase is desired, though the phase-angle error is decreased by increased ϕ'. If a tachometer designed for operation from a voltage source, such as the ARMA Corporation type *1B400* tachometer,[1] is operated from a current source, its speed errors are likely to be larger than the errors associated with operation from a voltage source.

Now if r_c is not omitted, it, in association with $\mathbf{I}_m$, can be replaced by a voltage source in series with r_c and the voltage-source equations of reference 1 can be applied with r_c substituted for r_{1m}, the self-resistance of the main-winding loop. The basic equation, adapted from equation 17 of reference 1, is

$$\mathbf{V}_L/\mathbf{I}_m = \alpha n r_c / \{[(b-a^2b)x_{11} + 2abr_c + a] + j[2abx_{11} - (b-a^2b)r_c - 1] + (a^2bx_{11} - a)n^2 - ja^2br_cn^2)\} \tag{15}$$

in which the self-reactance of the main-winding loop and the equivalent voltage source are represented respectively by

$$x_{11} \equiv x_\phi + x_{1m} \tag{16}$$

$$\mathbf{V}_m = \mathbf{I}_m r_c \tag{17}$$

For high r_c the results are essentially the same as given by the equations herein and are identical when r_c becomes infinity. In fact, for general analysis using a current source in association with any input network, and using any output network, the equations of reference 1 can be used simply by transforming the current source and its shunt impedance to the equivalent voltage source and series impedance, so that all possibilities can readily be studied merely by slight adjustment of existing equations. When a current source is used, r_{1m} and x_{1m} are replaced by the real and imaginary components of impedance seen by looking out from the terminals of the magnetizing reactance of the tachometer when the current source is opened. A considerable variety of possibilities for adjustment by means of terminal networks exists when a current source is used, just as when a voltage source is used, but when a current source is placed elsewhere than directly in series with the input winding, or a voltage source is placed elsewhere than directly across the winding terminals, the type of source used becomes indistinguishable from the point of view of the tachometer.

Although use of a current source directly in series with the input winding theoretically eliminates errors due to change in resistance of that winding with change in temperature, serious errors caused by change in temperature still may arise from change in resistance of the cup and change in resistance of the iron; also secondary effects may remain due to slight changes in reluctance of the iron or in dimensions of parts. Hence use of a current source is only a partial, and may be only a minor, influence in the reduction of temperature errors.

Operation with Varying Speed

The acceleration error for operation with a current source is not the same as for a voltage source connected directly to the terminals of the tachometer. When the input terminals of the tachometer are open (which corresponds to removal of a current source directly in series with the tachometer terminals), the characteristic equation (obtained by using r_c in place of r_{1m} in equation 195 of reference 1) is

$$(L_{11}L_{22}^2 - L_\phi^2 L_{22})s^3 + (r_cL_{22}^2 + 2r_2L_{11}L_{22} - r_2L_\phi^2)s^2 + (r_2^2L_{11} + 2r_cr_2L_{22} + L_{11}L_{22}^2\omega^2n^2 - L_\phi^2L_{22}\omega^2n^2)s + (r_cr_2^2 + r_cL_{22}^2\omega^2n^2) = 0 \tag{18}$$

For the ARMA Corporation tachometer mentioned, the roots of equation 18 are

$$s = -27{,}060 \text{ and } -5{,}365 \pm j1{,}270 \text{ second}^{-1} \tag{19}$$

When the terminals of the tachometer are short-circuited (which corresponds to removal of a voltage source directly across the tachometer terminals), the characteristic equation is obtained by using $r_{1m}' r_c/(r_{1m}' + r_c)$ in place of r_{1m} in equation 195 of reference 1, or in place of r_c in equation 18 here. Actually r_{1m}' may be used instead of $r_{1m}' r_c/(r_{1m} + r_c)$ with little error unless core loss is usually large. For the ARMA Corporation tachometer mentioned, the roots of the characteristic equation then are

$$s = 13{,}704,\ -5{,}791, \text{ and } -170 \text{ second}^{-1} \tag{20}$$

These figures can be compared with the corresponding figures in equation 196 of reference 1, which show no oscillation and no root less than 1,800. If a current source is placed directly in series with the input winding of an unloaded tachometer, the character of the transient in the response of output voltage to a step in speed depends only upon certain tachometer parameters themselves and on the size of the speed step, and is uninfluenced by the parameters of any external circuit elements.

Conclusions

The examination outlined herein indicates that use of a current source offers little promise in the reduction of speed and temperature errors below the levels already achieved or theoretically achievable with operation from a voltage source. In the hope of achieving very little, if any, reduction of error, one must pay the price of designing and constructing an adequate current source having acceptable wave form and very close tolerances on amplitude and frequency fluctuation.

Reference

1. An Analysis of the Drag-Cup A-C Tachometer by Means of 2-Phase Symmetrical Components, R. H. Frazier. *AIEE Transactions*, volume 70, part II, 1951, pages 1894–1906.

Discussion

Herbert H. Woodson (United States Naval Ordnance Laboratory, Silver Spring, Maryland): An auxiliary result of this study, especially interesting to those who work with tachometer-stabilized magnetic-amplifier servo systems, is contained in the transient analysis of the tachometer. From equation 20 the tachometer, when excited from a voltage source, has one time constant of approximately 6 milliseconds. When a tachometer is excited in this manner and is used to stabilize a magnetic amplifier servo system, the tachometer time constant in conjunction with the time delay in the magnetic amplifier may give sufficient phase shift to seriously limit the bandwidth obtainable with such a system. This limitation has been observed at the Naval Ordnance Laboratory.

The time delay through a 400-cycle 2-stage half-wave magnetic amplifier is 3.75 milliseconds.[1] To make the tachometer time constant negligible when used with such an amplifier, it must be decreased by a factor of ten or more. Equation 19 shows that tachometer excitation from a current source will effect such a decrease in tachometer time constant; however, such a drastic step need not be taken. A sufficient reduction in time constant can be achieved by raising the internal impedance of the excitation source to an appropriate value.

Reference

1. An Improved Magnetic Servo Amplifier, C. W. Lufey, A. E. Schmid, P. W. Barnhart. *AIEE Transactions*, volume 71, part I, 1952, pages 281–89.

Charles M. Edwards (Bendix Aviation Corporation, Detroit, Mich.): Professor Frazier's paper invites consideration of developing a device which utilizes a tachometer that has an output accurately proportional to the product of shaft speed and impressed voltage. While I was at the Dynamic Analysis and Control Laboratory, Massachusetts Institute of Technology, tests were made on an Arma 1B400 unit, to determine the linearity of output with impressed voltage. Over a range of voltages of approximately 10 to 1, the output-to-input ratio for full speed changed several per cent. Undoubtedly, most of this nonlinearity was due to effects in the core, although some might have been due to temperature changes.

It is reasonable that a combination voltage and current source, as might be provided by a feedback amplifier, could be developed to give partial compensation for the iron effects and possibly some of the temperature effects.

Professor Frazier is to be commended for his pioneering efforts in quantitative analysis of the a-c tachometer.

R. H. Frazier: The author appreciates the discussions by Mr. Edwards and by Mr. Woodson, which are valuable supplements to the paper. The drag-cup a-c tachometer represents in principle a type of device that can be adapted to a large variety of uses as a motor or a generator, especially when used in association with auxiliary terminal networks or other apparatus, as a component in a complex system, and invites much inventive speculation. When excited with direct current, the device can be used as an accelerometer. Some quantitative studies of such operation are in progress under the author's direction.

Diesel-Electric Locomotives in Canada

J. D. SYLVESTER
MEMBER AIEE

D. F. HANEY
ASSOCIATE MEMBER AIEE

Synopsis: This paper explains briefly the progress of dieselization on the two major railways in Canada. It outlines specific electrical problems encountered and suggests the developments desired to meet their particular type of operation. Information given is in terms of technical reciprocity with the numerous railways in the United States.

THE CANADIAN National Railways and the Canadian Pacific Railway are the two principal railway systems in Canada. These systems have over 40,000 miles of track from the Atlantic seaboard to the Pacific coast and comprise the two largest railway systems on the North American continent. Although there are other class I railroads operating in Canada, this paper will limit the discussion to the two roads which operate about 95 per cent of the total track mileage.

The railways were built in Canada not to meet a direct economic need for transportation but as a connecting link for the unification of the country. It subsequently became necessary for the railways to encourage settlement and development of primary industries in order to pay for the initial capital expenditure.

The two transcontinental railways are basically single-track lines with many branches feeding into the main line. They were constructed when modern machinery and methods were not available and consequently are characterized by numerous curves and grades. The railways operate through varied climatic conditions. A train could leave Vancouver at 50 degrees Fahrenheit and in a few hours be in a snow storm at a temperature of −40 degrees Fahrenheit. In general, the temperature ranges from −50 degrees Fahrenheit to 100 degrees Fahrenheit.

Locomotive 9000

The Canadian railways were the first to operate a diesel-electric locomotive

---

Paper 53-68, recommended by the AIEE Land Transportation Committee and approved by the AIEE Committee on Technical Operations for presentation at the AIEE Winter General Meeting, New York, N. Y., January 19–23, 1953. Manuscript submitted October 22, 1952; made available for printing December 29, 1952.

J. D. Sylvester is with the Canadian National Railways, Montreal, Quebec, Canada. D. F. Haney is with the Canadian Pacific Railway Company, Montreal, Quebec, Canada.

Table I. Comparison of Number of Steam and Diesel-Electric Units in Service at the End of 1942 and 1952

Year	Number of Steam Locomotives	Number of Diesel Units	Total Number of Units in Service
1942	3,977	5	3,982
1952	3,780	610	4,390

in main line service on this continent. Canadian National 9000, placed in passenger service in 1928, comprised a 2,660-horsepower diesel-electric locomotive of two units, the largest in the world for many years. This locomotive was built by the Canadian Locomotive Company at Kingston, Ontario, using 800-rpm Beardmore engines built in Scotland, and Westinghouse electrical equipment built in the United States. This was an experimental locomotive, the notable foresight of C. E. Brooks, former chief of motive power of the Canadian National Railways. The units accumulated 250,000 miles in revenue service and were retired in 1946 because spare parts became unavailable.[1]

Dieselization

After the initial investigation into diesel-electric units, the Canadian railways had little opportunity to develop the locomotive further because of the adverse economic conditions which started in 1929. Four locomotive units, totaling 3,710 horsepower, were owned in Canada by the Canadian National at the end of 1937.

In 1942 the Canadian railways began purchasing modern diesel-electric locomotives. A program for purchasing switching units was set up, but at that time no road units were considered for the following reasons:

1. Units for road service were not sufficiently reliable to perform satisfactorily in Canada's varied climate.
2. The fuel economics of a diesel switcher over a steam switcher, especially at idling, were sufficient to make purchasing diesel switchers obvious.
3. Canada had to import most of her fuel oil and because of war conditions was not assured of a continued supply of oil required for expansion to road units.

In 1947 the opening of the Alberta oil fields provided an assured domestic source of oil. In the meantime, the diesel-electric road locomotives had become more reliable and their purchase was now more attractive.

The assignment of new diesel-electric road power can be made either by dieselization of selected runs or by complete dieselization of a territory. The Canadian National assigns new diesel power to selected high-mileage runs, where the greatest return is obtained on the original capital expenditure.[2] The Canadian Pacific, on the other hand, assigns new diesel power to a specific territory with provision for extended service during off-peak traffic conditions. This avoids duplication of steam and diesel maintenance and servicing facilities and permits operating and maintenance personnel to become thoroughly familiar with one type of power.

The number of diesel-electric units operated by the Canadian National and Canadian Pacific has increased from five units totaling 4,710 horsepower at the end of 1942 to 610 units totaling 728,750 horsepower at the end of 1952. This growth is shown graphically in Figure 1.

The decrease in the number of steam locomotives in operation has not balanced the increase in diesel-electric units. Table I compares the steam and diesel-electric units in service at the end of 1942 and 1952. The decrease of 197 steam locomotives has been balanced by an increase of 605 diesel-electric units. It should be mentioned that the railways' steam inventory had not remained static. During the period from 1943 to 1948 a total of 314 modern steam locomotives were purchased, and from 1942 to 1952 a total of 511 obsolete steam locomotives were retired from service or scrapped. The increase in the number of motive power units is indicative of the expanding economy and the increase in population of Canada.

Prior to 1948, all diesel-electric units were manufactured in the United States. Since that time the American manufacturers have realized the importance of the Canadian market and are now manufacturing units in three subsidiary plants. At present, the Canadian content of the units varies from 65 per cent to 90 per cent of the value of the units and efforts are being made to increase this.

Table II. Service Miles of Diesel-Electric Units From 1943 to 1952 Inclusive

Type of Service	Service Miles
switching	49,900,000
road	46,100,000
total	96,000,000

Units manufactured in Canada are of American design with certain modifications to suit our climatic conditions. The railways are purchasing 1,500- and 1,600-horsepower road units with 4-wheel trucks for freight and passenger service, 1,200- and 1,500-horsepower road-switching units for wayfreight and branch-line service, and 660- to 1,200-horsepower units for switching and work-train service.

The diesel-electric units of the two railways have accumulated 96,000,000 miles in service to the present time. As shown in Table II, over one-half of this mileage is in switching service. The miles in road service have been accumulated since 1948.

Electrical Problems

Our problems, especially the electrical problems in diesel-electric locomotive operation, have been very few to date because the equipment is comparatively new and because the operation at relatively low schedule speeds does not subject the traction equipment to both high thermal stresses and high centrifugal forces.

Typical problems have been some flashovers on the main generators on one rail-

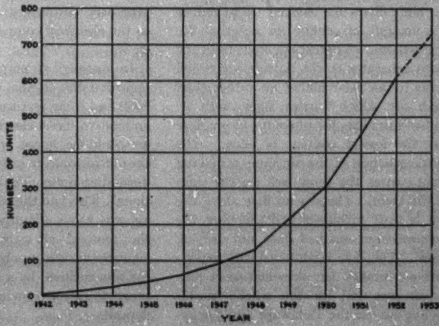

Figure 1. Graph showing increase of diesel-electric units on Canadian National and Canadian Pacific Railways

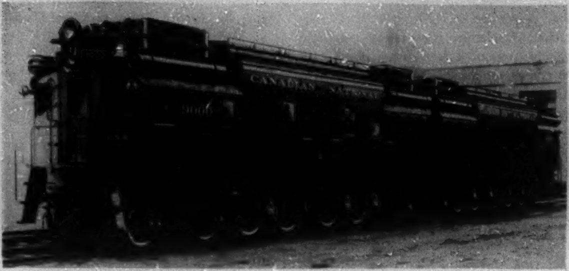

Figure 2. Canadian National Locomotive Number 9000. The first diesel-electric in main line service on the American continent

way, and marked commutator burns on traction motors in the beginning on the other railway. The causes of the flashovers have not as yet been determined definitely. Commutator burns were found to be due to starting the freight trains before the brakes were released. This problem ceased when operators were instructed to wait 5 minutes after releasing brakes before applying power to the wheels.

Some of our problems, which may not be typical elsewhere on this continent, are those caused by fine dry powdered snow blown by high winds so common in the extreme cold. This snow will pass through filters to build up to a foot and more in the interior passageways of the locomotive and will enter the main generator, traction-motor blowers, and electrical control compartments. This results in frequent moisture grounds which are partially alleviated by continuing the operation of the locomotive so that the electrical equipment is dried out by its own generated heat.

Late in the fall the locomotives are winterized to restrict the entry of powdered snow to the most critical areas of the engineroom. Up to 50 per cent of the car body filters are blocked off to reduce the amount of cooling air entering the engineroom. Exhaust openings from the main generator to the outside are closed so as to use recirculated air rather than fresh air which carries snow with it. Outside air along the top of the locomotive has the lowest content of snow. The swirling action of the air along a moving train carries the snow well up the sides of the train. The stream flow along the top is least turbulent and therefore the cleanest from roadbed dust and drifting snow. This is in accordance with experience on intakes for air-conditioned passenger cars and for the traction-motor cooling air on the Delaware and Lackawanna Western electric multiple-unit cars.

To take advantage of the relatively snow-free air above the locomotive, some units have a roof air intake placed over one of the engine cooling radiator blowers and so baffled that some of the exhaust from the radiator blowers is drawn into the engineroom with the outside air taken in at this point. The control temperature of this radiator blower is set to have it operate first and so supplement the outside air with preheated air whenever heat is available from the engine cooling radiators. The amount of air drawn through the roof intake will depend upon how many car body filters are blocked off and whether the engine room shutters are open or closed. The Canadian railways look forward to further developments to overcome the powdered snow problems and the resulting moisture grounds. Any means to reduce air intake and air leakage below or along the side of the locomotive is to be desired. Pressurizing the engine room and particularly the electrical compartments with clean air would be a step towards this objective. One manufacturer has a means of passing the cooling air from the main generator through a duct with a filter to the electrical compartment to pressurize it.

In passing, it may be significant to note that the original Canadian National 9000 had some features not yet available on modern diesel-electric power. Engine air could be taken either directly from the outside or from inside the engineroom, depending upon climate and track conditions. This had the advantage that when air was taken directly from the outside the amount of snow drawn into the engineroom was much less. The generator was enclosed in a separate compartment, thus free from snow and oily vapor deposits.

In winter, the electrolyte of our starting batteries is often down to a temperature of 5 degrees Fahrenheit and therefore the engines are kept idling when not in an engine house. It is the findings of our National Research Council that a diesel engine cannot be expected to ignite on starting if the engine block temperature is below 20 degrees Fahrenheit. Auxiliary steam generators are of value in our winter operation although they have not yet been arranged to heat the battery compartment.

Precautions are taken in cold weather to inspect locomotives indoors as soon as possible after being released from service. The electrical equipment therefore, does not cool down to the point where condensation would occur across insulated parts when subsequently brought into the shops.

In the United States there are many nonrailway shops which specialize in repairing electric traction equipment. In Canada there are none to date. The two major railways therefore are planning to equip several of the main shops to do these repairs. These will be staffed by reassigned personnel trained for the new work. It is not likely that there will be the advantage of competitive repair costs such as are available in the United States.

Our only schedule for traction motors is the inspection and clean-up at wheel change. This has been satisfactory to date but insufficient experience has been obtained to establish a definite overhaul interval. The first of our diesel-electric yard switchers has just seen 10 years of service. The first of our diesel-electric road locomotives has just had 600,000 miles of operation in freight service. A definite pattern of life expectancy of traction motor bearings is developing on some of the power. This more than anything else is dictating when the traction motors are taken into the main shops for whatever overhaul is required. Road failures of traction motors have been due mostly to mechanical failures and accidents.

Desired Developments

The Canadian railways note with interest recent developments which give better and more reliable locomotive performance. With the improvement in the diesel engine and the reduction in mechanical failures, more emphasis is being placed on the electrical components to ensure trouble-free service. Although many automatic controls are necessary, there is a need to make these of few moving parts and to have their functioning as simple as possible.

The use of class *H* insulation has increased the continuous rating of the electrical equipment. This allows the railways to use a higher gearing without reducing the haulage capacity in heavy freight service. This increase in "operating range" permits the better performance of a locomotive in heavy freight and in medium-speed passenger service. Further developments along these lines are anticipated.

Recently the capacity of the dynamic brake has been increased and danger of current overloads has been reduced by the development of an automatic control to replace the manual control. This will allow greater use to be made of the dynamic brake without burning out the resistors or overspeeding the cooling fans.

References

1. Oil Electric Motive Power on the Canadian National, C. E. Brooks. *Railway Age* (New York, N. Y.), volume 84, June 9, 1928, page 1319.

2. Application of Diesel Electric Locomotives, P. L. Mathewson. Engineering Institute of Canada, volume 33, September 1950, page 762.

◆

Discussion

P. H. Hatch (General Electric Company, Erie, Pa.): This year marks the 30th anniversary of the first diesel-electric locomotive. This was a switching locomotive used as a demonstrator on a number of railroads in the United States and subsequently purchased and put into regular service by one of them. It is especially interesting to note that the next two anniversaries in point of years belong to Canada. These are the first diesel-electric rail car in road service in 1925 and the first main-line diesel-electric locomotive in road service in 1928.

As the paper states, the discovery of large oil reserves in Alberta in 1947 has initiated full-scale dieselization of Canadian railways, which is well under way today.

One interesting question is touched upon by the authors in this connection. This is whether dieselization should be progressed on the "area" or the "cream-of-the-service" basis. There are advantages and disadvantages to both; probably the ultimate answer is one of economics.

Locomotive-wise the Canadian railways are adding to our store of knowledge in tackling squarely the problem of operating diesel-electric locomotives in very low temperatures and with continuing exposure to fine, dry snow. This should in the end enable locomotives to be built to be less vulnerable to low temperatures and it should lead to improvement in cab and apparatus ventilation generally, which knowledge will be of extensive use for both diesel-electric and electric locomotives in contending not only with snow but with rain, dirt, and dust as well.

In conclusion, it is very refreshing to have this paper by our Canadian friends and a great deal of interest and value is to be found in it.

Design Factors Favoring Diesel-Locomotive Electrical Maintenance

J. STAIR, JR.
MEMBER AIEE

Synopsis: Many details of design of electric apparatus and its installation in the locomotive have a profound effect on the amount and quality of maintenance attention it requires and receives in service. Simplicity and ruggedness are basic. The influence of design upon diesel-locomotive electrical maintenance cannot be overemphasized. This applies not only to the design of the electrical apparatus but also to the design of the conduit and wiring, electrical cabinets, cab structure, and even the diesel engine itself. Taken separately, the following features peculiar to the diesel-electric locomotive must be kept in mind.

Electric Apparatus

ELECTRIC apparatus must conform to the appropriate standards of the industry, with proper selection and use of traction motors, generators, auxiliaries, control and protective devices, and with some leeway in the capacity of the apparatus with respect to the work to be done. Modern inorganic materials should be used for the insulation of traction motors and generators. A detailed discussion of these items is beyond the scope of this paper.

Dirt, moisture, and oil fumes are inevitable. Consequently, an oily conductive film develops on the apparatus. Panels, connections, and interiors of motors and generators must be designed with adequate creepage paths and no portion of the power circuits should be exposed except where adequate creepage paths are provided.

Relays should be enclosed in dust-tight containers, with glass or plastic covers permitting visual inspection of the operation of the relay. Rotating apparatus should be equipped with grease-lubricated sealed bearings to exclude foreign matter and extend maintenance periods.

Electric devices suitable for railway service should be used throughout. Bearings and contacts of industrial-type devices, such as relays, contactors, and instruments often will not stand up under the shocks of running over the road and the vibration of the diesel engines.

Protective and control devices should be inherently sealed to prevent tinkering by crews and others who too often are more interested in experimenting with the various items of apparatus than with proper operation.

All electric apparatus and wiring should be designed to permit pressure spray cleaning of the interior and exterior of the locomotive without water entering the electric apparatus or wiring.

Conduit and Wiring

Conduit, wire and cable troughs, and wiring within the engine room should be located overhead or on the side walls well up from the floor and above the air intake filters.

Conduit should be of ample size to permit pulling in additional wires if required in the future, and to permit freely pulling out the original wiring for repairs or renewal.

Insulation on all wires and cables should be of heat-resistant material with fire-resistant nonabsorbent neoprene exterior.

All conduit, fittings, and junction boxes should be absolutely waterproof to permit pressure spray cleaning.

Cables cleated to the underside of the cab structure should be out of the way of

---

Paper 53-50, recommended by the AIEE Land Transportation Committee and approved by the AIEE Committee on Technical Operations for presentation at the AIEE Winter General Meeting, New York, N. Y., January 19–23, 1953. Manuscript submitted October 20, 1952; made available for printing November 19, 1952.

J. Stair, Jr., is with the Pennsylvania Railroad, Philadelphia, Pa.

or protected from brake shoe sparks, and should be clear of wheel wash and of any location subject to seepage of oil or water from engine room. They must also be protected from direct impact of jets from running-gear high-pressure cleaning devices. Cables and cable protection should not form pockets which will catch leaves, paper, or other combustible material.

Connections between motor leads and cab-structure leads should be easily disconnected, reconnected, and reinsulated. Leads must be sufficiently flexible to avoid breakage, and so cleated, located, and protected as to eliminate chafing.

To facilitate the replacement of cables under the cab structure, the bolts which secure the cleats to the underside of the cab structure should be attached firmly to the cab structure.

Sharp corners in conduit and cabinets, which may cause damage to wire and cable, should be eliminated or the wire and cable given special protection at such points.

Electrical Cabinets

Electrical cabinets should be a minimum of 4 inches above the floor to permit mopping the floor, and all wiring should be kept several inches above the bottom of the cabinets.

Doors should be dust-tight and waterproof to prevent entry of road dust, dirt, and cleaning solutions.

All wires and cables should enter and leave cabinets in conduit or in wiring troughs. These should be so designed that the entry of dirt or water will be reduced to a minimum, and fires originating on the running gear cannot spread to the cabinets.

Cab Structure

Engine room floors should be oil and watertight to prevent seepage of oil and water onto the traction motors and the cables below the floor.

All openings through floors for pipes, conduits, cables, and drains should be sealed against leakage or provided with raised dams around the opening; they should have suitable barriers to prevent a fire originating on the running gear from spreading to the interior of the unit.

Cab air filters should be provided to clean all air entering the engine room to prevent ingress of dirt and to minimize the entry of snow and rain as well.

Cab and doors should be automatically self-closing, not readily susceptible to being blocked open.

All doors and windows should be as dust-tight as practicable.

Adequate quantities of clean cooling air to main generators, traction motors, and electrical cabinets must be provided.

To keep oil fumes out of the electric apparatus, cooling air streams should not previously pass over the diesel engine and its appurtenances.

Suitable sumps should be provided beneath diesel engines and air compressors to catch and drain off all leakage of oil and water.

Diesel Engines

Diesel engines should be designed and constructed to provide the absolute minimum of oil leakage from top deck covers, inspection covers, crankcase breathers, piping, frame joints, and so forth.

Exhaust manifolds and all their connections must be absolutely free of leaks to avoid the entry of exhaust fumes and soot into the engine rooms and thence to the electric apparatus.

General

The diesel locomotive is a complicated piece of machinery. Unlike a stationary power plant or the machinery of a ship, it must, on a large railroad, be operated and maintained continually by many different persons.

In the interests of reliability and economical maintenance, simplicity of design and ruggedness of apparatus are of fundamental importance. Rugged does not necessarily mean massive. Although efficiency is to be desired, refinements to attain it to a high degree are not warranted if they result in complications of maintenance and in failures.

To facilitate both operation and maintenance, standardization of apparatus is desirable. Therefore, a modification in the design of a piece of apparatus which prevents its interchangeability with the older piece is to be avoided unless it sufficiently improves the operation or benefits the maintenance.

Likewise, in any given type of locomotive, both operation and maintenance are facilitated by standardization of the location of the various pieces of apparatus in the operating cab and in the engineroom.

◆

Discussion

C. A. Atwell (Westinghouse Electric Corporation, East Pittsburgh, Pa.): In this paper, at first glance very brief, Mr. Stair has done a good job of listing the essential design features of diesel locomotives that will help the operater in good maintenance.

Many of his listed items apply to locomotive arrangement with which designers of rotating apparatus will wholeheartedly agree because such things as accessibility to brushholders, ease of cleaning, and proper supply of ventilating air are items which mean much to the trouble-free operation of generators or motors. They know that if the arrangement is unhandy, the parts will be neglected, and such neglect can offset the efforts of the most careful and thorough design efforts.

It is almost heartbreaking to the designer when he climbs on a locomotive that has been in service only a few months to see apparatus, which was clean and shiny when it left the factory after thorough test, with field coils and brushholders dripping oil or detergent cleaning fluid.

Mr. Stair says dirt, moisture, and oil fumes are inevitable. This is probably true, but it is also a simple undeniable fact that generators and motors of the power and voltages required for diesel locomotives will not operate correctly if these enemies of commutators, brushes, and insulation are not kept to the minimum by continuous maintenance.

Designers of rotating apparatus are doing their utmost, or at least near their utmost, to produce machines that are rugged and reliable, but it is this writer's belief that without improved maintenance efforts to keep electric apparatus clean and dry, much design effort will be offset in the first few months of operation of a new locomotive.

R. L. Chapman (General Electric Company, Erie, Pa.): Mr. Stair's paper, treating as it does the design factors affecting maintenance from the viewpoint of a locomotive user, should be of particular interest to a locomotive manufacturer since the latter's knowledge of conditions of use must necessarily be less complete and continuous than that of the user. Conversely, the designer and manufacturer is usually more keenly aware of the limitations imposed by design considerations and how these affect the detail design of apparatus and its placement in the locomotive.

Mr. Stair, as a representative of one of the larger users of diesel-electric locomotives, is certainly well qualified to discuss these problems. He should be listened to as one who speaks with authority on this subject. Speaking for a manufacturer I want however to point out that the complete fulfillment of the requirements laid down by Mr. Stair would, in most cases, require additional space—an item at a premium in locomotives. Steady progress is being made in the direction indicated by this paper. Motor output is well on the way to being double what it was a few years ago; but the space available for that motor—fixed by wheel diameter, distance between wheel flanges, and clearance to rail—has not increased. Likewise the control has grown in size and complexity with the trend to higher horsepower, better utilization, increased fault protection, and more automatic operation; yet the space it occupies has not increased correspondingly.

This trend toward more horsepower and improved performance without a corresponding increase in size and weight is in the right direction. It is good, but it means that both the manufacturer and the user will have to be increasingly alert; the manufacturer to avoid design compromises that unnecessarily increase the cost of maintenance, and the user to find and adopt new and improved materials and procedures for servicing and maintaining the complex piece of machinery we call a locomotive.

That Mr. Stair is aware of the manufacturer's problems as well as his own is shown by his judicious use of the words should and must, and we cannot but agree with him that full consideration should and must be given to these factors.

J. Stair, Jr.: The design factors outlined in this paper were accumulated through continuing surveys of maintenance practices which have been found necessary for many different makes and models of diesel-electric locomotives. They are presented with the expectation that they could enable railroad personnel to maintain electric apparatus on diesel locomotives economically and efficiently.

While the quality of prevalent maintenance practices is somewhat beyond the scope of this paper, it seems appropriate to suggest that costly quality maintenance has been experienced because of certain unfavorable design factors, despite the fact that the apparatus left the factory "clean and shiny."

It is also significant that despite the premium on space, railroads have been forced to modify designs on many diesel locomotives to reduce maintenance costs and to improve reliability of performance.

Railroads are interested in better performance and lower maintenance costs from diesel locomotives and believe that more comprehensive designs can do much to accomplish both objectives.

Equipment and Functions of a Modern Diesel Locomotive Heavy Electric Repair Shop

F. THOMAS
NONMEMBER AIEE

Synopsis: Various requirements, procedure, and equipment for maintenance of electric equipment on diesel-electric locomotives are outlined.

Growth of the Electrical Maintenance Problem

With the rapid development and widespread employment of diesel-electric locomotives in recent years, the problem of electrical maintenance has grown with equal rapidity. Since the electric equipment on steam locomotives is relatively small and simple compared to that on diesel locomotives, the problem of educating electricians already in the employ of the railroad and of hiring and educating new men for electrical work has increased the magnitude of the maintenance headache. Aside from the procurement and education of competent personnel for the railroad electrical shop, there is the problem of securing the proper equipment for the shops and arranging this equipment so that it can be utilized to its fullest extent. Arranging and converting certain pieces of equipment from a steam locomotive back shop for use in new duties in the repair of electric equipment has been done to a limited extent.

Centralization of Repair

A large part of the equipment on today's diesel locomotive is electrical, and inspection and repairs on electric equipment must be far more specialized than similar work on steam locomotives, which makes the centralization of such repairs more essential. A great number of small pieces of equipment, such as relays, excitation controls, governor controls, and so forth, require specialized expensive repair and test equipment which cannot be duplicated in each small repair shop on the road. Traction motors and main generators and in general the larger types of electric equipment require periodical overhauling as well as overhaul when the locomotive unit is in the shop for complete general repairs. It is, therefore, necessary in planning these facilities to provide adequate space for general overhaul work, as well as work on equipment which has been sent in from outside points for repair. The repair of traction motors can be arranged to operate on a flow production basis overhaul system. The traction motor repair on a flow chart basis should utilize specialized machinery designed and placed for each specific task. It will, of course, become necessary to determine the volume of work anticipated in order to know if duplications of operations on some items are required. In general, it can be said that a field frame stand and an armature winding stand are required for each armature rewind job and heavy repair passing through the shop per 8-hour working day.

Traction Motors

The general procedure followed in a traction motor repair shop should be as follows: Every piece of equipment entering the shop goes through a preliminary cleaning process in a vapor degreaser and receives a shop index card, index number, and so forth, according to the type of indexing system selected. A test is made to determine what repairs are necessary and a colored tag indicating whether a complete rewind job or a partial overhaul job is to be done is attached. The next step in this operation is the removal of the traction motor pinion from the shaft which is done with a hydraulic pinion puller or an induction pinion heating device. The induction heating method has been found to save time and to be more efficient. The armature is removed from the traction motor housing and, if it is a rewind job, placed in an old lathe which is suitable for use in stripping the armature. A simple cutting tool is used in the lathe to cut the armature coils immediately behind the risers as the armature is rotated. The coils are then ripped out by means of a frog clamp attached to a 1-ton crane. The soldered parts of the winding and commutator are heated by a high-frequency soldering machine and the soldering slots cleaned with a low-pressure stream of air. The armature goes from here to the mild abrasive blast. After this abrasive blast

---

Paper 53-76, recommended by the AIEE Land Transportation Committee and approved by the AIEE Committee on Technical Operations for presentation at the AIEE Winter General Meeting, New York, N. Y., January 19–23, 1953. Manuscript submitted October 21, 1952; made available for printing December 4, 1952.

F. Thomas is with the New York Central System, New York, N. Y.

the commutator is tested by approximately 3,000 volts to ground and 200 to 250 volts bar to bar. Following necessary repairs, the commutator is ground, polished, and seasoned. The equalizing coils are then applied and preheated to about 200 degrees Fahrenheit. Next, follow the different winding steps such as bottom and top coils, temporary banding, further testing against ground, and finally brazing back end connections and soldering the commutator. The temporary banding wire is removed and permanent banding is applied. The vacuum impregnating process using insulating varnish is followed by a 24-hour baking at approximately 250 degrees Fahrenheit. The commutator is tightened, if necessary, undercutting is done, alignment checked, and the armature is dynamically balanced. Another ground and bar-to-bar test follows using new-type high-voltage surge tester, and if found to be all right the armature is ready for the traction motor assembly. Armatures which do not require rewinding are cleaned in a mild abrasive blast, dipped in varnish, baked for 24 hours, and from here go through the same operation as those armatures which received complete rewinding jobs.

Following cleaning in the vapor degreaser and removal of the armature, the field coils are tested inside the frame, and it is decided at this point whether it is necessary to rebuild these coils or have them cleaned and revarnished. The coils are then removed from the frame and go to their respective repair section. The frame as well as the poles are cleaned by a mild abrasive blast. Care should be taken that this abrasive blast material is suitable for this type of work and not too sharp or too hard. It should also be rather fine grained for best results. Frames should be inspected, the necessary ground insulation replaced, new or reinsulated field coils applied, and all leads and connections resoldered and reinsulated where necessary. The entire assembly of frame, coils, leads, and so forth, is baked for 24 hours at approximately 250 degrees Fahrenheit and then sent to assembly. After cleaning, the traction motor bearing housing is inspected, repaired and sent to assembly. In some instances it will become necessary to build up and remachine the traction motor bearing housing.

The traction motor armature bearings are sent to a special dustproof room, cleaned, inspected, and "miked" and are returned to service if in suitable condition. The bearings not passing inspection are returned to the manufacturer for reconditioning. The section of the frame which holds the traction motor suspension bearing should be inspected and if necessary should be built up by welding and remachining. The traction motor suspension bearing caps may likewise necessitate welding and remachining. All repaired and rebuilt components of the traction motor are assembled and the motor undergoes a 2-hour running test at various speeds and loads.

Generators and Auxiliary Motors

The rebuilding of the main generator, auxiliary generator, and blower motors follows approximately the same steps as the traction motor except for those types of main generators which have an a-c generator on the same shaft as the d-c generator. Inasmuch as the a-c generators supply current for all vital auxiliary apparatus, a rebuild and test procedure is developed handling the a-c side as a separate repair item.

Electric Equipment on Steam Generators

The specialized electric equipment used on steam generators should be repaired in a subsection of a small parts electrical section and tested for its particular functions. Motors and similar equipment used on steam generators can be incorporated in the general motor overhaul area previously mentioned.

Control Apparatus

The diesel-powered locomotive with electric drive demands a relatively new type of apparatus in railway service to be placed in quantity on each locomotive. This apparatus is used to co-ordinate the function of the diesel-power unit, the electric drive, and the engineman. Commonly, this type of apparatus is referred to as the electric control equipment. With the installation of this new type of control equipment came the need for specialized shop facilities for overhaul and maintenance. The following outline of shop procedures is intended to be a typical sequence but should not be taken as an ironclad procedure to be used in every instance. It can, however, be taken as an aid in enumerating the items which should be considered in planning a shop to meet a particular set of conditions and requirements for equipment obtained from various manufacturers.

DISASSEMBLY

Electric control equipment which is removed from the locomotive unit to be overhauled should at once be tagged and marked as to model, size, and number. While this extensive tagging appears to be rather unnecessary, it will be of great value in maintaining correct equipment records and permit the interchangeability of parts in conformance with manufacturers' parts books. For example, a transition relay removed from an early passenger locomotive unit may be installed on a passenger unit of later manufacture and different type if the part number for this particular item corresponds. All devices which must be cleaned in chemical solution should use tags which withstand the cleaning operation and remain legible. Preliminary cleaning will in general, remove the accumulation of dirt, grease, oil, and other foreign substances. Due to the fact that control equipment consists of a number of nonmetallic parts as well as various metallic parts, it becomes necessary to separate the different types of parts so that they may not be damaged by the warm cleaning agent. A plain suction vacuum cleaner is often useful in removing carbon and steel dust particles.

On all electropneumatic devices it is advisable first to remove the specifically electric equipment such as coils, and so forth, and clean the devices connected with the air operation separately.

DISTRIBUTION

All cleaned equipment designated for overhaul should be checked at one central inspection station, and at this time it should be determined if the part is fit for overhaul or should be replaced. The equipment which has been found worthy to be overhauled is forwarded to the designated shop repair section for each particular part and placed on storage racks marked so that individual parts may be properly identified. The same part when completely overhauled will be placed on the other side of these racks indicating that it is ready for installation or shipment

A small shop truck is best suited for handling the traffic between the various departments. Most of the control equipment is not too heavy and can be handled without large crane facilities. However, handling some parts on roller conveyors will speed operation in sections where traffic of small parts is extremely heavy. To utilize test equipment to the fullest extent, high potential test sets should be mounted on insulated boards on top of a table which can be wheeled around the test area of a small-parts section. Sufficient pans, boxes, and containers should be provided to facilitate the rapid assembly of equipment composed of comparatively small parts.

PRELIMINARY TESTING

Each repaired part should undergo a preliminary test which reproduces the action it must take when operating on the locomotive unit by means of a simple but accurate test device. It is necessary to have a constant voltage of 74 volts d-c as well as 110 volts a-c available at all points in the small-parts repair section. A source of high current will be required to test the battery-charging voltage-regulating relay and the current-limit controls on certain units as well as excitation panels. In general, an old electric welding set can be modified to produce the necessary results.

REPAIR EQUIPMENT

Compressed air should be available at all work benches. The benches used for repair of control equipment should be located close to rotary bins which contain all the bolts, nuts, washers, and other small items necessary. Most of the electric control equipment work will be concerned with the handling of comparatively small parts which require careful adjustment. It is essential to have good lighting. Small drills, hand tools, wrenches, pliers, and so forth, play an important part in this electrical shop. It is advantageous to hang tools, such as small power tools on a steel cable directly over the work bench and control the vertical movement of these tools by means of spring balancers. Some insulated benches should be provided for testing certain electric equipment, and for some devices it becomes necessary to have benches constructed of nonmagnetic material to permit the calibration of magnetic devices. It also becomes necessary to provide some kind of overload protection on all test outlets on benches. Small circuit breakers are most suitable for this application. To improve the appearance of a finished job and also in some instances to restore the insulation characteristics, it is necessary to repaint or respray certain parts of the control equipment. Extreme care should be taken to prevent paint being deposited on electric contact surfaces.

TEST PANELS

It is advisable to build portable test panels adaptable to a general test bench for testing a specific piece of equipment. The test panels should be designed to fit on the end of the bench, and the connections should have lead blocks which fit on the bench outlets and if necessary have self-closing air couplings. Controls, switches, meters, lights and rheostats necessary for conducting tests should be mounted on shock absorbing material to prevent changes of settings due to vibration. Wherever there is a great amount of a particular control device to be tested, a permanent test panel installation will be justified. Special attention should be paid to arranging the mounting brackets of any device to be tested so that it is in the same position as the mounts for this device located on a locomotive unit, and in critical cases surrounding vibration conditions on a locomotive should be duplicated on the test panel. For contactors it is possible to develop a mounting fixture which can be effectively used for all types of large contactors of various manufacturers. Small relays should not be mounted on the same contactor stand, since the vibrations set up by the constant opening and closing of large contactors during the test period might affect the previous test settings of small relays. Each shop should try to develop additional mounting fixtures to meet the requirements of particular jobs and reduce the time required to set up this special type of equipment.

Small devices which can be tested in multiple operations should be so grouped and connected to mechanical counting devices to indicate the number of cycles performed by each relay and also connected to a system of lights which will indicate a defective relay. It is our ultimate goal to develop a frame structure which permits the preassembly of the major portion of the control equipment on the shop floor where it can be tested as a complete assembly and then mounted as a unit on the locomotive. As a further attempt to decrease the number of men working in the limited space within a locomotive unit, there appears to be the possibility of utilizing a development of the radio industry of having a large amount of control wires moulded in a newly developed plastic transparent board or panel. This should reduce the amount of control difficulty encountered on the road caused by broken wires, chafed insulation, and so forth.

Governors and Fuel Injection Equipment

It is advisable to separate the overhaul and repair of governors and fuel injection equipment from the normal shop reconditioning areas and locate this type of work in a pressurized dustproof section of the shop. Since the manufacturers of diesel locomotives employ vastly different principles of governor control, it is necessary to segregate test equipment in the governor repair section for each particular type of governor to be tested. It becomes necessary to purchase specialized test equipment developed for the type of equipment involved from such manufacturers as American Bosch, General Electric, and so forth. Most engine governors employ mechanical and electric equipment coupled together to produce the desired mechanical actions as dictated by the requirements of the electric power transmission system of the locomotive unit. It is for this reason that the repair of electric as well as mechanical parts for governors is done in the same location, and that the injector equipment, which is of mechanical nature, is also placed in this dustproof section of the shop. It appears advisable to have men trained for the specialized work on the equipment handled in this particular section of the shop.

Work Remaining in Locomotive Unit

Although the greatest amount of repair work performed on diesel locomotive equipment is done outside the locomotive unit in specialized repair sections, there still is a large amount of work remaining which must be completed in the locomotive unit which is time consuming. While progress has been rather slow to find ways and means to expedite this type of work more efficiently, I believe that we have started in the right direction. In the near future we hope to be able to report further progress in this specialized field of work. We would appreciate greatly if the members of the American Institute of Electrical Engineers would continue to give us their co-operation and help, and any constructive criticism would be most welcome.

◆

Discussion

J. W. Teker (General Electric Company, Erie, Pa.): The magnitude of the tasks confronting railroads undergoing revolutionary changeover of motive power is not generally appreciated. Especially so, when we consider that the move from steam to diesel-electric power is being accomplished without perceptible interruption of service. The scope of this subject is certainly wide enough for several papers. Mr. Thomas has most effectively condensed present-day thinking in his presentation of the subject. My remarks only serve to supplement what Mr. Thomas has outlined.

Centralization of shop facilities is fundamentally sound. The concentration of volume allows a repetitive division of work, so each man acquires proficiency at his assigned task. Many of these tasks on electric apparatus are mechanical in nature and can be done by machinists or men with some mechanical background or training. The strictly electrical aspects of the job can then be handled by comparatively fewer electrically trained men. Such an arrangement makes it possible to direct the effort of a large electric repair organization with a few, and for the time being, harder-to-find capable electrically trained supervisors. These advantages would be lost if heavy repairs were wide spread.

Furthermore, centralization fixes responsibility which, in turn, stimulates proficiency and excellence of work quality. A case in point is the pulling of motor pinions. The hydraulic method can be used over an entire railroad system without hazard to the heat treatment of the pinion. But the setup time and labor may be greater than with the induction method which, in turn, involves the potential hazard of overheating a pinion if used improperly. Centralization should make it feasible to provide the right sizes, implements, and control so that induction heating can be used on the various makes of motors without damage to pinions or bearing assemblies. One man can be trained, kept busy, and held responsible for the proper execution of this duty.

The same arrangement would apply to the mounting of pinions. However, where the practice is followed of keeping pinions matched with gears, this training and responsibility problem is more difficult as the pinions are pulled and mounted at the several points of motor changeouts.

Practices vary and might be considered still in their evolutionary stages. In time best practices tend to be standardized. For instance, the seasoning of commutators before winding is certainly the best kind of precaution. Seasoning after winding to stabilize the commutator which has been subjected to the impacts of setting leads and high soldering temperatures is also desirable. But only after careful economic study over a period of time will it be known whether both seasoning operations are justified.

In addition to the repair and reconditioning of equipment, the shop may also conduct a continuous modernization program. Locomotive units are brought up to date and go back into service with increased ratings, higher horsepower, or with greater uniformity and standardization of parts. This alone is a sizeable but very worth-while task.

Centralization of shops provides opportunity for the study of returned equipment, permits analysis of defects by capable personnel, and aids in the accumulation of data which should provide a basis for corrective action in operation, running maintenance, and design for the improvement of motive power.

F. Thomas: It is with pleasure that I note in Mr. Teker's discussion that the policy which I outlined is looked upon by manufacturers' representatives and possibly other railroads as being sound.

The paper covers the thoughts of the larger railroads who, of course, maintain many types of various manufacturers' diesel-electric locomotives, and in order to keep the cost per mile for operation down, these railroads must purchase the finest of machines necessary for the repair and testing of the electric equipment.

The shop picked must be large enough to set up a production line of work, must have ample equipment installed, and must be well lighted; also as good a supervising personnel as possible must be selected. In this way it can be run efficiently and economically, requiring a fewer number of trained personnel for the various tasks performed.

I believe papers of this kind will do much to help the railroads in their changeover from steam to diesel when properly publicized and certainly will mean a closer relation between the railroads and the various manufacturers. This should, as time goes on, give the railroads and the manufacturers a much improved piece of motive power.

An Analytical Solution of Heat Flow Versus Wire Temperature for Electric Cables Buried in Plaster

J. E. GOFF
ASSOCIATE MEMBER AIEE

COMPLETE electric heating installations are becoming quite general throughout certain areas. A popular type is the resistance cable embedded in plaster to form a radiant panel heater. For long cable life and maximum safety, the cable temperature must not exceed a definite limit. Various investigators have derived equations describing the temperature throughout the panel. However such equations do not relate temperature to heat input or else they are based on conditions not met in electric cable heating. K. Kalous[1] developed equations for embedded pipe using hot water based upon the simplified assumption that heat flows laterally through the panel. This assumption is valid for panel thicknesses near pipe diameter and for pipe spacing, which is large when compared to panel thickness. Neither condition is met in electric cable heating. T. Napier Adlam[2] publishes curves for pipe buried in plaster. The pipe sizes and spacings however, are quite large as compared to electric cable sizes and cable spacing.

Shoemaker[3] presents a solution for temperature throughout a panel, using embedded pipe for conditions based upon an equivalent conductivity panel. It presumes a known pipe temperature and describes the temperature at any point in the panel, while the wire temperature of heating cable is an unknown factor. Also the work does not present a solution that will enable one to solve the pipe temperature for a known British thermal unit (Btu) output, nor solve for Btu output for a known pipe temperature. The cable temperature for a known Btu per foot input is one of the most important design considerations. Due to the intrinsic characteristics of cable heating, there is a constant heat input per foot of heating cable and the cable temperature must adjust to dissipate this input. Hence the need to determine maximum cable temperature is apparent. Previous cable designs have been made largely from experimental data and this does not always lend itself to optimum design.

This paper will show how the work of Shoemaker can be extended to give analytical solution of this problem, and will include experimental data to verify the solution.

Discussion of Work by Shoemaker

In the derivation of his solution for the temperature function in the panel, Shoemaker[3] replaced the actual heating panel by an equivalent panel. The relation between the actual panel and equivalent panel is shown in Figure 1. The actual heating panel consists of layers of materials of different conductivity and

---

Paper 53-71, recommended by the AIEE Domestic and Commercial Applications Committee and approved by the AIEE Committee on Technical Operations for presentation at the AIEE Winter General Meeting, New York, N. Y., January 19–23, 1953. Manuscript submitted March 12, 1952; made available for printing December 3, 1952.

J. E. Goff is with the Ceil Heat Division of Homes, Inc., Knoxville, Tenn.

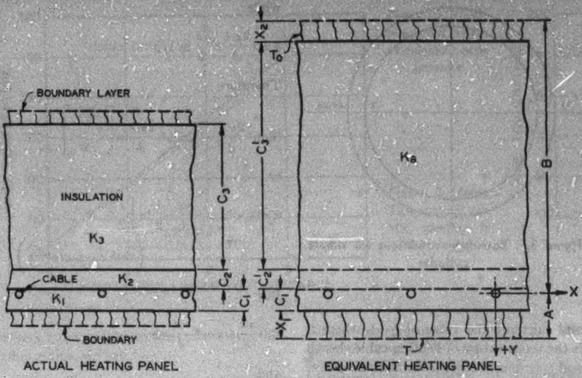

Figure 1. Actual and equivalent heating panel

thickness. In the equivalent panel, the different materials are replaced by one material of conductivity k_a. In order to keep the net thermal resistance of each layer constant, it is necessary to adjust the thickness of that layer in the equivalent panel by the following equation

$$c_j' = c_j \frac{k_a}{k_j} \tag{1}$$

where

k_a = equivalent conductivity used in equivalent panel.
k_j = actual conductivity of jth layer of actual panel.
c_j = actual thickness of jth layer of actual panel.
c_j' = equivalent thickness of jth layer of actual panel used in equivalent panel.

This is justified if the flow lines are perpendicular to the parting plane of the two media of different conductivity. Electric cables have small diameters, are closely spaced, and only materials of relatively high conductivity are used near the cable. Also the cables are embedded in the surface layer so that no change in conductivity occurs between cable and panel surface. These combine to make this simplifying assumption valid.

The second assumption replaces the film coefficient by an equivalent layer x_i of conductivity k_a as follows

$$x_i = \frac{k_a}{f} \tag{2}$$

This presumes that the film coefficient f is a constant while it is actually a function of panel surface temperature.

Here again the close spacing and high conductivity combine to give nearly constant panel surface temperature so that the variation in f will be less than the error in measurement in the actual system. Therefore this assumption should be readily accepted.

It is well known that steady-state heat flow must satisfy Laplace's equation which follows

$$\frac{\partial^2 T}{\partial x^2} + \frac{\partial^2 T}{\partial y^2} = 0 \tag{3}$$

Shoemaker shows the solution for $T(x,y)$ subject to the boundary conditions outlined in Figure 1 to be as follows

$$T(xy) = \alpha\theta(x,y) + \beta y + \gamma \tag{4}$$

where

$$\theta(x,y) = \frac{1}{2}\ln\left[\sin^2\frac{\pi x}{d}\cosh^2\frac{\pi y}{d} + \cos^2\frac{\pi x}{d}\sinh^2\frac{\pi y}{d}\right] - \frac{1}{2}\ln\left[\sin^2\frac{\pi x}{d}\cosh^2\frac{2A-y}{d} + \cos^2\frac{\pi x}{d}\sinh^2\frac{2A-y}{d}\right]$$

$$\alpha = \frac{1}{\Delta}[A(t_w - t_0) + B(t_w - t)]$$

$$\beta = \frac{1}{\Delta}[\theta(r,0)(t - t_0) + \theta(0,-B)(t_w - t)]$$

$$\gamma = \frac{1}{\Delta}[A\theta(r,0)t_0 + B\theta(r,0)t - A\theta t(0,-B)_w]$$

$$\Delta = (A+B)\theta(r,0) - A\theta(0,-B)$$

Other constants as defined in Figure 1.

Note that Btu per foot of pipe does not enter into this solution. The constant α is related to heat input but cannot be used directly to calculate this data.

Heat Flow for Concentric Cylinders

Let us digress for a moment and examine the problem of electrostatic fields. It is known that the boundary conditions for temperature in steady-state heat flow are formally identical with those for electrostatic potential. James Clerk Maxwell[4] developed the equations for the electrostatic field of a wire grating which is shown in Figure 2. Figure 2 shows that the closer one approaches the wire, the more nearly the equipotential lines approach circles, and correspondingly the more nearly the isotherms approach

Table I. Values of Film Coefficient Versus Panel Surface Temperature

Panel Temperature, Degrees Fahrenheit	Film Coefficient
90	1.48
100	1.49
105	1.50
110	1.51
115	1.52

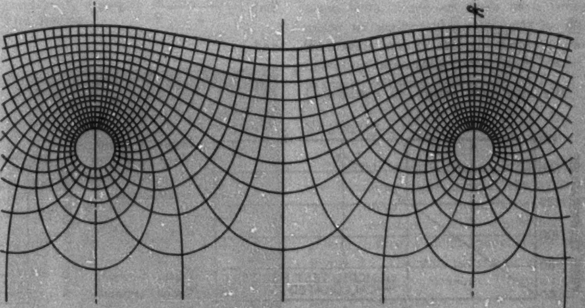

Figure 2. Maxwell's lines of force near a grating

circles in heat system. At a distance Δr from the wire, these isotherms are circles. This is an important result. The isotherms are circles so that the boundary values reduce to constants, and one may easily calculate the heat flow between two cylinders separated by a distance Δr and a medium of constant conductivity. The heat flow from a single cable through a ring Δr under these boundary conditions can be calculated quite easily; substitute for temperature difference across the boundary as determined by equation 2 and the result will give the heat flow temperature relation for each cable in the grid arrangement. Figure 3 shows such a simple arrangement.

Let us determine the temperature heat flow of the simple case in Figure 3 as follows

$$H=-kA\frac{dt}{dx}$$

This may be written

$$t=-\int\frac{H}{kA}\,dx$$

where

$A=(2\pi rZ)/12=$area of cylinder through which heat flows radially outward
$r=$radius of cylinder
$Z=$length of cylinder
$H=$heat input to cylinder Btu per hour
$k=$thermal conductivity

Substituting

$$t=-\int\frac{12H}{2\pi k_aZ}\frac{dr}{r}$$

where

$t_1\geqq t\geqq t_2$
$r_1\geqq r\geqq r_2$

or

$$t_1-t_2=\frac{12H}{2\pi k_aZ}\ln\left(\frac{r_2}{r_1}\right)$$

and

$$\frac{H}{Z}=\frac{\pi k_a}{6\ln\left(\frac{r_2}{r_1}\right)}(t_1-t_2) \qquad (5)$$

We may now return to equation 4 and calculate the value of t_1-t_2 where t_1 is the temperature of heating cable sheath and t_2 is temperature a distance Δr away. Since we are dealing with a circle of constant temperature, we may select any point on the circle to calculate t_2. Let us select the point $(x+\Delta x,\ 0)$ to calculate t_2.

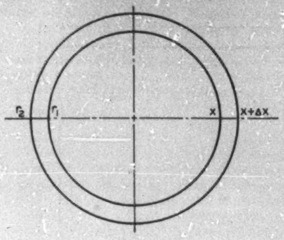

Figure 3. Boundary conditions for simple cylinder

Therefore

$$t_1=T(x,\ 0)$$
$$t_2=T(x+\Delta x,\ 0)$$
$$t_1-t_2=T(x,\ 0)-T(x+\Delta x,\ 0)$$
$$t_1-t_2=\alpha\theta(x,\ 0)+\beta(0)+\gamma-\alpha\theta(x+\Delta x,0)-\beta(0)-\gamma$$
$$t_1-t_2=\alpha[\theta(x,\ 0)-\theta(x+\Delta x,\ 0)] \qquad (6)$$

Substituting equation 6 into equation 5 we get

$$\frac{H}{Z}=\frac{\pi k_a}{6\ln\left(\frac{r_2}{r_1}\right)}(\alpha)\ [\theta(x,\ 0)-\theta(x+\Delta x,0)] \qquad (7)$$

This can be greatly simplified as follows

$$\theta(x,\ 0)=\ln\sin\frac{\pi x}{d}-\frac{1}{2}\ln\left[\sin^2\frac{\pi x}{d}\times\cosh^2\frac{2\pi A}{d}+\cos^2\frac{\pi x}{d}\sinh^2\frac{2\pi A}{d}\right]$$

But

$$\text{Sinh}\ x=\frac{\epsilon^x-\epsilon^{-x}}{2}=\frac{\epsilon^x}{2} \qquad x>4$$

and

$$\text{Cosh}\ x=\frac{\epsilon^x+\epsilon^{-x}}{2}=\frac{\epsilon^x}{2} \qquad x>4$$

while

$$4\pi>\frac{2\pi A}{d}>\frac{3\pi}{2}\ \text{in typical panels}$$

Therefore

$$\text{Sinh}^2\frac{2\pi A}{d}=\text{Cosh}^2\frac{2\pi A}{d}=\left[\frac{\epsilon^{\frac{2\pi A}{d}}}{2}\right]^2$$

or

$$\theta(x,0)=\ln\sin\frac{\pi x}{d}-\frac{1}{2}\ln\left[\frac{\epsilon^{\frac{4\pi A}{d}}}{2}\times\left(\sin^2\frac{\pi x}{d}+\cos^2\frac{\pi x}{d}\right)\right]$$

But

$$\sin^2\frac{\pi x}{d}+\cos^2\frac{\pi x}{d}=1$$

and

$$\frac{1}{2}\ln\frac{\epsilon^{\frac{4\pi A}{d}}}{2}=\frac{2\pi A}{d}-\ln 2$$

Therefore

$$\theta(x,0)=\ln\sin\frac{\pi x}{d}-\frac{2\pi A}{d}+\ln 2$$

Similarly replacing x by $x+\Delta x$

$$\theta(x+\Delta r,0)=\ln\sin\frac{\pi(x+\Delta x)}{d}-\frac{2\pi A}{d}+\ln 2$$

and

$$\theta(x,0)-\theta(x+\Delta r,0)=\ln\sin\frac{\pi x}{d}-\ln\sin\frac{\pi(x+\Delta x)}{d}=\ln\frac{\sin\frac{\pi x}{d}}{\sin\frac{\pi(x+\Delta x)}{d}} \qquad (8)$$

By similar process noting that B is large compared to d

$$\theta(0,-B)=-\frac{2\pi A}{d} \qquad (9)$$

and Δ becomes

$$\Delta=(A+B)\ln 2\sin\frac{\pi x}{d}-\frac{2\pi AB}{d} \qquad (10)$$

Substituting equations 8, 9, and 10 into equation 7 and noting that $x=r_1\equiv r$ (the cable radius) and $x+\Delta x=r_2\equiv r+\Delta r$

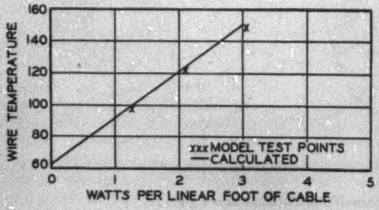

Figure 4 (left). Watts per foot of cable versus temperature

Figure 5 (right). Cable temperature versus cable spacing

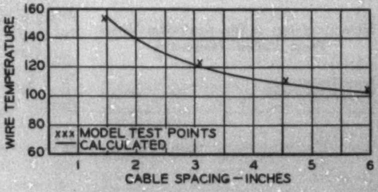

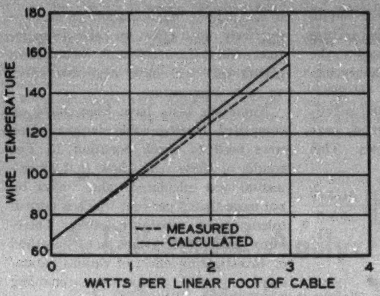

Figure 6 (left). Measured versus calculated temperature

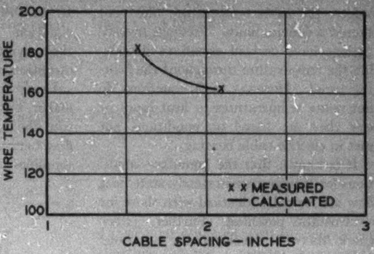

Figure 7 (right). Temperature versus spacing in test house

where r and $r+\Delta r$ are distance along the plus x axis, we get

$$\frac{H}{Z}=-\frac{\pi k_a}{6}\left[\frac{A(t_w-t_0)+B(t_w-t)}{(A+B)\ln 2\sin\frac{\pi r}{d}-\frac{2\pi AB}{d}}\right]\times\left[\frac{\ln\dfrac{\sin\frac{\pi(r+\Delta r)}{d}}{\sin\frac{\pi r}{d}}}{\ln\dfrac{r+\Delta r}{r}}\right] \quad (11)$$

But

$$\sin x=x-\frac{x^3}{3}+\frac{x^5}{5}+\ldots+$$

This is a convergent alternating series. The error in using N terms is always less than the $N+1$ term. When x is less than 0.2, the error in using only the first term of the series is less than 0.5 per cent. In this case $(\pi r)/d$ will always be small and less than 0.2. Therefore

$$\frac{\ln\dfrac{\sin\frac{\pi(r+\Delta r)}{d}}{\sin\frac{\pi r}{d}}}{\ln\frac{r+\Delta r}{r}}=\frac{\ln\frac{r+\Delta r}{r}}{\ln\frac{r+\Delta r}{r}}=1$$

and

$$\frac{H}{Z}=-\frac{\pi k_a}{6}\left[\frac{(A+B)t_w-At_0-Bt}{(A+B)\ln 2\sin\frac{\pi r}{d}-\frac{2\pi AB}{d}}\right] \quad (12)$$

or

$$t_w=\frac{-6H}{\pi k_a Z}\left[\ln 2\sin\frac{\pi r}{d}-\frac{2AB\pi}{d(A+B)}\right]+\frac{At_0+Bt}{A+B}$$

where

t_w = wire temperature
H/Z = Btu per foot of cable
r = radius of cable
d = spacing between wires center to center
t = room temperature
t_0 = temperature behind panel
t_w = temperature of cable
k = thermal conductivity of equivalent medium (for k_a, see Figure 1)
A = see Figure 1
B = see Figure 1

Discussion of equation 12 shows several interesting results.

1. t_w is a simple direct function of H, which was an expected result.

2. t_w is a simple function of K_a for a fixed A and B, where A is depth of bury of cable in equivalent panel. This was unexpected since where the physical configuration of actual panel is fixed, t_w is a complex function of K. The equivalent depth of bury A is $K_a/f+\Sigma c_j(K_a/K_j)$. When this is substituted for k_a, f, c_j, K_j one finds that relatively large changes in K_a have a small effect on cable temperature.

3. Wire temperature is only slightly affected by changes in t_0, that is, in the well insulated panel, $B>>A$ so that cable temperature is little affected by flooring or a heated room over the panel.

4. Cable temperature is directly related to A, which is directly related to depth of bury and film coefficient.

5. In most cases $\ln 2\sin\frac{\pi r}{D}$ is small compared to $\frac{2\pi(AB)}{d(A+B)}$ so that wire temperature is a simple inverse function of wire spacing.

Figure 8

Experimental Results

These equations were derived as a consequence of work done with an electrical analogue computer that used the same equivalent panel. The obvious steps were to compare the results obtained with the two systems. Two items were checked. The first was a curve of wire temperature versus power per foot for a constant spacing. The result is shown in Figure 4. The second test was to compare the effect of spacing on the wire temperature for a constant input per linear foot. The results are shown in Figure 5.

Since the model and mathematics were both based upon the same assumption, it was felt that an actual check should be made in a test house to compare results. Consequently a house 4 feet by 8 feet by 8 feet was constructed with heat loss factors adjusted to give the same conditions as a typical room with zero outside temperature. It was operated with $1^1/_2$-inch spacing and the power per foot was varied. The results of the test are presented in Figure 6.

Tests using cable embedded in sand over gypsum board were conducted as part of the test house work. The results are shown in Figure 7. In addition to these tests, numerous tests have been made to verify cable designs. In all such tests, one is able to calculate the operating temperature of a cable buried in plaster within a few degrees.

Summary

Complete electric heating installations are becoming quite general throughout certain areas. A popular type is the electric resistance cable embedded in plaster to form a radiant panel heater, see Figure 8. The intrinsic characteristic of cable heating is a constant I^2R input per foot of heating cable and the cable temperature must adjust to dissipate this heat. For long cable life and maximum safety, the cable temperature must not exceed a definite limit. Previous investigations have derived equations describing the temperature throughout the heating panel. However such equations do not relate temperatures to heat input or else they are based on conditions not met in electric cable heating.

It is known that the boundary conditions for temperature in steady-state heat flow are formally identical with those for electrostatic potential. Further, James Clerk Maxwell[4] developed the equations for the electrostatic field of a wire near a grating. Examination of this work shows that the closer one approaches the wire, the closer the equipotential lines approach circles and correspondingly the more nearly the isotherms approach circles in the heat system. It can be shown that at a distance Δr from the wire these isotherms are circles. Thus a simple method of obtaining a relation between cable temperature and heat input is suggested. The isotherms at a distance Δr from the round cable are circles and since the heat flow between concentric circles can be readily calculated, it only remains to find a way to calculate the temperature difference (Δt) between the isotherm circles (Δr) apart in the heating panel to relate cable temperature to heat input. R. W. Shoemaker in his book[3] derived an equation describing the temperature throughout a heating panel, based on the conditions normally met in cable heating.

Using the equation derived by Shoemaker, one may calculate Δt and substitute the value in the equation for heat flow between the isotherm circles. This simplifies to the following

$$t_w=\frac{-6}{k_a\pi}\frac{(H)}{(Z)}\left[\ln 2\sin\frac{\pi r}{d}-\frac{2\pi AB}{A+B}\right]+\frac{At_0+B_t}{A+B} \tag{1}$$

where

t_w = cable temperature
H/Z = cable input in Btu per foot
K_a = equivalent thermal conductivity of media
r = radius of cable
d = spacing of cable center to center
A = depth of bury of cable in equivalent panel
B = depth of equivalent panel behind cable
t_0 = temperature behind panel
t = room temperature

Examination of equation 1 shows that t_w is a simple direct function of heat input per foot of cable and of the equivalent depth of cover of cable. Cable temperature is approximately an inverse function of spacing. The most surprising result is that A is a function of K_a so that when typical values are substituted in the equation, one finds that variations in K_a have relatively small effect on cable temperature. Thus the usual small variations in plaster mix will have negligible effect on cable temperature.

Numerous tests have been made on completed heating cable designs which were used to check equation 1. The results of these tests show that experimental and calculated values differ by not more than 5 per cent which is normal tolerance on resistance cable. Therefore equation 1 represents an easy method of investigating effect of various parameters on cable temperature, enabling cable manufacturers to prepare general installation instructions prescribing safe installation practices. Experimental work is required only to verify the original design data as with any new product.

References

1. GENERAL THEORY OF RADIANT HEAT, **K. Kalous.**

2. RADIANT HEATING (book), **T. Napier Adlam.** The Industrial Press, New York, N. Y.

3. RADIANT HEAT (book), **Richard Woolsey Shoemaker.** McGraw-Hill Book Company, New York, N. Y. 1948.

4. A TREATISE ON ELECTRICITY AND MAGNETISM (book), **James Clerk Maxwell.** Clarendon Press, Oxford, England, volume I, Figure XIII, article 203.

Discussion

S. B. Hammond (Stanford University, Stanford, Calif.): A solution of Laplace's equation in two dimensions attributed to Shoemaker[1] is the basis of this paper by Goff. Shoemaker's solution, equation 4, is in an unwieldy form which Goff has solved for cable temperature as functions of cable size and spacing, depth of bury, British thermal units per foot of cable, and conductivities and dimensions of panel.

The mathematics is fairly straightforward. There are several approximations necessary to simplify the results which must be kept in mind if the final equation, equation 12, is to hold with any accuracy. The first requires the ratio A/d to be greater than $\pi/4$. The definitions of terms A and d are given in Figure 1. Now A is the equivalent thickness of a single homogeneous heat conductor between the electric cables and the heated room, including plaster and boundary layer. If this ratio were smaller, say $A/d=1/2$, an additional error of maybe 5 per cent would be introduced into equation 12 for cable temperature. However, as this ratio decreases further, the error increases at a rapidly increasing rate. A similar restriction is imposed on the ratio of B/d.

A further assumption requires r, cable radius, to be very small compared to d, the distance between adjacent cables, in order to simplify equation 11. This seems to conform well with practice.

Equation 12 for cable temperature may be further simplified by noting the log term in the brackets is usually considerably smaller than the second term in the brackets. Thus the equation can be written with little additional error

$$t_w=-\frac{12ABH}{kZd(A+B)}+\frac{At_0+Bt}{A+B}$$

Mathematically the minus sign is correct in this equation, but from physical considerations it appears this sign should be plus.

Consider next the case in ordinary house wiring where d is very large. It would appear that the preceding equation would give the temperature of the cables. However, the restriction was previously made that the ratio of A/d must be greater than $\pi/4$. Actually, equation 12, or the preceding equation, can only be used where the cables are uniformly spaced and cover a large surface area. From the methods used by Shoemaker and Goff it should be possible to derive an equation that would give the temperature of a single cable. These equations will not.

REFERENCE

1. See reference 3 of the paper, pages 264–67.

J. E. Goff: Mr. Hammond points out that one cannot calculate the temperature of a single conductor embedded in plaster using the equations devised in the paper under discussion. If one uses the simplified formula in Mr. Hammond's discussion, one finds that the temperature of a single conductor is the same as room temperature, regardless of the heat input. This is obviously not true. If one uses the equation in the form quoted in the paper, one finds that the single wire temperature is infinite regardless of the input to the cable. This too is impossible, so that one must agree that the final result can not be applied to calculation of temperature for a single conductor. However, I would be greatly surprised if we got any other result.

Shoemaker states,[1] "For a single source, the temperature function that satisfies Laplace's equation for unity intensity is $\ln(1/R)$, if combined with an image, $\ln(1/R)-\ln(1/R')$. To represent an infinite string of sources, we need a periodic function with similar singularities; this is known to be $\ln\sin Z$ where $Z=K(x+iy)$." Thus in the very beginning of his development, Shoemaker admits that he is not attempting a solution for a single conductor but is developing a solution for an infinite number of conductors.

Further it must be recognized that A/d must be greater than $1/2$. This fact is used to neglect certain terms in making the solution easier to use. However, if one notes how A was defined and the restrictions imposed upon it, then one immediately discovers that an almost constant surface temperature was assumed. This condition is met in electric heating cable installations where the spacing is seldom greater than 3 inches. However, if D is large, the surface temperature becomes $f(x)$ and A is no longer a constant, and a boundary assumed constant for mathematical reasons is not a constant.

These equations were devised for use in design of cable heating systems for many conductors, spaced reasonably close together and covering a large area. Therefore, great care should be used in applying these equations to other types of systems.

Mr. Hammond also calls attention to an error in sign. Equation 12 should have a minus sign in front of the first term. It was also omitted in copying the same equation later in the paper. This equation should read as follows:

$$t_w = -\frac{6H}{\pi k_a Z}\left[\ln 2 \sin \frac{\pi r}{d} - \frac{2\pi AB}{d(A+B)}\right] + \frac{At_0+Bt}{A+B}$$

REFERENCE

1. See reference 3 of the paper, page 264.

A Differential-Analyzer Study of Certain Nonlinearly Damped Servomechanisms

R. R. CALDWELL
ASSOCIATE MEMBER AIEE

V. C. RIDEOUT
ASSOCIATE MEMBER AIEE

A SERVOMECHANISM must hold its error or the difference between input and output, to as small a value as possible. If a large error appears as a result of a rapid change in the value of an input position signal, then high acceleration and high output speed are desirable, and these in turn are favored by a low damping ratio. When the error is near zero, the speed should be reduced rapidly so that overshoot does not occur, and this requires a high damping ratio. Thus the use of nonlinear damping which has some inverse relationship to the error has been proposed by several investigators.[1–5]

Another approach to the design of a nonlinear servomechanism involves a consideration of the practical limit of the available torque of the servo motor. If some maximum torque T_m is available, then the best servo performance in response to an input step will be obtained if T_m is first applied in such a direction as to accelerate the load and reduce the error, and is then reversed so that $-T_m$ is applied to reduce output speed to zero. Such a servo is called a relay servo and for optimum response it requires a sensing and swtiching device.[3,6,7]

The nonlinear damping approach has certain advantages, such as the fact that the ordinary stability criteria may be applied for small errors, but it cannot ordinarily be expected to give as rapid a response to an input step as the relay or maximum-torque servo. However, the relay servo has difficulty with other than step-function inputs, and is not too satisfactory in its operation when errors are small.

In the course of investigating a number of nonlinearly damped servos with the aid of a high-speed differential analyzer[8] it was discovered that one of these nonlinearly damped servos tended to operate at very nearly maximum torque except when errors were small. Thus this servo combines the best feature of the relay servo and of the nolinearly damped servos. It was first built in simple form and tested for response to an input step by J. B. Lewis.[4] The differential analyzer study made it possible to compare the Lewis servo with others, and to extend the study to other than step inputs, and to the case where the servo contained more than one lag. As a result of this work some major modifications of this servo are suggested which give significant improvement in its operation.

Response Criteria

A number of criteria for comparison of servo responses have been suggested.[9,10,11] In this work the integral

$$I = \int |e|\, dt \qquad (1)$$

was used, where $|e|$ is the absolute value of the error. For a step-function input applied to the simple linear second-order servo this integral is minimized by a damping ratio of $\zeta = 0.65$, giving an error overshoot of 7 per cent.

The choice of this criterion was based on a compromise between computer adaptability and suitability of the measure obtained. Thus use of the absolute value of error rather than error squared reduces the unwanted emphasis on the large initial error, which is unavoidable with step-function inputs. The per cent of overshoot obtained with this criterion is within the range generally accepted as suitable for a large class of servo applications. The use of time weighting, although desirable from some points of view, gives rise to difficulties in computer setups which are not in proportion to the advantages gained.

Unfortunately the absolute-value-error integral is not easily handled analytically. However, an analytic solution can be obtained for the second-order linear system. For a step-function input of amplitude P and the underdamped case, the absolute value integral is

$$I = \frac{p}{\omega_0}\left[\frac{2\epsilon^{\sigma\theta}}{1-\epsilon^{-\sigma\pi}} + \sigma \sin\theta + \cos\theta - 2\epsilon^{\sigma\theta}\right] \qquad (2)$$

where

$\sigma = \zeta(1-\zeta^2)^{-1/2}$
$\tan\theta = (1-\zeta^2)^{1/2}\zeta^{-1}$

The computer setup used to determine this integral is shown in Figure 1. This setup was used with various servos tested with different inputs to give a numerical basis for comparison.

Computer Solution of Linear and Nonlinear Servomechanisms

Figure 2 shows the basic servo used in this study.[8] If the nonlinear device is inactivated and the amplifier has no lags, we have a simple second-order linear servo in which

$$\left[p^2 + \left(\frac{B+N}{I}\right)p + \frac{K}{I}\right]c = \frac{K}{I}r \qquad (3)$$

where

I = the inertia of motor plus load
B = the viscous friction damping coefficient
$N = k_t k_1 k_2$ is the tachometer damping coefficient
$K = k_1 k_2$ is the loop stiffness or gain

Paper 53-107, recommended by the AIEE Feedback Control Systems Committee and approved by the AIEE Committee on Technical Operations for presentation at the AIEE Winter General Meeting, New York, N. Y., January 19–23, 1953. Manuscript submitted October 23, 1952; made available for printing December 12, 1952.

R. R. Caldwell and V. C. Rideout are with the University of Wisconsin, Madison, Wis.

The material in this paper is based in part on a thesis presented by R. R. Caldwell in partial fulfillment of the requirements for the Doctor of Philosophy degree at the University of Wisconsin.

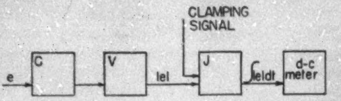

Figure 1 (left). Analogue computer setup for determination of absolute-error-integral criterion. Here the A-unit is an adder, the J-unit is an integrator, and the V-unit a full-wave rectifier, or absolute-value unit

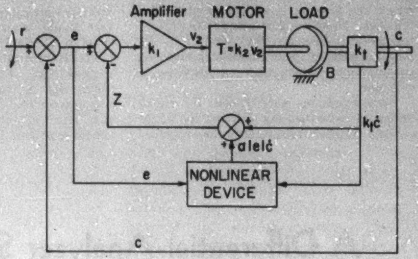

Figure 2 (right). Block diagram of basic servo studied in the paper. The linear form results if the nonlinear device is inoperative

We are chiefly concerned with the case where $B<<N$. The reference damping ratio is therefore chosen as

$$\zeta=\frac{N}{\sqrt{2KI}} \tag{4}$$

The characteristic frequency is

$$\omega_0=\sqrt{\frac{K}{I}} \tag{5}$$

By choosing a new time scale we can normalize with respect to ω_0 so that equation 3 becomes

$$[p^2+2\zeta(1+\alpha)p+1]c=r \tag{6}$$

where $\alpha=B/N$.

An analogue computer setup for solution of this second-order linear case is shown in Figure 3. A limiter has been added to limit the maximum motor torque. One or more lags, such as the one shown dotted in Figure 3, may be added if a higher order servo is to be investigated.

The type of nonlinear damping found to be most effective in this study was the kind in which a term proportional to the product of absolute error and output velocity $|e|\dot{c}$, was subtracted from the tachometer damping term.[4] This results in a total damping term (if $B/N<<1$) of $2\zeta\dot{c}-a|e|\dot{c}$. The block diagram of Figure 2 indicates how this damping may be applied in a servo. In practice, a rectifier might be used to obtain $|e|$, which might then be applied to the field of the tachometer to produce the $a|e|\dot{c}$ term. Thus normalized equation 6 becomes, for the Lewis nonlinearly damped case

$$\ddot{c}+2\zeta\dot{c}-a|e|\dot{c}+c=r \tag{7}$$

The analogue computer setup for this case is shown in Figure 4. The error integrals were computed as shown in the figure and used to aid in the comparison of transient responses.

Results

Step Input Signals

The peculiar advantages of the nonlinear servo of Figure 2 result from the fact that the nonlinear term not only reduces the damping when error is large but may actually make it negative if the proper magnitude relationship exists in equation 7. The constants were so adjusted that the damping did become negative for all but small initial errors. Thus, not only is the response to a step function better than the linear case, as shown in Figure 5(A), but the initial reduction in error is even faster than for the linear case with zero damping, as shown in Figure 5(B). The absolute-error-integral I is 4.0 units for the linear case and 2.8 units for the nonlinear case. The results of Figure 5 are for a servo of second order, with viscous damping B equal to zero, and with no torque limiting.

This servo, as shown in 5(C), gives much the same form of response for a wide range of input amplitudes, and in no case does overshoot occur. Reduction of overshoot is an advantage found in many nonlinear servos, but the smaller time of recovery obtained for smaller input steps is a unique advantage of this servo. The phase plane plot of Figure 5(D) also indicates improvement in response of the nonlinear servo in this simple case, for, as shown by MacDonald,[2] the area under this curve is inversely proportional to recovery time.

Figure 5 also shows the effect of torque limiting in this servo. Torque limitation was set at a value equal to the maximum torque attained by the linear system. This limitation had little effect on the time of response of the nonlinear system. The output torque is shown for the linear case in Figure 5(E) and for the corresponding nonlinear case in Figure 5(F). Note that in the latter case the torque tends to switch between values of $+T_m$ and $-T_m$, until the error is nearly reduced to zero. Thus, for this torque-limited case the operation of the nonlinear system is essentially the same as that of the optimum relay servo.

Figure 6 shows a comparison of the phase-plane trajectories for the optimum relay servo and the continuously damped torque-limited Lewis servo. Thus the torque-limited condition of this servo makes the best possible use of the maximum available torque.

Double-Step Input Signals

If, in the nonlinear system, the error is allowed to overshoot zero, the system may become unstable. Such a case is shown in the phase-plane plot of Figure 7(A), where stability is marginal, and the error is reduced to zero in only one out of three cases. This instability is the result of a change in the sign of the restoring torque which occurs when the nonlinear damping term $a|e|\dot{c}$ becomes too large. At the critical point the torque sign reversal causes the error to increase rather than decrease.

For the simple step input the parameters may easily be adjusted to eliminate the possibility of overshoot. However,

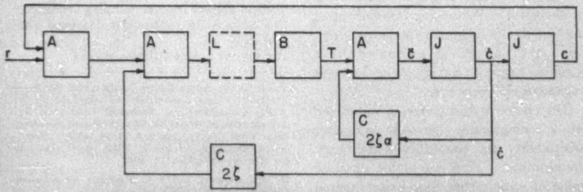

Figure 3. Computer setup used in the solution of the linear form of the servo of Figure 2. Here the B-unit is a limiter, and the L-unit is a lag (1/1+pT) which can be added as shown, or in other positions

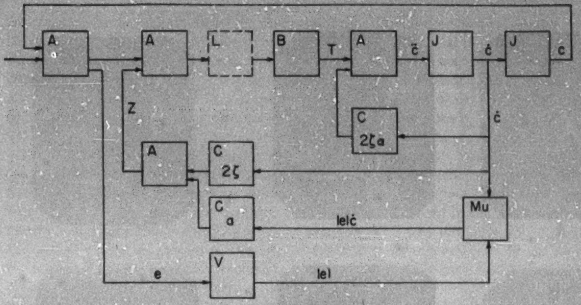

Figure 4. Computer setup used in solution of the nonlinear form of the servo in Figure 2; the Mu-unit is a multiplier

an input pulse, or a double-step input consisting of a positive step followed by an unequal negative step, can easily cause unstable action of the nonlinear system. This occurs when the input is suddenly reduced before the error caused by the original step is fully corrected. This may result in a change to a negative error while the velocity $\dot{c}$ is in the direction to correct a positive error. If the new negative error reduces the damping to zero, instability may result. The error will tend to increase without limit in either the first or third quadrant of the phase plane, much as in the case shown in Figure 7(A).

This tendency towards instability can be reduced by limiting the magnitude of the nonlinear term $a|e|\dot{c}$ to some experimentally determined maximum value. Using this type of limiting, it was found that a considerable improvement in stability could be obtained without substantially increasing the transient response time. This limiting treatment was also particularly effective in improving the servo response to sinusoidal input functions. Another very promising scheme, which has not yet been investigated, uses the $a|e|\dot{c}$ term only if the product $e\dot{c}$ is positive. This would always give full linear damping in the first and third phase-plane quadrants where $\dot{c}$ and e have opposite signs.

SINUSOIDAL AND SAW-TOOTH INPUTS

For a linear system, if either the transient or the frequency response is known then the other is completely determined. For the nonlinear system this is not the case. Thus it is necessary to extend the investigation of the nonlinear system beyond the study of transient response to

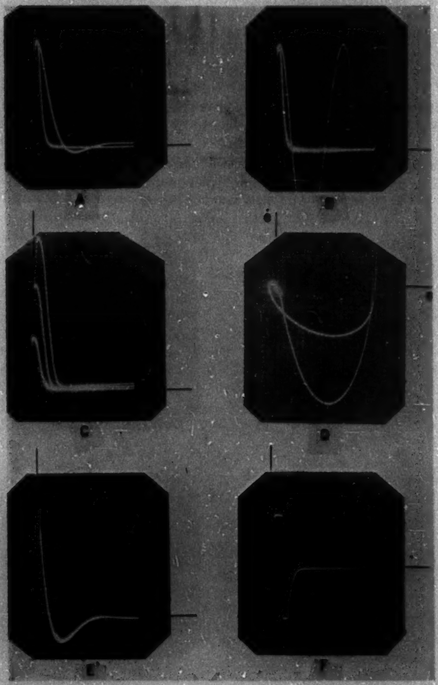

Figure 5 (left). Comparison of a nonlinearly damped servo with a linear second-order servo

A. Upper curve is the error for a step input to a linear servo ($\zeta=0.65$) and the lower curve is the error for a step input to the Lewis servo ($\zeta=2.2$, $a=0.7$)

B. Nonlinear servo error for an input step compared to that for the linear case with zero damping

C. Nonlinear servo error for three values of input step

D. Phase-plane plots for equal input steps; upper curve for the linear case, lower curve for the nonlinear case

E. Torque in the linear case (scale = 5 volts per large division)

F. Torque in the nonlinear case, with torque limited to the peak value found in the corresponding linear case, shown in D (scale = 10 volts per large division)

Figure 6 (below). Comparison of the phase-plane trajectories for an input step to the Lewis nonlinear and to the optimum relay servo

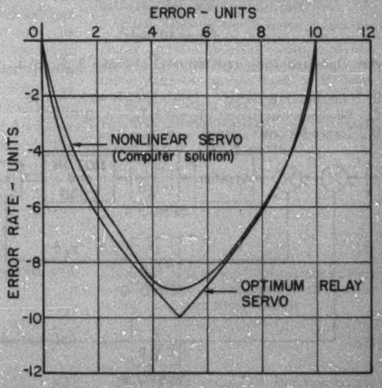

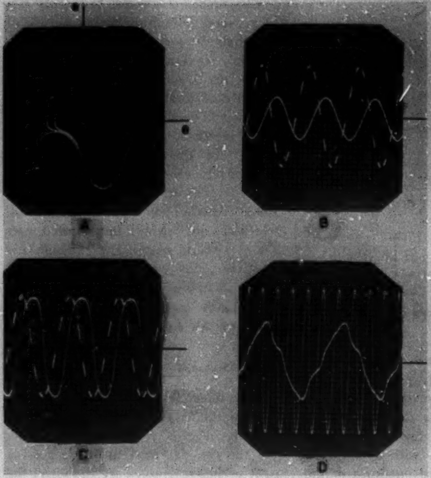

Figure 7

A. Instability in a nonlinearly damped servo
B. Response of a linear second-order servo ($\zeta=0.65$) to a sine wave, ($f=1.57$ cycles per second, input shown dotted)
C. The torque-limited Lewis nonlinear servo response to the sine wave of B
D. Frequency dividing (by five times) in a nonlinear servo ($f=4.92$ cycles per second)

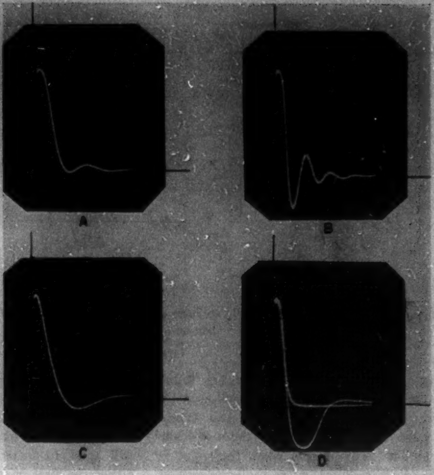

Figure 9

A. Optimized linear case, servo A of Figure 8, $T_A=0.6$, $\zeta=0.87$, $I=4.3$
B. Nonlinear case, servo A, $T_A=0.6$, $\zeta=2.2$, $a=0.7$, $I=3.9$
C. Optimized linear case, servo B of Figure 8, $T_B=0.6$, $\zeta=0.9$, $I=4.5$
D. Nonlinear case, servo B, $T_B=0.6$, $\zeta=3.7$, $I=3.3$ (upper trace), $\zeta=2.2$, $I=5.6$ (lower trace)

various step-function inputs. The computer setup used for the transient study is quite satisfactory for sinusoidal inputs. An audio oscillator was used as a sine-wave source since for this high-speed computer 382 cycles per second is equivalent to 1 cycle per second in real time.

The first noticeable effect of the nonlinear system is distortion of the output wave. This of course is to be expected, since the behavior of a nonlinear system is a function of amplitude. For the higher frequencies the nonlinear system does give an improvement in response as shown by a comparison of Figures 7(B) and (C). This improvement is in the form of increased output amplitude. At the higher frequencies larger torques

Figure 8 (below). Servo block diagram showing locations of added lags

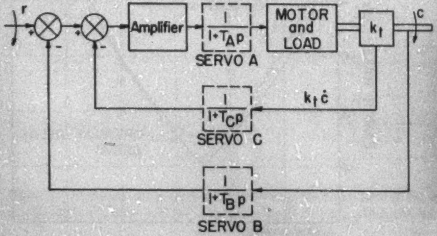

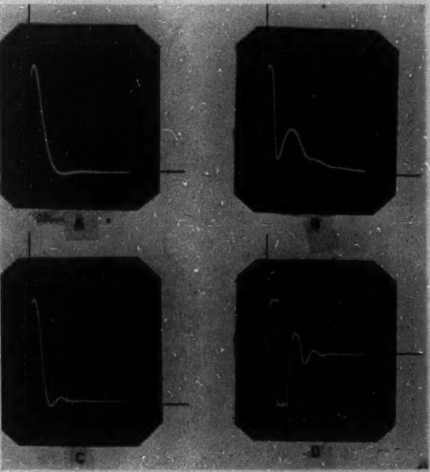

Figure 10 (right)

A. Optimized linear case, servo C of Figure 8, $T_C=0.3$, $\zeta=0.65$, $I=3.4$
B. Nonlinear case, servo C, $T_C=0.3$, $T_m=\pm 20$, $I=4.15$
C. Nonlinear case, servo C, $T_C=0.3$, $T_m=\pm 10$, $I=3.0$
D. Torque for case C above

are required for the output to follow the input. These increased torques can be supplied by the nonlinear system. The improvement of the phase of the output relative to the input is negligible. A lead network is more effective for the reduction of the phase lag.

Figure 7(D) shows a pathological effect caused by the nonlinear damping. This frequency division occurs for certain combinations of input amplitude and frequency. For magnitudes above or below the critical values the system will return to normal operation. This frequency division results when the $a|e|\dot{c}$ term is too large, so that a torque condition results which is similar to that discussed for the double-step case. Limiting the magnitude of $a|e|\dot{c}$ will return the system to normal operation. Varying degrees of limiting were found to be effective depending on the input amplitude and frequency. However, even with substantial limiting sufficient to remove all frequency-dividing effects, the high-frequency response of the nonlinear system is better than that of the linear.

Triangular input waves were also used, but gave no more information than the sine-wave inputs.

STEP INPUTS FOR HIGHER ORDER SERVOS

Although an unlimited number of higher order systems is possible, this study was limited to three cases corresponding to the addition of one or two simple lags in each of three positions in the system. The three locations of the inserted lags are shown by the broken-line blocks in Figure 8. The response of the nonlinear system is quite different in each case. Relatively large time-constant lags were used in an effort to emphasize the effect of lag. For smaller time constants, responses will differ from the second-order case by correspondingly smaller amounts.

For servo A, the nonlinear system transient response had a smaller error integral than the linear system, but had a rather large overshoot. The linear and nonlinear responses are shown in Figures 9(A) and (B). Thus for this servo the linear system may be preferred to the nonlinear if small overshoot is desirable.

With additional lags inserted, as in servos B and C, the transient responses of the linear and nonlinear systems are each similar in shape to their second-order counterparts. Figures 9(C) and (D) show the linear and nonlinear responses resulting for servo B. The two traces of Figure 9(D) result from use of the optimum damping ratio $\zeta=3.7$, and the damping ratio $\zeta=2.2$ used in the second-order system. This new optimum adjustment of ζ is of course necessary to fit the new system resulting because of the insertion of the lags.

For servo C, the linear and nonlinear responses are shown in Figures 10(A) and (B). The response of the nonlinear system is far from desirable. The unusual increase of the error in the positive direction is the result of excessive reverse torque brought about by the lagging $\dot{c}$ term. This condition may be corrected by another nonlinearity, such as the torque limiting which is present in any servo motor. This results in the nonlinear transient response shown in Figure 10(C), with the corresponding torque as in Figure 10(D).

NOISE

The operation of the nonlinear servo was studied for the case where random noise was added to various input signals. Noise peaks, if large enough, were found to give rise to the same instability problems found with double-step inputs. Smaller noise voltages gave effects which were much the same as those observed for the linear servo.

Conclusions

The nonlinearly damped servo described here has been shown by computer studies to have significant advantages over the corresponding linear servo, as well as over a number of other nonlinear servos. These studies have also shown that the responses to the various types of input signals must be carefully examined. Thus in the Lewis servo the nonlinear term $a|e|\dot{c}$, which is used to modify the damping, must in turn be modified to prevent undesirable responses or actual instability from occurring in the case of other than simple step input signals. In the computer studies made at the University of Wisconsin, a limiting of the $a|e|\dot{c}$ term was found to be helpful. It appears that servo performance may also be improved by reducing $a|e|\dot{c}$ to zero when the product $e\dot{c}$ is negative.

The complexities of even this relatively simple nonlinear servo are such that when the time constants and other constants are known for a practical case, it should probably be studied on a computer for the various input signals which might be encountered before the design is crystallized. It is hoped, however, that the study reported here will provide some kind of a guide in such design work, and act as an aid to future investigation.

References

1. Nonlinear Techniques for Improving Servo Performance, **Donald McDonald.** *Proceedings*, National Electronics Conference (Chicago, Ill.), volume 6, 1950, pages 400–21.

2. Multiple Mode Operation of Servomechanisms, **Donald McDonald.** *Review of Scientific Instruments* (New York, N. Y.), volume 23, January 1952, pages 22–30.

3. A Topological and Analog Computer Study of Certain Servomechanisms Employing Nonlinear Electronic Components, **R. C. Lathrop.** *Thesis*, University of Wisconsin, Madison, Wis., 1951.

4. The Use of Nonlinear Feedback to Improve the Transient Response of a Servomechanism **J. B. Lewis.** *AIEE Transactions*, volume 71, part II, 1953, pages 449–53.

5. A Phase-Plane Approach to the Compensation of Saturating Servomechanisms, **Arthur M. Hopkin.** *AIEE Transactions*, volume 70, part I, 1951, pages 631–39.

6. Theory of Servomechanisms, **H. L. Hazen.** *Journal*, Franklin Institute (Philadelphia, Pa.), volume 218, September 1934, pages 279–331.

7. Fundamental Theory of Servomechanisms (book), **L. A. MacColl.** D. Van Nostrand Company, Inc., New York, N. Y., 1945.

8. Catalog and Manual. George A. Philbrick Researches, Inc., Boston, Mass., 1951.

9. Calculation of the Optimum Parameters for a Following System, **C. Mack.** *Philosophical Magazine* (London, England), volume 40, September 1949, pages 922–28.

10. A Note on Control Area, **T. M. Stout.** *Journal of Applied Physics* (New York, N. Y.), volume 21, November 1950, pages 1129–31.

11. Some Design Criteria for Automatic Controls, **Paul T. Nims.** *AIEE Transactions*, volume 70, part I, 1951, pages 606–11.

◆

Discussion

Thomas M. Stout (University of Washington, Seattle, Wash.): I would like to offer a simplification of equation 2 of the paper and describe a related experimental procedure for determining the integrated absolute or squared error. This equation may be simplified by observing that

$$\sin\theta=(1-\zeta^2)^{1/2} \tag{1}$$

and

$$\cos\theta=\zeta$$

With these substitutions, the second and third terms reduce to

$$\sigma\sin\theta+\cos\theta=2\zeta \tag{2}$$

It is also convenient to write the equation in terms of an angle θ_1, such that

$$\tan\theta_1=-\tan\theta \tag{3}$$

and

$$\theta_1=\pi-\theta \tag{4}$$

where $\pi/2<\theta_1<\pi$. This angle is a direct measure of the time required by the system to first reach zero error, which is

$$t_1=\frac{\theta_1}{\omega_0\sqrt{1-\zeta^2}} \tag{5}$$

Making this change, the equation for the

Table I. Integrated Absolute Error for a Second-Order Servomechanism Subject to a Step Input of Magnitude P

ζ	$\frac{I\omega_0}{P}$
0.1	6.384
0.2	3.341
0.3	2.364
0.4	1.924
0.5	1.712
0.6	1.618
0.65	1.606
0.7	1.608
0.8	1.631
0.9	1.804
1.0	2.000

integrated absolute error of a second-order system subjected to a step input becomes

$$I=\frac{2P}{\omega_0}\left[\frac{\epsilon^{-\sigma\theta_1}}{1-\epsilon^{-\sigma\pi}}+\zeta\right] \qquad (6)$$

This form of the equation is particularly useful when ζ approaches unity, where the other equation leads to an indeterminate form. For $\zeta=1$, equation 6 of the discussion gives directly

$$I=\frac{2P}{\omega_0} \qquad (7)$$

which can also be obtained by direct integration of the error for the critically damped case. For $\zeta>1$, the integrated absolute error is the same as the integrated error and can be found[1] by adding the time constants of the closed-loop transfer function.

For purposes of comparison and to save future workers some labor, values computed from equation 6 are given in Table I of the discussion.

In some experimental studies similar to those described in the paper, we have been using a slightly different method for determining the integral of the error. In our case, a voltage proportional to the error was applied to an integrating amplifier in which the usual input resistor had been replaced by a diode rectifier. With this arrangement, only errors of one sign are integrated; the diode characteristics determine whether the absolute or squared error, or some intermediate power of the error, is used. Part of the integral is found by application of a positive signal to the input of the simulated servomechanism, and the remainder is found by applying an equal negative input, which simply means removing the previous signal.

This technique, although less elegant than the procedure described in the paper, is useful when the time constants in the computer simulation are fairly large, and it eliminates the need for an absolute value unit.

REFERENCES

1. See reference 9 of the paper.

R. R. Caldwell and V. C. Rideout: We wish to thank Mr. Stout for pointing out the simplifications possible in equation 2 of the paper.

Diesel-Electric Locomotive Ground Relays

G. R. McDONALD
ASSOCIATE MEMBER AIEE

Synopsis: The following paper lists and describes the various protective functions of the ground relay as used on diesel-electric locomotives. The connections are described, and comments are made on the control features initiated by the operation of the relay.

General Functions

THE USE of ground relays started in the early 1920's in automatic substations. These relays were primarily for the purpose of limiting the damage caused by armature breakdown. Prompt operation of an instantaneous-type relay limited damage to conductors and armature stackings. The relay also furnished similar protection for commutator flashovers.

The first use of a ground relay on a diesel-electric locomotive was about 1930. The first relays installed for this purpose were low-resistance high-current devices. In fact, some of these early relays did not have enough resistance to be self-protecting on the high currents imposed by flashovers, and as a consequence the relays were severely damaged by a flashover. Higher resistance, higher voltage relays were, therefore, in order. Along with the tendency in this direction, other miscellaneous functions were entrusted to the ground relay until now the list of protective features which it provides is quite imposing. Any discussion of this relay, therefore, involves having a clear concept of these various functions and their interrelations.

The following list covers most of the protective functions now performed by the ground relay.

1. Armature grounds in either the main generator or in the traction motors.
2. Accidental power circuit grounds:
   (a) On the positive power circuits.
   (b) On the power cables which are at one-half of the generator voltage during series-parallel operation.
   (c) On the negative power circuits.
3. High resistance creepage grounds, such as those caused by moisture and dirt:
   (a) On the positive circuits.
   (b) On the half-voltage circuits.
   (c) On the negative circuits.
   (d) On the armatures of generator or motors.
4. Flashover protection:
   (a) Generator armature.
   (b) Motor armature with motors operating in parallel.
   (c) Motor armature on the positive side when operating in series parallel.
   (d) Motor armature on the negative side when operating in series parallel.
   (e) Positive side contactor flashover.
   (f) Negative side contactor flashover.
   (g) Series contactor flashover (one-half generator voltage).
5. Protection during dynamic braking:
   (a) Motor flashover.
   (b) Ground in braking resistor.
   (c) Leakage or moisture ground.
   (d) Resistor blower motor ground or flashover.
6. Ground protection during engine starting.

A short discussion of each of the preceding points will help to clarify the functions of this relay. This discussion is based on an Alco-GE road locomotive. The ground relay considered has a pickup

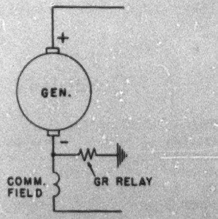

Figure 1. Ground relay connected on negative side of generator

---

Paper 53-77, recommended by the AIEE Land Transportation Committee and approved by the AIEE Committee on Technical Operations for presentation at the AIEE Winter General Meeting, New York, N. Y., January 19–23, 1953. Manuscript submitted October 20, 1952; made available for printing December 3, 1952.

G. R. McDONALD is with the General Electric Company, Erie, Pa.

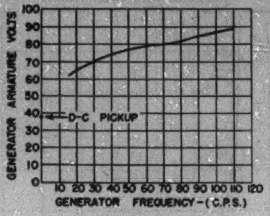

Figure 2. Ground relay pickup with generator armature grounded

of 38 volts with a coil current of 0.056 ampere. The coil resistance is 680 ohms. This relay is connected as shown in Figure 1.

Armature Ground

Consider a ground at one point on a generator armature. As the armature rotates this ground will travel from one polarity to the other. A relay connected as shown by Figure 1 will have applied to it an undulating voltage practically the equivalent of a completely displaced a-c wave. The relay pickup when operating on this voltage will be as shown by Figure 2. With this connection of the relay the drop through the generator commutating field will modify the actual voltage required by a small amount resulting from the drop through this field.

Operation in detecting an armature ground for a parallel connected motor is identical with that described for a generator, except for the slight modification caused by the commutating field drop. If the armature ground were on a series-parallel connected motor operating on the positive side of the line, the voltage applied to the relay would be equal to one-half of the generator voltage plus the undulating voltage from this armature. The relay would pick up at a slightly lower voltage than indicated by Figure 2 because of the larger d-c component. If the ground were in the armature of a series-parallel connected motor operating on the negative side of the line, conditions would be the same as for a generator armature except that this relay would be subjected to the voltage of this negative armature. This would be one-half of the generator voltage, and therefore, the pickup of the relay with respect to generator voltage would be double that shown by Figure 2.

These comments on armature grounds presupposed a zero resistance ground in an armature. If the armature ground actually has appreciable resistance as compared to the relay, then the voltage required to operate the relay will be correspondingly increased.

Accidental Power Circuit Grounds

(a) If a ground takes place on the positive side of the power system, generator voltage would be applied directly to the ground relay. If this ground were of zero resistance, the relay would operate when the generator voltage reached 38 volts. If the ground had appreciable resistance, the operating voltage would be correspondingly increased.

(b) If the ground took place in the connection between positive and negative motors when operating in the series-parallel connection, the same comments would apply except that the relay pickup in terms of generator voltage would be doubled.

(c) If a ground took place on the negative of a system it would appear, at first thought, that the ground relay coil would be short-circuited. Figure 3 illustrates this circuit. If the ground took place on the lead *B*, the coil of the ground relay would be short-circuited. If, however, the ground took place on leads *C* or *D*, the series field would be intermediate between the ground location and the circuit through the ground relay. Ordinary steady-state voltages developed across the series field would not be sufficient to operate the relay; however, any fluctuations in current would create enough inductive voltage across the series field to provide operation if the ground were on either *C* or *D*. An improvement on this circuit is to move the ground relay connection from *A* to *E*. In this case the transient inductive voltages of both the generator commutating field and the motor series field are effective for producing relay operation with grounds on either *C* or *D*, and the generator commutating field inductive voltage is available for producing operation with a ground on *B*.

Moisture or Creepage Grounds

One place where the ground relay does, if anything, too good a job is in connection with moisture or creepage grounds. These are always a matter of degree and most types of ground relays overprotect, causing unnecessary interference with locomotive operation. However, this matter is, somewhat involved, particularly from the standpoint that all of the leakage current does not necessarily pass through the relay coil.

(a) If leakage is taking place from the positive cable terminations and connections of the system, then conditions are identical with item (a) in the preceding section. Taking into account the equivalent resistance of the leakage path, the generator voltage with respect to relay pickup may readily be calculated.

(b) The same comments apply for leakage taking place on the cable terminations and connections between two or more series connected motors.

(c) Similar leakage from the negative does not tend to cause relay operation for the same reason as discussed under item (c) in the preceding section. The change in relay connections already mentioned would improve this situation, but the leakage resistance from the negative alone would have to be of a low value before relay operation could be expected.

(d) Leakage may be experienced from armatures because of the collection of dirt and moisture. This would usually be expected to occur at the commutator string bands or at the ends of the armature coils. If distributed leakage of this

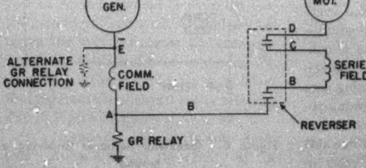

Figure 3 (left). Schematic diagram of negative power circuits

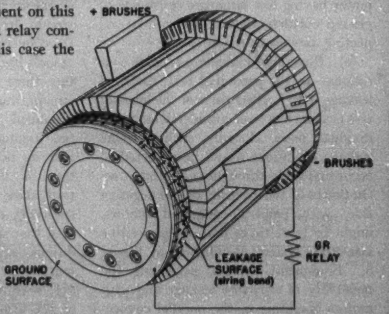

Figure 4 (right). Paths of distributed leakage over commutator string band

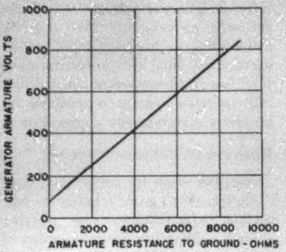

Figure 5 (left). Ground relay pickup with distributed armature leakage

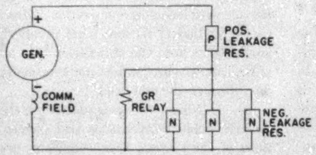

Figure 6 (lower left). Equivalent circuits for distributed cable leakage, parallel connected motors

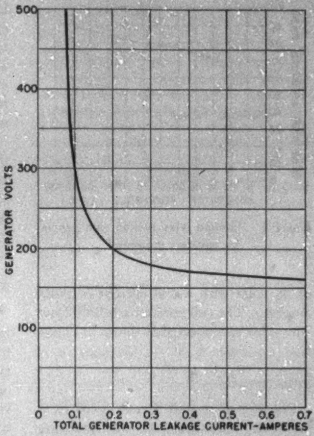

Figure 7 (right). Total leakage current at ground relay operation

type takes place, the voltage applied to the leakage paths varies between brushes or polarities around the armature. The leakage is in all directions even from one segment to the next, as shown by Figure 4. The relay sees only a small part of this total leakage current. Tests indicate that with uniform leakage around an armature, relay operation may be expected as shown by the curve of Figure 5. The armature insulation resistances used in plotting this curve are, of course, resistances taken at standstill. The armature insulation resistance values shown are surprisingly low, yet tests did not indicate any tracking or damage to the armatures as a result of these creepage grounds. This point is mentioned because ordinarily armature resistance to ground measurements might be expected to be on the order of megohms. Obviously an armature having low leakage resistance is badly in need of maintenance. The implication is that in emergency cases motive power having low armature resistance to ground could be dispatched without expecting damage to the armature.

(e) Generalized moisture leakage conditions: In the preceding text, moisture leakage from various parts of the locomotive circuits has been considered on an individual basis. Usually such extreme leakage conditions would be expected to occur uniformly throughout a locomotive. On this basis the exposure on the negative side, with parallel connected motors, might be three times that of the positive side of the system, as indicated by Figure 3. Equivalent circuits, neglecting the possibility of armature leakage and with motors operating in the parallel connection, would be as indicated by Figure 6. Total leakage current supplied by the generator, as plotted against generator voltage at the point where ground relay operation is produced would be as shown in Figure 7. Similar plots could be made for the series-parallel connection. The point illustrated is that the total leakage current which is causing damage to the equipment may be very many times the actual current that goes through the ground relay.

Flashover Protection

One of the main duties of the ground relay is to detect generator or motor armature flashovers. A point which can be made in connection with the equipment under discussion is that an armature flashover always involves ground in the circuit.

(a) Consider a generator armature flashover involving ground, as indicated by Figure 8. From the positive of the armature there is an anode drop, an arc stream drop, and a cathode drop where the connection is made to ground. From ground back to the negative of the armature there are corresponding anode, arc stream, and cathode drops. It may be presumed, therefore, that ground potential assumes a position approximately midway between the positive and negative of the armature. Oscillographic tests show that this assumption is substantially correct. It must be appreciated that during a flashover, arcing conditions vary continuously and ground potential may, therefore, fluctuate considerably with respect to potential at one side of the armature. The ground relay in this case received half of the armature voltage. Experience has shown that with the type of relay here discussed, and the connections shown in Figure 1 or modified as suggested in Figure 3, the ground relay always received sufficient voltage to reliably detect a generator flashover.

(b) The operation of the ground relay in detecting a parallel connected motor flashover is identical with that of detecting a generator flashover. The current in a flashover of this type will be partly generator current—which serves as exciting current for the motor by returning to the generator via the motor field—and partly current generated by the motor armature because the motor is being driven by train movement. A motor flashover will very frequently result in a generator flashover.

(c) If the motors are operating in the series-parallel connections and a positive

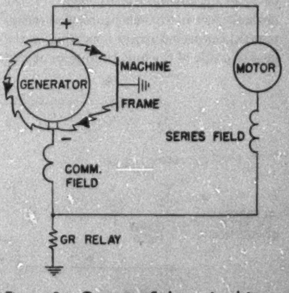

Figure 8. Generator flashover involving a ground

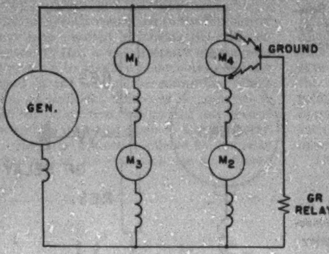

Figure 9 (left). Flashover of positive connected motor in series-parallel connection

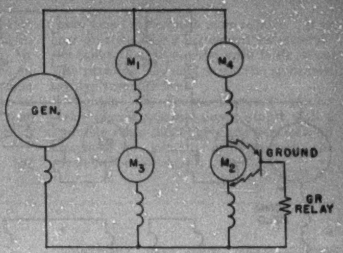

Figure 10 (right). Flashover of negative connected motor in series-parallel connection

connected motor flashes over the voltage across this motor will tend to collapse. The voltage across the negative motor connected in series will be increased as a result of the increase in generator current. The voltage available for operating the ground relay will be the sum of the voltage across the negative connected motor and half the voltage across the positive connected motor, see Figure 9.

(d) If in the series-parallel connection a negative connected motor flashes over, the relay will be operated by one-half of the voltage across this armature as indicated by Figure 10. In this case the inductance of the motor field may also be considered as contributing toward operating the relay and the net result is that reliable indication of negative connected motors flashing while operating in the series-parallel connections is obtained.

(e) Positive side contactors flashover: A commonly used locomotive power circuit for a typical 4-motor locomotive using series-parallel and parallel connections is shown in Fig 11(A).

The restricted space available on a locomotive makes it impossible to supply completely adequate arc distance for taking care of circuit interruptions of unusual severity on the main line contactors. Contactor flashover to ground although rare is always a possibility. A well-designed contactor tends to build up a fixed voltage across its contacts during circuit interruption and maintains this voltage until the arc is extinguished. This type of operation is indicated by Figure 11(B). Normally a contactor will maintain about 150 per cent of the circuit voltage across its contacts during circuit opening. If the contactor arc goes to ground it would be expected that the ground voltage would be midway between the voltages across the contactor tips. For a flashover of contactor *P1* operation of the ground relay may be estimated from the assumed vector relationship of Figure 11(C).

(f) Negative side contactor flashover: An analysis of the ability of the ground relay to detect a flashover of the *P2* contactor, which is on the negative side of the system, may also be made from Figure 11(B). Because of the inductive voltages involved, it will be observed that no difficulty should be experienced with the operation of the ground relay on this type of flashover.

(g) Series contactor flashover: A similar diagram may be drawn for a flashover of the series contactor *S1*.

GROUND PROTECTION DURING DYNAMIC BREAKING

A dynamic braking circuit is shown in Figure 12. The motor armatures and braking resistors are located to illustrate the direction of their voltage departure from the positive of the generator. The actual voltage developed by the generator during dynamic braking is quite small as compared to motor armature voltage. It will be noted that during dynamic braking all of the features previously discussed—armature grounds, creepage grounds, and flashovers—produce action of the ground relay. Hence it affords full protection during this type of locomotive operation.

ENGINE STARTING

While the generator is being used as a motor to start the diesel engine, the power circuits of the locomotive are connected to the control battery. The ground relay then responds to any ground that might exist on the control battery. If the ground relay is connected to the point *E* of Figure 3, it will be noted that when voltage is first applied to the generator, the armature drop is quite small consequently the ground relay will, in effect, be connected to the positive side of the battery. Most of the voltage will be across the generator starting field. As the generator comes up to speed the armature develops back electromotive force, the current decreases and the ground relay, in effect, becomes connected to the negative side of the battery. The relay is thus responsive to a ground at any location along the length of the control battery and circuits.

Relay Connections

A ground relay connected as in Figure 1 has provided very good protection on a large number of equipments. As discussed in connection with Figure 3, it is considered better to change the connections from point *A* to point *E* of Figure 3 in order to minimize the possibility of making the relay inoperative by having a ground on a negative lead.

A resistance bridge connection has sometimes been used in order to provide

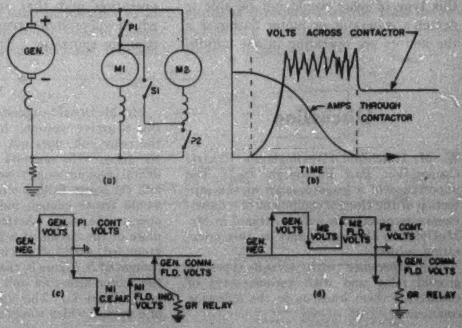

Figure 11. Diagrams relating to power contactor flashovers

A. Simplified schematic of circuits
B. Voltage and current during contactor opening
C. Vector diagram for flashover of P1
D. Vector diagram for flashover of P2

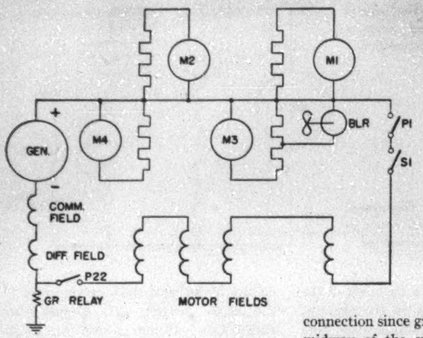

Figure 12 (left). Schematic diagram of dynamic braking circuit

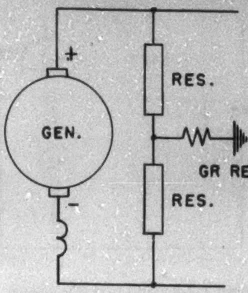

Figure 13 (right). Resistance bridge connection for ground relay

mid-point grounding of the generator voltage as indicated by Figure 13. Referring to the preceding headings, it would appear that this type of connection will detect armature grounds of either generators or motors. A relay so connected would recognize power circuit grounds except those during series-parallel operation which might occur on the cables operating at potential between the positive and negative motors. A bridge-connected relay should provide successful protection in the case of a creepage ground on either the positive or negative of the power circuits. It would not however respond to this type of ground on the cables connected between the positive and negative motors during series-parallel operation. Neither would it tend to detect generalized armature leakage since such leakage would produce a ground potential midway between the terminals of the generator or motor on which it existed. For generalized leakage conditions from the power cables the bridge-connected relay could give good operation on the basis that there would be more leakage from the negative of the system than from the positive. Theoretically this type of relay would not be able to detect a generator or motor flashover if the motors are operating in the parallel connection since ground voltage should be midway of the system. Actually there are fluctuations in this voltage and these might produce operation of such a relay. The bridge-type relay should provide protection for a motor flashover if the motors are being operated in the series-parallel connection and only one armature flashes over. For contactor flashovers it might be expected that this type relay would supply adequate protection.

There has been some thought that the bridge-connected relay relieves voltage stress on the equipment by grounding the mid-point of the system. Actually machine designers are mostly concerned with providing sufficient insulation and creepage distances in series windings such as commutating fields and series fields. A negative connected ground relay will normally keep all of these field windings at or near ground potential except in series parallel operation when some of the motor fields are raised to 50 per cent of system voltage above ground.

The functions performed by the ground relay should not interfere with emergency plugging of a locomotive.

The ground relay is normally arranged to control a generator field contactor. Particularly in case of a flashover it is necessary that the ground relay be fast in operation and that it control circuits which will promptly remove the excitation from the generator. The equipment here discussed has a generator provided with a single shunt field winding. The ground relay operates a field contactor which inserts a field killing resistance in the field circuit having approximately 16 times the resistance of the field. The voltage of the generator is thus quickly reduced below the point which will sustain a flashover.

With all ground relay systems it is customary to provide a cutout switch in series with the relay coil. This may be opened to permit emergency operation of the locomotive with a ground on the power circuit. Making the ground relay inoperative will, of course, eliminate its protective functions and such things as a flashover or a double ground on the system might cause considerable damage. The ground relay function should be retained during any load test since there is ordinarily no other way provided to clear a flashover.

The foregoing discussion illustrates the point that the ground relay has a large number of functions to perform. In most cases the exact operating current or voltage of the relay is not too critical; however, any changes made in the relay operating characteristics should be carefully considered with respect to all of the functions.

Considerable work is being done in connection with moisture grounds which, it is believed, will result in further improvements in locomotive operation.

◆

Discussion

W. M. Hutchison (Westinghouse Electric Corporation, East Pittsburgh, Pa.): The importance of a ground relay to the protection of the electric equipment of a diesel-electric locomotive is well illustrated in Mr. McDonald's thorough paper on this interesting subject.

Our experience with several types of ground relay and with various ways of connecting them leads us to the following comments.

Mr. McDonald suggests that a ground on the negative system, by short-circuiting the relay coil, does not necessarily nullify the relay. He suggests that if the accidental ground occurs between the motor and the series field, fluctuations in current would create enough inductive voltage to operate the relay. Actually there is much more of the circuit at a potential which, if grounded, would short-circuit the relay coil (potential *B*, Figure 3) than there is between the motor armature and field (potential *C* or *D*, Figure 3). Therefore, the probability of a ground which would nullify the relay is correspondingly great. Even if the ground occurs between the armature and field, only a violent change in generator or motor armature current, such as a motor flashover to ground, will cause it to operate. These are the greatest objections to this type of ground protection.

Tests with a certain relay with one side grounded showed no response to a single armature ground and erratic response to flashover.

Several years ago ground relays connected equivalent to one side grounded were used. So many accidental grounds to the conductor directly connected to the line side of the relay resulted in making the relay inoperative that it was necessary to reconnect the relay to another point which was not used in the locomotive wiring and which was at sufficient difference in potential to all the locomotive circuits that any ground would be depended upon to trip the relay.

Since the protection offered by the relay depends on its operation on an induced voltage supplied by either the generator commutating field or a motor series field, both of which have only a few turns, it appears that more data should be offered on the current surge required through these fields to develop the 38 volts required to operate the relay. It appears unlikely that such voltages can be developed in normal operation.

The resistance bridge connection has been found to be much more reliable. It is our practice, in our permanent series-parallel connection, to put the main fields all on the negative side and to use the resistance bridge ground relay.

Biasing the bridge-connected ground relay from a separate power supply with a suitable relay should give the best over-all response to grounds anywhere on the system from all causes.

Hydraulic Servos Incorporating a High-Speed Hydraulic-Amplifier Actuated Valve

ROBERT L. SCRAFFORD
ASSOCIATE MEMBER AIEE

ELECTROHYDRAULIC systems have certain advantages over pure electromechanical systems, which make them particularly suitable as an adjunct to electronic control for high-power level actuation. The main factor which has limited the application of hydraulic actuators until recently has been the awkardness of the control systems required. However, developments in the technique of controlling hydraulic flow electrically now permit the flexibility of electronic control to be applied to the linear operation of hydraulic valves at high speeds.

The advantages of hydraulic systems stem mainly from their ability to provide large amounts of power from a "hydraulic battery" (accumulator) with minimum of apparatus and storage volume, and with a small time constant. One-shot hydraulic systems have many applications in guided missiles, where high-power output to operate control surfaces is required for short period of flight. Another advantage of hydraulic systems is the ease of obtaining either linear or rotational motion.

Applications requiring continuous operation may also benefit from the minimum apparatus-to-horsepower ratio by providing a recharging system in a less restricted location than the actuator, and conveniently connected to it by copper tubing.

It is the purpose of this paper to describe a d-c transfer valve developed at Cornell Aeronautical Laboratory, Inc., and to call to the attention of servo engineers, especially in industrial positions, the progress that has been made in the field of hydraulic control, which may be familiar to engineers associated with the aircraft industry.

This valve, operating in conjunction with a hydraulic strut or piston, has a combination of gain, power output, and torque-to-inertia ratio which is difficult to obtain in an electrical actuator. However, ratings are particularly difficult to apply to hydraulic systems because of the inherent nonlinear relationships. It is desirable, for the sake of simplicity, to make a comparison on the basis of closed servo loops. These analyses indicate superiority over other servo systems operating at power levels of 1 to 10 horsepower, even when used in a control loop which does not fully realize the potentialities of the device.

Typical Hydraulic Control Systems

A typical control system is shown in block diagram form in Figure 1. In the case of a hydraulic system, the power source consists of a source of hydraulic fluid under pressure, and the power amplifier is a transfer or control valve. The actuator may be either of the linear or rotational-motion variety.

The General Servo Problem

We may divide all servomechanisms into two parts:

1. Intelligence section, which includes voltage-amplifying and phase-compensating functions;
2. Power output and driver stages

The first part contains devices which perform the various signaling and computing functions. These are shown as dotted lines in Figure 1. They provide no power to the load and may accomplish intelligence transmission by means of any of the systems used by communications and telemetering engineers. The second part contains the power-converting devices, in which power from some energy source is transferred to the load, in response to a signal from the intelligence portion of the loop.

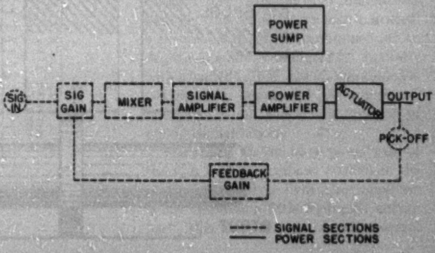

Figure 1. Servo block diagram

Paper 53-103, recommended by the AIEE Feedback Control Systems Committee and approved by the AIEE Committee on Technical Operations for presentation at the AIEE Winter General Meeting, New York, N. Y., January 19–23, 1953. Manuscript submitted September 29, 1952; made available for printing December 19, 1952.

ROBERT L. SCRAFFORD is with the Cornell Aeronautical Laboratory, Inc., Buffalo, N. Y.

The d-c transfer valve described in this paper was developed in the Cornell Aeronautical Laboratory Hydraulic Laboratory under the direction of W. C. Moog.

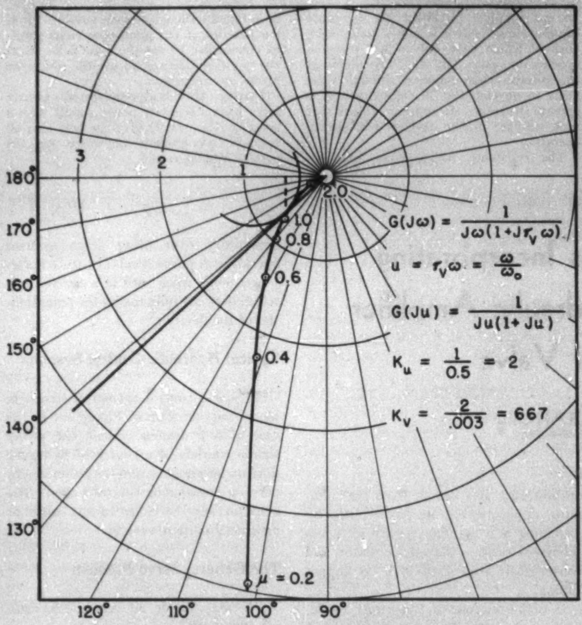

Figure 2 (above). Nyquist plot and computation of Kv for d-c valves

All mechanical servos are required to accomplish some motion at the output in response to a variable at the input. This motion will be opposed, as are all mechanical movements, by the three roots of force, namely, the act of doing work, acceleration of the structure, and mechanical friction. The frequency response of the servo is determined mainly by the second of these, which is brought about by the mass of the structure This mass is dictated by factors of allowable deflection for a given load and safety factor.

Often, in electric-positioning servos, the designer will find that the inertia of the load is a small fraction of the total inertia, which includes that of the actuator. This is aggravated by the fact that motors are essentially high-speed devices usually geared down to the load. At the motor end of this gear train, then, we have the situation of a large inertia which must accelerate very rapidly. This situation may be circumvented to some extent by the use of a constant-speed motor in conjunction with an electric clutch. However, this is a rather inefficient combination.

In the hydraulic servo, the picture is entirely different. The actuator may conveniently be designed for a wide range of speeds or for linear or rotational motion; hence, the need for a gear train is eliminated. Furthermore, the inertia of the hydraulic actuator plus hydraulic fluid is not high, resulting in a substantial advantage in high-frequency performance.

Figure 3 (below). Schematic of Cornell Aeronautical Laboratory's d-c nozzle-drive transfer valve

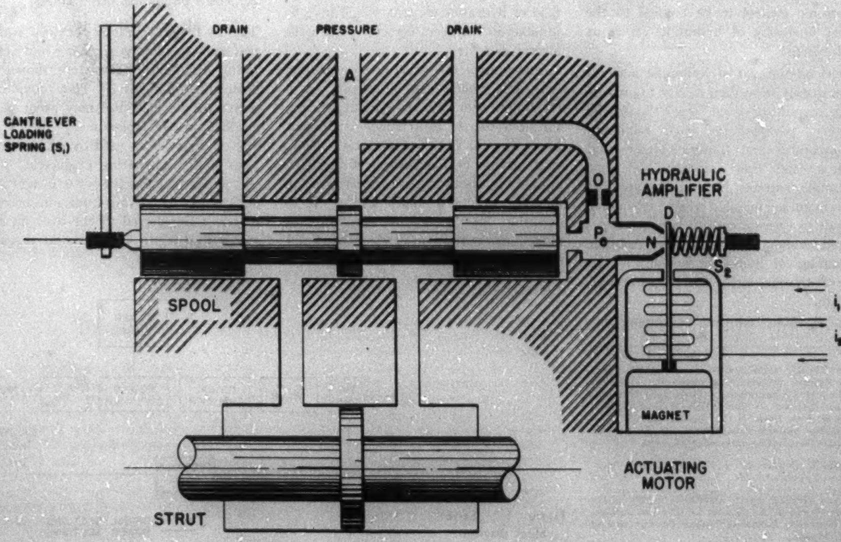

Figure 4. Valve control characteristics (output flow versus input current)

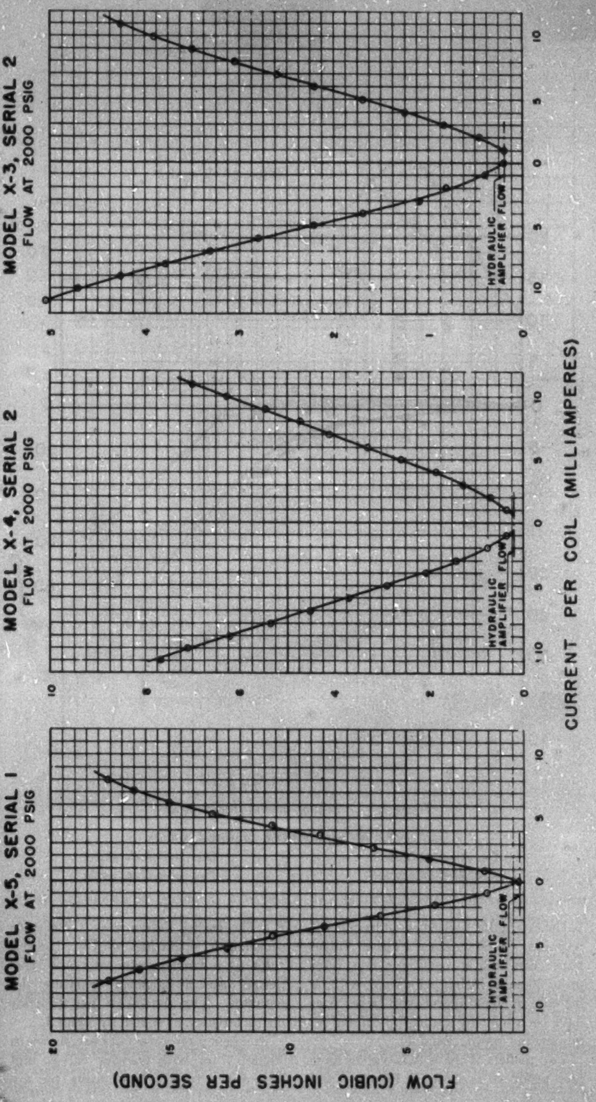

A proportional hydraulic servo requires a device which will control the flow of fluid to an actuator in response to a signal. This device is known as a transfer valve, and one having extremely fast operating characteristics is described in the following paragraphs.

The Cornell Aeronautical Laboratory Transfer Valve

The ideal transfer valve is a device which controls the flow of hydraulic fluid, under pressure, to some actuating device in response to a low-level electric signal. Hence, it is a power amplifier as well as a transducer. The input to the valve is usually supplied from an electronic amplifier, which is fed by the signal portion of the servo. The Cornell Aeronautical Laboratory's (C.A.L.) d-c transfer valve can be driven to full-output flow rates of 30 cubic inches per second, at pressures of 1,500 to 2,000 pounds per square inch, with an electric signal on the order of 20 milliwatts into one side of its center-tapped input impedance of 6,000 ohms.

The time constant of this valve is of the order of 3 milliseconds. Since the electric signal portions of the system have negligible time constants with respect to this valve, the system transfer function becomes

$$\frac{\theta_o}{\epsilon}=K_v\left[\frac{1}{p(1+p\tau)}\right]$$

In a hydraulic motor or piston as in an electric motor, integration is obtained. This is evident from the following

$$v=\frac{Q}{A}=\frac{dx}{dt}$$

and

$$x=\int\frac{Q}{A}dt$$

where

x = distance of piston travel
Q = oil flow
A = area of piston
v = velocity of piston

Using a time constant of 3 milliseconds and the transfer function just indicated, a theoretical K_v of 667 is obtained for an M_p of 1.5, as shown in Figure 2. Actually with a loaded system, the K_v mentioned is not reached, because of the compressibility of the oil, which is a function of piping configuration.

The reason for the large power gain of the C.A.L. valves (about 80,000) is the incorporation of a hydraulic amplifier. While consuming little hydraulic energy itself, this amplifier permits the control

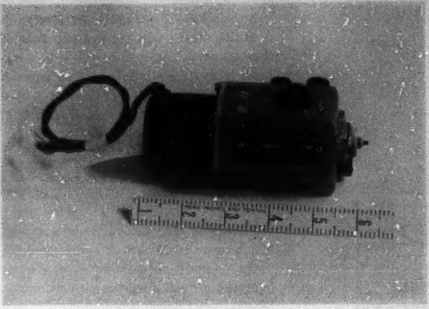

Figure 5. A-c valve

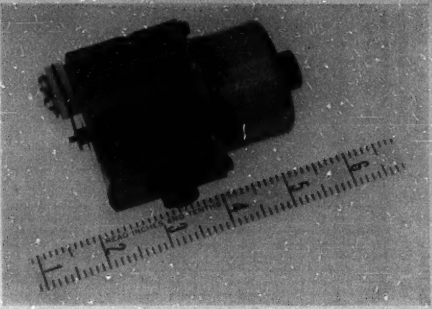

Figure 6. D-c valve

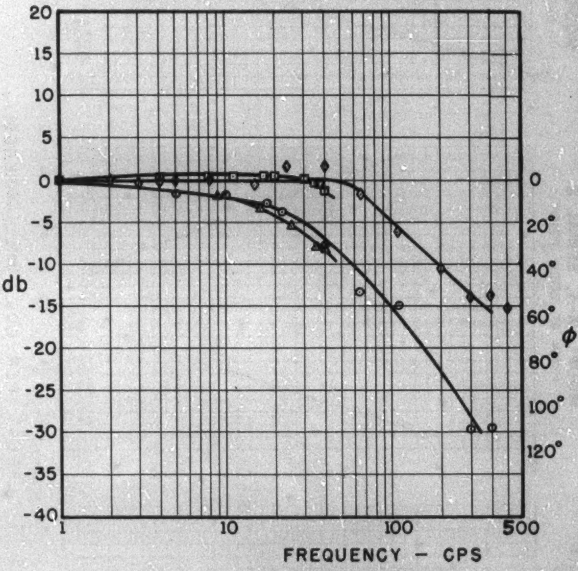

Figure 7. Open-loop transfer characteristics

Input, motor current; output, spool-spring position

◇ D-c valve amplitude
□ A-c valve amplitude
○ D-c valve phase angle
△ A-c valve phase angle

of large hydraulic energy with a minimum of electric power.

The C.A.L. transfer valve is shown schematically in Figure 3. Hydraulic pressure is applied at A. There is a very small amount of hydraulic flow past the orifice O, into the chamber P_c, and out the nozzle N. Control of oil flow through the nozzle is by the flapper D, actuated by an electric device. Pressure drop along this path is shared between the orifice and the nozzle. Chamber pressure is applied to the valve spool, which controls the flow of oil to the actuated device. The resulting force is opposed by a spring S_1. With no signal into the valve and a supply pressure of, say, 1,500 pounds per square inch, let us assume equal drops across the orifice and the nozzle. Chamber pressure is then 750 pounds per square inch and the centering spring may be adjusted to give zero output flow.

Now, if a signal is applied to the coils of the electric actuator, the flapper will move in or out, either increasing or decreasing the nozzle pressure drop and, hence, the chamber pressure. An increase in chamber pressure results in the valve spool being moved to the left against the spring, until a new force balance is obtained. A decrease in chamber pressure has the opposite effect.

The resulting control characteristics for a typical valve are shown in Figure 4. It should be noted that oil which flows through the nozzle is retained inside the unit and returned to the drain lines.

The salient features of the design can now be indicated. In the first place, the flapper does not move any appreciable amount in controlling oil flow from the nozzle. Secondly, there is a comparatively large force, something on the order of 50 pounds, available for positioning the spool. Both of these factors contribute to the fast action and excellent frequency-response characteristics. These valves have been built in maximum flow rates up to 30 cubic inches per second, with no increase in signal power, and larger sizes have been built by scaling up driving requirements proportionately.

Two models of the C.A.L. valves have been produced as shown in Figures 5 and 6. The earlier design uses a 400-cycle servomotor operating with a blocked rotor as a flapper actuator. The later design uses a balanced armature d-c actuator. The d-c valve has superior characteristics, as shown by Table I.

Frequency response data are shown in Figure 7 for both transfer valves, and data for a typical loop, using the a-c

Table I. Characteristics of A-C and D-C Servo Valves

	Alternating Current	Direct Current
Flow rate	30 cubic inches per second	30 cubic inches per second
Signal power required for full output	15 watts	20 milliwatts
Electrical input impedance	400 ohms	12,000 ohms (center tapped)
Time constant (input current to spool position)	0.05 second	0.003 second
Weight	2 pounds	1.1 pounds

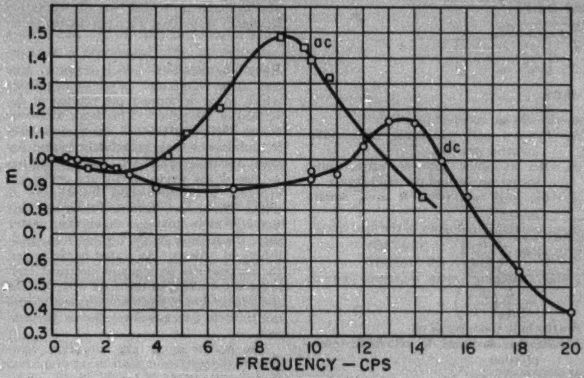

Figure 8. Closed-loop characteristics

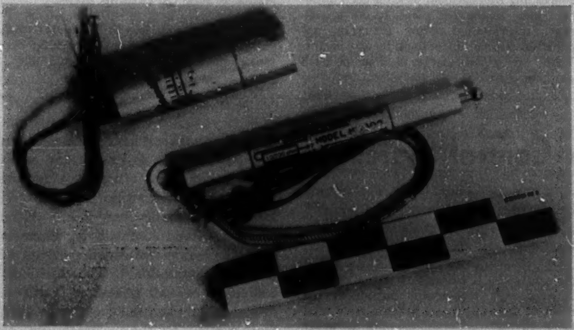

Figure 9. Linear-pickoff devices

valve, are shown in Figure 8. The d-c valve has never been tested in a loop having enough gain to realize its full capabilities.

Testing Procedure

The performance of the valve is measured in the following manner: The input is considered to be the variable-phase voltage in the case of the a-c valve, and the motor-differential current in the case of the d-c valve. The valve output is considered to be spool position and is measured by means of strain gages on the backing spring.

The strain-gage signal is amplified in a phase-calibrated Brush Development Company strain analyzer, and compared in phase with the input current or voltage signal, with a sinusoidal input signal. The relative phase shift is then obtained by either a phasemeter, or an oscillographic method, and corrected for unequal shifts in the two channels.

All data were taken with a level of signal sufficiently low to insure operation within the linear range. In the case of the open-loop data, Figure 7, this merely means that the valve was operated within its rating. In the tests which obtained the data shown in Figure 8, a piston was used with an autosyn pickoff. The follow-up signal was added to the driving signal in the driver-unit input transformer. The driver unit consisted of a simple twin-triode demodulator. In these tests the low-frequency piston motion was held to a value which prevented hydraulic flow-rate limiting for the particular piston in use as the frequency was increased.

No attempt was made to correlate the open- and closed-loop data.

Signal Transmission and Pickoffs

Although applications dealt with to date at the C.A.L. have been concerned with linear actuation, rotational motion equipment is available.

Since linear-motion actuation is a little uncommon, a word on pickoff devices seems in order. Linear pickoff devices are either linear-motion potentiometers or linear differential transformers (see Figure 9 for pictures of these components). The linear potentiometers have the same inherent resolution problems found in the rotary variety and are somewhat specialized for each application, in that the length must match the stroke of the linear actuator. Differential transformers correspond to the rotational microsyn device[1] and are equally susceptible to harmonic and quadrature-component generation. Because of a scarcity of good linear-motion instruments, it has been common practice in the past to use rotational devices connected by a crank arm.

Conclusions

The development of the servo valve has opened a new field for automatic control in those applications requiring high-speed operation at high-power levels. In addition, linear motion may be obtained simply, without gearing systems. It seems likely that there would be many industrial-control applications for such a system.

Reference

1. COMPONENTS HANDBOOK, Blackburn. MIT Radiation Laboratory Series, Massachusetts Institute of Technology (Cambridge, Mass.), volume 17.

Discussion

D. G. O'Brien and **S. J. Jatras** (Midwestern Geophysical Laboratory, Tulsa, Oklahoma): Mr. Scrafford's comments concerning the desirability of using hydraulic-control elements in certain servo applications are very much in order. Considerable research and development have been devoted to the task of obtaining suitable hydraulic elements. To date there appears to be two basic types of hydraulic valves—the single-stage valve in which the electromechanical transducer (torque motor) directly strokes the power piston, and the 2-stage valve in which the electromechanical transducer strokes the power piston through an intermediate amplifier stage. The valve described by Mr. Scrafford is of the second class, since it uses a hydraulic amplifier. Other valves of the first class which are now in production seem to have better frequency response than that indicated in Figures 7 and 8 of the paper. A direct comparison is not possible, however, since all the operating conditions are not specified in connection with Figures 7 and 8.

One of the disadvantages of the valve described by Mr. Scrafford is the dependence of the zero current (or null) position of the valve piston upon supply pressure. Later versions of this valve use two sets of orifices, one controlling each end of the piston. The single-stage valves now available are not susceptible to this difficulty. In fact, through the use of proper design techniques, the static gain of a single-stage valve has also been made insensitive to variations in pressure drop across the valve.

We should like to take exception to the open-loop transfer function given in the paper. It is not clear whether the output displacement referred to is that of the valve piston or the load ram. If the piston displacement is meant, then the integration does not belong in the denominator of this function. If the ram displacement is intended, the given function neglects some important load-circuit dynamics.

It is likely that Mr. Scrafford meant the load-ram displacement. The authors have found that the following transfer function is much closer to the actual situation, and is very useful in the preliminary analysis of a servo application problem

$$\frac{x}{\epsilon}=\frac{\dfrac{K_1K_h}{A_R}}{s\left[\dfrac{s^2}{\omega_n{}^2}+\dfrac{2\xi}{\omega_n}s+1\right]}$$

where

x = the displacement of ram

K_1 = forward path electronic gain, milliamperes per volt

K_h = the hydraulic gain of valve, cubic inches per second per milliampere

A_r = the load ram effective area, square inches

ω_n = the natural frequency of the load circuit $=A_R\left(\dfrac{B}{VM}\right)^{1/2}$

ξ = the damping ratio of load circuit $=\dfrac{L}{2A_R}\left(\dfrac{BM}{V}\right)^{1/2}$

B = the bulk modulus of oil

V = the total volume of oil under compression

M = the load mass

L = the leakage coefficient

We feel that Mr. Scrafford's comments concerning translational pickoffs need qualifications. In the first place, to our knowledge, translational-motion actuation applications are not uncommon by any means. There are a very large number of such applications in existence. Secondly, translational pickoffs of high quality are commercially available. For instance, translational potentiometers utilizing deposited-carbon resistance elements have been highly developed and are available in a wide range of resistance and power ratings. This type of potentiometer has excellent resolution characteristics and a long life expectancy. Differential transformers with very good quadrature and harmonic characteristics (less than 0.1 per cent of full output) are also available, provided that the excitation frequency is specified when purchasing them.

Robert L. Scrafford: It is certainly true that today hydraulic valves are available which equal or surpass the equipment described in the paper. This work was done before 1950, and the not uncommon delay in publication has been accompanied by great advances in the art. This period has witnessed the development and wider acceptance of linear-motion transducers as well. The author believes, however, that the fact that advances have been made since the writing should not deter the publishing of articles. As stated in the paper, the purpose was to acquaint electrical engineers not working in this field with some of the advantages of hydraulic apparatus, and not to write a technical treatise on the subject.

The author must take exception, however, to the statement made in the discussion that the zero of the hydraulic-amplifier type valve will shift with supply pressure. In this particular valve it has been found possible, by proper choice of spring constants, to hold the chamber pressure essentially constant over a variation of supply pressure of several hundred pounds. This action may be likened to the constant-current characteristics of a pentode amplifier.

Limiting in Feedback Control Systems

RALPH J. KOCHENBURGER
ASSOCIATE MEMBER AIEE

Synopsis: Limiting effects exist in feedback control systems because of the restricted range of operation of components or because of purposeful limiting introduced for the protection of equipment. Such limiting effects increase the difficulties associated with the analysis and synthesis of systems because of the nonlinear mathematical relations which result. As such effects can markedly modify system performance, there is a practical need for a simplified method for taking them into account. The effect of limiting on system performance is studied here in terms of the frequency response of the system. It is found that limiting of the most elementary form—simple limiting—improves system stability, except in those systems which are conditionally stable or have a conditional degree of stability. In such instances, precautions are suggested to prevent the limiting action from adversely affecting system performance. It is found that the velocity limiting of a servomotor introduces the effect of phase lead and hence can be used to improve system stability. On the other hand, the limiting of servomotor acceleration directly or indirectly (as by means of current or pressure limiting) is found to introduce a phase-lag effect which can be detrimental to system performance. Electronic analogue computer techniques were employed to obtain much of the data presented here.

THE conventional linear treatment applied to feedback control systems does not account for the fact that all of the physical elements involved have specific ranges of operation beyond which they cannot or are not permitted to operate. Electronic amplifiers have practical ranges of input voltage. Hydraulic and pneumatic servomotors often have specific ranges of safe operating pressures and are limited by pressure-relief valves. Generators used as amplifying elements have limits imposed by the effects of magnetic saturation. The hydraulic equivalent of such generators (variable-displacement pumps) have their output flows limited by the maximum obtainable pump displacement.

In addition to the natural limits inherent in each control system component,

---

Paper 53-109, recommended by the AIEE Feedback Control Systems Committee and approved by the AIEE Committee on Technical Operations for presentation at the AIEE Winter General Meeting, New York, N. Y., January 19–23, 1953. Manuscript submitted October 21, 1952; made available for printing December 18, 1952.

RALPH J. KOCHENBURGER is with the University of Connecticut, Storrs, Conn.

The author wishes to acknowledge the aid and co-operation of students, staff members, and employees of the Electrical Engineering Department, University of Connecticut. The suggestions made by Prof. V. B. Haas were particularly appreciated.

additional limits may be artificially introduced for protective purposes or to improve the system performance. As will be shown, velocity limiting of a servomotor can be used to improve the response damping (degree of stability) following the application of large disturbances. The torque or acceleration of a servomotor, or some related quantity such as armature current or hydraulic pressure, may be limited to protect the equipment. Artificially introduced limiting is often accomplished by the introduction of an auxiliary discontinuous negative-feedback path. Figure 1 illustrates the application of this method to velocity limiting. More direct mechanical methods might also be employed, such as the application of a centrifugally-actuated brake mechanism. Regardless of the mechanization employed, the same qualitative effects on system performance generally result. The remainder of this paper does not treat the methods for accomplishing the limiting action but rather deals with the effect of the limiting, once achieved, upon control system performance.

Figure 2 is a plot showing typical relationships between the input and output quantities of a limited control system element under steady-state conditions. Curve *a* shows the abrupt type of limiting sometimes encountered, particularly when negative-feedback limiting is employed. Curve *b* represents less abrupt limiting action as might be caused by saturation effects. In the quantitative treatments given here, it will be assumed that the limiting is abrupt, as in curve *a*. The conclusions thus reached can be qualitatively applied as well to the less abrupt forms of limiting.

In this discussion and the studies to follow, it will be shown that there will be instances when the limiting is beneficial to the performance of the feedback control system, and other instances when it is detrimental. While the mathematical method employed is approximate, its application should permit the designer to evaluate the effects of limiting in a given practical application and to select accordingly any modifications that might be necessary to improve performance.

Sinusoidal Response Method of Analysis and Synthesis

The analysis and synthesis of linear feedback control systems can be more expeditiously achieved by means of the now well-known sinusoidal response approach. The advantages of this method over the direct transient response approach become particularly apparent when the system being studied contains a large number of energy-storage elements.

When nonlinear phenomena, such as limiting, are encountered, the sinusoidal response method cannot be directly employed with mathematical exactness. An approximate method has been generally proposed[1] which preserves the advantages of the sinusoidal response approach. This method was further developed and applied to contactor servomechanisms by two independent contributors, Goldfarb[2] in Russia and the author[3] in this country. The method expresses the response of the nonlinear element in terms of a describing function. This describing function representation is based upon the assumption that a sinusoidal input signal is applied to the nonlinear element. The resulting output signal is, of course, nonsinusoidal because of nonlinear distortion. However, if only the fundamental harmonic component of this output signal is considered, it then becomes possible to describe the relation between input and output in terms of an amplitude ratio and a phase shift. This can be described in terms of a complex ratio between input and output signals; it is this latter complex ratio which is called the describing function.

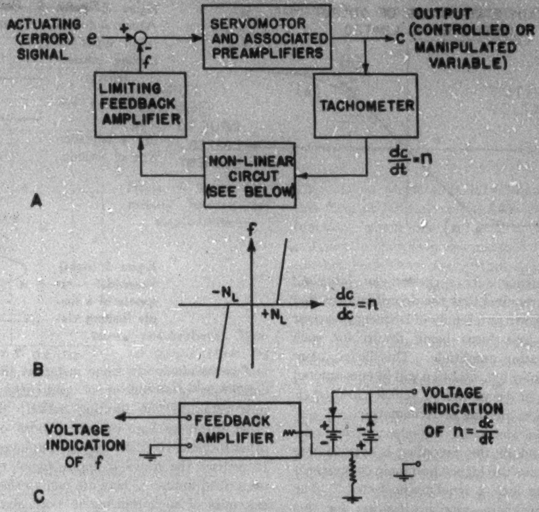
ACTUATING (ERROR) SIGNAL
e
+
-
f
SERVOMOTOR AND ASSOCIATED PREAMPLIFIERS
c
OUTPUT (CONTROLLED OR MANIPULATED VARIABLE)
LIMITING FEEDBACK AMPLIFIER
TACHOMETER
NON-LINEAR CIRCUT (SEE BELOW)
$\frac{dc}{dt}=n$
A
f
$-N_L$
$+N_L$
$\frac{dc}{dc}=n$
B
VOLTAGE INDICATION OF f
FEEDBACK AMPLIFIER
VOLTAGE INDICATION OF $n=\frac{dc}{dt}$
C

Figure 1. A feedback method of tachymetric limiting applied to a servomotor

(A) Block diagram illustrating feedback limiting
(B) Characteristic of limiting feedback path
(C) Method for obtaining feedback limiting

The describing function thus obtained is similar to the transfer function used to describe the response characteristics of linear control elements, except for the fact that the describing function of a nonlinear element will depend upon signal amplitude as well as frequency. In certain instances, the nonlinear element involves no energy storage and the describing function then depends upon amplitude only. This is often the case when contactor servomechanisms are considered or when simple limiting is encountered, as will be described later. In such instances, a simple graphical procedure becomes possible wherein a frequency-dependent locus representing the transfer function of the linear portion of the system and an amplitude-dependent locus representing the nonlinear describing function are superposed.[3] By means of elementary graphical constructions, conclusions can be reached regarding the system's degree of stability and speed of response and system modifications necessary to improve performance may be selected. This superposition method will be employed later in this paper.

There are other instances when the feedback element does involve energy storage. In this case, the describing function depends on both amplitude and

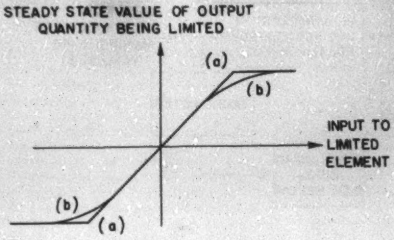

Figure 2 (left). Abrupt and saturation types of limiting characteristics

(a) Abrupt limiting
(b) Saturation type of limiting

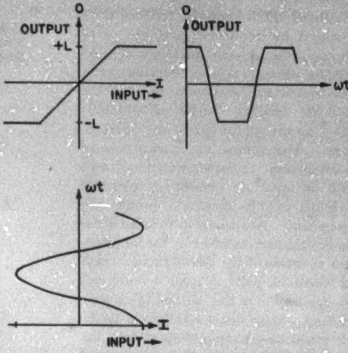

Figure 3 (right). Sinusoidal response of a simple limiting element

frequency. As suggested by Johnson,[4] this requires that the describing function be shown as a family of frequency-variant loci, one locus being drawn for each operating amplitude. This latter, more complicated, situation will be encountered here in discussions of velocity and acceleration limiting of servomotors.

The sinusoidal response method described in the preceding is approximate because the higher harmonic components of the output signal are neglected.* The major engineering justification for this approximation is the low-pass filter characteristics exhibited by most control-system components. It has been found that contactor control systems can be successfully designed with the aid of this method of analysis and synthesis. Inasmuch as the nonlinear distortion encountered with limiting is less severe than that arising from the abrupt action of contactor devices, it would be expected that the neglected higher-harmonic components would be even less significant in the case of limiting. It would therefore appear that the describing function approach proposed here would, in general, be a better approximation for the purpose of studying the effects of limiting than it proved to be when applied to contactor servomechanisms.

Simple Limiting in Feedback Control Systems

There are many instances of limiting where the limited component does not involve significant energy storage elements. An example is the limiting which occurs in a conventional electronic amplifier. Here the limiting arises because of the restricted range of input signal which can be handled. In some instances the conditions of cutoff or of grid-current flow establish the limiting action; in other instances high-vacuum diodes or other forms of rectifiers may be employed to restrict the range of input signal to prescribed limits. There are many other examples of such limiting in both electrical and mechanical components employed in feedback control systems. Limiting of this type is called simple limiting since no energy storage elements are directly affected by the limiting action. Simple limiting exists if a plot of output versus input, such as in Figure 2, can be used to describe the action of the limited component for transient as well as steady-state operation. The describing function of a component subject to simple limiting is not frequency dependent.

Figure 3 shows the effect of simple limiting when a sinusoidal input signal is applied to the limited component. It is assumed in the case shown that the limiting is abrupt and that it is symmetrical

Nomenclature

A_L = maximum acceleration magnitude as imposed by acceleration limiting

c = controlled variable (output); instantaneous value at a given time

C = value of capacitance (farads) representing inertia in the electric analogue of a servomotor

e = instantaneous value of the actuating signal (error) applied to the feed-forward portion of a feedback control system

E = complex representation indicating amplitude and phase angle of e when e is a sinusoidal function of time

e_0 = voltage representing n_0 in the electric analogue of a servomotor

e_1 = voltage representing n_1 in the electric analogue of a servomotor

G = general symbol for a feed-forward transfer function in a control system

G_{D1} = general symbol for the describing function, representing a nonlinear element

H = general symbol for a feedback transfer function in a control system

i = instantaneous value of the input signal applied to a limited element

I = magnitude of i when i is a sinusoidal function of time

$j = \sqrt{-1}$

L = general symbol for the maximum output magnitude imposed by limiting

M_p = peak value of the output-input amplitude ratio describing the control system response to sinusoidal input signals

n_0 = actuating signal applied to a servomotor and expressed in terms of corresponding steady-state output velocity; instantaneous value at a given time

N_0 = amplitude of a sinusoidal variation of n_0 (or of fundamental harmonic component of n_0 when n_0 is periodic but nonsinusoidal)

n_1 = instantaneous output velocity of a servomotor

N_1 = amplitude of a sinusoidal variation of n_1 (or of fundamental harmonic component of n_1 when n_1 is periodic but nonsinusoidal)

N_L = maximum magnitude of n_1 as imposed by velocity limiting

o = instantaneous value of the output signal of a limited element

O = magnitude of o when o is a sinusoidal function of time (or of the fundamental harmonic component of o when o is periodic but nonsinusoidal)

r = reference input signal applied to a control system; instantaneous value

R = amplitude of r when r is sinusoidal function of time

R_1, R_2, R_3 = electrical resistances in the equivalent electric analogue representation of a servomotor

s = Laplace transform operator

t = elapsed time

φ = general symbol for phase shift in angular degrees

τ = time constant associated with the dynamic response of a servomotor

ω = angular frequency $= 2\pi$ times frequency in cycles per second

---

* Johnson[4] has developed a method for taking these neglected higher harmonics into account. His method requires considerably more computational labor than is encountered with the cruder approach where these harmonics simply are neglected. Johnson's method provides a valuable means for checking the accuracy of this cruder approach for specific control problems. It was not considered applicable for deriving the general conclusions discussed in this paper.

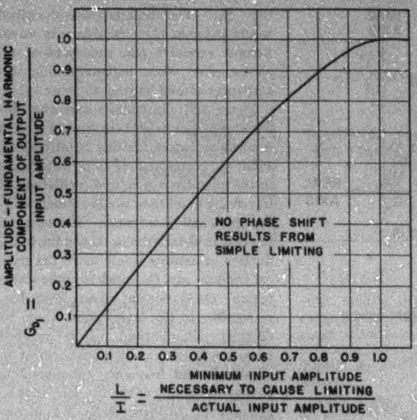

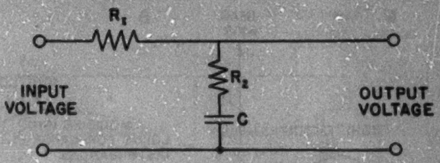

Figure 4 (left). Describing function for simple limiting

Figure 6 (above). Typical passive phase lag (undercompensated proportional plus integral) controller network

in that the limited magnitudes are the same for positive and negative signals. The result of this form of limiting is simply a flattening of the top of the sinusoidal wave form. The input signal is assumed to be expressed by

$$i(t)=I\cos\omega t \tag{1}$$

where I is the input signal magnitude. The output without limiting would be

$$o(t)=i(t) \tag{2}$$

when $I<L$ (no limiting action), where L the limited amplitude.

When $I>L$, limiting occurs, and the output is given by

$$o(t)=I\cos\omega t \tag{2A}$$

whenever $-L/I<\cos\omega t<L/I$, and by

$$o(t)=L \tag{2B}$$

whenever $\cos\omega t>L/I$, and by

$$o(t)=-L \tag{2C}$$

whenever $\cos\omega t<-L/I$.

The fundamental harmonic component of the output signal $o_1(t)$ is, by Fourier analysis

$$o_1(t)=O_1\cos\omega t \tag{3}$$

where o_1, the magnitude of the fundamental component, is mathematically expressed by

$$O_1=I\left\{\frac{2}{\pi}\left[\frac{L}{I}\sqrt{1-\left(\frac{L}{I}\right)^2}+\sin^{-1}\left(\frac{L}{I}\right)\right]\right\} \tag{4}$$

The describing function for the limiting action is therefore

$$G_{D1}=\frac{O_1}{I}=\frac{2}{\pi}\left[\frac{L}{I}\sqrt{1-\left(\frac{L}{I}\right)^2}+\sin^{-1}\left(\frac{L}{I}\right)\right] \tag{5}$$

whenever limiting occurs, that is, when $I>L$.

When no limiting occurs ($I<L$), the describing function is simply unity.

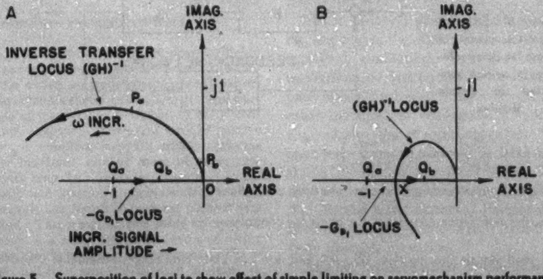

Figure 5. Superposition of loci to show effect of simple limiting on servomechanism performance

(A) Effect on a stable control system
(B) Effect on an unstable control system

There is no phase shift introduced by this form of limiting and the describing function, which may in general be a complex number, is in this instance a real number indicating the output-to-input amplitude ratio. Figure 4 is a plot of this describing function as obtained from equation 5.

It may be seen that simple limiting results merely in a decrease in the gain of the limited component and hence a decrease in the magnitude of the control system's transfer function. The effect of this change of gain upon system performance can be described by a variation of the well-known Nyquist diagram.[5,6] This variation, illustrated in Figure 5, is obtained by plotting the inverse of the system's transfer function, that is, the locus $(GH)^{-1}$. For linear systems, the system performance can then be evaluated by observing the orientation of this inverse locus with the point $-1+jO$. In the case of nonlinear systems, the same considerations which apply to the point $-1+jO$ now apply to the superposed locus representing the negative of the amplitude-variant describing function, that is, the function $-G_{D1}$. In other words, the negative describing function locus can be considered as though it were the locus of the point $-1+jO$ as the effective gain is varied because of the nonlinear action. The mathematical basis for employing superposed loci has been treated elsewhere[7] and will not be elaborated further.

The describing function locus for the case of simple limiting is shown in Figure 5. Since the limiting action introduces no phase shift, this locus lies entirely on the negative real axis. For low-amplitude disturbances which do not result in limiting, the operating point on this locus is the original $-1+jO$ point, that is, point Q_a. As the amplitude of the signals applied to the limited element increases, the quantity G_{D1} decreases and the operating point on the describing function locus moves to the right, say to point Q_b. This effective motion of critical point Q (corresponding to the $-1+jO$ point in linear systems) is equivalent to changing the scale of the inverse transfer locus in accordance with the gain change caused by limiting.

Once the superposed loci are con-

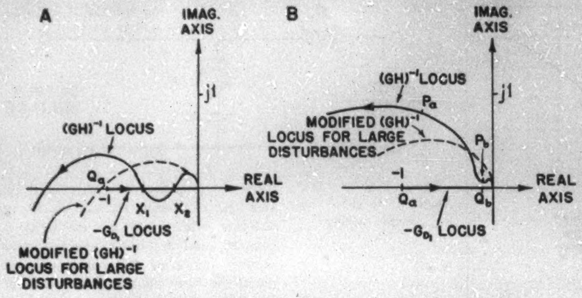

Figure 7. Effect of simple limiting on performance of conditionally stable systems

(A) Effect on a conditionally stable system
(B) Effect on a system having a conditional degree of stability

structed, it is then possible to investigate the stability and speed of response for various signal amplitudes. Point Q on the describing function locus for the particular signal amplitude involved is first determined. The question then must be answered as to whether point Q lies in a stable or unstable region. If the control system is stable under open-loop conditions, the test for this is fairly simple. If point Q lies to left of the inverse-transfer locus, as the latter is traversed in the direction of increasing frequency (in the direction of the arrows in Figure 5), then Q lies in a stable region; if Q lies to the right of the inverse-transfer locus it is in an unstable region. In Figure 5(A), points Q_a and Q_b represent stable operating regions. In Figure 5(B), point Q_a is in the unstable region while point Q_b is stable. A somewhat more complicated test for stability must be applied when the control system is unstable under open-loop conditions. The method for determining stability under these conditions has been described[6,7] for linear systems and can be applied to nonlinear systems, since point Q is equivalent to the point $-1+j0$.

If a given point Q is found to lie in a stable region, the response damping (degree of stability) and speed of response can be approximately determined by the following method. Point P on the inverse-transfer locus is found which is nearest to Q. The ratio of distance OQ to distance QP is then determined, where point O represents the origin. This ratio corresponds to the quantity frequently referred to as M_p, that is, the maximum ratio of output to input amplitude as the frequency is varied over the entire range of interest. Values of M_p between unity and 1.3 generally represent satisfactory response damping; values in excess of 1.3 indicate insufficient damping. When point P occurs at the origin, excessive damping and, consequently, a slow response may be expected. The frequency corresponding to the location of P on the inverse-transfer locus is an indication of the speed of response; higher frequencies indicate faster transient responses. The rules of thumb just described are not mathematically exact and precautions must be observed in their application. These precautions have already been discussed in texts dealing with linear feedback control systems.[6,7]

The inverse transfer locus shown in Figure 5(A) represents a system which is stable and adequately damped without limiting. Until limiting occurs, point Q is at Q_a. The value of M_p is 1.3, and adequate but not excessive response damping might be expected. As the signal amplitude increases because of the application of large disturbances, point Q moves to, say, Q_b. The criteria just described would indicate that the damping would become excessive and the speed of response slow when high-amplitude disturbances caused limiting to occur.

Figure 5(B) illustrates a somewhat different situation where the control system is unstable before limiting is introduced. Point Q_a, corresponding to no limiting, is in the unstable region, and oscillations of increasing amplitude would result following any small disturbance. However, an increase in signal amplitude and the introduction of limiting would move the critical point to, say, Q_b, which is in the stable region. Oscillations at an amplitude corresponding to this latter point would be damped. Equilibrium will be reached when steady-state oscillations occur at an amplitude and frequency corresponding to the intersection of the two loci, that is, at point X. In Figure 5(*B*), X is a convergent equilibrium point representing a condition of sustained oscillations.

It may be seen from the discussion so far that when limiting is applied to an already adequately damped system an increase in response damping and a decrease in speed of response results. These effects are evident only in the early part of the correction process following large disturbances; once the signal level is small enough to no longer cause limiting, the system damping returns to the original value. On the other hand, limiting applied to an unstable system results in the systems exhibiting self-sustained oscillations of a definite amplitude.

An intermediate situation may exist where the response of the unlimited system is stable but inadequately damped. The introduction of limiting will then improve the response damping for larger disturbances. Such an application of limiting can be of practical value in that

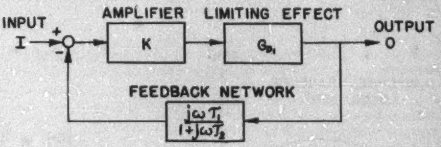

Figure 8. Effect of feedback means of phase lag compensation in system subjected to simple limiting

In general $\frac{O(j\omega)}{I(j\omega)}=KG_{D_1}\left(\frac{1+j\omega\tau_2}{1+j\omega\alpha\tau_2}\right)$

Quantity in parentheses indicates phase lag controller effect

α, the attenuation constant of the phase lag controller $=1+KG_{D_1}\frac{\tau_1}{\tau_2}$

For small signals (no limiting) $G_{D_1}=1$ and $\alpha=1+\frac{\tau_1}{\tau_2}\gg 1$, indicating considerable phase-lag controller action

For large signals (with limiting) $G_{D_1}\rightarrow 0$ and $\alpha\rightarrow 1$, indicating negligible phase-lag controller action

Figure 9. Equivalent circuit of a simple servomotor

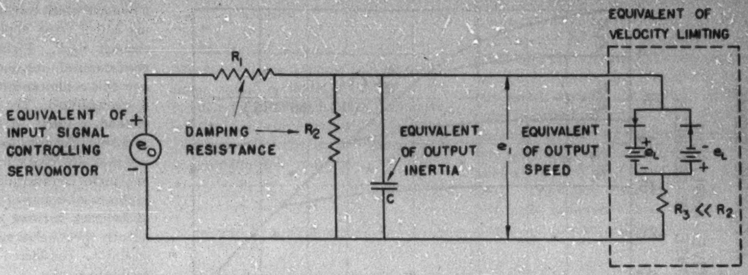
EQUIVALENT OF VELOCITY LIMITING
R_1
EQUIVALENT OF INPUT SIGNAL CONTROLLING SERVOMOTOR
+
e_0
−
DAMPING RESISTANCE
R_2
EQUIVALENT OF OUTPUT INERTIA
C
e_1
EQUIVALENT OF OUTPUT SPEED
e_L
e_L
$R_3 << R_2$

most control systems can tolerate a higher percentage transient overshoot in response to small disturbances than can be tolerated following the application of larger disturbances.

The conclusions which were derived previously by the describing function concept merely serve to correlate obvious conclusions which could be reached by qualitative physical reasoning. The instances were presented to bridge the gap between these simpler cases and the more complicated situations which are now to be discussed.

Simple Limiting with Conditionally Stable Systems

The conclusions indicated could have been reached without the sophistication of the sinusoidal response approach. The effect of limiting upon a conditionally stable control system is somewhat more subtle and can best be described in terms of this approach.

Conditionally stable systems are those which are stable for some specified range of feedback loop gain but which become unstable if the gain is sufficiently reduced or increased. The systems having transfer loci as indicated in Figure 5 became unstable only when the gain is sufficiently increased. Conditionally stable systems are encountered when:

1. The control system employs a highly effective phase-lag controller network (sometimes called an undercompensated proportional-plus-integral controller) for the purpose of permitting a higher velocity constant. Figure 6 shows one form of passive electric coupling network which performs this function; one or more of these networks may be placed in cascade. Pneumatic and hydraulic equivalents of such a network are found in process control systems. The result of this form of compensation is a reduction in the error resulting from slowly varying disturbances (such as ship roll in a gun-stabilization system), or from static disturbances such as coulomb friction.
2. The open-loop transfer function is unstable, that is, the control system contains either an unstable component or an unstable minor loop. This frequently occurs in missile guidance systems and less frequently in the control of conventional aircraft.

The solid-line curve of Figure 7(A) is a typical inverse transfer-function locus for a system which is conditionally stable because of the inclusion of a phase-lag controller. The locus of $-G_{D1}$, corresponding to simple limiting, is superposed on this plot, and the loci intersect at points X_1 and X_2. In the case of small disturbances of an amplitude insufficient to cause limiting, operation is at point Q_a on the describing-function locus: stable operation will then result. The intersection point X_1 represents a divergent equilibrium condition; it therefore represents a boundary on the describing function locus. Large amplitude disturbances, which cause limiting sufficient to move the operating point beyond X_1, will initiate unstable operation. The resulting oscillations of increasing amplitude will then move the operating point still farther to the right, until the convergent equilibrium point X_2 is reached. The final steady-state result will therefore be self-sustained oscillations of a relatively large amplitude and low frequency, as determined by the location of the intersection point X_2 on the two loci.

In the situation just described, simple limiting makes the system capable of self-sustained oscillations provided these oscillations are first initiated by a disturbance of sufficient magnitude. There are other instances of conditional stability, particularly those resulting when the open-loop transfer function is itself unstable (item 2 just described) where there is no second convergent intersection point X_2. In this latter instance, disturbances of sufficient magnitude would result in truly unstable operation.

Another instance where simple limiting can have an adverse effect upon performance exists in the case of systems having a conditional degree of stability. Such systems can also result from the application of phase-lag type compensating networks. They represent a less extreme case than do conditionally stable systems in that, while a reduction of gain will not cause instability, it can result in a higher value of the quantity M_p and hence in a lower degree of stability, that is, less response damping. The solid-line curve of Figure 7(B) is a typical inverse transfer function locus for such a system. As before, small disturbances insufficient to cause limiting correspond to operation at point Q_a, where the value M_p obtained in the manner previously described is 1.3. Adequate response damping is therefore indicated following such small disturbances. Larger disturbances causing limiting result in the operating point moving to, say, point Q_b. Here the value of M_p is 3 and poor response damping can be expected; furthermore the speed of response, as indicated by point P_b on the transfer locus, is considerably reduced. These results correlate with the following observations concerning the transient response of such a system: The response to small disturbances is adequately damped. The response to larger disturbances exhibits a slow initial speed of response and excessive overshoots of the response at the beginning of the correction process; the final part of the response becomes adequately damped as the limiting becomes less effective.

The above considerations indicate that limiting can have a particularly adverse effect when applied to conditionally-stable systems. These results are particularly significant when phase-lag compensating networks, that is, undercompensated proportional-plus-integral controllers, are employed. A scheme for avoiding these adverse effects is discussed next.

Phase-Lag Compensation Methods in Limited Systems

The preceding discussion, illustrated by Figure 7, showed the adverse effects that

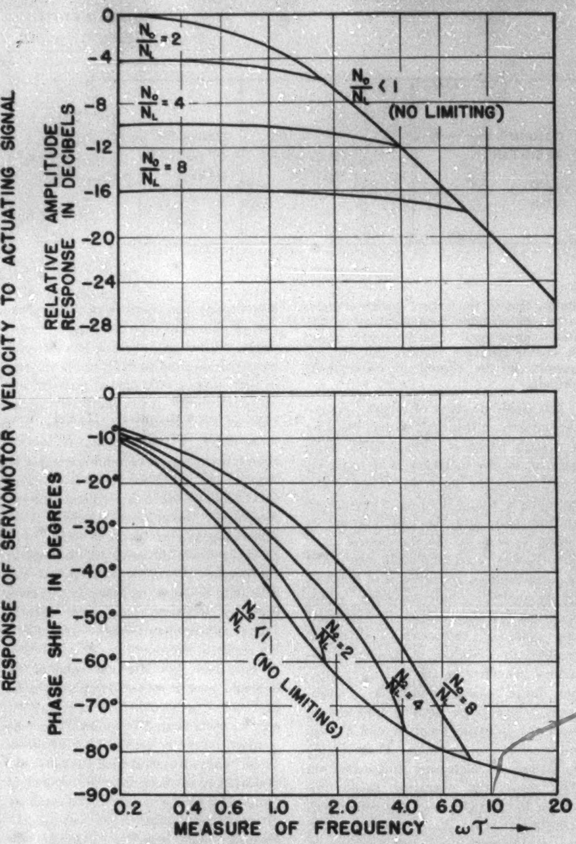

Figure 10. Describing function of a simple servomotor subjected to velocity limiting

limiting can have upon a system employing phase-lag compensation, particularly if a passive network, such as the type shown in Figure 6, is used to achieve this compensation. The most direct way of eliminating these effects is by making the phase-lag compensation effective only when low-signal amplitudes are involved. In other words, the inverse transfer function locus may have the conditionally stable forms shown by the solid-line curves of Figure 7 when small disturbances are involved, provided the locus is modified to the form shown by the broken-line curves of Figure 7 when large disturbances are applied of an amplitude sufficient to cause limiting. The broken-line curves do not respresent conditional stability. They represent the removal of most of the phase-lag compensation.

The block diagram of Figure 8 indicates how this can be accomplished if a feedback rather than passive method is used for obtaining the phase-lag type of compensation. The important requirement is that the minor loop involving the feedback path include the element being limited. (The same problem exists in contactor servomechanisms and phase-lag compensation is often best applied to such contactor systems by means of a minor feedback loop which includes the contactor element.) When this is not physically practical, the amplifying element in the forward portion of the feedback path should be artificially limited in a manner which corresponds to the limiting action being applied to the limited element itself. Figure 8 includes the mathematical relations which explain how this nonlinear form of compensation is accomplished. The describing function method is used. Actually, one of the major justifications for this method—the low-pass filter characteristic of the control loop under consideration—does not apply in this case because of the phase-lead type of feedback network employed. Consequently the conclusions shown in Figure 8 should be considered as being of only qualitative value.

Velocity Limiting of Servomotors

The simple form of limiting described before did not directly affect an energy storage element and the describing function representing this limiting merely accounted for a change in gain but had no effect upon the phase-shift characteristics of the system transfer function. When the speed of a servomotor, or the analogue of speed in some other control system element, is subject to limitations imposed on its maximum permissible magnitude, it generally will be found that this velocity form of limiting introduces a phase-lead effect and, furthermore, that the describing function for the limiting action is dependent upon frequency as well as amplitude.

The phase lead caused by velocity limiting exists in both the dynamically simple forms of servomotors, involving but one significant energy-storage effect, and in more complicated forms which may involve a multiplicity of such effects. This treatment will be concerned with the simpler case where only one energy storage effect, output inertia, need be taken into account in describing the servomotor's dynamics. Examples of such servomotors are

1. Shunt-type d-c servomotors with fixed field excitation and variable armature supply voltage. This type actually has a second energy storage element because of the armature circuit inductance. It is found, however, that in many applications the inductance can be neglected and that the combined inertia of the rotor, gearing, and load represents the only energy storage effect which need be considered.

2. The familiar 2-phase a-c servomotor employing fixed excitation on one phase winding and a variable control excitation on the other.

3. Hydraulic servomotors of the speed-gear type involving a variable displacement pump and a fixed displacement motor. The analogue of inductance in this application is the compressibility of the hydraulic fluid, including the elasticity of the housings transmitting and containing the fluid. If

these are negligible, and if the speed variations of the pump's drive motor can be neglected (as it can when an effective flywheel is used), then the output shaft inertia is the only energy storage element which need be considered.

4. Hydraulic servomotors of the linear actuator type where the pressure differential across the actuator piston is controlled by a pilot valve. Here again, the only energy storage element which need be considered is the output load inertia, provided that the fluid compressibility may be neglected and that the piston is not spring-loaded. Pneumatic servomotors of the linear actuator type do not fall into this simple category because of the compressible fluid used.

All of the types described are single energy storage devices only if there is negligible resilience in the coupling between the servomotor and its output load. All of the types except possibly the first type described are highly nonlinear, even apart from any limiting effects which might be involved. These nonlinear effects could be handled by the describing function method. This, however, is not the subject of this paper, and the servo elements considered here will be assumed to be linear except for the limiting action itself.

All the types can be represented by the equivalent electric network of Figure 9. The voltage source e_0 corresponds to the input signal controlling the servomotor. For electric servomotors, it would correspond to the equivalent source voltage applied by the amplifier (electronic or electromagnetic) which excites the servomotor. In a hydraulic speed gear, it would correspond to the pump displacement rate, as expressed in terms of equivalent output revolutions per minute. In a hydraulic linear actuator controlled by a pilot valve, it would correspond to the pilot valve position.

The series resistance R_1 contributes damping to the servomotor; the lower R_1, the greater the damping. This corresponds to the effective armature circuit resistance in electric servomotors and to the effects of leakage and hydraulic flow resistance in hydraulic servomotors of both the speed gear and linear actuator type. Resistance R_2 represents mechanical output damping of the viscous type; the greater the damping, the lower will be R_2. The value of shunt capacitance C varies directly with the output inertia. Voltage e_1 across capacitance C corresponds to the actual output speed of the servomotor.

If linear operation is assumed, the R's are constant, and the system dynamics can be described in terms of a single time constant

$$\tau = \frac{C}{\dfrac{1}{R_1}+\dfrac{1}{R_2}} \text{ seconds} \tag{6}$$

The steady-state response to a sinusoidal input signal e_0 would then be of the familiar form shown plotted versus frequency in the curve marked "no limiting" in Figure 10; that is, the servomotor's transfer function would be

$$\frac{e_1(j\omega)}{e_0(j\omega)} = \frac{R_2}{R_1+R_2}\,\frac{1}{1+j\omega\tau} \tag{7}$$

Velocity limiting is represented in the equivalent circuit of Figure 9 by a second additional damping resistance R_3, which is connected so that it is effectively in shunt with the resistance R_2 whenever the voltage e_1, representing servomotor output speed, exceeds the critical limited value in output magnitude. For effective limiting, $R_3 << R_2$; for flat limiting, where the speed is never permitted to even minutely exceed the limited value, $R_3 \rightarrow$ zero. Truly flat limiting cannot be physically achieved although it can be closely approached; the analyses to fol-

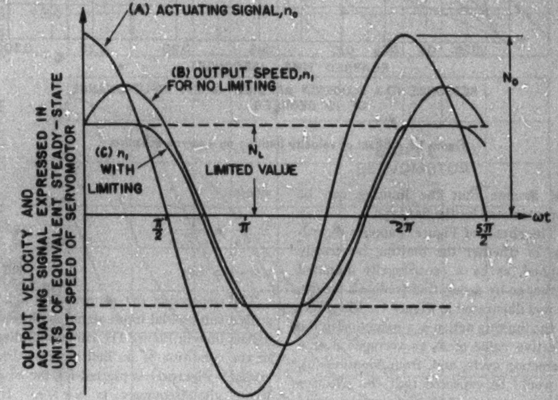

Figure 11 (above). Effect of velocity limiting on a simple servomotor subjected to a sinusoidal actuating signal

Conditions of plot:
$\omega = 1/\tau$
$N_L = 0$ (curve b)
$N_L = 1/2\ N_0$ (curve c)

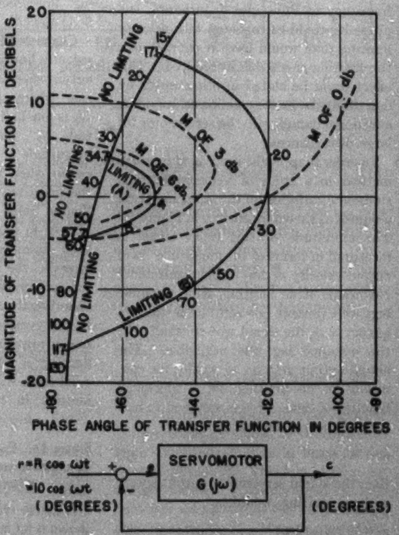

Figure 12 (right). Effect of velocity limiting on the transfer function of an elementary servomechanism

Values of points on loci represent values of ω
Curve a: $N_L = 800$ degrees/second
Curve b: $N_L = 200$ degrees/second
Without limiting, $G(j\omega) = \dfrac{200}{j\omega(1+0.1j\omega)}$
τ = servomotor time constant = 0.1 second
R = input amplitude = 10 degrees

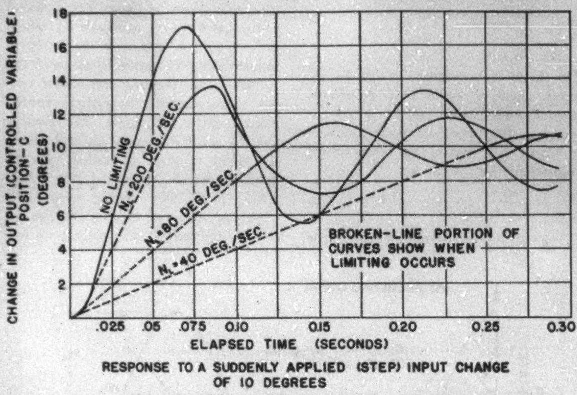

Figure 13. Effect of velocity limiting on a servomechanism

low assume that the limiting can be approximated by the flat type.

The circuit of Figure 9 applies regardless of whether the limiting is directly applied, as by a centrifugally actuated brake, or by a negative feedback means, as was illustrated in Figure 1. The effect of the limiting action is a reduction in the effective value of R_2 as averaged over a correction cycle, and, from equation (6), it would be expected that the effective time constant τ of the servomotor would be made lower. Therefore, for a given frequency of sinusoidal disturbance, less phase lag could be expected with velocity limiting than would have resulted before the limiting effect was introduced. This effect could be stated in other words by describing the limiting action as providing additional damping to the servomotor for large disturbances.

In order to apply the describing function method to a study of velocity limiting, sinusoidal variations of the input signal are assumed as shown by curve *a* in Figure 11. The amplitude of this input signal is measured in terms of the amplitude N_0 of output velocity n_0 that would result under conditions of no limiting, if no dynamic lags were present (τ=zero) or if the frequency ω of the signal was so small that the dynamic lag was negligible. The actual output velocity n_1 would, for conditions of no limiting, be a sinusoidal function of time. If n_0 is assumed to be a cosine function, that is, if

$$n_0 = N_0 \cos \omega t \tag{8}$$

then the actual servomotor output speed, without limiting, would be

$$n_1 = N_1 \cos (\omega t + \varphi) \tag{9}$$

where

$$N_1 = \frac{N_0}{\sqrt{1+(\omega\tau)^2}} \tag{9A}$$

$$\varphi = -\tan^{-1} \omega\tau \tag{9B}$$

The response of the output speed n_1 to such a suinusoidal input signal is plotted versus time in Figure 11; curve *b* applies to the condition of no limiting just discussed. Figure 11 is plotted for the case where the frequency is $\omega = 1/\tau$. In Figure 10, the curves marked "no limiting" are directly obtained from equations 9(*A*) and (*B*).

Curve *c* of Figure 11 shows the effect of velocity limiting on the wave shape of the output speed n_1. This plot represents the case where the limited value of speed N_L is one-half the actuating signal amplitude N_0. Limiting will start when the magnitude of n_1 becomes N_L. Limiting ceases when the speed representation of the input signal n_0 again falls below the limited value N_L. During limiting, the plot of n_1 is flat, since flat limiting has been assumed. Between the limiting intervals the speed n_1 follows a transient time relationship which can be derived by operational methods of transient analysis. In any event, it should be noted that the speed response resulting from velocity limiting is not the simple clipped sinusoidal form shown for the case of simple limiting in Figure 3. The significant effect of the limiting action is that the response with limiting, curve *c*, tends to lead in phase the response which would have resulted, curve *b*, if limiting were absent.

The describing function of a servomotor subject to such limiting could be determined by straightforward computational methods. The major steps to be pursued would be a determination of the time response, such as shown in Figure 11, for each condition of operation and then the determination of the fundamental harmonic component of this periodic time function. This respresents a straightforward, but nevertheless laborious, computational process. For this reason, an analogue computer representation of a velocity limited servomotor was constructed. The transfer function of this device was measured as a function of frequency for various conditions of limiting. The experimental means used to determine the transfer function had the property of being able to ignore all except the fundamental harmonic component of the output signal.

The transfer function of a velocity limited servomotor is shown plotted in Figure 10, as derived experimentally in the manner just mentioned. A family of curves is shown for various input amplitudes, represented by the ratio N_0/N_L. As would be expected in any form of limiting, the limiting action results in a reduction of output amplitude. More interesting than this is the effect upon the phase shift. The servomotor phase lag is less with limiting than it would have been before the limiting was introduced. In other words, the limiting action can be described as having produced a phase lead effect. This experimentally derived conclusion is in agreement with the qualitative discussion of velocity limiting based upon the equivalent circuit of Figure 9.

Effect of Velocity Limiting on Control System Performance

Under most circumstances, the gain reduction and phase lead introduced by velocity limiting can be expected to have a beneficial effect upon system stability. Exceptions might exist with conditionally stable systems, as discussed previously. Excluding such conditionally stable systems, velocity limiting ordinarily would improve the response damping for large

Figure 14. Example of an unstable servomechanism

*Transfer function shown is for no limiting

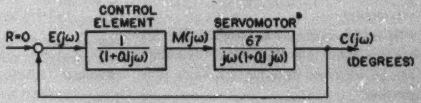
R=0
E(jω)
CONTROL ELEMENT
$\frac{1}{(1+0.1j\omega)}$
M(jω)
SERVOMOTOR*
$\frac{67}{j\omega(1+0.1j\omega)}$
C(jω)
(DEGREES)

disturbances. If the limiting is excessive, considerable overdamping could, of course, result, with a consequent slowing down of the speed of response of the system.

The effect of velocity limiting on the performance of a simple feedback control system is illustrated in terms of the frequency response in Figure 12. The system represented here could, for example, be a simple servomechanism having the following simple form of transfer function under nonlimited conditions

$$G(j\omega)=\frac{c(j\omega)}{e(j\omega)}=\frac{200}{j\omega(1+0.1j\omega)}$$

(for no output limiting) (10)

where

G = transfer function in the feed-forward part of the control loop
H = transfer function in the feedback part of the loop, assumed to be unity (direct output feedback)
c = output variable being controlled—in this case, output angle
$e=r-c$, the actuating (error) signal
r = reference input (desired value of the output variable)
τ = time constant associated with the servomotor response lag—in this case, equal to 0.1 second
ω = angular frequency (2π times the frequency in cycles per second) of the assumed sinusoidal test signal, radians per second

The quantities c, e, and r would all be in the same consistent measure of output units. In this particular servomechanism, the velocity constant k_v used to indicate system gain would be

$$k_v=200\ (\text{seconds})^{-1}=\frac{\text{steady-state rate of output correction } dc/dt}{\text{actuating signal } e}$$

In this particular instance, such a velocity constant would result in a stable but poorly damped system response unless some suitable form of limiting was introduced.

In Figure 12, the transfer locus of this system is shown plotted in logarithmic form; that is, the magnitude of $G(j\omega)$ is expressed in decibels on the vertical scale and the phase angle is expressed in degrees on the horizontal scale.[8] The M contours are mapped on this plot, where M, the magnitude of the system's output-input response ratio, $c(j\omega)/r(j\omega)$, is indicated in decibels. Attention is first called to the locus corresponding to no limiting, that is, that derived from equation 10. It may be noted that a high response peak is indicated at the frequency $\omega=45$ radians per second ($f=7.1$ cycles per second). This peak, corresponding to an M of about 13 decibels, indicates a very poorly damped transient response.

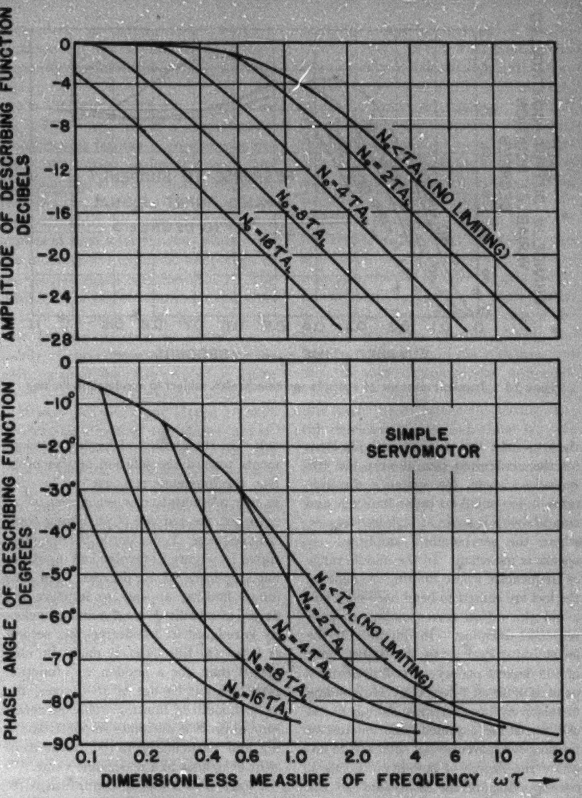

Figure 15. Describing function of simple servomotor subjected to acceleration limiting

This transfer function may be modified to show the effects of velocity limiting (limiting of $n=dc/dt$) by using the data plotted in Figure 11. In this case the quantity n_0, the actuating signal applied to the servomotor (expressed in terms of the equivalent steady-state output velocity), would be simply

$$n_0=k_ve=200e \text{ degrees per second} \qquad (11)$$

and, for a sinusoidal error signal $e=E\sin(\omega t+\phi)$, the amplitude of n_0 or N_0 would be

$$N_0=k_vE=200E \text{ degrees per second} \qquad (12)$$

Figure 11 shows the effect of limiting expressed in terms of the ratio N_0/N_L, where N_L is the maximum limited value of the output velocity. This ratio now becomes simply

$$\frac{N_0}{N_L}=200\frac{E}{N_L} \quad \text{(limiting ratio)} \qquad (13)$$

for this particular system. Limiting may be taken into account by recomputing the transfer function given in equation 10 and substituting the transfer function data plotted in Figure 11 for that portion of the relation represented by the expression

$$\frac{1}{1+j\omega\tau}$$

representing the dynamic response lag of the servomotor.

It is more convenient to show transfer loci for constant values of the reference input amplitude R than in terms of the error amplitude E. This can be done by straight-forward computational means. Such loci are shown for two conditions of limiting in Figure 12. It may be seen that

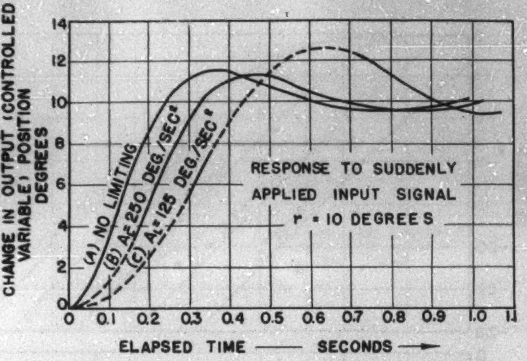

Figure 16. Transient response of a simple servomechanism subject to acceleration limiting

these transfer loci coincide with the locus for the nonlimited case at very low frequencies, where the system's dynamic error is too small to cause limiting, and coincide with it again at high frequencies, where the servomotor's amplitude response is too small. In the middle range of frequencies where limiting is effective, the loci are caused to bend backward and avoid the region corresponding to poor response damping. In Figure 12, the locus corresponding to the higher limit of 800 degrees per second still indicates a peak *M* of about 7 decibels, corresponding to relatively poor response damping. At the amplitude assumed, this amount of limiting is apparently not sufficient to improve the degree of stability. Locus *b*, corresponding to the lower limit of 200 degrees per second, indicates a peak *M* of about 1.5 decibels, representing adequate response damping.

The loci of Figure 12 represent various values of the limited velocity N_L for a specified input signal amplitude *R*. In general, one such locus can be drawn for a given ratio R/N_L. If the velocity limit N_L were specified, one locus would then apply for each value of input signal amplitude *R*.

In the case of linear control systems, it is possible to predict the nature of the transient response from frequency response data. Usually an approximate rule-of-thumb procedure is used,[6] but there is also a more exact (but more laborious) procedure available which was developed by Dr. George Floyd, described in chapter 11 of reference 6.

In the case of a nonlinear system such as the type considered here, such a prediction of the transient response from frequency response data becomes more difficult. In the absence of further developments toward the solution of this problem, the frequency response can be used in only a qualitative or semiquantitative sense for the purpose of predicting transient response. For example, the case illustrated by Figure 12 involved an input signal amplitude of 10 degrees. For this input, limiting appears to improve the degree of stability once the limited velocity is reduced to 200 degrees per second or less. On this basis, it might be estimated that, for a sudden step-function type of input change of 10 degrees, the same amount of limiting would be necessary to provide adequate response damping and particularly to reduce the transient overshoot to a reasonable value.

Figure 13 is a plot of the transient response of the same control system previously considered in Figure 12. Initial conditions of rest are assumed and a sudden (step-function) input signal *r* is considered as being applied at time $t=0$. It may be noted that the velocity limit must be reduced to at least 200 degrees per second before a significant improvement in response damping takes place, and that optimum response for this magnitude of signal input occurs when the velocity limit is still lower, that is, in the range of 40 to 80 degrees per second.

For a specified percentage overshoot, the velocity limit would have to be adjusted linearly, with the magnitude of the input disturbance anticipated. This would not be practical ordinarily in a physical system. In practice, the velocity limit ordinarily would be fixed at a value where it would serve to reduce the percentage overshoot resulting from large disturbances; it would then not be effective for smaller disturbances of a magnitude not sufficient to cause limiting action.

The transient response of this simple system could be determined easily by exact methods. In the many more complicated systems used in practice, such an exact determination would be difficult, and it would be far easier for the system designer to predict the effects of limiting by studying the frequency response and to then use these results to make approximate predictions concerning the transient performance. This procedure is more amenable to the synthesis of systems because the frequency response technique gives definite indications of how loci should be reshaped by compensating networks so that performance might be improved.

Experimental Verification of Method

The effect of velocity limiting upon an unstable servomechanism was considered in order to check the data of Figure 10 and the describing function method in general. The servomechanism is shown in Figure 14. Without limiting, the system is unstable for the velocity constant (67 degrees per second per degree) indicated.

The effect of a velocity limit of ±10 degrees per second ($N_L=10$) is then considered and the condition of steady-state oscillations are determined by the describing function method. The method for determining the nature of these oscillations is not explicit and a graphical solution is necessary. For the operating conditions given, the following steady-state conditions are found to prevail, assuming no input signal is being applied

1. The frequency of oscillation will be $\omega=12.6$ radians per second ($f=2$ cycles per second).

2. The output amplitude will be 0.96 degree, that is

$C=0.96\underline{/0}$ degree

3. Since the input is zero ($R=0$), the error signal will be

$E=-C=0.96\underline{/-180}$ degrees

4. For this frequency, the transfer function of the control element is

$\frac{M}{E}=\frac{1}{1+j1.26}=0.62\underline{/-52}$ degrees

5. So that the manipulated variable is

$M=0.60\underline{/-232}$ degrees

6. Since the velocity constant is 67 (seconds)$^{-1}$, the actuating signal applied to the servomotor is

$N_0=67M=40\underline{/-232}$ degrees

7. The ratio $N_0/N_L=4$.

8. From Figure 10, using the values $\omega\tau=1.26$ and $N_0/N_L=4$, the transfer function of the servomotor is -10.4 decibels at a phase angle of -38 degrees, or

$$G_{D1}=0.302\underline{/-38 \text{ degrees}}$$

9. And the servomotor velocity is

$$N=G_{D1}N_0=12.1\underline{/-270 \text{ degrees}}$$

10. The output variable is

$$C=\frac{N}{j\omega}=0.96\underline{/-360}=0.96\underline{/0 \text{ degrees}}$$

as initially stated

Actual analogue computer tests of this system demonstrated the same frequency of oscillation as predicted above, that is, 2 cycles per second (measured to within ±2 per cent). The actual output signal was, of course, nonsinusoidal with a peak value of 0.92 degree or 4 per cent less than the equivalent sinusoidal amplitude predicted by the describing function method.

In addition to providing the experimental check just described, this study also demonstrates the general principle that, while velocity limiting cannot prevent an otherwise unstable system from oscillating, it will limit the amplitude of oscillation to some specific value. For some feedback control applications, such self-sustained oscillations might be permissible.

Acceleration Limiting of Servomotors

In some instances the acceleration itself of a servomotor is artificially limited to protect various mechanical elements. More frequently, some other variable determining acceleration is limited instead, such as the current supplied to an electric servomotor or the pressure supplied to a hydraulic servomotor. When the output load is primarily characterized by the effect of inertia, this is equivalent to acceleration limiting.

If the discussion is confined to simple servomotors of the type represented by the equivalent circuit of Figure 9, the effect of acceleration limiting can be treated in a manner similar to the previous treatment of velocity limiting. The conclusions reached will apply as well in a qualitative sense to servo elements having more complicated transfer functions.

In Figure 9, the velocity limiting action was shown to be equivalent to a decrease in the resistance, designated as R_2, representing output viscous damping. This corresponded to an increase in effective damping action; a phase lead effect consequently resulted from velocity limiting. On the other hand, acceleration limiting action is equivalent to increasing the inertia of the system, that is, increasing the equivalent capacitance C. This corresponds to an increase in the system's dynamic lag, and a phase-lag effect consequently results with acceleration limiting.

The effect of acceleration limiting on the transfer function of a simple servomotor having but one energy storage element, and having negligible viscous output damping, is shown by the frequency response plot of Figure 15. These data were obtained by analogue computer studies of such a servomotor, where only the fundamental harmonic component of the output signal was considered. The symbol A_L is used to represent the magnitude of the acceleration limit imposed. The transfer function is plotted as a family of curves, one curve applying for each value of the ratio $(N_0/\tau A_L)$, where τ and N_0 have been previously defined.

It may be seen from Figure 15 that acceleration limiting introduces a pronounced phase-lag effect, and when this form of limiting is operative, an adverse effect on the stability of the control system may often be expected. This effect was also considered from the transient response standpoint for one example of a simple servomechanism having the following transfer function whenever limiting action is not operative

$$g(s)=\frac{10}{s(1+0.1s)}$$

Unity feedback transfer function, $h(s)=1$, is assumed. With no limiting, the response of such a system would be reasonably well damped (one-half of critical damping). The transient response to a 10-degree step function change in input r appears as shown in curve a of Figure 16. A 16-per-cent overshoot is observed and the correction time (arbitrarily defined as the time required for the error to be reduced to, and stay within the range ±2 per cent) is about 0.60 second. Curve B of Figure 16 shows the effect of an acceleration limit of 250 degrees per second-squared. The response damping shows a very slight improvement, but the correction time has been extended to about 0.68 second. Curve C of Figure 16 shows the effect of a lower acceleration limit of 125 degrees per second-squared. Now the response damping is obviously poorer in that the peak of the first overshoot has been increased from 16 per cent to 26 per cent. Furthermore, the correction time has been extended to about 1.15 seconds.

The application of even lower acceleration limits would tend to make the system still more poorly damped. It may be noted that, in Figure 16, the periods during which limiting is effective are indicated by broken-line portions of the response curves. In case b the limiting was effective only during the acceleration portion of the response, and a slight improvement in response damping resulted. From a frequency response standpoint, this might be explained as follows Reference to Figure 15 shows the limiting action causes a reduction in gain, usually tending to improve response damping, and an increased phase lag, tending to reduce the response damping. In case b, corresponding to a relatively high acceleration limit, the former effect of gain reduction predominated and some improvement in damping was noted. In case c the limiting was also effective during the deceleration portion of the response, and the response damping was decreased. From a frequency response standpoint this might be explained by stating that the detrimental effect of phase lag was predominant. In general it will be found that, whenever a marked reduction in the permissible acceleration of a servomotor is caused by limiting action, a reduction in response damping and in speed of response can be expected.

Conclusions

The effect of limiting on the performance of feedback control systems can be studied in terms of the frequency response of the system if the describing function method is employed. Data obtained using this method can then be shown graphically by means of transfer loci; unlike linear systems, such transfer loci will depend on amplitude as well as frequency and hence must be plotted as a family of curves.

From such frequency response data, predictions can be made concerning the nature of the system's transient response. It is possible to predict the general effect of various types of limiting on the response of the system and also to select means of compensation which are adapted to the improvement of such limited systems. The correlation between transient and frequency responses is qualitative as it is presented in this paper, and there is need for further work in this field so that a more quantitative method of correlation might be established.

Limiting is described as simple when no energy storage elements are directly affected by the limiting action. Such limiting action is equivalent to a simple reduction in system gain and hence presents stability difficulties only in those systems described as being conditionally stable. Conditionally stable systems often result from the application of phase-lag type of compensating networks and, in this instance, it is suggested that stability difficulties be avoided by using feedback means to achieve such compensation with the limited element included in the minor loop associated with such a feedback path.

More complicated forms of limiting are discussed, such as the velocity or acceleration limiting of servomotors. The former type of limiting is found to be generally beneficial as far as system stability is concerned; however, an excessive amount of such limiting can lead to an unduly slow response. The improvement in response damping associated with velocity limiting can be explained in terms of the phase lead effect such limiting introduces.

Forms of limiting which tend to restrict the acceleration of a servomotor, such as current limiting of electric servomotors and pressure limiting of hydraulic servomotors, cause an increased phase lag as far as the frequency response of the servomotor is concerned. Hence it is found that the damping associated with the transient response is adversely affected when such limiting action is applied.

Most of the data presented here were obtained from electronic analogue computer studies. It is felt that the combination of analogue computer studies with analysis and synthesis techniques based upon the describing function method constitutes the most effective engineering approach to the design of such nonlinear control systems.

References

1. Dynamics of Automatic Control (book), R. C. Oldenbourg, H. Sartorious (translated by Dr. H. L. Mason). *American Society of Mechanical Engineers*, New York, N. Y., February 1948.

2. On Some Nonlinear Phenomena in Regulatory Systems (in Russian), L. C. Goldfarb. *Avtomatika i Telemekhanika*, Moscow, Russia, volume 8, number 5, 1947, pages 349–83. Translated in *Report 1691*, National Bureau of Standards, Washington, D. C., 1952.

3. A Frequency Response Method for Analyzing and Synthesizing Contactor Servomechanisms, Ralph J. Kochenburger. *AIEE Transactions*, volume 69, part I, 1950, pages 270–84.

4. Sinusoidal Analysis of Feedback Control Systems Containing Nonlinear Elements, E. C. Johnson. *AIEE Transactions*, volume 71, part II, July 1952, pages 169–81.

5. Parallel Circuits in Servomechanisms, H. Tyler Marcy. *AIEE Transactions*, volume 65, 1946, pages 521–29.

6. Principles of Servomechanisms (book), G. S. Brown, D. P. Campbell. John Wiley and Sons, Inc., New York, N. Y., 1948.

7. Servomechanisms and Regulating System Design, Volume I (book), H. Chestnut, R. W. Mayer. John Wiley and Sons, Inc., New York, N. Y., 1951.

8. Theory of Servomechanisms (book), H. M. James, N. B. Nichols, R. S. Phillips. McGraw-Hill Book Company, New York, N. Y., 1947.

Discussion

Emile S. Sherrard (Naval Research Laboratory, Washington 25, D. C.): In this paper, Dr. Kochenburger has achieved an excellent survey of the effect of limiting in feedback control systems. This is a remarkable achievement if it is recognized that significant treatments of the surveyed subjects are rare or nonexistent.

The effect of limiting upon the stability of conditionally stable systems has been known to engineers for some time. Bode[1] in 1945 stated that amplifier saturation may cause conditionally stable systems to execute large amplitude oscillations. E. H. Bennett and H. Chestnut arrived at the same conclusion in 1949 in unpublished work. Bode's statement seems to be based on experience; Bennett and Chestnut performed transient calculations on typical servomechanisms. In this paper, the same conclusion is reached. However, the employment of the describing function method of analysis shortens the work, clearly exhibits the assumptions of the analysis, and suggests methods of compensating for the effects of limiting.

The author states that limiting applied to an "already adequately damped system" will result in "an increase in response damping and a decrease in speed of response." E. Levinson[2] has obtained contrary results. Levinson discusses the case of amplifier limiting in the feedback circuit of a tachometer-through-high-pass-filter stabilized servomechanism. As shown in Figures 5(A) and (B) of Levinson's paper, such feedback path limiting results in less response damping and an increase in speed of response. In the light of Levinson's work, it would seem that the statement of this paper holds, at most, for the case of series stabilization with a lag type or low-pass filter.

Nonlinearities other than the velocity limiting discussed in this paper may be deliberately introduced into a control system to compensate for unavoidable nonlinearities. Although individual systems may vary greatly, this writer believes the most profitable place for the insertion of non-linearities is generally in the system's stabilizing filter. The use of such simple limiting circuits as biased diodes, thyrite, or perhaps rectifiers with a high forward resistance for low voltages will not add appreciable size or weight to the system. Nor does the introduction of such nonlinearities add moving parts or complicate the mechanical design of the system.

A previous paper[3] has discussed the application of a simple limiting circuit to the lag network of Figure 6 when such a network is used for the series stabilization of a conditionally stable servomechanism. This paper shows that if a limiting circuit is not used, the system describes large amplitude oscillations as a result of saturation of one of its amplifiers. If a limiting circuit is used to prevent the magnitude of the capacitor's voltage from exceeding a certain value, the system will be stable for both large and small signal operation. In this writer's opinion, the same simple technique may be used to prevent large amplitude oscillations in a conditionally stable system stabilized by tachometer feedback through a 1- or 2-section lead network. A limiting circuit across one of the capacitors of the lead network might be used to prevent the large amplitude oscillations that could result from amplifier saturation in the system.

References

1. Network Analysis and Feedback Amplifier Design (book), H. W. Bode. D. Van Nostrand Company, Inc., New York, N. Y., 1945, pages 162–63.

2. Some Saturation Phenomena in Servomechanisms with Emphasis on the Tachometer Stabilized System, E. Levinson. *AIEE Transactions*, volume 72, part II, March 1953, pages 1–9.

3. Stabilization of a Servomechanism Subject to Large Amplitude Oscillation, Emile S. Sherrard. *AIEE Transactions*, volume 71, part II, November 1952, pages 312–24.

Howard Hamer (Electronic Associates, Long Branch, N. J.): Dr. Kochenburger is to be commended for his continued interest in nonlinear feedback control systems. His introduction of the describing function concept presented a most powerful tool to the servo designer who is willing to admit the existence of nonlinear systems.

I must, however, take issue with the author about certain aspects of his paper. An analysis using describing functions is, of necessity, only as good as are the functions used, and such a function, derived from an equivalent circuit or other analogue of the physical system, is only valid to the same degree as the analogue. To fully discuss this paper in this light would require, I fear, another paper. I will therefore discuss only the question of velocity limiting.

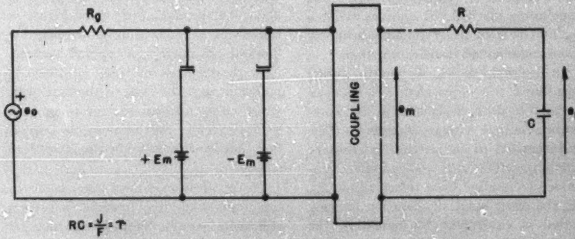

Figure 1. Equivalent circuit of servomotor with input limiting

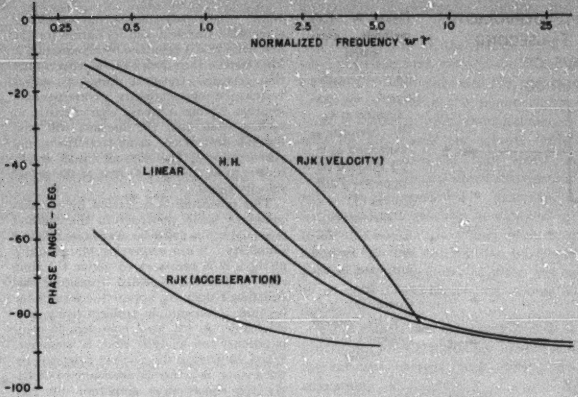

Figure 2. Phase angle of output velocity for a saturated servo

The equivalent circuit shown by the author as Figure 9 seems to me to be a rather naive picture of the behavior of a servo system. It is true that the author calls it the servomotor equivalent, but a motor divorced from its driving system is somewhat useless. In most practical systems, involving physical servos and not their analogues, the maximum velocity obtainable from the motor is well in excess of the system requirements, if one assumes infinite driving power and infinite rating on the motor. (An exception is the 2-phase a-c motor, but even in this instance synchronous speed is seldom reached.)

The designer then introduces limiting ahead of the servomotor, either deliberately to protect the motor or as a result of limits on such things as size of components or available supply power. The end result is that limiting occurs at the input to the motor rather than at the output. If we accept the author's approximate analogue for the motor alone (removing the output limit since it will not be reached) and include a limit on the driver, the equivalent circuit shown in figure 1 of the discussion is obtained. In this circuit, the resistor R_g and the diodes represent the fact that the driving power (and therefore the force or torque) is limited. The box marked "coupling" is used to indicate that limiting of driving power does not affect the output damping. It is a unilateral, zero-output-impedance, unity ratio device, which, on a computer, would be an isolating amplifier. The R and C represent motor parameters.

Application of a voltage e_0 large enough to saturate the driver will result in a driving function of approximately square wave shape at the input to the servomotor. The amplitude of the square wave will be held at the limit, although the input to the limiter may increase. The gain through the limiter will then fall off at 6 decibels for each 6-decibel rise of the voltage e_0. This variation in gain with input amplitude will be independent of frequency. The phase of the voltage e_m will be zero if the miscellaneous reactances such as motor inductance are neglected.

The voltage appearing at the output of the equivalent circuit, and the output velocity of the servomotor, will be independent, in amplitude and phase, of the amplitude of e_0, so long as the amplitude of e_0 is sufficient to saturate the limiter. The voltage e_1 is given by

$$e_1=e_m\left\{1-2\frac{\epsilon^{-t/\tau}}{1+\epsilon^{-\alpha}}\right\}0<t<\frac{1}{2f} \qquad (1)$$

where

e_m = the limited value

$\tau=RC=J/F$

$\alpha=\frac{1}{2f\tau}$

The (linearized) phase angle of this function can be determined from the zero-axis crossing as

$$\phi=\frac{180}{\alpha}\ln\frac{2}{1+\epsilon^{-\alpha}}\text{ degrees} \qquad (2)$$

and the peak magnitude, which occurs at $t=0$ is

$$\frac{e_{1m}}{e_m}=1-\frac{2}{1+\epsilon^{-\alpha}} \qquad (3)$$

These functions are easier to use than Fourier components, and are sufficiently accurate a representation of the amplitude and phase for stability studies.

The output velocity phase function is shown in Figure 2 of the discussion as the curve marked *H.H.;* those marked *RJK* are taken from Figures 10 and 15 of the paper for $N_0=8$. There is a similar difference between the amplitude ratios for the two equivalent circuits.

The equivalent circuit shown in Figure 1 of the discussion has been verified by stability studies on actual servos. Analogue computer studies using this equivalent circuit should give parallel results.

Ralph J. Kochenburger: The author appreciates the comments made by the discussers and the number of interesting suggestions they have made.

Mr. Sherrard calls attention to a statement made in the paper which the author should have expressed in more specific terms. Simple limiting, when applied in the feed-forward portion of an already adequately damped system, will result in an increase in response damping and a decrease in the speed of response. The example mentioned in Levinson's paper represents a different situation where the limiting is applied to the feedback path associated with a minor loop.

The scope of the paper did not include the introduction of nonlinear effects in stabilizing filters for the purpose of improving response. It is, however, believed that the describing function method could be used to study such effects.

The paper discussed one possible means for avoiding the unstable or poorly damped response often associated with conditionally stable systems when large amplitude disturbances are applied. This was illustrated in block diagram form in Figure 8. Mr. Sherrard's paper (his reference 3) proposes an alternative scheme for accomplishing the same purpose. There are a number of different methods available to the designer and the selection of the most appropriate will, of course, depend upon which method proves most convenient for the specific application involved. Mr. Sherrard has presented a significant treatment of this problem.

One issue questioned by Mr. Hamer was in regard to the use of equivalent circuit representations—or analogue computer representations—of actual system components. Such representations were employed in this paper so that general conclusions could be reached applicable to a class of control components. The process of generalizing always introduces errors. In any specific application it is obviously desirable, when possible, that the analysis be applied to the component itself rather than to some approximate equivalent.

The equivalent circuit of a servomotor, shown in Figure 9, is an approximate representation which is used to describe the operation of many servomotors used in practice and which will provide sufficiently correct answers in many control design problems. As mentioned in the paper, there will be some instances where this representation is too oversimplified. The motor is not to be considered divorced from its driving system and the resistance designated as R_1 should include the driving impedance of the source supplying power to the motor.

Mr. Hamer mentions that the designer would ordinarily limit servomotor speed indirectly, that is, by limiting the actuating signal applied to the servomotor. His Figure 1 is an equivalent circuit diagram corresponding to such a method. It is true that this is the method of speed limiting most frequently employed in practice. This method is an example of simple limiting as discussed in the first portion of the paper. Since the limiting action is isolated from the servomotor dynamics, the describing function for this type of limiting introduces no phase change (see Figure 4 of the paper). One of the purposes of the paper was to point out the advantages of output velocity limiting over the use of

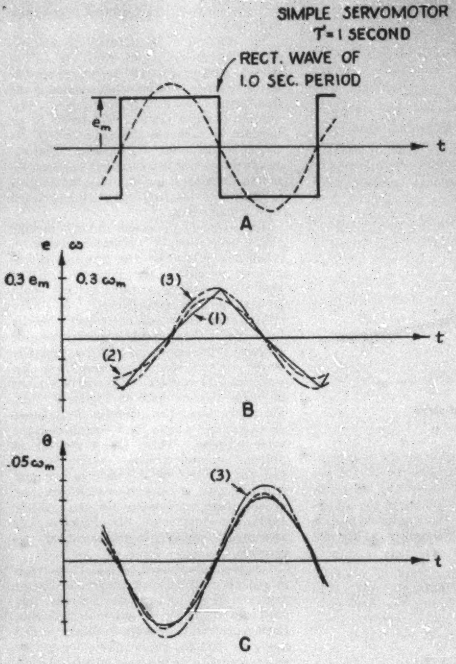

Figure 3. Two methods compared

(A) Actuating signal ω_m expressed as e_m

(B) Velocity ω expressed as e

(C) Angular position $\theta = \int \omega dt$

Curves (1) Actual values

Curves (2) Values by method proposed in paper

Curves (3) Values by method proposed by Mr. Hamer

simple limiting applied to the servomotor's driving circuit. Limiting of the actual output velocity has two basic advantages: It provides a more definite speed limit when compared with input limiting and would limit speed even when the load itself was of a nature which might tend to drive the motor and cause overspeeding. Furthermore, it introduces an effective phase lead which can be used to improve the degree of stability associated with the response to large disturbances.

Mr. Hamer proceeds to analyze the response of the simple servomotor represented in his Figure 1 for the case where the input signal is well in excess of the limited value. The steady-state output velocity is a repeated transient and its nature for the first half-cycle is described by his equation 1. Mr. Hamer then proposes, in effect, that this repeated transient form of output velocity be represented by a corresponding sinusoid having a phase characteristic of such a value that the sinusoid will pass through zero at the same time the actual velocity does. The sinusoid's peak amplitude is to be the same as that of the actual velocity signal.

This procedure is suggested by the discusser as being preferred to the method proposed in the paper because of its inferred simplicity. When employing Mr. Hamer's method, it is necessary to derive the time relation for the repeated transient; his equation 1 does not appear too formidable because of the simple problem being considered but, even here, considerable computational and analytic labor is necessary. When employing the method proposed by the author, it is merely necessary to multiply the square-wave amplitude by 1.27 (or $4/\pi$) to obtain the equivalent sinusoid upon which the describing function method is based. From this point on, the analysis is carried out on the basis of the conventional linear steady-state sinusoidal analysis.

Figure 3 of the discussion compares the two methods for the case where the limited rectangular-wave signal of frequency 1 cycle per second is applied to a servomotor of 1-second time constant. The difference in accuracy obtained by the two methods is particularly evident in the plot shown in part *c* of this diagram where the servomotor's predicted angular positions are compared with the actual values. In the case where the describing function method was employed, the curve corresponding to the predicted value is almost indistinguishable from the true curve. The maximum amplitude predicted by Mr. Hamer's method is 24 per cent greater than the true value.

The author wishes to thank Mr. Sherrard and Mr. Hamer for their interest in this paper and for the significant points of discussion they have raised.

Application and Operation of D-C Drives on Rubber Calenders

J. F. SELLERS
FELLOW AIEE

B. G. WHEELER
MEMBER AIEE

A. C. HALTER
MEMBER AIEE

D-C MOTORS are used almost universally on rubber calenders to obtain a wide speed range, good speed regulation, maximum braking under emergency conditions, suitable matching of speeds of the auxiliaries with the calender, and on the modern drives, electrical tension regulation of the fabric. The majority of the calenders in operation are driven by adjustable speed d-c motors with conventional armature resistor starting and with rheostat control of the motor field for speed regulation. The more modern installations are equipped with adjustable voltage systems to obtain greater flexibility of operation, better synchronization with auxiliary machines, more suitable power for the constant torque requirements of calender loads, and improved electrical braking under emergency conditions.

To obtain maximum production of a high-quality ply stock from a calender train, it is necessary that the line be capable of operating at the highest speed that it is possible to properly coat the cord with rubber, and that proper tension be maintained at all points in the line However, the safety of the personnel is always placed above the production requirements both by the rubber industry and the governmental bodies which have

---

Paper 53-145, recommended by the AIEE General Industry Applications Committee and approved by the AIEE Committee on Technical Operations for presentation at the AIEE Winter General Meeting, New York, N. Y., January 19–23, 1953. Manuscript submitted October 20, 1952; made available for printing December 4, 1952.

J. F. Sellers and A. C. Halter are with the Allis-Chalmers Manufacturing Company, Milwaukee Wis. B. G. Wheeler is with Cutler-Hammer Inc , Milwaukee, Wis.

an interest in the safety of the working men. With careful selection, design and application of electric equipment it is possible to meet and better the code requirements for safe operation and stopping. R. S. Ferguson states in an unpublished paper presented at the 1950 AIEE Conference on Electrical Engineering Problems in the Rubber and Plastics Industries, "The proper time to obtain a good safety stop is before placing orders for equipment and not after the drive has been installed."

Motors

There are four choices of type of d-c motor for the main calender drive:

1. 40-degree-centigrade rise self-ventilated.
2. 60-degree-centigrade rise self-ventilated.
3. 40-degree-centigrade rise separately ventilated.
4. 60-degree-centigrade rise separately ventilated.

The 60-degree-centigrade separately ventilated motor gives the lowest possible inertia and quickest stopping. A self-ventilated motor usually has greater inertia than the separately ventilated motor for two reasons. The first is that there is practically no restriction except shaft strength in ratio of armature core length to armature diameter in the separately ventilated motor. Thus a separately ventilated motor may have a core length of 130 to 150 per cent of the core diameter, whereas a self-ventilated motor is restricted to a ratio of 80 to 100 per cent for core length to core diameter, because of the pressure required to force the cooling air through the motor. The same comments apply to the comparison of self- or separately ventilated 40 or 60-degree-centigrade drive motors.

The second reason for the higher inertia of self-ventilated compared to separately ventilated motors is the necessity of keeping within 15 degrees centigrade additional rise for operation with full rated armature current at minimum continuous speed, which is usually less than 30 yards per minute. At this corresponding motor speed the attached fan must have a peripheral speed of about 1,700 to 1,800 feet per minute at the fan tip for a 40-degree-centigrade motor and and about 1,500 feet per minute for a 60-degree-centigrade motor.

The choice between 40-degree-centigrade or 60-degree-centigrade rise motor therefore is based on expected insulation life, knowledge of power requirement, and importance of emergency stopping distance.

A comparison of the inertia (WK^2) values of these four types of motor for a typical drive will illustrate the problem involved in making the motor choice. Take a calender with 28-inch-diameter rolls for 100 yards per minute fabric speed. This gives 41 rpm speed of calender roll. Since a direct drive motor will not be economically practical, a single reduction gear can be obtained up to about 11-to-1 ratio, which would give a motor speed of 451 rpm for 100 yards per minute. The power required will be such that a 400-horsepower motor is ample.

From calculations in appendix I, it is found that for 100 yards per minute and 300-per-cent current peak during deceleration:

1. A 40-degree-centigrade separately ventilated motor has 11.6 inches stopping distance, or 0.33 per cent of travel per minute.
2. A 40-degree-centigrade self-ventilated motor has 21.2 inches stopping distance, or 0.59 per cent of travel per minute.
3. A 60-degree-centigrade separately ventilated motor has 10.9 inches stopping distance, or 0.31 per cent of travel per minute.
4. A 60-degree-centigrade self-ventilated motor has 14.9 inches stopping distance, or 0.42 per cent of travel per minute.

Control

A simple d-c drive for a calender motor operating from a constant voltage bus requires only conventional line contactors, accelerators, field relays, and a rheostat for field adjustment to obtain a 3/1 or 4/1 range of speed adjustment. If a wider speed range is desired a 115/230-volt bus may be used. A separate adjustable voltage system for the auxiliaries is about the only practical way of co-ordinating electrically driven auxiliaries with a 2-voltage main drive. If a line shaft is used, tensioning must be accomplished by mechanical means such as air cylinders or weighted festoons with concurrent difficulties in compensating for coil build-up and build-down. All auxiliary machines depend on the calender motor for their power and cannot be operated or regulated separately.

Although this type of equipment may be very satisfactory for general purpose calenders, the mass production of automobile tires requires that the major portion of the ply stock be produced on calender trains which will produce a uniform grade of stock at high speed. As a result adjustable voltage drives, such as illustrated in Figure 1 are used on a line of this type. Tension regulators maintain tension at at least five points in the line; at the letoff, ahead of the calender, after the calender, at the windup, and at the liner. Storage is provided between the letoff and drying drums, and between the cooling drums and windup, so that the calender may remain in continuous operation while a splice is being made in the cord fabric whenever a new roll is started.

A regulator is provided for the main drive motor with a feedback from a tachometer coupled to that motor to provide a constant operating speed as selected by the calender operator. The result is maximum production and the quality of the ply stock is uniform. The operators can set the tension at the five points requiring tension in the line merely by adjusting potentiometers at the operators panels. The auxiliary motors may be individually jogged forward or reverse whenever the line is not running. Threading the line is simplified by providing for group operation of the motors on those machines ahead of or after the calender. With the arrangement illustrated in Figure 1, it is possible to start, thread the line, accelerate, operate at a maximum speed, decelerate, and stop the line either normally or under emergency conditions without unduly stretching the fabric or allowing it to loosen at any point in the line.

Electrical Braking

Maximum braking torque requires maximum motor flux and sustained maximum armature current throughout the braking cycle. Designing the motor with low WK^2 per horsepower, small field time constant and good commutation will all aid materially in effective braking. Three types of electrical braking are used on d-c calender drives; dynamic, uncontrolled regenerative, and controlled regenerative. Dynamic braking allows the energy in the drive to dissipate in a resistor connected across the motor armature in two or more successive steps. Each step of braking is limited by the ability of the motor to commutate the peak current. On adjustable speed motors, the first step must allow for reversal of the flux in the interpoles. The succeeding steps may be set for higher peak currents. Since dynamic braking may be applied to either constant or adjustable voltage drives, it is used more universally than regenerative. Even on adjustable voltage drives, motors will generally commutate more braking current than the supporting generators.

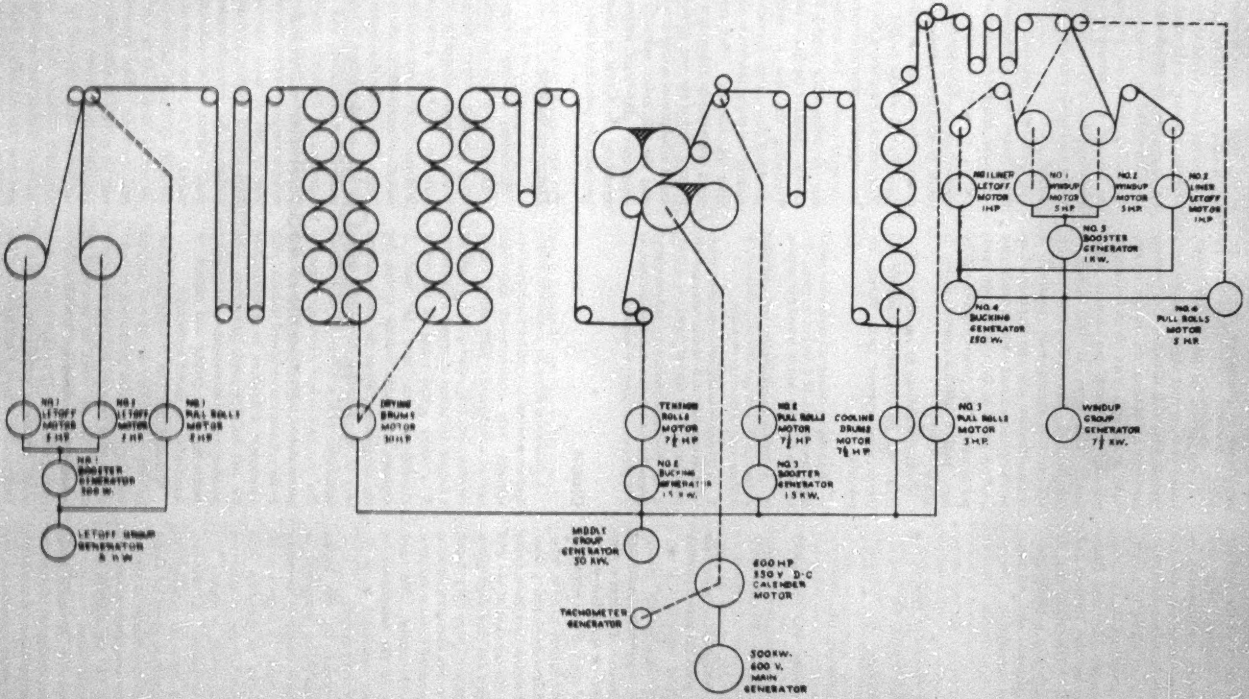
NO.1 LETOFF MOTOR 2 HP
NO.2 LETOFF MOTOR 2 HP
NO.1 PULL ROLLS MOTOR 3 HP
NO.1 BOOSTER GENERATOR 300 W.
LETOFF GROUP GENERATOR 5 KW.
DRYING DRUMS MOTOR 10 HP
TENSION ROLLS MOTOR 7½ HP
NO.2 BUCKING GENERATOR 1.5 KW.
MIDDLE GROUP GENERATOR 50 KW.
NO.2 PULL ROLLS MOTOR 7½ HP
NO.3 BOOSTER GENERATOR 1.5 KW.
COOLING DRUMS MOTOR 7½ HP
NO.3 PULL ROLLS MOTOR 3 HP.
600 HP 350 V D-C CALENDER MOTOR
TACHOMETER GENERATOR
500 KW. 600 V. MAIN GENERATOR
NO.1 LINER LETOFF MOTOR 1 HP
NO.1 WINDUP MOTOR 5 HP
NO.2 WINDUP MOTOR 5 HP.
NO.2 LINER LETOFF MOTOR 1 HP
NO.5 BOOSTER GENERATOR 1 KW.
NO.4 BUCKING GENERATOR 250 W.
NO.4 PULL ROLLS MOTOR 5 HP.
WINDUP GROUP GENERATOR 7½ KW.

Figure 1. Typical layout of adjustable voltage d-c drive for modern high-speed continuous-processing rubber calender train

Regenerative braking has the following advantages:

1. Small contactors operate to initiate the braking.
2. Average current is high for given peak currents.
3. Appreciable braking effort is available at low speeds.
4. Motors may be used which have a narrow speed range and low enough field time constant to provide sufficient flux for best braking.

The simplest form of uncontrolled regenerative braking involves the use of a generator with a time constant in the field such that on discharge of the field the flux, and thereby the voltage of the generator, will decay at a rate which will tend to maintain the armature current at a value which the generator and motor will commutate. A refinement of the simple regenerative braking scheme is the use of a nonlinear resistor in the discharge circuit of the generator field. Hence when the generator field discharge voltage is high the effective discharge resistance is low and the energy in the field slowly dissipates limiting peak currents. The effective resistance in the discharge path increases with decrease in voltage to reduce the time constant of the circuit and cause more armature current to flow at low speeds. Thus the current in the armature is maintained more nearly constant throughout the braking cycle. This resistor may be a rectifier, a thyrite resistor, or similar nonlinear resistance device.

On a controlled regenerative braking scheme, such as we are illustrating with the test data presented in this paper, a regulator is used to control the rate at which the generator discharges to maintain armature current at the maximum value commensurate with the commutating ability of the machine throughout the braking cycle. For equivalent peak currents the braking power will exceed that available from dynamic braking and uncontrolled regenerative braking because of higher average current. The generator is usually the limiting machine since its speed is maintained, whereas the calender motor speed is decreasing as the voltage decreases. However, the decreasing generator voltage allows higher currents than would be permissible if the voltage were maintained.

Since the rotating regulator allows the reversal of current through its armature it is well suited to regenerative braking applications. For speed regulation the reference field is supplied from a constant direct voltage source and a tachometer on the calender motor feeds a signal back to another field on the regulator for magnetic comparison with this reference. During braking, the fields of the regulator are reconnected to obtain maximum forcing of the generator field in the reverse direction until the current in the loop reaches its limiting value. At this point the current limit field of the regulator must take over and allow the generator voltage to decay at a rate which will maintain the armature current.

Since stopping distance is of prime importance on calenders used in the rubber industry, the need is evident for comprehensive data on an operating installation. The balance of this paper will describe the tests conducted on an adjustable voltage drive installed within the past 2 years and analyze the data obtained in these tests. The calender train corresponds to the layout illustrated by Figure 1 and the ratings of the motor and generators are as marked in that figure. The 2-horsepower letoff motors and the 5-horsepower windup motors are low-inertia separately ventilated machines with a 4.2/1 speed range. All other motors are of conventional self-ventilated design. The 600-horsepower 550-volt d-c calender motor has a speed range of 300/450 rpm and a field rated 115 volts. The field is reconnected to the 250-volt exciter bus during braking to obtain maximum flux. The 500-kw 600-volt supporting generator is of standard design and has the customary pole face windings. The commutation is exceptionally good up to 300-per-cent load and at 400 per cent there is no progressive damage to brushes or commutator on emergency stops. The field is rated 40 volts.

The rotating regulator supplying excitation to the generator is a 5-kw 167-volt Regulex exciter. The voltage drop across the combined interpole field of the motor and generator is used as the current signal to limit the loop current by controlling the Regulex exciter. This voltage drop is compared with the armature voltage of a small, heavily compounded d-c exciter and the difference between the two signals is fed into the current-limiting field of the regulator. The series field on the reference exciter compensates for the ohmic losses in the current-limiting circuit by reducing its terminal volts as the loop current increases. An additional field is wound on the interpoles of the main generator in a direction opposite the main winding, and connected in series with the signal leads, to reduce the inductive effect of the d-c transient through the interpole field. This additional winding on the main generator precludes the necessity of using a high-wattage resistor in the main power circuit.

When a safety switch is tripped all fields on the Regulex exciter are disconnected except the feedback from the tachometer and the current limit. As rapidly as practicable the reference field is reconnected in suicide across the 600-volt main generator armature even though the continuous rating of this field is only 30 volts. The relay initiating the emergency stop is provided with a low-inductance coil and with a nonmagnetic spacer between the armature and the core so that it opens extremely fast when the circuit is interrupted.

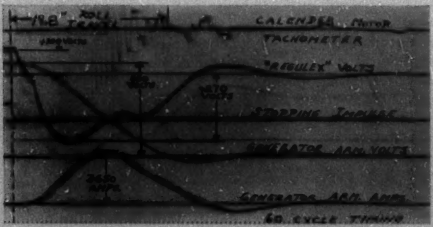

Figure 2. Oscillogram of electrical data on regenerative braking stop from 100 yards per minute with 430-per-cent braking current

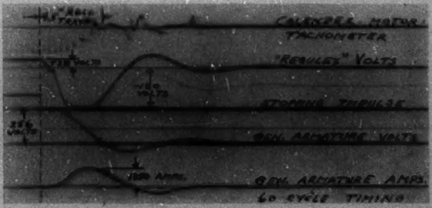

Figure 3. Oscillogram of electrical data for regenerative braking stop from 30 yards per minute with same constants as Figure 2

Testing Procedure and Results

On a d-c calender drive the variables affecting stopping distance are operating time of relays, time constant of the regulator, time constant of the main generator, time constant of the armature loop, armature current, and motor field strength. For a thorough analysis of these variables in the regeneration cycle, the following traces were recorded:

1. Calender revolutions.
2. Motor armature volts.
3. Motor armature current.
4. Generator field current.
5. Regulex exciter voltage.
6. Current-limit field current.
7. Tripping impulse.
8. Timing wave.

A 6-element oscillograph was used to record these variables so that it was necessary to repeat certain runs to obtain the eight traces. An a-c 6-pole tachometer generator signal was recorded to serve a twofold purpose. First, the magnitude of the voltage wave gave a good instantaneous calender speed indication and, second, a count of the total cycles between any two points gave a very accurate indication of the total strip travel during a particular period of time. For each given set of operating conditions eight sets of data were taken by initiating stops from operating speeds of 20, 30, 50, 60, 70, 80, 90, and 100 yards per minute.

Figure 2 is the oscillogram of a regenerative braking stop made from 100 yards per minute without destructive sparking of the generator brushes. The 3,650 amperes is 430 per cent of full-load rated current. By counting the cycles of the a-c tachometer and multiplying by a suitable factor to account for gearing and calender roll diameter, a stopping distance of 19.8 inches was ascertained. The additional oscillations on this trace were oscillations of the armature after it had stopped its forward rotation. The dashed line near the left of the oscillogram is drawn through the break in the stopping impulse line to show the point at which the safety switch was tripped, and the distance from that point to the point at which the Regulex voltage started to decrease is the time required to open the fields on the Regulex exciter. This is approximately 1 cycle. After about 4 additional cycles there is a break in the Regulex exciter volts indicating that the suicide contacts have closed forcing the Regulex exciter volts down even more rapidly. As the loop current increases, the current-limiting field forces the Regulex exciter to reduce its negative voltage and maintain the braking current as long as possible. As the tachometer and generator volts both decay to zero the Regulex volts return to zero.

Figure 3 is a similar stop from 30 yards per minute and with the lower energy in the system the current in the loop reaches 1,350 amperes.

Since only six elements were available in the oscillograph, two stops were made from 100 yards per minute with the same operating conditions. Figures 4 and 5 are the oscillograms of these stops. The current-limit reference was set slightly lower than the stop shown in Figure 2. These traces also illustrate the change in generator field current and the current flowing in the current-limit field of the regulator. All data recorded in these two oscillograms have been plotted in Figure 6 as a function of the elapsed seconds from the time the safety switch is tripped.

An analysis of these variables plotted as a function of time provides an insight into where the important distances are lost in the braking of a machine. Emphasis should be placed on the point that most of the distance lost is at the high speed of the calender because even with low braking torque at low speed, the time is long in comparison with the inches traveled. At 100 yards per minute on this particular drive and a 60-cycle time base, approximately 1 inch of fabric per cycle travels through the rolls.

The time between the opening of the safety switch and the initiation of the braking cycle by the control on this application was only about 1 cycle or 0.016 second. This time is about as short as it is practical to design.

The next time delay is in the Regulex exciter. This machine with its laminated steel construction has an inherently fast response and curve *8* indicates that it changes voltage rapidly and satisfactorily. The Regulex exciter effectiveness is somewhat reduced by its current-limit action as illustrated by curve *4*. Curve *4* shows that the current-limit signal leads the armature current, curve *7*, indicating that the reverse turns from the interpole field were not sufficient to entirely buck out the transient effect of inductance in the interpole field of the main motor and generator. However, this slight lead does check the negative rise of the Regulex voltage in time to prevent too large an overshoot and possible resulting oscillation. The initial in-rush of current in the current-limit field is due to the mutual inductance of the Regulex exciter fields when the suicide voltage is applied across the reference field.

The next time constant to consider is the field of the main generator. With a 40-volt field on this generator, curve *6* indicates that the Regulex exciter is able to force it from full field to zero in less than 0.17 second. This is very satisfactory and about as low a time constant as is practical in a machine of this type. There is very little difference in results between supplying this field directly with the Regulex exciter with no series resistance and maximum forcing, and supplying it through a ballast resistor which lowers the time constant but also lowers the effective forcing.

Curve *2*, a record of the terminal volts of the generator, indicates that the great-

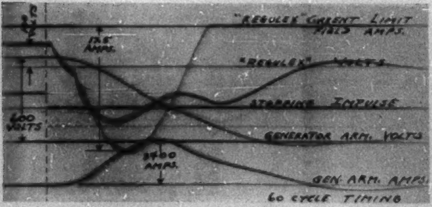

Figure 4. Oscillogram of electrical data for regenerative braking stop from 100 yards per minute with current limited to 400 per cent of full load

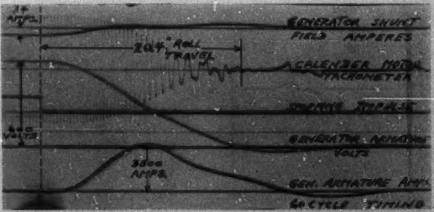

Figure 5. Oscillogram of electrical data for regenerative braking stop with same conditions as Figure 4

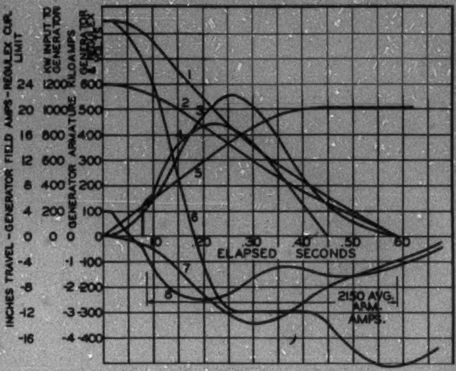

Figure 6. Response of electric equipment as a function of elapsed time after tripping a safety switch. Stopping test of Z calender from 100 yards per minute

Curve 1.	Effective generator field amperes
Curve 2.	Generator armature volts
Curve 3.	Generator kilowattage input
Curve 4.	Regulex current-limit field
Curve 5.	Inches stopping distance
Curve 6.	Generator field amperes
Curve 7.	Generator armature amperes
Curve 8.	Regulex armature volts

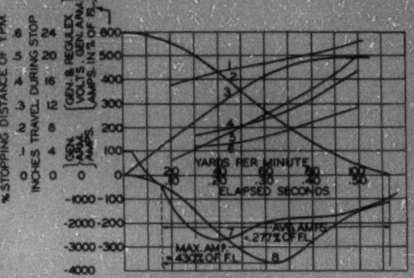

Figure 7. Response of electric equipment as a function of speed at which calender is running and of elapsed time after tripping safety switch. Sixty-horsepower 550-volt 300/450-rpm motor, 500-kw 600-volt 900-rpm generator. Twenty-eight-inch diameter rolls, 11.1 gear motor $WK^2=4,780$ pound-feet squared. Calender $WK^2=74,000$ pound-feet squared. Stopping test of 2 calender from 100 yards per minute. Curves 1, 4, and 5 are topping from a series of initial calender speeds from 20 to 100 yards per minute

Curve 1.	Stopping distance
Curve 2.	Generator armature volts
Curve 3.	Inches travel
Curve 4.	Peak armature amperes in per cent of full load
Curve 5.	Inches travel
Curve 6.	Average armature amperes in per cent of full load
Curve 7.	Regulex terminal volts
Curve 8.	Generator armature amperes

est time delay encountered in the entire braking is the failure of the generator voltage to follow its field current. Inasmuch as there is no other winding on the main field poles, the flux must be damped by some extraneous losses in the magnetic circuit such as eddy currents. Laminating the entire field structure including both the poles and yoke is the only effective way of overcoming this delay. Curve *1* illustrates the shunt field current which would be required to provide the voltage illustrated in curve *2* if no extraneous losses were present. The deviation between curves *1* and *6*, therefore, represents the greatest loss in the entire system and the one which must be overcome if stopping distances are to be reduced further than those obtained.

The average armature current from the time that the regulator reference field was suicided on the main armature until the drive stopped, was 2,150 amperes. The braking would be much more effective if curve *7* could be forced to a more nearly square shape, but this is impossible unless the flux damping can be eliminated.

Curve *5* indicates that although 0.6 second was used in stopping the drive, very little distance was sacrificed in the last 1/3 of this time.

If the current could be forced to its maximum value sooner, curve *3*, the kilowatt input to the generator, would rise more rapidly so that the appreciable effective braking would start at a higher speed with a resulting improvement in the stopping distance.

The series of curves in Figure 7 are derived from the eight stops which were made with conditions illustrated by Figures 2 and 3. Curves *2*, *3*, *7*, and *8* are similar to the corresponding curves in Figure 6 except that the current limit was set for a slightly higher value allowing a somewhat higher peak current. The data plotted in these curves are derived from the oscillogram shown in Figure 2.

Curve *6* of Figure 7 is a plot of the average armature amperes during braking in per cent of full-load current versus the speed in yards per minute that the calender was traveling at the time of the braking stop. Likewise the peak armature amperes during braking in per cent full-load current versus speed is plotted as curve *4*. These currents are approximately proportional to the increase in calender speed. However, from 70 to 100 yards per minute the speed is increased by motor field weakening rather than increase in voltage so that the slope, particularly of the percentage peak current, increases in this range.

Curve *1* is a plot of the stopping distance as a percentage of the speed at which the calender is running versus the calender speed in yards per minute. It is interesting to note that the stopping distance illustrated by curve *5* is almost directly proportional to the speed that the calender is running and that the percentage stopping distance illustrated by curve *1* does not change greatly for various initial speeds, with a specific calender and control set up.

Another interesting point is that the ratio between average and peak currents is almost constant at 65 per cent. If it had been possible to force the generator current to higher values more rapidly and to eliminate the inductive effects of the current-limit circuit, the average current would have been a greater percentage of the peak current under higher speed conditions.

No records were made of the motor field change during the braking cycle although the field was in all instances reconnected for twice its rated voltage and undoubtedly did have some effect on the braking. However, calculations of the increase in field flux and observations of the field current during the tests indicate that it could not change materially in the

0.6 second in which the calender was stopped.

A discrepancy still exists between the measured to calculated horsepower seconds of 1.2 to 1. The calculated values are based on a WK^2 of 4,780 pound-feet squared for the motor and 74,000 pound-feet squared for the calender and gears. These values may not be accurate. It is possible to check the total WK^2 by first taking running light tests to determine friction and windage and then observing speed at given intervals of time as the calender and drive coast to a stop without any braking.

Conclusions

The most outstanding conclusion to be drawn from the tests on this application is that a very satisfactory safety stop can be obtained by proper design and application of d-c motors and control on a rubber calender. Nineteen and eight-tenths inches is far below the code requirements set up by any state or federal safety commission and is well within the requirements usually specified by the rubber plants. The American Standards Association has set up rubber mill and calender safety codes for drives up through 250 feet per minute but has listed drives of higher speeds as special applications with higher percentage stopping distances subject to the approval of the enforcing authority. However, their most stringent code listed is 1.75 per cent as the stopping distance in percentage of the surface speed of the rolls. The stops obtained on this calender were equal to 0.55 per cent of the roll surface speed.

The second conclusion to be drawn from these data is that d-c transients must be carefully considered in every aspect of electrical braking if safety stops of minimum roll travel are to be obtained.

The design of the motor, control, calender, and gears must be carefully scrutinized if fast stops are to be realized when the equipment is installed and operating.

All auxiliary equipment on the line must be capable of performing as well as the main drive if undesirable looping or stretching of the material is to be avoided. On this particular application with the low inertia motors at the letoff and windup, it is possible to stop the entire line with an emergency stop and the control and the storage festoons will change length by only a very few inches. Also, the braking of the auxiliary motors must be such that men working at the auxiliary machines are as safe as the men working at the calender.

Probably the most satisfactory drive from the standpoint of production, quality, and safety to personnel is the adjustable voltage drive since it provides individual control of tensioning, flexibility of machine operation, high operating speeds, smooth acceleration and deceleration, and minimum rotation on safety stops.

Appendix I. Deceleration Calculation for a 400-Horsepower Drive at 100 Yards Per Minute or 450 RPM Motor Speed

Nomenclature

D_a = armature core diameter, inches
L_a = armature core length, inches
P = number of main poles
D_f = fan diameter, inches
rpm = motor revolutions per minute
hp = motor horsepower output at rated voltage
WK^2 = inertia, pounds-feet squared
D_1 = inches traveled during initial period of deceleration cycle, at approximately initial speed
D_2 = inches traveled during deceleration of motor speed
D_t = total inches traveled during complete decleration cycle
t = seconds of travel during time D_2

From design and test experience the output factor for a 40-degree-centigrade-rise motor in the type required for a calender is 0.00011 horsepower per rpm per cubic inch of armature core volume so

$$0.00011=\frac{400}{450\times\pi/4D_a^2L_a} \quad \text{or } D_a^2L_a=10{,}310 \qquad (1)$$

where

D_a = armature diameter, inches
L_a = armature core length, inches

For a separately ventilated motor assume $L_a=1.5\,D_a$, so

$$1.5D_a^3=10{,}310 \text{ or } D_a=19 \text{ inches and } L_a=28.5 \text{ inches} \qquad (2)$$

For a self-ventilated motor the attached fan at 135 rpm (30 per cent of 450 rpm = 30 yards per minute should have a tip velocity of 1,750 feet per minute.

$$\text{Fan diameter } D_f=\frac{1{,}750\times12}{\pi\times135}=49.6 \text{ inches} \qquad (3)$$

The relation between maximum possible fan diameter and armature diameter for the usual range of motor size is approximately

$$\text{Fan diameter } D_f=2.7\times D_a^{0.866} \qquad (4)$$

From equation 4

$$D_f=49.6=2.7D_a^{0.866} \text{ or } D_a=28 \text{ inches}$$

From equation 2

$$0.00011=\frac{400}{450\times\pi/4\times28^2\times L_a} \quad \text{or } L_a=13 \text{ inches} \qquad (5)$$

A 60-degree-centigrade-rise motor will have an output factor of 0.00013, so for a separately ventilated motor

$$0.00013=\frac{400}{450\times\pi/4\times1.5D_a^3} \quad \text{or } D_a=18 \text{ inches} \qquad (6)$$

and

$$L_a=1.5\times18=27 \text{ inches}$$

For a 60-degree-centigrade self-ventilated motor

$$D_f=\frac{1{,}500\times12}{\pi\times135}=42.5 \text{ inches} \qquad (7)$$

From equation 4

$$D_f=42.5=2.7D_a^{0.866} \text{ or } D_a=24 \text{ inches} \qquad (8)$$

$$\text{Core length } L_a=\frac{400}{450\times\pi/4\times24^2\times0.00013}=15.5 \text{ inches} \qquad (9)$$

An empirical rule for WK² value of preceding armatures of this class is:

$$WK^2 \text{ in pound-feet squared} =D_a^{3.75}\left(0.0013\,\frac{D_a}{P}+0.00019L_a\right) \qquad (10)$$

where P = number of main poles in motor.

Applying equation 10 to the preceding armature sizes, and using 6-pole motors throughout

6-19-28.5 armature = 592 pound-feet squared WK^2 (11)

6-28-13 armature = 2290 pound-feet squared WK^2 (12)

6-18-27 armature = 460 pound-feet squared WK^2 (13)

6-24-15.5 armature = 1170 pound-feet squared WK^2 (14)

where 6-19-28.5 represents 6 poles, 19 inch armature core diameter and 28.5 inch core length.

The calender, gears, and couplings for a typical 4-roll arrangement have a WK^2 of 72,000 which is 595 WK^2 at the motor shaft for 11 to 1 gear, so the total WK^2 is

40-degree-centigrade separately ventilated = 592 + 595 = 1187 pound-feet squared (15)

40-degree-centigrade self-ventilated = 2290 + 595 = 2885 pound-feet squared (16)

60-degree-centigrade separately ventilated = 460 + 595 = 1055 pound-feet squared (17)

60-degree-centigrade self-ventilated = 1170 + 595 = 1765 pound-feet squared (18)

A distance D_1 inches is traveled before the generator armature current rises appreciably and this has been found to be a time interval of 0.08 second, which represents 4.8 inches of fabric travel at 100 yards per minute speed, or 0.133 per cent of travel per minute.

The time to decelerate while reducing armature voltage to zero, with constant motor armature and field current is

$$t \text{ seconds} = \frac{\text{rpm}^2 \times WK^2}{1.615 \times 10^6 \times \text{hp}} \qquad (19)$$

$$= \frac{450^2 \times WK^2}{1.615 \times 10^6 \times 400 \times 0.55 \times 3.00}$$

$$= 0.000190\ WK^2$$

where rpm and hp are at full armature voltage. The distance D_2 traveled in t seconds will be at an average speed close to one-half of the speed when $t=0$, so

$$\text{distance } D_2 = \frac{t \times 100 \times 36}{60 \times 2}$$

$$= 30\ t \text{ inches} = 0.0057\ WK^2 \text{ inch} \qquad (20)$$

The total distance D_t traveled during an emergency stop is $D_t = D_1 + D_2$ or in terms of per cent of travel per minute it is

$$\text{per cent } D_t = \frac{100(D_1+D_2)}{100 \times 36} = 0.0278\ (D_1+D_2) \text{ per cent} \qquad (21)$$

The final comparison is then

40-degree-centigrade separately ventilated = 11.6 inches stopping or 0.33 per cent of per minute travel (22)

40-degree-centigrade self-ventilated = 21.2 inches stopping or 0.59 per cent (23)

60-degree-centigrade separately ventilated = 10.9 inches stopping or 0.31 per cent (24)

60-degree-centigrade self-ventilated = 14.9 inches stopping or 0.42 per cent (25)

These values are based on a peak stopping current of 300 per cent of rated, with the average being 55 per cent of this value after an initial 0.08-second period for the armature current to build up appreciably.

References

1. SAFETY CODE FOR MILLS AND CALENDERS IN THE RUBBER INDUSTRY. *Publication Number ASA B28.1—1949*, American Standards Association, New York, N. Y., 1949.

2. RUBBER MILLS AND CALENDERS—A COMPARISON OF STATE SAFETY CODES AND STANDARDS WITH A.S.A. B28.1—1949. United States Department of Labor, Bureau of Labor Standards (Washington, D. C.), April 1952.

Discussion

Francis A. Green (B. F. Goodrich Company, Akron, Ohio): I wish to congratulate Mr. Sellers, Mr. Wheeler, and Mr. Halter for a painstaking and thorough study of the braking problem which has confronted our industry over the years. They have isolated and identified the important factors and have indicated the characteristics which may be improved.

Safety is everybody's business and it is heartening to see this concrete evidence of the interest taken by the equipment manufacturers. A machine which will commutate 430-per-cent braking current is an achievement. The design of the *Z*-type calender coupled with mechanical feeding of rubber to the rolls and the described braking characteristics should considerably reduce the operator hazards. It is hoped that this degree of safety can be extended to the auxiliaries and the entire train.

The points mentioned for adjustable voltage drives and the inadequacy of 3/1 and 4/1 adjustable speed motors, dual voltage, and mechanically driven auxiliaries are being increasingly appreciated by the industry and should be emphasized.

The statement is made that a 400-horsepower motor is adequate for a *Z* calender with 28-inch rolls for 100 yards per minute. This may not be an altogether safe assumption as plasticity of stock, tension, length of rolls, width of stock, and other factors vary among the manufacturers. From a maintenance standpoint it is also worth while to have a margin of motor rating over load requirements.

The braking tests have provided a remarkably complete picture of the reactions which take place in the equipment described. They also provoke speculation of what might have happened with slightly different conditions. Two questions arise which I should like to state. First, if a motor with full field, speed controlled only by voltage, had been used, could braking have been improved? Second, if a magnetic amplifier or electronic regulator instead of rotating regulation had been used, could a faster response be obtained increasing the average braking current?

In conclusion I believe that it should be stated that the rubber industry owes a debt of gratitude to the authors, their principals, and the rubber manufacturer who provided the facilities.

J. F. Sellers, B. G. Wheeler, and **A. C. Halter:** The authors wish to thank Mr. Green for his discussion particularly since his viewpoint is that of a user of the type of equipment described in this paper. Mr. Green has posed two questions on which we would like to comment as follows.

First, what would be the stopping distance if a single speed motor had been used instead of a field weakening motor, for driving the calender on which tests were made, that is, a 600-horsepower 450-rpm motor instead of 600-horsepower 300/450-rpm motor? The single-speed motor would have a WK^2 value of 2,200 pound feet squared compared to 4,670 pound feet squared for the 300-rpm base speed motor. Using each total value of motor + calender WK^2 in the deceleration equation shows that for the same armature current peak the stopping distance would be shortened by 7 inches with the single-speed motor, for a total of about 14 inches. However, as discussed in the paper it would not be possible to realize all this improvement because of the damping action in the solid generator frame, which will not allow much reduction in the time required to bring the generator voltage to zero. Perhaps one-third of calculated gain could actually be obtained with the lower inertia motor, but with a laminated generator frame a much larger gain could be realized.

Second, if a magnetic amplifier or an electronic regulator had been used, instead of rotating regulation, could a faster response be obtained increasing the average braking current? An analysis of the various times involved in the braking cycle as illustrated in Figure 6 indicates that the time involved in bringing the regulator to its maximum voltage is a small part of the total total time required for stopping the drive. However, this loss of time is at the high speed and is therefore very important. It is difficult to estimate the degree to which the performance would be improved by changing to another type regulator since although some components such as tubes do not have appreciable time constant, practically all circuits have some time constants involved in the other components. Also, some damping might have to be used to prevent the regulator from going into continuous oscillation. In fact this particular rotating regulator was damped through a transformer connected to an auxiliary field so that it would retain its stability. With either electronic or magnetic amplifier type of regulator the forcing voltage could have been brought to its maximum value faster, but we do not believe that this would have appreciably improved the braking distance since the other elements in the system have a much greater time lag. Against the fact that the figure of merit is better for the magnetic amplifier and electronic regulators, we must balance the complication necessary to regenerate power through the regulator since the rotating regulator performs equally well in either direction and the other two types required duplicate units for current flow in the reverse direction.

Multitransformer Welding Presses

JACK OGDEN
NONMEMBER AIEE

USERS OF resistance welding equipment are finding "presswelding" to be ideally suited to many of their high-production applications. In its general concept, presswelding may be likened to present-day stamping-press practice; however, instead of forming or trimming, the weld press produces from 16 to 160 spot welds practically simultaneously on a given assembly. The welding press also differs from the usual stamping press in that the ram or movable platen is generally located in the lower part of the machine. This arrangement facilitates the location of the welding units and usually favors loading of the parts to be welded. Figure 1 shows three typical press types. The 4-post machine is used for large assemblies while the 2-post or open press is used for smaller operations.

The press platens are operated by motor-driven linkage systems or fluid-pressure cylinders. On large presses, the platen weight is usually counterbalanced with an air-cylinder system.

The welding electrode units, see Figure 2, correspond to the dies used in a stamping press; the upper or stationary electrode usually consists of a framework supporting the electrode pressure units, the welding transformers, the cooling and pressure medium manifolds. The lower electrode assembly support the backup electrodes and part locators.

In some more complicated units, the electrode pressure cylinders and welding transformers may be located both in the upper and lower electrode assemblies. To fully utilize the advantages of the press system, the electrode assemblies should be designed to permit easy removal and replacement of the entire electrode unit. This makes it practical to utilize a given press line for several different operations.

In early forms of the presswelder, comparatively large transformers were attached to the crown or base of the press and connected to the electrodes by long secondary cables. The advent of the small package transformer permitted locating the transformers on the electrode assembly, thus greatly facilitating electrode changes and reducing primary current demands.

Presswelding has several distinct advantages in high-production applications. Some major advantages of this sytem are the following:

1. Permits accurate and uniform locations of spot welds.

Figure 1. Typical press types

A. Four post, cam type
B. Four post, crank type
C. Two post, hydraulic type

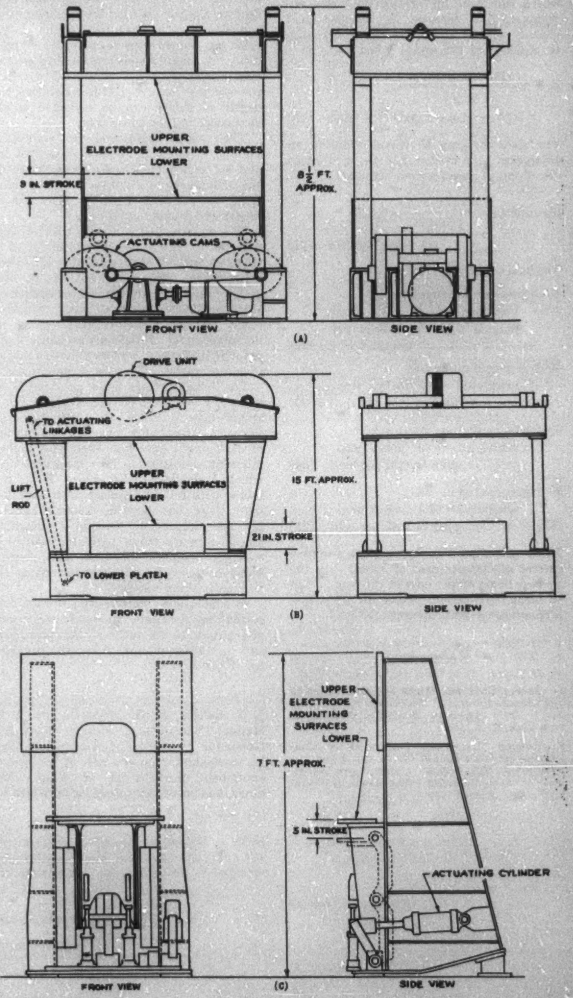
UPPER
ELECTRODE MOUNTING SURFACES
LOWER
9 IN. STROKE
8½ FT. APPROX.
ACTUATING CAMS
FRONT VIEW
SIDE VIEW
(A)
DRIVE UNIT
TO ACTUATING LINKAGES
LIFT ROD
UPPER
ELECTRODE MOUNTING SURFACES
LOWER
15 FT. APPROX.
21 IN. STROKE
TO LOWER PLATEN
FRONT VIEW
(B)
SIDE VIEW
UPPER
ELECTRODE
MOUNTING
SURFACES
LOWER
7 FT. APPROX.
5 IN. STROKE
ACTUATING CYLINDER
FRONT VIEW
(C)
SIDE VIEW

Paper 53-180, recommended by the AIEE Electric Welding Committee and approved by the AIEE Committee on Technical Operations for presentation at the AIEE Southern District Meeting, Louisville, Ky., April 22–24, 1953. Manuscript submitted November 28, 1950; made available for printing March 12, 1953.

Jack Ogden is with the General Motors Corporation, Detroit, Mich.

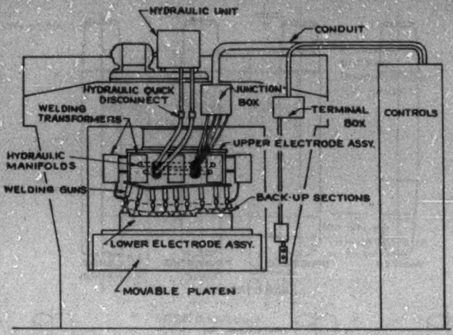
HYDRAULIC UNIT
CONDUIT
HYDRAULIC QUICK DISCONNECT
WELDING TRANSFORMERS
JUNCTION BOX
TERMINAL BOX
CONTROLS
UPPER ELECTRODE ASSY.
HYDRAULIC MANIFOLDS
WELDING GUNS
BACK-UP SECTIONS
LOWER ELECTRODE ASSY.
MOVABLE PLATEN

Figure 2. Welding press showing electrode installation

2. The welding of a large number of assemblies on one high-production fixture rather than on a number of like lower-production fixtures eliminates a particularly vexing problem of fixture co-ordination.

3. Permits the use of one or a group of presses for a number of different welding operations in the same manner that a stamping press can be used for producing different parts by changing dies.

4. As individual electrodes produce only one or two welds per assembly, their life is increased and production shutdowns for electrode dressing can be virtually eliminated.

5. Lends itself exceedingly well to automatic part handling equipment, particularly in progressive operation setups.

The successful employment of presswelding to improve quality and reduce production cost requires particular emphasis on the following items:

1. Loading and unloading of parts and assemblies.

2. Development of simple, accurate part locators.

3. Design and maintenance of equipment to reduce production "down time." This becomes extremely important on progressive operation installations where four or more presses may be synchronized in line.

4. Proper maintenance of electrode tips and backups.

Welding Equipment and Process Considerations

The following discussion covers some of the equipment requirements and techniques which are applicable to multitransformer presswelding.

Secondary Voltage Control Methods

The use of tap changing welding transformers permits the maximum voltage flexibility where accessibility and space considerations permit their installation.

Some systems employ one large autotransformer per phase with multiple switching devices feeding groups of two or more welding transformers, see Figure 3. Economy and space considerations make it impractical to individually adjust welding transformer voltages by this method. However, fixed ratio welding transformers may be more compact in design for the same secondary current outputs.

Although not as widely used as the first two methods, the variation of secondary output by means of phase shift heat control has many interesting possibilities. It provides stepless heat control with minimum space requirements and compares quite favorably costwise with the other methods if transformers are grouped as in the autotransformer system.

Welding Transformers

This subject has been thoroughly covered in another paper,[1] but it will probably not be amiss to emphasize that the welding transformer should be as compact as possible and extremely rugged as it usually is mounted in exposed locations. It will probably be subject to more severe water and oil exposure than the average transformer. Particular attention should be given to secondary terminal bracing and location. Mounting must be convenient and flexible. Polarity indication should be obvious in view of its importance in this type of welding.

In practice, most transformers of this type fail either for mechanical reasons or because of moisture breakdown of the insulation.

Secondary Circuit Arrangements (Figure 4)

Series Method. From a machine design standpoint, this is an ideal arrangement and consequently is very widely used. Series-welding has been a large factor in the widespread adoption of presswelding. The number of secondary circuits required for direct welding are reduced by half due to the fact that feed and return path are both on the same side of the part. The secondary impedance can be kept to a minimum and consequently primary current requirements may be re-

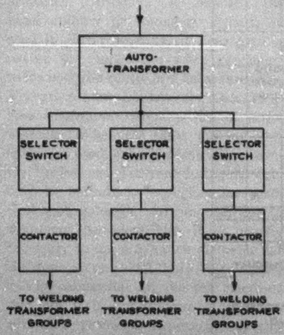
AUTO-TRANSFORMER
SELECTOR SWITCH
SELECTOR SWITCH
SELECTOR SWITCH
CONTACTOR
CONTACTOR
CONTACTOR
TO WELDING TRANSFORMER GROUPS
TO WELDING TRANSFORMER GROUPS
TO WELDING TRANSFORMER GROUPS

Figure 3. Voltage control by autotransformer method

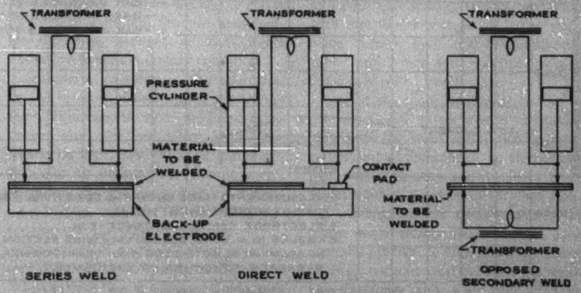
TRANSFORMER
TRANSFORMER
TRANSFORMER
PRESSURE CYLINDER
MATERIAL TO BE WELDED
CONTACT PAD
MATERIAL TO BE WELDED
BACK-UP ELECTRODE
TRANSFORMER
SERIES WELD
DIRECT WELD
OPPOSED SECONDARY WELD

Figure 4. Typical secondary circuit arrangements

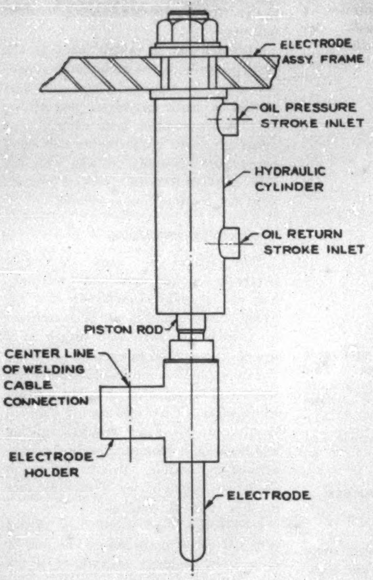
ELECTRODE ASSY. FRAME
OIL PRESSURE STROKE INLET
HYDRAULIC CYLINDER
OIL RETURN STROKE INLET
PISTON ROD
CENTER LINE OF WELDING CABLE CONNECTION
ELECTRODE HOLDER
ELECTRODE

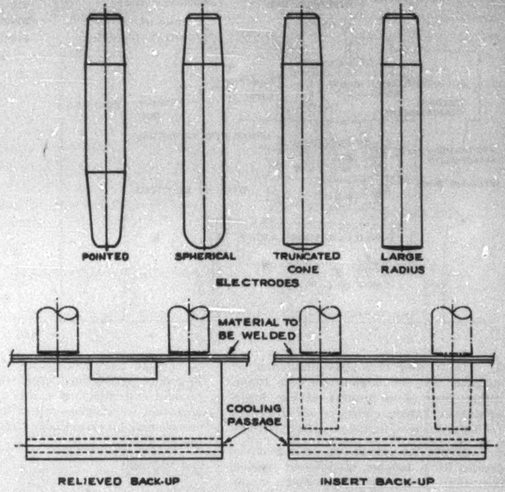
POINTED
SPHERICAL
TRUNCATED CONE
LARGE RADIUS
ELECTRODES
MATERIAL TO BE WELDED
COOLING PASSAGE
RELIEVED BACK-UP
INSERT BACK-UP

Figure 5 (left). Typical welding gun

Figure 6 (above). Typical welding electrodes and backups

duced. Inherently this circuit tends to produce very little indentation on the backup side of the part and rather deep indentation on the "hot" electrode side due to the tendency of the stock adjacent to the hot electrode to shunt part of the current from the weld. The metal on this side is usually less than 0.050 in thickness.

Direct Method. As shown in Figure 4, this differs from the usual spot-welding secondary circuit only in the fact that there is no permanent connection between the transformer and the backup electrode. The use of a contact pad or wiping con-

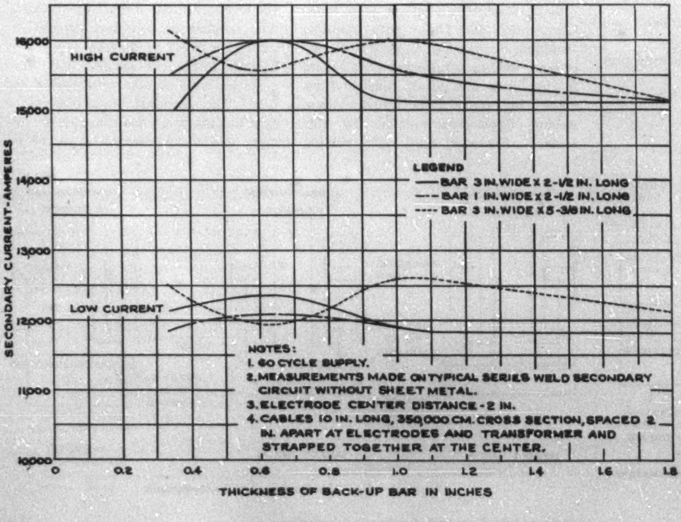

Figure 7. Effect of backup bar size on secondary current in series welding

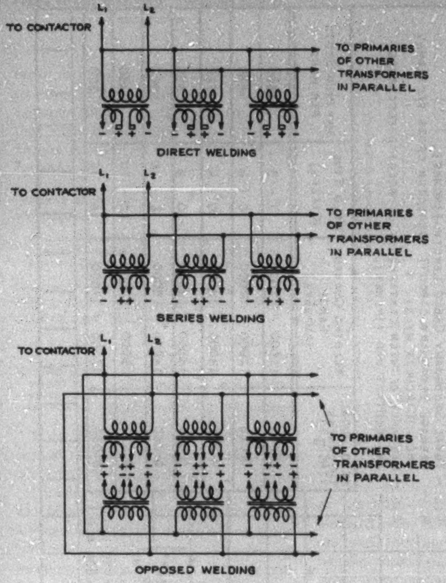

Figure 8. Polarity requirements

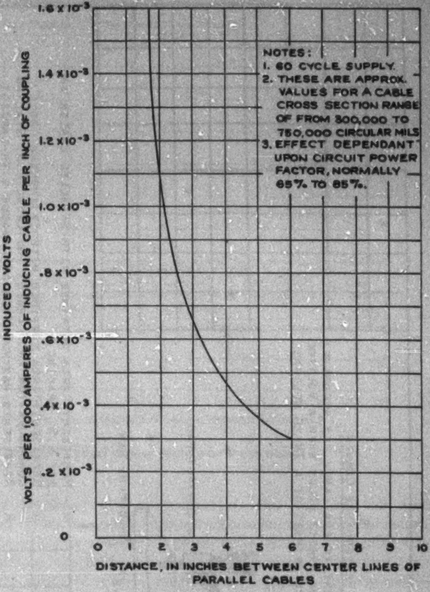

Figure 9. Impedance effect of adjacent secondary cables

tact simplifies the mechanical machine design and improves the loading conditions. The direct welding circuit is frequently used for stock thicknesses of over 0.050 where the welds are close to the edge of the assembly.

Opposed Secondary Method. Again referring to Figure 4, we see that this method combines the series- and direct-welding principles. Although it requires the same number of secondary circuits as used in direct welding, it does greatly reduce the impedance when producing welds near the center of a large assembly. This process does not have the stock thickness limitations characteristic of series welding. When the same contour electrodes are used on both sides of the assembly, the leakage of current during the weld may be considered negligible for practical spot spacings. In practice, due to alignment considerations, it is usually necessary to use a 5/8-inch diameter flat electrode on one side; this does increase leakage somewhat on the flat electrode side but it is not sufficient to interfere with the practical application of this process.

Polarity Considerations. When producing multiple spot welds simultaneously it is essential that proper polarity relations exist between adjacent electrodes. In general it may be stated that adjacent electrodes connected to separate transformer secondaries shall be of the same polarity if on the same side of the assembly. The application of this rule to series, direct, and opposed secondary circuits is illustrated in Figure 8. When multiphase connections are used on a machine, the welding guns on a given phase should be grouped separately from those on another phase. Failure to observe polarity requirements will produce considerable difference between adjacent welds under production-operating conditions.

Secondary Impedance Characteristics. In the interest of reducing primary current requirements and welding transformer size, the secondary impedance should be kept to a practical minimum. In order to maintain weld uniformity, secondary circuits controlled by a common voltage regulator should be of approximately the same impedance.

The effect of current flowing in adjacent conductors is shown in Figure 9. When current flow in adjacent conductors is in the same direction, it tends to reduce welding current flow; and when in the opposite direction, it tends to increase the current flow. In practice, "opposite polarity" cables are tied together and "like polarity" cables separated to obtain the most favorable conditions. These induced voltages are additive or subtractive vectorially at 90 degrees to the current vector.

Typical series-weld secondary-circuit impedances vary from 350 microohms with 78-per-cent power factor when using 18-inch long 750,000-circular-mil cables at 4-inch spot spacing to 250 microohms with over 95-per-cent power factor when using 8-inch long 600,000-circular-mil cables and 2-inch spot spacing (welding 0.035 cold rolled steel).

One of the most significant factors in the impedance of series-weld secondary circuits is the sheet metal and its associated contact resistance. In view of this fact, particular attention should be given to the effect of the sheet metal when making welding current measurements. In many spot-welding shops it has been common practice to take primary current readings without steel between the welding electrodes and then calculate the secondary current using a correction

TR-38 DIRECT WELDING PERFORMANCE CURVES

THESE CURVES INDICATE THE CURRENTS AVAILABLE PER SECONDARY FOR PRODUCING TWO SIMULTANEOUS DIRECT WELDS WHEN A VOLTAGE OF 440 VOLTS IS APPLIED TO THE PRIMARY OF A TR-38 WELDING TRANSFORMER.

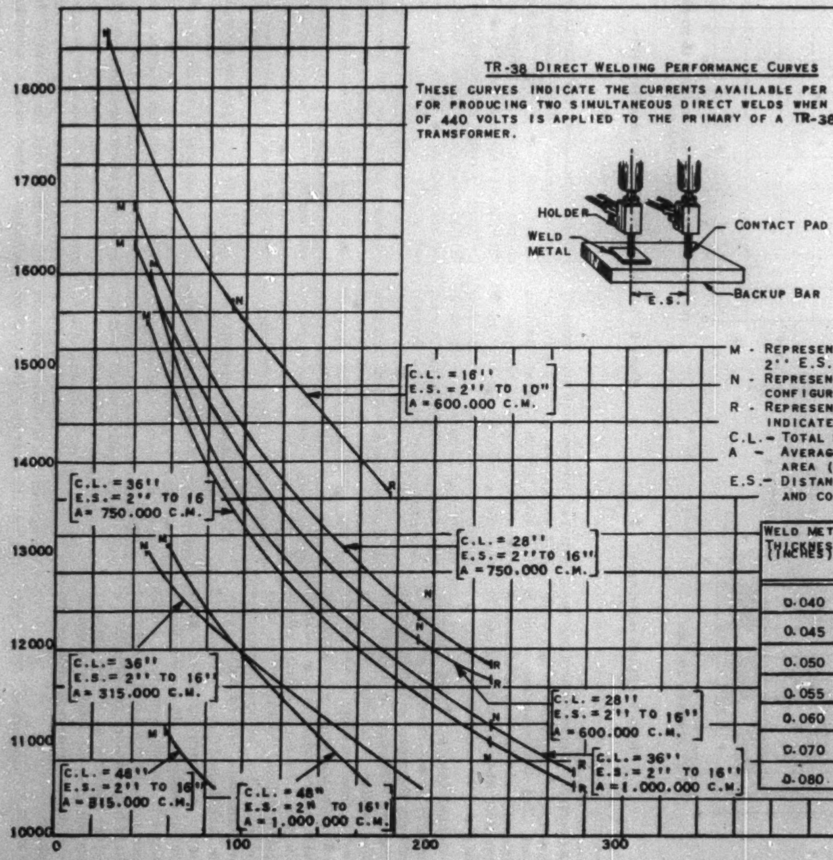

M - REPRESENTS AREA OBTAINED WITH PARALLEL CABLES AND 2'' E.S. SPACING.

N - REPRESENTS AREA OBTAINED WITH TRIANGULAR CABLE CONFIGURATION AND LARGEST INDICATED E.S. SPACING.

R - REPRESENTS MAXIMUM AREA OBTAINABLE WITH LARGEST INDICATED E.S. SPACING.

C.L. – TOTAL SECONDARY CABLE LENGTH (INCHES)

A – AVERAGE SECONDARY CIRCUIT CONDUCTOR CROSS SECTIONAL AREA (CIRCULAR MILS)

E.S. – DISTANCE BETWEEN CENTERLINES OF WELDING ELECTRODE AND CONTACT PAD (INCHES).

WELD METAL THICKNESS (INCHES)	WELDING CURRENT RANGE (AMPERES)	WELD TIME (CYCLES)	MAXIMUM SPOTS PER HOUR
0.040	11000 - 12000	7 - 5	1500
0.045	12000 - 13000	10 - 8	850
0.050	13000 - 14000	10 - 8	750
0.055	14000 - 14500	10 - 8	650
0.060	14500 - 15000	12 - 10	500
0.070	15000 - 16000	12 - 10	450
0.080	16000 - 17500	14 - 12	350

Figure 10 (on page 206). Welding performance curves

factor of 10 to 15 per cent to compensate for the welded metal. The following example illustrates the possible error that might occur if this method were to be used in a typical series-welding application:

Welding transformer—96-to-1 ratio. Two secondaries in parallel.

Primary resistance	0.22 ohm
Primary reactance	0.26 ohm
Line voltage	440 volts

Secondary circuit—8-inch long 600,000-circular-mil cables—electrode spacing 2 inches 0.035 to 0.035 being welded.

	With Sheet Metal	Without Sheet Metal
Primary current	302 amperes	603 amperes
Current per secondary	14,500 amperes	29,000 amperes

It is therefore recommended that all current readings on presswelders be taken while stock is being welded.

Utilizing experimental data obtained on typical circuits, Figure 10 illustrates a chart prepared as a ready reference for the welding machine designer for selecting equipment and making his electrode layout.

Pressure Heads

Although spring or air cylinder loaded devices are sometimes used, oil actuated cylinders are generally preferred as they are compact, independent of electrode wear, may be retracted easily for part clearance, and do not load the platen while in motion. Figure 5 illustrates a typical construction with attached electrode holder. The hydraulic power system for cylinder operation should have rapid follow-up characteristics to prevent loss of pressure during the weld.

Welding Electrodes

Conventional class no. 2 alloy water-cooled tips are generally used in either 1/2-inch or 5/8-inch diameter. Typical tip contours are shown in Figure 6. Our experience has shown that a $1^1/_2$-inch radius produces the best welding results on mild steel in the 0.030 to 0.090 thickness range. In view of the relative inaccessibility of many tip locations, a nonlocking taper (6- or 8-degree including angle) is frequently used in place of the usual Morse taper on the holder end.

In the design of the stationary or backup electrodes, either inserts or lands are used at the weld location. Solid backups following the contours of the panel are very satisfactory when new, but present an excessive "tuning problem" when localized wear occurs. If short inserts are used, they may be indirectly cooled by the water passages in the holder. While investigating the effects of series welding backup electrode geometry, some very interesting observations were made. Figure 7 illustrates the effect of varying the width, length, and thickness of the backup electrode when using a single pair of electrodes at 2-inch center distances. Although this effect is intriguing from a theoretical point of view, we have not yet been able to take full advantage of this phenomenon in practical designs.

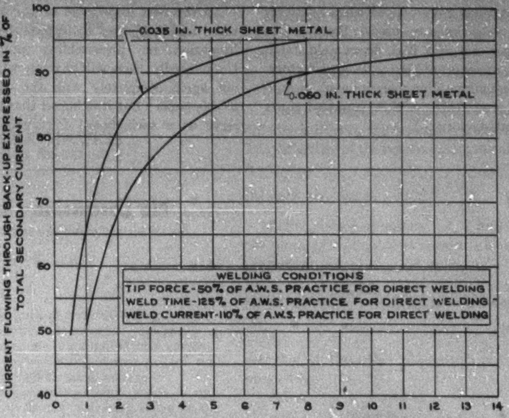

Figure 11. Effect of spot spacing on series welds

Stock Thickness Limitations

When direct or opposed secondary circuits are used, the presswelding of mild steel in thicknesses up to 0.100 inch is quite practical. Although greater thicknesses may be series-welded under ideal conditions, in practice considerable trouble is frequently encountered when thicknesses over 0.050 inch are exceeded on the hot electrode side. Although results may be improved by increasing weld spacing, the maintenance of good part fitup becomes a major problem. The stock on the backup electrode side may be two to four times the thickness of the thinner sheet.

Weld Spacing

When using direct or opposed secondary welding methods, the spacing in a series of welds is usually determined by the electrode holder and pressure cylinder construction. One and one-half inch centers are a common practical minimum.

When series-welding, the shunt current effect determines the practical minimum spacing. Figure 11 gives an indication of the effect of weld spacing on useful weld current for various metal thicknesses. A spacing of $1^1/_2$ to 2 inches is a good practical minimum.

Electrode Force

To avoid excessive current requirements and excessive indentations, series presswelds are usually made with approximately one-half the electrode force recommended by American Welding Society (A.W.S.) for direct welding.

A.W.S. force recommendations are well suited to direct or opposed secondary presswelds. When conditions permit increasing weld time, somewhat lower forces may be used with lower currents.

Welding Current

Series welds require approximately 110 per cent of A.W.S. recommended current values (for direct welding) when using 50 per cent of force and 100 to 125 per cent of weld time recommendations. Although series-weld currents may exceed direct weld current values by 10 or 15 per cent, each circuit produces two welds; thus actual primary current per weld may be only 55 or 60 per cent of the direct weld requirements.

Weld Time

Using electrode force and weld currents previously described, the most consistent series welds are produced when relatively long weld times are used. From 100 to 125 per cent of A.W.S. direct weld standards appears to be quite satisfactory. When making direct or opposed secondary presswelds, A.W.S. standard times are satisfactory.

To the best knowledge of the author there has been very little published information on presswelding practices. Undoubtedly, there will be many who will not agree completely with the context of this paper; but it is hoped that it will serve as a springboard for some lively discussions and profitable investigations of the subject.

Reference

1. ELECTRIC ARC AND RESISTANCE WELDING—II. *AIEE Special Publication S-26A*, "Design of Transformers for Resistance Welding Machines," Dean L. Knight, Dec. 1950, pp. 164-76.

◆

No Discussion

Power Equalizer Systems for Aircraft Alternators

JOHN A. GRANATH
ASSOCIATE MEMBER AIEE

ALBERT K. HAWKES
ASSOCIATE MEMBER AIEE

FOR EFFICIENT parallel operation of alternators it is necessary that both real and reactive load be distributed equally among the alternators. A 400-cycle a-c aircraft electric system presently in use employs both reactive and real power equalizers which are interconnections of the respective voltage and speed regulating systems of the paralleled alternators, giving an automatic correction for load unbalance while maintaining best system voltage and frequency regulation.

Reactive Power Equalizer

To achieve equal division of reactive load, a single current transformer is placed on corresponding phase leads of each of the alternators and is connected to the primary winding of the mutual reactor in the associated alternator's voltage regulator as shown in Fig. 1. The current transformers and mutual reactors are interconnected to form the equalizer loop of Fig. 2. When each alternator is delivering its share of current, the same current flows through all of the current transformers and zero current flows in the equalizer coils (mutual reactors).

The design of the voltage regulator used is such that when reactive current flows in the secondary winding of the mutual reactor, a voltage is superimposed on the normal voltage input to the regulator. The normal input is proportional to the terminal voltage of the alternator which is, when the alternator is on the bus, system voltage. Thus, when reactive current flows in the mutual reactor, the regulator will act to change excitation in a direction to reduce the superimposed voltage to zero. In this way the generated voltages of the machines on the system will be adjusted to that necessary for equal load sharing while rated system voltage is maintained. The relationship in the voltage regulator can be stated

$$(|V_o|-|V|)=B|I_m|\sin\theta \qquad (1)$$

where

$|V|$ = magnitude of terminal voltage
$|V_o|$ = magnitude of reference voltage
$|I_m|$ = magnitude of mutual reactor current
θ = angle by which the mutual reactor current lags terminal voltage
B = a proportionality factor which is constant in the operating range of the regulator

Next, an expression for $|I_m|$ in terms of load currents is to be obtained.

Referring to Fig. 2, if the currents in each of the n machines are $I_1, I_2, \ldots I_n$ and the current transformer ratios are all c, then $(1/c)I_1, (1/c)I_2, \ldots (1/c)I_n$ are the currents in the current transformers. If machine 1 has its load increased for any reason, I_1 will be different from the other (I_n) currents. Thus $I_1 \neq I_2 = I_3 = \ldots = I_n$.

If the currents are summed at points A and N in Fig. 2, two expressions are obtained

$$\frac{1}{c}I_1=i_1+i \qquad (2)$$

$$\frac{1}{c}I_n=i_n+i \qquad (3)$$

Subtracting equation 3 from equation 2 gives

$$\frac{1}{c}(I_1-I_n)=i_1-i_n \qquad (4)$$

The sum of the voltages around the loop containing the primaries of the n mutual reactors, if the impedance of the interconnecting leads is negligible, is expressed by

$$i_1Z_1+i_2Z_2+\ldots+i_nZ_n=0 \qquad (5)$$

or if $Z_1=Z_2=\ldots=Z_n$ this reduces to

$$i_1+(n-1)i_n=0 \qquad (6)$$

since $i_2=i_3=\ldots=i_n$. Substituting for i_1 in equation 4 yields

$$i_n=-\frac{1}{cn}(I_1-I_n) \qquad (7)$$

Substituting equation 7 in equation 6

$$i_1=\frac{n-1}{cn}(I_1-I_n) \qquad (8)$$

Equations 7 and 8 express the mutual reactor currents as functions of the difference current (I_1-I_n), which is in general a vector with both real and reactive components. Under normal conditions only the reactive component of this difference affects the voltage regulator. The difference of the reactive components is

$$|I_1|\sin\theta_1-|I_n|\sin\theta_n \qquad (9)$$

Making use of equations 1, 7, 8, and 9, the terminal voltage of alternator 1 is expressed by

$$|V|=|V_{o1}|-K\frac{(n-1)}{n}(|I_1|\sin\theta_1-|I_n|\sin\theta_n) \qquad (10)$$

and that of the other alternators is expressed by

$$|V|=|V_{on}|+\frac{K}{n}(|I_1|\sin\theta_1-|I_n|\sin\theta_n) \qquad (11)$$

where

$|V_{o1}|$ = reference voltage of alternator 1
$|V_{on}|$ = reference voltage for other alternators
$K=B/c$, a constant of proportionality which is a measure of the over-all effect of the equalizer

The value of K can be obtained by test using a single alternator and a load of low power factor. If the current transformer of the alternator under test is not connected to any other current transformers and is not short-circuited, current proportional to load current will flow in the mutual reactor. From a plot of terminal voltage as a function of reactive load current obtained under these conditions, the value of K, the negative of the slope of the line, can be read.

Equations 10 and 11 are useful in predicting system behavior during error or malfunction of a voltage regulator or exciter.

REDUCTION IN SYSTEM CAPACITY

When an equalizer system is used, a loss of available system capacity due to current unbalance can be caused by errors in the voltage regulator setting. These errors may be due to inaccuracy in original setting or to variation in the characteristics of the components during operation. The total available capacity of a system in which paralleled alternators do not share load equally is less than the sum of the capacities of the individual machines, since one or more alternators will be overloaded before full system capacity is reached.

Suppose that in a system of n alternators operating in parallel, the regulator of one alternator is in error by 2.5 per

---

Paper 53-179, recommended by the AIEE Air Transportation Committee and approved by the AIEE Committee on Technical Operations for presentation at the AIEE Southern District Meeting, Louisville, Ky., April 22–24, 1953. Manuscript submitted August 6, 1952; made available for printing March 2, 1953.

JOHN A. GRANATH and ALBERT K. HAWKES are with the Armour Research Foundation of Illinois Institute of Technology, Chicago, Ill.

The work described in this paper was carried out as part of a study of aircraft electric systems for the United States Air Force.

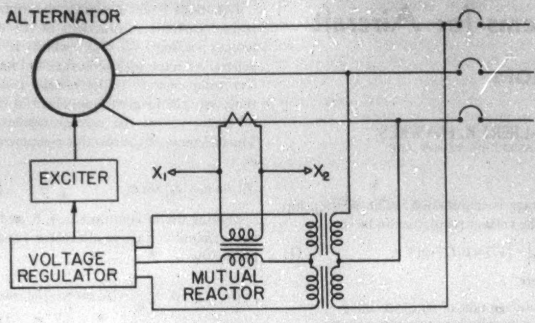

Fig. 1. Schematic diagram of voltage regulator

cent and the regulators of the other alternators are at their proper setting. For this condition, the capacity of the system can be determined by calculating the total system load at the time that any alternator reaches its rated capacity.

Since the terminal voltages of the two machines must be equal when paralleled and if equation 11 is subtracted from equation 10 there results

$$O=|V_{o1}|-|V_{on}|-K(|I_1|\sin\theta_1-|I_n|\sin\theta_n)$$

or

$$|I_1|\sin\theta_1-|I_n|\sin\theta_n=\frac{1}{K}(|V_{o1}|-|V_{on}|) \tag{12}$$

To compute the available capacity when the setting of one regulator is set or drifts to 2.5 per cent below normal, equation 12 becomes, using per-unit notation

$$|I_1|\sin\theta_1-|I_n|\sin\theta_n=\frac{1}{K}(-0.025)$$

Using a typical value of $K=0.106$ per unit obtained from test, and the fact that at the point just prior to overloading any machine $|I_n|=1.00$ per unit or $|I_n|\sin\theta_n$ at rated power factor (0.75) is equal to 0.661, equation 12 gives

$$|I_1|\sin\theta_1=0.425 \text{ per unit}$$

The total quadrature current supplied to the load is

$$|I_L|\sin\theta_L=|I_1|\sin\theta_1+(n-1)|I_n|\sin\theta_n$$

For a 4-machine system ($n=4$)

$$|I_L|\sin\theta_L=0.425+(3)(0.661)=2.41 \text{ per unit}$$

Assuming that the alternators share real load equally, the in-phase component of load current is

$$|I_L|\cos\theta_L=(4)(1.00)(0.75)=3.00 \text{ per unit}$$

Neglecting the change in system voltage which is 0.6 per cent, the total load vector power in per unit is

$$S_L=3.00+j2.41=3.85\underline{/38.8^\circ} \text{ per unit}$$

and the per cent of installed kva capacity which is available is

$$\frac{3.85}{4.00}\times 100=96.2 \text{ per cent}$$

If the regulator setting is 2.5-per-cent low, the reduction in system capacity with the value of K used is small (7 per cent for $n=2$) and decreases as the number of machines on the system increases. However, if the error in regulator setting is high, the reduction in system capacity increases, approaching 14 per cent as a limit, as the number of alternators on the bus becomes very large. An increase in the value of K decreases the reduction in system capacity resulting from errors in reference voltage. However, an increase in K could lead to hunting of the voltage regulating system due to transient unbalanced currents. Thus a value of K must be selected which is sufficiently large to insure adequate available system capacity in the presence of inherent error in regulator setting while maintaining voltage regulator stability.

System Performance During Abnormal Excitation

Another use of the equalizer analysis is to predict system voltage and the amount of circulating reactive current during abnormal excitation of one of several alternators operating in parallel. Such information may be of value in a study of protective devices for a system or in the choice of circuit parameters.

The two extremes of abnormal field excitation are when the field excitation goes to maximum value, as due to regulator failure, and complete loss of field excitation, as due to an open field winding. Overexcitation, if sustained, would cause alternator and exciter to overheat. Loss of excitation causes the faulty alternator to draw excessive reactive power from the system and limits that machine's real power output to 25 per cent of its rated value or less, beyond which the machine would pull out of synchronism.[1]

The method of analysis which follows was checked by tests on a system consisting of two 40-kva alternators and standard associated components. Calculated values of system voltage and reactive power delivered by each machine during abnormal excitation of one alternator were compared with measured values obtained from oscillograph records and found to be in reasonable agreement.[1]

Overexcitation

When the excitation of one alternator goes to its ceiling value, that alternator delivers more than its share of reactive power. The reactive power equalizer circuit indicates a deficiency of reactive power output from the other alternators, causing the exciters of these machines to increase excitation. Since the alternator

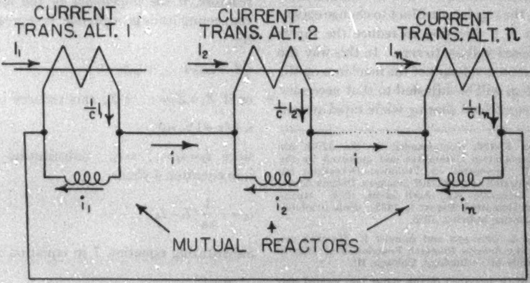

Fig. 2. Schematic diagram of reactive equalizer connections

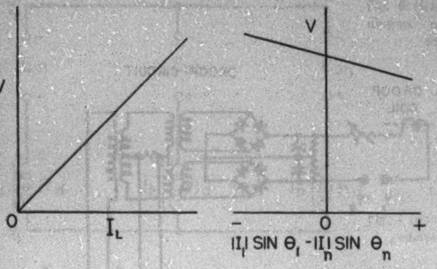

Fig. 3. Voltage characteristics of load and normal machine

with the defective regulator is incapable of reducing its excitation, bus voltage is sustained at a value above normal.

To examine an n alternator system in which one alternator has abnormal excitation, three volt-ampere characteristics are required. These are the characteristics of

1. The load Z_L.
2. Alternators with voltage regulator and reactive equalizer control.
3. The faulty alternator.

Expressed in the terms used in this analysis, these characteristics are, for the load

$$V = Z_L[I_1 + (n-1)I_n] \tag{13}$$

and for the regulated alternators equation 11 can be rewritten as follows because the in-phase components are equal (real power equalizer operating)

$$|V| = |V_{on}| + j\frac{K}{n}(I_1 - I_n) \tag{14}$$

See Figure 3.

In an alternator on which the voltage regulator is not effective and the excitation goes to ceiling value, the relationship between the alternator terminal voltage and its armature current is determined by the ceiling voltage and the saturated synchronous reactance of the alternator. Neglecting saliency and armature resistance, the voltage equation for the alternator is then written as follows:

$$V = E_1 - jX_{d_1}I_1 \tag{15}$$

where

V = terminal voltage
E_1 = internal voltage
X_{d_1} = direct axis reactance (saturated)
I_1 = armature current of alternator 1

Equations 13, 14 and 15 yield the following expression for the bus voltage

$$V = \frac{\frac{|E_1|}{X_{d_1}}\cos\delta_1 + \frac{|V_o|(n-1)}{K} + j\frac{|E_1|}{X_{d_1}}\sin\delta_1}{\frac{1}{X_{d_1}} + \frac{n-1}{K} + \frac{\sin\theta_L}{n|Z_L|} + j\frac{\cos\theta_L}{n|Z_L|}} = |V|(1+j0) \tag{16}$$

The angle δ_1 is the torque angle by which the internal voltage of alternator 1 leads the terminal voltage. The vertical bars signify magnitude.

Both the numerator and the denominator of equation 16 are complex numbers. Since the bus voltage was assumed to lie along the real axis, the quotient of the two complex numbers must be real, which means V is given by the quotient of either the reals or the imaginaries. For the alternator which has gone to ceiling excitation, the angle δ_1 is small (about 7 degrees), which means cos δ_1 may be assumed equal to unity with negligible error. Therefore, the quotient of reals can be approximated as

$$|V| = \frac{\frac{|E_1|}{X_{d_1}} + \frac{|V_o|(n-1)}{K}}{\frac{1}{X_{d_1}} + \frac{n-1}{K} + \frac{\sin\theta_L}{n|Z_L|}} \tag{17}$$

Equations for real and reactive power may be derived. The real power supplied by each of the n machines is given by the following

$$P_1 = P_n = \frac{|V|^2 \cos\theta_L}{n|Z_L|} \tag{18}$$

The expressions for the reactive power from the machine which has gone to ceiling excitation and from each of the other machines on the system are

$$Q_1 = |V|\left[\frac{|V| \sin\theta_L}{n|Z_L|} + \frac{(n-1)(|V| - |V_o|)}{K}\right] \tag{19}$$

and

$$Q_n = |V|\left[\frac{|V| \sin\theta_L}{n|Z_L|} - \frac{|V| - |V_o|}{K}\right] \tag{20}$$

Real and reactive components of current can be calculated, if desired, by dividing the expressions for P and Q by V and changing the sign of the reactive components.

The expressions derived are arranged for convenient substitution of parameters, that is, the effect of load, number of machines on the system, etc.

UNDEREXCITATION

An alternator operating in parallel with others may lose excitation due to an open-alternator or exciter field circuit. The resulting conditions can be analyzed in a manner similar to the overexcitation case described previously within limitations dependent upon the real power load on the system. At some value of real power load, depending on the characteristics of the generator and generator controls, an alternator with loss of field cannot convert its mechanical power input to electric power. Under this condition the alternator accelerates, pulls out of step with the system, and operates above synchronous speed. During loss of synchronism, the large fluctuations of power and bus voltage which occur, and the induced rotor currents in the alternator with open field, introduce complexities which hinder analytical treatment. The analysis which is developed is applicable for determining the voltage, current, and power for the condition where the alternator, due to saliency, is capable of carrying its share of the real power load which is on the system at the time of loss of excitation.

Since the excitation is zero during loss of alternator field, equation 15 must be modified to meet the new condition. E_1 now is zero, and the reactance of the machine is no longer the saturated synchronous reactance, but is somewhat less than the unsaturated synchronous reactance. A reasonable approximation for the machine reactance for this condition is to let $X = (X_{du} + X_q)/2$ where

X_{du} = unsaturated direct-axis synchronous reactance
X_q = unsaturated quadrature-axis synchronous reactance

This approximation is based on the fact that, during loss of field, the amount of magnetic saturation is small and the torque angle δ_1 approaches 45 degrees as

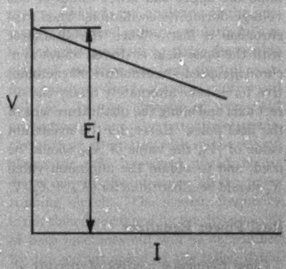

Fig. 4. Volt-ampere characteristic of faulty alternator during regulator failure

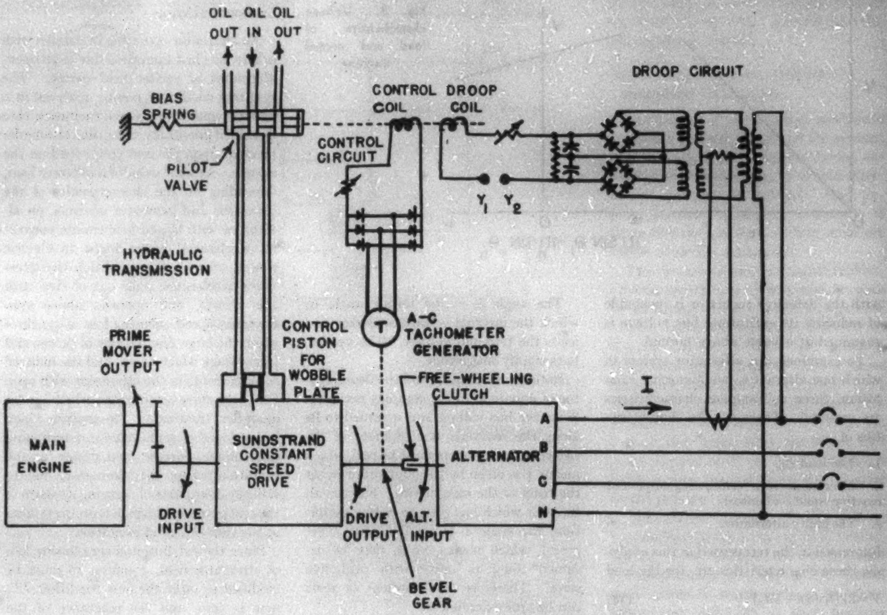

Fig. 5. Schematic diagram of alternator, drive, and associated equipment

the real power load approaches the magnitude at which synchronism is lost.

Equation 17 then is reduced to

$$|V| = \frac{\dfrac{|V_o|(n-1)}{K}}{\dfrac{2}{X_{du}+X_q}+\dfrac{n-1}{K}+\dfrac{\sin\theta_L}{n|Z_L|}} \qquad (21)$$

Expressions for real and reactive power and current can be obtained as before.

Theoretically, a modification of equation 21 should make it possible to determine the upper and lower limits of bus voltage during its oscillations when synchronism is lost. When the alternator with the open field is driven above synchronous speed, the armature magnetomotive force acts alternately along the direct axis and along the quadrature axis of the field poles. Hence, for the maximum value of $|V|$, the value of X_{du} should be used, and to obtain the minimum value X_q should be substituted for $(X_{du}+X_q)/2$.

Real Power Equalizer

Close frequency control of aircraft alternators depends on governing of their speeds. The alternator is driven by a variable ratio constant-speed drive,[2,3] the output speed of which is maintained at 6,000 rpm for input speeds between 2,800 and 9,000 rpm. Governing is effected by movement of a variable position wobble plate which changes the drive gear ratio. The pistons which fix wobble plate position are controlled by a solenoid operated sleeve valve. Fig. 5 shows the governing system in use today in operating aircraft, though in the last few years a system which eliminates the tachometer and control circuit has been devised. This newer system includes a flyball-type governor and trimmer load division circuits somewhat similar to the present droop circuit. The manufacturer states that closer frequency limits can be held with the new system, but vibration difficulties in adapting it to existing drives have caused the new governor to remain in the developmental stage with respect to operating aircraft.

The detailed view of Fig. 5 shows that the control coil is energized by a frequency reference voltage source. This voltage is the d-c output of a 3-phase bridge-type rectifier fed by a tachometer generator geared to the output shaft of the drive; thus the control coil voltage is proportional to drive output speed.

The droop coil voltage, provided by the droop circuit output, is proportional to the real power load on the alternator. The control coil alone gives constant frequency operation but the droop circuit acts as a trimmer on this reference frequency and introduces speed or frequency droop with load, which is necessary if paralleled alternators are to share load equally.

Fig. 6 shows the interconnection of the droop circuit outputs and droop coils of an n-machine system to form the real load equalizer. When all of the alternators carry the same real load, each droop circuit has the same output voltage and there is no current flow in any of the branches. If one of the alternators should pick up an increment of real load and each of the other machines still carries the same load, current will flow in the branches in such a direction as to correct the unbalance and restoration of equal load division by the action of all drive governors will occur.

The following development will be aimed at finding an expression for bus

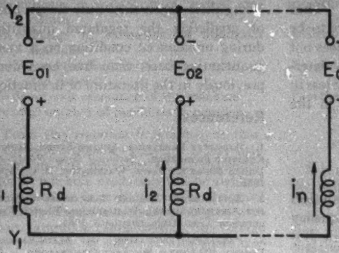

Fig. 6 (left). Schematic diagram of real load equalizer

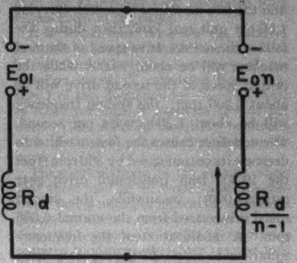

Fig. 7 (right). Simplified equivalent circuit

frequency as a function of unbalance in power component of current (component in-phase with reference voltage) among the n machines.

If alternator 1 is carrying a current I_1 and each of the other alternators carries the same current I_n, then, since the droop circuits are sensitive only to in-phase component of current, the direct voltages E_{o1} and E_{on} are given by

$$E_{o1}=M|I_1|\cos\theta_1 \tag{22}$$

$$E_{on}=M|I_n|\cos\theta_n \tag{23}$$

where

E_{o1} and E_{on} = the outputs of the droop circuits of the first and nth machines ($E_{o2}=E_{o3}=\ldots=E_{on}$)
M = droop circuit constant of proportionality
$|I_1|$ and $|I_n|$ = the magnitudes of the currents I_1 and I_n
θ_1 and θ_n = the angles by which I_1 and I_n lag the line to neutral reference voltage

Fig. 6 can be reduced to the simple circuit of Fig. 7, which yields

$$i_1=\frac{(n-1)}{n}\,\frac{(E_{o1}-E_{on})}{R_d} \tag{24}$$

where

R_d = resistance of each solenoid droop coil

Further

$$i_1=\frac{M}{R_d}\,\frac{(n-1)}{n}(|I_1|\cos\theta_1-|I_n|\cos\theta_n) \tag{25}$$

Tests on a single machine indicate that the frequency is approximately a linear, decreasing function of the droop coil voltage when the machine is delivering load. This is expressed by

$$f=f_0-N\,V_d=f_0-N\,i\,R_d \tag{26}$$

f = frequency
f_0 = reference frequency setting (frequency at no-load where tachometer setting alone determines drive speed)
N = positive constant
V_d = direct voltage across the droop coil
i = current in the droop coil

For the n-machine system, the bus frequency must satisfy the frequency equation of each machine with each droop coil current substituted for i and each setting substituted for f_0. For the first machine

$$f=f_{o1}-N\,i_1\,R_d \tag{27}$$

$$=f_{o1}-MN\frac{(n-1)}{n}(|I_1|\cos\theta_1-|I_n|\cos\theta_n) \tag{28}$$

If a new constant K' is defined by

$$K'=M\,N \tag{29}$$

then

$$f=f_{o1}=K'\,\frac{(n-1)}{n}(|I_1|\cos\theta_1-|I_n|\cos\theta_n) \tag{30}$$

The expression for the nth machine is

$$f=f_{on}+K'\,\frac{1}{n}\,(|I_1|\cos\theta_1-|I_n|\cos\theta_n) \tag{31}$$

since for machine n

$$i=-i_n=-\frac{i_1}{(n-1)} \tag{32}$$

The constant K' can be determined by loading a single machine and plotting frequency against load current. K' will be the negative of the slope of this line. A typical value for K' is 0.05 per unit or 20 cycles droop at a value of 1.0 per-unit current (power factor = 1.0).

The value of the constant K' can be changed by varying a droop adjusting resistor, shown in Fig. 5, which changes the value of the voltage E_o, fed to the equalizer system. When this resistance is set for maximum droop, K' is approximately 0.16 per unit, while the K' for minimum droop setting is about 0.04 per unit. Also, if frequency were to be plotted against in-phase component of current for a single machine with its droop circuit open, there would be a slight amount of droop inherent in the drive and alternator, showing that energizing only the control coil does not furnish a constant speed with load characteristic. This droop, however, amounts to only a few cycles in 400 for an in-phase current of 1.00 per unit, so a value of $K'=0$ for an open droop circuit is not significantly in error.

The equations for bus frequency, 30 and 31, are analogous to the equations for bus voltage, equations 10 and 11, so one would expect their ranges of application to be similar, but it will be shown that this is not so in every case.

REDUCTION IN SYSTEM CAPACITY

The frequency equations can be used to determine the loss of capacity due to error in setting as was done for the reactive equalizer. For example, in a 2-machine system, if the reference frequency of one machine is set 2.5 per cent above the normal no-load setting, and the other machine is assumed to carry rated load at rated power factor, then the available system kva capacity is only 83 per cent of the installed capacity ($K'=0.05$ per unit).

ABNORMAL SPEED CONDITION

Further applications of the frequency expressions are somewhat limited since the speed-regulating system is not completely analogous to the voltage-regulating system. The reason for this can be readily seen by examination of a failure which appears to offer application of the correspondence between the two systems. The failure in the frequency regulating system which is the analogue of the previously described voltage regulator failure is the loss of speed sense, where the wobble plate of one drive moves to the full overdrive position due to a loss of control coil voltage. In the absence of overspeed protection, if one alternator overspeeds, carrying its alternator with it, the second alternator will freewheel ahead of its drive due to the presence of the overrunning clutch. The system frequency is not then determined by the drive speeds of both machines but will be determined by the output speed of the failed drive. If the input speed of the first drive had been 9,000 rpm at the time of the failure and the two machines were each carrying 1.00-per unit real load, then during the failure the output drive speed of the first machine will be about 19,000 while the output speed of the second drive will be about 6,300 rpm; the system frequency will be about 1,200 cycles per second. The equalizer causes the first machine to decrease its output speed by 300 rpm from the 19,300 rpm (maximum drive gear ratio×9,000); meanwhile, the second speed is increased from the normal 6,000 rpm. A modification of the frequency equations to represent the separate drive speeds must be made if the equations are to be applied at all to this failure. Thus the bus frequency, which appears to be the analogue of the bus voltage, does not have the characteristic that it is determined by both machines during the loss in speed sense as was the voltage in the regulator failure.

Summary

It is possible to obtain analytical expressions for the voltage and frequency in the 400 cycle, a-c aircraft electric system where real and reactive load division are accomplished by equalizer systems. Using these expressions puts the problem of predicting the regulated quantities during unbalanced condition on a more quantitative basis than had been done previously in the literature or in practice.

References

1. AIRCRAFT ELECTRICAL SYSTEM STUDY, **Armour Research Foundation.** *Technical Report No. 52–49*, United States Air Force, Washington, D. C., April 1952.

2. ALTERNATING-CURRENT ELECTRICAL SYSTEMS FOR AIRCRAFT (book), Westinghouse Electric Corporation, Lima, Ohio, chapter 3, 1951.

3. PARALLEL OPERATION OF MAIN-ENGINE-DRIVEN 400-CYCLE AIRCRAFT GENERATORS, L. G. Levoy. *AIEE Transactions (Electrical Engineering)* vol. 64, Dec. 1945, pp. 811–15.

◆

Discussion

S. C. Caldwell (General Electric Company, Schenectady, N. Y.): The authors have made a useful and timely contribution in developing a general analysis for these systems, which is in general agreement with tests which I have witnessed. However, under some conditions, disagreements between test and analytical data were observed and it is the purpose of this discussion to explain these discrepancies in terms of limitations on the assumptions used in the analysis.

If equation 1 of the paper is to be valid or all conditions, the following assumption must be made: a machine with a normal regulator may be represented as an infinite sink or source whose terminal voltage is determined only by the signals applied to the input of its regulator.

With present excitation systems, the maximum reactive current that a machine can absorb at rated terminal voltage, at no real load, is the magnetizing current required for the machine at this voltage. This current will approximate the terminal voltage divided by synchronous reactance. Hence, once the excitation of a machine with a normal regulator is reduced to zero, the machine can absorb no more reactive power and is therefore no longer an infinite sink. It becomes simply a reactance across the bus equal to the synchronous reactance of the machine. It is evident then that, whatever the bus voltage is, the analyses based upon equation 1 do not hold, once the excitation of the normal machine has been reduced to the minimum obtainable from the excitation system. In practice, residual flux in the exciter, together with some conduction through the carbon pile at its limit of travel, results in a minimum possible excitation of about 0.10 to 0.30 per unit. (These figures may vary considerably with different machines and excitation systems.) The next question is whether this condition can occur in practice.

Aircraft machines in the larger sizes are characterized by high synchronous reactances which may be as large as 2.6 per unit. It is seen from the preceding reasoning that, with terminal voltage anywhere in the neighborhood of rated value, this value of reactance would permit absorption of less than 0.4 per unit reactive current. Beyond this, the regulator is at its limit of operation and terminal voltage will rise faster than would be indicated by equation 17. (This equation holds since the power angle is small at small loads.)

To test this, two machines were operated in parallel at no load. The load division circuit was connected but separate excitation was used on one machine to represent faulty regulator action. As this excitation was varied, readings of excitation on the voltage regulated machine were recorded and the curve shown in Fig. 1 of the discussion was obtained. Machines used were variable-speed machines rated at 30 kva, 0.85 power factor at 400 cycles, 120/208 volts. Their synchronous impedances were 1.66 per unit. The constant K in the reactive division circuit was set to 0.1. As noted on the curve, the regulation of the normal machine became nonlinear at about 2.0 per unit excitation on the separately excited machine: normal machine excitation remained constant for abnormal excitation greater than this value, and bus voltage was seen to rise more sharply. It was noted that, just beyond this point, the armature of the regulator fell suddenly into the magnet with an audible click, which signified that maximum travel had been obtained. Calculations of terminal voltage from equation 17 are in good agreement with test results up to the aforementioned point but, at an excitation of 2.67 per unit on the overexcited machine, equation 17 predicts bus voltage equal to 1.08 per unit; the observed value was 1.21 per unit.

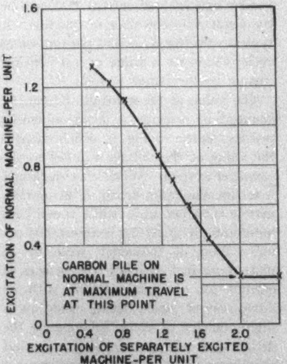

Fig. 1. Excitation characteristics on a paralleled system at no load

It should be noted that in the machines tested the saturation characteristics were such that no appreciable saturation existed in the regulated machine for any of the points on the curve. It is possible, perhaps, that machines with sharp saturation characteristics above rated voltage may not exhibit this effect, in that bus voltage may rise so slowly that the difference between the overvoltage signal and the differential reactive signal never becomes great enough to drive the regulator of the normal machine to maximum travel. However, since this characteristic varies considerably with different machines, the regulator limitations must be recognized and the analysis must be confined to the range over which the regulator can operate linearly.

In the paper, the authors refer to the effect of the differential reactive signal into the regulator as follows: "When the excitation of one alternator goes to its ceiling value, that alternator delivers more than its share of reactive power. The reactive power equalizer circuit indicates a deficiency of reactive power output from the other alternators, causing the exciters of these machines to increase excitation."

This is somewhat misleading since, with most aircraft systems at normal loads, the bus overvoltage signal under this condition will be larger than the reverse reactive power signal into the normal machines, and the regulator will therefore operate to reduce excitation in the normal machines. What is probably meant is that this reverse reactive power signal will tend to increase excitation in the normal machines over what it would be without the reactive power equalizer circuit. Actually, in the test described in this discussion, excitation in the normal machines was reduced to its minimum value long before ceiling excitation had been reached on the abnormal machine. It can be shown that, at no load, with unsaturated machines (and within the regulator range)

$$\Delta E_1 = \Delta E_2 \frac{K-Z}{(n-1)Z+K}$$

where

ΔE_1 = change in excitation of normal machines

ΔE_2 = change in excitation of abnormal machine

K = the proportionality constant used in the paper

Z = direct-axis reactance of the machine

n = total number of machines in parallel

From this equation it is apparent that, if the proportionality constant is less than the direct-axis reactance of the machines, normal machine excitation will be reduced by an increase in excitation of the abnormal machine. Again it is conceivable that with sharp saturation characteristics, bus voltage rise may not be sufficient with some machines to prevent the reactive power equalizer signal from overriding the bus overvoltage signal and cause excitation in the normal machines to increase when very large excitation is applied to the abnormal machine. In addition, if the load is sufficiently large, bus voltage rise may be small enough to permit the equalizer signal to override and cause normal machine excitation to rise. However, in the systems examined so far, this load appears to be much greater than rated system load.

Caution is necessary also in using the factor K. On some modern regulators, the equalizing reactor has been made nonlinear to limit bus voltage droop if the equalizing loop is opened. Hence K may be a function of the current flowing in the reactor, and may not be a constant for large values of this current.

Emil S. Sherrard (Naval Research Laboratory, Washington, D. C.): The analyses in this paper show that the steady-state operation of equalizer circuits may be described simply whether the equalizer circuit is used in conjunction with a complex electromechanical voltage regulator or an even more complex electrohydraulic speed governor. This simplification is of great value to the systems engineer who must analyze the behavior of such components in a system and who may have neither the time nor the background to consider the detailed operation of a voltage regulator or speed governor.

The reader might profit from a clear explanation of the phrase "magnitude of reference voltage" used to define the symbol $|V_0|$ of equation 1. Equation 1 implies that this quantity is a voltage measured either at the machine terminals or at the bus. However, the authors do not state whether it is a particular phase voltage or an average phase voltage, a no-load or a rated-load voltage, a voltage in a single generator or a multiple-generator system.

This analysis of reactive load unbalance assumes that, except for one generator, all generator currents are equal. Such an assumption is correct for a 2-generator system, but it may not be a realistic assumption for a multiple-generator system. An equation relating the reactive equalizer circuit sensitivity and the worst reactive unbalance has been derived without the use of this assumption. In per unit quantities, this equation may be written

$$S(X_1-X_a)=V_{a0}-V_{10} \qquad (1)$$

where

S = the sensitivity of the reactive load division circuit

subscript a denotes the average for all the parallel generators

subscript 1 denotes the generator carrying the largest reactive current

X = reactive generator current in the parallel system

V_0 = the average of the regulated phase voltages for a generator delivering rated current to the bus with a short-circuited equalizer

It is my impression that in the section of the paper entitled "Reduction in System Capacity" the calculations are applicable to large multiengine and multigenerator aircraft whose crews contain one or more flight engineers rather than to smaller aircraft containing only two generators which must operate satisfactorily in parallel with little or no attention from the flight crew or pilot. In the paper, the authors have assumed a sensitivity of 0.106 per unit, and calculated that one machine of the system supplies 0.425 per unit reactive current to the bus. For a 2-generator system, the second machine might be able to deliver its rated reactive current of 0.661 per unit to the bus. Therefore, for a 2-generator system, the reactive current supplied to the bus or the available reactive capacity, as we shall term it, is 1.086 per unit, which is 1.086/2×0.661 = 82.1 per cent of the installed or total generator reactive capacity.

A calculation of the ratio of installed to total generator reactive capacity will be made for the case of an aircraft containing a 2-generator system which is required to operate satisfactorily without any manual adjustment of reactive load balance. In order that this ratio may be compared with the value of 82 per cent just given, S will be taken equal to 0.106, and the rated reactive current of a generator assumed to be 0.661 per unit.

Present specifications require the average regulated phase voltage to be within a 5-volt band about a nominal value. Therefore, one generator could exhibit a rise in regulated voltage between no load and full load, and the other generator's regulated voltage could decrease between no load and full load. In an extreme case, the no-load voltages of the two generators could be equal and their full-load voltages could differ by 0.05 per unit, or approximately 5 volts. If flight crew attention is required to be at a minimum, the generator voltages might be adjusted to the nominal value at no load, at different times, or under different warm-up conditions. Such an adjustment procedure might easily cause the no-load voltage of one machine to be 1 per cent, or 0.01 per unit, higher than the nominal value, while the no-load voltage of the other machine could be 1 per cent lower than the nominal value. This difference of 0.02 per unit in no-load voltages, together with the 0.05 per unit difference in the regulation of the two machines, causes the regulated voltages of the two machines at full load and before paralleling to differ by 0.07 per unit. The term $V_{a0}-V_{10}$ in equation 1 of the discussion will be half this difference, or 0.035 per unit. Therefore, for $S=0.106$, and $X_1=0.661$ per unit, X_a, calculated from equation 1 of this discussion is 0.331 per unit. The reactive component of bus current is twice X_a or 0.662, and the ratio of available to installed capacity is 0.662/2×0.661 = 50.1 per cent. This 50-per-cent ratio differs appreciably from the 82-per-cent ratio calculated from values given in the paper.

If a 90-per-cent value for the ratio of available to installed reactive capacity is to be obtained, then the sensitivity of the equalizer circuit S, calculated from equation 1 of this discussion for $V_{a0}-V_{10}$ equal to 0.035 per unit, is found to be 0.53 per unit. This value of sensitivity contrasts with the typical value of 0.11 used in the paper.

These calculations, in my opinion, show that there may be no single value of sensitivity that is usable or typical for all parallel generator aircraft electric systems. The desirable or necessary values of sensitivity required to insure satisfactory reactive load division may differ from one system to another. Before the minimum equalizer sensitivity required for a particular system may be determined, it seems to me that at least the following must be determined:

1. The number of generators in parallel on the bus.
2. Whether or not flight personnel are available for monitoring and trimming of reactive current unbalance.
3. Whether present voltage regulators meet, do not meet, or exceed specified performance.
4. Whether or not the sensitivity of the reactive load division circuit is to be chosen equal to the minimum sensitivity necessary for acceptable steady-state reactive load division or equal to some higher value which will result in improved transient performance without sustained oscillation.

Russell W. Stineman (Boeing Airplane Company, Seattle, Wash.): The operation of the reactive power equalizing loop may be more fully understood if the case of unrestricted alternator currents is considered. An analysis may be made using the notation of Fig. 2 of the paper. Beginning with equation 5 of the paper and assuming $Z=Z_1=Z_2=Z_3=\ldots=Z_n$ gives

$$i_1Z+i_2Z+i_3Z+\ldots+i_nZ=0 \qquad (5A)$$

or

$$i_1+i_2+i_3+\ldots+i_n=0 \qquad (5B)$$

but

$$i_1=\frac{I_1}{c}-i, \quad i_2=\frac{I_2}{c}-i\ldots \qquad (5C)$$

Letting $i=I/c$ and substituting equations 5C and 5D in 5B gives

$$I=\frac{I_1+I_2+I_3+\ldots+I_n}{n} \qquad (5E)$$

and

$$i_1=\frac{I_1-I}{c} \qquad (5F)$$

It may be noted from the foregoing analysis that I is the average current of the n alternators; hence, i_1 is proportional to the difference between the current in alternator 1 and the average current of the n alternators.

The differential current i_1 is applied to the primary of the mutual reactor. This mutual reactor is essentially a transformer with a high reluctance core and a high

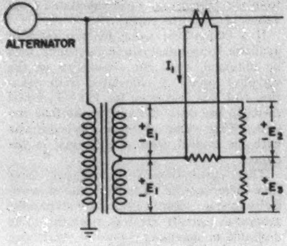

Fig. 2. Power sensing circuit

impedance secondary load, so that the primary current is almost entirely magnetizing current. However, due to hysteresis and and eddy current effects, the voltage induced in the secondary does not lead the primary current by a full 90 degrees. Tests conducted by me indicated that the phase shift is actually about 75 or 80 degrees in a typical circuit. Consequently, equation 1 is only an approximation, sufficiently accurate for most purposes.

For small values of mutual reactor primary current, the proportionality constant B is approximately related to the mutual reactance of the reactor X_m by

$$B \cong \frac{X_m}{\sqrt{3}} \tag{1A}$$

a relation that may be easily derived from the geometry of the vector diagram, after recognizing that the voltage regulator responds to the average of the three line-to-line voltages applied to its terminals. For larger signals, equation 1A becomes inaccurate and B is no longer a constant.

The real power-equalizing circuit shown in Fig. 5(A) of the paper may also be analyzed for the more general case of unrestricted alternator currents. Letting E be the voltage at the point Y_1, and summing the currents into Y_1

$$\frac{E_{01}-E}{R_d}+\frac{E_{02}-E}{R_d}+\frac{E_{03}-E}{R_d}+\ldots+\frac{E_{0n}-E}{R_d}=0 \tag{24A}$$

whence

$$E=\frac{E_{01}+E_{02}+E_{03}+\ldots+E_{0n}}{n} \tag{24B}$$

and

$$i_1=\frac{E_{01}-E}{R_d} \tag{24C}$$

As with the equalizing loop, the current i_1 is proportional to the difference between the signal voltage E_{01} and the average signal voltage of the n alternators.

The signal voltage E_{01} is derived from a circuit of the basic type shown in Fig. 2 of this discussion, where

$$E_{01}=|E_2|-|E_3| \tag{24D}$$

Analysis of the circuit gives a solution of the form

$$E_{01}=|E_1+KI_1|-|E_1-KI_1| \tag{24E}$$

For small values of I_1 or θ

$$E_{01} \cong 2KI_1 \cos\theta \tag{24F}$$

where θ = angle between E_1 and I_1.

For this case the proportionality constant M is approximately $2K$. For larger values of I_1 and θ, equation 24F is inaccurate and M is not a constant, although in all cases $E_{01}=0$ where $\theta=90$ degrees.

It is thus evident that the equalizing circuits are not perfectly selective; that is, the reactive power equalizer has a small sensitivity to real power unbalance, while the real power equalizer may respond to reactive currents. However, these features do not ordinarily have a qualitative effect on the circuits, and the quantitative effect becomes negligible if the unbalances are small.

In determining the effect of unbalance on system capacity, the authors selected rated alternator armature current as a criterion of full load. This criterion is questionable, since the greatest temperature rise occurs in the alternator field winding. A more realistic criterion would be the value of alternator field current at rated load. Assuming a constant power factor load, the critical alternator during a reactive power unbalance would be supplying current at a low power factor, more field current would be required, and the system capacity based on the field current criterion would be less than the capacity based on rated armature current. On the other hand, the critical alternator during a real power unbalance would be supplying current at a high power factor, so that more than rated armature current could be safely delivered, subject to the limitations of the alternator drive.

John A. Granath and Albert K. Hawkes: The authors are grateful for the interest shown in their work as evidenced by the constructive comments presented.

S. C. Caldwell's comments on the characteristics of newer alternators and regulators, as these affect the reactive equalizer analysis, are significant. Most general and important is the fact that a regulated machine, operating in parallel with a machine which is at ceiling excitation, is not an infinite sink. In the general case this is quite true. Quantitative prediction of system conditions should then perhaps be made in two steps, to consider each of the two approximately linear regions. It may be of interest to note, however, that the reactance of the paralleled machines and the magnitude of maximum generated voltage possible (ceiling) in a given type of machine may lie in a range of values such that one machine cannot deliver more reactive power than any other machine is capable of absorbing. This was the case with the particular equipment tested to verify the analysis. The no-load terminal voltage at ceiling excitation of one machine, determined by exciter characteristics and minimum regulator carbon stack resistance, was measured 1.3 per unit. The worst case for a given type alternator with associated exciter and regulator is a 2-machine system with no load, since one machine must absorb all the excess reactive power from the faulty machine. The second, or regulated, machine tested was capable of absorbing the full reactive output of the first. However, as Mr. Caldwell points out, a high level of excitation or large synchronous reactance values can (and does, on newer alternator designs) produce voltage drops in the regulated machine sufficiently great that the regulated machine would have to adjust excitation to produce negative voltage to maintain 1.00 per unit voltage at the bus. As a consequence, the regulated machine may be driven to minimum excitation, after which it offers a fixed impedance to the system. The two conditions, regulating and fixed impedance, make the two segments of the curve shown in Fig. 1 of the discussion.

The wording of the statement about the effect of the differential reactive signal should have been clarified. The sequence of events, as Mr. Caldwell surmised, was meant in the paper to be as follows:

1. One alternator goes to ceiling (regulator failure).
2. Other paralleled alternators have a voltage signal to regulator to reduce excitation to maintain 1.00 per unit bus voltage.
3. Other paralleled alternators have a current signal to regulator to increase excitation to maintain equal load sharing.
4. Net result is an equilibrium condition with bus voltage slightly elevated, and substantial circulating currents.

Both R. W. Stineman and E. S. Sherrard suggest that a more general approach to the n machine system would be to use the average current of the $n-1$ generators as a reference in discussing current unbalance. The assumption of equal currents among the $n-1$ machines was used instead, in order to bring out the relationships involved, with the possibility of using superposition for the more realistic cases where current from each machine is different, should it be desirable to analyze this case.

The quantity $|V_0|$ represents, in general, the desired voltage at the bus, regardless of the method by which this is achieved. In the particular regulator described, $|V_0|$ is the relationship between the characteristics of a spring and a solenoid which are matched over a range such that the resultant force is zero for predetermined combinations of spring travel and solenoid magnetic air gap. This representation of the reference voltage is compared, in this regulator, with the average of three line-to-line voltages such that the average voltage will be maintained at a constant value at the point of regulation over the no-load to rated-load range, in a single or multiple generator system.

The example of calculation of reduction in system capacity was given to show how the analysis can be used in a practical problem. The figures cited were not intended to indicate the worst possible case. Using the same method, with the assumption of greater errors in regulator performance owing to one regulator being set high and another set low, regulation or droop permitted by specification, errors in reading the meter used to set the adjustment of the regulators, phase unbalances on the system, and random errors, quite different numerical results may be obtained. Justification of such assumptions is difficult but important, and is felt by the authors to be another problem beyond the scope of this paper. Along this same line, the term "typical," ascribed to the value of equalizer constant K, was meant to indicate the value of this constant as measured in specific items of equipment which are in use, and which is implied in the United States Air Force Specification *MIL-R-5292A* for the type *L*-1 regulator. The analysis in this paper is not sufficiently extensive to draw conclusions as to the optimum or most desirable value of constant *K*. The word "typical" should not be construed as meaning desirable but rather as existing or in use. Before conclusions can be drawn as to an optimum, there is a need for further work, particularly on transient considerations such as Mr. Sherrard mentioned. We are in full agreement that additional work is needed to determine desirable power equalizer characteristics for particular applications, considering aircraft operating conditions as well as power system conditions.

Mr. Stineman has pointed out that an approximation is used in the representation of the reactive and real power sensing circuits. The fact that these circuits may be treated as having outputs proportional to reactive and real power flowing from the machine in question is not unreasonable.

For the real power sensing circuit, referred to by Mr. Stineman, the error in absolute value of the difference in the phasor quantities E_2 and E_3 is only about 5 per cent when the in-phase component of current is 1.00 per unit, and the quadrature component of current is 1.00 per unit. Thus, as he finally concludes, there is very little error involved in assuming that the output of this droop circuit is independent of quadrature current. Similarly, it has been found that little error exists in the reactive power sensing circuit because of the in-phase component of current.

The authors regret the error of oversight in not defining the *Z* terms first used in equation 5. These *Z*'s denote the impedance of the *n* mutual reactors.

REFERENCE

1. ANALYSIS AND REDESIGN OF A CARBON PILE VOLTAGE REGULATOR FOR AIRCRAFT GENERATORS, W. B. Kouwenhoven, G. J. Thaler. *AIEE Transactions*, vol. 67, pt. II, 1948, pp. 1197–1203.

A-C Versus D-C Power for Underground Mines

J. Z. LINSENMEYER
MEMBER AIEE

A. G. OWEN
NONMEMBER AIEE

IN THIS paper a comparison will be made of a-c and d-c systems and motor characteristics, the merits of power-factor correction will be discussed, the possibilities and effects of a good choice of conductors will be examined and the solutions to simple a-c distribution problems will be offered.

The provision of electric power to underground-mining machinery is a highly specialized problem requiring more rigid restrictions of installation than any other industry. This fact is particularly true in underground coal mining.

General Comparison of A-C and D-C Systems

Until recent years, d-c power transportation was the chief demand for electric power; and, as a result, not too much effort was required or expected in the direction of good voltage regulation or an adequate supply of power. Today the needs of good voltage regulation and adequate supply of power are greater than ever, yet 275-volt power commonly winds up as 160 volts at the machinery load. While such extremes in regulation can be lived with on d-c systems, even though highly undesirable, such conditions cannot be tolerated in an a-c powered system.

The distribution problem will divide into two parts: first, the primary transmission of power from the point of entry to the load centers; and second, the distribution at utilization voltages to the mining machinery and transportation equipment.

The primary transmission will invariably be a-c in either an a-c or a d-c system, and the identical nature of the problems involved therefore deletes any necessity of a comparison. However, basic design considerations will be discussed later. The primary distribution will terminate in a-c substations or d-c conversion units, the location of which will be chiefly a function of fire hazard, accessibility, and necessity for portability. The lack of restrictions on primary voltages will permit an optimum choice.

In the discussion of power utilization, the assumption is made that generally speaking either a-c or d-c drives may be successfully applied to all equipment except haulage applications.

State Mining Laws

The utilization voltage chosen will be closely related to the regulation problem, but in many cases an optimum choice is prevented by state laws. As an example, a survey of the 18 states with a published code shows seven limiting the voltage at the face to 300 volts, eight making no mention of voltage at all, and three allowing voltages over 300 volts under certain circumstances.

Effect of Line-Voltage Regulation on Motors

In the comparison of a-c and d-c systems, voltage regulation is an important factor. Both a-c motors and controls require much better regulation than their d-c counterparts. The added elements of power factor, line reactance, high motor-starting currents, and high contactor drop-out voltages tend to offset the greater voltage-compensating characteristics of the a-c system. The regulation of a d-c system is subject only to line resistance and relatively low motor-starting currents, and is not subject to the previously mentioned factors inherent in a-c systems.

The greatest problem in a-c regulation occurs during the motor start-up, and as a result, the a-c conductor choice will be determined chiefly by the motor starting current and torque demand, and the a-c contactor drop-out ratings.

For approximately equal torques of 200-per-cent full-load ratings, the starting current for a-c motors will be approximately $2^{1}/_{2}$ times that for d-c motors. The a-c motor will require a regulation half that for a d-c motor to meet these conditions.

If cable impedance is assumed to be a direct function of cable cross-section, the a-c motor will require approximately 4.62 times more copper at 220 volts than the d-c motor at 230 volts. At 440 volts, this figure would be reduced to 1.15. However, because of the effect of cable reactance and power factor, these ratios are not actually true but rather will vary from a fraction of, to a larger figure than 4.62. A proper selection of conductors will keep this ratio at a minimum, as will be described later.

Paper 53-185, recommended by the AIEE Mining and Metal Industry Committee and approved by the AIEE Committee on Technical Operations for presentation at the AIEE Southern District Meeting, Louisville, Ky., April 22–24, 1953. Manuscript submitted June 2, 1952; made available for printing March 19, 1953.

J. Z. LINSENMEYER and A. G. OWEN are with the Westinghouse Electric Corporation, East Pittsburgh, Pa.

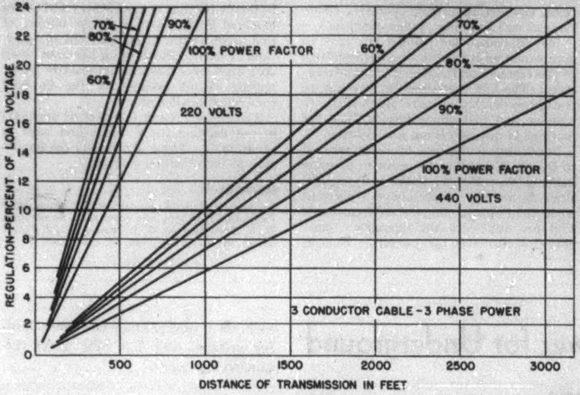

Fig. 1. Transmission distance versus regulation for 200 kw, using 4/0-circular-mil cable—1-inch spacing

It should be noted here that for a fully loaded motor, the copper required for a 440-volt cable is approximately one fourth that for a 220-volt cable for equivalent regulation, while for a motor-starting load, the 440-volt cable may require as low as one eighth the copper of a 220-volt cable, for the same regulation. Since it is obvious that the first case will be the limiting factor, the 440-volt cable can be but one fourth the size of a 220-volt cable for equivalent regulation; likewise, the starting regulation at 440 volts may be half that at 220 volts.

Effect of Power Factor and Voltage Regulation on Conductor Size

Fig. 1 shows the relative distances that a load of 200 kw can be transmitted over a 4/0 cable at 220 volts alternating current and 440 volts alternating current for power factors ranging from 60 per cent up to 100 per cent. A line is drawn across the chart at the 10-per-cent regulation level, which has tentatively been set as the desired maximum. Note that the transmission distance at 440 volts is four times that for 220 volts; and that the lower the power factor of the load, the shorter the possible transmission distance for the same per-cent regulation.

Fig. 2 shows the transmission distances for the same considerations as before, except for a 500,000-circular-mil cable. Again a straight line drawn across the chart at the 10-per-cent level shows the transmission distance at 440 volts to be four times that at 220 volts for the same regulation. As before, the lower power factors greatly reduce the transmission distance possible for a given regulation.

These comparisons graphically illustrate the saving in copper, which is an item of tremendous importance; and from a safety angle, we have a line-to-ground voltage of only 256 in the 440-volt system, as compared with a voltage of 275 on a d-c system. In addition, a safer grounding system is possible with the a-c system than has yet been devised for the d-c system.

Importance of Line Reactance to Voltage Regulation

The minimum power factor always present during a motor start-up will cause the line reactance to take precedence over the line resistance in the determination of voltage drop. Reduction of line reactance will be better accomplished by a minimum conductor spacing and the use of paralleled 3-conductor cables, since reduction of conductor size in a cable produces very little, if any, increase in reactance.

In the solution of the regulation problem, two choices are available: either increase conductor sizes and numbers or use power-factor correction to minimize the effect of motor-starting currents, or line reactance, or both.

Let us take a typical sample case and see what can be done. A continuous mining machine 1,000 feet from the low-voltage transformer, with one 50-horsepower-traction and two 70-horsepower cutter motors imposes a 25-per-cent traction-motor load, and a starting load for both cutter motors, which is the worst condition we would experience. Assuming a 35-per-cent and 85-per-cent power factor for the starting and running power factors, the line currents will be 1,800 and 475 amperes respectively.

Assuming unloaded starting for the cutter motors, we will choose a maximum regulation of 20 per cent as practical, from contactor drop-out considerations. Such a regulation will reduce the starting current to 1,440 amperes.

A 1,500-000-circular-mil cable would give 24-per-cent regulation but would not achieve a 20 per cent regulation, since further increase in conductor size serves to produce a net increase in conductor spacing and reactance. Quite obviously too, such a cable is impractical from a

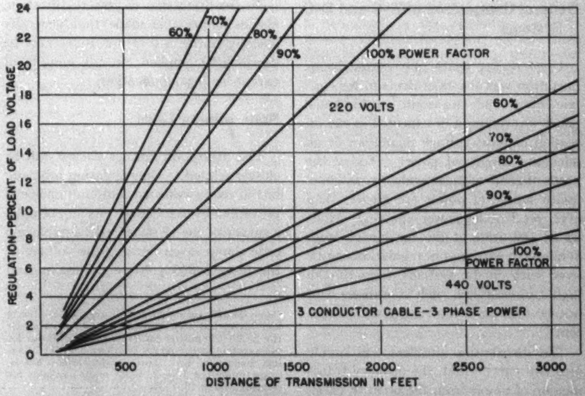

Fig. 2. Transmission distance versus regulation for 200 kw, using 500,000-circular-mil cable—1-inch spacing

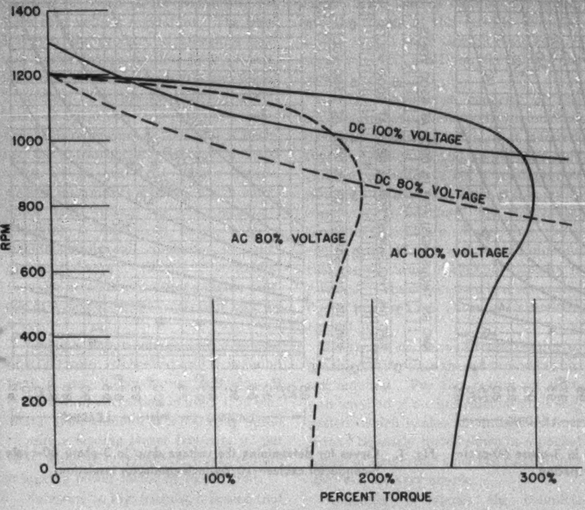

Fig. 3. Comparison of a-c and d-c motor speed-torque characteristics

weight and handling standpoint.

The use of two paralleled 3-conductor cables would permit 300,000-circular-mil conductors to give 20-per-cent regulation, or three paralleled 3-conductor cables with 2/0 conductors may be used. The important point here is the total copper cross section of the three 2/0 cables, which is less than one third of that of the 1,500,000-circular-mil cables, is made possible by closer spacing. Again, line reactance is a most important factor in a-c voltage regulation.

Power-Factor Correction Aids Voltage Regulation

Now let us explore power-factor correction as a means of improving regulation. In order to avoid the necessity of additional kilovolt-ampere capacity in the system feeding the load under consideration, the total line current, with capacitors added, must be no greater than before. The capacitor will therefore be 190 kva, and the full load-line power factor will be 85-per-cent leading, instead of lagging.

Since a capacitor will allow the two paralleled cables to be reduced from 300,000-circular-mil to 4/0-circular-mil conductors for the same 20-per-cent regulation, while the three paralleled 2/0 cables could not be reduced to 1/0 conductors, without increasing the regulation to 21 per cent. It is interesting to note that only 95-kva capacitors, which would give a full-load power factor of 100 per cent would require 250,000 circular mils for 2 cables, and the same 1/0 for 3 cables with 22-per-cent regulation. In all these cases the full-load regulation is less than 11 per cent. Reduction of line reactance is more beneficial than the addition of capacitors.

The discussion of shunt capacitors thus far has assumed them as connected continuously to the line. However, they may be installed at the motors in order to be switched from the line with the motors. The disadvantage of this method is the possibility of overvoltage from self-excitation, unless the capacitor size is limited to a kilovolt-ampere-rating approximately one fourth of the connected motor horsepower. The maximum capacity possible with the two 70-horsepower motors would then be about 35 kva. Since the small benefit of the 95-kva capacitors has already been determined, it follows that this method would be unsatisfactory.

The addition of capacitors will, however, correct power factor and reduce voltage drop throughout the feeder system. It may be concluded, therefore, that some combination of capacitors and cable division will give the best answer in the problem of voltage regulation, but that shunt capacitors cannot do the job alone.

Comparison A-C and D-C Motor Characteristics

Let us briefly compare the characteristics of a-c and d-c motors. Over the normal operating range of voltages, the d-c motors will maintain essentially the same peak value of torque, while reducing speed approximately in direct proportion to reduction in line voltage. The a-c motor starting and maximum-available torque will vary as the square of the line voltage, while maintaining an essentially constant speed. In addition, the starting current will be approximately five times normal running current, and the starting power factor will be very low. The d-c starting current will be in direct proportion to the torque required, and will be limited by a starting resistance. Loss

Fig. 4 (below, left). A-C feeder line (see Appendix 1 for calculations)

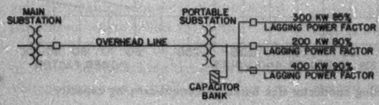
MAIN SUBSTATION
OVERHEAD LINE
PORTABLE SUBSTATION
300 KW 85% LAGGING POWER FACTOR
200 KW 80% LAGGING POWER FACTOR
400 KW 90% LAGGING POWER FACTOR
CAPACITOR BANK

Fig. 5 (right). Relation between kilowatts and kilovars at various power factors

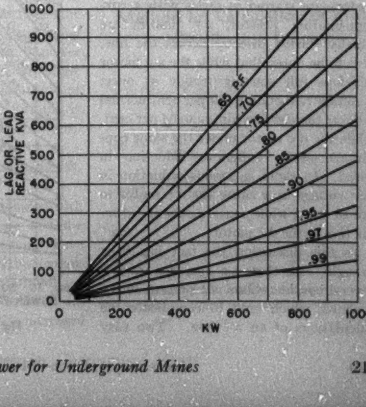

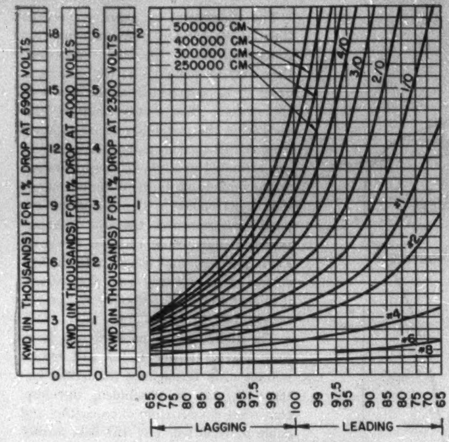

Fig. 6. Curves for determining the voltage drop in 3-phase 60-cycle overhead lines—34-inch equivalent spacing

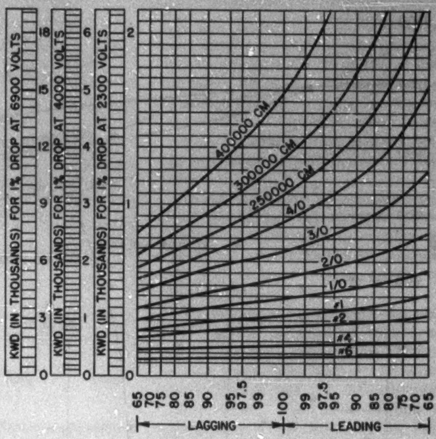

Fig. 7. Curves for determining the voltage drop in 3-phase 60-cycle 3-conductor cables—10/64-inch conductor insulation

of torque in the a-c motor may be compensated for to some degree by the use of a motor design approaching a National Electrical Manufacturers Association design *C*, in order that the high starting torque will more closely approach the pullout-torque values; and also the low starting current will aid in keeping the line loss at a minimum.

Considering the speed-torque curves for a d-c compound-wound motor and a low-slip, high-pullout and starting torque a-c squirrel-cage induction motor, as shown in Fig. 3, the stalled torque or zero-speed torque of the d-c motor is not shown, since this is not considered to be a safe operating point because the resultant high-armature current may cause a commutator flashover.

While all but the smaller sizes of d-c motors are started in series with a current-limiting resistor, a-c motors are usually started directly across the line. It is to be noted that while the a-c motor develops full starting torque at once, a voltage reduction to 80-per-cent normal reduces the starting torque to 64 per cent, while the d-c motor under the same conditions merely suffers a reduction in speed. In short, a serious reduction in line voltage may cause the a-c motor to fail to start, while causing only speed reduction in the d-c motor.

In this discussion the fact has been brought out that a-c systems involve several considerations not present in d-c systems, which tend to complicate the calculations of an a-c line. Two easy methods which are fairly accurate, in solving a-c distribution systems, at either primary or utilization voltages will be considered here.

Method of Determining Size of A-C Feeders

For an example, taking a small section of an a-c distribution system, as shown in Fig. 4 and calculated in Appendix I, the problem is to determine the conductor size required to maintain a 5-per-cent voltage regulation and the best transmission voltage.

The first step is to determine the total load and combined power factor appearing at the low-voltage substation. Adding the kilowatt loads directly, the total is found to be 900 kw. Using Fig. 5 to determine the reactive kilovolt-amperes of each load, the total is found to be 525 kilovars for the 900-kw load, and again, from Fig. 5 it is seen that this represents a power factor of 86-per-cent lagging. We are now ready to choose a conductor size.

Fig. 6 shows the conductor sizes as a

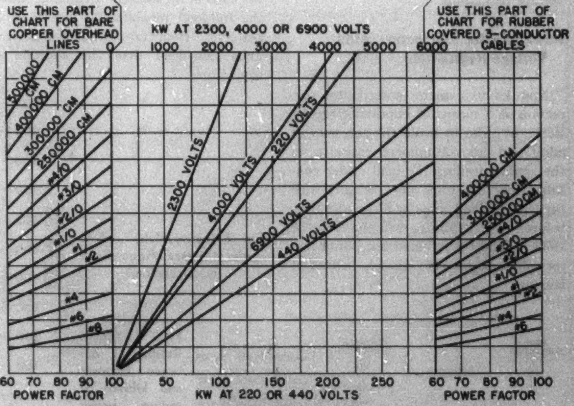

Fig. 8. Curves for selecting conductor size based on current-carrying capacity

function of power factor and KWD for 1-per-cent voltage regulation. The term KWD is the product of kilowatts load and feeder length in thousands of feet, for a nominal mean conductor spacing of 34 inches. The 900-kw load for a distance of 9,000 feet at 5-per-cent regulation, then, represents, 1620 KWD. Checking for a transmission voltage of 2,300 volts, at 86-per-cent power factor, we find no conductor curve, which eliminates this voltage as unsatisfactory. Checking a voltage of 4,000 volts, a 400,000-circular-mil conductor is found to be satisfactory. Should it be decided that this is too large, either a higher voltage or a power-factor correction can be tried.

Trying a higher voltage first, a voltage of 6,900 volts is checked and it is found that a no. 2 conductor will do. If power-factor correction is used, it is seen that a 4/0 conductor at 2,300 volts would require a leading power factor of 97 per cent, while at 4,000 volts it would require a lagging power factor of 95 per cent.

Referring to Fig. 5 again, it is seen that a power factor of 95-per-cent lagging shows 300 kilovars for 900 kw, leaving 225 kilovars to be compensated for by capacitors. By the same method we would find 750 kva of capacitors would be required for a 97-per-cent leading power factor. The capacitor cost may then be balanced against the cost of conductors and higher transmission voltages.

Let us check the same problem, using a 3-conductor cable. Referring to Fig. 7, which is a duplicate of Fig. 6 but is for cable spacings, it is found again that 2,300 volts is not a suitable transmission voltage, that 4,000 volts requires a 3/0 conductor, and that 6,900 volts requires a no. 2 conductor. Note here how the conductor size for the cable is smaller than for the pole line for each corresponding voltage.

If we wish to improve the power factor, the same procedure would be followed as before, but a closer look at the slopes of the curves in Fig. 7 will show that little reduction in conductor size can be achieved. As an example, to reduce the conductor size from 3/0 to 2/0, the power factor must be improved from 85-per-cent lagging to 98-per-cent lagging and to reduce to the next conductor size of 1/0 requires an improvement to 85-per-cent leading power factor. Here again is seen the importance of a small line reactance, and the small benefit derived from shunt capacitors, where cables are used.

These curves may be used for voltages of 230 or 460 by taking the square of the voltage ratios as a multiplier. For example, 2,300 volts is 10 times 230 volts, and the square of this ratio is 100. 10 KWD at 230 volts then is read as 100 times or 1,000 KWD on the 2,300-volt scales.

Lastly, the thermal capacity of the conductor sizes previously chosen must be checked. Referring to Fig. 8, it is found that at 4,000 volts and 85-per-cent lagging power factor, a no. 4 conductor is adequate for the pole line, and a no. 1 conductor is adequate for the cable. Since these sizes are smaller than those chosen from Figs. 6 and 7, it is obvious that the condition of thermal capacity is satisfied. The curves used here are reproduced from a Coal Division Committee Report.[1]

There are occasions where conductor spacings, other than those discussed so far, are required. For this reason an alternate method of a-c line calculation is suggested, which is also advantageous since it may be easily jotted down in a pocket memo or diary, and since the calculations involved are very simple.

Appendix II shows the complete method, which is more accurate than many short-cut methods. These formulas may be worked in either direction, in that we may assume a conductor size, and all but any one of the other variables, and determine the last variable; or we may assume a load, and all but any one of the other variables, and determine the remaining variable.

The term KWD, as before, represents the load in kilowatts per 1-per-cent regulation per 1,000 feet of line one way. Should it be desired to use R and X as the resistance and reactance respectively per mile of line instead of per 1,000 feet, then the KWD will be per mile of line instead.

If trigometric tables are not available to determine the term tan θ from the power factor, it may be easily calculated from the power factor as shown. Lagging and leading power factors are taken into consideration by the sign between the R and X terms, being plus for a lagging power factor and minus for a leading power factor. Either 3-phase or single-phase lines may be calculated. The resultant kilowatts obtained from the formula is for a 3-phase line, and dividing this result by 2 will give the kilowatts for a single-phase line of the same size, length, and so forth.

This discussion may be concluded with the observation that both a-c and d-c motors and distribution systems have their limitations, which are further magnified by laws limiting utilization-voltage maximums, but the trend towards increased mechanization and the increased demand for electric power at points remote from the power sources may gradually force a turning to a-c powered equipment, and a revision of mining laws to permit utilization voltages which are best suited to the needs of the industry, as well as the safety of the equipment-operating personnel.

Appendix I. Calculation of an A-C Feeder Line: Circuit Constant

1. Voltage at load = 4,000 or 6,900 volts.

2. Kilowatts of the load = total of 900 kw.

3. Power factor of load = 86 per cent.

4. Voltage drop to the load = 5-per-cent load voltage.

5. Conductor spacing of feeder = 34 inches for aerial line; 10/64-inch conductor insulation for cable.

6. Length of feeder = 9,000 feet.

7. Conductor size as determined from curves

A. 300,000 circular mils at 4,000 volts; no power factor correction; with aerial line.

B. No. 2 at 6,900 volts; no power factor correction; with aerial line.

C. 4/0 at 4,000 volts; power factor corrected to 95 per cent lagging; with aerial line.

D. No. 1 at 4,000 volts; power factor corrected to 97 per cent lead; with aerial line.

E. 3/0 at 4,000 volts; no power-factor correction; with 3-conductor cable.

F. No. 2 at 6,900 volts; no power-factor correction; with 3-conductor cable.

Total kilovars of 900-kw load, at 86 per cent lagging power factor = 525 kilovars.

4,000-volt aerial line, corrected to 95 per cent lagging power factor = 225-kva capacitor.

4,000-volt aerial line, corrected to 97 per cent leading power factor = 750-kva capacitor.

Appendix II. Short-Cut Method for Calculation of A-C Distribution Lines

$$(\mathrm{KWD}) = \frac{E^2(10^{-5})}{R + X(\tan\theta)} \qquad (1)$$

$$\tan\theta = \frac{\sqrt{1-(\mathrm{PF})^2}}{(\mathrm{PF})} \qquad (2)$$

$$(\mathrm{KW}) = \frac{(\mathrm{KWD})(\%\mathrm{VR})}{D} \qquad (3)$$

where

KWD = load in kilowatts per 1-per-cent regulation per 1,000 feet of line
E = voltage at the load
R = resistance per 1,000 feet of one conductor

X = reactance per 1,000 feet of one conductor, for spacing used
tan θ = trigometric tangent of angle, the cosine of which is the power factor of the load
PF = power factor of the load
KW = power in kilowatts to be transmitted
D = length of the feeder in thousands of feet
Per cent VR = per-cent voltage regulation desired

In equation 1, use $R+X(\tan\theta)$ for lagging power factors; use $R-X(\tan\theta)$ for leading power factors. For 3-phase power, multiply KW by 1; for single-phase power, divide KW by 2.

Reference

1. **Coal Division Committee Report.** *American Mining Congress*, Washington, D. C., May 1946.

◆

No Discussion

Open-Loop Frequency Response Method for Nonlinear Servomechanisms

R. L. COSGRIFF
ASSOCIATE MEMBER AIEE

Synopsis: This paper develops a useful graphical representation similar to the common Nyquist diagrams for the measured or calculated open-loop frequency response data of nonlinear systems.[1,2,3,4] This representation indicates the frequency response characteristics and other phenomena such as limit cycles[5] and response hysteresis, or jump phenomenon,[6] of closed-loop systems. Likewise, this open-loop representation is convenient for the synthesis of linear filters, which can be inserted in the error amplifier to improve the closed-loop response of such nonlinear systems. In fact, the closed-loop frequency response of the nonlinear system with a linear filter in the error or forward section of the loop can be determined if both the transfer function of the linear filter and the open-loop frequency response of the nonlinear servo without the filter are known. Many who have measured the response of servo systems assumed to be linear have realized that the assumption of linearity is not always satisfactory. For very small input signals, backlash and coulomb friction cause nonlinear distortion, as does saturation when the input signal is large.[7] It is hoped that the method used in this paper will help the servo engineer improve the response of nonlinear systems.

Representation of Nonlinear Frequency Response

A BLOCK diagram of a typical servomechanism is shown in Fig. 1. The input r to the servo causes the output c. The error signal e is defined by

$$e=r-c \tag{1}$$

The open-loop frequency response is taken by opening the loop at point a, Fig. 1, and directly exciting the input of block G. In this paper the error will be considered to consist of a constant e_0 and the fundamental term $e_1 \sin(\omega t+\theta)$. Notice that terms such as c_0, c_1, and r_0, r_1, etc., are constants and that only the terms r, c and e are functions of the independent variable t. Let

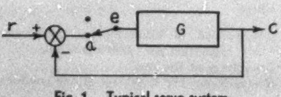

Fig. 1. Typical servo system

$$e=e_0+e_1 \sin(\omega t+\theta) \tag{2}$$

In this case the output c will generally be

$$c=c_0+c_1 \sin \omega t + c_2 \times \sin(2\omega t+\beta_2)\ldots c_n \sin(n\omega t+\beta_n) \tag{3}$$

It is necessary when measuring the open-loop response of a system whose approximate loop transfer function is of the form $1/(p)(k_0+k_1p\ldots)$ to allow the open-loop input e to have a small constant value e_0; otherwise, because of unbalance and nonlinearity of the system, the output c will contain a term of the form qt in addition to the terms indicated in equation 3. The term qt will distort the output and will make it difficult to measure the desired frequency components.

For a linear system $c_2\ldots$ and c_n of equation 3 are all 0 and it has been customary to represent the gain of block G in the complex form

$$G(j\omega)=\frac{c_1}{e_1}e^{-j\theta} \tag{4}$$

The gain expressed by equation 4 has the same meaning for the fundamental components of e and c given in equations 2 and 3 when the system is nonlinear. In fact, it has more, for one can then consider the ratio c_1/e_1 and θ as functions of the frequency ω and of e_1 or c_1.

It is desirable to plot the open-loop frequency response data on paper with real and imaginary axes. Often $G(j\omega)$ or the inverse $G^{-1}(j\omega)$ is plotted directly, but in nonlinear systems a different approach is necessary. If e and the output c are as expressed by equations 2 and 3 respectively, the input signal r is

$$r=e+c=e_0+e_1 \sin(\omega t+\theta)+ c_0+c_1 \sin \omega t+c_2 \sin(2\omega t+\beta_2)\ldots \tag{5}$$

The representation of the open-loop frequency response data used in this paper is the fundamental component of the input signal r, equation 5, written in the complex form

$$R(j\omega)=e_1e^{j\theta}+c_1 \tag{6}$$

The information conveyed by this equation is certainly the same as that conveyed by the complex gain given by equation 4. In addition, the representation of $R(j\omega)$ given by equation 6 indicates directly the fundamental input amplitude and its phase with respect to the fundamental output phasor c_1. (Notice that equation 2 implies that the input contains harmonic terms as given by equation 5.)

It is necessary that the open-loop frequency response data be taken in an orderly fashion so that the maximum information will be conveyed by these data when plotted in the $R(j\omega)$ plane. The following procedure is recommended in determining and plotting these open-loop frequency response data. First a set of angular frequencies ω covering the frequency range of interest and a set of fundamental output amplitudes c_1 covering the amplitude range of the system output are chosen. Then the error amplitude and phase are determined experimentally or analytically, which will produce each of the chosen fundamental output amplitudes at each of the chosen frequencies. (The phase of the error is determined with respect to the funda-

---

Paper 53-253, recommended by the AIEE Feedback Control Systems Committee and approved by the AIEE Committee on Technical Operations for presentation at the AIEE Summer General Meeting, Atlantic City, N. J., June 15–19, 1953. Manuscript submitted October 27, 1952; made available for printing May 12, 1953.

R. L. Cosgriff is with Ohio State University, Columbus, Ohio.

This paper is based upon work done at the Antenna Laboratory of the Electrical Engineering Department, Ohio State University, supported in part by a contract between the Wright Air Development Center and the Ohio State University Research Foundation. The author is indebted to the many who have helped make the paper possible, in particular, to Professors C. E. Warren and V. H. Rumsey, and to R. Fouty and J. Bacon.

c_1 \ ω	0	0.25	0.5	1.0	1.5	2.0	3.0
1.635	1.635 $\angle 180°$	1.70 $\angle 173.5°$	1.87 $\angle 176.56°$	2.45 $\angle 180°$	3.8 $\angle 203.8°$	6.93 $\angle 225°$	21.6 $\angle 245.4°$
1.5	1.268 $\angle 180°$	0.133 $\angle 172.4°$	1.48 $\angle 169.1°$	2.02 $\angle 180°$	3.28 $\angle 205.4°$	6.2 $\angle 226.6°$	19.8 $\angle 246°$
1.155	0.578 $\angle 180°$	0.630 $\angle 167.5°$	0.753 $\angle 163.3°$	1.155 $\angle 180°$	2.175 $\angle 210°$	3.78 $\angle 230.3°$	15.05 $\angle 247.4°$
0.5	0.047 $\angle 180°$	0.0859 $\angle 136.9°$	0.139 $\angle 141.8°$	0.297 $\angle 180°$	0.769 $\angle 217.6°$	1.83 $\angle 235°$	6.43 $\angle 249.1°$
0.25	0.00586 $\angle 180°$	0.0325 $\angle 115°$	0.060 $\angle 128.4°$	0.131 $\angle 180°$	0.371 $\angle 219.3°$	0.904 $\angle 236°$	3.21 $\angle 249.4°$

Fig. 2. Tabulation of phase and magnitude of error for various frequencies and fundamental output amplitudes

mental component of the output.) Each of these values of $E(j\omega)$, both amplitude and phase, can then be recorded in a table of the form shown in Fig. 2. Each column of this table corresponds to one of the chosen frequencies, and each row to one of the fundamental output amplitudes. After the open-loop response data have been obtained, these data can be recorded as points in the $R(j\omega)$ plane. A locus is then drawn through each set of points in the $R(j\omega)$ plot obtained for c_1 constant. The set of loci so obtained is called the constant amplitude or c_1 loci. A second set of loci can be drawn connecting points in the $R(j\omega)$ plane determined at each of the chosen frequencies. These loci are called the constant frequency or ω loci.

The open-loop frequency response data of a small instrument servo employing a 2-phase 400-cycle induction motor as an output device have been determined, and the c_1 loci and the ω loci of this servo are shown in the $R(j\omega)$ plane in Fig. 3. To illustrate the meaning of this $R(j\omega)$ plot, consider point P_2 in Fig. 3. This point, lying on the 1-cycle-per-second locus, has the polar co-ordinates of 1.33 units radius and an angular displacement of 56 degrees, or 0.977 radian from the horizontal or real axis. This indicates that the fundamental input signal represented by P_2 is of the form 1.33 sin $(6.28t+0.977)$. The amplitude of the fundamental output is estimated as 1.34, since P_2 lies between the 1.25 and the 1.50 loci; and for this reason, the fundamental output is of the form 1.34 sin $6.28t$.

Use of Linear Filters to Improve the Response of Nonlinear Systems

Considerable material is available concerning methods for improving the response of linear systems by the introduction of linear filters in the forward loop or error amplifier section of the servo system. The same techniques can be used in the case of nonlinear servomechanisms. For example, consider the block diagram shown in Fig. 4. This system is similar to that shown in Fig. 1 except that a linear filter F is in the forward loop. Observe that a set of values of $E'(j\omega)$, the input signal to block G, which produces the desired set of fundamental output amplitudes at the chosen frequencies, is the open-loop frequency response data without filter F. The values of $E(j\omega)$ which will produce the same set of output components as $E'(j\omega)$ can be found by dividing the set of values of $E'(j\omega)$ by the gain of filter F. Each value of $E(j\omega)$ for the table similar to that shown in Fig. 2 can be obtained for the system with filter F by dividing the $E(j\omega)$ term in the corresponding position of the table for the system without filter F by the gain of filter F.

The $R(j\omega)$ plot can also be modified in a like manner. To illustrate this process, consider the case where F, which has a gain of two, is inserted in a system whose original $c_1=1$ locus is as shown by the solid curve in Fig. 5. First observe that the input phasor from the origin to any point on the $c_1=1$ locus is the sum of two phasors, namely the output c_1 phasor along the real axis, and the error or $e_1\epsilon^{j\theta}$ phasor extending from the end of the c_1 phasor to the $c_1=1$ locus. Points on the new $c_1=1$ locus can therefore be determined by dividing the original error or $e_1\epsilon^{j\theta}$ phasors

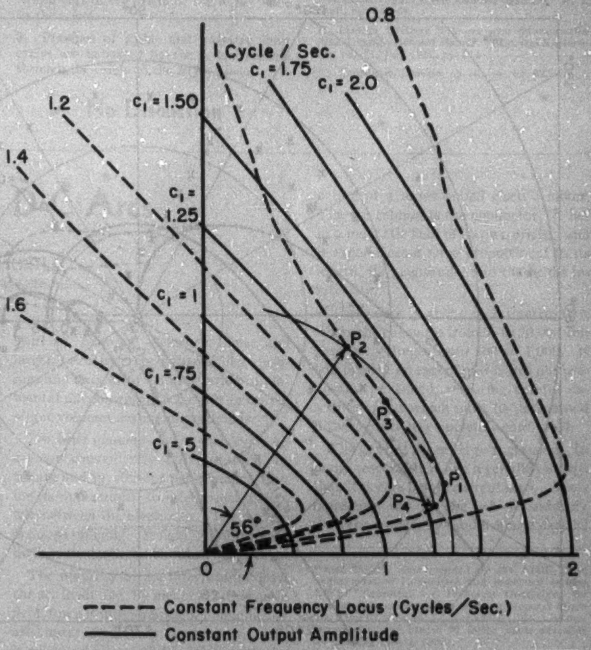

Fig. 3. Complex representation of response of a typical servo system

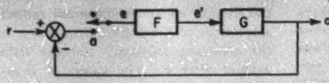

Fig. 4. Nonlinear system with a linear filter F for improving the response

by two and drawing the new $c_1=1$ locus through the points so obtained, as is shown in Fig. 5.

Stability

Nyquist's criterion can be used to determine the system stability by observing the enclosures of the origin by a small c_1 locus. For example, in Fig. 6 the $c_1=0.25$ locus has been drawn (part of the locus is shown by the crosses). Notice that this locus encloses the origin twice, indicating that the system has an unstable equilibrium point. This criterion can be justified only for nonlinear systems which have analytic equations of motion,[8] namely, systems which do not have backlash or static and coulomb friction; but it appears that it can be used with systems which do not have analytic equations of motion as well.

Notice also that the $c_1=1.155$ and the $\omega=1$ loci cross on the origin. This indicates that an output fundamental $1.155 \sin t$ can exist when the fundamental input $R(j\omega)$ is 0. As the input signal contains harmonics, terms of the form $r_3 \sin (2\omega t+\phi)$, etc., this type of response is classified as a subharmonic response. Actually the system has a stable limit cycle, and the term $1.155 \sin t$ very closely approximates the fundamental term of the output in both amplitude and frequency when the system is in this limit cycle state. A second set of loci, the $c_1=1.635$ and $\omega=0$, lies on the origin. This second point corresponds to a second singular point, as the frequency ω is zero.

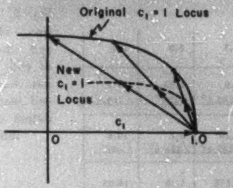

Fig. 5. Modification of measured response after inserting a linear filter F of gain two

Response Hysteresis (Jump Phenomenon)

In testing the closed loop response of a servo using a 2-phase induction motor as the power output device, it has been observed that the amplitude response depends upon the past history of the input signal. This phenomenon is very noticeable if the frequency is held constant and the input amplitude is varied. This characteristic of nonlinear systems can be best described with the aid of Fig. 7. If the fundamental input amplitude r_1 is increased, the fundamental output amplitude c_1 increases until r_1 reaches r_m. If r_1 becomes larger than r_m, then c_1 jumps to the lower curve. If r_1 is initially larger than r_m and then is decreased, it will be found that the jump between the two curves does not occur until r_1 is less than r_m. This characteristic is often called

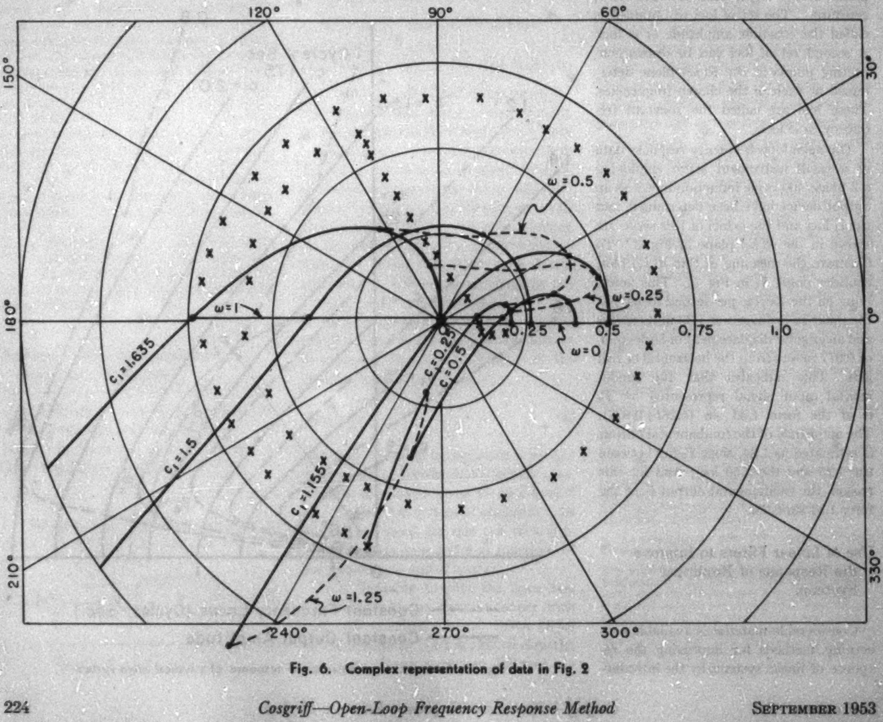

Fig. 6. Complex representation of data in Fig. 2

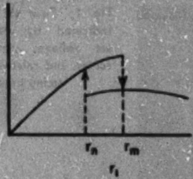

Fig. 7. Fundamental output amplitude as a function of the fundamental input amplitude for a system having response hysteresis

jump phenomenon, because of the jump in the steady-state response. However, a definite and often a very gradual transition occurs between the two states. For this reason this phenomenon is called response hysteresis by the author.

The presence of this phenomenon can be determined from the $R(j\omega)$ plot, Fig. 3. Consider an input with a frequency of 1 cycle per second whose magnitude is slowly increased until the state of the system is determined by point P_1. There is no point near P_1 on the 1-cycle-per-second locus corresponding to a radius greater than 1.33, the radius of P_1, except in the neighborhood of point P_2. For this reason the first jump of the hysteresis cycle occurs when the input amplitude becomes larger than 1.33. As the input magnitude is decreased from above 1.33, a second transition occurs when the input amplitude becomes less than the radius to point P_3, as there is no point near P_3 with a radius less than that of P_3. The operation of the system is then described by locating the point P_4 which has the same radius as P_3 on the 1 cycle-per-second locus. This completes the hysteresis cycle. The points P_1 and P_3 occur wherever the frequency locus is tangent to circles of constant input magnitude. For this servo the most prominent characteristic of this hysteresis cycle is the change of phase of the output with respect to the input.

Conclusion

The following properties of the $R(j\omega)$ representation of nonlinear servomechanisms can be utilized when the error signal consists of only a fundamental component (the d-c term in the error signal is usually sufficiently small that it can be neglected):

1. The closed-loop fundamental frequency response is indicated directly by the $R(j\omega)$ plot.

2. Stability can be determined by the encirclements of the origin of the $R(j\omega)$ plane by the c_1 loci.

3. Presence of stable and unstable limit cycles are indicated by the c_1 loci passing through the origin of the $R(j\omega)$ plane.

4. The restriction on the harmonic components of the error signals justifies a synthesis procedure for compensating networks, in that the open-loop frequency response can be determined from the open-loop frequency response of the servo without the filter and the transfer function of the filter.

5. Presence of response hysteresis is indicated by circles about the origin of the $R(j\omega)$ plane becoming tangent to the constant frequency or ω loci.

References

1. Non-Linear Mechanics (book) **N. Minorsky.** Edwards Brothers, Inc., Ann Arbor, Mich., 1947, pp. 233–71.

2. A Frequency Response Method for Analyzing and Synthesizing Contactor Servomechanisms, **Ralph J. Kochenburger.** *AIEE Transactions*, vol. 69, pt. I, 1950, pp. 270–84.

3. Theory of Relay Servomechanisms, **J. R. Dutilh.** *L'Onde Electrique*, Paris, France, Oct. 1950, pp. 438–45.

4. Sinusoidal Analysis of Feedback-Control Systems Containing Nonlinear Elements, **E. Calvin Johnson.** *AIEE Transactions*, vol. 71, pt. I, July 1952, pp. 169–81.

5. Theory of Oscillations (book), **A. A. Andronow, C. E. Chaikin.** English Language edition, Princeton University Press, Princeton, N. J., 1949, pp. 182–83.

6. Automatic and Manual Control (book), **D. A. Tustin.** Academic Press, Inc., New York, N. Y., 1951, "An Introduction to the Analysis of Non-linear Closed Cycle Control Systems," **W. E. Scott**, pp. 249–61.

7. Linear Circuit Theory and Servomechanism Design, **Howard Hamer.** *Electrical Engineering*, vol. 71, July 1952, pp. 614–15.

8. **Andronow, Chaikin,** *op. cit.*, pp. 61, 62.

No Discussion

Controlling D-C Arcs

R. L. HURTLE
ASSOCIATE MEMBER AIEE

Synopsis: A method of controlling d-c power arcs is presented, with the emphasis on eliminating retrogressive motion of the arc. Stills from motion pictures of power arc interruptions in a normal atmosphere present the fundamental nature of arc retrogression. The various characteristics of an arc which cause such motion are detailed, and countered by simple design principles. Control of the arc reduces erosion of the metal parts, gives better protection to the circuit, and reduces total arcing time.

AFTER nearly 60 years of intense study by learned and persistent scientists, the power arc in a gas is by no means completely understood. This is not to be wondered at in view of its 4,000 to 8,000 K temperature; its chaotic swirl of photons, electrons, ions, and larger particles; its lightninglike dashings and twistings; and its varied fundamental phenomena which occur in microscopic volumes during microseconds.

For brief moments twice each cycle an a-c arc conveniently terminates its intricate and mysterious performance, giving an opportunity to interpose a dielectric between the electrodes. The d-c arc is not so obliging. It fights hard from its birth to its death, and hardest at death.

The majority of d-c interrupters draw the arc in air and, by means of a magnetic field, force it into a refractory chamber or arc chute. Ordinarily the magnetic field is produced from a coil in series with the arc itself. Magnetic blowout is like the action of a series-wound electric motor. The arc column is the conductor; it lies in a magnetic field of its own origin; and it experiences a force proportional to its length, its magnitude, and the field's intensity.

This paper is about such interrupters, where the current is from 50 to 20,000 amperes at voltages from 100 to 1,000. It will present an aspect of d-c arcs not previously published, requiring careful description, but which must be understood if the arc is to be completely controlled.

The general aspect is retrogression. In many respects it is like a restrike, except that it occurs before current zero. A retrogressing arc is one which suddenly shortens, usually by establishing a parallel

---

Paper 53-305, recommended by the AIEE Land Transportation Committee and approved by the AIEE Committee on Technical Operations for presentation at the AIEE Summer General Meeting, Atlantic City, N. J., June 15–19, 1953. Manuscript submitted March 20, 1953; made available for printing May 1, 1953.

R. L. Hurtle is with the General Electric Company, Erie, Pa.

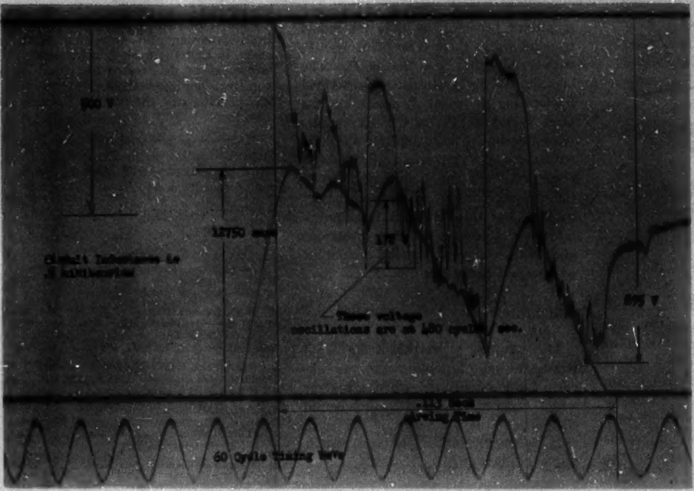

Fig. 1. Poor arc control, indicated by oscillating arc voltage, current resurges, and relatively long arcing time

arc behind the main arc. Ordinarily the parallel arc is struck from the existing cathode melt to an anode melt recently vacated by the anode end of the arc. Since the shorter of the two parallel arcs offers the lower resistance, the outer arc rapidly subsides. At the very least, retrogressions produce excessive erosion of contacts, of arc runners, and of arc chutes by sweeping across still-molten surfaces. The melts are blasted clean by the explosive action of the arc. On those arc chutes whose surfaces do not glaze, the erosion is by means of thermal shock. An improperly controlled arc can set up oscillating voltages which may feed a resonant part of the circuit which is external to the interrupter, and produce failure there by voltage breakdown.* Note the oscillating voltages appearing in Fig. 1. Excessive retrogression causes such frequent retracking along arc-running surfaces that the ability of these surfaces further to absorb thermal energy is diminished. When their thermal reservoirs are filled, the melts become excessively large in area. These, in turn, produce a breakdown of the gaseous dielectric, provide high stability of both arc termini, and a failure results. Not all failures, unfortunately, are precipitated in such fashion. An interruption where the retrogressions resulted in current resurges is recorded in Fig. 1. Resurges of such magnitude have long been observed on oscillographic records of arcs. J. D. Cobine[1] describes a form of retrogression where the arc shortens by reignition across the shortest gap length.

New Aspect of Retrogressions

The particular retrogressions not identified by published information and not generally recognized are those which do not result in a change in the existing rate of current decay. In many interruptions they precede those which do. If eliminated by proper arc control, the more apparent and spectacular aberrations represented by Fig. 1 usually will be prevented. In contrast to Fig. 1, Fig. 2 records an interruption where the retrogressions, if any, were not detected by the current-tracing element of the oscillograph. (An oscillographic, voltage-tracing element will record variations in volt-

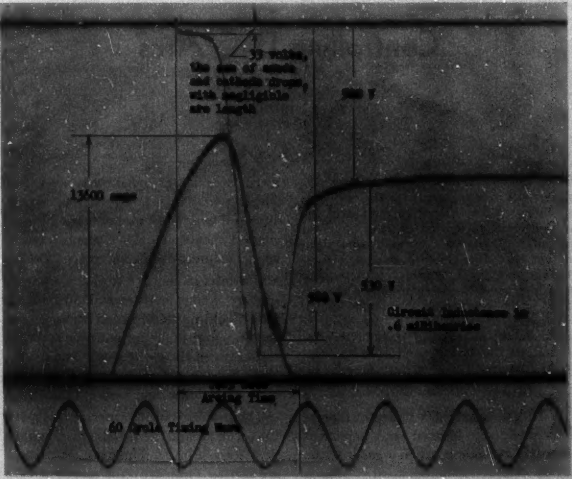

Fig. 2. Good arc control, indicated by relatively constant arc voltage, no observable current resurges, and relatively short arcing time

---

*This possibility was brought to the writer's attention by F. H. Catlin, General Electric Company, Erie, Pa.

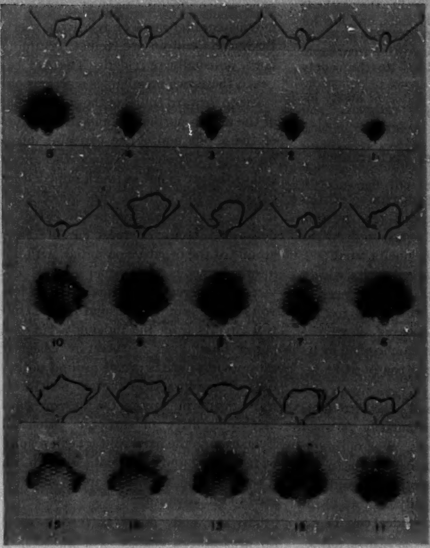

Fig. 3. Stills from a high-speed movie of an arc interruption. The frames were taken at approximately 2,000 per second. The arc duration was 1/2 cycle. Time is measured from right to left. The right-hand surface is fixed, and was positive during this interruption. The diamond-shaped lattice is expanded steel used as a magnetic pole piece on the camera side. The arc chute side on the camera side is a piece of ordinary window glass. In the last frame the arc length is 12 inches. For this interruption the line voltage was 100, and the peak amperes 1,450

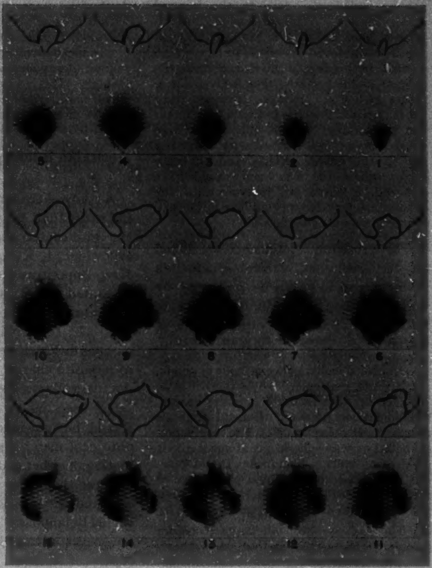

Fig. 4. Stills from a high-speed movie of an arc interruption. The conditions for this interruption differ from those of Fig. 3 only in having the fixed, or right-hand, surface negative. The peak amperes were 1,386

age, but cannot differentiate between normal changes in arc voltage and those resulting from retrogressions.) One would say that this arc was almost perfectly controlled. However, the oscillograms taken of the interruptions represented by Figs. 3 through 6[†] are, like those in Fig. 2, devoid of detectable retrogressions, yet all of the photographs except Fig. 4 clearly show them. Note Fig. 3, where the arc in frame 9 is in the process of striking toward the anode to provide a parallel arc. In frame 10 the outer arc has collapsed and the shorter one is about one-seventh as long as the main arc was in frame 9. In spite of the decreased arc length, the interrupter maintained the current at essentially a constant rate of decay. Frame 4 of Fig. 5 portrays a similar retrogression.

Often the frame showing a retrogressed arc will bear a remarkable resemblance to a previous frame. This is strikingly true in Fig. 5, where the arc is nearly identical in frames 2 and 4, and again in frames 7 and 10. In all frames in Fig. 5 the cathode, or left-hand end, did not travel well. The cathode melt thus became a danger point. Even though the anode end travelled well, by its stepping nature it left anode melts in close proximity to the cathode melt, thus affording the arc an opportunity to retrogress. In studying Fig. 3 through 6 one should keep in mind that although they are titled high-speed movie, from the arc's viewpoint they are strictly low-speed. They are but brief and widely separated glimpses of the arc's incandescent halo as it twists and thrashes about.

Arc Characteristics

Before discussing retrogressions further, a listing of some arc characteristics is in order:

1. On a continuous metal surface the cathode end of the arc moves readily and smoothly. This has been observed in various departments of the General Electric Company, and a paper on the subject appeared in 1949.[2]

2. On a continuous metal surface the anode end of the arc moves forward in steps.[3]

3. Discontinuities in a metal surface affect the travel of arc ends. For the cathode end to cross a discontinuity it must pause until the arc column impinges on the path ahead and forms a new melt. When the new melt develops sufficient boil of metal vapor, the gaseous mixture adjacent to it ionizes sufficiently to maintain an arc. The current path then shifts from the old melt to the new one. The cathode end is then free to travel forward. Since the anode end naturally travels in steps, its progress is not greatly impeded by a discontinuity unless either or both of the following occur: 1. Turbulence resulting from the change in path may prevent the arc column from

---

[†] The line diagrams above each frame show the shape of the arc-running surfaces and the location of the arc. The interrupter used in Figs. 3 through 6 has a fixed copper contact $3^3/_8$ inches long. Its outer end makes an interference fit against a bronze arc runner. The moving contact is $1^1/_8$ inches long. When at full gap, its outer end is $^1/_4$ inch from a brass arc runner. The arcing chamber has a volume of 45 cubic inches. The glass arc chute side was not glazed by interruptions up to and including the magnitude of that in Fig. 6. Beyond this level, however, the glass glazed or shattered, which of course would not permit normal arc interruption. The interrupter used in Fig. 2 is the same device described except for the arc chute, the volume of which remained the same. The interrupter used in Fig. 1 is a different device, but has the same size of arc chute.

coming sufficiently close to the forward anode surface. A forward anode melt is formed when the electric gradient between the arc column and the anode surface is high enough to produce a discharge from the column to the surface. For a given interrupter at a given voltage, therefore, there exists a critical distance between the column and the surface, beyond which a discharge will not occur; 2. If the discontinuity is a gap in the anode surface, and this gap occurs where the new melt would have occurred, a pause will prevail until the column has traveled on to where it can discharge to an anode surface.

The preceding statements are based on the nature of current conduction in metal and in gases, as presented by various authorities, and on the tracking records left by arcs on various kinds of surfaces.

4. Uncooled melts, either cathode or anode, are hazards, particularly when there is little distance between melts of opposite charge. The ionization potential of metal atoms is about 8 electron volts. The ionization potential of atmospheric gas atoms is about 14 electron volts. This means that a gaseous region containing a high percentage of metal atoms will ionize much more readily than a normal atmospheric gas.

5. The voltage drop in an arc occurs principally in the column, from which therefore most of its energy must be dissipated. Authorities generally credit the cathode with a drop of about 20 volts, and less for the anode. Note the 33-volt drop in Fig. 2.

6. Inductive voltages resulting from rapid current decay are additive to the supply voltage. This is a well-known phenomenon, which makes the interruption of highly inductive circuits difficult.

Desirable Interrupter Performance

A study of the foregoing characteristics indicates that to prevent retrogression the interrupter should accomplish the following: 1. Keep the melts small; 2. Keep oppositively charged melts widely separated; 3. Between close surfaces of opposite charge keep the gases free of ions; 4. To avoid breaking down the gaseous dielectric between uncooled melts of opposite charge, keep the positive inductive voltages low.

To keep melts small, the arc ends should be moved continuously forward onto cool metal surfaces. For optimum motion of either end of the arc, the metal surfaces should be smooth and continuous, and the gas flow adjacent to them should be laminar. These ideal conditions are never attained in practical interrupters. At least one of the contacts must move. For mechanical reasons the moving contact must be relatively short. Beyond its end an arc runner, or arcing horn, is usually provided. The gap between these two members is a serious obstacle to forward travel of the cathode end of the arc, in particular, and slows travel of the anode end. The gap also introduces gas turbulence. Since the anode end of the arc is not as much impeded by gaps as is the cathode end, making the moving contact positive in the circuit is desirable. However, most circuits have ground at the negative potential, with the interlocks, coils, and other control devices, as differentiated from power, a few volts above ground. Insulating the control circuits from the moving parts of a power interrupter is therefore easier if those moving parts are at ground potential. These practical factors nearly always result in having the moving contact at negative, or cathodic, potential. Even though the fixed contact can readily be made long and continuous, seldom can it be made negative in the circuit and thus used to full advantage.

The arc ends move better on some metals than on others. Fortunately, of the commercial metals, copper is the best

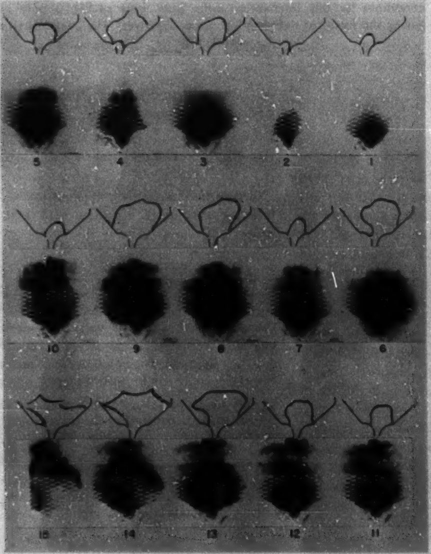

Fig. 5. Stills from a high-speed movie of an arc interruption. The conditions for this interruption differ from those of Fig. 3 only in line voltage, which was 150. The peak amperes were 2,220

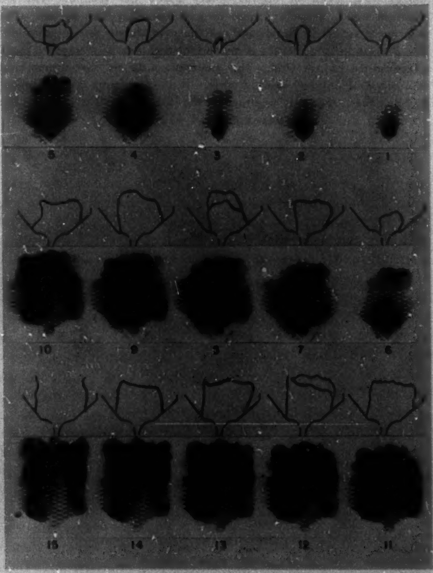

Fig. 6. Stills from a high-speed movie of an arc interruption. The conditions for this interruption differ from those of Fig. 3 only in line voltage, which was 200, and in having the fixed, or right-hand, surface negative. The peak amperes were 2,930

for good arc tracking. Its excellent thermal conductivity also aids in keeping melts small. Brasses and bronzes are frequently used as arc runners. They are next best in tracking quality and have the advantage of greater strength and economy.

Keeping oppositely charged melts widely separated requires that the contact gap be large and that the moving contact assembly does not bounce partially closed. Ordinarily, the moving assembly and its actuater will provide low initial velocity and high final velocity, while the reverse is required if the initial melts are to be kept small and closing bounces are to be eliminated. The greatest hazard, however, is usually at the ends of the contacts, particularly when they are short. Although rigorous proof of this statement by photographic evidence is prevented by the arc's halo and its extreme speed, yet most of the photographed retrogressions occurred in the region of the contact tips. Also, on power interrupters, erosion is generally pronounced at the contact tips, indicating large melts.

Since in the arc's travelling the first large melts occur at the contact tips, contacts should be so contoured that their surfaces diverge at a wide angle. The fixed contact should have at least twice the length of the moving contact, so that its end will be far from the opposite potential. Both contacts should be provided with arc runners which will readily take transfer of the arc. For the fixed contact, butt joints are possible. For the moving contact the ideal arrangement would be for the runner to take the arc from the moving contact in a streamline gas flow at the instant the arc reaches its end. Unfortunately, the position of the moving contact at this instant is difficult to determine. If the horn projects far into the gas flow, turbulence may carry the arc behind the runner, and control is lost. A reasonable compromise must be made, depending upon contact opening velocity, armature rigidity, and contact contour.

Keeping arc chute gases free of ions, where surfaces of opposite potential are near each other, requires a continuous flow of air. Because of space and in the interest of economy of materials, arc chutes usually incorporate arc splitters, arc baffles, arc-quenching grids, or rough-surfaced sides. These promote turbulence, which is desirable in dissipating arc energy. When the turbulence is excessive, however, volumes of ionized gas may be ejected backward. The explosive force of high-capacity interruptions will cause the arc to recoil, if there is insufficient space for it to travel outward. Turbulence in the first third of the arc chute is undesirable because it produces erratic running of the arc ends.

Interrupters which are enclosed except for their arc chute openings may contain insufficient air. If the interruption is protracted, cooling of the gases within the main portion of the enclosure will result in a partial vacuum. The resulting inrush of air through the arc chute opening will carry ionized gases toward the contacts, and may have sufficient force to carry the arc there as well.

Keeping positive inductive voltages low generally requires that the arc be elongated slowly. Arc splitters, arc baffles, arc-quenching grids, or arc chute sides when designed for sudden or extreme turbulence can provide too rapid cooling. Cooling results in deionization, which is a loss of conductivity and produces a drop in current. The decay of the current reacts with the circuit inductance to produce positive voltages. Although the actual change in current may be negligible, if the rate of change is high, the induced voltage will be high. These voltages can easily be sufficient to produce breakdown of the gaseous dielectric between uncooled melts which are not widely separated. Larger voltages produce breakdown between uncooled cathode melts and cooled anode surfaces.

Most interrupters produce large inductive voltages from too rapid current decay just prior to arc extinction. As the arc current approaches zero the arc suddenly loses its ionizing ability, and collapses. This collapse produces a rate of current decay greatly in excess of the prior rate. Where the circuit is inductive, large voltages are produced, enabling the arc with its dying gasp to reignite across hazard zones. To prevent this, just prior to its extinction the arc should not be elongated further. If also at this time the cathode and anode ends of the arc are stabilized upon large metal bosses at the ends of the arc runners, the resultant ionization will enable the arc to decay very slowly.

Excessive magnetic blowout force will produce large inductive voltages. In the ignition region the force cannot be too high, because there it results only in arc movement, not in current decay. In Fig. 2 note that for over one-third of the arc duration the current was increasing. The magnetic blowout field should taper off in the main body of the chute, and should be close to zero at the chute opening. To prevent high currents from producing forces proportional to the current squared, a portion of the steel magnetic circuit should saturate at a current value just above the interrupter's continuous rating. This will provide maximum force on the arc when the device acts as a contactor or switch. There is little danger of retrogression in such duty, and the contacts will be saved from excessive erosion. When overloads or short circuits must be interrupted, the saturated portion of the magnetic circuit will decrease the tendency for too rapid elongation.

Design Details

The causes of retrogression can now be summarized, together with mitigating design features, bearing in mind that some of the arc's characteristics are admittedly unknown, and that the interrupter discussed is one which draws the arc in air and elongates it by means of magnetic force from a series coil.

Short metal surfaces promote retrogression by causing pauses in travel of the arc ends, particularly the cathode. To counteract, make the fixed contact quite long, and the entire tracking surface on the fixed side as continuous as possible. Make the moving contact as long as permitted by good mechanical design. Where possible, make the fixed contact negative in the circuit. Otherwise, locate the moving contact's horn close to the moving contact for a quick and streamline transfer of the arc from the end of the moving contact to the horn.

A slow separation of the moving contact from the fixed contact will delay initial motion of the arc. This will result in large melts, which are hazards, and excessive contact erosion will follow. Moreover, the interruption will be prolonged because of the copious metallic evaporation caused by the slow separation. An impact type of separation will provide high initial velocity. Triggering of tension springs is a more complicated but more effective way to obtain high initial velocity. The moving contact support must receive the opening force at its center of percussion or between there and the line of contact, or it will rotate in a closing motion during the armature opening.

A limber or a bouncing armature and contact assembly will result in a closing action of the moving contact. The assembly should be rigid in the plane of motion, and should have negligible bounce.

Ferrous or aluminum arc runners do not provide good tracking surfaces. In no design should an arc runner be of magnetic material, because of the short-circuiting effect on the magnetic blowout force. Copper and its alloys provide good tracking and small melts.

Parallel arcing surfaces result in too close proximity of melts of opposite charge. The contacts should diverge immediately beyond the ignition region. Beyond the contact ends an included angle of about 120 degrees is most desirable.

Barriers in the arc's path which produce high turbulence or arc recoil will result in retrogression because of the ionizing of the gaseous dielectric between uncooled melts of opposite charge. They should be placed well toward the opening, and should have sufficient space between them for the arc to escape.

Arc quenchers, whether of metal or not, which suddenly dissipate large quantities of energy from the arc, will produce dangerous inductive voltages. The energy dissipation should be gradual. If, in addition, the quenchers act as barriers they may have some of the faults listed in the foregoing.

Enclosed interrupters which have openings for ejection of arc gases will experience retrogression if they have small air storage or require long periods of time for interruption. Louvred sides will permit replacement air to enter the enclosure, or the arc must be interrupted before the internal gas cools.

Rapid decay of the arc current just prior to current zero will often induce excessive voltage. Stabilization of the arc ends just prior to current zero, and cessation of arc elongation will permit a gradual collapse of current which will not induce voltage.

In final and brief summary, the arc should be moved rapidly at first, slowly or not at all at the last, smoothly at all times, and its metal runners should be as continuous as possible. If handled in such fashion, it will retrogress infrequently, it will do minimum damage to the interrupter, and its circuit will be given excellent protection.

References

1. GASEOUS CONDUCTORS (book), J. D. Cobine. McGraw-Hill Book Company, Inc., New York, N. Y., 1941, p. 386.

2. CHARACTERISTICS OF ARCS BETWEEN MOVING ELECTRODES, W. B. Kouwenhoven, T. B. Jones. *Electrical Engineering*, vol. 68, Oct. 1949, p. 834.

◆

Discussion

C. C. Whittaker (Westinghouse Electric Corporation, East Pittsburgh, Pa.): A paper on a subject like this can properly be written every few years because of its fundamental nature. Some of the information given in previous articles must of necessity be repeated, but it seems that periodically there is additional knowledge obtained to make instructive reading, especially for many of the younger engineers.

I would raise one question as to the procedure of the tests shown in Figs. 3 to 6. Here the switch undergoing test had on one side a solid iron pole piece, and on the camera side, an expanded metal pole piece, through the interstices of which the photographs were obtained. It would seem that the expanded metal would offer in the order of ten times the reluctance, so that the resulting arc-moving field would not be straight across the arc gap, which would thus cause the arc to be forced to one side of the arc box.

If further tests are contemplated, we suggest the use of a switch having an air-core blowout coil. Such a switch is shown in Fig. 7 with its arc box removed. For a number of test shots, say 25 to 30, the arc box is not required. With the arc-moving flux passing straight through the two blowout coils, as is the case with this switch design, the arc is forced straight forward between the coils.

Within the switch capacity, the arc itself is always extinguished within the coil area although luminous gases will be expelled beyond the coil boundary. Because the arc path is much more brilliant than the gases, these may be filtered out, leaving a definite arc path. Thus, instead of having to interpret a more or less blurred photograph, you would have a clear-cut arc path showing a definite arc shape from one arc terminal to the other.

R. L. Hurtle: Mr. Whittaker's discussion has two salient points: 1. The pole-piece design distorted the magnetic blowout field, thus forcing the arc to one side of the chute; 2. The arc better could be photographed if the magnetic field were derived from air-core blowout coils around the arc chute.

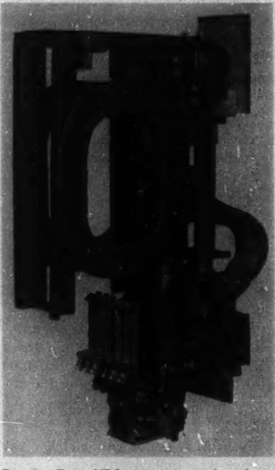

Fig. 7. Type UPC-525 unit switch with arc box removed

Because of fringing outward from the magnetomotive source, the magnetic field in an arc chute is always curved. The field is perpendicular to the chute through only one plane of space. If the chute is symmetrical on each side of its midplane, then the field will be perpendicular at that plane and distorted on each side. For practical purposes, then, the arc is always magnetically thrust toward one side or the other. The asymmetry of the arc chute used in the tests under discussion displaced the plane away from the glass side so that it lay at about the 0.6 point. The effect upon interruption characteristics was probably minor, but an understanding of such details is important. I appreciate Mr Whittaker's presentation of the improvement in technique.

The use of air-core blowout coils would permit clearer pictures. If the device being studied uses air-core coils around the arc chute as standard design, they should be used when interruptions are studied. However, the field resulting from such coils differs from that obtained from a steel-core coil in four important respects: 1. More turns are required for a given field intensity, resulting in greater inductive reactance; 2. External to the coils the field is reversed, in contrast to that of a steel-core coil where the field is in the same direction throughout the arc chute, with some fringing beyond the arc chute; 3. Between two separated air-core coils the field is radially symmetrical about their common axis, whereas in an arc chute using a steel-core coil the field is shaped as described above; 4. Within an air-core coil the density is uniform, in contrast with a tapering density in the field from a steel-core coil. I contend that the intensity should be high in the arc-ignition region, and should taper to a low value in that region of the arc chute where extinction is effected.

In summary, the principal reason for using a steel-core coil and an expanded pole piece was that this resulted in the least change from standard design which would permit photographing the arc.

Change in Resistance of Aircraft Current Limiters and Its Effect on Current Division in Networks

HENRY OMAN
MEMBER AIEE

Synopsis: When an aircraft current-limiter element is subject to sufficient overcurrent, it heats and finally melts, thus interrupting the circuit. The ohmic resistances of limiters at the instant before melting have been measured in the laboratory and have been found to be about 5.2 times the cold resistance, for copper-element limiters, and about 4.2 times the cold resistance for silver-element limiters. This increase in resistance results in an equalizing effect in parallel-connected limiters. A method is developed in this paper for predicting the extent of such current-equalization; in addition, it was discovered that the present method of predicting whether a limiter is damaged by a given current transient appears conservative.

IN ELECTRIC POWER systems, current limiters and fuses are used to protect wires, generating equipment, and switching equipment from excessive currents. They are also used to isolate faulted feeders and busses in appropriately designed multiple-path circuits:

1. Fuses are commonly used in industrial and domestic electric-power systems; a fuse has its fusible element made from a low-melting-point alloy.
2. Current limiters are used in aircraft electrical installations where an attempt is made to protect cable from overheating, generally under fault conditions. An aircraft limiter's fusible element is made from pure silver, copper, or copper alloy, all of which have high melting points. This high melting point gives the limiter greater insensitivity to ambient temperature.

The blowing-time versus current characteristics of aircraft limiters are well known.[1–4] The design procedure for coordinating the limiter blowing-time versus current curve with the damage characteristics of aircraft wire and cable has been well developed.[5] These two subjects are not within the scope of this paper.

A question which apparently had not been explored previously is this: What happens to the resistance of an aircraft limiter between the instant when fault current starts to flow, and the instant just before the limiter melts and clears the circuit? As the fusible element of the limiter heats, the resistance will obviously increase; but the amount of resistance increase was not known.

The next logical question is: What is the quantitative effect of this change in resistance on practical aircraft circuits? In previous tests of a mocked-up 120-volt d-c aircraft-electric system, it was discovered that parallel-connected limiters displayed an equalizing effect during the blowing period. The limiter that was supposed to blow first because of its lower resistance path, diverted some of its current to the parallel path.

Description of Aircraft Limiters

There are two types of limiters that are commonly used in aircraft, see Fig. 1. One has its fusible element and terminals stamped out of a sheet of copper of appropriate thickness. A refractory case is then built around the fusible element. This type of limiter is used on 28-volt d-c aircraft circuits and is available in various sizes in the range of 35 to 500 amperes. It is mounted by bolting to a bus or stud.

The other type of limiter has a fusible element fabricated from silver wire of appropriate diameter and length. The wire is welded to comparatively heavy terminals. The fusible element is surrounded with a glass tube, filled or coated on the inside with sand or glass cloth. The terminals are attached to the glass tube with a phenolic cap, which also serves as a grip and shield. This type of limiter is installed in clips. These silver-element limiters are used in 120 volt-to-ground circuits, and are available in various sizes in the current range of 5 to 100 amperes. Melting points for the fusible elements of limiters are 960.5 degrees centigrade for silver and 1,083 degrees centigrade for copper.

In studying limiters, one must keep in mind that limiter blowing is not a precise phenomenon, but rather a statistical phenomenon. To illustrate, limiters are at present considered acceptable if they will blow within a 12-per-cent band on the current-time characteristic. It naturally follows that there is no exact value for the resistance at the instant before melting.

Description of Laboratory Tests

The increase in resistance of limiter elements, from the time of initiation of current flow to the time of melting, was measured in the laboratory. The initial resistance was measured with a Kelvin bridge, and the final resistance was computed from current and voltage traces on oscillograms.

Current transients were recorded with an oscillograph galvanometer, connected directly to a suitable ammeter shunt. A direct-coupled amplifier had to be interposed between the limiter blades and the voltage-recording galvanometer, to protect the galvanometer from the open-circuit voltage across the blown limiter.

The amplifier showed signs of drift and nonlinearity. Nonlinearity effects were minimized by taking calibration oscillograms at expected test voltages; but drift could not be controlled. The error from these factors in some cases may have been as high as 7 to 10 per cent. However, enough oscillograms were taken to insure reasonably accurate results. Better amplifiers capable of driving the high-frequency-response oscillograph galvanometers have recently become available, and further tests could undoubtedly produce more accurate results.

Of the 28-volt copper-element limiters, 100 were blown and 64 useful oscillograms were obtained. Of the 208/120-volt silver-element limiters, 106 were blown and 62 useful oscillograms were obtained. In addition, 18 pairs of limiters were blown in parallel to verify experimentally the equalizing effect of parallel limiters.

Figs. 2 and 3 are typical oscillograms of the voltage and current in limiters during blowing. Figs. 4 and 5 show the ratios of premelting resistance to cold resistance of copper- and silver-element limiters, for various blowing times.

On the basis of these data, the ratios of premelting resistance to cold resistance have been determined to be, approximately:

1. 5.2 for copper-element 28-volt limiters;
2. 4.2 for silver-element 208/120-volt limiters.

It will be observed that the test results

Paper 53-272, recommended by the AIEE Air Transportation Committee and approved by the AIEE Committee on Technical Operations for presentation at the AIEE Summer General Meeting, Atlantic City, N. J., June 15–19, 1953. Manuscript submitted October 24, 1952; made available for printing April 20, 1953.

HENRY OMAN is with the Boeing Airplane Company, Seattle, Wash.

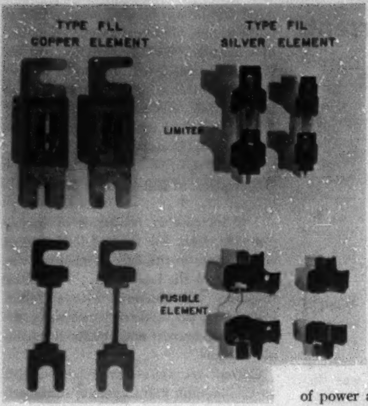

Fig. 1 (left). Types of current limiters used in aircraft. Left, for 28-volt power circuits; right, for 208/120-volt power circuits

produced a pattern of preblowing resistances, from which the values of 4.2 for silver-element limiters and 5.2 for copper-element limiters were picked. It must be kept in mind that these figures are not precise values, but rather, useful approximations. Further research could establish more precise values, and also could result in an understanding of the relation of this premelting resistance to blowing time.

It was originally expected that this change in resistance of a limiter might cause appreciable change in the current flowing through a circuit. However, tests and analyses indicate that, in practically all overloads and faults, circuit components other than limiters will offer the major portion of resistance. For example, Table I shows the maximum sustained fault currents expected in two types of airplane electric systems. An actual airplane fault will, in all probability, involve much smaller limiter voltage drops. Consequently, all limiter computations in this paper are based on constant total current.

Analysis of Limiter Resistance During Blowing

If a limiter blows in less than 0.1 second, the element does not lose any appreciable amount of heat through conduction, radiation, or convection.[1] Therefore, all the heat generated by the passage of current through the resistance of the limiter element is converted into increased temperature, up to the point where fusion starts taking place.

When the limiter element starts to melt, the metallic circuit is broken, an arc is formed, and relatively large amounts of power are released in the arc voltage drop. After that, the circuit is usually cleared in a relatively short time. In the analysis of blowing-time versus current characteristics of limiters, it has been found that any correction for the heat of fusion brings about less agreement between theoretical and experimental results.[1] In any event, the change in resistance of a limiter after the metallic path is broken is not within the scope of this paper.

If the blowing time is greater than 0.1 second, then there may be appreciable heat dissipated from the limiter element. If the blowing time is long, say many seconds, then only a small part of the total heat generated will go toward heating the element to its melting temperature. Thus, it would be extremely difficult to make a general mathematical analysis of the resistance of a slow-blowing limiter. Fortunately, as will be seen, a parallel circuit that is safe from an equalization standpoint with fast-blowing limiters, will be even safer if the limiters blow slowly.

Thus, the desired practical results can be accomplished by the use of an expression which will give the value of limiter resistance as a function of time for the quick-blowing condition. In deriving such an expression, two assumptions are made:

1. That the limiter blows in less than 0.1 second;
2. That constant current flows through the limiter.

The expression for the temperature rise of copper is

$$\text{Temperature rise, degrees centigrade} = \frac{0.018 \times \text{watt-seconds}}{\text{volume, cubic inches}} = \frac{0.018 I^2 Rt}{\text{cubic inches}}$$

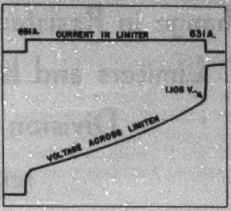

Fig. 2. Oscillogram showing voltage drop across a 200-ampere 28-volt copper-element limiter during blowing. The blowing time was 0.99 second

or

$$\Delta T = pRt$$

where

ΔT = temperature rise, degrees centigrade
$p = \dfrac{0.018 I^2}{\text{cubic inches}}$
R = resistance of element
t = time, seconds

The expression for the resistance change in a conductor when it heats is

$$R = R_0[1 + \alpha(T - T_0)]$$

where

R = resistance at temperature T
R_0 = resistance at initial temperature
T = final temperature
T_0 = initial temperature
α = thermal resistance coefficient

Revising

$$R = R_0 + R_0\alpha T - R_0\alpha T_0$$

Let $b = R_0\alpha$ and $a = R_0 - bT_0$

$$R = a + bT$$

In a given limiter having a constant current passing through it, the variables will be time, temperature, and resistance

$$\Delta T = pR\Delta t$$

Substituting

$$\Delta T = p\Delta t\,(a + bT)$$

$$\frac{dT}{a + bT} = p\,dt$$

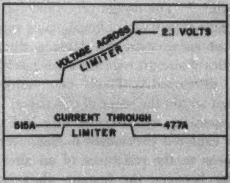

Fig. 3. Oscillogram showing voltage drop across a 40-ampere 208/120-volt silver-element limiter during blowing. The blowing time was 0.043 second

Fig. 4. Resistance at instant before melting of 28-volt copper-element limiters

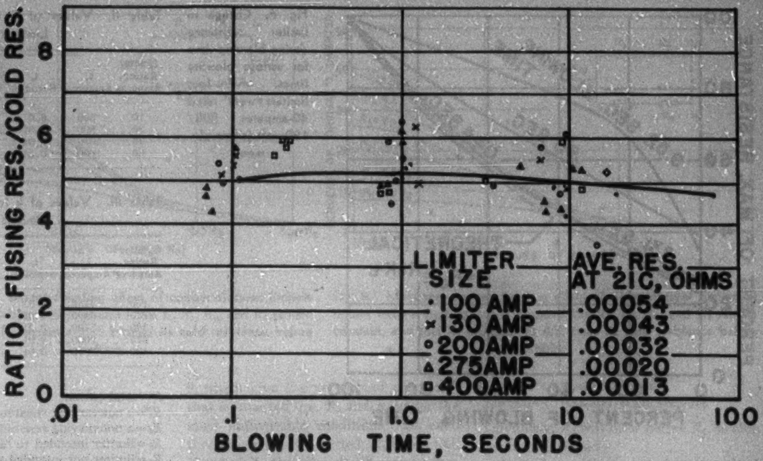

Fig. 5. Resistance at instant before melting of 208/120-volt silver-element limiters

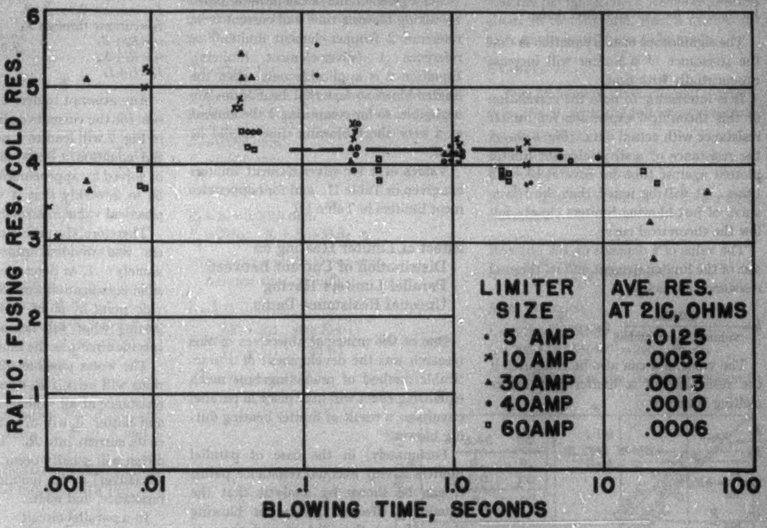

Integrating

$$\int \frac{dT}{a+bT} = \int p\,dt$$

$$\frac{1}{b}\log(a+bT) = pt + C$$

$$a+bT = \epsilon^{bpt+bC}$$

$$T = \frac{\epsilon^{bpt+bC}-a}{b} = \frac{\epsilon^{bpt}\epsilon^{bC}-a}{b}$$

At

$t=0, \quad T=T_0$

$$T_0 = \frac{\epsilon^0\epsilon^{bC}-a}{b} = \frac{\epsilon^{bC}-a}{b}$$

$$\epsilon^{bC} = bT_0 + a \quad a = R_0 - bT_0$$

$$\epsilon^{bC} = bT_0 + R_0 - bT_0 = R_0$$

Substituting to eliminate the constant of integration

$$T = \frac{R_0\epsilon^{bpt}-a}{b}$$

However

$$R = a + bT$$

Therefore

$$R = a + b\left[\frac{R_0\epsilon^{bpt}-a}{b}\right]$$

$$= a + R_0\epsilon^{bpt} - a = R_0\epsilon^{bpt}$$

$$= R_0\epsilon^{R_0\alpha pt} \qquad (1)$$

In conclusion

$$R_t = R_0\epsilon^{kR_0I^2t} \qquad (2)$$

where

R_t = limiter resistance at time t
R_0 = initial resistance of limiter
I = current which remains constant

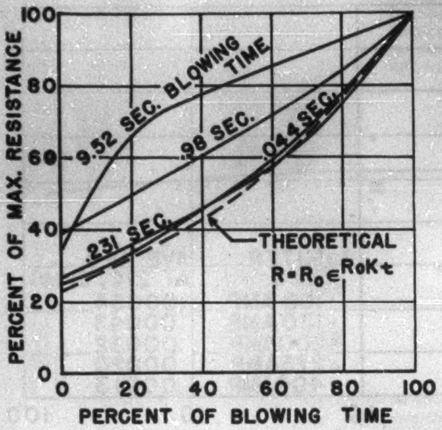

Fig. 6. Change in limiter resistance during blowing time for various blowing times. All four limiters were rated 40-amperes 208/120-volt (silver element)

t=time, seconds
k=constant for a given limiter design

The significance of this equation is that the resistance of a limiter will increase exponentially with time.

It is interesting to note the correlation of this theoretical expression for limiter resistance with actual data. Fig. 6 shows the resistance of a silver-element limiter plotted against time for several blowing times. It will be noted that the resistances of fast-blowing limiters closely follow the theoretical curve.

The value of k depends on the physical size of the limiter element and its thermal resistance coefficient

$$k=\frac{0.018\alpha}{\text{volume, cubic inches}}\text{ for copper}$$

The value of k can also be computed if the resistance of a limiter just before melting is known

$$\frac{R}{R_0}=\epsilon^{kR_0I^2t}$$

$$\log\frac{R}{R_0}=kR_0I^2t$$

$$k=\frac{\log\dfrac{R}{R_0}}{R_0I^2t}$$

Table I. Maximum Fault Current Expected in Airplanes

Type Circuit	Maximum Fault Current, Amperes	Size Limiter, Amperes	Limiter Resistance, Ohms	Voltage Drop	
				Limiter Cold	Limiter Hot
28 volt d-c	6000	275	0.0002	1.2	6.24
110 volt a-c	4000	60	0.0006	2.4	10.1

For a given limiter, k can be determined by taking blowing time and current from reference 2 (copper-element limiters) or reference 4 (silver-element limiters). Equation 2 is applicable only when the limiter blows so fast that heat losses are negligible, so for computing k the current at a very short blowing time should be used.

Values of k for silver-element limiters are given in Table II, and for copper-element limiters in Table III.

Effect of Limiter Heating on Distribution of Current Between Parallel Limiters Having Unequal Resistance Paths

One of the principal objectives of this research was the development of a practicable method of predicting how much equalizing effect will take place in parallel circuits as a result of limiter heating during blowing.

Fortunately, in the case of parallel limiters having unequal resistance paths, it can be shown by analysis that the equalizing effect is greater at blowing times of less than 0.1 second than at longer blowing times. This fact has been confirmed in the laboratory by blowing parallel limiters with various series resistances.

In this analysis of parallel circuits, two assumptions are made:

1. That the total current through the combination of limiters remains constant;
2. That the limiter blows in less than 0.1 second.

The following symbols will be used, see Fig. 7.

Table II. Values of k for Silver-Element Limiters

Limiter Rating, Amperes	I, Amperes	t, Seconds	R₀, Ohms	k
10	330	0.01	0.0052	0.253
30	800	0.01	0.0013	0.1725
40	1070	0.01	0.0010	0.125
60	1600	0.01	0.0006	0.0934

Table III. Values of k for Copper-Element Limiters

Limiter Rating, Amperes	I, Amperes	t, Seconds	R₀, Ohms	k
100	3150	0.01	0.00054	0.0307
130	3800	0.01	0.00043	0.0266
200	5700	0.01	0.00032	0.0158
275	9000	0.01	0.00020	0.0102
400	13800	0.01	0.00013	0.00667

I_t=total current
R_1=a nonvarying resistance
R_3=a nonvarying resistance
R_2=limiter intended to blow first
R_4=limiter not intended to blow first
I_1=current through R_2
I_2=current through R_4
$r_1=R_1+R_2$
$r_2=R_3+R_4$
$I_t=I_1+I_2$

Any attempt to derive an exact expression for the currents or limiter resistances in Fig. 7 will lead to a nonlinear differential equation. Such an equation could be solved by approximations, but it would be so unwieldy that it would have little practical value in airplane design.

Therefore, the problem of parallel limiters was divided into two categories, namely: 1. to determine the worst possible equalization conditions; 2. to provide point-by-point method of approximating what will actually happen in a specific circuit as the limiters heat.

The worst possible equalization conditions will exist if R_4 does not increase its resistance at all. Thus, as R_2 gets hotter and hotter, it will divert more and more of its current into R_4. The limiting condition will usually occur when R_2 reaches 4.2 (silver) or 5.2 (copper) times its cold resistance, and melts.

In a parallel circuit

$$I_1=\frac{I_tr_2}{r_1+r_2}\qquad I_2=\frac{I_tr_1}{r_1+r_2}$$

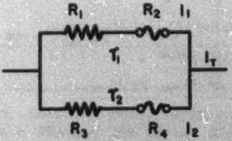

Fig. 7. Parallel circuit with limiters

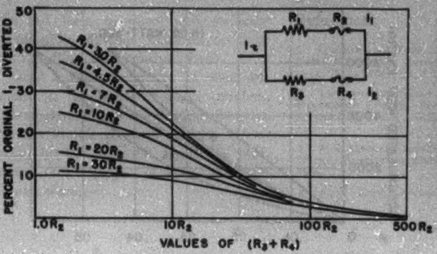

Fig. 8. Maximum current-diverting effect of copper-element limiters at instant before melting. It is assumed that I_t, R_1, R_3, and R_4 remain constant, and that R_2 increases to 5.2 times its cold resistance before melting

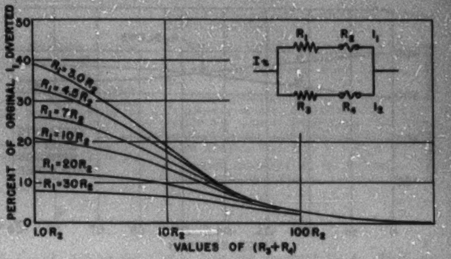

Fig. 9. Maximum current-diverting effect of silver-element limiters at instant before melting. It is assumed that I_t, R_1, R_3, and R_4 remain constant, and that R_2 increases to 4.2 times its cold resistance before melting

In Fig. 7

$$I_1=\frac{I_t(R_3+R_4)}{R_1+R_2+R_3+R_4}$$

Just before R_2 blows

$$I_1'=\frac{I_t(R_3+R_4)}{R_1+xR_2+R_3+R_4}$$

where

$x=4.2$ for silver
$=5.2$ for copper

The percentage of initial current I_1 that will be diverted into R_4 is

$$D=100\left[\frac{I_1-I_1'}{I_1}\right]=100\left[1-\frac{I_1'}{I_1}\right]$$

where $D=$per-cent current diverted.

$$D=100\left[1-\left\{\frac{(R_3+R_4)I_t}{R_1+xR_2+R_3+R_4}\times\frac{R_1+R_2+R_3+R_4}{I_t(R_3+R_4)}\right\}\right]$$

$$=100\left[1-\frac{R_1+R_2+R_3+R_4}{R_1+xR_2+R_3+R_4}\right]$$

By using various ratios for R_1/R_2 and $(R_3+R_4)/R_2$, the data for Figs. 8 and 9 were calculated.

Most parallel limiter equalizing problems can be solved quickly with Fig. 8 or 9, which give the per cent of current I_1 that is diverted into R_3 and R_4 under the most unfavorable conditions. If, even though current is diverted, R_2 blows well ahead of R_4, then the circuit may be considered safe from an equalization standpoint.

Table IV. Step-by-Step Computation of Resistances of Parallel Limiters

Current at Beginning, Branch Amperes		$\epsilon^{2.24t}\left(\frac{I}{100}\right)^2$	R at End of Period, Per Unit	t at End of Period, Seconds
1	400	1.431	1.431	0.01
2	296	1.218	1.218	0.01
1	391	1.409	2.02	0.02
2	306	1.234	1.50	0.02
1	378	1.378	2.78	0.03
2	318	1.253	1.88	0.03
1	365	1.348	3.74	0.04
2	331	1.279	2.40	0.04
1	353	1.325	4.96	0.05
2	343	1.303	3.13	0.05

EXAMPLE 1:

R_2 and R_4 are 30-ampere silver-element limiters

$R_1=0.026$ ohm
$R_3=0.052$ ohm

From Fig. 9

$R_2=R_4=0.0013$ ohm
$R_1=20R_2$; $R_3+R_4=41R_2$

Diverted current$=5$ per cent.

Assume that initially

$I_1=400$ amperes

$$I_2=I_1\frac{(R_1+R_2)}{(R_3+R_4)}=\frac{400(20+1)}{40+1}=205 \text{ amperes}$$

After diversion

$I_1=0.95\times400=380$ amperes
$I_2=205+(0.05\times400)=225$ amperes

Obviously, R_2 will blow before R_4, so this problem is solved.

If the foregoing check leaves a question about R_2 clearing first, then a more complete analysis will have to be made.

EXAMPLE 2:

Two 30-ampere silver-element limiters, as in Fig. 7, with the following constants

$R_2=R_4=0.0013$
$R_1=3.46R_2=0.0045$ ohm
$R_3=5.0R_2=0.0065$ ohm

From Fig. 9, diversion of $I_1=25$ per cent.

Assume

$I_1=400$ amperes at start

$$I_2=400\frac{(R_1+R_2)}{(R_3+R_4)}=296 \text{ amperes}$$

After diversion

$I_1=0.75\times400=300$ amperes
$I_2=296+(0.25\times400)=396$ amperes

On the basis of Fig. 9, there is reason to

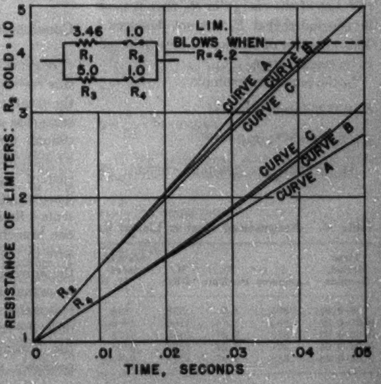

Fig. 10. Time-resistance plot of parallel 30-ampere 208/120-volt silver-element limiters. Total current is 696 amperes

Curve A contains no correction for current diversion

Curve B shows currents corrected every 0.01 second

Curve C shows currents corrected every 0.005 second

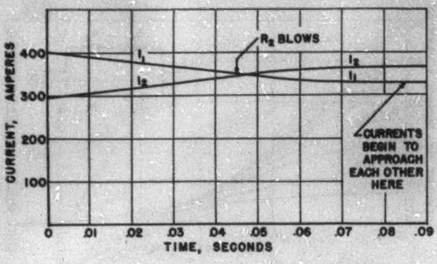

Fig. 11. Current division between parallel limiters with unequal resistance paths, as shown in Fig. 10. Currents are based on curve C resistances

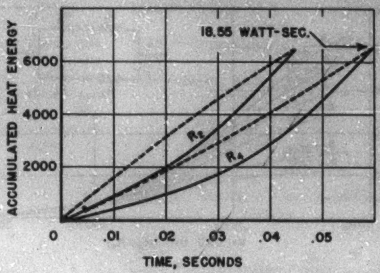

Fig. 12. Accumulated heat in parallel limiters having unequal resistance paths, as shown in Fig. 10. Dotted lines are based on H=kI²t. Solid lines are based on H=I²Rt, using curve C resistances from Fig. 10 and currents from Fig. 11

question which limiter will blow first.

The following method, based on point-by-point approximations, will provide a reasonably accurate picture of current distribution in a parallel circuit, where the equalization effect is in question. This analytical approach has been verified by laboratory tests where limiters in parallel were instrumented and blown.

As long as the limiters will blow in less than 0.1 second, the resistance of each limiter will be

$$R=R_0\epsilon^{kR_0I^2t} \tag{2}$$

With a current that will blow the limiter in 0.04 second, the resistance is tabulated against time. The current in each branch is corrected each 0.01 second. From the resulting data, the accumulated heat energy in each limiter can be computed from the formula

$$H=\int_0^t I^2Rdt$$

Limiter R_2 will blow after its resistance reaches 4.2 (silver element) or 5.2 (copper element) times its cold resistance. If the energy in R_4 at this time is less than 52 per cent of the energy in R_2, then it may be concluded that R_4 was not damaged.[6] This criterion of damage is now believed to be conservative.

In the preceding example

$k=0.1725$ (from Table II)

$$R=R_0\epsilon^{0.1725R_0I^2t}=R_0\epsilon^{2.24t\left(\frac{I}{100}\right)^2}$$

At 400-amperes constant current, R_2 would blow in 0.04 second.

Table V. Accumulated Heat in Limiter R_2

Time Period, Seconds	I_1, Amperes	R_2, Per Unit	H, I^2Rt	Accumulated H
0–0.01	395	1.2	838	838
0.01–0.02	385	1.75	1160	1998
0.02–0.03	373	2.37	1480	3478
0.03–0.04	361	3.22	1880	5358
0.04–0.05	353	3.97	1111	6469

Calculating R_2 and R_4 in a step-by-step manner produces the data in Table IV. For convenience, resistance is computed on a per-unit basis. Curves *B* in Fig. 10 shows the Table IV resistances R_2 and R_4 plotted against time; curves *C* show the same resistances, calculated with corrections in current made every 0.005 second instead of every 0.01 second. Fig. 11 shows the current I_1 and I_2 plotted against time, based on curve *C* resistances. From Figs. 10 and 11, the accumulated heat energy in each limiter can be computed. The values for R_2 are given in Table V.

The solid lines in Fig. 12 show the accumulated energy in each limiter. Apparently R_2 will blow first, but R_4, having absorbed 56 per cent of its blowing heat energy, would be considered damaged by present standards.[6] This step-by-step procedure is applicable to circuits having more than two limiters in parallel. It is also applicable to circuits having heterogeneous limiters.

Conclusions

In general, the laboratory test results of this research project seem to concur with the mathematical analysis. It would seem that only under extremely rare conditions would there be danger of the wrong limiter blowing first, as the result of current equalization in a circuit with limiters in parallel. Example 2 represents a limiter and about 6 feet of wire in one branch; and a limiter and 5 feet of wire in the other branch. This is about the worst condition that could be expected in actual practice. Longer wires, with reasonable differences in length, will reduce the equalizing effect. Nevertheless, the blowing time of a limiter can be appreciably delayed by its current being diverted to another path. In some cases, this delay may influence the limiter coordination of a system.

A new concept of limiter damage was a by-product of this limiter research project. The traditional method of determining heat content, and hence proximity to melting temperature, is to assume that the limiter resistance is constant. The energy content of a fast-blowing limiter will then be proportional to I^2t. This method appears conservative and tends to indicate that the damage in unblown limiters is greater than actually is the case. A more realistic approach would be to go back to the original formula

$$\text{Heat}=\text{watt-seconds}=I^2Rt$$

The resistance of a limiter that blows in less than 0.1 second under constant-current conditions is

$$R=R_0\epsilon^{kR_0I^2t} \tag{2}$$

Just before melting, the resistance of a limiter is 4.2 (silver-element) or 5.2 (copper-element) times its cold resistance. Thus the limiter will be absorbing energy 4.2 times or 5.2 times faster just before melting than it was at the beginning of the transient. Fig. 12 illustrates this point. In this case, both limiters have variable current, and the current was corrected every 0.005 second in the equation. Limiter R_2 blows at 0.045 second. On the basis of an I^2t analysis, R_4 has absorbed 13.5 watt-seconds. Actual energy absorption of R_4 was only 10.4 watt-seconds.

The application of this philosophy to slow-blowing limiters, and hence limiters in general, would be justified only after more thorough analysis. Such analysis is beyond the scope of this paper. In this connection, a number of limiters which had been subject to near-blowing transients were tested. These "used" limiters did not seem to have been seriously damaged by previous transients, for their blowing times were nearly normal.

Only a limited amount of time was spent on the limiter damage problem, inasmuch as it was not a major objective of this limiter research project. However, further research might be warranted on the subject of what constitutes limiter damage.

References

1. Limiter and Fuse Characteristic Curves, Irving Matthysse. Burndy Engineers' Club, Norwalk, Conn., 1947, pp. 1–11.

2. Twenty-Eight-Volt D-C Limiter Test Procedure. *Boeing Document D-10958*, Boeing Airplane Company, Seattle, Wash., 1950, pp. 7–15.

3. D-C Aircraft Limiters (drawing no. *G128-3*). Burndy Engineering Company, New York, N. Y., 1950.

4. Fuse, Single-Phase, 400 Cycle, Aircraft. *USAF Specification 32552*, United States Air Force, Dayton, Ohio, 1946, p. 3.

5. Wire and Circuit Breaker Guide for Airplane Design. *Boeing Document D-7900*, Boeing Airplane Company, Seattle, Wash. 1946, pp. 27 30.

6. Memorandum Report on A-C System Fuse Coordination Study. *USAAF Serial No. TSEPE-656-669-BJ*, United States Army Air Forces Technical Service Command, Engineering Division, Dayton, Ohio, Dec. 4, 1945, p. 32.

7. Fusing Currents, G. W. Stubbings. *The Electrician*, London, England, no. 3530, 1946, pp. 217–19.

◆

Discussion

J. C. Lebens (Bussmann Manufacturing Company, Saint Louis, Mo.): The author is to be complimented upon his analysis and solution of the fundamental question concerning the effect of change in aircraft limiter resistance with load on aircraft circuits. Actually the problem is not unique to aircraft circuits but is of vital importance wherever limiters or fuses are used in parallel.

A superficial study of the problem leads to the conclusion that the change in resistance of the fuse or limiter tends to maintain an even distribution of current when operated in parallel. However, the degree of the correction afforded by the change in fuse resistance with change of current in the two or more parallel paths has not been investigated fully. Mr. Oman does an excellent job in analyzing this problem and establishing the effect of the variables involved.

It might be of interest to report that further development has been made on the 28-volt d-c aircraft limiter since the paper was originally submitted. Electrically the new limiter is interchangeable with the one tested by Mr. Oman and is available in various sizes in the range from 35 to 500 amperes. The time-current characteristic of the new limiter is the same as that of the old one, except that greater accuracy can be maintained with the new limiter because positive spacing is maintained between the reduced section of the link and the housing of the limiter. This assures that the cooling effect of the housing will be the same on all samples. Hence, on low overloads where the time of opening is long enough for thermal conduction, greater accuracy is obtained.

The primary reason for the development of the new aircraft limiter was to increase the mechanical strength of the housing and to improve its performance under heavy short-circuit conditions. The fusible element and terminals are stamped out of a sheet of copper of appropriate thickness but the terminals extend into the case to obtain a superior keying action. The glass in the window is replaced with mica and the refractory case is replaced with laminated melamine sheet sections which are riveted together to complete the assembly. The rivets extend through the terminal extensions to lock the terminals to the housing.

Even though the new limiter has greater mechanical strength and superior short-circuit performance, its time-current characteristic is substantially the same as that of the limiter tested by Mr. Oman. Hence, his results could apply equally well to the new type.

The author also touched on another very important question affecting the application of fuses and limiters. This is the question of limiter damage which affects the selection of the limiter rating used in a co-ordinated system. Unfortunately Mr. Oman did not have sufficient time to pursue this avenue further inasmuch as it was not a major objective of his project. However, I agree with him that the subject of "what constitutes limiter damage?" is one that justifies further research.

I. Matthysse (Burndy Engineering Company, Norwalk, Conn.): Mr. Oman has presented a very thorough analysis of the effect of the increase in the resistance of the fusible element of a limiter as it approaches its melting point. He indicates in his conclusion that the current equalization in parallel paths, caused by the increase of limiter resistance, may influence the limiter co-ordination of a system.

It is assumed that both limiters in the parallel circuit of Fig. 7 are carrying the fault or overload current. If the paths have equal resistance the circuit will be cleared by the blowing of both limiters simultaneously, and the clearing time (neglecting arcing time) will be found from the time-current characteristic curve using the current through one limiter (half the total current) and finding the time from the curve. However, if the parallel paths are of unequal resistance, one limiter will blow first, at which time its current will transfer to the second limiter, causing the second one to blow very rapidly thereafter. The total clearing time is the time to clear both limiters. Comparing this total clearing time with the clearing time if the paths had been of equal resistance shows the effect on co-ordination of the paths being of unequal resistance.

The total clearing time may be determined for paths of unequal resistance using the step-by-step procedure developed by Mr. Oman. Using this procedure the blowing time for the first limiter would be determined, and then the additional time to blow the second limiter carrying the total current would be found.

The increase in the resistance of the limiter as it approaches the blowing point greatly complicates the general mathematical solution for parallel paths, as Mr. Oman points out. However, it is instructive to analyze the problem on the asumption that the current is unchanged by the increase of limiter resistance. For fast blowing (less than 0.1 second) the total value of I^2t up to blowing is a constant for a given limiter size. Let this constant be k. Then, referring to Fig. 7, if path 1 has the lower resistance the time t_1 to blow the limiter in this path is given by

$$I_1^2t_1=k$$

or

$$t_1=\frac{k}{I_1^2}$$

In this time the I^2t generated in the limiter in path 2 is equal to $I_2^2t_1$. After the first limiter blows the current in the second limiter is I_1+I_2. Therefore, the additional I^2t generated, after an additional time t_2 has elapsed up to the blowing of the second limiter, is

$$(I_1+I_2)^2t_2$$

The total I^2t in the second limiter must also equal k, thus

$$I_2^2t_1+(I_1+I_2)^2t_2=k$$

Substituting the value of t_1 given previously

$$I_2^2\frac{k}{I_1^2}+(I_1+I_2)^2t_2=k$$

Therefore

$$t_2=\frac{k(I_1^2-I_2^2)}{I_1^2(I_1+I_2)^2}=\frac{k(I_1-I_2)}{I_1^2(I_1+I_2)}$$

The total clearing time t_T is

$$t_T=t_1+t_2=\frac{k}{I_1^2}\left(1+\frac{I_1-I_2}{I_1+I_2}\right)$$

$$=\frac{k}{I_1^2}\frac{2I_1}{I_1+I_2}=\frac{2k}{I_1(I_1+I_2)}$$

If we let I be the average current in the two paths

$$t_1=\frac{k}{I_1I}\text{ (for unequal paths)}$$

If the resistances of both paths were equal, then I_1 would be equal to I, so that

$$t=\frac{k}{I^2}\text{ (for equal paths)}$$

Therefore

$$\frac{t_T}{t}=\frac{I}{I_1}$$

or

$$t_T=t\frac{I}{I_1}$$

Thus, the total clearing time is less when the resistances are unequal than when they are equal, by the factor of the ratio of the equal current to the larger of the unequal currents. In the second case cited by Mr. Oman the greater current was 400 amperes, whereas if the paths had been equal it would have been 348 amperes.

Therefore

$$t_T = t\frac{348}{400} = 0.87t$$

The total clearing time for the unequal paths is 87 per cent of the time if both paths were equal.

Thus, the effect on co-ordination of parallel paths of unequal resistance is to clear the limiters a little sooner than if the paths were of equal resistance. The question now is, how does the increasing resistance of the limiter influence this effect. As the author pointed out, the increasing resistance has a current equalizing effect. This results in the currents in each path differing less from each other than they would if the resistances remained constant. Therefore the decrease in the total clearing time due to the paths being of unequal resitance should not be as great as if the resistances remained constant. Thus, in the example cited, the total clearing time would be somewhere between the clearing time if the paths were of equal resistance and 87 per cent of this time. This small change in blowing time will probably have a negligible effect on co-ordination, and, in addition, Mr. Oman points out that this example is about the worst condition that could be expected in actual practice.

Mr. Oman discovered that the I^2t criterion for damage of an unblown limiter is conservative on the basis of the actual heat energy absorbed by the limiter. In addition, tests conducted by other researchers confirm his tests, indicating that much greater energy absorption leaves the limiters undamaged. Further research would be warranted on this subject.

Henry Oman: The interest shown by the discussers is very much appreciated.

Mr. Lebens' description of the improved limiter is a valuable supplement to the paper; and it would appear that the new design should result in more uniform limiter performance.

The conclusion derived by Mr. Matthysse relative to the blowing time of parallel limiters is very interesting. The reasoning certainly seems valid, and the discussion is welcomed as a useful addition to the paper

---

Design of Transformers for Resistance Welding Machines

D. L. KNIGHT
NONMEMBER AIEE

A DISCUSSION OF transformer design and characteristics would have been a rather controversial subject 15 years ago, as in those days the name-plate kilovolt-ampere rating of the transformer meant little other than that it was printed in English. Oftentimes in the early years, if the power companies limited the maximum connected kilovolt-amperes for a particular installation, a machine was supplied with this name-plate kilovolt-ampere rating, regardless of the actual load drawn by the machine. It was rather common practice to use excessive amounts of copper in the secondaries, and a very small amount of primary copper. There was no logical reason for this except perhaps that the secondaries could be seen, while the primaries were covered. In general, confusion existed, no standard ratings were used, and it was extremely difficult for power companies or users to determine actual ratings and demand figures. Of course, this condition could not continue, and several years ago the AIEE and the Resistance Welder Manufacturers' Association (RWMA) drew up specifications for the standardization of welding-transformer ratings.

No attempt will be made in this paper to discuss design procedures such as specific current densities, flux densities, etc., but rather to discuss the basis of transformer ratings, and factors affecting the design as well as factors which should be of primary interest to power companies and users of welding equipment.

Factors to be discussed are as follows (but not necessarily in the order of their importance):

1. Basis of transformer ratings.
2. Construction.
3. Transformer impedance.
4. Transformer efficiency.
5. Excitation and core loss.
6. Types of secondaries.
7. Insulating materials.

Basis of Transformer Ratings

The operation of a welding transformer differs from that of a conventional power transformer, in that the load on the power transformer is of a continuous nature, whereas the load on a welding transformer is a rapidly recurring one, usually approaching short-circuit values. In order to obtain a closer agreement between the actual instantaneous kilovolt-ampere demand and its kilovolt-ampere rating, it was decided to use a 50-per-cent duty-cycle rating, rather than the normal 100-per-cent duty-cycle rating used for most other transformers. The 50-per-cent duty-cycle rating, maximum temperatures, and conditions and methods of making temperature tests were established by the AIEE and adopted by RWMA as standards.

These standards have eliminated much of the confusion that formerly existed, in that they definitely give a meaning to the name-plate rating. All resistance-welding transformers manufactured today by members of the RWMA have a standard rating. The definition is: "The Standard Rating shall be the periodic rating based on a 50 per cent duty cycle and a one-minute integrating period." The name-plate rating does not necessarily indicate the maximum demand of the machine, but definitely does give the thermal limitations of the transformer.

Some confusion still exists in interpreting the ambient temperature to be used in transformer tests. Because the transformers as a rule are water-cooled devices, it is generally agreed that the ambient temperature should be determined by the inlet water temperature. This is now being considered by members of the RWMA and the standards will be revised in this respect.

Construction

The shell-type core with interleaved pancake windings is generally considered the most suitable type of construction for a low-voltage high-current transformer. The most economical disposition of material is possible, and the problems of

---

Paper 53-296, recommended by the AIEE Electric Welding Committee and approved by the AIEE Committee on Technical Operations for presentation at the AIEE Summer General Meeting, Atlantic City, N. J., June 15-19, 1953. Manuscript submitted November 28, 1950; made available for printing April 29, 1953.

D. L. Knight is with the National Electric Welding Machines Company, Bay City, Mich.

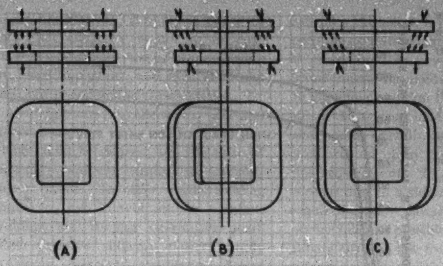

Fig. 1. Forces between flat primary and secondary coils

A. Electrical centers in line
B. Electrical centers out of line
C. Electrical centers in line, but coil of different dimensions

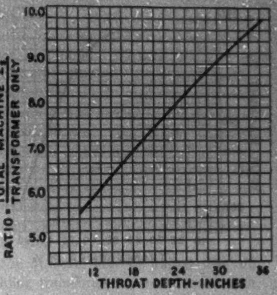

Fig. 2 (right). Relationship between transformer impedance and total impedance

Transformer $Z_s = 30$ micromhos
Power factor = 80 per cent

bracing the coils to withstand the mechanical stress is more easily accomplished.

The primaries are usually pancake-wound with fully annealed rounded-edge copper strip, varying in width and thickness depending upon the rating. The secondaries are single-turn pancake coils of cast rolled-copper or copper tubing. The coils are assembled in a shell core with interlacing of the primary and secondaries.

A welding transformer must be able to withstand repeated overloads up to six times its rated capacity at reduced duty cycles. The mechanical stresses which are developed in the windings of the transformer under these conditions are many times higher than would be expected if the unit was operated at rated load. A problem is involved in bracing of the coils to prevent their injury under these operating conditions.

When the primary and secondary coils of a transformer winding are assembled, the currents in these two elements are opposite in direction. Due to the magnetic field present, a force is set up which tends to separate the coils. For flat primary and secondary coils, having the same overall dimensions and identical electrical centers, the forces act in the direction shown in Fig. 1(A). The repelling forces are all at right angles to the plane of the coils. When the electrical centers are separated, however, as shown in Fig. 1(B), there is a component of force parallel to the planes of the coils as well as at right angles to them. This component may be quite large, and sufficient to damage the coils by driving them apart. If the coils are concentric with reference to one another, but one having smaller dimensions that the other, the forces acting between the coils are shown in Fig. 1(C). In addition to repelling forces at right angles to the plane of the coils, there are components parallel to these planes which tend to force the sides of the smaller coils inward and the sides of the larger coils outward.

These forces may be sufficient to damage the coils and, for this reason, the coils should be made to conform as nearly as possible to the arrangement shown in Fig. 1(A). The force acting between coils may be a few pounds, or several hundred, depending upon size of transformer. The parts of the coils within the transformer are held so that movement cannot take place, while the ends outside the the core are braced by plates forced against the coils by means of tie bolts or pressure screws in the core frames.

Impregnation of the coils is accomplished several ways by different manufacturers. Some impregnate the primary coils before assembly, and do not dip the entire transformer. Others do not dip and bake the primaries before assembly, but assemble the transformer and impregnate as a unit. The others dip and bake the primaries before assembly, assemble, then impregnate the entire transformer. The transformer should be dipped and baked as a unit. Whether the primary coils are impregnated before assembly depends on the penetration obtained at all points during the impregnation of the unit as a whole. Dipping and baking the entire transformer increases its oil and water resistance and also increases the efficiency of heat transfer by filling the voids present.

Transformer Impedance

Impedance rating of transformers is defined by RWMA standards as: "The per cent impedance of the transformer shall be expressed in terms of per cent primary voltage required to force rated primary current thru the combined resistance and reactance of the transformer proper. For this purpose the secondary windings shall be considered to consist of only that portion of the winding which is covered by the primary coils." In the past few years, considerable effort has been expended to reduce transformer impedance as much as possible without increasing the cost of construction. From the formula for inductance of flat pancake-type primary and secondary coils

$$L = 3.2T_1^2\frac{MT}{l}\left(S+\frac{d_1+d_2}{6}\right)\times 10^{-8}$$

where

L = inductance, henrys
T_1 = turns in primary coil
MT = mean turn, inches
l = height of primary coil, inches
s = distance between primary and secondary coil, inches
d_1 = width of primary coil, inches
d_2 = width of secondary coil, inches

it can be seen that the following factors affect the transformer impedance:

1. Thickness of primary and secondary coils.
2. Space between primary and secondary coils.
3. Number of turns in the primary.
4. Mean length of turn.
5. Number of primary and secondary coils.

Present-day welding transformers generally use relatively more primary and secondary coils of thinner section and thinner insulation between coils, resulting in closer coupling between the primary and secondaries. The secondary of a welding transformer is inherently a 1- or 2-turn coil, hence the number of turns in the primary is a direct function of the secondary voltage required.

Little improvement can be made in the mean turn, since the mean turn depends greatly on the cross-sectional area of core iron. Because the device is inherently a single-turn secondary transformer, the volts per turn is dependent

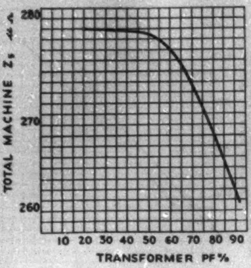

Fig. 3 (left). Change in total impedence with varying transformer power factors

100 air-operated press type 18 inches; Z_s = constant loop only
Transformer per cent Z = constant = 10 per cent
Loop Z = 180 microhms

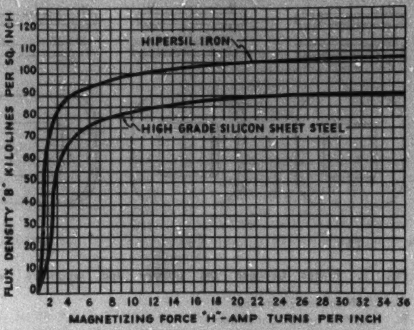

Fig. 4. Comparison of the saturation curves for the special cores and high-grade silicon-steel laminations

entirely on the secondary voltage required therefore the section of core iron is fixed.

What effect does transformer impedance have on the total impedance of the welder? Fig. 2 shows the relationship between transformer impedance and total impedance, for various loop or throat areas, when a transformer of 30-microhms total impedance (referred to the secondary) is connected to various loops. The curve is not a straight line, because, the power factor of the loop changes as the throat area increases, while the transformer power factor remains the same. It is apparent that the effect of the transformer impedance on the overall impedance becomes decreasingly less as the throat area increases.

In comparing per-cent impedance of transformers with the same kilovolt-ampere rating, it is necessary that the turn ratio be considered, when considering their effect on over-all welder impedance. Although the per-cent impedance may be the same, the transformer impedance in ohms, referred to the secondary, will be different if the turn-ratios are not the same.

The following example illustrates two transformers with the same kilovolt-ampere rating and per-cent impedance, but with slightly different secondary voltages and turn-ratio. The impedance referred to the secondary in one case is 94.5 microhms, while in the other it is only 79.2 microhms. If these transformers are connected to the same secondary loop, the maximum secondary current will be approximately the same, despite the fact that one secondary voltage is lower than the other.

EXAMPLE: RELATIONSHIP BETWEEN PER-CENT IMPEDANCE AND TURN-RATIO

(Assume both transformers connected to the same loop area and configuration)

Loop Values

Impedance = 0.0001 ohm
Power factor = 40 per cent
Resistance = 0.00004 ohm
Reactance = 0.0000916 ohm

Transformer No. 1

KVA = 50 (name plate)
Per-cent impedance = 10 per cent
Primary impedance = 0.388 ohm
Power factor = 70 per cent
Turn-ratio = 64
Secondary impedance = 0.0000945 ohm
Secondary resistance = 0.0000662 ohm
Secondary reactance = 0.0000676 ohm
R_t (total loop and transformer) = 0.0001062 ohm
X_t (total loop and transformer) = 0.000159 ohm
Z_t (total loop and transformer) = 0.000191 ohms
Maximum secondary current = 35,900 amperes
Kilovolt-amperes = 247

Transformer No. 2

KVA = 50 (name plate)
Per-cent impedance = 10 per cent
Primary impedance = 0.388 ohm
Power factor = 70 per cent
Turn-ratio = 70
Secondary impedance = 0.0000792 ohm
Secondary resistance = 0.0000555 ohm
Secondary reactance = 0.0000566 ohm
R_t (total loop and transformer) = 0.0000955 ohm
X_t (total loop and transformer) = 0.000148 ohm
Z_t (total loop and transformer) = 0.000176 ohm
Maximum secondary current = 35,700 amperes
Kilovolt-amperes = 224

The transformer impedance is very important with low-load impedance, while it assumes less importance as the load impedance increases. However, this does not mean that the per-cent impedance of the transformer should not be kept at a minimum regardless of the load impedance for which it is designed. Usually, in welding machines the transformer is designed for a given secondary-loop or load impedance. In any kilovolt-ampere size, the maximum secondary voltage (turn-ratio) is changed for appreciable differences in throat depth or configuration. The intent is to maintain approximately the same maximum kilovolt-ampere demand regardless of the load impedance. Under these conditions a change in per-cent impedance of a transformer designed for a high load impedance will cause the same percentage change in output as an equal change in per-cent impedance of a transformer designed for low load impedance.

Another factor that influences the effect of transformer impedance on the total impedance is the power factor of the transformer. Although the per-cent impedance may be the same, if the power factor or ratio of R and X in the transformer changes, the effect on the over-all impedance will change.

Fig. 3 is a curve showing the change in total impedance with varying transformer power factors, using constant loop impedance and constant per-cent transformer impedance.

Transformer Efficiency

Distribution transformers are designed for a very high light-load efficiency, because they are permanently connected to the power lines. On the other hand, welding transformers are energized only a small fraction of the time. If a machine operates on a duty cycle of 5 per cent for 8 hours a day, 5 days a week, it is only on the line 2 hours per week, as compared to 168 hours for a distribution transformer. Losses, therefore, in a welding transformer assume minor importance, while impedance, space, weight, cost, and mechanical construction assume major importance. It is not intended to infer that efficiency is not to be considered; however, these other factors are more important, and high efficiency must not be secured at their expense.

More important to the welder user and power company as a welder efficiency which could be defined as: the ratio of secondary ampere output to kilovolt-ampere input. In other words, welding amperes per kilovolt-ampere input. Welding, with its high intermittent load, often presents difficult power supply problems; therefore, any design change that increases the welder efficiency simplifies the power problem, and results in a more economical installation. As shown previously, proper transformer design can increase the welder efficiency.

Excitation and Core Loss

Distribution transformers are permanently connected to the power-company lines, and it is important that excitation current and no load losses be kept to a minimum. Since welding transformers never are operated at no load under normal conditions, the excitation current and no load losses are of no consideration, except as they affect the normal load current, performance, and over-all power factor.

With the importance of compactness and weight, the tendency is to work the core iron at higher densities than would be used for distribution transformers. The RWMA Standards have specified that the maximum exciting current is not to exceed 10 per cent for transformers up to 100 kva, and not to exceed 5 per cent for all transformers 100 kva and over. These values would not be tolerated in a distribution transformer, but they represent practical limitations for welding transformers.

In general, shell type cores are used, except in the smaller kilovolt-ampere sizes. Using the shell type core, adequate bracing to withstand the mechanical stresses involved during the momentary overloads are easier and more economically accomplished.

What type of electrical steel is best for welding transformers? The important limitation for core design is not core losses, but is the excitation or no-load current. Although it is not necessary to keep the excitation current to a low value, as is required in power or distribution transformers, the excitation current must be low enough so that it does not seriously affect the normal load current, performance, and overall power factor. The standards set up by the RWMA do meet this requirement. In order to keep the core section to a minimum, the designer requires a core material with as high a permeability as possible at high induction. Where space is not too important a consideration, the choice of electrical sheet is a matter of economics. The designer must balance the cost of the core material against increased size and weight of the transformer, to determine the most economical construction.

In the past few years a considerable number of welding transformers have been built using special types of core material. Special cores are made from high-quality cold-rolled silicon steel having preferred crystal orientation. This preferred orientation results in very low losses and low excitation current in the direction of rolling. With the preferred orientation of the crystals, the knee of the saturation curve is raised, so that the core can be operated at least at 30 per cent higher flux density, with the same magnetizing force or excitation current. A comparison of the saturation curves for the special cores and high-grade silicon steel laminations is shown in Fig. 4. The increased flux densities result in transformers smaller in over-all size and weight. It is this factor, and this factor alone, that has to date chiefly determined the use of special core iron for welding transformers. Figs. 5 and 6 show welding transformers manufactured with these cores.

Fig. 5 shows a 35-kva 2-secondary unit used in multitransformer welders where space is limited. Without the use of special core iron with high permeability at high induction, it would be impossible to obtain a transformer of this rating in the space allowed. Fig. 6 shows a standard 100-kva 50 per-cent duty cycle transformer for a pedestal type welder. The cubic space occupied by this unit is approximately 75 per cent of that necessary if standard high-grade electrical laminations were used.

The question may be raised why all welding transformers are not made with special high-permeability high-induction cores. Here again, it is a matter of economics. The cost per pound of the core material is considerably higher, and the designer must balance this cost against the saving in all material due to the decreased size and weight, and the labor saving involved in shearing and stacking standard laminations.

Types of Secondaries

The secondary of a welding transformer is a high-current low-voltage winding carrying instantaneous currents sometimes in excess of 200,000 amperes. Except in the very small sizes, the high currents make it necessary to have large cross sectional areas of copper. To reduce their size, by working at higher current densities, they are usually water cooled. At the same time, the primaries, are cooled by conduction of the heat to the secondaries. Numerous types of secondaries have been used in welding transformers. For the purpose of this paper, we will discuss the four major types used today, as shown schematically in Fig. 7.

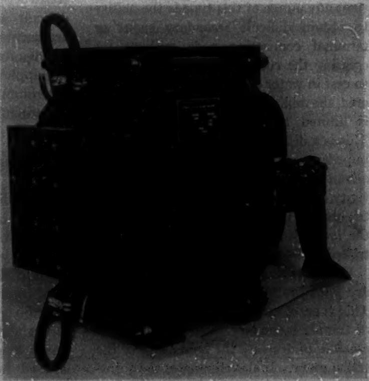

Fig. 5 (left). 35-kva 2-secondary special-core iron welding transformer

Fig. 6 (right). Standard 100-kva special-core welding transformer with rolled - copper secondaries

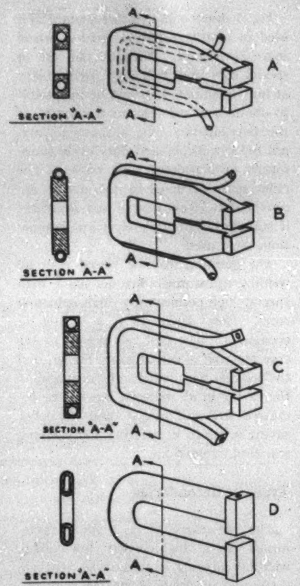

Fig. 7. **Types of secondaries used in welding transformers**

A. Cast copper, water cooling internal
B. Cast copper, water-cooling tube brazed
C. Fabricated secondary
D. Copper tubing

Fig. 7(A) shows a cast-copper secondary with cast-in water cooling tubes. This type is the one most commonly used today. The cost of construction is low, and efficient cooling is obtained with the cast-in water cooling tubes. One distinct advantage of this type is the ability to obtain difficult secondary snout or terminal connecting pads without increasing the cost appreciably. In order to cast in water cooling tubes of sufficient area, the minimum width of the secondary is limited to approximately 5/8 inch. This is a disadvantage where transformer impedance is important. Another disadvantage is the relatively low conductivity of the cast copper and the inability to obtain uniform conductivity unless the foundry practice is very closely controlled.

Fig. 7(B) shows a cast-copper secondary with brazed-on water cooling tubes. This type of construction allows the use of thinner secondary sections, making it possible to decrease the impedance of the transformer. It also eliminates the porosity sometimes experienced in casting internal water-cooling tubes. The cooling tubes sometimes collapse during the casting operation, resulting in a defective casting. However, tests indicate that the cooling is usually not as efficient as that which is obtained with cast-in cooling tubes.

Fig. 7(C) shows a secondary fabricated from rolled-copper plate, with water-cooling tubes brazed to the fabricated assembly. Electrolytic rolled copper, having a greater conductivity than cast copper, permits higher current densities to be used, resulting in reduced copper cross section and size. The smoother surface of the rolled-copper secondary results in a lower thermal gradient between the primary and secondary windings. The higher allowable current densities decrease the over-all size of the transformer. This type of construction also allows the designer to use thinner sections for reduced transformer impedance. The most serious disadvantage is the increased cost of construction.

Fig. 7(D) shows a secondary fabricated from copper tubing. Round copper tubing is bent and formed to a rectangular section by a special process. The efficiency of cooling is superior to any of the other types and permits the use of much higher current densities. This type of construction is difficult to manufacture. Minimum radii must be maintained at the bends, resulting in definite limitations to the designer. Because of the much higher current densities used and the smaller section of copper, the unit has relatively low thermal inertia. In other words, the transformer would reach dangerously high operating temperatures in a much shorter time if the cooling water is lost momentarily.

To definitely state which secondary construction is best would be extremely difficult and would lead to an endless argument. All have their advantages and disadvantages; which is used depends on the application, cost, preferences of the individual designer, and available manufacturing facilities.

Insulating Materials

In welding transformers the insulating problems are similar to those found in other low-voltage types. The primary and secondaries must be adequately insulated from each other and both insulated from the core. In general the practice today is to use class *B* insulation throughout, except, in some cases, a small amount of class *A* insulation is used for mechanical purposes. The insulating materials should be oil and water, resistant at the operating temperatures used. One of the problems confronting the designer is water condensation. In high humid weather, if the machine is operated at a reduced capacity, considerable condensation may occur on the secondaries. If this condition exists over prolonged periods, failure may occur if the insulating materials do not have good water-resistant characteristics. Even then, under prolonged periods of condensation, it is difficult to prevent insulating failures. The transformers are often used on hydraulic machines and, despite all precautions, leaks will occur. Therefore the insulating material should also be oil-resistant.

In large welding transformers, the volts per turn seldom exceed 30 volts, thus presenting no difficult insulating problem. Usually mica plate or varnished glass cloth is used. Sometimes the insulating material used is cut slightly wider than the width of the primary copper. However, this has a disadvantage, in that the efficiency of heat transfer between primary and secondary coils is reduced.

The ideal barrier material between primary and secondaries would be one with high dielectric strength, high mechanical strength, and high thermal conductivity. Unfortunately, insulating materials with high dielectric strength have relatively low thermal conductivity. Laminated phenolic material or varnished glass cloth are most widely used as a barrier.

In the past few years some work has been done with silicone insulating materials. These materials can be operated at much higher temperatures than can be safely used with other materials. Experimental units have been built and operated at temperatures exceeding 350 degrees Fahrenheit. The material offers much promise for the future, but at present it is difficult to justify the high cost, unless unusual operating conditions are encountered.

Conclusions

1. AIEE—RWMA standards for transformer ratings have gone a long way towards eliminating the confusion that existed before the standards were adopted.

2. The importance of transformer impedance becomes decreasingly less as the throat area (or load impedance) increases.

3. Losses in a welding transformer assume minor importance, as other factors are more important and high efficiency must not be secured at their expense. More important is welder efficiency (secondary amperes versus kilovolt-amperes input).

4. The excitation current is of no consideration, except as it affects the normal load current, performance, and overall power factor.

5. Major improvements have been made in the performance of welding transformers in the past 20 years, and reliable information on operating characteristics is now available.

References

1. Resistance Welding Manual. Resistance Welder Manufacturers' Association, Philadelphia, Pa., 1946.

2. Electrical Engineers' Handbook, Harold Ponder, William Del Mar. John Wiley and Sons, New York, N. Y., vol. 1, section 10, 1949.

3. Transformer Construction and Operation, Emerson Reed. McGraw-Hill Book Company, New York, N. Y., 1928.

4. Characteristics of Resistance Welding Transformers, F. E. Murray, R. C. Jones. *AIEE Transactions* (*Electrical Engineering*), vol. 65, Nov. 1946, pp. 726–28.

◆

No Discussion

Describing Function Method of Servomechanism Analysis Applied to Most Commonly Encountered Nonlinearities

H. D. GREIF
ASSOCIATE MEMBER AIEE

MOST OF THE literature dealing with the analysis and synthesis of servomechanisms confines itself to treating only linear systems in which all relationships can be expressed mathematically in the form of ordinary differential equations. However, in actual practice many systems are encountered containing elements which exhibit marked nonlinearities. The principal reason for ignoring such nonlinearities in much of the analysis and design of feedback-control systems is mathematical expediency. There is no simple mathematical method available to cope with nonlinear systems. There are certain types of nonlinear differential equations which are solvable, and techniques such as step-by-step solutions exist for more general nonlinear differential equations. Even to use these, however, involves so much tedious labor that the effort is rarely justifiable.[1]

A relatively simple technique for treating some types of nonlinear servomechanisms has been developed in recent years. This technique is based on the assumption that if a sinusoidal signal is applied to a nonlinear element the resulting output of the element can be represented by its fundamental Fourier component. This method of handling the analysis and synthesis of nonlinear feedback-control systems has been referred to as either the describing-function method or the frequency-response method.

A detailed discussion of the frequency-response method, as applied to contactor servomechanisms or discontinuous controllers, is contained in a paper by R. J. Kochenburger.[2] Another paper, written by E. C. Johnson,[3] deals primarily with a rigorous derivation showing the validity of applying the frequency-response method to nonlinear servomechanisms and the inaccuracies that can be expected in employing this method.

The describing-function method can be employed for treating any nonlinear system meeting the requirements that the output of the nonlinear element in response to a sinusoidal input is dominated by the first harmonic of a Fourier series, and that the linear elements of the system sharply attenuate all higher harmonics. Fortunately, most servomechanisms contain elements which act as low-pass filters and thus attenuate all higher harmonics. In general the filtering action tends to improve with the complexity of the system, thus making this method particularly valuable in cases of complicated systems.

Dr. Kochenburger's paper[2] includes a set of curves of the contactor-describing function for various typical contactor characteristics. These curves facilitate the analysis and synthesis of a contactor servomechanism considerably. It is the primary purpose of this paper to present curves of describing functions for other commonly encountered nonlinearities in feedback-control systems. Specifically, curves will be presented for hysteresis, dead space, negative deficiency, saturation, and variable-gain elements.

Theory of Describing-Function Method

In reviewing the theory of the describing-function method, for purposes of concreteness it will be assumed that the physical manifestation of a typical nonlinear servomechanism can be represented by the block diagram of Fig. 1. Although the block diagram appears to represent a very simple system, methods for network transformations make it possible to reduce most practical systems to such a simple form.[4]

The following symbols will be employed (refer to Fig. 1):

$G(s)_{em}$ = transfer function of the series controller
$G(s)_{nc}$ = transfer function of the linear unalterable elements
$G(s)_{cb}$ = transfer function of all linear feedback elements

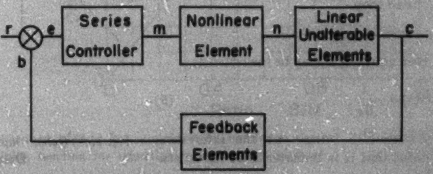

Fig. 1. Block diagram of a typical nonlinear servomechanism system

---

Paper 53-254, recommended by the AIEE Feedback Control Systems Committee and approved by the AIEE Committee on Technical Operations for presentation at the AIEE Summer General Meeting, Atlantic City, N. J., June 15–19, 1953. Manuscript submitted Feb. 24, 1953; made available for printing May 1, 1953.

H. D. Greif is with the Hughes Aircraft Company, Culver City, Calif.

The material presented in this paper is based largely upon results obtained as part of a Master of Science thesis research program conducted by the author at the University of California at Los Angeles. The author wishes to acknowledge with sincere gratitude the many helpful suggestions offered during the course of the research by Professors T. A. Rogers and J. R. Moore of the College of Engineering.

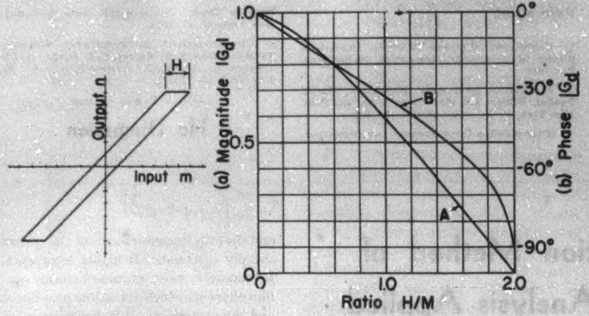

Fig. 2(A) (left). Input-output relation for hysteresis type nonlinear element. (B) (right). Describing function for hysteresis-type nonlinear element

G_d = equivalent transfer function of the nonlinear element, referred to as the describing function

The describing-function method is based on the assumption that the input or driving force *m* impressed on the nonlinear element is sinusoidal, and that the resulting response of the element *n* can be represented satisfactorily, as far as the overall system performance is concerned, by its fundamental Fourier component. The describing function G_d is therefore simply the amplitude and phase of the fundamental component of the response, relative to the assumed driving sinusoid. The derivation of equations for determining G_d for various types of nonlinearities is given in the Appendix.

Treating G_d just like any ordinary transfer function, the overall sinusoidal response characteristic of the system shown in Fig. 1 can be expressed as

$$\frac{c}{r}=\frac{G(s)_{em}G(s)_{nc}G_d}{1+G(s)_{em}G(s)_{nc}G(s)_{cb}G_d} \tag{1}$$

Consideration of equation 1 shows that the system will become unstable when

$$1+G(s)_{em}G(s)_{nc}G(s)_{cb}G_d=0 \tag{2}$$

or

$$G(s)_{em}G(s)_{nc}G(s)_{cb}=-\frac{1}{G_d} \tag{3}$$

If $G(s)$ is now defined as the product of all the linear transfer functions around the closed loop.

$$G(s)\equiv G(s)_{em}G(s)_{nc}G(s)_{bc} \tag{4}$$

then equation 3 may be rewritten as

$$G(s)=-\frac{1}{G_d} \tag{5}$$

Equation 5 brings out the interesting point that it is immaterial as far as stability is concerned where the nonlinearity occurs, either in the forward or the feedback part of the loop.

The describing-function method can be used in conjunction with either the familiar Nyquist stability criterion[5] or the root-locus technique,[6] depending on the exact nature of the problem. If the Nyquist criterion is used, only two curves in the complex plane must be plotted. One is the locus of the negative reciprocal of the describing function $-1/G_d$ and the other is the locus of the product of the linear transfer functions around the loop $G(s)$. The application of the root-locus technique is quite simple in those cases where the nonlinearity introduces no phase shift; however, in the more general case where there is a phase shift due to the nonlinear element, the application of the root-locus method requires the construction of a family of root loci for various angles of $G(s)$. The application of both the Nyquist stability criterion and the root-locus technique will be explained in greater detail in an example further on in this paper.

In discussing the various types of nonlinearities in this paper, two assumptions are always made. First, the nonlinearity must be symmetrical about the zero point. For simplicity the equations were all set up on this basis, and hence the values of the describing function are correct only if this assumption applies. Second, the gain of the nonlinear element must be unity. Although this second assumption frequently does not apply to a nonlinear element, it is a simple matter to break up the element into two separate units; one becomes a constant gain unit that can be lumped in with the linear elements, and the other becomes the nonlinear element with the required unity gain.

Describing Functions for Typical Nonlinearities

Hysteresis, backlash, or free play are frequently encountered nonlinearities in elements of servomechanisms. Some good examples are hysteresis in magnetic elements (although this is idealized here in assuming sharp breaks in the hysteresis loop and no saturation), backlash in gear trains, or free play in mechanical linkages. In any of the above examples output follows input after sufficient change, but always remains behind a certain fixed amount. Upon reversal of the input, the output remains constant until the input has proceeded by this fixed amount in the reverse direction. Since hysteresis, backlash, and free play are essentially similar in nature, they may all be treated together. Whenever the term hysteresis is used in a statement it may be considered

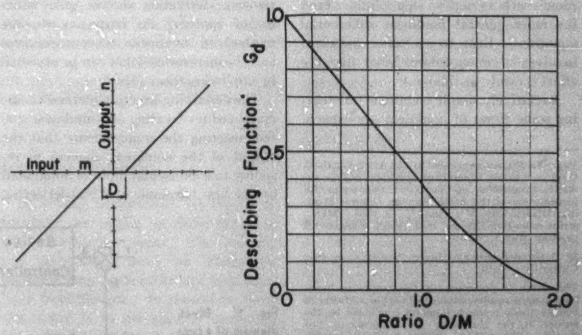

Fig. 3(A) (left). Input-output relation for dead-space-type nonlinear element. (B) (right). Describing function for dead-space-type nonlinear element

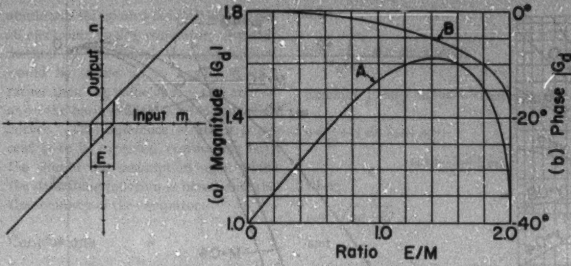

Fig. 4(A) (left). Input-output relation for negative-deficiency-type nonlinear element. (B) (right). Describing function for negative-deficiency-type nonlinear element

equally applicable to backlash or free play.

As mentioned earlier, let it be assumed that the hysteresis is symmetrical and the gain of the element is unity. Since an equation relating input and output of a hysteresis element cannot be written easily, it is simpler to describe the relationship geometrically as shown in Fig. 2(A). The symbol H is used for the width of the hysteresis loop, and must obviously be expressed in the same units as the input m. The amplitude and phase of the fundamental Fourier component of the response relative to the assumed driving sinusoid is derived in the Appendix, and is shown graphically in Fig. 2(B) for a hysteresis type element. The symbol M is used to denote the peak amplitude of the input, that is, $m = M \sin \omega t$, as explained in the Appendix.

Dead space is another commonly encountered nonlinearity in various elements of servomechanisms. Dead space is also sometimes referred to as positive deficiency or inert zone. One good example of dead space is a fluid pilot valve with "underlapped" ports. The input-output relation for a dead-space type element is shown in Fig. 3(A), and the corresponding describing function in Fig. 3(B). The symbol D is used to denote the total dead space, and must also be expressed in the same units as the input m.

Negative deficiency, superfluency, overlap, or click-over are the terms generally used to describe the nonlinearity that is just the reverse of dead space. A good example of an element in which negative deficiency is often present is a vane type torquer. The input-output relation for a negative-deficiency element is shown in Fig. 4(A), and the corresponding describing function in Fig. 4(B). The symbol E is used to denote the total deficiency, and is expressed in the same units as the input m.

Saturation or limiting is another type of nonlinearity frequently encountered in elements of servomechanisms. Good examples are motion stops, valve limits, magnetic saturation, or any other kind of inherent or artificially imposed limit. Fig. 5(A) shows the input-output relation for a saturation element, and Fig. 5(B) shows the corresponding describing function. The symbol B is used to denote the input at which saturation starts.

The last element included here is one having variable gain. A good example of an element displaying this characteristic is an ordinary fluid-flow-measuring device, where the output is proportional to the square of the flow. The input-output relation for a variable gain element can be expressed very simply as

$$n = m^y \text{ where } y > -2 \tag{6}$$

The describing function of a variable gain element is shown in Fig. 6.

Illustrative Example

In order to give a clearer picture of the application of the describing-function method, in conjunction with either the Nyquist stability criterion or the root-locus method, a typical simple example of a nonlinear system will now be considered. Let the linear transfer function of all the elements around the loop be given by

$$G(s) = \frac{K}{s(1+0.1s)(1+0.5s)} \tag{7}$$

Furthermore, let the system include a hysteresis-type nonlinear element such that

$$H = 0.5 \tag{8}$$

Thus, knowing the value of H, the describing function G_d can be readily ascertained from Fig. 2(B) as a function of the amplitude of the input to the nonlinear element M.

If the Nyquist criterion is employed, the next step is to compute the locus of $G(s)$ by substituting various values of $j\omega$ for s in equation 7. The loci of $G(s)$ and $-1/G_d$ are then plotted in the complex plane. Fig. 7 shows such a plot for this example for values of $K = 8.0$, 4.95, and 4.0, respectively. The locus of $-1/G_d$ can be thought of as the locus of the critical point corresponding to the $(-1, j0)$ point in conventional servomechanism theory. When the critical point lies to the right of the $G(s)$ locus, the poles have positive real roots and the system tends to be unstable. As can be seen readily from Fig. 7, when the gain $K = 4.0$, the system is completely stable. When the

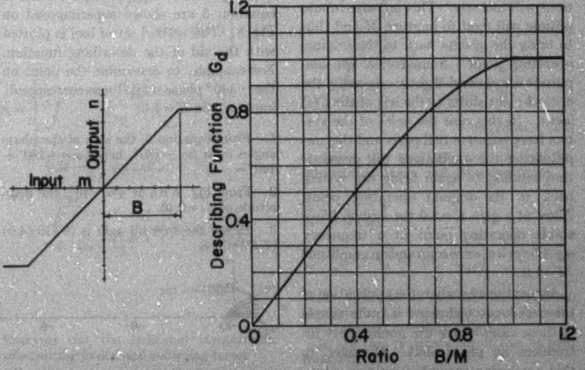

Fig. 5(A) (left). Input-output relation for saturation-type nonlinear element. (B) (right). Describing function for saturation-type nonlinear element

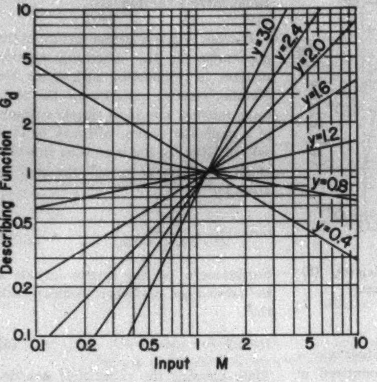

Fig. 6. Describing function for variable-gain element, $n=m^y$

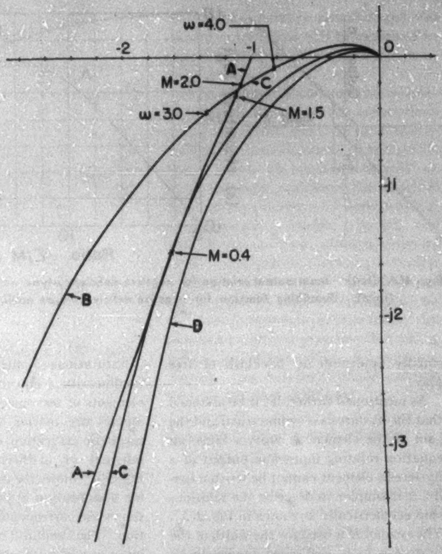

Fig. 7. Complex plane plot

(A). $-1/G_d$ for $H=1/2$

(B), (C), and (D). $G(s)=\frac{K}{s(1+0.1s)(1+0.5s)}$ for $K=4.0$, 4.95, and 8.0

gain is increased to $K=4.95$, the $G(s)$ locus is just tangent to the $-1/G_d$ locus, and hence this is the maximum gain for which the system is stable. (It might be noted at this point that this same system without hysteresis would be stable up to a gain $K=12.0$.) When the gain is increased further, as for the case of $K=8.0$, shown in Fig. 7, the $G(s)$ and the $-1/G_d$ loci intersect. Suppose the system is initially operating at a point corresponding to the intersection of the two loci, that is, a frequency $\omega=3.5$ cycles per second, and an amplitude of the input into the nonlinear element, $M=1.8$. If the amplitude M is decreased slightly for any reason whatsoever, the critical point will shift to the right of the $G(s)$ locus. Since the poles of the system now have positive real parts, the amplitude of the oscillations will increase. This increase in amplitude will tend to increase M and thus to bring the system back to the original operating point. Similarly, if the amplitude is increased slightly originally, the critical point shifts to the left of the $G(s)$ locus. In this case the poles of the system have negative real parts and the amplitude of the oscillations will decrease, thus tending to again bring the system back to its original operating point. Thus, at a gain $K=8.0$ the system has a stable operating point at a frequency $\omega=3.5$ cycles per second and an amplitude $M=1.8$.

As mentioned earlier, the application of the root-locus technique is quite simple in those cases where the nonlinearity introduces no phase shift. However, in this particular example involving a hysteresis element, the application of the root-locus method requires the construction of a family of root loci for various angles of $G(s)$, since G_d introduces a phase shift. Fig. 8 shows the phase angle loci of $G(s)$ for $-180°$, $-170°$, $-160°$, $-150°$, $-140°$, and $-130°$. Since the loci above and below the real axis are symmetrical, only the loci in the upper half-plane are shown. Another set of loci satisfying both the magnitude and phase requirements of equation 5 are shown superimposed on Fig. 8. This second set of loci is plotted with the aid of the describing function. For example, to determine the point on the $-140°$ phase-angle locus corresponding to a gain $K=4.0$:

1. From equation 5, the sum of the phase angles must be $-180°$, hence $\phi=-180°+140°=-40°$.
2. From Fig. 2(B), at $\phi=-40°$, the magnitude of $G_d=0.46$.
3. Hence the over-all gain is $(2)(10)(4.0)(0.46)=36.8$.
4. The points on the $-140°$ locus satisfying equation 5 occur where the product of all the vectors is 36.8. These points are located by trial and error.

In order to verify the validity of the describing-function method, the above ex-

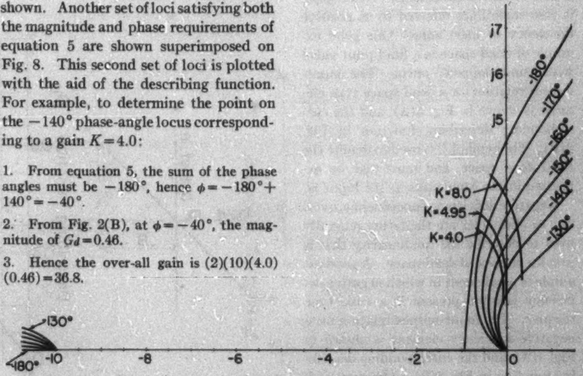

Fig. 8. Root locus of $G(s)=\frac{K}{s(1+0.1s)(1+0.5s)}$ and gain loci for hysteresis element where $H=1/2$

ample was set up on a *GAP/R* high-speed all-electronic analog computor. By this method it was found that the system would be stable up to a gain $K=5.2$ rather than the value of $K=4.95$ arrived at on the basis of the describing-function curves. This difference of about 5 per cent is to be expected, considering both the simplifying assumption upon which the describing function is based and also the accuracy of the computor.

Conclusions

A few simple graphs have been plotted which make it relatively easy to predict the behavior of a servomechanism containing a component whose characteristics include either hysteresis, dead space, negative deficiency, saturation, or variable gain. In most cases, the outlined method of treating nonlinear elements is accurate to within 5 to 10 per cent, which is sufficiently good for most engineering-design calculations. In general, in the case of the Nyquist stability criterion, the greatest accuracy can be expected when the intersection between the $G(s)$ locus and the $-1/G_d$ locus is perpendicular, while the least accuracy can be expected when the two loci approach each other almost tangentially.

The describing function curves are not only valuable tools in predicting the stability of a servomechanism containing a nonlinear element, but also in finding the proper network to possibly improve the performance of such a system. They are also useful in some cases where the performance of a linear system may be improved by purposely introducing a nonlinearity in one of the components. For example, if small sustained oscillations are permissible, it is sometimes possible to increase the gain of a system quite considerably by designing either saturation or the proper type of variable gain into one of the components.

Appendix

The output n of any nonlinear element in response to a sinusoidal input m, where

$$m=M\sin\omega t \tag{9}$$

can be expressed as a Fourier series

$$n=\frac{a_0}{2}+a_1\cos\omega t+b_1\sin\omega t+a_2\cos 2\omega t+b_2\sin 2\omega t+\dots \tag{10}$$

where

$$a_i=\frac{2}{\pi}\int_0^\pi n(t)\cos i\omega t d(\omega t) \tag{11}$$

and

$$b_i=\frac{2}{\pi}\int_0^\pi n(t)\sin i\omega t d(\omega t) \tag{12}$$

Equation 10 may also be written in the form

$$n=\frac{c_0}{2}+c_1\sin(\omega t+\phi_1)+c_2\sin(2\omega t+\phi_2)+\dots \tag{13}$$

where

$$c_i=\sqrt{a_i^2+b_i^2} \tag{14}$$

and

$$\phi_i=\tan^{-1}\frac{a_i}{b_i} \tag{15}$$

Since the describing function method is based on the assumption that all harmonics except the fundamental are negligible, the describing function is

$$G_d=\frac{c_1}{M}\underline{/\phi} \tag{16}$$

In the case of hysteresis, it can be seen from Fig. 2(A) that

$$n=M-\frac{H}{2} \text{ for } \frac{\pi}{2}\leqq\omega t\leqq\pi-\sin^{-1}\frac{M-H}{M} \tag{17A}$$

$$n=m+\frac{H}{2} \text{ for } \pi-\sin^{-1}\frac{M-H}{M}\leqq\omega t\leqq\frac{3\pi}{2} \tag{17B}$$

Substituting equation 17 in equations 11 and 12

$$a_1=\frac{2}{\pi}\left[\int_{\frac{\pi}{2}}^{\pi-\sin^{-1}\frac{M-H}{M}}\left(M-\frac{H}{2}\right)\cos\omega t d(\omega t)+\int_{\pi-\sin^{-1}\frac{M-H}{M}}^{\frac{3\pi}{2}}\left(M\sin\omega t+\frac{H}{2}\right)\times\cos\omega t d(\omega t)\right] \tag{18}$$

$$b_1=\frac{2}{\pi}\left[\int_{\frac{\pi}{2}}^{\pi-\sin^{-1}\frac{M-H}{M}}\left(M-\frac{H}{2}\right)\sin\omega t d(\omega t)+\int_{\pi-\sin^{-1}\frac{M-H}{M}}^{\frac{3\pi}{2}}\left(M\sin\omega t+\frac{H}{2}\right)\times\sin\omega t d(\omega t)\right] \tag{19}$$

Carrying out the indicated integrations, substituting limits, and collecting terms

$$\frac{a_1}{M}=\frac{H}{\pi M}\left(\frac{H}{M}-2\right) \tag{20}$$

$$\frac{b_1}{M}=\frac{1}{\pi}\left[\frac{\pi}{2}+\sin^{-1}\frac{M-H}{M}+\left(\frac{M-H}{M}\right)\cos\sin^{-1}\frac{M-H}{M}\right] \tag{21}$$

From equations 20 and 21 the describing function for a hysteresis-type nonlinear element is readily computed.

In the case of dead space, it can be seen from Fig. 3(A) that

$$n=m-\frac{D}{2} \tag{22}$$

$$\text{for } \sin^{-1}\frac{D}{2M}\leqq\omega t\leqq\pi-\sin^{-1}\frac{D}{2M}$$

Inasmuch as the fundamental of the output is in phase with the input in the case of symmetrical dead space, it can be seen that

$$a_1=0 \tag{23}$$

Substituting equation 22 in equation 12

$$b_1=\frac{2}{\pi}\int_{\sin^{-1}\frac{D}{2M}}^{\pi-\sin^{-1}\frac{D}{2M}}\left(M\sin\omega t-\frac{D}{2}\right)\times\sin\omega t d(\omega t) \tag{24}$$

Carrying out the indicated integration, substituting limits and collecting terms

$$\frac{b_1}{M}=1-\frac{2}{\pi}\sin^{-1}\frac{D}{2M}-\frac{D}{\pi M}\cos\sin^{-1}\frac{D}{2M} \tag{25}$$

From equation 25, the describing function for a dead-space type nonlinear element is readily computed.

In the case of negative deficiency, it can be seen from Fig. 4(A) that

$$n=m+\frac{E}{2} \text{ for } \sin^{-1}\frac{E}{2M}\leqq\omega t\leqq\pi+\sin^{-1}\frac{E}{2M} \tag{26}$$

Substituting equation 26 in 11 and 12

$$a_1=\frac{2}{\pi}\int_{\sin^{-1}\frac{E}{2M}}^{\pi+\sin^{-1}\frac{E}{2M}}\left(M\sin\omega t+\frac{E}{2}\right)\times\cos\omega t d(\omega t) \tag{27}$$

$$b_1=\frac{2}{\pi}\int_{\sin^{-1}\frac{E}{2M}}^{\pi+\sin^{-1}\frac{E}{2M}}\left(M\sin\omega t+\frac{E}{2}\right)\times\sin\omega t d(\omega t) \tag{28}$$

Carrying out the indicated integrations, substituting limits, and collecting terms

$$\frac{a_1}{M}=-\frac{1}{\pi}\left(\frac{E}{M}\right)^2 \tag{29}$$

$$\frac{b_1}{M}=\frac{1}{\pi}\left(\pi+\frac{2E}{M}\cos\sin^{-1}\frac{E}{2M}\right) \tag{30}$$

From equations 29 and 30, the describing function for a negative-deficiency type nonlinear element is readily computed.

In the case of saturation, it can be seen from Fig. 5(A)

$$n=B \text{ for } \sin^{-1}\frac{B}{M}\leqq\omega t\leqq\pi-\sin^{-1}\frac{B}{M} \tag{31A}$$

$$n=m \text{ for } \pi-\sin^{-1}\frac{B}{M}\leq\omega t\leq\pi+\sin^{-1}\frac{B}{M} \tag{31B}$$

In as much as the fundamental of the output is in phase with the input in the case of saturation, it can be readily seen that

$$a_1=0 \tag{32}$$

Substituting equation 31 in equation 12

$$b_1=\frac{2}{\pi}\left[\int_{\sin^{-1}\frac{B}{M}}^{\pi-\sin^{-1}\frac{B}{M}} B\sin\omega t\, d(\omega t)+\int_{\pi-\sin^{-1}\frac{B}{M}}^{\pi+\sin^{-1}\frac{B}{M}}(M\sin\omega t)\sin\omega t d(\omega t)\right] \tag{33}$$

Performing the indicated integration, substituting limits, and collecting terms

$$\frac{b_1}{M}=\frac{2}{\pi}\left[\sin^{-1}\frac{B}{M}+\frac{B}{M}\cos\sin^{-1}\frac{B}{M}\right] \tag{34}$$

From equation 34, the describing function for a saturation-type nonlinear element is readily computed.

In the case of variable gain, since the output is in phase with the input, it can be readily seen that

$$a_1=0 \tag{35}$$

Substituting equation 6 in equation 12

$$b_1=\frac{4}{\pi}\int_0^{\frac{\pi}{2}}(M\sin\omega t)^y\sin\omega t d(\omega t)$$

$$=\frac{4}{\pi}M^y\int_0^{\frac{\pi}{2}}(\sin\omega t)^{y+1}d(\omega t) \tag{36}$$

Let

$$y+1\equiv z \tag{37}$$

Then

$$b_1=\frac{4}{\pi}M^y\int_0^{\frac{\pi}{2}}(\sin\omega t)^z d(\omega t) \tag{38}$$

$$\frac{b_1}{M}=\frac{4}{\pi}M^{y-1}\left[\frac{\sqrt{\pi}\,\Gamma\frac{z+1}{2}}{2\Gamma\frac{z+2}{2}}\right]$$

$$=\frac{2}{\sqrt{\pi}}M^{y-1}\left[\frac{\Gamma\frac{z+1}{2}}{\Gamma\frac{z+2}{2}}\right] \tag{39}$$

Then, with the aid of a table of Gamma functions, the describing function for a variable gain nonlinear element is readily computed from equation 39.

References

1. Automatic Feedback Control (book), **W. R. Ahrendt, J. F. Taplin.** McGraw-Hill Book Company, Inc., New York, N. Y., chapter 8, 1951.

2. A Frequency Response Method for Analyzing and Synthesizing Contactor Servomechanisms, **Ralph J. Kochenburger.** *AIEE Transactions*, vol. 69, pt. I, 1950, pp. 270–84.

3. Sinusoidal Analysis of Feedback-Control Systems Containing Nonlinear Elements, **E. Calvin Johnson.** *AIEE Transactions*, vol. 71, pt. II, July 1952, pp. 169–81.

4. Block Diagram Network Transformation **T. D. Graybeal.** *Electrical Engineering*, vol. 70, Nov. 1951, pp. 985–90.

5. Principles of Servomechanisms, **G. S. Brown, D. P. Cambell.** John Wiley and Sons, Inc., New York, N. Y., chapters 6 and 7, 1948.

6. Control System Synthesis by Root Locus Method, **Walter R. Evans.** *AIEE Transactions*, vol. 69, pt. I, 1950, pp. 66–69.

◆

No Discussion

Aircraft Protection from Thunderstorm Discharges to Antennas

J. M. BRYANT
FELLOW AIEE

M. M. NEWMAN
ASSOCIATE MEMBER AIEE

J. D. ROBB
ASSOCIATE MEMBER AIEE

Synopsis: The transport aircraft is inherently provided nearly complete thunderstorm-discharge protection by the metal fuselage, which forms a safe path for discharge currents that the aircraft may intercept. External elements such as movable surfaces and antennas can be protected. Airline experiences have shown that antennas frequently intercept discharges; a current surge conducted along the antenna lead-in frequently damages radio equipment and, in some cases, has resulted in fires. An effective antenna-protection unit was consequently developed, which besides protecting the ratio equipment, also records the bypassed current and charge magnitudes. Analysis of the sphere-gap pitting indicates the total-charge transfer, and small magnetic links indicate the peak currents by their magnetization. Because of the research importance of the data, these experimental units have been made available to airlines interested in cooperating with the Lightning and Transients Research Institute's program of protection researches. The discharge-current records and supplementary information from questionnaires are providing data for improved protection, and also help resolve statistically such questions as discharge-probability variations to be expected with various operating factors of geographical location, altitude, temperature, and size and speed of the aircraft.

AIRCRAFT FLYING under thunderstorm conditions may intercept electrical discharges. These discharges may be between different cloud-charge areas, or in a channel progressing towards and terminating at ground; they differ from familiar concepts of lightning only to the degree that they are most generally in lower-current regions of lightning channels. However, a low-flying aircraft may intercept a main discharge channel, and therefore discharge protection must also be adequate for the higher current intensities encountered in lightning strokes to ground.

Both theory and experience prove that the metal surface of the aircraft inherently forms a safe discharge-current-diverting path around occupants and equipment in the interior. However, it has been determined that certain external elements such as movable control surfaces, plastic sections, and outside antennas require protection.

Development of aircraft protective methods has been continuing at the Lightning and Transients Research Laboratory, in co-operation with several airlines and under research programs sponsored by the Office of Naval Research and the Navy Department's Bureau of Aeronautics and, more recently, by the Air Force's Wright Air Development Center.

Consequent progress in protective methods was presented and discussed with aircraft manufacturer's and airline participation in a Symposium under the Navy's Bureau of Aeronautics sponsored program

---

Paper 53-196, recommended by the AIEE Transportation Committee and approved by the AIEE Committee on Technical Operations for presentation at the AIEE Summer General Meeting, Atlantic City, N. J., June 15–19, 1953. Manuscript submitted March 25, 1952; made available for printing March 27, 1953.

J. M. Bryant is with the University of Minnesota, Minneapolis, Minn., and M. M. Newman and J. D. Robb are with the Lightning and Transients Research Institute, Minneapolis, Minn.

Acknowledgment is made of research support of the Navy Department, Office of Naval Research, and Bureau of Aeronautics, of the Air Force, Wright Air Development Center, and of the co-operation of American Airlines and the Joslyn Manufacturing Company in flight evaluation and development of the lightning protector.

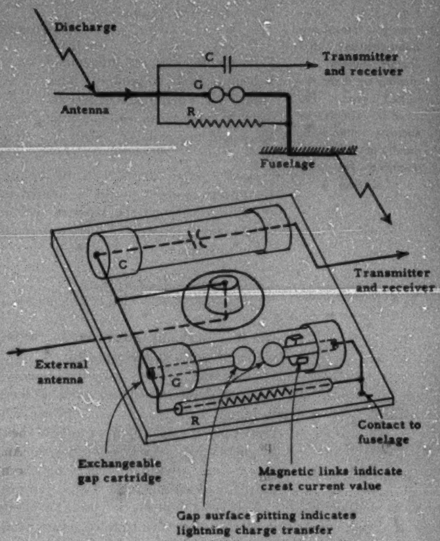
Discharge
C
Transmitter and receiver
G
Antenna
R
Fuselage
C
Transmitter and receiver
External antenna
G
R
Contact to fuselage
Exchangeable gap cartridge
Magnetic links indicate crest current value
Gap surface pitting indicates lightning charge transfer

Fig. 1 (above). Schematic diagram and illustrative sketch of protective and current-recording arrester for discharges to antenna

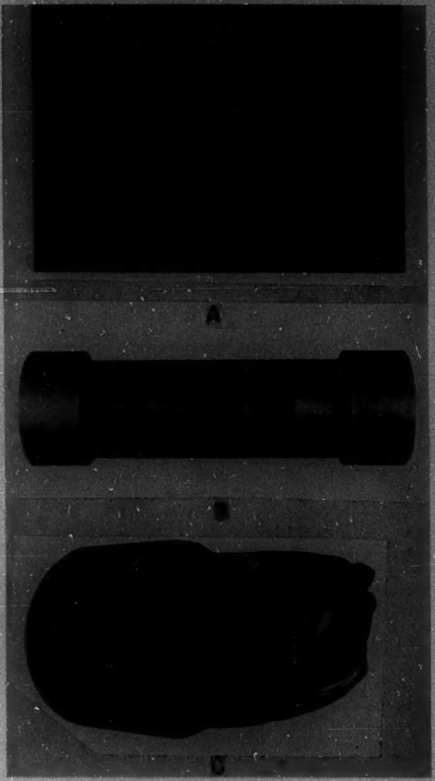

Fig. 2. Aircraft antenna-protective unit and typical gap cartridges

A. Aircraft antenna protective recorder
B. Gap cartridge which intercepted a discharge to the antenna of about 25,000 amperes, 10- to 20-microsecond duration. Magnetic strips record crest current values, and character of sputtering indicates types of discharge
C. Melting of gap sphere by intercepted long-duration discharge to the aircraft antenna of about 100 coulombs, though crest current did not exceed 5,000 amperes. Most of the gap records were of this long duration type

at the Lightning and Transients Research Institute.[1]

The greatest need of improved protection for transport aircraft proved to be in relation to discharges to external antennas entering inside the aircraft, damaging equipment, and occasionally starting fires. A protective scheme, developed under our Office of Naval Research program, as presented in the Symposium proceedings,[1] was since used successfully on an experimental basis by American Airlines, and is presented in this paper.

Protection from Discharges to Antennas

From records of airline experiences, it is seen that antennas frequently intercept discharges. A current surge conducted along the antenna lead-in frequently damages radio equipment and, in some cases, has resulted in fires. Simple bypass gaps which have been in use at the antenna post are ineffective for many discharge-current wave shapes, as indicated by airline experiences, and vividly illustrated by the following excerpt from a pilot's report:

> "Checked ship for damage, found wires leading in from top antenna burned to a powder. Both transmitter and receiver on high frequency burned out. Flight engineer's hat sitting in radio rack was full of small holes."

An effective antenna-protection unit, shown in Figs. 1 and 2, was consequently developed which, besides protecting the radio equipment, also records the bypassed lightning-current and charge magnitudes. The principal merit of the method described is that it provides protection against all types of discharge-current surges, regardless of wave shape, with a minimum of energy transfer into the radio equipment.

The operation of this protective method is as follows: A capacitor *C*, as shown in Fig. 1, having approximately ten times the capacity of the antenna, is placed in series with the antenna lead-in wire, and as close to the feed-through insulator as possible. A spark gap *G* to ground is provided from the antenna side of the capacitor, to divert the discharge current to the structure of the airplane. The setting of the spark gap should be such

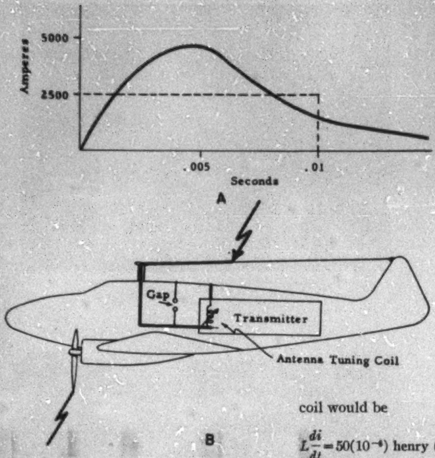
Amperes
5000
2500
.005
.01
Seconds
A
Gap
Transmitter
Antenna Tuning Coil
B

Fig. 3(A). Low-current rate-of-rise thunderstorm discharge current indicated by flight returned gaps. (B) Lead-in circuit to antenna tuner with usually provided gap intended for protection

that transmitter voltages will not cause it to arc over. The capacitor should have a breakdown voltage higher than that of the spark gap, with adequate safety margin. When discharges strike the antenna, the capacitor will charge to the spark-gap breakdown voltage, and the discharge current will be diverted across the gap to the aircraft structure. Thus the maximum surge energy that can go to the radio equipment is the charging energy for the series capacitor, which is relatively negligible. For a typical case of a gap set for 10,000 volts and a 1,000-micromicrofarad protection capacitor, the energy transfer would be

$$\frac{1}{2}CE^2=\frac{1}{2}(10^{-9}\text{farad})(10^4\text{ volts})^2=0.05\text{ joule}$$

The purpose of the resistor R is to bleed stray charge off the antenna, which might otherwise cause corona and associated radio interference.

The need for the series capacitor, in addition to the gap used heretofore, is illustrated by the following considerations: Many strokes to aircraft involve relatively low-current rates of rise, as indicated in later paragraphs on flight researches. A typical discharge of this type is shown in Fig. 3(A). Such a discharge would not necessarily flash a simple gap, as may be shown by reference to the circuit of Fig. 3(B). This input circuit, with simple gap protection at the feed-through point, consists essentially of an antenna-tuning inductance of about 50 microhenries between the lead-in and the aircraft skin. With the current wave of Fig. 3, the maximum voltage across the coil would be

$$L\frac{di}{dt}=50(10^{-6})\text{ henry }(10^6)\text{ amperes per second}=50\text{ volts}$$

which is considerably less than that required to flash the protective gap, which must be set higher than possible transmitter voltages of 5,000 to 10,000 volts. The charge transfer for this current wave would be the integral of the current waveshape, and therefore would be approximately

$$(0.01\text{ second})(2{,}500\text{ amperes})=25\text{ coulombs}$$

a charge transfer not uncommon for a lightning stroke to ground. This charge transfer, in a period of 0.01 second is sufficient to damage an antenna-tuning coil, but would not, as shown, flash a protective gap.

With a series capacitor in this circuit, the charge transfer would be limited to the charge through the capacitor before the gap breaks down and therefore would be, in this case

$$CE=1(10^{-9}\text{ farads})(5{,}000\text{ volts})=5\times10^{-6}\text{ coulombs}$$

which is negligible compared to the 25 coulombs without the capacitor.

Recording features are simply incorporated by mounting steel strips, as seen in Figs. 1 and 2, so located as to indicate crest-current values by the degree of their magnetization. Analysis of the sphere-gap pitting, after a discharge has been passed, indicate the total charge transfer.

New types of protection units are being developed for very-high-frequency stub antennas, and for high altitude operations as shown in Figs. 4(A) and 4(B). The unit for very-high-frequency stub antennas is being designed with coaxial fittings so that the unit will merely be inserted at the point where the trans-

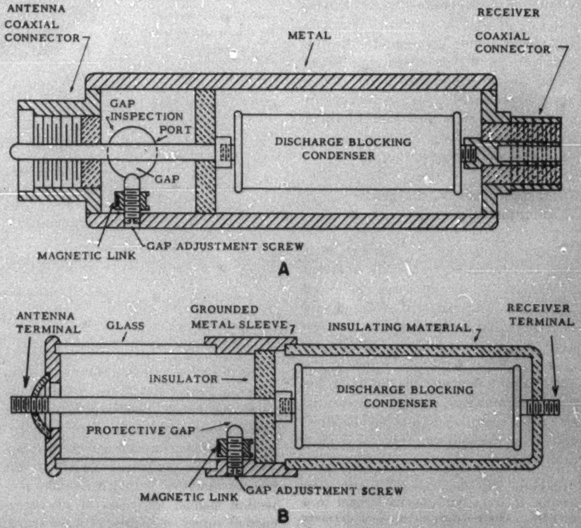
ANTENNA COAXIAL CONNECTOR
METAL
RECEIVER COAXIAL CONNECTOR
GAP INSPECTION PORT
DISCHARGE BLOCKING CONDENSER
GAP
MAGNETIC LINK
GAP ADJUSTMENT SCREW
A
ANTENNA TERMINAL
GLASS
GROUNDED METAL SLEEVE
INSULATING MATERIAL
RECEIVER TERMINAL
INSULATOR
DISCHARGE BLOCKING CONDENSER
PROTECTIVE GAP
MAGNETIC LINK
GAP ADJUSTMENT SCREW
B

Fig. 4(A). Very-high-frequency coaxial antenna protection unit. (B) High-altitude antenna-protection unit

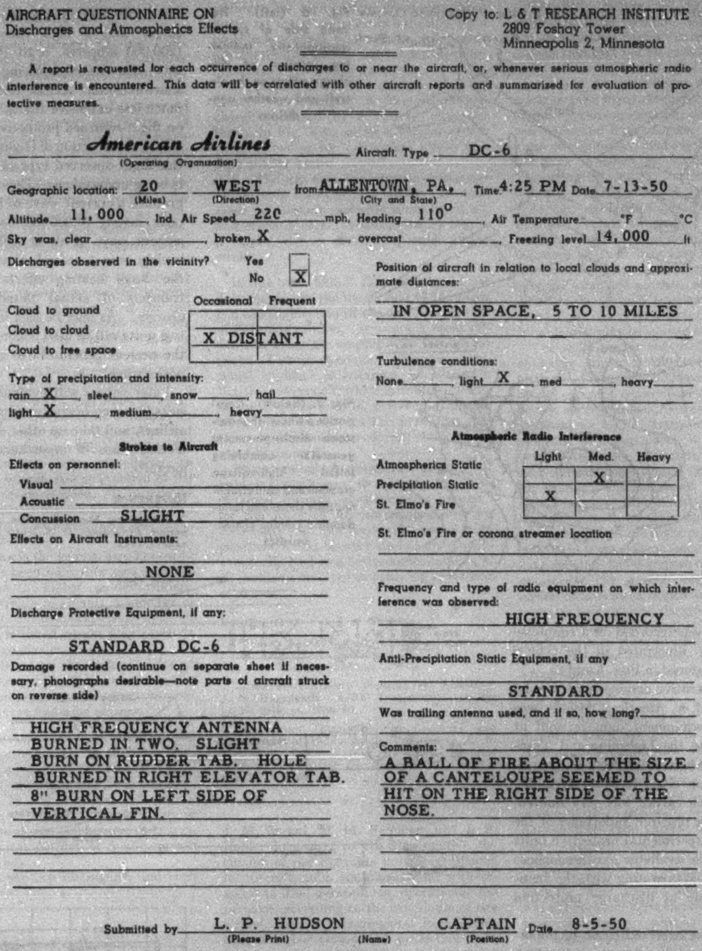

AIRCRAFT QUESTIONNAIRE ON
Discharges and Atmospherics Effects

Copy to: L & T RESEARCH INSTITUTE
2809 Foshay Tower
Minneapolis 2, Minnesota

A report is requested for each occurrence of discharges to or near the aircraft, or, whenever serious atmospheric radio interference is encountered. This data will be correlated with other aircraft reports and summarized for evaluation of protective measures.

American Airlines (Operating Organization) Aircraft Type DC-6

Geographic location: 20 (Miles) WEST (Direction) from ALLENTOWN, PA. (City and State) Time 4:25 PM Date 7-13-50

Altitude 11,000 Ind. Air Speed 220 mph. Heading 110° Air Temperature ____ °F ____ °C

Sky was, clear ____, broken X, overcast ____, Freezing level 14,000 ft

Discharges observed in the vicinity? Yes ☐ No ☒

	Occasional	Frequent
Cloud to ground		
Cloud to cloud	X DISTANT	
Cloud to free space		

Type of precipitation and intensity:
rain X, sleet ____, snow ____, hail ____
light X, medium ____, heavy ____

Strokes to Aircraft

Effects on personnel:
Visual ____
Acoustic ____
Concussion SLIGHT

Effects on Aircraft Instruments:
NONE

Discharge Protective Equipment, if any:
STANDARD DC-6

Damage recorded (continue on separate sheet if necessary, photographs desirable—note parts of aircraft struck on reverse side)
HIGH FREQUENCY ANTENNA BURNED IN TWO. SLIGHT BURN ON RUDDER TAB. HOLE BURNED IN RIGHT ELEVATOR TAB. 8" BURN ON LEFT SIDE OF VERTICAL FIN.

Position of aircraft in relation to local clouds and approximate distances:
IN OPEN SPACE, 5 TO 10 MILES

Turbulence conditions:
None ____, light X, med ____, heavy ____

Atmospheric Radio Interference

	Light	Med.	Heavy
Atmospherics Static		X	
Precipitation Static	X		
St. Elmo's Fire			

St. Elmo's Fire or corona streamer location

Frequency and type of radio equipment on which interference was observed:
HIGH FREQUENCY

Anti-Precipitation Static Equipment, if any
STANDARD

Was trailing antenna used, and if so, how long? ____

Comments:
A BALL OF FIRE ABOUT THE SIZE OF A CANTELOUPE SEEMED TO HIT ON THE RIGHT SIDE OF THE NOSE.

Submitted by L. P. HUDSON (Please Print) (Name) CAPTAIN (Position) Date 8-5-50

Fig. 5. Typical questionnaire return involving a discharge to the antenna. The protective recording arrester prevented damage to equipment

mission line connects to the antenna mast. The entire unit would be replaced, in event of a discharge, by unscrewing the connectors and replacing with a new unit. The size of this unit can be varied to meet the power requirements of the particular equipment: for low-power very-high-frequency equipment the unit should be no larger than a few cable diameters. The unit shown in Fig. 4(B) would replace the present protection units where high-altitude operation required greater leakage distance.

Through the initiative and co-operation of American Airlines, fifty of the experimental protective and recording units were placed in operation over a 2-year period. Whenever the antenna was struck, the protective gap cartridge was replaced by a spare and the original gap sent to the Lightning and Transients Research Institute for analysis. The gap shown enlarged in Fig. 2(C) is typical of about 90 per cent of the returns. In all cases, the protective unit provided protection to the equipment and, at the same time, also contributed new data. It was thus determined that most of the intercepted discharges were of low current magnitudes (of the order of 5,000 amperes) but of relatively long duration and high-charge (of the order of 100 coulombs) transfer. Related data on the discharge

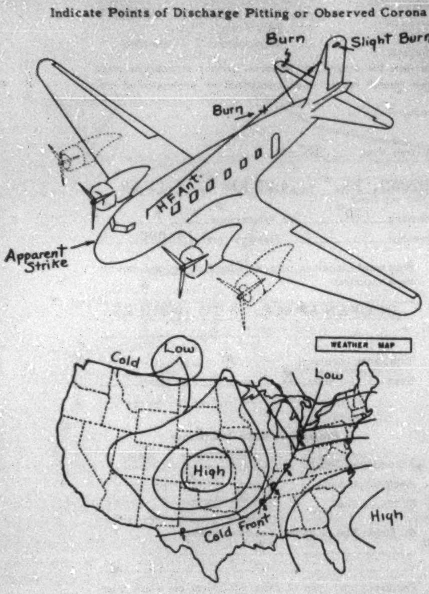
Indicate Points of Discharge Pitting or Observed Corona
Burn
Slight Burn
Burn
HF Ant.
Apparent Strike
WEATHER MAP
Cold
Low
Low
High
Cold Front
High

Fig. 6 (left). Reverse side of typical questionnaire, indicating location of discharge points on the aircraft and weather conditions

encountered was recorded on a simplified questionnaire, illustrated in the typical returns reproduced in Figs. 5 and 6.

This co-operative arrangement worked out very well, as American Airlines was saved radio-equipment damage, and at the same time the Lightning and Transients Research Institute received quantitative data on cloud-to-cloud type discharges, which earlier was very limited. Because of the research importance of the data, these experimental protective units are being made available to other airlines interested in co-operating with the Institute's program of discharge protection researches.

The data are expected to be of importance in determining the extent to which protection safety margins need to be carried. Also, the data from the returned gaps and questionnaire program should eventually resolve questions as to intensity of discharge currents at various altitudes and locations. Through wider and continued use of the questionnaires it is hoped to also resolve such questions as discharge stroke probabilities to be expected with various operating factors of geographical location, altitude, temperature, speed, and aircraft size.

The maximum burning and melting effects possible with present test facilities, which include a high-voltage generator (1,500,000-volt d-c or 3,000,000-volt surge) and a high current generator (200,000 amperes, 5 to 10-microsecond wave-shape) for producing the standard short-duration *AIEE* test waves, are much less extensive than those observed on flight-returned protective gaps. As a result, construction of facilities to produce this flight-observed type of current wave is being undertaken. These facilities will produce a current wave of 5,000-amperes peak, lasting 10,000 microseconds, and a current wave of about 100 amperes d-c lasting over 1 second, thus reproducing the large heating effects and charge transfers of actual thunderstorm discharges. As may be seen in Fig. 7, these two units will be used in conjunction with the present generators to give one composite wave.

Later papers will evaluate further results of our co-operative program with the airlines, and take up other discharge protection phases of importance to transport aircraft.

REFERENCE

1. LIGHTNING PROTECTION FOR AIRCRAFT. *Symposium Proceedings*, U. S. Navy Bureau of Aeronautics, 1948.

Fig. 7. (below) Composite artificial-thunderstorm discharge-current generator combining initial high-voltage gradient and consequent multiple short- and long-duration current characteristics

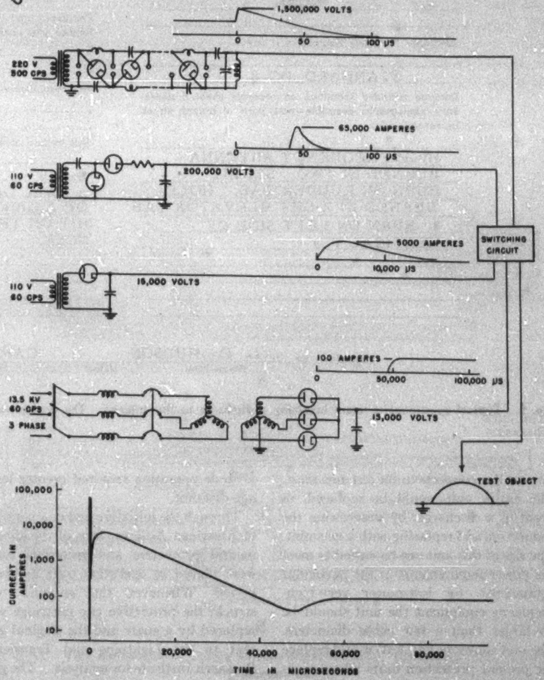
1,500,000 VOLTS
0
50
100 μs
220 V
500 CPS
65,000 AMPERES
0
50
100 μs
110 V
60 CPS
200,000 VOLTS
5000 AMPERES
0
10,000 μs
SWITCHING CIRCUIT
110 V
60 CPS
15,000 VOLTS
100 AMPERES
0
50,000
100,000 μs
13.5 KV
60 CPS
3 PHASE
13,000 VOLTS
TEST OBJECT
100,000
10,000
1,000
100
10
CURRENT IN AMPERES
0
20,000
40,000
60,000
80,000
TIME IN MICROSECONDS

Discussion

J. H. Hagenguth (General Electric Company, Pittsfield, Mass.): The protective scheme for protection of radio equipment disclosed in the paper is a good means of preventing long duration discharges from flowing through the radio equipment. It would be interesting to know how many cases of operation of these devices are known to have occurred.

The writer wonders whether the same purpose cannot be achieved by using heavier wire and better insulation on these coils. Quite obviously this scheme does not prevent high voltages from being applied to the coil for steep current or voltage waves, and certainly during spark-over of the gap the voltage existing across the capacitor is being applied to the coil. Of course, if the coil should break down, permanent disabling damage may not occur since the driving surge voltage will be quickly removed. Unfortunately, even this protection does not provide continuity of radio communication at all times as shown in Fig. 5 and 6, where it is stated that the antenna is burned in two. Perhaps larger sized wire could be used to prevent such damage. Fig. 1 of this discussion shows the coulombs required to burn a No. 6 wire in two as function of the mechanical tension applied. It is evident that a reduction in tension greatly increases the probability of withstanding a long duration discharge.

A No. 4 wire is the largest wire known to me which has been burned in two near the ground. With the higher coulomb content expected in strokes to aircraft, a wire size of perhaps No. 3 should be relatively safe. Of course, the additional weight may preclude the use of large-diameter wires.

It is not clear how the authors arrive at the current wave of Fig. 3(A) as indicated by flight-returned gaps. Such deductions seem impossible for the following reasons.

1. There is only one magnetic link used to indicate current crest through the gap. If there is any current reversal, the indicated current amplitude may be in considerable error.[1] In Fig. 4 of this reference a current reversal of only 8.34 per cent, or 2,600 amperes of a 31,000-ampere discharge, indicates a crest current of 5 kiloamperes on the inner link.

2. While one can distinguish and even calibrate for high-current discharges from burns on metal surfaces as indicated by a multitude of small, bright burns, these burns are obliterated by any subsequent low-current discharges of long duration.

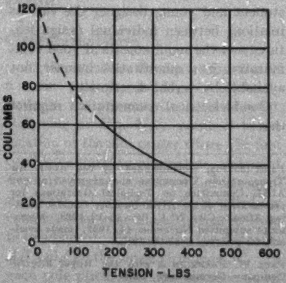

Fig. 1. Arc to no. 6 copper wire under mechanical tension requires indicated coulombs to cause failure

3. Neither of the two measurements indicates wave shape. A 25-coulomb discharge produced by a current wave, as shown in Fig. 3(A), or by a current of 200 amperes lasting for 1/8 second would produce similar burns.

4. The gap does not necessarily register all currents involved in a stroke. In most cases the antenna probably is not hit at all, and in many cases, as illustrated by Fig. 6, it carries only an unknown fraction of the stroke.

It has been found[2] that the size of the holes burned in the metal skin of the plane is a good indication of the coulomb content of lightning strokes. It is much more difficult to assess the amplitude of the current peaks of short duration. However, occasional evidence is obtained, as shown in Fig. 6 of reference 2, which indicates currents of the order of 100,000 amperes with relatively steep fronts. In this particular case the estimated coulomb content of the stroke was 500 coulombs.

Much valuable statistical material on lightning discharges to aircraft has been obtained through questionnaires prepared for the National Advisory Committee for Aeronautics.[3] The continued use of such practices would be very useful, and should eventually lead to a better understanding of all problems involved in lightning protection of planes.

REFERENCES

1. DIRECT MEASUREMENT OF SURGE CURRENTS, C. M. Foust, J. T. Henderson. *AIEE Transactions*, vol. 54, April 1935, pp. 373–78.

2. LIGHTNING STROKE DAMAGE TO AIRCRAFT, J. H. Hagenguth. *AIEE Transactions*, vol. 68, pt. II, 1949, pp. 1036–46.

3. LIGHTNING DISCHARGES TO AIRCRAFT AND ASSOCIATED METEOROLOGICAL CONDITIONS, L. P. Harrison. *Technical Note No. 1001*, National Advisory Committee for Aeronautics, Washington, D. C., May 1946.

J. M. Bryant, M. M. Newman, and J. D. Robb: In answer to Mr. Hagenguth's discussion of our lightning protection scheme for aircraft radio equipment, and with respect to the question on operational experience, according to the experience of one airline, with 50 experimental installations over a 2-year period, the protective units have operated in about 30 cases of lightning strokes to aircraft antennas, and operation has been 100 per cent successful in protecting the radio equipment from damage. In regard to Mr. Hagenguth's suggestion that protection of radio equipment could be achieved by using heavier coils and better insulation, the problem is one of attempting to protect the equipment in operation at present, and consequently redesign and modification of all radio equipment installed in aircraft is hardly practical compared with the addition of the small arrester unit at the antenna feed-through. In addition, it should be pointed out that the antenna is used for reception also and that heavy coils would hardly be practical for receiver circuits which normally utilize relatively fine wire.

Regarding the question raised that continuity of radio communication would be lost by lightning damage to the antenna, it may be said that not all antennas are necessarily destroyed by lightning, for example, wing cap or fin cap antenna designs can be made to take many discharges. The problem of developing long-wire antennas which will withstand direct strokes has also been given consideration; and a research program has been in effect at the Lightning and Transients Research Institute (LTRI), under a research grant by the Copperweld Wire Corporation, in regard to more suitable wire for aircraft antennas. Precipitation-static radio interference requiring the use of insulated antenna wire and fittings makes the change to new larger current-carrying capacity standard antenna wire sizes more difficult; however it is expected that with more flight discharge current data, a more suitable wire may be worked out.

The wave shapes indicated in the paper obviously cannot be as accurate based on pitting and magnetic link data as it would be if oscillographic records had been obtained. Some oscillographic recording has been achieved by LTRI, under an earlier joint program with Air Force Wright Air Development Center laboratories, in which an airplane was instrumented with six cathode-ray oscillographs and flown through many thunderstorms. The stroke probability for a single aircraft, however, turned out to be very low, so that the flight program was discontinued after several records intercepting long-duration 5,000-ampere discharges were obtained. The present program providing airline data returns, which includes general questionnaire data on the stroke as well as a gap cartridge indicating stroke characteristics, has been more fruitful because of the greater number of records involved, from which the wave shape of Fig. 3(A) was derived as reasonably representative. The gap cartridges, as may be seen in the gap close-up photograph of Fig. 2, contain two magnetic links, not one, in answer to Mr. Hagenguth's point with which we agree concerning the inaccuracies of using only one link. However, we cannot agree that equal burns would be produced by a 200-ampere current lasting 1/8 second, as in the case of a 5,000-ampere crest current discharge of the same coulomb transfer. LTRI composite long-duration current tests indicated that equal charge transfers do not necessarily produce the same burning, and that the actual wave shapes and crest current affect the pitting considerably. Also by reproducing in the laboratory both sputtering and pitting effects on the gaps, and by the use of magnetic-link crest-current data, representative wave shapes may be reasonably reconstructed.

It was one of the objects of the paper to indicate that aircraft intercept not only high rate of rise discharges, but also that a majority of the strokes intercepted are intercloud and have low rates of rise, and thus require specific protection means, such as the capacitor scheme described, which will work for any discharge wave shape.

Comprehensive questionnaires by the United States Weather Bureau have provided valuable information but, because they were many pages in length, relatively few were regularly filled out. The LTRI program questionnaires have the advantages of being brief, and in many cases data in the form of discharged protection gaps accompany the questionnaire. Through a co-operative research program with the Joslyn Manufacturing and Supply Company of Chicago the gap replacements are made available by LTRI, in exchange for the research data, to any airline that will co-operate in sending in the gap elements which have intercepted discharges together with the relevant questionnaire data on flight conditions at the time of the discharge. LTRI at present receives, in addition to its own questionnaire, reports from co-operating airlines, also condensed lightning strike reports from many other organizations such as the Civil Aeronautics Administration. It is felt that this information, in addition to its general value from an over-all statistical viewpoint, is also valuable in determining relative needs of protection and provides necessary data for researches being continued at our laboratory, under joint Navy Bureau of Aeronautics and Air Force Wright Air Development Center support as well as industry research grants, on further reduction of thunderstorm discharge hazards to aircraft.

Commutation of Low-Voltage D-C Aircraft Generators

PAUL W. FRANKLIN
MEMBER AIEE

Synopsis: A considerable number of failures of d-c aircraft generators are caused either directly or indirectly by unsuccessful commutation. Difficulties encountered are related either to electromagnetic design features of the machine or to mechanical or chemical-physical phenomena in connection with the commutator, brush holders, and brush material. In the following, some of these features bearing upon the quality of commutation will be analyzed.

A D-C generator is primarily a polyphase salient pole type a-c generator, with rotating armature, connected to a device which collects the current and transforms the output frequency to zero. This device does not produce any power and acts merely as a switching component. As such, it may even be operated remotely from the generator, and it is only for reasons of simplicity and compactness that it is made a part of the machine. It now so happens that the requirements for the successful operation of this element of secondary nature impose severe restrictions upon the basic design of the power-generating equipment. It can be shown that for a large d-c machine for high speed and sudden load changes or for an aircraft generator, almost every design detail must be proportioned with regard to successful commutation.

Faulty commutation in aircraft generators may lead to a general failure in several ways. For instance, brushes may wear at an accelerated rate and the resulting carbon dust may lead to grounding caused by accumulation on surfaces or within slots and under slot wedges. Poor commutation also causes high brush temperatures which, in turn, may contribute to commutator distortions, or raise the temperature of the armature with ensuing wedge lifting or insulation failure. Occasionally, commutation, which has taken a trend to the worse, may be self-healing, particularly if load and speed are reduced but, normally, poor commutation will get progressively worse until destruction of another component of the machine follows.

To simplify this survey, it will be split into two groups, namely, commutation troubles caused by:

1. Inherent electromagnetic design features, or
2. Mechanical-physical-chemical features related to commutator and brush holder design, brush composition, and environmental effects.

Difficult as the requirements for successful commutation are with regard to electromagnetic features, they are by far surpassed by the severity of those of the second group. Summarizing, this writer believes that normally a d-c aircraft generator can be designed to have acceptable electrical commutation characteristics, and this within the weight and bulk required by the application. As to the requirements of the second group, they are of an extremely complex nature and sometimes dependent upon factors beyond the feasible control of both the generator and component manufacturer. Finally, very often primarily technological difficulties without immediate solution force acceptance of compromises on desired performance features in the hope that further development will remove these limitations.

Electrical Design Factors

The theory of electrical commutation is a rather old one, already well developed during the first decade of this century. In the writer's belief, available theory is capable of furnishing to the designer whatever guidance he requires, provided he is willing to spend the time needed for computation. This guidance ranges from the well-known rule of thumb to design the interpole winding 15 to 30 per cent stronger than the armature reaction, to the highly advanced approach of Dreyfus.[1] The intricacy of a method chosen by a designer must be commensurate with the accuracy required and the relevance of the results obtained. For instance, if the electrical commutation difficulties expected are of first magnitude and little trouble is expected with brush holders, commutators, and brushes, it would be well worth while to make a detailed study using Dreyfus' methods, in the case of a large rating. On the other hand, if, regardless of the excellence of the electrical design, severe obstacles will have to be overcome with regard to brush holders and brushes, a refinement of electrical calculations beyond a certain point is unnecessary. This, in the writer's belief, is the case with a d-c aircraft generator.

In the Appendix, a compilation of design formulas with regard to commutation is presented for convenience, based essentially upon Arnold's work.[2] It is believed that in view of the mechanical difficulties, and the fact that each aircraft generator design must be calibrated by the black-band method, these equations are adequate for a good design. In particular, they demonstrate clearly to the student and young designer the various relations between individual design features and the requirements of good commutation in a quantitative manner, not available by verbal description.

Good electrical commutation requires that:

Paper 53-305, recommended by the AIEE Air Transportation Committee and approved by the AIEE Committee on Technical Operations for presentation at the AIEE Summer General Meeting, Atlantic City, N. J., June 15–19, 1953. Manuscript submitted November 14, 1952; made available for printing April 28, 1953.

PAUL W. FRANKLIN is with the Royal Electric Company, Germantown, Ohio.

The writer wishes to express his grateful appreciation and thanks to John Gartner for advice and comment regarding mechanical and commutation details.

1. The commutation process shall take place in a zone undisturbed by the main-pole stray flux.

2. The uncompensated differential reactance voltage of the commutating coil shall be as small as possible.

3. Magnetic interlinkage conditions at the moment of interruption of the commutating coil must be favorable.

4. Interpole magnetic circuits must remain linear (unsaturated).

Nomenclature

P = number of pole pairs
a = number of pairs of armature circuits
m = multiplicity of armature winding
D_a = armature diameter, inches
D_c = commutator diameter, inches
y = coil pitch in slots, that is, pitch 1 to 8, $y=7$
N = number of armature slots
$\delta = +\left|\frac{N}{2_p} - y\right|$ = absolute value of coil pitch deficiency
τ_c = commutator bar pitch, inches
b = peripheral brush contact length along commutator Fig. 4, inches
u = commutator bars per slot
j = thickness of mica in between two commutator bars, inches
α = electrical pole arc ratio, usually 0.6–0.75
τ = pole pitch, inches
I = total armature current, amperes
S = total number of armature conductors
$A = \frac{IS}{2aD_a\pi}$ ampere conductors per inch armature circumference
n_c = number of compensating slots per pole
I_c = current volume per compensating slot
d = main-pole air gap (mechanical), inches
t = armature slot pitch, inches
d_{IP} = interpole air gap (mechanical), inches
k_{cIP} = Carter factor in interpole gap
s = armature slot opening, inches
L_a = armature core length, inches
L_{IP} = axial interpole shoe length, inches
w = turns per commutator bar in armature winding
v_a = armature circumferential speed, feet per minute
b_{IP} = circumferential interpole shoe width, Fig. 1(A), inches
μ = friction coefficient
ν = ratio
η = ratio

COMMUTATION ZONE

As the armature slot leaves the area of a main pole, its conductors gradually undergo the process of current reversal. Referring to Fig. 1(A), point B is the location of the slot center where the first conductor starts to commutate, and point C where the last conductor finishes commutation. The distance BC is called the commutation zone Z and is spaced from both adjacent pole horns by the distances AB and CD, the single clearance SC. Of each pole pitch, only the distance under the pole itself is power-producing. The commutation zone, per equation 3, depends primarily upon commutator and brush dimensions and the type of winding chosen. In larger d-c aircraft generators, the number of commutator bars per slot u is usually unity, and δ, the coil pitch deficiency, small but preferably not zero. Whereas commercial designs make Z = 10 to 18 per cent of the pole pitch, aircraft designs use 20 to 25 per cent and even more, only limited by an economical single clearance. With a given brush density, the larger the commutation zone and the smaller the permissible single clearance, the wider the brushes and the shorter the commutator.

What is now the minimum permissible value for the single clearance in aircraft designs? Commercial designers, blessed with fewer restrictions, usually use 1/4 to 1/3 of the available space between the pole horns. The aircraft generator designer will try to cut the unproductive distances AB, CD, and BC to a minimum and will usually deal with single clearances of 0.100 to 0.250 inch. Both when entering and leaving the commutation zone, the stray flux from the main pole should be as small as possible. In this respect, the trailing edge, interrupting commutation, is more critical then the leading one. As may be seen from Fig. 1(E), a generator is more favored in this respect than a motor, since the magnetic pressure at point D, straying into the trailing commutation zone, is lower than the one at the leading edge point A.

The expressions for the magnetic pressures at the pole horns are given by equations 9 and 10 and a very approximate expression for the stray densities at points B and C are indicated by equation 11. The ratios of these stray densities to the maximal interpole density $B_{IP_{max}}$ equa-

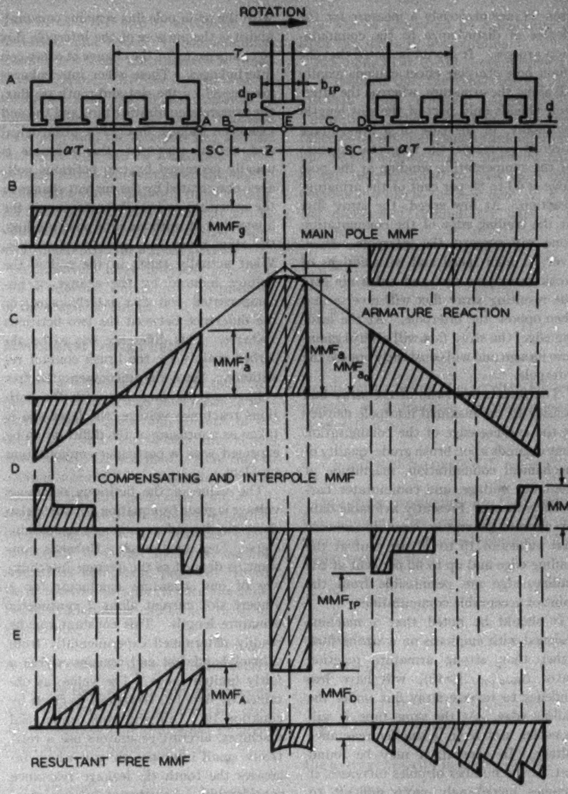

Fig. 1. MMF distribution of a compensated d-c machine (generator)

tion 25, are obviously a measure for the degree of disturbance to the commutation process. It should be noted that the main pole straying effect extends axially all along the armature, whereas the interpole shields only part of the slot length. Normally, in the case of a low-voltage aircraft generator, the magnetic pressure of the compensating winding at the pole edge is 60 to 85 per cent of the armature reaction. At low speed, the stray flux at the trailing edge of the commutation zone will support the interpole. However, at high speed and with designs of weak main pole flux and small air gap, the resulting stray flux will reverse and then oppose the interpole. At the leading edge, the stray flux will always maintain its sign and will constantly oppose the interpole.

The permissible ratio of the stray flux density to the maximal interpole density at the trailing edge of the commutation zone depends upon brush grade, quality of mechanical commutation, magnitude of reactance voltage, and commutator bar-to-bar voltage. Presently available data for aircraft generators seem to indicate that values of 15 to 20 per cent at the trailing edge and up to 60 per cent at the leading edge are permissible from the point of acceptable commutation.

It should be noted that a machine designed with emphasis on a strong flux, rather than strong armature reaction (ratio $B_{\text{main pole}}/A>40$), will have less tendency to reverse stray flux under the trailing edge. At the same time, it will be cooler and have a smaller reactance voltage. In general, it may be found that, as the number of poles increases, it becomes increasingly more difficult to maintain sufficient single clearance.

REACTANCE VOLTAGE

In between two commutation periods, an armature coil is interlinked with the main pole flux; the change of this interlinkage produces the output voltage. During commutation, this interlinkage with the main pole flux remains constant, and it is the purpose of the interpole flux to compensate for the change of other coil interlinkages. These other interlinkages are caused by the slot-and-tooth tip flux, the armature quadrature flux, and the end extension leakage flux. For pedagogical and design purposes, this relation is usually expressed by two fictitious voltages, one created by the current change in the armature coil in the presence of the interpole but without interpole winding, the other by cutting interpole flux lines. What actually exists in the coil is the voltage induced by the change of uncompensated coil flux interlinkages, or the difference between the two fictitious voltages. This difference has to be absorbed mainly by the brush contact resistance. Since the uncompensated free voltage usually increases with the fictitious reactance voltage, the later one is taken as a measure of the difficulty to be expected with a particular commutation problem.

The value of the fictitious reactance voltage is given by equation 20, which also shows the dependency upon design parameters. The constant k_H, Hobart's constant, is defined as the average interlinkage of one armature conductor for 1 ampere slot current along 1 centimeter armature length. This constant can be readily determined experimentally from a black-band test and remains within a fairly limited range. The value, as obtained by Arnold's equations, is given by equation 19. Differing from commercial machines, aircraft generators use a relatively small interpole air gap which increases the tooth tip leakage reactance considerably. An attempt to save interpole turns by reducing the interpole gap may lead to high reactance voltages and, in addition, will deprive commutation of the healthy smoothing effect of a large interpole gap upon local flux variations.

It is quite difficult to specify permissible values for the reactance voltage. It depends upon brush material, upon the constancy of brush contact, that is, mechanical brush vibrations and therefore also commutator circumferential speed. It also depends upon the means available to the designer to keep disturbances out of the commutation zone and his chances to compensate the reactance voltage. It may be too early to define limitations for d-c aircraft generators, but a crude survey seems to indicate that present altitude-treated brushes will, at maximal speed, withstand 2 to 3 volts of fictitious reactance voltage without detriment to commutation. In all probability, with more experience and better brushes, also more weight allowance, this limit could be extended should higher ratings require. It should be noted that the deviation of this value from commercial values, up to 12 volts and more, must be charged primarily to the altitude treatment, the mechanical difficulties, to be described, and the high current densities.

Usually, the designer will not find it difficult to match the theoretically required interpole flux shape, since normally only two conductors per armature slot are being used.

MAGNETIC INTERLINKAGE CONDITIONS AT MOMENT OF CIRCUIT INTERRUPTION

In general, at the moment of interruption, the commutating coil should be interlinked with other short-circuited coils so that magnetic energy may be transferred. It should not, however, be coupled with another coil being interrupted at the same time instant as the first one.

In aircraft generators with simplex wave windings and two conductors per slot, the commutating coil is coupled with other circuits in the following manner:

1. Top-to-bottom interlinkage with other slot conductor.
2. Common tooth tip permeance.
3. Interlinkage within the end extension.
4. Common interlinkage with other commutating coils and short-circuited turns (metal field coil bobbins) along the main-pole axis. This also includes eddy currents.

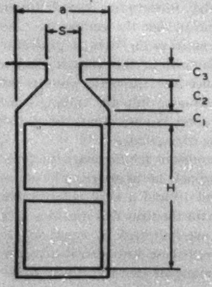

Fig. 2 (left). Typical slot

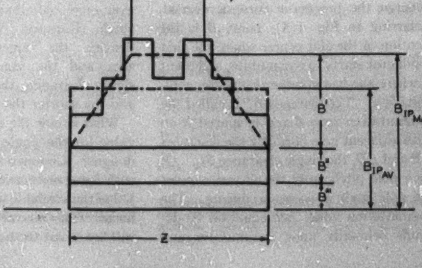

Fig. 3 (right). Interpole flux shape

in the solid parts of the main-pole magnetic circuit.

The coupling coefficient of all these circuits varies of course, but it is believed that because of the relatively small main-pole gap, the coupling to field coil bobbins, etc., is a closer one than on commercial machines. Whereas in the previous details the designer will attempt to choose favorable conditions, in this particular case his hands are more or less tied and he will try rather to evade definitely unfavorable conditions as, for instance, simultaneous interruptions of several interlinked coils. This, in the case of a lap winding, would call for an odd number of slots or bars per pole pair which, in turn, should not contradict the requirements of an equalizer winding.

If a design permits a choice between a wave and a lap winding, the lap winding will provide improved commutation only if the current volume per slot is decreased, that is, the number of slots increased above those of the wave winding. As is well known, this requires more room for insulation.

LINEARITY OF INTERPOLE MAGNETIC CIRCUITS

To insure that none of the resulting densities in any one of the components of the interpole magnetic circuit exceed saturation, the designer will do well to analyze graphically the leakage flux of the interpole structure. For a compensated machine, the leakage coefficient will vary between 1.5 and 3.0, and the ratio of the interpole body flux, including leakage, to main-pole flux at minimum speed will vary from 15 to 35 per cent. At higher speeds, this ratio will of course increase. If there are as many interpoles as main poles, superposition and consequent flux weakening will occur within the armature and stator yoke; if the number of interpoles is reduced, superposition will also occur within the armature teeth and the main-pole body. This is a type of interpole–main-pole feedback where an increase of either flux will always weaken the other one. Thus, increasing load current will cause a main-pole flux drop which, in turn, will appear as an increase in series resistance. Because of the weight limitations and the enforced high magnetic densities, this effect is felt particularly in aircraft generators.

Assume that an interpole winding is tuned by the black-band method at minimum speed and full load. As the speed is increased, owing to decrease of saturation, in the parts common with the main-pole flux, it will increase in strength. This in turn will lead to advanced commutation, and hence overcompounding. Assume now that the interpole is tuned at high speed. At low speed, due to saturation and loss in flux because of superposition with the now increased main-pole flux, the interpole flux and the main-pole flux will be weakened. Both of these effects will require an increase in minimum speed to maintain rated voltage. All these phenomena may or may not be noticeable in a particular design; however, inherently, they always exist.

A relatively large interpole gap, if it can be afforded, will improve the linearity of the magnetic circuit.

Mechanical Design Factors

Even a well-designed commutator cannot be considered as a geometrically perfect cylinder; a certain amount of eccentricity and bar-to-bar unevenness must always be accepted. Referring to commutators of 3- to 4-inch diameter, as used in aircraft generators, an eccentricity of 0.0004-to 0.0006-inch full-indicator reading and a bar-to-bar unevenness of 0.00007 to 0.0001 inch may be considered as acceptable practice. It will be of interest to approximate the radial brush accelerations caused by these imperfections.

ACCELERATION CAUSED BY ECCENTRICITY

Rather than delving into a mathematical derivation, we assume in crude approximation that the radial excursion of an eccentric commutator is

$$X=\frac{d_0}{2}\sin(\omega_R t)$$

where

d_0 = total eccentricity, full indicator reading, inches
ω_R = rotational angular velocity

We obtain the average velocity to

$$\dot{X}_{av}=\frac{2}{\eta}\frac{d_0}{2}\omega_R=\frac{d_0(\text{rpm})}{30}\text{ inches per second}$$

and the maximal acceleration to

$$\ddot{X}_{\max}=\frac{d_0}{2}\omega_R^2$$

and

$$\frac{\ddot{X}_{\max}}{g}=1.42\times10^{-6}d_0(\text{rpm})^2$$

expressed as a multiple of gravitational acceleration $g=386$ inches per second.[2]

BAR-TO-BAR ACCELERATION

To verify the slightly surprising results, the magnitude of the maximal acceleration will be bracketed by calculating it from two different assumptions.

Assuming a bar-to-bar unevenness of d_c, it is assumed that the brush travels this distance with constant acceleration. Theoretically, the brush jumps this distance in an infinitely small time interval; but we will assume that it takes one half of the time required to pass from one commutator bar to the next one. If K is the number of commutator bars, this time is

$$T_c=\frac{60}{(\text{rpm})2K}$$

and since

$$d_c=\ddot{X}\frac{(T_c)^2}{2}$$

we obtain as before the acceleration expressed as a multiple of gravitational acceleration to

$$\frac{\ddot{X}_{\max}}{g}=5.76\times10^{-6}d_c(\text{rpm}\times K)^2$$

As a check, we assume now that, rather than jumping, the brush travels the unevenness in a sinusoidal motion. The radial travel is then

$$X=\frac{d_c}{2}\sin(\omega_c t)$$

and with

$$\omega_c=\frac{2\pi(\text{rpm}\times K)}{2\times60}$$

$$\frac{\ddot{X}_{\max}}{g}=3.55\times10^{-6}d_c(\text{rpm}\times K)^2$$

the average velocity in both cases is

$$\dot{X}_{AV}=\frac{d_c(\text{rpm}\times K)}{30}\text{ inches per second}$$

We see that both results are fairly close, in spite of the different underlying assumptions. A numerical example will illustrate the conditions.

Given a typical aircraft generator brush with an area 7/16 by 1.00 inches and height 1.25 inches. The brush weighs 0.030 pound, and with a specific pressure of 5 pounds per square inch the brush arm pressure is 2.18 pounds, or approximately 70 times the brush weight. Evaluating the developed equations, we assume that $d_0=0.0008$ inch, $d_c=0.0001$ inch, $K=40$, and rpm$=6{,}000$ and $8{,}000$. We obtain the results shown in Table I.

Whereas the accuracy of these figures may be doubted on account of the underlying assumptions, it may be concluded that, during operation, the brush is subjected to extremely heavy impacts of high frequency. Consequently, the nature of the brush contact is by no means

Table I

RPM		6,000	8,000	
$\ddot{X}_{max}/g$		0.819	1.46	caused by eccentricity
$\dot{X}_{av}$	inches per second	0.16	0.213	
Rotational Frequency	**Cycles per Second**	**100**	**133**	
$\ddot{X}_{max}/g$	(b1)	33.2	59	caused by bar-to-bar unevenness
	(b2)	20.5	36.5	
$\dot{X}_{av}$	inches per second	0.80	1.068	
shocks	frequency of cycles per second	4,000	5,333	

a steady one, but one of continuous vibration, even under favorable conditions. This, incidentally, together with the absence of a reactance voltage, is one of the reasons why brush life tests performed on slip rings should be viewed with caution.

It has been attempted to approach the brush contact phenomenon as a mutual indentation of two elastic bodies, the area in mutual contact being a Hertzian surface with a surrounding zone of incomplete contact. For a geometrically perfect slip ring and rigid brushes, this may hold true; however, in view of the permanent bouncing, that is, change of contact, a statistically uniform contact is obtained. This is also borne out by the uniform surface gloss usually noticed. It should be added, with regard to the following, that this does not necessarily imply uniform current density.

The current transfer from or to the brush across the commutator film to or from the commutator copper is a complicated phenomenon beyond the scope of this paper. It is generally accepted that the transfer takes place in local highly concentrated current filaments of very high temperature, which continuously change location. The generally observed decrease of friction coefficient in the presence of current transfer is attributed to lubrication by small carbon particles plasticized by the intense local temperature of the electric arc. This change of the friction coefficient with applied load may be observed neatly by the change of brush-chattering noise. As is well known, the friction coefficient also depends upon the moisture content of the air, which, in aircraft machines, will vary between very wide limits. Using humidity contents of 0.1 to 200 grains water per pound air, it may be found that this amounts to from approximately one water molecule out of 20 average air molecules down to one in 40,000 air molecules.

Under otherwise constant conditions, the friction coefficient does not necessarily remain constant. It may cycle or change gradually or abruptly and may also display signs of frictional hysteresis. There seem to exist mutual relations between the quality of commutation and the friction coefficient. For instance, a certain change in friction causes a change in the quality of commutation which in turn either restores or continues to change friction or, to use another nomenclature, the film. This ability of the friction coefficient, the film in short, the contact condition either to restore itself or to deteriorate, is essentially a brush characteristic. All the designer can do in helping the brush is to provide good electrical commutation; and well-designed commutator and brush holder, to prevent the altitude-treated brush from becoming unmanageable.

A change of the friction coefficient will change the tangential force acting upon the brush, and with this the relative brush position within the holder may change. This changes the statistical center of current collection under the brush, or the distribution of circulating currents superposed upon the uniform current density distribution, and this in turn changes the position of the armature reaction. To elaborate on this important feature, brush stability must be discussed. See Fig. 4.

Three principal forces act upon the brush body:

1. The force exerted by the brush holder arm *F*.
2. The force exerted by the commutator *R*.
3. The force exerted by the brush holder wall *W*.

Whereas the brush arm force *F* is distributed either within a small area or along a line, the other forces extend along a surface and, in the following, are replaced by their resultant. The small friction forces along the brush holder wall and under the brush arm are neglected in the following discussion.

A stable brush holder is designed so that the force *W* required to keep equilibrium to the other forces *R* and *F* can be provided by the geometrical location of the brush holder wall. This means that the projection of the intersection point *A* of forces *F* and *R* upon the supporting surface, point *A'*, must be located within the physical extent of the brush holder wall. If not, equilibrium will be achieved by brush cocking and support from the edges of the box. This general requirement of equilibrium, insisting upon a specific geometrical arrangement, must be maintained for all possible operating conditions, namely, new and worn brush length, variations of brush friction, and accidental shifts of the center of brush contact along a considerable portion of the brush width.

Whereas the point of attack of force *F* is more or less defined, the position of the other two forces may vary considerably. The wall force *W* is the resultant of several point or small area forces, which may vary in location from one brush holder to the next one, because of local unevenness or intermittent distortion, burrs, toolmarks, etc.

The center of current collection under the brush, equivalent to a fictitious center of gravity of current density is, if not equivalent, at least closely related to the location of point *C*. It is the location of the electrical neutral of the machine, and any movement of this point will shift the location of the armature reaction, thus causing a positive or negative feedback into the main-pole axis. It is now a particular feature of aircraft generators that, owing to the relatively wide brush width and the high number of ampere conductors per inch armature circumference, they are particularly sensitive to nonmechanical shifts of the armature reaction, that is, the electrical neutral. Aside from the feedback to be discussed, a shift of armature reaction in space against the fixed compensating winding and interpole will create a mismatch of the magnetomotive forces (*MMF*), increase the uncompensated part of the commutation reactance voltage, and thus worsen commutation. This in turn may further change the film or friction coefficient, which may either shift the armature reaction back or further away, creating either a self-healing or an essentially unstable condition.

This shift in armature reaction may be observed very neatly in the change of field current, if the generator is run with a voltage regulator. Assume a machine with $A = 1{,}200$ *A* per inch, a commutator diameter of 3.00 inches, armature diameter of 4.250 inches, brush width 0.4375 inch and 75 turns per shunt coil. Let it further be assumed that the center of current collection changes for 0.025 inch out of 0.7 inch of the brush width. This will amount to an additional magnetomotive force in the main-pole axis of

$$\Delta MMF = 0.025\frac{4.250}{3.000}1{,}200 = 42.5 \text{ ampere-turns per pole}$$

which causes a change of the regulated field current of

$$\Delta T_{field} = \frac{42.5}{75} = 0.566 \text{ ampere}$$

These field current variations are often observed during heat runs and life tests and cannot be interpreted as changes due to heating effects.

The displacement of the electrical neutral may be caused (aside from by actual shifting of the brushes) either by a strong or weak interpole winding and the aforementioned change in friction coefficient. A change caused by the interpole is, however, a permanent one; it is caused essentially by the change in superposed circulating currents under the brush which are the result of advanced or retarded commutation. Advanced commutation, usually more favorable than delayed, will also strengthen the main pole and lower the permissible minimum speed, but may cause decreasing field current values with increasing loads at high speeds, creating a possibility of instability in the regulator, and forcing it to work at high resistance values. The opposite, causing undercompounding at high speeds, weakens the main pole and may require a higher minimum speed than permissible.

The displacement of the neutral, caused by the change in friction coefficient, or a change in film or contact condition, may be explained by Fig. 4. Starting with a condition of equilibrium, based on a certain value of the friction coefficient μ, the three brush forces F, R and W meet at point A. Suppose now, that the brush and the wall have indented each other into a permanent contact pattern then the location of the wall force W is fixed. If now, due to an external disturbance, the friction coefficient μ changes the new commutator force R may be found by drawing a tangent to the new friction coefficient circle through point A, since both arm and wall force will remain constant as to location. The changed commutator forces R_2 or R_3, drawn through A, will result in a new contact center on the commutator, C_2 or C_3, depending in which direction friction changes. If a scale drawing is made for a conventional brush size in a typical trailing brush holder, it may be found that this shift $C_1 C_2$ or $C_1 C_3$ will easily amount to as much as 0.020 to 0.030 inch. Furthermore, for a configuration such as Fig. 4, an increase in friction will move the current collection center against the direction of rotation, thus strengthening the main-pole axis, and lowering the value of the field current in the presence of a voltage regulator. On the other hand, the increase in brush friction may cause an increase in brush temperature, which could be read by a thermocouple. Again, such a simultaneous change in field current and temperature, usually opposite to each other, may often be observed during life tests.

Very often, these observed field current variations are ascribed to changes in the general film condition, meaning that with a change in film contact resistance, the circulating currents under the brushes vary, and hence the armature feedback into the main pole axis is changed. In the writer's opinion, this is not borne out by theory. Assuming that the brushes are located in the electrical neutral (as, for instance, determined by a shunt field-armature mutual inductance test) and assuming further a simple lap winding, with a brush width equal to commutator bar width, a uniform brush density or local contact drop indicates linear commutation, without a feedback from the armature to the main field. In such a condition, there should be no contribution by the armature to the main-pole excitation. If, however, the local brush density and the contact drop along the brush is uniformly slanted, this indicates advanced or retarded commutation, which in turn, may be interpreted as linear commutation plus a superposed circulating current in the commutating coil. This additional circulating current is the cause of the feedback. Another explanation, often used, demonstrates a shift in the commutator potential curve, and hence the neutral, caused by the uneven brush density curve. This consideration is of general nature and applies to all windings with wide brushes. It can now be shown mathematically that a mere change in the film resistance cannot cause the type of brush current density distribution which causes a feedback. As a matter of fact, uniform film resistance, regardless of value, is the basic reason for linear commutation, additional circuit resistance (coil, risers) only distoring the brush current distribution in a symmetrical manner. The unsymmetrical brush current distribution, causing feedback, can be achieved only by the insertion of a phase-shifted voltage into the commutat-

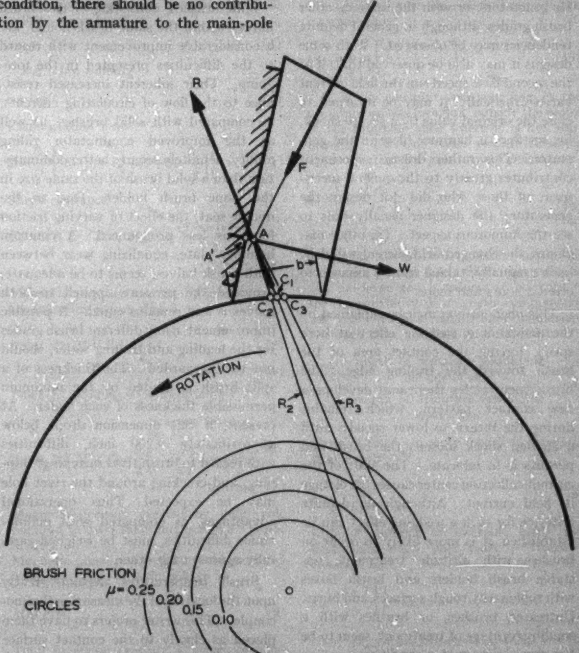

Fig. 4. Distribution of forces in a trailing brush holder

ing coil, as, for instance, from the outside, by the interpole, or within the coil, by uncompensated coil inductivity. The change of internal resistance within the machine, caused by a general change in brush drop voltage, is too small to account for the relatively large field current changes. It follows therefore that a change in film contact resistance, although being eminently important from the point of view of general commutation quality, brush wear, radio noise, and heating, has no direct bearing upon the observed armature feedback and consequent changes in required field current.

Another interesting phenomenon is observed occasionally. Suppose a generator is run for a longer period at minimum speed, full-load, and the field current is read. The machine is then run at top speed, full-load for an extended period, and returned at the same load to base speed. It will be found that often the field current values before and after the high-speed run will vary, sometimes as much as 0.8 to 1.0 ampere for conventional 30-volt generators. This change is erratic. It may or may not occur regularly with the same generator, with similar generators, or with the same or other brush grades, although in general definite tendencies may be observed. With some designs it may also be observed that, if at the second base speed run the field current varies drastically, it may be returned to close the original value by a severe shock, for instance a hammer blow in the generator. This rather drastic experiment contributes greatly to the general merriment of those who did not design the generator; the designer usually fails to see the humorous aspect. On other machines, the changed field current will drift back gradually, taking from 5 minutes to often 2 hours and more.

This phenomenon may be explained by the action of a wedging effect at high speed, forcing the contact area of the brush toward the trailing edge. The brush then settles there and develops a new contact pattern, which remains during the return to lower speeds, until a sudden shock loosens the brush and permits it to relocate. The shift of the current collection center causes the change in field current. Although no definite criterion for such a wedging effect can be established, it is more likely to occur on brushes with altitude treatment, unstable brush holders and brush boxes with tool marks, rough surfaces, and burrs. Untreated brushes, or brushes with a small percentage of treatment, seem to be less sensitive to such a condition.

Conditions under all brushes are by no means identical, as thermocouple readings will readily prove. As a matter of fact, the well-known tendency of the simplex wave winding toward selective commutation may, after a certain time, aggravate conditions. It is conceivable that, among all brushes of the same polarity, the one with the lowest drop or most advanced position will hug or suck in a larger share of the armature current. As a result of the increasing temperature and the negative temperature coefficient of the brush and contact drop, an unstable process may set in. It is often observed during life tests, particularly altitude runs, that resulting brush wear is quite uneven, some brushes being worn down to the rivets and others of the same polarity showing litle wear. This again depends upon brush grade in general, and individual brush pressure; and also upon minor individual inaccuracies in the tangential and axial brush adjustment not necessarily reproducible within generators of the same type. Further investigations along this line, correlating individual brush pressure, temperature, current, and wear would be of considerable advantage to the art.

Split brushes, consisting of two brush halves within the same brush holder, are a considerable improvement with regard to the difficulties presented in the foregoing. Their inherent increased resistance to the flow of circulating currents, as compared with solid brushes, as well as the improved commutator riding ability, definitely secures better commutation than a solid brush of the same size in the same brush holder. Due to the double seat, the effect of varying friction forces is less pronounced. A common hammer plate, equalizing wear between both brush halves, seems to be adequate, provided the pressure applied to both halves is and remains equal. A possible improvement, using different brush grades for the leading and trailing wafer, should not be disregarded. The thickness of a split brush is limited by the minimum permissible thickness of each wafer. At present, if this dimension drops below approximately 0.200 inch, difficulties with regard to brush rivet fastening, chipping, and cracking around the rivet hole may be expected. Thus operational advantages, as compared with maintenance difficulties, must be weighed carefully against each other.

Brush temperatures depend greatly upon the location of the measuring thermocouple. This writer prefers to have them placed as closely to the contact surface as possible, approximately 3/32 to 1/8 inch for detecting the highest temperature extant as well as to serve as an early wear indicator. To obtain fairly accurate results, the thermocouple should be cemented to the brush, and the ends of the wire should be welded together rather than relying upon solder. Temperatures thus read vary from 150 to 240 degrees centigrade, centering around 180 to 200 degrees centigrade. It is interesting to observe that some altitude-treated brushes do not change much in temperature when the speed is changed between the extremes of the range. The brush temperature is not necessarily an indication for the average commutator surface temperature, and does not seem to be a function of the specific cooling surface of the commutator.

A continuous brush temperature of about 200 degrees centigrade for full load seems to be acceptable, provided that the commutator bar material will not fatigue at this value. Brush rivets joints and pigtails should not either loosen or oxidize at these temperatures.

Helical grooves, as used occasionally on slip rings and commutators of commercial designs, should be tried out on aircraft generators, and this writer feels that they may be beneficial from the point of view of ventilation as well as that of uniform seating of the brush. A continuous-low frequency rocking action would prevent any wedging of the nature described previously, and would probably result in a steady field current; in addition, there would be a constant supply of fresh air directly under the brush.

All these features have been purposely described in detail to show that brush operation in aircraft generators under otherwise constant operational and design parameters, is subject to occasionally wide variations, caused either by environmental effects or features not always controllable by the manufacturing process. Brush operation becomes more erratic as the design becomes marginal and the life of the generator is expended.

Brush wear is a complex function of brush material, brush temperature, brush pressure, and current density, commutator circumferential speed and roughness, water content in the air, and the presence of arcs under the brush, that is, the magnitude of the uncompensated reactance voltage.[4] For aircraft generators normal values will range from 2 to 4×10^{-4} inches per hour. The individual brush wear should not vary more than ±25 per cent from the average for a complete machine. Depending upon brush grade, the average brush wear will either increase, remain constant, or decrease with increasing altitude. It is also affected by commutator and bar breathing, brush box deformation, and striction, grease deposits on the commutator, etc.

Fortunately, most brushes possess a recuperational tendency, that is, if commutation conditions have worsened and a reduction in load, speed, and altitude is made, former conditions may be restored. The relative frequency and the type of such a recuperation period will depend upon normal load conditions, design parameters, and of course the brush grade. This ability to reform the film or the original beneficial contact condition is the reason why brushes which failed to perform under extended artificial altitude cycles perform satisfactorily under actual conditions. It is however, a subject open to discussion as to how far this margin of safety should be relied upon.

Based upon the inherent erratic quality of brush performance, caused by a multitude of features difficult to trace or to control, the writer feels that brush life testing must be conducted over extended periods actually in the generator. The resulting wear of a 20-hour test at altitude, extrapolated to 500 or 1,000 hours, does not always give a true picture of the capability of both the generator and the brushes. On the other hand, failure during an extended run at continuous load and constant altitude does not necessarily condemn a design, although a successful completion of such a test would by all means be highly desirable. It appears that, in such a case, a representative load cycle, including variations in load, speed, and altitude with recuperation periods simulating those actually occurring could be established, still including a sufficient margin of safety. In such a case it should be required to accumulate a certain number of hours of life by running a sufficient number of typical cycles. It is realized that the specification of such a typical cycle, differing for commercial and military flying, and also dependent upon the type of the airplane and mission, must be attempted in close co-ordination and co-operation by all concerned.

Appendix. Compilation of Design Equations

Commutation Design Equations

The following assumptions are made:

1. Linear current change in each coil exists.

2. Tooth tip permeance is assumed to be constant, and equal to its maximum. This will result in a slightly higher reactance voltage and a larger commutation field slope at the edges of the commutation zone. It is not believed that the error committed is prohibitive.

3. Decrease of slot inductance due to skin effect is neglected. This effect is undoubtedly present, particularly at conductors' heights above 0.200 inch and speeds in excess of 6,000 to 8,000 rpm for 4- and 6-pole machines. The companion effect of the decrease in inductance, the resistance increase, is definitely evident and may be calculated by Dreyfus' equations.[4] Fortunately, the internal slot inductance, changed by the skin effect, is a small component of the total reactance; hence the error committeed is not too large. It should be noted, however, that the decrease of slot reactance, as the speed increases, could lead to a progressively stronger interpole with ensuing overcompounding.

4. The interpole is designed to compensate only for inductive reactance voltages. The slot constant is based on an average value between self-inductance and mutual inductance, thus eliminating the coupling problem. The difference between the two constants could be considered as, for instance, by Richter's[5] or Dreyfus' equations, but this is not considered necessary for this particular case.

5. Fluctuations in interlinkage are considered only for the slot portion but not for end extension leakage or armature quadrature flux. First, in these components, the fluctuations are smaller than in the slot; second, the components, as such, are small.

For a wave winding

$$a=m \tag{1}$$

For a lap winding

$$a=mp \tag{2}$$

Commutation zone

$$Z=\frac{D_a}{D_c}\left\{(b-j)+\tau_c\left[u(1+\delta)-\frac{a}{p}\right]\right\} \tag{3}$$

Single clearance

$$SC=AB \text{ or } CD \text{ of Fig. 1}=\frac{(1-\alpha)\tau-Z}{2}, \text{ inches} \tag{4}$$

Magnetic pressure exerted by armature at the following points, Fig. 1

$$\text{Point } A\text{:}\quad MMF_a'=\frac{\alpha}{2}\tau A \tag{5}$$

$$\text{Point } E\text{:}\quad MMF_{a_0}=\frac{\tau}{2}A \text{ for infinitely narrow brushes} \tag{6}$$

$$\text{Point } E\text{:}\quad MMF_a=\frac{A}{2}\left(\tau-\frac{Z}{2}\right) \text{ for finite brushes} \tag{7}$$

Magnetic pressure exerted by main pole required to drive main flux across air gap = MMF_g.
Magnetic pressure exerted by compensated winding at edge of main pole to be

$$MMF_c=\frac{n_c}{2}I_c \tag{8}$$

Total magnetic pressure at edges of poles for a generator with direction of rotation as shown in Fig. 1

$$\text{Point } A\text{:}\quad MMF_A=MMF_g+(MMF_a'-MMF_c) \tag{9}$$

$$\text{Point } D\text{:}\quad MMF_D=MMF_g-(MMF_a'-MMF_c) \tag{10}$$

Usually MMF_g is about 0.6 to 0.8 of MMF_a' for 30-volt d-c aircraft generators.

In crude approximation we obtain the main pole stray flux density at points B and C to

$$B_{BC}\cong\frac{4\pi}{10}2.54\frac{MMF_A \text{ or } MMF_D}{\sqrt{(SC)^2+d^2}} \text{ lines per inch}^2 \tag{11}$$

Commutation Reactance Voltage

λ_{slot} is the conventional slot constant. For a slot shown in Fig. 2

$$\lambda_{slot}=\frac{H}{3a}+\frac{c_1}{a}+\frac{2.3c_2}{a+s}+\frac{c_3}{s} \tag{12}$$

λ_{TT_1} is the tooth tip constant under the interpole shoe at its maximal value, neglecting the variation during the commutation process

$$\text{For } b_{IP}<2t,\ \lambda_{TT_1}\sim\frac{b_{IP}}{4d_{IP}k_{cIP}} \tag{13}$$

$$\text{For } b_{IP}>2t,\ \lambda_{TT_1}\sim\frac{t}{2d_{IP}k_{cIP}} \tag{14}$$

λ_{TT_2} is the tooth tip constant outside the interpole shoe

$$\lambda_{TT_2}=\frac{1}{\pi}\ln\left[\frac{s+\pi(t-s)}{s}\right] \tag{15}$$

λ_q is the constant corresponding to the armature quadrature flux, outside the realm of the interpole shoe where it is not suppressed. For this value we use Arnold's approximation for unsaturated pole horns

$$\lambda_q\sim\frac{\left[1-\frac{n_cI_c}{A\tau}\right]}{(1-\alpha)} \tag{16}$$

λ_e is the constant corresponding to the end extension leakage flux. Since this value is not too large and is subject to corrections for the proximity of magnetic components, we use Arnold's simple approximation, although more accurate formulas exist.

$$\lambda_e\sim0.4\frac{\text{length of armature conductor outside of slot}}{\text{length of armature conductor within slot}} \tag{17}$$

Ratio of total armature length to interpole shoe length

$$\nu=\frac{p}{p'}\frac{L_a}{L_{IP}} \tag{18}$$

with p' number of interpole pairs, not necessarily main pole pairs p. Hobart's constant k_H

$$k_H=\frac{8\pi}{10}\frac{1}{\nu}\left\{\frac{t}{Z}[(\lambda_{slot}+\lambda_{TT_1})+(\nu-1)\times(\lambda_{slot}+\lambda_{TT_2})]+(\nu-1)\lambda_q+\nu\lambda_e\right\} \tag{19}$$

Average fictitious reactance voltage

$$e_r = 1.015 w L_a A k_H v_a \times 10^{-8} \tag{20}$$

Arnold replaces the theoretically required interpole flux shape by a trapezoid, for which he then derives certain constants of shape (Fig. 3).

$$B_{IP_{av}} = 2.54 A k_H \nu \text{ lines per inch}^2 \tag{21}$$

$$B' = 2.54 A \frac{8\pi}{10} \frac{t}{\eta Z} [(\lambda_{slot} + \lambda_{TT_1}) + (\nu - 1)(\lambda_{slot} + \lambda_{TT_2})] \tag{22}$$

$$B'' = 2.54 A \frac{8\pi}{10} (\nu - 1) \lambda_q \tag{23}$$

$$B''' = 2.54 A \frac{8\pi}{10} \nu \lambda e \tag{24}$$

$$B_{IP_{max}} = B' + B'' + B''' \tag{25}$$

$$B_{IP_{av}} = \eta B' + B'' + B''' \tag{26}$$

To calculate the shape constant η, the effective brush width b' is required

$$b' = \frac{D_a}{D_c} \left[(b - j) + \left(1 - \frac{a}{p}\right) \tau_c \right] \tag{27}$$

Now, the proper condition must be chosen.

$$\text{a.} \quad |u\delta| = 0 \quad t > b' \quad \eta = \frac{t}{Z} \tag{28}$$

$$\text{b.} \quad |u\delta| = 0 \quad t < b' \quad \eta = \frac{b'}{Z} \tag{29}$$

$$\text{c.} \quad |u\delta| \neq 0 \quad t > (b' + \delta t) \quad \eta = \frac{t}{Z} \tag{30}$$

$$(b' + \delta t) > t > (b' - \delta t) \quad \eta = \frac{2tb'}{Z(t + b' - \delta t)} \tag{31}$$

$$(b' - \delta t) > t \quad \eta = \frac{b'}{Z} \tag{32}$$

Required interpole MMF

$$MMF_{IP} = MMF_a + \frac{B_{IP_{max}} d_{IP} k_{cIP}}{\frac{4\pi}{10} 2.54} + MMF_{IP}'' - MMF_c \tag{33}$$

with MMF_{IP} an estimated addendum for ampere turns required within the normally unsaturated interpole circuit excluding the interpole air gap.

References

1. Commutation of Large DC Machines (book), **L. Dreyfus.** Springer-Verlag, Berlin-Charlottenburg, Germany, 1929.

2. The DC Machine (book), **Arnold-la-Cour.** Springer-Verlag, Berlin-Charlottenburg, Germany, 1923.

3. Design Considerations for D-C Aircraft Generators, **J. D. Miner.** *AIEE Transactions*, vol. 63, 1944, pp. 1234–40; discussion, pp. 1459–60.

4. Resistance Commutation, **Frank D. Olney.** *AIEE Transactions*, vol. 69, pt. II, 1950, pp. 1207–18.

5. Electrical Machinery (book), **Richter.** Springer-Verlag, Berlin-Charlottenburg, Germany, 1924.

No Discussion

Optimization of Nonlinear Control Systems by Means of Nonlinear Feedbacks

R. S. NEISWANDER
ASSOCIATE MEMBER AIEE

R. H. MacNEAL
NONMEMBER AIEE

Synopsis: The first portion of this paper is devoted to the logical selection of a category of nonlinear systems—systems having: 1. controllers with any number of time lags or leads, and usually operating in their saturated region (velocity saturation, force saturation, etc.), and 2. loads consisting of combinations of nonlinear masses, nonlinear dampers, and nonlinear springs. (Nonlinearities which involve explicit functions of time, such as mass and inertia of a controlled rocket motor missile, introduce special considerations not included here.) In the second part of the paper, characteristics of an intentionally nonlinear element added to the feedback are considered. In the final part, the nonlinear element is shaped to provide optimum response in the saturated region of operation.

THE USE of intentionally nonlinear elements to improve automatic control performance is not a new idea in servomechanism history; it has been recognized for a number of years that the overshooting tendency of saturated control systems could be reduced by increasing damping at saturated velocities. However, the problem of shaping the nonlinear element for best over-all performance has been considered only recently, and in many respects this can be regarded as a completely new branch of the servomechanism field. The work of Tustin[1,2] and others in England has led Porter[3] to predict that servo system analysis of the future may be directed principally toward introducing nonlinear elements as means of optimizing control systems, in contrast to the present emphasis upon linearization by mechanical and electrical design.

The growing interest both here and abroad in nonlinear control systems is probably mostly the result of necessity. McDonald[4] in his survey of the state of the art, points out that the improvement of linear systems by engineering design, reducing time delays and energy storages, and improving acceleration characteristics of servo motors is rapidly reaching a point of diminishing return. As a next step, nonlinear techniques come into being.

There are at present at least three methods of treating nonlinear servomechanisms and, as is common to all nonlinear techniques, each method is applicable to a certain restricted category of control systems. Each of these methods is an outgrowth of an on-off servomechanism analysis technique, although the original techniques did not include the concept of performance optimization. Hazen[5] in his classic (1934) paper proposed analyzing, by operational techniques, on-off controls which were essentially linear except for discontinuities at switching instants. MacColl[6] in 1945, and Weiss[7] in 1946 proposed the use of phase-plane analysis to determine responses of certain second-order on-off servomechanisms. More recently, Kochenburger[8] in 1950 introduced a frequency response method applicable to pseudo-linear on-off controls, that is, although actually nonlinear, several linearizing assumptions may be made regarding certain control systems.

By the introduction of an intentionally nonlinear element into the control system, each of the on-off servo techniques has been extended to provide a means of improving control system performance. The sectionally linear technique has been adapted by Schwartz[9] to improve a linear

---

Paper 53-252, recommended by the AIEE Feedback Control Systems Committee and approved by the AIEE Committee on Technical Operations for presentation at the AIEE Summer General Meeting, Atlantic City, N. J., June 15–19, 1953. Manuscript submitted February 24, 1953; made available for printing April 20, 1953.

R. S. Neiswander and R. H. MacNeal are with the California Institute of Technology, Pasadena, Calif.

servomechanism by means of a superimposed discontinuous control. Sherrard[10] has suggested a means, based upon the more general frequency analysis technique, of determining a nonlinear filter which improves the response of a saturated linear servomechanism. The phase-plane technique has been used by Hopkin[11] for the optimization of certain second-order control systems in which the force applied to the load is assumed to be saturated. In Hopkin's method the resultant error signal includes an intentionally nonlinear function of the static error and a linear function of the output velocity.

The intent of the present paper is to outline a method, in many respects an extension of Hopkin's proposal, which can be applied to complex control systems. The method accounts for various kinds of saturations (velocity, force-rate, force, etc.) occuring in control systems having nonlinear loads, and a number of time lags and leads. Although optimization is accomplished by nonlinearizing rate feedback, it should be noted that most of the features of the method are applicable to optimization by nonlinearizing static error signal. For other than simplified control systems, automatic computers are substituted for graphical phase-plane constructions.

The method to be developed is applicable to the saturated region of operation and is therefore not directly concerned with operation near the control system null. Excluding on-off systems, a large number of control systems are reasonably linear in their null regions and can be designed for optimum null region performance by means of well-known linear techniques. If the resulting parameters (loop gain, and correction networks) are assumed to be invariable and necessary elements of the basic control, the present method can be applied to the resultant system. In other words, the goal of null tightness does not conflict with the goal of optimum saturated performance; both can be attained in the same system.

In considering the class of control systems termed nonlinear, one should keep in mind that they can only be defined negatively: all which are not linear. They constitute an infinitely large and diverse class which defies generalization or general analysis. Consequently, any method of treating nonlinear systems must necessarily be restricted. The restrictions of the method to be presented are not precisely known, for this would require the nearly impossible task of investigating a great number of nonlinear control systems; therefore the limitations noted throughout this paper should not be considered to be exact.

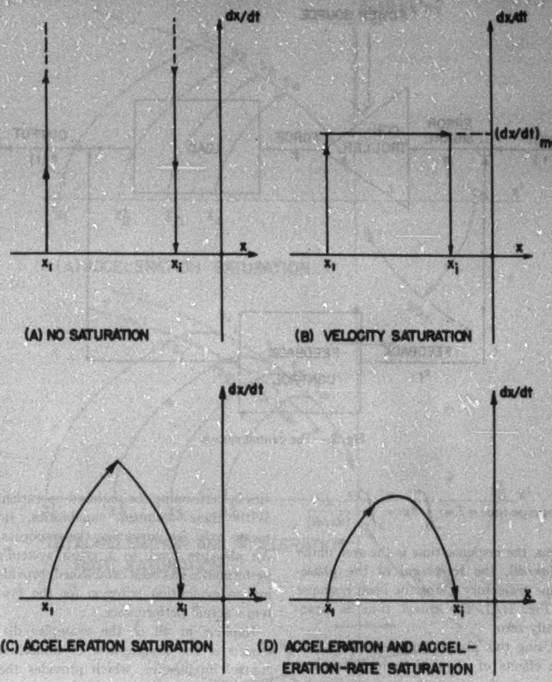

(A) NO SATURATION

(B) VELOCITY SATURATION

(C) ACCELERATION SATURATION

(D) ACCELERATION AND ACCELERATION-RATE SATURATION

Fig. 1. Optimum saturated responses

The Optimum System

Contemporary control system analysis evolved from feedback amplifier design and electrical circuit theory, and it deviates with reluctance from the original concept of the completely linear system. In fact, linear control systems with their neat, analytic solutions are so easily treated that there is a tencency to regard the linear system as the optimum system. Nonlinearities are considered undesirable and are neglected, eradicated, or occasionally admitted by approximate extrapolation from linear theory.

On the other hand, there is an interesting and quite different interpretation of system optimization, which perhaps may best be described by a series of examples. Let it be assumed that the objective of a control system is to move its output, x, from an initial point, x_1, to a final point $x_i \pm \delta$, δ being the tolerated error, in the shortest possible time. It will be advantageous to present the response of such a system by means of a displacement-velocity plot, such as those illustrated in Fig. 1. For a second-order control system, this plot is the phase-plane representation, and for a higher order system this is a phase-plane cross-section of the corresponding multidimensional phase space. However, in either case, the position-velocity plot presents sufficient information, and will be subsequently referred to here as the phase plane.

If the system has almost unlimited available force and perfect control intelligence, its quickest route to the final point is by means of a nearly infinite acceleration to some midpoint and then a nearly infinite deceleration to the final point. The corresponding response trajectory, Fig. 1(A), rises vertically from the initial point, x_1, to an almost infinite velocity, and then descends vertically down to x_i. The relation between the phase-plane trajectory and the response time is apparent

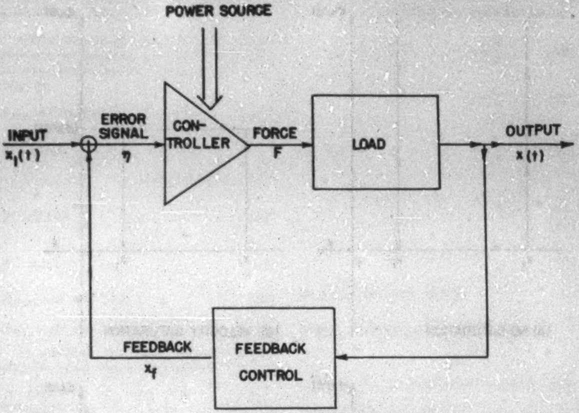

Fig. 2. The central system

$$\text{Response time} = T = \int_0^T dt = \int_{x_1}^{x_f} \frac{dx}{(dx/dt)}$$

Thus, the response time is the area under $1/(dx/dt)$, the reciprocal of the phase-plane trajectory. For the ideal response of Fig. 1(A), the travel time is practically zero.

Using this phase-plane representation, the effects of physical limitations upon the system's responses can readily be seen. Velocity saturation prevents the trajectories from rising above a velocity limit, $(dx/dt)_{\max}$. Thus, a control having no limitations except this velocity limit best performs the task of moving from x_1 to x_f by means of an infinite acceleration up to the bounding velocity, and then a constant velocity up to the end point where an infinite deceleration stops the motion. The resultant trajcetory, Fig. 1(B), now has a finite response time.

In all practical systems the output acceleration must be finite, limited by the inertia of the load and the available force. For example, a system having a pure inertia load and limited available force but no other restrictions has, as its best response, maximum acceleration (maximum available force) to the midpoint, and maximum deceleration to the end point. This produces the trajectory of Fig. 1(C).

Furthermore, if the control force is not able instantaneously to reverse itself, the slope of the trajectory cannot abruptly change, and the resultant trajectory has a rounded apex, Fig. 1(D).

Each of these four examples utilizes its absolute maximum physical capabilities in performing the required operation. With these assumed capabilities, no means exist for improving the responses. An absolute limit to a given system's performance has been established, providing an evaluation criterion for the system's actual performance.

Implicit in all of the examples discussed is the assumption of unlimited control intelligence, which provides the perfect saturated approach to the final point. In actual fact, real systems here will be allowed to become unsaturated and possibly linearly controlled in the null region. This provision results in a less than perfect response.

As a basis for the optimization procedure, the foregoing can be summarized: An absolute optimum control system is one which has physical limitations only, having sufficient control intelligence to perform all requested operations at saturated levels.

For all of the foregoing examples, the performance requirement to move from position x_1 to position $x_f \pm \delta$ within the shortest possible time, was employed, and will continue to be used throughout the remainder of this paper. Other performance demands, such as following a sinusoidal input, $A \sin \omega t$ within tolerated error δ, maximizing ω; following a constant velocity input v within tolerated error δ, maximizing the velocity; or minimizing output error for large variations of the load, will in general require different optimizing techniques. Since superposition of solutions is not permissible in nonlinear analysis, correlation between optimization for any two requirements, such as the first two mentioned, is difficult.

The Method

The task is to devise an intentional feedback which sponsors the optimum response defined in the previous section. Fig. 2 represents the typical control system to be optimized. The controller, which may have various linear and nonlinear elements, imposes a force F on the load, which may be a combination of nonlinear masses, nonlinear dampers, and nonlinear springs (excluding explicit functions of time). Saturated system optimization assumes complete saturation of the controller and thus does not, in general, provide useful information for the final portions of the response trajectories. A technique for determining the limit, the boundary of the unsaturated region surrounding the end point, will be presented later. Within the completely saturated region, the error signal must be large, and has no influence on the output except to initiate reversal when the error reverses polarity.

To discover just what intelligence is required of the optimum feedback element, it is worth while to re-examine the optimum response trajectories of the system. Consider, for example, a system which has a mass plus damping load and a controller which is force-saturated but which can instantaneously reverse the direction of the force. The perfect responses of this system are shown in Fig. 3(A), for final position x_f and various initial values x_1, x_2. . . . (A convenient rule to remember is that all trajectories in the upper half-plane must progress to the right since $\dot{x}$ is positive; and all in the lower half-plane to the left.) It is convenient to shift the x co-ordinates so that the final position, x_f, always lies at the origin, that is, $x' = x - x_f$. Along the early portions of the trajectories, from x_1' to s_1, x_2' to s_2, etc., the system is saturated, accelerating positively. At s_1, s_2. . .the control intelligence reverses the signal, and the force is reversed to become oppositely saturated. Near the origin (the null) the method is not valid and trajectories must be determined by linear analysis or other means. Therefore, for optimum saturated response the only duty of the control intelligence is to select the initiation of reversal, the optimum switching line $s_1s_2s_3\ldots$. Any saturated trajectory which is switched, upon crossing this line, is properly directed towards the origin.

The load mass and damping elements

of this example may be nonlinear without changing the character of the perfect response trajectories. If either of these elements is a function of x, or if a spring is added to the load, perfect responses such as those of Fig. 3(A) will be different for different final positions, and a series of phase planes is required, each representing a specific final position and a complete range of initial positions.

If the load is not an explicit function of x, that is, only a function of time derivatives of x, the various phase-plane plots for different final points will be identical. The optimum switching line can either be considered as a function of x', which is in reality the static error signal, or as a function of output velocity. Using static error signal as the independent variable, Hopkin[11] devised a phase-plane method of optimizing second-order control systems by intentionally nonlinearizing the static error. The method presented here utilizes output velocity as the independent variable, with consequent optimization by nonlinearizing the rate feedback. These two viewpoints are very closely related, and many of the features of the nonlinear rate optimization described here are applicable to nonlinear static error optimization.

It would appear that this optimum saturated control is in many respects similar to that of an on-off servo; and, indeed, in some respects the relay appears to be the ideal controller. However, as mentioned previously in discussing required intelligence, is it assumed that the null accuracy of response is improved if the system is approximately linear.

Admitting a maximum rate of change of controller force $dF/dt_{\max}$ the family of optimum responses becomes those of Fig. 3(B). Note that the optimum switching line $s_1s_2s_3$. . .has been advanced to allow for reversal time, the intervals s_1t_1, s_2t_2. . .being the portions of the trajectories during reversal. Again, when any saturated trajectory has its signal switched, upon crossing the optimum switching line, reversal is initiated in such a way that the trajectory is properly deflected towards the origin.

If, in addition, the system has an absolute velocity barrier, the optimum switching line may take the odd form shown in Fig. 3(C).

In brief, the optimum switching line can be expressed as a function of dx/dt for certain systems (loads independent of x), and in general as a function of dx/dt and the input, or null, value, x_t. In other words: The sufficient control intelligence for the optimum control system (always saturated) is an optimum switching line $S\{dx/dt, x_t\}$ determined by the perfect response trajectories of the system. Throughout this paper, the brackets $\{\}$ will mean a function of. . . .

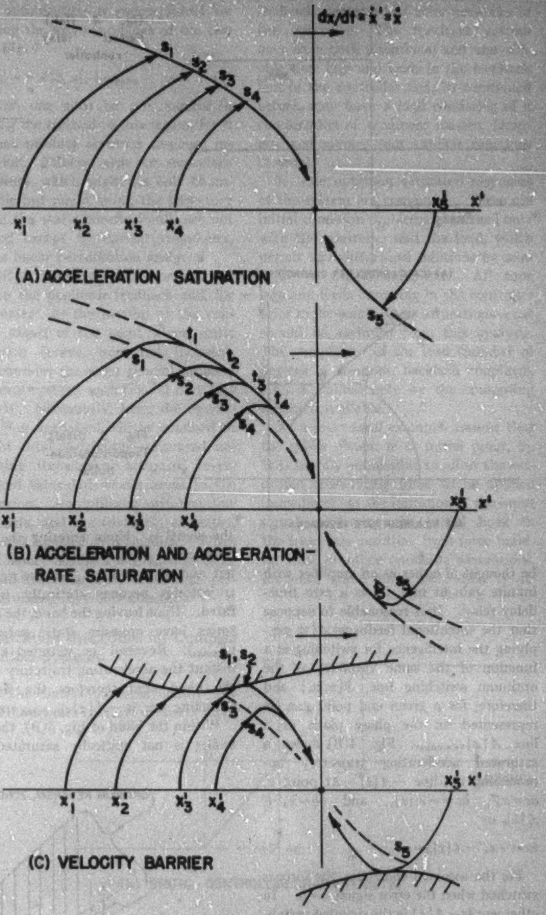

(A) ACCELERATION SATURATION

(B) ACCELERATION AND ACCELERATION-RATE SATURATION

(C) VELOCITY BARRIER

Fig. 3. Switching lines for optimum responses

Since the optimum switching line is the entire intelligence required by an optimum control, it must be provided by the feedback. But just what is the nature of influence of the feedback? First, the feedback must transfer $-x$ to the linear summing element, for it is implicitly assumed that the output should follow the input. Second, it must have some sort of optimizing function $A\{\}$ to provide the optimum switching line. The resultant feedback signal to the summing element is therefore $x_f = -x - A\{\ \}$, and the corresponding error signal is $\eta = x_t - x - A\{\}$. Shifting the x axis to maintain the end point at the origin $(x' = x - x_t)$

$$\eta = -x' - A\{\} \tag{1}$$

As is usual with nonlinear phenomena, simple examples perhaps best demonstrate the important features of equation 1. Consider first a hypothetical system having a static controller characteristic as shown in Fig. 4(A). The controller can

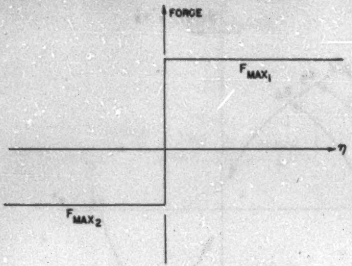

(A) STATIC CONTROLLER CHARACTERISTIC

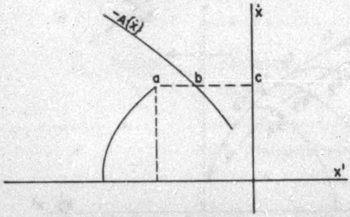

(B) NONLINEAR RATE FEEDBACK

Fig. 4 (left). Perfect relay controller

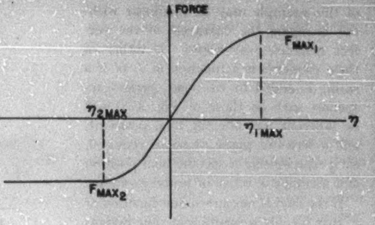

(A) STATIC CONTROLLER CHARACTERISTIC

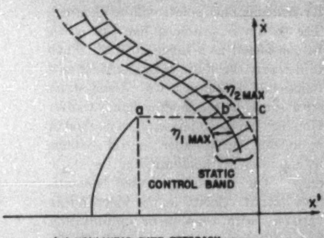

(B) NONLINEAR RATE FEEDBACK

Fig. 5 (right). Proportional controller

be thought of either as an amplifier with infinite gain at null, or as a zero time-delay relay. It is reasonable to suppose that the intentional feedback $A\{\ \}$ supplying the intelligence for switching is a function of the same variables as the optimum switching line, $S\{\dot{x}, x_t\}$ and therefore, for a given end point can be represented on the phase plane as a line $A\{\dot{x}\}_{x_t=\text{const}}$. Fig. 4(B) shows a saturated accelerating trajectory approaching the line $-A[\dot{x}]$. At point a, $ac=x_a'$, $bc=-A[\dot{x}]_a$, and $ab=x_a'+A[\dot{x}]_a$ or

$$ba=-x_a'-A\{\dot{x}\}_a=\eta \tag{2}$$

For the assumed controller, the force is switched when the error signal $\eta=0$. In other words $-A\{\dot{x}\}$ is the signaled switching line. When the signaled switching line is coincident with the optimum switching line, the feedback sponsors perfect control, and the system optimization has been accomplished. In the selected example, this is extremely simple

$$S\{\dot{x}\}_{x_t=\text{const}}=-A\{\dot{x}\}_{x_t=\text{const}}$$

or

$$S\{\dot{x}, x_t\}=-A\{\dot{x}, x_t\}$$

Now consider the more practical controller static characteristic shown in Fig. 5(A), which has force limits of $F_{\max_1}$ and $F_{\max_2}$ but which is unsaturated and nearly linear between these limits. From equation 2, the length ba of Fig. 5(B) is the signal η. Upon entering the band between $-A\{\dot{x}\}$ displaced $\eta_{\max_1}$ to the left and displaced $\eta_{\max_2}$ to the right, all trajectories become statically unsaturated. Upon leaving the band, the trajectories have opposite static saturation ($F_{\max_2}$). Reversal is initiated at the instant the accelerating trajectory enters the band, and therefore the signaled switching line is $-A\{\dot{x}\}_{x_t=\text{const}}-\eta_{\max_1}$.

Within the band of Fig. 5(B), the controller is not statically saturated and consequently unsaturated control of the system will result unless other saturations occur. Accordingly, this zone is labeled the static control band. It presents an important problem in connection with the method of optimization being described. If no other saturations occur, the system does not perform saturated reversals, and the present method is not strictly applicable. The saturated reversal and the unsaturated reversal must be treated differently.

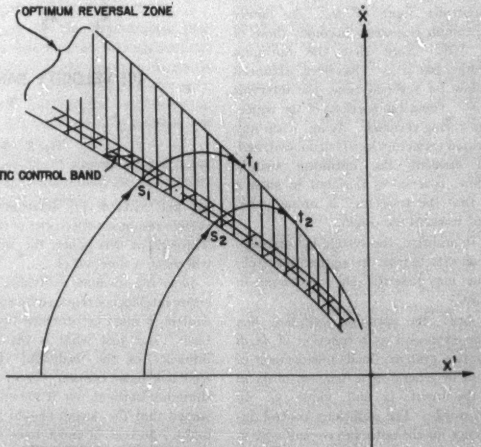

Fig. 6. Optimum saturated reversal

1. *Saturated reversal.* Nonstatic saturations produce optimum trajectories such as those of Figs. 3(B) and 3(C); as an example, the force-rate saturated trajectories of 3(B) are reproduced in Fig. 6. When a controller is force-rate saturated, its output force is changing at the maximum rate permitted by the physical limitations of the controller. The region between $s_1s_2s_3$. . .and $t_1t_2t_3$. . . , where saturated reversal is effected, is termed here the optimum reversal zone. Trajectories reversed within this zone have maximum curvature, for it is physically impossible to reverse any trajectory more quickly than its force-rate saturation permits.

Reversal within a static control band narrower than the optimum reversal zone would imply a greater than possible curvature of the reversing trajectories, therefore in this case saturated reversal is assured. The controlled trajectories will thus be identical with the optimum trajectories, and the signaled switching line will be identical with the optimum switching line

$$S\{\dot{x}, x_1\} = -A\{\dot{x}, x_1\} - \eta_{\max_1} \tag{3}$$

Graphically, this amounts to matching the leading edges of the static control band and the optimum reversal band.

2. *Unsaturated reversal.* By similar reasoning, one would expect that, when the static control band is wider than the optimum reversal zone, the trajectories would be unsaturated, at least for the latter portion of the reversal. This prohibits unrestricted use of the present method. If, as in the case of many simple systems, once captured, the trajectories forever remain within the static control band, optimization is accomplished by matching the exit boundaries of the two zones, Fig. 7

$$T\{\dot{x}, x_1\} = -A\{\dot{x}, x_1\} + \eta_{\max_1} \tag{4}$$

However, one must be very careful in applying the method to this region, for it may not produce accurate response information. Effects such as secondary oscillations, which might not only be undesirable but might swing the trajectory outside the static control band, are not revealed except by special techniques, such as linear perturbation analysis.

In all of these examples, time lags and leads in the nonlinear feedback and, for that matter, in the portion of the controller ahead of the point where static saturation occurs, were not included. Now consider the more general problem of control systems with several time lags or leads. Necessarily, here, the operating region optimized will be confined to that of total saturation—saturated accelerating trajectories, saturated reversals, and saturated decelerations to the null region. An optimum switching line still exists, and the feedback, as before, sponsors a signaled switching line. When the arbitrary feedback is shaped to make the two switching lines coincident, perfect saturated control is attained.

Optimization Procedure for Complex Control Systems

1. The control system is linearly optimized in its null region by means of linear feedback elements and error networks in the controller. The resultant system may have both intentional and unavoidable time lags and leads in the feedback and in the controller and, as mentioned before, may have a load consisting of a combination of nonlinear masses, dampers, and springs (not explicit functions of time).

2. The optimum saturated responses of the system are computed. These are initial condition problems concerned only with the controller and the load, which permit straightforward solutions by analogue or digital computers. All time lags and leads occurring in the controller prior to the points where saturations occur should be excluded from this analysis. The complexity of the load (number of degrees of freedom, backlash couplings, etc.) is limited only by the computing facilities available.

As a procedural example, assume that the given system is at initial point, x_1. It is usually permissible to allow the saturated accelerating force to be applied immediately at the initiation of the input signal, neglecting the initial hook in the trajectory resulting from force build-up time or other nonstatic saturations, for once static force saturation is at-

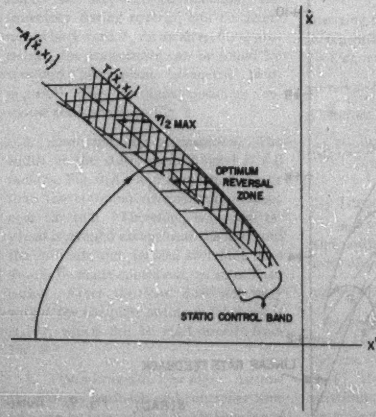

Fig. 7. Optimum unsaturated reversal

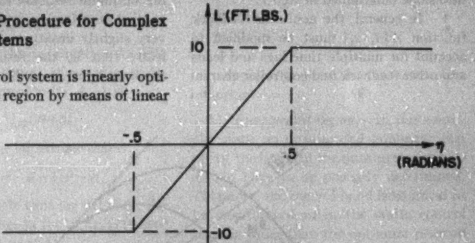

(A) STATIC CONTROLLER CHARACTERISTIC

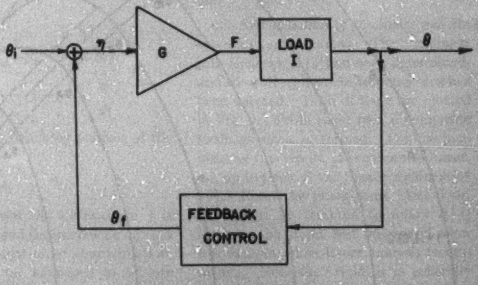

(B) BLOCK DIAGRAM

Fig. 8. Simplified control system

tained, the problem is unconcerned with initial conditions. During the acceleration phase, the solution is that of a known force acting upon a known load. At an arbitrary time, τ_1, reversal is initiated by reversing the signal, and a new initial value problem is created with known initial conditions, forces, and load. This solution is continued until the output velocity is zero, producing final position$_{x_{f1}}$. Using various switch initiation times and various initial points x_1, x_2, etc. the complete set of saturated responses can be obtained. As an accuracy refinement, the final portions of the trajectories, where, in the actual system, linear operation occurs, can be computed by linear analysis. Fortunately, all final trajectories for any one final position are identical.

From the optimum responses, the optimum switching line, $S\{\dot{x}, x_f\}$ is immediately obtained.

3. Assuming no time lags (or leads) in the feedback or in the controller prior to static saturation point, the first approximation of the feedback function is simply

$$A_0\{\dot{x}, x_f\} = -S\{\dot{x}, x_f\} + \eta_{\max_1}$$

The value of $\eta_{\max_1}$ results directly from the controller static force limit and the null slope determined in step 1.

4. In general, the nonlinear feedback function $A\{\dot{x}, x_f\}$ must be modified to account for multiple time lags and leads and other feedback and controller characteristics neglected in the foregoing analysis. The basic procedure proposed is this: The desired responses, x versus time are known from step 2. If the control system loop is broken just prior to the feedback and the perfect responses (along with proper control system inputs) applied as forcing functions, then the actual output responses of the system should coincide with the applied perfect responses. If outputs do not correspond, the nonlinear feedback $A\{\ \}$ must be adjusted to produce proper responses.

A suggested procedure for accomplishing this is as follows: The first estimate of the nonlinear feedback has already been found. This function can be tried in the form of $kA_0\{\dot{x}, x_{f_n}\}$ for some specific perfect response applied as a forcing function to the feedback, and the factor k adjusted until proper switching is obtained. This provides a point on the improved $A\{\dot{x}, x_{f_n}\}$ curve. Repeating with the balance of the perfect responses, the second approximation $A\{\dot{x}, x_f\}$ results.

5. It is clear that this method is applicable, strictly only to the operating region which is continuously saturated, and it is therefore very important to determine the limits of this region. Fortunately, the unsaturated boundaries are the immediate results of step 4. A limiting optimum response exists which when applied as a forcing function produces a very slightly unsaturated reversal of the load; that is, the resultant trajectory deviates slightly from the optimum trajectory (by displaying less curvature). In an exact sense, this trajectory is the limit of usefulness of the method.

6. The final step in the design of the control system is the reconciliation of the linear and saturated results. The control system has been optimized for its linear null region operation and for its saturated operation. Furthermore, the limits of the saturated operation are known. An unsaturated but very nonlinear zone of operation may exist between the two solved regions. When this gap is relatively small and the system's nonlinear functions are well-behaved, interpolation of $A\{\dot{x}, x_f\}$ across the zone is fairly simple. If the nonlinear, unsaturated zone is large compared to the other two operating regions, optimization can in many instances be accomplished (see previous discussion of unsaturated reversal) but requires considerable caution. In complex systems the innocent-appearing static control band of the position-velocity plot is in reality an n-dimensional space tube with the associated freedoms for instabilities.

A SIMPLE EXAMPLE

Optimization of a simplified control system will be carried out, first to demonstrate the problems of reconciliation in dual optimization, and second to show by comparison of dual with linear optimization alone, the marked improvement in system response. The control system chosen has the following inherent features:

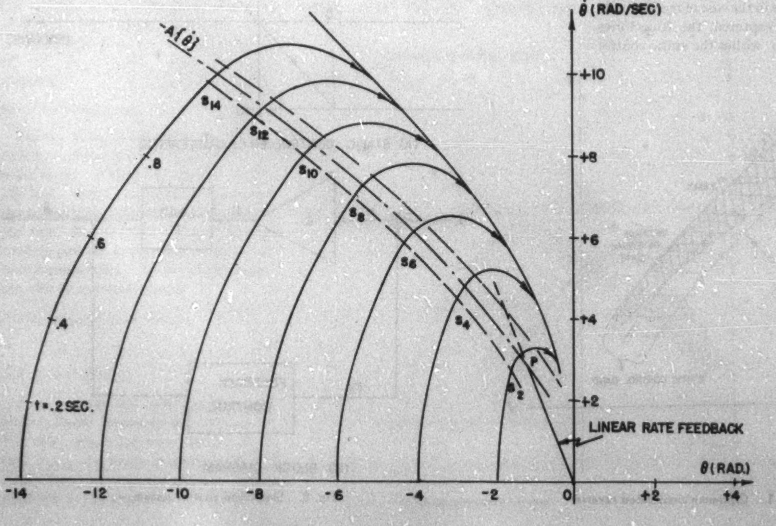

Fig. 9. Determination of $A\{\dot{\theta}\}$

1. Controller, linear up to the static torque saturation, which occurs when $|L|=10$ foot-pounds. Rate of reversal of torque cannot exceed 50 foot-pounds per second.

2. Load, constant inertia, $I=1$ slug-foot².

1. *Linear optimization.* The imposed means of linear optimization is a linear rate generator driven by the system output, that is, the feedback $\theta_f=-\theta-a_1\dot{\theta}$. By means of a linear analysis which includes a consideration of system time lags of the order of 0.02 second, the optimum controller gain is selected as $G=20$ foot pounds per radian; and for a little less than critical damping, the rate feedback coefficient, a_1, becomes 0.4. Therefore, the static controller characteristic is that of Fig. 8(A), and the basic control system, (neglecting the small time lags) is that of Fig. 8(B).

2. *Optimum response trajectories.* The saturated torque, $L_{\max}$, acting upon a constant inertia, produces the parabolic acceleration and deceleration trajectories of Fig. 9. During saturated reversal

$$\left(\frac{dF}{dt}\right)_{\max}=-50=\frac{d}{dt}(\ddot{\theta})=\dot{\theta}\frac{d}{d\theta}\left[\dot{\theta}\frac{d\dot{\theta}}{d\theta}\right]$$

$$=\dot{\theta}^2\frac{d^2\dot{\theta}}{d\theta^2}+\dot{\theta}\left(\frac{d\dot{\theta}}{d\theta}\right)^2$$

Hence

$$\frac{d^2\dot{\theta}}{d\theta^2}=-\frac{50}{\dot{\theta}^2}-\frac{(d\dot{\theta}/d\theta)^2}{\dot{\theta}} \qquad (5)$$

At an arbitrary point on the deceleration trajectory, $\dot{\theta}$ and $d\dot{\theta}/d\theta$ are known, which allows equation 5 to be solved for $d^2\dot{\theta}/d\theta^2$, the rate of change of trajectory slope. By stepwise construction, the trajectory during reversal can be determined backwards. As an alternative procedure, the trajectories can be found by standard phase-plane geometric techniques.[12] The resultant optimum response set is shown in Fig. 9.

3. *Zero time-lag optimization.* The width of the static control band is 1.0 radians, Fig. 8(A), and is much narrower than the optimum reversal zone, except near the null. Therefore, saturated reversal is assured except near the null, and the optimum and signaled switching lines should be made coincident, as mentioned earlier. Since the load does not vary with θ, the complete optimum feedback is $A_0\{\dot{\theta}\}$, which can be read directly from Fig. 9.

4. *Optimizing with time lags.* Assume the various feedback and controller time lags can be lumped as a single time lag of 0.02 second. This lag delays the actual error signal by some small increment which can be estimated as follows:

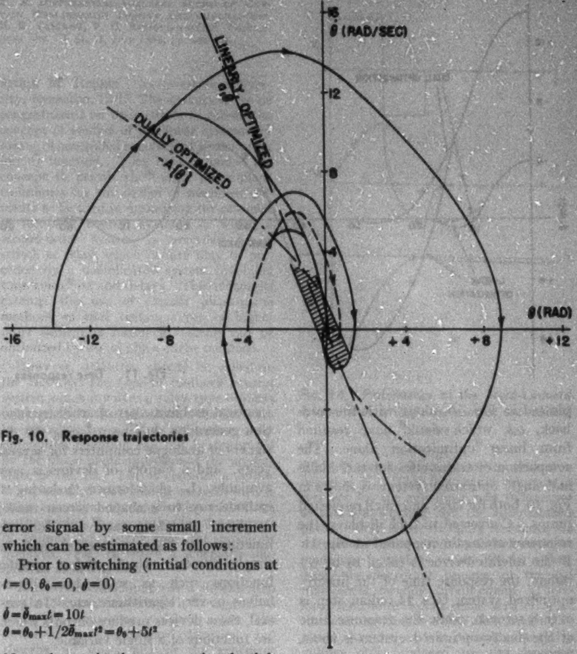

Fig. 10. Response trajectories

Prior to switching (initial conditions at $t=0$, $\theta_0=0$, $\dot{\theta}=0$)

$$\dot{\theta}=\ddot{\theta}_{\max}t=10t$$
$$\theta=\theta_0+1/2\ddot{\theta}_{\max}t^2=\theta_0+5t^2$$

Note that θ_0 is always negative for left half-plane trajectories. From Fig. 9, an approximate expression for $A\{\}$ is

$$A_0\{\dot{\theta}\}=0.06\dot{\theta}^2+0.3\dot{\theta}=6t^2+3t$$

And the zero time lag error signal is

$$\eta_0=-(\theta+A_0\{\dot{\theta}\})=-\theta_0-11t^2-3t$$

Inserting the single time lag network, the incremental change in the signal is (where $s=d/dt$, $\tau=0.02$ second)

$$\eta-\eta_0=\Delta\eta=-\tau s\eta$$

Therefore

$$\Delta\eta(s)=\frac{\theta_0}{s+50}+\frac{3}{s(s+50)}+\frac{22}{s^2(s+50)}$$

(By Laplace convention, $s=\frac{d}{dt}$.)

And noting t at switching point is of the order of unity

$$\Delta\eta(t)\backsim 0.06+0.44t$$

At switch point, s_{14} for example, t is about 1 second, and the increment $\Delta\eta\backsim 0.5$ radians. As a first-order approximation, $A_0\{\dot{\theta}\}$ should be advanced to initiate switching 0.5 radian earlier. Obviously, for trajectories nearer the origin the correction is smaller, and for trajectories more remote the correction becomes quite important.

5. *Unsaturated region.* In this example, since no unsaturated nonlinear gap exists, the limits of the unsaturated region do not have to be precisely determined. Therefore, the control band is assumed to be unsaturated when the static control band is wider than the optimum reversal zone, which is indicated in Fig. 9 by the discontinuation of both zones near the null.

6. *Reconciliation of the linear and the saturated optimizations.* The nonlinear rate feedback $A\{\dot{\theta}\}$ had been determined, and the null region rate feedback $a_1\cdot\dot{\theta}$ has been selected. Both of these are plotted in Fig. 9. From these two, a composite feedback must be formed. For the purposes of this report, it is chosen as linear, $a_1\dot{\theta}$, up to point P and thence nonlinear, $A\{\dot{\theta}\}$. From the phase-plane plots alone, one might be tempted to follow $A\{\dot{\theta}\}$ closer to the origin, but this would allow less damping than linear analysis recommends. Near the origin, it is generally wise to let linear analysis take precedence.

The resultant nonlinear feedback is

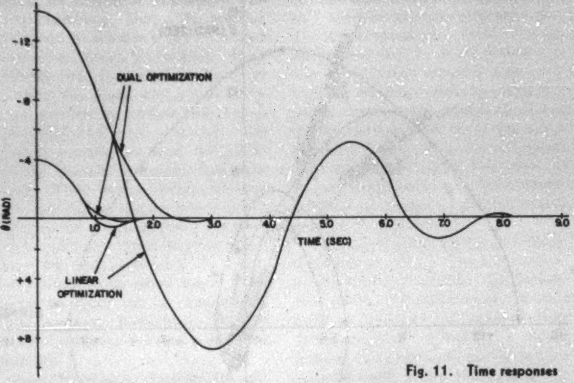

Fig. 11. Time responses

plotted in Fig. 10, along with the feedback, $a_1\dot{\theta}$, which would have resulted from linear optimization alone. The comparison of trajectories for the dually and singly optimized systems is shown in Fig. 10, both for large and small requested jumps. Converted to time displays, the responses are again compared in Fig. 11. If the tolerated error is taken to be 0.1 radian, the response time of the linearly optimized system to a 14-radian step is over 8 seconds, while the response time of the dually optimized system is about 2.3 seconds.

Discussion

The engineering problem of producing the desired nonlinear function is one which cannot be completely answered at present. It should be noted that the identical problem, that of arbitrary function generation, has been facing the designers of analogue computers for several years; and a variety of devices is now available: 1. photoformers,[13] slaving a cathode ray to a shaped screen mask; 2. diode switching arrays,[13] forming functions by linear segments; and 3. simple elements which product specific functions such as square-law, three-halves power, logarithmic, etc. In general, these devices produce outputs which are functions of a single variable.

If a function of two independent variables, $A\{\dot{x}, x_i\}$, is desired, the product approximations $A_1\{\dot{x}\}\cdot A_2\{x_i\}$ or $A_1[\dot{x}\cdot A_2\{x_i\}]$ should be considered, noting that multiplication by means of the rate sensor excitation is often possible.

If, as in some servomechanisms, output rate is not conveniently nonlinearized, the optimization method may be considered from the viewpoint of nonlinearizing the error signal rather than the rate feedback.

References

1. The Effects of Backlash and Speed-Dependent Friction on the Stability of Closed-Cycle Control Systems, **A. Tustin.** *Journal*, Institution of Electrical Engineers, London, England, vol. 94, pt. IIA, no. 1, 1947, pp. 143–51.

2. Analyzing the Effect of Non-Linearity in Closed-Cycle Systems. *Ibid.*, pp. 152–60.

3. An Introduction to Servo-mechanisms, Menthuen's Monographs on Physical Subjects (book), **A. Porter.** John Wiley and Sons, Inc., New York, N. Y., 1950.

4. Nonlinear Techniques for Improving Servo Performance, **Donald McDonald.** *Proceedings*, National Electronics Conference, Chicago, Ill., vol. 6, 1950, pp. 400–21.

5. Theory of Servo-mechanisms, **H. L. Hazen.** *Journal*, Franklin Institute, Philadelphia, Pa., vol. 218, no. 3, Sept. 1934, pp. 279–331.

6. Fundamental Theory of Servomechanisms (book), **L. A. MacColl.** D. Van Nostrand Company, New York, N. Y., 1945.

7. Analysis of Relay Servomechanisms, **H. K. Weiss.** *Journal of Aeronautical Sciences*, New York, N. Y., vol. 13, July 1946, p. 364.

8. A Frequency Response Method for Analyzing and Synthesizing Contactor Servomechanisms, **Ralph J. Kochenburger.** *AIEE Transactions*, vol. 69, pt. I, 1950, pp. 270–84.

9. Piecewise Linear Servomechanisms, **J. W. Schwartz.** *AIEE Transactions*, vol. 71, pt. II, Jan. 1953, pp. 401–5.

10. Stabilization of a Servomechanism Subject to Large Amplitude Oscillation, **Emile S. Sherrard.** *Ibid.*, pp. 312–24.

11. A Phase-plane Approach to the Compensation of Saturating Servomechanisms, **Arthur M. Hopkin.** *AIEE Transactions*, vol. 70, pt. I, 1951, pp. 631–39.

12. Introduction to Nonlinear Mechanics (book), **Nicolas Minorsky.** J. W. Edwards, Ann Arbor, Mich., 1947.

13. Electronic Techniques Applied to Analogue Methods of Computations, **G. D. McCann, C. H. Wilts, B. N. Locanthi.** *Proceedings*, Institute of Radio Engineers, New York, N. Y., vol. 37, no. 8, Aug. 1949.

◆

Discussion

D. M. Collier (Oak Ridge National Laboratory, Oak Ridge, Tenn.): As an addendum to the authors' section entitled "Discussion," it should be noted that the nonlinear feedback originally proposed by J. B. Lewis[1] is one practical example of the type of nonlinear rate feedback under discussion. This feedback is rather easily achieved in practice and can be modified to produce the desired nonlinear function $A\{\dot{x}, x_1\}$ certainly for the specific case of a second-order system with a linear load and possibly for other systems. As Caldwell and Rideout[2] point out, the Lewis feedback network, when applied to a torque-limited system, gives performances which approach optimum. The system has a phase-plane plot similar to that shown in Fig. 1(D).

Lewis approached the problem somewhat differently, starting from the well-known second-order linear system with error and derivative feedback. Then by extrapolation from the performance of the linear system with a constant damping coefficient, he devised a modification which makes the damping coefficient a linearly decreasing function of the error. For step inputs his system gives a marked improvement in performance over that obtainable with a linear system.

Briefly, Lewis' feedback network is as follows. A second-order linear system is adjusted so that the tachometer feedback gives approximately critical damping for the linear system. Then another tachometer feedback has the system error applied to its excitation field, and its shaft connected to the system output. This nonlinear tachometer thus feeds back the product of output derivative times the position error, and this voltage is added to the motor input in the manner shown in Fig. 12. As will be noted, the system has a differential equation of the general form

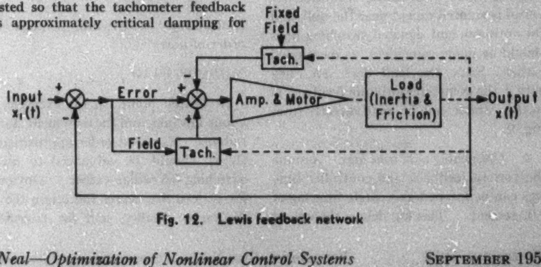

Fig. 12. Lewis feedback network

$$\ddot{x}+[A-B(x_1-x)]\dot{x}+cx=cx_1$$

It is apparent that this is a decided improvement over the linear system in response to positive-step inputs; but this system is even slower than the linear one for negative-step inputs, as may be seen from considering the equation. For this reason, Lewis added another nonlinearity which takes the absolute value of the error voltage before applying the error to the field of the nonlinear tachometer, with the result that the second term in the foregoing equation becomes

$$[A-B|x_1-x|]\dot{x}$$

In truth, this allows the system to follow both positive and negative input steps, but the system has overshoot for large input steps and is unstable for input steps larger than a certain level determined by the relative values of A and B.

Even in the above form, this nonlinear feedback gives performance approaching optimum for some inputs to a torque-limited motor. It is this writer's opinion that, using the methods outlined in the above papers, the Lewis feedback can be adjusted to give optimum nonlinear performance with a torque-limited motor (the usual case in practice) by removing the absolute value nonlinearity and substituting a polar relay type of device which changes the derivative term in certain combinations at the boundaries of the various phase-plane quadrants. The performance of such an arrangement should be much like that of Hopkin's (see ref. 11 of the paper) "anticipator" system optimized for both step and constant-velocity inputs. The system would be rather like the one described in the authors' section entitled, "A Simple Example." A network of this general type is being investigated by the writer with the objective of obtaining a simple practical feedback network for application in systems which have heretofore largely been investigated only with computers.

REFERENCES

1. THE USE OF NONLINEAR FEEDBACK TO IMPROVE THE RESPONSE OF A SERVOMECHANISM, J. B. Lewis. *AIEE Transactions*, vol. 71, pt. II, Jan. 1953, pp. 449–53.

2. A DIFFERENTIAL-ANALYZER STUDY OF CERTAIN NONLINEARITY DAMPED SERVOMECHANISMS, R. R. Caldwell, V. C. Rideout. *AIEE Transactions*, vol. 72, pt. II, July 1953, pp. 165–70.

Arthur M. Hopkin (Northwestern University, Evanston, Ill.): The authors are to be congratulated on their efforts to extend the concept of control of nonlinear systems by means of controlled reversals of a saturating forcing function. They have extended the concept to permit the use of phase-plane techniques for the design of nonlinear elements to be used in optimizing the response of feedback control systems in which a second-order system is preceded by a switch or relay, which in turn may be preceded by a complicated system involving time constants and delays. This technique extends the use of certain phase-plane methods so that certain types of higher order saturating feedback systems can be optimized by use of phase-plane methods.

However, attention should be called to the fact that the type of feedback control system which involves a relay-type element followed by a system whose behavior may be described by a third- or higher order differential equation can not be optimized by the phase-plane approach at the present state of the art. Let us consider a simple Ward-Leonard positioning system with a relay contolling the application of voltage to the field of the generator for the purpose of gaining an insight into the problems involved. Fig. 13 shows a schematic diagram of such a system.

If the reference input r is a sudden step in the forward direction, it is logical to have the controller suddenly close the switch S_1 in the forward direction, and thereby set up a flux in the generator which results in an armature voltage, which drives the motor to reduce the error and hence to make c approach r. If the controller will control the time of reversal of the switch s_1 in such a way that the motor velocity becomes zero at the same instant that the error becomes zero, and if the controller will then open the switch s_1, it might at first seem that there would be an ideal controller for step inputs. However, when $e=0$ and the speed $\omega=0$, and S_1 is open there is still a flux in the generator field in such a direction as to produce a negative V_a. This flux would decay at a rate set by the resistance and inductance of the field-winding and the eddy-current paths. Even if the damping resistance R_D were made infinite, and the switch could be made arc free, there would still be a flux-decay time constant because of the parameters of the eddy current circuit. Therefore, the motor would reach zero error at zero velocity, but it would then back up to give a negative error as a result of negative voltage still produced by the decaying field. The controller might go through another control cycle to counteract the remaining error, but it could not be considered an optimum controller. The performance described is delineated graphically in Fig. 14.

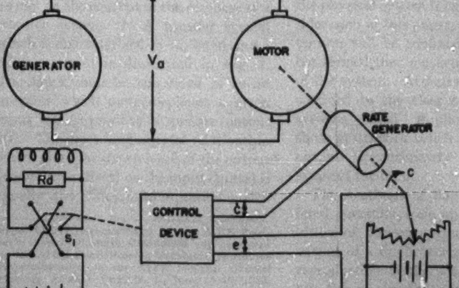

Fig 13 (left). A Ward - Leonard positioning system controlled by a field-reversing relay

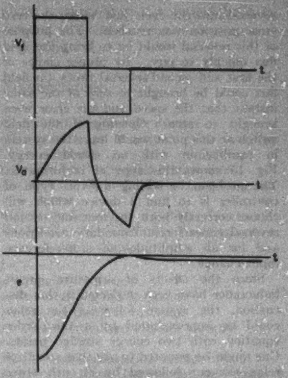

Fig. 14. Performance of the Ward-Leonard system with a single reversal of the control relay

This performance could be made to approach an optimum by introducing a second

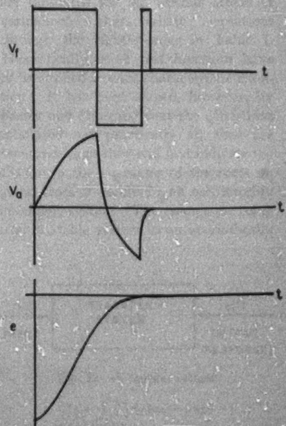

Fig. 15 (right). Performance of the Ward-Leonard system with two reversals of the control relay reversal into the cycle just before the zero error position was reached. The purpose of this reversal would be to bring the field flux quickly to zero. By proper choice of the first and second reversal times, the field flux could be brought to zero at the same instant that the speed and the error were brought to zero. Opening of the field switch at this point would leave the system in equilibrium with no stored energy. Fig. 15 shows this type of performance. The problem in setting up this type of controller is to find a device which will choose correctly both the first and second reversal times for all boundary conditions and for all amplitudes of stop-reference input change.

Since the effects of armature circuit inductance have been neglected in this discussion, the system following the relay could be approximated by a third-order equation with two energy storage points. One might be tempted to say that a control relay element followed by an nth order system would be required to make $(n-1)$ reversals give optimum response to a step input, based on the discussion involving second- and third-order systems. However, a much more careful study of higher order systems would be required before such a statement could be made. It is evident that, as the system controlled by the relay element becomes of higher order, more reversals would be required for optimum response to a step input.

The authors have helped advance the frontiers of knowledge in this field by their contributions. However, where the problem is that of optimizing the step response of a feedback system which involves a relay device followed by a higher order system, there are still many unsolved problems.

R. S. Neiswander and **R. H. MacNeal:** The authors would like to express their gratitude to Prof. Hopkin and Dr. Collier for their generous comments and contributions concerning the paper.

With the growing enthusiasm in nonlinear control and consequent large number of excellent papers, the engineer is sometimes a little overwhelmed at the apparent diversity of techniques. A general criticism of the paper is that it does not make its intentions sufficiently clear. Therefore a highly simplified classification of techniques is given now to show more precisely the application of the proposed method; the system's region of operation has been used as a basis for classification.

Null Region Methods. The null region is the region of small motions. Linear methods are often satisfactory, and several methods are available for considering nonlinear null region effects such as backlash and coulomb friction.

Unsaturated Region Methods. Excepting on-off controllers, there is a dynamic operating region away from the null which is unsaturated. The most common approach has been to keep this region as linear as possible, allowing linear analysis. Techniques by McDonald (ref. 4 of the paper) and Lewis (ref. 1 of Mr. Collier's discussion) have been proposed recently to improve response of systems otherwise linear in this region by intentionally nonlinearizing elements. A frequent result of such methods is decreasing the rate feedback over that specified by linear criteria. When prominent unintentional nonlinearities exist in the system, no general methods are available.

Saturated Region Methods. A quite common design practice is to designate the point at which saturations occur as the boundary of the system's usefulness. Excepting special situations such as that introduced by severe noise limiting, the reason for imposing the boundary is simply that linear analysis breaks down. Actually, control systems are capable of much wider dynamic regions of operation. The present method is intended to handle a specific performance requirements in this region, and at the same time be compatible with methods used in the null region. A frequent result of this method is to increase rate feedback over that dictated by linear null criteria.

In general, methods which apply to one region do not necessarily apply to another region. A system required to operate over a wide dynamic range might well be designed by a combination of two or three applicable methods.

Prof. Hopkin's discussion is concerned primarily with on-off control systems in which there is no region of linear or unsaturated response. In the type of system envisaged in our paper there is a small region of linear response near the null within which the system transients are allowed to decay naturally. Hence there will be no steady-state position error regardless of the order of the equation describing the system. The response time of such a system to a step input will be somewhat longer than that obtainable with an ideal on-off control, but it has compensating advantages in stability and simplicity. The method described in our paper is not essentially a phase-plane technique and the phase-plane cross sections should be considered as helpful response "pictures" not actually vital to the method.

Dr. Collier has pointed out a family of useful, nonlinear optimizing elements which were completely overlooked by the authors. As he has suggested, the feedback arrangement utilized by Lewis can be simply extended to supply a large assortment of functions. For example, the feedback function of Fig. 9 was in the paper assumed to be $A\{\dot{\theta}\}$. It would be just as appropriate to consider the feedback as $a\{\theta\}\dot{\theta}$ (linear rate feedback with a variable coefficient); or $b\{\dot{\theta}\}\theta$ (linear static error with a variable coefficient); or any of a multitude of combinations of functions of θ and $\dot{\theta}$. The real advantage of these rephrasings appears when attempting to physically create nonlinear elements.

The Synthesis of "Optimum" Transient Response: Criteria and Standard Forms

DUNSTAN GRAHAM
MEMBER AIEE

R. C. LATHROP
ASSOCIATE MEMBER AIEE

Synopsis: Methods for synthesizing servomechanisms are reviewed, and it is pointed out that stability criteria, frequency, and root-locus methods reduce to conditions on the transfer-function constants. These may be made mathematically specific following Whiteley's suggestion of "standard forms." Eight mathematical criteria for optimum transient responses are critically examined, and the clear superiority of the minimum integral of time-multiplied absolute-value of error is demonstrated. The application of this criterion results in the selection of standard forms, which are presented in tables.

TRANSIENT BEHAVIOR is an attribute of many measurement, control, and communication devices. Engineering design of such physical systems often involves the choice of design variables which will insure optimum transient behavior. Mathematical techniques applicable to this engineering design problem have been rapidly developed and extended during the past ten years. The lack of a practical mathematical definition of optimum transient behavior, however, has forced empiricism into the design procedures, and the procedures themselves, for the most part, are esoteric and laborious. Development of a unitary figure of merit for transient behavior and the tabulation of optimum system characteristics would be valuable to the designer.

Mathematical methods applied to the problem of optimizing the transient behavior of physical systems depend uniformly on the concept of the response of a transfer system.[1–3] A transfer system which is characterized by an input and a related output is illustrated in Fig. 1. The block may be conceived of as an operator which metamorphoses a given input $r(t)$ to produce a unique output $c(t)$. The most fundamental relationship which gives the dependence of the output (response or effect) on the input (cause) is usually the differential equation which describes the physical system. A simple positioning servomechanism, its linear second-order equation, and its transfer function are illustrated in Fig. 2. The transfer functions of the linear systems considered in this paper are always reduced to the normalized form

$$\frac{C(s)}{R(s)}=\frac{p_ms^m+\ldots+p_2s^2+p_1s+p_0}{s^n+q_{n-1}s^{n-1}+\ldots+q_2s^2+q_1s+1} \quad (1)$$

Procedures for deriving the normalized transfer function from the system differential equation are outlined in Appendix I.

Three distinct problems occur in the application of differential equations and operational mathematics to physical systems. These problems have been named the analysis, instrument, and synthesis problems.

1. The analysis problem is: Given the input and the mathematical description of the system, find the output.
2. The instrument problem is: Given the output and the mathematical description, find the input.
3. The synthesis problem is: Given the input and the desired output, determine the mathematical description.

It is clear that the synthesis problem is intimately related to engineering design. Typical inputs are often known and the "desired" output may be subject to specification. The mathematical description of the required system is a preliminary to its physical realization. Realization of the physical system is excluded from consideration in this paper, however, and attention will be confined to what Bubb[4] has termed the "mathematical attorney" of the system. Attention will be further confined to the class of linear transfer systems called "duplicators," that is, those systems in which the shape of the output approximately duplicates the shape of the input.

The synthesis of duplicators has suffered, generally, from an inadequate definition of desired output. The desired output of a duplicator usually is perfect reproduction of the shape of the input, but this is physically impractical. The desired output is, therefore, often formulated rather loosely on a frequency-response basis in terms of gain margin and phase margin, or on a transient basis in terms of intuitive concepts of rise time and overshoot.

Nomenclature

$r(t)$ = input to a transfer system
$c(t)$ = output, or response, of a transfer system
$e(t)=r(t)-c(t)$ = transfer system error
$E(s)=R(s)-C(s)$ = Laplace transform of error
$w(t)$ = transfer-system weighting function
$W(s)=C(s)/R(s)$ = transfer function of a linear system
$j=\sqrt{-1}$
ω = angular frequency
ω_0 = natural angular frequency
λ = Laplace complex variable
$s=\lambda/\omega_0$ = normalized Laplace variable
t = time
P_i, Q_i = transfer-function coefficients
p_i, q_i = normalized transfer-function coefficients
$a_i, b, c, d, \ldots$ = normalized transfer-function coefficients
ζ = damping ratio
$\alpha+j\beta$ = a root of a transfer-system characteristic equation
C_i = error coefficient

Synthesis Methods

The first and most obvious condition on the output is stability. The output of a duplicator is unequivocally desired to be stable. Fortunately, stability can be precisely defined, and conditions for stability can be rather easily calculated. There are certain conditions on the coefficients of the characteristic equation which must be satisfied in order to insure that the system is stable.

The functional relations between the coefficients defined by the Routh-Hurwitz criterion must hold. These test functions are tabulated for the various orders of normalized characteristic equations through the eighth order in Table I. Theoretically, $n-1$ test functions have to be applied to each characteristic equation. It has been shown, however, by Frazer and Duncan,[5] that the conditions tabulated are practically all that are necessary since they will first indicate the change in the character of the roots on going from a stable to an oscillatorily divergent system. The change on going from a stable system to an aperiodically

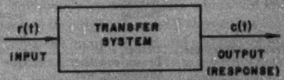

Fig. 1. A transfer system

$$C(t)=\int_{-\infty}^{+\infty}r(\tau)w(t-\tau)d\tau$$
$$C(s)=R(s)W(s)$$

Paper 53-249, recommended by the AIEE Feedback Control Systems Committee and approved by the AIEE Committee on Technical Operations for presentation at the AIEE Summer General Meeting, Atlantic City, N. J., June 15–19, 1953. Manuscript submitted March 19, 1953; made available for printing May 5, 1953.

DUNSTAN GRAHAM and R. C. LATHROP are with the Wright Air Development Center, Wright-Patterson Air Force Base, Ohio.

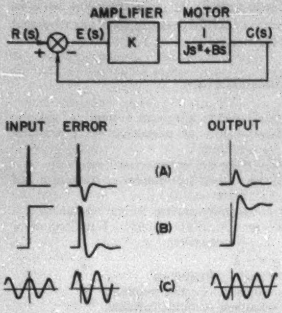

Fig. 2. A linear positioning servomechanism defined by the differential equation $J\frac{d^2c}{dt^2}+B\frac{dc}{dt}+Kc=Kr$ **and the transfer function** $\frac{C(s)}{R(s)}=\frac{K}{Js^2+Bs+K}$

Typical responses illustrated are:

A. The impulse response, or weighting function

B. The step-function response

C. The sinusoidal response

Table I. The Routh-Hurwitz Stability Criterion

Characteristic Equation	Criterion
$s^2+bs+1=0$	$b>0$
$s^3+bs^2+cs+1=0$	$bc-1>0$
$s^4+bs^3+cs^2+ds+1=0$	$bcd-d^2-b^2>0$
$s^5+bs^4+cs^3+ds^2+es+1=0$	$bcd+b-d^2-b^2e>0$
$s^6+bs^5+cs^4+ds^3+es^2+fs+1=0$	$(bcd+bf-d^2-b^2e)e+b^2c-bd-bc^2f-f^2+bfe+cdf>0$
$s^7+bs^6+cs^5+ds^4+es^3+fs^2+gs+1=0$	$(bcd+bf-d^2-b^2e)e+b^2cg-bdg-bc^2f-f^2-bc+d+bfe+cdf>0$
$s^8+bs^7+cs^6+ds^5+es^4+fs^3+gs^2+hs+1=0$	$(bcde+b^2cg+bef-bdg-b^2e^2-bc^2f-d^2e-f^2-bch+dh+bfe+cdf)f+b^2cfg+bc^2dh-b^2ceh-bcd^2g-b^2g-b^2cd+b^2e+b^2edg+b^2gh+bd^2-b^2f-bdfg-cd^2h+cdf^2+d^2g+b^2gh-bfdg-bh^2+dfh>0$

divergent one is first indicated by a change in the sign of the last coefficient. Familiar theorems of the theory of equations point out additional relations between the roots and the coefficients of the characteristic equation.

A method much in vogue among aerodynamicists for the approximate synthesis of airplane dynamics involves plotting the Routh-Hurwitz test function, equated to zero, as a function of two design variables, with all others held fixed. This gives a graphical representation, called a stability diagram, of the boundary between stable and unstable combinations of the two selected variables. An extension of this method due to W. Brown[6] enables one, at the cost of considerable labor, to superimpose lines of constant oscillatory period and lines of constant logarithmic decrement (damping) on such a plot. The degree of stability provided by a selected combination may be determined in this fashion. A stability diagram for third-order systems is shown in Fig. 3, which may be used for the solution of the cubic equation, since the real and imaginary parts of the complex pair of roots are available directly, and the third root is the negative inverse of $\alpha^2+\beta^2$.

In the case of closed loop systems, such as servomechanisms and feedback amplifiers, the Nyquist criterion is often applied to determine stability.[7] The shape of the complex frequency-response function

$$\frac{C(j\omega)}{R(j\omega)}=\left[\frac{P_m\lambda^m+P_{m-1}\lambda^{m-1}+\ldots+P_1\lambda+P_0}{Q_n\lambda^n+Q_{n-1}\lambda^{n-1}+\ldots+Q_1\lambda+Q_0}\right]_{\lambda=j\omega} \quad (2)$$

is, of course, dependent on the various coefficients of the numerator and denominator polynomials. It appears that, as in the case of the Routh-Hurwitz criterion, the stability and degree of stability of the system, judged by the Nyquist criterion, depend on certain relations between the coefficients of the transfer function.

The synthesis of servomechanisms is often carried out using the logarithmic plots of the frequency-response function developed by Bode[8] and Nichols.[3] Appropriate rules governing maximum amplitude ratio, gain margin, phase margin, and the length of asymptotes between break points, if applied with care, may result in a system with adequate transient performance. The outcome of the analysis, however, is not necessarily the optimum system, and the result indicates only approximately the changes in the system which would bring about improved transient performance. All this is in decided contrast to the situation usually facing an amplifier or filter designer, to whom the frequency response is all important and is susceptible to precise specification.

The root-locus method developed by Evans[9,10] is also widely used in the synthesis of closed-loop systems. Both the frequency and transient responses of the system may be inferred from such a plot. There are, however, no generally known

Table II. Methods of Servomechanism Synthesis

Method	Author	Assumed Input	Criterion	Remarks
Stability Diagram	Routh and Hurwitz Brown	None necessary	Stability	Determines stability only. Brown shows how the degree of stability may be determined.
Frequency Response	Nyquist Bode Nichols	Constant amplitude sinusoids of all frequencies	Stability, maximum gain, stability margins	Most widely used method. Depends on rules of thumb for shaping the frequency response. Essentially a cut and try method.
Root Locus	Evans Moore	None necessary	Stability and degree of stability. Transient and frequency response may be inferred and suitable criteria applied.	Criteria are not explicit. A graphical method easy to apply. Only one gain may be adjusted at a time.
Rms-Error	Wiener Phillips Bubb	Input and noise must be stationary time series. Power spectral density must be known	Minimum root mean square error.	A powerful method, but difficult to apply. Leads explicitly to required transfer characteristic.
Transient Response	Draper, *et al* Brown and Hall Oldenbourg and Sartorius Bretoi Others	Step function or other simple type	Speed of response, overshoot, minimum $\int e^2$, error coefficients	Charts available for first, second and third order systems. Higher ordered systems must be cut and tried. Analog computers a great help.
Standard Forms	Whiteley	Step function	Maximally flat frequency response, or a given peak overshoot.	The standard form essentially is the desired transfer characteristic. Very easy to apply. The criteria may be questioned.

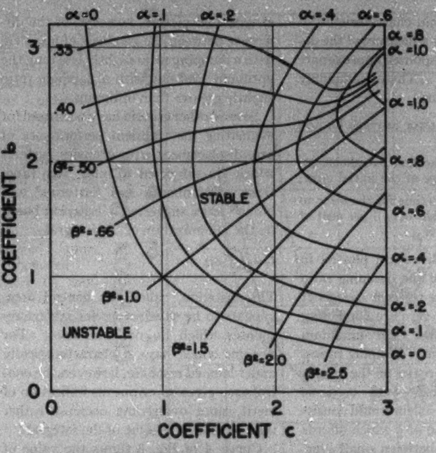

Fig. 3. Stability diagram for third-order systems defined by the transfer function $\frac{C(s)}{R(s)} = \frac{1}{s^3+bs^2+cs+1} = \frac{1}{\left(s+\frac{1}{\alpha^2+\beta^2}\right)[(s+\alpha)^2+\beta^2]}$ **showing contours of constant logarithmic decrement** α **and undamped frequency, squared** β^2

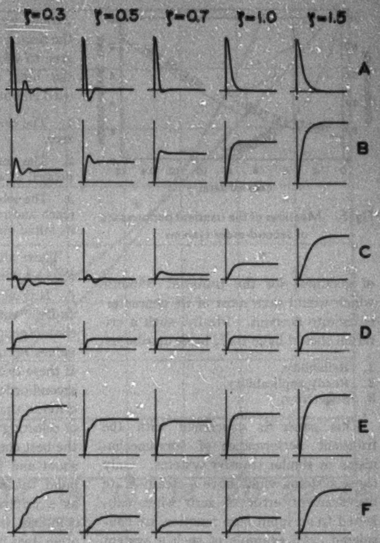

Fig. 4. Step-function responses of second-order systems and figures of merit

(A). $e(t)$

(B). $\int_0^t e(t)dt$

(C). $\int_0^t te\,dt$

(D). $\int_0^t e^2dt$

(E). $\int_0^t |e|dt$

(F). $\int_0^t t|e|dt$

specifications for the optimum location of the poles and zeros beyond the bare specification of stability or degree of stability (damping ratio, time to damp). If it were possible to specify the optimum location of the poles and zeros, that would amount to the specification of the form and the coefficients of the system transfer function.

In the design of filters (or servomechanisms) operating on noisy inputs, the elegant mathematical methods of Wiener[11] may be applied. The result is an explicit mathematical statement of the desired weighting function for the system. Phillips[9] has simplified the application of this method to the synthesis of duplicator servomechanisms by assuming a form for the system transfer function, and leaving only one parameter open to adjustment so as to obtain the minimum rms error.

For a few cases, the direct synthesis of transient response is possible. Charts showing the transient responses as functions of nondimensional system parameters are given by Draper and Schliestett,[12] G. Brown,[13] Bretoi,[14] and others for first and some second- and third-order systems. In very special cases, as in the synthesis of pulse-amplifier interstage circuits, Wallman[15] and others[16,17] have presented such charts for transient responses of higher-ordered systems. Note that the method of specifying the exact form of the transient response in terms of the system parameters is equivalent to the specification of a desired system transfer function.

Whiteley[18] has taken the indicated step and has tabulated the coefficients of the polynomial denominators of system transfer functions for desirable systems of various orders, and with three different kinds of numerators. He has named these explicit numerical functions for the polynomial denominators standard forms. The criteria which Whiteley[18] used to judge the "goodness" of desired outputs were, in one case, a maximally flat frequency response, and in others, the magnitude of the peak overshoot.

Some other criteria of goodness for transient responses which have been applied by the authors of transient-response charts and by users of such charts and of differential analyzers are:

1. Delay time.
2. Solution time.
3. Time to first zero.
4. Peak ratio.
5. Overshoot.

While suitable values for all these or other applicable quantities may be known in general, this knowledge usually does not give much insight into the most favorable adjustments to make to the system. In many cases where several figures of merit are applied, it is possible to "trade" part of one for a better value of another. The direct synthesis of transient responses, whether from charts, from Whiteley's[18] standard forms, or by means of a differential analyzer, is subject to the objection that the desired output has not been defined precisely enough.

Table II summarizes the various methods of synthesizing servomechanisms (and other dynamic systems) which have been discussed above, cites the criteria which are applied, and summarizes the limitations of each method.[19]

Criteria for Transfer System Response

The choice of specific design variables in the synthesis of duplicators depends completely on the criteria which are applied in judging how well the output follows the input. Speed and stability of response are desirable. These qualities may be indicated numerically by defining solution time, time to first zero, overshoot, and so forth. A more fruitful approach to the problem, however, would be to develop a unitary figure of merit or criterion

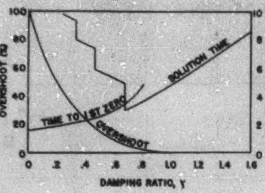

Fig. 5. Measures of the transient performance of second-order systems

of goodness for the transient response which would take most of its characteristics into account. Ideally, such a criterion should have three basic attributes:

1. Reliability.
2. Ready applicability.
3. Selectivity.

This paper is concerned with the transient performance of servomechanisms or similar transfer systems. Only those systems which have a steady-state displacement error of zero when subjected to an input step function are considered. An example of such a system would be a simple linear second-order system which has the normalized transfer function

$$\frac{C(s)}{R(s)}=\frac{1}{s^2+2\zeta s+1} \tag{3}$$

Fig. 4(A) shows the error responses of this system for various values of ζ, when the input is a unit step function. These responses differ from a perfect response in various ways. Certain characteristics of the responses provide a measure of the degree to which the responses approximate the ideal response. Three commonly used characteristics are:

1. The time for the error to reach its first zero.
2. The amount of the first overshoot, expressed as a percentage of the initial error.
3. The solution time (time for the error to reach and remain within only 5 per cent of its initial value).

These three quantities are plotted in Fig. 5 as functions of the damping ratio ζ. It is clear that the per-cent overshoot and the time to first zero are conflicting characteristics, in that their minimum values occur at different damping ratios. If these two characteristics of the simple second-order responses were used as criteria, the design problem would consist of selecting that value of ζ which affords the best compromise between small overshoot and fast rise time. On the other hand, the solution time can be used alone as a criterion of performance, since it combines, in a sense, the properties of the other two characteristics. Applied to a linear second-order system, it appears to have some of the characteristics of an ideal criterion. It is reliable, in that it selects a damping ratio of about 0.7, a value which is commonly considered to be optimum. It is fairly easy to apply, given the time responses of a system. It is also selective, in that the difference between the optimum value and other values is easy to distinguish. It gives an exaggerated picture, however, of the difference between the goodness of a system with a damping ratio slightly less than the optimum, and one with a damping ratio slightly greater than optimum.

Several other criteria have been used for evaluating the transient performance of zero-displacement-error transfer systems which are subjected to input step functions. Oldenbourg and Sartorius[8] and Nims[20] have suggested a criterion based on the minimization of the integral

$$I_1=\int_0^\infty e\,dt \tag{4}$$

This criterion, called the control area, appears to be satisfactory for system responses which do not overshoot. For systems which have a characteristically underdamped response, however, the control area gives an erroneous indication of merit, since overshoots decrease rather than increase the value of the integral.

Curve *A* of Fig. 6 shows the value of the criterion I_1 as a function of the parameter ζ for a system with the transfer function of equation 3 subjected to a unit step function of input. It can be seen that the minimum value of I_1 occurs at the damping ratio $\zeta=0$, a value which is certainly not optimum. The failure of this criterion to select a reasonable linear second-order system is sufficient grounds for its rejection from further consideration.

A modification of this criterion to provide for weighting of the error with time was proposed by Nims.[20] This modified criterion is defined by the integral

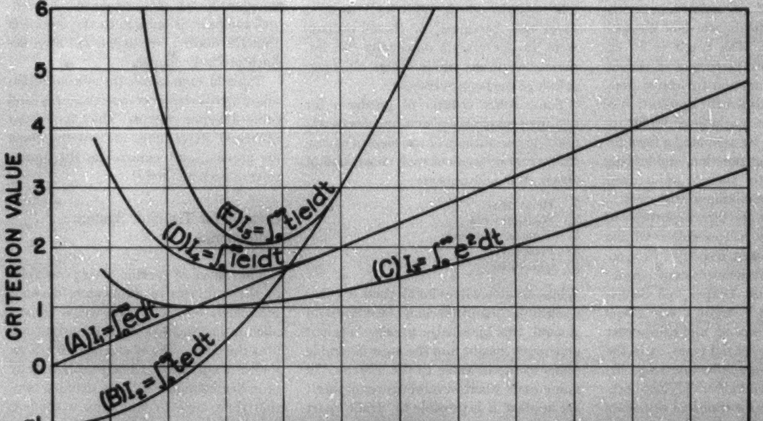

Fig. 6. Criteria for the step-function responses of second-order systems $\frac{C(s)}{R(s)}=\frac{1}{s^2+2\zeta s+1}$

Curve A: Integral of error, the control area

Curve B: Integral of time-multiplied error, the weighted control area

Curve C: Integral of squared error

Curve D: Integral of absolute value of error

Curve E: Integral of time-multiplied absolute value of error

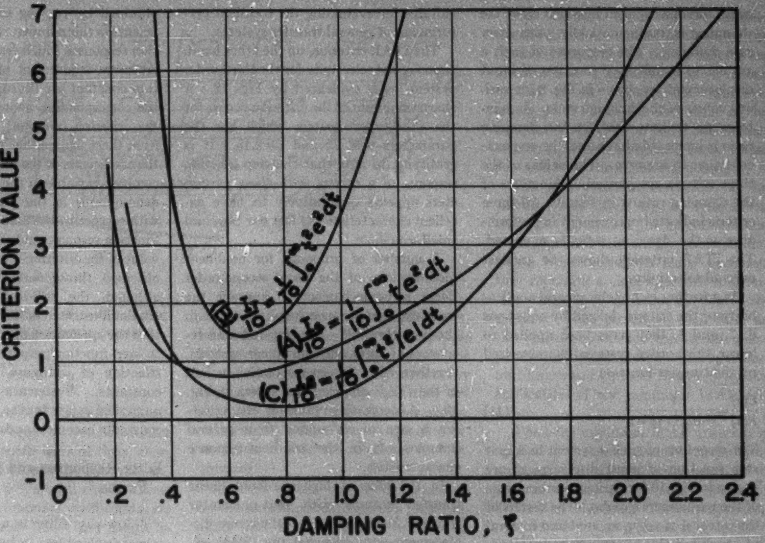

Fig. 7. Three additional criteria for the step-function responses of second-order systems

Curve A: integral of time-multiplied squared error

Curve B: integral of time-squared error-squared

Curve C: integral of time-squared absolute value of error

$$I_2=\int_0^\infty te\,dt \tag{5}$$

The weighted control area I_2 provides an increasingly heavy penalty for a sustained error. As before, that system is considered optimum which produces a minimum value of I_2. Curve *B* of Fig. 6 is a plot of the value of this criterion applied to the second-order system. It can be noted that the minimum value of the weighted control area occurs at the damping ratio $\zeta=0$. Therefore, this criterion fails in the same way as the control area.

Hall[21] has suggested the integral

$$I_3=\int_0^\infty e^2dt \tag{6}$$

as a figure of merit. In this case either positive errors or negative errors due to overshoots will produce positive contributions to the value of the integral. If this criterion is applied to the step-function responses of the simple linear second-order transfer system, curve *C* of Fig. 6 is the result. The minimum criterion value occurs at $\zeta=0.5$, which is not an obviously undesirable damping ratio. Furthermore, the criterion can be handled analytically or mechanized with relative ease on a differential analyzer. It also exhibits limited selectivity.

Another figure of merit which has been investigated is given by the integral

$$I_4=\int_0^\infty |e|dt \tag{7}$$

Curve *D* of Fig. 6 shows the results of testing this criterion in connection with the transient response of the simple linear second-order transfer system. The minimum value of the criterion occurs at about $\zeta=0.7$. It is moderately selective, and although it is not analytic, it is easily mechanized on an analogue computer.

If time weighting is introduced, this criterion is modified to

$$I_5=\int_0^\infty t|e|dt \tag{8}$$

This function is known as the integral of time-multiplied absolute-value of error (ITAE) criterion. If, as before, it is tested on the simple second-order system, curve *E* of Fig. 6 is the result. The minimum occurs at $\zeta=0.7$. The ITAE criterion is selective and easy to mechanize on an analog computer. Applications to other systems to test its reliability will be discussed later.

Still other figures of merit can be formed with more complex combinations of error and time weighting. Three such criteria are

$$I_6=\int_0^\infty te^2dt,\quad I_7=\int_0^\infty t^2e^2dt,\quad I_8=\int_0^\infty t^2|e|dt \tag{9}$$

The values of these criteria as functions of ζ for the step-function responses of the simple second-order system are presented in Fig. 7. Although these criteria show promise with respect to reliability and selectivity, they are excluded from further consideration because they are difficult to handle, either analytically or on the analogue computer.

Of the several criteria mentioned here, only those defined by equations 6, 7, and 8 are considered worthy of further investigation. In order to test the general applicability of these three criteria, they are applied to a second-order linear zero-velocity-error system, which has the normalized transfer function

$$\frac{C(s)}{R(s)}=\frac{2\zeta s+1}{s^2+2\zeta s+1} \tag{10}$$

This transfer function describes a second-

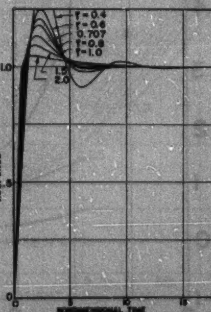

Fig. 8. Step-function responses of zero-velocity-error second-order systems

order servomechanism in which all of the damping is mathematically pure error rate damping. The responses of such a system to a unit step function of input displacement are shown in Fig. 8 for various values of the damping ratio. It is interesting to note that, as the damping ratio is increased above one, the response continues to improve. The values of the three criteria are plotted as functions of the damping ratio ζ in Fig. 9. All three criteria indicate improvement in performance as the damping ratio is increased. The ITAE criterion shows the greatest over-all selectivity.

As a further test of the general applicability of the criteria defined by equations 6, 7, and 8, they have been applied to linear third-order systems characterized by the transfer function

$$\frac{C(s)}{R(s)}=\frac{1}{s^3+bs^2+cs+1} \tag{11}$$

The responses of such a system to a unit step function of input displacement are shown in Fig. 10 for various combinations of the parameters b and c. The results of the integral of error-squared and integral of absolute-value-of-error criteria as applied to this system are presented in Fig. 11. It is clear that these two criteria fail to achieve selectivity. Additional tests indicate that these criteria become even less selective for higher-order systems, and it is doubtful that they are suitable for evaluating the transient performance of general transfer systems.

The ITAE criterion, on the other hand, retains good selectivity for the third-order system, as is evidenced by Fig. 12. A sharp minimum of the criterion occurs for the third-order system which has the parameters $b=1.75$ and $c=2.15$. It is gratifying to note that the step-function response of a system with these parameters appears qualitatively to have excellent characteristics of fast rise time and small overshoot.

A number of proposals for nonlinear modifications of the basic second-order linear servomechanism to improve the transient performance have appeared in the literature.[22,23] The step function responses of three such nonlinear systems, together with the corresponding values of the ITAE criterion, are shown in Fig. 13. A decreasing value of the criterion is seen to correspond to a general improvement in the transient-response characteristics.

In the case of higher-ordered linear transfer systems with unit-numerator transfer functions (also called zero-displacement-error systems) the ITAE criterion may be represented as a surface in a multidimensional space which has the dimensions of the transfer-function coefficients. The surface (line), its shape, and minimum point have already been illustrated for the second- and third-order cases in Figs. 6 and 12. The multidimensional surface itself cannot be graphically represented for systems of order higher than the third. Instead, Figs. 14 and 15 show sections through the surface for the fourth- and fifth-order systems. These sections are obtained by adjusting all but one of the coefficients of the system transfer function to their optimum values. This one coefficient is then varied throughout a range on either side of its optimum value, and the corresponding variation in the value of the ITAE criterion is plotted. In Figs. 14 and 15, the curves denoted by the letters b, c, etc., are the sections through the multidimensional surface obtained by varying the indicated coefficients in this manner. Several step-function responses which result from the nonoptimum adjustment of a transfer-function constant are illustrated, adjacent to the corresponding nonminimum value of the criterion function. It may be seen from these figures that the adjustment of the coefficients of the lowest powers of the complex variable in the transfer-function denominator is the most critical, both with respect to the character of the step-function response and with respect to the value of the criterion. The same situation obtained throughout the investigation, although the still-higher-ordered cases are not illustrated in this way. It appears that the application of the ITAE criterion to step-function responses results in the selection of optimum transfer-function constants. Systematic tabulations of numerical values for the transfer function constants become standard forms.

Filter Responses and Standard Forms

A low-pass filter is a duplicator, and other duplicators, including servomechanisms, may be designed by analogy to filters.[2] In general, transfer systems with good low-pass filter characteristics have correspondingly good transient responses. One of the simplest possible low-pass filters is an n-stage resistance-capacitance-coupled pulse amplifier, in which the stages are identical.[16] The characteristic function of such a system is the binomial expansion of an appropriate order. The response of a physical system with such a characteristic equation is composed of equally and critically damped modes. This response has been suggested by Imlay[24] as an optimum in connection with the response of an aircraft under the control of an automatic pilot, and by Oldenbourg and Sartorius[3] in connection with regulators and servomechanisms.

The precise definition of desired output afforded by the requirement that all modes of the response be equally and

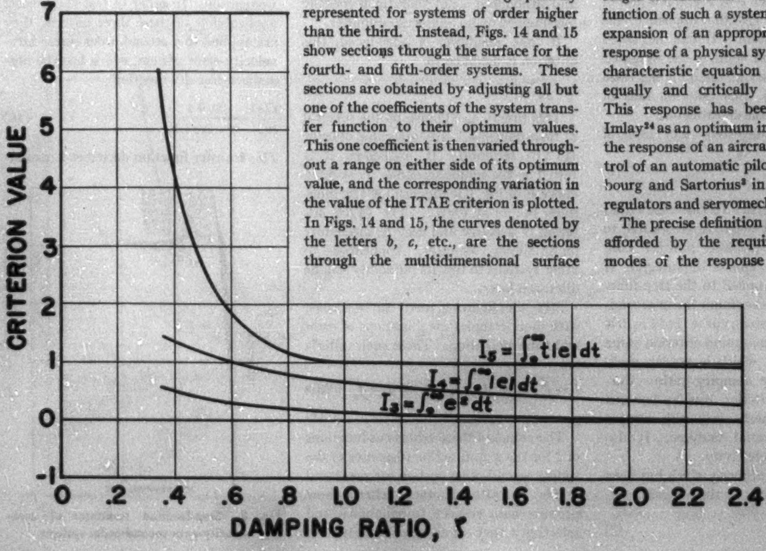

Fig. 9. Criteria applied to the step-function responses of zero-velocity-error second-order systems

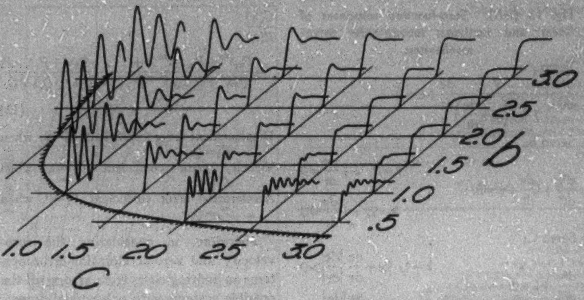

Fig. 10. Step-function responses of third-order systems with the transfer function

$$\frac{C(s)}{R(s)}=\frac{1}{s^3+bs^2+cs+1}$$

critically damped leads readily and explicitly to the required system transfer function. The coefficients of these characteristic functions are the binomial coefficients. The polynomial characteristic functions with binomial coefficients are tabulated in Table III. They might be considered to be a set of standard forms for the synthesis of duplicators with unit-numerator transfer functions. In fact, lacking more suitable forms, Whiteley[18] has suggested the binomial coefficients for certain higher-order system transfer-function constants. The step-function responses of the binomial filters are shown in Fig. 16, and the corresponding frequency-response functions in Fig. 17. It has been noted that, in the language of operational mathematics, these methods of describing the response are equivalent. Therefore, the adjustment of a linear transfer system's parameters, resulting in a transfer function with a unit numerator and a characteristic equation with binomial coefficients, guarantees the responses indicated. The transient responses of the binomial filters are not optimum for many applications, in the sense that they are relatively slow. The frequency-response characteristics show a corresponding attenuation of even the relatively low frequencies.

Another rather simple configuration for the interstage couplings of a pulse amplifier has been suggested by Butterworth.[25] These interstage circuits are designed so that the poles of the normalized system transfer function are evenly distributed on the unit circle in the left half of the complex plane. Such a location of the poles is illustrated for systems of orders one through eight in Fig. 18. The corresponding step-function and frequency responses are shown in Figs. 19 and 20. The standard forms for the Butterworth filters are shown through the eighth order in Table IV. It would be possible to extend this table by analysis, since the definition of the distribution of the poles implies the definition of the characteristic function.

The standard forms for the Butterworth[25] filters are similar to those for the binomial filters, in that the coefficients are symmetrical. This phenomenon is indeed typical of all characteristic functions whose poles lie on the unit circle in the complex plane. (The binomial characteristic equations are special cases, whose roots all lie at the minus one point.)

The step function responses of the Butterworth[25] filters are, by comparison with the responses of the binomial filters, faster, and not surprisingly, more oscillatory. Nevertheless, for many purposes, they represent a close approach to intuitive concepts of optimum duplicator responses. They served, in each case, as the starting point for the iterative experimental determination of the optimum unit-numerator transfer functions by the application of the minimum ITAE criterion.

When the minimum ITAE criterion is applied to the determination of the optimum unit-numerator transfer functions of various orders, the standard forms of Table V are obtained. The corresponding pole locations, step-function responses, and frequency responses are shown in Figs. 21, 22, and 23. With regard to these various mathematical equivalents, it can be seen that the application of this arbitrary criterion has not resulted in the selection of a family of systems with similar and progressive characteristics as the order of the system is increased. This is, in a way, a disappointing result, for it had been hoped that it would be possible to extrapolate the experimental results to the selection of standard forms for systems of still higher orders than it was possible to investigate. In general, the standard forms defined here have coefficients which are slightly higher for the

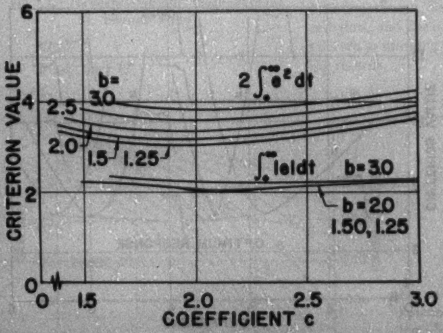

Fig. 11. Integral of squared error and integral of absolute value of error criteria applied to the step-function responses of third-order systems

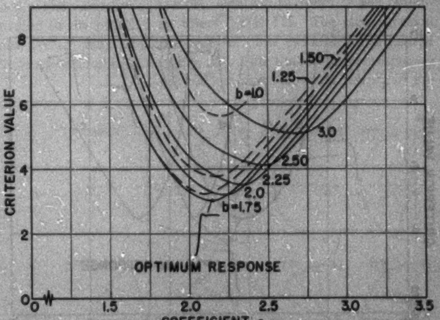

Fig. 12. The integral of time-multiplied absolute value of error criterion applied to the step-function responses of third-order systems

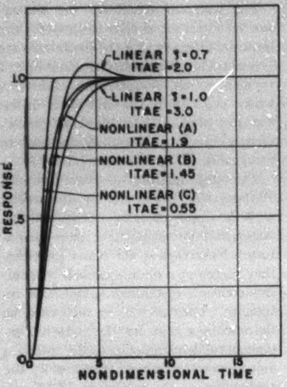

Fig. 13 (left). Step-function responses of linear and nonlinear second-order servomechanisms

Servo A:

$$\frac{d^2e}{dt^2}+\frac{2}{1+4\left(e+\frac{de}{dt}\right)}\frac{de}{dt}+e=0$$

Servo B:

$$\frac{d^2e}{dt^2}+k\frac{de}{dt}+e=0 \qquad \begin{array}{l} k=0,\ e+\frac{de}{dt}\neq 0 \\ k=2,\ e+\frac{de}{dt}=0 \end{array}$$

Servo C:

$$\frac{d^2e}{dt^2}+k=0 \qquad \begin{array}{l} k=1,\ 2e+\frac{de}{de}\left|\frac{de}{dt}\right|>0 \\ k=-1,\ 2e+\frac{de}{dt}\left|\frac{de}{dt}\right|<0 \end{array}$$

low orders of the complex variable, and slightly lower for the higher orders of the complex variable than the corresponding Butterworth[28] standard forms. No inferences on this basis, however, seem warranted.

The criterion has selected responses which are much faster than those of the binomial filters, but which are less oscillatory than those of the Butterworth[28] filters. The goodness of the selected responses might be classed as a fortunate phenomenon of engineering science. Presumably, the value of the congruent standard forms is correspondingly high.

Zero-Velocity and Zero-Acceleration-Error Systems

The class of linear duplicators with unit-numerator transfer functions, while basic, represents only a small fraction of the possible linear systems. The numerators of possible system transfer functions are almost infinitely variable. By confining attention, however, to duplicators with no steady-state displacement error, the normalized transfer-function numerator polynomials are limited to those which include a constant term of unit magnitude. This would still leave open for consideration a large number of polynomial numerators, of an order equal to or less than the corresponding denominator, if an arbitrary choice of polynomial coefficients were allowed. In servomechanism design practice, however, there are two limiting cases, the zero-velocity-error and zero-acceleration-error systems.

The steady-state error of a servomechanism may be shown[2] to be

$$\underset{t\to\infty}{e(t)}=C_0r+C_1\frac{dr}{dt}+\frac{C_2}{2}\frac{d^2r}{dt^2}+\dots \tag{12}$$

In terms of the generalized transfer-function constants shown in the transfer function

$$\frac{C(\lambda)}{R(\lambda)}=\frac{P_m\lambda^m+P_{m-1}\lambda^{m-1}+\dots+P_2\lambda^2+P_1\lambda+P_0}{Q_n\lambda^n+Q_{n-1}\lambda^{n-1}+\dots+Q_2\lambda^2+Q_1\lambda+Q_0} \tag{13}$$

Displacement error coefficient $C_0=0$, when $P_0=Q_0$

Velocity error coefficient $C_1=0$, when $P_1=Q_1$

Acceleration error coefficient $C_2=0$, when $P_2=Q_2$

Therefore, in considering the zero-velocity and zero-acceleration-error systems as limiting cases from among all the possible systems with polynomial-numerator transfer functions, only two different numerators for each order of the denominator will be selected. The optimum transfer functions (standard forms) for systems with normalized transfer functions

$$\frac{C(s)}{R(s)}=\frac{1}{s^n+q_{n-1}s^{n-1}+\dots+q_2s^2+q_1s+1} \tag{14}$$

have already been found by applying the ITAE criterion. The possibilities of finding standard forms for zero-velocity-error systems characterized by the transfer function

$$\frac{C(s)}{R(s)}=\frac{q_1s+1}{s^n+q_{n-1}s^{n-1}+\dots+q_2s^2+q_1s+1} \tag{15}$$

and zero-acceleration-error systems with the transfer function

$$\frac{C(s)}{R(s)}=\frac{q_2s^2+q_1s+1}{s^n+q_{n-1}s^{n-1}+\dots+q_2s^2+q_1s+1} \tag{16}$$

will now be examined in turn.

It may be noted that $C_1=\int_0^\infty e\,dt$ and

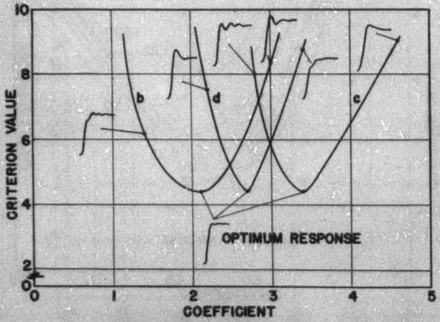

Fig. 14. Sections through the minimum point of the ITAE surface, fourth-order unit-numerator system

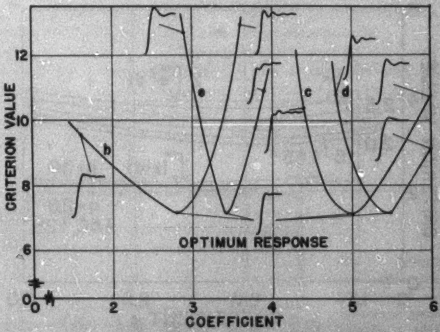

Fig. 15. Sections through the minimum point of the ITAE surface, fifth-order unit-numerator system

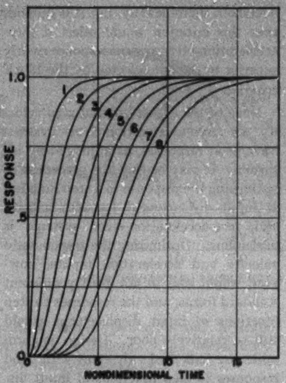

Fig. 16. Step-function responses of the binomial filters, defined by the transfer functions

$$\frac{C(s)}{R(s)}=\frac{1}{(s+1)^n}\quad (n=1, 2, \ldots 8)$$

Table III. The Binomial Standard Forms

$$s+\omega_0$$
$$s^2+2\omega_0 s+\omega_0^2$$
$$s^3+3\omega_0 s^2+3\omega_0^2 s+\omega_0^3$$
$$s^4+4\omega_0 s^3+6\omega_0^2 s^2+4\omega_0^3 s+\omega_0^4$$
$$s^5+5\omega_0 s^4+10\omega_0^2 s^3+10\omega_0^3 s^2+5\omega_0^4 s+\omega_0^5$$
$$s^6+6\omega_0 s^5+15\omega_0^2 s^4+20\omega_0^3 s^3+15\omega_0^4 s^2+6\omega_0^5 s+\omega_0^6$$
$$s^7+7\omega_0 s^6+21\omega_0^2 s^5+35\omega_0^3 s^4+35\omega_0^4 s^3+21\omega_0^5 s^2+7\omega_0^6 s+\omega_0^7$$
$$s^8+8\omega_0 s^7+28\omega_0^2 s^6+56\omega_0^3 s^5+70\omega_0^4 s^4+56\omega_0^5 s^3+28\omega_0^6 s^2+8\omega_0^7 s+\omega_0^8$$

Table IV. The Butterworth Standard Forms

$$s+\omega_0$$
$$s^2+1.4\omega_0 s+\omega_0^2$$
$$s^3+2.0\omega_0 s^2+2.0\omega_0^2 s+\omega_0^3$$
$$s^4+2.6\omega_0 s^3+3.4\omega_0^2 s^2+2.6\omega_0^3 s+\omega_0^4$$
$$s^5+3.24\omega_0 s^4+5.24\omega_0^2 s^3+5.24\omega_0^3 s^2+3.24\omega_0^4 s+\omega_0^5$$
$$s^6+3.86\omega_0 s^5+7.46\omega_0^2 s^4+9.13\omega_0^3 s^3+7.46\omega_0^4 s^2+3.86\omega_0^5 s+\omega_0^6$$
$$s^7+4.5\omega_0 s^6+10.1\omega_0^2 s^5+14.6\omega_0^3 s^4+14.6\omega_0^4 s^3+10.1\omega_0^5 s^2+4.5\omega_0^6 s+\omega_0^7$$
$$s^8+5.12\omega_0 s^7+13.14\omega_0^2 s^6+21.84\omega_0^3 s^5+25.69\omega_0^4 s^4+21.84\omega_0^5 s^3+13.14\omega_0^6 s^2+5.12\omega_0^7 s+\omega_0^8$$

Table V. The Minimum ITAE Standard Forms, Zero-Displacement-Error Systems

$$s+\omega_0$$
$$s^2+1.4\omega_0 s+\omega_0^2$$
$$s^3+1.75\omega_0 s^2+2.15\omega_0^2 s+\omega_0^3$$
$$s^4+2.1\omega_0 s^3+3.4\omega_0^2 s^2+2.7\omega_0^3 s+\omega_0^4$$
$$s^5+2.8\omega_0 s^4+5.0\omega_0^2 s^3+5.5\omega_0^3 s^2+3.4\omega_0^4 s+\omega_0^5$$
$$s^6+3.25\omega_0 s^5+6.60\omega_0^2 s^4+8.60\omega_0^3 s^3+7.45\omega_0^4 s^2+3.95\omega_0^5 s+\omega_0^6$$
$$s^7+4.475\omega_0 s^6+10.42\omega_0^2 s^5+15.08\omega_0^3 s^4+15.54\omega_0^4 s^3+10.64\omega_0^5 s^2+4.58\omega_0^6 s+\omega_0^7$$
$$s^8+5.20\omega_0 s^7+12.80\omega_0^2 s^6+21.60\omega_0^3 s^5+25.75\omega_0^4 s^4+22.20\omega_0^5 s^3+13.30\omega_0^6 s^2+5.15\omega_0^7 s+\omega_0^8$$

$C_2=2\int_0^\infty te\,dt$ for the error response to a unit step input, and that low (or zero) values of these integrals have already been rejected as suitable criteria for optimum response. On an experimental basis, at least, no suitable combination of system parameters could be found which would give displacement step-function responses in accord with intuitive concepts of a good response for many of the zero-velocity and zero-acceleration-error systems. This is by no means to say, however, that the ITAE criterion may not be applied to select the best possible response.

Figs. 8 and 9 have already been presented to show the possible responses of second-order zero-velocity-error systems and the corresponding values of the ITAE criterion. An arbitrary selection of the damping parameter $\zeta=1.6$, as optimum, may be made on the basis that further increases in the damping parameter result in a negligible improvement in the response.

Very much the same situation obtains with regard to the third-order zero-velocity-error system with the transfer function

$$\frac{C(s)}{R(s)}=\frac{cs+1}{s^3+bs^2+cs+1} \qquad (17)$$

For any given value of b, the step-function response will improve indefinitely as the parameter c is increased. The value $b=1.75$ is optimum, according to the ITAE criterion, and the value $c=3.25$ may be selected as marking the onset of diminishing returns.

The standard forms corresponding to the minimum value of the ITAE criterion for the zero-velocity-error systems, through the sixth order, are shown in Table VI. The corresponding responses to step functions of input displacement are illustrated in Fig. 24. Large peak overshoots and rapid accelerations are a concomitant of zero-velocity error. The alternatives suggested by Whiteley,[18] who used peak overshoot as a criterion, tend to have a persistent error which the ITAE criterion will not tolerate. A compromise which may have some merit in this case is afforded by the zero-velocity-error systems which have transfer-function denominators identical to those of the binomial filters, Table III. The step function responses of these systems are presented in Fig. 25. Note that while the responses exhibit less overshoot and less rapid ac-

Fig. 17. Frequency-response functions of the binomial filters

$$\frac{C(j\omega)}{R(j\omega)}=\frac{1}{(j\omega+1)^n}\quad (n=1, 2, \ldots 8)$$

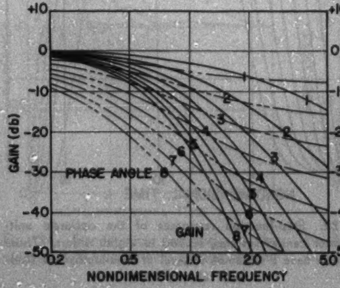

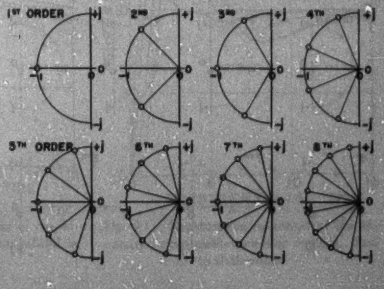

Fig. 18 (right). Pole locations of the Butterworth filters, first to eighth orders

celerations than the optimum responses of Fig. 24, they are, at the same time, appreciably slower.

The case of the third-order zero-acceleration-error transfer system is similar to the third-order zero-velocity-error system, in that the ITAE criterion diminishes in value indefinitely as the value of the b parameter is increased. The value $c=4.9$ is optimum, and the value $b=3.0$ marks the point where little improvement in response results from further increases in this parameter.

Other optimum standard forms for the zero-acceleration-error systems through the sixth order are shown in Table VII, and the corresponding step-function responses appear in Fig. 26. As in the case of the zero-velocity-error systems, the step-function responses, while best according to the ITAE criterion, may still leave something to be desired with respect to peak overshoot. The systems defined by Whiteley's[18] standard forms suffer from the same defect as before; that is, they tend to have a persistent error. Binomial zero-acceleration-error systems, therefore, may again prove to be a suitable compromise. The step-function responses of the binomial zero-acceleration-error systems are shown in Fig. 27.

It is worth reiterating that while these responses are relatively slow, they may, theoretically at least, be reproduced to an arbitrary time scale. The ITAE criterion lays heavy emphasis on a rapid response in nondimensional time, and the overshoots, undershoots, and rapid accelerations are an inevitable feature, if rapid responses of zero-acceleration-error systems are required. Another criterion, such as $\int_0^\infty |e|\,dt$, would penalize the first overshoot more heavily, but it is dubious that this criterion would select a zero-acceleration-error system response clearly superior to the one selected by the ITAE criterion $\int_0^\infty t|e|\,dt$.

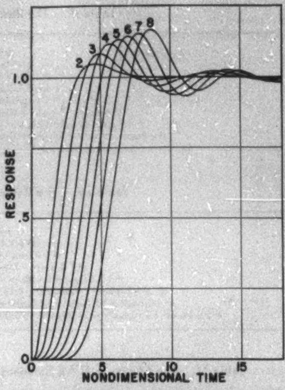

Fig. 19. Step-function responses of the Butterworth filters, second to eighth orders

None of the higher-ordered zero-velocity or zero-acceleration-error systems have good responses, as adjudged by intuition. It may be that the procedure of optimizing the response to a step function of input displacement for zero-velocity and zero-acceleration-error systems is misleading. Optimizing the responses to velocity and acceleration inputs, however, would lead to not greatly different standard forms, and the responses to step functions of input displacement would still be relatively poor. Design compromises are indicated. Systems with good responses to step functions of input displacement, and small but finite velocity and acceleration errors, probably represent an over-all optimum. Standard forms for such systems remain to be discovered.

Suggested Application of the Criterion and of Standard Forms to Design

If a standard form is available for the type of transfer function involved in a particular design problem, its use repre-

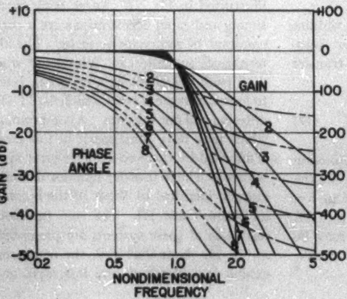

Fig. 20 (left). Frequency - response functions (amplitude and phase) of the Butterworth filters, second to eighth orders

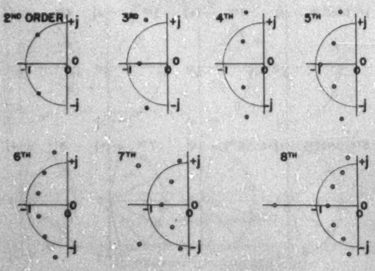

Fig. 21 (left). Pole locations of the optimum unit - numerator transfer systems, second to eighth orders

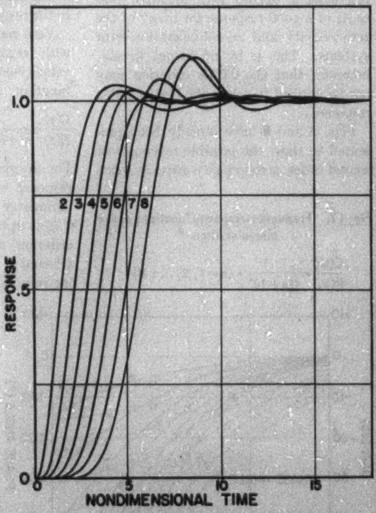

Fig. 22. Step-function responses of the optimum unit-numerator transfer systems, second to eighth orders. These responses have a minimum integral of time-multiplied absolute value of error

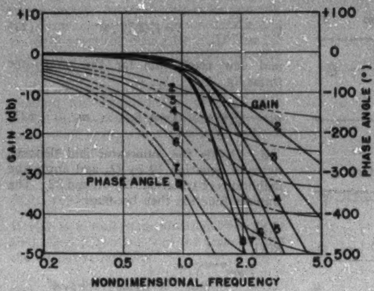

Fig. 23 (left). Frequency-response functions of the optimum unit-numerator transfer systems, second to eighth orders

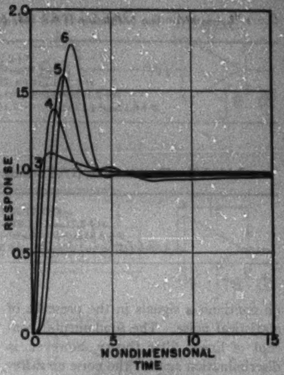

Fig. 26. Step-function responses of the optimum zero-acceleration-error systems, third to sixth orders

sents a simple, powerful, and accurate synthesis procedure. The elementary steps involved would be:

1. Write the differential equations of the system.
2. Develop the system transfer function, leaving in literal form the constants which may be adjusted by design.
3. Normalize the transfer function (equivalent to a time-scale change in the time domain).
4. Solve algebraically for the values of the design variables which will make the transfer-function denominator conform numerically to the appropriate standard form.
5. If it is a matter of choice, the real time scale of the response may be adjusted by the selection of suitable design variables.
6. The system will have the desired response.

Mathematical operations involved comprise the simplest algebra and the direct Laplace transformation (usually accomplished by inspection). The use of standard forms does not involve solving for the roots of equations, plots or graphical constructions, integration, or inverse Laplace transformations. It is a true synthesis method, in that it leads directly and unequivocally to a description of the required system in terms of its design parameters.

The standard forms for the zero-displacement-error systems appear to have immediate application to the design of the many servomechanisms, regulators, and instruments which have transfer functions with unit numerators. They further give rise to a new class of multistage pulse amplifiers with a novel and unique adjustment for optimum response. In those cases where standard forms are unavailable for the exact type of transfer function involved, the use of the most nearly approximate standard form will lead to a very rapid estimate of suitable system adjustments. This estimate may then be refined by other methods. Of course, it may be hoped that standard forms will eventually be developed for all cases of practical interest to the designer of linear systems.

If analogue computation is employed in the study of linear or nonlinear systems for which no standard forms are available, the ITAE criterion may still be used as a unitary figure of merit for the rapid evaluation of a large number of configurations. In the case of systems with multiple outputs, such as an aircraft under automatic control, the criterion, suitably weighted, could be applied to the several outputs simultaneously and the sum of the weighted ITAE criterion values would be an over-all figure of merit for the system.

Finally, since the application of the criterion requires an origin in time, it may appear that the standard forms developed from it are not suitable for the optimum synthesis of servomechanisms operating

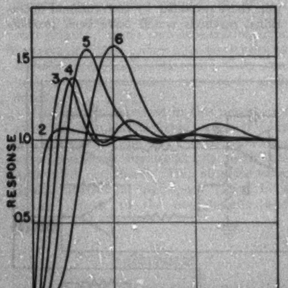

Fig. 24. Step-function responses of the optimum zero-velocity-error systems, second to sixth orders

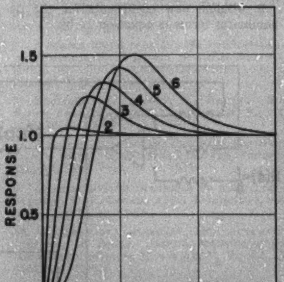

Fig. 25. Step-function responses of the binomial zero-velocity-error systems, second to sixth orders

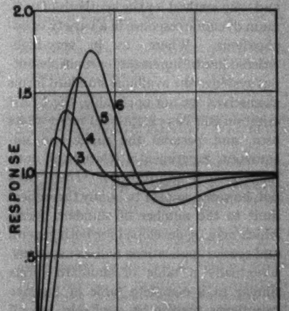

Fig. 27. Step-function responses of the binomial zero-acceleration-error systems, third to sixth orders

Table VI. The Minimum ITAE Standard Forms, Zero-Velocity-Error Systems

$s^2+3.2\omega_0 s+\omega_0^2$
$s^3+1.75\omega_0 s^2+3.25\omega_0^2 s+\omega_0^3$
$s^4+2.41\omega_0 s^3+4.93\omega_0^2 s^2+5.14\omega_0^3 s+\omega_0^4$
$s^5+2.19\omega_0 s^4+6.50\omega_0^2 s^3+6.30\omega_0^3 s^2+5.24\omega_0^4 s+\omega_0^5$
$s^6+6.12\omega_0 s^5+13.42\omega_0^2 s^4+17.16\omega_0^3 s^3+14.14\omega_0^4 s^2+6.76\omega_0^5 s+\omega_0^6$

Table VII. The Minimum ITAE Standard Forms, Zero-Acceleration-Error Systems

$s^3+2.97\omega_0 s^2+4.94\omega_0^2 s+\omega_0^3$
$s^4+3.71\omega_0 s^3+7.88\omega_0^2 s^2+5.93\omega_0^3 s+\omega_0^4$
$s^5+3.81\omega_0 s^4+9.94\omega_0^2 s^3+13.44\omega_0^3 s^2+7.36\omega_0^4 s+\omega_0^5$
$s^6+3.93\omega_0 s^5+11.68\omega_0^2 s^4+18.56\omega_0^3 s^3+19.3\omega_0^4 s^2+8.06\omega_0^5 s+\omega_0^6$

on continuous signals in the presence of statistical noise. The fundamental concept of linear filter theory, however, is discrimination against the noise on a frequency basis. Phillips,[3] as has been pointed out, suggests the selection of a form for the servomechanism system transfer function, and subsequent adjustment of a design parameter to minimize the rms error in the presence of given spectra of signal and noise. There is no reason why the form which is selected should not be one of the standard forms defined by application of the ITAE criterion. The design parameter which is reserved for the optimizing process is the time scale of the standard-form response. This is the equivalent of saying that the natural frequency of the system is placed between the signal and noise frequencies in a way which gives the least rms error in following the signal and rejecting the noise.

Conclusion

Standard forms can provide a quick and easy method for the synthesis of optimum dynamic response in a variety of applications. Where, as in very-high-ordered linear, nonlinear, or multiple-output systems, the available standard forms themselves are not applicable, the ITAE criterion still has exceptional merit of its own, and permits the rapid and unequivocal experimental selection of optimum system adjustments. There does not, however, appear to be any theoretical limit to the number of standard forms which may be developed for both general and special applications to linear systems. Eventually a table of standard forms similar to a complete table of Laplace transforms should be available for all cases of interest; at that time the synthesis of linear systems to have optimum transient response will become a simple, straightforward matter of algebra instead of the involved and often baffling problem which it has been in the past.

Appendix I. Derivation of the Normalized Transfer Function

In general, linear transfer systems of the class known as duplicators may be described by an explicit differential equation of the form

$$\left(Q_n\frac{d^n}{dt^n}+Q_{n-1}\frac{d^{n-1}}{dt^{n-1}}+\dots+Q_2\frac{d^2}{dt^2}+Q_1\frac{d}{dt}+Q_0\right)c(t)=\left(P_m\frac{d^m}{dt^m}+P_{m-1}\frac{d^{m-1}}{dt^{m-1}}+\dots+P_2\frac{d^2}{dt^2}+P_1\frac{d}{dt}+P_0\right)r(t)\qquad(18)$$

in which P_i and Q_i are constants and $m\leqq n$. The corresponding transfer function is

$$\frac{C(\lambda)}{R(\lambda)}=\frac{P_m\lambda^m+\dots+P_2\lambda^2+P_1\lambda+P_0}{Q_n\lambda^n+\dots+Q_2\lambda^2+Q_1\lambda+Q_0}\qquad(19)$$

Equation 19 may be put in a more convenient form for some purposes by a normalization process, which is accomplished as follows:

1. Define a constant ω_0 such that

$$\omega_0^n=\frac{Q_0}{Q_n}\qquad(20)$$

2. Define new coefficients for the denominator terms in equation 19 by

$$q_i=\frac{Q_i}{\omega_0^{n-i}Q_n}\qquad i=1,2,\dots n\qquad(21)$$

and new coefficients for the numerator terms by

$$p_i=\frac{P_i}{\omega_0^{n-i}Q_n}\qquad i=0,1,2,\dots m\qquad(22)$$

3. Divide the numerator and denominator of equation 19 by Q_n and apply the definitions of equations 20, 21, and 22. The transfer function then becomes

$$\frac{C(\lambda)}{R(\lambda)}=\frac{p_m\omega_0^{n-m}\lambda^m+\dots+p_2\omega_0^{n-2}\lambda^2+p_1\omega_0^{n-1}\lambda+p_0\omega_0^n}{\lambda^n+q_{n-1}\omega_0\lambda^{n-1}+\dots+q_2\omega_0^{n-2}\lambda^2+q_1\omega_0^{n-1}\lambda+\omega_0^n}\qquad(23)$$

4. Introduce a new complex variable s such that

$$s=\frac{\lambda}{\omega_0}\qquad(24)$$

Then the transfer function reduces finally to the normalized form

$$\frac{C(s)}{R(s)}=\frac{p_ms^m+\dots+p_2s^2+p_1s+p_0}{s^n+q_{n-1}s^{n-1}+\dots+q_2s^2+q_1s+1}\qquad(25)$$

Equation 24 is equivalent to the substitution of a new independent variable τ in the original differential equation, where $\tau=\omega_0 t$. It is important to note that the transfer function of the system has been reduced to a form in which the coefficients of the first and last terms of the denominator are unity.

Appendix II. Analogue Computer Techniques

The development of the standard forms outlined in this paper depended on the availability of the transient responses associated with a very large number of combinations of transfer function coefficients. The computational labor necessary to obtain these responses by conventional operational methods would have been prohibi-

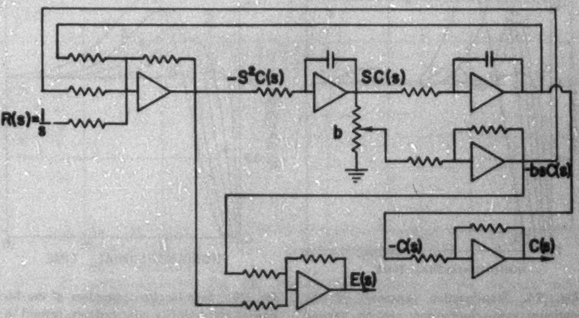

Fig. 28. Analogue computer circuit for obtaining the responses of a second-order transfer system

tive, especially for the higher-order systems. An electronic analogue computer afforded the only practical means for obtaining the transient responses and the corresponding criterion values.

Fig. 28 shows the basic computer circuit diagram for obtaining the response of a second-order zero-displacement-error system which has the normalized transfer function

$$\frac{C(s)}{R(s)}=\frac{1}{s^2+bs+1} \qquad (26)$$

If $r(t)$ is a unit step function applied at $t=0$, then $R(s)=1/s$, and the transform of the output response is

$$C(s)=\frac{1}{s(s^2+bs+1)} \qquad (27)$$

The transform of the error response is given by

$$E(s)=R(s)-C(s)=\frac{1}{s}-\frac{1}{s(s^2+bs+1)}$$

$$=\frac{s^2+bs}{s(s^2+bs+1)}=(s^2+bs)C(s) \qquad (28)$$

It is possible, with the aid of a computer technique developed by Beck,[26] to simultaneously extract the error response from the basic computer circuit, which is used to generate the output response without using differentiators. The method involves summing selected responses which are available within the computer loop, as illustrated in Fig. 28.

The Laplace transforms of the output response and error response of a second-order zero-velocity-error system are given by

$$C(s)=\frac{bs+1}{s(s^2+bs+1)} \qquad (29)$$

and

$$E(s)=\frac{s^2}{s(s^2+bs+1)} \qquad (30)$$

for an input step function. Beck's[26] method may be applied to extract these responses from the basic computer circuit of Fig. 28, although the required connections are not shown. In a similar manner, the output and error responses of zero-displacement, zero-velocity, and zero-acceleration-error systems of higher orders may be developed without using differentiators. Only one basic computer circuit is required for each order.

The criteria discussed in this paper were mechanized on the analogue computer using the circuits of Fig. 29. Criterion values were produced simultaneously with the associated responses. The absolute-value device utilized a high-speed relay, in a circuit similar to the one described by Bennett and Fulton.[27]

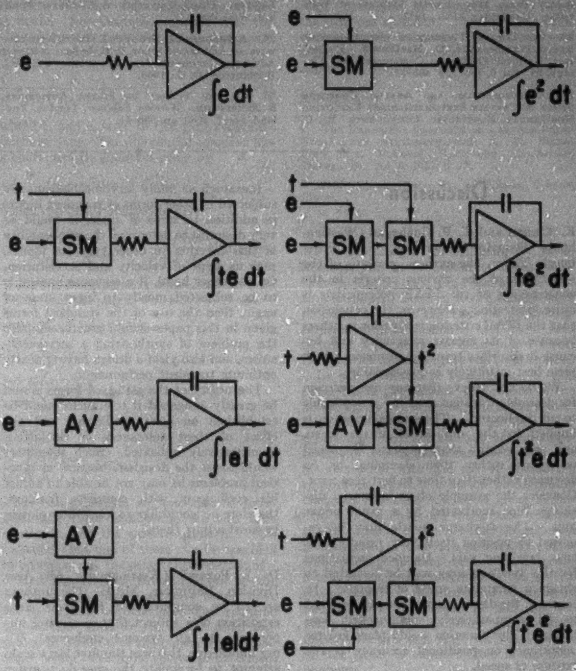

Fig. 29. Circuits for mechanizing performance criteria on an electronic analogue computer

SM = servo multiplier AV = absolute value unit

References

1. Response of Physical Systems (book), J. D. Trimmer. John Wiley and Sons, Inc., New York, N. Y., 1950.

2. Theory of Servomechanisms (book), H. M. James, N. B. Nichols, R. S. Phillips. McGraw-Hill Book Company, Inc., New York, N. Y., 1947.

3. The Dynamics of Automatic Controls (book), R. C. Oldenbourg, H. Sartorius. The American Society of Mechanical Engineers, New York, N. Y., 1948.

4. A New Linear Operational Calculus, F. W. Bubb. United States Air Force *TR No. 6581*, Wright Air Development Center, Wright-Patterson Air Force Base, Ohio, May 1951.

5. On the Criteria for the Stability of Small Motions, R. A. Frazer, W. J. Duncan. *Proceedings*, Royal Society of London, England, vol. A-124, 1929, pp. 642–54.

6. A Simple Method of Constructing Stability Diagrams, W. S. Brown. *R and M No. 1905*, British Aeronautical Research Committee, London, England, 1942.

7. Regeneration Theory, H. Nyquist. *Bell System Technical Journal*, New York, N. Y., vol. 11, 1932, pp. 126–47.

8. Network Analysis and Feedback Amplifier Design (book), H. W. Bode. D. Van Nostrand Co., Inc., New York, N. Y., 1945.

9. Control System Synthesis by Root Locus Method, W. R. Evans. *AIEE Transactions*, vol. 69, pt. I, 1950, pp. 66–69.

10. Aerodynamic Stability and Automatic Control, W. Bollay. *Journal*, Institute of the Aeronautical Sciences, New York, N. Y., vol. 18, 1951, pp. 569–617.

11. The Extrapolation, Interpolation, and Smoothing of Stationary Time Series (book), N. Wiener. John Wiley and Sons, Inc., New York, N. Y., 1949.

12. General Principles of Instrument Analysis, C. S. Draper, G. V. Schliestett. *Instruments*, Pittsburgh, Pa., vol. 12, 1939, pp. 137–42.

13. Dynamic Behaviour and Design of Servomechanisms, G. S. Brown, A. C. Hall. *Transactions*, American Society of Mechanical Engineers, New York, N. Y., vol. 68, 1946, pp. 503–22.

14. Automatic Flight Control—Analysis and Synthesis of the Lateral Control Problem, R. N. Bretol. *Transactions*, American Society of Mechanical Engineers, New York, N. Y., vol. 74, 1951, pp. 415–30.

15. Vacuum Tube Amplifiers (book), G. E. Valley, Jr., H. Wallman. McGraw-Hill Book Company, Inc., New York, N. Y., 1948.

16. Networks Designed to Approximate a Specified Transient Response, J. A. Blickensderfer, H. P. Blanchard. *Technical Report No. 1*, Electronics Research Laboratory, Stanford University, Palo Alto, Calif., March 1950.

17. The Synthesis of Lumped-Element Circuits for Optimum Transient Response, G. W. C. Mathers. *Technical Report No. 38*, Electronics Research Laboratory, Stanford University, Palo Alto, Calif., Nov. 1951.

18. The Theory of Servo Systems, With Particular Reference to Stabilization, A. L. Whiteley. *Journal*, Institution of Electrical Engineers, London, England, vol. 93, 1946, pp. 353–72.

19. A Survey of Stability Analysis Techniques for Automatically Controlled Aircraft, A. L. Jones, B. R. Briggs. National Advisory Committee for Aeronautics *TN 2275*, Ames Aeronautical Laboratory, Moffett Field, Calif., Jan., 1951.

20. Some Design Criteria for Automatic Controls, Paul T. Nims. *AIEE Transactions*, New York, N. Y., vol. 70, 1951, pt. I, pp. 606–11.

21. The Analysis and Synthesis of Linear Servomechanisms (book), A. C. Hall. The Tech-

nology Press, Massachusetts Institute of Technology, Cambridge, Mass., 1943.

22. Non-Linear Techniques for Improving Servo Performance, **D. MacDonald.** *Proceedings*, National Electronics Conference, Inc., Chicago, Ill., vol. 6, 1951, pp. 400–21.

23. A Topological and Analog Computer Study of Certain Servomechanisms Employing Non-Linear Electronic Components, **R. C. Lathrop.** *Thesis*, University of Wisconsin, Madison, Wis., 1951.

24. A Theoretical Study of Lateral Stability with an Automatic Pilot, **F. H. Imlay.** National Advisory Committee for Aeronautics *TR 693*, Washington, D. C., 1940.

25. On the Theory of Filter Amplifiers, **S. Butterworth.** *Wireless Engineer*, London, England, vol. 7, 1930, pp. 536–41.

26. Symposium I on REAC Techniques. Reeves Instrument Corporation, New York, N. Y., "A Method for Solving Problems on the REAC by the Use of Transfer Functions Without Passive Networks," **C. Beck.** March 15–16, 1951, pp. 131–36.

27. The Use of High-Speed Relays in Electric Analogue Computers, **R. R. Bennett, A. S. Fulton.** *AIEE Transactions*, vol. 70, pt. II, 1951, pp. 1553–55.

◆

Discussion

K. Kinnen and **K. P. Geohegan** (Westinghouse Electric Corporation, East Pittsburgh, Pa.): The authors' analysis of the selectivity of the various criteria in the construction of the ITAE polynomials is quite interesting. However, the conclusion that the ITAE criterion is superior to others because of its greater selectivity and because it describes transient responses which seem best intuitively is questionable.

We do not believe that any one criterion for desirable transient response is applicable to all duplicators. The proper criterion is implied by the application of the servo, and may require that emphasis be placed on speed rather than damping, or on accuracy rather than time to first-zero error. Consider the example of an industrial discharge pipe motivated by a given power unit. The discharge nozzle may be required to position itself very rapidly over large receiving vats. Damped oscillations for this function may well be tolerated to obtain a maximum speed of response. In contrast, the discharge pipe may be required to fill comparatively small-necked containers. This function would place greater importance on positional accuracy at the expense of speed.

Using a gun-mount drive as a second example, the proper servo design is that which maximizes the kill-probability integral regardless of which criterion this requires. It would seem, therefore, that the system cannot be most effectively designed by any one criterion, ITAE or otherwise, until the complete application is considered.

Donald C. McDonald (Cook Research Laboratories, Skokie, Ill.): The need is extremely great for a criterion which will define the optimum transient response of a servomechanism. A large number of the operational problems or inadequacies of existing automatic-control systems are the result of an improper choice during the design stage of the type of transient response desired for the system.

The ITAE criterion appears to be a criterion which does define or evaluate adequately the transient performance of a servomechanism to a step of angle input. The adequacy of this criterion is based upon the fact that it gives recognition to the concepts that the sign of the error is not important (only the existence of an error is important in evaluating transient performance), and that the existence of an initial large error must be accepted, but the system should be penalized if any error exists after this initial period. In addition, the form of that criterion is the simplest which contains the aforesaid features, and is still discriminatory in nature.

Inasmuch as many servomechanisms are subjected to other forms of transient inputs in addition to steps of angle, it would be very desirable to determine the applicability of this criterion to other types of inputs, such as steps of velocity and acceleration. On the other hand, if a servomechanism is to be subjected mostly to input steps of angle, then the use of the standard forms given in this paper should greatly simplify the problem of synthesizing a servomechanism, and also yield a design having nearly optimum transient performance.

The utility of the standard forms would be greatly enhanced if tolerances could be established on each coefficient, and the effect of these tolerances or deviations quantitatively indicated. Such tolerances would assist the designer, because in practical problems he may not be able to adjust his coefficients with complete freedom; therefore he would like to know how closely he must adjust them.

D. J. Povejsil (Westinghouse Air Arm Division, Baltimore, Md.): The authors are to be congratulated for their clear exposition of a subject that is of vital importance to all systems engineers. To my knowledge, this was the first large-scale attempt to formulate the specific transfer functions that satisfy a given error criterion. Thus, the systems engineer is empowered to perform the legislative and judicial function of systems design simultaneously. That is to say, he may attempt to mold his system into a standard form and at the same time have a quantitive measure of system goodness. Contrast this with the methods of Routh,[1] Nyquist,[2] and their many respective variations, which are capable only of passing judgment upon a system already formulated; or with the binomial or Butterworth[3] forms, which permit the formulation of a stable system, but not necessarily an optimum one.

There may be those who will be critical of the error criterion used by the authors as the basis for their standard forms. The authors themselves have admitted possible inadequacies of this criterion for zero-velocity and zero-acceleration error systems. Such arguments are mere sophistry, however, since the only alternatives to the authors' standard forms are other standard forms, shown to be inadequate, or the usual cut-and-try methods. The important fact is that the authors have taken a long step in the right direction towards a more logical approach to systems design.

For some time, we have investigated the problem of designing automatic flight-control systems to fit predetermined desired characteristics. A procedure was devised for the logical formation of automatic flight-control systems. Using this procedure for the initial gain settings, and then optimizing gains by observation of computer results, we were able to formulate fundamental autopilot systems far more rapidly and efficiently than before. The characteristic equations for these systems were recorded to use as a basis for future design. In the cases where enough data was taken for comparison (fourth-, fifth-, and sixth-order polynomial denominators), we found that our results fall between the authors' expressions and those for the Butterworth[3] filters. Thus, we are grateful to the authors, not only for establishing the validity of our work, but also for pointing the way towards further refinements in our methods.

In connection with autopilot systems, it should be mentioned that the formation of an autopilot system to fit one of the polynomials is a rather simple matter, provided that the system has a sufficient number of adjustable variables of the proper type. This last provision is the real clue to the power of the method suggested by the authors, because it leads to the following theorem for all linear systems:

Theorem: "A linear system whose characteristic equation is

$$p^n+a_1p^{n-1}+\ldots+a_{n-1}p+a_n=0$$

can be molded into any desired form if the following conditions are met:

1. The total number of system variables must at least equal the order of the characteristic equation.
2. Each constant a_j of the characteristic equation must be a function of at least one of the system variables.
3. Any combination of m a_j's must contain m system variables."

To illustrate the theorem, consider the characteristic equation

$$p^3+a_1p^2+a_2p+a_3=0$$

In order to mold this equation into any desired form:

1. There must be three variable parameters, A_1, A_2, A_3.
2. a_1, a_2, and a_3 equal functions of A_1, A_2, A_3.
3. The following type of condition does not exist

$$a_1=f_1(A_1)$$

$$a_2=f_2(A_1)$$

That this simple theorem has been ignored in autopilot work is obvious when it is found that almost none of the standard autopilot systems satisfy the three conditions. Almost invariably, there are insufficient control parameters to effect the desired optimization.

Concerning the standard forms themselves, can any conclusion be drawn from the increasing similarity of the authors' forms and the Butterworth[2] forms as the order of the equation increases? If this were a trend, the Butterworth[3] forms could be used for equations higher than eighth order that satisfy the ITAE criterion.

There is one other evidence of a trend in the authors' standard forms for unity numerators. If phase shift is plotted as a function of frequency, it is found that phase shift is almost a linear function of frequency, except for the final $\pi/2$ radians of phase shift. Furthermore, the slope of the linear portion of the phase shift versus frequency curve is approximately

$$\frac{\phi}{\omega}=\frac{n}{1.45}$$

where

ω = frequency, radians per second
ϕ = phase shift, radians
n = order of polynomial

Unfortunately, the relationship is not exact, and its accuracy decreases with the order of the equation. Nevertheless, it would appear that the property of linear phase shift bears some relationship to the ITAE criterion.

REFERENCES

1. See reference 5 of the paper.
2. See reference 7 of the paper.
3. See reference 25 of the paper.

G. H. Fett (University of Illinois, Urbana, Ill.): The authors have set up a unique and definite method of determining what is considered an optimum response of a dynamic system, and the standard forms which they give should be useful in simple control systems. Where the control is not linear, or where the degree of the characteristic equation is high, the mathematical difficulties become rather great when the method is applied.

Other criteria, as the authors suggest, might well be used in place of the ITAE one; a suggested criterion which is much simpler to visualize is the value of the output displacement at the first overshoot, when a unit step displacement is applied to the input, multiplied by the time required to reach the maximum deflection. This measure is simply the area, on the displacement-time curve, of the rectangle bounded by the maximum deflection and the overshoot time. When this criterion is used for a second-order differential equation, corresponding to a servomechanism with a time delay in the load, a minimum occurs at a damping ratio of 0.5, with a relatively flat region between damping ratios of 0.4 and 0.6, and the curve shows selectivity against values other than these.

This same criterion may be applied to equations of any order, with considerable selectivity of suitable values. An advantage of this criterion is the ease with which it can be applied to combinations of linear and nonlinear systems, or those involving switching between time constants at different points on the phase-plane trajectory. For a complete discussion, see references 1 and 2.

The method suggested by the authors does lead to considerable complexity when the determination of the required quantities is made. For example, suppose that the control system gives rise to an open-loop expression given by

$$\frac{C}{E}=\frac{K}{s(1+\tau_1 s)(1+\tau_2 s)} \tag{1}$$

where τ_1 and τ_2 refer to two time constants in the system. The differential equation has a characteristic equation given by

$$\tau_1\tau_2 s^3+(\tau_1+\tau_2)s^2+s+K=0$$

which can be normalized to give

$$s^3+\frac{\tau_1+\tau_2}{\tau_1\tau_2}\left(\frac{\tau_1\tau_2}{K}\right)^{1/3}s^2+\frac{1}{\tau_1\tau_2}\left(\frac{\tau_1\tau_2}{K}\right)^{2/3}s+1=0$$

Using the corresponding standard form from Table V of the paper, which is

$$s^3+1.75\omega_0 s^2+2.15\omega_0^2 s+\omega_0^3$$

it is seen that

$$\frac{\tau_1+\tau_2}{\tau_1\tau_2}\left(\frac{\tau_1\tau_2}{K}\right)^{1/3}=1.75\omega_0$$

and

$$\frac{1}{\tau_1\tau_2}\left(\frac{\tau_1\tau_2}{K}\right)^{2/3}=2.15\omega_0^2$$

Thus two equations are available to determine the three unknowns, the two time constants, and the gain constant K. This indicates that one of these can be specified in advance and the other two determined.

Had the original equation been of the fourth order, three equations would have to be solved to determine the required quantities. Thus for the eighth order suggested in Table V of the paper, seven equations would have to be solved to determine the design parameters—not a simple procedure.

An interesting point results from a control system having an open-loop response given by

$$\frac{C}{E}=\frac{K(1+\tau_3 s)}{s(1+\tau_1 s)(1+\tau_2 s)} \tag{2}$$

for which the normalized form of the characteristic equation may be written

$$s^3+\frac{\tau_1+\tau_2}{\tau_1\tau_2}\left(\frac{\tau_1\tau_2}{K}\right)^{1/3}s^2+\frac{1+\tau_3}{\tau_1\tau_2}\left(\frac{\tau_1\tau_2}{K}\right)^{2/3}s+1=0$$

Now, if the standard form of Table V of the paper is applied, it is seen that

$$\frac{\tau_1+\tau_2}{\tau_1\tau_2}\left(\frac{\tau_1\tau_2}{K}\right)^{1/3}=1.75\omega_0$$

and

$$\frac{1+\tau_3}{\tau_1\tau_2}\left(\frac{\tau_1\tau_2}{K}\right)^{2/3}=2.15\omega_0^2$$

If the time constants τ_1 and τ_2 were specified, then the constant of the lead network τ_3 and the gain constant K can be readily computed. In this example, the solution for the optimum parameters is not difficult. It may be that the authors had in mind situations such as that just described.

I am glad that the authors included the word "optimum" in quotation marks when the title was specified. The word has been overused in the literature, and must be very indefinite in its connotation because each application implies a different "optimum."

REFERENCES

1. THE TRANSIENT RESPONSE OF A SINGLE POINT NON-LINEAR SERVOMECHANISM, K. N. Burns. *Proceedings*, National Electronics Conference, Chicago, Ill., vol. 8, 1952, p. 22.
2. *Ibid.*, Thesis, University of Illinois, Urbana, Illinois.

W. O. Brehaus, W. F. Milliken, Jr., C. L. Muzzey, and **I. C. Statler** (Cornell Aeronautical Laboratory, Inc., Buffalo, N. Y.): In this paper, Graham and Lathrop have proposed a simple criterion for optimizing transfer system response and have also included a presentation of standard forms for use with systems up to the eighth order.

In our opinion, the real impact of this paper lies in the authors' recognition of the design utility of a criterion, and in the underlying reasoning and choice of the ITAE criterion. There are many practical situations, notably in nonlinear mechanics, and in connection with the use of computing equipment, where a criterion for optimum transient responses will be of great usefulness. If we have any suggestion relative to this paper, it is the fact that the criterion presentation, in itself, is a sufficiently worthwhile package to stand on its own, and that it may be somewhat obscured by the general completeness of the historical background material which proceeds it, and the development of the standard forms which follow. Be this as it may, the 3-in-1 nature of this paper is commendable in its thoroughness.

In general, this paper stands as a thoroughly fine piece of work. The authors' presentation is factual and impartial, and because of recent refinements necessitating the optimization of systems, is in addition timely. From the viewpoint of those engaged in airplane artificial-stability and feel systems, and automatic-control applications in general, it is believed that the standard forms, up to and including the eighth order, are sufficient for present practice. While it is easy to visualize in this work, systems of higher order, in general they can be simplified to an eighth or less order. In cases, where the system under consideration does not permit application of the standard forms, it will still be practical and useful to evaluate the criterion integral directly.

The authors wisely make no strong case for the finality of the criterion proposed, but rather that it appears reasonable in light of experience with both lower- and higher-order systems. Many criteria can of course be promulgated, and whether the present criterion is completely reliable, selective, and easy to use for higher-order systems, can only be decided through experience. In our own systems-design work we contemplate using the proposed integral unless other evidence suggests modification.

Considerable advantage will attend the use of one criterion by those engaged in systems design, and this is true even if the criterion is not absolutely perfect for all situations.

We would like to take this opportunity to congratulate the authors on a straightforward, well conceived, and well executed paper.

Philip C. Rapp (Bell Aircraft Corporation, Buffalo, N. Y.): It is necessary, in the first place, to express the gratitude of the engineering profession to the authors for the excellent job they have done in exploring the characteristics of so many different systems. We may congratulate ourselves upon living at a time when mechanical aids to analysis have made possible the execution of a task which would formerly have been so laborious as to be almost impossible.

On the whole, however, the results are slightly disappointing; not, one hastens to add, because of any deficiency on the part of the authors, but because the theory yields so little of regular behavior. This may be due to the fact that the criterion on which the systems are optimized is, itself, somewhat awkward to manipulate. The non-analyticity of the absolute value function makes it awkward to manipulate by classical techniques. This hampers the exploration of the reasons for the absence of any fraternal resemblances between the responses of systems of increasing order. At the same time, one suspects that the optimum values of the higher coefficients become less and less sharply determined as the order increases. This leads to a speculation that there may exist families whose behavior is very close to the optima presented here, but whose behavior is considerably more regular. The distribution of poles in Fig. 21 is somewhat suggestive of a family whose poles are distributed on a normal curve whose vertex lies at $-k$, $k<1$.

Finally, it is always necessary to keep in mind in investigations of this nature that the optimal criterion is a function of the application of the servomechanism. The criterion used here is certainly one of wide applicability, but there are services in which it is necessary to minimize the integral of the error regardless of the oscillatory behavior of the functions thus determined. Very frequently, the oscillations of such a system can be filtered by a large inertial impedance on the output. Likewise, it is important to the servomechanism engineer to remember that it is the conditions at the final output that must be optimized. The writer has known cases in which the servomechanism engineer carefully optimized the characteristics of the block of the diagram subject to this own immediate surveillance, ignoring the fact that the output of this block was fed to another subsystem whose characteristics had a much stronger effect on the whole system behavior than the servomechanism itself. Unfortunately, the optimum, so-called, for the servomechanism gave far from optimum characteristics for the whole system. Thus, the criterion proposed here, or any other, must be applied at the output.

Dunstan Graham and **R. C. Lathrop**: The authors wish to express their appreciation to all the discussers who have contributed their observations and comments.

Mr. Povejsil's concept of systems synthesis seems to be in remarkable consonance with our own. We should like to hazard the guess that this may be attributed to the fact that his experience in the synthesis problems connected with high order, multiple-loop, aircraft automatic control systems is very similar to ours. It is, of course, gratifying to note that he has arrived at such similar standard forms independently.

The theorem which he proposes is interesting, valuable, and undoubtedly correct. We cannot do otherwise than concur in his observation that disregard of the implied law has been prevalent, to date, in the synthesis of aircraft automatic controls. It has been our experience that additional feedback loops often provide the desired control parameters. While algebraic difficulties may arise in solving for the optimum values of the control parameters, the difficulties are not considered to be by any means insuperable.

It is apparently true that the high-order ITAE standard forms approach those of the Butterworth filters, but the direction of this approach is not regular. Reference to the first few coefficients of the seventh- and eighth-order standard forms illustrates this point.

Mr. Povejsil's evidence concerning the linearity of the phase characteristic (and other possible family traits) certainly merits further investigation. Linvill,[1] however, indicates that a large class of transfer systems, comprising also the Butterworth filters, have approximately linear phase characteristics. The possibility also exists that there may be some regular distributions of poles which would yield transfer functions approximately equal to the ITAE standard forms, as suggested by Mr. Rapp. Several different families of pole locations are proposed in references 15, 16, and 25 of the paper. We are not, however, sanguine in the expectation of finding regular characteristics for the minimum ITAE transfer systems.

It appears that the connotation of the word duplicator, as employed in the paper, is not entirely clear. To our minds, the characteristics of a high-performance duplicator must comprise simultaneous speed, stability, and accuracy. There may, of course, on occasion, be good and sufficient reasons for sacrificing one of these qualities. The ITAE criterion is proposed as an adjunct to, not a substitute for, engineering judgment. With regard to the design requirements of the vat discharge tube, as discussed by Mr. Kinnen and Mr. Geohegan, it would seem that the criteria to be applied to the performance of the mechanism are the ones applied to a switch rather than those applied to a continuous, closed-loop duplicator. In the case of the gun mount drive, the evaluation of the effect of all possible variations in servo system parameters on the kill probability may be impractical. It is indicated in the paper how the ITAE criterion may be used in conjunction with the rms error criterion. All valid criteria, maybe excluding the ITAE criterion, will have to be applied to each systems design. An example of the simultaneous application of several integral criteria is given by Boksenbom and Hood.[2]

It is still our opinion, however, that the ITAE criterion alone will provide a sound basis for design in a variety of useful applications.

In anticipation of Mr. McDonald's suggestion, the authors have successfully applied the ITAE criterion to the evaluation of systems subjected to step functions of input velocity and load disturbance. The results of these tests will be available for publication in the near future. Of course, adjustment of systems for optimum transient response to these inputs yields standard forms which are different, in general, from the input positional step-function standard forms.

The further suggestion that tolerances on the standard-form coefficients be established has considerable merit. Unfortunately, however, the presentation of data associated with all of the possible simultaneous variations of the coefficients would be rather formidable. The results of varying the coefficients, one at a time, about their optimum values are given in Figs. 6, 12, 14, and 15 of the paper, for unit-numerator transfer functions of orders two through five.

Mr. Rapp is quite correct in his assertion that cascading two transfer systems which have been optimized individually may not yield the over-all optimum adjustment. The reader can easily verify this fact by multiplying two low-order standard forms together.

The criterion propounded by Dr. Fett is certainly easy to apply, and it may be adequate for certain systems. It has several serious shortcomings, however, when it is applied to general duplicator systems. First, it is not defined for systems which do not overshoot. Second, when it is applied to some higher-order systems it may select system coefficients which yield transient responses obviously unsuitable for duplicators. For example, in the case of the third-order zero-displacement-error system, Dr. Fett's criterion selects transfer-function coefficients in the neighborhood of $b=0.5$, $c=2.0$. Reference to Fig. 10 of the paper shows that this point lies on the stability boundary.

The open-loop transfer function given in equation 2 of Dr. Fett's discussion represents an important practical case. The closed-loop normalized transfer function, however, reduces to the form

$$\frac{C}{R}=\frac{c's+1}{s^3+bs^2+cs+1}$$

where $c'<c$. Standard forms for such systems are not given in the present paper, but we expect to make them available for publication soon.

REFERENCES

1. THE APPROXIMATION WITH RATIONAL FUNCTIONS OF PRESCRIBED MAGNITUDE AND PHASE CHARACTERISTICS, J. G. Linvill. *Proceedings*, Institute of Radio Engineers, New York, N. Y., vol. 40, 1952, pp. 711–21.

2. AUTOMATIC CONTROL SYSTEMS SATISFYING CERTAIN GENERAL CRITERIONS ON TRANSIENT BEHAVIOR, A. S. Boksenbom, R. Hood. *NACA TN 2378*, National Advisory Committee for Aeronautics, Washington, D. C., 1951.

Approximation of Transient Response from Frequency Response Data

CHARLES H. DAWSON
MEMBER AIEE

Synopsis: A relatively short method yielding the time response to an impulse-input from the Nyquist or Bode presentation of the real frepuency open-loop response is outlined. This method has been found to give good agreement for linear feedback systems up to and including those having fifth-order closed-loop transfer functions.

ALTHOUGH automatic feedback control design requirements usually specify the output time response to some standard form of input signal, the design process is commonly performed on a frequency response basis. This procedure is justified by the existing wealth of knowledge and experience in steady-state alternating current theory and in feedback amplifier performance. To check the completed design, the response information must be transformed from the frequency to the time domain.

Exact mathematical methods of performing these transformations exist for linear systems under very general conditions but unfortunately do not lead to closed-form results except in certain special cases. Since even completely random inputs may be considered as composed of successions of impulses, knowledge of impulse response leads easily to the response for any specified input.

This paper presents an approximate solution of the inverse Laplace transform for linear systems under certain restrictions which are satisfied by all well-stabilized feedback control systems. Zero initial energy storage is assumed. The solution for a particular example is illustrated in the figures; the actual equations of this example are given in the Appendix.

Mathematical Basis

If the closed-loop transfer function, $G(s)$, of a linear system has no poles in the right-hand plane, the response $c(t)$ to an input unit impulse, $\delta(t)$, reduces to

$$c(t)=\frac{1}{2\pi}\int_{-\infty}^{\infty}G(\omega)\epsilon^{j\omega t}d\omega \qquad (1)$$

Each of the two functions, under the integral sign may be considered as the sum of a real and an imaginary part, each real part being an even function of ω and each imaginary part an odd function of ω

$G(\omega)=R(\omega)+jI(\omega)$ and
$\epsilon^{j\omega t}=\cos\omega t+j\sin\omega t$

where

$R(\omega)$ and $\cos\omega t$ are real and even
$I(\omega)$ and $\sin\omega t$ are imaginary and odd

Therefore

$$c(t)=\frac{1}{2\pi}\int_{-\infty}^{\infty}[R(\omega)\cos\omega t-I(\omega)\sin\omega t]d\omega+ j\frac{1}{2\pi}\int_{-\infty}^{\infty}[R(\omega)\sin\omega t+ I(\omega)\cos\omega t]d\omega \qquad (2)$$

Since the integrand in the second integral is odd, the value of the integral is zero. Since the integrand of the first integral is even, integration over the range from minus to plus infinity yields a value equal to twice that given by integration over the range from zero to plus infinity. Equation 2 may therefore be expressed as

$$c(t)=\frac{1}{\pi}\int_{0}^{\infty}R(\omega)\cos\omega t\,d\omega- \frac{1}{\pi}\int_{0}^{\infty}I(\omega)\sin\omega t\,d\omega=c_r(t)+c_i(t)$$

where

$c_r(-t)=c_r(t)$
$c_i(-t)=-c_i(t)$

Since for all negative values of time, a physical system can show no response to an impulse occurring at $t=0$

$c(-t)=0=c_r(-t)+c_i(-t)=c_r(t)-c_i(t)$

and therefore

$c_r(t)=c_i(t)$

The response to a unit impulse at $t=0$ can thus be expressed either as

$$c(t)=\frac{2}{\pi}\int_{0}^{\infty}R(\omega)\cos\omega t\,d\omega$$

or as

$$c(t)=-\frac{2}{\pi}\int_{0}^{\infty}I(\omega)\sin\omega t\,d\omega \qquad (3)$$

Obtaining the Imaginary Component

To evaluate the integral of equation 3, a plot of $I(\omega)$ as a function of ω is required. Assuming that the open-loop frequency response of the system is available as a Nyquist plot in polar co-ordinates or as a Bode diagram of magnitude in logarithmic units against phase angle, loci of constant values of the imaginary component may be added from equation 4 or equation 5. The curve of $I(\omega)$ against ω is then readily determined from the composite plot.

The loci of constant I on the Nyquist plot are circles of radius $1/(2I)$ having their centers at $x=-1$ and $y=1/(2I)$ as defined by

$$[x+1]^2+[y-1/(2I)]^2=[1/(2I)]^2 \qquad (4)$$

These loci are shown in Fig. 1 superimposed on the Nyquist plot of the Appendix example. The resulting plot of $I(\omega)$ against ω is given in Fig. 2. The loci on the Bode diagram are more cumbersome to draw, being defined by

$$\phi=180^\circ-\tan^{-1}1/(2I)\pm \cos^{-1}[(r+1/r)/(4+[1/I]^2)^{1/2}] \qquad (5)$$

where

ϕ = the phase angle of the open-loop response in degrees
r = the magnitude

Approximating the Integral

The response to a unit impulse is given by equation 3 as

$$c(t)=-\frac{2}{\pi}\int_{0}^{\infty}I(\omega)\sin\omega t\,d\omega \qquad (3)$$

$$=-\frac{2}{\pi}\int_{0}^{\omega_0}I(\omega)\sin\omega t\,d\omega- \frac{2}{\pi}\int_{\omega_0}^{\infty}I(\omega)\sin\omega t\,d\omega \qquad (6)$$

Since the response of a physical system falls off rapidly at high frequencies, the contribution of the second integral of equation 6 will be negligible for reasonably large values of ω_0 allowing the assumption that $I(\omega)=0$ for $\omega\geq\omega_0$. However, if ω_0 is further and further reduced, it must reach a value such that the second integral is no longer negligibly small compared with the first integral.

Leaving for the present, the determination of a suitable value of cut-off frequency ω_0, assume that $I(\omega)=0$ for

---

Paper 53-248, recommended by the AIEE Feedback Control Systems Committee and approved by the AIEE Committee on Technical Operations for presentation at the AIEE Summer General Meeting, Atlantic City, N. J., June 15–19, 1953. Manuscript submitted February 25, 1953; made available for printing May 13, 1953.

CHARLES H. DAWSON is with the University of Rochester, Rochester, N. Y.

This paper is a revision of a doctoral thesis by the author at Iowa State College of Agriculture and Mechanic Arts, Ames, Iowa.

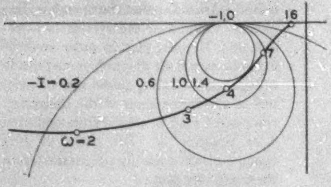

Fig. 1 (above). Loci of constant I superimposed on the Nyquist plot of

$$C/E=[5(1+j\omega)^2]/[(j\omega)^3](1+j0.05\omega)^2$$

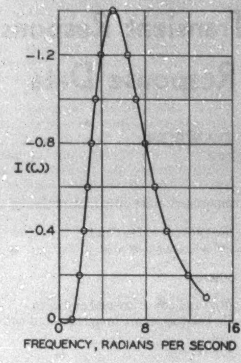

Fig. 2 (right). The curve of I(ω) against ω derived from Fig. 1

$\omega \geq \omega_0$. Under this assumption, and noting that $I(0)$ is zero since $G(0)$ is real, $I(\omega)$ may be expanded in a Fourier sine series in the interval $0 \leq \omega \leq \omega_0$ as

$$I(\omega)=\sum_{n=1}^{\infty} a_n \sin\frac{n\pi\omega}{\omega_0} \qquad (7)$$

where

$$a_n=\frac{2}{\omega_0}\int_0^{\omega_0} I(\omega)\ \sin\ \frac{n\pi\omega}{\omega_0}$$

If equation 7 is substituted in equation 6

$$c(t)=-\frac{2}{\pi}\int_0^{\omega_0}\left[\sum_{n=1}^{\infty} a_n \sin\frac{n\pi\omega}{\omega_0}\right]\times \sin \omega t\, d\omega$$

Since the integration is over only a finite range, the integral and summation processes may be interchanged giving

$$c(t)=-\frac{2}{\pi}\sum_{n=1}^{\infty} a_n \int_0^{\omega_0} \sin\frac{n\pi\omega}{\omega_0} \sin \omega t\, d\omega$$

$$=-\frac{1}{\pi}\sum_{n=1}^{\infty} a_n \int_0^{\omega_0}\left[\cos\left(\frac{n\pi}{\omega_0}-t\right)\omega - \cos\left(\frac{n\pi}{\omega_0}+t\right)\omega\right] d\omega \qquad (8)$$

since $(\sin a)(\sin b)=1/2\ [\cos(a-b)-\cos(a+b)]$. When equation 8 is integrated

$$c(t)=-\frac{1}{\pi}\sum_{n=1}^{\infty} a_n\left[\frac{\sin\left(\frac{n\pi}{\omega_0}-t\right)\omega}{\frac{n\pi}{\omega_0}-t}-\frac{\sin\left(\frac{n\pi}{\omega_0}+t\right)\omega}{\frac{n\pi}{\omega_0}+t}\right]_0^{\omega_0}$$

$$=-\frac{\omega_0}{\pi}\sum_{n=1}^{\infty} a_n\left[\frac{\sin(n\pi-\omega_0 t)}{n\pi-\omega_0 t}-\frac{\sin(n\pi+\omega_0 t)}{n\pi+\omega_0 t}\right]$$

Now, letting $\tau=\omega_0 t$ and noting that

$\sin(n\pi-\omega_0 t)=-(-1)^n \sin \omega_0 t$ and
$\sin(n\pi+\omega_0 t)=(-1)^n \sin \omega_0 t$

$$c(t)=\frac{\omega_0}{\pi}\sum_{n=1}^{\infty}(-1)^n a_n\left[\frac{\sin\tau}{n\pi-\tau}+\frac{\sin\tau}{n\pi+\tau}\right]$$

$$=2\omega_0 \sin\tau \sum_{n=1}^{\infty}\frac{(-1)^n n a_n}{(n^2\pi^2-\tau^2)} \qquad (9)$$

Numerical values of $c(t)$ are most simply obtained through the use of tables of $[(-1)^n 2n \sin\tau]/[n\pi^2-\tau^2]$ calculated for various n's at suitable intervals of τ. These values are given in Table I for $n=1$, 2, 3, 4, and 5, and for $\pi/6$ intervals for τ.

Determination of Cutoff Frequency

In the current investigation the Fourier sine coefficients, a_n, for $I(\omega)$, were determined by 18-point graphical integration; $I(\omega)$ was assumed to decrease linearly between the frequency, $\omega_{0.1}$ at which $I(\omega)=-0.1$ and is decreasing in absolute value, and ω_0; only the first four terms of the series for $c(t)$ were retained; and ω_0 was chosen empirically as equal to 1.3 $\omega_{0.1}$. The ratio of ω_0 to $\omega_{0.1}$ was chosen after four examples (one of second order, two of third order, and one of fifth order) had been examined, and the variation between predicted and exact values determined for a wide range of ratios. The selected value of 1.3 represents a compromise value which gave highly satisfactory results in the four examples considered. ω_0 was also investigated as a function of other potentially significant frequencies such as that where $I(\omega)$ attains its negative maximum, but no correlation was found for the four examples.

The degree of fit was arbitrarily measured by taking the square root of the average of the squares of the differences between the predicted and actual responses at 20 points equally spaced over a convenient interval equal to or slightly greater than that of the first positive alternation of $c(t)$. To establish a percentage reference, the same error was computed assuming that a difference equal to 1 per cent of the actual $c(t)$ existed at each of the 20 times. The ratio of 1.3 gave errors of less than 5 per cent on this

Table I. Values for n and for π/6 Intervals for τ

	$\frac{-2n \sin\tau}{n^2\pi^2-\tau^2}$ for $\tau=k\frac{\pi}{6}$				
k	n=1	n=2	n=3	n=4	n=5
1	0.104	−0.051	0.034	−0.025	0.020
2	0.197	−0.090	0.059	−0.044	0.035
3	0.269	−0.108	0.069	−0.051	0.041
4	0.314	−0.099	0.062	−0.045	0.036
5	0.330	−0.065	0.037	−0.026	0.021
6	0.318	0.000	0.000	0.000	0.000
7	0.279	0.077	−0.040	0.028	−0.021
8	0.225	0.158	−0.073	0.050	−0.038
9	0.161	0.237	−0.090	0.059	−0.044
10	0.098	0.288	−0.085	0.053	−0.040
11	0.043	0.316	−0.054	0.032	−0.023
12	0.000	0.318	0.000	0.000	0.000
13	−0.027	0.292	0.071	−0.036	0.025
14	−0.040	0.244	0.149	−0.067	0.045
15	−0.039	0.180	0.221	−0.083	0.054
16	−0.029	0.113	0.279	−0.079	0.049
17	−0.014	0.050	0.312	−0.051	0.030
18	0.000	0.000	0.318	0.000	0.000
19	0.011	−0.034	0.296	0.068	−0.034
20	0.017	−0.049	0.250	0.144	−0.063
21	0.018	−0.049	0.185	0.216	−0.079
22	0.014	−0.037	0.119	0.275	−0.076
23	0.007	−0.019	0.053	0.310	−0.049
24	0.000	0.000	0.000	0.318	0.000
25	−0.006	0.015	−0.036	0.298	0.066
26	−0.010	0.024	−0.054	0.253	0.141
27	−0.011	0.025	−0.053	0.191	0.213
28	−0.008	0.020	−0.041	0.122	0.272
29	−0.005	0.010	−0.031	0.055	0.308
30	0.000	0.000	0.000	0.000	0.318

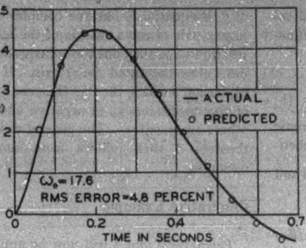

Fig. 3. Actual and predicted impulse responses for

$\omega_0/\omega_{0.1}=1.29$

basis. Fig. 3 shows the predicted and actual impulse response curves for the Appendix example.

Discussion of the Method

As has already been noted, ω_0 must be large enough to allow the assumption that the second integral of equation 6 is negligible compared with the first. Since $I(\omega)$ is never greater than $G(\omega)$ and $G(\omega)$ decreases for higher frequencies at a rate of at least 12 decibels per octave, setting ω_0 greater than $\omega_{0.1}$ minimized error from this assumption.

The use of 18-point graphical integration should not cause difficulty unless ω_0 is chosen so large that the curve of $I(\omega)$ cannot be adequately represented by points at $\omega_0/18$ intervals. Since the behavior of $I(\omega)$ in the range between $\omega_{0.1}$ and ω_0 is not readily determined by the loci of constant I method, linear behavior is assumed. Since interest was centered on the first positive alternation of the response, and since the major contribution of the fifth and higher ordered terms all fell beyond this range in the examples considered, use of only the first four terms of the series for $c(t)$ appears justified. The errors resulting from the use of 18-point integration and to the assumption of linearity between $\omega_{0.1}$ and ω_0 are random functions of ω_0; the error resulting from neglecting the fifth and higher ordered terms increases with increasing ω_0.

Conclusion

The method as outlined in the foregoing, and illustrated by the Appendix example, gives excellent results with a small amount of computation for the systems considered. However, no investigation of higher order systems and systems having multiple loops has been made, since computational aids were not available to determine exact solutions. The random nature of the errors introduced by the assumptions of the preceding paragraph precludes the possibility of establishing an exact theoretical basis for choosing the cutoff frequency. The same procedure can, of course, be applied whenever an approximation of the inverse Laplace transform is desired, provided the behavior of the transform is known on the real frequency axis.

Appendix I. Illustration of the Method

The example chosen to illustrate the method is for a system whose transfer function is

$$C/E=[5(1+j\omega)^2]/[(j\omega)^2(1+j0.05\omega)^2]$$

The corresponding closed-loop Laplace transform is

$$C/R=[5(1+s)^2]/[0.0025s^5+0.1s^4+s^3+5s^2+10s+5]$$

Taking the inverse transform yields the exact impulse response as

$$c(t)=0.09\epsilon^{-.729t}-6.36\epsilon^{-3.4t}+3.58\epsilon^{-28.13t}+22.76\epsilon^{-4.37t}\sin(4.18t+6.8°)$$

Eighteen-point graphical integration applied to Fig. 2 yields for the Fourier coefficients of the first four terms in the series for $I(\omega)$ for $\omega_0/\omega_{0.1}=1.29$: $a_1=-0.781$, $a_2=-0.519$, $a_3=-0.066$, and $a_4=0.134$. Thus

$$c(t)=\sin\tau\times\left[\frac{27.56}{\pi^2-\tau^2}-\frac{36.52}{4\pi^2-\tau^2}+\frac{6.96}{9\pi^2-\tau^2}+\frac{18.88}{16\pi^2-\tau^2}\right]$$

where $\tau=17.6t$.

◆

No Discussion

A Relative Damping Criterion for Linear Systems

J. FRANK KOENIG

ASSOCIATE MEMBER AIEE

MANY feedback controls and other physical systems are designed on the basis of linear theory, that is, linear differential equations with constant coefficients. A. Leonhard[1-3] and A. Vazsonyi[4] have given graphical methods for determining whether all roots of the characteristic equation are located within certain sectors of the complex plane. Vazsonyi's method determines whether all dimensionless damping rates ζ of any linear system are greater than any prescribed value. Each pair of complex conjugate roots of the characteristic equation of a linear system has its own value of ζ. Any such pair can be expressed as

$$[-\zeta\pm j(1-\zeta^2)^{1/2}]\omega_n \qquad (1)$$

where

ω_n is the undamped natural frequency
$\zeta<1$ corresponds to an oscillatory transient response
$\zeta=1$ corresponds to critical damping

In Fig. 1 is shown the complex plane in which the roots of the characteristic equation may be plotted. A linear system is stable if and only if all roots of the characteristic equation have negative real parts. Consider a complex conjugate pair located on the boundaries of a sym-

---

Paper 53-247, recommended by the AIEE Feedback Control Systems Committee and approved by the AIEE Committee on Technical Operations for presentation at the AIEE Summer General Meeting, Atlantic City, N. J., June 15–19, 1953. Manuscript submitted February 6, 1953; made available for printing May 5, 1953.

J. FRANK KOENIG is with the National Bureau of Standards, Washington, D. C.

The work presented in this paper was conducted under a co-operative program of Basic Instrumentation Research and Development sponsored by the United States Office of Naval Research, United States Office of Scientific Research of the Air Research and Development Command, and the United States Atomic Energy Commission, Washington, D. C. Thanks are expressed to Dr. H. L. Mason of the National Bureau of Standards for helpful discussions.

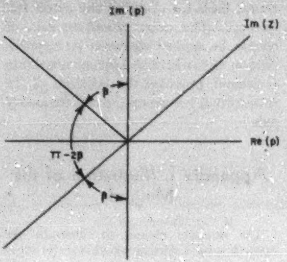

Fig. 1. Superposed complex planes

metrical sector $\pi-2\beta$, Fig. 1. This pair has a value of ζ

$$\zeta=\sin\beta,\quad 0\leq\beta\leq\pi/2 \tag{2}$$

If all roots are located within some sector $\pi-2\beta,\beta$ fixed, then all roots have damping ratios greater than $\zeta=\sin\beta$. By use of either the Leonhard graphical method or the Vazsonyi graphical method, the number of roots inside and outside each such sector $\pi-2\beta$ can be determined. Leonhard plots a transformed characteristic equation while Vazsonyi plots a transformed Nyquist[5] transfer function.

Theorems on Root Regions

This section presents an analytical procedure for determining the information obtainable by the graphical methods of Leonhard and Vazsonyi.

A theorem by E. Frank[6] follows:

Theorem 1. The zeros of the complex polynomial

$$P(z)=z^n+(A_1+jB_1)z^{n-1}+\ldots (A_n+jB_n),\quad (A_i \text{ and } B_i \text{ real}) \tag{3}$$

all have negative real parts if and only if all coefficients c_p are positive and the k_p are pure imaginary or zero in the continued fraction expansion

$$\frac{Q(s)}{P(s)}=\frac{1}{c_1z+k_1+1}+\frac{1}{c_2z+k_2+}\,\frac{1}{c_3z+k_3+}\cdots\frac{1}{+c_nz+k_n}\text{*} \tag{4}$$

where

$$Q(z)=A_1z^{n-1}+jB_2z^{n-2}+A_3z^{n-3}+jB_4z^{n-4}+\ldots$$

Theorem 1 may be extended, to yield information concerning the sectorial regions of roots of a real polynomial equation as follows:

Theorem 2. Let

$$p^n+a_1p^{n-1}+a_2p^{n-2}+\ldots+a_n=0 \tag{5}$$

be a polynomial equation (characteristic equation) with real coefficients. Substitute $p=z\epsilon^{-j\beta}, 0<\beta<\frac{\pi}{2}$, into equation 5 and obtain the complex polynomial

$$P(z)=z^n+(A_1+jB_1)z^{n-1}+\ldots+(A_n+jB_n) \tag{6}$$

in which the A_i and B_i are real. Form

$$Q(z)=A_1z^{n-1}+jB_2z^{n-2}+A_3z^{n-3}+jB_4z^{n-4}+\ldots \tag{7}$$

All roots of equation 5 are located within the sector $\pi-2\beta$ if and only if the c_p are real and positive, and the k_p are pure imaginary or zero, in the continued fraction expansion

$$\frac{Q(z)}{P(z)}=\frac{1}{c_1z+k_1+1}+\frac{1}{c_2z+k_2+}\cdots\frac{1}{+c_nz+k_n} \tag{8}$$

Proof of Theorem 2. The transformation $p=z\epsilon^{-j\beta}$ relates the z-plane to the p-plane. If the p-axes and z-axes are considered to be coincident, then this substitution rotates the z-zeros counterclockwise by an angle β with respect to the p-roots. Suppose the z-zeros are then made coincident with the p-roots, by rotating the z-plane clockwise through β with respect to the p-axes. Subsequent discussion relates to this latter configuration, shown in Fig. 1. Suppose theorem 1 is applied successfully (the c_p real and positive and the k_p pure imaginary or zero) to polynomial 6. Then all zeros of polynomial 6 have negative real parts and all roots of equation 5 are located within the sector $\pi-2\beta$, Fig. 1, since p-roots and z-zeros now coincide, and complex p-roots always occur in conjugate pairs. This completes the proof.

Another theorem by E. Frank[6] follows:

Theorem 3. The complex polynomial 6 has r zeros with positive real parts and $(n-r)$ zeros with negative real parts if, in the expansion 8, r of the coefficients c_r are negative and the remaining $(n-r)$ are positive.

Theorem 3 may be extended as follows:

Theorem 4. Given equation 5 having all roots with negative real parts, substitute $p=z\epsilon^{-j\beta}$ into it and obtain polynomial 6. Then form polynomial 7. Equation 5 has $2r$ roots outside the sector $\pi-2\beta$ and $(n-2r)$ roots inside the sector if, in the expansion 8, r of the coefficients c_p are negative, and the remaining $(n-r)$ are positive.

Proof of Theorem 4. For a fixed value of β, if equation 5 has one complex conjugate pair of roots outside of the sector $\pi-2\beta$, Fig. 2, then one root of equation 5 lies below the tilted $Im(z)$ axis. If the expansion 8 exists, then by theorem 3 one of the coefficients c_p is negative and all others are positive. The general case of theorem 4 then follows from similar reasoning.

Illustrative Example

Theorems 2 and 4 will now be applied to one of the characteristic equations to which Leonhard[3] applied his criterion

$$p^{6}+7p+121.25p^4+535.5p^3+1061p^2+1021p+630=0 \tag{9}$$

Leonhard chose five values of β:0 degrees (°) 11.25°, 22.5°, 45° and 67.5°. His results show that there is one pair of roots in each of these conjugate sectors:

1. Between $\beta=0$ and $\beta=11.25$
2. Between $\beta=22.5$ and $\beta=45$
3. Between $\beta=45$ and $\beta=67.5$

Choose $\beta=22.5°$ and apply theorems 2 and 4. Substitute $p=z\epsilon^{-j22.5}$ into equation 9 and obtain

$$P(z)=z^6+7(\cos\beta+j\sin\beta)z^5+121.25(\cos 2\beta+j\sin 2\beta)z^4+\ldots+630(\cos 6\beta+j\sin 6\beta) \tag{10}$$

or, with slide-rule accuracy

$$P(z)=z^6+(6.47+j2.68)z^5+(85.6+j85.6)z^4+(205+j494)z^3+(0+j1061)z^2+(-391+j942)z+(-445+j445) \tag{11}$$

Now form

$$Q(z)=6.47z^5+j85.6z^4+205z^3+j1061z^2-391z+j445 \tag{12}$$

Frank has shown that the continued fraction expansion $Q(z)/T(z)$ gives the same information as expansion 8, where

$$T(z)=z^n+jB_1z^{n-1}+A_2z^{n-2}+jB_3z^{n-3}+A_4z^{n-4}+\ldots \tag{13}$$

since

$$\frac{Q(z)}{T(z)}=\frac{1}{c_1z+k_1}+\frac{1}{c_2z+k_2}+\cdots+\frac{1}{c_nz+k_n} \tag{14}$$

gives the coefficients c_p and k_p. Expansion 14 is used to save some computational labor. From polynomial 11 form

$$T(z)=z^6+j2.68z^5+85.6z^4+j494z^3+0z^2+j942z-445 \tag{15}$$

Using slide-rule computation again, expansion 14 is obtained by dividing $T(z)$ by $Q(z)$ until a remainder R_1 is obtained which is of lower degree than $Q(z)$; then $Q(z)$ is divided by this remainder, and so on. If we write only the coefficients, the computation may be arranged as follows

---

* This short form of the continued fraction has the same meaning as

$$\frac{Q(s)}{P(s)}=\cfrac{1}{c_1s+k_1+1+\cfrac{1}{c_2s+k_2+\ldots+\cfrac{1}{c_ns+k_n}}}$$

$$\begin{array}{r}
0.155-j1.63=c_1+k_1 \\
\hline
Q(s)\big)\,1+j2.68+85.6+j494+0+j942-445=T(s) \\
1+j13.23+31.7+j164-60.5+j69 \\
\hline
-j10.55+53.9+j330+60.5+j873-445 \\
-j10.55+139.5-j334+1730+j637+725 \\
\hline
-85.6+j664-1669+j236-1170=R_1
\end{array}$$

$$\begin{array}{r}
-0.076-j1.59=c_2+k_2 \\
\hline
R_1\big)\,6.47+j85.6+205+j1061-391+j445=Q(s) \\
6.47-j50.2+126-j18+89 \\
\hline
+j135.8+79+j1079-480+j445 \\
+j135.8+1058+j2655+376+j1860 \\
\hline
-976-j1576-856-j1415=R_2
\end{array}$$

$$\begin{array}{r}
0.087-j0.819=c_3+k_3 \\
\hline
R_2\big)\,-85.6+j664-1669+j236-1170=R_1 \\
-85.6-j138-75-j124 \\
\hline
+j802-1594+j360-1170 \\
+j802-1291+j702-1160 \\
\hline
-303-j342-10=R_3
\end{array}$$

$$\begin{array}{r}
3.23+j1.55=c_4+k_4 \\
\hline
R_3\big)\,-979-j1576-856-j1415=R_2 \\
-979-j1105-32 \\
\hline
-j471-824-j1415 \\
-j471+531-j15 \\
\hline
-1355-j1400=R_4
\end{array}$$

$$\begin{array}{r}
0.224+j0.021=c_5+k_5 \\
\hline
R_4\big)\,-303-j342-10=R_3 \\
-303-j313 \\
\hline
-j29-10 \\
-j29+30 \\
\hline
-40=R_5
\end{array}$$

$$\begin{array}{r}
33.9+j35=c_6+k_6 \\
\hline
R_5\big)\,-1355-j1400=R_4 \\
-1355 \\
\hline
-j1400 \\
-j1400 \\
\hline
R_6=0
\end{array}$$

Note that five of the c_ν are positive and one is negative. Therefore, by theorem 4, one complex pair of roots of equation 9 is located outside the sector $\pi-2\beta, \beta=22.5°$. The computation was repeated for other β. For $\beta=11.25°$, we find again that five c_ν are positive and one is negative. Therefore one pair is located outside the sector $\pi-2\beta$, $\beta=11.25°$. For $\beta=45°$, four of the c_ν were found positive and two negative; therefore two root-pairs of equation 9 are outside of the sector $\pi-2\beta, \beta=45°$. It follows that one pair is located in the region outside of the sector $\pi-2\beta, \beta=45°$ and inside the sector $\pi-2\beta, \beta=22.5°$. For $\beta=67.5°$, all c_ν were found negative; therefore all roots of equation 6 are complex and are located outside the sector $\pi-2\beta, \beta=67.5°$. It follows that one pair is located in the region outside of the sector $\pi-2\beta, \beta=67.5°$ and inside the sector $\pi-2\beta, \beta=45°$. These results are the same as Leonhard's. As β nears the value corresponding to a pair of roots on the sectorial boundary, the remainder $R_{n-1}=R_5$ approaches zero.

Evaluating Root with Lowest Damping Ratio

The complex roots of any real polynomial equation can be evaluated (values determined) by an extension of the methods of the previous sections. As a simple example, it is here applied to finding the roots of

$$p^2+2p+2=0 \qquad (16)$$

Substitute $p=se^{-j\beta}$ into equation 16 and obtain

$$s^2+2(\cos\beta+j\sin\beta)s+2(\cos 2\beta+j\sin 2\beta)=0 \qquad (17)$$

The substitution corresponds to Fig. 1 in which the s-axes are rotated clockwise with respect to the p-axes and s roots and p roots are coincident. For a given β, if equation 16 has a complex pair of roots with negative real parts so that one p root is located on the negative imaginary axis of the s plane, then equation 17 has a negative pure imaginary root. This root of equation 17 can be obtained in the following manner. Assume $\beta=22.5°$. Then equation 17 becomes

$$s^2+(1.848+j0.765)s+(1.414+j1.414)=0$$

As in the section entitled "Illustrative Example," form $Q(s)/T(s)$, where

$$Q(s)=1.848s+j1.414$$

and

$$T(s)=s^2+j0.765s+1.414$$

We obtain the coefficients of the continued fraction $Q(s)/T(s)$ from the following calculation

$$\begin{array}{r}
0.542s=c_1s \\
\hline
Q(s)\big)\,s^2+j0.765s+1.414=T(s) \\
s^2+j0.765s \\
\hline
+1.414=R_1
\end{array}$$

$$\begin{array}{r}
1.305s+j1=c_2s+k_2 \\
\hline
R_1\big)\,1.848s+j1.414=Q(s) \\
1.848s \\
\hline
+j1.414 \\
+j1.414 \\
\hline
R_2=0
\end{array}$$

Since c_1 and c_2 are both positive, all roots of equation 17 are located above $Im(s)$ of Fig. 1, for $\beta=22.5°$, by theorem 1. Upon repeating the procedure for $\beta=67.5°$ it was found that $R_1=-1.414$. It follows from the theory given in Frank's paper[6] that $R_{n-1}=0$ for a value of β corresponding to a pure imaginary root whose value is obtained by setting R_{n-2} to zero. If it is assumed as a first approximation that R_1 varies linearly with β, then in this example we may expect $R_1\approx 0$ for $\beta=45°$. We test our assumption with $\beta=45°$, in equation 17, obtaining

$$s^2+(1.414+j1.414)s+(0+j2)=0 \qquad (18)$$

and

$$T(s)=s^2+j1.414s$$

and

$$Q(s)=1.414s+j2$$

and

$$\begin{array}{r}
0.707s=c_1s \\
\hline
Q(s)\big)\,s^2+j1.414s=T(s) \\
s^2+j1.414s \\
\hline
0=R_1
\end{array}$$

Since $R_1=0$, we obtain the value of the pure imaginary root of equation 18 from the prior remainder $R_{n-2}=R_0=Q(s)$ which gives $s=-j\sqrt{2}$. Since, in Fig. 1, p roots and s roots are coincident, it follows that the p roots of equation 16 are $-1\pm j1$. In general, R_{n-1} will not vary linearly with β; however, the linear assumption will usually give a close approximation to the root.

This root evaluation method can be used to obtain any root pair, and in particular the root pair with the smallest damping ratio, without first solving for the other roots. It can be applied equally well to polynomial equations with complex coefficients. It is related to the methods of Wall[7] and Hitchcock.[8]

Regions of Root Frequencies and Evaluation of the Roots

In theorems 2 and 4 the transformation $p=se^{-j\beta}$ was used. If $p=-j(s+\omega)$ is used in theorem 2, ω fixed and positive, and if all c_ν are positive, then all roots of equation 5 have frequencies (imaginary parts) less than ω. If the same transformation is used in theorem 4, ω fixed and positive, and if r of the c_ν are negative and $(n-r)$ are positive, then $2r$ of the roots have frequencies greater than ω and $(n-2r)$ less than ω.

In the section entitled "Theorems on Root Regions," for the evaluation of roots, the transformation $p=-j(s+\omega)$

could have been used instead of $p=ze^{-j\beta}$.

Evaluating Root with Lowest Frequency

Leonhard can evaluate all root pairs of any characteristic equation by the use of a family of transformed characteristic equations; however, his method gives first the root pair with the lowest frequency, which is not necessarily the root pair with the smallest or largest damping ratio. By analogy with Leonhard's method, Vazsonyi's method can be extended in order to evaluate first the root pair with the lowest frequency; then the root pair with the next lowest frequency is obtained, etc. Leonhard gave no proof for his statement that his method evaluates first the root pair with the lowest frequency. The proof is given here for the extension of Vazsonyi's method, and essentially the same proof applies to Leonhard's method.

Vazsonyi plots the locus of the open-loop transfer function (a function of the complex variable p) as p travels, starting at the origin, along the second-quadrant boundary of the sector, Fig. 1, for various values of β. For each value of β we obtain what may be called a transformed Nyquist locus. If the point traveling on a sector boundary passes through a root of the characteristic equation, the corresponding transformed Nyquist locus passes through the critical point -1. When plotting a set of transformed Nyquist loci one actually varies ω along the positive imaginary axis of the p plane, at the same time that points p (one point on each arbitrarily chosen sector boundary) travel along the sectorial boundaries. For any characteristic equation in which all roots have negative real parts, suppose one has chosen sector boundaries which pass through the complex roots. As ω increases from 0 to ∞ the points p pass through all the roots. Since, for any value of ω, all points p are the same distance from the negative real axis, it follows that as ω increases from 0 the root with the smallest frequency will be passed over first by one of the points p. This completes the proof.

In actual application, the sector boundaries chosen can be, as in Leonhard's method, those corresponding to $\beta=11.25°$, 22.5°, 45° and 67.5°. The root pair with the lowest frequency is approximated from the plots of the transformed Nyquist loci corresponding to these chosen sector boundaries. This procedure is essentially the same as in Leonhard's method.

Summary of Results

Most of the results given now are based on the new theorems presented herein.

Criteria were presented which yield information on the following, concerning the characteristic equation of any linear system: 1. the sectorial regions of the complex plane in which roots are located; 2. a lower limit to the damping ratios of the roots, in order to be certain that all oscillatory transient components disappear quickly; 3. whether the frequencies of all roots are less than any given value; 4. the number of roots with frequencies greater than any given value.

A method was presented which yields the solution for any root pair of a polynomial equation with real coefficients, and in particular the pair with the smallest damping ratio. It also applies to complex polynomial equations.

The method of Vazsonyi, for the determination of the number of roots within sectorial regions, was extended to yield solutions for root pairs, but it has been pointed out that the pair with the lowest frequency is necessarily the first one evaluated.

References

1. Stabilitatskriterium insobesondere von Regelkreisen bei vorgeschriebener Stabilitatsgute, A. Leonhard. *Archiv fuer Elektrotechnik*, Berlin, Germany, no. 2/3, 1948, p. 100.

2. Die selbsttatige Regelung (book), A. Leonhard. J. Springer, Berlin, Germany, 1949.

3. Automatic and Manual Control (book), edited by A. Tustin. Academic Press, Inc., New York, N. Y., 1952, "Relative Damping as Criterion for Stability and as an Aid in Finding the Roots of a Hurwitz Polynomial," A. Leonhard, pp. 25–35.

4. A Generalization of Nyquist's Stability Criteria, A. Vazsonyi. *Journal of Applied Physics*, New York, N. Y., vol. 20, 1949, pp. 863–67.

5. Regeneration Theory, H. Nyquist. *Bell System Technical Journal*, New York, N. Y., vol. 11, 1932, pp. 126–47.

6. On the Zeros of Polynomials with Complex Coefficients, E. Frank. *Bulletin*, American Mathematical Society, New York, N. Y., vol. 52, 1946, pp. 144–57.

7. Analytic Theory of Continued Fractions (book), H. S. Wall. D. Van Nostrand Company, Inc., New York, N. Y., 1948, pp. 185–90.

8. Algebraic Equations with Complex Coefficients, F. L. Hitchcock. *Journal of Mathematics and Physics*, Cambridge, Mass., vol. 18, 1939, pp. 202–10.

Discussion

K. P. Geohegan (Westinghouse Electric Corporation, East Pittsburgh, Pa.): It may be of interest to know that parts of this problem have been studied before and that an alternate method of calculation is available.[1] Instead of using a continued fraction expansion, Sherman presents a generalized Routh array and a generalized set of Hurwitz determinants which apply to equations with complex coefficients.

Sherman uses Cauchy's index theorem to count the number of roots in the sector of the s plane to be investigated by counting the number of encirclements of the origin in the w plane. He evaluates this number of encirclements by a method based on the reasoning used in deriving Sturm's theorem.

To duplicate the example given in the paper, using Sherman's method, substitute $p=re^{i}\frac{112.5\pi}{180}$ and simplify as the author did.

$$P(r)=r^{6}+(-2.68-j6.47)r^{5}+(-85.6+j85.6)r^{4}+(494+j205)r^{3}+(-j1061)r^{2}+(-942+j39^{1})r+(445+j445)$$

Arrange the coefficients in two rows, the real coefficients above the coefficients of the imaginary parts. Then use the cross-multiplication scheme described in Sherman's paper or in Frazer, Duncan, and Collar[2] for constructing a Sturm sequence. The scheme is the same as that used in the ordinary Routh criterion test except that the starred rows are derived from the two preceding unstarred rows; the unstarred rows are derived from the two preceding rows. Then the number of sign changes in the sequence of unstarred leading elements is the number of roots in the half-plane $112.5°<\theta<292.5°$.

	1	−2.68	−85.6	494	0	−942	445
	−6.47	85.6	205	−1061	391	445	
*	−6.83	34.9	−214	−39.1	565	−288	
	−3.59	−27.8	69.9	9.86	−49.0		
*	−4.87	−2.83	+38.7	−17.19	−15.96		
	1.25	−2.02	−1.097	1.814			
*	−4.21	8.36	1.886	−6.14			
	−1.994	2.25	0.0595				
*	1.201	2.11	−3.62				
	6.92	−7.14					
*	1.324	0.412					
	−1.230						

The five sign changes in the sequence of unstarred leading elements indicate that five roots lie in the half-plane investigated by the author. This method is not much shorter but the operations are easier on a desk calculator.

Sherman's paper explains how to count the number of roots in any polygon, sector, circle, strip, etc., for an equation with real or complex coefficients.

REFERENCES

1. Generalized Routh-Hurwitz Discriminant, Seymour Sherman. *Philosophical Magazine and*

Bulletin of Science, London, England, vol. 37, series 7, no. 271, Aug. 1946, pp. 537–51.

2. Elementary Matrices, R. A. Frazer, W. J. Duncan, A. R. Collar. Cambridge University Press, Cambridge, England, 1947, pp. 152–53.

J. Frank Koenig: Mr. Geohegan has made some interesting comments. Dr. Sherman did his work[1] in connection with the problem of the flutter of aircraft surfaces. In this problem it is necessary and sufficient for stability (absence of flutter) that all zeros of a complex polynomial be located outside of the first quadrant. Dr. Sherman apparently was not aware of the fact that some of his mathematical results could be applied to any linear system described by a characteristic equation (real polynomial equation); in his mathematical paper (see ref. 1 of Mr. Geohegan's discussion) he states, "It is suspected that this method can be applied to other calculations arising in mechanical, aeronautical, and electrical engineering." Mr. Geohegan has confirmed Dr. Sherman's suspicions.

Mr. Geohegan states that the calculation of Dr. Sherman's array is shorter than that of Dr. Evelyn Frank's continued fraction. His statement is not in agreement with the findings of H. S. Toney who, in an unpublished report, prefers the Frank method because of its "simplicity of form and of operation," with regard to flutter calculations. Both methods are described in a recent book.[2]

Still another method (a determinant criterion) was presented recently[3] which determines whether all zeros of any real polynomial are located in any given sector or infinite strip. In that paper the extension of the theorem to the determination of the number of zeros in any sector (or infinite strip) was implied by reference to a theorem in Dr. Marden's book.[4]

The author thanks Mr. Geohegan for his helpful discussion of a portion of the paper.

References

1. The Simplification of Flutter Calculations by Use of an Extended Form of the Routh-Hurwitz Discriminant, S. Sherman, J. DiPoala, H. F. Frissel. *Journal of the Aeronautical Sciences*, New York, N. Y., vol. 12, 1945, pp. 385–92.

2. Introduction to the Study of Aircraft Vibration and Flutter (book), R. H. Scanlan, R. Rosenbaum. The Macmillan Company, New York, N. Y., 1951.

3. On the Zeros of Polynomials and the Degree of Stability of Linear Systems, J. F. Koenig. *Journal of Applied Physics*, New York, N. Y., vol. 24, no. 4, 1953, pp. 476–82.

4. The Geometry of the Zeros (book), M. Marden. American Mathematical Society, New York, N. Y., 1949, p. 140.

Automatic Control of Gas Turbines for Natural Gas Pipeline Pumping

C. R. INGEMANSON
ASSOCIATE MEMBER AIEE

ARNE LOFT
NONMEMBER AIEE

H. J. WILT
ASSOCIATE MEMBER AIEE

IN AN EXPANSION era in the natural-gas pumping field, rivaling the building of the railroads, considerable interest has developed in the application of gas turbines, driving centrifugal compressors, for the pumping of natural gas. Since overall system reliability and continuity of service are the watchwords in natural gas pumping, the gas turbine fulfills all requirements. Its features—relatively simple construction, automatic operation, self-sustentation, self-protection, low installation and maintenance costs—indicate that the gas turbine is an excellent prime mover for pumping natural gas through long distance pipelines.

A detailed description of the application of the gas turbine for gas pipeline pumping was given in 1951.[1] Recently, the design details of the 5,000-horsepower gas turbine have been presented.[2] The purpose of this paper is to describe the automatic control equipments for the 5,000-horsepower gas turbine designed for natural gas pipeline pumping.

Pumping stations often are located in isolated areas. Therefore, control equipment must be arranged so that the gas turbine can be controlled with a minimum of skilled operating personnel. Also, provision must be made for starting, loading, and stopping the pumping equipment in the shortest possible time with the least number of manual operations. Automatic control, given a single start or stop signal by a station operator or remote dispatcher, fulfills these requirements.

Fig. 1 shows, in schematic form, the components of natural-gas pipeline pumping 5,000-horsepower gas-turbine equipment which must be controlled to place a pumping unit in or out of operation. Fig. 1 also includes the schematic gas line piping for a 4-unit natural-gas pipeline pumping station with a total rated capacity of 20,000 horsepower. This is the maximum contemplated for any one station at the present time.

Essentially, the control equipment for a pumping unit consists of three components:

1. The main control equipment;
2. The mechanical, electrical, and hydraulic control elements of the turbine;
3. The Cabinetrol* panels for the station and turbine auxiliaries.

Main Control Equipment

The main portion of the automatic control circuits and the associated control devices for pipeline-pumping gas-turbine equipment is centralized in a duplex control board, which is shown in Fig. 2.

Control Devices

Speed-responsive relays and motor-driven timing relays are the heart of the automatic-control equipment for starting and stopping a gas turbine pumping unit. These relays function to control the various steps in the operating sequence.

The speed relays operate in response to the rectified output of tachometer generators coupled to the shafts of the high- and low-pressure turbines.

The motor-driven timing relays, which operate either directly or indirectly from speed-relay signals, control such functions as turbine and duct purging, gas-compressor purging and pressurizing, valve operation, and turbine cooling.

Contact-multiplying auxiliary relays provide the necessary interlocking for correct-sequence operation.

A pressure regulator which responds to a station discharge-pressure signal controls the gas-turbine speed and loading to maintain the desired station discharge pressure.

Operation Sequence

The control circuits are arranged so that the starting signal will initiate the starting sequence of the gas-turbine pumping equipment only when all prestarting conditions have been satisfied. When the circuit breakers for the auxiliary and emergency lube oil and emergency nozzle-cooling water pumps are closed, protective-device trip contacts are reset, and

---

Paper 53-323, recommended by the AIEE Chemical, Electrochemical and Electrothermal Applications Committee and approved by the AIEE Committee on Technical Operations for presentation at the AIEE Pacific General Meeting, Vancouver, B. C., Canada, September 1–4, 1953. Manuscript submitted October 23, 1951; made available for printing July 1, 1953.

C. R. Ingemanson is with the General Electric Company, Philadelphia, Pa., and Arne Loft and H. J. Wilt are with the General Electric Company, Schenectady, N. Y.

* Reg. U. S. Pat. Off.

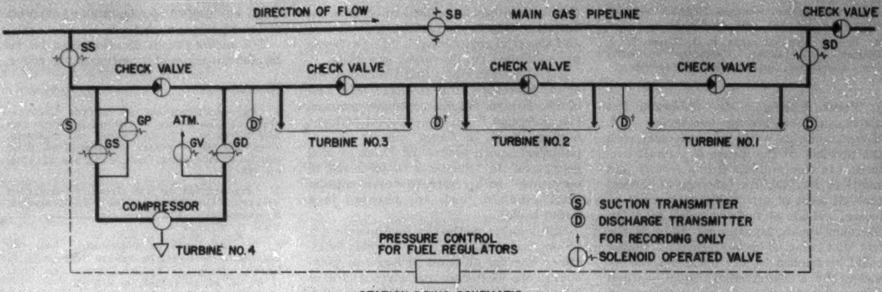
DIRECTION OF FLOW
SB
MAIN GAS PIPELINE
CHECK VALVE
SS
SD
CHECK VALVE
CHECK VALVE
CHECK VALVE
CHECK VALVE
S
GP
ATM.
GS
GV
GD
D†
D†
D†
D
TURBINE NO.3
TURBINE NO.2
TURBINE NO.1
COMPRESSOR
TURBINE NO.4
S SUCTION TRANSMITTER
D DISCHARGE TRANSMITTER
† FOR RECORDING ONLY
SOLENOID OPERATED VALVE
PRESSURE CONTROL FOR FUEL REGULATORS

STATION PIPING SCHEMATIC

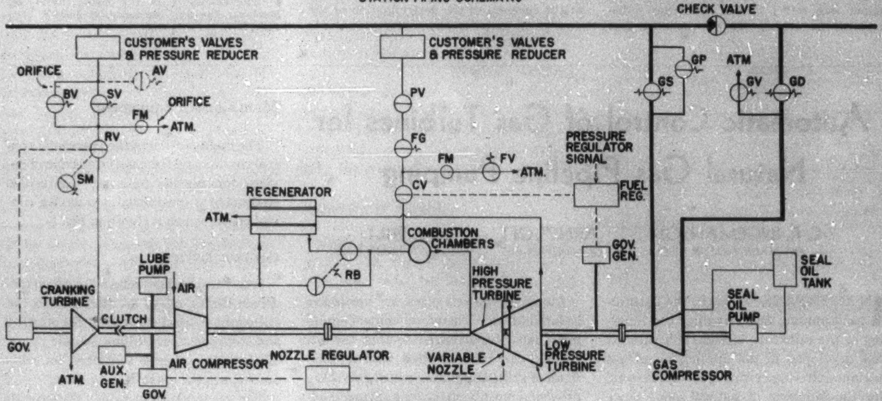
CHECK VALVE
CUSTOMER'S VALVES & PRESSURE REDUCER
CUSTOMER'S VALVES & PRESSURE REDUCER
ORIFICE
AV
BV
SV
ORIFICE
FM
ATM.
RV
SM
PV
FG
FM
FV
ATM.
CV
PRESSURE REGULATOR SIGNAL
FUEL REG.
REGENERATOR
ATM.
COMBUSTION CHAMBERS
GOV. GEN.
RB
LUBE PUMP
AIR
CRANKING TURBINE
CLUTCH
HIGH PRESSURE TURBINE
GOV.
ATM.
AUX. GEN.
GOV. GEN.
AIR COMPRESSOR
NOZZLE REGULATOR
VARIABLE NOZZLE
LOW PRESSURE TURBINE
GAS COMPRESSOR
GP
ATM
GS
GV
GD
SEAL OIL TANK
SEAL OIL PUMP

UNIT PIPING SCHEMATIC

Fig. 1. Typical piping schematic for gas turbine pumping station

AV—Alcohol valve
BV—Starting by-pass valve
CV—Gas control valve
FG—Fuel gas stop valve
FM—Flow meter
FV—Fuel gas vent valve
GD—Gas compressor discharge valve
GP—Gas compressor pressurizing valve
GS—Gas compressor suction valve
GV—Gas compressor vent valve
PV—Pressure ratio valve
RB—Regenerator by-pass valve
RV—Starting regulating valve
SB—Station by-pass valve
SD—Station discharge valve
SM—Starting mechanism
SS—Station suction valve
SV—Starting stop valve

control air pressure and battery charge are normal, three green lamps are lighted, indicating that starting conditions are correct. The failure of one of these lamps to light will indicate to the operator which one of the three control components is the source of prestarting trouble.

The starting sequence is initiated when the operator turns the master control switch to the "start" position. The automatic-control circuits will then complete the operations, as shown in Fig. 3. When the first unit in a station is started, the operator closes the station by-pass valve at a convenient time and the pressure regulator maintains the desired station discharge pressure. The operator can have manual control of either station or unit loading by means of selector valves which operate in conjunction with the pressure-regulating equipment. He also can control manually the pressure-control signal to the fuel regulator, if the control air supply should fail. Full-load condition can be reached in approximately 20 minutes after the starting indication has been given.

During starting, failure of the clutch to engage the starting and high-pressure turbines, failure of the unit to fire, or failure of the automatic starting sequence to be completed within a definite period of time will cause the pumping equipment to be shut down.

A pumping unit also is shut down when the operator turns the master control switch to the "stop" position, operates the emergency stopping devices, or when protective devices operate in response to abnormal temperatures or pressures, overspeed, and loss of flame. The stopping signal automatically initiates the shutdown sequence shown in Fig. 3.

When the high-pressure turbine coasts to approximately 2-per-cent speed, a motor-driven timing relay is started to determine the length of time the d-c lubricating and cooling water pumps will run to cool the bearings and the turbine. Restarting of the turbine can be initiated any time below 2-per-cent speed.

At the instant any unit is given the shutdown signal, the station by-pass valve is automatically opened and the other units which are running in the station are brought to a minimum load speed by reduction in fuel supply. This is done to minimize the heating of the gas compressor and associated piping. These units will assume normal speed and load when the operator recloses the station by-pass valve.

Annunciation and Alarms

A 36-drop annunciator together with an alarm bell and lamp provide both audible and visual warnings when an abnormal operating condition exists, or when a protective device operates to shut down the turbine.

The annunciator alarms are arranged in three groups:

1. Warning only for an abnormal operating condition;
2. Warning for an abnormal operating condition with subsequent shut down if the condition persists;
3. Shut down indication.

This arrangement provides an easy means of advising a remote dispatcher of the nature of the trouble when an alarm signal is received. Provision for operating a station siren and any additional alarm devices which may be required is included in the alarm circuits.

Remote Control

Local operators will control the first pipeline-pumping gas-turbine equipments being installed. However, it is contemplated that the units eventually will be controlled by a remote dispatcher. Arrangement of the automatic-control circuits permits a remote dispatcher to place a unit into operation or shut it down with one start or stop signal. He also will have control of the operation of the station by-pass, suction, and discharge valves. Provisions are included for transmitting prestarting condition, complete sequence, alarm and station suction and discharge pressure indications to a remote station.

Indicators and Recorders

Instruments and meters enable the operator to check turbine and gas compressor speeds, turbine variable nozzle position, turbine running time and auxiliary generator output. Recorders provide a continuous record of the pumping equipment temperature and vibration conditions, the station suction and discharge pressures and the unit discharge pressure.

Other Features

A mimic bus on the duplex control board depicts the unit gas line piping. If the operator desires to alter the operating sequence of the gas line valves from that determined by the automatic sequence, selector switches placed in the mimic bus permit manual control. Indicating lamps furnish a visual check of the valve positions at all times. Selector switches enable the operator to check the operating sequence, ignition and fuel regulator operation. Sound power telephone jacks are provided to facilitate communication between the various components of the pumping equipment.

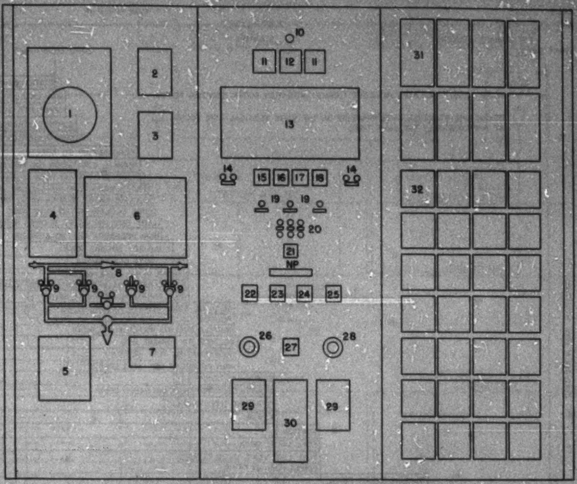

Fig. 2. Front view of the duplex control board for a natural-gas pipeline pumping gas-turbine equipment

1. Gas pressure indicator-recorder
2. Station pressure regulator hand-auto selector valve
3. Unit pressure regulator hand-auto selector valve
4. Vibration recorder
5. Vibration recorder control and power unit
6. Temperature recorder
7. Temperature recorder control unit
8. Gas compressor piping mimic
9. Control switches and position indicating lamps for gas compressor valves
10. Alarm lamp
11. Speed indicators
12. Variable nozzle position indicator
13. Annunciator
14. Regenerator by-pass valve position indicating lamps
15. Auxiliary generator field ammeter
16. Auxiliary generator voltmeter
17. Auxiliary generator ammeter
18. Running time meter
19. Flame indicating lamps
20. Sequence indicating lamps
21. Master control switch
22. Voltage regulator transfer switch
23. Ignition test switch
24. Fuel setting test switch
25. Operation selector switch
26. Exciter field rheostat
27. Phone jack
28. Voltage regulator voltage adjusting rheostat
29. Speed relays
30. Auxiliary generator watt-hour meter
31. Motor driven timing relays
32. Auxiliary relays

Duplex Control Board Construction

Reference to Fig. 2 shows that the duplex control board consists of three units. Basically, the front panels of the three units are arranged from left to right in order to accommodate the following functions:

1. Recording;
2. Control;
3. Relaying.

The exterior of the rear panels are free from devices, thus permitting the control board to be placed against a wall. Walk-in type construction of the control board, with entrance doors at both ends, provides ready access to all devices for maintenance and adjustment.

Actually, two types of control boards, a station duplex and a turbine duplex, may be used in a pumping station. The first gas-turbine pumping unit installed in a station requires a station-type duplex control board. A turbine duplex board

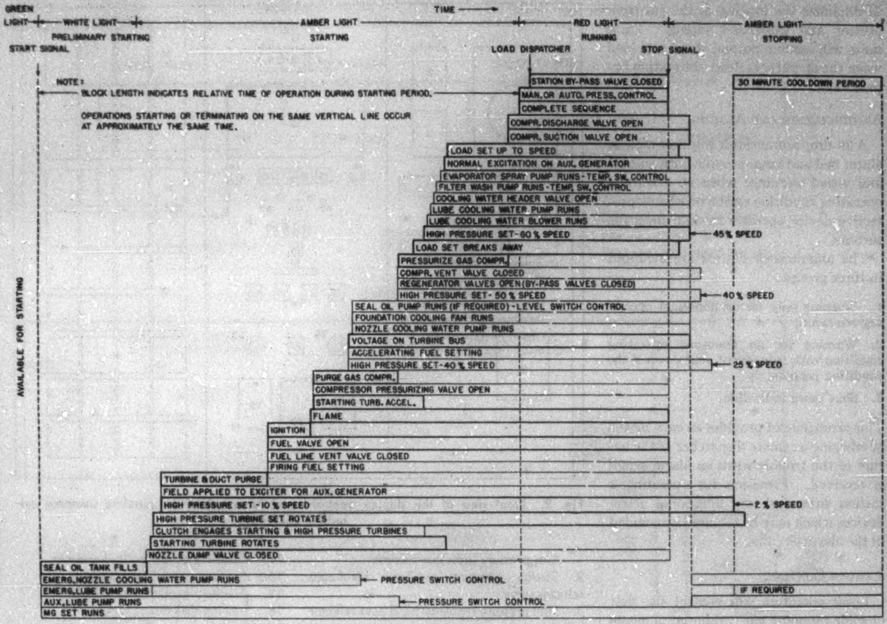
TIME
GREEN LIGHT
START SIGNAL
WHITE LIGHT
PRELIMINARY STARTING
AMBER LIGHT
STARTING
LOAD DISPATCHER
RED LIGHT
RUNNING
STOP SIGNAL
AMBER LIGHT
STOPPING
NOTE:
BLOCK LENGTH INDICATES RELATIVE TIME OF OPERATION DURING STARTING PERIOD.
OPERATIONS STARTING OR TERMINATING ON THE SAME VERTICAL LINE OCCUR AT APPROXIMATELY THE SAME TIME.
AVAILABLE FOR STARTING
STATION BY-PASS VALVE CLOSED
MAN. OR AUTO. PRESS. CONTROL
COMPLETE SEQUENCE
COMPR. DISCHARGE VALVE OPEN
COMPR. SUCTION VALVE OPEN
LOAD SET UP TO SPEED
NORMAL EXCITATION ON AUX. GENERATOR
EVAPORATOR SPRAY PUMP RUNS - TEMP. SW. CONTROL
FILTER WASH PUMP RUNS - TEMP. SW. CONTROL
COOLING WATER HEADER VALVE OPEN
LUBE COOLING WATER PUMP RUNS
LUBE COOLING WATER BLOWER RUNS
HIGH PRESSURE SET - 60 % SPEED
45 % SPEED
LOAD SET BREAKS AWAY
PRESSURIZE GAS COMPR.
COMPR. VENT VALVE CLOSED
REGENERATOR VALVES OPEN (BY-PASS VALVES CLOSED)
HIGH PRESSURE SET - 50 % SPEED
40 % SPEED
SEAL OIL PUMP RUNS (IF REQUIRED) - LEVEL SWITCH CONTROL
FOUNDATION COOLING FAN RUNS
NOZZLE COOLING WATER PUMP RUNS
VOLTAGE ON TURBINE BUS
ACCELERATING FUEL SETTING
HIGH PRESSURE SET - 40 % SPEED
25 % SPEED
PURGE GAS COMPR.
COMPRESSOR PRESSURIZING VALVE OPEN
STARTING TURB. ACCEL.
FLAME
IGNITION
FUEL VALVE OPEN
FUEL LINE VENT VALVE CLOSED
FIRING FUEL SETTING
TURBINE & DUCT PURGE
FIELD APPLIED TO EXCITER FOR AUX. GENERATOR
HIGH PRESSURE SET - 10 % SPEED
2 % SPEED
HIGH PRESSURE TURBINE SET ROTATES
CLUTCH ENGAGES STARTING & HIGH PRESSURE TURBINES
STARTING TURBINE ROTATES
NOZZLE DUMP VALVE CLOSED
SEAL OIL TANK FILLS
EMERG. NOZZLE COOLING WATER PUMP RUNS
PRESSURE SWITCH CONTROL
EMERG. LUBE PUMP RUNS
AUX. LUBE PUMP RUNS
PRESSURE SWITCH CONTROL
MG SET RUNS
30 MINUTE COOLDOWN PERIOD
IF REQUIRED

Fig. 3. Control sequence diagram for pipeline pumping gas turbine

is furnished with each additional unit. The station board differs from the turbine type in that it houses the master regulating equipment and the common station auxiliary relays. Both boards are constructed for rapid conversion between the two types with a minimum number of modifications. This conversion feature permits the user to purchase pumping equipment without having to determine the exact details of his expansion plans. It also allows him to shift equipment between new and existing stations to meet changes in load conditions.

Mechanical, Electrical, and Hydraulic Turbine Control Components

The load of each unit is determined by the load-turbine speed control, which is overridden by turbine exhaust temperature, as follows: The speed signal from the governor generator, the temperature signal from the gas-filled bulb, and the called-for speed signal from the pressure regulator are fed into the fuel regulator, which in turn positions the gas-control valve to supply the desired amount of fuel to the combustion chambers. Ahead of the gas-control valve is a pressure-ratio valve which holds a fixed ratio between the control valve-inlet pressure and the combustion-chamber pressure, thereby limiting the required range of the gas-control valve. An electrically operated stop valve is located between these two valves to shut off fuel when desired, see Fig. 1.

Maximum efficiency of the gas turbine over the full load range is obtained by compressing the minimum amount of air required to operate the unit within the turbine-inlet temperature limit, as follows: The required air flow which results in maximum turbine-inlet temperature is produced by controlling the speed of the high-pressure set. Positioning of the variable second-stage nozzle determines the high-pressure set speed. Nozzle position is controlled by a nozzle regulator, which responds to high-pressure set speed and turbine exhaust temperature. Regulation of the fuel supply, in turn, compensates for the energy change on the load turbine.

The retractable spark plugs and follow-up flame detectors ignite the fuel and detect the fire in the combustion chambers. Mechanical overspeed and overtemperature limits trip the units in case of control failure.

Cabinetrol Panels for Station and Turbine Auxiliaries

Cabinetrol is a standard system of centralized low-voltage control. Each turbine will have its own Cabinetrol panel. The station auxiliaries will be in a separate panel. Therefore, in a 4-unit pumping station, there will be four turbine panels and one station panel, all of which can be located to suit the station requirements. Thus, the diverse functions of this application are co-ordinated into similar panels, providing a minimum of installation time, and simplification of plant construction and operation. The complete Cabinetrol equipment for a two unit station is shown by the 1-line diagram, see Fig. 4.

Since many of these pumping stations are located in isolated areas, the electric-power supply for each station is designed

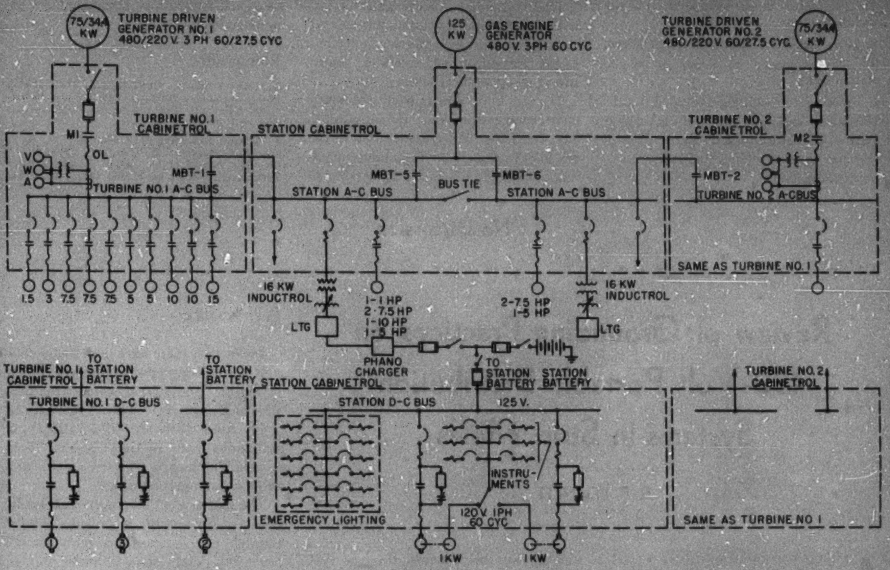
75/344 KW
TURBINE DRIVEN GENERATOR NO. 1 480/220 V. 3 PH 60/27.5 CYC
125 KW
GAS ENGINE GENERATOR 480 V. 3PH 60 CYC
TURBINE DRIVEN GENERATOR NO. 2 480/220 V. 60/27.5 CYC
75/344 KW
TURBINE NO. 1 CABINETROL
STATION CABINETROL
TURBINE NO. 2 CABINETROL
M1
OL
V
W
A
MBT-1
TURBINE NO. 1 A-C BUS
MBT-5
BUS TIE
MBT-6
STATION A-C BUS
STATION A-C BUS
MBT-2
M2
TURBINE NO. 2 A-C BUS
SAME AS TURBINE NO. 1
1.5
3
7.5
7.5
7.5
5
5
10
10
15
16 KW INDUCTROL
1-1 HP
2-7.5 HP
1-10 HP
1-5 HP
2-7.5 HP
1-5 HP
16 KW INDUCTROL
LTG
LTG
PHANO CHARGER
TO STATION BATTERY
STATION BATTERY
TURBINE NO. 1 CABINETROL
TO STATION BATTERY
TO STATION BATTERY
STATION CABINETROL
TURBINE NO. 2 CABINETROL
TURBINE NO. 1 D-C BUS
STATION D-C BUS
125 V.
INSTRUMENTS
120 V. 1PH 60 CYC
EMERGENCY LIGHTING
SAME AS TURBINE NO. 1
1 KW
1 KW

Fig. 4. Single-line diagram of turbine and station auxiliaries for two 5,000-horsepower gas turbine pipeline pumpers

to be completely self-contained. Each station has three independent sources of electric power:

1. A station storage battery;
2. A gas-engine driven a-c generator;
3. An a-c generator, gear driven from the high-pressure shaft of each gas turbine.

The 60-cell 400-ampere-hour (8-hour rate) station battery, together with a 25-ampere 125-volt d-c phano-charger (two chargers in parallel are used for a 3- or 4-unit station) furnishes d-c power for the main turbine control and supervisory circuits, emergency lighting, and the essential auxiliaries, such as the auxiliary and emergency lube oil and the emergency nozzle-cooling water pumps, if the turbine-driven generator fails and the gas-engine driven generator is shut down.

The gas-engine driven generator can be used to supply power to the station a-c busses, or, if a turbine-driven generator is out of service, to feed the auxiliaries of that turbine. The latter can be accomplished by closing the bus tie contactor between the station and turbine busses.

The turbine-driven auxiliary generators supply all of the a-c power for their own auxiliaries under normal operating conditions. However, the station auxiliaries can be supplied from the turbine bus if required. Normal starting will be without any external supply of a-c power available. At approximately 45-per-cent turbine speed, the turbine generator is connected to the turbine bus. To prevent overloading of the generator by simultaneous starting of the turbine auxiliaries, a sequence timing relay energizes the auxiliaries at 5-second intervals. The auxiliaries are designed for operation over a range of 220 volts to 480 volts at 27.5/60 cycles on a constant volts-per-cycle basis.

Since the generator frequency varies from 36 to 60 cycles, from zero to full load of the gas compressor, and the voltage varies as the square of the speed on a self-excited machine, it is necessary to have a constant volts-per-cycle regulator. This regulator maintains the volts-per-cycle ratio constant to prevent overheating the squirrel-cage induction motors, and also maintains constant voltage (at any given frequency) with load. An exciter-field rheostat mounted on the duplex control board provides manual voltage control of the auxiliary generator through a transfer switch which removes the constant volts-per-cycle regulator from service. During the period that the auxiliaries are being connected to the turbine bus, the generator is overexcited.

The Cabinetrol panel for the turbine auxiliaries consists of:

1. Turbine incoming line fused switch, bus contactor, bus tie contactor, and associated relays;
2. A-c motor starters for the nozzle-cooling water pump, foundation cooling fan, compressor-seal oil pumps, lube water-cooling blowers, and lube cooling water, filter wash, and the evaporator spray pumps;
3. D-c motor starters for the auxiliary and emergency lube oil, and the emergency nozzle-cooling water pumps.

The Cabinetrol panel for the station auxiliaries consists of:

1. Feeders to Inductrol* power packs (dry-type induction voltage regulators) for regulating the lighting load;
2. A-c motor starters for the air compressors and control-room ventilating fan;
3. Spare starters for the turbine auxiliaries;
4. Emergency lighting panels;
5. Control for two motor-generator sets which supply regulated a-c power for metering, recording, and ignition;
6. Master switching control for the power busses.

Here the maximum in flexibility is provided. In each station provision is made to supply:

---

* Reg. U. S. Pat. Off.

1. The station busses from any one of the turbine busses;

2. Any turbine bus from the station busses;

3. One turbine bus from another via the station bus.

Complete interlocking is provided to prevent interconnection of any of the turbine generators, since it is impossible to synchronize these machines under the varying turbine loads.

Each station panel has a mimic bus layout of the turbine and station busses, with control switches and indicating lights for a 4-unit station. The indicating lights show the status of each circuit.

The possibility of completely-automatic unattended gas-pipeline pumping stations has been taken into consideration in the design of these panels. Only minor modifications would be required to install conventional supervisory equipment for remote control.

References

1. Gas Turbine Centrifugal Compressor Stations for Gas Pipeline Pumping, J. F. Eichelmann, J. S. Quill. *Gas*, Los Angeles, Calif., vol. 27, July 1951, pp. 80, 82, 85–6, 88.

2. Design Features of a 5000 HP Gas Turbine, B. O. Buckland, D. C. Berkey. *Transactions*, American Society of Mechanical Engineers, New York, N. Y., vol. 74, no. 5, July 1952, pp. 655–63.

No Discussion

Review of Grounding Practices on 480-Volt Portable Distribution Systems in Strip Mines

R. B. BENNETT
NONMEMBER AIEE

A NUMBER of unfortunate experiences in the past, resulting in the loss of lives, have made many persons conscious of the hazards which can exist on the high-voltage systems serving strip-mining operations. Several years ago a system design employing the neutral grounding resistor was adopted. This has greatly minimized the number of shock accidents caused by equipment and cable failures.

The same hazards exist in lower degree in the operation of the lower voltage circuits serving auxiliary equipments such as pumps, drills, air compressors, etc. These circuits and the equipment they serve, because of the nature of their job, are subjected to abuse from the elements, rough handling, overloading, falling rocks, and many other things which would be considered intolerable on any well and permanently installed equipment. Some of these abuses, such as rough handling, overloading, etc., can be eliminated. It must be assumed, however, that these equipments will continue to be mistreated and, since it is not economical to provide complete protection against the elements, the best that can be done is to design the low-voltage systems to minimize the shock hazards caused by circuit and equipment failures.

Typical Systems

It appears to be in order to review certain of the more common low-voltage systems in use and to analyze them from the standpoint of their potential shock hazard.

Fig. 1 is representative of a typical distribution system used in a strip-mining operation. It is of interest in this discussion only because it shows the manner in which the auxiliary transformers are associated with the 4,160-volt system.

In the majority of 480-volt portable distribution systems the auxiliary transformer banks consist of conventional transformers rated 2,400/4,160*Y* to 480/240 volts, connected wye to the 4,160-volt system through enclosed fuse cutouts. The low-voltage windings of the three transformers in the bank are connected delta for 480 volts. There are three commonly used sizes of auxiliary transformer banks, namely: three 10-kva units; three 15-kva units; and three 25-kva units. Occasionally, small loading shovels may be supplied from the 480-volt auxiliary transformers. In such instances the auxiliary transformer bank may consist of three $37^{1}/_{2}$-kva or three 50-kva units.

Past Practice

In the past there have been many 480-volt portable systems arranged as shown in Fig. 2. Actually, in spite of the fact that such a system is in direct violation of safety codes, there are still occasional installations made in this manner. This system employs a simple 3-conductor cable without ground wires.

The motor may have been completely insulated from earth, or grounded solidly through pipe connections to a direct-connected pump, or in intimate contact with soil. In the first case the resistance R_g of the motor frame to absolute ground is infinite. Should the motor winding, for example, phase *A*, come into contact with the motor frame, the phases *B* and *C* are then at rated phase potential with respect to the motor frame. Under this condition, the motor frame may develop a dangerous potential with respect to ground, depending upon the amount and the division of charging currents. Suppose that now, because of a skinned place in the cable insulation, phase *C* comes in contact with the earth, through a resistance R_x, which may vary over a range from zero to infinity, depending upon soil conditions and the degree of contact. Assume that R_x is 1,000 ohms, which is a quite reasonable value. Since R_g is infinite, because the motor is insulated from earth, no current will flow in the circuit between phases *A* and *C*. With no current flowing through R_x, the voltage drop across this contact resistance is zero, hence phase *C* is at ground potential. The motor frame is at the potential of phase *A*, therefore the voltage E_g between the motor frame and earth is the voltage of phase *A-C*. A man touching the motor frame under these conditions is subjected to full-phase voltage and may receive a very serious shock.

The thought may arise—why not ground the motor frame so that it will always be at earth potential; then, regard-

---

Paper 53-329, recommended by the AIEE Mining and Metal Industry Committee and approved by the AIEE Committee on Technical Operations for presentation at the AIEE Pacific General Meeting, Vancouver, B. C., Canada, September 1–4, 1953. Manuscript submitted October 26, 1952; made available for printing July 13, 1953.

R. B. Bennett is with the General Electric Company, Cincinnati, Ohio.

less of the type of fault, the voltage E_g between the motor frame and earth would be zero and no hazard would exist? This is a perfectly logical thought; however, it is not practical with this class of portable equipment to provide the low resistance grounds which are required. Generally, the only ground practical in these cases is a driven ground rod. Experience has shown that this type of ground will provide ground resistance R_g anywhere from infinity to approximately 10 ohms, depending upon soil conditions. More often than not, the average resistance of driven rods will be in the order of 100 to 200 ohms. Assume, for example, that a driven ground provides a resistance R_g of 150 ohms between the motor frame and earth, and that the resistance R_x, because of contact of phase *C* with earth, is 150 ohms. Under these conditions, if phase *A* should become short-circuited to the motor frame, a circuit is established in which a current *I* will flow.

$$I=\frac{480}{R_g+R_x}=\frac{480}{150+150}=1.6 \text{ amperes}$$

The voltage which constitutes the shock hazard is voltage drop E_g which will appear across R_g.

$$E_g=IR_g=1.6\times150=240 \text{ volts}$$

This voltage is sufficient to cause serious injury. It is therefore obvious that the circuit shown in Fig. 2 is unsafe and should not be used.

Simple Driven Ground

In an attempt to overcome the shortcomings of this scheme, the practice was adopted of connecting the motor to the 480-volt source at the auxiliary bank through a portable cable which, in addition to the phase conductors, included a ground conductor or conductors as shown in Fig. 3. The ground conductor is solidly attached to the motor frame at one end, and to a driven ground at the other end.

In looking at this arrangement from the standpoint of potential shock hazard, it seems appropriate to consider only that type of cable with the multiple ground wires located in the interstices of the phase conductors, since it appears to be a safer cable than that with only a single ground conductor.

Consider again that phase *A*, due to a winding failure, becomes connected to the motor frame. This places a voltage on the motor frame, depending again on the distribution of charging currents flowing through resistance R_g. If R_g is of a very low value, the voltage drop caused by the small charging currents is negligible, and the shock voltage E_g is low. Unfortunately, R_g may be very high. If, because of soil conditions, it approaches infinity, as it very easily may, the motor frame potential will become equally as elevated because of grounds in the motor winding, as it does in the case of the circuit using the simple 3-conductor cable.

Now assume a solid short circuit occurring in the cable, between a phase conductor and the ground wire or wires such as shown as fault *A* in Fig. 3. This type of fault results in relatively high short-circuit currents, which very likely will blow at least one of the low-voltage backup fuses, assuming that they exist. During the interval of the short circuit, the shock voltage E_g is the voltage drop in the ground wire between the point of fault and the motor frame. Assuming the point of fault to be near the auxiliary transformers, and that the resistance of the ground wire or wires is equal to that of the phase conductor, the voltage E_g is one-half the circuit voltage, which may be of the order of 350 volts. This voltage was determined from tests of typical transformer regulation under short-circuit conditions on a length of no. 6 portable cable, supplied from a bank of 3 to 15 kva transformers. Thus it is possible, in the case of the faults just described, to obtain with this type of system shock voltages E_g as high as 175 volts.

The question may be raised, why not make the resistance of the cable ground conductors, say, one-third that of the phase conductors? It is not unreasonable to build such a cable, so it is in order to analyze conditions in which a cable of this kind would be used, as in fault *A*, Fig. 3. Here again the voltage E_g is the drop in the ground conductors from the point of fault to the motor frame. However, with the resistance of the ground conductor one-third that of the phase conductor, only one-fourth of the circuit voltage appears as E_g, the drop in the ground wires. Thus the shock voltage is 90 volts instead of 175. This is not generally a dangerous voltage and perhaps could be tolerated. Unfortunately, however, all faults may not occur between the phase and ground conductors. It is entirely

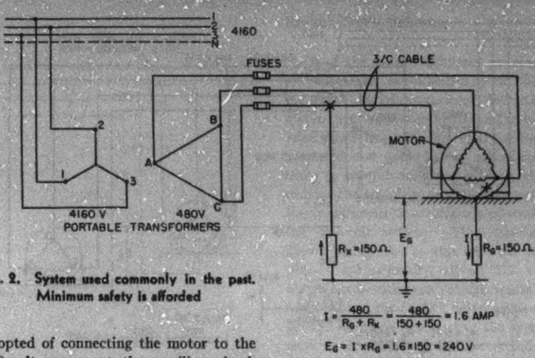

Fig. 2. System used commonly in the past. Minimum safety is afforded

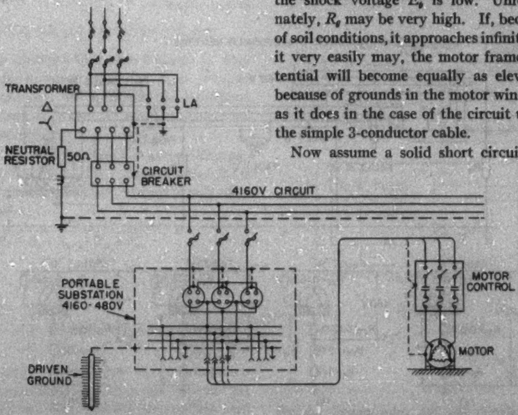

Fig. 1. General arrangement of typical distribution system for strip-mining operations

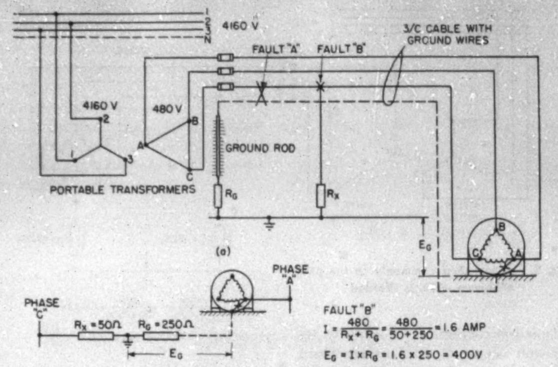
1
2
3
N
4160 V
3/C CABLE WITH GROUND WIRES
FAULT "A"
FAULT "B"
4160 V
480 V
2
B
A
1
3
C
GROUND ROD
PORTABLE TRANSFORMERS
R_G
R_X
E_G
B
C
A
(a)
PHASE "A"
PHASE "C"
R_X = 50Ω
R_G = 250Ω
E_G
FAULT "B"
I = 480/(R_X + R_G) = 480/(50+250) = 1.6 AMP
E_G = I x R_G = 1.6 x 250 = 400V

Fig. 3. System using simple driven ground

possible for the cable to be injured in some such manner as to cause the phase conductor to come into contact with earth, creating a condition similar to fault *B* in Fig. 3. With this condition the phase wire may be in contact with earth through a resistance R_x and still be insulated from the ground conductor.

An analysis of the circuit of fault current will indicate a circuit such as Fig. 3 (A), in which E_g, the shock voltage, still depends on the resistance R_g of the driven ground. Because of the indefinite nature of ground and contact resistance, we are justified in assigning any value for R_x and R_g. Purposely to make the answer appear discouraging, assume $R_x = 50$ ohms and $R_g = 250$ ohms, then:

$$I = \frac{480}{R_x + R_g} = \frac{480}{50+250} = 1.6 \text{ amperes}$$

$$EG = IR_g = 1.6 \times 250 = 400 \text{ volts}$$

This is of course a dangerous shock voltage. Although it appears that the portable cable with the ground wire or wires is less hazardous than the simple 3-conductor cable, it is still possible to obtain dangerous shock voltages, when used with driven grounds of indefinite resistances.

Use of 4,160-Volt System Neutral

Since the most dangerous conditions which have been analyzed have been attributed to high resistance values of driven grounds, the question naturally arises, why not reduce the resistance of the ground? Low values of ground resistance are difficult and expensive to obtain, and because of the portable nature of the equipment being considered, it is not practicable to try to obtain the low value of ground resistance which is required, at each transformer location. It may have been overlooked, however, that the neutral of the 4,160-volt system is perhaps the best ground obtainable. Since it is part of the 4,160-volt circuit which supplies the auxiliary transformers, there is no reason why it should not be considered as a low-resistance ground for the 480-volt portable circuits. Such a system will be as shown in Fig. 4, and might consist of a 300-foot length of no. 6 portable cable having an approximate resistance of 0.15 ohm for the phase and ground conductor. The overhead neutral wire can be assumed to be 2/0 conductor, 2 miles long, having a resistance between points *X* and *Y* of 1.0 ohm. The resistance R_g of the ground at the substation for the neutral resistor can be assumed to be 5 ohms. It is desirable to have a lower value than this. However it is a reasonable value to hope to obtain in practice. To analyze this type of system, the following four types of faults will be considered:

1. *Fault A*. Phase conductor *C* solidly grounded and insulated from the ground wire.
2. *Fault B*. Phase conductor *C* and ground wire solidly connected together.
3. *Fault C*. Phase conductor *C* and ground wire connected together with high resistance connection.
4. *Fault D*. Phase conductor *C* connected to earth through a high resistance and insulated from ground wire.

All of these faults will be investigated, assuming that phase *A* is solidly connected to the motor frame because of an internal motor fault.

The circuit for fault *A* is shown schematically in Fig. 4(A). The fault current *I* will then be

$$I = \frac{480}{R_{az}+R_{zy}+R_{yz}+R_g}$$
$$= \frac{480}{0.15+0.15+1.0+5.0} = 76.5 \text{ amperes}$$

$$E_g = I(R_{zy}+R_{yz}+R_g)$$
$$= 76.5(0.15+1.0+5.0)$$
$$= 76.5 \times 6.15 = 470 \text{ volts}$$

This is a dangerous voltage and cannot be overlooked even though this type of fault may occur infrequently.

The circuit for fault *B* is shown schematically in Fig. 4(B). The fault current *I* will be

$$I = \frac{350}{R_{az}+R_{zy}} = \frac{350}{0.15+0.15} = \frac{350}{0.3} = 1{,}160 \text{ amperes}$$

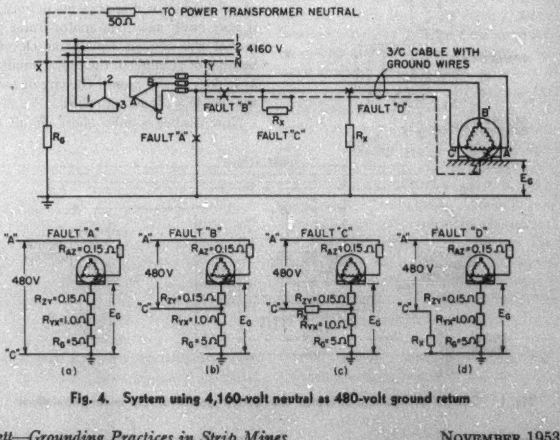
50Ω
TO POWER TRANSFORMER NEUTRAL
1
2
3
N
4160 V
X
Y
3/C CABLE WITH GROUND WIRES
2
B
1
3
A
C
FAULT "B"
R_X
FAULT "D"
FAULT "C"
FAULT "A"
R_G
R_X
B'
C'
A'
Z
E_G
"A"
FAULT "A"
R_AZ=0.15Ω
480V
R_ZY=0.15Ω
R_YX=1.0Ω
R_G=5Ω
E_G
"C"
(a)
"A"
FAULT "B"
R_AZ=0.15Ω
480 V
"C"
R_ZY=0.15Ω
R_YX=1.0Ω
R_G=5Ω
E_G
(b)
"A"
FAULT "C"
R_AZ=0.15Ω
480V
"C"
R_X
R_ZY=0.15Ω
R_YX=1.0Ω
R_G=5Ω
E_G
(c)
"A"
FAULT "D"
R_AZ=0.15Ω
480 V
"C"
R_ZY=0.15Ω
R_YX=1.0Ω
R_X
R_G=5Ω
E_G
(d)

Fig. 4. System using 4,160-volt neutral as 480-volt ground return

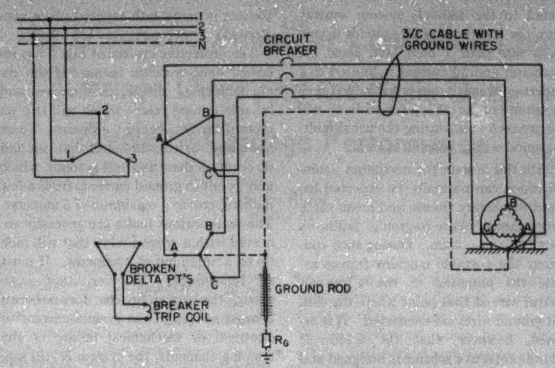

Fig. 5. System using broken delta potential transformers to tripoff ground faults

(Tests on similar systems indicate that, because of regulation of the transformers, the available voltage will be approximately 350 volts.)

$$E_g=0(R_{yz}+R_g)+I(R_{zy})=1{,}160\times0.15 =175 \text{ volts}$$

The voltage E_g corresponds to the voltages obtained for similar fault conditions in the circuit shown in Fig. 3, and likewise can be reduced 50 per cent by trebling the capacity of the ground conductors.

The circuit for fault *C* is shown schematically in Fig. 4(C). Assume that R_x is 100 ohms; then the fault current *I* will be

$$I=\frac{480}{R_x+R_{zy}+R_{az}}=\frac{480}{100+0.15+0.15} =4.8 \text{ amperes}$$

$$E_g=0(R_g+R_{yz})+4.8\times0.15=0.72 \text{ volt}$$

It is obvious that this voltage is negligible, however, since, as R_x is reduced toward zero, we approach the conditions of fault *B*, where E_g reached dangerous levels.

The circuit for fault *D* is shown schematically in Fig. 4(D). Assume that R_x is 100 ohms; the fault current *I* will be

$$I=\frac{480}{R_x+R_g+R_{yz}+R_{zy}+R_{az}}$$

$$=\frac{480}{100+5+1+0.15+0.15}=\frac{480}{106.3}$$

$$I=4.5 \text{ amperes}$$

$$E_g=I(R_g+R_{yz}+R_{zy})=4.5(5+0.15+0.15) =4.5\times5.3=24 \text{ volts}$$

Although this value of E_g does not constitute a shock hazard, it can be seen that as R_x becomes less and approaches zero the shock voltage approaches the dangerous values obtained for fault *A*.

It appears therefore that with this type of system there is nothing to be gained by utilizing the 4,160-volt neutral as a ground since it is still possible for hazardous shock voltages to occur.

Phase Wire in Contact with Earth

One very important fact is that in any of the systems discussed up to this point, should a phase wire come into accidental contact with earth, the potential of the other two phases goes to full voltage above ground. If anyone, in handling the cable, should come in contact with either of the other two phase wires, which may be exposed because of injury to the insulation, he will be subjected to severe shock.

Broken Delta Scheme

All of the points discussed previously are recognized, as evidenced by the thinking which has been expressed both orally and in print on systems proposed to minimize shock hazard. One of the schemes proposed and doubtless in use is essentially a ground detecting scheme which utilizes the so-called broken delta potential transformer to establish a neutral for the 480-volt system. This scheme is shown in Fig. 5. In this case the three phases are normally all at 277 volts above earth with zero voltage across the open ends of the broken delta. Should a ground occur on any part of the system, such as shown between phase *A* and the motor frame, the neutral of the system assumes phase *A* potential and maximum voltage appears across the open ends of the delta to energize the circuit breaker trip coil, thereby disconnecting the defective motor.

The advantages of this scheme are that grounds are removed instantly from the system, if the fault current is of sufficient magnitude to displace the neutral to a point which will provide tripping voltage across the open ends of the delta.

The disadvantage is that dangerous voltages can exist during that interval from the inception of the fault until the breaker opens. Furthermore, should the breaker fail to open for any reason, the system is not fail-safe.

In most installations there are two or more circuits supplied from the transformer bank. This type of ground detector is unable to select the feeder on which the ground exists, hence all the feeders must be tripped by the main

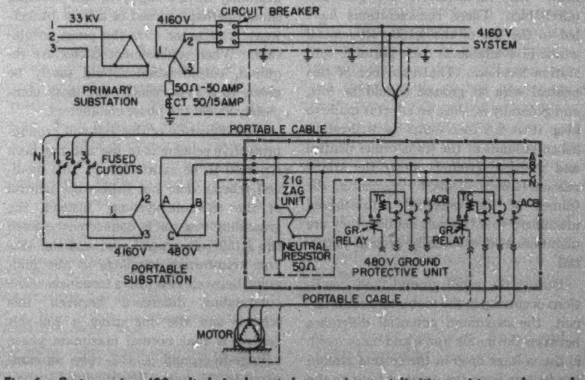

Fig. 6. System using 480-volt derived neutral, ground-current limiting resistor, and ground relays

breaker and a search made for the feeder in trouble.

480-Volt Derived Neutral and Current-Limiting Resistor

In the search for a system to eliminate the shock hazards which exist in the system arrangements described, the one presently receiving the greatest acceptance on established systems is based on principles borrowed from the ground-protective scheme which has been used for many years on 4,160-volt distribution circuits. This system is shown schematically in Fig. 6. A neutral is established for the 480-volt transformer bank by means of a small zigzag grounding transformer, the neutral being connected to ground through a suitable resistor. A 50-ohm resistor having a continuous rating of 5 amperes is commonly being used. It limits the maximum ground current to 5 amperes and permits the use of a small zigzag unit which is given a continuous rating of 5 amperes neutral current. A simple plunger-type overcurrent ground relay with pickup adjustable down to 2 amperes is used to detect ground current. This relay, utilizing phase voltage, energizes a potential trip device in the main transformer or feeder breaker to clear the faulted circuit. Tripping potential is taken from the load side of the breaker, thereby eliminating the need for an auxiliary switch on the breaker to clear the trip coil.

The degree of protection afforded by this system depends solely upon the resistance of the ground to which the ground conductors in the cable are connected. Driven grounds at these portable installations cannot be justified economically and, furthermore, are generally unreliable. These considerations have led to the use of the 4,160-volt neutral which is available at each portable substation location. The resistance of this neutral wire to ground should be low, and generally is, since an effort is made to keep it at 2.5 to 5 ohms by well-established grounds at the transformer neutral and multiple grounds along the transmission circuit. Thus, by connecting the frames of the portable motor-driven machinery to 4,160-volt neutral, they are maintained at essentially ground potential.

During the usual ground fault conditions occurring in the motor and cable circuit, the maximum potential difference between the motor frame and mean earth is the voltage drop in the system ground conductors from the point of fault to the ground end of the protective resistor connected to the 480-volt system neutral. Since the resistance of this circuit is generally less than 1 ohm, and since the maximum ground current is limited to 5 amperes, the maximum potential between the frames of portable pit machinery will not exceed 5 volts during the usual fault-to-ground on the 480-volt system.

With this system the maximum potential which can normally be expected between machinery frames and mean earth occurs during phase-to-ground faults on the 4,160-volt system. During such conditions the portable machine frames assume the potential of the 4,160-volt neutral wire at that point where the 480-volt ground wires are connected. It is assumed, however, that the 4,160-volt ground protective scheme is designed and installed to limit the maximum potential at the most extreme point of its neutral wire to 100 volts. This voltage, except in rare instances, is not hazardous. Fortunately, the 4,160-volt circuits are kept short enough, for the purpose of improving voltage regulation, to keep the maximum potential on the 4,160-volt neutral wire to less than 50 volts.

There is a hazard against which this system affords no protection. The majority of low-voltage portable cables consist of three insulated phase conductors and one or three bare-ground wires. It is quite possible for this type of cable to be injured mechanically, exposing a phase conductor. A person coming in contact with this exposed portion will be subjected to a potential of 277 volts to ground.

Fully to utilize the benefits of the protection afforded by this system, consideration should perhaps be given to a type of cable in which the phase conductors are completely shielded. That the cable flexibility be not impaired, this shielding should perhaps consist of a loose basket-weave conductor over the phase insulation. When replacement cables are required, consideration should surely be given to a type which will most completely shield the phase conductors.

A modification of this 480-volt ground-protective scheme is in use and has been reported to be satisfactory. This modified scheme does not utilize the neutral of the 480-volt system; instead, the grounding resistor is connected between the 4,160-volt neutral wire and the 480-volt transformer windings at the mid-point between two phase terminals. The outstanding difference between this scheme and the one using a 480-volt neutral is that normal maximum phase voltage-to-ground is 415 volts as compared to 277 volts. The modified system is therefore less safe, particularly when contact is made with exposed phase conductors.

The protective system of Fig. 6 has received some criticism because of the unavailability of simple, inexpensive, and reliable ground relays which will trip on ground currents below 2 amperes. There are many varieties of faults that can and do occur on these 480-volt systems, which may result in ground currents from a few milliamperes to a maximum of 5 amperes. The more serious faults are generally removed with a ground relay that will pick up on a minimum of 2 amperes. It must be remembered, however, that even though the backup breaker does not open because of insufficient ground current or electrical or mechanical failure of the tripping elements, the system is still safe from the hazards of contact with machine frames. An electrician at one operation has designed an electronic circuit to use with this protective scheme, which is sensitive to ground currents of a few milliamperes.

Wye-Connected 480-Volt Windings

It should be emphasized that the system illustrated in Fig. 6 applies to existing installations already having wye-delta auxiliary transformers. On new jobs permitting choice of delta-wye transformers, all the advantages of the system just described can be obtained without need for a derived neutral. Greater simplicity, less over-all cost, and improved reliability result with the 480-volt neutral connected directly through the current limiting resistor to the 4,160-volt ground wire. With the exception of the delta-wye connection, and omission of the zigzag transformer, connections are as shown in Fig. 6.

Conclusion

Many needless accidents occur each year in all industries, many of them the result of lack of foresight. It is very encouraging to see the consciousness which has developed in the past few years of the hazards that exist, and the thought and effort which is being given toward their prevention. Unfortunately, too many preventive measures come into being only through hindsight. Even though conditions arise that may defy the imagination, it is the engineer's job to analyze each new design with the question, "Have I done all I can to make this world a safer place in which to work?"

◆

No Discussion

The Magnetic-Amplifier Controlled Log-Carriage Drive and the Basic Duty Cycle of Carriage Performance

H. A. ROSE
MEMBER AIEE

Synopsis: The drive for the log carriage is probably the most important of all sawmill drives. The mill's output is directly related to the speed and agility with which the carriage will respond to the sawyer's needs. The carriage represents a load of high inertia, and to propell it at required degrees of acceleration, deceleration, and speed demands large amounts of power. In making electric log-carriage applications it is economic practice to load the drive units to the maximum currents for which they are capable in rapidly recurring duty-cycle operation. This paper deals with the significance of this loading as related to:

1. The cost of the drive as affected by the production requirements of specific applications.

2. The introduction of modern magnetic-amplifier controls to permit loading the drive components to their maximum load capabilities.

3. The introduction of a "basic duty cycle" for carriage operation. Based on this cycle, simple equations are developed to afford better understanding and appreciation of the important factors involved

$$\text{Dollar cost} \sim (\text{HP})_{\text{rms}} = \frac{P_m{}^3 d^2 W}{86{,}600{,}000}$$

For example, this basic equation states that the cost of a drive is approximately proportional to the cube of the maximum production requirement (P_m), measured in continuous round trips per minute, that the carriage must make. Other important equations are developed, and the solution of a specific problem according to the theory is presented in graph form.

ELECTRIC drives for log carriages are rapidly becoming established in the forest product industries. A large number of new and rehabilitated installations have been made in the last few years and a high percentage of these have been equipped with electric drives instead of the long established twin-cylinder steam engines and "shotguns."

It is logical that the log carriage would be among the last of the industries' machinery drives to be electrified. Practically all other machines except those subject to severe loading in the form of reciprocating or oscillating motions[1] are presently driven by electric motors. The log carriage being one of these high-peak load applications has, until recently, been most economically powered by low cost, although inefficient, steam-driven equipment. Waste wood and bark for production of steam power was cheap and in plentiful supply.

During recent years, however, the economic pattern has been steadily changing. Waste wood is being put into pulp or other higher-valued products. "Hogged" fuel is becoming scarce. Steam, once available in unlimited quantity, has become both scarce and a high-value item. Steam plants have become costly to install and expensive to operate, except in the case of a comparatively few large integrated mills which operate dry kilns, a planing mill, or other by-product plants in conjunction.

These unfavorable conditions to steam-driven equipment and the present-day general availability of moderate-cost electric power are responsible for the marked increase in electric log-carriage installations. Also, modern electric carriage drives operate at high efficiency, since much of the energy taken for their operation is cyclically returned to the power system as inertia energy during the working periods of deceleration of the carriage.

Electric carriage drives are available in two principal forms, commonly referred to as the "geared" type and the "gearless" type, as illustrated in this paper. Both types are similar as regards major elements of equipment, the essential difference being in the carriage propulsion unit. In the geared-type, a high-speed motor is coupled to a speed reducer and cable drum, all mounted on a common bedplate. In the gearless type, a slow-speed very-high-torque motor and cable drum are mounted on a common armature shaft between two heavy-duty pedestal bearings. The high-torque motor eliminates the need for a gear unit and provides a simple way of connecting the motor directly to the carriage.

In the geared-type drives, motor inertia presents a problem because it must be accelerated to speeds of 1,200 to 2,000 rpm in 1 to 2 seconds or less, during which the carriage reaches full speed. To minimize motor inertia and thereby reduce the portion of gross power absorbed by it, a 75-degree-centigrade rise machine is generally employed. Since gearless drives have to reach only 50 to 120 rpm for full carriage speed, the angular acceleration involved is so low that motor inertia is of little consequence. This permits economic use of 40-degree-centigrade rise machines.

General Requirements for Log-Carriage Drives

Carriage drives should have sufficient reserve power to quickly accelerate and decelerate the carriage without distress at the commutators of the propulsion motor or generator. The drive must respond quickly to movements of the sawyer's controller. The system should create the feeling of being "alive" at the controls. The sawyer should not be burdened with conflicting mental requirements of having to manipulate his controller to prevent overloading the equipment while striving to attain maximum lumber output.

To attain these requirements economically requires motors and generators having high momentary commutating capability, that can be used continually in rapidly recurring duty-cycle operation. Since the motor is at rest or reduced speed a considerable portion of the time, forced air cooling is required to dissipate its losses. The drive motor of the motor-generator set must have high-breakdown torque, commensurate with the peak reversing power demands placed against it by the generator. Current and speed regulating equipment is required to force the machines to respond quickly to the prescribed limits of their commutating capabilities.

The Magnetic Amplifier, Speed and Load Controller

Much of the success attained to date by electric carriage drives is due to mod-

---

Paper 53-316, recommended by the AIEE General Industry Applications Committee and approved by the AIEE Committee on Technical Operations for presentation at the AIEE Pacific General Meeting, Vancouver, B. C., Canada, September 1–4, 1953. Manuscript submitted May 28, 1953; made available for printing July 20, 1953.

H. A. Rose is with the Westinghouse Electric Corporation, Seattle, Wash.

The author wishes to give credit and express his appreciation to T. M. Greer who assisted in the formulation of certain concepts of the theory of the "basic duty cycle" and for other important mathematical work leading to preparation of the material for this paper.

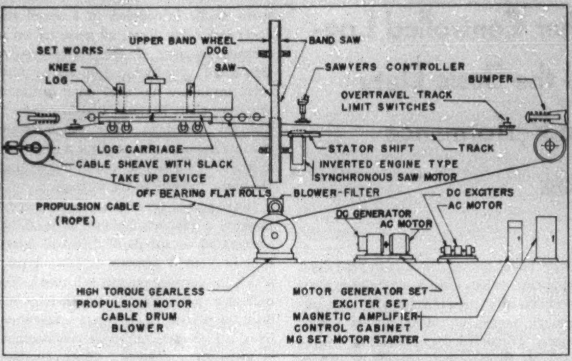
UPPER BAND WHEEL
BAND SAW
SET WORKS
DOG
KNEE
LOG
SAW
SAWYERS CONTROLLER
BUMPER
OVERTRAVEL TRACK LIMIT SWITCHES
LOG CARRIAGE
STATOR SHIFT
TRACK
CABLE SHEAVE WITH SLACK TAKE UP DEVICE
INVERTED ENGINE TYPE SYNCHRONOUS SAW MOTOR
OFF BEARING FLAT ROLLS
BLOWER-FILTER
DC EXCITERS
AC MOTOR
PROPULSION CABLE (ROPE)
DC GENERATOR
AC MOTOR
HIGH TORQUE GEARLESS PROPULSION MOTOR CABLE DRUM BLOWER
MOTOR GENERATOR SET
EXCITER SET
MAGNETIC AMPLIFIER CONTROL CABINET
MG SET MOTOR STARTER

Fig. 1. Diagram showing the principal pieces of equipment for the gearless type of electric log-carriage drive, including the inverted engine-type synchronous-drive motor for the band saw

ern types of load- and speed-regulating systems. Rotating regulators[2,3] were first used. The latest advancement in this type of control is the magnetic amplifier.[4,5] This device has the principal advantages of being a small static piece of equipment, which having once been adjusted requires no further attention.

In the drive described by this paper, the magnetic amplifier supplies the entire excitation requirements for a conventional variable-voltage reversing-polarity exciter which, in turn, excites the propulsion generator.

The larger generator ratings have sufficiently high field inductance to prevent rapid rise in voltage (carriage acceleration) if natural circuit time constants are allowed to prevail. To overcome this, generator field forcing is employed. The forcing action is obtained from the magnetic amplifier, arranged to simultaneously force and limit the generator output voltage through the exciter. A push-pull type of magnetic amplifier is used, since the generator and exciter must operate with reversing polarity. The push-pull amplifier consists of two matched amplifiers operating in opposition.

As illustrated, see Fig. 13, the magnetic amplifier is provided with four intelligence windings, which act jointly to determine the exciter field current required:

1. Speed control winding, actuated by sawyer's controller.

2. Bias winding, for extending the magnetic amplifier's range; excited at constant potential.

3. Current limit winding, for limiting the degree of current loading permitted; excited by load voltage drop across series and commutating field windings of propulsion generator. Restraining bias prevents this winding becoming effective for current less than the permissible value.

4. Antihunt winding, for maintaining stable carriage speed as determined by sawyer's controller position; excited by damping transformer from exciter voltage.

The magnetic amplifier control, see Fig. 12, is the heart of the entire control system. Through its control windings, the sawyer sets the direction and speed of the carriage by positioning his controller. The magnetic amplifier forces the generator (voltage) and propulsion motor (speed) to respond at a constant rate of acceleration for all speed selections. The rate of acceleration is determined by the current loading permitted for the drive units, and is established by the bias setting given the current-limit winding.

The magnetic amplifier uses the self-saturating effect[6] of the load current i_f it controls to assist in producing the flux changes required in its magnetic circuit. The control energy i_c required to swing the output from zero to maximum value is, therefore, very small. High values of control-circuit amplification and exciter-field forcing action are thereby obtained. The current duty on the sawyer's controller is very small.

Sawyer's Controller

The sawyer's controller is of special design for easy and essentially stepless speed control. Movement of the handle in either direction results in progressive closure of a single series of contacting leaves and buttons. There are no sliding contacts. Forward and reverse controller movements automatically excite the corresponding directional speed amplifiers through integrally built speed selection switches.

Fig. 2. A heavy-duty gearless propulsion motor, with integrally built grooved cable drum, d-c electric solenoid brake, forced-air blower, and air filter. Note split construction of motor frame, commutator inspection covers, large shaft and pedestal bearing

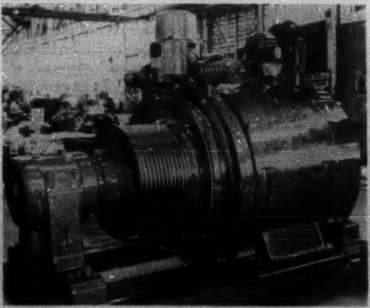

Fig. 3 (right). Typical installation of gearless propulsion motor. Note wooden face guide for propulsion cable in foreground. Airfilter prevents entrance of sawdust and dirt to motor. Long tension bolts hold motor securely to foundation

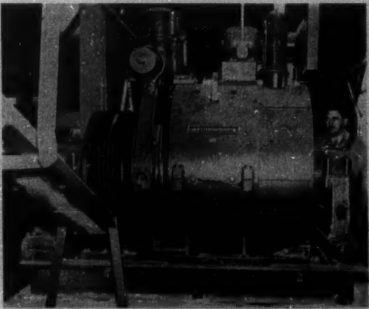

Fig. 4. Power-supply motor-generator set for gearless log-carriage drive. Components are open-drip proof, 40-degree-centigrade rise

Fig. 5 (right). Typical installation of power-supply motor-generator and separately driven 3-unit excitation motor generator set for gearless log-carriage drive

Analysis of Power Requirements

The electric energy required to drive log carriages is nominal, and may be almost negligible compared with other costs of mill operation. This is because a large portion of the energy put into accelerating the loaded drive is returned to the power system as inertia energy during periods of deceleration.

The electric power needed to propel the carriage, however, is considerable, and requires propulsion equipment of comparable power rating. The cost of the drive is approximately proportional to the required power rating. The yearly investment charges covering the installation may be considerably larger than the cost of the energy.

Without regard to equipment cost, it is of paramount importance that the drive have adequate power and speed to meet the mill's daily production requirements, as measured in properly sawn board-foot output. Too small a drive, although of low first cost, may be tremendously expensive through losses in production. An oversize powerful drive, with correspondingly high investment charges, can also curtail production by having too low a carriage return speed. A high-speed lightweight carriage may lose production by slow accelerating and decelerating capability in the drive, the characteristic of feeling "sluggish" at the controls.

The following theoretical treatment is intended to show the importance and relationship of the factors which affect cost and production performance of log carriage drives. It is not the author's intent to present the more involved equations treating the various forms of carriage movements. These become so complicated that perspective regarding the basic elements of the problem are lost. The nomenclature identifies the most important factors which characterize electric carriage drives.

Nomenclature

P_m = rate of production in round trips of the carriage, per minute

d = average one-way distance the carriage moves in normal sawing, feet

W' = weight of the carriage, log, propulsion cable, and equivalent sheaves, pounds

W = total equivalent weight of the entire moving system, pounds of carriage weight, including equivalent weight of the drive motor and gear unit

S = the level running speed of the carriage, feet per minute

a = accelerating and decelerating rate of the carriage, feet per second squared.

Δt = time required to accelerate the carriage from stand-still to speed S, seconds.

$(HP)_a$ = torque horsepower developed to accelerate the loaded system W to speed S in time Δt

$(HP)_{rms}$ = rms torque horsepower developed when continuously propelling the loaded system W over track distance d to speed S, accelerating and decelerating in time Δt

$(HP)_{rms}'$ = rms torque horsepower developed when continuously propelling the loaded system W over track distance d to speed S, accelerating and decelerating in time Δt with the carriage active $\alpha = 1/1$ of the time

α = the per unit, 1/1, time the carriage is active during normal sawing operations

F' = pull on the propulsion cable required to accelerate the load inertia W', pounds

F = the propulsion motor air gap rope pull (fictitious) in equivalent pounds on the propulsion cable required to accelerate the total equivalent weight W

P_m (mechanical) = the mechanical capability of a given drive for different carriage speeds S for rate of acceleration a, round trips per minute

P_m (thermal) = the thermal capability of a given drive for different carriage speeds S for rate of acceleration a, round trips per minute

v = speed, feet per second

T = time for one-way trip, seconds

T_{rt} = time for round trip, seconds

Δt = time for acceleration or deceleration, seconds

Δt_r = time at level running speed, seconds

d_r = distance traveled at level running speed, feet

Δs = accelerating or decelerating distance, feet

S_m = maximum carriage speed, feet per minute

v_m = maximum carriage speed in feet per second

g = acceleration of gravity, feet per second squared

f = force, pounds

w = weight, pounds

s = speed, feet per minute

$1/1i$ = torque "gain," expressed in per unit of nominal full-load value = 1

$1/1s$ = rpm speed "gain," expressed in per unit of nominal rated value = 1

(hp) = horsepower

1/1 = a per unit value (1.75 1/1 = 175 per cent)

To attain maximum production, the sawyer inherently returns the carriage at the maximum speed capability of the drive. The speed in making the cut depends principally on the character of the wood being sawed and on the depth of the cut. For soft woods, under normal sawing conditions, maximum carriage speed may be expressed approximately as

$$S \approx \frac{500}{D} \text{ feet per minute}$$

and for hard woods

$$S \approx \frac{250}{D} \text{ feet per minute}$$

where D is the depth of the cut in feet.

Fig. 6. Typical sawyer's control station, showing sawyer's master controller, push-button console, foot button, and "nigger" stick

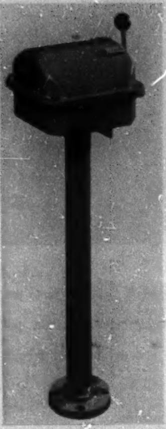

Fig. 7. Sawyer's pedestal-mounted master controller. Controller head is dust-tight. External wiring is made through pedestal

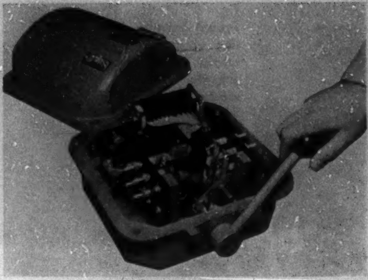

Fig. 8. Sawyer's controller with cover removed. Note travel selection switches in foreground and factory wired resistor assembly in background. Controller has no sliding contacts. Resistor assembly in controller head reduces external wiring connections to a minimum

Fig. 9. Magnetic amplifier and control device cabinet. Constant potential exciter-field rheostat, exciter voltmeter, and d-c ammeter are mounted on swinging door

These semiempirical equations are the result of certain investigations of the author regarding carriage-sawing speeds for large band and circular saws. They are based on the principle that carriage speed times depth of cut governs the rate of kerf removal for properly filling the saw gullets.

It follows that sawing speeds for softwood logs approximating 1-foot diameter approach carriage-return speeds. For this reason, and to simplify carriage-drive comparisons, it is common practice to measure the capability of a given electric drive by the maximum number of round trips per minute P_m it will make if assumed to operate continuously over a travel distance d, propelling a loaded carriage of weight W', with zero idle time. ($\alpha=1.0$.)

The Basic Duty Cycle

To simplify equations governing log-carriage drive performance a basic duty cycle of operation was adopted. It was found that a cycle using one-fourth the travel distance d for acceleration, and another one-fourth for deceleration could, for practical purposes, be accepted as an "ideal cycle," for the following important reasons:

1. In moving a given weight a given distance in a given time, the cycle requires a minimum of accelerating horsepower.
2. With considerable degree of accuracy, the cycle also results in near minimum amounts of motor heating (rms torque horsepower).
3. That $1/4d$ accelerating distance, $1/4d$ decelerating distance, and $2/4d$ for full-speed travel represents fairly closely the performance exercised by the sawyer for high-speed carriage operation.
4. That the cycle results in one-third time for acceleration, one-third time for full speed travel, and one-third time for deceleration, which simplifies the mathematical development and resulting equations.

This theoretical cycle is called the basic duty cycle, and it results in an "optimum mode" of performance for any drive. The characteristics of the cycle are shown by Fig. 14.

In the theoretical development, friction effects are neglected to simplify the basic equations. Friction for the entire system may be conservatively assumed at 50 pounds per ton of loaded carriage weight. As a coefficient, this is a force of 0.025 1/1 weight. By comparison, acceleration rates range from 6 to about 15 feet per second squared. In terms of gravity, these are forces of about 0.186 to 0.465 1/1, compared to 0.025 1/1 for friction. Friction can therefore decrease the accelerating ability of a drive about 5.4 to 13.4 per cent below what it would be without friction. Since friction also increases decelerating rates by similar percentages, production performance of a drive suffers little from the effects of friction. Neglecting its effects therefore seemed justified for the purposes of this paper.

Characteristic Equations of the Basic Duty Cycle

The following principal equations were derived from the characteristics of the basic cycle. The developments are given in the Appendix.

Note 1: Equations with an asterisk apply only for the basic cycle or optimum mode; those not so identified may be applied generally. The subscript o identifies a factor or value applying only in the optimum mode.

Note 2: P_m (mechanical) and P_m (thermal) determine the rates of production in round trips per minute for different carriage speeds S, but for constant values of carriage travel d and acceleration rate a. P_m (mechanical) is in no way limited by thermal considerations of the propulsion motor; likewise P_m (thermal) is not limited by mechanical considerations.

Note 3: The crossing of curves P_m (mechanical) and P_m (thermal) gives the carriage speed S' for which maximum production is obtained commensurate with thermal capability; see equation 13.

$$S_o=3P_m d \text{ feet per minute} \qquad (1)^*$$

$$\Delta t_o=\frac{30d}{S_o} \text{ seconds} \qquad (2)^*$$

$$(\mathrm{HP})_{e_o}=\frac{WS_o^2}{63{,}700{,}000\,\Delta t_o} \text{ torque horsepower} \qquad (3)$$

$$(\mathrm{HP})_{\mathrm{rms}_o}=\sqrt{\frac{2}{3}}\,(\mathrm{HP})_{e_o} \text{ rms torque horsepower} \qquad (4^*)$$

$$(\mathrm{HP})_{\mathrm{rms}}'=\sqrt{\alpha}\sqrt{\frac{2}{3}}\,(\mathrm{HP})_{e_o} \text{ rms torque horsepower} \qquad (5)^*$$

$$F'=\frac{P_m^2 dW'}{6{,}450} \text{ pounds cable pull (neglecting friction)} \qquad (6)^*$$

$$(\mathrm{HP})_{e_o}=\frac{P_m^3 d^2 W}{71{,}000{,}000} \text{ torque horsepower} \qquad (7)^*$$

$$(\mathrm{HP})_{\mathrm{rms}_o}=\frac{P_m^3 d^2 W}{86{,}600{,}000} \text{ rms torque horsepower} \qquad (8)^*$$

$$(\mathrm{HP})_{\mathrm{rms}_o}'=\sqrt{\alpha}\,\frac{P_m^3 d^2 W}{86{,}600{,}000} \text{ rms torque horsepower} \qquad (9)^*$$

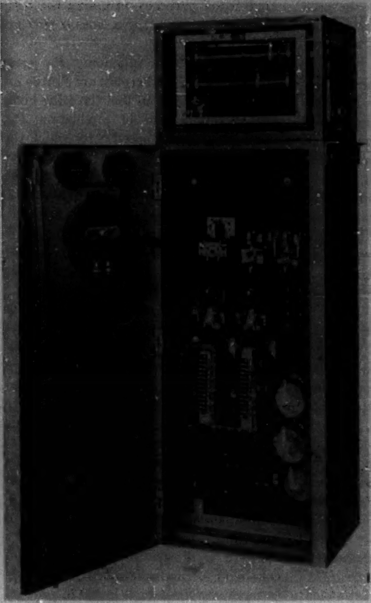

Fig. 10. Control cabinet with open door showing magnetic amplifiers and rectifier units on bottom panel section, and auxiliary control relays on top section. Control resistors mounted in grilled top frame

$$F=\frac{P_m{}^3dW}{6,450}\text{ (fictitious) pounds of motor air-gap rope pull}\quad(10)^*$$

$$P_m\text{ (mechanical)}=\frac{1,800S}{S^2+3,600da}\text{ round trips per minute}\quad(11)$$

$$P_m\text{ (thermal)}=\frac{900a}{1/1i^3S}\text{ round trips per minute}\quad(12)$$

$$S'=60\sqrt{\frac{da}{2\,1/1i^2-1}}\text{ feet per minute}\quad(13)$$

Discussion of Basic Equations

Accurate values for d, W, P_m, and α should be available for a proposed application, such as the example given by Fig. 15. Consecutive use of equations 1 to 6, inclusive, may then be used to solve the problem for operation in the optimum mode. It is important that the value W be the total equivalent weight of the entire moving system, expressed in pounds of carriage weight.

The importance of equations 7 and 8 should be appreciated. As indicated in the synopsis, the cost of a drive is proportional to the horsepower rating necessary to produce the required carriage performance. The equations therefore show the relative importance of the three principal factors influencing the cost.

It is important that unnecessary weight be eliminated from the propelled system W since it is dead load that must be repeatedly raised and lowered in speed, and increases the drive cost proportionately. The log weight may be that of the average log carried. Technically, it should be less than the average log weight.

The carriage-travel distance d is determined by the mill layout and length of the average log. This value is substantially fixed for a given application. It is important that the correct value be accurately determined, as the cost of the drive is proportional to the square of this factor.

The most important factor affecting drive cost is production capability P_m. Its influence is proportional to the cube of the round trips per minute the drive should be capable of making under sustained maximum production speeds. Once values for W and d have been established for the conditions pertaining to maximum production P_m, the cost of the drive will vary rapidly with changes in assumed values of P_m. For example, changing

Fig. 11. Cross-the-line 2,300- or 4,160-volt motor-generator-set motor starter, usually employed for largest drives. Smaller ratings use either 440- or 220-volt starters

P_m from 12 to 15 essentially doubles the cost of the drive. It is therefore very important that the desired value of P_m be determined as accurately as possible. There may be little sense in powering a heavy duty long-side carriage for 25-percent excess production P_m (doubles drive cost), unless the large log supply and the rest of the mill facilities will maintain its operation.

General equation 3 is important, as it may be applied outside the optimum mode to determine independently the increase in drive horsepower required to obtain

1. Greater carriage agility Δt (rates of acceleration) than the specific value Δt_o which obtains for the optimum mode.
2. Higher carriage ceiling or return speeds S than is provided for by the optimum mode S_o.

S_o and Δt_o should first be determined. Other values of S and Δt may then be substituted and the change in horsepower noted. The example illustrates the effect on $(HP)_o$ of changing the agility factor Δt. The increase in inertia horsepower $(HP)_a$ will not be great for agility values downward to 0.75 Δt_o. As a general rule, full speed accelerating times less than this value are impractical.

Determination of Propulsion Motor Rating

The lifetimes of carriage drives are spent continually accelerating and decelerating inertia. Economic application of electric drives to this unusual type of load requires motors of low inertia effect, high load-current commutating capacity, and wide speed-range capability.

These characteristics are best met by the nominally-rated Association of Iron and Steel Engineers (AISE) standardized d-c mill motors (for geared-type drives) and by Electric Traction Elevator motors (for gearless-type drives).

When properly applied, these heavy-duty motors may be operated to maximum speed and current values in the order of 1.5 to 2 times their nominal ratings. The requirements, as applied to a specific application, are:

1. Safe speeds must not be exceeded.
2. Maximum current-commutating ability must not be exceeded.
3. Rms loading shall not result in excessive temperatures with forced ventilation.
4. The load-cycle requirements and the rating of the machines shall permit the commutators to maintain satisfactory polish and acceptable performance.

The maximum momentary horsepower

capability for carriage propulsion motors therefore becomes

$$(\mathrm{HP})_e = (\text{nominal HP rating}) \times (1/1 \text{ speed gain}) \times (1/1 \text{ torque gain}) \qquad (14)$$

$$(\mathrm{HP})_e = (\text{nominal HP rating}) \times (1/1s) \times (1/1i)$$

Or, the nominal motor rating for a particular application would be

$$(\mathrm{HP})\,(\text{nominal rating}) = \frac{(\mathrm{HP})_e}{(1/1\,s)(1/1\,i)} \qquad (15)$$

For the example of Fig. 15, if 1/1 s and 1/1 i are chosen as 2.0 and 1.8, the total horsepower "gain" becomes 2×1.8=3.6. The nominal motor rating would be 225/3.6=62.5 horsepower, which corresponds to the AISE frame-610 force-ventilated mill-motor rating. For $s=2$, this motor would have thermal horsepower capability of 2×62.5=125 horsepower. The duty cycle assumed however, requires a thermal capability of 164 rms horsepower for $\alpha=0.8$. This requirement is met with reserve by the 94-horsepower, AISE frame-612 motor, having 188 rms horsepower capability for $s=2$. In fact, it meets the optimum rms horsepower of 183 for $\alpha=1.0$.

Proper values to assign the gain factors can best be arrived at by consultation with the electric machinery manufacturer, after all facts concerning the actual sawing cycle have been established. In general, the higher-gain values will apply to light and moderate duty applications, such as log-breakdown plants for pulp mills. The lower values should be used for heavy-duty sawmill applications, involving high-carriage speeds S and production rates P_m.

Equation 11 gives the mechanical production capability of a drive, P_m (mechanical) for different carriage-speed values S, and for constant accelerating and decelerating rate a. This equation applies between limits of $S=0$ to $\sqrt{2}S_o$. Fig. 16 gives the plot of P_m (mechanical) for the example of Fig. 15. The maximum carriage speed attainable S_m is $\sqrt{2}$ times the optimum speed S_o. The corresponding maximum production P_m (maximum) is $3/4\sqrt{2}=1.06$ times the optimum production P_{m_o}.

Equation 12 gives the thermal production capability of a drive, P_m (thermal) for different carriage speed values S, for constant accelerating and decelerating rate a and for assigned accelerating capability i. This formula applies between limits of $S=0$ and $S=\sqrt{2}S_o$.

Curves 1 to 6 of Fig. 16 are plots of equation 12 for different horsepower-rated motors, each having assigned accelerating capabilities i such as to give the same accelerating capability $a=10$ feet per second squared. The motor of curve 6 is one half the horsepower size (1/1 $p=0.5$) of curve 1, but is worked to twice its nominal current rating (1/1 $i=2$). The curves cover the normal range of motor loading (1/1 $i=1$ to 2) used for application purposes, including the optimum case, where 1/1 i becomes $1/\sqrt{2/3}=1.22$.

When the two functions, P_m (mechanical) and P_m (thermal) are plotted for the same value of a, their crossing gives the maximum rate of production P_m, and corresponding speed S for which the cycle may be maintained continuously. The particular speed value S at which the crossing occurs is given by equation 13.

Curve 1 represents a motor thermally capable of continuous operation at 1 1/1 i, continuously accelerating and decelerating, attaining a maximum center distance speed of $\sqrt{2}\,S_o$ and developing a maximum horsepower of $\sqrt{2}\,(\mathrm{HP})_{e_o}$.

The portion of the thermal curves above P_m (mechanical) are fictitious, since the production values, although thermally feasible, are mechanically nonattainable. All portions of curve 1 are fictitious, except the single point value representing maximum possible production. The production values of the thermal curves below P_m (mechanical) are real, and can be realized continuously without exceeding thermal capability of the motor.

Curve 6 illustrates the thermal incapability of undersized carriage drives to meet sustained high levels of production, as obtains for high speed lumber-sawing rigs in sawmills, where cants and logs run small and of even size. Too small

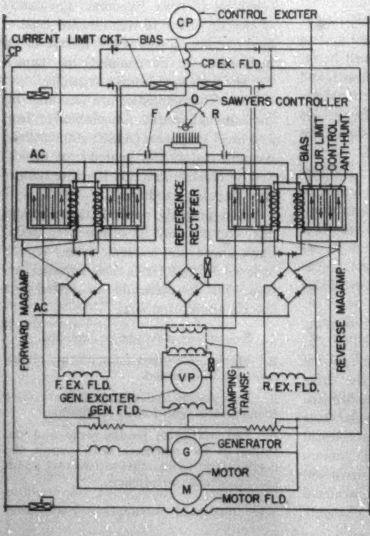

Fig. 12 (left). Schematic connection diagram showing principal circuits for magnetic-amplifier controlled electric log-carriage drive

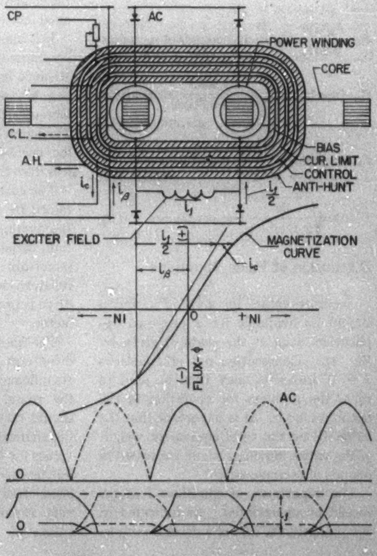

Fig. 13 (right). Simplified diagram showing parts and illustrating principle of operation of magnetic amplifier as used with log-carriage drives

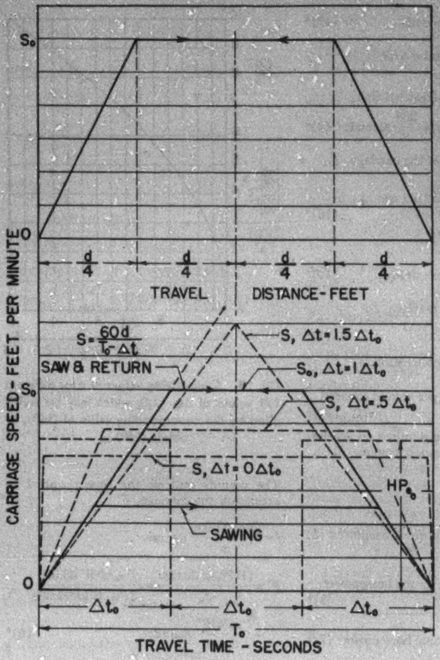

Fig. 14 (left). Diagram defining the basic duty cycle. Solid line pertains to basic cycle operation S_o. Dashed lines S apply for rates of acceleration and speed on either side of the basic cycle characteristic S_o. All cycles illustrated obey the condition $S=60d/(T-\Delta t)$ in order that each shall be completed in time $T=T_o$

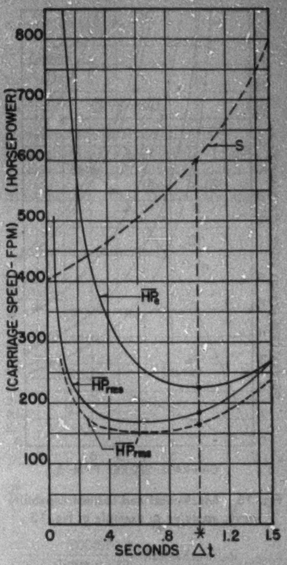

Fig. 15. Curves showing solution of an assumed log-carriage application. The equations give successive steps in the solution according to the "optimum mode"

Application information: d=20 feet; W=40,000 pounds; $P_m=10$; $\alpha=0.8$

$$S_o=3P_m d=600$$

$$\Delta t_o=\frac{30d}{S_o}=1^*$$

$$T_o=T=3\Delta t_o=3$$

$$\boxed{\begin{gathered} S=\frac{60d}{T-\Delta t} \\ (HP)_e=\frac{WS^2}{63{,}700{,}000\Delta T} \\ (HP)_{rms}=\alpha(HP)_e \\ (HP)_{rms_o}'=\sqrt{\alpha}(HP)_{rms} \end{gathered}}$$

$$(HP)_{e_o}=\frac{WS^2}{63{,}700{,}000\Delta t_o}$$
$$=225$$

$$(HP)_{rms_o}=\sqrt{\frac{2}{3}}(HP)_{e_o}$$
$$=183$$

$$(HP)_{rms_o}'=\sqrt{\alpha}\sqrt{\frac{2}{3}}(HP)_{e_o}$$
$$=164$$

$$'\Delta t_o=\frac{30d}{S}=1$$

Note: The boxed equations are not used in the successive step solution of the problem

a drive in this class of service can also suffer from poor commutation, due to insufficient periods of light loading for maintenance of proper commutator polish. An application made according to curve 6 would, however, be ideal for log-breakdown service in pulp mills.

Applications according to curve 1 are uneconomical since no advantage is taken of the overload capabilities of the equipment, and the idle time and reduced-speed operation inherent to log carriage operation.

Curve 2, which contains the point of basic-cycle operation represents only 1.22 1/1 *i* loading, and is conservative. The usual application involves sufficient idle time and reduced-speed sawing to permit working the commutators between 1.5 to 2 1/1 *i*, and still meet rms horsepower requirements. Cycles for long-side head rigs, sawing large variable-diameter logs, contain considerable idle time and slow speed sawing, so as to permit use of 1/1 *i*=1.65 to 2.

Conclusions

1. Electric drives may be economically applied to all classes of log-carriage service where electric power is available.

2. The cost of energy to power electric carriages is small, because of regeneration from the inertia of the mechanical system.

3. Electric drives are available in both geared and gearless types of drum and rope propulsion equipments.

4. The power components of the drive should possess high momentary load capability, for use in rapidly recurring duty-cycle operation.

5. The propulsion motor should possess low-inertia effect, to minimize self-consumption of power and recirculation of energy.

6. A speed-forcing current-limiting type of speed regulator is required to insure maximum output, adequate rates of acceleration and deceleration, and smooth even running speed during sawing.

7. The drive should be properly matched to the duty it is to perform as regards:

   A. Production capability—round trips of the carriage per minute.

   B. Agility of movement—the feeling of being "alive" at the controls.

   C. Adequate return speed capability.

   D. Thermal capacity matched to rms horsepower of the carriage cycle.

8. The sawyer's controller should be easily operated and the control should respond instantly to all controller movements.

9. A basic duty cycle of optimum carriage

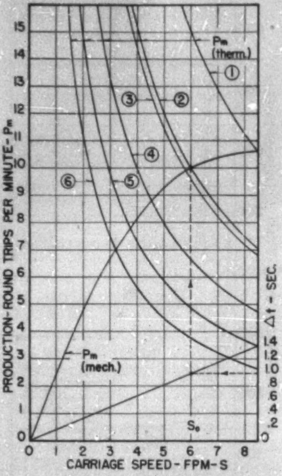

Fig. 16. Mechanical and thermal capability curves applying to example of Fig. 15

$$P_m\text{ (mechanical)}=\frac{1{,}800S}{S^2+3{,}600da}$$

$$P_m\text{ (thermal)}=\frac{900\,1/1\,p^2a}{S}$$

$$=\frac{900a}{1/1\,i^2S}$$

	1/1 p	1/1 i
①	1	1
②	0.816	1.22
③	0.800	1.25
④	0.667	1.50
⑤	0.572	1.75
⑥	0.500	2.00

performance approximates the manner in which the sawyer manipulates the carriage for maximum round-trip production.

10. Simple characteristic equations based on the cycle aid in better understanding and appreciation of important factors involved in the application and operation of electric carriage drives.

Appendix. Development of Equations

Prime Equations of the Basic Cycle

Based on the concepts of the basic duty cycle as given in the text, see Fig. 14

Δt_o (acceleration) $=\Delta t_o$ (deceleration)

$$=\frac{d/4}{v/2}=\frac{d}{2v}\text{ seconds}\qquad(16)^*$$

$$\Delta t_o\text{ (run)}=2\frac{d/4}{v/2}=\frac{d}{2v}\text{ seconds}\qquad(17)^*$$

where v = feet per second $=S/60$

Therefore

Δt_o (acceleration) $=\Delta t_o$ (deceleration)

$$=\Delta t_o\text{ (run)}=\frac{30d}{S_o}\text{ seconds}\qquad(2)^*$$

Time for a round trip of the carriage, T_{rt}

$$T_{rt}=6\Delta t_o=\frac{180d}{S_o}\text{ seconds per round trip}\qquad(18)^*$$

Production $P_m=60(1/T_{rt})$

$$P_{m_o}=\frac{S_o}{3d}\text{ round trips per minute}\qquad(19)^*$$

Required speed of the carriage, S_o

$$S_o=3P_{m_o}d\text{ feet per minute}\qquad(1)^*$$

The required rate of acceleration, a_o

$$a_o=\frac{S_o}{60\Delta t_o}=\frac{S_o^2}{1800d}\text{ feet per second squared}\quad(a=v/t)\qquad(20)^*$$

The torque horsepower required to accelerate the inertia of the loaded system, $(HP)_e$

$$(\text{hp})=\frac{fs}{33{,}000};\ f=\frac{wa}{g}$$

$$(HP)_e=\frac{WS^2}{63{,}700{,}000\Delta t}\text{ torque horsepower}\qquad(3)$$

$$(HP)_{e_o}=\frac{WS_o^2}{63{,}700{,}000\Delta t_o}\text{ torque horsepower}\qquad(3)^*$$

$$(HP)_{e_o}=\frac{P_{m_o}{}^3d^3W}{71{,}000{,}000}\text{ torque horsepower}\qquad(7)^*$$

The rms torque horsepower (heating effect) required to maintain any cycle; $(HP)_{rms}$

$$(HP)_{rms}=\sqrt{\frac{2(HP)_e{}^2\Delta t}{T}}=\sqrt{\frac{2\Delta t}{T}}(HP)_e\qquad(21)^*$$

The rms torque horsepower (heating effect) required to maintain the basic cycle; $(HP)_{rms_o}$

$$(HP)_{rms_o}=\sqrt{\frac{2\Delta t}{3\Delta t}}\,(HP)_{e_o}=\sqrt{\frac{2}{3}}(HP)_{e_o}\qquad(4)^*$$

$$=\frac{P_{m_o}{}^3d^3W}{86{,}600{,}000}\text{ rms torque horsepower}\qquad(8)^*$$

The rms torque horsepower (heating effect) developed if the carriage is active $\alpha 1/1$ of the time, $(HP)_{rms}'$

$1/1\alpha$ = active time
$1/1\beta$ = idle time

$1/1\alpha+1/1\beta=1=1/1T$ (one way trip)

$$(HP)_{rms}'=\sqrt{\frac{(HP)_{rms}{}^2\alpha+0^2\beta}{\alpha+\beta=1}}$$

$$=\sqrt{\alpha}(HP)_{rms}\text{ (for any cycle)}\qquad(22)^*$$

$$(HP)_{rms_o}'=\sqrt{\alpha}\sqrt{\frac{2}{3}}(HP)_{e_o}\text{ rms torque horsepower}\qquad(5)^*$$

$$(HP)_{rms_o}=\sqrt{\alpha}\ \frac{P_{m_o}{}^3d^3W}{86{,}600{,}000}\text{ rms torque horsepower}\qquad(9)^*$$

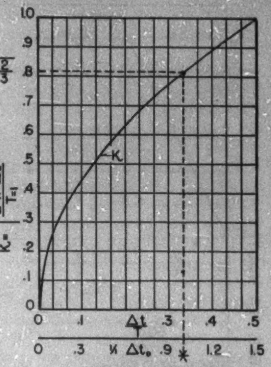

Fig. 17. Curve giving values of κ for different 1/1 values of $\Delta t_o=1.0$, which may be multiplied by the corresponding value of $(HP)_e$ to obtain $(HP)_{rms}$

The pounds pull on the rope required to accelerate the carriage, F'

$$f=\frac{(\text{hp})\,33{,}000}{s}\text{ pounds}$$

$$F'=\frac{(HP)_{rope}\,33{,}000}{S_o}=\frac{P_{m_o}{}^3d^3W'33{,}000}{3P_{m_o}d71{,}000{,}000}$$

$$=\frac{P_{m_o}{}^2dW'}{6{,}450}\text{ pounds}\qquad(6)^*$$

The fictitious air-gap rope pull required to accelerate the carriage, F

$$F=\frac{P_{m_o}{}^2dW}{6{,}450}\text{ pounds}\qquad(10)^*$$

Explanation of $\kappa=(2\Delta t/T)^{1/2}$ (Refer to Fig. 17)

The term $(2\Delta t/T)^{1/2}$ in equation 21 is the amount κ by which $(HP)_e$ may be multiplied to obtain $(HP)_{rms}$ for any paired values of Δt and T on either side of the optimum mode. The values of κ were determined from 1/1 values of $\Delta t/T$ and Δt_o, and the results given by the curve of Fig. 17. The limits of accelerating time over which $1/1\Delta t_o$ and $\Delta t/T$ can apply are given by the abscissa. For a given problem, if S_o is determined from equation 1, followed by Δt_o from equation 2, $(HP)_{e_o}$ for the optimum mode is then directly available from general equation 3. Other values of $(HP)_e$ on either side of Δt_o may then be calculated by equation 3. Corresponding values for $(HP)_{rms}$ may then be obtained by multiplying $(HP)_e$ by κ. Corresponding values for $(HP)_{rms}'$ are next obtained by multiplying $(HP)_{rms}$ by $\alpha^{1/2}$.

Development of $S=60d/(T-\Delta t)$ (Refer to Figs. 14 and 15)

A specific rate of production P_m requires a one-way trip be made in definite time T. This condition can be met by different paired values of S and Δt, including the optimum values S_o and Δt_o

$$d=\frac{v\Delta t}{2}+v\Delta t_r+\frac{v\Delta t}{2} \quad (\Delta t_r=T-2\Delta t) \qquad (23)$$

$$d=v\Delta t+v\Delta t_r \quad (v=a\Delta t) \qquad (24)$$

$$d=a\Delta t^2+a\Delta t \quad (T-2\Delta t)$$

$$v=\frac{d}{T-\Delta t} \quad (v=S/60)$$

$$S=\frac{60d}{T-\Delta t} \qquad (25)$$

$$S_o=\frac{60d}{3\Delta t_o-\Delta t_o}=\frac{30d}{\Delta t_o} \qquad (26)^*$$

Development of P_m (Mechanical) $=\frac{1{,}800aS}{S^2+3{,}600da}$ (Refer to Fig. 16) (11)

$$P_m\,(\text{mechanical})=60/2T=\frac{60}{2(\Delta t+\Delta t_r+\Delta t)}$$

$$P_m\,(\text{mechanical})=\frac{60}{2(2\Delta t+\Delta t_r)} \qquad (27)$$

$$d_r=d-2\Delta s \quad (\Delta s=v\Delta t/2)$$

$$v\Delta t_r=d-v\Delta t$$

$$\Delta t_r=\frac{d-v\Delta t}{v} \quad (\Delta t=v/a)$$

$$\Delta t_r=\frac{da-v^2}{av}$$

$$P_m\,(\text{mechanical})=\frac{30av}{v^2+da} \quad (v=S/60)$$

$$P_m\,(\text{mechanical})=\frac{1{,}800aS}{S^2+3{,}600da}$$

round trips per minute (11)

Development of P_m (Thermal) $=\frac{900a}{1/1i^2S}$ (Refer to Fig. 16) (12)

Time for 1-way trip $T=2\Delta t+\Delta t_r$

Time for round trip $=2(2\Delta t+\Delta t_r)$

1/1 heating effect of continuous cycle

$$=\sqrt{\frac{2(1/1i^2\Delta t+0^2\Delta t_r+1/1i^2\Delta t)}{2(2\Delta t+\Delta t_r)}} \qquad (28)$$

To avoid overheating equation 28 must be equal to 1.

$$\sqrt{\frac{2(2\,1/1i^2\Delta t)}{2(2\Delta t+\Delta t_r)}}=1$$

$$2(2\,1/1i^2\Delta t)=2(2\Delta t+\Delta t_r)$$

Number of round trips per second

$$=\frac{1}{2(2\Delta t+\Delta t_r)}$$

$$P_m\,(\text{thermal})=\frac{60}{2(2\Delta t+\Delta t_r)}=\frac{60}{4\,1/1i^2\Delta t} \qquad (29)$$

$$\Delta t=\frac{v}{a};\quad v=\frac{S}{60}$$

$$P_m\,(\text{thermal})=\frac{900a}{1/1i^2S} \qquad (12)$$

Note that $1/1i$ and a must be companion quantities. That is, $1/1i$ must produce acceleration a.

Development of S' $=60\sqrt{da/(2\,1/1\,i^2-1)}$ (13)

The particular speed point S' at which P_m (mechanical) equals P_m (thermal) establishes the rate of maximum continuous production capability for the particular assumed overloading value $1/1i$. S' is found by equating P_m (mechanical) $=P_m$ (thermal)

$$\frac{1{,}800aS}{S^2+3{,}600da}=\frac{900a}{1/1i^2S} \qquad (30)^*$$

$$S'=60\sqrt{\frac{da}{2\,1/1i^2-1}}$$

Development of $S_m=\sqrt{2}S_o\,(a=a_o)$ (See Text)

For an accelerating rate corresponding to S_o, the maximum speed the carriage can attain and not overrun the midpoint of travel is S_m.

$$\frac{d}{4}=\frac{a_o\Delta t_o^2}{2}$$

$$\frac{d}{2}=\frac{a_o\Delta t_m^2}{2}$$

$$\Delta t_m=\sqrt{2}\Delta t_o$$

$$v_m=a\Delta t_m=\sqrt{2}a\Delta t_o$$

$$v_o=a\Delta t_o$$

$$v_m=\sqrt{2}v_o$$

$$S_m=\sqrt{2}S_o \qquad (31)^*$$

Development of P (Maximum Mechanical) $=3/4\sqrt{2}P_{m_o}=1.06P_{m_o}$ (See Text)

Time for a round trip at maximum speed $=4\Delta t_m$

$$P\,(\text{maximum mechanical})=\frac{60}{4\Delta t_m}$$

$$\frac{d}{2}=\frac{v_m\Delta t_m}{2}$$

$$v_m=\sqrt{2}v_o$$

$$v_o=S_o/60$$

$$\Delta t_m=\frac{60d}{\sqrt{2}S_o}$$

$$P_{m_o}=\frac{S_o}{3d} \qquad (1)^*$$

P (maximum mechanical)

$$=\frac{3}{4}\sqrt{2}\frac{S_o}{3d}=\frac{3}{4}\sqrt{2}\,P_{m_o}=1.06P_{m_o} \qquad (32)^*$$

References

1. HANDLING LOGS BY ELECTRIC MOTOCYLINDER, H. A. Rose. *AIEE Transactions*, vol. 70, pt. II, 1951, pp. 1613–20.

2. AMPLIDYNE-CONTROLLED LOG CARRIAGE DRIVE, W. D. Vincent. *AIEE Transactions*, vol. 69, pt. II, 1950, pp. 1124–29.

3. MAGNETIC AMPLIFIER AND HEAVY-INERTIA CYCLIC LOADS, C. H. Storey, Jr. *Westinghouse Engineer*, East Pittsburgh, Pa., vol. 12, no. 3, May 1952.

4. HOW MAGNETIC AMPLIFIERS OPERATE, G. H. Stearley. *Product Engineering*, New York, N. Y., Jan. 1951.

5. APPLICATION OF MAGNETIC AMPLIFIERS, F. N. McClure. *Electrical Engineering*, vol. 69, June 1950, pp. 538–43.

6. SELF-SATURATION IN MAGNETIC AMPLIFIERS, W. J. Dornhoefer. *AIEE Transactions*, vol. 68, pt. II, 1949, pp. 835–50.

◆

Discussion

W. D. Vincent (General Electric Company, Seattle, Wash.): Electric log-carriage drives have now become firmly established in the lumber industry. Over 100 of the d-c, current-forcing type of high-speed drives have been installed within the past few years in various manufacturing plants throughout the world. This is evidence of the acceptance of these drives by their users. Mr. Rose's paper attests to his extensive knowledge and experience in this field.

Mr. Rose presents a basic duty cycle of carriage traverse which assumes that optimum results will be obtained with the traverse time apportioned such that one-third is used for acceleration, one-third for full speed travel, and one-third for deceleration. The principal equations presented in his paper were derived, based on the characteristics of this basic cycle.

The writer questions that this cycle will actually result in optimum performance as stated. It is easily proved that the basic duty cycle results in the minimum horsepower for moving a given mass a given distance in a given time. However, in a practical log-carriage application the distance traveled by the given weight is not a given constant, as the motor equivalent weight travels a distance depending on gear ratio or drum diameter chosen. Thus for a given set of practical conditions the basic duty cycle will probably not produce the optimum performance.

In moving a given weight a given distance with a given accelerating horsepower, it can be proved that an optimum, maximum velocity exists which will result in minimum traverse time. This optimum velocity (for the carriage in this application) may be obtained by selecting the proper gear ratio between the motor and the cable drum with the geared drive or by selecting the proper cable drum diameter with the gearless drive. Several trial calculations showed that the optimum cycle is actually a variable depending upon the accelerating horsepower, the carriage weight, and the traverse distance. The accelerating time actually amounted to between 41 and 49 per cent of the total traverse time in the examples tried.

The use of magnetic amplifiers and a 2-field exciter as presented in this paper should result in a very acceptable type of carriage drive. This type of amplifier has been used successfully for many other applications in industry. In general we have had better results using the amplidyne amplifier for applications involving a reversing duty cycle such as that required for a log-carriage drive.

D. S. Smith (British Columbia Research Council, Vancouver, B. C., Canada): Mr. Rose is to be complimented on his contribution to the theoretical study of log-carriage drives but I am a little apprehensive of some of his assumptions. Our own studies, which include speed-time measurements on carriages, suggest that it may be difficult to reconcile theory and practice. In this connection I would like to ask three questions. First, our speed-time records show considerable rounding off of curves between the acceleration and constant speed portions. Have you observed this and do you not feel that it affects your theory appreciably? Second, how do you arrive at values of α for a mill and have you found that the values obtained with actual installations agree reasonably well with estimated values? Third, what information have you from tests on the amount of regenerated energy to be expected with your drives?

H. A. Rose: The author appreciates the points of constructive criticism raised by Mr. Vincent and Mr. Smith.

Mr. Vincent is correct in emphasizing that the equivalent weight of the propulsion motor and the drum diameter have very marked influence in the calculations of drive performance. As pointed out under "Discussion of Basic Equations," it is essential to proper application of the theory of the basic duty cycle that W be the total weight of the entire moving system in equivalent pounds on the carriage. This should include the propulsion motor, speed reducer, motor coupling, cable, cable sheaves, and the rotational inertia of the carriage wheels. The minimum drum diameter should be at least 30 times the cable diameter. The diameter is also set by the permissible maximum revolutions per minute of the propulsion motor, which speed will correspond to about $\sqrt{2}$ times the basic carriage speed S_0. Since the motor's inertia contributes to the total weight propelled as the square of the gear ratio, a specific application may make it desirable to use a lower gear ratio and larger drum diameter than would be set by the maximum permissible motor speed, $\approx\sqrt{2}\ S_0$. Equation 15 takes this consideration into account by the value assigned $1/1\ s$. By definition $(HP)_e$ contains the portion of inertia horsepower required to propel the motor at the assigned value of $1/1\ s$. In some applications, it will be found that 25 to 50 per cent of the total inertia horsepower is required to propel the propulsion motor and its associated cable drum and gear unit. This percentage can readily be determined from equations 6 and 10 for the conditions of the basic cycle.

Mr. Smith raises some important points on which the lumber industry needs much more information than is presently available. It is hoped that the rapidly increasing use of electric carriage drives will afford users the opportunity to determine and report their findings.

The rounding-off of the speed-time records between acceleration and constant speed running makes it necessary in practice to compensate for the loss in production P_m by providing for slightly increased rates of acceleration, and when permissible by slightly higher sawing and return speeds.

The active time value α can be arrived at with sufficient accuracy by observation of operation of the existing drive, or by comparison with similar drives, with such corrections made as may be considered advisable. The range of α for different applications is considerable. As a general rule, it is unsafe in sawmill practice to assign α values of less than 80 per cent, unless a detailed accurate study of the requirements are made. The calculation of α should not include long periods of idle time not directly associated with normal log handling and sawing operations.

Adequate test information on the percentage amount of regenerated energy was not available for the paper. Tests are contemplated to obtain factual information on this important subject. Theoretical calculations indicate that between 65 to 85 per cent of the input energy to the drive should be returned.

In conclusion, it should be emphasized that the equations of the basic duty cycle are not intended to fulfill all the detail requirements for solution of electric log-carriage applications. The author and his associates have found that they constitute a set of powerful tools by which most preliminary drive calculations can be made. Further, they set forth in simple form the important considerations of a complex problem which could otherwise not be readily appreciated.

The Spreading and Interface Resistances of Electric Contacts

CLARENCE W. LITTLE, JR.
ASSOCIATE MEMBER AIEE

WILLIAM B. KOUWENHOVEN
FELLOW AIEE

IN ALMOST every electric circuit there are one or more places where current passes from one continuous metal body to another across the interface separating the two. The presence of the interface introduces an additional resistance into the circuit, and this additional resistance has for many years been called contact resistance. For over a century the contact resistance was thought to arise entirely from the potential drop through which charge must pass in going across the interface from one body to the other, and this was considered to be the only resistance of a contact. Today, it is known that the deviation from a uniform current field caused by the constriction of the current to a few small conducting areas at the interface also contributes to the contact resistance. A recent paper[1] by one of the authors describes some of the more important effects of this latter phenomenon.

Aim of Investigation

In resistance welding, contact resistance is one of the major factors determining the amount and location of heat energy delivered to the weld. Existing techniques allow more accurate control of the magnitude and duration of the current supplied to the weld than of the magnitude and location of the contact resistance at the weld. Even though much excellent work on contact resistance has been done, there is still a gap between the formulas of theory and the control procedures in practice. In the hope of narrowing this gap, the authors set out to determine whether the contact resistance between the butt ends of right circular solid cylinders could be qualitatively and quantitatively predicted when all known, controllable factors affecting the resistance were taken into account and controlled. The results of the investigation are intended to promote a better understanding of the factors which determine the initial magnitude of the contact resistance at electrode-workpiece and workpiece-workpiece interfaces.

Paper 53-353, recommended by the AIEE Electric Welding Committee and approved by the AIEE Committee on Technical Operations for presentation at the AIEE Pacific General Meeting, Vancouver, B. C., Canada, September 1–4, 1953. Manuscript submitted October 20, 1952; made available for printing July 2, 1953.

CLARENCE W. LITTLE, JR., was with The Johns Hopkins University, School of Engineering, Baltimore, Md., when this paper was written, and is now with the Research Division, Allis-Chalmers Manufacturing Company, Milwaukee, Wis. WILLIAM B. KOUWENHOVEN is with The Johns Hopkins University, School of Engineering, Baltimore, Md.

The authors would like to express their appreciation to the Office of Naval Research for supplying funds for investigation, to the Resistance Welding Committee of the Welding Research Council for their suggestions and help, and to Dr. William B. Sackett for his helpful comments on the work.

Investigation and Results

The investigation was limited to the d-c contact resistance of single-metal contacts made between the butt ends of 1/2-inch diameter, solid, right circular cylinders under static mechanical axial loads. Two pure metals, silver and aluminum, and three alloys, a bronze, a brass and a stainless steel, were used as contact materials to provide desired variations of hardness, volume electric resistivity, and surface film properties. All tests were made in air at ambient temperatures and the contacts were arranged to provide minimum or zero temperature gradients in the contact bodies.

Using the theory outlined in the following, and the experimental procedures outlined later, results were obtained which indicated only a qualitative fit to theory. The quantitative discrepancies, however, were fairly consistent for a given metal. Possible causes of this quantitative discrepancy are given in the discussion of results.

Theory

GENERAL

The total resistance between two points in a circuit is actually a measure of the energy lost as heat in transporting electric charge from one point to the other. In d-c circuits the energy is consumed in maintaining the stationary current field in the conducting media, according to the existing boundary conditions, and in maintaining the current flow through potential barriers which may exist at interface surfaces if a contact is included between the points. A contact, then, may introduce resistance into the circuit in three known ways: First, by introducing new boundary conditions for current flow in the conducting bodies in contact; second, by introducing surface potential barriers through which the current must flow in leaving or entering a conductor; and third, by introducing material (sometimes semiconducting or insulating) through which current must flow in the interface region between the conducting bodies in contact. The resistance arising from the first is called the spreading resistance and that from the second and third the interface resistance.

The current flow lines in a symmetrical contact, where the actual area of contact is symmetrically located in the interface, are sketched in Fig. 1(A). The interface resistance represents the electric energy needed to transport charge from the metal body of one contact to that of the other across the interface, while the spreading resistance represents the additional resistance in the metal contact bodies themselves because of the constriction of the current flow lines through the conducting area. The actual flow lines are solid, while the normal path of the flow lines, in the case where the bodies are in complete metallic contact across the entire interface area, is shown in dotted lines. The difference between the actual body resistance resulting from the solid line field and the body resistance resulting from the dotted line field is the spreading resistance part of contact resistance.

INTERFACE RESISTANCE

The actual resistance of a film material is present only when a thick (30 Ångström units or greater), continuous film remains in the interface after the contact is made. Most contacts have either sufficient contact voltage or mechanical load to rupture a thick film, and the current flows through fissures or bridges, by-passing the film material itself. This does not mean that the effect of thick films always disappears when they are ruptured, because the delimitation of current to small parts of the interface area will increase the resistance introduced by the first and second effects. The portion of the interface resistance represented by the third effect—the resistance of a thick intervening film—is not considered further here because, in the range studied, contact loads ruptured such films on the metals used.

Unless the contact surfaces are carefully cleaned and then degassed and mated in a vacuum, there is still a thin film (less than 30 Ångström units) of adsorbed gas or a monomolecular layer of oil separating the metal surfaces of the contact bodies, even if a thick film is absent. This thin film is maintained under large mechanical loads. If the film is not present, the metal atoms of one of the contact bodies can approach those of the other to within normal atomic spacings, and the contact is welded shut. It is difficult, then, to achieve perfect metallic contact in an ordinary contact interface, and is even undesirable to eliminate all films in most electric contacts because of the welding or sticking which would result. For the majority of contacts, then, the current must pass through at least a thin film at the interface and so actually leave and re-enter a metal surface. One of the more satisfactory theories explaining the conduction of current through thin films is adequately described by Holm.[3] The two major independent variables that affect this part of the interface resistance are the total film thickness or separation between the contact bodies, t, and the work function, ϕ_e, for the emission of electrons from the metal or film. The unit-area resistance of thin films, according to the Holm-Kirschstein equation, is

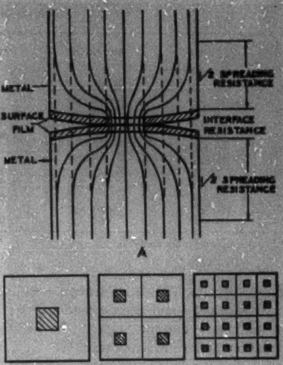

Fig. 1. Current flow lines

A. Symmetrical contact interface
B. Subdividing contact area

$$\gamma=\left(\frac{10^{-22}}{1.29}\,\frac{A^2}{1+AB}\right)\epsilon^{AB} \tag{1}$$

where

$$A=(7.32\times10^{-5})\left(1-\frac{7.2}{t\phi_e}\right)$$

$$B=(1.265\times10^{-6})\left(\phi_e-\frac{10}{t}\right)^{1/2}$$

In equation 1 γ is in ohm-inches^2 when ϕ_e is in electron volts and t in Ångström units (Å). Assuming, then, only thin films, the interface resistance may be expressed by

$$R_t=\frac{\gamma}{S_t} \tag{2}$$

where S_t = the conducting area at the contact interface. This term represents the energy expended by the current in crossing the interface from one contact body to the other. An interesting feature is that, both theoretically and experimentally, it is virtually independent of temperature and the material of the film itself.

SPREADING RESISTANCE

The other term that contributes to the total resistance introduced into a circuit by a contact is that caused by the spreading resistance mentioned. There are rigorous equations defining the relation-

Table I. Analyses of Specimen Materials

	Silver	Aluminum	Bronze	Brass	Stainless Steel
Al	0.01*	99.90 as remainder			C 0.11
Cu	0.05*	0.02 sp	89.50	61.48	Si 0.89
Fe	0.01*	0.02 sp	0.02 sp	0.05 sp	Ni 10.16
Pb	None*		1.96	3.00	Cr 17.29
Ag	99.89 as remainder				Mo 0.16
					Fe remainder
Sn	None*		0.01 sp	0.02 sp	
Zn	None*		8.26	35.62	
Ni	None*		0.40 sp	0.02 sp	
Si	0.01*	0.01 sp			
Sb	0.02*	0.05 sp	0.05 sp	0.05 sp	

* From spectrographic analysis.

ship between space variation of potential, current density, and electric conductivity in stationary current fields. One such equation, derived in many texts,[3] is

$$\nabla\mathbf{J}=-(\nabla\Phi\nabla 1/\rho+1/\rho\nabla^2\Phi)=0 \qquad (3)$$

where $\mathbf{J}$ = the current density space vector, Φ the electric potential, and ρ the resistivity of the conductor. ∇ is the familiar vector differential operator $\nabla\equiv \mathbf{i}\partial/\partial_x+\mathbf{j}\partial/\partial_y+\mathbf{k}\partial/\partial_z$ in Cartesian coordinates. Equation 3 holds even if the conductor is inhomogeneous, but not if it is aeolotropic, for then $1/\rho$ becomes a tensor of the second rank. In the case of a homogeneous, isotropic conductor, equation 3 reduces to the familiar Laplace equation

$$\nabla^2\Phi=0 \qquad (4)$$

as $\nabla 1/\rho$ is zero.

To calculate the total resistance between two points in a circuit (isotropic conductor) resulting from the energy needed to maintain the stationary current field there, equation 3 or 4 could be solved for the potential difference between the points arising from a specific current. Unfortunately, the solution is quite difficult except for certain simple boundary conditions. To determine the true effect of a contact present between the points, two solutions would be used, one with the conductor assumed to be continuous through the whole contact interface, dotted flow lines in Fig. 1(A), and the other with additional boundary conditions resulting from the actual current constrictions at the interface, solid flow lines, Fig. 1(A). The difference of resistance obtained between these two solutions is the spreading resistance.

For solid cylindrical conductors of circular cross-section, Kouwenhoven and Sackett[1] found the spreading resistance, which was due to a circular constriction, concentric with the cylinder axis

$$R_s=\rho\left(\frac{1}{d_c}-\frac{1.409}{d_a}+0.296\frac{d_c^2}{d_a^3}+\right.$$
$$\left.0.0525\frac{d_c^4}{d_a^5}+\ldots\right) \qquad (5)$$

where ρ is the electric resistivity, d_c the diameter of the conducting circular constriction at the interface, and d_a is the apparent interface diameter (cylinder diameter). If a single constriction is divided into n equal-area constrictions of the same shape, symmetrically and uniformly located over the interface area, the spreading resistance is reduced by the factor of $n^{-1/2}$. The effect, qualitatively, of such a subdivision is to reduce the maximum displacement perpendicular to its normal direction of flow that a current flow line must experience to find a continuous path through the interface. Fig. 1(B) shows clearly that if the number of contact areas symmetrically placed is increased by a factor of 4, while maintaining the same total contact area, the maximum distance that a current flow line must travel is cut in half. The total contact area (shaded portion) is the same for the three cases shown but is divided into four parts in the middle specimen and 16 parts in the right specimen.

CONTACT AREA

One of the important factors in determining the magnitude of both the spreading resistance R_s and the interface resistance R_t is the actual conducting area of the contact at the interface. This conducting area S_c may be different from either the load-bearing contact area S_b, or the apparent contact area S_a. The apparent contact area may be defined as the area of a contact surface. The load-bearing area requires further explanation.

Actual contact between two solid bodies can occur only when the atoms of one body approach those of the other to within a few Å. Since surface roughness, even on flat, smooth surfaces, is usually greater than several tens of Ångström units, there are relatively large hills and valleys initially in each of the mating contact surfaces. The actual area in contact supporting a particular mechanical load is determined largely by the maximum stress that the contact materials will support without irreversibly deforming. This maximum stress H determines the load-bearing area of the contact, and for a given load F Holm[4] gives the relations

$$S_b=\frac{F}{H} \qquad (6)$$

where the contact area is plastically produced, and

$$S_b=\frac{2F}{H} \qquad (7)$$

when the contact area is produced by light loads on flat surface contacts.

In this study of contacts, where no thick films existed at the interface, the conducting and load-bearing contact areas were assumed to be equal, and neither depended directly on the apparent area. This is important, for it shows that contact resistance, for a given contact material and a given contact load, is relatively independent of the apparent contact area. In fact, the apparent area enters the contact resistance only through the second and succeeding terms of equation 5, which are negligible when the actual contact area is less than 1/10 the apparent area.

CONTACT RESISTANCE

The contact resistance R_c, made up of the sum of R_t and R_s, is the difference between the total resistance R_T between two points spanning the contact and the body resistance R_b that the conductor would exhibit between the points if it were continuous through the entire interface area. This may be expressed as

$$R_c=R_T-R_b=R_s+R_t \qquad (8)$$

Equations 2 and 5, coupled with the effect of area subdivisions, may be combined to give an expression for the d-c contact resistance of a contact made under static mechanical load between thick-film-free butt ends of solid right circular cylinders. It is

$$R_c=\frac{\rho}{n^{1/2}}\left(\frac{1}{d_c}-\frac{1.409}{d_a}+\ldots\right)+\frac{4\gamma}{\pi d_c^2} \qquad (9)$$

This is valid only under the conditions stated, that is,

1. The resistivity ρ is constant throughout the conductor body.

Table II. Specific Resistance and Hardness for Specimen Materials

Material	Specific Resistance (at 24 Degrees Centigrade), Ohm-Inches	Hardness, Pounds per Square Inch
Silver	0.685×10^{-6}	33,000
Aluminum	1.08×10^{-6}	15,000
Bronze	1.70×10^{-6}	90,000
Brass	2.80×10^{-6}	128,000
Stainless steel	28.5×10^{-6}	244,000

2. Only thin films, thickness <30 Å, exist at the interface.

3. The n subdivisions of conducting contact area are symmetrically and uniformly distributed over the interface area.

4. d_c and d_a are diameters of true circles.

If, in addition, equation 6 is accepted and combined with equation 9, the expression for contact resistance may be expanded to include the effects of mechanical load F

$$R_c = \frac{\rho}{n^{1/2}}\left(\frac{(\pi H)^{1/2}}{(4F)} - \frac{1.409}{d_a} + \ldots\right) + \frac{H\gamma}{F} \quad (10)$$

This is subject to the two additional requirements that:

5. The load-bearing area is plastically produced.

6. The load-bearing area and conducting contact area are equal.

Equation 10 is a valuable aid in understanding the factors affecting the contact resistance at interfaces meeting the conditions stated. The experimental work, described in the following, was designed to test equation 10.

Experimental Procedure

GENERAL

The major variables in equation 10 are:

1. Contact material resistivity ρ.
2. Number of the conducting contact area equal subdivisions n.
3. Contact material hardness, H.
4. Contact mechanical load F.
5. Apparent contact area diameter d_a.
6. Unit-area film resistance γ which in turn depends on the material electron work function Φ_e, and the spacing between interface surfaces t.

Indirectly, temperature enters equation 10, for a temperature gradient at the interface would change the nature of the field equation solution upon which the spreading resistance terms are based, and thus change the contact resistance. Also, the temperature of the metal affects the magnitude of the resistivity and the stress limit H. Time has some effect if the metals are such that they age-harden or age-anneal to change H.

The various variables entering equation 10 were generally controlled and varied in the following ways. Selection of different contact materials were made to provide variations in ρ, H, and ϕ_e. Use of an adsorbed air film on clean surfaces or use of a monomolecular oil film gave rough control of t. The number of subdivisions n were controlled by surface preparation, and the apparent diameter d_a was fixed by the cylinder diameter. The load F was applied and controlled by a dead-weight loading arrangement. Temperature gradients were reduced to a minimum by a series contact arrangement, and measurements were made over sufficient periods of time to encompass the effects of aging. A more detailed account of these various techniques follows.

Fig. 2. Specimen unit

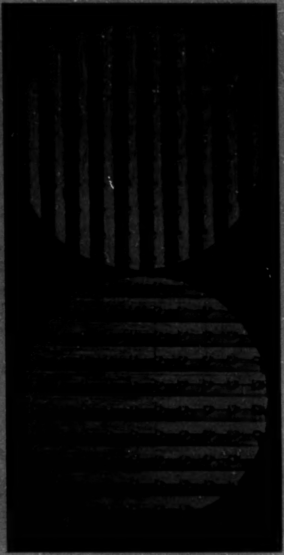

Fig. 3. Contact pattern

SPECIMENS

A specimen set consisted of six identical units, each unit being a 2-inch-long, solid, right circular cylinder of 1/2-inch diameter. To provide reasonable uniformity, the units for each material were cut from the same rod, and sample sets were prepared of silver, aluminum, bronze, brass, and stainless steel. Analyses of the specimen materials are given in Table I, and the specific resistance and hardness measured for the specimen materials are given in Table II.

For reference and correlation with other contact studies, one specimen set of each material was prepared with flat-milled butt ends on each unit. To provide control of n in other sets, equidistant parallel 90-degree grooves were milled in the unit cylinder end surfaces. Six units were assembled into a specimen set by tandem alignment in a V block, contact being made between the butt ends of the units. This provided five equidistant contacts for measurement. The V block was removed after insertion of the sample set in the loading machine. The ridges of adjacent units in the grooved sets were at right angles so that contact was initiated at the discreet ridge crossover points, and the contact area was enlarged at increasing loads by plastic flow at these points. The number of ridges employed provided values for n of 21, 80, 320, and 1,300, by count. Fig. 2 shows a specimen unit and Fig. 3 a resulting subdivision pattern. Each spot is a small contact area subdivision. The holes in Fig. 2, each of 0.02-inch diameter and spaced 0.4 inch apart, were drilled through the cylinder diametrically. They served a dual purpose, namely, making possible the insertion of thermocouples, and serving as points of contact for the resistance measuring leads.

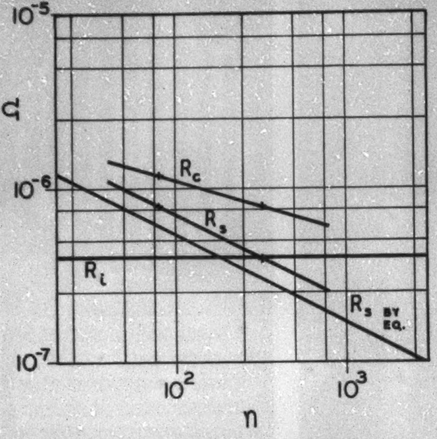

Fig. 4 (above). Contact resistance versus n for silver at 230 pounds

Fig. 5 (right). Contact resistance versus n for aluminum at 230 pounds

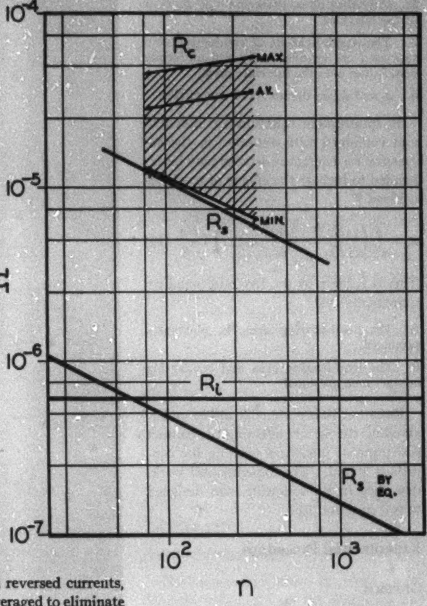

APPARATUS AND TECHNIQUES

Apparatus

The loading machine was of the dead-weight type. Force was applied axially to each specimen set through steel loading rods mounted on spherical joints at the upper and lower ends of the machine. The lever arm ratio on the loading member allowed addition of load increments without dynamic overshoot. To provide uniform subareas at each contact spot, it was necessary that the loading be almost ideally axial. A system of eight strain gauges monitored the strain balance around the periphery of the loading members. Comparison of computed force values with the reading of a calibrated strain gauge cell showed no detectable error from friction or binding.

The current source for the sample set was a 24-volt, 600-ampere rated d-c generator. The ripple factor was much less than 1 per cent, and a cross check using a battery current source gave identical results. A potentiometer was used to measure the voltage drops in the sample set. Its reference standard cell was cross-calibrated against three other standard cells, which in turn had been recently calibrated by the National Bureau of Standards. A 190-microhm shunt, rated at 400 amperes, was used to determine the current in the sample set. The potentiometer was also used with 22 thermocouples to measure the temperature along each sample set. All resistance measurements were made with reversed currents, and the results were averaged to eliminate errors.

Measurements

A specimen set with a given value of *n* contact subareas, with the thermocouple and voltage leads in place, was assembled in a *V*-block, placed between the loading members of the testing machine, and a load of 10 pounds was applied. The no-load readings (10 pounds) of the strain gauges were noted, then an axial load of 230 pounds was applied to the specimen set. The strain gauge readings were checked for uniformity of loading, then a direct current of 10 amperes was sent through the set. When temperature equilibrium was reached, the voltage drop across each of the five contacts and the voltage drop across the body of each of the six units in the set were measured.

The initial run at 10 amperes was followed by runs at 40, 80, and 120 amperes. After these runs had been completed, the 10-ampere run was repeated. In addition, a number of resistance values were measured when transient currents were used of the order of 2,000 amperes and with a duration of 1.5 milliseconds.

The specimen sets with 21 contact points were tested at 230-pound load at the current values stated in the foregoing; they were then removed from the testing machine.

The sets with 80 contact points were first tested at 230 pounds and the current values. Then the load was increased to 920 pounds, and the current runs repeated. They were then removed from the testing machine.

The specimen sets with 320 and 1,300 contact points, and the set with flat-milled end surfaces were tested first at 230-pound load, then at 920 pounds, and lastly at 1,575 pounds, the current runs being made at each load. When these were completed, the sets were removed from the machine.

After each set had been removed from the testing machine, the diameter of the indentations in the ridges was measured with the use of a Jones and Lamson bench comparator at a magnification of 150. The total contact area S_c in square inches was calculated from these measurements. The diameters were quite uniform in size on a uniformly loaded surface, only 6 per cent to 8 per cent of the total number, deviating from the average value by as much as 5 per cent. Sets mated without current had the same contact surface appearance as those through which 200 amperes was passed continually, and there was no welding or sticking of contacts when separated. This indicated the presence of thin films at all loads.

The contact resistance of each contact was determined by subtracting the corresponding body resistance from the resistance measured for a span that included the contact. The data used in the computation of contact resistance R_c were based on the measurements taken at 10 amperes after the current cycle had been completed. Under these conditions the temperature variation between individual contacts was negligible.

Computations

To determine the measured contact resistance of each contact, it was necessary to subtract from the total resistance, measured between probes, the resistance of the contact bodies themselves. Normally, this body resistance would be the resistance of a length of the solid cylinder equal to the separation between the measuring probes. The presence of the surface ridges introduced an additional body resistance which varied with the ridge height and indentation depth of the contact spots. This correction term for the body resistance was computed, and in almost all cases amounted to less than 10 per cent of the nominal cylinder body resistance. Tests measuring the same contact resistance with different probe spans, and tests using 60- and 45-degree angles for the ridges instead of the 90 degrees used in the majority of the measurements, showed that the actual measured contact resistance was accurate to slightly better than ±5 per cent. Even though the technique was one of difference measurement, the two measured values and the difference were all of the same order of magnitude, so that accuracy approaching the intrinsic experimental accuracy was not surprising.

For comparison with equation 10, it was necessary to separate the measured contact resistance into spreading resistance, given by the first term of the equation, and interface resistance, given by the second term. The only variables common to both terms are H and F, which determine the actual contact area, and they enter the terms in different powers. However, n, which was accurately established by count, affects only the spreading resistance, and R_c may be expressed as

$$R_c=\frac{C_1}{n^{1/2}}+C_2 \tag{11}$$

when all variables but n are fixed. The method chosen for determining the spreading resistance and interface resistance was to solve simultaneous equations for C_1 and C_2 using the values of R_c measured for different n values with other variables fixed. The experimentally determined spreading resistance was taken to be $C_1/n^{1/2}$ and the interface resistance to be C_2. This method was shown to be a true division of R_c into R_s and R_i by plotting $C_1/n^{1/2}$ against ρ, H, and F on log-log paper and plotting C_2 against H and F on log-log paper. They were found to vary with these variables to the proper power. The R_i term, C_2, was also solved for γ, and γ was solved for t, the film thickness. These thicknesses were consistent, lying between 4.9 Å and 5.2 Å for all metals but aluminum, and for all contacts.

Results

For the smallest probe spacing (0.4 inch) there was a maximum possible total error of ±5 per cent in the resistance determinations. In general, the error of measurement was much smaller. In 420 measurements of body resistance the variation between readings on the same material was less than ±2 per cent, and the average resistivity values computed from these measurements were within 1

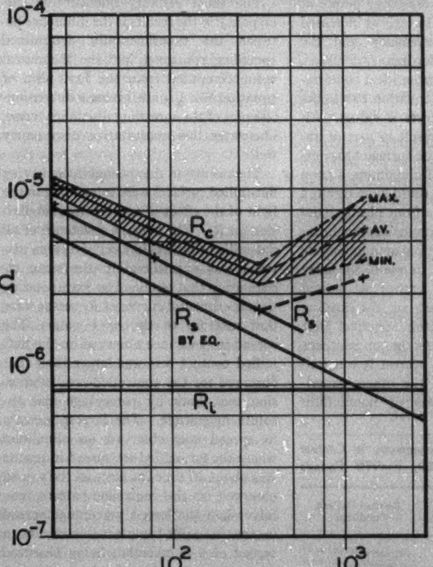

Fig. 6. Contact resistance versus n for bronze at 230 pounds

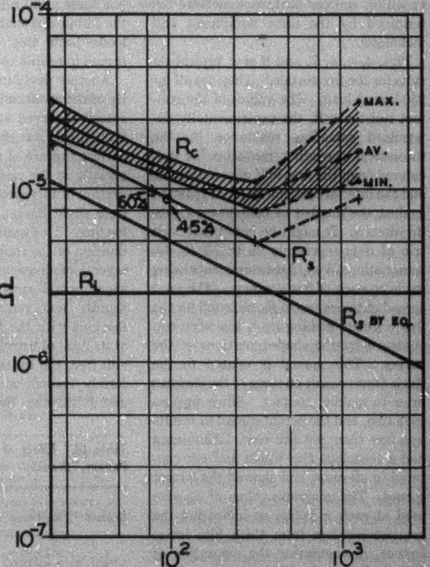

Fig. 7. Contact resistance versus n for brass at 230 pounds

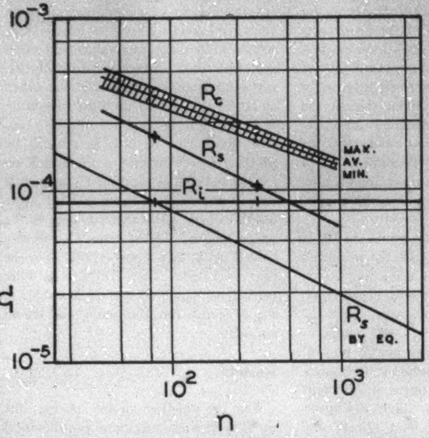

Fig. 8. Contact resistance versus n for stainless steel at 230 pounds

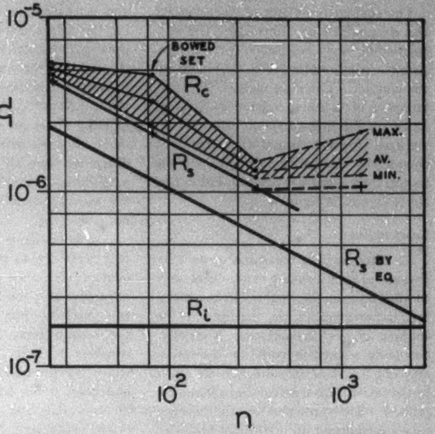

Fig. 9. Contact resistance versus n for bronze at 920 pounds

per cent of the material resistivities determined by more accurate means. As the body resistance and contact resistance measured values were of the same order of magnitude, it was assumed that the contact resistance values were also accurate to within ±5 per cent, as they were determined by the same equipment and technique.

Figs. 4, 5, 6, 7, and 8 give typical results for the five metals.[6] They are all for 230-pound load. The values of the contact resistance R_c the experimentally determined spreading resistance R_s, the theoretical spreading resistance as calculated from the first half of equation 10, and the interface resistance R_i, are plotted against the number of contact area subdivisions *n*. It might be noted that each trio of dots represents 25 to 75 R_c determinations, 5 to 15 measurements being made on each of five contacts. The total spread of the values of R_c, as found for the five contacts making up a specimen set, is shown by the shaded portions of the curves. This spread is related to the thick films present on some of the surfaces prior to making contact. Silver had no such film, and the actual spread in results was less than ±2 per cent. Aluminum had a tenacious film which was not ruptured in all cases, and showed the largest spread. The minimum values of R_c were used at each *n* value, as indicating the greatest freedom from thick film interference, in computing the separation of R_c into R_s and R_i. This may be eristic, but was given validity by a series of cross-checks.

At $n=1{,}300$, the values of R_c are not in line with those for the other values of *n*. This was found to be the result of the lack of height uniformity in the fine ridges of the $n=1{,}300$ units. Inspection of these specimen sets showed that contact was not made at all ridge crossover points at the 230-pound load. In tests at increased loads both this discrepancy and the spread in results became less.

Another deviation from ideal conformity of the results with equation 10 was the spread observed at lower *n* values. Although this was the result in part of imperfect rupture of thick surface films, especially in the case of aluminum, a good portion of this spread could have resulted from slight deviations from ideally axial loading. This would produce nonuniform division of the conducting area among its several subdivisions. In one of the early experimental runs a bronze set bowed slightly and remained in the loading machine with the bottom spherical joint at its limit of travel. As the top joint was still free, the contact nearest it was uniformly loaded, while the others experienced varying degrees of nonuniform loading. The effects of the unequal area subdivision are shown in Table III; these results are plotted in Fig. 9 for $n=80$, and show the increased spread compared to the uniformly loaded $n=21$ and $n=320$ sets.

Table III. Effect of Asymmetry in Contact Pattern, Bronze: $n=80$, $F=920$ Pounds

Contact	R_c, Ohms	Contact Pattern Condition
1	2.2×10^{-6}	symmetrical
2	3.6×10^{-6}	asymmetrical
3	5.1×10^{-6}	maximum asymmetry
4	3.3×10^{-6}	asymmetrical
5	2.6×10^{-6}	slightly asymmetrical

The most striking quantitative discrepancy in the results is the difference between the experimentally determined spreading resistance and the theoretical value computed from the first term of equation 10. Fig. 10, giving a dimensionless plot of the spreading resistance terms, illustrates this quantitative discrepancy well.

The results on the specimen sets having flat-milled surfaces were interesting in the light of the effect of contact area subdivision on R_i. The average resistance of all flat-milled contacts in a set of a given material was approximately the same resistance as that obtained by extrapolating the experimental curves of R_c versus *n* for that material to the $n=1$ value. The spread in resistance observed on the flat-milled contact sets was larger than that observed for the controlled-area-subdivision sets, both by percentage and absolute magnitude. The largest increase in spread was observed on aluminum where the flat-milled set spread in results was about 40 times as large as the spread observed on the controlled-pattern sets. Silver had the lowest percentage spread in the flat-milled contact set results, a spread of 0.16 microhm being observed for an average value of 1.4 microhms at 230 pounds. However, since the controlled pattern sets of silver showed no

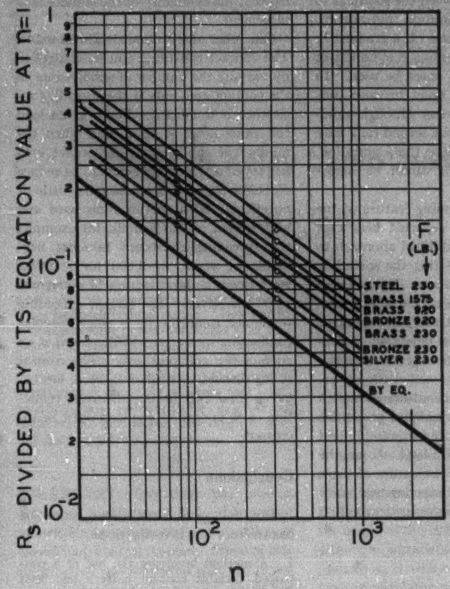

Fig. 10. Dimensionless R_s versus n for silver, bronze, brass, and stainless steel

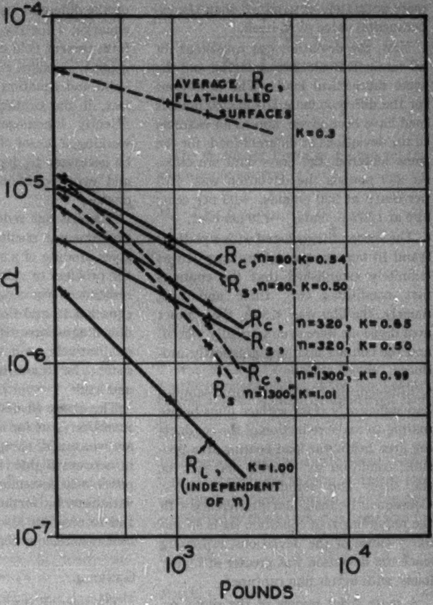

Fig. 11. Contact resistance versus load for brass

spread at all, this is still significant. For a given load and material the flat-milled set contact resistance did not exceed, as an upper limit, the extrapolated experimental spreading resistance value for a single spot contact eccentrically placed,[1] nor did it fall below, as a lower limit, the contact resistance observed for any of the controlled-pattern multispot contact sets of that material.

In addition, it is interesting to note the effect of the arrangement to reduce temperature gradients and the results of the area measurements. With the series contact arrangement providing five equidistant heat sources (at 10 amperes each contact dissipated from 0.1 to 10 milliwatts), the temperature gradient in the four central specimen units was less than 0.02 degree centigrade per inch, as observed among the 20 equidistant thermocouples monitoring the temperature along that 8-inch section. The gradient on the end units was about 0.1 degree centigrade per inch at 10 amperes because of the heat sink afforded by the steel loading members. The area measurements were surprisingly close to theory. Table IV shows some typical results.

Discussion of Results

DEVIATION OF R_s EXPERIMENTAL FROM EQUATION VALUE

Referring again to Fig. 10, it may be seen that the experimentally determined R_s for silver, bronze, brass, and stainless steel, at the 230-pound load, are higher than the values obtained from the first term of equation 10 by percentages of 30, 43, 75, and 150 respectively, based on equation 10. However, the spread in results for these metals at 230-pound load was only about ± 2 per cent, ±15 per cent, ±14 per cent, and ±10 per cent respectively. Remembering that the experimental accuracy was, at worst, ±5 per cent virtually eliminates the possibility of the discrepancy being due to faulty measurements. This leaves two possibilities; either the separation of the total experimentally determined contact resistance into spreading resistance and interface resistance was made incorrectly, or else the first term of equation 10 does not completely describe the true conditions in the actual contacts measured.

Table IV. Comparison of Calculated and Measured Areas

	Brass F=1,575 Pounds H=128,000, Pounds per Square Inch	Bronze F=920 Pounds H=90,000, Pounds per Square Inch
Area calculated from $S_b=F/H$, square inches	0.0123	0.0102
Measured area using 150-times magnification, square inches	0.0124	0.0103

As was mentioned under "Computations," the separation of R_t into R_s and R_i was tested by three other methods, all of which showed the separation to be valid. This leaves only the fit of the experimental R_s to the first term of equation 10 to consider. For convenience, this term is restated

$$R_s=\frac{\rho}{n^{1/2}}\frac{(\pi H)^{1/2}}{(4F)}-\frac{1.409}{d_a}+\dots \qquad (12)$$

The variables F, d_a, H, and n were directly measured by nonelectric means, and an additional determination of the ratio H/F was made through the load-bearing area measurements. The resistivity was determined to better than 2 per cent so that the values of all variables used in, computing R_s from equation 12 were more accurately determined than the experimental value of R_s itself.

Now, the deviation was consistent for all contacts of the same material and the same mechanical load. The deviations for the different materials at 230 pounds load have been given, and as an example of the deviations at different loads for the same material, the brass data are cited. At 230 pounds the deviation was +75 per cent; at 920 pounds, +95 per cent; and at 1,575 pounds, + 120 per cent.

The six conditions listed with equations 9 and 10 were considered in turn. It was definitely established that the contacts met conditions two, three and five; namely, the film was <30Å, the contact area divisions were symmetrically placed, and the contact area was plastically produced.

Although the brass and bronze samples had sufficiently thick surface films before mating to make reduction of the conducting area below the load-bearing area possible, condition six ($S_b = S_c$) was met for the silver and stainless-steel samples. Consequently, thick film interference with the requirement of condition six is an unlikely cause of the deviations, especially since the deviation was greater at higher loads, with better film rupture.

A more strict review of the shape requirements on d_c and d_a showed that a multiplier of $4/\pi^{1/2}$, or about 1.12, would give a more accurate expression of R_s, since the apparent area was square instead of circular in shape when subdivided into n subdivisions. This fixed increase of the equation value by 12 per cent does not account for the deviations observed.

By a process of elimination, then, not satisfying the first condition (constant value of ρ) seemed to be the major cause of the deviations. Holm[6] has shown that relatively small temperature gradients can give an appreciable increase in contact resistance. Even though the gradient in the sample set was nearly zero, there was no guarantee that the 0.02-degree-centigrade per-inch value observed over the contact bodies was maintained up to the interface boundary itself. In addition to the slight nominal increase in the value of ρ which a small temperature increase at the boundary could cause, the more serious effect is that of producing a space variation or gradient in ρ. Another possible cause of a gradient in ρ in the critical interface region of the contact bodies is the cold-working of the material there as a result of plastic flow. The seriousness of a ρ gradient may be realized by referring to equations 3 and 4. Every equation given for spreading resistance, including equation 12, is based on the difference between the solutions of equation 4 for the uniform and nonuniform current field cases. If a gradient in ρ (or $1/\rho$) exists, equation 4 is no longer valid and equation 3 must be used. In fact, if the contact body becomes sufficiently inhomogeneous through cold-working, a tensor of the second rank may be necessary to describe the ρ variation, and even equation 3 would be inadequate.

There is one redeeming feature of the experimental results reported here that gives promise of a simplified approach to the problem of calculating the spreading resistance term in contacts. Even though equation 12 and the experimental results do not agree quantitatively, they do agree qualitatively, and the deviation is consistent for quantitative given material and load.

The observed deviation increases with ρ and/or H as far as material properties are concerned, except for aluminum, and it increases slightly with load. It may be possible to determine the nature of these variations by further experimental work and to combine the necessary correction factors with equation 12.

General

The over-all results point out some interesting features in the resistance of contacts of the type studied. One of these is the relative magnitude of R_s and R_t. Since each varies with the load to different powers, R_t becomes dominant at light loads and R_s becomes dominant at high loads, and there is a unique load for each set of other conditions, at which the two are equal. If the contact pattern were completely controlled and the apparent area much larger than the actual conducting area, the contact resistance would be a function of the load F, according to

$$R_c = \frac{C_1}{F^{1/2}} + \frac{C_2}{F} \tag{13}$$

This would account for the numerous equations[7−10] giving the variation of contact resistance with load as

$$R_c = \frac{C}{F^k}$$

or

$$R_c = \frac{C_1}{F^k} + C_2 \tag{14}$$

with various values assigned to C, C_1, C_2, and with k values between one-half and one. Fig. 11 shows values of k greater than one and also less than one-half were found when the load change also altered the boundary conditions for R_s by changing n or the symmetry of the contact area placement.

One other observation should be made. The contact resistance can be controlled by varying the number of subdivisions of the contact area only if the spreading resistance is dominant. For a given load the value of R_t is fixed, and when the number of subdivisions of contact area employed are increased enough to reduce R_s below R_t, further increase has little or no effect. With the air films used and with a load of 230 pounds, for example, the spreading resistance becomes negligible at about $n = 3{,}000$ for stainless steel, brass, and bronze, and at about $n = 1{,}000$ for silver. The largest spreading resistance would be for a single circular conducting spot eccentrically placed at an edge of the apparent area. The control of R_c, through control of R_s by n, lies between these two limits. If further reduction of R_c is desired, the load must be increased.

Conclusions

The following conclusions may be drawn from this investigation:

1. A method involving the use of a controlled variable contact pattern has been developed which makes it possible to separate contact resistance into its two components, spreading resistance and interface resistance.
2. The value of the spreading resistance R_s was found to vary inversely as the square root of the number of contact points n, as predicted by theory.
3. The experimentally measured values of spreading resistance were found to be higher than those predicted by theory.
4. The spreading resistance is larger than the interface resistance for values of n of less than 1,000 at loads greater than 100 pounds. It is a major component of the contact resistance for thin-film metal contacts made in air under static loads.
5. The contact resistance can be controlled and accurately reproduced with materials having only thin surface films at the interface when under mechanical load.

References

1. Contact Resistance—The Contribution of Nonuniform Current Flow, W. B. Kouwenhoven, W. Sackett. *Electrical Engineering*, vol. 71, March 1952, pp. 264–68. (Their equation is based on a solution to the Laplace equation made by L. C. Roess of the Texas Company.)

2. Electric Contacts (book), Ragnar Holm. Gebers, Stockholm, Sweden, 1946, pp. 106–20.

3. Electromagnetic Fields (book), Ernst Weber. John Wiley and Sons, Inc., New York, N. Y., vol. I, 1950, pp. 66–71.

4. See ref. 2, pp. 71–87.

5. Contact Resistance, W. B. Kouwenhoven, C. W. Little, Jr. *Welding Journal*, New York, N. Y., vol. 31, Oct. 1952, p. 457s.

6. See ref. 2, pp. 23–41.

7. Electric Contacts, G. Windred. Macmillan and Company, Ltd., London, England, 1940, p. 38.

8. Contact Resistance, L. Binder. *Elektrotechnik und Maschinenbau*, Berlin, Germany; vol. 30, 1912, pp. 781–88.

9. Contact Resistance and Microphonic Action, F. S. Goucher, F. Gray. *Physical Review*, New York, N. Y., vol. 36, 1930, pp. 375.

10. Measurement of Contact Resistance, William B. Kouwenhoven, J. Tampico. *Welding Journal*, New York, N. Y., vol. 19, 1940, pp. 408s–413s.

◆

No Discussion

Errors in Relay Servo Systems

LOUIS F. KAZDA
MEMBER AIEE

Synopsis: This paper presents some of the errors that are present in a nonlinear second-order feedback-control system. In order to investigate some of the errors that exist in a piece-wise (See Appendix for definitions) linear control system, the phase-plane method of analysis is used. Along with a description of some of the errors that exist, equations are presented for determining these errors, and curves covering the normal operating range are included.

IN RECENT years there has been a gradual build-up of a body of technical knowledge on various aspects of nonlinear closed-loop control systems. Some of this information has indicated that errors are present in such a system, but there has been almost no definitive documentation of the errors themselves. This paper presents the results of a study of some of the errors that are present in a nonlinear second-order relay servomechanism under varying conditions of operation.

Background

In linear analysis of closed-loop control systems, it is assumed that the system errors are small so that no part of the system is saturated and, therefore, linear relationships exist among the various transfer functions. Many control systems can be approximated by a simple second-order linear system which consists of an inertia J, viscous damping f, and a control torque k that is proportional to the error. This system has been extensively treated in technical literature[1-8] during the past decade. For numerous industrial applications, a compensated proportional error control system provides satisfactory operation. However, many applications exist where it would be desirable to increase the speed of response of the system or decrease the weight of a given system that has satisfactory response. A relay control system will provide a reduction in weight for the same maximum available control torque. A relay control system containing a simple error-sensing element will normally have a dead zone. If the system sensitivity is increased, one finds that the system will oscillate around the origin of the E-$\dot{E}$ plane. This system, although unsatisfactory in many applications, is widely used at the present time in regulator applications due to its simplicity. The applications considered in this paper are concerned with high-performance servo systems in which it is essential to reduce the error and its time derivatives to zero in a minimum amount of time. In order to utilize the full capabilities of this type of control system, a more complex error-sensing computer must be employed. The details of such a computer are not presented at this time, although, for the systems considered here, construction is no great problem. There are many relay servo systems which have only a small amount of viscous damping and negligible time delays within the controller. For purposes of analysis, they can be approximated by a system containing only output inertia.

In Fig. 1 is shown a relay servo of this type which is characterized by a controller P, an inertia J, and an error detecting device N. The controller P will, in general, contain an electronic amplifier and computer, as well as the output element which supplies torque to drive the inertia load.

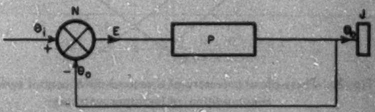

Fig. 1. Block diagram of a nonlinear feedback control system

The system of Fig. 1 is defined by the following equations

$$J\ddot{\theta}_o = T \text{ for } \dot{E}\times|\dot{E}|+\frac{2T}{J}E>0 \tag{1}$$

$$J\ddot{\theta}_o = -T \text{ for } \dot{E}\times|\dot{E}|+\frac{2T}{J}E<0 \tag{2}$$

$$E=\theta_i-\theta_o \tag{3}$$

where

J = the system inertia
T = the developed controller torque
θ_i = the angular position of the input shaft
θ_o = the angular position of the output shaft
E = the error
$\dot{E}$ = the error rate

In linear systems, the controller supplies a torque proportional to error and error-rate in a predetermined fashion. In the case considered in this paper, it is necessary for the computer to detect the boundary equation

$$\dot{E}\times|\dot{E}|+\frac{2T}{J}E=0 \tag{4}$$

which separates the positive and negative torque regions. A plot of this equation is shown in Fig. 2 by curve C_3. When the input shaft is given a step function of position or a step function of velocity, $\ddot{\theta}_i$ is zero, and the system is defined by the following equations of motion:

$$J\ddot{E} = -T \text{ for } \dot{E}\times|\dot{E}|+\frac{2T}{J}E>0 \tag{5}$$

$$J\ddot{E} = T \text{ for } \dot{E}\times|\dot{E}|+\frac{2T}{J}E<0 \tag{6}$$

where E, $\dot{E}$, and $\ddot{E}$ are the error, the error rate, and the error acceleration and T and J are as previously defined. Equations 5 and 6 have as their solution equations 7 and 8

$$-\frac{J}{2T}\dot{E}^2=E-K_0 \tag{7}$$

$$\frac{J}{2T}\dot{E}^2=E+K_0 \tag{8}$$

K_0 in the equations represents the initial error and/or error rate in the system

Paper 53-354, recommended by the AIEE Feedback Control Systems Committee and approved by the AIEE Committee on Technical Operations for presentation at the AIEE Pacific General Meeting, Vancouver, B. C., Canada, September 1–4, 1953. Manuscript submitted April 27, 1953; made available for printing July 20, 1953.

Louis F. Kazda is with the University of Michigan, Ann Arbor, Mich.

Part of this work was sponsored by the United States Air Force, under contract no. AF 33-038-21673, in conjunction with Cook Research Laboratories, Skokie, Ill.

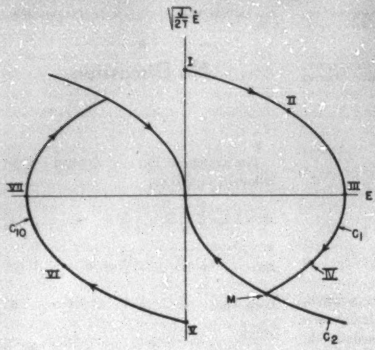

Fig. 2 (left). Phase-plane trajectory of a second-order control system for various initial conditions

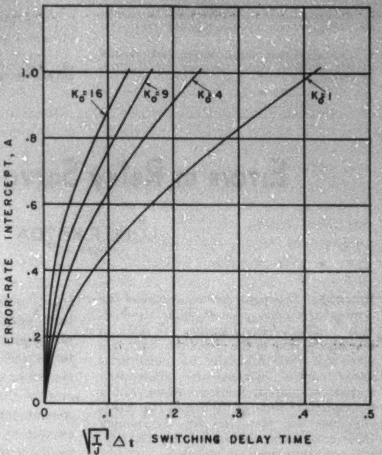

Fig. 4 (right). Error-rate intercept versus switching-time delay for various initial conditions

caused by the input shaft being subjected to a step function of position, a step function of velocity, or a combination of the two. Equations 7 and 8 are represented in the phase plane shown in Fig. 2 by curves C_1 and C_{10} respectively.

A system satisfying these equations has been shown[4] to be one that gives maximum speed of response to an input error. Given an initial positive error (represented by point III, Fig. 2), the representative point (See Appendix) follows the parabolic path until the midpoint M, by applying full accelerating torque. At point M, torque is reversed, and the representative point follows curve C_2 to the origin. However, it is possible to have other initial conditions. If given an initial error rate (represented by point I), the representative point follows the parabolic curve again to point M before torque is reversed, and then follows curve C_2 to the origin. Points II, IV, V, VI, and VII represent other possible initial conditions.

Switching Errors

If an attempt is made to construct a system that will satisfy these specifications, numerous inaccuracies have to be considered. Since physically it takes time to reverse the torque in the system, even after the computer has detected the switching curve given by equation 4, the true phase trajectory (See Appendix) is not one as shown in Fig. 2, but will take on the form shown by curve C_3 in Fig. 3. It can be seen from Fig. 3 that the error and error rate do not reduce to zero simultaneously, but an error rate exists when the error is zero, due to the delay time in switching. As time progresses, the representative point will continue to follow trajectory C_3 until it again crosses the switching curve determined by equation 4, which is located in the second quadrant. With time delay still present, reverse torque will not be applied until after the representative point crosses the switching curve. After reverse torque is applied, the representative point will follow a new trajectory similar to curve C_1, see Figs. 2 and 3. In general, as time progresses the representative point will encompass the origin in a manner that depends upon the particular delay time of the system under consideration. Since the time delays normally encountered in practice are small for the values chosen, the representative point will encompass the origin in an ever-decreasing fashion.

The equation representing the phase trajectory C_1 is defined by equation 7.

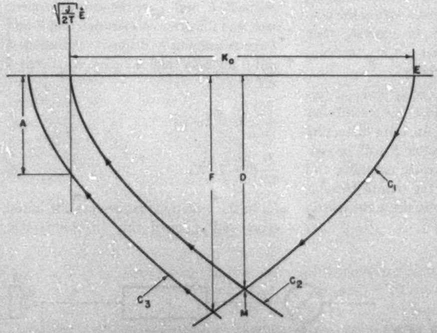

Fig. 3. Phase-plane trajectory of a second-order control system under the condition of improper switching

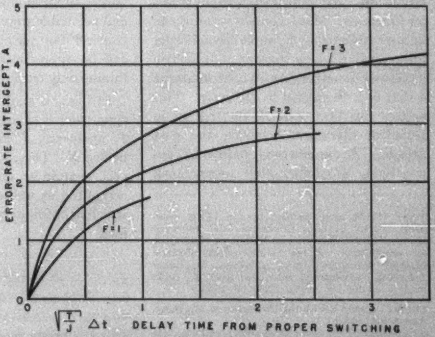

Fig. 5. Error-rate intercept versus switching-time delay for various switching velocities

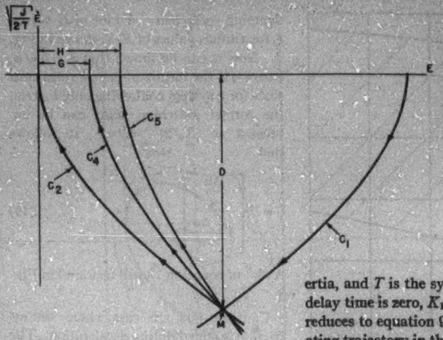

Fig. 6. Phase-plane trajectory of a second-order control system under the conditions of coulomb and viscous damping after switching

The equation representing the correct decelerating curve C_2 is defined by

$$\frac{J}{2T}\dot{E}^2-E=0 \tag{9}$$

The equation defining the overshoot curve C_3, is

$$\frac{J}{2T}\dot{E}^2-E=K_1 \tag{10}$$

where K_1 is the error in the system when the error rate is zero, J is the system inertia, and T is the system torque. If the delay time is zero, $K_1=0$, and equation 10 reduces to equation 9, the proper decelerating trajectory in the phase plane. From equation 10, the value of the intercept A, the error velocity when the error is reduced to zero is found to be

$$A=\sqrt{K_1}=\left|\sqrt{\frac{J}{2T}}\dot{E}\right|_{\text{intercept}} \tag{11}$$

From equations 7 and 9, the value of D, the velocity for correct switching is found to be

$$D=\sqrt{\frac{K_0}{2}} \tag{12}$$

From equations 7 and 10, the value of F, the velocity existing at actual switching, is found to be

$$F=\sqrt{\frac{K_0+K_1}{2}} \tag{13}$$

Although F is a measure of the switching time delay, a more useful form of the information is to determine the delay time directly. The time required to go from one point to another in the phase plane can be determined, in general, by the following integral equation

$$t_{a\rightarrow b}=\int_{E_a}^{E_b}\frac{dE}{\dot{E}} \tag{14}$$

When applied to equation 7, equation 15 is obtained

$$t_{a\rightarrow b}=\sqrt{\frac{J}{T}}\left[\sqrt{K_0+K_1}-\sqrt{K_0}\right] \tag{15}$$

where a is the time at proper switching.

A plot of A versus $(T/J)^{1/2}\Delta t$ is shown in Fig. 4 for various initial conditions, K_0. In Fig. 5 is shown a similar plot with F, the maximum velocity, as the parameter instead of K_0. Dimensionless time and error rate are used to keep the values as general as possible. Inspection of the curves in Fig. 4 reveals that for a given delay time, the error rate intercept A increases for increasing initial conditions K_0. Inspection of the curves in Fig. 5 reveals that for a given delay time, the error rate intercept A increases for increas-

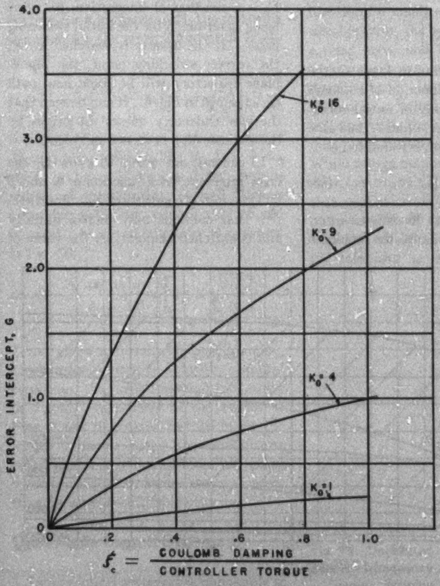

Fig. 7. Error intercept G versus coulomb damping coefficient ξ_c for various initial conditions

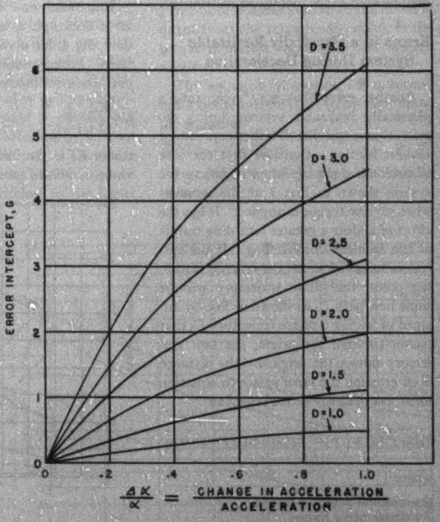

Fig. 8. Error intercept G versus change in acceleration/acceleration ratio for various switching velocities

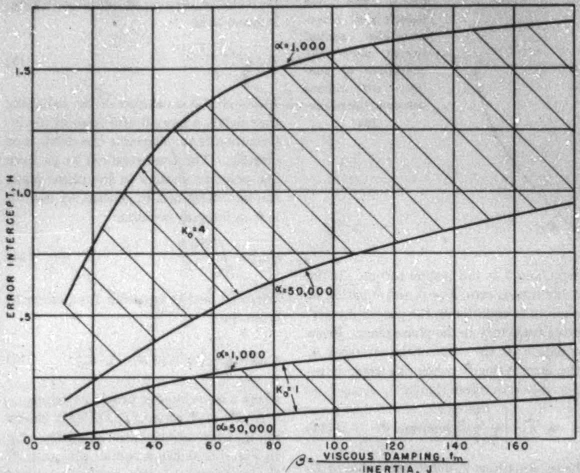

Fig. 9. Error intercept H versus viscous damping-inertia ratio for various initial conditions and accelerations

ing switching velocities F. In an experimental system, it is possible to determine the switching delay time by measuring the error rate intercept A using the curves of Figs. 4 or 5, and knowing either K_0 or F. An x-y recorder or a cathode-ray oscillograph having a long-persistence screen may be used as the measuring instrument.

Errors in a Physically Realizable System During Deceleration

Another error that may creep into a physically realizable system during deceleration is one due to either coulomb or viscous friction. Consider first the case of coulomb damping when added to the system shown in Fig. 1 at the moment when reverse torque is applied. It has the effect of adding a greater retarding torque at the moment of switching. If the system is switched at M, the correct switching point, the phase trajectory will be some new path C_4 as shown in Fig. 6. Instead of having a phase trajectory C_2 that passes through the origin, the new trajectory misses the origin by the distance G on crossing the error axis. In equation form, curve C_4 can be expressed as

$$J\ddot{E}=T+Q=\left(1+\frac{Q}{T}\right)T=(1+\xi_c)T\triangleq T' \quad (16)$$

where

Q = coulomb damping torque
T = decelerating torque
$\xi_c=\frac{Q}{T}$ = coulomb damping coefficient

Thus, integrating equation 16, equation 17 is obtained

$$E=\frac{J}{2T}\dot{E}^2+K_2 \quad (17)$$

$$=\left(\frac{1}{1+\xi_c}\right)\left[\frac{J}{2T}\dot{E}^2+K_2\right]$$

In general, one wants to know G, the error intercept, as a function of coulomb damping ξ_c for a variety of initial conditions. From equations 17 and 7, the value of G, the error intercept, is found to be

$$G=\frac{K_0}{2}\left[\frac{\xi_c}{1+\xi_c}\right] \quad (18)$$

where K_0 is the initial condition as previously defined and ξ_c is the coulomb damping coefficient. A plot of G versus ξ_c for various values of K_0 is shown in Fig. 7. Now it can be shown that $\xi_c=\Delta\alpha/\alpha$, where α is the torque-to-inertia ratio, and since for a system containing only inertia, the correct switching point can be expressed as $(K_0/2)^{1/2}=D=F$, it follows that

$$G=D^2\left[\frac{\frac{\Delta\alpha}{\alpha}}{1+\frac{\Delta\alpha}{\alpha}}\right] \quad (19)$$

A plot of equation 19 will be found in Fig. 8.

Consider now the case where viscous friction is added during deceleration. The effect of viscous friction is to add retarding torque at the moment of switching, but on that varies with velocity. In equation form this can be expressed as

$$J\ddot{E}=T+f_m\dot{E} \quad (20)$$

where J, T, $\ddot{E}$, and $\dot{E}$ have been previously defined and f_m is the viscous friction coefficient. Again letting $\alpha=T/J$ and letting $\beta=f_m/J$, equation 20 when integrated becomes

$$E=-\frac{\dot{E}}{\beta}-\frac{\alpha}{\beta^2}\ln\left(1-\frac{\beta}{\alpha}\dot{E}\right)+K_4 \quad (21)$$

K_4 is a constant of integration, its value being determined by the initial switching point. If the system is switched at M, the correct switching point, the phase-plane trajectory will be some new path C_5, as shown in Fig. 6. It can be seen that the new trajectory misses the origin by the distance H, a new error intercept.

In general, one wants to know H, the error intercept, as a function of α and β and the initial conduction K_0. For a system that contains only inertia initially and is switched at point M, the value of

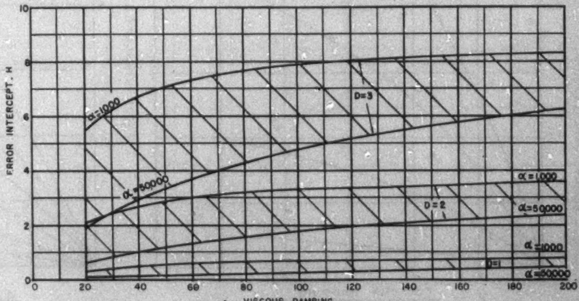

Fig. 10. Error intercept H versus viscous damping-inertia ratio for various switching velocities and accelerations

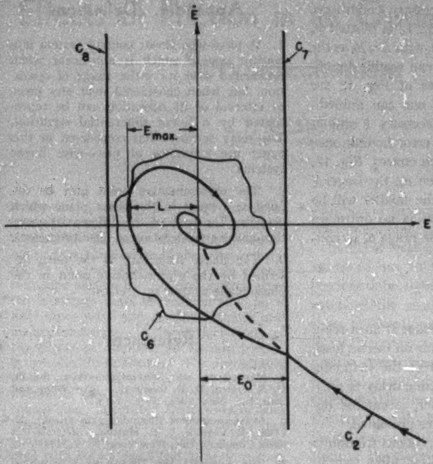

Fig. 11. Phase-plane trajectory of a dual-mode control system

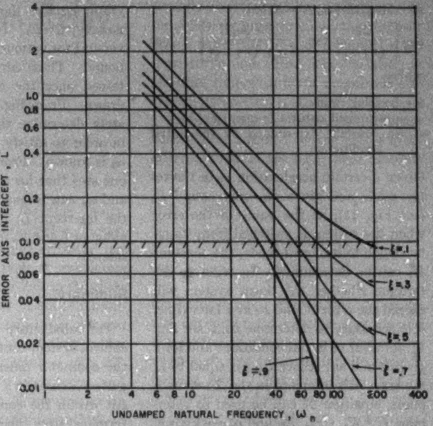

Fig. 12. Error intercept L versus undamped natural frequency ω_n for various damping ratios

K_4 can be found from equation 22

$$K_4=\frac{K_0}{2}-\frac{\sqrt{K_0\alpha}}{\beta}+\frac{\alpha}{\beta^2}\ln\left[1+\beta\sqrt{\frac{K_0}{\alpha}}\right] \quad (22)$$

Setting $\dot{E}=0$ in equation 21, the following equation for the error intercept H is obtained

$$H=\frac{K_0}{2}-\frac{\sqrt{K_0\alpha}}{\beta}+\frac{\alpha}{\beta^2}\ln\left[1+\beta\sqrt{\frac{K_0}{\alpha}}\right] \quad (23)$$

A plot of H versus β for various values of K_0 and α is shown in Fig. 9. If it is desired to have H versus β for various values of acceleration α and various switching velocities, equation 24 should be used. A plot of equation 24 is shown in Fig. 10.

$$H=D^2-\frac{\sqrt{2D^2\alpha}}{\beta}+\frac{\alpha}{\beta^2}\ln\left[1+\beta\sqrt{\frac{2D^2}{\alpha}}\right] \quad (24)$$

Thus, given a certain viscous damping, acceleration, switching velocity, or initial condition, the error intercept can easily be found. Inspection of the curves of Figs. 9 and 10 reveals that the larger the torque-to-inertia ratio, the smaller the error intercept. For a large switching velocity, a greater error intercept exists than for a small switching velocity.

Dual-Mode Control Systems

In a practical system it is impossible to have a computer that will detect the equation

$$\dot{E}\times|\dot{E}|+\frac{2T}{J}E=0$$

precisely. Erratic servo performance may result from computer errors. One method of overcoming this difficulty is to add a second mode (a linear one) that will function for small errors. Thus, given a sizeable error, the system will function as a relay servo and have the phase-plane trajectory shown in Fig. 2. At a predetermined point in the phase plane, the system is switched to a linear one that will approach the origin. A plot of this dual-mode trajectory is shown in Fig. 11. While a large number of switching boundaries (see curve C_6) could be chosen, one that can be readily detected by a computer is that of error only. These are shown as straight lines C_7 and C_8. Once the computer has switched to the linear system, it is important that the linear trajectory does not exceed this predetermined error bound. If it should, the system would return to its relay mode, and may or may not eventually return to the origin, depending upon the value of ξ and positions of C_7 and C_8. In any event, it would not be operating under the best conditions. An attempt has been made to relate the defining quantities, namely ξ and ω_n of a linear system to the defining quantity of the relay mode, which is the torque-to-inertia ratio or α the system acceleration.

The equation of motion for a second order linear system is given by the following equation

$$\ddot{E}+2\xi\omega_n\dot{E}+\omega_n^2E=0 \quad (25)$$

Integrating equation 25, one obtains equation 26

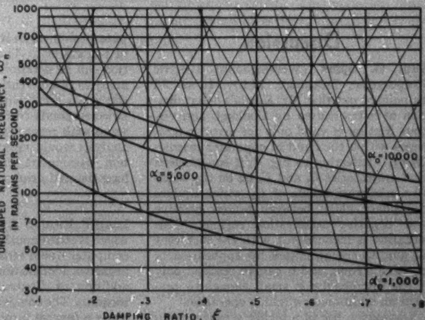

Fig. 13. Undamped natural frequency ω_n versus damping ratio ξ for various initial conditions

$$\dot{E}^2+2\xi\omega_n E\dot{E}+\omega_n^2E^2=K_3\times$$
$$\exp\left[\frac{2\xi}{\sqrt{1-\xi^2}}\tan^{-1}\frac{\dot{E}+\xi\omega_n E}{\omega_n E\sqrt{1-\xi^2}}\right] \qquad (26)$$

where

ξ = damping ratio
ω_n = undamped natural frequency
K_3 = a constant determined by the initial conditions

Given a certain acceleration α_0 in the relay mode and given an error bound E_0 (see Fig. 11), as the value of the error when the system is switched from its relay mode to its linear mode, the constant K_3 can be determined. In order to determine whether the linear system will exceed the error bound E_0 at a later time, it is necessary to determine E_{max}, see Fig. 11, for a set of initial conditions and for a given ξ and ω_n. Since E_{max} is equal to L, the error axis intercept in the $\dot{E}$ versus E plane, equation 27 can be used to determine L if K_3, ξ, ω_n, E_0, and α_0 are known.

$$L^2=\left[E_0^2+\frac{\dot{E}_0^2}{\omega_n^2}+\frac{2E_0\dot{E}_0}{\omega_n}\right]\times$$
$$\exp\left[\frac{2}{\sqrt{1-\xi^2}}\tan^{-1}\frac{-E_0\sqrt{1-\xi^2}}{\omega_n E_0+\xi\dot{E}_0}\right] \qquad (27)$$

A plot of equation 27 is shown in Fig. 12 for various values of ξ and ω_n, with α_0 as a parameter. If it is assumed that proper switching has occurred and the system is decelerating on the C_2 trajectory, equation 4 will then describe the path of the system. Solving equation 4 one can see that in general

$$\dot{E}=\sqrt{\frac{2T}{J}E}=\sqrt{2\alpha E}$$

Applying this result to the case of a particular error bound E_0, the equation $\dot{E}_0=\sqrt{2\alpha_0 E_0}$ is obtained. Thus, given E_0 and α_0, the value of $\dot{E}_0$ may be obtained, which is the only remaining unknown in equation 27. From the curves of Fig. 12, one sees that only a limited region of the graph satisfies the necessary conditions, namely, $L=E_0$. In Fig. 13 is plotted ω_n versus ξ for various α_0's, with $L=E_0$ as the bound. These curves can readily be obtained once the curves of Fig. 12 are drawn. From Fig. 13 one can immediately determine the necessary ξ and ω_n in order to satisfy the error bound, once α_0 is known. From the curves, Fig. 12, one sees that for a given α_0, the larger ξ and ω_n can be made, the smaller will be the intercept L. There is no optimum value of ξ and ω_n for the range of α_0 considered.

Summary

For satisfactory response from a relay control system containing an inertia load, the computer must detect the switching curves accurately. If time delay is present within the controller, it can be determined from the curves presented.

If either coulomb or viscous friction is present within the system after switching, the system's error and error rate will not be zero simultaneously. The error within the system when the error rate is zero can be determined from the included curves.

In a physically-realizable relay control system with an inertia load, a small variation in any of the parameters would lead to unstable operation. Some modification of this system is therefore essential. One solution to the problem would be the addition of a second mode of operation; namely, a linear mode with positive damping. For small errors, the system would operate as a linear one. Given a large error, however, the system would function as a relay servo where full torque of proper sign would be applied until that time when the error is brought within a predetermined error bound. At this point, the controller would switch to its linear mode to reduce the error to zero.

Appendix. Definitions

1. A piece-wise linear control system is a control system which is non-linear when considered over its entire range of operation, but when considered over any piece or interval of its operation can be represented by a linear differential equation. The relay servosystems considered in this paper are examples of piece-wise linear systems.

2. The representative point may be defined as a point in the phase plane which describes the path of the differential equation under consideration as time progresses.

3. The phase trajectory is the path described by the representative point in the phase plane as time progresses.

References

1. Principles of Servomechanisms (book), G. S. Brown, D. P. Campbell. John Wiley and Sons, Inc., New York, N. Y., 1948.

2. Servomechanism Fundamentals (book), H. Lauer, R. Lesnick, L. E. Matson. McGraw-Hill Book Company, Inc., New York, N. Y., 1947.

3. The Analysis and Design of Servomechanisms, Herbert Harris, Jr. *Report No. 454*, Office of Scientific Research and Development, Washington, D. C., Dec. 1941.

4. Non-Linear Techniques for Improving Servo Performance, D. McDonald. *Proceedings*, National Electronics Conference, Chicago, Ill., vol. 6, 1950, pp. 400–21.

5. Introduction to Non-Linear Mechanics (book), N. Minorsky. Edwards Brothers, Inc., Ann Arbor, Mich., 1947.

6. Theory of Non-Linear Oscillations (book), A. A. Andranow, C. E. Chaikin. Princeton University Press, N. J., 1949.

7. Analysis of Relay Servomechanisms, H. K. Weiss. *Journal of the Aeronautical Sciences*, New York, N. Y., July 1946, pp. 364–76.

8. Multiple Mode Operation of Servomechanisms, D. McDonald. *Review of Scientific Instruments*, New York, N. Y., vol. 23, no. 1, 1952, pp. 22–30.

9. Contributions to the Theory of Non-Linear Oscillations (book), S. Lefschetz. Princeton University Press, Princeton, N. J., 1950.

10. Introduction to Non-Linear Mechanics (book), N. Kryloff, N. Bogolinboff. Princeton University Press, Princeton, N. J., 1949.

11. A Phase-Plane Approach to the Compensation of Saturating Servomechanisms, Arthur M. Hopkins. *AIEE Transactions*, vol. 70, pt. I, 1951, pp. 631–39.

◆

Discussion

Paul G. Spink (Westinghouse Electric Corporation, Baltimore, Md.): It should be pointed out that Mr. Kazda's determination of errors caused by Coulomb and viscous friction is valid only for error magnitudes within the band of computer insensitivity. Referring to Fig. 6, it can be seen that trajectories C_4 and C_5 lie on the negative acceleration side of C_2, which divides the phase plane between desired positive and negative acceleration regions. This situation is inconsistent with the fact that C_4 and C_5 are generated by application of positive torque, and it can be realized only if the discrepancy is small enough to prevent an additional switching operation.

Obviously, use of a highly sensitive computer would result in an oscillatory behavior of the system. The nature of this oscillation can be determined by methods used in analysis of conventional relay servos, since the servo error with respect to trajectory C_2 corresponds to that of the conventional servo with respect to the $\dot{E}$ axis. Such an analysis would necessarily consider all system parameters, including computer differential and dead zone.

Louis F. Kazda: It is true that in a system which is continuously operating the detecting computer would sense the deviation into the negative acceleration region caused by the addition of Coulomb or viscous damping torque. The computer in this system would cause a reverse torque to be applied to the system. The results obtained under this condition of operation would cause the system to oscillate about the C_2 curve. The width of the oscillation depends on the computer dead time, which in turn is a function of the computer sensitivity to the E and $\dot{E}$ components. Given these components the oscillating phase plane trajectory can be obtained.

It is obvious from such operation that it would be impossible to determine either the Coulomb or viscous damping coefficient experimentally using a cathode-ray oscillograph. Although not explicitly stated in the paper, in order to determine the constants mentioned it is necessary to have a 1-shot computer, one that will maintain its status quo once the $\dot{E}\times/\dot{E}/+(2T)/JE=0$ curve has been crossed.

Effects of Friction in an Optimum Relay Servomechanism

T. M. STOUT
ASSOCIATE MEMBER AIEE

Synopsis: A recently proposed relay servomechanism employs maximum torque at all times, with the sense of the torque determined by a comparison of the error and the square of the error rate. With correct switching and no friction, this system gives the minimum possible response time for a step input with the specified inertia and maximum torque. A theoretical study of the effects of Coulomb or viscous friction is described in this paper. The degradation of the step-function response as a result of friction is measured by the change in response time, integrated absolute error, and integrated squared error. It is found that moderate amounts of friction can be tolerated with only a small loss in performance, if a slight change is made in the switching device.

RELAY SERVOMECHANISMS have been used and studied[1–10] for a number of years. In the usual system, the sense of the torque applied to the output shaft is controlled by a relay whose operation is based on the sign of the error. Such systems can be made small and simple, but have a tendency to oscillate at small amplitudes if the system has moderate amounts of dead space or time delay. Friction helps to stabilize a relay system but is otherwise objectionable. Lead networks, which make the torque dependent on a linear combination of error and error rate, have been used as stabilizing devices.

McDonald,[11–13] Hopkin,[14] and others[15] have recently proposed that the usual relay system be modified by the substitution of a nonlinear lead network or "anticipator" for the conventional linear lead network. In the proposed system, the sense of the torque is based on a comparison of the error and the square of the error rate. For a step input and neglecting all friction torques, this system uses maximum accelerating torque until the error is reduced to half its original value, and maximum decelerating torque until the error is reduced to zero.

The proposed system is called an "optimum" system, since it gives the minimum response time possible with the specified inertia and maximum torque. Because the response time varies with the magnitude of the initial error and the response to a step input does not give a precise description of the response for other inputs, the system must be considered nonlinear.

In linear systems, slight errors in the values of any of the system parameters produce only slight variations in the character of the response. This common-sense observation is based on a theorem in mathematics which states that, under certain conditions, the solution of a differential equation is a continuous and differentiable function of parameters in the equation.[16] While the equations of linear servomechanisms meet the conditions of the theorem, those of off-on systems may not. For this reason it seemed desirable to remove some of the assumptions on which previous analyses of the proposed optimum system have been based, in order to determine whether the presence of friction might produce serious effects.

The investigations to be described are concerned with changes in the response of this system due to Coulomb or viscous friction. The systems considered become optimum in the absence of friction.

Response Criteria

Several criteria are used to measure degradation of the response due to the presence of friction. The speed of response to an abrupt change in the input signal is an important characteristic of a control system. In linear systems, the response time is defined somewhat arbitrarily as the time needed for the error to become and remain less than a specified fraction, usually a few hundredths, of the initial magnitude.[17] This sort of definition is perfectly satisfactory for linear systems whose behavior is independent of the input magnitude.

This definition is not so useful for nonlinear systems where the character of the response may vary widely with changes in the input magnitude, and the error may actually become zero in a finite time. In the following investigations, the response time is defined as the time required for the error to become zero. The variation of response time with input magnitude and system parameters is studied.

Ambiguities in the definition of response time can be avoided by the use of other criteria, such as the integrated absolute error

$$A_1=\int_0^\infty |e|dt$$

or the integrated squared error

$$A_2=\int_0^\infty e^2dt$$

for a step input. These integrals, which also depend on the input magnitude and the system parameters, are finite even when the error takes an infinite time to become zero. They have been used in other theoretical and experimental studies of linear and nonlinear servomechanisms[18–20]. Both integrals are computed, either analytically or numerically, for the systems with friction studied here.

The Idealized System

To provide a standard to which the systems with friction can be compared, the theory of the proposed optimum system will be reviewed and the various response criteria applied to it.

System Equations

The load presented to the motor by the output shaft is assumed to be an inertia load, and all friction torques are ignored. The motor delivers a torque which is either constant ($\pm T_m$) or zero. The response of the system to a step input is then determined from the equation

$$J\ddot{e}=\pm T_m \tag{1}$$

where e is the error, dots denote differentiation with respect to time, and the sign of the torque depends on e and $\dot{e}$ in a manner to be described. This equation may be integrated directly to obtain the error rate

$$\dot{e}=K_1\pm\frac{T_m}{J}t \tag{2}$$

and the error

$$e=K_2+K_1t\pm\frac{T_m}{2J}t^2 \tag{3}$$

as functions of time, where K_1 and K_2 are constants which depend on the initial conditions.

The output shaft is assumed to be stationary when the step input is applied. Because of its inertia, the velocity of the output shaft cannot change instantane-

---

Paper 53-355, recommended by the AIEE Feedback Control Systems Committee and approved by the AIEE Committee on Technical Operations for presentation at the AIEE Pacific General Meeting, Vancouver, B. C., Canada, September 1–4, 1953. Manuscript submitted April 27, 1953; made available for printing July 2, 1953.

T. M. STOUT is with the University of Washington, Seattle, Wash.

This work was supported by the Office of Naval Research.

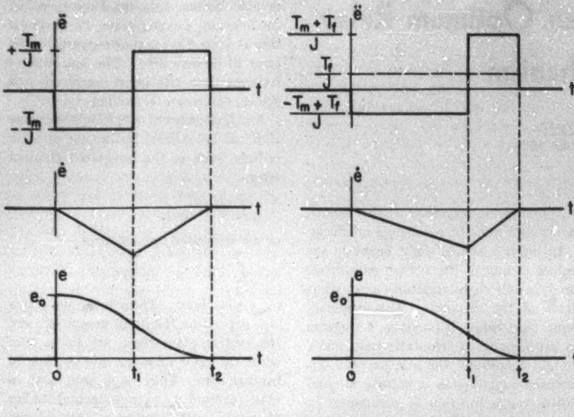

(A) IDEAL CASE

(B) WITH COULOMB FRICTION

Fig. 1. Error and error rate for a relay servomechanism

ously, and the initial error is thus equal to the magnitude of the step input. For the acceleration interval the initial conditions are therefore $\dot{e}(0)=0$ and $e(0)=e_0$, and the equations of motion are

$$\dot{e}=-\frac{T_m}{J}t \tag{4}$$

$$e=e_0-\frac{T_m}{2J}t^2 \tag{5}$$

At a time t_1, the error is reduced to half its original value, the torque is reversed by the action of the nonlinear anticipator, and the equations for the subsequent interval are

$$\dot{e}=\frac{T_m}{J}t-2\sqrt{\frac{T_m}{J}}\sqrt{e_0} \tag{6}$$

$$=-\frac{T_m}{J}(t_2-t) \tag{7}$$

$$e=2e_0-2\sqrt{\frac{T_m}{J}}\sqrt{e_0}t+\frac{T_m}{2J}t^2 \tag{8}$$

$$=\frac{T_m}{2J}(t_2-t)^2 \tag{9}$$

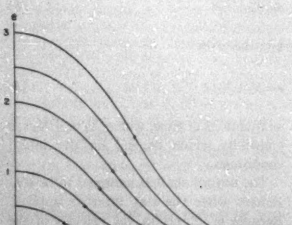

Fig. 2 (left). Error as a function of time for a relay servomechanism without friction

In equations 7 and 9 t_2 is the time required for the error to become zero, that is, the response time. Plots showing the relations between error and error rate are given in Fig. 1(A). A family of curves of error as a function of time are given in Fig. 2; similar curves, based on experimental data, are given by McDonald[13] and Hopkin.[14]

RESPONSE CRITERIA

The switching time t_1 can be found by substituting $e=e_0/2$ in equation 5; the result is

$$t_1=\sqrt{\frac{J}{T_m}e_0} \tag{10}$$

The response time t_2 can be found from equations 6 or 8 or, more simply, by noting that

$$t_2=2t_1 \tag{11}$$

$$=2\sqrt{\frac{J}{T_m}e_0} \tag{12}$$

It can be seen by inspection that the integrated absolute error is

$$A_1=\frac{1}{2}e_0t_2$$

$$=\sqrt{\frac{J}{T_m}}e_0^{3/2} \tag{13}$$

The integrated squared error, somewhat more difficult to evaluate, turns out to be

$$A_2=\frac{23}{30}\sqrt{\frac{J}{T_m}}e_0^{5/2} \tag{14}$$

All three measures of response are functions of J/T_m, as would be expected and become smaller with a decrease in J or an increase in T_m. They also depend on a power of e_0 which could have been predicted from dimensional requirements. With the torque-to-inertia ratio given, the response time, integrated absolute error, and integrated squared error can easily be calculated for any initial error from these equations.

SWITCHING

To simplify graphical work, it has been assumed that $T_m=1$ and $J=1$, with the result that $\dot{e}$ is equal to t and e varies as $t^2/2$. This assumption amounts to a change of variable which can be specified more precisely if the need arises.

With the substitution of these numerical values, the error can be written

$$e=e_0-\frac{\dot{e}^2}{2} \tag{15}$$

for $0<t<t_1$, and

$$e=\frac{\dot{e}^2}{2} \tag{16}$$

for $t_1<t<t_2$. These equations are the basis of the phase-plane plots given in

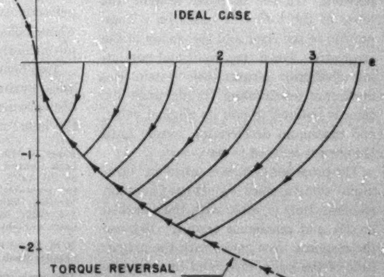

Fig. 3 (right). Phase-plane plot for a relay servomechanism without friction

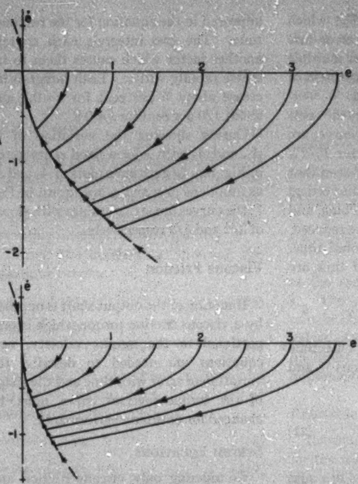

Fig. 4. Phase-plane plots for a relay servomechanism with Coulomb friction

A. $T_f=0.4T_m$
B. $T_f=0.8T_m$

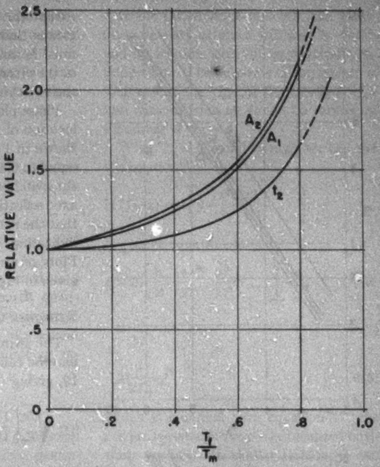

Fig. 6 (right). Relative response time, integrated absolute error A_1, and squared error A_2, as functions of T_f/T_m

Fig. 3. All of the trajectories coincide approaching the origin; equation 16 therefore gives the values of e and $\dot{e}$ at the time of torque reversal and divides the phase plane into regions of positive and negative torque. Points above or to the right of this curve correspond to $-T_m$, and points below or to the left correspond to $+T_m$. The curve appears in the second and fourth quadrants, and is symmetrical about the origin.

In general terms, the equation of the torque-reversal or switching curve (in the fourth quadrant) is

$$\dot{e}_s^2=\frac{2T_m}{J}e_s \tag{17}$$

where s denotes a switching point. The function of the switching device is to compare $\dot{e}^2$ with the proper multiple of e, determine the position of the system with respect to the boundary, and supply a signal to the relay which will result in the proper torque.

Hopkin[14] describes two methods for converting the theoretical torque-reversal curve into a physical switching device. In one method the phase-plane plot is reproduced on the face of a cathode-ray tube in which the horizontal and vertical deflections of the beam depend directly on the error and error rate. An opaque mask covers the region on one side of the torque-reversal curve, and a photocell determines from the location of the spot whether positive or negative torque is required. This scheme, which permits any required torque-reversal curve to be easily realized, is bulky and complicated.

His other method, which is more commonly used,[11,13,15] requires a comparison of two voltages, one proportional to the error and the other proportional to the square of the error rate.* The nonlinear function is generated by biased-diode networks whose design is based on equation 17 and the symmetry requirements.

Coulomb Friction

Previous studies have not been concerned with a quantitative measurement of the detrimental effects of incidental Coulomb or viscous friction. It is known that a slight change in the shape or location of the torque-reversal curve will preserve the desirable features of the original system,[11,15] and McDonald has suggested the deliberate use of Coulomb friction to assist in the decelerating process.[11] While it would be possible to study the behavior of the system with friction and the original switching procedure, it seems more fruitful to determine how much sacrifice in performance is produced by friction if the best possible switching procedure is used.

System Equations

If motion of the output shaft is opposed by a Coulomb friction torque T_f which is independent of velocity, the net accelerating torque is decreased but the decelerating torque is increased. The motion is still described by equations 2 and 3, except that T_m must be replaced by (T_m-T_f) during the interval when the output shaft is accelerating, and by (T_m+T_f) during the deceleration interval. To obtain the desired type of response, switching must be delayed until the error is less than half its original value, as indicated by Fig. 1(B).

The error and error rate will become zero simultaneously if the switching is carried out in such a way that

$$t_1\left[\frac{T_m-T_f}{J}\right]=(t_2-t_1)\left[\frac{T_m+T_f}{J}\right] \tag{18}$$

$$\frac{1}{2}\left[\frac{T_m-T_f}{J}\right]t_1^2+\frac{1}{2}\left[\frac{T_m+T_f}{J}\right](t_2-t_1)^2=e_0 \tag{19}$$

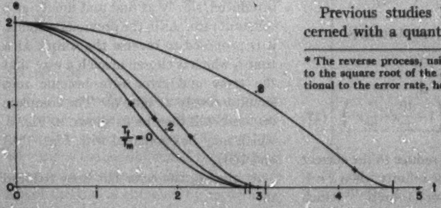

Fig. 5. Error as a function of time for a relay servomechanism with Coulomb friction

---

* The reverse process, using a voltage proportional to the square root of the error and another proportional to the error rate, has also been used.[11]

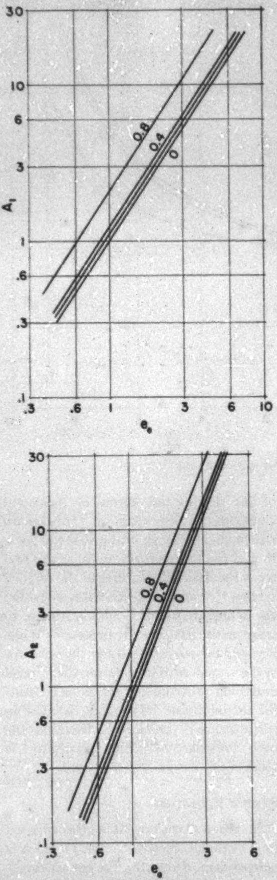

Fig. 7. Integrated absolute error A_1, and squared error A_2, as a function of initial error for $T_f/T_m = 0, 0.2, 0.4, 0.8$

Equation 18 states that the velocity is continuous at t_1, and equation 19 states that the total motion of the output shaft is e_0. To satisfy these conditions for all initial error magnitudes, it is necessary to make the switching boundary

$$\dot{e}_s^2 = 2\left[\frac{T_m+T_f}{J}\right]e_s \tag{20}$$

$$= 2\left[\frac{T_m}{J}\right](1+T_f/T_m)e_s \tag{21}$$

in the fourth quadrant. This boundary equation is identical with equation 17 except for the factor $1+T_f/T_m$, which means that the square of the error rate must be compared with a larger multiple of the error. Only a slight adjustment of the switching device is required.

Phase-plane plots, showing the new location of the torque-reversal curve, are shown in Figs. 4(A) and 4(B) for T_f/T_m equal to 0.4 and 0.8. It will be seen that the switching curve is closer to the vertical axis, reflecting the delay in switching, and that the maximum velocities are reduced, indicating an increase in response time. Plots of error as a function of time are given in Fig. 5.

RESPONSE CRITERIA

The switching time and response time may be calculated from equations 18 and 19, giving

$$t_1 = \sqrt{\frac{Je_0}{T_m}}\left[\frac{1+x}{1-x}\right]^{1/2} \tag{22}$$

$$t_2 = \frac{2}{1+x}t_1 \tag{23}$$

$$= 2\sqrt{\frac{Je_0}{T_m}}\left[\frac{1}{1-x^2}\right]^{1/2} \tag{24}$$

where, for brevity, $x = T_f/T_m$. These expressions reduce to the friction-free values when $x=0$ and become infinite when $x=1$, as expected. When x is small, the response time is approximately

$$t_2 \cong 2\sqrt{\frac{Je_0}{T_m}}\left(\frac{1+x^2}{2}\right) \tag{25}$$

For $x=0.2$, the response time is increased about 2 per cent; for $x=0.8$, the increase is 67 per cent. The effect of friction is small because the friction torque is put to use in decelerating the output shaft.

That a moderate amount of friction is not too serious may also be concluded from consideration of the integrated absolute or squared error, although these integrals increase more rapidly with x than the response time does. Some straightforward integration and algebra establishes that the integrated absolute error is

$$A_1 = \sqrt{\frac{J}{T_m}}e_0^{3/2}\left[\frac{1}{1-x^2}\right]^{1/2}\left(1+\frac{x}{3}\right) \tag{26}$$

and the integrated squared error is

$$A_2 = \frac{23}{30}\sqrt{\frac{J}{T_m}}e_0^{5/2}\left[\frac{1}{1-x^2}\right]^{1/2}\left(1+\frac{10}{23}x-\frac{1}{23}x^2\right) \tag{27}$$

These equations also reduce to the correct form for $x=0$, become infinite when $x=1$, and contain the factor $(1-x^2)^{-1/2}$ which appeared in the equation for the response time. The two integrals each contain another factor which causes them to increase rapidly with x. Both integrals increase about 5 per cent for $x=0.2$ and about 120 per cent for $x=0.8$.

Curves showing the variation of t_2, A_1, and A_2 with x for a fixed e_0 are given in Fig. 6. Logarithmic plots of A_1 and A_2 as functions of x and e_0 are shown in Fig. 7; the curves are straight lines with slopes of 3/2 and 5/2 respectively.

Viscous Friction

If motion of the output shaft is opposed by a viscous friction torque which is proportional to the output velocity, new equations are needed to describe the variation of error with time and the shape of the torque reversal curve must be changed for optimum performance.

SYSTEM EQUATIONS

Considering only viscous friction and inertia, the equation describing the response of the system to a step input is

$$J\ddot{e}+f\dot{e} = \pm T_m \tag{28}$$

where f is the friction coefficient and the sign of the torque will again depend on e and $\dot{e}$.

The general solutions of this equation are

$$\dot{e} = \pm\Omega + K_1\epsilon^{-t/\tau} \tag{29}$$

$$e = \pm\Omega t - K_1\tau\epsilon^{-t/\tau} + K_2 \tag{30}$$

where

$\Omega = \frac{T_m}{f}$, the maximum or limiting velocity

$\tau = \frac{J}{f}$, the time constant

K_1 and K_2 depend on the initial conditions

For the same initial conditions as before, the error rate and error during the accelerating interval are

$$\dot{e} = -\Omega(1-\epsilon^{-t/\tau}) \tag{31}$$

$$e = e_0 - \Omega t + \Omega\tau(1-\epsilon^{-t/\tau}) \tag{32}$$

The error rate increases exponentially toward the limiting value, while the error is reduced, slowly at first and finally at a constant rate. As in the previous systems, it is proposed to reverse the torque at a time t_1 which is chosen in such a way that the error and error rate become zero simultaneously at time t_2. The complete response will then be as shown in Fig. 8, which may be compared with Figs. 1(A) and 1(B).

At time t_1, the error has been reduced to

$$e(t_1)=e_0-\Omega t_1+\rho\Omega\tau \tag{33}$$

and the error rate is

$$\dot{e}(t_1)=-\rho\Omega \tag{34}$$

where

$$\rho=1-\epsilon^{-t_1/\tau}) \tag{35}$$

the fraction of the limiting speed which is attained by the output shaft at the switching point. Equations 33, 34, and 35 give the initial conditions for the decelerating interval between t_1 and t_2.

During the deceleration interval, the equations become

$$\dot{e}=\Omega-(\rho+1)\Omega\epsilon^{-(t-t_1)/\tau} \tag{36}$$

$$e=\Omega t-2\Omega t_1-\Omega\tau+(\rho+1)\Omega\tau\epsilon^{-(t-t_1)/\tau}+e_0 \tag{37}$$

Imposing the conditions $\dot{e}(t_2)=0$ and $e(t_2)=0$ we obtain, after some algebraic manipulation, two equations

$$0=\Omega-(\rho+1)\Omega\epsilon^{-(t_2-t_1)/\tau} \tag{38}$$

$$0=\Omega(t_2-t_1)-\Omega t_1+e_0 \tag{39}$$

which are analogous to equations 18 and 19. Except for the nature of the equations, it would be possible to solve equations 35, 38, and 39 to determine ρ, t_1, and t_2 for any particular e_0.

It is much more convenient, however, to consider that t_1 is given. Using the value of ρ computed from equation 35, we then find (t_2-t_1) from

$$\epsilon^{-(t_2-t_1)/\tau}=\frac{1}{\rho+1} \tag{40}$$

which is derived from equation 38. The response time is then

$${}_s=t_1+\overline{(t_2-t_1)} \tag{41}$$

and the initial error is

$$e_0=2\Omega t_1-\Omega t_2 \tag{42}$$

Some typical response curves for a system of this type are given in Fig. 9 for $\tau=0$ and $\tau=1$. When τ is made zero by eliminating the inertia, switching occurs at $e=0$; with no inertia, the output shaft rotates only when torque is applied and comes to rest immediately when the torque is removed. The switching point for $\tau=1$ occurs at relatively small values of e, increasing to $e_s=0.308$ for large initial errors. Phase-plane plots are given in Fig. 10.

SWITCHING

The required torque-reversal curve in the phase plane can be determined numerically, using equations 33 and 34, which give the coordinates of the switching point for a particular value of e_0. A more direct method is obtained by recognizing that the switching boundary is also a particular trajectory of the system, passing through the origin. Noting that $+T_m$ is used along this curve, we return to equations 29 and 30, substitute the conditions $\dot{e}(0)=0$ and $e(0)=0$, and obtain

$$\dot{e}_s=\Omega(1-\epsilon^{-t/\tau}) \tag{43}$$

$$e_s=\Omega t-\Omega\tau(1-\epsilon^{-t/\tau}) \tag{44}$$

Eliminating t, we obtain[8]

$$e_s=-\Omega\tau\ln\left[1-\frac{\dot{e}_s}{\Omega}\right]-\tau\dot{e}_s \tag{45}$$

as the required relation between e_s and $\dot{e}_s$. The boundary for the fourth quadrant is obtained by substituting negative values of $\dot{e}_s$; the boundary in the second quadrant is obtained by symmetry requirements.

RESPONSE CRITERIA

Inasmuch as no neat analytic expression for the response time is available, discussion will be confined to two limiting cases, and a graph based on numerical calculations will be presented.

If the initial error is small, the maximum velocity attained will also be small, and the friction term will be relatively unimportant. The behavior of the system is then essentially that of the idealized system without friction, as can be verified in a number of ways.

When $\dot{e}_s/\Omega$ is small enough, we can use the relation[21]

$$\ln(1-x)=-\left[x+\frac{x^2}{2}+\frac{x^3}{3}+\ldots\right]$$

to reduce equation 45 to

$$e_s=\Omega\tau\left[\frac{\dot{e}_s}{\Omega}+\frac{\dot{e}_s^2}{2\Omega^2}+\frac{\dot{e}_s^3}{3\Omega^3}+\ldots\right]-\tau\dot{e}_s \tag{46}$$

$$=\frac{\tau}{2\Omega}\dot{e}_s^2+\ldots \tag{47}$$

$$\cong\frac{J}{2T_m}\dot{e}_s^2 \tag{48}$$

which is identical with equation 17, the torque-reversal curve of the idealized optimum system. In similar fashion, it can be shown that the trajectories, and therefore the response time, integrated absolute error, and integrated squared error,

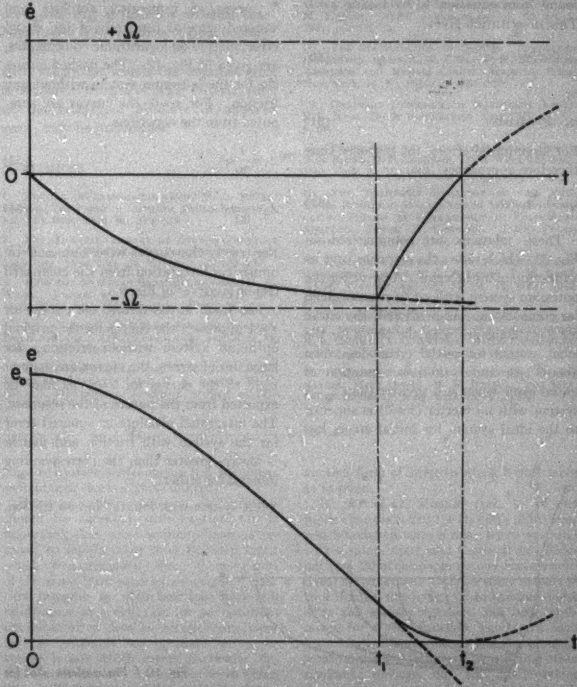

Fig. 8. Error and error rate for a relay servomechanism with viscous friction

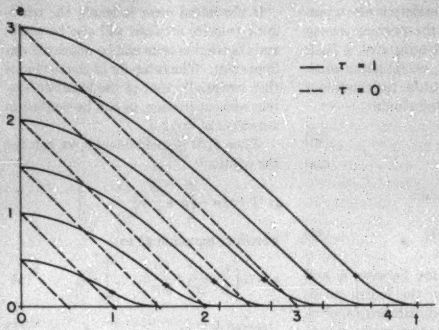

Fig. 9. Error as a function of time for a relay servomechanism with viscous friction

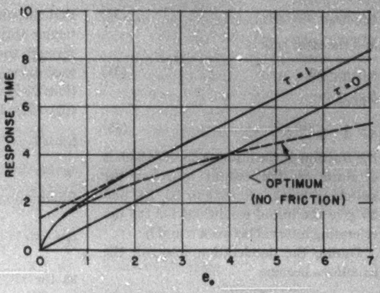

Fig. 11. Response time as a function of initial error for relay servomechanisms with viscous friction

reduce to the simpler form given earlier.

If the initial error is large, it is convenient to write equation 42 in the form

$$t_2 = \frac{e_0}{\Omega} + 2(t_2 - t_1) \tag{49}$$

since the limiting value of $(t_2 - t_1)$ can be found from equation 40 by taking $\rho = 1$. This substitution gives

$$\epsilon^{-(t_2 - t_1)/\tau} = \frac{1}{2} \tag{50}$$

or

$$(t_2 - t_1) = 0.693\tau \tag{51}$$

For large initial errors, the response time therefore approaches

$$t_2 = \frac{e_0}{\Omega} + 1.386\tau \tag{52}$$

These relations are summarized in Fig. 11, which shows the response time as a function of initial error. A curve for the optimum system without friction is given for comparison. As predicted, the curve for $\tau = 1$ coincides with the curve for the ideal system for initial errors less than about 1/2, and is a linear function of initial error when e_0 is greater than 2. A system with no inertia ($\tau = 0$) is superior to the ideal system for initial errors less than 4. This result may be expected from the fact that the inertialess system reaches its maximum velocity immediately and wastes no time in acceleration; for large initial errors, the greater maximum velocities possible in the ideal system result in a smaller response time.

Curves of integrated absolute and squared error as functions of the initial error, plotted on logarithmic co-ordinates, are given in Fig. 12. The dashed curves are for the optimum system without any friction. For $\tau = 0$, the curves are computed from the equations

$$A_1 = \frac{1}{2\Omega} e_0^2 \tag{53}$$

$$A_2 = \frac{1}{3\Omega} e_0^3 \tag{54}$$

For $\tau = 1$, the curves were obtained by numerical integration from the computed response curves of Fig. 9.

For small initial errors, the curves for $\tau = 1$ approach the curves for the original optimum system without friction; for large initial errors, the curves are asymptotic to the curves for $\tau = 0$, as may be expected from the nature of the response. The integrated absolute or squared error for the system with friction and inertia is always greater than the corresponding integral for either:

1. A system with intertia and no friction.
2. A system with friction and no inertia.

The limiting curves evidently supply lower bounds for the integrals and indicate the best possible performance to be expected from a given system. Any method of control other than the optimum switching methods will result in poorer performance, shown by an increase in the integrated absolute or squared error for any step disturbance.

Although the special values $T_m = J = f = 1$ were used to compute the response and phase-plane curves presented in the various figures, the curves for $\tau = 1$ may be treated as functions of dimensionless variables. To apply these results to other systems, it is necessary to consider that time has been measured relative to τ and error relative to $\Omega\tau$. With these scale changes, the curves apply to any similar system.[3]

Combined Coulomb and Viscous Friction

No detailed study has been made of the effects of combined Coulomb and viscous friction. Additional degradation of the response is, of course, to be expected.

It should be mentioned, at least, that the effects of combined Coulomb and viscous friction will be minimized by a suitable selection of the torque-reversal curve and a corresponding adjustment of the switching device. As already noted, the torque-reversal curve must be a trajectory of the system under deceleration conditions, passing through the origin. For this case, the required curve can be computed by substituting

$$\Omega' = \frac{T_m + T_f}{f} \tag{55}$$

$$= \Omega\left(1 + \frac{T_f}{T_m}\right) \tag{56}$$

for Ω in equation 45.

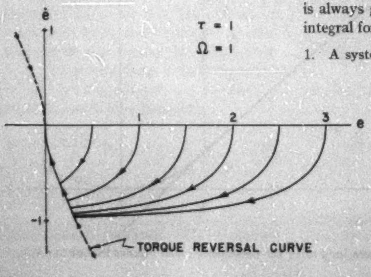

Fig. 10. Phase-plane plot for a relay servomechanism with viscous friction

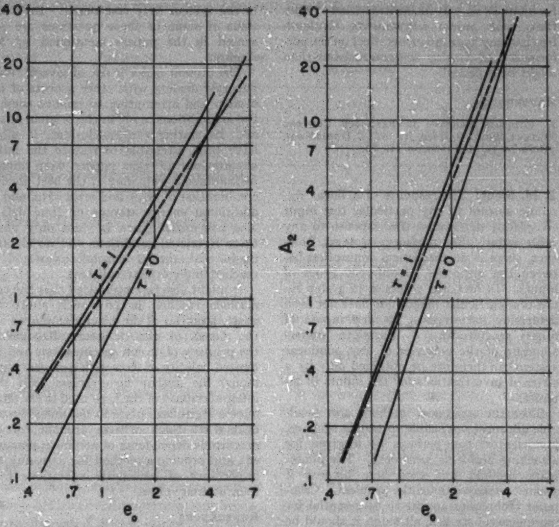

Fig. 12. Integrated absolute error A_1, and squared error A_2, as functions of initial error for relay servomechanisms with viscous friction. (Dashed curve is for a system without friction)

Conclusions

A surprisingly large Coulomb-friction torque, as much as 50 per cent, can be permitted without much sacrifice in system performance, if a simple adjustment is made in the switching device. Viscous friction is not significant for small errors, that is, errors which can be reduced to zero without reaching the maximum available speed, if a similar adjustment is made.

The time required for the error to become zero after a step disturbance is a measure of system quality and is readily computed for the systems considered here.

For comparisons of these systems with others for which the response time is not finite, the use of other criteria, such as the integrated absolute or squared error, may be preferable.

References

1. Theory of Servomechanisms, **H. L. Hazen.** *Journal*, The Franklin Institute, Philadelphia, Pa., vol. 218, Sept. 1934, pp. 279–330.

2. Fundamental Theory of Servomechanisms (book), **L. A. MacColl.** D. Van Nostrand Company, Inc., New York, N. Y., 1945, pp. 107–25.

3. Analysis of Relay Servomechanisms, **H. K. Weiss.** *Journal of Aeronautical Sciences*, New York, N. Y., vol. 13, July 1946, pp. 364–76.

4. An Analysis of Relay Servomechanisms, **David A. Kahn.** *AIEE Transactions*, vol. 68, pt. II, 1949, pp. 1079–88.

5. Relay Servomechanisms: The Shunt-Motor Servo with Inertia Load, **T. A. Rogers, W. C. Hurty.** *Transactions*, American Society of Mechanical Engineers, New York, N. Y., vol. 72, Nov. 1950, pp. 1163–72.

6. Theory of Relay Servomechanisms, **J. R. Dutilh.** *Onde Electrique*, Paris, France, vol. 30, Oct. 1950, pp. 438–45.

7. A Frequency-Response Method for Analyzing and Synthesizing Contactor Servomechanisms, **R. J. Kochenburger.** *AIEE Transactions*, vol. 69, pt. I, 1950, pp. 270–84.

8. On Some Nonlinear Phenomena in Regulatory Systems, **L. C. Goldfarb.** *Automatika i Telemekhanika*, Moscow, USSR, vol. 8, Sept.-Oct. 1947, pp. 349–83. (Translated in *Report No. 1691*, National Bureau of Standards, Washington, D. C., May 29, 1952.)

9. On the Computation of Relay Servomechanisms, **E. Y. Lechtman.** *Automatika i Telemekhanika*, Moscow, USSR, vol. 12, Jan.-Feb., 1951, pp. 15–27. (Translated in *Report No. 1691*, National Bureau of Standards, Washington, D. C., May 29, 1952.)

10. Discontinuous Automatic Control of Missiles, **I. Flugge-Lotz.** *Technical Report No. 14*, Division of Engineering Mechanics, Stanford University, Stanford, Calif., June-Aug., 1950.

11. Nonlinear Techniques for Improving Servomechanism Performance, **D. McDonald.** *Proceedings*, National Electronics Conference, Chicago, Ill., vol. 6, 1950, pp. 400–21.

12. Multiple Mode Operation of Servomechanisms, **D. McDonald.** *Review of Scientific Instruments*, New York, N. Y., vol. 23, Jan. 1952, pp. 22–30.

13. Basic Research in Nonlinear Mechanics as Applied to Servomechanisms, **D. McDonald.** *Technical Report No. T16-1*, Cook Research Laboratories, Chicago, Ill., Jan., 1952.

14. A Phase-Plane Approach to the Compensation of Saturating Servomechanisms, **Arthur M. Hopkin.** *AIEE Transactions*, vol. 70, pt. I, 1951, pp. 631–39.

15. The Stabilization of On-Off Controlled Servomechanisms, **A. M. Uttley, P. H. Hammond.** *Automatic and Manual Control*, Academic Press, New York, N. Y., 1952, pp. 285–307.

16. Ordinary Differential Equations (book), **E. L. Ince.** Dover Publications, New York, N. Y., p. 69.

17. Principles of Servomechanisms (book), **G. S. Brown, D. P. Campbell.** John Wiley and Sons, New York, N. Y., 1948.

18. The Transient Behavior of the Two-Stage Rototrol Main Exciter Voltage Regulating System as Determined by Eelctrical Analogy, **James T. Carleton.** *AIEE Transactions*, vol. 68, pt. I, 1949, pp. 59–63.

19. Analogue Methods for Optimum Servomechanism Design, **F. C. Fickeisen, T. M. Stout.** *AIEE Transactions*, vol. 71, pt. II, Nov. 1952, pp. 244–50.

20. A Differential Analyzer Study of Certain Nonlinearly Damped Servomechanisms, **R. R. Caldwell, V. C. Rideout.** *AIEE Transactions*, vol. 72, pt. II, July 1953, pp. 165–70.

21. Tables of Integrals and Other Mathematical Data (book), **H. B. Dwight.** The Macmillan Company, New York, N. Y., 1947.

◆

Discussion

George S. Axelby (Westinghouse Electric Corporation, Baltimore, Md.): Mr. Stout's paper is interesting and informative. Although the effects of Coulomb friction on linear servo performance have been analyzed,[1] few papers have attempted to determine the effects of Coulomb and viscous friction on the operation of a nonlinear servomechanism. Mr. Stout's conclusions are indeed surprising when it is considered that a large Coulomb friction torque can be permitted with a magnitude equal to 50 per cent of the motor torque without much sacrifice in system performance if a nonlinear switching device is slightly altered.

However, this conclusion, in general, should be accepted with caution. It is important that some servomechanisms respond to inputs other than the step input which was discussed here. Comparisons of the error, error squared, or weighted error time integrals for step functions have less significance as a criterion for an optimum nonlinear servo than for an optimum linear system. Actually, an optimum servo response is one which meets particular design specifications. A nonlinear servo which has an ideal response for a particular input may not have an acceptable response for another form of input to which it may have to respond.

In particular, Hopkin (ref. 14 of the paper) has discussed the stability difficulties which occurred when a relay servo was used with a ramp input, and Caldwell and Rideout (ref. 20 of the paper) showed that a nonlinear servo became unstable when subjected to a double step input or to random noise after the system response had been optimized for a step function input. In each instance, the performance for the troublesome inputs was improved by utilizing other nonlinear devices, but the modifications degraded the response for the step input.

Other servos are required at times to reproduce sinusoidal inputs. Although nonlinear servos necessarily produce some distortion in the sinusoidal output, it is, in many instances, not important because of the low-pass filter characteristics of the servo actuator. However, if a large Coulomb friction force should be present in the mechanical output linkages, the desired sinusoidal output might deteriorate and be useless.

Apparently, the method of inducing the switching or other nonlinear characteristics in a system is important, particularly if sinusoidal outputs are desired. For instance, Caldwell and Rideout had to modify their nonlinear system to prevent the servo from becoming a frequency divider with certain input amplitudes and frequencies.

From the preceding discussion, it appears that a servo which is designed to work with general inputs is different from the servo which is originally designed and optimized for step inputs, and, as Mr. Stout suggests, it is difficult to predict what a change in nonlinear system parameters will have on the character of the response. Accordingly, it would be difficult to predict whether the effect of a given Coulomb friction torque on a modified system would be much different from that which was predicted for the original servo.

Variations of system parameters and additional time lags, which are inherent in any complex servo, also affect performance of an idealized system and make modifications necessary. Such effects are not easily analyzed on the phase plane, the necessary modifications are difficult to synthesize, and consequently the actual effects of friction on the final system performance cannot be as readily calculated as they were in this paper.

However, Mr. Stout is to be commended for his analysis. It illustrates rather vividly that, with proper adjustments, Coulomb friction may have much less effect on the performance of a relay servomechanism than might be expected.

REFERENCE

1. COULOMB FRICTION IN FEEDBACK CONTROL SYSTEMS, Vinton B. Haas, Jr. *AIEE Transactions*, vol. 72, pt. II, May 1953, pp. 119–26.

T. M. Stout: The response of a linear dynamic system to any particular test input completely determines the response to any other input. For nonlinear systems, however, there is no theoretical connection between the responses to different types of inputs. In fact, the response to a step input of a particular magnitude does not even determine the response to step inputs of other magnitudes. A complete understanding of the behavior of any nonlinear system can therefore be obtained only by a series of investigations for the inputs of interest.

Since the analytical methods now available are most applicable to simple systems, investigators can perhaps be forgiven for attacking problems piecemeal. The phase-plane method was used here because it seemed appropriate for the problem. Computer techniques appear to be essential for more general studies, although it should be mentioned that phase-space methods have been applied to higher order switching servomechanisms of the type discussed here.[1]

When a relay servomechanism employing a nonlinear lead network was first proposed, some engineers felt that the apparent superiority of this system might disappear if other inputs and various possible defects in the system were considered. Investigations of some of these questions are presented in the papers mentioned by Mr. Axelby.

The present paper is one of several recent papers[2,3] dealing with other aspects of this system and attempting to remove some of the assumptions made in the original analysis. In stating the conclusions, it might have been advisable to restate the initial assumptions of this paper: step inputs, instantaneous switching at the best possible combination of error and error rate, and no additional energy storage or time delays. The conclusion given is valid only under these restricted conditions and no claim is made that similar conclusions would be reached under other conditions.

It might also be emphasized that the conclusions reached in any such study are partly a matter of the criteria employed and the tastes of the designer. Recognizing the primacy of design specifications and the limited validity of tests with a single type of input, the author nevertheless feels that integral criteria of the type used in the paper have a legitimate place in nonlinear system evaluation. Such criteria account for the magnitude dependence of nonlinear phenomena and provide a method for assessing the importance of parameter variations from their desired values.

REFERENCES

1. AN INVESTIGATION OF THE SWITCHING CRITERIA FOR HIGHER ORDER CONTACTOR SERVOMECHANISMS, I. Bogner. *Ph D. Thesis*, University of Michigan, Ann Arbor, Mich., 1953.

2. ERRORS IN RELAY SERVO SYSTEMS, Louis F. Kazda. *AIEE Transactions*, vol. 72, pt. II, Nov. 1953, pp 323–28.

3. SWITCHING ERRORS IN AN OPTIMUM RELAY SERVOMECHANISM, T. M. Stout. *National Electronics Conference*, Chicago, Ill., Sept. 28, 1953.

Characteristic Power Requirements for Performing Various Functions in Underground Coal Mines

H. P. MUSSER
MEMBER AIEE

MANY CHANGES in coal mining methods have been taking place during the past two decades as a result of mechanization. Electrical motor drives are now used for a great variety of functions. In order to design proper underground power transmission and distribution circuits, to select the correct size and location of transforming or converting units, and to estimate power supply needs and costs, it is desirable to determine typical demand and energy-consumption requirements for both individual operations and area needs.

The size of a motor used to operate certain mining equipment does not necessarily fix the demand and energy consumption that might be expected in comparison to similar requirements of other smaller or larger motors. There are many factors affecting the demand and energy consumption per connected horsepower, such as the type and condition of a particular piece of equipment, the rate at which a mining operation is performed, and the human element of handling equipment. The data assembled from many tests and studies show sufficiently consistent results to draw definite conclusions regarding demands and energy consumptions related to horsepower ratings for performing various functions in underground mining.

The Tortoise and Hare Race of Tonnage and Power

An excellent way to illustrate the growth of mechanization in coal mining is to compare the tons of coal produced per horsepower connected at two widely separated periods. For instance, in 1931 a group of 23 companies with outputs in the 30,000 to 60,000 ton-per-month class produced an average of 30.22 tons of coal

---

Paper 53-360, recommended by the AIEE Mining and Metal Industry Committee and approved by the AIEE Committee on Technical Operations for presentation at the AIEE Middle Eastern District Meeting, Charleston, W. Va., September 29–October 1, 1953. Manuscript submitted June 29, 1953; made available for printing July 29, 1953.

H. P. MUSSER is with the West Virginia Engineering Company, Charleston, W. Va.

Table I. Variation of Power Consumption with Rated Horsepower of Mining Machines

Connected Horsepower	Number of Places Cut	Number of Seams	Average Demand in Kilowatts	Average Watt-Hours per Square Foot of Kerf
30	6	1	19.54	32.84
35	20	7	27.16	46.77
50	22	4	28.54	47.16
65	68	1	24.82	31.32*
75	17	1	41.47	48.95

* This seam of coal easier to cut than average seam

per month for each horsepower in electric equipment connected, whereas in 1951 a similar group in the same tonnage class produced only 16.39 tons for each connected horsepower. Naturally, as the amount of connected load increased, the over-all demand and energy consumption followed in nearly direct proportions, but in certain individual applications or mining operations, the demands and energy requirements are more or less constant and do not change with changes in rated horsepower.

The power consumption in underground coal mines as related to connected horsepower for certain operations or areas will be discussed in this paper. All data presented are based upon actual tests extending over a long period of time. Unless otherwise stated, all values apply to the demand and energy consumption at the face. These values of necessity are less than those registered at the metering point or center of distribution because of transmission, conversion, and transformation losses.

Mining Machines

POWER REQUIREMENTS AS RELATED TO CONNECTED HORSEPOWER

The mining machine used to cut coal at the face is the one piece of equipment which was almost universally used in bituminous coal mines before the automatic miners such as Colmol, Continuous Miner, and others made their appearance several years ago. It is still the piece of machinery common to more mines than any other item of equipment unless fans are considered.

Table II. Variation of Power Consumption with Age of Bits, 65-Horsepower Mining Machine

Age of Bits	Number of Places Cut	Average Demand in Kilowatts	Average Watt-Hours per Square Foot of Kerf
Worn out	13	25.94	37.80
Half used	8	25.11	25.60
New	5	24.33	18.50

Actual tests have shown that the demand and energy requirements of mining machines do not vary with the horsepower rating as directly as might be expected. In fact, a mining machine of 50-horsepower rating will normally create demand and consume energy in quantities just slightly larger than a 35-horsepower machine, see Table I.

It is obvious that energy-consumption figures for mining machines based on tonnage would provide no true basis of comparison between cutting coal in a seam 3 feet high and in a seam 6 feet high. The only basis of comparison for power consumption by mining machines is in energy use per square foot of kerf. Kerf is defined as the undercut (or other types of cuts) made to assist the breaking of the coal. For example, if the mining machine has a 6-foot cutter bar, and is undercutting a face 20 feet wide, there would be 120 square feet of kerf. For convenience, the term watt-hours per square foot of kerf will be used.

By referring to Table I, marked similarity in demand and energy requirements can be noted between the 35-horsepower and 50-horsepower mining machines. The low energy consumption as listed in the table for the 65-horsepower machine is not representative of that horsepower rating, because all of the tests for that category were made in one seam, which seam is more easily cut than the average. The 75-horsepower mining machine created a larger demand than the machines of lower horsepower rating, but the energy consumption for a definite unit of work performed was almost identical. This is exactly as it should be, since demand, expressed in kilowatts, is a measure of the rate of doing work and the watt-hours, required to cut a square foot of kerf, are a measure of a definite amount of work done, regardless of the time required for doing the work. By contrast with the power consumption data as shown in Table I, one 75-horsepower mining machine cutting 20 places in the Chilton seam, where sandstone streaks existed, used an average of 142.39 watt-hours per square foot of kerf, or almost three times as much energy. This clearly illustrates the range of energy use that is possible under varying conditions. However, many tests by machines of different horsepower ratings in a variety of seams substantiate the generalization that cutting coal under normal conditions with ordinary bits consumes about 50 watt-hours per square foot of kerf.

POWER REQUIREMENTS AS AFFECTED BY TYPE AND CONDITION OF BITS

Table II outlines the variation of power consumption with the new or worn condition of bits used on the mining machine cutter bar chain. The mining machine using new or sharp bits consumed less than one-half the energy of the machine using old worn out bits. This points out quite strikingly how bit sharpness effects energy consumption. However, in contrast, the demands created by machines using new, half used, or worn out bits were almost the same. This indicates that the dull bits do not consume power at a faster rate but because of the bit dullness the machine must operate for a longer period of time to make the cut, thereby using more energy. The demand or rate of using power remains about the same, but the time element increases the energy consumption required to cut a unit of kerf when dull bits are used.

As might be expected in the operation of mining machines, energy consumption varies considerably with the use of different types of bits, but surprisingly the demand does not vary in a similar manner. Table III shows this variation quite clearly, with one type of bit using almost twice the energy used by another type. Several different types of bits are in general use for mining machines:

1. A bit which is used and then resharpened repeatedly by heat treatment;
2. A bit which is used once and then thrown away;
3. Several types of bits which are carbide tipped and hold their cutting edge so well that they can be used for cutting longer than any of the other types before resharpening.

Only small variations in demand are

Table III. Variation of Power Consumption with Different Type Bits, 65-Horsepower Mining Machine

Type Bit	Number of Places Cut	Average Demand in Kilowatts	Average Watt-Hours per Square Foot of Kerf
Type No. 1	5	24.33	18.50
Type No. 2	18	22.67	29.70
Type No. 3	15	25.63	32.90

Table IV. Variation of Power Consumption with Rated Horsepower of Loading Machines

Type Loader	Connected Horsepower	Substation Demand	Kilowatt-Hours per Ton
Type No. 1	20	10	0.423
Type No. 2	25	20	0.405
Type No. 3	50	12	0.364

caused by using different type bits and therefore the energy variation results from the time required to cut a place. The tests outlined in Tables II and III were both made with a 65-horsepower mining machine, and were a part of the 68 places cut by the 65-horsepower machine in Table I in a seam which is easier to cut than the average coal seam, thereby accounting for the low power-consumption figures. Although these figures are not representative power-consumption figures, they reflect quite accurately how energy use varies with bit dullness and with different types of bits.

Loading Machines

Although there have been numerous machines designed through the years to load coal, the modern-type loading machines in general use today only came into wide acceptance in the bituminous coal industry about 1935. Since that time there has been a trend to wider use of loading machines as mechanization at the mines increased, and although the automatic miners made their appearance about 1948, the loading machine is still widely used. Even though the automatic miners were designed to replace the loading machine as well as the mining machine and drill, in practice it is observed that many loading machines are operating behind automatic miners so that the room floor can act as a surge bin and thereby permit the automatic miners to more nearly fulfill their mission, that is, continuous operation. This practice is in use because the coal-hauling facilities at many mines do not remove the coal from the automatic miners as rapidly as it is mined. Actual tests over the years have shown that between 0.35 and 0.5 kilowatt hours per ton are required by loading machines. As was found with mining machines, the energy consumption for loading machines does not vary directly with horsepower rating.

Table IV outlines the results of tests where three different types of loading machines of varying horsepower ratings were operated in the same mine. It should be noted that the demand figures listed in this table were recorded at the substation and therefore are slightly higher than the demands at the face because of transmission losses. The loader type no. 1, with 20-horsepower rating, created the lowest demand of the three types but used the most energy. The explanation for this fact is that the machine operates slower, creating less demand, but takes longer to load a ton of coal, and thereby uses more energy. Loader type no. 2 created a much higher demand than the other two loaders, as a result of the manner in which it loads coal but, operating considerably faster than loader type no. 1, it consumed less energy to load a ton of coal than the no. 1 type. Loader type no. 3, with much the largest horsepower rating, consumed the least energy of any of the three types and created only slightly more demand than no. 1 loader. This no. 3 loading machine is faster in its operation than no. 1 loader, therefore uses less energy, and its operating cycle is smoother than type no. 2 and creates much less demand.

Automatic Miners

About 1948, two automatic miners were placed on the market: one, the Continuous Miner, was built by Joy Manufacturing Company, Pittsburgh, Pa., and the other, the Colmol, was built by the Jeffrey Manufacturing Company, Columbus, Ohio. Since that time several other manufacturers have built machines designed to do the same job. These machines were planned to replace the mining machine, drill, and loading machine, and to cut and load the coal in one operation. These automatic miners created new electrical problems as soon as they began operation. These problems are:[1]

1. "The miner combines in one operation what were formerly three separate machine operations: cutting, drilling, and loading. When "all eggs are in one basket," as in the continuous miner, any stoppage means total loss of production. As ways are devised to make these miners more truly "continuous," this problem becomes increasingly important.

2. "The rate of advance of the miner is comparatively rapid, requiring corresponding measures for rapidly advancing the electrical system.

3. "We have far more horsepower in the continuous miner than formerly concentrated in any one machine. In a system where several miners are operating in a limited area, the concentration of power is quite considerable."

It is extremely important to maintain a good voltage supply to these machines since the torque requirements are considerable, and for a special reason with machines operated by direct current. Since under d-c operation, motor speed is a function of voltage, it follows that voltage means tonnage. In fact, one company raised the voltage 18 per cent and the tonnage increased nearly 50 per cent. The automatic miners are an ideal application for a-c power, and so long as the voltage is maintained above the critical "pull out" level, the motors operate at practically constant speed. The importance of maintaining good voltage regulation for the supply to a-c motors is emphasized by the fact that the torque of an a-c motor varies as the square of the voltage.

The automatic miners are rated between 150 and 163 horsepower. In a series of 10 tests using two of the automatic miners, the average energy use was 2.25 kilowatt-hours per ton. The average demand created in two tests, each in a different seam, for one automatic miner was 87.5 kw. The average demand created in seven tests in four different seams for another automatic miner was 86 kw, or almost identical in amount with the other machine.

One test was made at a substation feeding a complete extraction unit having a total connected load of 285 horsepower, which consisted of an automatic miner and gathering and haulage conveyors necessary to transport the coal to the tipple. Naturally taking data at the substation means the transmission losses will be included and therefore both the energy and demand values are higher than would be the case for values taken at the face. This test was recorded for a period of $6^1/_2$ hours, during which the automatic miner advanced 80 feet in a coal seam $3^1/_2$ feet high and at a face 20 feet wide. The energy consumed by this

Table V. Power Use for Gathering Coal with Locomotives Operating in Series or in Parallel, 60-Horsepower Locomotives

Motors Connected	Rated Speed in Miles per Hour	Tons Gathered per Day	Energy Use per Day, Kilowatt-Hours	Kilowatt-Hours per Ton
Series	3	176.3	54.2	0.307
Parallel	6	154.8	108.2	0.698

285 horsepower of connected load was 4.18 kilowatt-hours per ton at the substation.

Gathering

Three primary methods are used to gather the coal from the faces where it is mined and to deliver it to the main haulageways. These are by rail, by either chain or shaker conveyors, and by shuttle cars. Energy use for either method varies between 0.25 and 0.5 kilowatt-hour per ton under average conditions, without appreciable difference between the methods. However, in considering demands a difference is found, since gathering locomotives would create demands in excess of conveyors or shuttle cars.

One demand test made on a face chain conveyor 50 feet long, with a 5-horsepower motor driving it, showed the average demand to be 2.3 kw. To operate this same conveyor empty required 1.3 kw, or 56.5 per cent of the average demand created while moving coal. This load, measured when the conveyor was empty, is the friction load, which was smaller for this installation than is normally found.

On another demand test made on a room chain conveyor 260 feet long, driven by a 10-horsepower motor, the average demand was found to be 7.38 kw, or almost the rated capacity of the motor. On this installation momentary overloads occurred. The load required to drive this chain conveyor empty was 5.2 kw, or 70 per cent of the average demand created while moving coal, which is a normal condition for chain conveyors. This forcefully demonstrates the magnitude of friction loads normally experienced with conveyor operation.

An interesting experiment in power use for gathering coal by rail was made in which two gathering locomotives were used, one rated at 3 miles per hour and the other at 6 miles per hour. Both locomotives were rated at 60 horsepower, the slow speed one having motors operated in series, and the fast speed one using motors operating in parallel. The results of this test are outlined in Table V, and show how greatly energy consumption can vary with locomotives of the same horsepower, but operating with different motor connections. It will be noted from the table that the parallel-connected locomotive, rated at twice the speed of the series-connected locomotive, actually gathered less coal and consumed more than twice the energy per ton. This condition exists, because with the faster speed, there is more spinning of the wheels, extra power required for acceleration, and considerable power wasted in the resistances (running on points).

Table VI. Equipment Horsepower Ratings

Number of Machines	Equipment	Horsepower
4	Mining machine	140
4	Face conveyor	20
2	Room conveyor	20
2	Blower	6
1	Car hoist	5
4	Coal drill	6
	Total	197

Table VII. Variation of Power Consumption by Haulage Locomotives with Distance and Grade

Test No.	Distance in Feet	Average Grade in Per Cent*	Average Coal Load in Tons	Momentary Peak Demand in Kilowatts	Average Demand in Kilowatts	Energy Used in Kilowatt-Hours	Energy Use per Ton Kilowatt-Hours per Ton
No. 1 Test	3,000	3.83	45	316	211	14.13	0.314
No. 2 Test	5,000	3.20	45	267	196	23.28	0.517

* Against loads

Conveyor Loading Section

Many mines operate sections in which the coal is cut, drilled, and shot in the traditional manner and then loaded by hand onto chain conveyors. A test was made on such a section to determine the demand and energy requirements. This section contained equipment with horsepower ratings as shown in Table VI.

As expected, the results indicate a large diversity of operation between the units during the six hours of the test, particularly the mining machines. The highest peak reached momentarily was 82.5 kw. The highest 15-minute period which would be the demand of interest for billing purposes was 44 kw. The energy consumption for this section was 0.79 kilowatt-hour per ton. This amount of energy drilled and undercut the coal at four faces, and then gathered it by conveyors to the point where the main haulage system received it.

Haulage

In a previous section, gathering was described as transporting the coal from the faces to a central point where the main haulage system received it. The means of transportation to move the coal from this central point to the tipple is known as the haulage system. Two principal methods of haulage are in widespread use today, namely, rail and conveyor belts. Naturally, for either system, power consumption will vary greatly with grades and the length of haulage. Therefore, any demand and energy figures will be dependent to a large extent on these factors. However, for most mines, the energy consumption for haulage will be between 0.5 and 1.5 kilowatt-hours per ton, with differences in grades and distance as previously pointed out, resulting in values both less and greater than this.

Tests were made on rail haulage in which two locomotives, one pulling and the other pushing, hauled the same load over different distances and slightly different grades. The locomotives used in the tests were a 13-ton unit rated at 156 horsepower and a 10-ton unit rated at 120 horsepower, or a total connected load of 276 horsepower. The results of the tests are outlined in Table VII.

In the second test the distance increased 66.6 per cent, and the energy use per ton increased 64.6 per cent to effectively illustrate the direct effect distance has on the energy consumption per ton of coal hauled by rail. However, as the distance increased 66.6 per cent in the second test, the average demand decreased 7.1 per cent, because of a reduction in grade against which the loads were hauled. In the second test the energy use per ton was 0.517 kilowatt-hour for a haulage distance of 5,000 feet. It is readily apparent that large energy use per ton is experienced with haulage distances of 25,000 feet and over, which are not uncommon.

A large part of the power to drive belt conveyors used for haulage purposes is consumed in overcoming the friction load. One test made on a 36-inch conveyor belt, 2,850 feet long and driven by a 75-horsepower motor, showed a demand of 65 kw, or indicated an overloaded condition. To run this same belt empty created a demand of 37.5 kw, or 57.7 per cent of the operating demand.

On another test of a 36-inch conveyor, 2,100 feet long, driven also by a 75-horsepower motor, the average demand was only 45.6 kw. This smaller demand reflects the reduced tonnage moved by this belt. The friction load created a 36-kw demand, or 79 per cent of the demand required to run coal on the belt. This friction load is unusually high and may have been caused by insufficient lubricant on the rollers.

Conclusion

The connected horsepower sometimes is an indication as to what the energy and demand requirements will be for a specific operation such as a haulage locomotive, but often the horsepower rating is not reflected, as in the case of mining machines. It is vital to bear in mind that each mine has certain conditions which are unique, and that the data presented here is based on the average figures for many mines unless otherwise stated. In the cases where specific tests are presented, it should not be assumed that these are necessarily made in mines with average conditions. On the other hand, the conditions affecting each test have been made a part of the data for that test.

Reference

1. Power for Continous Miners, W. A. MacCalla. *Proceedings*, Coal Mining Institute of America, Pittsburgh, Pa.

No Discussion

The Effect of Reactive Components in the Measurement of Grounding Circuits

L. H. HARRISON
MEMBER AIEE

KNOWLEDGE CONCERNING the electrical characteristics of the earth's surface is important in safe operation of electric equipment. Such knowledge is helpful in application of lightning protection to power systems, protection against shock hazards, and protection against premature blasting accidents where electric shot firing is used.

Various devices are available for measuring the resistivity of circuits through the earth, and have been in wide use for a number of years. The method generally used is based upon work by the National Bureau of Standards in 1918, and alternating current is used for measuring, on the theory that the readings will then be unaffected by stray or extraneous voltages in the earth. The devices are calibrated to read directly in ohms, and it has been generally assumed that Ohm's law is applicable to circuits through the earth.

Electric current does not always flow from a power system into the earth in accordance with Ohm's law, when the ohmic values used have been determined by tests made with commercial ground testers. Investigation has indicated that there is a reactive component that must be considered, and this involves the test leads as well as the earth circuit itself.

Tests from Power Circuits

An investigation conducted in the Pittsburgh district of western Pennsylvania involved transmission of voice-modulated signals through the earth. The antenna system for such transmission usually consisted of a section of earth strata between two electrodes driven into the earth; or, in a coal mine, between the mine track and an electrode in the roof. It was possible to put more power into the earth circuit through the same electrodes with the higher frequencies. The curve, Fig. 1, indicates this relationship for some of the tests made.

Comparative tests using direct current and alternating current from mine power circuits were also made. Data typical of these tests are shown in Tables I and II. These data were obtained with current flowing into a circuit made up of two ground rods installed in the bottom of a mine entry and the earth between. Voltages were measured from one electrode to various points in the earth. When measured with a commercial-type ground tester, these electrodes indicated values of 48 and 68 ohms, or a total for the earth circuit through the electrodes of 116 ohms. There was some fluctuation in the d-c voltage during these tests, and this accounts for the variation in the current. The alternating voltage remained steady; therefore the current values remained constant.

Comparison of these tables shows that the d-c resistance checked with the measured 68 ohms at $5^{1}/_{2}$ feet from the electrode; however, the impedance of the same circuits with alternating current indicated considerably lower values.

Tests with Higher Frequencies

To investigate further the impedance characteristics of the earth surface, tests were made using frequencies from 30 cycles to 200 kc, inclusive, as well as with direct current. For these tests, two metal-pipe electrodes were driven into the ground about 45 feet apart, *A* and *B*, Fig. 2. In line with these, and approximately 11 feet from each, two additional electrodes, *C* and *D*, were driven. Each electrode then was measured with a standard-type ground resistance tester, and the resistance to ground of each elec-

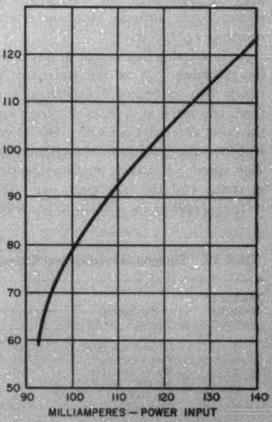

Fig. 1. Frequency versus power input

Paper 53-359, recommended by the AIEE Mining and Metal Industry Committee and approved by the AIEE Committee on Technical Operations for presentation at the AIEE Middle Eastern District Meeting, Charleston, W. Va., September 29–October 1, 1953. Manuscript submitted June 29, 1953; made available for printing August 5, 1953.

L. H. Harrison is with the United States Bureau of Mines, Birmingham, Ala.

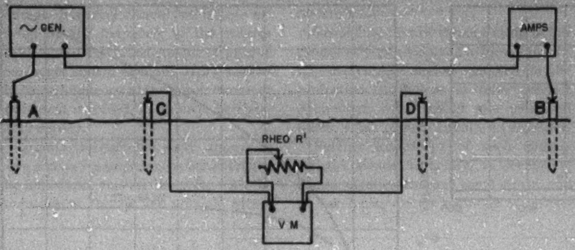

Fig. 2. Typical test circuit for various frequencies

Rheostat R' adjusted to halve the normal voltage; then $R' = R$

Ground tests
Rod A = 90 ohms
Rod B = 110 ohms
Rod C = 150 ohms
Rod D = 250 ohms

trode was indicated as follows: $A = 90$ ohms, $B = 110$ ohms, $C = 150$ ohms, and $D = 250$ ohms. The ground circuit between *C* and *D* was measured, using direct current, and it indicated a resistance of 730 ohms.

To make the tests, a signal generator was then connected to electrodes *A* and *B* with a milliammeter in series with the circuit. A vacuum-tube voltmeter was connected between inner electrodes *C* and *D* to measure the voltage drop across the earth circuit when current flowed in the ground. To save time in calculating the resistance or impedance of the circuit, a 0- to 1,000-ohm variable rheostat was connected across the terminals of the voltmeter, and 100 milliamperes of alternating current was caused to flow through the ground between electrodes *A* and *B*. The current value was held constant, and the signal generator adjusted for various frequencies. Rheostat *R*, Fig. 2, was adjusted to halve the voltage reading, and thus the position of the rheostat indicated the value of impedance in the circuit under test. The graphic curve, Fig. 3, shows the relationship of impedance to frequency indicated in these tests.

Measurements of voltage drops across a section of earth with 100 milliamperes flowing in the circuit indicated a difference of 40 per cent in voltage drop, between electrodes for frequencies from 30 to 200 kilocycles. The fact that about 25-per-cent difference is indicated for a variation in frequencies from 0 (direct current) to 1,000 cycles appears significant in the consideration of ground measurements. Fig. 4 shows the relationship of impedance to frequency from 0 to 1,000 cycles.

Tests were made with unmodulated carrier signals transmitted through various thicknesses of overburden from an underground mine to the surface, without the aid of metallic conductors. It was found that stronger signals were received with transmission at the lower frequencies. The output power of the transmitter was held constant. These results were thought to have been accomplished by a greater spread of the current from the transmitter, because of the increased impedance of the antenna path at the lower frequencies.

Ground Measurements

Ground-resistance measurements are usually associated with safety in operation of electric equipment around coal mines. Because ground measurements made with commercial ground testers usually are read directly in ohms, it is generally thought that Ohm's law can be applied. This is true only when the entire circuit is considered; even then, it does not always hold true.

If a grounding electrode is measured and the probable current flow calculated, using the ohmic value indicated and the line voltage, the result is likely to be at great variance with the actual current. The curves, Fig. 5, show results of typical tests of this kind, using power from a mine power circuit. To obtain these data, copperweld ground rods were driven into the earth 1 foot at a time. Resistance measurements were made, and the current was measured and calculated for each foot of electrode depth.

At a coal-gasification project in Alabama, electrocarbonization was used as a means of igniting the coal bed. Four holes about 60 feet apart were drilled from the surface into the coal lying about 180 feet below. The holes were cased with 6-inch steel pipe, and electrodes installed inside the pipe. The electrodes consisted of 4-inch stainless-steel cylinders, 17 inches in length, to which was attached a 2-inch steel pipe with a copper cable inside, both of which extended from the coal bed to the surface. These elec-

Table I. Test Data with Direct Current

Distance from Electrode, Inches	Amperes Flowing	Voltage Readings	Ohms Calculated
6	1.68	86	51.2
12	1.73	89	51.4
18	1.75	95	54.3
24	1.82	96	52.7
30	1.83	101	55.3
36	1.85	104.5	56.5
42	1.86	108.3	58.3
48	1.86	110	59.2
54	1.90	115	60.6
60	1.86	118	63.4
66	1.78	122	68.5

Table II. Comparative Test with Alternating Current

Distance from Electrode, Inches	Amperes Flowing	Voltage Readings	Ohms Calculated
6	1.52	13	8.55
12	1.52	16	10.53
18	1.52	25	16.45
24	1.52	30	19.74
30	1.52	35	23.03
36	1.52	40	26.32
42	1.52	45	29.61
48	1.52	48	31.58
54	1.52	50	32.89
60	1.52	52.2	34.34
66	1.52	55	36.18

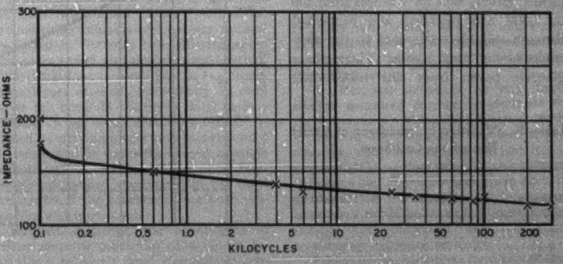

Fig. 3. Relationship of impedance to frequency

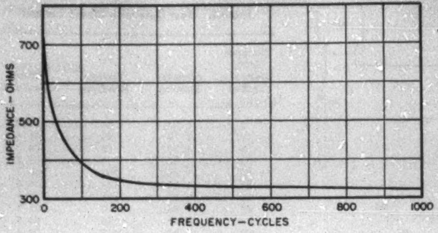

Fig. 4 (above). Change in impedance, 0 to 1,000 cycles

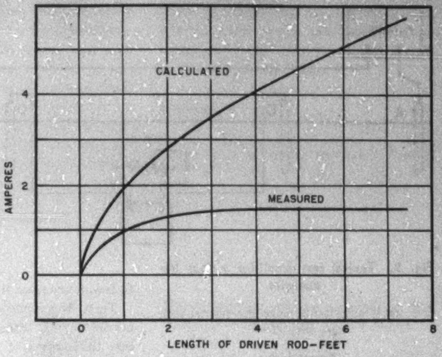

Fig. 5. Impedance measured and calculated with different depths of electrode

trodes were insulated from the steel casings by means of transite pipe and insulating-fiber centering disks at the surface terminals. The electrodes were embedded in the coal, and the 6-inch casings were in contact with the top of the coal seam. The resistance between the electrode and the casing in the no. 2 hole measured 7.5 ohms.

To determine the best value of voltage to apply for the initial carbonizing tests, a series of very careful ground-resistance measurements were made. Because power would be applied to the nos. 2 and 3 electrodes first, most of the tests were made on these holes. The no. 2 electrode measured 8.37 ohms, and the no. 3 electrode 7.9 ohms. The casing in the no. 2 hole measured 2.5 ohms to ground, and that in the no. 3 hole 2.75 ohms to ground. The circuit, including electrodes 2 and 3 with the earth circuit in series, measured 17 ohms. Later, after water had been removed from the holes, the circuit resistance was indicated at 20.9 ohms.

Alternating current, at 60 cycles, from an isolated circuit was then applied to the no. 2 electrode and the no. 3 electrode in series. Current and voltage readings were taken at short-time intervals, and the resistance was calculated, with results shown in Table III. The ohms calculated from the first readings varied considerably from the ohms measured. The impedance of the circuit dropped gradually as the test voltage was continuously applied.

A 500-kva variable-voltage autotransformer, having taps for voltages from 200 to 1,800 was installed and connected through suitable equipment to the electrodes in nos. 2 and 3 holes. Single phase 60-cycle power from this transformer was applied at 800 volts, but the switchboard ammeter failed to indicate current flowing. It was expected, having applied 800 volts to a circuit which had measured 21 ohms, that a current of 38 amperes would flow. After a check of the circuits and metering equipment had been made, 800 volts was again applied, with the same results. A portable ammeter was then used to measure the current in the circuit, which at that time measured 3 amperes.

Table III. Variation in Impedance of Circuit Through the Coal Seam

Amperes	Volts	Ohms (Calculated)
1.95	75.5	38.7
2.15	73.0	33.9
2.50	66.0	26.4
2.75	62.0	22.5

Subsequent voltage and current readings taken at short-time intervals indicated a lowering impedance as the current path through the coal bed was gradually carbonized. The graphic curve, Fig. 6, shows the relationship of the impedance calculated to impedance measured.

It is interesting to note that, in this instance, three different values of impedance were indicated:

1. A value of 21 ohms when measured with a ground tester;
2. A value of 38.7 ohms when a 60-cycle voltage of 75.5 was applied to the circuit;
3. A value of 266 ohms when a 60-cycle voltage of 800 was impressed on the circuit.

This apparent phenomenon has been noted in other instances, where ground measurements were made with ground testers and with current from industrial power circuits.

Conclusions

The flow of electric current in circuits through the earth is affected by reactive components, which must be considered in the accurate calculation of current flow or voltage drop in such circuits,

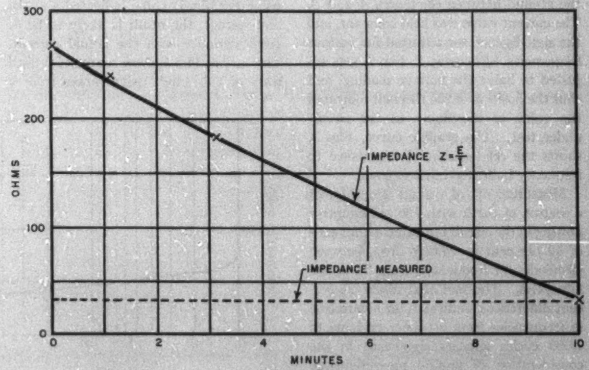

Fig. 6. Relationship of calculated impedance to measured impedance

Voltage drop and current values are affected by the frequency of the voltage applied, and the measurement of ground impedance should be made with power of the same frequency as the power circuit or equipment involved, in order to be rigorously correct.

Circuits through the earth appear to have a negative impedance characteristic, the impedance varying inversely with the frequency of the applied voltage, within certain limits.

Grounding circuits through earth strata cannot be depended upon to blow a fuse or trip overcurrent devices installed for the protection of motors or other electric equipment, even though the measured ohmic value of such circuits so indicates.

Further knowledge of such characteristics should be helpful in developing communication through earth strata, and in developing better methods of protection against shock and premature blasting hazards.

References

1. Applicability of Radio to Emergency Mine Communications, E. W. Felegy, E. J. Coggeshall. *Report of Investigations 4294*, United States Bureau of Mines, Washington, D. C., 1948.

2. Some Characteristics of the Earth as a Conductor of Electric Current, M. C. McCall, L. H. Harrison. *Report of Investigations 4903*, United States Bureau of Mines, Washington, D. C.

◆

Discussion

E. B. Curdts (James G. Biddle Company, Philadelphia, Pa.): This paper is interesting in that it reveals the existence of problems in mining activities which may call for a better understanding of the characteristics of electrodes associated with or surrounded by earth in general.

In dealing with problems involving the flow of electric current in the earth, it has been generally agreed that opposition to such flow is usually an electrolytic phenomenon and does not conform to accepted theories describing the transmission of electric charges through metals. Furthermore, the relative geometry of the elements of ground circuits usually does not conform with that involved in ordinary metallic circuits, requiring a somewhat different treatment in reaching conclusions concerning current flow and voltage gradients.

In commenting on this paper exception can first be taken to the broad statements in the third paragraph concerning Ohm's law and the ohmic values obtained from commercial ground testers. Commercial ground testers are logically calibrated to indicate the ratio of voltage to a current, which is what the user wishes to know, but there is no reason to assume that the linearity of Ohm's law must apply in such measurements because the device is calibrated in ohms.

Commercial ground testers of the more commonly used types are provided with either a-c or polarity reversing sources, and are available in the frequency range of from about 25 to 100 cycles or reversals per second. In the case of the crossed-coil ohmmeter type of ground tester which uses a hand-cranked generator for its source of supply, the frequency or reversals per second may be varied by the cranking speed to avoid objectionable beat frequencies with commercial 25-, 50-, and 60-cycle extraneous voltages in the earth. Those commercial instruments using battery-vibrators are usually designed for one fixed frequency in the order of 100 cycles for the same reason.

The crossed-coil ohmmeter type ground tester, recognized in section 3.43 of AIEE Standard no. *550*,[1] does not have an alternating output in the ordinary sense, but through dead zones in the mechanical reversers the current is forced to zero at the instant of the voltage zero so there can be no phase displacement between the two. In other words, at least this particular type of commercial ground tester is intended to measure resistance and not impedance. Even if the ground circuits should have any reactive properties they would not be measured as such by ground testers of this type since there are no quadrature components in the measuring circuit.

The author's statement concerning test leads is also open to question, particularly in connection with the current interrupter type of ground tester. It has been demonstrated by practical field measurements with such instruments that self- and mutual reactances between leads causes no significant errors, even with a very close and very long coupling. It has been claimed that lead reactance has caused errors when using ground testers of the current interrupter type when measuring large grounding grids. Since the design features used in this type of ground tester are such that reactive components are suppressed, it is more likely that any errors encountered were the result of mutual resistance effects between the earth under test and the current reference, these effects being caused by the current reference electrode not being sufficiently remote from the electrode under test.

As is generally known, the reason why commercial ground testers use alternating or reversing current rather than direct current in making ground tests is to eliminate for practical purposes the effects of electrolytic polarizations. Unless the volumes of earth surrounding the electrodes are entirely free of electrolytic moisture, a d-c test of one polarity would indicate higher resistance values than those obtained with alternating or reversing voltages due to gas films forming and being sustained at the surfaces of the electrodes. Therefore, under conditions of electrolytic dissociation there should be no reason to expect that measurements made with commercial and higher frequencies, or with commercial ground testers, should conform to those made with direct current. However, experience has indicated that there are no difficulties in co-ordinating ground-fault protection on d-c circuits with currents determined from commercial ground-tester measurements where natural variations in electrode to earth resistances are given sound engineering consideration. Wide variations in conditions in the immediate layers of earth surrounding an electrode can occur in relatively short periods of time. More stable conditions can be obtained by driving longer rods to permanent moisture and by properly spaced multiple rods to reduce current density. Mr. Harrison's unqualified statements in the third paragraph of the conclusions are both misleading and questionable.

Without disputing the possibilities of minor reactive properties of a circuit involving a relatively small electrode in contact with an infinite mass such as the earth, it would appear likely that the anomalies encountered in the cases cited by the author, at least at the lower frequencies, could be due to unstable or nonreproducible conditions surrounding the electrodes. Such instabilities, not only due to electrolytic dissociation in the case of the d-c tests, can be caused by changes in electrode to earth contact conditions such as moisture variations, and thermal changes due to the magnitude of the test current used, including the drying out of the earth immediately surrounding the electrodes. The geometrical characteristics of an electrode to earth contact cannot be overlooked in considering the voltage gradients that exist as a result of current. It can be simply shown that the greatest voltage gradient, and therefore most of the resistance, appears in the earth layers immediately surrounding the electrode. Thus, any physical, chemical, or thermal changes occuring in these immediate layers may greatly affect the measure resistances without any reactive properties existing.

The results of the test, as shown in Fig. 5, are extremely puzzling. It has been demonstrated in numerous instances that ground resistance measurements can be relied upon to determine current flow unless the actual current is of sufficient magnitude and duration to increase the earth temperature or to dry out the earth immediately surrounding the electrode. Where steep wave-front high-amplitude current impulses are involved it has been found that actual breakdown of high gradient layers occurs, resulting in deviations from the calculated current values.

The calculated current values shown in Fig. 5 seem to conform with practical and theoretical results when the resistance measurement is made to remote earth. The actual current curve does not, but instead shows a flatness with increasing rod depth which one would expect to find if the reference rod forming the 2-terminal network were of such high resistance, compared to the rod under test, that it became the controlling factor.

Mr. Harrison attributes the very much smaller measured current to electrode to earth reactance. Using the 7-foot rod depth in Fig. 5, the calculated current is 5.5 amperes, and the measured current is 1.5 amperes. Calculating the relative values of resistance and reactance from these data, it is found that the reactance component of impedance would be about 3.5 times that of the resistance component. Such a situation would seem extremely unlikely.

The measuring technique for a test of this kind is simple, so there should be no cause to question the one used in this case. Although the technique is not described, it would be natural to assume that the same 2-terminal network was used for both the calculated and measured tests, which would give comparable results. However, the results indicate that a 2-terminal network was used to determine the actual 60-cycle current, and a 3-terminal network to determine the resistance to remote earth of the rod being tested. Any attempt to compare a 2-terminal with a 3-terminal test would be invalid. It is also assumed that the power system used was either an ungrounded one, or if not, then the system ground was used as reference (the rod under test being connected to the ungrounded side of the source).

In summarizing this particular phase of the investigation covered by this paper, I cannot but help being left with the feeling that because of the lack of information concerning measurement technique, and because of the great difference in measured and calculated currents as shown in Fig. 5, that there is no conclusive evidence that this great current difference can be accounted for by reactive effects in the rod to earth contact.

Mr. Harrison discusses, in the section entitled "Tests with Higher Frequencies," and shows in Fig. 2, some details of the technique used in making the frequency-impedance measurements. Actually this test, from the information given, turns out to be a measure of the combined impedance characteristics of two unrelated parts of the circuit. One of these parts involved the mutual impedance between points *A* and *B* when measured with a high impedance voltmeter and with R' at infinity. The other part involved the net impedance of rods *C* and *D*. The measurements as described in this paper actually resulted in the sums of the mutual impedance of rods *A* and *B*, and the net impedance of rods *C* and *D*.

The question then arises as to just what information was being sought in this investigation. If the electrode to earth impedance was the information desired, then an additional question arises. Were the measurements which resulted in values of 150 ohms and 250 ohms for the *C* and *D* rods taken to remote earth; if so, what was the mutual resistance between these two rods? In other words, did this investigation have as its purpose the determination of the impedance-frequency effects of an electrode to remote earth, or just between two rods chosen to be spaced 23 feet apart?

Even assuming that the measuring circuit was valid for the purpose intended, some assurance should be given by Mr. Harrison that the ammeter, voltmeter, and rheostat involved were accurate over the wide range of frequencies used in these tests. It is conceivable that skin effect alone in the rheostat could account for the negative-impedance characteristic shown in Fig. 3.

Mr. Harrison makes reference to the Bureau of Mines report no. *4903* on this subject, which he co-authored. However, the information given in the Bureau of Mines report conflicts with that given in this paper. A comparison of the two shows that the test described in the paper is not represented by Fig. 3 as stated, but represents data from an entirely different 2-terminal test as described in the Bureau of Mines report. Fig. 4 apparently represents data resulting from the 4-terminal test described in the AIEE paper. Data tabulated in the Bureau of Mines report roughly checks the curve shown in Fig. 4 of the AIEE paper. Assuming that the tabulated data in the Bureau of Mines report are valid, the 30-cycle impedance is 450 ohms and the 60-cycle impedance is 420 ohms, a reduction of 6.7 per cent in the range of these commercial frequencies. The 730-ohm figure for the d-c test can be discarded as irrelevant unless the measurement was made before electrolytic dissociation developed, which was unlikely.

The anomalies encountered in the test in connection with the coal-gasification project are challenging, to say the least. However, a study of the information given leads one to believe that these anomalies are caused entirely by changing conditions around the electrode between the different tests. Again it must be emphasized that the resistance of electrodes surrounded by earth is confined largely to the immediate layers of earth and is greatly influenced by conditions of moisture and temperature.

Summarizing this discussion, Mr. Harrison is to be commended for pointing out the wide variations that can occur in electrode to earth contacts, even though the reactive effects may not be as pronounced as his paper may lead one to believe.

REFERENCE

1. MASTER TEST CODE FOR RESISTANCE MEASUREMENT. *AIEE Standard No. 550*, May 1949.

Richard W. Inman (Associated Research, Inc., Chicago 18, Ill.): To properly evaluate Mr. Harrison's paper, one must ask several questions, any one of which has a distinct bearing on the accuracy of the statements made and the conclusions reached. Consequently this discussion must take the nature of a question rather than a comment.

Very little reference is given to the equipment used in the performance of the various measurements and tests. For instance, was the commercial type of ground tester a d-c or an a-c unit? If it was an a-c tester, of what frequency and voltage were the output?

Where d-c data were submitted, was any considerations given to reversed readings to eliminate the possibility of error due to electrolytic potentials or stray currents within the area of measurement?

There are various types of commercial ground resistance testers presumedly designed to measure resistance to earth of man-made grounds and to do so on the basis that Ohm's law is applicable to circuits through the earth. Experience has indicated, however, that while these testers may be calibrated directly in ohms under various conditions to be found in conjunction with the measurement of ground resistance, it is impossible to closely check the readings of one type of tester with another; yet it is possible to obtain repetitive readings of the same magnitude for the same tester under the same given set of conditions.

It is a known fact that some testers are materially affected by the resistance of the auxiliary probes while others are not. The sensitivity and response of other testers are affected by the relation of the auxiliary probe resistance to that of the resistance of the man-made ground under test.

It is apparent, therefore, that considerations of the measurements technique involved, the relative spacing of the auxiliary probes, the depth of rod, and several other factors are essential. Equally important in evaluation of the material presented would be data as to the depth of penetration of the man-made ground rods as well as depth of penetration of the auxiliary probes and whether one or two were used and what the spacing of them was.

It is true that measurements with commercial testers are usually made directly in ohms, but in so doing it is natural that operation of the over-all circuit must be understood. The same would seem to apply to the information in Fig. 5 concerning which the statement is made that power was used from the mine power circuit. Equally important would be the method of measurement used in determining the factors making up the curves contained in Fig. 5.

Here reference is made to the question of whether consideration was given to the theory of the sphere of influence of a ground rod in relation to its depth and the consequent spacing of auxiliary probes in the ground-resistance measurement. As the water content of the earth has a material effect upon the resistance of any ground rod driven into the earth, and as all too often the water content is changing, unless the timing of any testing is relatively short in duration, it would appear extremely difficult to propose absolute statements and conclusions.

If one compares the readings of Table III with the final reading taken after the water had been removed from the holes, then the variations are not too great and on the basis of the statement that the impedance of the circuit dropped gradually as the test voltage was continuously applied one would certainly be lead to believe that a change in circuit conditions resulting from the watts in the circuit under test was a contributing factor rather than an error in reading resulting from the change in impedance. Is it not reasonable to assume that possibly due to a continuous application of current potentials to the circuit under test a drying-out effect was taking place, which in turn would naturally affect what was assumed to be the impedance of the circuit rather that its d-c resistance?

The flow of electric current into the earth is affected not only by the apparent resistance to earth of the man-made ground connection but also by the character of the earth surrounding the ground, by electrolytic potentials and currents in the earth, and by the earth resistivity in the area of the ground contact. The fact that there is variation between calculated current values and actual measured current values can be considered more as a summation of these grounding factors than as a conclusion that it is entirely due to the reactive components in ground resistance. It would seem very possible that we are dealing with a nonlinear active resistance, the value of which is frequency dependent. Perhaps we are also dealing with a combination of nonlinear resistances and reactances, any or all of which could be present and effect measurements made if cognizance is not taken of effect upon measurements of man-made grounds located within the sphere of influence of the test electrodes.

L. H. Harrison: Some very interesting points have been brought out in these discussions. Mr. Curdts' statement to the effect that there is no reason to assume that the linearity of Ohm's law must apply in such measurements is strange indeed. It would seem that where a resistance measurement is given in ohms this would be the logical assumption.

Reference is made to the crossed-coil, mechanical-reverser type of ground tester by Mr. Curdts, who states that, even if the ground circuits should have any reactive properties, they would not be measured as such by this type of ground tester. It is hard to conceive of phase displacement with the square-wave form of alternating current produced by the mechanical reverser; nevertheless, it can be demonstrated that the addition of capacitance to the resistance of the circuit under test will lower the reading obtained with this type of instrument in about the same proportions as that of the battery-powered vibrator types.

Many textbooks, Bureau of Standards papers, and technical bulletins on ground-resistance testing give the equation $R = \rho(1/2\pi C)$ for the resistance to the flow of current away from an electrode in the earth, where C = the combined electrostatic capacity in free space of the electrode and its image above the surface of the earth. If this equation is valid, then every circuit comprising one or more grounding electrodes and a section of the earth's surface has capacitive reactance as one of its component parts. Mr. Inman states that it would seem very possible that we are dealing with a nonlinear active resistance, the value of which is frequency dependent. This is merely another way of saying that we are dealing with circuits having resistance components and reactance components, which was my original contention.

It is regrettable that these discussions either ignore or pass lightly over the results of tests made at the coal-gasification project. The theory of electrolytic dissociation is inadequate to cover the anomalies indicated, since such wide variations in impedance were observed with the same frequency of applied voltage. Neither can they be explained by changing conditions around the electrodes in the time elapsed between the different tests, as the power for carbonization was first applied within a matter of minutes after the low-voltage 60-cycle resistance test was completed. The suggestion that the increased resistance might be due to a drying-out effect caused by the continuous application of current is not acceptable because it is shown in Table III and by the curve of Fig. 6 that the impedance of the circuit was gradually lowered by the continuous application of current. If, however, we can conceive of this circuit as comprising a capacitance with a high leakage dielectric, it is possible to work out a plausible explanation of the phenomena observed.

My paper deals primarily with the measurement of grounding circuits intended to limit the voltages that might appear on the frames of electric equipment upon occurrence of a ground fault within the equipment. If such ground measurements do not indicate accurately the impedance of this fault-current circuit, they are valueless as a means of determining the degree of protection provided. There is need to distinguish between ground measurements for system protection against lightning and those made to provide protection from shock hazard.

I am indebted to Mr. Curdts and Mr. Inman for their valuable contributions to the available knowledge of ground-testing procedure, and their interest in this paper is greatly appreciated.

Wanted: A Modern Diesel-Electric Rail Car

K. O. ANDERSON
ASSOCIATE MEMBER AIEE

THE self-propelled rail car is returning to a place of popularity as the railroads seek to reduce costs and attract additional passenger business. Current rail-car application in the United States covers relatively long main-line runs with diesel-hydraulic cars, and branch line service with light diesel-electric cars. Between these two extremes there lies a need for a main-line type of car capable of performing suburban service. Certain characteristics of the electric drive are well suited to this application.

Trends in Rail Passenger Business

A ghost has returned to our nation's railroads. Considered dead for the past 20 odd years, the diesel-powered rail car has come back in numbers as railroads are reawakening to the advantage of providing adequate passenger service for their patrons.

Not all roads, it is true, are trying to better their passenger service. Almost every week the Interstate Commerce Commission is petitioned to permit abandonment of another run. But there are some reversals to this trend. The New Haven, most notably, in the past year has added more than 50 new passenger trains to its schedules. It is planning even more, because it has found the passenger business lucrative. Rail cars are used on most of these new runs.

Other roads, too, are finding rail cars the answer to many of their passenger problems. Through their use, deficit operations have been turned into moneymakers, or losses have been cut down considerably. Many of these roads are finding that rail cars make new services both possible and profitable. The New York Central, for instance, has restored passenger service to Midland, Mich., for the first time in 25 years.

As the number of automobiles and trucks in operation continues to increase, our nation's highway system becomes ever more crowded. This problem, existing everywhere, but particularly critical in our more crowded areas, brings traffic to a literal crawl, and makes driving extremely hazardous, to say nothing of the human frustration involved.

Thus there is a natural tendency to turn to the rails for relief, wherever adequate service is offered. The word adequate here means clean, comfortable equipment, operating on a fast schedule, and with reasonable frequency. Even crowded highways are preferable to a dirty, green-plush-upholstered coach of 1900 vintage creaking along behind a steamer at 20 miles per hour. Passengers will simply refuse to ride in such cars.

Place of the Rail Car

Locomotive-hauled streamliners are suitable for long-distance runs, where enough demand exists to fill several cars. But on many of the shorter and interurban schedules, only one or two cars are required, which makes locomotive power and investment excessive and therefore uneconomical. Diesel-powered rail cars appear to answer these requirements very well. The new ones being put into service today are clean and quiet, have high accelerating rates and high top speeds, and are economical to operate.

The well-known Budd *RDC*, of which 116 are in operation or on order, is used on 13 United States railroads and in three foreign countries. Its two 275 gross horsepower engines and 63 tons

---

Paper 53-361, recommended by the AIEE Land Transportation Committee and approved by the AIEE Committee on Technical Operations for presentation at the AIEE Middle Eastern District Meeting, Charleston, W. Va., September 29–October 1, 1953. Manuscript submitted June 29, 1953; made available for printing August 4, 1953.

K. O. ANDERSON is with the General Electric Company, Erie, Pa.

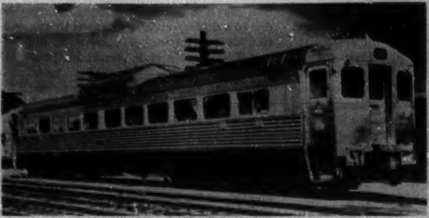

Fig. 1. Type of diesel-hydraulic rail car in current use on a number of American railroads

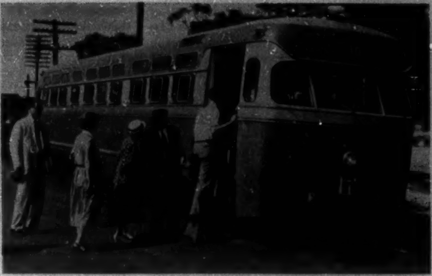

Fig. 3. Mack FCD diesel-electric rail car in service

loaded weight give it an exceedingly high horsepower per ton ratio and consequently good acceleration characteristics. The hydraulic transmission—the first to be introduced for main-line rail service in the United States—has proved itself in service despite the skepticism of many experts. Operating costs reasonably close to those predicted have been obtained.

Best of all is the flexibility that this new railroad tool has provided, as compared with locomotive-hauled trains. On the Pennsylvania-Reading Seashore lines, for instance, six cars in multiple unit with only one crew leave Camden. At Tuckahoe, two cars are cut off, and taken by another crew to Ocean City, while the other four proceed on the main line to Wildwood Junction. Again two are cut off for Cape May while the original crew proceeds with the remaining cars to Wildwood. On the return trip to Camden, a reverse procedure is followed.

Flexibility is the keynote of every rail car. Because it is a self-contained unit, it can be operated singly or in multiple as scheduling demands, and can be changed from one to the other with a minimum of effort.

Another, smaller, diesel-powered rail car with electric drive has been introduced on the New Haven. Named the Mack *FCD* rail car, the single pilot model has now been in operation more than a year. After a lapse of 24 years, Fall River, Mass. now has passenger service provided by this "Little Shoreliner."

The original car has a Mack 180-horsepower engine. The General Electric drive consists of a traction generator of the variety used on industrial diesel-electric locomotives and four Presidents' Conference Committee (PCC)-car type traction motors, together with suitable single-end single-unit control. It seats 45 passengers, has a top speed of 54 miles per hour, and is equipped with air brakes. Essentially then, it is a Mack highway bus mounted on PCC trucks for rail operation.

The New Haven likes this car so well it has placed an order for nine additional units. These new cars will seat 50 passengers, and have 150-horsepower engines, and top speed of 60 miles per hour. They will have double-end control and be equipped to operate two in multiple, thus giving additional flexibility.

Electric Drive for Main-Line Cars

These two different types of modern diesel-powered rail cars are not fundamentally competitive. They are far apart in total weight, horsepower, and seating capacity, as well as first cost. Their respective operating costs compare favorably to these factors. The Budd *RDC* is intended for main-line operation and has the necessary speed to stay out of the way of other traffic. The Mack rail car is an ideal unit for light branch line service.

But a gap still exists in the needs of railroads for modern rail-car equipment of main-line size. A car is needed to do several things that any car equipped with a hydraulic transmission, in its present state of development, cannot do. These needs are:

1. Good acceleration characteristics at low speeds.
2. Ability to pull trailers.
3. Ability to operate in electrified tunnels, such as at Grand Central Terminal, N. Y.

Electric drive can fill this gap!

The hydraulic transmission used on rail cars has its maximum torque at zero speed versus torque at maximum speed limited to about 3-to-1 ratio. This ratio is commonly called wraparound. In contrast, an electric drive, even with a single motor connection, can easily provide six or seven to one wraparound.

Therefore, of two cars with the same horsepower per ton ratio, the one with

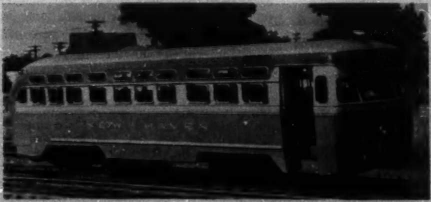

Fig. 2 (left). Original Mack FCD diesel-electric rail car built for the New York, New Haven and Hartford Rail Road

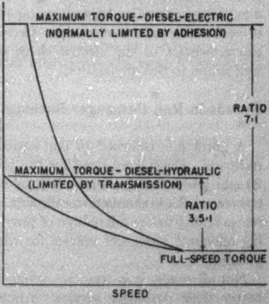

Fig. 4. Typical wraparound characteristic for diesel-electric drive compared with that for diesel-hydraulic transmission

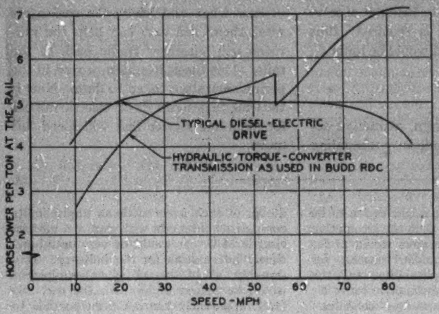

Fig. 5. Transmission characteristics for diesel-powered rail cars

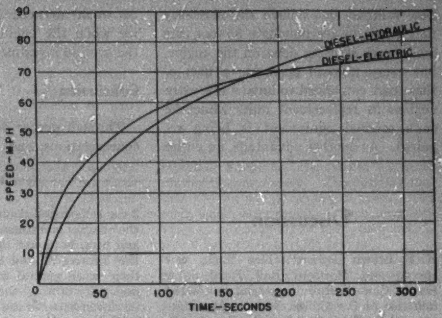

Fig. 6. Speed-time characteristics for a diesel-electric and a diesel-hydraulic rail car (equal horsepower per ton ratios)

electric drive can accelerate up to approximately 65 miles per hour more quickly than can the one with hydraulic transmission. This means that the former can cover a run of 5 to 6 miles or less more quickly than can the latter. Many commuter schedules call for stops only 1 or 2 miles apart. Obviously, a car with electric drive will do such jobs better.

For runs of greater length, the hydraulic transmission car has the advantage, since it goes into "locked-up" direct drive, where the only loss is in the gearing. Here, it should be noted, it is the practice to run the engine at higher speeds than when the transmission is in use, thus actually producing more horsepower, since engine torque is essentially constant.

Use of Trailers

In addition to the high rate of acceleration at low speeds, the rail car equipped with electric drive can easily pull trailers without harm. Thus much greater flexibility of operation without excessive added investment can be obtained. The diesel-hydraulic car, as now applied to United States railroads, is not designed for pulling trailers. While the diesel-electric rail car will have somewhat lower acceleration when pulling a trailer than when running by itself, it will not deteriorate in performance so much as to be unusable. The balancing speed on level tangent track of a motor car-trailer car combination (of equal weights) will be only about 10 per cent less than that of a motor car alone.

Ordinary passenger coaches could be used as trailers with this rail car so long as they were self-contained units. That is, they need not be dependent upon the power car for either train heat or electric power. Since the required heating load of a passenger car in zero degree Fahrenheit weather is approximately equal to the air-conditioning load in summer, the diesel-electric undercar power plant would provide both these services, thus making the car truly independent. As an added benefit, this car would not then have the axle generator type of power supply which provides an additional drag on the prime mover of the train.

Operating and Maintenance Advantages

Railroads are already finding difficulty in operating diesel-powered rail cars when they must enter electrified tunnel zones, where the engines cannot be run underground. In the case of the diesel-hydraulic car, the only recourse is to pull the car with an electric locomotive, but in the case of the diesel-electric car it would be a comparatively simple matter to provide third-rail pickup and additional control to operate the car from third-rail power.

At the present time, the hydraulic transmission is still a mystery to most railroad shops. Consequently, this transmission is often returned to the manufacturer when it needs repair. On the other hand, with but one exception, all the class-I railroads in the United States now have diesel-electric locomotives and could easily service a diesel-electric rail car. It is even conceivable that many of the same components could be used on the rail cars that are now in use on the locomotives, thereby easing the renewal parts problem.

In all railroad equipment, reliability and low maintenance costs are the key to success. For a new design of diesel-electric rail car, then, reliability must be built into it. Most of all, as the heart of the car, the engine or engines must be thoroughly reliable. Many railroad men are inclined to look down their noses at a high-speed (1,800 to 2,100 rpm) engine because they doubt its reliability. Some of them feel that an engine operating at 1,000 rpm or less is inherently more reliable. Unfortunately, several high-speed engines have been improperly applied in railroad service and thus the whole series of these engines has suffered in reputation. On the other hand, high-speed engines have performed well on industrial locomotives and in thousands of automotive applications. Fundamentally a high-speed engine properly applied can be just as reliable as a low-speed engine. And the lower weight, smaller space, and probable lower cost of a high-speed engine are not to be taken lightly in design of the over-all car.

The problem of maintenance should not be overlooked in a car's design. This will mean that the entire engine or perhaps the complete power unit must be easily removed from the car so that it can be taken to a convenient place for work.

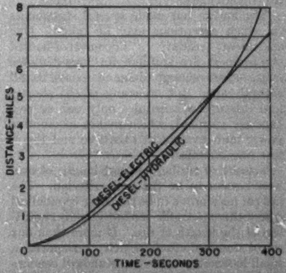

Fig. 7. Distance-time characteristics for a diesel-electric and a diesel-hydraulic rail car (equal horsepower per ton ratios)

Few railroad shops have the necessary floor space to accommodate 85-foot cars while work is being done on the engine, but every railroad operating a fleet of these cars can afford to have a few extra engines as replacement units while the car's original equipment is being repaired. As another advantage, an entire car would not need to be held out of service while the engine is repaired; thus the over-all investment would be lower.

Conclusion

Through proper design, attractive accommodations, and judicious scheduling of runs when and where the passengers want them, rail cars can help the railroads win passenger traffic back to the rails. This thesis has been proved in the preliminary steps taken to date. Now is the time to design a diesel-electric rail car for main-line service that will speed this move.

Discussion

H. F. Brown (Retired) (New York, New Haven and Hartford Rail Road, New Haven, Conn.): Rail cars are not new on the railroads of the United States. Manufacturers have been building them and railroads have been using them continuously for the past 45 years. They have been gasoline-electric (General Electric 1907), gasoline with mechanical drive (Keene 1912, Mack 1920), high-pressure steam (Sentinel, Bessler, 1935), and diesel-electric (Goodyear-Westinghouse "Comet," 1936), to mention but a few. Each was supposed to be the solution for declining or nonprofitable passenger traffic on branch lines, or for local traffic on sections of main lines where this traffic was being lost to the highways.

What happened to all these cars? The answer is simple: they became too expensive to maintain, and were too expensive in first cost to replace. Present-day types, to survive, must not have either of these shortcomings. The Budd Rail Diesel Car mentioned in the paper is one of the latest and one of the best designs to date. It is not exactly a ghost; it is a very live descendant of famous ancestry. Whether it has inherited the short life of its predecessors or not is too early to say.

Rail cars are used abroad for passenger service much more than in this country, and handle a large portion of the passenger traffic. They are used for the same economic reasons that make railway electrification more extensively used in those countries than here. Very few of these single car units have electric drive. There are, however, many 3- and 5-car units of the most "modern" design with electric drive operating throughout Europe today. In view of this, the title of the paper is somewhat misleading, as it implies that modern diesel-electric cars do not exist.

The author has made several statements to which exceptions may be taken. One statement reads: "Locomotive-hauled streamliners are suitable for long-distance runs, where enough demand exists to fill several cars. But on many of the shorter and interurban schedules only one or two cars are required, which makes locomotive power and investment excessive and therefore uneconomical."

Volume of traffic, and not length of run, would seem to be the real criterion. The rail car may prove to be the more economical where there is traffic for but one car regardless of the length of run. If more than one car of standard coach capacity is required, a small locomotive with two standard coaches might well prove to be the more economical investment when compared with the cost of two rail cars. If 2-car or 3-car operation is a known requisite, possibly a 2-car or 3-car self-propelled unit might prove to be the cheaper investment than the locomotive and cars, but most operators would prefer the locomotive and standard coaches for their more general applicability, and the possibility of using the locomotive for other service in between the passenger schedules.

The operation cited of the 6-car train all made up of self-propelled units, and broken up during the run into three 2-car trains, represents an investment of nearly $1,000,000 which is at least $250,000 greater than the investment required for three 1,000-horsepower diesel-electric locomotives and six new standard coaches. It is thus apparent that "excessive investment" is not always on the side of locomotive operation, and that other factors may govern.

If it has been possible by careful design and good engineering to build a good diesel rail-car with just enough power for the acceleration and speed required and with control features for multiple-unit operation with other similar units, why penalize its cost and performance as a single unit by adding capacity to haul a trailer. Regardless of the type of drive, the acceleration and speed will be impaired with the trailer. Thus, the combination will not be able to render the service for which the single car unit was designed. If instead, another self-propelled unit is added, to be operated in multiple with the first, the design characteristics for acceleration and speed are retained. If this operation is thought to be uneconomical as to investment, then possibly the same criticism can be made of 1-car operation.

No self-propelled car yet designed, either here or abroad, regardless of whether mechanical or electrical drive, can equal the economical performance in operation or maintenance of the electric multiple-unit car taking power from a contact conductor. The author states that a diesel-electric rail car is wanted "to operate in electrified tunnels, such as at Grand Central Terminal, New York." Such a suggestion seems utterly inconceivable. It is doubtful if there would be space in such a busy terminal for single-car operation. To operate such cars in trains made up of the number of cars required would mean a large duplication of investment which would be useless over the greater portion of the run. If it is desirable to operate through suburban service from parts of lines not now electrified into the Grand Central Terminal, it would be far more economical to extend the electric operation to include such lines, rather than to operate such high cost cars on their own power, or even to haul them through the electrified zone into the electrified terminal.

If, as the author states, it is "a comparatively simple matter to provide third-rail pickup and additional control to operate the car from third-rail power," a paper on the design of such a car with an approximate comparison of its cost with that of a modern electric M.U. car would be very useful and timely information for the industry. Presumably, all of this additional equipment would be placed underneath the car. So far it apparently has not been possible to even design a diesel-electric locomotive for such operation with reasonable cost, or to justify the economics of operating such a locomotive beyond the electrified territory.

The diesel rail car, like the diesel locomotive, undoubtably has its economic place in modern railroad transportation. The operation of neither can be economically justified in underground or totally enclosed suburban passenger terminals already electrified.

P. H. Hatch (General Electric Company, Erie, Pa.): After World War I the railroads of this country were faced with serious difficulties in branch-line passenger train operation arising from increasing highway competition and mounting expenses involved in running passenger trains of the conventional type (steam locomotive and cars). In an attempt to retain traffic and reduce expenses they resorted to the use of lightweight cars powered by internal combustion engines. Initial success with rather crude vehicles equipped with mechanical drives led to an intensive development of rail cars. As sizes of both cars and prime movers increased, electric drives were developed and applied. Starting with a few cars scattered among a few railroads the number grew until many hundreds were in use all over the country.

Then, even more suddenly than it had started, the rail car boom collapsed about 1930 as it became clear that most branch-line passenger traffic could not economically be retained.

The ensuing growth and application of the diesel-electric locomotive, first as a switcher and then as passenger and freight units, occupied the attention of the railroads through the 1930's and the years of World War II. Again, as after World War I, the problem of passenger train operation came to the fore. This time, however, the trouble involved the main line rather than the branch lines. In both cases the reasons were the same: diminishing passenger traffic and rising expenses.

This situation, logically enough, led to the development of the diesel-hydraulic rail car manufactured by Budd and the smaller diesel-electric rail car manufactured by Mack, both of which are described in Mr. Anderson's paper.

In railroad service, electric drive has proved itself superior to all other types in respect to reliability, low maintenance, and flexibility. If rail cars, singly or in multiple, are going to be the answer to the large-scale handling of passenger service in the future, then these advantages cannot be overlooked. This is well presented by Mr. Anderson and it warrants careful consideration. Unfortunately, however, several factors contribute to make the area of usefulness of the diesel rail car rather vulnerable, so the future of this type of railroad equipment is at present somewhat uncertain.

K. O. Anderson: The author wishes to thank Mr. Hatch and Mr. Brown for their constructive discussions.

Mr. Brown is quite correct in stating that, where more capacity than provided by one standard coach is required, a small locomotive with two standard coaches might well prove to be more economical in first cost than two rail cars. By "small" locomotive, it is assumed that he means light in weight, not just small in horsepower.

But the fact remains that United States class-I railroads, in general, have been reluctant to buy lightweight locomotives for any purpose. When the first cost of a 1,500- or 1,600-horsepower locomotive and two standard coaches is compared with the first cost of two rail cars of equal seating capacity, the latter will normally have a lower original investment.

Other factors may well govern the choice of equipment. These factors are so numerous and vary so widely among different operations and various railroads that each case must be considered specifically. It is exceedingly difficult to make valid generalizations that will apply to all. Some of these factors are utilization of equipment for other than passenger services, labor costs as determined by particular union agreements, maintenance costs of "standard" versus "nonstandard" motive power, fuel costs, and revenues as influenced by passenger acceptance of different types of equipment.

In regard to this last factor, modern rail cars have found high favor among passengers wherever introduced. In the few instances where these new cars have been displaced by old coaches and locomotives, for varying reasons, the traffic created by the rail cars was quickly dissipated again, because the older cars were dirty and uncomfortable and the schedules were slow.

Certainly, as Mr. Brown points out, the acceleration and top speed of a rail car will suffer when pulling a trailer as compared to operating by itself. But, if the motor car has an electric drive, it can pull a trailer without harm to the drive when the operating conditions warrant this operation. In this case, the electric drive provides flexibility of operation that other type drives may not provide.

The growth of automobile traffic, like a parasitic vine, is strangling our cities. Some solution must be found which will be more desirable to the commuter than driving his automobile into the city. One possibility would be to have high-speed rail service available on many branch lines. These lines would converge as they neared the city and quickly deliver the commuter to a central terminal, such as at Grand Central. Better yet, the cars could even be operated onto the subway system, thus bringing the commuter right to the front door of his place of business. This latter possibility is being actively considered in at least one large American city.

It is questionable that these many branch lines could be economically electrified, especially as the suburbs expand and commuting distances grow. The deciding economic factor will be density of traffic. The main track, after several branch lines converge, could certainly be electrified, since it would have enough traffic density.

It was not meant to imply that addition of third-rail pickup and suitable control to a diesel-electric rail car for operation off third-rail power was easy—to be done without considerable thought and development. But is it not "comparatively simple" to add this equipment to a car already equipped with electric traction motors, as opposed to a car with a hydraulic transmission?

As both discussers state, the rail car has a place in railroad operation. The many railroad companies have had varying degrees of success in finding this niche in their own operations. Electric drive on a rail car does provide certain advantages. The author sincerely believes that diesel-electric rail cars will eventually be widely applied on the American railroads, and that a suitable solution for commuting problems, perhaps with dual-power rail cars, will be found.

Technical Aspects of Application of Electric Equipment in Coal Preparation Plants

W. R. MORTON
ASSOCIATE MEMBER AIEE

THE INCREASED cleaning required to provide coal which will meet present-day market requirements has greatly expanded the use of processing equipment in coal preparation plants. This places increased emphasis on the selection of the electric equipment to obtain the utmost in safety, reliability, and efficiency. The various phases of the electric system should be considered early in the planning stages so that the location of the mechanical and electric equipment may be properly co-ordinated.

In viewing the electric equipment, the following should be carefully considered:

1. Total power requirements
2. Power distribution equipment
3. Motors
4. Control equipment
5. Selection of cable

The following discussion is intended to point out many of the present-day concepts which should be given due consideration.

Power Requirements

There is no fixed ratio of connected horsepower (hp) to tons of coal cleaned per hour since the power depends upon the process used and whether or not there is a large quantity of fine coal to be cleaned. However, in the early stages, before the complete plant is well defined, it is desirable to have some yardstick of approximate power requirements. A check of quite a number of plants already built indicates that, where there is little or no fine coal cleaning, between 2 and 3 connected hp per tons per hour (tph) has been required. When considerable fine coal cleaning is involved the figures may well be as high as 4 to 5 hp per tph. If we consider a plant designed for 750 tph, the connected hp requirement may then fall somewhere between 1,500 and 3,750.

Since the power system is designed upon the basis of kilovolt-ampere (kva) requirements, the hp must be converted to kva required. Fig. 1 shows the kva requirements of totally enclosed normal torque motors up to 150 hp for speeds of 1,800 and 1,200 rpm. Totally enclosed motors are shown since they are becoming widely used in new plants. While the kva requirements of motors below 25 hp may slightly exceed 1 kva per hp the larger motors require less. For the normal spread of hp ratings encountered in preparation plants, a figure of 1 kva per hp is considered satisfactory.

Also, since the actual selected hp rat-

Paper 53-358, recommended by the AIEE Mining and Metal Industry Committee and approved by the AIEE Committee on Technical Operations for presentation at the AIEE Middle Eastern District Meeting, Charleston, W. Va., September 29–October 1, 1953. Manuscript submitted May 27, 1953; made available for printing August 24, 1953.

W. R. Morton is with the General Electric Company, Schenectady, N. Y.

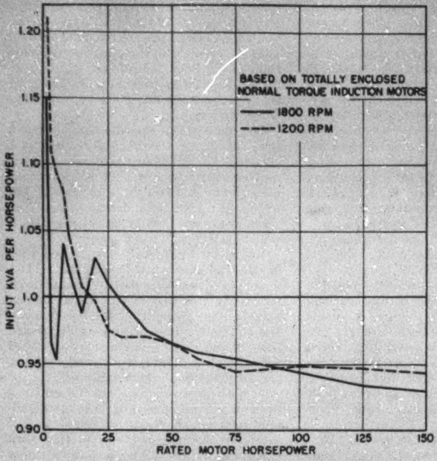

Fig. 1. Input kva per hp for various motor hp ratings

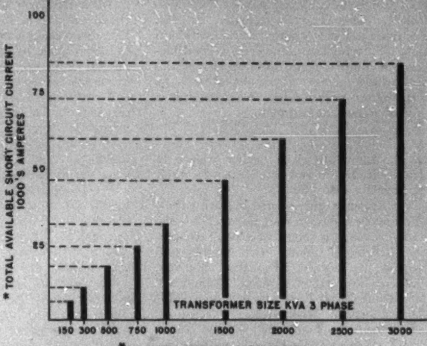

* INCLUDE MOTOR CONTRIBUTION
FOR 250,000 KVA PRIMARY SHORT CIRCUIT DUTY
IMPEDANCE NOT MORE THAN 5.5 %
480 VOLT SECONDARIES

Fig. 3 (above). Short-circuit current levels for various substation sizes

ing in most cases exceeds the calculated hp requirements because of the range of standard motor hp and because all motors are not always fully loaded at the same time, a diversity factor is used in arriving at the estimated power requirements. A diversity factor of 60 to 65 per cent will in most cases be satisfactory.

Taking all of these factors into account, the kva requirements of a preparation plant may be considered to be 65 per cent of the connected horsepower. For a 750-tph plant the range of kva might then be considered as anywhere between 975 and 2,435 kva, and in certain cases even more.

Power Distribution Equipment

Motor Voltages

Having arrived at the total kva requirements for the plant, the next consideration is how the power will be distributed to the various drives. To arrive at the best and most economical system, the hp range and the available incoming high-voltage supply should first be determined.

Knowing the hp sizes and available voltage, Fig. 2 can be used to determine whether the larger motors and control would be more economical at 440 volts or at high voltage. The comparison shown in Fig. 2 is based upon the use of the following:

1. Open, *40 C*, 1,800 rpm squirrel-cage motors.
2. Group control, type C 440-volt starters.
3. Current limiting fused starters for 2,300- and 4,000-volt starters.
4. Load center substations for 440 volts (curve *A*) at $9.00 per hp.
5. Master substations for 2,400 volts (curve *C*) at $4.00 per hp.

Variations from any of the above conditions would tend to vary the price level but by replotting all the curves on the same basis the same approximate cross-over points would result. This would then establish the following approximate economic limits:

1. If 2,300-volt power is available without use of stepdown transformers, use 440 volts for motors up to 150 hp and 2,300-volt motors, 200 hp and above.
2. If 4,160-volt power is available without use of stepdown transformers, use 440 volts for motors up to 250-hp and 4,000-volt motors, 300 hp and above.
3. If incoming lines are above 4,160 volts, use 440-volt motors up to 250 hp and 2,300-volt motors, 300 hp and above.

Use of high-voltage motors below 150 hp is not only uneconomical from the first-cost standpoint but also the windings of motors of this size are not as strong mechanically as the low-voltage motors

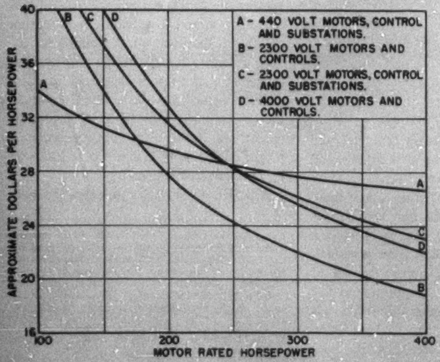

Fig. 2 (left). Approximate costs of motors, control, and substations, as a function of motor hp

Table I. Suggested Maximum Transformer Bank for Various IC Levels

IC Level	Maximum Transformer Bank
15,000 amperes	300 kva
25,000 amperes	750 kva
50,000 amperes	1,500 kva

Fig. 4. Load center unit substation

Fig. 6 (right). Comparison of line-to-ground voltage on grounded and ungrounded neutral systems

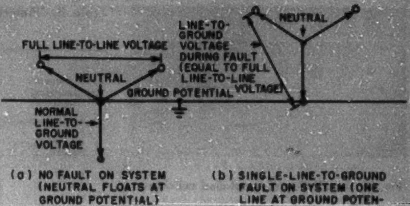
FULL LINE-TO-LINE VOLTAGE
NEUTRAL
NORMAL LINE-TO-GROUND VOLTAGE
GROUND POTENTIAL
LINE-TO-GROUND VOLTAGE DURING FAULT (EQUAL TO FULL LINE-TO-LINE VOLTAGE)
NEUTRAL

(a) NO FAULT ON SYSTEM (NEUTRAL FLOATS AT GROUND POTENTIAL)

(b) SINGLE-LINE-TO-GROUND FAULT ON SYSTEM (ONE LINE AT GROUND POTENTIAL)

because of the smaller wire sizes usually encountered.

SUBSTATIONS

Since the majority of the drives encountered in a coal preparation plant fall below the 150-hp range, it follows that there is usually a large amount of 440-volt power required. Before deciding upon the size of step-down transformer to be used, it is well to consider the short-circuit interrupting capacity (IC) available in standard low-voltage control equipment. The following interrupting levels are available: 15,000, 25,000 and 50,000 amperes rms asymmetrical. These same interrupting capacity levels as well as higher ratings are available in standard low-voltage switchgear. However, to use standard controllers the three mentioned IC levels are all that should be considered. Fig. 3 shows the total short-circuit current available, including motor contribution from various sizes of transformer banks with 250,000-kva primary short-circuit duty. Many mining properties may have considerably lower primary short-circuit duty than this. However, from the long range viewpoint it is not wise to take too much advantage of this, since the power company system may change in a few years and what was once an adequately protected low-voltage system may become inadequate. Table I indicates the suggested maximum transformer bank for the various IC levels.

Where load conditions indicate that a 1,000-kva transformer bank would be desirable, and that it is desirable to have circuit-breaker starters, the most economical solution is to use a transformer with 8 per cent impedance rather than the standard 5.5 per cent impedance. This will then lower the secondary short-circuit duty to within the 25,000-ampere IC level.

Use of transformer banks larger than 1,500 kva will usually require the use of current limiting reactors ahead of each group control, and the over-all economics in the majority of cases has been shown to be in favor of using a number of smaller transformer banks, each feeding only a portion of the load.

Since the motor load is spread over a wide area, often involving several buildings, the load center unit substation as shown in Fig. 4 is gaining wide acceptance as the best means of distributing the power. There are several factors which determine the most economical size of load center unit, as follows:

1. High-voltage feeder length
2. Low-voltage feeder length
3. Substation size

A given total load may be supplied by several different combinations of load center units. As the number of substations are increased to handle a given load, the length of high-voltage feeder cable is increased, the low-voltage feeder cable length is decreased, and the substation size is decreased. Conversely, the fewer the number of units used, the shorter the high voltage cable becomes, the longer the low-voltage cable, and the larger the substation. Fig. 5 shows how the cost, including average cable lengths, will vary as a function of substation size. It can be seen that for 480-volt secondary power, the most economical ratings are between 750 and 1,500 kva where the curve is relatively flat.

LOW-VOLTAGE GROUNDING

In the past year or so there has been considerable activity in the direction of using load centers with wye-connected low voltage, and of grounding the neutral of the 480-volt system, as contrasted to the old practice of using delta-connected low voltage and leaving the system ungrounded.

In the ungrounded system, as shown on Fig. 6, the actual neutral floats somewhere near the true electric neutral as long as there is no ground on any of the lines. However, when one line does become grounded, none of the protective devices will be tripped and the other two lines are then at 480 volts above ground.

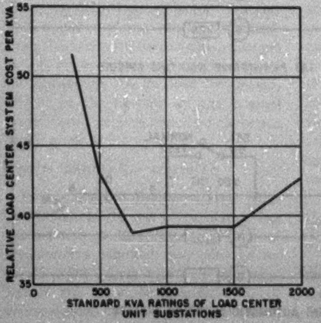

Fig. 5 (left). Relative cost of load center system as a function of substation size

Fig. 7. Possible ground-fault connection in ungrounded neutral system

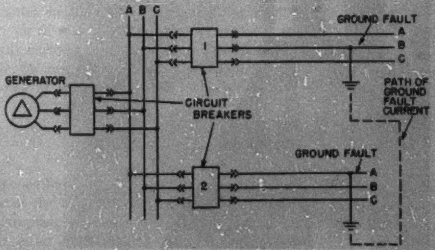

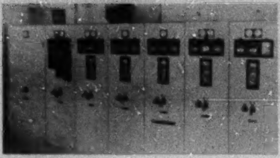

Fig. 8. Installation of metal-clad switchgear

Table II. Protective Devices and Applicable Starter Size for Various Short-Circuit Current Levels

RMS Amperes Asymmetrical IC	Type of Protective Device	NEMA* Starter Size	
		Separate Starters	Grouped Control
15,000	Molded case breaker, 225 amperes	1 to 4	1 to 4
25,000	Molded case breaker, 600 amperes	5	
	Molded case breaker, 225 amperes, backed up by magnetic 25,000 IC breaker		1 to 4
	Magnetic type breaker, 225 amperes or 600 amperes		3 to 6
	Fused switch with necessary silvered fuses	1 to 5	1 to 3
50,000	Magnetic type 25,000 IC breaker in cascade with 50,000 IC main line breaker		3 to 6
	Fused switch with low voltage current limiting fuses	1 to 3	1 to 3

* National Electrical Manufacturers Association.

Hence the ground fault remains there until the operator tracks it down and removes it.

The grounded neutral system is the safer of the two since there are only 277 volts to ground at any time. With the neutral grounded, as soon as any one of the phase conductors becomes grounded there is sufficient current flow to trip the circuit breaker or fuse protecting the circuit on which the ground occurs. This greatly simplifies the job of locating the ground fault since the breaker immediately ahead of the fault will be tripped. If the fault occurs beyond the load terminals of the motor starter, as is frequently the case, operation of the rest of the system may continue while the fault is being repaired.

Neutral grounding minimizes transient overvoltages to ground from such conditions as arcing ground faults and switching surges. Experience has shown that on ungrounded systems transient overvoltages of several times normal have occurred under such conditions and caused simultaneous failure of several pieces of electric equipment in the plant.

Another advantage is that only one motor or feeder is involved in the fault On ungrounded systems, shown in Fig. 7, phase *B* may become grounded in one motor and the operator would not know it existed, unless a ground detector were connected to the system, in which case the ground would usually be left on the system until the end of the shift. Some time later, phase *A* may go to ground in another motor in the area. In this case two motors will be involved in the fault and considerable time may be lost in clearing up the trouble.

An additional advantage is that the voltage stress-to-ground on the cables is limited to 277 volts and should therefore mean that longer cable life should be obtained and fewer ground faults arise.

The usual first reaction to using the grounded neutral 480-volt system is that there will be too much production time lost, because as soon as a ground occurs, the protective equipment shuts the unit down. However, actual experience of many operators indicates that there are fewer shutdowns with the grounded system than with the ungrounded system.

Existing delta-connected 480-volt systems can be arranged for grounding the neutral by use of a zigzag wye-connected grounding transformer which derives a neutral for the system which may be grounded.

SWITCHGEAR

When using the load center distribution system, it is often desirable to have one common point to interrupt power to the various load center units spread around the plant. In such cases, metal-clad switchgear line ups such as shown in Fig. 8 are used. The number of feeder panels needed in such a line-up will depend upon the total amount of power and the general plant layout. One breaker may be used to feed several load center substations, each with its own disconnect switch on the high voltage, provided the total kva connected to any one breaker

Fig. 9. Installation of grouped control in preparation plant

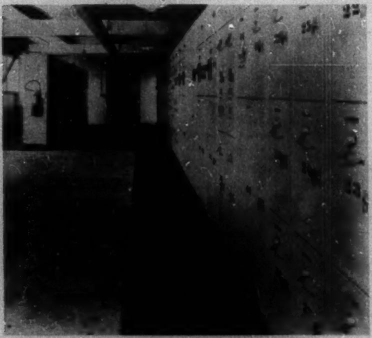

Fig. 10 (right). Typical sequence control circuits

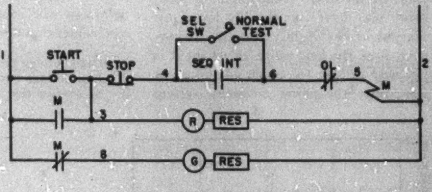

(A) PERMISSIVE STARTING CIRCUIT

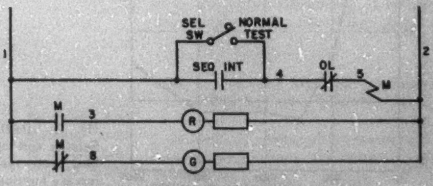

(B) AUTOMATIC STARTING CIRCUIT

Fig. 11. Desk-type push button panel

does not exceed 6 times the kva rating of the smallest bank connected to that feeder. This limitation has been selected to insure that the overcurrent devices on the breaker may be set to trip for a fault on the low-voltage side of any of the transformers.

CAPACITORS FOR POWER-FACTOR CORRECTION

Another important consideration in the modern preparation plant is that of overall plant power factor. The majority of the plant load is induction-type motors which operate at a lagging power factor. Most power companies have a penalty clause for poor power factor but there is no fixed pattern of the various clauses. Some power companies charge a penalty for anything below 80 or 85 per cent, and have a bonus for better power factor. In either case the cost of improving power factor by means of capacitors can be repaid in a relatively short time by the saving on the power bill. The amount of corrective kilovolt-amperes (kva) can very easily be determined. Knowing the required kva at a given plant, power factor will give the actual kilowatt (kw) load. Next, the desired power factor for a particular power clause must be decided. Once this is known, the corrective kilovars (kvar) of capacitors may be determined by multiplying the kw load by the difference of the tangents of the original power factor angle θ_1 and the final power factor angle θ_2.

$$\text{kvar} = \text{tangents } \theta_1 - \text{tangents } \theta_2$$

In addition to improving the plant power factor, the use of capacitors has the advantage that the total kva of transformers required may also be reduced. The degree to which the transformer size may be affected will of course depend upon the actual amount of power factor correction used.

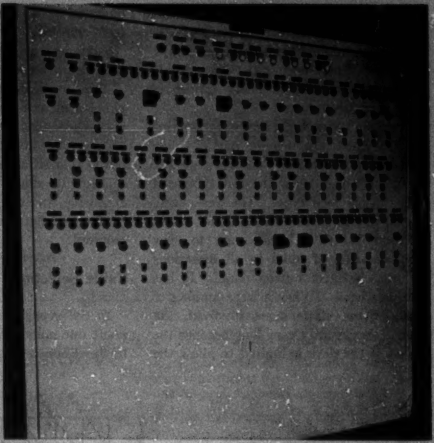

Fig. 12 (right). Vertical-type push button panels

One factor to remember in using capacitors is that the total connected kilovars on a substation should be kept below two-thirds of the substation rating to avoid the possibility of a resonant condition developing.

MOTORS

After the hp and voltage ratings have been determined, the motor type and enclosure must be selected. On drives such as blowers, pumps, air-compressors, valves and small conveyors, normal starting torque motors may be used. On medium-sized conveyors, screens, crushers and breakers, high-starting torque motors are frequently used. For the large conveyor drives, such as *ROM* conveyors, wound-rotor motors are applied so that belt stresses may be kept within predetermined limits. Centrifugal-type filters very often have a very high inertia and in such cases a careful check should be made to see whether wound-rotor motors or specially designed squirrel-cage motors are required.

When selecting the motor enclosure, the location of the motor in the plant should be considered. In the dusty portions of the plant totally enclosed motors are most suitable. In the wet cleaning sections, either dripproof or splashproof motors may be used.

Control Equipment

The control starters considered for coal preparation should be of the types having short-circuit interrupting capacity. Starters are available either separately mounted or as group controls. Both types are available in interrupting ratings of 15,000, 25,000, and 50,000 rms amperes asymmetrical, as shown in Table II.

In some preparation plants separate starters are selected and mounted throughout the plant near the motor which they control. In other plants, where separate starters are used, it has been found desirable to mount the starters on pipe racks in one or more central locations. The large majority of present-day plants utilize standard grouped control starter assemblies which are completely wired and mounted in enclosed, dead-front enclosures, such as shown in Fig. 9. In some cases these assemblies are mounted in pressurized control rooms.

One of the important considerations in the control equipment is proper sequence-interlocking to prevent costly coal pile-ups in the modern large-tonnage plants. The plant operation in conjunction with proper sequencing can be arranged for either permissive starting or for automatic starting, or a combination of both.

In permissive starting, Fig. 10(A), the control circuit is arranged so that each starter is energized by means of a push button or other initiating device, but not before the starter preceding it in sequence has been energized, unless the circuit is set up for a test operation of a unit.

The automatic starting circuit, Fig. 10(B), is arranged so that only the first unit is started by push button and then successive units start in sequence as a function of the preceding starter's being energized. In this type of circuit it is usually advisable to insert time-delay relays at various intervals in the sequence, to allow units to come up to speed before units which feed them are started. Without the addition of the time-delay relays, units would pick up in order limited only by the inherent time delay pickup of each successive starter.

In plants that use permissive starting circuits there are usually one or more master push-button control panels. These may be either of the desk type or of the vertical face type. The desk type, as shown in Fig. 11, is suitable for use in locations where it is necessary to view the operation of units in all directions around the push button panel. It has one drawback. When a large number of push button stations are involved, the panel is necessarily very long because the depth of the desk is limited to allow the operator to reach all of the push buttons from one side.

A typical application for this type of panel is in the boom operators station.

The vertical-face-type push button panel, such as shown in Fig. 12, is usually used where a large number of push button stations are involved and over-all visibility is not absolutely essential. Because of its simple construction it is less expensive, and the greater mounting area per foot of length results in less floor space required.

Cable Selection

In the over-all electrical design of the plant due consideration should be given to the selection of the cable. In selecting cable there is considerable information available to choose cable which has sufficient insulation for the system voltage and proper copper cross section to handle the load current with a reasonable voltage drop to the particular load. However, there is another important consideration: the short-circuit current which the cable must handle and the length of time that the short-circuit current will flow before the protective device trips. Fig. 13 shows the relationship between the short-circuit current magnitude and the time for the protective device to clear the fault. From this it may be seen that on a low-voltage system with 25,000-ampere IC breaker is used, the minimum feeder conductor size should be no. 1. If the IC duty is 50,000 amperes, the minimum feeder conductor size would become no. 3/0. These factors should be borne in mind and given careful consideration if maximum cable life is desired.

The short-circuit current on the load side of the starter terminals will be less than that available on the incoming line terminals, provided overload relay heaters are included in the starter. This is because of the resistance of the heaters, which limits the short-circuit current.

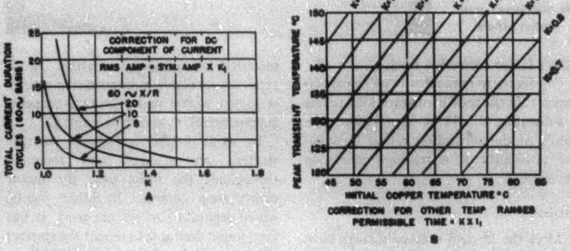

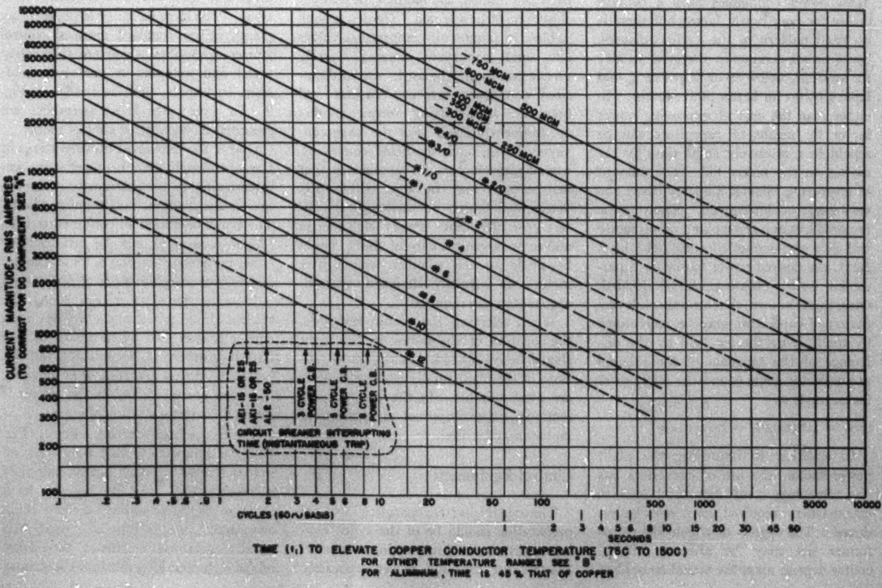

Fig. 13. Short-circuit capacity of various size cables as a function of time before clearing fault

For example, a size 1 starter for a $7^1/_2$ hp would have a through current of approximately 7,500 amperes on a system having 25,000-amperes duty on the control center bus. This starter would normally be protected by a molded case breaker which would clear the fault in about 1/2 cycle. This would mean that at least a no. 8 wire should be used for the motor leads, whereas, from a current-carrying capacity only, a no. 14 wire would be required.

Summary

In summary, when considering a new coal preparation plant the following suggestions bear careful consideration:

1. Determine substation size, taking into account the short-circuit protective levels available in the control.
2. Select motor voltages on the basis of the economics of the power distribution system, and of obtaining best life of motors.
3. Select control having proper interrupting capacity and properly sequenced for best over-all plant efficiency.
4. Use solidly grounded low-voltage distribution to obtain maximum reliability of the power system.
5. Apply capacitors to improve power factor and reduce required substation size where the economics will justify their use.
6. Select cables to withstand the particular short-circuit level as well as for proper ampere and voltage levels.

No Discussion

A Low-Height 15-Ton Mine Locomotive for Low Vein Haulage

J. W. BRAUNS
NONMEMBER AIEE

MECHANIZATION has opened up new possibilities to the coal mining industry. One of these is the mining of coal seams formerly considered too narrow for practical working. Such operations impose severe restrictions on much of the equipment employed. To meet these requirements, a low-height haulage locomotive was designed with the objective of keeping vertical dimensions to a minimum. The fact that a number of these units are now operating successfully on various properties attests the basic soundness of the design.

General

The problem of mining coal that lies in narrow seams has been present since the beginning of the industry. For many years it was necessary to cut and remove sufficient shale to provide the clearance required for working. As a result, the cost of obtaining coal from such mines was high and the operation often proved unprofitable. Even the early machines were not designed to fit such restricted space, but the passage of time saw this difficulty overcome.

Mechanization of operations at the face has speeded up the tempo of mining all along the line. More coal is produced in a shorter time in a smaller working area. This has placed a greater load on the transportation system—heavier trains must be moved at higher speeds.

Design Problem

The problem facing the locomotive designers was to produce a haulage locomotive capable of handling the production of coal in seams 30 to 42 inches high. This meant using every precious inch of available space. Moreover, the locomotive must meet the following requirements laid down for standard haulage-type locomotives:

1. Sufficient motor capacity to give high continuous tractive effort ratings at high locomotive speeds.
2. Improved traction motor designs, insulation, and construction to reduce motor maintenance.
3. Sturdy, welded frame construction.
4. Equalization of locomotive weight to give smoother riding, better pulling power, and fewer derailments on rough track.
5. Journal bearings of ample capacity for increased speeds and loads.
6. Improved accessibility of wearing parts, and the use of better materials with hardened surfaces to reduce wear.
7. Convenient location of equipment to promote easy and safe operation.
8. Sufficient controller steps to permit rapid acceleration at high adhesion.
9. Accelerating resistors of the edgewise-wound ribbon type to eliminate breakage, and reduce size and weight.

With mechanical mining and high production rates any breakdown in the transportation system results in a large loss of output so failures must be kept to a minimum. Locomotives must have the ability to stand up day after day in continuous heavy service.

Locomotive Description

To meet these requirements a 15-ton, low-height trolley locomotive has been developed with an over-all height of 26 inches with 23-inch wheels. With 25-inch wheels, a higher speed is obtained but the over-all height is increased to $27^3/_8$ inches. It is 248 inches long and 78

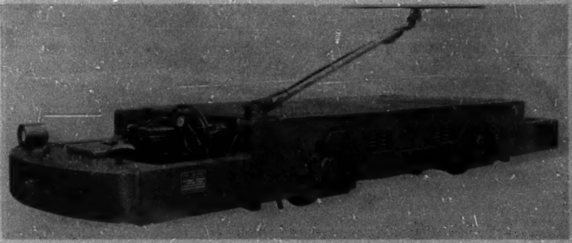

Fig. 1. Typical 15-ton low-height haulage locomotive

Paper 53-365, recommended by the AIEE Land Transportation Committee and approved by the AIEE Committee on Technical Operations for presentation at the AIEE Middle Eastern District Meeting, Charleston, W. Va., September 29–October 1, 1953. Manuscript submitted July 1, 1953; made available for printing August 10, 1953.

J. W. Brauns is with the General Electric Company, Erie, Pa.

Fig. 2. Motorman's end of locomotive, showing controls

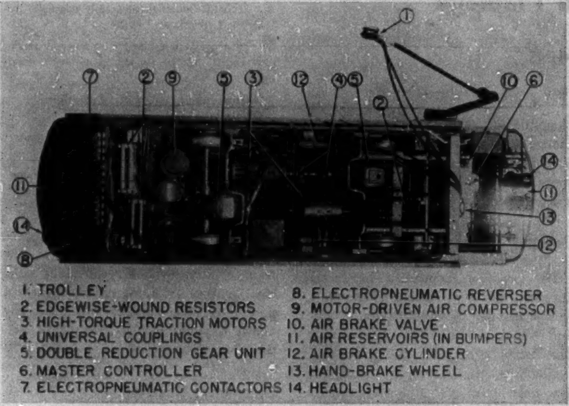
①
⑦
②
⑨
⑤
③
⑫
④
⑤
②
⑩
⑥
⑪
⑭
⑧
⑭
⑪
⑬
⑫
1. TROLLEY
2. EDGEWISE-WOUND RESISTORS
3. HIGH-TORQUE TRACTION MOTORS
4. UNIVERSAL COUPLINGS
5. DOUBLE REDUCTION GEAR UNIT
6. MASTER CONTROLLER
7. ELECTROPNEUMATIC CONTACTORS
8. ELECTROPNEUMATIC REVERSER
9. MOTOR-DRIVEN AIR COMPRESSOR
10. AIR BRAKE VALVE
11. AIR RESERVOIRS (IN BUMPERS)
12. AIR BRAKE CYLINDER
13. HAND-BRAKE WHEEL
14. HEADLIGHT

Fig. 3. View from above with principal pieces of equipment identified

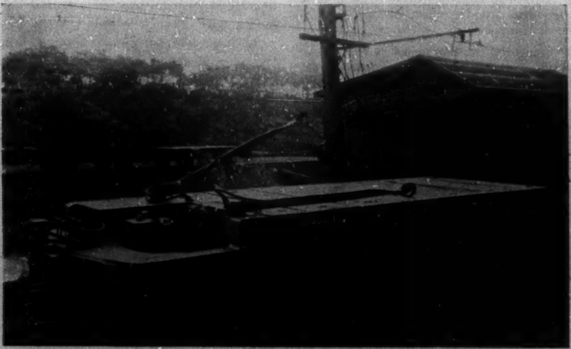

Fig. 4. Two locomotive units combined for separable tandem operation

inches wide over journal boxes. The addition of trolley pole sockets outside the side frames increases the width to 90 inches.

Each of the two axles is powered with a frame-mounted traction motor of the d-c series-wound commutating-pole self-ventilated type having a 1-hour rating of 95 horsepower at 250 volts. Class-*B* insulation is used throughout, and the armature is carried on antifriction bearings mounted in separate frameheads. A drive shaft with a double universal joint and a slip joint connects the motor to the double-reduction gear box mounted on the axle. The first reduction is a spiral-bevel-type pinion and gear, and the second reduction is a spur-type pinion and gear. All drive bearings are of the antifriction type with the exception of the suspension bearings on the locomotive axle. With 23-inch wheels the rated drawbar pull is 7,500 pounds at a speed of 7 miles per hour, with 250 volts on the trolley. The use of 25-inch wheels and high-speed gearing gives a rating of 7,500 pounds drawbar pull at 10.5 miles per hour. The maximum starting tractive effort (30-per-cent adhesion) is 9,000 pounds. Both motors are permanently connected in parallel for operation from a 250-volt trolley.

An electropneumatic control system provides ten steps in motoring to give smooth, rapid starting of trains and maximum tractive effort for accelerating heavy loads. Seven steps of dynamic braking are also provided to help brake the train on down grades. The master controller actuates electropneumatic contactors and an electropneumatic reverser. A motor-driven compressor supplies air for the locomotive brake system, the locomotive control, and the sanding equipment. A motorman's valve controls the application of air to two equalized brake cylinders which operate the locomotive brakes.

A low-height controller with cam-actuated contacts was used which could be mounted in the normal upright position. The controller, reverser, hand brake wheel, and valves for the air brake, sander and whistle are all conveniently located and compactly arranged for easy and safe operation. The hand brake, operated by the brake wheel, is used for emergency only and as a parking brake to hold the locomotive at standstill.

Trolley poles may be mounted on either or both sides of the locomotive. A special type of trolley pole socket with an air-actuated lifter is available. By merely operating an air valve, the trolley base can be raised enough to permit the pole, in the down position, to be swung across the top of the locomotive. Thus the pole can easily be set for trailing, regardless of the direction of locomotive travel.

A fuse in the trolley circuit affords protection for the locomotive. Each traction motor is protected by an overload relay. These relays are set for a value of current corresponding to 35-per-cent adhesion on the locomotive. To secure reapplication of power once a relay has tripped, the controller handle must be returned to the off position.

A trolley retriever, used to prevent damage if the pole leaves the wire, functions on no voltage and automatically lowers the pole if it leaves the wire. The operation can be made either automatic or manual, thus permitting the locomotive to pass insulated joints in the trolley wire without the pole being retracted.

The locomotive can be arranged for separable tandem operation of two units, that is, two units connected together with one operator. In this case provision is made for emergency brake application if, for any reason, the units should separate. A safety drawbar, in addition to the regular drawbar, is provided between units. As an additional safety feature, clips may be located below the drawbar pins to prevent a pin falling out if, by any chance, it should shear.

Headlights have been greatly improved by the use of sealed beam units which retain high brilliance throughout their life.

Conclusion

In spite of its strictly limited dimensions, this low-height locomotive has the same advanced design features and sturdy construction that have proved eminently successful in the standard line of haulage locomotives. Adequate space is provided for both the motorman and the trip rider. Particular attention has been paid to details that serve to promote safety and reduce fatigue resulting from working in close confines.

Field experience has demonstrated that the objectives of the designers have been achieved. A powerful and efficient locomotive has been produced which is helping to increase the efficiency and economy of extracting coal from low-height seams. As such, it fits admirably into the picture of progress through mechanization in the coal industry.

No Discussion

Split-Pole Exciters: Their Design and Application on Diesel-Electric Locomotives

H. R. STIGER
ASSOCIATE MEMBER AIEE

THE development of the diesel-electric locomotive posed the problem of utilizing full engine horsepower over a wide range of locomotive operating conditions. One means devised to solve this problem was the use of a split-pole exciter, so designed as to give a generator load characteristic closely matching the constant horsepower output of the diesel engine over most of its range. Since the regulation results from the inherent exciter characteristics, this system employs a minimum of control equipment.

General

The past decade has witnessed the development of many refinements in diesel-electric locomotive control. The application of load-control systems has made it possible to utilize full engine horsepower under all normal operating conditions. As a result, fuel economy has been improved and engine stalling has been reduced to a negligible amount.

Application of load control, however, has been considered feasible only on large road locomotives. The natural question then is: What of the smaller locomotives which do switching, classification, and light road work at moderate speeds? They operate intermittently at full and partial throttle, giving their diesel engines a variable workout. This duty requires a locomotive with quick pickup. Such applications demand a control system which will give good engine utilization at an economically justifiable cost.

For a number of years the General Electric Company has been using split-pole exciters in this service with excellent results. A machine of this type has electrical characteristics such that it automatically furnishes suitable excitation to the traction generator under full horsepower operating conditions. It provides for low generator voltage when the traction-motor current demand is high, high generator voltage when the current demand is low, and good regulation between these extremes. As a result, the load demand on the diesel engine approximately equals the maximum power available at full throttle setting over most of the locomotive operating range.

Construction

A knowledge of the construction of the split-pole exciter will help in understanding its operation. Essentially, it is similar to an ordinary d-c exciter, except that the field poles are of a special split construction—hence its name. One part of the split pole is called the differential-pole section, and the other the shunt-pole section. A brass spacer block separates these two, causing them to act magnetically as individual poles. The complete pole piece is held together by brass rivets. Two windings are used, corresponding in name to the pole sections. Fig. 1 shows a typical split pole with a section of the windings cut away. Notice that the differential winding surrounds the differential-pole body only, while the shunt winding surrounds both pole bodies. Fig. 2 shows the pole construction with the windings removed. As can be seen here, the differential-pole section is considerably smaller in cross section than the shunt-pole section.

The exciter is housed in the same frame with the auxiliary generator and the combined machine is often mounted on the main generator frame; see Fig. 3. The two armatures are on the same shaft,

---

Paper 53-362, recommended by the AIEE Land Transportation Committee and approved by the AIEE Committee on Technical Operations for presentation at the AIEE Middle Eastern District Meeting, Charleston, W. Va., September 29–October 1, 1953. Manuscript submitted June 29, 1953; made available for printing August 4, 1953.

H. R. Stiger is with the General Electric Company, Erie, Pa.

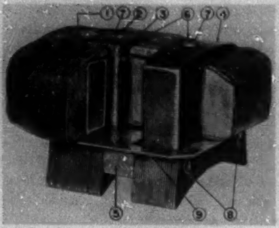

Fig. 1. Sectional view of a typical split pole, showing location of parts and windings

1. Shunt winding
2. Differential winding
3. Differential pole section
4. Shunt pole section
5. Brass spacer
6. Pole bodies
7. Frame bolt holes
8. Brass rivets
9. Brass supporting plate

which is usually belt-driven from the main generator shaft. A typical exciter-auxiliary generator equipment is approximately 16 inches in diameter and weighs 780 pounds. The size of the exciter end of the machine and number of its poles depend upon the power requirement for excitation of the traction-generator field. Naturally, the auxiliary power requirements of the locomotive determine the size of the other end of the machine. Both factors affect the over-all machine size.

Elementary Circuit

The basic circuit of the split-pole excitation system is shown in Fig. 4. The differential winding of the exciter field is connected in series with the generator and traction motors so that it carries the load current of the generator. The shunt field winding is connected in parallel with the exciter armature and the locomotive battery through resistors, as shown in Fig. 4. These two power sources supply self- and separate-excitation, respectively, to the field. The exciter terminals are connected to the traction-generator field winding.

Exciter Characteristics

The output characteristic of the split-pole exciter represents the amount of field excitation needed by the traction generator to match the diesel-engine output. The exciter characteristic required for any particular generator is determined from the generator design curves. For instance, curve *R* in Fig. 5 represents the excitation characteristic for a typical 600-horsepower diesel-driven generator. It is plotted in terms of exciter internal volts *E* (terminal volts plus armature, commutating field, and brush drops) and generator load amperes.

The exciter characteristic results from the combined effect of the shunt- and differential-pole sections. These effects are shown respectively by curves *A* and *B*, which may be imagined to be the exciter characteristics that would result if each of the two magnetic fields were applied independently over the entire operating range of the machine. In actual practice, the design and construction of the exciter pole pieces and field windings are such as to combine the effects of these two magnetic fields to produce the desired characteristics.

The differential winding is so arranged that, when energized, the magnetic field it creates opposes the effect of the magnetic field created by the shunt winding in the differential-pole section. With heavy generator load currents, such as occur when starting and accelerating a heavy train, the effect of the magnetic field created by the differential winding overcomes and exceeds that of the magnetic field created by the shunt winding. This causes the magnetic field in the differential-pole section to create a voltage in the armature which subtracts from the voltage created by the magnetic field in the shunt-pole section. The net result is low output voltage on both the exciter and the traction generator.

As the locomotive accelerates, the generator load current decreases. This lowers the effect of the differential field until a point is reached where it just balances that of the shunt field. When this occurs the effect of the differential-pole section is neutralized, and the voltage output of the exciter is entirely the result of the magnetic field produced by the winding around the shunt-pole section. At this point curves *A* and *R* in Fig. 5 cross.

Further increase in the locomotive speed results in still lower generator load current. The shunt magnetic field then overcomes the differential magnetic field on the differential-pole section. As a result, the magnetic fields of the two pole sections add, producing still higher output voltage on both the exciter and the traction generator.

The shunt field winding is largely supplied from the locomotive battery through the separate resistor shown in Fig. 4. A relatively small amount of current is also

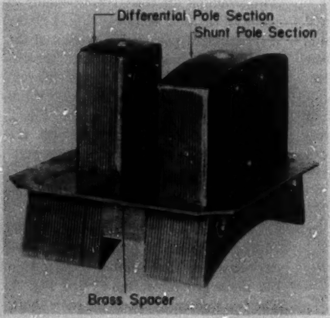

Fig. 2 (left). Split-pole body, showing construction details

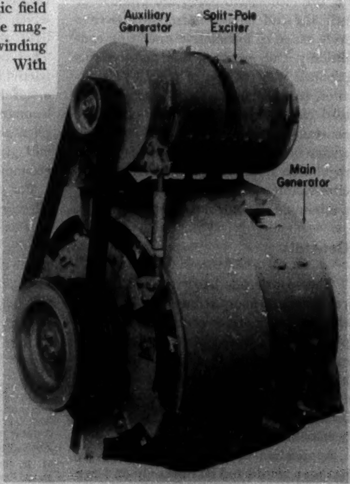

Fig. 3 (right). Exciter-auxiliary generator set mounted on main generator

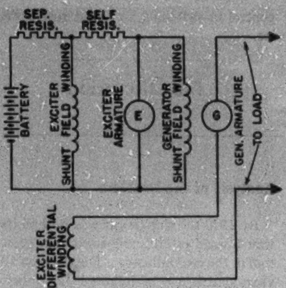
SEP. RESIS.
SELF RESIS.
BATTERY
EXCITER SHUNT FIELD WINDING
EXCITER ARMATURE
E
GENERATOR SHUNT FIELD WINDING
G
GEN. ARMATURE
TO LOAD
EXCITER DIFFERENTIAL WINDING

Fig. 4. Simplified diagram of basic circuits for the split-pole exciter

supplied from the exciter armature through the self-resistor. The separate and self-resistances provide a means for adjusting the characteristics of the shunt-pole section of the field, curve *A* in Fig. 5. The straight line *A'* represents the characteristic resulting from the excitation supplied by the battery. The shaded area between *A'* and *A* represents the influence of the self-excitation. Adjustments in the high-current range are made by changing the value of the separate resistance. In the low-current range, adjustments are made by changing the value of the self-resistance. The proper values of these resistances are determined by the manufacturer during test of the locomotive and, under normal operating conditions, need not be changed.

An example of how the output characteristic is designed into both the exciter and the traction generator is shown in Fig. 6. The solid curve represents the actual power available for traction from a 600-horsepower diesel-driven generator equipped with a properly adjusted split-pole exciter. The dotted curve represents power theoretically available for traction from the same set if the generator were to fully utilize the diesel-engine horsepower. This curve is slightly less than the rated engine horsepower, and is approximately constant over the entire operating range. The two curves do not coincide exactly. They are, however, close enough over the operating range of the locomotive so that it is practically correct to say that all power available under normal conditions is properly utilized.

Advantages

The split-pole exciter system offers a simple and inexpensive control scheme because the desired characteristics are largely inherent in the exciter itself, and little external equipment is necessary. The components are sturdy and require a minimum of maintenance. The simplicity of the control used makes it relatively easy for the operator to understand and service. Excellent matching ability assures utilization of practically full engine horsepower. This results in a good locomotive which can cover a lot of ground in a short time. Changes in normal operating conditions produce immediate and automatic response from the excitation system.

The split-pole exciter and main generator were designed for a normal ambient temperature range within which maximum horsepower can be very nearly realized. However, by external adjustments, this equipment can be made to operate with excellent results at other mean ambient temperatures. This assured efficient performance in various climates encountered throughout the world.

Limitations

Variations in engine ability, such as would result from a clogged injector or other engine trouble causing loss of power, are not recognized by the split-pole equipment. Consequently, some degree of engine stalling is experienced under these conditions. Inherently, however, this is not as bad as might be expected, since the power demanded by the generator decreases approximately as the square of the speed. This is true because the voltage generated is proportional to both the speed and the field excitation. Since the exciter is driven from the generator shaft the field excitation is also proportional to the speed, and thus the generator power demand varies approximately as the square of the speed.

The split-pole excitation system could result in engine stalling when starting up a locomotive after it has been shut down for some time in cold weather. Under this condition both the exciter and main generator fields will have abnormally low resistance. This results in field currents that are higher than normal, which imposes a greater than normal load demand on the engine. In actual practice this situation has not proved at all serious. In the first place, the diesel engine will be run long enough to bring its oil and water temperature up to suitable values before it is called upon to deliver any power. This engine warm-up period will serve to heat the air in the cab and indirectly take the chill off the exciter and generator. It is also a fact that the cooler a shunt-excited winding may be, the more rapidly it will approach its ultimate operating temperature. A combination of these factors effectively reduces the engine stalling on a "cold" locomotive to acceptable values.

Application

At present, the split-pole exciter system of control is being successfully used by the General Electric Company on its 44-, 70-, and 95-ton diesel-electric switching locomotives. It is also being applied on many diesel-electric locomotives furnished for all types of service in foreign countries. In the Alcoa-GE line of locomotives for

Fig. 6 (right). Performance curves of a diesel-engine generator set equipped with a split-pole exciter

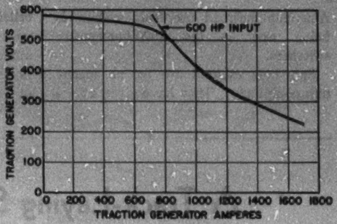

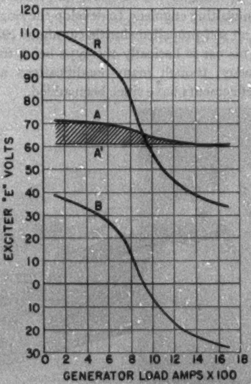

Fig. 5. Split-pole exciter characteristics

American railroad use, this system is being used on the 1,000-horsepower switchers.

Split-pole exciters are by no means new equipment. They have given an excellent account of themselves performance-wise for years. In view of this past record and the present applications, the split-pole exciter evidently has a definite place in the future of diesel-electric locomotive control in switching and light road service.

◆

No Discussion

A Track-Laying Shuttle Car

J. W. BRAUNS
NONMEMBER AIEE

THE shuttle car was developed to meet the demand for rapid transportation of coal from the working face to the secondary haulage system in the mine. Rubber-tired cars generally have been used, but certain limitations pointed to the desirability of a track-laying vehicle. Such a car was designed, with electric drive and an electrohydraulic control system. Nearly 3 years of operating experience indicate that the design is fundamentally sound and that this type of vehicle has a definite place in mining operations.

General

Development over the past 25 years of a variety of mechanical coal mining equipments has resulted in a veritable underground revolution in the coal industry. Cutting machines quickly slice their way several feet into a coal face, neatly outlining the block to be broken away with the next blast. Drilling machines make holes in just the proper places for the blasting charge. Then loading machines reach out and gather up the broken coal onto their conveyors, transfer it back away from the face, and dump it into a waiting vehicle, which transports it to the secondary rail haulage system. Where conditions are suitable, continuous mining machines performing all these operations may be applied.

Evolution of the Shuttle Car

As the use of the mechanical loading machine increased, a bottleneck began to develop in the operation behind the loading machine. The transportation schemes in use 20 years ago could not move the coal away from the loader to the secondary haulage systems fast enough to utilize fully the potentialities of the loader. A change was inevitable and many were tried, but one which met with greatest success was a scheme which eliminated the necessity for tracks in the gathering area.

This scheme was conceived by a Chicago consulting engineer named James Fletcher about 1935. He advanced the idea of two or three rubber-tired tractor-trailer units working behind a mechanical loader to keep a steady flow of coal moving from the loader to the secondary track system. That was the forerunner of today's shuttle car.

Even though the tractor-trailer units formed a successful beginning to the solution of the efficient gathering of the coal, they were still inefficient from the standpoint of their coal carrying capacity relative to the amount of space they occupied.

It remained for A. L. Lee, a Pittsburgh consulting engineer, to develop the single-unit self-propelled shuttle car about 1939. This car is basically the type being used today, though many modifications and refinements have since been added.

Analysis of the Problem

By 1940 the shuttle car was well on its way toward establishing itself as a basic tool in the coal industry. For the next 10 years shuttle cars all followed the rubber-tired 4-wheeled pattern. In 1950 General Electric introduced its track-laying shuttle car. Before deciding to enter this field, full advantage was taken of the opportunity to review shuttle-car performance during several years of operation with rubber-tired vehicles. Features of existing shuttle cars which might be improved upon were carefully investigated. One of the predominant complaints against the rubber-tired vehicles was that they were unsuited for wet mines. The comparatively high ground pressure resulting from the small area of contact between the tire surface and the ground made these vehicles tend to dig ruts in the haulage ways and bog down in the soft bottoms. In addition, a considerable amount of tire trouble accompanied the use of these cars. This pointed the way to the adoption of the track laying design. This design affords a much larger ground contact area over which the weight of the car with its load is distributed, thus lessening the tendency to form ruts. In fact, it tends rather to pack down the surface of the haulage way into a firm roadway.

Description of the Car

Basically, this car consists of a material-receiving body with an adjustable dis-

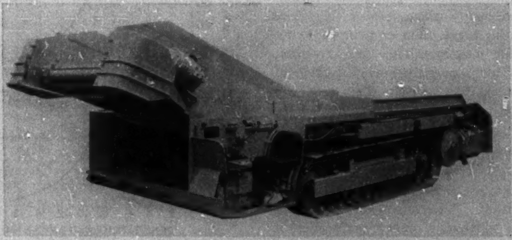
Fig. 1. Oblique view from discharge end of car, showing conveyor raised

---

Paper 53-366, recommended by the AIEE Land Transportation Committee and approved by the AIEE Committee on Technical Operations for presentation at the AIEE Middle Eastern District Meeting, Charleston, W. Va., September 29–October 1, 1953. Manuscript submitted July 1, 1953; made available for printing August 10, 1953.

J. W. Brauns is with the General Electric Company, Erie, Pa.

Fig. 2. Closeup view of traction motor, reduction gear, and chain and sprocket track drive

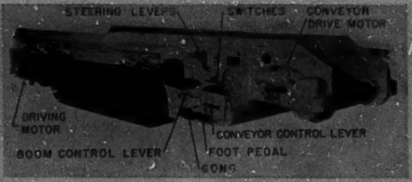

Fig. 4. Oblique view of car, showing operator's position with principal controls identified

charge boom at the front end, a chain-driven conveyor running the length of the car, and two crawler-type tracks on which the car runs, see Fig. 1. The car is equipped with a vertically mounted cable reel with a capacity of 500 to 600 feet of 2-conductor cable having a safety ground wire. A small hydraulic motor, operating in conjunction with a differential pressure valve, serves to keep correct cable tension for automatic spooling and unspooling during operation of the car. The reel also has a level-wind feature similar to that on a fishing reel. Tractive power for the car is furnished through two 20-horsepower d-c series motors. One motor drives each track through a right-angle gear box plus a chain and sprocket arrangement, as shown in Figs. 2 and 3. Automatically timed magnetic contactors accelerate the traction motors in three steps. The control equipment is of the sealed type, and control compartments are force-ventilated where necessary to remove corrosive gases generated by arcing.

Steering is accomplished by breaking one or the other of the tracks in much the same way as a conventional crawler-type tractor. The traction motor on the side being braked is disconnected during braking.

Brakes are of the clasp type, and are spring-set, fail-safe so that they automatically apply if the power supply to the car is interrupted for any reason. They operate on a drum mounted on a shaft extension at the commutator end of the traction motor, and are controlled hydraulically from brake valves located at the operator's position. Hydraulic pressure is furnished by a double-section pump, a high-capacity section for the discharge boom lift, and a smaller section for the cable reel and brakes. The pump is driven by a 3-horsepower compound-wound d-c motor. The operator's compartment is located near the front of the car on the side opposite the cable reel, see Fig. 4. It contains two cushioned seats, one for either direction of operation, plus all controls necessary for normal operation of the car. Within easy reach are levers for raising and lowering the adjustable boom and for 2-speed operation of the conveyor, a forward and reverse pedal, two steering levers, control and headlight switches, and a foot gong.

Characteristics

The car is highly maneuverable. By changing the braking force on one of the tracks with the hand steering lever, the operator can execute varying degrees of turns. If desired, he can lock one track and the car will actually pivot about that track. This feature is particularly useful when operating behind a loading machine, as the loading end of the car may be moved from side to side merely by applying a slight amount of forward or reverse motion to the unlocked track.

The track carriages are pivoted to the main car body on the rear or drive end and spring-loaded at the front end by means of a torsion spring and knuckle. This arrangement allows the car to follow an uneven mine bottom and still give a smooth comfortable ride to the operator. It also reduces the body frame stresses which would normally occur if the carriage were firmly mounted at both ends to the car body.

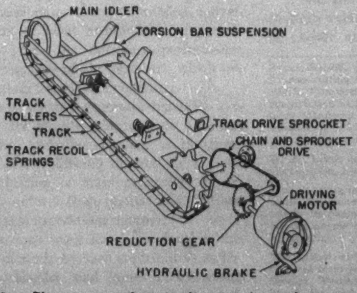

Fig. 3. Phantom view showing elements of propulsion equipment for track-laying shuttle car

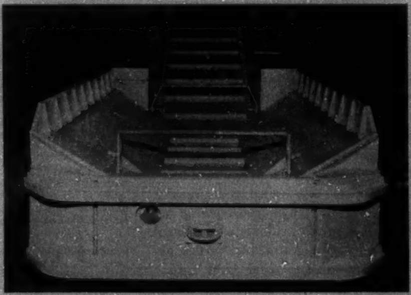

Fig. 5. View of car from loading end with discharge end raised

Fig. 6. Shuttle car in operation in a wet-bottom mine

Another advantage of the track-laying design is that it eliminates the need for wheel wells in the sides of the body. This permits the use of a wider body bed and wider conveyor, thus giving greater coal carrying capacity and faster unloading. Two 5-horsepower motors with gear reduction drive the conveyor chains. These are designed for two speeds—fast for unloading into the mine car and slow for shifting the coal toward the front of the car as it is loaded into the rear by the mechanical loader.

Operation

Operation of the car is simple and practically effortless. To move the car straight ahead, the operator need only press down the pedal in the direction he faces. To execute a turn he need only operate the hand lever corresponding to the direction he wishes to turn. Thus, for a left turn, he operates the lever in his left hand and for a right turn he operates the lever in his right hand. This is true regardless of his seated position. Normally, operators require only a few minutes of oral instruction plus a few more minutes of actual operating practice before they are ready to begin working behind the loading machine and on the loading ramp.

Experience to date indicates that a track-laying shuttle car capable of working behind a mechanical loader and moving with its burden over the toughest of working roadbeds is the answer to the need for fast, efficient transfer of coal from the working face to the secondary haulage system.

◆

Discussion

F. R. Hugus (Joy Manufacturing Company, Franklin, Pa.): Mr. Brauns stated, "It remained for A. L. Lee, a Pittsburgh consulting engineer, to develop the single unit self-propelled shuttle car, about 1939." Since this implies that Mr. Lee was the first to develop a shuttle car, I feel that this impression should be corrected and wish to present the following facts:

1. The complete records of a Joy Manufacturing Company single-unit self-propelled shuttle car, which was designated as *1ET-1E*, were released for production on January 8, 1938. Also, this company released complete records for *2ET-1D* shuttle car on May 16, 1938. The first was a 250-volt machine securing power through a trailing cable, and the second was a battery-powered machine. It is safe to assume that considerable engineering and development work was done in 1937, because such work of necessity must precede the act of releasing records for production.
2. The shuttle car designated as *2ET-1D* and assigned serial number *ET-101*, was displayed by the Joy Manufacturing Company at the American Mining Congress exhibition in 1938. This same shuttle car was subsequently sold to the Hanna Coal Company and shipped on July 14, 1938.
3. The company records indicate that in 1939 Joy Manufacturing Company shipped more than 40 shuttle cars. The majority were battery operated but several cable reel types were also sold.
4. John D. Russell was granted Patent no. 2,192,650 covering a single unit self-propelled shuttle car on March 5, 1940. This was assigned to the Joy Manufacturing Company. The application for this patent was filed on July 14, 1938.
5. The first shuttle car developed by A. L. Lee was installed in The Union Coal Company Mine at Renton, Pennsylvania. G. A. Shoemaker, who was the manager of this mine at the time that the Lee shuttle car was installed, has stated that this event took place in 1939.

Too often historical information concerning the birth of a new idea which later develops into a vital and important part of our industrial economy, is, in the course of time, lost or unintentionally modified. In this instance recorded facts are available and I feel that they should be used to provide as accurate a record as possible concerning the first stages of the development of shuttle cars in mines.

The Use of an Analogue Computer to Optimize the Transient Response of an Aircraft-Type Generator-Regulator System

H. B. JAMES
ASSOCIATE MEMBER AIEE

IN THE past 5 years, a great deal of interest has been centered on the use of electronic analogue computing machines for the study of dynamic systems. The transient solution of even the simpler problems is difficult and laborious to obtain by classical mathematical methods, and for this reason analogues of these systems are being used extensively to facilitate their study and design. Since large quantities of data for a considerable range of variables are required to properly evaluate system performance, the analogue method of study is most useful. When the systems under study contain elements which are erratic or involve nonlinearities, the analogue computer is even more important.

The analogue computer is a combination of high-gain d-c amplifiers and passive networks which simulate the devices or process whose operation is being computed. Circuits capable of performing arithmetic operations, differentiation, and integration are combined to perform a sequence of operations producing directly a variation of current or voltage which represents the desired solution. Because the computer is analogous to the dynamic system under investigation, it will react to any stimulus in the same manner as would the dynamic system.

Questions as to how to stabilize a given system or what combination of parameters gives the optimum performance are examples of the problems which are solved on this type of computer.

Thus, electric generator-regulator systems are readily adaptable to analogue studies, and the problem of designing feedback stabilizing devices for a given combination of main generator, its exciter, and a voltage regulator is obtained in a most expeditious manner.

Previous work has been done in this field of study by such contributors as Dr. E. L. Harder[1] and James T. Carleton.[2] This paper, in contrast to these cited, covers the use of the analogue computer to simulate a part of the generator-regulator system, the balance of the system being provided in its real and true form. In this particular case, the analogue computer simulated the main generator and its exciter. An actual voltage regulator was used to control the voltage of the simulated machines. The various feedback circuits which were studied were also analogued on the computer to allow rapid changes of their parameters. This study was rather the inverse of that normally encountered, for here we were using a given regulator while the major parameters of the main generator and its exciter were varied to find their effect on the over-all system characteristics. There were two reasons for such a study:

1. In the case of the particular regulator used for this study, a carbon-pile regulator, it has so far been impossible to properly convert its transfer function to the electronic analogue computer without loss of many of its important characteristics.
2. The particular regulator under study had been used in application with other generator-exciter combinations, and in the interests of standardization, which have become increasingly important in military operations, it was felt that new generator-exciters should, if possible, be designed in accordance with the results obtained from such an analogue study.

It was the main purpose of this paper to study certain reasonable combinations of exciter and main generator with a fixed voltage regulator to determine the optimum transient response as a function of the following parameters:

1. Main generator open-circuit time constant.
2. Exciter shunt-field time constant.
3. Feedback transformer time constants.

Curves are presented to show the change in response of the output voltage transient when a given load was suddenly removed from the system as these parameters were varied.

Main Discussion

Generator-Regulator System Studied

Fig. 1 shows all the components of a typical aircraft a-c electric power system: an a-c generator with its integral exciter, a carbon-pile voltage regulator, a control panel with field relay and protective devices, and necessary current transformers for both the voltage-regulator and the control panel. This paper deals with typical generator-regulator combinations similar to the one shown in this figure. In fact, the voltage regulator used in this study is the one shown in Fig. 1.

The a-c generator is a conventional salient-pole machine which provides a frequency of 800 cycles per second at a rotational speed of 8,000 rpm. A rotating field is used with damper windings to improve the wave shape. This machine is rated at 20 kva, 115 volts.

The exciter is a 6-pole d-c shunt generator with pole-face windings and a full set of interpoles. The a-c generator and exciter are mounted on the same shaft.

The a-c generator voltage is controlled by varying the exciter output voltage which supplies power directly to the a-c generator field. The carbon-pile voltage regulator provides a variable resistance in series with the shunt field. This resistance is changed in accordance with the speed and load conditions to maintain the a-c generator output voltage within narrow limits.

This carbon-pile voltage regulator is similar to conventional d-c generator voltage regulators. It is a self-contained unit, which, when properly adjusted, will operate to maintain the a-c generator output voltage within 2 to 3 per cent over the rated load and speed range of the system. A feedback transformer is used to provide an anticipatory signal to the voltage regulator to stabilize the excitation system during transient conditions.

Fig. 2(A) is a schematic diagram of the system being studied. Fig. 2(B) is a block diagram of this same system.

Paper 53-368, recommended by the AIEE Air Transportation Committee and approved by the AIEE Committee on Technical Operations for presentation at the AIEE Aircraft Electric Equipment Conference, Seattle, Wash., September 30-October 2, 1953. Manuscript submitted July 1, 1953; made available for printing August 24, 1953.

H. B. James is with the Westinghouse Electric Corporation, Lima, Ohio.

This paper is part of a Master's thesis submitted to the Graduate School of the University of Pittsburgh, in partial fulfillment of the requirements for the degree of Master of Science in Electrical Engineering.

The author wishes to acknowledge the assistance received from James T. Carleton of the Analytical Section, Westinghouse Electric Corporation, Pittsburgh, Pa., and many of the author's associates of the Aviation Engineering Department, Small Motor Division, Lima, Ohio.

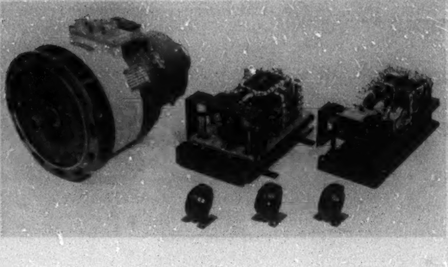

Fig. 1 (left). A typical a-c generating system showing generator, regulator, control panel, and current transformers

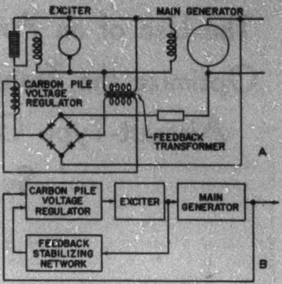
EXCITER
MAIN GENERATOR
CARBON PILE VOLTAGE REGULATOR
FEEDBACK TRANSFORMER
A
CARBON PILE VOLTAGE REGULATOR
EXCITER
MAIN GENERATOR
FEEDBACK STABILIZING NETWORK
B

Fig. 2(A). Schematic diagram of the system used for this study. (B) Block diagram of the system used for this study

This paper considered certain typical combinations of the exciter and the a-c generator constants as encountered on aircraft electric systems. For each combination of the machine constants, different feedback stabilizing constants were set into the analogue computer and the transient response was observed with load applied and removed.

Since the time available for this study was rather limited, certain parameters of the system were held constant through the investigation. First, the voltage regulator was adjusted properly on an actual machine as shown in Fig. 1. No further adjustments of the regulator were made during the investigation. The value of current flowing through the carbon pile for any particular excitation condition was always the same. The gain of the exciter was held constant. The synchronous reactance, transient reactance, and load reactance were all maintained constant. The parameters which were varied are:

1. Main generator open-circuit time constant T_{do}.
2. Exciter shunt-field time constant T_f.
3. Feedback transformer primary time constant T_p.
4. Feedback transformer turns-ratio n.

Analogue of the System

The system analogue used for this study is shown in Fig. 3. As stated before, the carbon-pile voltage regulator was used in its real form; the exciter was analogued as a simple time delay or lag circuit using an operation amplifier (no. 1); the a-c generator was simulated by means of a passive network which represented its open-circuit time constant T_{do}', its synchronous reactance X_d, its transient reactance X_d', and its load X_L. The feedback stabilizing transformer was reproduced by a lead network using an operational amplifier (no. 3).

Appendix I shows the proof of the analogies used for the exciter, the a-c generator, and the feedback transformer.

To provide the proper level of signals into the voltage regulator, two auxiliary circuits were necessary to augment the standard analogue computer components.

The sensing circuit of the voltage regulator normally operates at a voltage of 115 volts a-c, while the maximum output of the operational amplifiers used for this study are nominally rated at ±50 volts. Therefore, a d-c amplifier, in the form of a cathode-follower, consisting of two *6L6* beam power amplifier tubes in parallel was connected to the output of the operational amplifier (no. 3) supplying the voltage-regulator sensing circuit. This circuit was designed so that the output voltage from the operational amplifier never exceeded 50 volts and the sensing circuit operated at its nominal value of 100 volts d-c.

The second auxiliary circuit was necessary to force a current through the carbon pile which was a measure of the current flowing in an actual exciter field circuit. For this purpose a special amplifier, consisting of a cathode-follower driving a saturable reactor, controlled the current supplied to the carbon pile. A *5881* tube was used for the cathode-follower and two 400-cycle-per-second saturable reactors were used for the higher power level amplifier. A conventional bridge-type selenium rectifier provided a unidirectional current through the carbon pile. This amplifier was designed to minimize any effects it might have on the system being analyzed.

Disturbances to the system were provided by switching various amounts of load on the a-c generator (R_8). Solutions were obtained by both oscilloscope display and pen recorder data.

Fig. 4 shows the entire analogue setup. The computer, a Boeing Electronic Analogue Computer (BEAC),[3] is shown at the extreme right. An oscilloscope and camera are shown in the center. To the left of the oscilloscope is the carbon-pile voltage regulator (rear) and the auxiliary amplifiers (front).

System Performance Criteria

The method of performance evaluation of any dynamic physical system is usually based on some "transient figure of merit,"

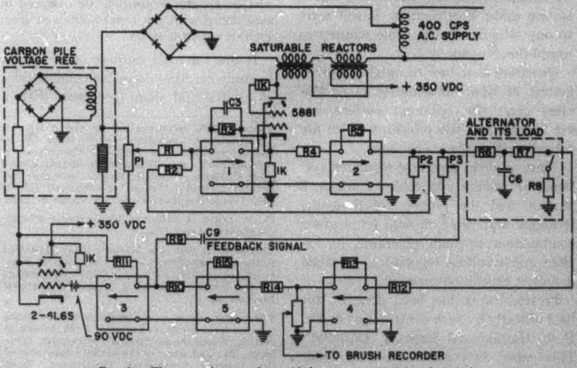

Fig. 3. The complete analogy of the system used for this study

Fig. 4. The entire analogue setup, showing the computer, auxiliary amplifiers, regulator, and recording device

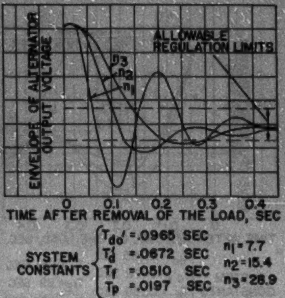

Fig. 5. Response of a particular system as the turns-ratio of the feedback transformer is varied

and to be useful, must have the following characteristics[2]:

1. It must be a measure of the performance of transient behavior of the system and be of physical significance.
2. It must be calculable.
3. It must be measurable.

When dealing with any physical system there are two important transient factors to consider: time of response and stability. Therefore, we must examine any transient behavior, such as the voltage output fluctuations of the alternator, for these two characteristics. We would ask: how much time elapsed from the application of a given disturbance till the voltage returned to its normal value? Also, were there any severe oscillations which occurred during this time?

A number of possibilities are available to make this evaluation. Carleton used the rms-error criterion.[2] Harder, in dealing with linear systems, reasoned that since the oscillation could be described by a single frequency and a logarithmic decay, the criteria could be expressed in terms of a system time constant, or time for the envelope to drop to 36.8 per cent of its initial value, and a single frequency, describing the oscillatory term.[1] Simpler methods can be used. Many of the military specifications governing the type of aircraft electric power system used for this study state that the a-c generator output voltage during load changes between full and no load shall recover to and remain within the regulation limits within a definite time and that no sustained oscillations shall develop.

For this investigation the latter method was used because of its direct application to the system being studied. Referring to the necessary characteristics for a transient figure of merit, this method adequately meets the first and third requirement. It is not easily calculable, but due to the nonlinear nature of the voltage regulator it was felt that it was impossible to expect a method of calculation. The very reason for using this type of electronic analogue representation implies difficult, if not impossible, direct analytic attack.

For this study, the output voltage transient was recorded by means of a pen recorder and photographs of an oscilloscope for a range of machine parameters considered reasonable. Examination of these results gave data sufficient to determine the time of recovery and the oscillatory nature of the system during the transient period.

Conclusion

General

The data presented by the analogy method of electric system study used in this paper provides solutions of the output voltage transient for a particular carbon-pile voltage regulator in combination with a reasonable range of exciter and a-c generator machine constants. It further demonstrates the degree of stability provided by a number of feedback stabilizing transformers used with these exciter and a-c generator combinations.

It is obvious that with a flexible analogue setup as used in this study many other parameter variations can be studied for their effect on the transient performance by merely varying the setting of a "coefficient potentiometer" or by plugging in different fixed resistors or capacitors in the circuit. At present, this analogue setup with modifications is being used to study the system performance as a function of the synchronous and transient reactance of the a-c generator, as a function of the exciter amplification factor, as a function of the voltage regulator adjustment, and many other important variables that are of interest to designers of aircraft electric power systems.

In general, this method of studying dynamic system performance is amenable to any case where a part of the system is either erratic, very complex, or highly nonlinear. Such a condition usually prevents an accurate representation by direct analogue methods and necessitates the use of the actual device itself in combination with simulated circuits.

Evaluation of Analogued Circuits

During the course of the investigation covered by this paper it was felt that better methods for simulating the system conditions were possible. However, due to the limited time, it was not feasible to explore other circuitry. Further work along this line of attack is being pursued

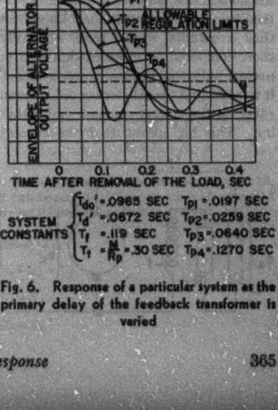

Fig. 6. Response of a particular system as the primary delay of the feedback transformer is varied

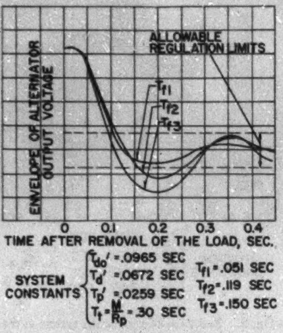

Fig. 7. Response of a particular system as the exciter time constant is varied

at this time and shows great promise. Nevertheless, the analogue circuits which were used in this study did serve a useful function and produced results, which, though they might not be precise enough for all purposes, did afford an insight into the system performance which could be expected under the conditions observed.

The auxiliary circuit which supplied the current through the carbon pile was limited in both maximum and minimum values of current. This restricted the study more or less to conditions where the machines are operating at high rotational speeds, or what is more important, where the excitation requirements of the a-c generator are low. Actually, this is not too serious since the stability and system performance, under these conditions, are usually most critical. If this case is controlled satisfactorily, operation at lower rotational speeds, or high excitation levels, should be more stable.

Another important consideration was the effect of time delay or lag in the saturable reactors. The use of the 400-cycle-per-second voltage supply for this circuit minimized this delay, but since the system being studied contained important time constants which were relatively short compared to those encountered in normal industrial electric power systems, it was felt that the reactor lag did have an effect on the system response and stability. This lag meant that the current flowing through the carbon pile was not a direct function of the exciter output voltage but was delayed in time behind the exciter voltage. This supposition was confirmed by the fact that when a combination of machine constants duplicating the system shown in Fig. 1 were set into the computer, the feedback requirements for proper stability of the analogued system indicated a damping transformer with about two to three times the anticipatory signal delivered by the actual transformer for a comparable degree of stability. An all-electronic power amplifier has corrected this condition. Another paper will cover these modifications, for with these changes very precise quantitive measurements are possible.

Output Voltage Transients as Affected by Variations in Parameters

Fig. 5 shows the response of a particular system used for this investigation as the turns-ratio of the feedback transformer was varied. The two dashed lines indicate the allowable regulation limits and define the region in which the oscillation must confine itself in determining the system time of recovery. It was evident that the greater the turns-ratio *n* of the feedback transformer the more stable the system became. However, it was equally evident that the time of response suffered if this parameter were increased indefinitely. Conversely, the speed of the initial excursion of the transient was increased as the turns-ratio was decreased. This resulted in a less stable system and so it was concluded that some intermediate value would produce the optimum results.

To further demonstrate the uses to which this type of analogue study can be applied, the response of the output voltage transient of a given system is shown for a change in the feedback transformer primary time constant. See Fig. 6.

There was, as in the previous case, a definite value of primary time constant which would give the optimum transient performance. In Fig. 6, a short-time constant produced an overdamped condition, while a long-time constant improved the time of response but only with a sacrifice in the stability.

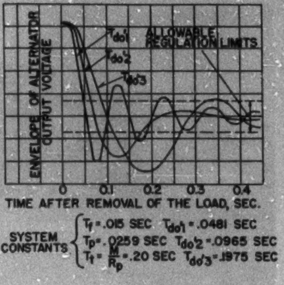

Fig. 8. Response of a particular system as the a-c generator time constant is varied

Fig. 7 demonstrates the effect of varying the exciter time constant with all other system parameters held constant. It can easily be seen that the faster the exciter responded to a signal, the more closely we approached the optimum condition for system response.

Fig. 8 shows the effect of varying the a-c generator open-circuit time constant. All other system parameters were held constant. As in the case of varying the feedback transformer turns-ratio and its primary time constant, it is easy to see that a definite value of the open-circuit time constant produced the "best" compromise between time of recovery and stability. Increasing the a-c generator time constant improved the stability but it also increased the time it took the system to recover. Decreasing the time constant had the reverse effect.

Discussion on Transient Figure of Merit Used in Paper

As can be seen from Figs. 5 through 8, it is rather difficult to evaluate the best system using the criterion of a time of recovery of the system voltage within a certain regulation limit. For a very small variation in the system parameters, the last point of intersection of the oscillation of the output voltage transient with the regulation limits may change a large amount, the change bearing little relationship to the parametric variation. The other methods of evaluating system performance overcome this condition by properly weighing the entire error over a period of time. From the results of

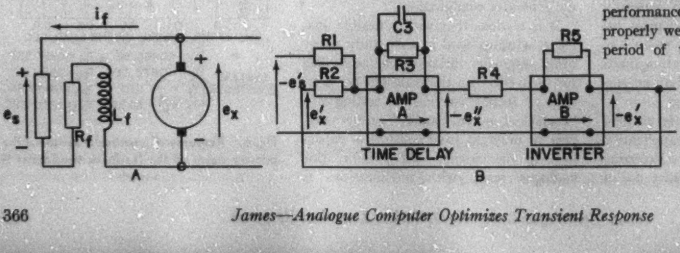

Fig. 9(A). Schematic of the shunt exciter. **(B).** Analogy used for the shunt exciter

Fig. 10(A). Schematic of the a-c generator. (B). Analogy used for the a-c generator

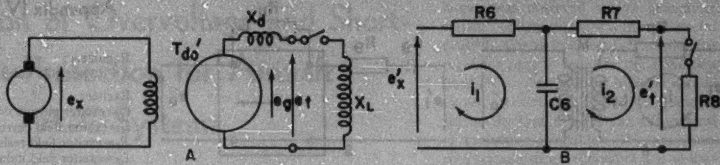

this study, it is recommended that the military specifications on aircraft electric systems be reevaluated as to the transient figure of merit in order that more uniform system performance will be obtained.

Since the first work on this paper was accomplished, an excellent treatise on the subject of the transient response of servomechanisms has been written by Graham and Lathrop.[4] Some of the criteria presented in this paper have been tried with success on this problem and show great promise for the future.

Appendix I. Proof of the Analogy Used for the Exciter, the A-C Generator, and the Feedback Stabilizing Transformer

Exciter

The exciter portion of the system is shown in Fig. 9(A). Using operational notation, we can write the differential equation describing this element as

$$e_x = e_s + R_f i_f + L_f p i_f \qquad (1)$$

and letting $T_f = L_f/R_f$

$$e_x - e_s = R_f i_f (1 + T_f p) \qquad (2)$$

Also, assuming we are operating the exciter at a relatively high speed which assures linearity between the field current i_f and the generated voltage e_x, we can write

$$e_x = K_f i_f \qquad (3)$$

or

$$i_f = e_x/K_f \qquad (4)$$

Substituting equation 4 into 2

$$e_x - e_s = R_f e_x / K_f (1 + T_f p) \qquad (5)$$

Rewriting equation 5 gives

$$e_x = \frac{K_f}{R_f}\left(\frac{1}{1+T_f p}\right)(e_x - e_s) \qquad (6)$$

Now if we connect two operational amplifiers as shown in Fig. 9(B), we can describe its functions by the following expressions

For amplifier B

$$e_x' = -(R_5/R_4)(-e_x'') \qquad (7)$$

and for amplifier A

$$-e_x'' = \frac{1}{1+R_3C_3p}\left[\frac{R_3}{R_2}e_x' + \frac{R_3}{R_1}(-e_s')\right] \qquad (8)$$

Combining equations 7 and 8

$$e_x' = \frac{-R_5/R_4}{1+R_3C_3p}\left[\frac{R_3}{R_2}e_x' - \frac{R_3}{R_1}e_s'\right] \qquad (9)$$

By inspection of equations 6 and 9, it can be seen that the correct analogy exists if the following three conditions are met:

$R_3C_3 = T_f$

$(R_5/R_4)(R_3/R_2) = K_f/R_f$

$(R_5/R_4)(R_3/R_1) = K_f/R_f$

A-C Generator

The usual expression for time constant of a generator with inductive reactance loading is[1]

$$T_d' = T_{do}'\left(\frac{X_d' + X_L}{X_d + X_L}\right) \qquad (10)$$

where

T_{do}' = transient open-circuit time constant of the field current, and equals L/R of the field circuit
T_d' = transient short-circuit (through external reactance in this case) time constant
X_d' = transient reactance
X_d = synchronous reactance
X_L = external reactance

The equation for generated armature volts e_g can be written as

$$e_g = \left(\frac{K_g}{1+T_d'p}\right)e_x \qquad (11)$$

where e_x is the exciter output voltage.

Further, the expression for the terminal voltage e_t is

$$e_t = \left(\frac{X_L}{X_d + X_L}\right)e_g \qquad (12)$$

or

$$e_t = \left(\frac{X_L}{X_d + X_L}\right)\left(\frac{K_g}{1+T_d'p}\right)e_x \qquad (13)$$

Fig. 10(A) shows the schematic of the a-c generator portion of the system. The a-c generator equivalent circuit is represented by a T-section network using two resistive elements, R_6 and R_7, and a capacitor element C_6. The load is also represented by a resistive element R_8. See Fig. 10(B).

Again using operational notation, we can write the differential equations describing this circuit as

$$e_x' = R_6 i_1 + \frac{1}{C_6 p}(i_1 - i_2)$$
$$(14)$$
$$o = (R_7 + R_8)i_2 + \frac{1}{C_6 p}(i_2 - i_1)$$

Solving for i_2 by determinants

$$i_2 = \frac{\begin{vmatrix} \left(R_6 + \frac{1}{C_6 p}\right) & -e_x' \\ -\frac{1}{C_6 p} & o \end{vmatrix}}{\begin{vmatrix} \left(R_6 + \frac{1}{C_6 p}\right) & -\frac{1}{C_6 p} \\ -\frac{1}{C_6 p} & \left(R_7 + R_8 + \frac{1}{C_6 p}\right) \end{vmatrix}}$$

$$= \frac{e_x'\left(\frac{1}{C_6 p}\right)}{\left(R_6 + \frac{1}{C_6 p}\right)\left(R_7 + R_8 + \frac{1}{C_6 p}\right) - \left(\frac{1}{C_6 p}\right)^2} \qquad (15)$$

Multiplying the numerator and denominator of equation 11 by $\frac{pC_6}{R_6 + R_7 + R_8}$

$$i_2 = \frac{\dfrac{e_x'}{R_6 + R_7 + R_8}}{\dfrac{(1 + R_6C_6p)\left(R_7 + R_8 + \frac{1}{C_6 p}\right) - \frac{1}{C_6 p}}{R_6 + R_7 + R_8}} \qquad (16)$$

Expanding the denominator of equation 16

$$i_2 = \frac{\dfrac{e_x'}{R_6 + R_7 + R_8}}{\dfrac{R_6 + R_7 + R_8 + R_6R_7C_6p + R_6R_8C_6p}{R_6 + R_7 + R_8}} \qquad (17)$$

$$= \frac{\dfrac{e_x'}{R_6 + R_7 + R_8}}{1 + \dfrac{R_6C_6p(R_7 + R_8)}{R_6 + R_7 + R_8}}$$

Now, if we wish the voltage across R_8, we must multiply equation 13 by R_8. Designating this quantity as e_t' we have

$$e_t' = R_8 i_2 = \left(\frac{R_8}{R_6 + R_7 + R_8}\right) \times \left(\frac{1}{1 + \dfrac{R_6C_6p(R_7 + R_8)}{R_6 + R_7 + R_8}}\right)e_x' \qquad (18)$$

By inspection of equations 10, 13, and 18, it can be seen that the correct analogy exists if the following conditions are met

$R_6C_6 = T_{do}'$

$R_6 + R_7 = X_d$

$R_7 = X_d'$

$R_8 = X_L$

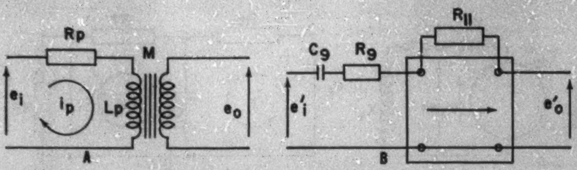

Fig. 11(A). Schematic of the unloaded feedback transformer. (B). Analogy used for the unloaded feedback transformer

$$\left(\frac{R_7+R_8}{R_6+R_7+R_8}\right)R_6C_6=T_d'$$

Since it is convenient to describe machine reactances in per-unit quantities, we do so in this analogy. A convenient base impedance is used in the analogue circuit. In this case 50,000 ohms represented a 1.0 per-unit impedance. Note that we assume linearity between the exciter output voltage e_x and the generated voltage of the a-c generator e_t. It is connected directly to the exciter and is therefore also operating at a high speed which makes this assumption reasonable.

Feedback Stabilizing Transformer

The feedback stabilizing transformer used to provide an anticipatory signal to the voltage regulator is shown in Fig. 11(A). Ideally this device has been shown to produce a voltage which is the rate of change of the voltage applied to its primary circuit. From Fig. 11(A), the current through the primary can be written as

$$i_p=\frac{e_t}{R_p} \tag{19}$$

This, of course, assumes that the primary delay L_p/R_p is negligible. Then

$$e_o=M_pi_p=M_p\frac{e_t}{R_p}=T_Tpe_t \tag{20}$$

where T_T is defined as the feedback transformer time constant M/R_p.

When it is desirable to introduce a primary delay in the transformer, the output voltage can be written as

$$e_o=\frac{T_Tpe_t}{1+T_pp} \tag{21}$$

where $T_p=L_p/R_p$, the primary time constant.

It can readily be seen that the relationship between the main time constant T_T and the primary time constant T_p is

$$T_T=nT_p \tag{22}$$

where n is the turns-ratio of the transformer.

Fortunately, we have a very simple analogue circuit to represent equation 21. This arrangement of the operation amplifier is known as a "lead" network, shown in Fig. 11(B). We can write

$$\frac{e_t'}{R_9+\frac{1}{C_9p}}=\frac{-e_o'}{R_{11}} \tag{23}$$

or

$$\frac{e_t'C_9p}{1+R_9C_9p}=\frac{-e_o'}{R_{11}} \tag{24}$$

Then

$$e_o'=-\left[\frac{R_{11}C_9pe_t'}{1+R_9C_9p}\right] \tag{25}$$

By direct comparison of equations 21 and 25, it can be seen that the correct analogy exists if the following conditions are met

$R_{11}C_9=T_T$
$R_9C_9=T_p$

Appendix II. Values of Analogue Computer Elements

Resistors (values given in megohms):
$R_1=0.0616$
$R_2=0.0616$
$R_3=2.0$
$R_4=4.86$
$R_5=1.0$
$R_6=0.050$
$R_7=0.0265$
$R_8=0.10$
$R_9=$ 0.259
$R_{10}=$ 1.0
$R_{11}=10.0$
$R_{12}=$ 0.518
$R_{13}=$ 1.0
$R_{14}=$ 1.0
$R_{15}=$ 1.0

Capacitors:
C_1 (used with R_1 determines T_f)
C_6 (used with R_6 determines T_{do}')
C_9 (used with R_9 and R_{11} to determine T_p and maximum T_T)

Potentiometers:
$P_1=0.734$
$P_2=0.734$
$P_3=$(used to determine T_T or n)

Appendix III. System Parameters Which Were Held Constant Throughout the Investigation

Regulator:
Westinghouse *AVR-90* voltage regulator adjusted to proper operation on a 20-kva a-c generator

Exciter:

Exciter field amperes:	0.75 ampere at no load
	1.42 amperes at 50 per cent, zero power factor load

Exciter amplification factor: $E_x/I_f=8.6/0.75=11.5$

A-C Generator:

Per-unit synchronous reactance:	1.53
Per-unit transient reactance:	0.53
Per-unit load reactance:	2.00

Appendix IV. Nomenclature

Regulator:
e_s = carbon pile voltage, volts

Exciter:
e_x = exciter output voltage, volts
i_f = exciter field current, amperes
R_f = exciter field resistance, ohms
L_f = exciter field inductance, henrys
T_f = exciter field time constant, seconds
K_f = exciter amplification factor, volts per ampere

A-C Generator:
X_d = synchronous reactance, per-unit ohms
X_d' = transient reactance, per-unit ohms
X_L = load reactance, per-unit ohms
T_{do}' = open-circuit time constant, seconds
T_d' = short-circuit time constant, seconds
K_g = a-c generator amplification factor, volts per volt
e_g = a-c generator generated voltage, volts
e_t = a-c generator terminal voltage, volts
(Primed quantities of voltage denote computer values.)

Feedback Transformer:
$T_p=L_p/R_p$ = feedback transformer primary time constant, seconds
$T_T=M/R_p$ = feedback transformer mutual time constant, seconds
R_p = feedback transformer primary resistance, ohms
L_p = feedback transformer primary inductance, ohms
$M=nL_p$ = feedback transformer mutual inductance, ohms
n = feedback transformer turns-ratio

References

1. Solution of the General Voltage Regulator Problem by Electrical Analogy, E. L. Harder. *AIEE Transactions*, vol. 66, 1947, pp. 815–25.

2. The Transient Behavior of the Two-Stage Rototrol Main Exciter Voltage Regulating System as Determined by Electrical Analogy, James T. Carleton. *AIEE Transactions*, vol. 68, pt. I, 1949, pp. 59–63.

3. Electronic Analog Computers (book), G. A. Korn, T. M. Korn. McGraw-Hill Book Company, Inc., New York, N. Y., 1952, pp. 341–43.

4. The Synthesis of "Optimum" Transient Response: Criteria and Standard Forms, Dunstan Graham, R. C. Lathrop. *AIEE Transactions*, vol. 72, pt. II, Nov. 1953, pp. 273–88.

5. Regulation of A-C Generators with Suddenly Applied Loads, E. L. Harder, R. C. Cheek. *AIEE Transactions (Electrical Engineering)*, vol. 63, June 1944, pp. 310–18.

6. Electrical Analogy Methods Applied to Servomechanism Problems, G. D. McCann, S. W. Herwald, H. S. Kirschbaum. *AIEE Transactions (Electrical Engineering)*, vol. 65, Feb. 1946, pp. 91–96.

7. Analogue Computers for Feedback Control Systems, Robert A. Bruns. *AIEE Transactions*, vol. 71, pt. II, Nov. 1952, pp. 250–54.

8. Analogue Methods for Optimum Servomechanism Design, F. C. Fickeisen, T. M. Stout. *AIEE Transactions*, vol. 71, pt. II, Nov. 1952, pp. 244–50.

◆

No Discussion

Co-ordination of Overvoltage and Short-Circuit Protection for Aircraft A-C Systems

M. TRBOVICH
MEMBER AIEE

R. E. KIDWELL, JR.
ASSOCIATE MEMBER AIEE

W. M. TUCKER
MEMBER AIEE

THE purpose of a circuit protector (CP) is to clear faults and thus permit the remainder of the system to continue normal operation. The function of overvoltage protection is to prevent damage to utilization equipment by de-energizing the generator when system overvoltage exists. Proper co-ordination is necessary to prevent nuisance tripping of the overvoltage relay (OVR) during low-resistance faults.

The protection required by all utilization equipment has not been established. In lieu of quantitative information regarding overvoltage requirements of utilization equipment, the problem of co-ordinating CP and OVR characteristics is approached in two ways:

1. The maximum time of fault duration is specified. Then the OVR performance is described in terms of the maximum line-to-neutral (L-N) voltage which must not operate the relay. The maximum CP rating is determined from the minimum L-N fault current which causes maximum or near maximum overvoltage on the unfaulted phases.
2. As an alternate procedure, the characteristics of an existing OVR can be assumed to meet the requirements. Then the maximum rating of CP's is prescribed so that the OVR does not operate on L-N faults.

Both methods require quantitative information regarding fault overvoltages.

Fault Overvoltages

The causes of overvoltage may be grouped into two categories: 1. those due to malfunctioning of the generator, regulator, or distribution system, and 2. those due to normal switching operations. The former category is of particular interest for this paper. The overvoltage may appear as a transient, or it may be continuous. Its influence persists until either the cause is removed or a protection device operates.

Investigations were made using presently available narrow-speed-range generators rated from 15 to 40 kva and controlled by either a carbon-pile or a static (magnetic-amplifier) regulator. The generators studied were:

A. A-c generator, 15 kva, 120/208 volts, 0.75 power factor, 3-phase, 320/480 cycles per second, 4,800/7,200 rpm. Carbon-pile regulator. (*XEL-24*).

B. A-c generator, 15 kva, 120/208 volts, 0.75 power factor, 3-phase, 320/480 cycles per second, 4,800/7,200 rpm. Carbon-pile regulator. (*XEL-24*).

C. A-c generator, 40 kva, 120/208 volts, 0.75 power factor, 3-phase, 400 cycles per second, 6,000 rpm. Carbon-pile regulator. (*AF-32509A*).

D. A-c generator, 15 kva, 120/208 volts, 0.75 power factor, 3-phase, 320/480 cycles per second, 4,800/7,200 rpm. Static regulator. (*MIL-G-6099*).

E. A-c generator, 30 kva, 120/208 volts, 0.75 power factor, 3-phase, 320/480 cycles per second, 4,800/7,200 rpm. Static regulator. (*MIL-G-6099*).

F. A-c generator, 30 kva, 120/208 volts, 0.75 power factor, 3-phase, 320/480 cycles per second, 4,800/7,200 rpm. Static regulator. (*MIL-G-6099*).

Transient voltages were recorded by an oscillograph. The method of describing transients in this paper is illustrated in Fig. 1. Curve *A* represents a hypothetical transient, and curve *B* describes the same transient by showing one-half of the envelope.

Short-Circuit Removal

When a 3-phase or 3-phase-to-neutral fault occurs at the generator terminals, the input voltage to the carbon-pile regulator drops to zero and the exciter terminal voltage increases to a value corresponding to ceiling excitation. After removal of a 3-phase or 3-phase-to-neutral fault, the terminal voltage builds up to a value corresponding approximately to ceiling excitation before the regulator can return the system voltage to normal. This behavior was observed for all generators tested. In the event of a line-to-line-to-neutral, line-to-line, or L-N fault, the regulator acts to increase the excitation until either the regulator input is normal or ceiling excitation is reached, depending on the type of fault and the amount of excitation available. The maximum overvoltages after removal of line-to-line-to-neutral, line-to-line and L-N faults were observed to be equal to or less than those after removal of 3-phase or 3-phase-to-neutral faults, depending on the excitation during the fault. Transient overvoltages due to fault removal are shown in Fig. 2 for a narrow-speed generator controlled by a carbon-pile regulator and driven at approximately average rated speed. The relative magnitudes of the short-circuit overvoltages vary with speed and generator design; however, the general trend indicated by the curves of Fig. 2 is typical of all the carbon-pile-controlled generators tested.

The same trend holds for short-circuit overvoltages on generators controlled by the static regulators used in these tests with one major exception; the removal of any fault which includes T_1 (*A* phase) results in a maximum voltage corresponding to ceiling excitation.

The results shown in Fig. 2 pertain to the no-load condition; that is, after the fault is removed, no load exists on the bus. If, after the fault is removed, the generator supplies current to resistive or inductive loads, the maximum bus voltage is less than that of the no-load condition because of the demagnetizing action of the armature current.

A comparison of overvoltages after removal of 3-phase faults, no-load condition, is given in Fig. 3 for several narrow-speed generators and a constant-speed genera-

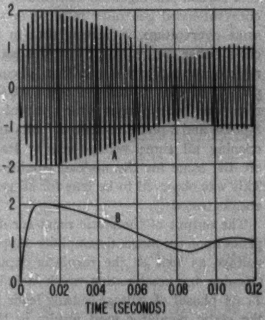

Fig. 1. Method of describing transient voltages

Paper 53-364, recommended by the AIEE Air Transportation Committee and approved by the AIEE Committee on Technical Operations for presentation at the AIEE Aircraft Electric Equipment Conference, Seattle, Wash., September 30–October 2, 1953. Manuscript submitted June 30, 1953; made available for printing August 28, 1953.

M. TRBOVICH, R. E. KIDWELL, JR., and W. M. TUCKER are all with the Naval Research Laboratory, Washington, D. C.

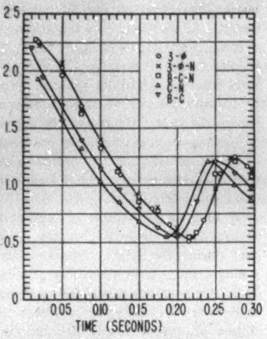

Fig. 2. Overvoltages after removal of faults. No load on bus after fault removal. Generator A. 420 cycles

tor driven at a speed equivalent to 420 cycles.

Open Sensing Leads

If all three voltage-sensing leads to a carbon-pile regulator are opened, the exciter goes to ceiling. If any one lead is opened, the output voltage of the regulator rectifiers drops to approximately 66 per cent of normal. (The value, 0.66, equals the ratio of the direct-voltage output of a single-phase, full-wave rectifier to the direct-voltage output of a 3-phase, full-wave rectifier.) The regulator then acts to increase the excitation until the phase voltage is approximately 1.5 per unit or less, depending on the extent of saturation. Overvoltages after opening sensing leads are shown in Fig. 4 for a narrow-speed generator controlled by a carbon-pile regulator and driven at approximately average rated speed. Opening any combination of sensing leads to a carbon-pile regulator controlling the constant-speed generator resulted in the same overvoltage, indicating that in all cases either the generator iron was saturated or the exciter was at ceiling. A comparison of Figs. 2 and 4 shows that the maximum overvoltages after removal of 3-phase and 3-phase-to-neutral faults and opening all three voltage-sensing leads are the same for the no-load condition. This was observed to be true for all generators tested.

The output of the static regulator depends upon the magnetic-amplifier supply voltage as well as the regulator input. Opening any combination which includes T_1 (A phase) of voltage-sensing leads to the static regulator used results in the generator voltage first dropping as the magnetic amplifier loses power, and then building up to ceiling after a relay operates to connect the exciter as a self-excited generator. Opening any combination of sensing leads which does not include T_1 results in a build-up to an overvoltage with the magnetic amplifier furnishing the exciter-field current. Fig. 5 shows the overvoltages for open-sensing leads to a static regulator controlling a narrow-speed generator driven at approximately average rated speed.

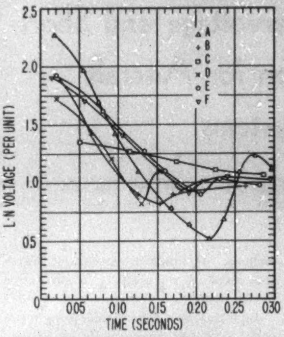

Fig. 3. Overvoltages after removal of 3-phase faults, no-load condition. Generators A, B, C, D, E, and F. 420 cycles

Unbalanced Fault Interim

Table I shows the phase voltages during line-to-line-to-neutral, line-to-line and L-N faults for a variety of generators. It also includes the ceiling voltages obtained by opening all three sensing leads. It is noted that, in general, overvoltages exist on the unfaulted phases. Fig. 6 shows the complete transient for an unbalanced fault. The example chosen is the worst condition for the generator controlled by a static regulator, that is, a fault on the phase from which the magnetic amplifier draws its power. Note that: 1. the time interval of overvoltage is a function of fault-clearing time, and 2. the voltage is transient after both fault initiation and fault removal.

Fault-Transient-Overvoltage Curve

The fault-transient-overvoltage curve, Fig. 7, is based on the removal of 3-phase faults, no-load condition. This curve represents the worst overvoltage transient likely to occur after fault removal. This curve does not take into account the overvoltages due to open sensing leads to the regulator or the overvoltages of the unshort-circuited phases during an unbalanced fault. It is assumed that the system will be protected by a relay from steady-state overvoltages. However, the overvoltage-protection relay should remain unaffected by the voltage transients caused by short circuits, assuming that the generator is to remain connected throughout. In the event of an unbalanced fault, an overvoltage can exist on the unshort-circuited phases for a time interval which depends on the characteristics of the fault-clearing device. Then, after fault removal, the transient voltages of all three phases can correspond to the fault-transient-overvoltage curve. Therefore, the fault-transient-overvoltage curve should be shifted to the right on the time axis by a suitable time interval.

Fig. 7 represents a composite of the transient envelopes of the generators investigated. The composite curve is determined as follows. The transient is considered to begin when the terminal voltage first rises above one per unit. The transient is considered to end when the voltage returns to one per unit for the first time. Since the voltage generally overshoots several times before a steady-state value is reached, each overshoot is considered as a separate transient. The composite curve is then determined from the worst transients. A factor of $2^1/_2$ per cent is allowed for errors in oscillography.

The composite curve is based on voltages observed at the generator terminals. No attempt has been made to take into account such factors as line drop, regulator tolerances, meter errors, and phase unbalance.

It is emphasized that the curve shown in Fig. 7 represents one-half of a hypothetical voltage envelope which indicates phase voltage as a function of time. A point on the curve is not to be interpreted as the length of time that a specified volt-

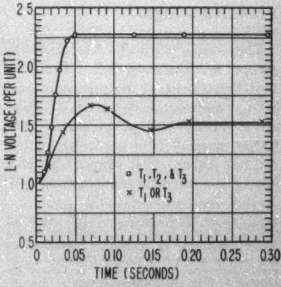

Fig. 4. Overvoltages after opening sensing leads, no-load condition. Generator A. 420 cycles

age exists. On the contrary, a point on the curve indicates the bus voltage at a specified instant of time.

It would be desirable if the overvoltage data could be presented in such form as to be useful in determining the overheating of system components due to overvoltage. For constant resistance, the energy input is proportional to V^2t, where V is the effective value of the transient voltage, and t is the time duration of the transient. If the rate of heat dissipation is constant during the transient, the energy dissipated is proportional to V_0^2t, where V_0 is the rms voltage (steady-state) prior to initiation of the transient. Then temperature rise is proportional to $(V^2-V_0^2)t$. However, the determination of the effective value of the worst transient voltage likely to occur requires the use of information in addition to the data presented in this section. Since the worst condition is the transient voltage of an unfaulted phase during an unbalanced fault plus (in time) the transient after fault removal, the additional data needed are: 1. transient voltage during the fault interval, and 2. the time that the fault exists. To determine the latter, it is necessary to co-ordinate limiter and circuit-breaker characteristics with the transient fault currents which can occur in a system.

Effect of Fault Duration on L-N Voltage

L-N Fault Current for Maximum Overvoltage

Tests on eight generator-regulator combinations (wide speed range, narrow speed range, static regulator, carbon-pile regulator) resulted in steady-state L-N fault currents of 7.2 to 9.0 per unit for low fault circuit impedance. Generator speed was 6,300 and 8,000 rpm for the narrow and wide speed range respectively. A single generator-regulator system (generator D) was assembled for test purposes, see Fig. 8.

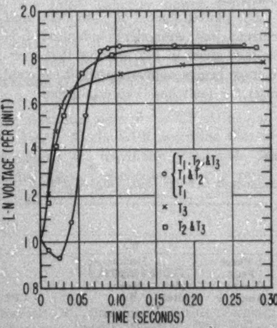

Fig. 5. Overvoltages after opening sensing leads, no-load condition. Generator D. 420 cycles

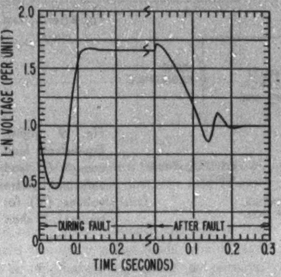

Fig. 6. Voltage of phase C during A-N fault and after fault removal. Generator D. 400 cycles

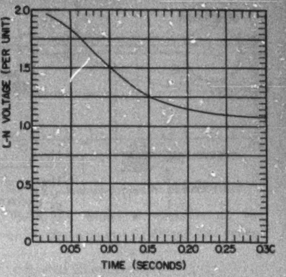

Fig. 7. Fault-transient overvoltage limits for controlled frequency range (380 to 420 cycles)

At a generator speed of 6,000 rpm, several L-N faults were established. Fault resistances from 0.2 to 0.05 per unit were used. Oscillographic records were made of the fault current and the L-N voltage.

When a ground fault is established, the L-N voltage on the faulted phase drops and the average rectified line-to-line voltage also drops. The regulator causes an increase in generator excitation until the average rectified voltage of the three phases is approximately the same as prior to the fault. For decreasing fault resistance, the unfaulted L-N voltage increases until ceiling excitation exists. When ceiling excitation exists, a decrease in fault resistance results in a small decrease in L-N voltage because of armature reaction effects. A fault resistance just low enough to cause exciter ceiling voltage therefore results in the higher overvoltage.

A fault resistance of approximately 0.1 per unit on the phase supplying power to the magnetic amplifier resulted in maximum overvoltage. The L-N steady-state fault current was 6.5 per unit. If a phase not supplying magnetic amplifier power were short-circuited, the fault resistance at which maximum unfaulted phase voltage occurred would be somewhat less than 0.1 per unit.

Equivalent Fault Current

In calculating available fault current, the variation in current following the initiation of a fault was considered. It was necessary to convert the varying current from the oscillographic record to a current value equivalent to the step-function current used in describing circuit protectors.

In this work, the expression used to compute approximate equivalent currents was

$$I=\frac{1}{\sqrt{2}}\left[\frac{\sum_{k=1}^{n} i_{pk}^{2}}{n}\right]^{1/2} \qquad (1)$$

Table I. Per Unit L-N Voltages (Steady-State) During Unbalanced Faults

Generator	Phase	Frequency, Cycles	Type of Fault: A-B-N	B-C-N	B-C	A-N	C-N	Three Open-Sensing Leads
A	A	420		1.15	1.60		1.18	2.30
	B			0	0.90		1.38	2.30
	C			0	0.90		0	2.30
B	A	420		1.35	1.52		1.13	1.90
	B			0	1.02		1.72	1.90
	C			0	1.00		0	1.90
C	A	420	0	0.69	1.55		1.26	1.38
	B		0	0	0.94		1.55	1.38
	C		0.73	0	0.93		0	1.38
D	A	420		0.90	1.42		1.07	1.83
	B			0	0.74		1.27	1.83
	C			0	0.69		0	1.83
E	A	420	0	0.98	1.58	0	1.08	2.00
	B		0	0	0.82	1.48	1.32	2.00
	C		1.06	0	0.80	1.78	0	2.00

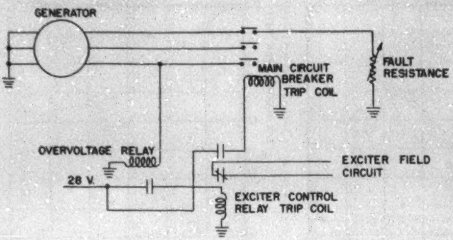

Fig. 8 (left). Test circuit

Fig. 9 (right). Equivalent fault current (I) and unfaulted phase voltage (V) for typical L-N short circuit

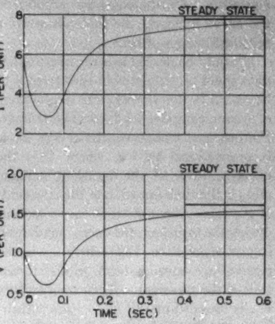

where

i_{pk} = the peak current of the kth half-cycle
n = the total number of half-cycles in the time interval t

For a fault circuit impedance of 0.1 per unit, the approximate equivalent current for the test circuit is given in Table II.

Table II

Fault Duration, Seconds	Equivalent Current, Per Unit
0.1	3.0
0.2	5.0
0.3	6.0

The equivalent current is identical to a step function current in the sense that limiters and thermal circuit breakers will be committed to trip in approximately the same time for equal magnitudes of the two currents. Obviously, however, the varying current from which the equivalent current is derived may have a relatively large magnitude at the time of circuit interruption. Since the current at the time of circuit interruption contributes to component damage, this value of current must also be considered in determining the current interrupting capacity required in a particular CP application.

CP Rating

From the assumed values of fault current magnitude and duration shown in Table II the maximum usable rating of CP's can be fixed. For example, the test generator-regulator unit furnished fault current equivalent to step-function current of 125 amperes when the fault duration was 0.1 second. Limiters[1] numbered 10 or lower, a proposed circuit breaker[2] of a 15-ampere rating or less, and an existing circuit breaker[3] rated less than 5 amperes would isolate a 125-ampere fault in 0.1 second. Further, the test generator-regulator unit furnished fault current equivalent to 210 amperes when the fault duration was 0.2 second. Again, limiters numbered 30 or lower, a proposed circuit breaker of 30-ampere rating, and an existing circuit breaker rated 7.5 amperes will isolate a 210-ampere fault in 0.2 second. The validity of these values of equivalent current and operation time for limiters and existing thermal circuit breakers has been verified experimentally. Similar data for a fault duration of 0.3 second and for generator E are given in Table III. Also shown in Table III is the maximum limiter rating permissible in mesh networks where limiter current is approximately one-half of fault current.

In the preceding discussion, an additional requirement was placed upon the CP, i.e., in addition to isolating a fault before a cable smokes or flames, a CP must clear a L-N fault before the overvoltage relay is committed to trip The additional performance requirement restricts the CP ratings which may be used in a given system. It is important to note that the maximum rating shown in Table III applies where circuit impedance is such that the specified fault current can exist. Where only lower values of fault current and, therefore, lower values of overvoltage can exist, additional voltage versus fault current data for higher values of fault resistance are necessary before co-ordination requirements can be determined.

Overvoltage for Assumed L-N Fault Duration

Calculations similar to those made for equivalent current were made to convert the varying voltage from the oscillographic record to an equivalent step-function voltage (V). The mathematical expression used was

$$V=\frac{1}{\sqrt{2}}\left[\frac{\sum_{k=1}^{n} e_{pk}^{2}}{n}\right]^{1/2} \qquad (2)$$

where e_{pk} is the peak voltage of the kth half-cycle.

The plotted curves of equivalent fault current and equivalent unfaulted L-N voltage given in Fig. 9 show that overvoltage begins approximately 0.1 second after the fault has been established.

Table III. Maximum CP Rating for Fixed Fault Duration

Effect of Environmental Condition on Circuit Protector is Not Included. Fault Circuit Impedance Is 0.1 Per Unit. 400 Cycles

	Fault Duration, Seconds														
	0.1					0.2					0.3				
Generator Rating, Kva	1-Phase Fault Current, Amperes	Single* Limiter	Limiter in Mesh Net	CB†	CB‡	1-Phase Fault Current, Amperes	Single* Limiter	Limiter in Mesh Net	CB†	CB‡	1-Phase Fault Current, Amperes	Single* Limiter	Limiter in Mesh Net	CB†	CB‡
15	125	10	5	15	<5	210	30	10	30	7.5	250	40	20	35	10
30	250	30	10	35	7.5	420	50	30	60	15	500	>80	40	>75	25

* Reference 1.

† Circuit breaker satisfying reference 2.

‡ Circuit breaker satisfying reference 3 (maximum permissible operating time).

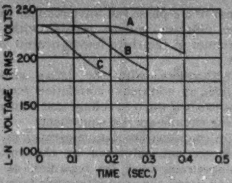

Fig. 10. Maximum voltage versus time characteristic for which OVR must not operate

A—Fault duration 0.3 second
B—Fault duration 0.2 second
C—Fault duration 0.1 second

Using the data in the preceding sections, the maximum voltage which must not energize the overvoltage relay can be described. The unfaulted phase voltage exists for approximately 0.1 second less than the duration of the fault, which in this discussion has been fixed at 0.1, 0.2, or 0.3 second. The maximum steady-state unfaulted phase voltage measured on the generators available at the Naval Research Laboratory is approximately twice rated generator voltage on narrow-speed-range generators under certain specified operating conditions. With the fault duration assigned, Fig. 6 shows the maximum instantaneous L-N voltage existing on the unfaulted phases which should not energize the OVR. For the narrow-speed-range generators studied, the calculated equivalent voltage for these voltage envelopes shows the maximum permissible L-N voltage versus time characteristic, Fig. 10, which can exist on two phases and which must not energize the OVR.

Establishing a single overvoltage curve for several generator ratings does not necessarily penalize the circuit protection in the lower capacity power systems. After an overvoltage curve has been standardized, it is necessary to examine the current and voltage relationship as a function of time and fault impedance for each power source. With these data, the maximum permissible CP rating can be fixed. As the OVR operating time is decreased, the maximum permissible CP rating also is decreased. For a rapid acting OVR, the decrease in permissible CP rating may influence the size of the main bus since many loads would have to be supplied through paralleled circuits.

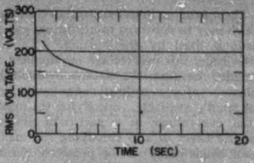

Fig. 11. Voltage versus time characteristic of test OVR (minimum operation time characteristic)

Effect of OVR Characteristic on CP Rating

Using the assumption that a specific OVR characteristic is satisfactory, the following procedure is used to determine the CP rating which may be used with that OVR. A test OVR was connected to the main circuit-breaker terminals. The operating characteristic of this relay is shown in Fig. 11. Several L-N faults were established, and oscillographic records were made of fault current and unfaulted L-N voltage. The equivalent fault current, calculated from the oscillograms with equation 1, for the time interval between fault initiation and the operation of the OVR is shown in Fig. 12, curve *A*. This curve shows the maximum time that L-N fault currents may persist before the voltage on the unfaulted phases energizes the OVR.

With a fault resistance of approximately 0.1 per unit on the phase supplying magnetic amplifier power, the voltage drop on the faulted phases causes the relay contacts in the exciter field circuit to close and connect the exciter field directly across the exciter armature. This relay action results in maximum steady-state unfaulted L-N voltage. For slightly higher fault resistance, however, a similar relay action takes place except that, when the exciter field is connected across the exciter armature, the resulting increase in faulted phase voltage is enough to open the relay contacts in the exciter field circuit. The regulator than takes control and reduces the unfaulted phase voltage and the fault currents. The preceding relay action accounts for the shape of Fig. 12, curve *A*. The OVR does not operate for the fault currents indicated by the dotted portion of curve *A*.

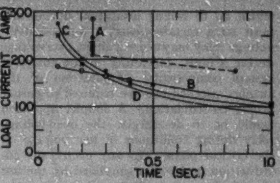

Fig. 12. Circuit protector characteristic

A. Maximum protector characteristic for co-ordination with test OVR and test generator
B. CB rated 25 amperes[3]
C. Fuse numbered 30[1]
D. CB rated 7.5 amperes[2]

Curves *B*, *C*, and *D* of Fig. 12 show the maximum fuse and circuit-breaker ratings that may be used in the low-impedance test circuit if the OVR characteristic shown in Fig. 11 is used. Co-ordinated protector performance at the critical point of curve *A* (minimum current—minimum time) was verified experimentally.

Conclusions

To make the operational requirements of fault and overvoltage components compatible, the maximum permissible ratings of circuit protection components must be established in relation to the current source capacity. A practical method has been proposed for establishing co-ordination of overvoltage protection with circuit protection.

References

1. Fuse, Enclosed Link, Aircraft. *Military Specification MIL-F-5372*, United States Air Force, Dayton, Ohio, Oct. 23, 1950.

2. Circuit Breakers, Three-Phase A-C, Trip-Free 115/200-Volt. *Bureau of Aeronautics Experimental and Developmental Specification XBL 809*, Bureau of Aeronautics, Washington, D. C., Nov. 7, 1952.

3. Circuit Breakers, Trip-Free, Aircraft. *Proposed Military Specification MIL-C-5809B*, Wright Air Development Center, Dayton, Ohio, Nov. 1952.

◆

Discussion

Russell W. Stineman (Boeing Airplane Company, Seattle, Wash.): The authors failed to discuss the application of 3-phase overvoltage relays. In a system employing carbon-pile regulators, or any regulator which is not peculiarly sensitive to a fault on a particular phase, an overvoltage relay which responds to the average line-to-line voltage will not sense any overvoltage during a fault. No co-ordination is required between the overvoltage relay and circuit protectors, thus greatly increasing the ease and flexibility of system design. The overvoltage relay need have only sufficient delay to override the transient voltage following removal of a 3-phase fault. Circuit protectors should then be chosen to give fault clearing that is fast enough to prevent damage to single-phase loads on an unfaulted phase.

In a system employing static regulators

which go to ceiling excitation during any fault on a certain phase, a 3-phase overvoltage relay may sense a slight overvoltage during a fault, depending on the choice of system components. Application of the authors' method may be required to ensure proper co-ordination. A simpler approach would be to de-energize the over-voltage relay during conditions of low voltage on the critical phase. In any event, the co-ordination problem is simplified by the use of a 3-phase overvoltage relay, since the voltage sensed during a fault will always be less severe than the worst phase voltage.

M. Trbovich, R. E. Kidwell, Jr., and **W. M. Tucker:** We thank Mr. Stineman for his discussion.

The maximum line-to-neutral overvoltage which may be delivered to utilization equipment is fixed by specification.[1] To our knowledge, this overvoltage requirement is included because the actual overvoltage tolerances of most utilization equipment are not readily available. Specifying the maximum overvoltage in a particular system has the effect of also specifying the maximum single-phase circuit protector rating because the protection functions must be accomplished before the line-to-neutral voltage exceeds the specified limits.

With the preceding data, the co-ordination of single-phase fault-protection devices in terms of line-to-neutral voltage and available fault current is straightforward. On the other hand, if 3-phase voltage sensing is used, it is also necessary to correlate the output of a 3-phase full-wave rectifier (with three different voltage inputs) with the maximum of the three line-to-neutral voltages.

Furthermore, with the latter sensing method, an additional correlation requirement exists if the overvoltage and regulator sensing circuits are not equivalent.

The co-ordination data presented in the paper are not influenced by the voltage sensing circuit used, for regardless of the sensing circuit the overvoltage relay characteristic must be correlated with the permissible line-to-neutral overvoltage.

REFERENCE

1. CHARACTERISTICS OF AIRCRAFT ELECTRIC POWER. *Military Specification MIL-E.7894*, Bureau of Aeronautics, Washington, D. C.

Directional Detection for Parallel Aircraft Alternators

F. MAMETT
ASSOCIATE MEMBER AIEE

J. A. GRANATH
ASSOCIATE MEMBER AIEE

AIRCRAFT electric system designers have several methods available for providing generator protection. These include overcurrent devices (thermal and magnetic), differential current devices (balanced current and zone type), and directional sensing devices (the familiar reverse current cutout).

Of these various protection methods, all but one are suitable, with appropriate modification, for use on either a-c or d-c systems. The exception is directional sensing, since alternating currents do not possess directional properties with respect to a fixed reference, as do direct currents. The directional properties of an a-c system can be determined only by the use of an alternating reference of the same frequency. When the relative phase angle between the current and the reference is established, and a voltage is chosen as the reference, the resultant power and reactive power do possess directional properties with respect to a fixed reference. The problem of directional sensing in an a-c system, therefore, requires consideration of the direction of power and reactive power, and consequently is more difficult than determining the direction of a d-c current.

In response to general interest expressed in the possible use of directional protection on aircraft a-c systems, several organizations have undertaken development programs and some devices have been built. It is the purpose of this paper to show a method useful in determining the requirements of a sensing element for a-c directional protection, which is based on system parameters and performance as predicted by analysis and observed by tests. System performance in terms of power and reactive power flow is discussed in general and an example is given to show the application of the method in the determination of the characteristics of a directional protection-sensing element for a given system, for the purpose of achieving an abritrarily chosen degree of protection.

The system to which this device is to be applied is as shown in Fig. 1, consisting of two or more 3-phase, 4-wire alternators connected in parallel. These alternators are supplied with shaft power at controlled speed by any of the means available; variable ratio hydraulic pump and motor, gas turbine, air turbine, auxiliary combustion engine, etc. Excitation is provided for the alternators by integral shaft-mounted rotating exciters or by static exciter-regulators. Power and reactive power load equalizing is provided by interconnection of the speed governor circuits and voltage regulator circuits respectively. The zone to be protected by the directional sensing device includes the alternator and cable length from the alternator terminals to the direction sensing element.

Directional Aspects of System Conditions

DEFINITION OF TERMS

The term directional, when applied to a d-c system, is self-explanatory. In a-c system analysis, direction of power flow can be defined by the phase relationship between current and voltage, holding one of the two quantities as reference, and adopting certain conventions. If the terminal voltage of a machine which is acting as a generator is defined as the reference and is represented by a phasor

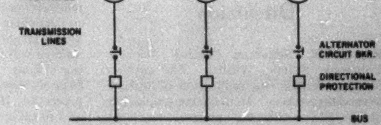

Fig. 1. Electric system line diagram

Paper 53-363, recommended by the AIEE Air Transportation Committee and approved by the AIEE Committee on Technical Operations for presentation at the AIEE Aircraft Electric Equipment Conference, Seattle, Wash., September 30–October 2, 1953. Manuscript submitted June 25, 1953; made available for printing September 2, 1953.

F. MAMETT and J. A. GRANATH are with the Armour Research Foundation, Illinois Institute of Technology, Chicago, Ill.

The work described in this paper was carried out for the United States Air Force, Electrical Branch, Equipment Laboratory, Wright Air Development Center, Dayton, Ohio.

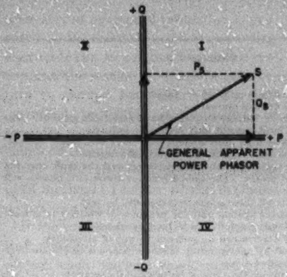

Fig. 2. Direction reference co-ordinates

lying along the positive abscissa of the co-ordinate axes, the relative position of any current or voltage phasor can be located, given the phase displacement of that quantity with respect to the reference phasor. If the convention that apparent power *S* is the product of a voltage and the complex conjugate of the associated current, a phasor representing apparent power can be located on another set of co-ordinate axes as shown in Fig. 2. In this diagram the real component of *S* is *P*, the power in watts delivered by the machine, and is represented by the component of *S* which is parallel to the abscissa. The region of positive power is to the right of the ordinate; negative power (absorbed power) is to the left. Similarly, reactive power *Q* in vars is the vertical component of *S*. Positive reactive power lies above the abscissa and indicates a generator delivering reactive power; that is, supplying an inductive load or lagging power factor. Thus a phasor in quadrant I represents a generator delivering power at lagging power factor. Quadrant II and III indicate power being absorbed by a generator at lagging (II) or leading (III) power factor. Quadrant IV operation is that of a generator supplying power to a leading power factor load, or operating underexcited on a paralleled system, that is, delivering power but absorbing reactive volt-amperes.

NORMAL CONDITIONS

In normal, steady-state operation, an alternator will be delivering power and reactive power to some load. The power phasor representing alternator output will be in quadrant I as shown in Fig. 2. The three phase voltages are equal in magnitude and are displaced from each other by an angle of 120 degrees. The currents are also balanced, and no neutral current exists. The system frequency is constant and the various alternators are sharing the total connected load.

Transients which occur in normal operation may cause the phasor *S* to lie momentarily in any position around the 360-degree arc. Such transient power swings are those which may occur during synchronizing or which may be caused by voltage regulator and speed governor recovery after sudden application or removal of load, or on recovery from a fault. The magnitude and direction of *S* during these synchronizing swings depends on system reactances and number of machines on the bus. The time duration of transient power swings, which will ultimately damp out if the system is stable, is a function of system constants including inertias, and can be calculated.[1,2]

Because the constant speed alternator drive cannot have infinitely fast speed of response, consideration must be given to possible power system transients resulting from sudden accelerations and decelerations of the prime movers. The maximum magnitude and time duration of these depends on the nature of the prime movers and control systems involved, but in general they should be of the same order of magnitude as the synchronizing disturbance.

ABNORMAL CONDITIONS

The four general types of short circuits which may occur are: single-line to neutral, double-line to neutral, line-to-line, and 3-phase. The voltages and currents present during these faults are a function of the fault impedance, the location, and the number of machines on the system.

Simple calculations made on the basis of solid faults on a 2-alternator system and no connected load are usually sufficient to give the direction and approximate magnitudes of the power and reactive power components.

The effect of having more than two machines on the system would be to increase the fault current. Any other assumptions necessary in these fault calculations should be made conservatively. Phasor diagrams showing the typical voltages and currents during short circuit are shown in Fig. 3. As would be expected, the fault voltage for a zero impedance fault at the terminals of the directional sensing element is zero (except for the line-to-line fault). The values listed in Table I are per phase, and are for the phase or phases involved in the fault.

An alternator can supply real power to a system to which it is connected only when it is receiving mechanical power input from a power source, that is, a prime mover. If for some reason the prime mover fails to supply this power, then the alternator, if kept connected to the electrical system, will function as a synchronous motor and will supply power to the prime mover. As long as the power required to drive the prime mover at synchronous speed is below the pull-out torque of the alternator, the alternator will remain in synchronism and the system will be stable.

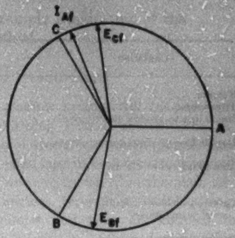

SINGLE LINE TO GROUND SHORT CIRCUIT

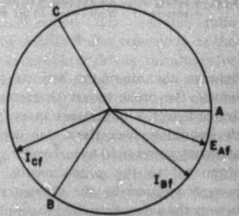

DOUBLE LINE TO GROUND SHORT CIRCUIT

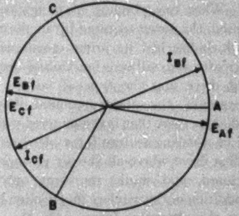

LINE TO LINE SHORT CIRCUIT

Fig. 3. Short-circuit phasor diagrams

The over-all effect on the system of an alternator losing its prime mover is a function of the type of prime mover and the type of coupling between them. When a free-wheeling clutch is employed

Table I. Tabulation of System Conditions

Condition	Power	Reactive Power	Comments
Normal	$+A$, $+B$	$+A$, $+B$	Machine delivering power to lagging power factor load
Transients	$\pm A$, $\pm B$, $\pm C$	$\pm A$, $\pm B$, $\pm C$	Random occurrence in a normal system
Single line-to-ground short-circuit	0	0	The two phases which have voltage available have zero fault current. The phase which has high fault current may have zero voltage
Double line-to-ground short-circuit	0	0	The two phases which have high fault current may have zero phase voltage. The phase which has voltage available has zero fault current
Line-to-line short-circuit	$-B$	$+B$	The fault voltage is the same on both faulted phases and the fault currents are 180 degrees out of phase. The indications for those two phases will be exactly opposite
	$+B$	$-B$	
Three-phase short-circuit	0	0	For zero impedance faults all three phase voltages will be zero
Loss of prime mover	$-A$, $-B$	0	Magnitude depends on drive system and the presence or absence of a free-wheeling coupling. Never greater than A for free wheeling
Dragging rotor	$-B$	0	Maximum reverse power determined by pull-out torque of alternator
Speed governor failure	$+A$, $+B$ $+C$	0	Amount of power supplied by overspeeding machine depends on the number of machines and the type of drive
Power equalizer failure	$\pm A$	0	Direction of power depends on the type of failure and its location
Excitation malfunctions	0	$\pm A$, $\pm B$	Direction of reactive power depends on the kind of failure

Key: + forward — A = less than 0.15 per unit — C = greater than 1.50 per unit
− reverse — B = 0.15 to 1.50 per unit — 1.0 per unit = alternator name-plate rating

between the alternator and its prime mover, the prime mover characteristics are no longer of importance in analyzing the condition, since the clutch does not allow any power to be transferred from the alternator to the prime mover. The power consumed by the alternator will be only the amount required to supply the I^2-R losses, iron losses, and the friction and windage losses. These are always a very small percentage (approximately 10 to 15 per cent) of the alternator rating.

When free-wheeling couplings are not used, the power required by an alternator which has lost its prime mover will be greater and will be a function of the kind of drive and the type of failure. For example, the power required may be slightly more than is encountered with the free-wheeling feature for a bleed air turbine drive where all the air passages are closed, and would represent only the addition of the windage and friction losses to the alternator losses. On the other hand, the power required may be of the same order of magnitude as the alternator rating for this same air turbine operating as a compressor. The most severe case would probably be encountered where the prime mover is a reciprocating engine of large capacity as compared to the alternator. If the load imposed on the alternator by the loss of the prime mover is in excess of the pull-out torque of the alternator, the alternator will lose synchronism and begin to slow down. Conditions of this sort are considered in the section which deals with dragging rotor conditions.

As long as the pull-out torque of the alternator is not exceeded, the alternator will take power from the system and continue to furnish its share of reactive power to the system.

The conditions referred to as dragging rotor are those in which the power consumed by the alternator is such that none of the prime mover input is utilized in supplying load power. Such conditions may be caused by rubbing of the alternator rotor, bearing seizure, loss of prime mover, and other mechanical failures.

These failures may result in the loss of relative motion between rotor and stator. Before this occurs, the machine in question passes through two intermediate stages. The first stage involves a reduction in the power supplied to the system. If this condition persists, it may result in the losses increasing to the point where the alternator is taking power from the system as well as from its prime mover (if the prime mover is operative). This condition appears to the system as a loss of prime mover, and the analysis of the preceding section holds. Should the mechanical load (the losses due to mechanical failure) become so large that it is impossible for the alternator to develop enough torque as a motor to carry this load, the alternator loses synchronism and rapidly slows down to either a greatly reduced speed or a completely stalled condition.

The power absorbed from the system as the losses increase reaches a value equal to the pull-out torque of the alternator and is usually two or three times the alternator rating by the time synchronism is lost. Once synchronism is lost, power oscillations take place which are similar to the power swings during out-of-phase synchronizing previously discussed.

As the alternator slows down, a point is reached where the machine is no longer able to maintain rated terminal voltage. This will take place on machines with integral exciters since the maximum exciter output, and consequently the maximum air gap flux is limited by the exciter speed. For machines which are excited by some other means, saturation of the magnetic circuit will limit the air gap flux even if sufficient current is supplied by the excitation system. In any event the alternator presents a highly reactive load to the rest of the system causing large currents to flow in the faulted alternator with an accompanying drop in system voltage. The severity of this voltage reduction is dependent on the number of machines on the system and is most severe for the 2-machine case.

During normal operation, the alternators comprising the electrical system operate at their normal frequency, corresponding to the rated shaft speed, and they share system load through the use of various interconnections between the alternator governors.

Faults may occur in the governor or control circuit, such as the failure of the speed-sensing element or its drive shaft, open or short circuits on various portions of the control leads, etc. These faults may have practically no effect on the system or may be so serious as to interrupt the production of power completely. The result is a function of the fault location, the size of the prime mover as compared to the size of the alternator, the type of coupling between the prime mover and the alternator, the relative rating of the paralleled machines, and other characteristics.

For example, if the paralleled alternators are driven by the main engines through a variable ratio transmission and a free-wheeling connection, it is possible for the alternator and its drive to operate at different speeds. Consider a loss of speed sense on the variable ratio transmission so as to cause the alternator coupled to it to increase its frequency. The result would be to accelerate the remaining alternators so they would experience reverse power on all phases and to raise the system frequency to that dictated by the overspeeding machine. If some sort of overspeed protection is provided on the drive unit, the overspeeding alternator can be removed from the system and the rest of the machines can return to normal operation. If no such overspeed protection is employed, or should it malfunction, then the other machines on the system can continue to draw power from the overspeeding machine until mechanical failure of the machines occurs as a result of the abnormal speed.

If the system was modified so that the free wheeling connection was not employed, each machine would attempt to operate at that speed determined by its governor and, as a result, loss of synchronism would occur on the system.

Many types of system faults may be grouped in the category of excitation malfunctions. Among them are loss of alternator field, loss of exciter field, loss of voltage regulator sense, and various failures in the reactive load division circuits.

Loss of alternator field or of exciter field causes the machine which has experienced this failure to take reactive power from the system instead of supplying it as is the normal condition. The effects on the system are serious in that they involve a reduction in the bus voltage and cause the remaining machines to operate at high currents and low power factors. If the total system load is small in magnitude, the system can stay in synchronism. During this period no reverse power is experienced by any of the machines on the system. For larger system loads, the excited machines of the system may not be able to supply the reactive power requirement of the unexcited machine and the system will lose synchronism, and large power swings will ensue. These will not die out and will persist until corrected by operator action or until mechanical failure takes place.

Failures occurring in the voltage regulator or equalizer system can also cause reactive power to be consumed by one or more alternators of the system. These failures may be accompanied by system overvoltage or undervoltage, unequal sharing of reactive load with its associated reduction in system capacity, etc. For failures of this nature reverse reactive power may be experienced by faulted or unfaulted machines, depending upon the type and location of the failure. In a properly functioning machine the reactive power consumed as a result of maximum excitation on another machine of the system may be of the same order of magnitude as the reactive power taken by a machine which has subnormal excitation. Because of this feature, it is not possible to determine by the direction of flow of reactive power alone whether or not a particular machine is operating properly.

Summary of Conditions

System conditions in terms of direction and magnitude of power and reactive power flow at the point of measurement are summarized in Table I with explanatory comments. Table values are given letter designations to indicate that certain bounds or orders of magnitude apply to systems in general, and to emphasize the fact that specific values depend on the circuit parameters of specific systems.

From Table I, it is possible to determine the feasibility of using directional indications to select the circumstances under which a protective device should function, and to determine where additional intelligence is needed for a particular application. Quantities which are available to be sensed or measured are power and reactive power, time duration of directional flow, or combinations of these quantities. The characteristics of malfunctions and of normal operation must be correlated in such a way that the combination of conditions chosen to indicate malfunction does not also occur for any normal or permissible operating conditions.

In using the table, certain considerations must be kept in mind:

1. The fact that sensed reverse power or reactive power of a certain magnitude occurs for each system condition for which trip is desired is not adequate in itself. Further investigation is required to ascertain that no permissible system condition also gives rise to the directional quantity, so that nuisance tripping will not occur.

2. When one machine is delivering power resulting from a malfunction, other machines on the system are absorbing power, or experiencing reverse power flow at the sensing element. Thus, whenever a source circuit malfunction occurs which causes an alternator to deliver an excess of power or reactive power, the remaining, properly operating alternators will be experiencing the reverse of these quantities. This is in conflict with the greater number of cases where a source circuit malfunction causes the defective machine to absorb real or reactive power. The possibility of removing a properly functioning alternator from the system as a result of the malfunction of another alternator is undesirable and should be prevented. This can be done by proper selection of the system property to measure, by setting the trip level, or by superimposing a requirement of additional intelligence for a signal to trip.

3. A combination of conditions should be selected which provide the minimum possibility of indecisions (trip or not-trip) on a set of conditions, and the minimum difficulty of co-ordination with other protective equipment.

An Example Application of the Method

System Description

The sample system will be one with the following characteristics. The alternators which operate in parallel are of the same kind in both construction and rating and are driven from the main aircraft engines through a variable ratio transmission and they are coupled to the transmission with a free-wheeling clutch.

Reference to Table I indicates that additional information is needed to evaluate system performance under governor malfunction. The variable ratio transmission (hereafter referred to as the drive) is capable of driving the alternator at about twice rated speed for normal engine cruising revolutions per minute if the speed governing system should fail. Because of this, overspeed protection in the form of a centrifugal switch mounted on the drive is provided. The switch operates when the drive output speed exceeds by a preset amount the rated drive output speed. When the switch operates, it causes the drive to assume its minimum shaft speed position and also trips the alternator breaker so the machine is electrically removed from the system. During the overspeed condition, reverse power occurs on the rest of the alternators connected to the system. This reverse power may be as high as four times the generator rating for two alternators in parallel and light system load with the maximum reverse power occurring in any case about t' seconds after the failure of the speed governor. If the centrifugal overspeed switch operates, the system will return to normal with the overspeeding machine removed in about t seconds where $t>t'>$ duration of a synchronizing disturbance. If the overspeed switch does not operate, then reverse power in excess of magnitude A will still be present after t seconds.

The various alternators on the system share the real and reactive load by virtue of equalizer loop connections among the machines. The real power equalizing system has small gain, that is, changing from no load to full load changes the prime mover speed only about 1/2 per cent for machines which are operating properly. Therefore the equalizer has only a small effect on the power-sharing during abnormal system conditions. Reverse power which flows as a result of faults in the real power equalizing circuits will be small, and it will not be in excess of the power taken by a free-wheeling alternator.

PROTECTION REQUIREMENTS

The following functional operating requirements have been arbitrarily selected for the purpose of demonstrating the use of directional protection methods. A justification of the assumed requirements, involving an analysis of the function of the aircraft, types of load devices, evaluation of weight, reliability, ease of operation, and other factors necessitating extensive analysis and judgments, is beyond the scope of this paper.

Directional protection shall be designed which will perform several functions. One is to detect any short circuit occurring in the protection zone and to remove such a fault from the system before the fuses blow. The directional protection shall also detect when any alternator is taking more power from the system than it would take during freewheeling operation, removing that alternator from the system if the condition persists for more than a transient period.

The directional protection shall not operate during any normal system transient such as synchronizing or sudden dropping of load, regardless of the direction or magnitude of the power during this period. It shall not operate for abnormal system conditions caused by failures in the real power division or governor circuit except when such failures jeopardize the entire system. The directional protection shall not operate for faults outside its own protection zone (through faults).

CORRELATION OF REQUIREMENTS AND CONDITIONS

Having specified the various system operating conditions, Table I will be used to determine the common characteristics of those conditions for which protection is desired. It will also be used to insure that system conditions for which protection is not desired do not possess these characteristics.

A survey of the table indicates that a device sensitive to reverse power in excess of A would perform all of the required duties with the following exceptions. It would not detect short circuits except for line-to-line faults, where it would operate improperly. It may act prematurely on loss of speed sense or during a synchronizing disturbance.

A device sensitive to reverse reactive power would not provide protection for any of the required conditions and would act improperly on a line-to-line fault. It could also remove the wrong machine from the system in the event of a voltage regulator failure.

It would appear then, that reverse power is the most suitable of these two quantities to sense.

The major deficiency in detecting reverse power in excess of magnitude A is the inability to detect line faults since, except for the line-to-line case, no voltage is available on the faulted phase. During the line-to-line fault, the line currents are 180 degrees out of phase and it is therefore impossible to determine which alternators are good and which are faulty by the direction of power alone.

On synchronizing disturbances reverse power transients always occur as a result of out-of-phase synchronizing, but they die out quickly. The reverse power produced by an overspeeding alternator will be transient if the overspeed switch functions, and it should not cause the directional protection to operate. If the overspeed switch does not operate in the required time, all the remaining alternators should be removed from the system before permanent damage to all the machines may be incurred.

MODIFICATIONS NECESSARY

To provide protection on line faults by reverse power protection, it is necessary to provide a reference voltage. This may be achieved by: 1. Some sort of memory device, a capacitor for example, to provide as voltage reference the line to neutral voltage of the phase prior to the fault (the product of the reference voltage and fault current would provide directional power components on all line faults); 2. A phase shift network which involves using the voltage of an adjacent phase or a line to line voltage, shifted in such a fashion that normal power and reactive power indications are produced during normal conditions (quadrant I) with the phase-shifted voltages.

The use of the voltage prior to fault as the voltage reference does not completely satisfy the protection requirements, since improper action will still take place on line-to-line faults. Shifting the line to neutral voltage so that the indicated power during the fault is the product I_aE_c, I_bE_a, and I_cE_b on each of the three phases, does satisfy the conditions. The phase shift should be of such a value that under normal conditions the shifted voltages E_c, E_a, and E_b occupy the positions of the normal voltages E_a, E_b and E_c respectively. Reverse power indications in excess of magnitude A for all of the line faults, except zero impedance 3-phase faults, are given for the phase shift specified.

If it is assumed that improper action on line-to-line faults is less desirable than insensitivity to zero impedance 3-phase faults, the use of phase-shifted line-to-neutral voltages to provide line fault protection is the most desirable of the methods indicated.

The improper removal of machines because of synchronizing disturbances can be prevented by utilizing a suitable time delay. The premature action on loss of speed sense can also be prevented by providing time delay. For the system of this example, a time delay of t seconds will be sufficient for both these conditions, and will still allow the directional power protection to function and prevent the destruction of the entire system if the overspeed protection should fail to operate.

The addition of the time delay, while improving the action of the protective device during transient conditions, does slow down the speed of protection in general. The only place where this is highly undesirable is on short circuits, since slow action may allow fuses to blow before the directional protection clears the fault. On all line faults, with the exception of 3-phase faults, reverse power will exist on one or two but not all three phases. On all other fault conditions, if reverse power does exist, all three phases will be involved. If a time delay is used under conditions of reverse power on all three phases, and no intentional time delay is provided when reverse power exists on some of the phases only, a device built with these characteristics will provide the required protection.

FUNCTIONAL CHARACTERISTICS OF DETECTOR

The functional characteristics of the device necessary to accomplish the protection desired for the system used in the example can be divided into four categories:

Phase Shift

A passive network is required which will give a voltage proportional to the input voltage, and which lags the input voltage to the network by an angle of 120 degrees.

Phase Demodulators

A circuit or device is necessary which can assume two stable states, one state corresponding to conditions of indicated reverse power (which is the same as the actual reverse power during conditions of balanced voltage) of magnitude A or greater, and the second state for conditions where the indicated power is positive, zero, or negative, and less than A in magnitude.

Time Delay

A time delay circuit or device is necessary to provide the required t seconds' time delay.

Balance or Unbalance

A device or circuit which has two stable states, one state corresponding to conditions where all 3-phase demodulators give the same indication, and the other when indication from one of the demodulators is different from the other two.

The conclusions arrived at in the example are not intended to imply that solutions to all protection problems may be attained by the use of directional protection or that the conclusions drawn are in any way general. For a different system and with protection against other failures or other combinations of failures required, different results will be obtained.

The system used in the example is an existing system, and the results obtained have actually been used in the construction of a directional protector with the specified characteristics.

Summary

The factors of system performance which affect directional sensing in aircraft a-c electric systems have been discussed in general and the requirements of a device to make use of the intelligence available from directional sensing have been developed for a specific case. To carry this development to completion, it is necessary to obtain quantitative values for sensitivity, time delay, current and voltage magnitudes, wave form distortion, etc., for application of the method to a specific system. There are also design problems to be solved to get components which will meet operating requirements of environment, size, weight and reliability, as well as the functional requirements here outlined. It is believed, however, that the establishment of the functional requirements must be the first step in successful development of a directional protection device for aircraft.

References

1. Alternating Current Machines (book), **Thomas C. McFarland.** D. Van Nostrand and Company, Inc., New York, N. Y., 1948, p. 356.

2. Electric Machinery, Vol. II, A-C Machines (book), **M. Liwschitz-Garik, C. C. Whipple.** D. Van Nostrand and Company, Inc., New York, N. Y., 1946, p. 368.

No Discussion

The Effects of Abnormal Conditions on Aircraft, Parallel A-C Power Systems

S. C. CALDWELL
ASSOCIATE MEMBER AIEE

A. J. WOOD
ASSOCIATE MEMBER AIEE

Synopsis: The purpose of this paper is to call attention to system malfunctions which may occur on parallel-connected, aircraft, a-c electric power systems. These malfunctions must be considered when an integrated study is made of the protection and operation of these systems. A list and discussion of these malfunctions is presented. It is hoped that this paper will stimulate discussion which will provide more nearly complete coverage of the problems associated with this type of system.

IN RECENT years the growth of electric power loads on aircraft has been extremely rapid.[1] As a result of this, and in an effort to reduce weight, an increasing number of aircraft power systems are being designed to operate at constant frequency with two or more alternators in parallel.[2,3] The application of this type of system brings with it new protective problems as well as those usually found on other types of electric power systems. The importance of these protective problems becomes magnified when it is realized that some projected aircraft cannot remain aloft without electric power.

In the basic design of aircraft power systems consideration should be given to the functioning of the system under abnormal conditions as well as normal conditions. This paper presents a list of possible malfunctions which have been encountered and considered in recent applications as well as those which have been known in the past. Different system configurations will emphasize different problems, so that each system configuration needs a separate analysis based upon its own peculiarities. This listing, however, is intended to present the general problems common to all such systems. With these problems in mind, the selection of a particular configuration and protective system may be based upon adequate consideration of all the factors.

Problems peculiar to isolated, variable-speed systems are not considered except where they appear related to parallel, constant-speed system conditions. Fig. 1 illustrates the components of an aircraft power system. This discussion is concerned with malfunctions in the electric distribution system, alternator, voltage regulator, drive, and drive-governing system.

Results

Table I presents the list of malfunctions discussed in this paper and briefly states some of the effects of these malfunctions on system operation. It may be seen that these problems are not purely generator problems, but also involve the drive and its control as well as the bus and distribution system. It is necesssary therefore that close co-ordination be maintained between manufacturers of drive, protective system, and airframe. The effects of these abnormal conditions on the functioning of the aircraft equipment or on the ultimate damage to the aircraft are not considered. This is a separate problem in itself and requires consideration for each particular aircraft.

System Malfunctions

The sequence of the following discussion does not imply any relative scale of importance or probability of occurrence of the malfunctions. Various system engineers will undoubtedly rank these malfunctions in different orders. In general, it is a primary design objective that no single failure should result in loss of all electric power.

Electric System Faults (Short Circuits)

At present aircraft electric distribution systems depend upon fuses, current limiters, and thermal breakers for fault

---

Paper 53-371, recommended by the AIEE Air Transportation Committee and approved by the AIEE Committee on Technical Operations for presentation at the AIEE Aircraft Electric Equipment Conference, Seattle, Wash., September 30–October 2, 1953. Manuscript submitted July 1, 1953; made available for printing August 13, 1953.

S. C. Caldwell and A. J. Wood are with the General Electric Company, Schenectady, N. Y.

Table I. System Malfunctions of Aircraft A-C Electric Systems

Malfunction	Possible Causes	Effects on System	Damage Which May Result	Remarks
System Faults (Short Circuits)	1. Accidental terminal faults 2. Broken lines due to vibration 3. Combat damage 4. Wear (abrasion)	1. Interruption or reduction in power available for affected loads 2. Possible loss of synchronism during fault 3. Possible overvoltage on unaffected phases 4. Large currents and reduced voltages on the affected phases	1. Overheating of lines 2. Damage to equipment 3. Loss of generating equipment 4. Loss of entire system by bogging or by failure to clear fault	Large motor loads present special protective problems and may require relatively long clearing times. Main busses generally require very long clearing times. Large drive power requirements for some types of faults
Excitation Failures				
Overexcitation of one machine	1. Loss of sensing lead to regulator 2. Regulator failure or fault within the exciter 3. Damage to reactive load division circuits 4. Accidental error in regulator settings	1. Rise in bus voltage; possible large system overvoltage 2. Excess of reactive current out of abnormal machine 3. Reduction in excitation and deficiency in reactive current out of normal machines 4. Possible loss of synchronism producing large, fluctuating currents and torques in all machines and fluctuation of bus voltage about an average tending to be somewhat higher than normal	1. Damage to generating equipment (most probably to abnormal machine) 2. Loss of synchronism 3. Damage to load equipment	
Underexcitation of one machine	1. Loss of lead to exciter field 2. Open in alternator field circuit within the machine 3. Regulator failure	1. Drop in bus voltage 2. Deficiency in reactive current in abnormal machine 3. Excess of reactive current in normal machines and possible large increase in excitation 4. Possible loss of synchronism producing large, fluctuating currents and torques in all machines and fluctuation of bus voltage about an average which is lower than normal	1. Damage to generating equipment (most probably to normal machines in 2-machine systems) 2. Loss of synchronism 3. Damage to load equipment	
Exciter polarity reversals	1. Random synchronizing 2. System faults 3. Initial build-up transient	1. Oscillating bus voltage which may produce system overvoltages (with carbon-pile regulators) 2. Fluctuating currents in all machines which can be large	1. Damage to load equipment 2. Damage to generating equipment 3. Damage to regulating equipment	This problem is disappearing with the application of effectively dampered alternators and static-type voltage regulators
Loss of Phase				
Isolated operation	1. Fault clearing 2. Broken line due to vibration 3. Poor connections 4. Combat damage	1. Loss or reduction of power to loads 2. Reduction of starting torque for 3-phase motors 3. Negative- and zero-sequence currents will flow in system and generator and sequence voltages will appear on affected portion of system 4. Possible overvoltages on two normal phases (if a machine feeder or stator winding is opened)	1. Possible overheating of alternators and rotating loads due to negative- and zero-sequence currents 2. Possible damage to loads from overvoltage on normal phases	Not a highly damaging condition except where generator feeders or windings are opened or where large unbalanced currents are produced
Parallel operation	1. Fault clearing 2. Broken line due to vibration 3. Poor connections 4. Combat damage	1. Same as items 1, 2, 3 above for open phases other than in machine feeders or stator windings 2. Small negative- and zero-sequence voltages 3. For opens in machine feeders or stator other than in electric load division phases, sequence currents will not be excessive 4. For opens in phases sensed by electric load division circuits: a. Bus voltage unbalance will be small b. Neutral currents in machines may be very large c. Circulating currents in normal machine phases may be very large d. Excitation on affected machine may be high e. Excitation on normal machines may be low f. Affected machine may carry most of real and/or reactive load g. The normal machines may produce a deficiency of real and/or reactive power	1. Possible overheating of alternators and rotating loads due to negative- and zero-sequence currents 2. Possible overheating of alternator rotor due to high excitation	Opening the phase without the load division circuits on machine feeders or stator windings will not seriously affect system operation
Random Synchronizing	1. Operational synchronizing 2. Resynchronizing after faults	1. Transient interchanges of power and current 2. Transient torques transmitted to the drives 3. Possible exciter polarity reversals	1. The continued application of transient torques may shorten the effective life of the drive	Automatic synchronizing equipments will reduce the frequency but not preclude these occurrences
Drive Malfunction				
a. Overspeeding drive	1. Mechanical malfunctions	1. Overspeeding machine takes on real load and tends to accelerate normal	1. Overheating of machine	

Table I (continued)

Malfunction	Possible Causes	Effects on System	Damage Which May Result	Remarks
	2. Loss of load division system	machines and raise system frequency a. Without overrunning clutches on drives, overspeeding machine may be forced to run out of synchronism b. With overrunning clutch, system frequency will rise and overspeeding machine may carry large currents; normal machines will draw small real current from system and overrun their clutches 2. System voltages and reactive current division will remain near normal unless synchronism is lost	2. Possible damage to clutch 3. Possible mechanical failure of generators or rotating loads	
b. Underspeeding drive	1. Mechanical malfunctions 2. Loss of load division system	1. Affected machine tends to drop real load and reduce system frequency a. Without overrunning clutches, machine may be forced to run out of synchronism (depending upon type of drive) b. With overrunning clutches, the machine will draw small real current to remain in synchronism by overrunning its clutch. System frequency will drop with present drives. 2. Bus voltage and reactive division will remain near normal unless synchronism is lost	1. Possible damage to overrunning clutch 2. Possible overloading of normal machines 3. Possible damage to loads from underfrequency operation	
c. Governor instability	1. Malfunction in the governing system 2. Excitation of a governing system oscillation by the electrical system	Governor instability may set up large oscillating currents and torques in machines and bus voltage may fluctuate appreciably	1. Possible damage to alternator 2. Possible damage to mountings	
Dragging Machine	1. Broken alternator shaft 2. Bearing failure 3. Rubbing rotor	May draw very large currents from the system	1. Overheating of dragging machine 2. Possible overheating of lines and normal machine	Stalled machine may draw from three to six per unit current from the bus. The current drawn (real and reactive components) depends upon the amount of dragging torque and speed of alternator
Loss of Load Division Circuits	1. Electrical faults in load division circuits (open circuits as well as short circuits)	1. Possible severe unbalance in real and/or reactive machine currents 2. Possible drop in voltage and/or speed	1. Possible overheating of alternators 2. Possible damage to overrunning clutches	Effect on the system operation depends upon the particular load division circuit(s) used and the malfunction which occurs

protection.[4,5] These devices require large fault currents and power to clear, and the clearing times range from a few milliseconds to several seconds. Generating systems (*viz.*, alternators, exciters, and regulators) are usually designed to yield a minimum of three per unit fault current for a 3-phase short circuit at the alternator terminals. This means even higher unbalanced fault currents since the negative- and zero-sequence impedances of the alternators are much less than the positive-sequence impedance.

Even with high fault current and sufficient power to clear faults, some faults may require longer than 1 second to clear. This has been found true particularly on main bus faults and faults on lines to large rotating loads which are protected by certain types of fuses and thermal breakers which will permit motor starting. These long fault clearing times require time delays in some of the generator protective devices so that generators will not be removed from the system during the time short circuits are being cleared. For instance, if neutral current actuates a protective relay, a time delay must be incorporated in the relay system so that this system will not remove the generator during unbalanced faults involving ground. This co-ordination problem requires that fault clearing times be calculated fairly accurately.[6]

Some types of faults may result in loss of synchronism during the fault since the available synchronizing torque may be very small. When this type of fault is cleared, the machines will have high excitation and very large system transients will occur. The protective devices must be able to override this condition without false trips.

Momentary interruption of voltage to motor loads will cause them to decrease in speed. If these loads constitute a high percentage of the system load or if generation is reduced by the fault, the system may not recover. Also, if the speed of induction motors drops sufficiently when the voltage is interrupted by a fault, the inrush current to the motor when the fault is cleared may be as high as the starting inrush current of the motor.

The distribution lines used in aircraft a-c electric systems have a relatively high resistance.[7] This fact, coupled with the high fault currents produced by the generating systems and large alternator losses for some types of faults, requires high fault power from the drive. The worst cases encountered to date by the authors have been single-line-to-ground faults and line-to-line faults. The actual magnitude of the fault power required is a function of the sequence impedances of the system, the character of the loads, and the characteristics of the particular generating system in question. With stiff drives, the fault power requirement does not present a particularly difficult problem either mechanically or electrically. If drives without overload capacity are used, these high power requirements under fault conditions may result in a large

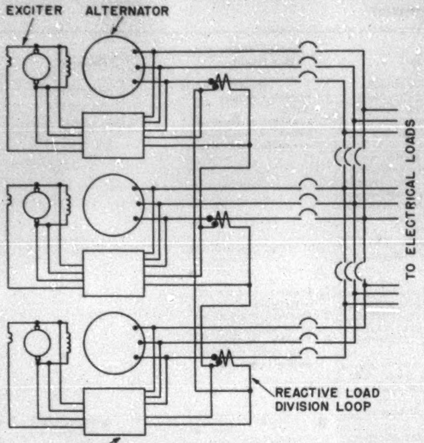

Fig. 1. Alternator, exciter, and regulator combination for aircraft, parallel a-c systems

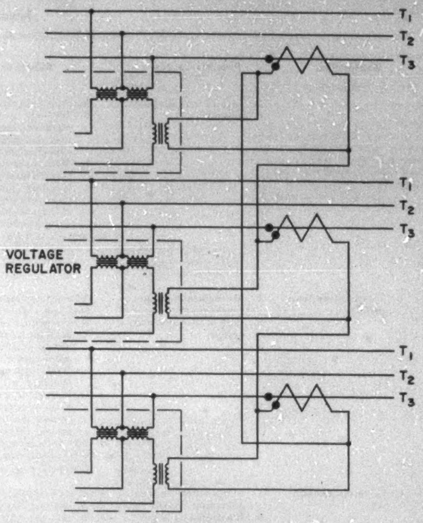

Fig. 2. Reactive load division loop

transient frequency droop which may reduce fault current capabilities below that required to clear the fault. This condition is one which must be considered also in the design of protective systems. If underfrequency or underspeed devices are utilized, they must be co-ordinated in such a way that the system is not shut down during or immediately following these speed dips.

EXCITATION FAILURES

Overexcitation on One Machine

If a regulator or exciter malfunction causes the excitation of one machine of a parallel system to rise, the terminal voltage of the system will tend to rise. The reactive load division circuits (shown in Fig. 2) presently being used will not prevent the excitation of the normal machines from being driven down. This action, as well as the amount of voltage rise, depends upon reactive division circuit and machine constants and load. At light load, the only effect will be a bus voltage rise coupled with circulating reactive currents. This condition can be detected and the machine which is generating the excessive reactive volt-amperes can be removed from the system, provided the system overvoltage is great enough to warrant its removal.

However, if the system load is large and real load division functions normally, the excitation on the normal machines will be driven low enough so that reactive currents will be severely unbalanced between machines. These currents may be large enough to overheat the alternators. Under some conditions of large system load and with alternators which have a high synchronous reactance, the excitation on the normal machines may be driven so low that synchronizing torque is less than load torque and synchronism is lost before the system voltage rises high enough to actuate overvoltage devices. The normal machizes will then act as induction generators and the system instantaneous power flow and voltage will fluctuate and large, fluctuating reactive currents will flow in all the machines. A system with a large number of machines may prevent the bus voltage from rising enough to actuate overvoltage devices.

If slipping takes place, pulsating torques will be transmitted to the alternator shafts at slip frequency. Since this frequency may be low (1 or 2 per cent of rated frequency), a danger of exciting mechanical resonance occurs, although use of a nonlinear coupling greatly reduces this hazard. Also, the pulsating real power may excite the real load division system at its critical frequency and set up a speed-governing-system oscillation. Again, use of nonlinear shaft couplings will tend to limit the amplitude of this oscillation.

Underexcitation on One Machine

If the reverse of the situation described in the foregoing occurs, that is, the excitation on one machine is reduced, the machine with low excitation will not generate its share of the reactive volt-amperes, and the system voltage will tend to decrease. If the alternator excitation is completely lost the power carrying capability of the alternator will be limited to that due to saliency. However, if only the exciter field current is reduced to zero, the power carrying capability of the alternator will include the effect of the exciter residual voltage as well as the saliency effect. With high system loads synchronism may be lost and the malfunctioning machine will slip and cause fluctuations of system voltage and power.

The characteristics of the system under this condition of slip are the same as given in the preceding section entitled "Overexcitation on One Machine." However, the bus voltage will fluctuate about an average lower than rated. This level will be determined by the gain and saturation characteristics of the reactive division circuits together with load conditions.

Under this condition the machine with low excitation must be removed from the system and the machines with high excitation must be left on the system. This is exactly the opposite situation to that described under the overexcitation condition. During the time that these excitation malfunctions are present the loads will continue to be supplied provided that the system stability limits are not exceeded.

Exciter Polarity Reversals

In addition to the excitation malfunctions just given, one of the troubles encountered in parallel system operation has been that of exciter polarity reversals. These reversals occur frequently in lightly dampered alternators that have been synchronized out of step or on the occurrence of a 3-phase fault. An exciter reversal will cause an unstable regulator condition so that the terminal voltage will oscillate. Several methods of preventing exciter reversals have been found, and it appears that this problem may not be prevalent in future systems.

Loss of Phase

The opening of a phase line either in the distribution system or inside of a machine is certainly a possible malfunction. Combat damage, vibration, fault clearing, and poor mechanical connections may all be causes of this malfunction.

Isolated Operation

Opening a generator lead when operating isolated, or opening a line anywhere in the distribution system (isolated or parallel operation), will cause a loss of power on that phase in the part of the system dependent upon that particular line. Three-phase motors on the system tend to balance the phase voltages by providing low zero-sequence impedances. Therefore, if 3-phase motors are being supplied from the section of line with an open phase in it, an appreciable voltage may still be present to supply single-phase loads on the opened phase.

An open line will reduce the full load and, to a greater extent, the starting capabilities of 3-phase motors. If the system load is large, the alternator supplying the load may become overheated due to the unbalanced currents. Also, an open line in the machine or between the machine and the voltage regulator sensing leads, will result in overvoltages on the other two phases if the regulator senses 3-phase quantities.

Parallel Operation

With a system operating in parallel, an open phase in a machine or in one of the lines between machines will have little effect on system operation. The system bus voltage will remain relatively well balanced at rated value since the alternator zero-sequence impedance is small compared to the other sequence impedances. Since system zero-sequence impedances are usually large compared to the alternator value, only small unbalanced currents will flow in the loads and little (if any) derating needs to be applied to the loads for this condition. Also, in the systems studied to date, continuous operation of the machine under this condition has been possible, since unbalanced currents are relatively small and electric coupling between the alternators is little affected.

However, if the phase containing the electric load division circuits is opened in an alternator or in the leads between machines, large unbalanced currents (zero and negative sequence) will flow in the machines and loads. This condition must be alleviated if overheating of the alternators and possible loss of the system are to be prevented. This condition is brought about by the fact that an open circuit in the phase which contains the load division sensing circuit appears as a load unbalance in the load division circuit. The differential load division circuit will then force excitation (and/or power) upwards in the machine with the open phase and force it downwards in the remaining machines. Therefore, the abnormal machine will supply a disproportionately large amount of reactive (and/or real) load and very large circulating neutral and phase currents (in the two normal lines) will flow. Since these currents may be of the order of two per unit or more, overheating can take place in both normal and abnormal alternators. This unbalanced condition will also produce large third-harmonic currents in some alternators, which tends to aggravate overheating in such machines.

Random Synchronizing

Past experience indicates that with manual synchronizing systems alternators are likely to be closed in out-of-step and out-of-phase.[8] When a low-impedance 2- or 3-phase fault is cleared, the system will be subjected to large resynchronizing surges. During such a fault the excitation of the machines rises to a high value and, since the electric coupling between machines is very small, the machines will usually slip out of step. These resynchronizing surges can be as large or larger than for initial synchronizing.

The large current and torque transients attendant with random synchronizing may result in shortening drive life, and with lightly dampered, carbon-pile-regulated machines exciter reversals have been induced by field current transients under these conditions. There have been reports of damage to machine and drive mountings resulting from the large torques characteristic of these conditions.

For these reasons, the industry has been greatly interested in automatic synchronizing equipment to prevent these major system disturbances and it appears that successful devices will be available soon. However, it should be noted that automatic synchronizing does not prevent random synchronizing upon clearing a multiphase fault. Therefore, drive and machine construction and mountings still must be able to withstand synchronizing surges if a high order of system reliability is to be obtained. Automatic synchronizing will reduce the frequency of occurrence, but it does not eliminate completely the transient currents and torques due to random synchronizing.

Malfunctions of the Drive[9]

The drive malfunctions which affect the electric system are those resulting in overspeed, underspeed, or governor instability causing oscillations in speed.

Overspeeding Drive

When one drive overspeeds, its alternator will generate a disproportionately large share of the system real power requirements. If the total system real power requirements are within machine capabilities, the overspeeding machine will take on all of the system real load and tend to accelerate the normal machines. If overrunning clutches are used, the system will operate at the overspeed with the normal machines continuously overrunning their clutches and drawing enough electric power from the system to overcome their losses. The normal machines will still supply their share of reactive load. Currents in the overspeeding machine will be very large if the load is heavy and damage due to overheating will ensue.

If overrunning clutches are not used, normal drives will be accelerated if power requirements for this acceleration are within the capabilities of the overspeeding machine. Again, the overspeeding machine will have very large currents. If there is insufficient power to accelerate the normal drives, the overspeeding machine will run out of synchronism and large current surges will flow in all machines and slip frequency torques on the shafts will be large.

Underspeeding Drive

In a system with overrunning clutches drive underspeed will cause the affected generator to drop real load and absorb enough real power from the system to remain in synchronism and overrun its clutch. Since this requires only small amounts of power and since the alternator still carries its share of reactive load, machine currents will be small and resulting system capacity may be greater than if the machine were dropped completely from the system. However, if differential real load division is used, system frequency will drop to a value dependent upon division circuit constants and upon load. Also, if the overrunning clutch cannot operate continuously in the overrunning condition, clutch failure may ensue and slow or stop the machine rotation.

In a system without overrunning clutches, if the generator has insufficient power capabilities to force the drive to operate at synchronous speed, the generator will run out-of-step and cause large pulsating currents and torques both in itself and in the normal machines.

If all drives are operating at underspeed due to low engine speeds, generator and regulator characteristics are such that bus voltage may be maintained down to 75 per cent speed or less. Saturation in transformers and induction motors may raise magnetizing currents to levels high enough to seriously damage the loads or to operate load overcurrent devices in addition to overloading the alternator field due to its own saturation characteristics. This last is true of both isolated and parallel systems.

Governor Instability

Governor hunting or instability may be caused by a malfunction in the governing system due to mechanical or electrical damage to control components. This hunting may then set up large current and torque oscillations in the alternators. These oscillations can cause severe mechanical damage to the alternator and its mountings.

DRAGGING MACHINE

Alternator speed may be reduced or an alternator completely stopped by mechanical failures such as a broken shaft, a bearing failure, or a rubbing rotor. If machine speed is reduced to the point where it is still running at synchronous speed but is dragging, real power will flow into the machine. If the alternator speed drops still further it will pull out of step with the system and system voltage and power flow will oscillate. A completely stalled machine acts as a reactance load on the system and will draw high currents. The magnitude of these currents depends upon the reactance of the alternator.

LOSS OF LOAD DIVISION CIRCUITS[10]

Reactive Load Division

The reactive load division circuit may suffer several types of failures. If the loop is opened the voltage regulators will revert to droop-type regulators where the terminal voltage is determined by the reactive load and by the amount of droop incorporated in the regulators. Reactive load division will be maintained between the machines to a degree dependent upon droop circuit characteristics and regulator settings. If a current transformer in the loop is open-circuited the regulator involved will increase the excitation of its alternator and decrease excitation on the normal machines. This excitation may go to high values but system voltage will remain near normal. The affected machine will carry large reactive load and may overheat.

Short-circuiting a current transformer in the reactive division loop will remove the droop signal from the associated voltage regulator. The subsequent action of the voltage regulator will depend upon the initial setting of affected voltage regulator with respect to settings on the normal regulators. The affected machine excitation may be driven to a high level or to a low level depending upon these relative settings. Reactive current unbalance between machines will depend upon these settings. For instance, if the initial setting of the regulator with the short-circuited current transformer is higher than the settings on the normal machines, the affected machine will tend to raise the bus voltage and generate an excessive share of reactive load.

Opening the line between the reactive division loop and the regulator drooping transformer will also cause a loss of reactive droop signal to the regulator. Since the loop is still intact, reactive load division will be maintained. However, if the voltage drop across the open drooping transformer in the regulator is significant, the excitation of its alternator will rise and tend to raise bus voltage. The ultimate bus voltage will depend upon the circuit constants.

Real Load Division

Real load division may be accomplished by a differential loop or by a drooping speed versus load characteristic in the governor. A failure in this latter type of governing system will cause the real load to be redistributed among the remaining machines on the system.

Failures in differential systems may take the form of open or short circuits or mechanical damage to servomotors or other components. The particular form of control system used will determine the effect on the electric system upon the occurrence of a fault in the differential real load division system. The usual results to be expected are that one machine will increase its speed slightly and generate all of the real power on the system. If overrunning clutches are used, the remaining machines will motor and overrun the clutches. Also, if the system load is heavy, the alternator which is generating the load power may become overheated.

Conclusions

1. A parallel a-c system is subject to a number of malfunctions which can impair its operation or cause complete loss of system function. These conditions have been discussed qualitatively in some detail with the intention of providing the system engineer with criteria with which to estimate the type and degree of protection needed to meet the increasingly reliable operational standards required in modern aircraft.

2. The authors feel that the compilation of the abnormal system conditions given in Table I, plus the evidences of their existence, will provide assistance in analyses of integrated aircraft power systems by bringing together in one place a list of abnormal conditions under which the system may be called upon to operate.

3. It is hoped that additions to this table and discussion will be forthcoming: this paper presents only those aspects which have come to the attention of the authors and it is thought that other problems undoubtedly exist in this field.

4. Due to considerable variations in system configurations and parameters, no attempt has been made to present quantitative results. It is felt that, for the present, each different system must be analyzed separately both quantitatively and qualitatively as an integral assembly if optimum compromises between reliability, complexity, weight, and space are to be obtained.

References

1. PROGRESS IN APPLICATIONS OF ELECTRICAL ENGINEERING TO AIR TRANSPORTATION, **D. E. Fritz.** *AIEE Transactions*, vol. 71, pt. II, 1952, pp. 261–69.

2. BASIC CONSIDERATIONS IN SELECTION OF ELECTRIC SYSTEMS FOR LARGE AIRCRAFT, **W. K. Boice, L. G. Levoy, Jr.** *AIEE Transactions (Electrical Engineering)*, vol. 63, June 1944, pp. 279–87.

3. PARALLEL OPERATION OF MAIN-ENGINE DRIVEN 400-CYCLE AIRCRAFT GENERATORS, **L. G. Levoy, Jr.** *AIEE Transactions (Electrical Engineering)*, vol. 64, Dec. 1945, pp. 811–16.

4. PROTECTION OF THE AIRPLANE MAIN BUS, **D. W. Exner.** *AIEE Transactions*, vol. 68, pt. II, 1949, pp. 979–82.

5. AIRCRAFT ELECTRIC POWER PROTECTIVE SYSTEMS, **B. O. Austin.** *AIEE Transactions*, vol. 66, 1947, pp. 1375–82.

6. A METHOD OF CALCULATING CURRENT LIMITER AND FUSE CLEARING TIMES IN A-C SYSTEMS, **S. C. Caldwell, L. E. Jensen.** *AIEE Special Publication S-57*, 1953.

7. IMPEDANCE DATA FOR 400-CYCLE AIRCRAFT DISTRIBUTION SYSTEMS, **D. W. Exner, G. H. Singer, Jr.** *AIEE Transactions*, vol. 71, pt. II, 1952, pp. 410–19.

8. AUTOMATIC SYNCHRONIZING FOR AIRCRAFT ALTERNATORS, **Fred B. McCarty, G. W. Hills.** *AIEE Transactions*, vol. 71, pt. II, 1952, pp. 454–58.

9. GOVERNOR REQUIREMENTS FOR AIRCRAFT ALTERNATOR DRIVES, **W. K. Boice, L. G. Levoy, Jr.** *AIEE Transactions (Electrical Engineering)*, vol. 64, July 1945, pp. 534–40.

10. POWER EQUALIZER SYSTEMS FOR AIRCRAFT ALTERNATORS, **John A. Granath, Albert K. Hawkes.** *AIEE Transactions*, vol. 72, pt. II, Sept. 1953, pp. 209–17.

Discussion

Paul F. Boggess (Westinghouse Electric Corporation, Lima, Ohio): The authors state that, "In general, it is a primary design objective that no single failure should result in loss of all electric power." Reliability of a parallel a-c power system is obtained because two or more sources of power are available to a single bus system. If a-c power is the primary power source, i.e., without a-c power the aircraft is unable to fly, then the primary design criterion must be that no single fault in the power system results in appreciable loss of electric power to the loads and continuity of a-c power to the bus is essential.

A parallel a-c power system is composed of the following components: engine, drive with frequency and real load control, a-c generator with voltage and reactive load control, a control and protective system and a bus system. System malfunctions cannot be limited in evaluation to the effect on an individual component, but must include evaluation of interrelations existing in the system. For example, if an excitation fault occurs, what effects are seen in frequency and real load civision control?

Electric short circuits in combination with certain system and fault impedances can impose heavy mechanical loads on the drives. If drives without the proper overload capacity are used, the high fault power requirements may result in a large transient frequency droop which may reduce fault current capabilities below that required to clear the fault. Under such a condition the system very likely will not recover. Such a-c power systems will not be satisfactory as the prime objective stated in one manner by the authors, and in another manner in this discussion, would not be satisfied. One fault could cause the loss of all power. It seems to be necessary that drives with sufficient overload capacity must be used in a-c power systems.

In considering over- and underexcitation faults, the number of machines in parallel, the strength of the reactive load division, and the type of regulator used must be considered when determining the rise or fall in system voltage when the fault occurs. A static-type regulator does not react the same as a carbon-pile-type regulator under extreme fault conditions. It is also true that static-type regulators from different manufacturers may not give the same results.

Exciter polarity reversals have been listed as an abnormal condition in a parallel a-c system. Again, we must consider the type of voltage regulator and a-c generator we are considering. With carbon-pile regulators, exciter polarity reversals can occur during build-up of the voltage, on the application of a short circuit and if water impinging on the commutator of the exciter causes commutator to brush separation, forcing the main field power to flow in the reverse direction in the exciter shunt field. Static-type voltage regulators, in general, are devices which provide separate excitation to the exciter. Polarity reversals do not occur as long as the static regulator provides the separate excitation. The authors state that effectively dampered a-c generators and static regulators are a cure to the problem of exciter polarity reversals. Will effectively dampered a-c generators with carbon-pile voltage regulators have a polarity reversal problem? Discussion has been presented on this subject in the past.[1]

REFERENCE

1. EXCITER POLARITY REVERSALS IN VOLTAGE-REGULATED AIRCRAFT ALTERNATORS, R. P. Judkins, H. M. McConnell. *AIEE Transactions*, vol. 71, pt. III, 1952, pp. 275–83.

S. C. Caldwell and A. J. Wood: We would like to thank Mr. Boggess for his comments and interest in this paper.

Reliability in aircraft electric systems is becoming increasingly important as the modern aircraft increases its dependence upon electric power to fulfill its mission and even in many cases to remain in flight. The objective that in a parallel system single malfunctions should not cause complete loss of power must be extended to cover the entire system. That is, if the reliability inherent in a parallel system is to be maintained, single faults in the alternators or voltage regulators controlling the alternators, drives, drive controls, or electric protective system should not cause complete loss of power. The authors do not believe that the statement "reliability of a parallel a-c power system is obtained because two or more sources of power are available to a single bus system" is complete. While a well-protected, parallel system can be made highly reliable, cognizance of the special problems attendant upon parallel operation is required if this high degree of reliability is to be obtained. The purpose of the paper was to point out these special problems so that they might be taken into account when designing a parallel, a-c system.

Mr. Boggess' comments on the effects of malfunctions are substantially those presented in the paper. The effects of any malfunction must be analyzed from a systems viewpoint. That is the aim of the data which are presented in Table I. In the instance noted by the discusser, part of his question is answered in the presentation. For the remainder: the reaction of the frequency controls depends upon the particular drive used, i.e., whether speed sensing is obtained from alternator voltage or from a separate sensing device or a combination of the two and, in the case of out-of-step operation, on the transient response characteristics of the drive system. With most drives that are available, basic speed control is obtained from a separate sensing device, and alternator output frequency sensed from the voltage (if used) performs only a trim function on the speed control. Hence, changes in frequency with changing bus voltage are limited and compared with the effects of the basic malfunction of over- or underexcitation these speed variations are not considered important.

Note has been made in the presentation of the possibility of exciting a resonance if out-of-step operation occurs and, should this occur, serious mechanical damage to the system may ensue.

The maximum power requirement on a given alternator drive must be considered from both a steady-state and transient basis. In a recent study of the alternator drive power requirements for a multigenerator installation on a large aircraft, it was found that the intermittent overload requirement and not fault power was the determining factor in choosing drive ratings. This situation arose because of the imposed requirement that a large percentage of the total electric load be supplied from a reduced number of alternators.

The magnitude of transient fault power required depends upon the following factors:

1. Type of fault.
2. Location of the fault in the system.
3. Duration of the fault.
4. Alternator parameters.
5. Voltage regulator parameters.

It was stated in the paper that single line-to-ground and line-to-line faults will generally produce the largest fault power requirement. These high fault power requirements are basically due to: 1. the necessity for large fault currents to clear thermal devices in the distribution system; 2. the use of relatively high resistance distribution lines; 3. the I^2R losses in the amortisseur circuits; 4. the increased load on the unfaulted phases.

The effects of requiring a larger amount of power output from a drive than it is capable of supplying will be seen in a transient frequency droop. The magnitude and duration of this droop depend upon the following factors:

1. System inertias.
2. Magnitude of power required.
3. Maximum power available from the drive.
4. Response characteristics of the drive governor.
5. Duration of the fault.
6. Amount of prefault load.

The duration of the fault is lengthened as larger sizes of thermal protective devices are used.

The steady-state fault power requirements on two large, multiengine aircraft have been studied and found to reach values of 2 to 3 per unit following the initial transient. However, the authors do not believe that these figures can be taken as a general rule for purposes of drive design. The fault power requirements should be considered on an energy basis. The high fault power must exist for a sufficiently long time to have a noticeable effect on system frequency, since the rotational energy of the machine and drive are large. On this basis a combination of long, high resistance lines plus long fault clearing times (such as would be obtained by the use of large thermal protective devices) are required to produce a significant frequency droop even without augmentation of energy input to the drive. The loads on many aircraft systems are well diversified and no large thermal protective devices are required on such systems. Therefore, system faults will be cleared rapidly enough to preclude any large frequency droop on unbalanced faults.

In view of this we agree fundamentally with Mr. Boggess' statement that "... drives with sufficient overload capacity must be used in (aircraft) a-c power systems." However, it is necessary to define precisely the phrase "sufficient overload capacity" in terms of what is actually needed.

Exciter reversals of electrical origin in carbon-pile regulated systems have been overcome by several methods. One is by means of heavy dampers in both axes (which are desirable for other reasons as well) on the alternator together with high-speed regulators and transient field bias; another is by means of series and shunt windings on the exciter which tends to lengthen rotor current decay time. These are discussed in detail in the reference noted by Mr. Boggess.

For these reasons, the authors feel that the reversal problem appears surmounted at the present time. It should be noted however, that, as long as carbon-pile regulators are used, new operating conditions affecting the mechanics of commutation and brushes may arise and the problem may return. Thus, the discusser's comments on static regulators are pertinent in that they point out the inherent superiority of the static regulator which, without recourse to special windings or devices, appears very effective in combating this problem.

We would like to include several worthwhile additions to the paper which were suggested by Jonn Ward.[1] All of the following comments apply to the data of Table I of the paper.

System Faults

Effects on system:

5. May cause very large ripple in transformer-rectifier d-c output.
6. May cause saturation currents to flow in iron core devices which may operate thermal protectors in these circuits before the fault is cleared by the system protection. This is particularly true in the case of line-to-line faults.
7. May require 3-phase loads to operate on 1 or 2 phases following the fault.

Exciter Polarity Reversals

Possible causes:

4. Worn-down or hung-up exciter commutator brushes.

Remarks:

Effectively dampered alternators will not prevent polarity reversals caused by worn-down exciter commutator brushes.

Dragging Machine

Effects on system:

System voltage may be depressed.

Remarks:

The current drawn depends upon the amount of dragging torque, speed of alternator, and characteristics of the reactive load division circuit.

REFERENCE

1. DISCUSSION by John Ward OF THE EFFECTS OF ABNORMAL CONDITIONS ON AIRCRAFT, PARALLEL A-C POWER SYSTEMS, S. C. Caldwell, A. J. Wood. *AIEE Special Publication S-57*, section II, 1954.

Continuous Current Capacity of Bundled Cables for Aircraft

M. SCHACH
ASSOCIATE MEMBER AIEE

L. D. SCHROEDER
ASSOCIATE MEMBER AIEE

ELECTRIC cables installed in aircraft are normally tied together in bundles for a portion of the cable run from the bus to the individual load device. As a consequence, the temperature of a particular cable depends not only on the current which it carries but also on the currents which flow simultaneously in other cables of the group. The problem of the current capacity of cables in bundles can be stated as follows: given any set of currents, how shall individual cables of the proper size be selected so that their limiting temperature is not exceeded when the cables are arranged in a bundle; or, stated conversely, given any specified bundle of cables, what is the combination of currents which may be carried by the cable group.

Sound cable ratings are necessary for the safety of the aircraft and for economy of cable weight. The inadequacy of the existing cable ratings is widely recognized. Since present bundled-cable ratings are not sound technically, it is possible seriously to underload or to overload cables in a given bundle. In addition the present method of rating cables severely restricts the number of cables which may be loaded simultaneously.

Each bundle of cables or currents constitutes a distinct problem in heat flow. It will become evident from the number and kinds of variables which are involved that finding an exact solution would be a lengthy and difficult process. The infinite variety of possible bundles makes it necessary to seek an approximate solution which can be applied easily to any given bundle.

This paper is concerned with only one of the criteria which limit current capacity, namely, the maximum permissible temperature of the insulation. The relative convenience of measuring conductor temperatures makes it desirable to state the thermal limitation as a maximum conductor temperature. This may be done because the conductor temperature is nearly constant over its cross section and because the temperatures of the conductor and insulation differ negligibly at their common boundary. When applied to a bundle of cables, this criterion requires that the hottest conductor must not exceed the maximum preassigned temperature.

The investigation has been confined to rating cables for direct current. The application of the method to rating cables for alternating current will depend primarily on how much the effective resistance of each conductor will vary as a result of the different possible proximity effects.

It is the aim of this article to show that a basis exists for an approximate solution of the problem of the continuous-current-rating of cables in bundles. In addition, a simple graphical method for selecting cables or current values for the bundled condition will be described. The method will be embodied in a cable-selection and cable-rating chart which can be drawn for any prescribed set of conditions Thus, charts can be drawn for various cable specifications, bundle construction, loading conditions, and environments. The cable charts are easy to draw and apply. Their application to bundled cables will provide a simple means of obtaining the lowest over-all cable weight consistent with the safety of the aircraft.

Factors Affecting Heat Transfer in Bundled Cable

Since the limiting criterion with which we are concerned is a maximum conductor temperature, a brief review of the factors affecting heat transfer in bundles is desirable. The factors affecting heat transfer for the case of uniform bundles (bundles composed of cables of a single size) have been described in a previous paper.[1] It will be shown later that mixed bundles (bundles composed of cables of more than one size), under conditions to be specified, dissipate heat at the same rate as uniform bundles having the same cross-section area. As a consequence of this fact it is possible to apply several of the results of the uniform-bundle study to mixed bundles.

An exact analysis of the effect of each parameter is not possible because of the complex heat-flow boundaries and the

---

Paper 53-375, recommended by the AIEE Air Transportation Committee and approved by the AIEE Committee on Technical Operations for presentation at the AIEE Aircraft Electric Equipment Conference, Seattle, Wash., September 30–October 2, 1953. Manuscript submitted June 15, 1953; made available for printing August 13, 1953.

M. SCHACH and L. D. SCHROEDER are with the Naval Research Laboratory, Washington, D. C.

The authors wish to acknowledge that R. E. Kidwell, Jr., of the Naval Research Laboratroy, Washington, D. C., contributed to the ideas from which the cable-selection and cable-rating chart developed.

nonlinear heat-transfer relations at the bundle surface. A subsidiary difficulty to be noted is the fact that the effect of changing one parameter (on the ability of the bundle to dissipate heat) depends on the concomitant values of the remaining variables. However, an approximate description is possible and is valuable for understanding the problem.

PROPERTIES OF INDIVIDUAL CABLES

The properties of the individual cables which are important for heat transfer are conductor diameter, insulation thickness, insulation thermal conductivity, and surface emissivity. The thermal conductivity of the conductor is so great compared to that of the insulation that its thermal impedance may be neglected. An approximate calculation of the effect of each of the parameters can be made for uniform bundles, and an example of the heat-flow equations required for such a calculation is given in Appendix I for a bundle of 19 cables.

An increase in the diameter of the individual conductors decreases both the internal and external thermal resistance, so that greater heat dissipation can occur. Similarly, an increase in the thermal conductivity or surface emissivity of the insulation of the individual cables increases the ability of the bundle to transfer heat. Calculation shows that a 50-per-cent increase in thermal conductivity of the insulation would improve the heat dissipation 8 per cent for a bundle of 19 *AN-18* cables and 12 per cent for a bundle of 19 *AN-1/0* cables. (*AN-18*, *AN-1/0*, etc., are the individual cable size designations given by Military Specification *MIL-W-5086*.[2]) The effect of increasing the insulation thickness of the individual cables on the bundle heat dissipation is less obvious. The thermal resistance of the bundle interior increases, while the exterior or bundle-surface resistance decreases; the latter effect follows from the enlarged surface area. For example, calculation shows that an increase of 100 per cent in insulation thickness for *AN-18* cables would permit 13 per cent more heat to be dissipated from a bundle of 19 *AN-18* cables, and that the same per-cent increase in insulation thickness for an *AN-1/0* cable would result in 6 per cent less heat dissipation for a bundle of 19 *AN-1/0* cables.

PROPERTIES OF BUNDLE

The effect of four bundle factors is considered: 1. bundle tightness, 2. position of loaded cables within the bundle, 3. presence of dummy (unloaded) cables, and 4. the number of cables loaded simultaneously.

Let us suppose that we start with an arbitrary bundle tightly bound at intervals of 1 inch and ask what happens to the heat dissipation for a given maximum conductor temperature as the interval of tie is increased to 6, 12, or 24 inches, i.e., the bundle is loosened. Measurements on uniform bundles showed that the heat dissipation changed gradually and either increased or decreased depending on the position and number of cables loaded simultaneously.[1] In no case did the heat dissipation fall more than 12 per cent below the original tight bundle condition. It can be assumed that the effect of the interval of tie would be the same for mixed bundles.

Measurements on uniform bundles show that there is some variation in heat transfer with the position of the loaded cables, but it does not appear practical to take advantage of the favorable configurations.[1]

The effect of dummy cables on the heat dissipation of the loaded cables depends on the number loaded simultaneously, the position of the loaded cables, and on the tightness of the bundle. For tight bundles and a given number loaded, the heat dissipation increases when dummy cables are added to the bundle. For example, if only one cable in a bundle of 37 *AN-18* cables bound at 1-inch intervals is loaded, it can dissipate 25 per cent more heat than a single cable in air subject to the same conductor temperature rise; if only seven of the cables in a bundle of 37 *AN-18* cables (bound at 1-inch intervals) are loaded, they can dissipate 12 per cent more heat than a bundle of seven *AN-18* cables (bound at 1-inch intervals) in which all cables carry current. When the bundle is loosely bound, the beneficial effect of dummy cables is reduced or eliminated. Measurements show that when only one cable in a bundle of 37 *AN-18* cables (bound at 2-foot intervals) is loaded, it dissipates heat at the same rate as a single cable in air.[1] Consequently, it does not appear practical to apply the favorable effect of dummy cables in a quantitative manner.

The effect of the number of cables loaded simultaneously cannot be described for the general case of the mixed bundle. For the special condition in which the loaded cables are of a single size and carry identical currents, P_n (the allowable heat dissipation per cable) was observed to satisfy approximately the relation

$$P_n = P_1/n^{\gamma} \qquad 0.33 \le \gamma \le 0.40$$

where

P_1 = the heat dissipated by a single cable in air
n = the number of cables loaded simultaneously

It will be seen in the section entitled "Basis for Rating Cables in Bundles" that heat dissipation for the general case of mixed bundles can be treated as a function of the cross-section area of the bundle.

Conditions of Problem

A standard set of conditions must be selected for the bundle and its environment to serve as a reference. These conditions are a prerequisite for a clear discussion, and are not intended to restrict the installation of cables in aircraft. (The application of the analysis and results to other sets of conditions will be described later.)

1. Cables whose dimensions and conductor resistance fall within the limits given by Military Specification *MIL-W-5086* for sizes *AN-22* and larger will be taken as standard. The thermal conductivity of the insulation of typical aircraft cables has been shown to lie in the range of 0.0034±0.0006 watt inch^{-1} degrees centigrade^{-1}.[3] This range of thermal conductivity will be taken as standard.

2. Bundle size is limited to a maximum cross-section area (insulation and conductor) of approximately 4 square inches. In terms of the number of cables per bundle, four square inches corresponds roughly to a bundle of 20 *AN-1/0* or a bundle of 450 *AN-18* cables.

3. An ambient temperature of 25 degrees centigrade, a maximum allowable conductor temperature of 65 degrees centigrade, and sea level pressure will be taken as standard conditions.

4. Heat transfer from the bundle surface is to occur only by natural convection and radiation, since the bundle is located in free air.

5. The bundle should be a compact group, roughly circular in cross section, and bound by ties or supports at intervals of 6 inches or less.

6. No limit will be placed on the number of cables in a bundle which may carry current simultaneously.

Basis for Rating Cables in Bundles

The standard conditions previously mentioned impose significant restrictions on the number and kinds of bundles to be considered. Nevertheless, a very great number of bundles are possible, and therefore there remain an equally large number of distinct heat-flow problems to be solved. It is clear that neither an exact analytical solution nor a graphica solution (i.e., a plot of the heat-flow lines) for each bundle is feasible.

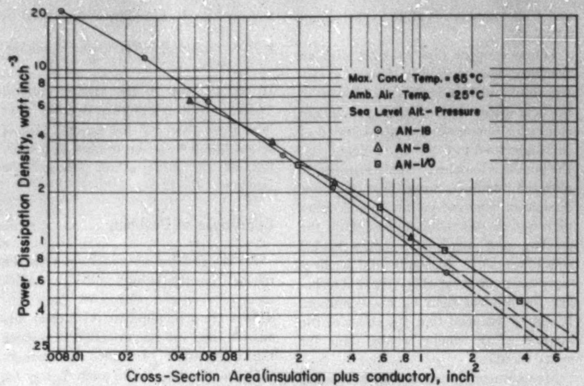

Fig. 1. P.d. for uniform bundles

The approach to the problem to be considered here is to determine the class of conditions for which heat transfer in bundles is poorest and to assume that these conditions apply to all bundles satisfying the standard conditions given in the preceding section. Cable ratings must be based on the poorest heat-transfer conditions if safe operation of the electric system is to be assured. The possibility of this approach to the rating of bundled cables was suggested by an analysis of heat dissipation of uniform bundles.

The term "power dissipation density" (p.d.) which will be employed in the following discussion is defined as the heat dissipated by a unit length of bundle divided by the cross-section area of the conductors and insulation of the current-carrying cables in the bundle. The heat dissipated is simply the sum of the electric power losses of the individual conductors loaded simultaneously.

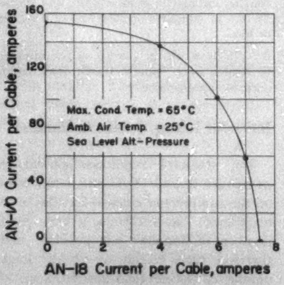

Fig. 2. Possible currents for a mixed bundle consisting of 19 AN-18 cables surrounded by 6 AN-1/0 cables. Every AN-18 cable and every AN-1/0 cable carries the current shown

P.D. of Uniform Bundles

If p.d. is plotted as a function of cross-section area for fully loaded uniform bundles, a distinct curve is obtained for bundles of each cable size. (A fully loaded bundle is one in which every cable carries current simultaneously.) Fig. 1 exhibits the experimental results for uniform bundles of *AN-18*, *AN-8*, and *AN-1/0* cables. The points plotted for size *AN-18* cables correspond to bundles of 1, 3, 7, 19, 37, and 169 cables. Bundles of 1, 3, 7, and 19 cables were used for both *AN-8* and *AN-1/0* curves. In addition to the conditions listed in the preceding section, every cable in any given bundle carried the same current. Fig. 1 is of particular interest because it shows that the p.d. for uniform bundles lies within a narrow band of values. For a cross-section area up to 4 square inches, it can be seen that the maximum p.d. for any given area is less than 40 per cent greater than the minimum for the same area.

The p.d. of uniform bundles of the same cross-section area (conductor plus insulation) is a function of the thickness of the insulation of the individual cables and the number of layers of insulation through which the heat must flow. If the insulation thickness were a constant for all cable sizes, it would follow that the p.d. for uniform bundles of large cables would be greater than that for uniform bundles of small cables for a given bundle cross-section area. Actually, it is observed for typical aircraft cables, satisfying Military Specification *MIL-W-5086*, that the insulation thickness ranges approximately from 25 mils for an *AN-22* conductor to 50 mils for an *AN-1/0* conductor. Calculation of p.d. by the method illustrated in Appendixes I and II for the range of bundles permitted by the preceding section shows that this limited variation in insulation thickness is negligible. Consequently, the uniform bundle p.d. curves for cable sizes between *AN-18* and *AN-1/0* will lie within the curves in Fig. 1. Furthermore, the minimum p.d. curve for uniform bundles will be that corresponding to the smallest individual cables. Isolated points corresponding to single cables may fall below the minimum p.d. curve; in Fig. 1 there is one measured point, corresponding to a single *AN-8* cable, which lies below the *AN-18* p.d. curve.

The term p.d. may be applied to any part of a bundle or number of cables as well as the whole bundle. It is evident for the case of uniform bundles that the p.d. is not constant throughout the bundle when every cable carries the same current. When steady-state conditions prevail, heat must flow out from the bundle, and the temperature at the center must be higher than that at the outer portion of the bundle. Consequently, the resistance of the outer cables must be less than that of the center cables. It follows, therefore, that the p.d. at the bundle center will be greater. This variation in p.d. through the bundle is small enough to be neglected for our purposes. For example, the variation in p.d. for the individual cables of a bundle of 169 *AN-18* cables was less than 5 per cent. Therefore, the p.d. for any uniform bundle in which each cable carries identical currents will be assumed to be constant throughout the bundle.

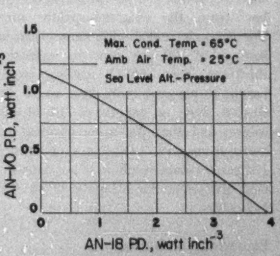

Fig. 3. Possible p.d. for a mixed bundle consisting of 19 AN-18 cables surrounded by 6 AN-1/0 cables. Every AN-18 cable and every AN-1/0 cable dissipates the p.d. shown

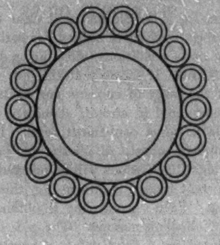

Fig. 4 Cross section of mixed bundle I, 1 AN-1/0 cable and 18 AN-18 cables

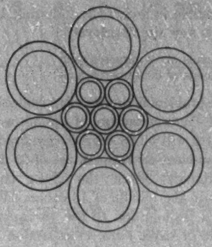

Fig. 5. Cross section of mixed bundle II, 7 AN-18 cables and 6 AN-8 cables

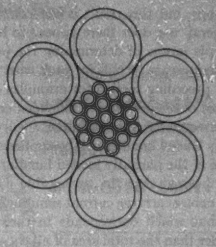

Fig. 6. Cross section of mixed bundle III 19 AN-18 cables and 6 AN-1/0 cables

A RESTRICTION ON P.D. OF MIXED BUNDLES

The application of Fig. 1 to mixed bundles will be considered after introducing a restriction on the loading of mixed bundles. It is apparent that for any bundle composed of cables of two or more different sizes there are many ways of assigning currents which satisfy the basic criterion of a given maximum temperature for the hottest conductor of the bundle. For example, Fig. 2 shows the possible current values for a mixed bundle consisting of 19 *AN-18* cables surrounded by 6 *AN-1/0* cables. Each point plotted represents a load condition which results in a 40-degree-centigrade rise for the hottest conductor when every *AN-18* cable and every *AN-1/0* cable carries the current shown. Corresponding to each point in Fig. 2 there is a pair of p.d. values. Fig. 3 shows the permissible pairs of p.d. values. The simplest restriction on the loading of mixed bundles would require uniform p.d. for all cables loaded simultaneously. Any other assumption would require a lengthy and complex graphical analysis for each group of cables loaded simultaneously, which which would be most unpractical. For these reasons we add to the basic criterion (of a maximum temperature of the hottest conductor) the requirement that the p.d. be the same for each cable of any one group of cables loaded simultaneously. This requirement will be referred to as the uniform p.d. requirement.

P.D. OF MIXED BUNDLES

The p.d. of a bundle of given cross-section area (insulation plus conductor) depends on: 1. the thermal resistance of the bundle interior, and 2. the ability to transfer heat at the surface to the surroundings. Measurements of uniform bundles show that the thermal resistance of the bundle interior changes slowly as a given bundle is loosened. This fact means that the presence or absence of a snug fit of adjacent, like cables does not critically affect the thermal resistance. This result suggests that the thermal resistance for the case where adjacent cables are of different sizes would not be markedly different from that of uniform bundles. Measurements on uniform bundles of a given cross-section area show that surface heat dissipation for a given average surface temperature rise is nearly independent of the constituent cable size. From this qualitative discussion we would conclude that the p.d. for mixed bundles should be approximately equal to the p.d. values of uniform bundles of corresponding area.

The heat-dissipation density was measured for four mixed bundles. Drawings of the cross section of bundles I, II, and III appear in Figs. 4, 5, and 6. In addition to conforming to the standard conditions of the preceding section, the cables in these bundles were arranged symmetrically so that cables of one size occupied a given layer. Bundles I and III were composed of *AN-18* and *AN-1/0* cables. These two bundles illustrated an extreme mixed-bundle condition in that very large and very small cables were placed in juxtaposition; in bundle I the *AN-1/0* cable was surrounded by *AN-18* cables while in bundle III the *AN-18* cables were surrounded by *AN-1/0* cables. Bundle IV was composed of 2 *AN-4* and 6 *AN-14* cables, but no attempt was made to attain any symmetry in grouping the cables. The currents in each size of cable were adjusted until uniform p.d. prevailed throughout the bundle. The p.d. values for the four bundles for a 40-degree-centigrade maximum conductor rise and the values for uniform bundles of the corresponding cross-section area are given in Table I. The table shows that the p.d. for the four bundles is as high or higher than that of uniform bundles of *AN-18* cables. Therefore, it will be assumed that the p.d. for any mixed bundle is equal to or greater than the minimum p.d. for uniform bundles of the smallest cable employed in the mixed bundle. Consequently, it will be adequate for general application to select the p.d. curve of uniform bundles of *AN-18* cables as the minimum curve. This curve is the maximum allowable p.d. curve and is called the "*R*" or "reference p.d." curve.

The results and conclusions of this section have been concerned thus far with fully loaded bundles. The result that the power dissipation of fully loaded uniform or mixed bundles is primarily a function of the cross-section area of the bundle (insulation and conductor) can be extended to the case in which only a fraction of the cables in the bundle are loaded simultaneously. (The expression "partially loaded bundle" will be used as a synonym for a bundle in which only a fraction of the total number of cables in the bundle are loaded simultaneously.) The presence of the unloaded cables in the bundle tends, in most cases, to permit an increase in the p.d. of the loaded

Table I. Mixed Versus Uniform Bundles

Mixed Bundle Designation	Constituent Cables	Cross-Section Area, Inches^2	Mixed Bundle Power Density, Watt Inch^{-3}	Uniform Bundle Power Density for Same Area, Watt Inch^{-3}	
				AN-18	AN-1/0
I	1 *AN-1/0* 18 *AN-18*	0.360	1.95	1.85	2.20
II	7 *AN-18* 6 *AN-8*	0.339	2.10	1.95	2.25
III	19 *AN-18* 6 *AN-1/0*	1.34	0.97	0.72	0.94
IV	2 *AN-4* 6 *AN-14*	0.260	2.80	2.30	2.60

group; but this result is not completely general, nor does there appear to be any simple means of determining the permissible increase in p.d. for each case. (See the preceding section for examples of the effect of the presence of unloaded cables.) Consequently, the minimum R curve for fully loaded bundles will be applied to the case of the partially loaded bundle. It is emphasized that the permissible p.d. for the cables carrying current simultaneously is that which corresponds to their area rather than the total area of all the cables in the bundle.

SUMMARY

Two general results affecting the p.d. of mixed bundles under steady-state conditions have been established:

1. The p.d. must be the same for each cable of a group of cables of different sizes which carry current simultaneously.
2. The point determined by the p.d. of a group of cables loaded simultaneously and their cross-section area must lie on the R curve.

Originally, result 1 was introduced as a simplifying condition. Measurements have shown that this condition is necessary if mixed bundles are to dissipate at a rate equal to or greater than uniform bundles composed of the smallest cable size. Result 2 is a necessary condition for making certain that the maximum allowable heat dissipation in mixed bundles will not be exceeded.

These two results will now be taken as a basis for rating cables in mixed bundles.

Cable-Selection and Cable-Rating Chart for Obtaining Ratings Graphically

The purpose of this section is to describe a method for drawing a cable-selection and cable-rating chart. The chart is used to find the graphical solution for: 1. the cable sizes when the group of currents is given, or 2. the currents when the bundle of cable sizes is given. The method can be applied generally to any prescribed set of conditions which characterize the individual cables, construction, loading, and environment of the bundle. For the particular chart to be described the conditions given in the section on "Conditions of Problem" will be assumed to apply. It should be remembered, too, that the chart will be based on the thermal limitation of the cables.

NEED FOR CHART

The need for a chart will become clear by studying a simple example. Consider a bundle in which the following 15 currents flow simultaneously:

10 loads of 8 amperes each
5 loads of 60 amperes each

The problem is to select two cable sizes so that the temperature of the hottest conductor will be 65 degrees centigrade (for an ambient air temperature of 25 degrees centigrade) when the given currents flow in the bundle of 15 cables. We are given, in addition to the 15 currents, a table of cable sizes, cross-section areas, and conductor resistances, and the reference p.d. curve previously mentioned.

The cable sizes are to be chosen so that the p.d. for each cable with the given current flowing in it satisfies the two basic conditions given in the foregoing summary: 1. The p.d. for every cable in the bundle must be the same. In our example, the p.d. for a cable carrying 8 amperes is to be equal to the p.d. of a cable which carries 60 amperes. 2. The point determined by the bundle p.d. (which is equal to the individual cable p.d.) and the total cross-section area of the cables of the bundle must lie on the R curve.

The correct cable sizes could be determined by a trial-and-error calculation. For example, as a first step, an *AN-20* cable could be chosen arbitrarily for the 8-ampere load. Knowing its conductor resistance at 65 degrees centigrade and its cross-section area (insulation and conductor), its p.d. is computed. Note that the conductor resistance is taken for 65 degrees centigrade for this cable as well as for all the remaining cables in the bundle. The next step is to select a cable for the 60-ampere load so that its p.d. will be equal to that for the *AN-20* cable carrying 8 amperes; let us suppose that an *AN-8* cable would suffice. The third step is to sum the cross-section area of the 15 trial cables (10 *AN-20* and 5 *AN-8*). The final step is to see whether the point having the trial p.d. and total area as coordinates falls on the R curve. If the point does not lie on the curve, the trial process must be repeated. After two or three trial points have been calculated, a curve of p.d. versus total cross-section area could be drawn through these points; the intersection of this curve with the R curve would represent the required values for the bundle p.d. and total area. The cable sizes could be obtained by one or more trial p.d. calculations for each current until cable sizes giving the graphically determined p.d. value are found.

CONSTRUCTION OF CHART

The discussion of the trial-and-error calculation for finding the correct cable sizes for a bundle makes it clear that a simpler method is needed for satisfying the two conditions affecting p.d. In particular, it shows that the p.d. values for the range of currents and cable sizes encountered in aircraft should be available in some convenient form. In the proposed chart, a family of parallel straight lines, which will be referred to as "current lines," is drawn for this purpose. Each current line is obtained in the following manner. The p.d. is calculated for a fixed value of current for each cable size from *AN-22* to *AN-1/0* for a set of typical aircraft cables, and the results are plotted as a function of cross-section area (insulation and conductor) on a logarithmic scale. It is found that the points lie on or close to a straight line. A considerable simplification of the chart is gained at small cost in accuracy if the mean straight line through the points is taken as the current line, rather than the irregular curve through all the points. As an example, the 10-ampere line is the mean straight line drawn through points on a logarithmic scale whose co-ordinates are

$$\text{ordinate} = \frac{I^2R_n}{A_n} = \frac{(10)^2R_n}{A_n} \tag{1}$$

$$\text{abscissa} = A_n \tag{2}$$

where

R_n = the conductor resistance per inch at 65 degrees centigrade
A_n = the cross-section area of insulation and conductor for the corresponding cable size

In the chart shown as Fig. 7, the current lines range from 1 to 2,000 amperes. The experimentally determined R curve, taken from Fig. 1, and the cable cross-section area indexes showing cable size complete the chart. The cross-section areas which are assigned to the *AN* cables by the chart are the same areas used in equations 1 and 2 for determining the current lines; these values were selected to give conservative results when applied to cables which satisfy Military Specification *MIL-W-5086*. It may be noted that the areas given by the chart are approximately the minimum values to be encountered in practice.

PROCEDURE FOR USING CHART TO FIND CABLE SIZES WHEN CURRENTS ARE GIVEN

The procedure will be illustrated for a bundle in which the following 15 currents flow simultaneously:

10 loads of 8 amperes each.
5 loads of 60 amperes each.

There may or may not be additional

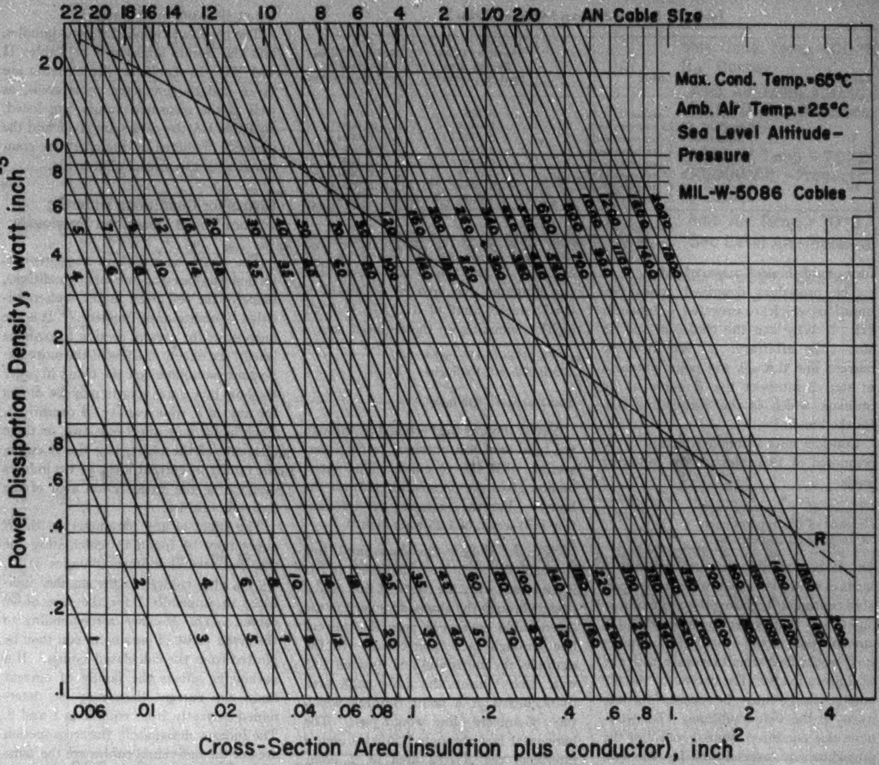

Fig. 7. Proposed Naval Research Laboratory cable-selection and cable-rating chart for bundled cables carrying continuous currents and satisfying conditions of the section entitled "Conditions of Problem." For application to other conditions see the section entitled "Charts for Conditions Differing from Those Described Previously"

cables in the bundle, but they do not carry current simultaneously with the 15 loads specified. It was noted earlier that the possible beneficial effect of the presence of dummy cables on the loaded cables does not warrant quantitative consideration. The procedure to be followed here neglects the effect of dummy cables.

Step 1: For some arbitrary value of ordinate, say 0.1 watt inch^{-3}, find the area required by each load. To do this, locate the current line and note its intersection with the horizontal line through 0.1 watt inch^{-3}. For this example, it is seen that

8 amperes require 0.044 inch^2 at 0.1 watt inch^{-3} p.d.
60 amperes require 0.250 inch^2 at 0.1 watt inch^{-3} p.d.

Step 2: Sum up the area for all loads which are to be carried simultaneously. In the example, we have

10 loads of 8 amperes each require $10\times0.044=0.44$ inch^2
5 loads of 60 amperes each require $5\times0.25=1.25$ inches^2

Total area required at 0.1 watt inch^{-3} p.d. $=1.69$ inches^2

The point whose co-ordinates are 1.69 inches^2 and 0.1 watt inch^{-3} represents a hypothetical bundle which satisfies condition 1 but does not satisfy condition 2 because the point which represents it does not lie on the *R* curve.

Step 3: Locate the current line through the point (1.69 inches^2, 0.1 watt inch^{-3}) and find its intersection with the *R* curve. In our example, the current line through the point (1.69 inches^2, 0.1 watt inch^{-3}) is the 540-ampere line. This line intersects the *R* curve at a point whose ordinate is 1.4 watt inch^{-3}.

Step 4: Follow the horizontal line through 1.4 watt inch^{-3} to its intersections with the 8- and 60-ampere lines. Follow the vertical line at each intersection to the top of the chart where the *AN* cable sizes are given. In the example the horizontal line through 1.4 watt inch^{-3} intersects the 60-ampere line at a point whose abscissa lies between the *AN-6* and *AN-4* cable areas. *AN-4* is the size required for each of the five 60-ampere loads. The horizontal line through 1.4 watt inch^{-3} intersects the 8-ampere line at a point whose abscissa lies between the *AN-14* and *AN-12* cable areas. *AN-12* is the cable size required

Table II. Predicted Versus Measured Areas

Bundle	Given Loads	Predicted Cross-Section Area per Load, Inches^2	Measured Cross-Section Area per Load, Inches^2
I	1 load of 198 amperes	0.205	0.198
	18 loads of 5.25 amperes each	0.0085	0.0084
II	7 loads of 5.5 amperes each	0.0088	0.0084
	6 loads of 40.5 amperes each	0.050	0.047
III	6 loads of 140 amperes each	0.240	0.198
	19 loads of 3.75 amperes each	0.0103	0.0084
IV	2 loads of 102.5 amperes each	0.108	0.0922
	6 loads of 11.5 amperes each	0.016	0.0126

for each of the 10 8-ampere loads.

The procedure described raises two questions which are answered in Appendix III: 1. Why can the choice of p.d. in step 1 be arbitrary. 2. Why does the current line through the point obtained in step 2 intersect the *R* curve at an ordinate which is the permissible p.d. for the bundle?

Consider next a bundle which is to be composed of 19 cables for the following loads:

10 loads of 8 amperes each
5 loads of 60 amperes each
4 loads of 20 amperes each

Let it be further supposed that the 5 loads of 60 amperes each were to be operated continuously during the entire time of flight, and that either the 10 loads of 8 amperes each or the 4 loads of 20 amperes each would flow simultaneously with the 60-ampere loads. The cables for the 60-ampere loads must be chosen for the worse of the two conditions. To determine this condition, steps 1 and 2 of the procedure are carried out for the two possibilities. The larger of the two total areas given by step 2 establishes which calculation is used to select the cables for the 60-ampere loads.

The extension of the procedure to a bundle in which the number of simultaneous loads is arbitrary is self-evident.

PROCEDURE FOR USING CHART TO FIND CURRENT CAPACITY WHEN CABLE SIZES ARE GIVEN

The procedure will be illustrated for a bundle in which the following cables are loaded simultaneously:

10 *AN-12* cables
5 *AN-4* cables

There may be additional cables in this bundle, but as in the converse procedure, we shall neglect any possible effect of the presence of unloaded cables.

Step 1: Sum up the cross-section area of the insulation and conductor of the cables which are to be loaded simultaneously. The area of each cable size is shown at the top of the chart. For our example, the area of 1 *AN-12* is 0.0175 inch^2, that of 1 *AN-4* is 0.092 inch^2. Summing up the required area

$$10\times0.0175=0.175 \text{ inch}^2$$
$$5\times0.092\ =0.460 \text{ inch}^2$$

$$\text{Total area}=0.635 \text{ inch}^2$$

Step 2: Follow the vertical line through the total area just obtained to the intersection with the *R* curve. The intersection gives the permissible p.d. for the bundle. For the example, the intersection is at a p.d. of 1.25 watt inch^{-2}.

Step 3: Follow the horizontal line through the p.d. just obtained to its intersection with the vertical line which passes through the abscissa for each of the given cable areas and note the current line through each intersection. In the example, the horizontal line through 1.25 watt inch^{-2} meets the *AN-4* cable area (0.092 inch^2) at a point through which the 65-ampere line would pass. The horizontal line through 1.25 watt inch^{-2} intersects the *AN-12* area at a point through which the 10-ampere line passes. The current capacities for the *AN-4* and the *AN-12* cables are 65 and 10 amperes respectively.

ACCURACY OF CHART

The chart has been prepared to give conservative results. (An exception to this statement is discussed in Appendix IV.) It is estimated that the maximum error is approximately 30 per cent, i.e., the area predicted by the chart for any given load falls within 30 per cent of the minimum allowable cable area when the conditions of the chart are met. Conversely, when the cables are given, the maximum error in current predicted by the chart is about 20 per cent. The largest contribution to the error is a result of the fact that the chart replaces the band of p.d. values of Fig. 1 by a single curve. Two smaller errors are introduced by the fact that the current lines are represented by straight lines and by the assumption that all cables are at the same temperature.

The chart was applied to four bundles, and the results are shown in Tables II and III. In Table II, the currents are given and the predicted cable areas, as well as the measured values, are listed. In Table III, the cables are given and the currents predicted by the chart are compared with the measured currents.

Charts for Conditions Differing from Those Described Previously

The chart described in the previous section was based on one set of conditions, namely, the set given in the section entitled "Conditions of Problem." It is the purpose of the present section to examine briefly the effects of a few of the more important parameters on the chart in order to show how cable charts may be drawn for any of a wide variety of conditions. Each factor may affect one, two, or three elements of the chart, i.e., the *R* curve, the family of current lines, or the indexes designating the cross-section area of the individual cables.

The effect of any parameter on the *R* curve may be found by calculating the p.d. for several uniform bundles (1, 7, 19, 37, etc., cables) in the manner indicated in Appendix I for the case of 19 cables. The *R* curve corresponding to the given value of parameter can then be plotted from the calculated points. If a parameter affects the family of current lines, the current lines may be determined correctly from equations 1 and 2. The indexes designating the cross-section area of the individual cables are the same as used in equation 2.

CONDUCTOR MATERIAL

Charts may be drawn for any conductor material. Fig. 7 applies to cables having copper conductors. If, for example, copper is replaced by aluminum and all other factors are held constant, only the family of current lines is affected. Without redrawing the current lines the chart can be made applicable to aluminum conductors by labelling the current lines

Table III. Predicted Versus Measured Currents

Bundle	Given Cables	Predicted Current per Cable, Amperes	Measured Current per Cable, Amperes
I	1 *AN-1/0*	197	198
	18 *AN-18*	5.2	5.25
II	7 *AN-18*	5.3	5.5
	6 *AN-8*	38.0	40.6
III	6 *AN-1/0*	120	140
	19 *AN-18*	3.2	3.75
IV	2 *AN-4*	90	102.5
	6 *AN-14*	9.2	11.6

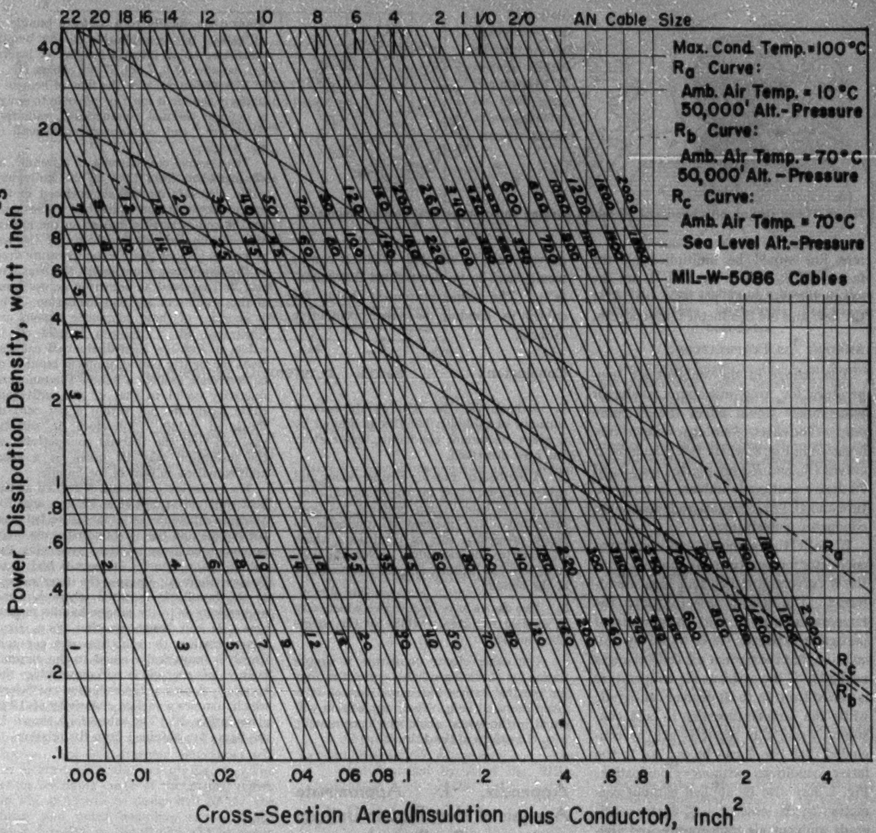

Fig. 8. Proposed Naval Research Laboratory cable-selection and cable-rating chart for bundled cables carrying continuous currents and satisfying conditions of the section entitled "Conditions of Problem" except for ambient air temperature, maximum conductor temperature, and altitude pressure

with current values valid for aluminum. If a given current line is to be applicable to both materials, the p.d. must be the same function of the area for the two cases. This result is obtained by setting

$$(I^2R_n)_{(\text{copper})} = (I^2R_n)_{(\text{aluminum})}$$

where R_n = resistance per unit length at the operating temperature. Therefore

$$I_{(\text{aluminum})} = \left[\frac{\text{resistivity of copper}}{\text{resistivity of aluminum}}\right]^{1/2} I_{(\text{copper})}$$

$$= 0.78 I_{(\text{copper})}$$

Thus, Fig. 7 could be used for aluminum cables if each current line were labelled with a current value equal to 78 per cent of the value which appears. It may be noted that a chart with two sets of current values and cable size designations could be applied to bundles containing both copper and aluminum cables. The dimensions of cables provided for aluminum cables by Military Specification *MIL-W-7072*[4] are sufficiently close to those specified by Military Specification *MIL-W-5086* for copper cables, so that any chart drawn for the latter can be applied to the former with the slight modification indicated.

INSULATION MATERIAL

If insulating materials with improved thermal conductivities are used, the *R* curve will require modification. The method for calculating the points of the *R* curve has been indicated in Appendix I.

DIMENSIONS OF CONDUCTOR AND INSULATION

Changes in these dimensions would require a complete revision of the chart, i.e., the cable area designation, *R* curve, and current lines would have to be modified.

MAXIMUM CONDUCTOR TEMPERATURE

If the maximum allowable temperatures were changed, e.g., as a result of improved insulation, the current lines and *R* curve would have to be modified. The ordinate of every point on each cur-

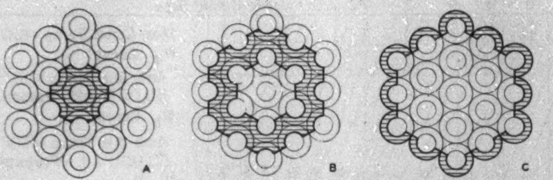

Fig. 9. Cross section of a bundle of 19 cables showing approximate heat-transfer boundaries

rent line would be multiplied by the factor R_0'/R_0, where R_0' and R_0 are the conductor resistance per unit length at the new and old conductor temperatures.

AMBIENT AIR TEMPERATURE

The change in the ambient air temperature for fixed maximum conductor temperature would affect the *R* curve only. The effect of ambient temperature is shown in Fig. 8, where two calculated *R* curves (R_a and R_b) are plotted for 10 and 70-degree-centigrade ambient air temperature and 100-degree-centigrade maximum conductor temperature.

If both the ambient and maximum conductor temperatures are changed, both the *R* curve and the current lines are affected. The special case in which the temperature rise is held constant is of particular interest. It is found by calculation that the current capacity changes negligibly if the ambient air temperature is varied from 25 to 60 degrees centigrade while the temperature rise is held constant. From this result is can be concluded that Fig. 7 can be applied to the latter conditions without modification. Fig. 7 may also be applied without correction to the case of a 57-degree-centigrade ambient air temperature and 100-degree-centigrade maximum conductor temperature.

ALTITUDE

The diverse ambient temperatures and pressure which occur at altitude will affect the *R* curve. Two calculated *R* curves for a pressure corresponding to 50,000 feet are drawn for 10 and 70-degree-centigrade ambient air temperatures in Fig. 8. The heat dissipated by convection for a pressure corresponding to 50,000 feet was computed from relations given by W. Elenbaas.[5] The effect of a change in pressure alone can be seen in Fig. 8 by studying the curves labelled R_b and R_c.

CABLES IN TROUGHS, CONDUIT, OR PROTECTIVE JACKETS

If cables were placed in a trough instead of being tied in bundles in air the *R* curve would be affected. New *R* curves would have to be determined experimentally. The same statement holds for cables in conduit or other protective jackets.

Conclusions

1. A basis for the steady-state current capacity of cables in bundles as limited by a given maximum conductor temperature has been described.

2. A method of drawing a cable-rating and cable-selection chart for the graphical solution of the cable-rating problem has been presented. The method is applicable to many prescribed sets of conditions which characterize the individual cables, the construction, the loading, and the environment of the bundle.

3. Two charts have been drawn which may be applied to aircraft cables for the conditions specified.

4. The cable charts constitute a simple means for obtaining reliable current ratings for bundled cables which are subject to a given thermal limit. Their application will result in the lowest cable weight consistent with the safety of the aircraft.

Appendix. I. Approximate Analysis of Heat Flow in Uniform Bundles

The discussion of heat flow in uniform bundles to be given here is a revision of that given in reference 1. The analysis will be applied specifically to a uniform bundle of 19 cables, but is applicable to any bundle consisting of an integral number of layers, i.e., bundles of 3, 7, 19, 37, 61 cables, etc.

In order to describe the flow of heat in a uniform bundle it must be possible to assign a definite thermal conductivity, radiation coefficient, and convection coefficient to the bundle.

The thermal conductivity of a bundle, as distinguished from that of the individual cable, depends on the air enclosed in the spaces between the individual cables and on the conductors as well as on the insulation of the individual cables. If the assumption is made that the temperature drop in the conductors is negligible, the heat flow can be conceived as occurring across composite regions of air and insulation. The boundaries of those composite regions are illustrated for a uniform bundle of 19 cables in Fig. 9. Heat-dissipation calculations for tightly bound, uniform bundles of cables which assume a bundle thermal conductivity equal to that of the individual cable insulation fall within 8 per cent of measured values. Therefore, it will be assumed that the thermal conductivity of the insulation may be taken as a good approximation to that of the bundle.

The radiation coefficient λ defined as the heat radiated in unit time by unit area for 1-degree difference in temperature between the bundle and the surrounding walls, may be computed from relations governing the net radiation transfer between a body and its surroundings. Because the outer surface of the bundle is indented, there is some uncertainty as to the precise bundle surface area. It can be shown that, as a good approximation, the radiating area per unit length is numerically equal to the circumference of the circle circumscribing the bundle.[6] A plot of the radiation coefficient which assumes a surface emissivity of 0.9 is given in Fig. 10. The values for λ shown in the figure are obtained from the relation

$$\lambda=\frac{Se(T_{sk}^4-T_{ak}^4)}{T_{sk}-T_{ak}}$$

where

S = Stefan's constant
e = emissivity of the cable surface
T_{sk} = average temperature of bundle surface in degrees absolute
T_{ak} = temperature of the surrounding walls

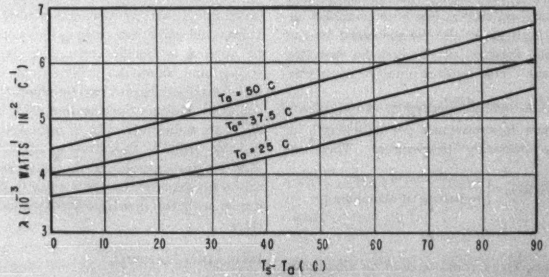

Fig. 10. Radiation coefficient λ versus average surface temperature rise T_s-T_a, for three ambient air temperatures T_a

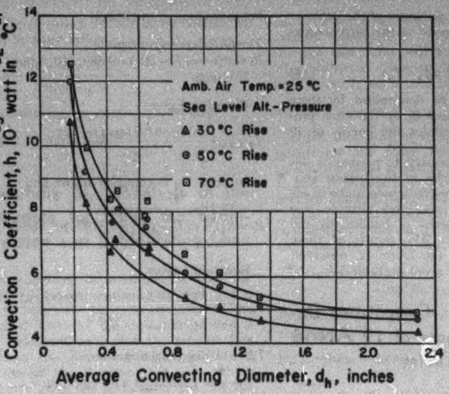

Fig. 11 (left). Convection coefficient h versus average convecting diameter d_h, for three values of average surface temperature rise

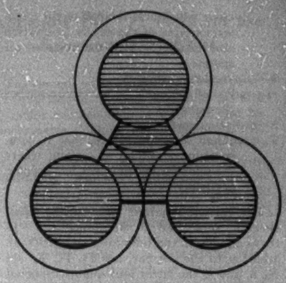

Fig. 12. Cross section of a bundle of three cables showing approximate heat-transfer boundaries

in degrees absolute. (It will be assumed that the wall temperature is the same as that of the air at a point where the gradient has become negligible.)

The convection coefficient h, defined as the heat transferred by natural convection in unit time by unit area for 1-degree difference between the bundle surface temperature and the ambient air temperature, was determined experimentally from bundle measurements. The results are shown in Fig. 11 where the convection coefficient is plotted as a function of the average convecting diameter d_h of the bundle surface. The average convecting diameter is defined as the diameter of a circle whose area is equal to the cross-section area of the cables and enclosed air spaces.

The heat flow may be calculated by treating the bundle as a series of concentric layers. The heat-transfer boundaries will be defined with the aid of Fig. 9. The outer bounding curve of the shaded region in Fig. 9(A) will be designated by *A;* the inner and outer bounding curve of the shaded region in Fig. 9 (B) will be designated by *B* and *C;* the inner bounding curve of the shaded region in Fig. 9(C) will be designated by *D*.

The heat produced by the center cable is conducted from the periphery of the center conductor to *A*, the outer boundary of the shaded region shown in Fig. 9(A). The rate of heat flow per unit length in this region is given by the relation

$$I^2R_1=\frac{2\pi K(T_1-T_2)}{\log_e(r_A/r_1)} \qquad (3)$$

where

I = current per cable

R_1 = conductor resistance per unit length at temperature T_1

K = thermal conductivity of the insulation

T_1 = temperature of the center conductor, arbitrarily assigned

T_2 = average temperature of the six conductors in the first layer

r_1 = conductor radius

r_A = radius of a circle whose area is equal to that bounded by *A* of Fig. 9(A); that is

$$\pi r_A^2=6\left[\frac{\sqrt{3}b^2}{4}-\frac{2\pi r_1^2}{3}\right]$$

where b = over-all diameter of an individual cable.

The approximation is now made that the temperature drop between *A* and *B* may be neglected. The heat produced by the six cables of the first layer is added to that from the center cable and is conducted from *B* to *C*. The relation governing the flow of heat in this region is

$$I^2(R_1+6R_2)=\frac{2\pi K(T_2-T_3)}{\log_e(r_C/r_B)} \qquad (4)$$

where

R_2 = conductor resistance per unit length at average temperature T_2

T_3 = average conductor temperature of the 12 cables of the second layer

r_B = radius of a circle whose area is equal to that bounded by *B* of Fig. 9(B); that is

$$\pi r_B^2=6\left[\frac{\sqrt{3}b^2}{4}+\frac{2\pi r_1^2}{3}\right]$$

r_C = radius of a circle whose area is equal to that bounded by *C* of Fig. 9(B); that is

$$\pi r_C^2=6\left[\sqrt{3}b^2-\frac{5\pi r_1^2}{3}\right]$$

The further approximation is made that the temperature drop between *C* and *D* may be neglected. The heat produced by the 12 cables of the second layer is added to that of the seven interior cables and total energy is conducted from *D* to the outer bundle surface. In the region from *D* to the periphery, we have

$$I^2(R_1+6R_2+12R_3)=\frac{2\pi K(T_3-T_s)}{\log_e(r_s/r_D)} \qquad (5)$$

where

R_3 = conductor resistance per unit length at average temperature T_3

T_s = average bundle surface temperature

r_D = radius of a circle whose area is equal to that bounded by *D* of Fig. 9(C); that is

$$\pi r_D^2=6\left[\sqrt{3}b^2+\frac{7\pi r_1^2}{6}\right]$$

r_s = average conducting radius of the bundle surface = r_D + insulation thickness of the cable

At the outer surface, heat is transferred by convection and radiation to the surrounding air and walls. The rate of heat transfer can be stated as

$$I^2(R_1+6R_2+12R_3)=2\pi(r_hh+r_\lambda\lambda)(T_s-T_a) \qquad (6)$$

where

r_h = average convecting radius of the bundle surface, defined as the radius of a

Table IV. Calculated and Measured Values

Bundle Designation	Calculated Values		Measured Values	
	Current, Amperes	Power Density, Watt Inch^{-3}	Current, Amperes	Power Density, Watt Inch^{-3}
3 *AN-18*	13.3	12.4	12.9	11.5
7 *AN-18*	9.6	6.3	9.7	6.5
19 *AN-18*	6.9	3.2	6.9	3.3
37 *AN-18*	5.5	1.94	5.5	2.05
169 *AN-18*	3.1	0.64	3.2	0.70
3 *AN-8*	55.0	3.9	54.0	3.8
7 *AN-8*	40.3	2.1	40.6	2.2
19 *AN-8*	28.5	1.0	29.5	1.1
3 *AN-1/0*	186	1.7	182	1.6
7 *AN-1/0*	135	0.92	137	0.94
19 *AN-1/0*	96	0.45	99	0.48

circle whose area is equal to the cross-section area of the cables (insulation and conductor) and the enclosed air spaces

h = convection coefficient

r_λ = radius of the circle which circumscribes the bundle

λ = radiation coefficient

T_a = ambient air temperature, that is, temperature of the air at a point where the temperature gradient has become negligibly small.

The current required must satisfy equations 3, 4, 5, and 6 simultaneously. In these equations the unknown quantities, in addition to the current, are T_2, T_3, T_s, R_2, R_3, h, and λ, the latter four quantities being dependent on the three preceding. In order to find I, the method of successive approximations is used, that is, one value of I is assumed and substituted in turn in equations 3, 4, and 5. By this means one determines a set of values of T_2, T_3, T_s, R_2, and R_3. The values λ and h, corresponding to $T_s - T_a$, and the average convecting bundle diameter d_h may now be selected from Figs. 10 and 11. Finally, a value of I can be computed with equation 6. If this value agrees with the one assumed initially, the correct current has been found. If the two currents differ, other assumed values must be tried and the calculation must be repeated.

The number of trial values needed may be limited to two or three by plotting the current calculated by equation 6 as a function of the assumed current. The intersection of this curve with the straight line, I (calculated) = I (assumed), gives the desired current. The extension of the method to bundles consisting of an integral number of layers is self-evident. Computation details for a bundle of 19 *AN-18* cables are given in Appendix II.

The heat dissipation of a bundle of three cables may also be calculated in the same manner if the boundaries are chosen suitably. The assumption is made that all three conductors are at the same temperature, T_1. E, the boundary of the shaded region of Fig. 12, is taken as an isotherm. The heat conducted from E to the bundle periphery is

$$3I^2R_1 = \frac{2\pi K(T_1 - T_s)}{\log_e (r_s/r_E)} \tag{7}$$

where r_E = radius of a circle whose area is equal to that bounded by E of Fig. 12; that is

$$\pi r_E{}^2 = \left[\frac{\sqrt{3}b^2}{4} + \frac{5\pi r_1{}^2}{2}\right]$$

$r_s = r_E$ + insulation thickness of the cable

The heat transferred to the surroundings is as follows

$$3I^2R_1 = 2\pi(r_h h + r_\lambda \lambda)(T_s - T_a) \tag{8}$$

The current can be determined by these two equations, 7 and 8, by the same procedure as that used for the bundle of 19 cables.

The current necessary to produce a 40-degree-centigrade rise in the hottest conductor for 25-degree-centigrade ambient air temperature and sea level altitude was calculated for a series of bundles by the method described. The results of these calculations and the currents observed experimentally are given in Table IV.

Appendix II. Computation Details for a Bundle of 19 AN-18 Cables

To determine: I, current per cable, and p.d., power dissipation density, when every cable in the bundle carries current simultaneously.

Given:

T_1 = 65 degrees centigrade
T_a = 25 degrees centigrade
Temperature coefficient of resistance = α = 0.00395 at 20 degrees centigrade
Conductor resistance per inch at 20 degrees centigrade = $R = 0.503 \times 10^{-3}$ ohm inch^{-1}
K = 0.0034 watt inch^{-1} degrees centigrade^{-1}
Insulation thickness = 0.0276 inch

r_1 = 0.024 inch
r_A = 0.088 inch
r_B = 0.106 inch
r_h = 0.233 inch
c = 0.181 inch
r_D = 0.199 inch
$r_s = r_D$ + insulation thickness = 0.227 inch
r_λ = 0.259 inch
Bundle area (insulation and conductor) = 0.1604 inch^2
$R_1 = R[1+\alpha(T_1 - 20)] = 0.593 \times 10^{-3}$ ohm inch^{-1}

From equation 3

$$T_2 = T_1 - \frac{I^2R_1 \log_e (r_A/r_1)}{2\pi K} \tag{9}$$

Assume that I = 7.0 amperes. Substituting in equation 9, we obtain

T_2 = 63.2 degrees centigrade
$R_2 = R[1+\alpha(T_2 - 20)] = 0.589 \times 10^{-3}$ ohm inch^{-1}

Equation 4 gives

$$T_3 = T_2 - \frac{I^2(R_1 + 6R_2) \log_e (r_C/r_B)}{2\pi K} \tag{10}$$

Substituting in equation 10, we find

T_3 = 58.2 degrees centigrade
$R_3 = R[1+\alpha(T_3 - 20)] = 0.579 \times 10^{-3}$ ohm inch^{-1}

Equation 5 gives

$$T_s = T_3 - \frac{I^2(R_1 + 6R_2 + 12R_3) \log_e (r_s/r_D)}{2\pi K} \tag{11}$$

T_s = 54.9 degrees centigrade

I is now calculated with equation 6

$$I = \left[\frac{2\pi(r_h h + r_\lambda \lambda)(T_s - T_a)}{R_1 + 6R_2 + 12R_3}\right]^{1/2} \tag{12}$$

which is evaluated for

$(T_s - T_a) = 54.9 - 25.0 = 29.9$ degrees centigrade

The radiation and convection coefficients can therefore be obtained from Figs. 10 and 11.

λ, for $T_s - T_a = 29.9$ degrees centigrade = 0.00415 watt inch^{-2} degrees centigrade^{-1}
h, for $T_s - T_a = 29.9$ degrees centigrade and $d_h = 2r_h$, = 0.00675 watt inch^{-2} degrees centigrade^{-1}

Substituting in equation 12 we find

I = 6.7 amperes

Since the value for I assumed and that calculated by equation 12 differs, additional trials are required. It is found that when I is assumed to be 6.7 amperes, the current calculated by equation 12 is 6.8 amperes. If the calculated values are plotted as a function of the assumed values, and if the straight line, I(calculated) = I(assumed), is drawn on the same graph, the intersection at 6.78 amperes gives the desired current. This result is shown in Fig. 13.

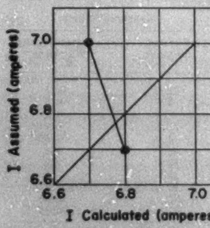

Fig. 13 (left). Graphical solution for current per cable for a bundle of 19 AN-18 cables

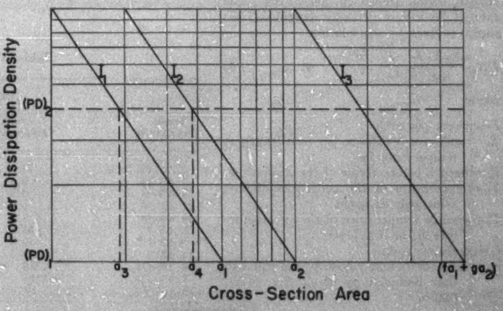

Fig. 14. Figure illustrating Appendix III

The p.d. power density of the bundle is given by the relation

$$\text{p.d.}=\frac{I^2(R_1+6R_2+12R_3)}{\text{bundle area}} \tag{13}$$

Substituting in equation 13, we find

$$\text{p.d.}=3.29 \text{ watts inch}^{-2}$$

Appendix III. Analysis of the Procedure for Using the Cable-Selection and Cable-Rating Chart

In describing the procedure for using the chart to determine the cable sizes for a bundle when the currents are given it was asserted that the p.d. selected in step 1 was arbitrary, and that the current line through the point determined in step 2 intersected the R curve at a point whose ordinate gives the permissible p.d. for the bundle. These statements will be justified by showing that the procedure satisfies the two conditions mentioned previously:

1. The p.d. for every cable loaded simultaneously must be the same.
2. The point determined by the p.d. and the total cross-section area of the cables loaded simultaneously must lie on the R curve.

In step 1 of the cable selection procedure, a p.d. was arbitrarily chosen, and from this the cable area for each of the given currents corresponding to this value of p.d. was found. Let $(\text{p.d.})_1$, I_1, and I_2 denote the value of p.d. selected and the given currents; let a_1 and a_2 represent the corresponding areas. See Fig. 14. In step 2, a total bundle area corresponding to $(\text{p.d.})_1$ was found which can be represented by (fa_1+ga_2), where f and g are the number I_1 and I_2 loads respectively. By steps 1 and 2, a point has been determined which satisfies condition 1. The current line through this point will be designated I_3. The horizontal distance between current lines I_2 and I_3 can be expressed as

$$\log(fa_1+ga_2)-\log a_2 \tag{14}$$

If the procedure of steps 1 and 2 is repeated for any other value of p.d., say $(\text{p.d.})_2$, the areas a_3 and a_4 are obtained for I_1 and I_2 respectively. The total bundle area for this case is fa_3+ga_4.

It will now be shown that the point with co-ordinates $[fa_3+ga_4, (\text{p.d.})_2]$ lies on current line I_3 by proving that

$$\log(fa_1+ga_2)-\log a_2 =\log(fa_3+ga_4)-\log a_4 \tag{15}$$

From the fact that current lines I_1 and I_2 are parallel, then

$$\log a_1-\log a_2=\log a_3-\log a_4 \tag{16}$$

Therefore

$$\frac{a_1}{a_2}=\frac{a_3}{a_4} \tag{17}$$

$$\frac{fa_1}{a_2}=\frac{fa_3}{a_4} \tag{18}$$

$$g+\frac{fa_1}{a_2}=g+\frac{fa_3}{a_4} \tag{19}$$

$$\frac{ga_2+fa_1}{a_2}=\frac{ga_4+fa_3}{a_4} \tag{20}$$

Taking the logarithm of both sides of equation 20, we obtain equation 15.

Equation 15 shows that the choice of any p.d. in step 1 results in a point which lies on the same current line. In addition, every one of these points satisfies condition 1. It then follows that the intersection of the current line and the R curve determines the permissible p.d. since it satisfies conditions 1 and 2.

Appendix IV. A Note on the Accuracy of the Chart

The current values predicted by the chart for fully loaded bundles composed entirely of cables smaller than *AN-18* will not be conservative. Thus, for a bundle of 100 *AN-22* cables, the current per cable given by the chart for a 40-degree-centigrade maximum conductor temperature rise is 2.9 amperes. It is calculated that 2.9 amperes per cable would produce a 54-degree-centigrade maximum rise.

However, if the currents are given, the chart yields cable sizes (including sizes *AN-20* and *AN-22*) which are conservative. For example, if we are given a bundle of 100 loads of 2.4 amperes each, the chart, Fig. 7, predicts a cable area corresponding to a cable between *AN-22* and *AN-20*. Calculation shows that 100 *AN-22* cables carrying 2.4 amperes per cable would produce a 40-degree-centigrade maximum rise.

References

1. Continuous Current and Temperature Rise in Bundled Cables for Aircraft, **Milton Schach, R. E. Kidwell, Jr.** *AIEE Transactions*, vol. 71, pt. II, 1952, pp. 376–84.

2. *Military Specification MIL-W-5086*, Washington, D. C., Nov. 30, 1950.

3. Continuous Current and Temperature Rise in Aircraft Cables, **M. Schach.** *AIEE Transactions*, vol. 71, pt. II, 1952, pp. 197–203.

4. *Military Specification MIL-W-7072*, Washington, D. C., Nov. 30, 1950.

5. Heat Dissipation by Free Convection, **W. Elenbaas.** *Philips Research Report*, Eindhoven, Holland, vol. 3, 1948, pp. 338–60.

6. The Calculation of Heat Transmission (book), **Margaret Fishenden, Owen A. Saunders.** His Majesty's Stationery Office, London, England, 1932, chap. II.

Discussion

E. P. Barlow (The Glenn L. Martin Company, Baltimore, Md.): In the past, our deplorable lack of knowledge on the continuous current capacity of cables installed in bundles in aircraft has not caused much actual service difficulty. In our low-voltage (28 volts d-c) systems most of the cables are designed for voltage drop. Past aircraft designs have tended to the use of bundles in which at any one time many of the cables would not be carrying current. For these and other reasons, our past installations have seldom pushed the cable to the maximum limits of its performance. In the future it appears that we will need to give much more attention to the matters presented in this paper if our installations are going to continue to give satisfactory service. The use of higher voltage systems will decrease the number of cables selected on a voltage drop basis. More continuously operating loads will decrease the number of unloaded cables in the bundles. Higher performance aircraft are decreasing the margin between the maximum permissible temperature for the cable and the environment of its installation. In short, future designs are likely to demand much more careful analysis of our cable ratings from the thermal standpoint and this paper presents valuable tools with which to accomplish this additional work.

With reference to Fig. 8, there appears to be a surprisingly small derating (less than 30 per cent for small bundles and approximately 15 per cent for large bundles) for altitude conditions. Previously available information, particularly in regard to the performance of single conductors in free air, have indicated considerably more derating with altitude. A discussion of the factors which cause the 50,000-foot 70-degree-centigrade R_b curve to lie so little below the sea-level 70-degree-centigrade R_s curve would be of interest.

M. Schach and **L. D. Schroeder:** We would like to thank Mr. Barlow for his discussion which places the problem of rating aircraft cables in proper perspective.

While our lack of knowledge has not caused much actual service difficulty, it may have imposed a significant weight penalty. In the past, it has been virtually impossible to evaluate the rating of cables. The proposed Naval Research Laboratory charts make it possible to obtain a quantitative estimate of the existing method of rating cables in bundles.

Military Specification *MIL-W-5088*[1] provides one current value for each cable size under bundle conditions. The proposed Naval Research Laboratory charts yield a range of current values for each size of cable, depending upon the specific currents which flow simultaneously in other cables of the bundle. A fair estimate of the validity of the current values given by *MIL-W-5088* can be obtained from Table V which indicates the range of allowable currents for three *AN* cable sizes for a few conditions. This table is based on Fig. 7. The lower rating for a given cable size and number loaded is obtained by assuming that all of the other cables loaded simultaneously with it are size *AN-2*. The upper current value for a given cable size and number of cables loaded is found by assuming that all of the other cables loaded simultaneously with it are size *AN-22*.

The small altitude-derating indicated by Fig. 8 is a consequence of our assumption that the ambient air and wall temperatures are the same and the two facts which follow: 1. the interior of the bundle of cables presents a larger proportion of the total thermal impedance than does the insulation of a single aircraft cable. For a bundle of 169 *AN-18* cables, this impedance at sea level constitutes 45 per cent of the total compared to about 15 per cent for a single cable. 2. Radiation accounts for a substantial part of the total heat transfer at the bundle surface. For a bundle of 169 *AN-18* cables, the relative amounts of heat transferred by radiation and convection at sea level are approximately 55 and 45 per cent respectively. For a single *AN-18* cable, these values are about 25 and 75 per cent respectively. It follows, therefore, that even though the convection coefficient at 50,000 feet is about one-third of its value at sea level, the relative decrease in heat dissipation with altitude will be much less for bundled cables than for single cables.

Table V. Comparison Between Current Ratings Given by *MIL-W-5088* and Fig. 7

Nominal AN Cable Size	MIL-W-5088 Bundle Rating of Nominal Cable, Amperes	Allowable Current Rating of Nominal AN Cable When Bundled with the Cables Shown. All Cables Carry Current Simultaneously. Current Values Based on Fig. 7		
		Bundle Composition		
		Total No. of Cables in Bundle	1 Nominal Cable and	Allowable Current Rating of Nominal Cable, Amperes
18	10	3	2 *AN-2*	5.7
		3	2 *AN-22*	14.0
		6	5 *AN-2*	4.0
		6	5 *AN-22*	11.5
		9	8 *AN-2*	3.5
		9	8 *AN-22*	10.0
8	46	3	2 *AN-2*	37
		3	2 *AN-22*	70
		6	5 *AN-2*	28
		6	5 *AN-22*	64
		9	8 *AN-2*	24
		9	8 *AN-22*	60
2	100	3	2 *AN-2*	122
		3	2 *AN-22*	175
		6	5 *AN-2*	94
		6	5 *AN-22*	170
		9	8 *AN-2*	82
		9	8 *AN-22*	164

REFERENCE

1. INSTALLATION OF AIRCRAFT WIRING. *Military Specification MIL-W-5088*, Washington, D. C., March 14, 1951.

Control of Metal Build-up in Minimum Pressure Sensitive Contact Systems

J. P. DALLAS
MEMBER AIEE

T. R. STUELPNAGEL
ASSOCIATE MEMBER AIEE

Synopsis: The race for automaticity has allowed little time for simplification and cost reduction. We have automatic jet engine control as a function of ten parameters employing 30 vacuum tubes. But do we have adequate reliability? In view of these problems, this paper investigates the simplest information sensing and control element for servomechanisms—sensitive electric contacts. Contact protection and reliability are carried beyond the scope of electric networks and a mechanical solution is proposed to the remaining problem of metal build-up. Reliable operation on 50 microwatts of input signal power, 200,000 times power amplification, 4-ounce weight, cigarette package size, no heat-dissipation problem, no stand-by power required for cathode heating, and tens of millions of cycles of operation may be the reward of further study of sensitive contact signal sensing devices.

Introduction

SECOND INDUSTRIAL REVOLUTION

A second industrial revolution is sweeping across America, invading industry and home alike. This is the revolution of automaticity spearheaded by servomechanisms. The first revolution resulted when technology produced machines that would replace men's muscles. This second industrial revolution is providing slave "brains" which will control these machines. Already whole plants, such as oil refineries and paper mills, are being controlled by skeleton crews of technicians. These men merely co-ordinate the slave "brains" with push buttons, mechanized data cards, or tape recorded program controls.

Automatic controls have invaded the home. Automatic furnaces, coffee makers, laundry equipment, and kitchen ranges with vacuum tubes have elevated the housewife to a domestic technician. Automobiles with power steering, power braking, automatic transmission, and photoelectric headlight dimmers have almost made it possible to transfer the control of the vehicle to the back-seat driver.

Automatic control involves the use of servomechanisms. Servomechanisms are power conversion devices which transform an input error signal into a controlled mechanical output. Typical servo controls turn valves in proportion to temperature or adjust the flight of an airplane as directed by the autopilot.

NEED FOR SERVOMECHANISM SIMPLIFICATION

The almost frantic race for more and better servomechanisms with which to propagate this second industrial revolution has left the servo engineer breathless and perhaps a little dismayed. The pace of the last few years has allowed little time for simplification. Performance has been the keynote. This has been particularly true in aircraft servomechanisms where the performance requirements have been fantastically high, such as control of fuel to a jet engine as a function of 10 parameters. Complexity, particularly in new developments, breeds high cost and unreliability; therefore, the purpose of this paper is to investigate the simplest information sensing and primary control element for servomechanisms—sensitive electric contacts.

OFF-ON PULSE-CONTROLLED CONTACTS

Off-on pulse-controlled contacts may compete in performance with vacuum-tube and magnetic amplifier systems and with transistor systems for low cost and weight. Contacts can be made to do the job of more complicated systems by modern servo-clutch pulse control tech-

---

Paper 53-376, recommended by the AIEE Air Transportation Committee and approved by the AIEE Committee on Technical Operations for presentation at the AIEE Aircraft Electric Equipment Conference, Seattle, Wash., September 30–October 2, 1953. Manuscript submitted July 2, 1953; made available for printing August 24, 1953.

J. P. DALLAS and T. R. STUELPNAGEL are at 8511 Vicksburg Avenue, Los Angeles, Calif.

niques and feedback systems working directly into the coils of the signal sensing relay. Such a method of using sensitive contacts has been discussed in an earlier paper.[1]

Reliable operation on 50 microwatts of input signal power, a power amplification of 200,000 times 4-ounce weight, cigarette package size, no heat-dissipation problem, no stand-by power required for cathode heating, and rugged designs to meet aircraft vibration and acceleration requirements are some of the rewards of learning how to use a sensitive contact relay signal sensing device. But the solution of many critical contact problems is essential before contacts of the order of sensitivity indicated here can be successful in high reliability servo systems. This paper and the references outline these problems and propose some solutions.

Problems with Sensitive Contact Application

There is no single solution to the contact problem. Contact making elements are in use in many types of systems with radically different requirements. Optimum engineering design consists in meeting the contact problem of a given design with minimum weight and cost. The contact protection system described elsewhere[2] outlines a general contact protection philosophy and a basic resistance-capacity-diode circuit for minimizing metal transfer by preventing contact arcing and sparking. However, this protection system does not prevent the formation of metallic spires which result from the low-voltage bridging phenomena. The basic resistance-capacity-diode protection circuit provides reliable long-life contact operation in systems where spire formation is prevented by occasional high-level signals. Such high-level signals change the particular contact area sufficiently to distribute the metal transfer. In sensitive contact systems where minimum pressure operation is the constant condition and the contacts are not regularly subjected to high-level signals, spires become a major problem. Such a circuit is typified by a close-range temperature control. The purpose of this paper is to investigate the problem of this latter type of application which is troubled by metallic spire formation. Such sensitive contact systems are even faulted by the effects of electrostatic attraction between the contacts at small gaps. This problem can be solved by the selection of appropriate contact configuration and detent circuits.[3]

Definitions

How sensitive are "sensitive contacts" and how small is "minimum pressure?" It is necessary to define such inexact descriptions. Therefore, these and other more or less boundless adjectives will be provided with more definite boundaries as follows:

Sensitive Contacts

As used in this paper, sensitive contacts refer to contact gaps of the order of 0.001 to 0.005 inch. Contact movement may be proportional to a gradually changing signal. In such systems where the contact gap is proportional to the signal, the actual operating separation of the contacts may be of the order of 0.0005 inch. The power controlled by the contacts is direct current.

Detent

Detent is a magnetic or mechanical means of increasing the contact pressure at the instant the circuit is made. For example, a detent force may be obtained by magnetically coupling the contact current to the contact armature, or by providing mechanical snap action. Such detent can only be obtained in exchange for signal sensitivity. Therefore, in high-sensitivity systems its use must be avoided or minimized.

Minimum Pressure Sensitive Contacts

These are considered to be contact systems in which initial contact closure pressure may be as little as 0.01 gram.

High Reliability

High reliability as herein considered is required in sensitive contact application where 100-per-cent operation must be sustained for tens of millions of operations. Such operation is to be contrasted to heating controls where an occasional out of tolerance or erratic operation can be tolerated. If such a heating control has a specified tolerance of ±2 degrees, an occasional 5-degree erratic operation will be tolerated. A gun sight control, on the other hand, could not tolerate any out of tolerance operation without endangering airplane, pilot, and mission. Therefore, high-reliability operation within the meaning of this paper would be required.

Contact Life

Reliability and long life go hand in hand. They result only when energy dissipation, and consequently metal transfer at the contacts, is small. To get some idea of required life an off-on modulated servo clutch type of control may be considered. In such an application the sensitive contacts might operate with 100 microwatts of signal power and control 10 watts of power at a rate of 10 cycles per second. One hour of continuous operation, therefore, can result in 36,000 operations. One thousand hours of continuous operation would require 36,000,000 contact cycles.

Bridging

Modern concepts of the physics of electric contact operation involve the following theory of metallic bridging. As metallic contacts are separated the contact area decreases in size and increases in resistance to current flow until the generated heat is sufficient to melt the metal. Then as the contacts are separated still further a molten metal bridge is drawn out between the contacts. Still greater contact separation, perhaps in the order of a few micro-inches, causes the bridge to rupture and the electric circuit to be broken. Unfortunately, the molten metal in the bridge does not divide evenly between the contacts. Instead, more than half ordinarily transfers to the negative contact for the conditions under consideration. The total consequence of this operation is to build protuberances called pips, domes, or spires on the cathode contact and to create a corresponding crater in the anode contact. Ragnar Holm (reference 4, sections 56–62) proves that all bridging metal transfer "is proportional to the square of the final current traversing the bridge at its rupture."

As the losses of metal due to vaporization and dissipation in sparks and arcs of cruder contact systems are eliminated by the refinement of contact protection networks, the problems arising from bridging metal transfer become more serious. Fig. 1 illustrates two types of bridging metal transfer protuberances.

Contact Domes

Contact domes are metal protuberances with rounded tops of the general form shown at *A* in Fig. 1.[4] This type of metal transfer is the result of bridging at currents above the values considered in this discussion. The shape of the dome is not always smooth. Irregular peaks develop which may eventually fail the contacts by closing the gap or mechanically interlocking the contacts. The dome type of metal transfer concerns this discussion only as a limiting condition since it results from contact currents which are excessive for long-life sensitive contacts or from less than optimum contact protection network design.

Contact Spires

Contact spires are metal protuberances with relatively sharp tops and small diameters of the general form shown at *B* in Fig. 1. This type of metal transfer results when current levels are kept low. The spire problem is not dealt with in Ragnar Holm's discussion. Holm's investigations are concerned with bridging transfer at currents above 75 milliamperes where the dome rather than the spire type of build-up is likely to occur. The present paper is concerned with the problem of reducing or eliminating the contact spire type of metal transfer.

The Dilemmas

The first dilemma confronting the designer of sensitive contact systems occurs when he discovers that the elimination of arcs and sparks through the use of protection networks can result in a critical metallic bridging problem.

The second dilemma which must be resolved by the designer occurs when he starts out to reduce metal transfer by following the procedure of reducing contact current. Since Ragnar Holm proved that metal transfer from metallic bridging was proportional to the bridge current squared, the obvious course is to reduce this current. But oddly and unfortunately, while the physical quantity of metal transfer does decrease as the square of the bridging current the actual linear growth or rate of height build-up of the cathode contact pip is not appreciably reduced by reducing the bridge currents. Investigation of these phenomena by the authors has established that while the volume of metal transferred at each break is roughly proportional to the bridge current squared, the height increase of a contact pip remains substantially constant for sensitive minimum-pressure contact systems as defined in the foregoing. The diameter of the contact protuberance decreases while the rate of height growth is affected very little by contact current change. Under the specified conditions this holds true for contact circuit currents ranging from less than 1 milliampere up to 500 milliamperes. Fig. 1 presents an illustration of the second dilemma in that the two cathode contact pips, while of different volume, are of equal height after the same number of cycles.

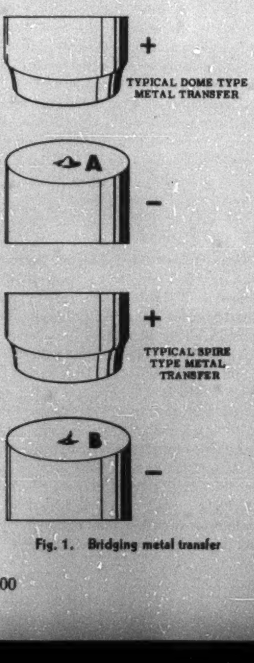
+
TYPICAL DOME TYPE METAL TRANSFER
A
–
+
TYPICAL SPIRE TYPE METAL TRANSFER
B
–

Fig. 1. Bridging metal transfer

This paper deals with the elimination of the spire type of metal transfer since it is these spires that persist in spite of reduced contact current or contact protection networks. In fact, the spire forms more readily in an environment where there are no arcs or sparks to neutralize it or no high currents to melt it down.

Nature of Contact Spires

Sensitive contacts operating with optimum resistance-capacity-diode networks at currents below 75 milliamperes with maximum contact pressures of the order of 1 gram will grow a typical metallic spire of 0.001 to 0.005 inch in diameter by 0.005 inch high in as little as 100,000 cycles of operation. Such spires eventually close the contact gap and result in the contacts failing to open. These observations apply to the use of platinum, silver, and gold. In general, those materials most desirable for contact use due to their low tendency to build up oxide film are the materials which form cathode spires the most readily (reference 4, table 61.01). Since a typical spire may be 0.001 inch in diameter, a microscope is usually necessary to observe it, and many failures from this cause are not correctly diagnosed and are commonly attributed to other causes.

Methods of Controlling Cathode Spires

The following conclusions were reached after testing to destruction 150 different contact systems.

Voltage and Current

While reducing contact current has little effect on the rate of height growth of contact spires, it does reduce the amount of metal transferred, making the mechanical elimination of the spires surer. It is apparent that by increasing the contact circuit voltage lower contact circuit currents will result for loads requiring the same amount of power. If a contactor operated by sensitive relay contacts requires a current of 50 milliamperes at 120 volts, it is obvious that more than 200 milliamperes will be required to do the same work in a 28-volt circuit. While all the factors affecting the selection of the optimum voltage for a sensitive relay contact circuit are not known, it is believed that somewhere between 100 and 200 volts may prove most desirable.

Detent

Since metallic spires of 0.001 to 0.005 inch in diameter have little mechanical strength and since in the initial stages of spire building high contact pressures will tend to shift the point of contact and reduce the spire building tendency, high detents may be thought of as a possible solution. Tests indicated that detent values required to be effective were of the order of tens of grams. This method obviously was incompatible with sensitivity requirements.

Low Current

Reduction in contact current only resulted in reducing the diametral dimension of the spires without appreciably slowing up the rate of their linear growth.

Balancing Bridging Growth by Spark Erosion

If the contact protection network is modified to allow a controlled amount of sparking, in theory one should be able to balance the tendendy toward spire growth with the losses from spark erosion. In practice such a balance has proved too critical; furthermore, erosion from either arcs or sparks introduces oxide films and other complications of the contact surface which tend to cause low-pressure sensitive contacts to malfunction; they fail to close within the signal tolerance design limits.

Preventing Spire Build-up with High Make Currents

High make currents can be used to prevent sharp spires from forming. This method of prevention has also proved to be impractical because the high current

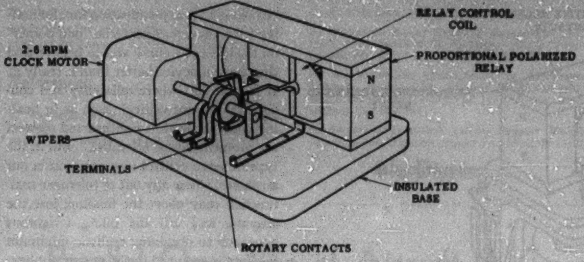

Fig. 2. Rotary cathode contacts applied to a sensitive proportional relay

transfers a much larger quantity of metal which in turn results in a serious dome build-up. Protrusions from the dome transfer eventually close up the contact gap or cause mechanical interlocking. High make currents also introduce the hazard of contact sticking.

BIMETALLIC CONTACT MATERIALS

Holm suggests that a nickel anode contact working with a silver cathode will reduce metallic bridging transfer to the cathode. The nickel has a tendency to oxidize so that in the initial pip forming stages the contact meeting areas shift about, thus not permitting a high rate of pip height growth. However, tests by the writers of both nickel-silver and nickel-platinum contact combinations gave erratic operation at contact closure pressures of less than 1 gram. Tests of bimetallic contacts of this nature also led to a theory of operation differing from Holm's. The nickel-platinum combination, when observed under a microscope, appeared to have a self-regulating property. The material from the platinum contact tended to transfer to the positive contact area of the nickel contact, coating it with a thin layer of platinum. When this reached a certain stage the metal transfer appeared to reverse and return to the original platinum contact. This operation produced over-all metal transfer equilibrium for several million cycles. However, the contact pressure required to maintain close tolerance contact operating signal conditions was too high to allow use of this method. Much further work on metallic combinations tending to inhibit spire building in sensitive low-pressure contact systems is needed.

NONMETALLIC CONTACT MATERIALS

These were tried and were found to introduce presently insoluble problems. With carbon and graphite contacts electrostatic bridging of contact dust particles, rapid wear, and adverse contact pressure versus contact resistance stopped further exploration of this method.

MECHANICAL SOLUTION

Finally, a mechanical solution to cathode contact spires proved most successful. Holm suggests that "by often turning the electrode so as to make contact in new spots" bridge metal transfer cathode pips may be avoided. This could be accomplished in many ways. Flexibly mounting the contact points or contact arms so that operation produces a change in the mating areas of the contacts may reduce the tendency toward spires. However, experiments were not successful in producing a nonpositively driven or turned low-pressure contact system.

A positively rotated and scraped cylindrical cathode contact has proved to be the best solution so far found to the cathode contact spire problem.

Motor-Driven Cathode Contact

A positive correction of the sensitive contact cathode spire problem was obtained by externally driving cylindrical cathode contacts of a sensitive relay. A polarized proportional relay with cylindrical motor-driven cathode contacts is shown in Figs. 2 and 3. The rotating contact wiper or brush continuously cleans the cathode contact through its burnishing action which ensures uniform low-contact pressure performance. The contacts were made of platinum 10 per cent iridium alloy in the experimental relay. While platinum iridium alloy contacts were used, it is believed that fine silver rings could have been used on the rotating contacts. Since the rotating contact cylinders employ a substantial amount of material, a significant cost reduction may thus be possible. Silver rotating contacts against the platinum iridium armature contacts are recommended for test evaluation. This assembly has the following advantages:

CONSTANTLY CHANGING CATHODE AREA

Constantly changing the cathode area prevents the accumulation of metal bridging deposits in any one spot, thus eliminating spires, domes, and pips.

FAIL SAFE

If the contact driving motor fails, the relay will continue to function in the ordinary manner for a limited life. The addition of the contact driving motor is not a complete series liability with regard to relay failure. Of course, in maximum sensitivity systems motor failure can cause out of tolerance contact opening operation. Closing tolerances will not be immediately affected.

BURNISHING ACTION

The cathode contact cylinders are burnished by the wiper bearing on them. The action of this wiper tends to burnish the contact so that uniform low-pressure operation is reliably assured. The mechanical strength of contact spires of the order of 0.002 inch diameter is low enough to allow the wiper to remove them if they form due to temporary failure of the driving motor or due to repetitive operation in the same area.

SIGNAL CONTACT SEPARATING FORCE REDUCED

Since the contacts driven by external power are moving, little or no signal separating force is required to open the contacts. This permits a large increase in contact sensitivity without reduction in reliability or sacrifice of signal opening

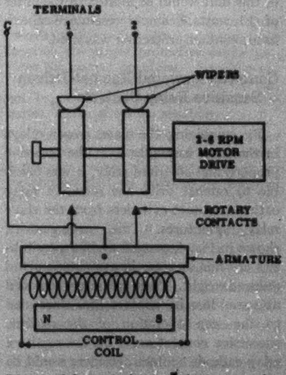

Fig. 3. Schematic diagram of sensitive relay with power-driven rotary cathode contacts

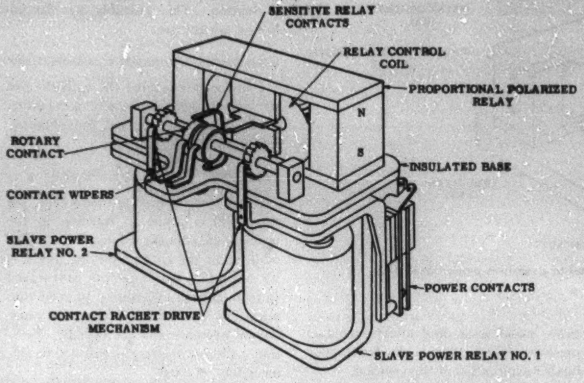

Fig. 4. Rotary cathode contacts of a sensitive relay ratchet driven by power relays

tolerance requirements. The basic principle of overcoming static contact hysteresis by power driving one of the contacts produces an important gain in the practical sensitivity of contact devices.

Preliminary Test Results of Experimental Rotating Cathode Contact Relay

These test results indicate reliable operation under aircraft conditions with a 50-microwatt input signal. Contact gaps of 0.004 inch were used. A 60-milliampere 120-volt inductive load was controlled for 20,000,000 cycles of operation with no observable deterioration of the contact surfaces or any change in the sensitivity of the relay. There was no indication that the control output power of this unit would be limited to the order of 10 watts. Simple resistance-capacitance contact protection was used.

Contactor Powered Ratchet-Driven Sensitive Relay Contacts

By combining the slave power relays in the same assembly with the sensitive proportional polarized relay, it was possible to ratchet drive the sensitive relay cathode contact cylinders from the slave relay armatures. This arrangement, shown in Fig. 4, seemed to offer possibilities of some increase in compactness and reduced weight. These gains were achieved at some loss in contact life, since, due to the step operation of the ratchet, successive contact areas on the sensitive relay cathode contact cylinders would be repeated. An undetermined increase in contact hysteresis could be expected compared to the motor-driven contact assembly because the contacts would not usually be in motion at the instant of opening. Tests have not been made to determine what effect this would have on probably useful life of the assembly. Problems are anticipated with magnetic interaction of the slave relays with the sensitive relay. Some advantages can be taken of this effect to provide a small amount of detent action.

The Testing Problem

Engineering opinion on sensitive contact devices varies between two extremes. One, there is no problem. Two, the problem is so complicated and complex that any attempt to solve it is all but hopeless. The reason for this extreme difference of opinion is that ordinary test procedures on identical assemblies can appear to justify either or both of these conclusions. If contact life is defined as the number of cycles within operation tolerances, then normal variation between successive test samples will be at least 4 to 1. That is, if a life of 4,000,000 cycles is obtained from one test, the minimum life may be found to be as low as 1,000,000 cycles. If less than precise mechanical and electrical design is employed in the relay, if anything less than precision flexure pivots or precisely flat joints in the magnetic circuit are employed, contact life variations may be in the order of 10 to 15 times. Only by the elimination of all mechanical ambiguities can close tolerances on sensitive contact operation be held for tens of millions of cycles as required for off-on pulse-controlled servo-clutch operation. It is very easy for test engineers to find justification for eliminating what they consider to be "odd points" on the life-cycle curve and to believe that they have a device better than it really is. It is true that where reliability and consistency are not critical, such as in heating controls, such a lighthearted view of the problem can be tolerated. But in the type of servo control now common in our airplanes, where any out of tolerance malfunction may abort the mission, lose the aircraft, and kill the pilot, a rigorous approach to obtaining realistic minimum life data is essential to the proper application of sensitive contact controls (reference 6, section 4.22).

Care must be taken in the testing of sensitive contact devices to insure that test procedures actually simulate operation. Early in the development of one servomechanism, it was reasoned that contact bounce was the critical problem. Therefore a high-level square-wave signal was used to drive the contact life-cycle test. No malfunction was observed in billions of operations. Yet when the complete servomechanism was life-cycled, failure occurred in less than 100,000 operations. It turned out that contact bounce was not the critical factor and that normal operation produced successive minimum pressure operation conducive to cathode contact spire formation. These spires caused the unexpected failures. The high-signal-level, square-wave life testing of the contact assemblies, while creating the severest contact bounce conditions, prevented the growth of cathode contact spires which, due to the minimum contact pressures in actual operation, were the critical problem limiting the life of the servomechanism.

Conclusions

1. Considerable research has been expended in trying to find the easy ways to solve the cathode spire problem in minimum pressure sensitive contact systems. The most reliable answer to date is that of rotating the negative contact against a contact burnishing wiper and employing a contact protection network designed to minimize the amount of metal transfer.

2. The neglect of mechanically driven cathode contact assemblies has been the result of a rather naive attitude toward the whole contact problem. When less elaborate methods are rigorously examined and other available methods of servo control employing vacuum-tube equipment or magnetic-amplifier designs are evaluated, then a simple clock motor driving a rotating contact of a proportional relay appears by comparison worthy of careful consideration.

3. Investigation of bimetallic contact combinations designed to minimize cathode spire formation is likely to be profitable.

Further investigation of nonmetallic contact materials for minimum pressure sensitive contact systems is considered desirable.

References

1. Consideration of Off-On Modulated Reversing Clutch Servo Systems, T. R. Stuelpnagel, J. P. Dallas. *AIEE Transactions*, vol. 71, pt. II, 1952 (Jan. 1953 section), pp. 406–10.

2. Sensitive Relay Contact Protection Systems, J. P. Dallas, T. H. McCully. *AIEE Transactions*, vol. 67, pt. II, 1948, pp. 1204–07.

3. Electrostatic Oscillation in Sensitive Contact Mechanisms, Thomas R. Stuelpnagel. *AIEE Transactions*, vol. 71, pt. II, 1952 (Jan. 1953 section), pp. 397–401.

4. Electric Contacts (book), Ragnar Holm. Almquist and Wilksells, Stockholm, Sweden, 1946.

5. Electrical Contacts (book), G. Windred. MacMillan and Company, London, England, 1940.

6. Report of Advisory Staff for Aircraft Electrical Systems. Wright Air Development Center and Bureau of Aeronautics, Dayton, Ohio, 1951.

7. A Polarized Relay as an Aircraft Control Element, Royce E. Johnson, Frank A. Glassow. *AIEE Transactions*, vol. 67, pt. II, 1948, pp. 1249–55.

No Discussion

Parallel Operation of Aircraft A-C Generators

L. R. LARSON
MEMBER AIEE

IN MILITARY aircraft, the growth of electric power consumption has been very large. The load requirements have led to the desirability of developing a-c systems rather than producing power as direct current and then converting to meet the a-c load requirements. For the most part, single-generator systems or combinations of single-generator systems using split-bus arrangements have been used. Need for higher-reliability systems, having greater reserve capacity, and making higher utilization of generator capacity through the diversification of load equipment leads to the conclusion that parallel systems should be used in future aircraft.

In ways, the problems involved in parallel operation of a-c systems are far more complex than those encountered in use of single-generator systems. Certain of the functions that are peculiarly applicable to single-generator systems may not be performed in a satisfactory manner and may cause system malfunction when used in parallel-generator systems. An attempt is made in this paper to define the various operating conditions and certain of the system malfunctions that may result from failure, mismatch, or lack of co-ordination of the various items used in paralleled-generator systems. While it is unnecessary at this time to place specific numerical limitations on the performance of various items, at least the interrelationships can be expressed and conclusions drawn therefrom. Careful analysis of the problem should point up the lack of certain desirable equipments necessary for proper operation of such systems. Past trends of development of components rather than integrated systems may lead to complete mismatch of many of these individual items of equipment when being combined into an operating system, unless great care is used in defining the compatibility requirements of each item of equipment.

Operational Requirements

Modern high-performance aircraft place a premium on the number of crew members that can be carried on a particular mission. In addition, these crew members have less time available to execute their assigned duties. Consequently, the electrical system should require little or no supervision for its operation. A reasonable design objective for the a-c system is that it should be as easy to operate as the older d-c system. In other words, the operator, having selected the generators need for the particular operation, should not be required to establish manually the conditions necessary for parallel operation and bring about synchronization.

Systems must be as simple as is compatible with the prior requirement of automaticity. Proper design and arrangement contribute to ease of maintenance and increased system reliability. Each individual component used in the system must be capable of withstanding normal service abuse without failure or malfunction. A device that will not meet these requirements can well cause more loss of weapon effectiveness than the use of a device having slightly lower performance but higher reliability.

Certain design principles can be applied during the consideration of a particular system configuration or items of equipment. Several of these are listed below:

1. The characteristics of the individual components must be carefully co-ordinated to meet the steady-state and transient requirements that are placed on the system by the present load equipments.

2. Though the control and protective functions must be co-ordinated with the remainder of the system, they should be physically integrated with the associated equipment whenever possible. In this manner, the supplier of the basic equipment can assure correct and proper assembly of these various components without dependence on another party for the proper installation of the interconnecting circuits, whether electric, hydraulic, or pneumatic.

3. Control and protective functions should not be operated through common circuitry or elements, when failure of the circuit or elements will result in simultaneous loss of control and protection.

4. Protective devices must be carefully co-ordinated so that during system malfunction the proper protective device provides the correct operation. Simultaneous tripping of cascaded protective devices can not be permitted while retaining the required degree of system reliability.

5. The principle that one fault shall not cause system collapse is of fundamental importance when discussing systems or components that are required for safety of flight.

The above list of design principles apply for either single-generator systems or for multigenerator parallel systems. The problem of proper co-ordination will be more complex in the case of the multigenerator system. Even in the case of a multigenerator system it is necessary that proper and reliable operation be achieved while using the individual generators in a split bus arrangement.

Paper 53-372, recommended by the AIEE Air Transportation Committee and approved by the AIEE Committee on Technical Operations for presentation at the AIEE Aircraft Electric Equipment Conference, Seattle, Wash., September 30–October 2, 1953. Manuscript submitted June 30, 1953; made available for printing August 24, 1953.

L. R. Larson is with the Naval Research Laboratory, Washington, D. C.

Engineering personnel of the following companies gave their wholehearted co-operation in relating equipment characteristics and personal observations of system performance: General Electric Company, Schenectady, N. Y., The Glenn L. Martin Company, Baltimore, Md., Jack and Heintz, Inc., Cleveland, Ohio, Sundstrand Machine Tool Company, Rockford, Ill., Westinghouse Electric Corporation, Lima, Ohio, and others.

Component Parameters

The normal sequence of events in the development of equipment is for the component design engineer to establish the requirements for his specific device with only incidental attention being given to the associated components going into the completed system. Certain of the requirements for satisfactory parallel operation of generators as a system will be listed for the particular components in the following discussion.

PRIME MOVER AND GOVERNOR

To produce narrow frequency range a-c power, the prime mover must be capable of accepting and controlling available energy to produce continuously-controlled output speed, held within acceptable limits. The energy source may be pneumatic, hydraulic, or mechanical. For the various sources, the conversion equipment will necessarily assume different forms. The power conversion device with its associated governor should result in similar operation, since the electric loads for a particular aircraft using any of the above energy sources are likely to be the same. For consideration as prime movers in parallel-generator systems, the units must be provided with a means of obtaining real load division. The prime mover must be capable of supplying the overload and transient requirements placed on it by the electric system. The governor system applied to a prime mover must be considered carefully so that a loss of the control function will result in a "fail safe" condition. An integral mechanical governing system holding speed tolerance to ± 5 per cent, with possibly an electric topping circuit to enable real load division and finer speed control, seems to be a reasonable solution to this particular problem.

GENERATOR AND REGULATOR

Generator and regulator must be capable of delivering controlled power as required by the loads of the particular system. These requirements place limitations on permissible voltage regulation, voltage unbalance, wave form, transient response, both for normal system load switching, and for abnormal system conditions to be discussed later. The regulator must incorporate a satisfactory means for providing reactive load division among machines being operated in parallel. The characteristics of the generator and regulator must be carefully integrated with those of the associated prime mover.

PROTECTIVE DEVICES

It is of fundamental importance that characteristics of protective devices be based on realistic system-operating conditions. In addition, the various devices must be co-ordinated so that predicted system operation can be maintained without malfunction or lack of co-ordination of the various protective devices used. To mention a few of the possible protective devices that must be co-ordinated would include the following: fuses, limiters, circuit breakers, overvoltage, differential, and over- and underfrequency protectors, reverse power relays, pressure relief systems in prime movers, overheat elements, etc. All of these various devices must be co-ordinated with control functions provided by such equipments as automatic synchronizing gear, voltage regulators, and governors. It is of fundamental importance that the protective equipment have the necessary capacity to perform satisfactorily its normal operating function under the most severe of abnormal system-operating conditions.

Integration of Components into a System

In the preceding section, certain operational requirements and characteristics of individual system components were described in general terms. The mention was made of the requirement of establishing the necessary co-ordination of certain protective devices to assure proper system operation. A further example of close co-ordination of component parameters is available from the analysis of the prime mover-generator combination. The final decision for the requirements to be placed on equipment to insure satisfactory parallel operation at all times is directly influenced by the detailed characteristics of the a-c generator-regulator combination and the parameters of the prime mover with its associated governor.

The complexity of the problem can be illustrated by assuming a situation where two hydromechanical drives are being operated in parallel, and the aircraft includes as an integral component a gas turbine driving a third generator having a capacity comparable to each of the other two machines. The gas turbine auxiliary unit is necessary for ground or water-based operation. For certain flight conditions, such as letdown and landing, parallel operation of the three generators as a system to achieve increased system capacity and reliability would be highly desirable. With the present state of the art, there have been difficult operational problems in achieving parallel operation for machines of identical rating and manufacture having prime movers of the same rating and manufacture. The illustration of introducing a third machine having an entirely different type of prime mover shows the number of parameters that must be closely integrated so that equalizer circuits for both real and reactive power can be reduced to a standard signal, and the resulting control functions have the same static and dynamic characteristics for each machine.

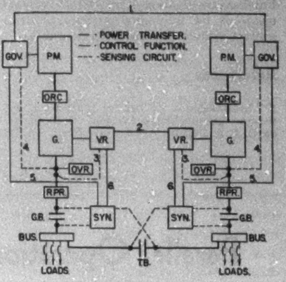

Fig. 1. Control and sensing paths for a 2-generator aircraft system

PM—Prime mover
GOV—governor
ORC—overrunning clutch
G—a-c generator
VR—voltage regulator
OVR—overvoltage relay
SYN—synchronizing equipment
GB—generator breaker
TB—tie breaker

1—real load division
2—reactive load division
3—reactive load signal
4—real load signal
5—speed correction
6—voltage correction

Fig. 1 is a schematic diagram of a 2-generator system used to illustrate the channels through which control information must be fed to make possible parallel operation. A paper by J. A. Granath and A. K. Hawkes[1] and an unpublished paper, "Sensitivity Requirements of Reactive Load Division Circuits in Aircraft Electrical Systems," by E. S. Sherrard define certain of the requirements for proper real and reactive load division among machines being operated in parallel. These requirements are based on achieving high utilization of system capacity—normally, on the order of 90 per cent of the total generator rating.

While there are many desirable facets to be achieved by using speed droop for real load division among drives operated in parallel, production tolerances in governors and drift in setting during the normal life of a unit very likely will make necessary the use of feedback circuits and interconnections among drives to insure real load division within ±10 per cent of the generator rating. Reactive load division by means of voltage droop has been found to be unsatisfactory. As a result of this experience, differential reactive-load-division circuits were introduced. The sensitivity of early load-division circuits was so low as to require manual monitoring to assure acceptable load division during normal flight operation. With operators not being available, the sensitivity and gain of these circuits must be increased so that reliable reactive load division can be achieved even though the individual generator voltages may be adjusted to the extreme permissible variation allowed by procurement specifications.

Many of the constant-speed drive and accessory drive developments have been initiated and carried out with little or no thought given to the ultimate requirement for parallel operation of these devices. This has resulted in governors being developed with no means available for introducing a signal to provide for accurate real load division.

The premise that a satisfactory generator should deliver power to the electrical system when its prime mover is capable of doing so leads to certain design guides. For example, the use of a reverse power relay that would automatically disconnect the generator from the system when power was flowing from the bus into the generator. The parameters of such a device must be such that the unit will override the normal energy transfer taking place during synchronization of machines with the remainder of the aircraft system. In addition, the device must not malfunction during periods when fault conditions exist on the aircraft bus or in the distribution system. To meet the design objective of automaticity, a reverse power relay must be associated with automatic synchronizing equipment. This equipment will sense the relationship existing between the generator and the aircraft bus and will automatically introduce corrective action to bring the generator within the acceptable band for paralleling with the system before initiating parallel operation. Perhaps an easier solution to this particular problem comes about through the use of an overrunning clutch located between the prime mover and the a-c generator. For this condition, once the a-c generator has been synchronized with the aircraft system, the generator will remain in a condition of readiness to deliver power to the system whenever its prime mover is capable of assuming its share of the system load. The overrunning clutch should be capable of withstanding continuous operation under slip conditions without failure or malfunction.

As has been pointed out, static and dynamic characteristics of the various devices being operated in parallel should be similar. Future carrier applications may require that not only the equipment in the aircraft be on prior to starting main engines, but the power flow to the equipment must not be interrupted during transfer from external to internal power. In this case, it may become necessary to parallel the aircraft system with either a ground power unit or perhaps large generators located aboard ship which may be feeding upwards of 20 aircraft simultaneously. Obviously, the difficulties encountered in such an operation will be manifold, and careful consideration should be given to the possibility of floating the aircraft electric system on the ground power unit with no requirement for real load division among these machines. The problem of reactive-load division, with the possibility of excessive circulating currents, will require detailed analysis. The use of proportional reactive-load division to establish reasonable reactive load division during such operation may be possible.

Abnormal Operating Conditions

In addition to assuring proper system operation during normal operating conditions, attention must be given to the satisfactory operation of the system for abnormal conditions. A properly integrated system should be capable of recovering from abnormal conditions without damage to either the power system components or to the load equipments. In addition, the return should be to a stable operating condition within the design range. Certain suggestions for protective devices can be made for specific failures. Ultimate use of such equipment must be based on detailed analysis of the particular aircraft system.

Various failures within the prime mover may give rise to conditions that make it desirable to remove the drive and its generator from the remainder of a parallel-operated system. Failure of a drive tending to force the machine to overspeed will result in that drive hogging the real load of the system and, where the drive is capable of doing so, of pulling the entire system frequency up to the limit of the drive. The use of an overrunning clutch between the drives and the individual generators may not materially influence the condition since the real load division circuits, if in operation, would tend to force division of load among the machines, bringing the normal machines to an overspeed condition in an attempt to take their share of the total system load. If topping governors are used, as previously discussed, when the limit of the topping circuit is approached, the machine tending to overspeed will carry the other machines to overspeed as synchronous motors. This discussion is based on the assumption that total loss of control has occurred on the machine going to overspeed. With a failure of this nature, the use of an overfrequency relay biased with a power signal could insure the removal of the faulty machine from the system. The setting of the overfrequency relay would, of necessity, be above the upper frequency limit of the topping governor. Where the control failure would be limited to the topping governor, the system frequency could rise to the maximum value permitted by that circuit. If this frequency is above the acceptable frequency range for the load equipment, the faulted machine can be found by automatically splitting the system up so that the generators would operate as single units. Having done this, the good machines would return to normal operating conditions, and the machine having suffered the failure would remain at maximum frequency permitting easy identification and removal from the system.

Prime movers can also fail by going to an underspeed condition. The use of an overrunning clutch between the prime mover and the generator would permit the generator to continue to operate as a synchronous motor, sharing reactive load with the other machines on the system. By the use of an underspeed switch built into the prime mover, this generator could be removed from the system at some predetermined prime-mover speed. If the failure has been the loss of the topping governor circuit and this failure causes the topping governor to force the prime mover's speed down, again the faulty machine could be removed from the system by splitting the system into its component parts, and then selecting and removing the faulty machine automatically.

The failure or loss of the real-load-division circuit may not cause immediate system malfunction; however, a disturbance of prime-mover speed or perhaps system load could initiate unbalanced conditions that would be detrimental to system capacity. Since the loss of the differential real load division circuit will probably cause drives to go to an underspeed condition, an underfrequency time-delay relay could be used to open the tie breakers, causing the system to operate in a split-bus arrangement. Continued operation at a dangerous underspeed by any drive should cause removal of that generator from the system.

Mechanical failures in a generator may occur in several ways. The failure may be gradual as for some bearing failures or for a dragging rotor. These failures can exist for considerable time before the rotor is blocked. Whether these conditions can be detected from the flow of power in the generator feeders is dependent on the prime-mover operating conditions and the nature of the failure. As long as the prime mover is capable of supplying the normal electric load and losses of a generator, along with the energy being dissipated by the dragging rotor or bad bearing, there will be no indication of failure detectable on the generator feeders. However, a complete stoppage of the generator rotor will result in a very large increase in electric power being fed into the bad machine from the remainder of the system. Excessive heating as a result of a gradual failure conceivably could be detected by an overtemperature device; however, these devices should not be looked upon with favor since nuisance outages occurring due to system overloads would be prohibitive. In addition, the location of such a thermal device is a critical problem. For example, on a 2-bearing machine, either bearing could be expected to fail. A blocked rotor condition can be detected by a reverse power relay. Depending on the nature of the ultimate failure, such devices as an underspeed switch in the prime mover or differential protectors on the generator and feeders could remove the generator from the system.

Other possible generator failures include loss of field. For the presently used machines, this could include both the exciter shunt field and the main a-c generator-field circuits. With present equipment, it seems more likely that the exciter field will be lost before the main field circuit would be opened.

The present design practice of not bringing the main field circuit outside the generator frame should be encouraged. This practice is in agreement with comments on integral design made earlier in this paper. With the loss of the exciter field of a generator being operated in parallel with other machines, the resulting system operation will be dependent on the generator characteristics and the magnitude and nature of the load on the system. Should the failure occur on a lightly loaded system, it is not likely that the machine would lose synchronism with the system. However, the action of the reactive-load-division circuits should tend to depress system voltage in an attempt to make the malfunctioning machine carry its proper portion of the system reactive load. In the case of an open circuit in the main generator field, similar operation can be expected. However, the faulty generator would be less capable of carrying real load than for the previous case. When the power capabilities of the machine have been exceeded the malfunctioning machine will be driven above synchronous speed by its prime mover through the action of the real-load-division circuits, and will be driven to the point where, as an asynchronous machine, it would be delivering its proper share of real load. However, the action of the reactive-load-division circuits will tend to force the system voltage down. Certain regulator-generator combinations tend to go to overvoltage conditions when supplying a leading-power-factor load, so that the final steady-state condition is dependent on the characteristics of all of the elements making up the system. During the transient period, the slip frequency may be sufficiently low to match the resonant frequency of the mechanical system, giving rise to damage to the prime mover. For these conditions, the malfunctioning machine must be selected and removed from the system for satisfactory system performance. If the slip frequency for the asynchronous generator is sufficiently high, an overspeed switch in the prime mover could be used to remove the malfunctioning machine.

Failures involving the voltage regulator and the associated circuitry may result in overexcitation for the generator. For this condition, the machine having incurred this malfunction will tend to increase the system voltage. Depending on the relative sensitivities of the reactive-load division and voltage-sensing circuits, the excitation on the normal machines may rise or fall. If the excitation of the normal machines is depressed far enough, these machines will lose synchronism and run as induction generators with a slip sufficient to carry their share of the real load. Again, as in the previous case, severe system oscillations may be incurred. In this case, for a 2-generator system, the use of the overspeed switch indicated for the condition of under excitation would result in the normal machine being removed from the system, while the malfunctioning machine would remain in operation and would force the system to a condition of overvoltage.

In a parallel-generator system, the loss of a phase by open circuiting in a particular generator may or may not cause a serious malfunction. If the failure occurs in those phases not being used for real-or reactive-load-division sensing, the power output of the machines suffering malfunction will drop to approximately two-thirds of its normal share of system load, with the remainder of the load being assumed by the other machines on the system. However, if the phase being lost is used for load-division sensing, serious system malfunction may result. A damaged machine will tend to assume full-system load, using the other machines on the system as transformers to accomplish the proper phase relationships. As occurred in some of the previously described malfunctions, the machine suffering the failure will tend to be driven at a speed above its normal operating condition. The remaining machines will tend to run as synchronous motors, provided an overrunning clutch is used. With this possibility of system malfunction, it would be desirable to place the current transformer's used in sensing real and reactive loads on the same phase, rather than in two different phases.

Another condition that perhaps should not be listed under the section "Abnormal Operating Conditions" is that occurring during the synchronizing of individual machines to establish a parallel-generator system. The various protective devices used throughout the drive, generator, and distribution systems must be co-ordinated properly so that the transient phenomena occurring during synchronizing will not cause nuisance outages. Even though automatic synchronizing gear may be used to insure that the initial synchronizing disturbances will not be excessive, system operating conditions, such as a 3-phase low-impedance fault, may result in machines losing synchronism during the fault. Upon removal of the fault, parallel operation must be re-established with the machines at ceiling excitation, considerable slip among machines, and possibly full out-of-phase. The resultant system disturbance could not be classed as a "normal" switching transient.

Various distribution-system faults may occur, and the system must be designed so that the fault can be removed without excessive system disturbance. Of prime importance in establishing these system stability criteria are the overload capabilities of the generators and prime movers. Military specifications for a-c generators require that the machines be capable of producing 3-per-unit fault current for a 3-phase low-impedance fault condition. In addition, the generators are required to produce 2-per-unit power for 5 seconds. Consideration of the external characteristics of a machine meeting these requirements shows that a generator is potentially capable of developing at least 3-per-unit power for a short period of time. Careful consideration of the distribution system to be used should show what fault impedances can be expected, and whether these impedances would result in such high levels of power. If such conditions do exist, very careful consideration has to be given to the overload potentialities of the prime mover being used. If the duration is sufficiently short prior to fault clearing, the inertia of the generator and prime mover may be sufficient to deliver the required energy without serious loss of speed. However, if this is not the case, the prime mover must be capable of supplying adequate power to insure the proper system operation. When a large portion of the system load is composed of rotating machinery, faults of considerable duration may permit these machines to slow sufficiently to cause the system to stall during recovery.

Of particular interest in component co-ordination is the problem of overvoltage protection. Unfortunate system experience has shown that overvoltage protection applied to a generator may operate before an overcurrent device, such as a fuse or circuit breaker, will clear a fault in the distribution system. This is particularly true when line-to-neutral overvoltage sensing is used. With a fault occurring on a phase other than that having overvoltage protection, the overvoltage relay is subjected to an overvoltage condition for the duration of the fault plus the normal system recovery time. With presently used fuses and circuit breakers, a mismatch of these devices with presently used overvoltage relays causes serious malfunctions, especially in those circuits where the higher-rating fuses and circuit breakers are used.

Conclusions

The following broad conclusions can be drawn from the foregoing discussion:

1. Due to the many divergent conditions encountered in obtaining proper system co-ordination, experience with complete system operation is necessary for intelligent selection of control and protective functions as well as basic system components, such as prime movers, generators, regulators, circuit breakers, etc.

2. Proper integration of the various items used in establishing a system is necessary for satisfactory system performance.

3. Well defined design data or, preferably, experimental test data are necessary to establish detail component requirements.

4. The use of mismatched system components can cause serious system malfunction.

5. Consideration should be given to the possibility of parallel operation of the aircraft system with external or ground power units.

6. Continued growth of parallel-operated systems may require specification of specific design data for drives, generators, regulators and other system components. This is particularly true if items of different manufacture are to be used interchangeably or placed in parallel or similar operation by operational requirements.

Reference

1. Power Equalizer Systems for Aircraft Alternators, John A. Granath, Albert K. Hawkes. *AIEE Transactions*, vol. 72, pt. II, Sept. 1953, pp. 209–17.

◆

No Discussion

Differential Reactive Current Protection Relay

RUSSELL W. STINEMAN
ASSOCIATE MEMBER AIEE

THE PAST few years have witnessed the increasing use of alternating current in large military aircraft, to the point where systems of paralleled alternators are required to meet the load demand. Such systems have problems and malfunctions of a type not encountered with isolated alternators or with paralleled d-c generators. As a result, new control and protective techniques must be developed for paralleled a-c systems if adequate reliability is to be obtained.

A particular 3-phase a-c power system which was designed for use in a large aircraft derives its power from four alternators which are normally paralleled through a central bus. A single-line diagram of the system is shown in Fig. 1. Loads are fed from the main busses, as indicated, so the alternators may be isolated during an emergency without interrupting service to the loads. Each alternator has an integral exciter, controlled by a carbon pile voltage regulator. Equalization of reactive current between alternators is obtained from a current transformer loop. The operation of the equalizing circuit serves to introduce a trimming signal into the voltage regulators whenever a reactive current unbalance exists, as is described more fully by Granath and Hawkes.[1] Externally controlled circuit breakers are used to connect the alternators to their respective main busses, and to connect the latter to the central bus, the interconnecting lines being multiple-wire fused feeders.

During developmental testing of the system in question, a number of problems were encountered involving unbalanced reactive currents of the several alternators. It was found that these difficulties could be overcome by a heretofore unknown device which the author has called a differential reactive current protection relay (DRCPR). With a DRCPR connected to each alternator, any condition resulting in an alternator supplying appreciably more than its share of lagging reactive current will actuate the corresponding DRCPR, sending a trip signal to the corresponding bus tie circuit breaker. More conventional protective devices may then be applied to the isolated alternator. The DRCPR is quite flexible and, if desired, may be connected to sense real as well as reactive current unbalance.

Paper 53-373, recommended by the AIEE Air Transportation Committee and approved by the AIEE Committee on Technical Operations for presentation at the AIEE Aircraft Electric Equipment Conference, Seattle, Wash., September 30–October 2, 1953. Manuscript submitted July 1, 1953; made available for printing September 2, 1953.

R. W. Stineman, is with the Boeing Airplane Company, Seattle, Wash.

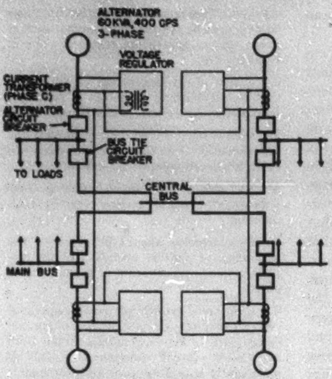

Fig. 1. Single-line diagram of an aircraft electric system, showing reactive equalizing circuit

Need for a New Protective Device

The problems which originally led to the conception of the DRCPR arose from the following three situations:

Voltage Regulator Fault

If a voltage regulator fault, such as a broken sensing lead, causes overexcitation of one alternator, that alternator will deliver a large reactive current to the system. The other voltage regulators will tend to hold the system voltage constant and hence will reduce the excitation of their respective alternators. However, the reactive equalizing circuit, sensing the unbalanced reactive currents, will reduce the excitation of the overexcited alternator and increase the excitation of the other alternators. As a result, the system stabilizes at a voltage appreciably above normal with the overexcited alternator overloaded. The calculated performance of the system for a particular fault is illustrated by the curves in Fig. 2, which show system voltage and the armature and field currents of the overexcited alternator as a function of initial load, power factor, and number of alternators operating. The calculated values were checked by tests for the case of two alternators in operation, the errors being less than about 10 per cent. Note that for initial loads in the neighborhood of 0.8 per unit, the overexcited alternator will be severely overloaded and the voltage may be high enough to damage some loads, yet the field current is not great enough to actuate a conventional exciter protection relay (connected across the alternator field) to shut down the overexciter alternator.

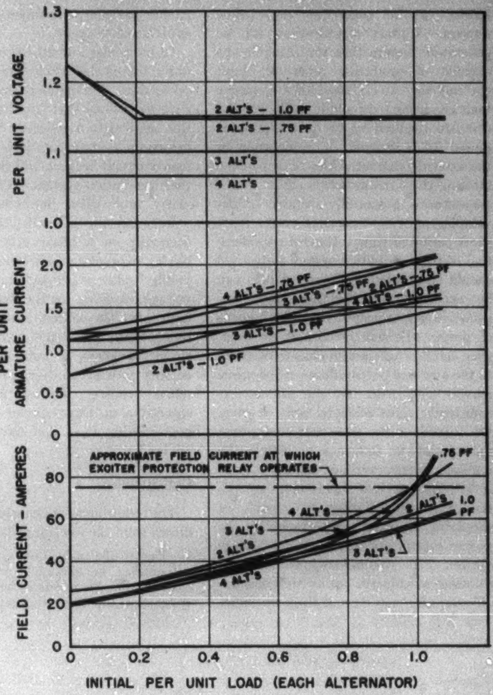

Fig. 2. Calculated performance of an alternator when the phase A or phase B voltage regulator-sensing lead has broken

Phase *C* Main Bus Fault

If a fault occurs at a main bus, the fuses in the line between the central bus and the faulted bus will quickly blow, since these fuses carry the fault current supplied by several alternators. Fault current will then be supplied only by the alternator closest to the faulted bus. If the fault is on the phase utilized by the reactive equalizing circuit (phase *C*), the fault current will pass through one of the current transformers shown in Fig. 1. The reactive equalizing circuit thus responds to the fault current, decreasing the excitation of the alternator still connected to the fault and increasing the excitation of the other alternators. As a result, the fault current stabilizes at a value slightly more than twice rated alternator current, yet the alternator fuses do not blow and the field current of the faulted alternator is too low to operate the exciter protection relay. In addition, the overexcitation of the other alternators causes either a sustained overvoltage or, in some cases, operation of the exciter protection relays, resulting in complete system failure.

Broken Equalizing Loop

If a break occurs in a wire connecting two of the current transformers shown in Fig. 1, the entire output of each current transformer circulates through the adjacent voltage regulator. The inductive component of alternator current causes line voltage depression; for example, an inductive component equal to rated alternator current would depress the voltage 18 per cent. In addition, any differences in voltage regulator settings result in unequal division of reactive load among the alternators.

Description of DRCPR

The common factor in these problems is the presence of a large signal from the reactive equalizing loop to the voltage regulators. The DRCPR was devised to respond to a large equalizing signal in such a manner as to open the bus tie circuit breaker whose corresponding alternator appears to be overexcited.

A circuit diagram of the DRCPR in its finally developed form, including the external connections, is shown in Fig. 3. The weight of this unit is 3.8 pounds. The operation of the reactive current sensing portion of the unit may be explained as follows: The output of the line transformers is applied directly to the upper 3-phase rectifier. During normal system operation, the bus tie circuit breaker is actuated, so the circuit breaker auxiliary contacts shown in Fig. 3 are open. Consequently, the output of the upper rectifier is applied only to the right-hand coil of the polarized relay, tending to pull the relay armature to the right. The output of the mutual reactor is added to one phase of the line transformer output, and the resulting voltage is applied through the lower 3-phase rectifier to the left-hand coil of the polarized relay, tending to pull the relay armature to the left. As long as the currents of the operating alternators remain balanced, the mutual reactor secondary voltage is small, the voltages applied to the polarized relay coils are equal, and the relay is not actuated. If, however, the alternator currents are unbalanced, then a current flows in the mutual reactor primary which is proportional to the difference between the current of the alternator shown in Fig. 3 and the average current of all the alternators. A vector diagram is shown in Fig. 4 for the case where the corresponding alternator is delivering more than its share of lagging reactive current. The angle by which the mutual reactor secondary voltage leads the primary current would ideally be 90 degrees. In practice, hysteresis and eddy current effects reduce this angle to about 75 degrees. For the case illustrated in Fig. 4, the vector relations are such that the voltage to the left-hand coil of the polarized relay is increased, actuating the relay and tripping the bus tie circuit breaker. Note from reference to Fig. 1 that tripping the bus tie circuit breaker does not remove power from any loads. If the alternator were delivering less than its share of lagging reactive current, then the mutual reactor vectors in Fig. 4 would be reversed, and the right-hand coil of the polarized relay would predominate. For real current unbalances, the mutual reactor vectors in Fig. 4 would be rotated 90 degrees and there would be no substantial effect on the polarized relay.

The reasons behind the choice of a name for this protective device should now be evident. "Differential" refers to the fact that the relay responds only when the alternator outputs are unbalanced. "Reactive" indicates that the sensing circuit discriminates between real and reactive unbalances, responding only to the latter. "Current" is used because the operating point is a function of the alternator currents. Note that the polarized relay will operate at essentially the same value of mutual reactor primary current over a wide range of line voltage, since any variations in line voltage will affect the two relay coils equally. Even an open circuit in one of the line transformer primary leads will have only a small quantitative effect on the operation of the DRCPR.

Whenever a bus tie circuit breaker is open, the overvoltage relay in the corresponding DRCPR is energized through the upper 3-phase rectifier in Fig. 3. Since this rectifier is connected directly to the line transformer, its voltage output is directly proportional to the average line-to-line voltage at the alternator terminals. High alternator voltage will, after a suitable time delay, actuate the overvoltage relay, sending a trip signal to the exciter control relay, which in turn shuts down the alternator and trips the alternator circuit breaker. The overvoltage relay need not be housed in the same enclosure as the reactive current sensing elements. However, for this particular application, no more suitable location for the overvoltage relay was apparent, and a weight saving could be realized by consolidating the differential reactive current and overvoltage functions in one unit.

With a DRCPR connected to each alternator, the system is adequately protected against the troublesome conditions previously described. If a voltage regulator fault results in overexcitation of an alternator, the corresponding DRCPR senses the high reactive current delivered by the alternator, and trips the bus tie circuit breaker. The voltage of the isolated alternator then rises to a high value, actuating the overvoltage relay and thus shutting down the alternator. Provision is made in the control system for subsequently reclosing the bus tie circuit breaker. The reactive current flow during a voltage fault was used to determine the operating level of the DRCPR, it being found that

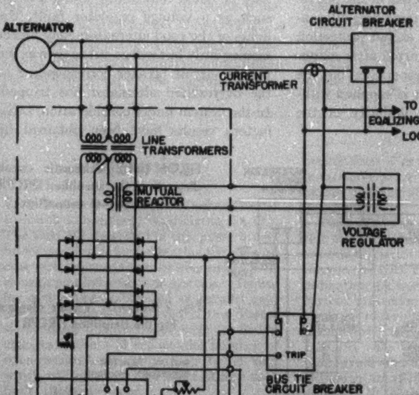

Fig. 3 (left). Schematic circuit diagram of the complete DRCPR and its external connections

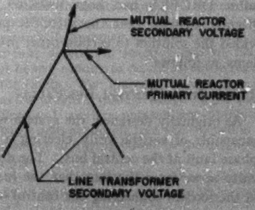
MUTUAL REACTOR SECONDARY VOLTAGE
MUTUAL REACTOR PRIMARY CURRENT
LINE TRANSFORMER SECONDARY VOLTAGE

Fig. 4 (right). Vector diagram of the reactive current sensing elements of the DRCPR when the external connections are as shown in Fig. 3

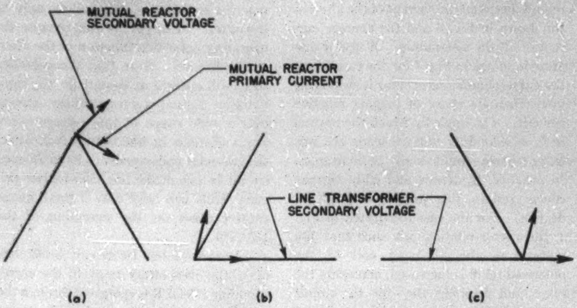
MUTUAL REACTOR SECONDARY VOLTAGE
MUTUAL REACTOR PRIMARY CURRENT
LINE TRANSFORMER SECONDARY VOLTAGE
(a)
(b)
(c)

Fig. 5. Vector diagrams for modified external connections to the DRCPR

operation at a differential reactive current of 0.6 per unit was low enough to detect any voltage regulator fault and high enough to prevent nuisance trips during synchronizing surges.

In the event of a phase *C* main bus fault, after the fuses have blown in the feeder to the central bus, the reactive component of the current unbalance is sufficient to operate the DRCPR of the faulted alternator. As the corresponding bus tie circuit breaker trips, one of its auxiliary contacts short-circuits the reactive equalizing circuit. As a result, the excitation of the faulted alternator is no longer restricted, and the fault clears in a normal manner.

If the reactive equalizing loop breaks, the full reactive component of current delivered by an alternator affects both its voltage regulator and its DRCPR. For the DRCPR operating setting chosen, an alternator will be isolated if its reactive current output exceeds 0.6 per unit, thus limiting the undervoltage to about 11 per cent. If this voltage drop were deemed excessive, the DRCPR could be set to operate at a lower current, in which case some trouble with nuisance trips during synchronizing might be encountered.

Additional Benefits Derived from DRCPR

During testing of the over-all system after DRCPR's had been installed, it became evident that the DRCPR provided the solution to certain other problems, as follows.

THREE-PHASE CENTRAL BUS FAULT

As originally designed, the system was incapable of satisfactorily clearing a 3-phase fault at the central bus. The difficulty arose from the fact that the fuses in the feeders connecting the central bus to the main busses had to have a fairly high rating to obtain proper fuse coordination during a load feeder fault. As a result, the relatively low line currents during a 3-phase central bus fault would not blow any fuses before the exciter protection relays would shut down all the alternators. However, with practically zero voltage at the central bus, the alternators do not remain synchronized. Hence, the currents delivered by the alternators, while approximately equal, have randomly varying phase angles, so that large and random signals are present in the reactive equalizing circuit. Under these conditions, the DRCPR's quickly operate and trip all but one of the bus tie circuit breakers. The remaining alternator is shut down by its exciter protection relay, but may be restarted after manually opening the corresponding bus tie circuit breaker. Power is supplied without interruption to a majority of the loads.

ALTERNATOR FAILURE

The most probable causes of alternator failure are loss of field and bearing seizure. In either case, a large reactive current flows into the faulty alternator. This has the same effect on the reactive equalizing circuit as if the alternator were delivering much less than its share of lagging reactive current to the system. The other alternators must therefore deliver more than their share of reactive current. Under heavy load conditions, the reactive current unbalance will be sufficient to operate the DRCPR's of the good alternators, thus preventing severe overloading of the good alternators. However, with light system loads, the current flowing into the failed alternator may be sufficient to cause serious damage, and the reactive equalizing signals will depress the system voltage, yet the DRCPR's of the good alternators will not be actuated. This situation may be remedied by a slight modification of the DRCPR wherein the right-hand contact of the polarized relay, as shown in Fig. 3, is connected to an alternator failure indicating light. The operator's instructions are to shut down the alternator if the light remains on for more than an instant. A light is employed in preference to tripping a circuit breaker because it would be undesirable to affect a good alternator's performance as the result of overexcitation of another alternator. It may be noted that during a malfunction such as a voltage regulator fault, the lights of the good alternators may flicker momentarily but will go out as soon as the bus tie circuit breaker corresponding to the overexcited alternator has tripped. In the system under consideration, satisfactory results have been obtained by

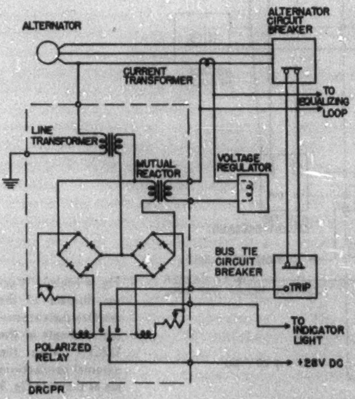

Fig. 6 (left). Schematic circuit diagram of the simplified DRCPR and its external connections

Fig. 7 (below). Vector diagram for the simplified DRCPR

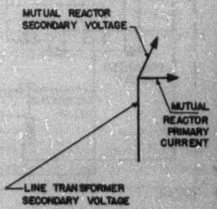
MUTUAL REACTOR SECONDARY VOLTAGE
MUTUAL REACTOR PRIMARY CURRENT
LINE TRANSFORMER SECONDARY VOLTAGE

setting the DRCPR so that the indicator light comes on at a reverse differential reactive current of 0.3 per unit.

Other Applications and Modifications of the DRCPR

While the discussion so far has been concerned with the application of the DRCPR to a particular aircraft electric system, it should be realized that the device has a high degree of inherent flexibility, which should permit its use in many applications. These applications need not be restricted to aircraft systems. Certain modifications in the external connections of the DRCPR will permit it to perform additional functions. These are:

1. A resistor may be placed across the input terminals of the mutual reactor (see Fig. 3) in order to rotate the mutual reactor primary current approximately 30 degrees. This condition is illustrated in Fig. 5(A) which shows the vector relations for the case where the corresponding alternator is delivering more than its share of lagging reactive current. Note that the DRCPR now has equal sensitivity to both real and reactive current unbalances. The bus tie circuit breaker will be tripped if the alternator delivers more than its share of either real or reactive current and the indicator light will come on if the alternator delivers less than its share of either real or reactive current. These responses could be reversed by interchanging the connections to the current transformer shown in Fig. 3.
2. By interchanging the phase B and C line transformer primary connections, the sensing circuit vector diagram may be modified to the form shown in Fig. 5(B) which again illustrates the case where the corresponding alternator is delivering more than its share of lagging reactive current. Again the DRCPR becomes equally sensitive to real and reactive current unbalances, but in this case the bus tie circuit breaker will be tripped when the alternator delivers more than its share of real current or less than its share of reactive current, while the indicator light will come on when the alternator delivers less than its share of real current or more than its share of reactive current. Again these responses may be reversed by interchanging the connections to the current transformer.
3. By interchanging the phase A and C line transformer primary connections, the sensing circuit vector diagram may be modified to the form shown in Fig. 5(C) which also illustrates the case where the corresponding alternator is delivering more than its share of lagging reactive current. The DRCPR will now be principally sensitive only to real current unbalances. The bus tie circuit breaker will be tripped when the corresponding alternator delivers either more or less than its share of real current, depending on the current transformer connections, as before.

It is thus evident that any combination of real and reactive current may be sensed. The DRCPR may be successfully applied to systems having alternators with different ratings by matching the current transformer ratios to alternator ratings.

For an application where an overvoltage relay is not to be included in a single housing with the reactive current sensing elements, the DRCPR may be simplified to the form shown in Fig. 6. The estimated weight of this unit is 2 pounds. This simplified version is connected to only one phase of the main power system when the unit is to perform the functions originally described in this paper. Consequently, the DRCPR in this form may be used in a single-phase system. A vector diagram for the simplified version is shown in Fig. 7, from which it is evident that the principles of operation are unchanged. When the simplified version is used in a 3-phase system, the modified external connections described previously may still be made.

Conclusion

The differential reactive current protection relay has provided an eminently satisfactory solution to a number of problems encountered in an a-c aircraft electric system. These problems were associated with voltage regulator malfunctions, faults on the phase used for reactive current equalization, a broken equalizing loop, a 3-phase fault at the central bus, and an alternator failure caused by bearing seizure or loss of excitation. In addition, the DRCPR has considerable inherent flexibility, which enables it to detect real as well as reactive current unbalances and to be employed in a wide variety of situations.

Reference

1. Power Equalizer Systems for Aircraft Alternators, John A. Granath, Albert K. Hawkes. *AIEE Transactions*, vol. 72, pt. II, Sept. 1953, pp. 200–17.

◆

Discussion

E. S. Sherrard and **W. M. Tucker** (Naval Research Laboratory, Washington, D. C.): The DRCPR described in this paper is useful for clearing or for facilitating the clearing of several types of faults or abnormal conditions in parallel generator systems. Its use for overvoltage protection of parallel generator systems is considered in this discussion. Also, this discussion suggests design changes which will reduce the number of open-circuited equalizer loop faults and which will minimize the effect of any such faults that may occur.

The DRCPR clears overvoltages in a single generator system and overvoltages in a parallel generator system that are characterized by abnormal reactive current unbalance. Not all parallel system overvoltages are characterized by abnormal reactive current unbalance, and consequently the DRCPR may not be relied upon for clearing all overvoltages in parallel systems. For example, a single-phase fault betwen lines A or B and neutral may result in excessive phase voltages on the unfaulted phases without abnormal reactive current unbalance.

Time delays in attaining abnormal reactive current unbalance or operating time of the bus tie circuit breaker and the polarized relay in the DRCPR may complicate the co-ordination between overvoltage and overcurrent protection or may prolong clearing times of overvoltages in parallel systems. Presumably, the overvoltage relay of the DRCPR has time-delay characteristics that avoid nuisance trips on fault and switching transients of a single generator system. If to this single generator time-delay characteristic is added the uncertain or varying time delay in reaching abnormal reactive unbalance and in polarized relay and bus tie breaker operation, the resultant overvoltage clearing times may become uncertain or excessive, or may no co-ordinate with the overcurrent fault—clearing characteristics or switching transients of the parallel system.

Because of the existence of overvoltages that may not be cleared by the DRCPR and the difficulty in obtaining good co-ordination between the time-delay characteristic of the overvoltage relay and the fault-clearing and switching transients in both a single generator and parallel generator system, it is our opinion that the DRCPR should not be used as the sole overvoltage protective device in a parallel generator system.

The authors' circuit has been designed for use with generators controlled by carbon-pile regulators. Undoubtedly the DRCPR will be extended to generators controlled by static (magnetic-amplifier) regulators. Laboratory texts conducted at the Naval Research Laboratory indicate that a 0.6-per-unit differential reactive current may not be low enough to detect all static regulator faults. For example, in one case it was found that a value of about 0.5-per-unit differential reactive current was obtained when a voltage sensing lead was opened in a phase not supplying power to the magnetic amplifier.

In his description, the author indicates that in typical systems the equalizer loop connections are made between current transformer (CT) terminals. A great increase in the reliability of these typical systems may be obtained by making additional equalizer loop connections between the corresponding regulator terminals. The circuit configuration would then consist of two parallel connecting loops and connections between corresponding CT and regulator terminals. An examination of this proposed circuit shows that its operation is independent of a single open circuit in an equalizer loop connection or in a connection between a CT terminal and its corresponding regulator terminal. Then, no equalizer malfunctioning occurs unless two or more connections in the equalizer circuit are opened.

Since CT's and regulators will be relatively remote from each other, this requirement of two or more open circuits for a malfunction in equalizer operation may greatly improve the reliability of a differential equalizer circuit.

Saturation of the mutual reactor (MR) may be utilized to prevent excessive drops in bus voltage that could result from the conversion of a differential equalizer circuit to a proportional equalizer circuit through an open circuiting of the equalizer loop connections. For no more than a 10-per-cent real or reactive current unbalance, the maximum normal MR primary current (nearly proportional to the difference between its generator line current and the average generator line current) will be 0.1 per unit, where base current for the MR primary is the CT secondary current corresponding to rated generator line current. If the MR begins to saturate at 0.1-per-unit primary current, it may be highly saturated at 0.15-per-unit primary current. For a per-unit sensitivity of 0.5, which is higher than the value of 0.18 employed in this paper, the maximum bus voltage reduction caused by proportional equalizer action would be 7.5 per cent for a zero power-factor load, and 3.3 per cent for 0.9 power-factor load.

This reduction in bus voltage probably would not cause damage to the system loads. However, the poor reactive balance that may result from equalizer signal saturation would have to be correlated with system power factor (many generators rated at 0.75 power factor are used in 0.9 power-factor systems and therefore reactive balance is less important than real balance), the excess generating capacity available, and the reduction of generator life caused by temporary reactive overloads.

The employment of MR saturation and an additional equalizer loop connection should, in our opinion, cause equalizer loop malfunctioning to be an extremely infrequent occurrence. Therefore, it may be advisable to consider that, on a statistical basis, protection against equalizer malfunctioning should not be provided unless such provision may be furnished without an increase in weight, space, or circuit complexity.

Russell W. Stineman: There appears to be little basis for the concern of Mr. Sherrard and Mr. Tucker about the performance of the DRCPR during single-phase faults if we merely note the generally accepted principle that an overvoltage relay should not operate during a fault. Protection for single-phase loads during a fault on another phase is attained by rapid fault clearing through the proper choice of circuit protectors. Consequently, any overvoltage protective scheme that does not operate during any fault has perfectly satisfactory performance with regard to faults. The overvoltage section of the DRCPR satisfies this requirement since: 1. it is not energized during paralleled operation; 2. during isolated operation it has the same type of sensing as the voltage regulator and hence senses no overvoltage during a fault; and 3. it has sufficient time delay to override the most severe recovery voltage after a fault has cleared. It is undesirable to use an overvoltage relay that might operate during a fault and then go to considerable pains to insure that it does so, when it is relatively simple to use an overvoltage relay that inherently will never operate during a fault.

The operating time of the reactive current sensing section of the DRCPR is such that the bus tie circuit breaker will open 50 to 80 milliseconds after a voltage regulator fault which causes overexcitation. This time will generally be small compared with the operating time of the overvoltage relay.

Obviously, the value of reactive current at which the DRCPR should be set to operate will depend on the parameters and components of the over-all system. It is desirable that the setting be as high as possible to avoid false trips when the alternators are initially paralleled. The suggested criteria are that the DRCPR be set to trip the bus tie circuit breaker in the event of any regulator fault that causes either flow of circulating currents large enough to significantly impair system capacity or an overvoltage that will damage important loads, and be set to energize the indicator light at about half the setting just indicated. The latter setting is somewhat limited by practical considerations in the design and adjustment of the polarized relay.

In some applications, it may be desirable to replace the indicator light with a delay relay that would shut down the alternator if the failure signal persisted for more than, say, 5 seconds, the exact time depending on the system under consideration. This was not done for the system considered in the paper, in order to completely exclude the possiblity of false shutdowns. A false shutdown was considered more serious than a false trip of the bus tie circuit breaker, since the latter does not interrupt power to loads or reduce system capacity.

Mr. Sherrard and Mr. Tucker have made an interesting suggestion in regard to the use of a saturable mutual reactor in the voltage regulator. They point out that one disadvantage to such a scheme is poor reactive load division when the reactors are saturated. It may be noted that a normal DRCPR will still protect the alternators against serious overload during such a condition. Other points which should be considered in regard to a saturable mutual reactor are as follows:

1. Saturation may result in a serious heating problem. If the reactor starts to saturate at 0.1-per-unit primary current, it will certainly be extremely saturated, with high core loss, at 1.0-per-unit current. Yet the reactor must be able to carry any current within the capacity of the alternator. Otherwise, an open loop, by causing mutual reactor failures, could result in malfunctions of all regulators and complete system failure.
2. A saturating reactor may have excessive departure from the ideal 90-degree phase angle between primary current and secondary voltage. If so, compensation in the form of magnetic shunts, tertiary windings, or capacitive networks would be required to prevent the regulator from responding to real current unbalances.
3. Real current unbalance causes current to flow in the reactor primaries, tending to saturate the reactors and cause poor reactive load division. It may be some time before real load division is accurate and reliable enough to permit consideration of saturable mutual reactors. In any event, this interaction between real and reactive load division will always be a disadvantage.

There are many conceivable malfunctions of the voltage regulating system, some of which do not require protection, some of which are handled by the DRCPR, and some for which there is no adequate protection yet devised. It is not considered feasible or practical to provide protection against every conceivable malfunction. Certainly a broken equalizing loop is one of the more probable failures, because the wires involved are relatively long. With duplicate wiring, as the discussers point out, protection which responds only to an open loop may be unjustified. This assumes that the system is thoroughly inspected frequently enough to assure detecting each failure before a second failure occurs. It may be noted, however, that the DRCPR was not installed solely or even primarily to protect against a broken loop. Consequently, the DRCPR may be considered to give protection against an open loop without complicating the circuitry.

Methods for Prediction of Steady-State Performance for Unbalanced Regulated 3-Phase Generators

B. J. WILSON
ASSOCIATE MEMBER AIEE

Synopsis: Based on simultaneous solutions of algebraic equations, resultant values of excitation voltage are obtained for a regulated a-c generator operating under unbalanced conditions. These equations result from a detailed consideration of the reaction to unbalance of the regulator system components. In general, solutions of the equations can be obtained graphically; in some cases, they can be attained analytically. Both methods are applied to representative examples of regulated aircraft generators operating at 400 cycles. Once the excitation voltage is determined for a given unbalance, symmetrical components are applied to obtain voltages and currents. An accuracy of better than 10 per cent is estimated.

THE FUNCTION of the voltage regulator in polyphase systems which become unbalanced has been neglected almost entirely in the history of this device. To remedy this situation, a method of analysis has been prepared for predicting steady-state operating conditions of faulted or unbalanced regulated generators. The method is valid for regulated generators currently in use, and for certain types anticipated in future applications.

The lack of information on the unbalanced operation of regulated generators can be attributed to two reasons. One is the idea that symmetry is normalcy in system operation and will ultimately be realized in the final system. Instead of being considered in the earlier stages of design, the problem of balancing the circuit is usually left to the operational stage. In practice, a system is never truly balanced. This fact should cause some concern, because a question immediately arises concerning the extent to which the unbalance influences regulator action. Most prominent among these unbalances are the common fault conditions that frequently arise. The other reason is the nonlinearity of typical regulator components. Computation is exceedingly difficult with the nonlinear functions encountered in an ordinary regulator, and this difficulty is widely recognized in regulator and servomechanism theory.

The extent to which the unbalance conditions at the regulator input terminals influence the generator field current can be resolved. The consequent excitation voltage then determines terminal conditions at the generator. With a satisfactory prediction of these terminal quantities, system designers can anticipate their needs for proper sized switchgear and protective devices.

Only those types of regulators which influence generator field current are considered here. If winding damages are discounted, the excitation condition of each generator phase is alike. Although the unbalance may anomalously affect the regulator, the regulator will not ameliorate any unbalance conditions.

In the methods presented here, algebraic and graphical techniques are outlined for calculating the steady-state operating conditions. These methods are equivalent to solutions of simultaneous nonlinear equations for the steady-state conditions considered here. For one type of regulator, an analytic method is developed, through the use of approximating functions, over restricted ranges of the nonlinear characteristics of the regulating system elements. The analysis is general for any type of regulator that influences generator field current. Finally, the method is applied to regulated aircraft generators operating at 400 cycles.

Background Discussion

For balanced operation, conventional round-rotor or salient-pole theory permits accurate predictions of operating voltages and currents from known excitation and impedance values. The assumptions of ideal balance of magnitude and phase conditions generally facilitate this in polyphase machines. A great simplification in the mathematical model of the machine is realized through these restrictions. At zero power factor, round-rotor theory leads to satisfactory results for regulation calculations on either salient-pole or round-rotor machines. However, when current or power calculations are made, extremely large errors can result from misuse of round-rotor theory on salient-pole machines. These points will bear on questions that arise in connection with the application of symmetrical components to the unbalance problem.

Balanced 3-phase short circuits are calculated from the ratio of excitation voltage to direct-axis synchronous reactance with sufficient accuracy for most engineering purposes, especially for low short-circuit ratio machines. Unbalanced faults generally are handled from stock symmetrical component expressions. Ordinarily, the excitation is assumed known for these calculations. If it is not, additional sources of information have to be exploited for its evaluation. As stated earlier, sources of this nature are not too widely known, and it is with considerable difficulty that success is met in such a search. As a further matter of concern, the use of symmetrical components in salient-pole machine calculations is seldom questioned. Yet round-rotor theory is employed in writing the basic voltage equation for the positive-sequence-current component. This fact bears more heavily on the general unbalance case, which is seldom considered, than on "typical" fault conditions. As a consequence, this practice is not deplored and is followed more often than not. It should be pointed out, however, as a source of error.

Obtaining final analytic forms of terminal conditions for any arbitrary degree of unbalance is not as simple as in the short circuit cases. The use of symmetrical-component analysis is retained, however, on the premise of avoiding entanglements with the complex mutual-coupling coefficients of rotating machines. Using condensed matrix methods, the develop-

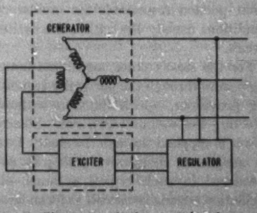

Fig. 1. Elementary 3-phase regulated system

Paper 53-374, recommended by the AIEE Air Transportation Committee and approved by the AIEE Committee on Technical Operations for presentation at the AIEE Aircraft Electric Equipment Conference, Seattle, Wash., September 30–October 2, 1953. Manuscript submitted May 28, 1953; made available for printing August 13, 1953.

B. J. Wilson is with the Naval Research Laboratory, Washington, D. C.

Table I. Comparison Between Predicted and Measured Values of Terminal Fault Conditions for Carbon Pile of Regulator, Current in Amperes, and Voltage in Volts

Fault Type	Predicted Values					Measured Values				
	E	I	V_a	V_b	V_c	E	I	V_a	V_b	V_c
Three-phase	511	134	0	0	0	511	130	0	0	0
Two-phase, L to L	420	155	81.8	81.8	163.6	477	168	68	68	128
Two-phase, L to L to N	502	184	0	0	79.6	492	188	0	0	82
One-phase, L to N	427	260	0	140	140	492	253	0	141	117

Table II. Comparison Between Predicted and Measured Values of Terminal Fault Conditions for the Magnetic-Amplifier Type of Regulator, Current in Amperes, and Voltage in Volts

Fault Type	Predicted Values					Measured Values				
	E	I	V_a	V_b	V_c	E	I	V_a	V_b	V_c
Three-phase										
L to L to L	910	217	0	0	0	900	214	0	0	0
Two-phase										
L to L (a to b)*	668	240	85	85	170	920†	318	80	80	154
L to L (b to c)	698	252	178	89	89	717	248	140	80	80
Two-phase										
L to L to N (a to b to neutral)	910	330	0	0	93	912	293	0	0	108
L to L to N (b to c to neutral)	790	286	91	0	0	782	283	101	0	0
One-phase										
L to N (a to neutral)	910	536	0	188	188	900	530	0	150	170
L to N (b to neutral)	558	322	144	0	144	531	313	146	0	130

* Magnetic-amplifier supply voltage on phase *a*.

† Ceiling excitation.

ment of the general unbalance case is outlined in Appendix I.

The Regulated Generator

The previous discussion indicates that if the excitation voltage can be determined, the faulted or unbalanced phase voltages and currents can be evaluated when the machine and circuit constants are known. All analytic expressions that follow are written in these terms.

The essential features of the voltage-regulated generator fall within the category of a basic single closed-loop feedback system. In fact, from an overall standpoint, the generator system under consideration, including its shaft mechanical input, has its analog counterpart in a self-excited oscillator. In variation to the usual case with the analog oscillator, the feedback portion of the system is a nonlinear amplitude limiting circuit. That portion responsible for oscillatory conditions usually lies within the exciter circuit.

For the steady state, amplitude limiting occurs through the particular regulating provisions, which function without affecting the output waveform. Steady power is supplied through the shaft. Due to component complexity ordinarily encountered in such typical systems, an oscillation criteria is difficult to formulate. For the steady state, it can be approximated roughly by evaluation of the exciter characteristics. Usually exciter conditions must be satisfactory if terminal voltage is to build up. For the self-excited shunt generators usually employed as synchronous machine exciters, critical oscillatory conditions can be formulated in terms of critical exciter shunt-field resistance. With other exciter units, such as the magnetic-amplifier types, critical conditions are still harder to define, even in the steady state. As a further feature of the regulated system, the value of excitation depends upon the conditions existing at that point of the system corresponding to the regulator input. For the polyphase systems, amount of unbalance is of paramount importance, as well as that of magnitude conditions. This fact is especially true for the classification of the regulated systems under discussion here, where only the generator field current is adjusted. On the other hand, the conditions existing at the regulator input location depend upon the value of the excitation voltage. The purpose of the analysis of the balanced or unbalanced regulated system is to predict the value of this excitation voltage. Thus, solution of terminal conditions can be obtained at once. When this prediction of excitation voltage is achieved, the problem is reduced to one of routine symmetrical-component calculations.

BALANCED OPERATION

Normally, each phase receives equal excitation. If balanced load impedances are provided as a sink for these excitation voltages, the system will be balanced throughout. At the regulator input, a reference adjustment may be made with respect to a predetermined system voltage. This adjustment may be considered as a manual throttle for controlling the current supply of the generator field. Any deviation from this reference adjustment causes the voltage regulator to influence the generator field current, and hence the excitation voltage, in a manner which tends to restore the system voltage (at the regulator input) to its former value.

Fig. 1 illustrates the type of regulator-exciter combination under discussion. Not all regulators that fall within this class have the type of input shown. Among the common variations are single-phase, line-to-line, and line-to-neutral sensing. Ordinarily, a sensing circuit is interposed between the line connection and the principle regulator mechanism. Most commonly, it consists of a rectifier to transform the a-c line signal to d-c, the form in which the control signal or automatic throttle reacting to the line voltage and accordingly directing the regulator action, is most often required.

These variations have no bearing on the fundamental method presented here. The manner of connecting the regulator input, however, may be responsible for vast differences in the resulting unbalanced voltage and currents for comparable unbalanced load conditions. In each instance, the procedure to be followed in predicting unbalance quantities is apparent when the analysis is understood. Details of this analysis are reserved for treatment in Appendix II.

In most instances, when a balanced 3-phase short circuit occurs on a regulated system, the excitation voltage increases to its ceiling value, that is, to a predeter-

Table III. Comparison of Predicted and Measured Values for a Regulated System with Specific Unbalance

The Load Impedance is One per Unit on Two Phases and One-Half per Unit on the Third Phase

Quantity Excitation Voltage E	Predicted Value, 310 Volts		Measured Value, 314 Volts	
I_a	100	amperes	82	amperes
I_b	55.2	amperes	43	amperes
I_c	56.8	amperes	44.2	amperes
V_a	138	volts	111	volts
V_b	149	volts	122	volts
V_c	168	volts	128	volts

Table IV. Symmetrical Component Expressions for Terminal Fault Quantities

Fault Type	Phase Currents	Phase Voltages
Three-phase	$\lvert I_a\rvert=\lvert I_b\rvert=\lvert I_c\rvert=\frac{\lvert E\rvert}{\lvert Z_1\rvert}$	
Two-phase	$I_a=\frac{(2+a)E}{Z_1+Z_2}$	$V_a=-E\frac{aZ_2}{Z_1+Z_2}$
	$I_b=-I_a$	$V_b=V_a$
	$I_c=0$	$V_c=E\frac{2aZ_2}{Z_1+Z_2}$
Two-phase-to-neutral	$I_a=\frac{E}{Z_1+\frac{Z_0Z_2}{Z_0+Z_2}}\left\{1+(1+a)\frac{Z_0}{Z_0+Z_2}-a\frac{Z_2}{Z_0+Z_2}\right\}$	$V_a=0$
	$I_b=\frac{E}{Z_1+\frac{Z_0Z_2}{Z_0+Z_2}}\left\{a^2-a\frac{Z_2}{Z_0+Z_2}-\frac{Z_0}{Z_0+Z_2}\right\}$	$V_b=0$
	$I_c=0$	$V_c=\frac{3aEZ_0Z_2}{Z_1Z_0+Z_1Z_2+Z_0Z_2}$
One-phase	$I_a=\frac{3E}{Z_1+Z_2+Z_0}$	$V_a=0$
	$I_b=0$	$V_b=\frac{E}{Z_1+Z_2+Z_0}\{(a^2-1)Z_0+(a^2-a)Z_2\}$
	$I_c=0$	$V_c=\frac{E}{Z_1+Z_2+Z_0}\{(a-1)Z_0+(a-a^2)Z_2\}$

mined maximum generator field current. In the test system considered here, ceiling value is alterable in terms of the shunt-field resistance of the exciter or in terms of the generator-field resistance. Hence, ceiling conditions are defined by the speed and minimum exciter-field resistance. This ceiling excitation can be determined by an overall test of the regulator-exciter, or by component examination of the regulator characteristics, principally the constant load-exciter external characteristic.

UNBALANCED OPERATION

The reaction of a regulator to a system-voltage unbalance naturally differs from that determined for the balanced case. The regulator, however, is powerless to restore a balanced condition. Further, the extent to which the regulator does affect the generator field current depends upon the type of fault, the magnitude of the line voltage applied to the regulator, and the manner in which the regulator is connected to the system. Usually, a fault will result in line-voltage conditions under which the regulator causes an increase in excitation. This increase is often cumulative and sometimes demands the maximum output that the exciter is set to deliver (ceiling excitation). On the other hand, although unbalanced line conditions cause the regulator to increase excitation, this excitation may reach a value at which the regulator input signal is large enough to halt the excitation increase at some final value. The equilibrium point of this process must be resolved. The regulator is controlled by its input from the unbalanced line and correspondingly influences the generator excitation. Yet the input to the regulator sensing circuit is directly related to the excitation.

To determine the final excitation attained, two aspects of the problem may be used for providing a key to the solution. In the first place, if the output current of the regulator rectifier is considered as a control over the excitation-voltage value, the manner in which the excitation voltage varies in response to this rectifier output can be determined. In the second place, the manner in which this control current varies in response to the sensing input from the line can be found for any degree of unbalance. Further, the line input voltage is directly related to the excitation. Simultaneous solution of these two cases then yields the operating point(s) or operating excitation voltage(s) for the given unbalanced load. This solution may be performed graphically or analytically. With this information, the symmetrical-component expressions in Appendix I can be used to calculate the magnitudes of the unbalanced voltages and currents. For any given line unbalance, details of the methods for evaluating the final excitation are described subsequently in Appendix II.

Two categories of unbalance are considered: one due to terminal short circuits; the other to arbitrary unbalance in load impedance. Once excitation is predicted for a given terminal fault, it is used in conjunction with the stock symmetrical-component expressions peculiar to that type of fault to solve for the terminal conditions. These formulas are derivable easily enough for such cases, and are widely published.[1,2,3] They are included in Appendix I, however, for completeness. The results of such calculations are presented in Tables I and II for cases of various terminal fault conditions. Table I represents resultant data for the test system employing the carbon-pile type regulator, while Table II shows results extended to the system utilizing a magnetic-amplifier type regulator. For the magnetic-amplifier unit, the magnitude of the amplifier supply voltage must be specified. The final excitation attained is a function of this supply voltage. Below a critical value the system resorts to ceiling excitation for the particular system tested.

When excitation is predicted for the case of arbitrary unbalanced load impedances, its subsequent application in the solution of the voltage equations does not lend itself so well to easy solutions—at least not to quick numerical evaluation. In this instance, coupled circuit phenomena complicate obtaining the explicit solution in such a way that is not so easily overcome as in the simpler short circuit cases. Results of calculations for the terminal conditions were made using the matrix expressions in Appendix I and are tabulated in Table III.[4,5] For this type of unbalanced loading, there is no doubt that armature reaction would result in larger values of net magnetizing force than would be found in the short-circuit cases, and magnetization would then be more nearly nonlinear at near normal excitation. This condition is plainly observed in the results. Measured current values are distorted from calculated current values to a degree

Table V. Matrix Expressions Applicable to General Unbalance

Quantity	With Negligible Line and Neutral Impedance	Including Line and Neutral Impedance
Phase currents	$\lVert \mathbf{I}\rVert = \lVert A\rVert\,\lVert \mathbf{Z}_{SC_T}\rVert^{-1}\lVert \mathbf{E}\rVert$	$\lVert \mathbf{I}\rVert = \lVert A\rVert\,\lVert \mathbf{Z}_{SC_T}'\rVert^{-1}\lVert \mathbf{E}\rVert$*
Phase voltages	$\lVert \mathbf{V}\rVert = \lVert \mathbf{Z}\rVert\,\lVert A\rVert\,\lVert \mathbf{Z}_{SC_T}\rVert^{-1}\lVert \mathbf{E}\rVert$	$\lVert \mathbf{V}\rVert = \lVert \mathbf{Z}\rVert\,\lVert A\rVert\,\lVert \mathbf{Z}_{SC_T}'\rVert^{-1}\lVert \mathbf{E}\rVert$
Symmetrical-component currents	$\lVert \mathbf{I}_{SC}\rVert = \lVert \mathbf{Z}_{SC_T}\rVert^{-1}\lVert \mathbf{E}\rVert$	$\lVert \mathbf{I}_{SC}\rVert = \lVert \mathbf{Z}_{SC_T}'\rVert^{-1}\lVert \mathbf{E}\rVert$

* Here $\lVert \mathbf{Z}_{SC_T}'\rVert = \lVert \mathbf{Z}_{SC}\rVert + \lVert \mathbf{Z}_{SC}'\rVert + \lVert \mathbf{Z}_{L,G}\rVert$, where line and neutral impedance

$$\lVert \mathbf{Z}_{L,G}\rVert = \begin{Vmatrix} (\mathbf{Z}_{L_0}+3\mathbf{Z}_g) & 0 & 0 \\ 0 & \mathbf{Z}_{L_1} & 0 \\ 0 & 0 & \mathbf{Z}_{L_2} \end{Vmatrix}$$ in terms of sequence components.

Table VI. Three-Phase Rectifier Output Under Specified Fault Conditions

Operation	Output, I_c, Amperes	Test Rectifier, I_c, Amperes*	Defined Voltage Relations
Balanced	$I_c = \dfrac{1.35V_L}{n(2R+r)}$	$I_c = 0.324V_L \times 10^{-2}$	V_L = Line voltage
L to L terminal fault	$I_c = \dfrac{1.8V}{n(3R+2r)}$	$I_c = 0.306V \times 10^{-2}$	$V = \dfrac{3\mathbf{E}\mathbf{Z}_2}{\mathbf{Z}_1+\mathbf{Z}_2}$
L to L to N terminal fault	$I_c = \dfrac{1.8V'}{n(3R+2r)}$	$I_c = 0.306V' \times 10^{-2}$	$V' = \dfrac{3\mathbf{E}\mathbf{Z}_0\mathbf{Z}_2}{\mathbf{Z}_1\mathbf{Z}_0+\mathbf{Z}_1\mathbf{Z}_2+\mathbf{Z}_0\mathbf{Z}_2}$
L to N terminal fault	$I_c \doteq \dfrac{1.8V''}{n(2R+r)}$	$I_c = 0.43V'' \times 10^{-2}$	$V'' = \dfrac{\sqrt{3}\mathbf{E}\sqrt{\mathbf{Z}_0^2+\mathbf{Z}_0\mathbf{Z}_2+\mathbf{Z}_2^2}}{\mathbf{Z}_1+\mathbf{Z}_2+\mathbf{Z}_0}$

* The numerical coefficients are dependent on rectifier circuit constants.

which might be expected from a discussion on the saturation effects for the single-phase short-circuit case. When round-rotor theory is used, the error is further aggravated, although this effect is somewhat submerged by virtue of the greater influence of the load impedance.

Two principal phenomena contribute to the accuracy of the predictions for excitation voltage. One is the temperature of the carbon-pile element for the type of regulator used in the particular test equipment employed to check the analysis. The other is the temperature of the dynamos involved, particularly the shunt-field resistance of the exciter, and to a lesser extent the temperature of the generator field. For a measured field current, the combination of these can cause an error up to 10 per cent in the prediction of the excitation voltage over that taken from the air-gap line. Fortunately, those elements with critical temperatures may be subjected to the abnormal current values encountered under short-circuit condition by means of no-load test methods. Thus, characteristics peculiar to the mechanics of prediction may be gained under representative operating temperature conditions.

Conclusions

The critical aspect of predicting the steady-state performance of a regulated generator with unbalanced loading is that of determining the excitation voltage after unbalance occurs. An intimate knowledge of the regulator and power supply for the generator field permits calculation of the regulator transfer characteristic. Difficulties with the nonlinearity of two system elements, the carbon pile and the exciter-generator, are overcome by the use of approximating functions or by graphical means. No attempt was made to approximate analytically the control characteristics of the magnetic amplifier. After the prediction of excitation, symmetrical-component analysis may then be employed to secure unbalanced phase voltages and phase currents.

Within the test limits to which this analysis was utilized, the results indicate that in general the accuracy of prediction can be better than 10 per cent. Results given in Tables I, II, and III show that accuracy is greatest where low saturation is present after fault or unbalance, and least when high saturation prevails.

Nomenclature

$\mathbf{E}$ = excitation voltage per phase taken on the air-gap line
$\mathbf{E}_1$ = positive-sequence excitation voltage
$\mathbf{Z}_1$ = positive-sequence impedance per phase
$\mathbf{Z}_2$ = negative-sequence impedance per phase
$\mathbf{Z}_0$ = zero-sequence impedance per phase
$\mathbf{Z}_a$, $\mathbf{Z}_b$, $\mathbf{Z}_c$ = polyphase load impedances
I = effective value of phase current
$\mathbf{I}_a$, $\mathbf{I}_b$, $\mathbf{I}_c$ = effective phase currents for phases a, b, and c, respectively
$\mathbf{I}_0$, $\mathbf{I}_1$, $\mathbf{I}_2$ = zero-, positive-, and negative-sequence current components
$\mathbf{V}_a$, $\mathbf{V}_b$, $\mathbf{V}_c$ = effective phase voltages for phases a, b, and c, respectively
$\mathbf{V}_0$, $\mathbf{V}_1$, $\mathbf{V}_2$ = zero-, positive-, and negative-sequence terminal-voltage components
V_L = effective line voltage
V_{DC} = rectifier output voltage
V = effective voltage between faulted and unfaulted lines on a line-to-line fault
V' = effective voltage between faulted and unfaulted lines on a line-to-line-to-neutral fault
V'' = effective voltages between unfaulted phases and neutral on a line-to-neutral fault
V''' = effective voltage between unfaulted phases on a line-to-neutral fault
L = line
N = neutral
I_c = average value of control current
r = resistance of carbon-pile solenoid
R = dropping resistance in rectifier circuit
n = turns ratio of sensing transformers
α = phase angle, $\alpha = \tan^{-1}\left[\dfrac{\sqrt{3}\mathbf{Z}_0}{\mathbf{Z}_0+2\mathbf{Z}_2}\right]$, where $\mathbf{V}_b = \mathbf{V}_c/\pi - 2\alpha$, for phasing between the two line-to-neutral voltages of the unfaulted phases in the case of a line-to-neutral fault
a = operator, $\epsilon^{j\frac{2\pi}{3}} = \epsilon^{j120^\circ}$
$\lVert A\rVert$ = symmetrical-component transformation matrix
r_{cp} = carbon-pile resistance
I_f = exciter shunt-field resistance
V_e = exciter terminal voltage
R_t = total shunt-field resistance in exciter
R_F = generator field resistance
I_F = generator field current
K_F = slope of fault-characteristic line for rectifiers
K = slope of air-gap line for synchronous alternator

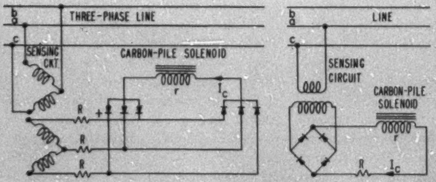

Fig. 2. Typical sensing circuits and rectifiers for carbon-pile regulators

A(left). Three-phase sensing and rectification

B (right). Single-phase sensing and rectification

Appendix I. Symmetrical-Component Expressions

The basic defining transformation for symmetrical components is

$$\begin{aligned} \mathbf{I}_a &= \mathbf{I}_0+\mathbf{I}_1+\mathbf{I}_2 \\ \mathbf{I}_b &= \mathbf{I}_0+a^2\mathbf{I}_1+a\mathbf{I}_2 \\ \mathbf{I}_c &= \mathbf{I}_0+a\mathbf{I}_1+a^2\mathbf{I}_2 \end{aligned} \qquad (1)$$

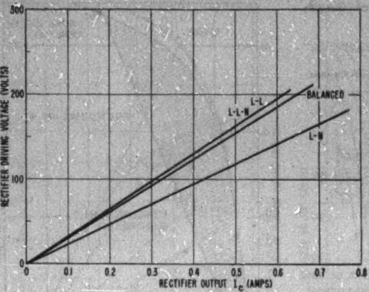

Fig. 3. Three-phase rectifier output as a function of line voltages for indicated faults

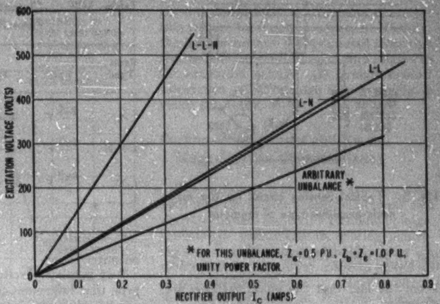

Fig. 4. Three-phase rectifier output versus excitation voltage for indicated types of unbalance

In matrix form

$$\|\boldsymbol{I}\| = \|A\|\,\|\boldsymbol{I}_{SC}\| \qquad (1A)$$

where

$$\|A\| = \begin{Vmatrix} 1 & 1 & 1 \\ 1 & a^2 & a \\ 1 & a & a^2 \end{Vmatrix}$$

which is the so-called transformation matrix. Subscripts 0, 1, and 2 represent zero, positive, and negative sequences, respectively.

For the case of common short circuits, the symmetrical-component voltage equations in conjunction with the terminal fault conditions allow relatively simple expressions to be obtained for the appropriate fault type. These are tabulated in Table IV for convenience.

For arbitrary unbalance, especially defined in terms of load impedance, matrix methods prove advantageous. The process of deriving the essential relations for the general unbalance case follows easily from the symmetrical-component voltage equations for any phase. This set of relations is shown as follows

$$0 = \boldsymbol{I}_0\boldsymbol{Z}_0 + \boldsymbol{V}_0$$
$$\boldsymbol{E}_1 = \boldsymbol{I}_1\boldsymbol{Z}_1 + \boldsymbol{V}_1$$
$$0 = \boldsymbol{I}_2\boldsymbol{Z}_2 + \boldsymbol{V}_2$$

or simply as

$$\|\boldsymbol{E}\| = \|\boldsymbol{Z}\|\,\|\boldsymbol{I}_{SC}\| + \|\boldsymbol{V}_{SC}\| \qquad (2)$$

where the symmetrical components of excitation and terminal voltages appear as

$$\|\boldsymbol{E}\| = \begin{Vmatrix} \boldsymbol{E}_0 \\ \boldsymbol{E}_1 \\ \boldsymbol{E}_2 \end{Vmatrix} = \begin{Vmatrix} 0 \\ \boldsymbol{E} \\ 0 \end{Vmatrix}$$

and

$$\|\boldsymbol{V}_{SC}\| = \begin{Vmatrix} \boldsymbol{V}_0 \\ \boldsymbol{V}_1 \\ \boldsymbol{V}_2 \end{Vmatrix}$$

The impedance matrix $\|\boldsymbol{Z}_{SC}\|$ for the generator is defined by

$$\|\boldsymbol{Z}_{SC}\| = \begin{Vmatrix} \boldsymbol{Z}_0 & 0 & 0 \\ 0 & \boldsymbol{Z}_1 & 0 \\ 0 & 0 & \boldsymbol{Z}_2 \end{Vmatrix}$$

The symmetrical components for the phase current are represented as

$$\|\boldsymbol{I}_{SC}\| = \begin{Vmatrix} \boldsymbol{I}_0 \\ \boldsymbol{I}_1 \\ \boldsymbol{I}_2 \end{Vmatrix}$$

It is common practice to reduce $\|\boldsymbol{V}_{SC}\|$ in the following manner

$$\|\boldsymbol{V}_{SC}\| = \|\boldsymbol{Z}_{SC}'\|\,\|\boldsymbol{I}_{SC}\| \qquad (3)$$

where $\|\boldsymbol{Z}_{SC}'\|$ is deducible from the load-impedance matrix

$$\|\boldsymbol{Z}\| = \begin{Vmatrix} \boldsymbol{Z}_a & 0 & 0 \\ 0 & \boldsymbol{Z}_b & 0 \\ 0 & 0 & \boldsymbol{Z}_c \end{Vmatrix}$$

and where

$$\|\boldsymbol{Z}_{SC}'\| = \|A\|^{-1}\|\boldsymbol{Z}\|\,\|A\|$$

$$= \frac{1}{3}\begin{Vmatrix} (\boldsymbol{Z}_a+\boldsymbol{Z}_b+\boldsymbol{Z}_c) & (\boldsymbol{Z}_a+a^2\boldsymbol{Z}_b+a\boldsymbol{Z}_c) & (\boldsymbol{Z}_a+a\boldsymbol{Z}_b+a^2\boldsymbol{Z}_c) \\ (\boldsymbol{Z}_a+a\boldsymbol{Z}_b+a^2\boldsymbol{Z}_c) & (\boldsymbol{Z}_a+\boldsymbol{Z}_b+\boldsymbol{Z}_c) & (\boldsymbol{Z}_a+a^2\boldsymbol{Z}_b+a\boldsymbol{Z}_c) \\ (\boldsymbol{Z}_a+a^2\boldsymbol{Z}_b+a\boldsymbol{Z}_c) & (\boldsymbol{Z}_a+a\boldsymbol{Z}_b+a^2\boldsymbol{Z}_c) & (\boldsymbol{Z}_a+\boldsymbol{Z}_b+\boldsymbol{Z}_c) \end{Vmatrix} \qquad (4)$$

Rank is preserved in this transformation to the equivalent form $\boldsymbol{Z}_{SC}'$.

These relations allow the substitution of

$$\|\boldsymbol{E}\| = \|(\boldsymbol{Z}_{SC}+\boldsymbol{Z}_{SC}')\|\,\|\boldsymbol{I}_{SC}\| = \|\boldsymbol{Z}_{SCT}\|\,\|\boldsymbol{I}_{SC}\| \qquad (5)$$

for the original voltage equations.

The currents are solved by

$$\|\boldsymbol{I}_{SC}\| = \|\boldsymbol{Z}_{SCT}\|^{-1}\|\boldsymbol{E}\| \qquad (6)$$

From the defining transformation

$$\|\boldsymbol{I}\| = \|A\|\,\|\boldsymbol{I}_{SC}\|$$

where

$$\|\boldsymbol{I}\| = \begin{Vmatrix} \boldsymbol{I}_a \\ \boldsymbol{I}_b \\ \boldsymbol{I}_c \end{Vmatrix}$$

which is the phase-current matrix. Equation 7 is the result

Table VII. Rectifier Output for Single-Phase Sensing Circuit, with Specified Types of Unbalance

Fault Type	Sensing Circuit Location (Lines)†	Driving Voltage	Current, I_c	Defined Voltage Relations
L-L (lines a to c)	a-b	$V = \lvert V_b^* - V_c^* \rvert$	$I_c = \dfrac{2\sqrt{2}V}{\pi n(R+r)}$	$V = \dfrac{3EZ_2}{Z_1+Z_2}$
	b-c	$V = \lvert V_b^* - V_c^* \rvert$	$I_c = \dfrac{2\sqrt{2}V}{\pi n(R+r)}$	
	c-a	$V = 0$		$V = 0$
L-L-N (line a to line c to neutral)	a-b	$V' = V_b$	$I_c = \dfrac{2\sqrt{2}V'}{\pi n(R+r)}$	$V' = \dfrac{3EZ_2Z_0}{Z_1Z_2+Z_1Z_0+Z_2Z_0}$
	b-c	$V' = V_b$	$I_c = \dfrac{2\sqrt{2}V'}{\pi n(R+r)}$	
	c-a	$V' = 0$	$I_c = 0$	$V' = 0$
L-N (line a to neutral)	a-b	$V'' = V_b$	$I_c = \dfrac{2\sqrt{2}V''}{\pi n(R+r)}$ ‡	$V'' = \sqrt{3}E\,\dfrac{\sqrt{Z_0^2+Z_0Z_2+Z_2^2}}{Z_1+Z_2+Z_0}$
	b-c	$V''' = \lvert V_b^* - V_c^* \rvert$	$I_c = \dfrac{2\sqrt{2}V'''}{\pi n(R+r)}$	$V''' = \sqrt{3}E\,\dfrac{(2Z_0+Z_2)}{Z_1+Z_2+Z_0}$
	c-a	$V''\ \ V_c$	$I_c = \dfrac{2\sqrt{2}V''}{\pi n(R+r)}$	$V'' = \sqrt{3}E\,\dfrac{\sqrt{Z_0^2+Z_0Z_2+Z_2^2}}{Z_1+Z_2+Z_0}$

† See Fig. 2(B).

‡ For b-c connection.

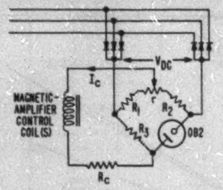

Fig. 5. Typical sensing circuit for the magnetic-amplifier type of regulator

$$||\boldsymbol{I}||=||A||\,||\boldsymbol{Z}_{SCT}||^{-1}||\boldsymbol{E}|| \tag{7}$$

From the fact that the phase voltages are given by

$$||\boldsymbol{V}||=||\boldsymbol{Z}||\,||\boldsymbol{I}||$$

where

$$||\boldsymbol{V}||=\begin{Vmatrix} V_a \\ V_b \\ V_c \end{Vmatrix}$$

substitution for $||\boldsymbol{I}||$ gives

$$||\boldsymbol{V}||=||\boldsymbol{Z}||\,||A||\,||\boldsymbol{Z}_{SCT}||^{-1}||\boldsymbol{E}|| \tag{8}$$

The pair of equations 7 and 8 for $||\boldsymbol{V}||$ and $||\boldsymbol{I}||$ constitutes the complete steady-state solution for the general case of unbalance.

The matrix formulas are summarized in Table V. The results are extended to cases where line and neutral impedance are present.

Appendix II. Mechanics of Predicting Excitation Voltage for a Regulated Generator

Gaining sufficient information to predict a post-fault or post-unbalance steady-state condition requires detailed facts on the regulator components and generator steady-state constants. This statement is particularly true if the prediction must be made solely from the design data. With test equipment available, however, it is possible to approach a solution for any specific unbalance more directly by using simple test measurements, which are essentially no-load in nature. These involve only the loading of the generator field-current power supply at power levels in the order of 10 per cent of the rated generator output.

Table VIII. Output Voltage of the 3-Phase Rectifier

Fault Type	V_{DC}	Defined Voltage Relations
L-L.......	$\frac{2\sqrt{2}}{\pi}V$.....	$V=E\frac{3Z_2}{Z_1+Z_2}$
L-L-N....	$\frac{2\sqrt{2}}{\pi}V'$....	$V'=\frac{3Z_0Z_2E}{Z_1Z_0+Z_1Z_2+Z_0Z_2}$
L-N.......	$\frac{4\sqrt{2}}{\pi}V''$...	$V''=\sqrt{3}E\frac{\sqrt{Z_0^2+Z_0Z_2+Z_2^2}}{Z_1+Z_2+Z_0}$

Any regulator-exciter combination of the type that influences generator field current can be subdivided into principal component parts. These are the regulator proper, which includes the line-voltage sensing device, and the generator-field power supply or exciter. Among regulator types that fit into this classification are those employing d-c generator-exciters, and those utilizing saturable reactor or magnetic-amplifier-controlled rectifiers for generator field-current power supplies. Both of these power supplies are controlled by a d-c signal from a line-voltage sensing device. This signal is usually an output from a 3-phase full-wave rectifier, or an output from a single-phase bridge-type rectifier. In any event, steady-state transfer characteristics may be obtained for the over-all regulator system, or for its component parts.

The types of regulator systems analyzed here include the d-c exciter-generator variety with both single-phase and 3-phase rectifier sensing control. In a broad sense, the resultant generator excitation is determined for any operating condition by a crossover point of two separate characteristics having a common parameter. This is the sensing-rectifier output current controlling the generator excitation. One characteristic is the generator excitation voltage as a function of the control current; the other is the control current as a function of the driving force applied to the rectifier. Through the symmetrical component expressions given in Appendix I, this second characteristic is, in turn, directly related to excitation voltage. Once the first characteristic is plotted, a series of curves drawn for various types of unbalance will intersect the excitation curve(s) at points that are representative of steady-state excitation for the respective types of unbalance. If it is possible to formulate analytic expressions for these curves, the root(s) of their equated expressions for a given unbalance will yield the desired excitation value(s) for that unbalance. This step was taken at the end of Appendix II for one of the regulated systems tested.

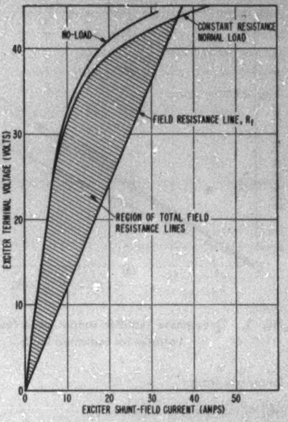

Fig. 7. Exciter magnetization characteristics

From a knowledge of the manner in which the regulator components are interconnected, the steps in attaining a desired characteristic are easily deduced. The rectified current, already defined as the control current, will be designated I_c for convenience.

Rectifier Output I_c for Carbon-Pile Control

Sensing networks often incorporate 3-phase full-wave and single-phase bridge-type rectifier circuits. Representative diagrams of such systems are given in Fig. 2.

Results of calculations for the 3-phase rectifier output under various conditions of unbalance are given in Table VI, and plotted in Fig. 3. They were obtained by assuming negligible rectifier forward resistance and infinite reverse resistance to inverse voltage.

An intermediary step was taken to correlate the actual unbalanced line voltage and the excitation voltage, by employing the

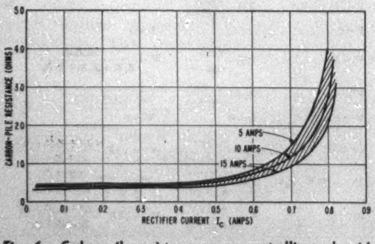

Fig. 6. Carbon-pile resistance versus controlling solenoid current for different values of current

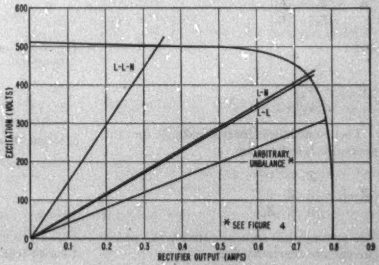

Fig. 8 (right). Excitation voltage versus rectifier control current

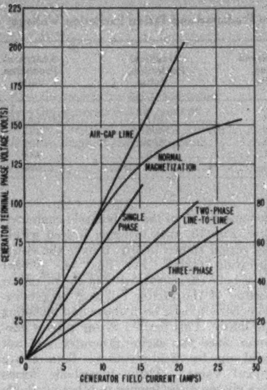

Fig. 9. Machine characteristics of 15-kva test generator at 400 cycles

results of symmetrical-component analysis. The results of this step are listed in Table VI; and Fig. 3 is converted to Fig. 4 by these relations.

When the single-phase sensing circuit is employed, Fig. 2(B), control current is dependent upon the lines on which the rectifier input is placed, as well as the type of fault or unbalance. This dependence is illustrated by Table VII. A set of curves analogous to and serving the same purpose as those of Figs. 3 and 4 can be constructed for the single-phase rectifier arrangement.

Subject to the assumptions stated, the results in all cases considered are general to any 3-phase generator employing these types of regulator rectifiers. The data illustrated in all the diagrams correspond to 400-cycle operation.

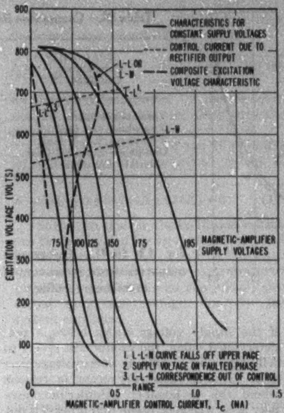

Fig. 10. Control characteristics for the magnetic-amplifier regulator

Rectifier Output for Magnetic-Amplifier Control Circuits

The circuit arrangement for obtaining regulator control through a magnetic amplifier usually differs somewhat from that used with the carbon-pile unit. A typical illustration (Fig. 5) shows that deviations from desired line voltages are sensed by comparison against a gas-tube reference voltage. A mechanical spring tension serves this purpose in the carbon-pile unit.

Calculations similar to those employed in the case of the carbon-pile regulator are used to obtain control current. The rectified voltage applied to the reference-comparison circuit is first obtained. This is given in Table VIII as a function of excitation voltage for various fault cases. Finally, the control current I_c is evaluated from this rectified direct voltage, and in turn related to the excitation voltage. A straightforward calculation on the bridge circuit of Fig. 5 yields this result.

Carbon-Pile Element and Exciter Magnetization Characteristics

The carbon pile injects a variable resistance into the exciter shunt-field circuit and thereby changes the exciter terminal voltage. Carbon-pile characteristics relating pile resistance and controlling solenoid current are illustrated in Fig. 6 for various values of steady carbon-pile currents. Heating effects in conjunction with the extreme steepness of the resistance curve do not allow a specific operating path to be defined. Instead, operation occurs within the region cross-hatched in Fig. 6. This fact obviates the ability to predict the exact resistance value inserted in the exciter shunt-field circuit. As a compromise, values are taken from the center line.

Exciter terminal voltage is determined by the intersection of the resultant shunt-field total-resistance line and the exciter magnetization characteristic for full load. If the total field-resistance line R_t, illustrated in Fig. 7, is taken as a minimum, intersections with the magnetization characteristic occur to the left, thereby defining the operating point. Large errors are expected at near critical field resistance.

Final Location of Excitation

After noting the values of exciter terminal voltage for a given rectifier output, the generator field current can be calculated. Thus, the final value of excitation is determined as a function of rectifier output current, since the unsaturated excitation voltage is directly related to generator field current by the air-gap line. The nonlinear curve of Fig. 8 illustrates this type of characteristic. The magnetization characteristics for the generator and the air-gap line are plotted in Fig. 9.

Similar intermediate steps were not executed for the magnetic-amplifier regulator. The principle illustrated, however, does imply that similar intermediate steps are possible with the magnetic amplifier.

As a final step in predicting excitation for a given condition of unbalance, the

Fig. 11 (below). Schematic diagram for the test carbon-pile regulated system

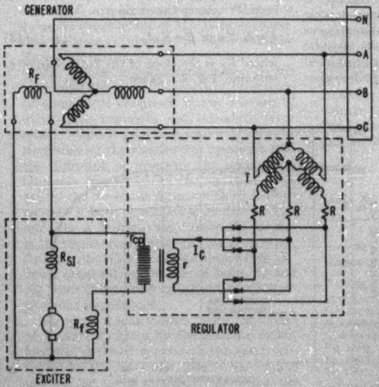

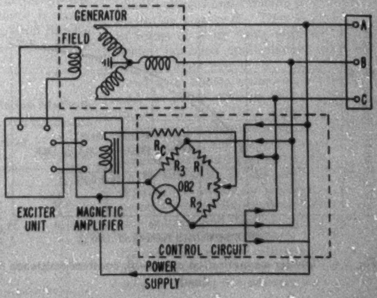

Fig. 12 (right). Schematic diagram for the test magnetic-amplifier regulated system

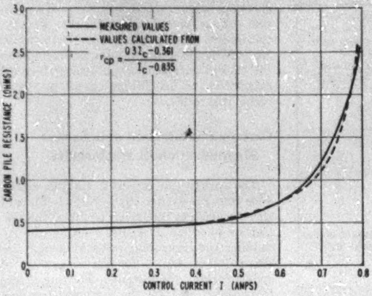

Table IX. Comparison Between Predicted and Tested Excitation Voltage

Unbalance Condition	Measured Value, Volts	Graphical Prediction, Volts	Analytical Prediction Volts
Three-phase fault	511	511	Indeterminate
Two-phase, L-L fault	420	466	452
Two-phase, L-L-N fault	502	505	501
One-phase-to-neutral fault	427	496	483
Arbitrary unbalance	314	310	302

Fig. 13 (left). Carbon-pile output resistance versus control current from rectifier

characteristics of Fig. 4 are superimposed on Fig. 8 for the carbon-pile unit. The curves of Fig. 4 show how the control current would vary if the excitation voltage were varied with a specific unbalance existing on the system. Intersection of any specific unbalance curve from Fig. 4 with the principal excitation characteristic thus defines the steady-state value of excitation.

Fig. 10 illustrates the process for the magnetic amplifier. Here, the resultant excitation-voltage curve, analogous to that of Fig. 8, is composite. For each value of magnetic-amplifier supply voltage, an individual excitation-voltage characteristic is defined. The totality of such curves for all values of supply voltage forms a family of curves. After considering the 1-to-1 relationship between the supply voltage and the excitation voltage, the resultant composite curve is formed for any given fault or condition of unbalance. This type of consideration was given previously when deriving rectifier response to unbalanced driving voltages, as shown in Table VI and Fig. 4.

The variation between control current and unbalanced driving voltages is shown as the lightly dashed curves in Fig. 10. These curves are analogous to those of Fig. 4.

Control-current values are obtained by applying the voltages given in Table VIII to the circuit of Fig. 5. The line-to-line-to-neutral curve does not lie within the region plotted. Again, when a curve for a control current intersects a curve for a composite excitation voltage, the steady-state value of excitation is defined for any unbalance. The magnetic amplifier is controlled so that if the supply voltage drops below a predetermined value, the exciter will revert to self-excitation as long as undervoltage persists. Intersections may occur in regions where this is possible. Borderline cases may arise when the prediction process is not accurate enough to estimate the critical undervoltage. This phenomenon was observed in the test of the line-to-line fault.

In obtaining more rapid predictions for calculating unbalance of machines already built, the excitation characteristic of Fig. 8 may be taken directly as a no-load test. Likewise, the straight-line unbalance curves, also shown in Fig. 8, may be measured directly. This process was followed for the magnetic amplifier, Fig. 10. In applying unbalanced voltages to the rectifier, such test procedures may entail special considerations of phase and magnitude. Immediate calculation of steady-state unbalance can then be made for regulated generators. Through such tests, operating performance is evaluated without actually submitting the machine to fault.

A complete schematic diagram of the carbon-pile regulated system is presented in Fig. 11. Fig. 12 shows the magnetic-amplifier regulator.

Analytical Prediction for the Carbon-Pile Regulator

Excitation can be calculated solely from analytical expressions. This prediction is possible if the exciter full-load characteristic and the carbon-pile output-resistance curve can be represented by suitable analytic approximations. For the test regulated system considered here, a hyperbolic equation was fitted to the carbon-pile characteristic, Fig. 13, thus bringing it well within the region shown in Fig. 6 over the entire operating range. For Fig. 14, another hyperbolic curve was fitted to the nonlinear portion of the exciter full-load magnetization characteristic both above and including the knee. This limited fitting proves adequate since the exciter-generator will not build up for field-resistance lines above critical value. These hyperbolic forms were chosen in preference to other available approximations because of a desire to avoid numerous trial and error solutions of transcendental equations or power series commonly applied by others.[6]

For the carbon-pile curve

$$r_{cp} = \frac{0.3I_c - 0.361}{I_c - 0.835} \tag{9}$$

where r_{cp} is the resistance of the carbon pile.

For the exciter magnetization curve

$$V_e = \frac{I_f}{0.134 + 0.019 I_f} \tag{10}$$

where V_e is the exciter terminal voltage applied to the generator field and where I_f is the exciter shunt-field current. The operating point on the exciter magnetization characteristic is given by

$$V_e = I_f R_t \tag{11}$$

where R_t is the total shunt-field resistance, $R_f + r_{cp}$, with R_f that portion due only to the winding. Equations 10 and 11 result in

$$V_e = 52.7 - 7.07 R_t \tag{12}$$

For any given fault or unbalance, the rectifier behaves according to

$$I_c = E/K_F \text{ or } E = K_F I_c \tag{13}$$

where K_F is the slope of the fault characteristic line, Fig. 4. Since

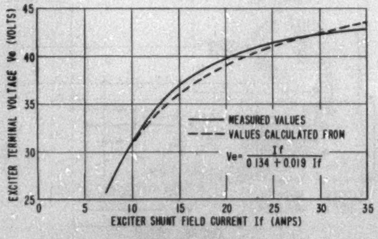

Fig. 14. Exciter magnetization curve with constant-resistance load

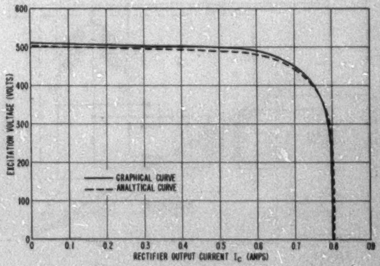

Fig. 15 (right). Comparison between graphically and analytically determined values of excitation voltage as a function of control current I_c

$$\frac{V_s}{R_F}=I_F=\frac{E}{K} \tag{14}$$

where

R_F = the generator-field resistance
I_F = the generator-field current
E = the generator excitation voltage
K = the slope of the air-gap line

combining equations 12 and 14 produces

$$E=\frac{K}{R_F}[52.7-7.07R_t] \tag{15}$$

With the assistance of equation 9, equations 13 and 15 can be equated to produce the final resulting control current I_c, thus establishing the excitation voltage through equation 13. A preferable procedure, however, consists in first writing equation 15 explicitly in terms of E. This is done with the help of equation 9. The result is

$$I_c=\frac{0.833E-424}{E-518} \tag{16}$$

for the system considered. A plot of equation 16 is given in Fig. 15, along with the graphically determined curve of Fig. 8.

Combining equations 13 and 16 produces an equation in the excitation voltage E, given by

$$E^2-(518+0.833K_F)E+424K_F=0 \tag{17}$$

For the test system, the excitation voltage can be determined for any unbalance which is characterized by K_F. Table IX illustrates the comparison between the measured, graphically predicted, and analytically predicted excitation voltages for the test system employed.

References

1. Electric Circuits (book). **Massachusetts Institute of Technology Staff.** John Wiley and Sons, Inc., New York, N. Y., 1943.

2. Electric Power Transmission (book), **M. P. Weinbach.** The Macmillan Company, New York, N. Y., 1948.

3. Symmetrical Components (book), **C. F. Wagner, R. D. Evans.** McGraw-Hill Book Company, New York, N. Y., 1933.

4. Linear Transformations in Three-Phase Circuits, **Louis A. Pipes.** *AIEE Transactions*, vol. 60, 1941, pp. 351–56.

5. Mathematical Methods in Electrical Engineering (book), **M. B. Reed, G. B. Reed.** Harper and Brothers, New York, N. Y., 1951.

6. Analytical Expressions for the Magnetization Curve of Electric Machines, **B. I. Arkhangelskii.** *Elektrichestvo*, Moscow, USSR, 1950, pp. 30–32.

◆

Discussion

T. B. Owen (Hughes Aircraft Company, Culver City, Calif.): Mr. Wilson has ably attacked a problem which is sure to have increased importance in the future when a-c systems become more prominent in aircraft. I do have the feeling, however, that Mr. Wilson has compromised the usefulness of his work by using the matrix notation, when the use of determinants would have made it much more understandable to the majority of people. The solution of the characteristic equations obtained by the use of symmetrical components is simple enough to become more widespread, and in any event, you always have to solve a determinant to solve a matrix.

I think it should be pointed out that Fig. 4, which is derived from Table VI and Fig. 3, is tied down to a definite generator, presumably the 15-kva machine of which Mr. Wilson speaks earlier. This must be so, since the values of Z_1, Z_2, and Z_0, which are the values for some particular generator, are a part of the defined voltage relations of Table VI. It is interesting to note that on larger kilovolt-ampere machines such as are being designed at present, the values of Z_0 and Z_2 are so much smaller than the values in the machine of Mr. Wilson's paper that the slopes of the lines in Fig. 4 would be changed radically.

Mr. Wilson notes several times in his paper that the use of round-rotor symmetrical-component equations in the analysis of salient-pole machines can introduce large errors. This is very true, and it is only the simplicity of the round-rotor approach and the difficulty of inserting the quadrature reactance component in the equations that justify the use of the former with its inaccuracies. I have developed a method of formulating a fictitious impedance Z_1' for use in the round-rotor equations that gives excellent results, this fictitious impedance Z_1' being obtained by the use of both X_d and X_q, the direct- and quadrature-axis synchronous impedances.

My method is as follows: with the values of X_d and X_q given by the machine manufacturer, internal generated voltage is obtained for the particular current I intend to use by the usual methods. Knowing the internal generated voltage, the terminal voltage, and the current, the fictitious internal impedance Z_1' is readily calculated. It varies considerably from X_d, having a large real component, and a somewhat smaller imaginary component. Using this value of Z_1' in the conventional round-rotor symmetrical-component equations gives excellent correspondence with test values. Obviously, this method gives results which are valid only when the regulator is operating under its ceiling value.

In closing, I wish to compliment Mr. Wilson in the organization and content of his paper. It should provide the basis for a number of other much needed papers in the future.

Russell W. Stineman (Boeing Airplane Company, Seattle, Wash.): The author has introduced unnecessary complexity and sources of error into the calculations by dealing with the internal nonlinear characteristics of the voltage regulator and exciter. It is the purpose of this discussion to present a simpler and more accurate method of calculating the desired quantities.

This method is based on the premise that, regardless of its internal characteristics, a regulated excitation system will hold constant the voltage which it senses, unless the excitation thus required exceeds ceiling excitation. For example, a 3-phase sensing circuit of the type shown in Fig. 2(A) will sense approximately the average line-to-line voltage, if the voltage unbalance is small. For larger voltage unbalance, each line-to-line voltage must be weighted by a factor which is proportional to the portion of each cycle during which the particular voltage governs the rectifier output. The exact expression is

$$V_s=\frac{V_{a-b}}{\pi}(\cos c+\cos b)+\frac{V_{b-c}}{\pi}\times(\cos a+\cos c)+\frac{V_{c-a}}{\pi}(\cos b+\cos a) \tag{18}$$

where V_s is the voltage sensed; V_{a-b}, V_{b-c}, and V_{c-a} are the line-to-line voltages; and a, b, and c are the corresponding interior angles of the line-to-line voltage phasor triangle. Rigorously, V_{a-b}, V_{b-c} and V_{c-a} are peak values of the voltage waves, but identical results will be obtained by consistently using effective values, a convention which will be employed here. For the case of normal balanced operation,

$$V_{a-b}=V_{b-c}=V_{c-a}=\sqrt{3}\text{ per unit and } a=b=c=60\text{ degrees}$$

from which

$$V_s=(3\sqrt{3})/\pi=1.654$$

This is the value of V_s which will be maintained, if possible, by the regulated excitation system.

The first step in the calculation of generator performance is to apply the conventional symmetrical-component methods given in Appendix III, determining the phase voltages and currents in terms of the excitation voltage E. Then V_s is calculated in terms of E by using equation 18, or a similar equation applicable to the type of sensing circuit employed. Since V_s is regulated to a known value, E is determined, and the phase voltages and currents easily follow. If E as thus determined exceeds ceiling excitation voltage E_{max}, then E is set equal to E_{max}, and the phase quantities are revised downward proportionally.

The simplicity of this method is obvious. A particular advantage is that only the alternator sequence impedances, ceiling excitation voltage, and the type of regulator sensing need be known to carry out the calculations. Even if the ceiling excitation voltage is unknown, many useful calculations may be carried out wherein it is known or

Table X. Comparison of Calculation Methods

Quantity	Calculated Value (Wilson)	Calculated Value (Stineman)	Measured Value
E, volts	310	245	314
I_a, amperes	100	79.2	32
I_b, amperes	55.2	43.7	43
I_c, amperes	56.3	44.5	44.2
V_a, volts	138	109	111
V_b, volts	149	118	122
V_c, volts	168	133	128

assumed that the required excitation will be less than ceiling, as with moderate unbalanced loads or single-phase faults.

When a magnetic-amplifier type of regulator is employed, the voltage of the phase supplying power to the amplifiers, say V_a, determines the value of E_{max}. If V_a drops below a certain critical value, a relay operates to directly self-excite the exciter. If this relay operation causes V_a to rise appreciably, cycling of the relay may take place. These factors may require several readjustments of the calculated values of E and V_a to finally evaluate the performance, but the basic method of calculation remains unchanged.

A comparision of the two methods of calculation for the arbitrary-load-unbalance example considered in the paper is given in Table X.

The only serious discrepancy between measured values and the values calculated by this writer is in the excitation voltage E. It is assumed that the measured value was determined from a measured generator field current and the slope of the air-gap line. It is the opinion of the writer that the abovementioned discrepancy is largely due to saturation, and that better correlation would be obtained if a correction factor had been applied to the slope of the air gap line to account for actual saturation. Using a correction factor estimated from Fig. 9 yields a measured excitation voltage of 250 volts.

The method of calculation presented in this discussion has been used by this writer for several years for routine fault calculations. However, the method appears so straightforward that no personal credit for its development is claimed.

B. J. Wilson: The matrix notation has been generally accepted by the engineering profession. Its use here is in the best interests of the applicability of analyses to the broadest range of unbalance situations we can anticipate, and accomplishes this in the clearest manner. By employing matrix notation, we incorporate into the problem the logic concomitant with systems of algebraic equations and their solutions. We could scarcely do better. At the same time, we anticipate certain advantages afforded us by the modern computer. Even in our deceivingly simple 3-phase case, the variables yield a 6-by-6 system of equations. By satisfying conditions for diagonal form, we were able to draw on the services of an iterative computer, thus sidestepping explicit matrix inversion—or solution processes involving determinental evaluations required in the final forms of our equations. More sophisticated computers are available for handling these forms, the solution of which is pretty much a brute force project by longhand methods.

As an additional point, it must be mentioned that a matrix is a symbolic array not in itself to be solved, but merely a convenient notation employed in the solution of equations.

In regard to the change of slope, Fig. 4, it must be pointed out once more that the method is general to machines with arbitrary values of sequence impedance.

For convenience, the presentation is designed so that matrix methods need not be used for the common fault unbalances.

Mr. Owen's comments are interesting regarding the alleviation of errors introduced by the compromised use of round-rotor theory. It is questionable, however, whether the constant ratio Z_1' that Mr. Owen advocates for use would be a satisfactory compromise for the wide range of complex current values encountered in the general application of the prediction methods described here.

The bases for Mr. Stineman's premise are subject to some formidable restrictions which should be observed before indiscriminate use of this tenet can be exercised. In the first place, the constancy of the effective "sensed" voltage is certainly not independent of the regulator internal characteristics. On the contrary, it is a direct function of them. The degree to which the sensed voltage remains constant over a given operating range depends on and is proportional to the sensitivity of the individual regulator. Consequently, the flatness of a regulated voltage over the load range depends on the extent of range over which the individual regulator component characteristics remain sensitive as mentioned above.

For regulators considered in the paper, which are characteristic of a wide class used with aircraft generators operating at per-unit balanced load or greater, the operating region remains in highly sensitive regions. This is true also for moderate unbalance from near normal impedance. For heavy loads or extreme unbalance, less sensitive operating regions are encountered, no longer making it possible to claim even approximately that the sensed voltage remains constant. These facts are born out upon inspection of Figs. 6 and 8. There exists also the possibility of instability and/or oscillations. For instance, change of slope in Fig. 6 at low abscissa values could induce an oscillating condition. Essentially then, the shortcoming of Mr. Stineman's recommendation lies in the fact that it does not consider the simultaneous effect of all the significant parameters present. It is straightforward at the expense of being limited to relatively high-quality regulators restricted to operation within the machine's rating or operation at nearly balanced conditions. The mechanics of the other steps outlined by Mr. Stineman are essentially those contained in the paper, which, however, is generalized to include any unbalanced condition.

The method prescribed in the paper provides a direct attack to the evaluations of excitation voltage without any of the reservations mentioned above. It is general to any load condition, regulator construction, or circuit connection, being subject only to those assumptions stated, which have a secondary effect on the results.

New Developments in Differential-Type Hydraulic Transmissions and Controls

R. H. EISENGREIN
ASSOCIATE MEMBER AIEE

Synopsis: The differential-type hydraulic transmission has been used as a constant speed drive for aircraft a-c generators for approximately 8 years. The experience gained in this time on both the *B36* and *P5M* airplanes has been a major factor in establishing future aircraft electrical system and component requirements. However, the final decision to establish closer electrical system tolerances for voltage and frequency, real and reactive load balance, and necessary fault protection should be determined on the basis of component and system reliability, simplicity, and performance. The following discussion considers these important characteristics for the components controlling system frequency, real-load division between paralleled a-c generators, and automatic paralleling of a-c generators. The improvements in new system performance were gained by utilizing components with faster response times, and also by the introduction of nonlinear circuit elements. Design and performance details are cited to substantiate steady-state frequency control to within 0.25 per cent of 400 cycles per second, real-load division to within 2 kw, and automatic paralleling of generators to maintain current transients within generator full-load ratings.

The Basic System

IN CONSIDERING future systems utilizing the differential-type hydraulic transmission and controls, there are various combinations of elements to be considered. The simplest combination for a single generator system would be the hydraulic transmission and basic mechanical-hydraulic flyball governor. This self-contained unit would have no external control connections, since the governor would be integral with the transmission. There would be an input and output shaft only.

Considering input speed variations to the drive between 3,000 and 9,000 rpm, the steady-state system frequency would remain between 395 and 400 cycles per second. The maximum steady-state frequency droop with load occurs at the low input speeds. For some applications, these frequency limits have been held between 400 and 398 cycles per second. Typical performance data for a 40-kva 0.75-power factor system are shown in Fig. 1. Fig. 1 is a record of system-frequency deviation and applied load for two different input speeds. As input speed is increased from 3,000 to 5,000 rpm, the steady-state frequency droop for full load decreases from 5 cycles per second to 3 cycles per second. Likewise, the transient recovery time and peak frequency deviation with load decrease with increasing input speed. These improvements in performance are a function of both increasing system sensitivity and decreasing transmission slip at the higher input speeds. An additional control available for this simple system would be an integrally-mounted mechanical-hydraulic overspeed device.

The major field for improvement in performance beyond the limits of this basic system lies in the control of the steady-state frequency. The solution to this problem, of course, is the establishment of an accurate frequency reference. The transient-response characteristics of the system are determined almost completely by the dynamic characteristics of the hydraulic transmission and governor and the system inertia. Improvements in system transient-response time might be achieved by utilizing some of the new high-speed electromechanical transducers, but only at the sacrifice of the simplicity of the present basic system.

An extension of the control elements to improve the steady-state frequency accuracy requires an accurate frequency reference, and also a device for shifting the basic governor setting as system frequency deviates from the reference frequency. The components utilized to perform these functions are shown in Fig. 2. The frequency reference consists of two tuned resistance-inductance-capacitance circuits, with their outputs rectified and differentially connected to provide a d-c null voltage for a system frequency of 400 cycles per second. The d-c output varies in magnitude with frequency error, and varies in polarity as a function of increasing or decreasing frequency error. This error signal drives the control coil of a push-pull magnetic amplifier. The magnetic amplifier, in turn, drives the control phase of a precision frequency-control motor. The fixed phase of the control motor receives power from an additional winding on the magnetic amplifier. Through a gear box and rack, the control motor positions an auxiliary speeder spring in the flyball governor to maintain the basic governor setting at 400 cycles per second.

The performance characteristics of the originally proposed 40 kva 0.75-power factor system with these additional controls are shown in Figs. 3, 4, and 5. These tests were run at input speeds of 3,000, 5,000, and 6,500 rpm respectively, for loads of 2, 8, 18 and 30 kw. The steady-state frequency deviation with load is now less than 1 cycle per second for all input speed conditions. The accuracy of this measurement is not obvious from these figures for the existing calibration. However, the accuracy has been established by measuring the difference in frequency between the system generator and a tuning fork reference for the same tests. These data are shown in Fig. 6. Curve *C* indicates the time of load application and load dump, curve *B* shows the transient frequency deviation, and curve *A* shows the steady-state frequency difference before and after load application. The curves show the frequency transient for a 30-kw load. The system frequency was set below the refer-

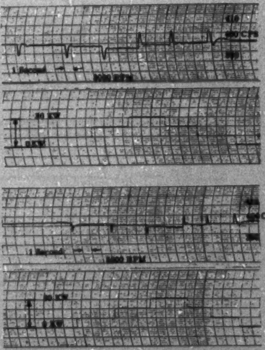

Fig. 1. Basic system characteristics at 3,000-rpm input speed for 9-, 18-, and 26-kw loads, and at 5,000-rpm input speed, 18- and 27-kw loads

---

Paper 53-369, recommended by the AIEE Air Transportation Committee and approved by the AIEE Committee on Technical Operations for presentation at the AIEE Aircraft Electric Equipment Conference, Seattle, Wash., September 30–October 2, 1953. Manuscript submitted June 30, 1953; made available for printing September 2, 1953.

R. H. EISENGREIN is with the Sundstrand Machine Tool Company, Rockford, Ill.

The author wishes to acknowledge the comments and advice of his colleagues in the Engineering Department.

Fig. 2. Basic system with frequency controller and control motor

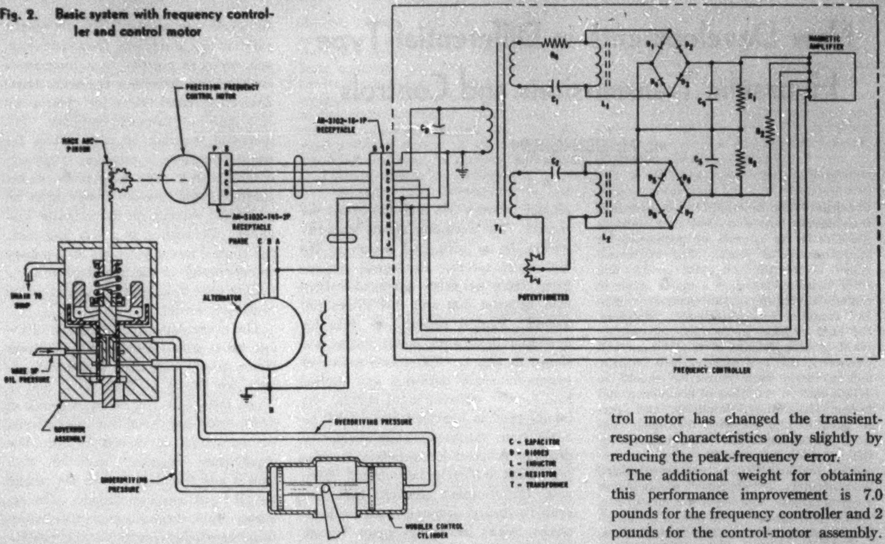
PRECISION FREQUENCY CONTROL MOTOR
RACK AND PINION
AN-3102-18-1P RECEPTACLE
AN-3102C-14S-2P RECEPTACLE
P S
A B C D
S P
A B C D E F G H I J
PHASE C B A
DRAIN TO SUMP
ALTERNATOR
MAKE UP OIL PRESSURE
GOVERNOR ASSEMBLY
OVERDRIVING PRESSURE
UNDERDRIVING PRESSURE
WOBBLER CONTROL CYLINDER
C - CAPACITOR
D - DIODES
L - INDUCTOR
R - RESISTOR
T - TRANSFORMER
R_3
C_1
L_1
C_2
L_2
C_3
T_1
D_1
D_2
D_3
D_4
D_5
D_6
D_7
D_8
C_4
C_5
R_1
R_2
R_3
MAGNETIC AMPLIFIER
POTENTIOMETER
FREQUENCY CONTROLLER

ence to show a definite beat frequency. Prior to the shock load, this difference frequency was 2.0 cycles per second; after the shock load was applied, the beat frequency was 2.25 cycles per second; and when the load was removed it was 2.0 cycles per second. These values show a deviation of less than 1 cycle per second for full load on the generator. The addition of the frequency controller and control motor has changed the transient-response characteristics only slightly by reducing the peak-frequency error.

The additional weight for obtaining this performance improvement is 7.0 pounds for the frequency controller and 2 pounds for the control-motor assembly. An additional factor to be considered is the reliability of the precision frequency control. The main source of trouble would be loss of sensing leads to either the control motor or frequency controller. For either fault, the system frequency

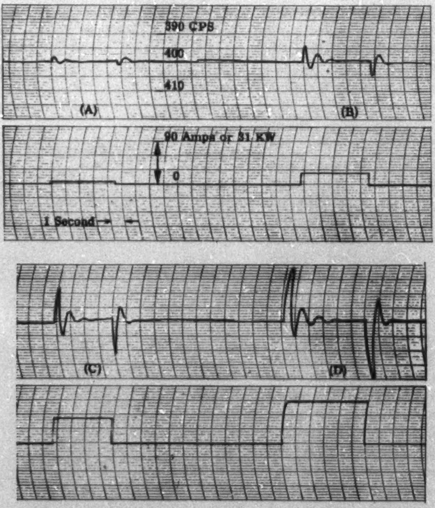

Fig. 3. Characteristics of basic system with frequency controller and control motor for 3,000-rpm input speed to drive and various kilowatt loads

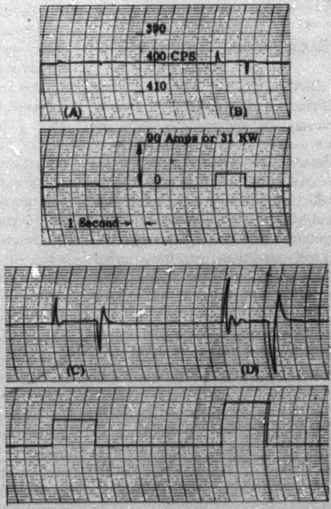

Fig. 4. Characteristics of basic system with frequency controller and control motor for 5,000-rpm input speed to drive and various kilowatt loads

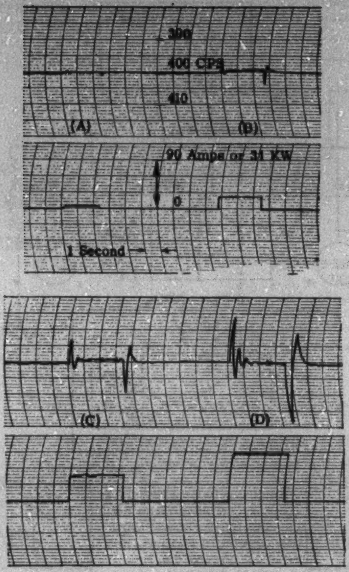

Fig. 5. Characteristics of basic system with frequency controller and control motor for 6,500-rpm input speed to drive and various kilowatt loads

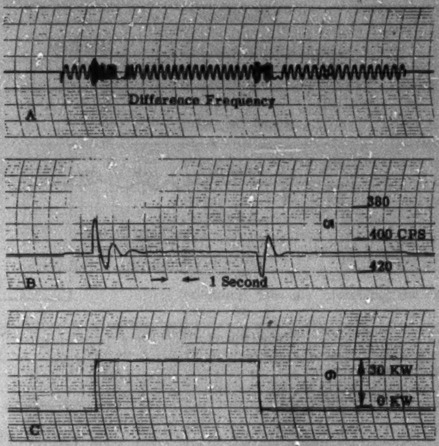

Fig. 6 (above). Accurate difference frequency measurement for various loads of basic system with frequency controller and control motor

would be controlled again by the basic governor; its basic setting would now be 390 cycles per second.

Multiengine Installations

The extension of the basic package with a frequency controller and control motor to permit paralleling of generators on multiengine installations involves only the addition of a circuit for sensing real load on each generator. The circuit is added to the frequency controller and is shown in Fig. 7. It provides a d-c signal proportional to the real load on its generator.[1] When two systems are paralleled, a similar circuit in the second frequency controller is differentially connected to the first real-load division circuit. A circulating current flows through a magnetic-amplifier control winding in each controller. The polarity and magnitude of this signal are a function of the direction and magnitude of real-load unbalance between the two generators, respectively. Through action of the control motor, the basic governor speed settings of each system are changed to establish a rebalance of real load between generators.

Typical performance data for a 2-generator paralleled system are shown in Fig. 8. The total system load is 30 kw. The records show an initial load of 15 kw on one machine, the temporary load unbalance during acceleration, and final rebalance of real load to the initial values. Steady-state load balance is maintained to within 2 kw for all input speed and load conditions. The additional weight of the load division circuit components is 0.5 pound.

An additional control could be added to provide for adjusting real-load division between generators. It would consist of a flight engineer's rheostat in one of the tuned resistance-inductance-capacitance circuits to permit unbalancing the circuit so as to temporarily accelerate or decelerate a drive, and thus its generator. This might be necessary if two frequency controllers with different frequency settings were paralleled. After paralleling, the system frequency would settle at some value between the two settings. An error would exist between each frequency refer-

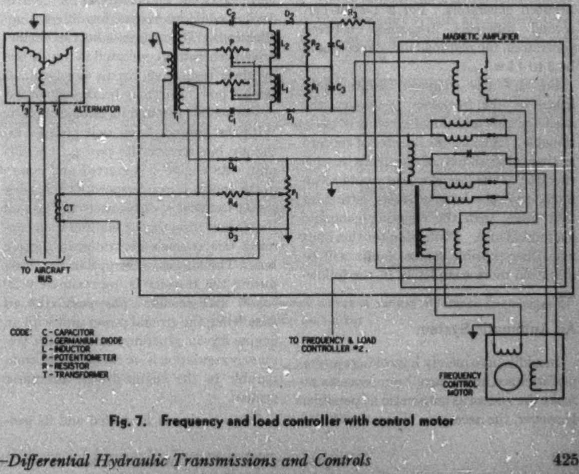

Fig. 7. Frequency and load controller with control motor

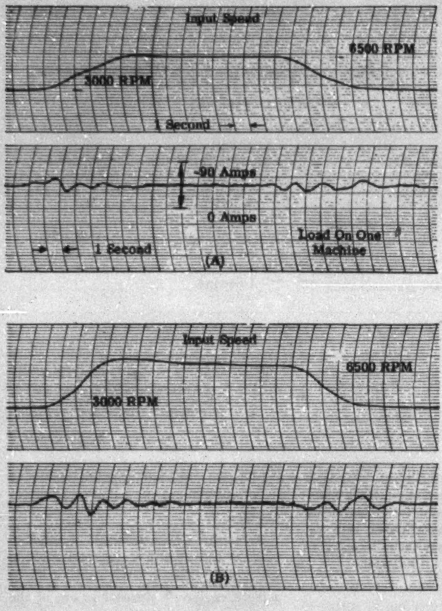

Fig. 8. Paralleled generator characteristics for input-speed accelerations of one drive. Second drive at 5,000-rpm input speed. System load of 30 kw

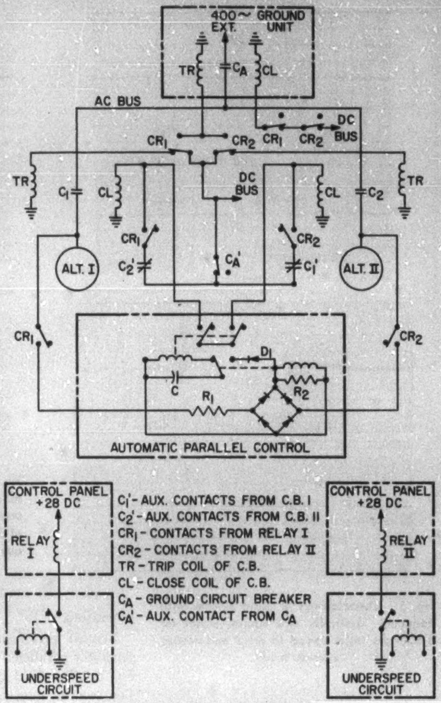
400~ EXT.
GROUND UNIT
TR
C_A
CL
AC BUS
CR_1
CR_2
CR_1
CR_2
DC BUS
TR
C_1
CL
DC BUS
CL
C_2
TR
CR_1
CR_2
ALT. I
C_2'
C_A'
C_1'
ALT. II
CR_1
CR_2
D_1
C
R_1
R_2
AUTOMATIC PARALLEL CONTROL
CONTROL PANEL +28 DC
RELAY I
UNDERSPEED CIRCUIT
C_1' - AUX. CONTACTS FROM C.B. I
C_2' - AUX. CONTACTS FROM C.B. II
CR_1 - CONTACTS FROM RELAY I
CR_2 - CONTACTS FROM RELAY II
TR - TRIP COIL OF C.B.
CL - CLOSE COIL OF C.B.
C_A - GROUND CIRCUIT BREAKER
C_A' - AUX. CONTACT FROM C_A
CONTROL PANEL +28 DC
RELAY II
UNDERSPEED CIRCUIT

Fig. 9. Automatic system block diagram

ence and the system frequency. The resulting error signal in each magnetic-amplifier frequency-control coil will be nullified by an error signal from the magnetic-amplifier load-division control coil. The load-division error signal can be created only by an unbalance of real load between generators. For a 1-cycle-per-second difference frequency between generators, the real-load unbalance would be 3 to 4 kw.

For the close frequency limits established by the frequency controller, the need for this additional control is questionable. An additional factor of concern is the vulnerability of the leads to this rheostat. The loss of a lead would mean a change in the basic governor setting for that drive, with the resulting complete load unbalance. Protection for this fault and other possible system faults will be discussed more completely in the following.

An Automatic System

In addition to merely improving system performance, there have been requests to make the system as automatic as possible. However, the necessary characteristics of reliability and simplicity were still of vital importance. A block diagram of a proposed automatic system is shown in Fig. 9. Other combinations of control devices could be devised for different applications. The system shows two engine-driven generators connected to the a-c bus by their respective circuit breakers. A ground power unit may be also connected to the a-c bus through its circuit breaker. With the ground power unit plugged in, the a-c bus receives its power from this unit. As engine I is started and comes up to speed, its underspeed switch, at a preset frequency, disconnects the ground power unit from the a-c bus and then connects this engine's generator to the a-c bus. The power interruption resulting during the transfer is approximately 20 to 40 milliseconds. The possibility of paralleling the ground power unit with an engine-driven generator exists if the frequency regulation is, or can be made, comparable to the engine-driven alternator system.

When engine II is started and its generator comes up to speed, it can only be connected to the a-c bus through an automatic paralleling control. The underspeed switch cannot put alternator II on the bus directly because contact C_1' is now open. However, with the automatic paralleling circuit now connected to both alternator outputs, it will connect alternator II to the bus at the correct time automatically.

The existence of system faults and the possibility of preventing resulting damage in the system was also a major factor in determining its reliability. In general, it was felt that faults to be considered should be loss of engine power, loss of sensing leads to various electrical components, and possible malfunctions in the constant-speed drive or generator.

For cases of no rotational input to the drive, which might be caused by either an engine shutdown or a sheared input shaft to the drive, the underspeed switch could not be closed, and this generator could not be connected to the a-c bus. This would be true whether the generator was

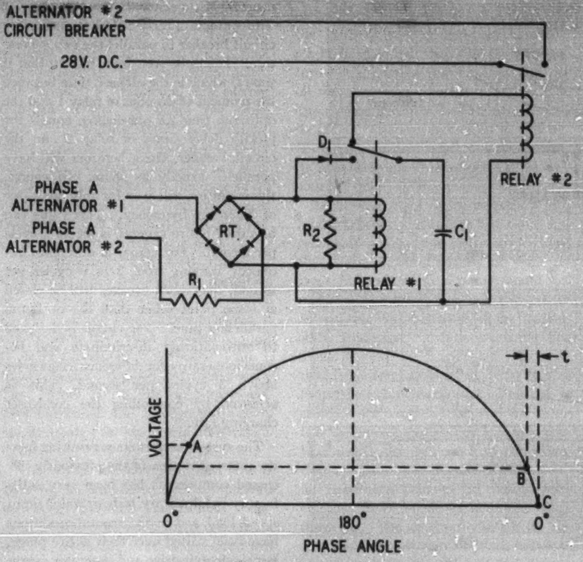

A-POINT WHERE RELAY #1 ENERGIZES
B-POINT WHERE RELAY #1 DE-ENERGIZES
C-OPTIMUM PHASE ANGLE FOR PARALLELING
t-DELAY TIME OF RELAY #2 PLUS CIRCUIT BREAKER

Fig. 10. Automatic paralleling circuit and voltage-phase-angle characteristic

connected to the first or second engine to be started. If the system generators were already paralleled, and the rotational input to one drive was lost, the underspeed switch would automatically disconnect the malfunctioning generator from the bus.

In case of an overspeed of a generator, a mechanical-hydraulic overspeed mechanism would automatically shift the drive control to the underdrive position. This action would cause the drive output speed to decrease and trip the underspeed switch. The malfunctioning generator would be disconnected from the a-c bus. Incidently, it should be noted that both the overspeed and underspeed protection mechanisms are mechanically connected on the drive side of an overrunning clutch which is located between the drive and the alternator.

For loss of voltage to the frequency controller, which might be caused by a generator or voltage-regulator malfunction, or loss of the sensing leads to the frequency controller, the precision frequency-control motor will lack power. The speed-control system will revert to the basic governor setting. Since this setting could be below the underspeed relay dropout point, the machine could be disconnected from the a-c bus. If the leads to the precision frequency-control motor were opened, the system would again revert to the basic governor setting, and this generator could be automatically disconnected from the a-c bus.

Since each of these possible faults could exist with generators in parallel, the resulting conditions should be investigated. For no rotational input to one drive, the underspeed switch will disconnect this generator from the a-c bus. Just prior to this time, real load will become unbalanced temporarily and system frequency will dip momentarily. The signal created by the real-load unbalance decreases system frequency 3 to 4 cycles per second, at which value the frequency-discriminator error signal prevents a further reduction. For an overspeed condition, the real load again will become temporarily unbalanced, with the accelerating machine absorbing the majority of load; system frequency momentarily will rise until the overspeed mechanism operates and puts the system in underdrive. The underspeed switch will be actuated and trip this alternator off the bus. To minimize the length of this transient, it might be desirable to have the overspeed mechanism directly take the malfunctioning system off the bus. For loss of voltage to one frequency controller, system frequency will momentarily droop as the operating frequency controller decreases system frequency as it tries to maintain real-load division between systems. However, since the faulty system will revert to basic governor setting, it will be disconnected from the a-c bus. If the leads to the precision frequency-control motor are opened, the same situation as previously discussed will exist. The faulty system will revert to the basic governor setting and be disconnected from the a-c bus.

Component Details

The details of the various components in the automatic system are of interest on the basis of analyzing performance and

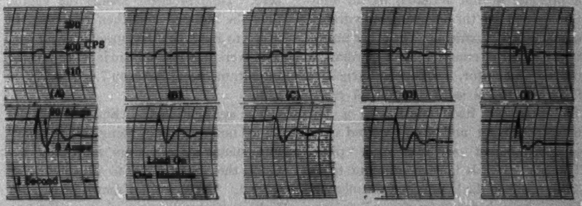

Fig. 11. Automatic paralleling unit. Performance curves at various difference frequencies of 30 kw initially on a-c bus

A. 0.1 cycle per second
B. +1 cycle per second
C. +2 cycles per second
D. −1 cycle per second
E. −2 cycles per second

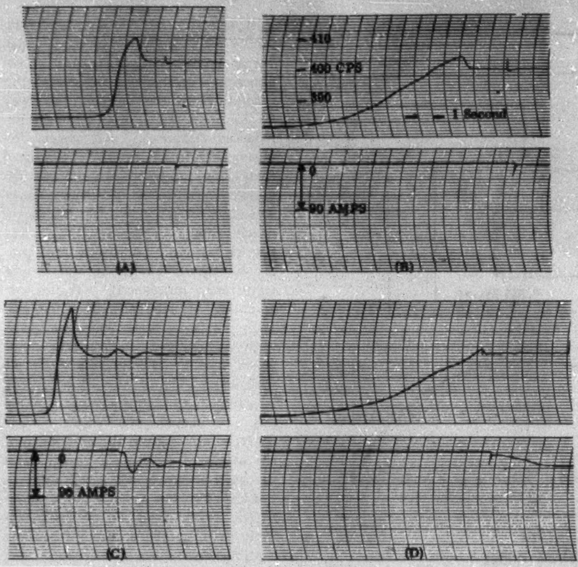

Fig. 12. **Automatic paralleling unit performance curves for starting tests**

A. 0 kw on bus initially
B. 15 kw on bus initially

also estimating possible malfunctions. In all cases, the units have been designed to operate in accordance with *MIL-E-7894* and *MIL-E-5272*. The only components mounted on vibration isolators are relays. The remainder of the components are passive elements which can withstand the extremes of vibrations without any special mounting provisions.

Two types of underspeed control devices are available. One unit consists of a pressure switch actuated by an additional land on the mechanical-hydraulic overspeed mechanism. The other underspeed control consists of a permanent magnet generator, a frequency sensitive network, and a sensitive control relay. The generator itself consists of a permanent magnet and a coil wound on a specially-shaped soft-iron pole piece. The pole piece is located adjacent to an output gear of the hydraulic transmission. The voltage induced in the coil is proportional to the speed of the output gear and the varying reluctance of the air gap between the gear teeth and the soft iron pole piece. The tuned circuit provides an output voltage which varies sharply with frequency over a limited range. It is in this range that the sensitive relay pickup and dropout voltage are set. By sharpening the slope in this limited range, close control of pickup and dropout voltage are maintained.

The overspeed-control mechanism consists of a flyball-actuated valve. During an overspeed, it drains to case the proper governor control line to cause the drive output speed to decrease. The overspeed mechanism may only be reset by dropping system-makeup pressure to zero. This, in effect means the engine must be stopped and then restarted, in order to reset the overspeed mechanism. The overspeed mechanism is set to actuate for output speeds between 7,000 and 7,500 rpm.

The automatic paralleling unit was designed on the basis of being able to maintain steady-state system frequency between the limits of 399 to 401 cycles per second. The circuit is shown in Fig. 10. Voltages from the same phase of the two generators to be paralleled energize relay 1 and cause it to pickup and dropout at the difference frequency of the two systems. When relay 1 is first energized, capacitor C is charged to approximately 35 d-c volts through a contact of the relay. When relay 1 is de-energized, its contact discharges capacitor C through relay 2. The contacts of relay 2 close the necessary circuit breaker to parallel the two generators. It can be seen from Fig. 10 that if time t, which is the elapsed time between the moment of dropout of relay 1 and the optimum time for paralleling, equals the pickup delay times of relay 2 and the circuit breaker, the generators will have paralleled exactly in phase. Of course, this condition will exist for only one value of difference frequency. This value can be varied but in general, is set for 1 cycle per second. For values of difference frequency varying from 2 to 0 cycles per second, the circuit breaker will be closed at some point other than the optimum paralleling time. The circuit is designed to automatically discriminate and become inoperative for difference frequencies above 3 cycles per second. This is achieved by controlling the condenser charging rate.

The system performance resulting from the interconnection of the previously discussed components has been very satisfactory in laboratory tests in which input speed, load, and environmental conditions have been varied over their entire range. For single-unit drive and generator operation, steady-state frequency limits have been within the ±1 cycle per second limits for all load, speed, and environmental conditions. These results have been verified by qualification tests for an airframe manufacturer. The transient frequency response characteristics for sudden load applications vary with input speed, and are shown in Figs. 3, 4, and 5. From the diagrams, it can be seen that for minimum frequency deviation with load, the drive input speed should be high. Thus, it would be beneficial, performance-wise, to make the drive input speed during cruise conditions a high input speed.

The performance characteristics for the automatic paralleling unit are shown in Figs. 11 and 12. Fig. 11 shows the initial current transient existing when paralleling at various difference frequencies. The initial load on the bus was 30 kw. The two generators were Westinghouse type *8QL40A*. It is seen that the current transient at all times is within the rating of one generator. Fig. 12 shows the current transient which is caused when a generator is autoparalleled as it is coming up to speed at different-acceleration rates. This would be the condition existing in the proposed automatic system as the second engine is started. Curve A shows the frequency of the incoming machine rising rapidly enough through the operating range of the autoparalleling unit so that condenser C cannot fully change in this time. The autoparalleling unit can operate only after the initial frequency transient. This is desirable, since it then operates near the optimum design point, and insures a minimum line-current transient. Curve *B* shows the same data for a slower input acceleration. There is no initial load on the system for these tests. Curves *C* and *D* reveal similar performance data for the case of 15 kw initially on the bus. The line current transient is well within the full-load rating of the 40-kva alternators used.

The frequency and load transients which exist when two units are paralleled are shown in Fig. 11. For the initial condition of full load on one machine, it can be seen that upon paralleling there is some overshoot before the load is finally equally divided between generators. From Fig. 8, the temporary real-load unbalance and frequency transient are illustrated for various input accelerations.

The effect of environmental conditions on the various system components has been previously mentioned. However, actual tests on a drive, generator, and a frequency and load controller soaked at −65 degrees Fahrenheit for 12 hours, indicated that as the input speed was increased to the governing level in a period of $2^1/_2$ minutes, the system frequency was initially 396 cycles per second. In a matter of 4 minutes from the time of starting, the frequency was at 398 cycles per second, and at 5 minutes it was at 400 cycles per second. The drive was kept operating at this ambient for 30 minutes and the frequency remained within 1 per cent of 400 cycles per second for this period. This particular test was run with no load on the alternator and as a consequence drive-oil temperatures remained low for a considerable time. If the system were loaded, as normally might be expected, the drive-oil temperature would increase more rapidly and the oil viscosity would be lower. This is of importance, because the control motor and its gearing operates immersed in this oil. With the motor's limited torque capacity, its response time is increased by the viscous oil drag.

Additional tests on a frequency and load controller alone, with the drive and generator at room temperature, indicated that the controller, soaked at −65 degrees Fahrenheit for 6 hours, could immediately be brought to an ambient of 80 degrees Fahrenheit without steady-state frequency deviation beyond the limits of ±1 cycle per second. An additional change of ambient to +200 degrees Fahrenheit likewise showed no change of steady-state frequency beyond the specified limits. The frequency and load controller was also subjected to the vibration specifications of *MIL-E-5272*, with no subsequent change in performance characteristics and no structural damage resulting. The automatic paralleling circuit was likewise exposed to the extremes of temperatures of −65 and 200 degrees Fahrenheit for 5 to 10 minutes, as might be expected in field service, and no apparent change in performance characteristics was noted. The underspeed control has operated satisfactorily in a transmission where oil inlet temperatures have varied to the operating temperatures of 225 degrees Fahrenheit, with no detrimental effect on performance characteristics. The overspeed mechanism has likewise been exposed to these operating conditions with similar results being obtained.

It is realized that these environmental conditions are rapidly becoming obsolete, and much time and effort is being expended to redesign present equipment and develop new equipment to meet the increasing temperatures to which the drive and its components will be subjected. Transmissions currently have been operating with oil inlet temperatures up to 325 degrees Fahrenheit. An additional potential source of trouble, the higher frequency vibrations reported by various airframe manufacturers, also are being considered in designing all new components. It is realized, of course, that despite the extensive laboratory tests made on these equipments, additional field problems will exist, as always. In addition to the need for meeting new environmental conditions, component design is reviewed periodically to consider the possibility of obtaining lighter weight units. Likewise, possible changes in system design are being studied which would minimize transient frequency deviations, improve steady-state real-load division, improve stability of paralleled systems, and permit paralleling of alternators driven by different prime movers.

References

1. Power Equalizer Systems for Aircraft Alternators, **Albert K. Hawkes, John A. Granath.** *AIEE Transactions*, vol. 72, pt. II, Sept. 1953, pp. 209–17.

2. A Constant-Speed Drive for Aircraft Alternators, **L. H. Schuette, R. Chrzanowski.** *Applied Hydraulics*, Cleveland, Ohio, July 1948, pp. 6–9, 22.

3. Alternating-Current Electrical Systems for Aircraft. Westinghouse Electric Corporation, Lima, Ohio, Jan. 1951.

4. Aircraft Electrical System Study, **H. J. Finison, L. W. Matsch, L. J. Stratton.** Armour Research Foundation, Illinois Institute of Technology, Chicago, Ill., April 1952. (Equipment Laboratory, *Contract No. 33(038)-35011, RDO No. 656-2112*, Wright Air Development Center, Dayton, Ohio.)

No Discussion

Bibliography on Feedback Control

AIEE COMMITTEE REPORT

THIS bibliography is an attempt to collect a reasonably complete set of references pertaining to the concept of feedback, its applications, and consequences, up to the year 1952. These references necessarily touch upon many fields of engineering and also contain a number of items on related topics. Although the material has been divided into a number of broad categories, it should be recognized that many references could appear with almost equal validity under more than one topic. The classification is therefore somewhat arbitrary and the reader is advised to look over related topics in all cases. Within each category the items are arranged chronologically. A list of periodicals is given on pages 460-62.

Classification Chart

Books and Related Bibliographies: Primarily devoted to feedback control systems, automatic control, and regulation.

Surveys and Reviews: General articles, basic concepts of measurement and control, forms of controllers, industrial applications of automatic control.

Terminology: Standards, symbols.

System Analysis: Transient and sinusoidal studies, analytical and graphical methods, linear and nonlinear problems.

Stability: Criteria for stability, their application to feedback control systems, consideration of degree of damping.

Servomechanisms: Position regulators, followers.

Relay-Type Servomechanisms and Feedback Controllers: Off-on, 2-position, and discontinuous controllers, sampling servos.

Industrial Process Control: Automatic process regulation, controllers and their adjustments, applications, instrumentation.

Temperature and Pressure Control: Laboratory and industrial controllers, thermostats, temperature measurements for automatic controllers, control of high and low pressures.

Flow and Liquid Level Control: Gases and liquids.

Generator Voltage Regulation: Surveys, generator characteristics, excitation systems, generator stability.

Generator Voltage Regulators, Rheostatic and Vibrating Types: Carbon pile, vibrating, multicontact, and electromechanical devices.

Generator Voltage Regulators, Electronic: Vacuum and gas-filled tubes used as regulators for a-c and d-c generators.

Generator Voltage Regulators, Dynamoelectric and Magnetic Types: Multifield exciter, magnetic amplifier.

Line Voltage Regulators, Electromechanical: Induction and step voltage regulators, adjustable ratio transformer.

Line Voltage and Current Regulators, Electronic: Series and shunt tube stabilizers for electronic power supplies.

Line Voltage and Current Regulators, Magnetic: Saturated magnetic circuit, resonant circuit, constant current source.

Constant Voltage and Constant Current Devices: Barretter, glow tube, corona tube, nonlinear bridge.

Motor Speed Regulation: A-c and d-c motors; tachometer, photoelectric, and governor control.

Prime Mover Speed Regulation: Steam and hydraulic turbines, internal combustion engines.

Power System Regulation: Frequency, load, and tie-line control, interconnected networks.

Boiler and Combustion Control: Regulation of boiler operation, feed-water regulation, electric boiler, multifuel furnace.

Industrial Drives: Steel, paper, machine tool, and textile drives, arc-furnace electrode control.

Transportation: Automatic pilots for aircraft, ship steering and stabilization, diesel-electric locomotives.

Electronic Regulators: Automatic gain and frequency control, oscillators.

Servo-Operated Instruments: Recorders, self-balancing instruments.

Feedback Amplifiers: Current and voltage feedback, effect of feedback on impedances and response, galvanometer amplifier.

Regulating Devices: Variable resistance, electromechanical, electronic, pneumatic, and hydraulic elements; servomotors, synchros, clutches, valves.

Dynamo Amplifiers: Amplidyne, Magnicon, Magnavolt, Metadyne, Regulex, Rotorol, multifield machines.

Experimental Studies: Test methods and devices, analogues.

Miscellaneous Regulators: Illumination, rectifier voltage control, acoustic applications.

Books and Related Bibliographies

1. Dynamische Probleme der Maschinenlehre, **R. v. Mises.** Volume IV, I, II, part 2 of Encyklopadie der Mathematischen Wissenschaften, B. G. Teubner, Leipzig, 1911.

2. Governors and the Governing of Prime Movers, **W. Trinks.** D. Van Nostrand Co., New York, N. Y. 1919.

3. Die Regelung der Kraftmaschinen, **M. Tolle.** Springer, Berlin, Germany, 1921.

4. Regelung und Ausgleich in Dampfanlagen, **T. Stein.** Springer, Berlin, Germany, 1926.

5. Regler fur Druck und Menge, **Guido Wunsch.** R. Oldenbourg, Munich, Germany, 1930.

6. Die Selbsttaetige Regelung Elektrischer Maschinen, **E. Juillard-Ollendorf.** Springer, Berlin, Germany, 1931.

7. Der Chemie-Ingenieur; Volume 2, Part 1, Kontroll-und Reguliereinrichtungen, edited by M. Jakob, P. Gmelin, J. Kronert. Akademische Verlagsgesellschaft M. B. H., 1932. (Lithoprinted by Edwards Bros., Ann Arbor, Mich. 1943.)

8. Unmittelbare Regelung, **W. Schmidt.** VDI-Verlag, Berlin, Germany, 1939.

9. The Wisdom of the Body, **Walter B. Cannon.** W. W. Norton and Co., New York, N. Y., 1939.

10. Untersuchung der Stabilitaet von Regulierungen anhand des Vectorbildes, **Rene Feiss.** A.-G., Gebr. Leemann and Co., Zurich, Switzerland, 1939.

11. Industrial Instruments for Measurement and Control, **T. J. Rhodes.** McGraw-Hill Book Co., New York, N. Y., 1941.

12. Temperature Measurement and Control, **R. L. Weber.** The Blakiston Co., Philadelphia, Pa., 1941.

13. The Analysis and Synthesis of Linear Servomechanisms, **Albert C. Hall.** The Technology Press, Cambridge, Mass., 1943.

14. Die Regelung der Kraftmaschinen, **Gustav Fabritz.** Springer, Vienna, Austria, 1940. (Lithoprinted by Edwards Bros., Ann Arbor, Mich., 1944.)

15. Mittelbare Regler und Regelanlagen, **F. V. A. Engel.** VDI-Verlag G.M.b.H., Berlin, Germany, 1944. (Lithoprinted by Edwards Bros., Ann Arbor, Mich., 1946.) Extensive bibliography including patent references.

16. Vektorielle Regeltheorie, **Paul Profos.** A.-G. Gebr. Leemann and Co., Zurich, Switzerland, 1944.

17. Stabilitaet Elektrischer Drehstrom-Kraftuebertragungen, Andreas Timascheff. Springer, Berlin, Germany, 1940. (Lithoprinted by Edwards Bros., Ann Arbor, Mich., 1944.) Bibliography.

18. Automatic Control Engineering, **Ed S. Smith.** McGraw-Hill Book Co., New York, N. Y., 1944.

19. Network Analysis and Feedback Amplifier Design, **Hendrick W. Bode.** D. Van Nostrand Co., New York, N. Y., 1945.

20. Principles of Industrial Process Control, **Donald P. Eckman.** John Wiley and Sons, New York, N. Y., 1945.

Papers **53-250** and **53-251**, recommended by the AIEE Industrial Control and Feedback Control Systems Committees and approved by the AIEE Committee on Technical Operations for presentation at the AIEE Summer General Meeting, Atlantic City, N. J., June 15–19, 1953. Manuscript for 53-250 submitted October 27, 1952; made available for printing April 17, 1953. Manuscript for 53-251 submitted March 16, 1953; made available for printing April 20, 1953.

Paper **53-393**, recommended by the AIEE Industrial Control and Feedback Control Systems Committees and approved by the AIEE Committee on Technical Operations for presentation at the AIEE Fall General Meeting, Kansas City, Mo., November 2–6, 1953. Manuscript submitted July 10, 1953; made available for printing August 13, 1953.

The personnel for the Subcommittee on Bibliography of the AIEE Committee on Industrial Control are: W. H. Elliot, E. E. Moyer, W. Schaelchlin, J. W. Picking, and R. W. Jones. The personnel for the Subcommittee on Bibliography of the AIEE Committee on Feedback Control Systems are: E. R. Behn, F. H. Ferguson, A. Porter, O. H. Schuck, C. N. Weygandt, and R. W. Jones.

The bibliography was edited by Richard W. Jones, Northwestern University, Evanston, Ill. The editor wishes to express his appreciation to the Northwestern Technological Institute for clerical and typing assistance which made this work possible.

21. Considerations sur le Probleme de la Stabilite, **Daniel Gaden.** Editions la Concorde, Lausanne, Switzerland, 1945.

22. Fundamental Theory of Servomechanisms, **LeRoy A. MacColl.** D. Van Nostrand Co., New York, N. Y., 1945.

23. Instruments and Process Control, **New York State Vocational and Practical Arts Association.** Delmar Publishers, Albany, N. Y., 1945.

24. Analysis and Design of Translator Chains, **H. Ziebolz.** Askania Regulator Co., Chicago, Ill., 1946.

25. Regelungstheorie, **Jost Hanny.** A. G. Gebr. Leemann and Co., Zurich, Switzerland, 1947.

26. Theory of Servomechanisms, **Hubert M. James, Nathaniel B. Nichols, Ralph S. Phillips.** McGraw-Hill Book Co., New York, N. Y., 1947.

27. Probleme General de la Stabilite du Mouvement, **A. Liapounoff.** Princeton University Press, Princeton, N. J., 1947.

28. Instrument and Control Manual for Operating Engineers, **Eugene W. F. Feller.** McGraw-Hill Book Co., New York, N. Y., 1947.

29. Servomechanism Fundamentals, **Henri Lauer, Robert Lesnick, Leslie E. Matson.** McGraw-Hill Book Co., New York, N. Y., 1947.

30. Grundgesetze der Regelung, **W. Oppelt.** Wolfenbutteler Verlagsanstalt G. m. b. H. Wolfenbuttel, Hanover, Germany, 1947.

31. Governors and Governing, **B. R. Parkinson.** Walter King, London, England, 1947.

32. Die Elektrische Selbsterregung, mit Einer Theorie der Aktiven Netzwerke, **F. Strecker.** Hirzel, Stuttgart, Germany, 1947.

33. Cybernetics, **Norbert Wiener.** John Wiley and Sons, New York, N. Y., 1948.

34. The Dynamics of Automatic Controls, **R. C. Oldenbourg, H. Sartorius** (1st edition), translated by H. L. Mason. The American Society of Mechanical Engineers, New York, N. Y., 1948.

35. Electronic Instruments, **Ivan A. Greenwood, Jr., J. Vance Holdam, Jr., Duncan MacRae, Jr.** McGraw-Hill Book Co., New York, N. Y., 1948.

36. Teleological Mechanisms, **L. K. Frank, G. E. Hutchinson, W. K. Livingston, W. S. McCulloch, N. Wiener.** New York Academy of Sciences, New York, N. Y., 1948.

37. Principles of Servomechanisms, **Gordon S. Brown, Donald P. Campbell.** John Wiley and Sons, New York, N. Y., 1948.

38. Stetige Regelvorgaenge, **Winfried Oppelt.** Wissenschaftliche Verlagsanstalt K. G. Hannover, in Gemeinschaft mit Wolfenbutteler Verlagsanstalt G. m. b. H. Wolfenbuttel, Germany, 1949.

39. Le Circuit de Regulation, **Gilbert Nasse.** Hermann et Cie, Paris, France, 1949.

40. The Geometry of the Zeros of a Polynomial in a Complex Variable, **Morris Marden.** American Mathematical Society, New York, N. Y., 1949.

41. The Instrument Manual. The United Trade Press, London, England, 1949.

42. Die Selbsttaetige Regelung, **A. Leonard.** Springer, Berlin, Germany, 1949.

43. Analyse, Synthese et Position Actuelle de la Question des Servomecanismes, **P. Colombani, G. Lehmann, J. Loeb, A. Pommellet, F. H. Raymond.** Societe d'Edition d'Enseignement Superieur, Paris, France, 1949.

44. Response of Physical Systems, **John D. Trimmer.** John Wiley and Sons, New York, N. Y., 1950.

45. Introduction to Servomechanisms, **A. Porter.** John Wiley and Sons, New York, N. Y., 1950.

46. La Commande Hydraulique, **C. R. Himmler.** Dunod, Paris, France, 1950.

47. Bibliography of Information on Servomechanisms and Related Subjects. Technical Information Bureau (TPA 3), Ministry of Supply, London, England, 1950.

48. Voltage Stabilizers, **F. A. Benson.** Electronic Engineering, London, England, 1950.

49. Bibliography on Industrial Control. *Special Publication S-39*, AIEE, New York, N. Y., 1950.

50. Automatic Controls, compiled by **F. Stenger, R. M. Stenger, R. M. Ancell.** Bureau of Reclamation, United States Department of the Interior, Denver, Colo., 1951. Bibliography.

51. Dynamik Selbsttaetiger Regelungen, Vol. I (2nd edition), **Rudolf C. Oldenbourg, Hans Sartorius.** R. Oldenbourg, Munich, Germany, 1951.

52. Bibliography of Magnetic Amplifier Devices and the Saturable Reactor Art, **James G. Miles.** *AIEE Transactions*, vol. 70, pt. II, 1951, pp. 2104–23.

53. An Introduction to the Theory of Control in Mechanical Engineering, **R. H. Macmillan.** Cambridge University Press, Cambridge, England, 1951.

54. Thermostats and Temperature - Regulating Instruments, **R. Griffiths.** Charles Griffen and Co., Ltd., London, England, 1951.

55. Fundamentals of Automatic Control, **G. H. Farrington.** John Wiley and Sons, New York, N. Y., 1951.

56. Servomechanisms and Regulating System Design, Vol. I, **Harold Chestnut, Robert W. Mayer.** John Wiley and Sons, Inc., New York, N. Y., 1951.

57. The Handbook of Measurement and Control, **M. F. Behar** (editor). The Instruments Publishing Co., Pittsburgh, Pa., 1951.

58. Automatic Feedback Control, **William R. Ahrendt, John F. Taplin.** McGraw-Hill Book Co., New York, N. Y., 1951.

59. Automatic and Manual Control, **A. Tustin** (editor). Butterworths Scientific Publications, London, England, 1952.

60. Cybernetics, Circular Causal and Feedback Mechanisms in Biological and Social Systems, **Heinz von Foerster** (editor). Josiah Macy, Jr., Foundation, New York, N. Y., 1952.

Surveys and Reviews

61. Automatic Regulators, Their Theory and Application, **E. S. Smith.** *Transactions*, American Society of Mechanical Engineers, vol. 58, May 1936, pp. 291-303.

62. Fundamental Concepts and Problems in Regulation (in German), **J. Kronert.** *Zeitschrift fur technische Physik*, vol. 18, no. 11, 1937, pp. 398–405.

63. Principles and Practice of Automatic Control. *Engineer*, vol. 163, 1937; Jan. 22, pp. 94–97; Jan. 29, pp. 122–24; Feb. 5, pp. 150–51; Feb. 12, pp. 176–77, 188; Feb. 19, pp. 204–05; Feb. 26, pp. 236–37; March 5, pp. 268–69; March 12, pp. 294–95; March 19, pp. 322–23; March 26, pp. 352–53; April 2, pp. 380–82; April 9, pp. 408–09; April 16, pp. 438–39; April 23, pp. 467–69.

64. Industrial Instruments, Their Theory and Application, **E. S. Smith, Jr., C. O. Fairchild,** *Transactions*, American Society of Mechanical Engineers, vol. 59, Oct. 1937, pp. 595–607.

65. Some Fundamental Considerations in the Application of Automatic Control to Continuous Processes, **E. S. Bristol, J. C. Peters,** *Transactions*, American Society of Mechanical Engineers, vol. 60, Nov. 1938, pp. 641–50; May 1939, pp. 358–63.

66. The Adoption of Regulating Drives in Industry (in German), **W. Schlotmann.** *Elektrotechnik und Maschinenbau*, vol. 57, May 24, 1939, pp. 557–67.

67. Comparison of Different Regulation Problems (in German), **W. Oppelt.** *Luftfahrtforschung*, vol. 16, Aug. 20, 1939, pp. 447–72. (Also *Technical Memo No. 966*, National Advisory Committee for Aeronautics, Feb. 1941). A comparison of pressure, speed, temperature, and autopilot regulation problems.

68. A Suitable and Systematic Classification of Various Regulating Systems, **A. Leonard.** *Elektrotechnik und Maschinenbau*, vol. 58, 1940, pp. 541–46.

69. Regulating Technique. The Technical Problem and its Economical, Social and Cultural Effect (in German), **H. Schmidt.** *Zeitschrift des Vereines deutscher Ingenieure*, vol. 85 Jan. 25, 1941, pp. 81–88.

70. The Automatic Control Problem, **F. J. van Antwerpen.** *Industrial and Engineering Chemistry*, vol. 34, April 1942, pp. 387–91.

71. Measurement and Control of Process Variables, *Chemical and Metallurgical Engineering*, vol. 50, May 1943, pp. 97–144.

72. Comparative Survey of Regulating and Control Problems in Industrial Plants (in German), **E. Courtin.** *Elektrotechnik und Maschinenbau*, vol. 62, Feb. 4, 1944, pp. 62–71.

73. Forms and Principles of Servomechanisms, **S. W. Herwald.** *Westinghouse Engineer*, vol. 6, Sept. 1946, pp. 149–54. Tabulations of various types of measuring element, suitable for servomechanisms and other regulating systems, amplifier, and final control element.

74. The Design of Automatic and Manually Operated Control Systems, **A. Porter.** *Transactions*, Society of Instrument Technology, vol. 1, Jan. 1947, pp. 23–40.

75. Servomechanisms, Semeiology, Stability, and Satisfaction, **M. F. Behar.** *Instruments*, vol. 20, Sept. 1947, pp. 804–11.

76. Some Industrial Electronic Servo and Regulator Systems, **E. W. Forster, L. C. Ludbrook.** *Journal*, Institution of Electrical Engineers, vol. 94, pt. 2A, May 1947, pp. 100–11.

77. Basic Principles of Automatic Control Systems, **A. Porter.** *Proceedings*, Institution of Mechanical Engineers, vol. 159 (War Emer. Issue No. 38), 1948, pp. 25–45.

78. Fundamentals of Automatic Control, **W. Oppelt.** *Engineers' Digest*, vol. 10, 1949; June, pp. 184–89; July, pp. 237–41; Sept., pp. 317–21.

79. Automatic Regulation (in Dutch), **C. Dellaert.** *Ingenieur*, vol. 61, Sept. 2, 1949, pp. W 63–69.

80. Automatic Regulation in Electrical Installations, **A. Ernst, P. Biveroni.** *Bulletin Oerlikon*, vol. 29, Dec. 1949, pp. 1971–82; vol. 30, March 1950, pp. 1991–2008.

81. Temperature Measurement and Control in the Process Industries, **D. H. Fuller.** *Instruments*, vol. 23, March 1950, pp. 246–47, 290–303.

82. Progress in Automatic Control Systems, **A. Tustin.** *Engineering*, vol. 170, Nov. 10, 1950, pp. 360–63.

83. Instrument Engineering. Its Growth and Promise in Process-Control Problems, **G. S. Brown, D. P. Campbell.** *Mechanical Engineering*, vol. 72, Feb. 1950, pp. 124–27, 136.

84. Seven Basic Types of Servomechanisms Analyzed, **R. Herst.** *Electrical Manufacturing*, vol. 45, May 1950, pp. 90–95.

85. Electrical and Mechanical Regulation Technique (in German), **W. Hunsinger.** *Zeitschrift des Vereines deutscher Ingenieure*, vol. 93, June 21, 1951, pp. 567–70.

86. On Regulation of Industrial Processes, **H. J. Roosdor.** *Philips Technical Review*, vol. 12, Feb. 1951, pp. 221–27.

Terminology

87. Attempt to Standardize and Germanize the Nomenclature in Regulation Technique (in German), **P. Gmelin, F. Ranke.** *Zeitschrift fur technische Physik*, vol. 18, no. 11, 1937, pp. 406–09.

88. Automatic Control Terms. *Mechanical Engineering*, vol. 68, Feb. 1946, pp. 134–38.

89. Unified Symbolism for Regulatory Controls, **G. A. Philbrick.** *Transactions*, American Society of Mechanical Engineers, vol. 69, Jan. 1947, pp. 47–67.

90. Instrumentation Flow Plan Symbols, **D. E. Hostedler.** *Instruments*, vol. 22, Oct. 1949, pp. 963–65.

91. Proposed Symbols and Terms for Feedback Control Systems, **AIEE Committee Report.** *Electrical Engineering*, vol. 70, Oct. 1951, pp. 905–09.

92. Standard Symbols in Control Technique (in German), **F. Ranke.** *Brennstoff-Warme-Kraft*, vol. 3, Nov. 1951, pp. 369–73.

System Analysis

93. On Governors, **James C. Maxwell.** *Proceedings*, The Royal Society, vol. 16, 1868, pp. 270–83.

94. On Direct Acting Regulators, **J. Wischnegradski.** *Der Civilingenieur*, vol. 23, 1877, pp. 95–131.

95. On the Theory of Regulators (in German), **R. v. Mises.** *Elektrotechnik und Maschinenbau*, vol. 26, 1908, pp. 783–89.

96. On the Dynamics of Automatic Amplifier Regulator (in German), **K. Kupfmuller.** *Elektrische Nachrichten-Technik*, vol. 5, 1928, pp. 459–67.

97. Self-Regulation, A New Law in Regulation Technique (in German), **T. Stein.** *Zeitschrift des Vereines deutscher Ingenieure*, vol. 72, Feb. 11, 1928, pp. 165–71; Feb. 18, pp. 209–14.

98. On Graphical Methods for the Study of Electric Oscillations (in German), **F. Kirschstein.** *Archiv fur Elektrotechnik*, vol. 24, 1930, pp. 731–62.

99. On the Oscillations of Regulators (in French), **Le Corbeiller.** *Proceedings*, Third International Congress for Applied Mechanics, Ab. Sveriges Litografiska Tryckerier, Stockholm, Sweden 1931, pp. 205–12.

100. Feedback Systems for Regulators (in German), **C. R. Himmler.** *Archiv fur technisches Messen*, vol. 5, Dec. 1935, T167–68, J060-2.

101. Principles Underlying the Rational Solution of Automatic Control Problems, **S. D. Mitereff.** *Transactions*, American Society of Mechanical Engineers, vol. 57, 1935, pp. 159–63. Discussion in vol. 58, 1936, pp. 55–65.

102. The Fundamental Laws of Regulation (in German), **K. Rummel.** *Archiv fur das Eisenhuttenwesen*, vol. 8, Jan. 1935, pp. 281–92.

103. Self-Oscillatory Systems Governed by Functional Equations (in French), **V. Bowschewerow.** *Physikalische Zeitschrift der Sowjetunion*, vol. 9, no. 5, 1936, pp. 529–32.

104. Time Lag in a Control System, **A. Callender, D. R. Hartree, A. Porter.** *Philosophical Transactions*, The Royal Society, vol. 235A, 1936, pp. 415–44.

105. Regulator Theory (in German), **T. Poschl.** *Elektrotechnik und Maschinenbau*, vol. 54, March 1, 1936, pp. 97–102.

106. Time Lag in a Control System, Part 2, **D. R. Hartree, A. Porter, A. Callender, A. B. Stevenson.** *Proceedings*, The Royal Society, vol. 161A, Aug. 20, 1937, pp. 460–76.

107. Periodic and Aperiodic Oscillations in Sensitive Regulating Systems (in German), **H. Koenig.** *Zeitschrift fur technische Physik*, vol. 18, no. 11, 1937, pp. 426–31.

108. The Problem of Indirect Governing (in Italian), **C. Possio.** *Ricerche di Ingegneria*, vol. 5, Sept.-Oct. 1937, pp. 123–35.

109. Laws of Direct Regulation on a General Basis (in German), **W. Schmidt.** *Zeitschrift des Vereines deutscher Ingenieure*, vol. 81, Dec. 11, 1937, pp. 1425–31.

110. Quantitative Analysis of Process Lags, **C. E. Mason.** *Transactions*, American Society of Mechanical Engineers, vol. 60, 1938, pp. 327–34; discussion, vol. 61, 1939, pp. 67–71.

111. Quantitative Analysis of Single Capacity Processes, **A. F. Spitzglass.** *Transactions*, American Society of Mechanical Engineers, vol. 60, 1938, pp. 665–74; vol. 62, 1940, pp. 51–62.

112. General Principles of Instrument Analysis, **C. S. Draper, G. V. Schliestett.** *Instruments*, vol. 12, May 1939, pp. 137–42.

113. Relations Between Attenuation and Phase in Feedback Amplifier Design, **H. W. Bode.** *Bell System Technical Journal*, vol. 19, July 1940, pp. 421–54.

114. On the Regulation Problem (in German), **T. Buchhold.** *Elektrotechnik und Maschinenbau*, vol. 58, 1940, Jan. 5, pp. 1–10, Jan. 19, pp. 31–40.

115. Design Factors Controlling the Performance of Instruments, **C. S. Draper, G. P. Bentley.** *Transactions*, American Society of Mechanical Engineers, vol. 62, July 1940, pp. 421–32.

116. The Stabilization of Regulating Systems with Electronic Amplifiers, by Means of Damping or Elastic Feedback (in German), **E. H. Ludwig.** *Archiv fur Elektrotechnik*, vol. 34, 1940, pp. 269–84.

117. Automatic Control in the Presence of Process Lags, **C. E. Mason, G. A. Philbrick.** *Transactions*, American Society of Mechanical Engineers, vol. 62, 1940, pp. 295–309.

118. Application of the Properties of Three Types of Determinants to the Calculation of the Natural Frequencies of Coupled Oscillating Circuits (in French), **M. Parodi.** *Revue Generale de l'Electricite*, vol. 47, May 11–18, 1940, pp. 358–63.

119. Method of Solving the Laplace Transformation for Transient Phenomena in Linear Networks, Applied to Automatic Regulation (in German), **E. Grunwald.** *Archiv fur Elektrotechnik*, vol. 35, Aug. 25, 1941, pp. 379–400.

120. Mathematics of Surge Vessels and Automatic Averaging Control, **C. E. Mason, G. A. Philbrick.** *Transactions*, American Society of Mechanical Engineers, vol. 63, Oct. 1941, pp. 589–601.

121. Control Problems, **N. Minorsky.** *Journal*, Franklin Institute, vol. 232, Nov. 1941, pp. 451–87; Dec. 1941, pp. 519–51.

122. Mathematical Representation of Control Mechanisms (in German), **H. Tischner.** *Hochfrequenztechnik und Elektroakustik*, vol. 58, Nov. 1941, pp. 145–48.

123. Behavior of Automatic Regulators (in German), **G. Wunsch.** *Zeitschrift des Vereines deutscher Ingenieure*, vol. 85, May 10, 1941, pp. 444–48.

124. Notes on Controlled Type of One-Dimensional Motion, (in German), **H. Bilharz.** *Zeitschrift fur angewandte Mathematik und Mechanik*, vol. 22, Aug. 1942, pp. 206–15.

125. The Laws Governing Regulating Processes (in German), **E. Gork.** *Wissenschaftliche Veroeffentlichungen aus den Siemens-Werken*, vol. 20, pt. 2, 1942, pp. 329–64.

126. The Damping Problem in Regulating Technique (in German), **A. Lang.** *Zeitschrift fur technische Physik*, vol. 23, 1942, pp. 280–95.

127. Regulator Oscillations and Oblique-Angled Vector Diagrams (in German), **A. Luthi.** *Schweizerische Bauzeitung*, vol. 119, April 11, 1942, pp. 171–74.

128. The Deviation Area in Quick-Acting Regulation. A Contribution to the Theory of Quick-Acting Regulation (in German), **I. Obradovic.** *Archiv fur Elektrotechnik*, vol. 36, June 30, 1942, pp. 382–90.

129. Design of Continuous Linear Regulating Systems (in German), **H. Rosenhamer.** *Archiv fur Elektrotechnik*, vol. 36, Dec. 31, 1942, pp. 693–715.

130. Graphical Analysis of Transient Phenomena in Industrial Processes, **K. J. DeJuhasz.** *Instruments*, vol. 16, Aug. 1943, pp. 466–72, 508, 509.

131. Forced-Oscillation Approach to the Problem of the Automatically-Controlled Continuous Process, **P. R. Ewald.** *Instruments*, vol. 16, Aug. 1943, pp. 474–76, 506.

132. An Iteration Method for Graphical Solution of Regulation Problems (in German), **O. Martin.** *Wissenschaftliche Veroffentlichungen aus dem Siemens-Werken*, vol. 21, 1943, pp. 238–46.

133. On the Degree of Damping in the Third-Order Differential Equation of Regulation (in German), **W. Oppelt.** *Archiv fur Elektrotechnik*, vol. 37, 1943, July 31, pp. 357–60; Oct. 31, p. 508.

134. Load Dependence of Automatic Regulators and Means for its Prevention (in German), **E. Weis.** *Elektrotechnische Zeitschrift*, vol. 64, May 20, 1943, pp. 261–67.

135. Process Lags in Automatic-Control Circuits, **J. G. Ziegler, N. B. Nichols.** *Transactions*, American Society of Mechanical Engineers, vol. 65, 1943, pp. 433–44.

136. Physics and Regulating Technique (in German), **M. Lang.** *Physikalische Zeitschrift*, vol. 45, Dec. 1944, pp. 209–23.

137. Contributions to the Theory of Automatic Controllers and Followers, **D. G. Prinz.** *Journal of Scientific Instruments*, vol. 21, April 1944, pp. 53–64.

138. Amplifier Theory Applied to Regulators **J. M. Cage.** *Electronics*, vol. 18, Jan. 1945, pp. 140–43.

139. Quantitative Analysis of Single and Multiple-Capacity Plants, **P. G. Kaufmann.** *Proceedings*, Institution of Mechanical Engineers, vol. 153 (War Emerg. Issue No. 8), 1945, pp. 237–48.

140. On the Theory of Automatic Control: Regulator Equations, **P. G. Kaufmann.** *Proceedings*, Institution of Mechanical Engineers, vol. 153 (War Emerg. Issue No 8), 1945, pp. 249–59.

141. On the Method of Van der Pol and its Application to Non-Linear Control Problems, **B. V. Bulgakov.** *Journal*, Franklin Institute, vol. 241, Jan. 1946, pp. 31–54.

142. The Effect of Measurement Dead Time in the Control of Certain Processes, **D. P. Eckman.** *Transactions*, American Society of Mechanical Engineers, vol. 68, Oct. 1946, pp. 707–11.

143. Relationship Between Stability and "Statism" in Electric Drives with Booster Generator (in Russian), **A. A. Feldbaum.** *Vestnik Elektroprommishlennosti*, vol. 17, no. 1, 1946, pp. 3–10. "Statism" is defined as the percentage variation in the regulated variable with change in load. A Rototrol system is described in detail.

144. Application of Circuit Theory to the Design of Servomechanisms, **A. C. Hall.** *Journal*, Franklin Institute, vol. 242, Oct. 1946, pp. 279–307.

145. Dynamic Behavior and Design of Servomechanisms, **G. S. Brown, A. C. Hall.** *Transactions*, American Society of Mechanical Engineers, vol. 68, July 1946, pp. 503–24.

146. The Frequency Response of Automatic Control Systems, **Herbert Harris, Jr.** *AIEE Transactions (Electrical Engineering)*, vol. 65, Aug.-Sept. 1946, pp. 539–46.

147. Parallel Circuits in Servomechanisms, **H. T. Marcy.** *AIEE Transactions*, vol. 65, Aug.-Sept., 1946, pp. 521–29.

148. The Solution of Complicated Regulation Problems by Means of the Frequency Relation of the Regulator Circuit (in German), **P. Profos.** *Schweizer Archiv fur angewandte Wissenschaft und Technik*, vol. 12, April 1946, pp. 105–13.

149. Frequency Co-Existence Laws in Stable Self-Oscillatory Systems (in Russian), **K. Teodorchik.** *Bulletin*, l'Academie des Sciences, URSS, Department des Techniques Scientifiques, no. 3, 1946, pp. 385–88. Nyquist's criterion applied to stationary oscillators with a single feedback path.

150. Wischnegradski's Problem in the Theory of Direct Regulation—I. Theory of the Direct Acting Regulator with Coulomb and Viscous Friction (in Russian), **A. Andronow, A. Mayer.** *Avtomatika i Telemekhanika*, vol. 8. 1947, pp. 314–34.

151. Regulation Technique (in Italian), **E. Buzzi.** *Energia Elettrica*, vol. 24, Jan. 1947, pp. 29–34.

152. The Inverse Nyquist Plane in Servomechanism Theory, **G. B. Criss.** *Proceedings*, Institute of Radio Engineers, vol. 35, Dec. 1947, pp. 1503–04.

153. Study of the Properties of Automatic Regulation (in French), **M. Cuenod.** *Bulletin Technique de la Suisse Romande*, vol. 73, 1947; April 4, pp. 105–15, May 10, pp. 121–25, Nov. 22, pp. 317–24, Dec. 6, pp. 329–32.

154. On Some Nonlinearities in Systems of Regulation (in Russian), **L. S. Goldfarb.** *Avtomatika i Telemekhanika*, vol. 8, 1947, pp. 349–383.

155. Theoretical and Experimental Methods for the Study of Closed Cycle Automatic Control Systems, **L. von Hamos.** *Transactions*, Instruments and Measurements Conference, Stockholm, Sweden, 1947, pp. 129–38.

156. Theory of Automatic Control Systems, **M. A. Melvin.** *Journal of Applied Physics*, vol. 18, August 1947, pp. 704–22.

157. The Frequency Response Method of Control Analysis, **W. C. Moog.** *Instruments*, vol. 20, Sept. 1947, pp. 811–16.

158. The Theory of Quadripoles Arranged in Closed Chains (in French), **P. Satche.** *Revue Generale de l'Electricite*, vol. 56, Oct. 1947, pp. 426–32.

159. The Application of Lead Networks and Sinusoidal Analysis to Automatic Control Systems, **George J. Schwartz.** *AIEE Transactions*, vol. 66, 1947, pp. 69–77.

160. The Frequency Response Method in the Theory of Regulation (in Russian), **V. V. Solodovnikov.** *Avtomatika i Telemekhanika*, vol. 8, 1947, pp. 65–88.

161. A Method of Analyzing the Behavior of Linear Systems in Terms of Time Series, **A. Tustin.** *Journal*, Institution of Electrical Engineers, vol. 94, pt. 2A, 1947, pp. 130–42.

162. A Method of Analyzing the Effect of Certain Kinds of Non-Linearity in Closed-Cycle Control Systems, **A. Tustin.** *Journal*, Institution of Electrical Engineers, vol. 94, pt. 2A, 1947, pp. 152–60.

163. Fundamental Principles of Automatic Regulators and Servomechanisms, **A. L. Whiteley.** *Journal*, Institution of Electrical Engineers, vol. 94, pt. 2A, 1947, pp. 5–22.

164. Static Determination of the Accuracy of Regulation of Electric Drives with Electro-Mechanical Amplifiers (in Russian), **E. L. Ettinger.** *Vestnik Elektroprommishlennosti*, no. 6, 1948, pp. 13–19.

165. Graphical Analysis of Control Systems, **Walter R. Evans.** *AIEE Transactions*, vol. 67, pt. I, 1948, pp. 547–51.

166. Integral Criteria for the Quality of Regulation (in Russian), **A. A. Feldbaum.** *Avtomatika i Telemekhanika*, vol. 9, 1948, pp. 3–19.

167. The Frequency Analysis Method Applied to Control Problems, **A. Garde.** *ASEA Journal*, vol. 21, Nov-Dec. 1948, pp. 123–38.

168. On the Conditions of Quality of Automatic Control (in Russian), **N. A. Kartvelishvili.** *Doklady Akademii Nauk, SSSR*, vol. 61, July 1, 1948, pp. 21–23. Establishes the requirements for the roots of the characteristic equation to lie within a given horizontal strip in the complex plane.

169. Tensorial Analysis of Control Systems, **G. Kron.** *Journal of Applied Mechanics*, vol. 15, June 1948, pp. 107–24.

170. Response Characteristics as Regulating Criteria, **H. Meyer.** *Brown Boveri Review*, vol. 35, May-June 1948, pp. 151–57.

171. On the Construction of Diagrams of Frequency of Oscillation (in Russian), **V. P. Nikitin, V. K. Turkin, N. P. Kunitski.** *Doklady Akademii Nauk, SSSR*, vol. 59, no. 1, 1948, pp. 57–60.

172. Locus Methods for Regulation Processes with Friction (in German), **W. Oppelt.** *Zeitschrift des Vereines deutscher Ingenieure*, vol. 90, June 1948, pp. 179–83.

173. The Analysis of Retarded Control Systems, **L. A. Pipes.** *Journal of Applied Physics*, vol. 19, July 1948, pp. 617–23.

174. Criteria for Absence of Overregulation and Criteria for Monotony (in Russian), **V. V. Solodovnikov.** *Doklady Akademii Nauk, SSSR*, vol. 62, Oct. 11, 1948, pp. 599–602.

175. A Quality Test of Regulation (in Russian), **V. V. Solodovnikov.** *Doklady Akademii Nauk, SSSR*, vol. 60, 1948, pp. 977–80.

176. Method of Dynamic Compensation in Automatic and Tele-Control (in Russian), **F. E. Temnikov.** *Elektrichestvo*, no. 3, 1948, pp. 8–14. Reference quantity is caused to follow saw-tooth wave form, and pulses are generated when regulated variable and reference quantity are equal. Frequency and relative position of pulses serve as control means.

177. On the Maximum Deviation of the Regulated Quantity in a Transient Process (in Russian), **G. M. Ulanov.** *Avtomatika i Telemekhanika*, vol. 9, 1948, pp. 168–75.

178. Stability of Linear Oscillating Systems with Constant Time Lag, **H. I. Ansoff.** *Journal of Applied Mechanics*, vol. 16, June 1949, pp. 158–64.

179. General Algebraic Method Applied to Control Analysis of Complex Engine Types, **A. S. Bosenbom, R. Hood.** *Technical Note 1908*, National Advisory Committee for Aeronautics, July 1949.

180. Method of Determining the Frequency Response Characteristics of an Element or Systems from the System Transient Output Response to a Known Input Function, **H. J. Curfman, Jr., R. A. Gardiner.** *Technical Note 1964*, National Advisory Committee for Aeronautics, Oct. 1949.

181. Servomechanisms and Regulators. Criteria of Stability. Examples of Applications (in French), **C. Galmiche.** *Review Generale de l'Electricite*, vol. 58, Jan. 1949, pp. 19–30.

182. Equations for the Approximate Solution of Dynamic Problems for Stable Linear Systems, **K. H. Hohenemser.** *Journal of the Aeronautical Sciences*, vol. 16, Dec. 1949, pp. 723–28.

183. The Behavior of Continuously Disturbed Automatic Linear Systems (in Russian), **V. S. Kulebakin.** *Doklady Akademii Nauk, SSSR*, vol. 68, 1949, pp. 855–58. It is shown that linear systems can be represented by homogeneous differential equations with constant coefficients for all positive values of time.

184. Methods of Determining Frequency Response of Engines and Control Systems from Transient Data, **E. LaVerne, S. Boksenbom.** *Technical Note 1395*, National Advisory Committee for Aeronautics, Aug. 1949.

185. A Classification of Linear Transfer Members, **H. L. Mason.** *Transactions*, American Society of Mechanical Engineers, vol. 71, 1949, pp. 407–12.

186. Principles of Design of Automatic Regulating Systems with Small Adjustment Error (in Russian), **M. V. Meerov.** *Avtomatika i Telemekhanika*, vol. 10, 1949, pp. 84–98.

187. The Effect of Pole and Zero Locations on the Transient Response of Linear Dynamic Systems, **J. H. Mulligan, Jr.** *Proceedings*, Institute of Radio Engineers, vol. 37, May 1949, pp. 516–29.

188. The Matrix Analysis of Linear Networks Containing Active Quadripoles (in Italian), **A. Pinciroli, A. Taraboletti.** *Alta Frequensa*, vol. 18, April 1949, pp. 73–82.

189. On the Freedom of Choice of the Parameters of Autonomic Processes of Regulation of Several Reciprocally Related Quantities (in Russian), **A. M. Popovskii.** *Avtomatika i Telemekhanika*, vol. 10, 1949, pp. 401–23.

190. On the Application of Trapezoidal Frequency Characteristics to the Analysis of the Behavior of Systems of Automatic Regulation (in Russian), **V. V. Solodovnikov.** *Avtomatika i Telemekhanika*, vol. 10, 1949, pp. 362–76.

191. A Method of Determining the Parameters of Linear Automatic Regulation Systems (in Russian), **E. G. Uderman.** *Avtomatika i Telemekhanika*, vol. 10, no. 2, 1949, pp. 113–21. Approximate representations of high order systems containing only one pair of complex roots, by 2nd or 3rd order equations.

192. Regulation Chains with Links Having Several Degrees of Freedom (in Russian), **B. V. Bulgakov.** *Prikladnaya Matematika i Mekhanika*, vol. 14, Nov.-Dec. 1950, pp. 619–34.

193. Contribution to the Study of Automatic Control (in French), **M. Cuenod.** *Bulletin*, Association Suisse des Electriciens, vol. 41, Sept. 2, 1950, pp. 673–78. Survey of Hurwitz and Nyquist methods with the latter formulated in rectangular co-ordinates.

194. Method for Determining the Frequency Response Characteristics of an Element or System from the System Transient Output Response to a Known Input Function, **H. J. Curfman, Jr., R. A. Gardiner.** *Report 984*, National Advisory Committee for Aeronautics, 1950.

195. Method of Relative Units Applied to the Calculation of the Accuracy of Regulation of Static Systems Under Transient Conditions (in Russian), **E. L. Ettinger.** *Elektrichestvo*, no. 11, Nov. 1950, pp. 57–63.

196. Control System Synthesis by Root Locus Method, **Walter R. Evans.** *AIEE Transactions*, vol. 69, pt. I, 1950, pp. 66–69.

197. Method of Calculation of Transient Processes in Linear Systems, in Particular in Control Systems, **H. Hochrainer.** *Paper 339*, International Conference on Large Electric High Tension Systems, 1950.

198. Transient Response of a Regulator Chain, **H. Jefferson.** *Wireless Engineer*, vol. 27, March 1950, pp. 83–85.

199. Frequency Response of Linear Systems From Transient Data, **M. E. LaVerne, A. S. Boksenbom.** *Report 977*, National Advisory Committee for Aeronautics, 1950.

200. Variations of the Parameters of Regulating Systems by Internal Linkages (in Russian), **D. I. Maryanovskii.** *Elektrichestvo*, no. 2, Feb. 1950, pp. 21–32.

201. General Method of Assessing Small Variations in Electric Systems by Means of Equivalent Circuits (in Russian), **V. N. Milshtein.** *Elektrichestvo*, no. 5, May 1950, pp. 47–54. Equivalent linear circuits and the corresponding variational equations are established for a number of nonlinear systems.

202. The Design of Control Circuits by Characteristic Curves (in German), **W. Oppelt.** *Archiv der elektrischen Uebertragung*, vol. 4, Jan. 1950, pp. 11–16.

203. Electronics and Experimental Mathematics, (in French), **F. H. Raymond.** *Onde Electrique*, vol. 30, Jan. 1950, pp. 30–44. A generalization of servomechanism theory leading to the general concept of the mathematical machine.

204. The Relations Between Regulation, Positive and Negative Feedback, and Negative Resistance (in German), **W. Reichardt.** *Elektrotechnik*, vol. 4, Feb. 1950, pp. 47–53; March 1950, pp. 73–80.

205. The Practical Application of Frequency Response Analysis to Automatic Process Control, **C. I. Rutherford.** *Proceedings*, Institution of Mechanical Engineers, vol. 162, 1950, pp. 334–54.

206. Analysis and Synthesis of Following and Regulating Systems Under the Influence of Stationary Random Disturbances (in Russian), **V. V. Solodovnikov.** *Isvestiya Akademii Nauk, SSSR.* Otdelenie Tekhnicheskikh Nauk, no. 11, Nov. 1950, pp. 1648–79.

207. A Graphic Method for Determination of Time Constants and Period of a Third Order Linear System (in German), **H. St. Stefaniak.** *Ingenieur-Archiv*, vol. 18, 1950, pp. 221–32.

208. A Note on Control Area, **T. M. Stout.** *Journal of Applied Physics*, vol. 21, Nov. 1950, pp. 1129–31.

209. Determination of Frequency Characteristics from Response to Arbitrary Input, **E. R. Walters, L. B. Rea.** *Journal of the Aeronautical Sciences*, vol. 17, July 1950, pp. 446–52.

210. Feedback Amplifiers and Servo Systems—Their Common Theoretical Basis, **E. E. Ward.** *Wireless Engineer*, vol. 27, May 1950, pp. 146–53.

211. Synthesis of Feedback Control Systems by Means of Pole and Zero Location of the Closed Loop Function, **M. R. Aaron.** *AIEE Transactions*, vol. 70, pt. II, 1951, pp. 1439–46.

212. On a General Treatment of Problems in Cybernetics (in French), **S. Colombo.** *Comptes Rendus*, l'Academie des Sciences, vol. 232, March 28, 1951, pp. 1287–88.

213. Regulation Theory. I. Direct Regulation. II. Regulation with a Servomotor (in Danish), **P. Draminsky.** *Ingenioren*, 1951; vol. 60, Sept. 1, pp. 602–06, Sept. 8, pp. 614–19.

214. Investigation of the Dynamics of Automatic Regulating Systems by the Method of the Generalized Integral Criteria (in Russian), **A. A. Feldbaum.** *Elektrichestvo*, no. 7, July 1951, pp. 18–24.

215. Survey of the Developments in Regulation Technique During Recent Years (in Swedish), **A. Garde.** *Ingenioren*, vol. 60, Aug. 4, 1951, pp. 549–57.

216. Nondimensional Study of Proportional-Plus-Reset Control of Single-Capacity System, **J. A. Hrones, J. B. Reswick.** *Transactions*, American Society of Mechanical Engineers, vol. 73, July 1951, pp. 511–17.

217. Importance of Extending Nyquist Servo-Mechanism Analysis to Include Transient Response, **R. L. Johnson, J. B. Rea.** *Journal of the Aeronautical Sciences*, vol. 18, Jan. 1951, pp. 43–49. Points out the possible errors in evaluating a high

order system by approximations to the Nyquist plot.

218. The Effects of Loads and Disturbances Upon Feedback Controllers, **R. W. Jones.** *AIEE Transactions*, vol. 70, pt. I, 1951, pp. 460–64.

219. Selection of Optimum Parameters of Automatic Regulators and Servomechanisms (in Russian), **V. S. Kulebakin.** *Doklady Akademii Nauk, SSSR*, vol. 77, 1951, pp. 265–67.

220. Sampled-Data Control Systems Studied Through Comparison of Sampling with Amplitude Modulation, **William K. Linvill.** *AIEE Transactions*, vol. 70, pt. II, 1951, pp. 1779–88.

221. Parametric Excitation, **N. Minorsky.** *Journal of Applied Physics*, vol. 22, Jan. 1951, pp. 49–54.

222. Combination Open-Cycle Closed-Cycle Systems, **J. R. Moore,** *Proceedings*, Institute of Radio Engineers, vol. 39, Nov. 1951, pp. 1421–32.

223. Some Design Criteria for Automatic Controls, **Paul T. Nims.** *AIEE Transactions*, vol. 70, pt. I, 1951, pp. 606–11.

224. A Graphical Method for Plotting Amplitude and Phase Angle of Transfer Functions of Dynamic Systems Without Factoring Polynomials, **E. F. Smith.** *Technical Note 2522*, National Advisory Committee for Aeronautics, Nov. 1951.

225. Dynamic Accuracy and Optimum Characteristics of Servomechanisms and Transforming Devices (in Russian), **V. V. Solodovnikov.** *Doklady Akademii Nauk, SSSR*, vol. 77, 1951, pp. 269–72.

226. A Note on the Design of Conditionally Stable Feedback Systems, **Paul Travers.** *AIEE Transactions*, vol. 70, pt. I, 1951, pp. 626–30.

227. Reduction of a Problem in Cybernetics to a Problem of Pursuit in Hilbert Space (in French), **R. Vallee.** *Comptes Rendus*, l'Academie des Sciences, vol. 232, March 28, 1951, pp. 1288–90.

Stability

228. On the Conditions Under Which an Equation Has Only Roots with Negative Real Parts, **A. Hurwitz.** *Mathematische Annalen*, vol. 46, 1895, pp. 273–84.

229. On Algebraic Equations Which Only Contain Roots with Negative Real Parts (in German), **J. Schur.** *Zeitschrift fur angewandte Mathematik und Mechanik*, vol. 1, pt. 4, 1921, pp. 307–11.

230. On the Criteria for the Stability of Small Motions, **R. A. Frazer, W. J. Duncan.** *Proceedings*, The Royal Society, vol. 124A, 1929, pp. 642–54. Routh's criterion is derived from that of Hurwitz. The question of when a stable system becomes unstable as one parameter is varied is investigated.

231. Regeneration Theory, **H. Nyquist.** *Bell System Technical Journal*, vol. 11, 1932, pp. 126–47.

232. Regeneration Theory and Experiment, **E. Peterson, J. G. Kreer, L. A. Ware.** *Bell System Technical Journal*, vol. 13, 1934, pp. 680–700.

233. The Nonlinear Theory of Electric Oscillations, **Balth. van der Pol.** *Proceedings*, Institute of Radio Engineers, vol. 22, Sept. 1934, pp. 1051–86. Extended bibliography.

234. Necessary Conditions for Instability, or Self-Oscillation, of Electric Circuits, **D. G. Reid.** *Wireless Engineer*, vol. 14, Nov. 1937, pp. 588–96.

235. Regulating Methods in Controllable Electric Systems, and the Criteria for Their Stability, **W. Artus.** *Elektrische Nachrichten-Technik*, vol. 17, Oct. 1940, pp. 231–44.

236. Regeneration Theory and the Stability of Regulating Systems (in German), **R. Feiss.** *Schweiserische Bauseitung*, vol. 115, March 2, 1940, pp. 97–99.

237. The Determination of Regulator Stability from the Vector Diagram, **R. Feiss.** *Zeitschrift des Vereines deutscher Ingenieure*, vol. 84, 1940, pp. 819–24.

238. The Stability of Regenerative Circuits, **R. S. Rivlin.** *Wireless Engineer*, vol. 17, July 1940, pp. 298–302. Alternative proof for Nyquist's theorem.

239. On the Treatment of Stability in Electro-Mechanical Systems (in German), **W. Artus.** *Wissenschaftliche Veroeffentlichungen aus dem Siemens-Konzern*, vol. 20, no. 1, 1941, pp. 186–206.

240. Geometrical Representation of Hurwitz' Criterion for Equation of the 5th and 6th Orders (in German), **H. Bilharz.** *Zeitschrift fur angewandte Mathematik und Mechanik*, vol. 21, April 1941, pp. 96–102.

241. A New Method for Determining the Stability of Regulation (in German), **R. Feiss.** *Schweiserische Bauzeitung*, vol. 118, Aug. 9, 1941, pp. 61–65.

242. Stability Investigation of Discontinuous Regulators, Graphical Representation of Contactor Control (in German), **F. Krautwig.** *Archiv fur Elektrotechnik*, vol. 35, Feb. 20, 1941, pp. 117–26.

243. The Stability Investigation of Mechanical Regulating Systems, **W. Artus.** *Feinmechanik und Praezision*, vol. 50, 1942, pp. 261–73.

244. Self-Excited Oscillations in Dynamical Systems Possessing Retarded Actions, **N. Minorsky.** *Journal of Applied Mechanics*, vol. 64, June 1942, pp. A65–71.

245. Stability and Aperiodicity of Motion of the 4th Order (in German), **K. Schmidt.** *Archiv fur Elektrotechnik*, vol. 37, April 30, 1943, pp. 217–20.

246. Investigation of Stability Conditions in Delayed Regulation (in German), **D. Stein.** *Elektrische Nachrichten-Technik*, vol. 20, Sept. 1943, pp. 205–13. Abstract in *Wireless Engineer*, vol. 21, May 1944, p. 238. Discusses automatic gain control for amplifiers in cases in which there is a delay before the regulation becomes effective.

247. Note on a Law of Hurwitz (in German), **H. Bilharz.** *Zeitschrift fur angewandte Mathematik und Mechanik*, vol. 24, 1944, pp. 77–82.

248. Notes on the Stability of Linear Networks, **En-Lung Chu.** *Proceedings*, Institute of Radio Engineers, vol. 32, Oct. 1944, pp. 630–37.

249. A New Method for Stability Investigations, **A. Leonard.** *Archiv fur Elektrotechnik*, vol. 38, 1944, pp. 17–28.

250. On Stability Under Constantly Acting Disturbances (in Russian), **I. G. Malkin.** *Prikladnara Matematika i Mekhanika*, vol. 8, 1944, pp. 241–45.

251. Theory of Nearly Linear Systems (in French), **J. Ville.** *Revue Generale de l'Electricite*, vol. 54, Feb. 1045, pp. 54–57. System admittance is resolved into linear and nonlinear parts.

252. The Analysis of Hunting by Means of Vector Diagrams, **B. Adkins.** *Journal*, Institution of Electrical Engineers, vol. 93, pt. 2, Dec. 1946, pp. 541–48.

253. The Generalization of the Nyquist and Leonard Stability Criteria, **W. Frey.** *Brown Boveri Review*, vol. 33, March 1946, pp. 59–65.

254. Stability of Linear Automatic Control Systems (in Russian), **D. I. Marianovski.** *Elektrichestvo*, no. 9, 1946, pp. 15–30. Hurwitz stability criterion is reduced to a single equation.

255. Generalized Routh-Hurwitz Discriminant, **S. Sherman.** *Philosophical Magazine*, vol. 37, Aug. 1946, pp. 537–51. A finite numerical algorithm for finding the number of such roots of a polynomial with complex coefficients as lie in a generalized polygon.

256. On the Theory of Sinusoidal Auto-Oscillations in Systems with Many Degrees of Freedom (in Russian), **K. Teodorchik.** *Comptes Rendus*, l'Academie des Sciences de l'URSS, vol. 52, no. 1, 1946, pp. 33–36.

257. A New Method for Assessing the Stability of Linear Regulation Systems (in German), **L. Cremer.** *Zeitschrift fur angewandte Mathematik und Mechanik*, vol. 25/27, Aug.-Sept. 1947, pp. 161–63. Based upon the Routh-Hurwitz criteria but permits calculation of the frequency in the neighborhood of the stability limit, as well as an estimate of the degree of stability.

258. On Systems of Autoregulation Stabilized for an Arbitrarily Large Coefficient of Amplification (in Russian), **M. V. Meerov.** *Avtomatika i Telemekhanika*, vol. 8, 1947, pp. 225–42.

259. A Note on Stability Calculations and Time Lag, **S. Sherman.** *Quarterly of Applied Mathematics*, vol. 5, April 1947, pp. 92–97. Application of the Cauchy-Sturm method to systems having a time lag.

260. On the Behaviour of Dynamical Systems with Small Violations of the Routh-Hurwitz Criteria (in Russian), **N. N. Bautin.** *Prikladnaya Matematika i Mekhanika*, vol. 12, Sept.-Oct. 1948, pp. 613–32.

261. Criteria for Unsafe and Safe Bounds of a Region of Stability (in Russian), **N. N. Bautin.** *Prikladnaya Matematika i Mekhanika*, vol. 12, Nov.-Dec. 1948, pp. 691–728.

262. Elementary Proof and Sharpening of the Hurwitz Stability Criterion (in German), **K. H. Grossmann.** *Schweizer Archiv fur angewandte Wissenschaft und Technik*, vol. 14, Aug. 1948, pp. 242–47.

263. Stability Criterion Applicable to Regulating Circuits of Specified Quality of Stability (in German), **A. Leonard.** *Archiv fur Elektrotechnik*, vol. 39, Sept. 1948, pp. 100–07.

264. On a Special Case of Investigation of Stability of Regulating Systems (in Russian), **A. M. Letov.** *Prikladnaya Matematika i Mekhanika*, vol. 12, Nov.-Dec. 1948, pp. 729–36. Considers the case of two equal roots.

265. On a Problem of Indirect Regulation (in Russian), **G. N. Nikolskii.** *Inshenernii Sbornik Akademii Nauk SSSR*, vol. 4, 1948, pp. 113–32. Analysis of stability conditions in a nonlinear servomechanism.

266. Recent Methods for Investigating the Stability of Regulating Processes (in German), **W. Oppelt.** *Die Technik*, vol. 3, July 1948, pp. 312–14.

267. On the Stability of Discontinuous Regulating Processes (in German), **W. Oppelt.** *Elektrotechnik*, vol. 2, March 1948, pp. 71–78 Approximate analysis, using the Nyquist diagram, of regulating systems having a single contact-making element.

268. Stability of Linear Oscillating Systems with Constant Time Lag, **H. I. Ansoff.** *Journal of Applied Mechanics*, vol. 16, June 1949, pp. 158–64.

269. On the Aperiodic Stability of Linear Systems (in Russian), **Z. S. Bloch.** *Avtomatika i Telemekhanika*, vol. 10, 1949, pp. 3–7.

270. Generalization of the Nyquist Stability Criterion (in French), **M. Demontvignier, P. Lefevre.** *Comptes Rendus*, l'Academie des Sciences, vol. 228, Jan. 31, 1949, pp. 360–62.

271. Study of Stability of a Linear System from the Generalized Phase Diagram (in French), **M. Demontvignier, P. Lefevre.** *Comptes Rendus*, l'Academie des Sciences, vol. 228, 1949, pp. 463–65.

272. A New Harmonic Method of Studying the Stability of Linear Systems (in French), **M. Demontvignier, P. Lefevre.** *Revue Generale de l'Electricite*, vol. 58, July 1949, pp. 263–79.

273. Stability Criteria of H. Nyquist (in German), **F. Kirschstein.** *Archiv der Elektrischen Ubertragung*, vol. 3, Sept. 1949, pp. 195–98. Develops additional rules to cover cases in which the Nyquist criterion presumably leads to incorrect results.

274. Mikhailov's Test and the Estimation of the Roots of the Characteristic Equation (in Russian), **N. N. Myasnikov.** *Avtomatika i Telemekhanika*, vol. 10, 1949, pp. 267–73.

275. On the Stability of Discontinuous Regulating Processes, **W. Oppelt.** *Elektrotechnik*, vol. 2, 1949, pp. 71–78.

276. Active Networks and the General Locus Criterion for Stability (in German) **F. Strecker.** *Frequenz*, vol. 3, March 1949, pp. 78–84.

277. A Generalization of Nyquist's Stability Criteria, **A. Vazsonyi.** *Journal of Applied Physics*, vol. 20, Sept. 1949, pp. 863–67. An extension of the Nyquist diagrams to permit evaluation of the lower limits of the values of damping ratios.

278. The Stability of Automatic Regulation (in Swedish), **E. Voipo.** *Kraft och Ljus*, vol. 22, Nov. 1949, pp. 247–65.

279. Methods of Investigating the Stability

of Regulating Systems with Distributed Parameters(in Russian), **Y. V. Vorobiev, V. I. Drozdovich.** *Avtomatika i Telemekhanika*, vol. 10, 1949, pp. 77–83.

280. Vysnegradskii Diagrams for an Isodromic Regulator with Non-Linear Action (in Russian), **N. A. Zelezcov.** *Avtomatika i Telemekhanika*, vol. 10, July 1949, pp. 424–36.

281. Nyquist Diagrams and Routh-Hurwitz Stability Criterion, **F. E. Bothwell.** *Proceedings*, Institute of Radio Engineers, vol. 38, Nov. 1950, pp. 1345–48.

282. Stability of Voltage Regulators, **Frank E. Bothwell.** *AIEE Transactions*, vol. 69, pt. II, 1950, pp. 1430–33.

283. Contribution to the Study of the Stability of Circuits for Control and for Servomechanisms (in French), **P. L. Dubois-Violette.** *Comptes Rendus*, l'Academie des Sciences, vol. 230, April 12, 1950, pp. 1380–83.

284. On the Stability of Automatic Regulators by Integral Action and Second Derivative Conjugates (in French), **P. L. Dubois-Violette.** *Comptes Rendus*, l'Academie des Sciences, vol. 230, 1950, pp. 1448–50.

285. Application of Stability Criteria to a Regulating System Containing an Amplidyne (in French), **F. van Geertruyden.** *H. F. Electricite, Courants Faibles, Electronique*, no. 6, 1950, pp. 169–76.

286. Stability Criteria (in German), **E. Gork.** *Archiv der electrischen Uebertragung*, vol. 4, March 1950, pp. 89–96.

287. The Effect of Transmission Distance on the Stability of Flow-Control Processes, **D. B. Kirk.** *Instruments*, vol. 23, Nov. 1950, pp. 1191–94.

288. Strictly Unstable Regulating Systems (in Russian), **A. M. Letov.** *Prikladnaya Matematika i Mekhanika*, vol. 14, 1950, pp. 183–92.

289. On the Character of the Bounds of the Region of Stability of Regulating Systems (in Russian), **A. I. Lurye.** *Prikladnaya Matematika i Mekhanika*, vol. 14, July-Aug. 1950, pp. 371–82.

290. Investigation of the Stability of a Regulating System When Minor Feedback Loops are Introduced (in Russian), **D. I. Maryanovskii.** *Elektrichestvo*, no. 3, March, 1950, pp. 51–56.

291. The Setting Diagram for Regulators (in German), **W. Oppelt.** *Zeitschrift fur angewandte Mathematik und Mechanik*, vol. 30, May-June 1950, pp. 188–89.

292. When Does Nyquist's Stability Criterion Hold? (in German), **J. Peters.** *Archiv der elektrischen Uebertragung*, vol. 4, Jan. 1950, pp. 17–22.

293. Auto-Oscillations in Some Servosystems Conditioned by the Presence of Dry (Coulomb) Friction (in Russian), **B. A. Ryabov.** *Doklady Akademii Nauk, SSSR*, vol. 73, July 1950, pp. 283–86.

294. On the Use of Hurwitz Determinants in the Representation of the Domain of Stability in Problems of Oscillation (in German), **E. Sponder.** *Schweiser Archiv fur angewandte Wissenschaft und Technik*, vol. 16, March 1950, pp. 93–96.

295. Stability Criterion from Closed and Open Loci (in German), **F. Strecker.** *Archiv der elektrischen Uebertragung*, vol. 4, June 1950, pp. 199–206.

296. The Nyquist Criterion of Stability, **J. C. West.** *Electronic Engineering*, vol. 22, May 1950, pp. 169–72.

297. The Generalized Transmission Matrix Stability Criterion, **Pierre M. Honnell.** *AIEE Transactions*, vol. 70, pt. I, 1951, pp. 292–98.

298. A Survey of Stability Analysis Techniques for Automatically Controlled Aircraft, **A. L. Jones, B. R. Briggs.** *Technical Note 2275*, National Advisory Committee for Aeronautics, Jan. 1951.

299. Interpretation Rule of the Generalized Phase Diagram (in French), **P. M. Lefevre.** *Comptes Rendus*, l'Academie des Sciences, vol. 232, Jan. 1951, pp. 381–83. Restatement of Nyquist and Bode criteria, which significantly reduces the numerical labor involved.

300. On the Problem of the Stability of Regulated Systems (in Russian), **A. I. Lurye.** *Prikladnaya Matematika i Mekhanika*, vol. 15, Jan.-Feb. 1951, pp. 67–74.

301. On Strictly Unstable Regulated Systems (in Russian), **A. I. Lurye.** *Prikladnaya Matematika i Mekhanika*, vol. 15, March-April 1951, pp. 251–54.

302. A General Criterion of Stability of Servomechanisms–Seats of Hereditary Phenomena (in French), **J. Loeb.** *Comptes Rendus*, l'Academie des Sciences, vol. 233, July 1951, pp. 344–45.

303. The Stability Problem in Feedback Amplifiers, **W. A. Lynch.** *Proceedings*, Institute of Radio Engineers, vol. 39, Sept. 1951, pp. 1000–08. A review paper in which Nyquist's criterion is used, and the properties of minimum phase-shift networks are described.

304. On the Theory of Stability of Regulated Systems (in Russian), **I. G. Malkin.** *Prikladnaya Matematika i Mekhanika*, vol. 15, Jan.-Feb. 1951, pp. 59–66.

305. Conditions of Stability and Instability of Active Systems, with Particular Reference to Electric Networks (in Italian), **A. Pinciroli.** *Elettrotecnica*, vol. 38, April 25, 1951, pp. 193–94.

306. On the Conditions of Stability of a Linear System (in Russian), **L. A. Varshavskii.** *Zhurnal Tekhnicheskoi Physiki*, vol. 21, Aug. 1951, pp. 907–19.

Servomechanisms

307. Theory of Servomechanisms, **H. L. Hazen.** *Journal*, Franklin Institute, vol. 218, Sept. 1934, pp. 279–331.

308. Design and Test of a High-Performance Servomechanism, **H. L. Hazen.** *Journal*, Franklin Institute, vol. 218, Nov. 1934, pp. 543–80.

309. A Position Regulator for Paper Slitters, **F. H. Gulliksen.** *AIEE Transactions* (*Electrical Engineering*), vol. 57, Nov. 1938, pp. 634–36.

310. Photoelectric Weft-Straightener Control, **C. W. LaPierre, A. P. Mansfield.** *AIEE Transactions* (*Electrical Engineering*), vol. 57, Sept. 1938, pp. 513–19.

311. Servo-Motors Control Double-Extraction Turbines, **O. N. Bryant.** *Power*, vol. 84, Sept. 1940, pp. 86–88.

312. Servomechanisms with Shunt Motor Fed from Ionic Rectifier (in Russian), **V. P. Nikitin, N. P. Kunitzki.** *Comptes Rendus*, l'Academie des Sciences, de l'URSS, vol. 34, no. 1, 1942, pp. 14–18.

313. Polarized-Light Servo System, **T. M. Berry.** *AIEE Transactions* (*Electrical Engineering*), vol. 63, April 1944, pp. 195–98.

314. Gyroscopic Stabilizer for Tank Guns, **C. R. Hanna, L. B. Lynn.** *Electrical Engineering*, vol. 63, Oct. 1944, pp. 355–60.

315. Considerations in Servomechanism Design, **S. W. Herwald.** *AIEE Transactions* (*Electrical Engineering*), vol. 63, Dec. 1944, pp. 871–76.

316. Regulator Circuits Without Relays Used in Conjunction with Induction Motors (in German), **W. Kramer.** *Electrotechnische Zeitschrift*, vol. 65, Oct. 26, 1944, pp. 351–55. Describes a number of servomechanisms consisting of 2-phase induction motor controlled by saturable inductors.

317. A Continuous-Control Servo System, **J. T. McNaney.** *Electronics*, vol. 17, Dec. 1944, pp. 118–25.

318. Servomechanisms, **D. C. Bomberger.** *Bell Laboratories Record*, vol. 23, Nov. 1945, pp. 409–11.

319. Wide Speed Ranges with Servomechanisms, **G. A. Caldwell.** *Westinghouse Engineer*, vol. 5, Sept. 1945, p. 157.

320. Electronic-Type Instruments for Industrial Processes, **P. S. Dickey, A. J. Hornfeck.** *Transactions*, American Society of Mechanical Engineers, vol. 67, July 1945, pp. 393–98.

321. The Servo Problem as a Transmission Problem, **E. B. Ferrell.** *Proceedings*, Institute of Radio Engineers, vol. 33, Nov. 1945, pp. 763–67.

322. Tracer-Controlled Position Regulator for Propeller Milling Machine, **C. R. Hanna, W. O. Osbon, R. A. Hartley.** *AIEE Transactions* (*Electrical Engineering*), vol. 64, April 1945, pp. 201–05.

323. Application of Electric Equipment for Ship-Propeller Milling Machine, **H. Earl Morton, Oren G. Rutemiller.** *AIEE Transactions* (*Electrical Engineering*), vol. 64, April 1945, pp. 205–08.

324. Electric Turret-Traversing Mechanism for Tanks, **S. J. Mikina.** *Journal of Applied Mechanics*, vol. 12, Dec. 1945, pp. A228–40.

325. Operational Methods in Servomechanism Design, **W. E. Restemeyer.** *Journal of the Aeronautical Sciences*, vol. 12, July 1945, pp. 313–19.

326. Servomechanisms–How They Work, **R. H. Rogers.** *Machine Design*, vol. 17, April 1945, pp. 119–24.

327. Electronically Controlled Contour Milling Machine, **O. G. Rutemiller, H. E. Morton.** *Machine Design*, vol. 17, Sept. 1945, pp. 103–07.

328. The Amplidyne Generator Applied to Speed-Controlled Electric Gun Turrets for Aircraft, **L. A. Zahorsky.** *AIEE Transactions* (*Electrical Engineering*), vol. 64, May 1945, pp. 221–25.

329. Electronic Register Control for Multicolor Printing, **W. D. Cockrell.** *AIEE Transactions* (*Electrical Engineering*), vol. 65, Aug.-Sept. 1946, pp. 617–22.

330. Linear Servo Theory, **R. E. Graham.** *Bell System Technical Journal*, vol. 25, Oct. 1946, pp. 616–51.

331. Fundamentals of Servomechanisms, **S. W. Herwald.** *Product Engineering*, vol. 17, June 1946, pp. 464–70.

332. Dimensionless Analysis of Servomechanisms by Electrical Analogy, **S. W. Herwald, G. D. McCann.** *AIEE Transactions* (*Electrical Engineering*), vol. 65, Oct. 1946, pp. 636–39.

333. Supplying D-C Motors Through Valve Amplifiers (in German), **H. Hochrainer.** *Elektrotechnik und Maschinenbau*, vol. 63, June 1946, pp. 135–41. Servomechanism applications are described, and the stability consideration are discussed in detail.

334. Electrical Analogy Methods Applied to Servomechanism Problems, **G. D. McCann. S. W. Herwald, H. S. Kirschbaum.** *AIEE Transactions* (*Electrical Engineering*), vol. 65, Feb. 1946, pp. 91–96.

335. New Servomechanism Theory; the Synthesis of Automatic Control Systems, **W. C. Robinette.** *Instruments*, vol. 19, Feb. 1946, pp. 75–81.

336. High Performance Demodulator for Servomechanisms, **K. E. Schreiner.** *Proceedings*, National Electronics Conference, vol. 2, 1946, pp. 393–403.

337. Theory of Servo Systems, with Particular Reference to Stabilization, **A. L. Whiteley.** *Journal*, Institution of Electrical Engineers, vol. 93, pt. 2, Aug. 1946, pp. 353–72.

338. Contributions to the Theory of Hydraulic Servomoters (in Russian), **Z. S. Blokh.** *Bulletin*, Academie des Sciences, Department des Techniques Scientifiques, vol. 11, no. 2, 1947, pp. 151–58. Piston stroke characteristics calculated for different types of valve action.

339. Obtaining Attenuation-Frequency Characteristics for Servomechanisms, **H. Chestnut.** *General Electric Review*, vol. 50, Dec. 1947, pp. 38–44. Tabulation of the frequency characteristics for a large number of networks.

340. Hydraulic Remote Position Controllers, **J. E. M. Coombes.** *Journal*, Institution of Electrical Engineers, vol. 94, pt. 2A, 1947, pp. 270–82.

341. The Use of Servos in the Army During the Past War, **E. J. H. Douch.** *Journal*, Institution of Electrical Engineers, vol. 94, pt. 2A, 1947, pp. 177–89.

342. Some Servo Mechanisms Used by the Royal Navy, **J. O. H. Gairdner.** *Journal*, Institution of Electrical Engineers, vol. 94, pt. 2A, 1947, pp. 208–21.

343. The Use of Servo Mechanisms in Aircraft, **A. A. Hall.** *Journal*, Institution of Electrical Engineers, vol. 94, pt. 2A, 1947, pp. 256–65.

344. The Analysis and Design of Servomech-

anisms, **H. Harris, Jr.** *Transactions*, American Society of Mechanical Engineers, vol. 69, April 1947, pp. 267–80.

345. A Comparison of Two Basic Servomechanism Types, **Herbert Harris.** *AIEE Transactions*, vol. 66, 1947, pp. 83–93.

346. Elements of Position Control, **K. A. Hayes.** *Journal*, Institution of Electrical Engineers, vol. 94, pt. 2A, 1947, pp. 161–76.

347. The Analysis and an Optimum Synthesis of Linear Servomechanisms, **Donald Herr, Irving Gerst.** *AIEE Transactions*, vol. 66, 1947, pp. 959–70.

348. Stabilizing Servomechanisms for Optimum Overall Performance, **S. W. Herwald.** *Product Engineering*, vol. 18, June 1947, pp. 132–37.

349. Naval Applications of Electrical Remote-Positional Controllers, **W. E. C. Lampert.** *Journal*, Institution of Electrical Engineers, vol. 94, pt. 2A, 1947, pp. 236–51.

350. Dimensionless Analysis of Servomechanisms by Electrical Analogy—I, **G. D. McCann, S. W. Herwald.** *AIEE Transactions*, vol. 66, 1947, pp. 111–18.

351. Hydraulic Variable Speed Transmissions as Servomotors, **G. C. Newton, Jr.** *Journal*, Franklin Institute vol. 243, June 1947, pp. 439–69.

352. The Effects of Backlash and Speed Dependent Friction on the Stability of Closed-Cycle Control Systems, **A. Tustin.** *Journal*, Institution of Electrical Engineers, vol. 94, pt. 2A, May 1947, pp. 143–51.

353. Electronic Servo Simulators, **F. C. Williams, F. J. U. Ritson.** *Journal*, Institution of Electrical Engineers, vol. 94, pt. 2A, 1947, pp. 112–29.

354. Designing Hydraulic Servos, **H. Ziebolz.** *Machine Design*, vol. 19, July 1947, pp. 123–26.

355. Designing Pneumatic and Electric Servos, **H. Ziebolz.** *Machine Design*, vol. 19, Sept. 1947, pp. 132–38.

356. Servomechanisms, **R. H. Bacon.** *American Journal of Physics*, vol. 16, Feb. 1948, pp. 79–92.

357. Designing Hydraulic Servo Circuits, **C. E. Grosser.** *Machine Design*, vol. 14, Jan. 1942, pp. 52–56, 128.

358. Frequency Response Measurement of Hydraulic Power Unit, **M. R. Hannah.** *Transactions*, American Society of Mechanical Engineers, vol. 70, 1948, pp. 525–39.

359. The Effect of Coulomb Friction on the Performance of Servomechanisms, **G. D. McCann, F. C. Lindvall, C. H. Wilts.** *AIEE Transactions*, vol. 67, pt. I, 1948, pp. 540–46.

360. Stabilizing Servomechanisms, **D. McDonald.** *Electronics*, vol. 21, Nov. 1948, pp. 112–16.

361. Stabilization of Carrier Frequency Servomechanisms—I. Gain-Phase Margin Diagrams of Controller Characteristics, **A. Sobczyk.** *Journal*, Franklin Institute, vol. 246, July 1948, pp. 21–43.

362. Stabilization of Carrier Frequency Servomechanisms—II. Design Formular for Proportional-Derivative Networks, **A. Sobczyk.** *Journal*, Franklin Institute, vol. 246, Aug. 1948, pp. 95–121.

363. Stabilization of Carrier Frequency Servomechanisms—III. Methods of Obtaining Required Carrier Phase Shift, **A. Sobczyk.** *Journal*, Franklin Institute, vol. 246, Sept. 1948, pp. 187–214.

364. Signal Generators for Servo System Measurements, **C. F. White.** *Proceedings*, National Electronics Conference, vol. 4, 1948, pp. 59–71.

365. A Variable Radio Frequency Follower System, **R. F. Wild.** *Proceedings*, Institute of Radio Engineers, vol. 36, Feb. 1948, pp. 281–85.

366. Phase Lead for A-C Servomechanisms, **A. H. Benner.** *Journal of Applied Physics*, vol. 20, March 1949, pp. 268–73.

367. A Servo Employing the Magnetic Fluid Clutch, **E. S. Bettis, E. R. Mann.** *Review of Scientific Instruments*, vol. 20, Feb. 1949, pp. 97–101.

368. Comparison of Steady-State and Transient Performance of Servomechanisms, **Harold Chestnut, Robert W. Mayer.** *AIEE Transactions*, vol. 68, pt. 1, 1949, pp. 765–77.

369. Automatic Servo and Remote Controls, **M. Lattmann.** *Microtecnic*, vol. 3, Jan.-Feb. 1949, pp. 3-9.

370. Electromechanical Lead Networks for A-C Servomechanisms, **D. McDonald.** *Review of Scientific Instruments*, vol. 20, Nov. 1949, pp. 775–79.

371. The Calculation of the Optimum Parameters for a Following System, **C. Mack.** *Philosophical Magazine*, Series 7, vol. 40, Sept. 1949, pp. 922–28.

372. Instrument Inaccuracies in Feed-Back Control Systems with Particular Reference to Backlash, **H. Tyler Marcy, Morris Yachter, Jerome Zauderer.** *AIEE Transactions*, vol. 68, pt. I, 1949, pp. 778–88.

373. Magnetic Fluid Clutch in Servo Applications, **G. Nelson.** *Electronics*, vol. 22, Nov. 1949, pp. 100–03.

374. Design Equations for Servomechanisms, **B. Parzen.** *Electrical Communication*, vol. 26, Sept. 1949, pp. 249–56.

375. Probability Criterion for the Design of Servomechanisms, **J. R. Ragazzini, L. A. Zadeh.** *Journal of Applied Physics*, vol. 20, Feb. 1949, pp. 141–44.

376. Servomechanisms and Remote Control (in French), **Y. Rocard, J. Loeb.** *Annales de Telecommunication*, vol. 4, Nov. 1949, pp. 397–404.

377. An Electronic D-C to A-C Converter for Use in Servo Systems, **E. E. St. John.** *Proceedings*, Institute of Radio Engineers, vol. 37, Dec. 1949, pp. 1474–78.

378. Graphical Determination of Transfer Function Loci for Servomechanism Components and Systems, **C. H. Thomas, E. C. Easton,** *AIEE Transactions*, vol. 68, pt. I, 1949, pp. 307–18.

379. Transient Conditions in the Simplest Circuit Using Servomechanisms (in Russian), **M. V. Belyaev.** *Elektrichestvo*, no. 6, June 1950, pp. 42–46. The effect of linear and nonlinear resistances in shunt with the compensating winding of an amplidyne are studied.

380. Carrier Compensation for Servomechanisms, **H. E. Blanton.** *Journal*, Franklin Institute, vol. 250, Nov. 1950, pp. 391–407; Dec. 1950, pp. 525–42.

381. A Note on the Error Coefficient of a Servomechanism, **J. L. Bower.** *Journal of Applied Physics*, vol. 21, July 1950, p. 723.

382. Integral Controller for Use in Carrier-Type Servomechanisms, **R. L. Cosgriff.** *AIEE Transactions*, vol. 69, pt. II, 1950, pp. 1379–83.

383. Servo Control Problems, **A. J. O. Cruickshank.** *Transactions*, Institution of Engineers and Shipbuilders in Scotland, vol. 94, pt. 5, 1950–1951, pp. 266–302.

384. Study of the Influence of Time of Propagation Upon the Stability of Regulating Servomechanisms by the Method of Fusion of Roots (in French), **P. L. Dubois Violette.** *Comptes Rendus*, l'Academie des Sciences, vol. 230, 1950, pp. 1499–501. Stabilization of a servomechanism with time lag.

385. An Electronic Simulator for Nonlinear Servomechanisms, **Charles M. Edwards, E. Calvin Johnson, Jr.** *AIEE Transactions*, vol. 69, pt. I, 1950, pp. 300–07. Limiting devices are incorporated into a linear analogue for autopilot simulation.

386. Mechanical and Electrical Factors in Servomechanism Design, **R. Herst.** *Electrical Manufacturing*, vol. 46, Nov. 1950, pp. 76–79, 184, 186.

387. A Phase-Plane Approach to the Compensation of Saturating Servomechanisms, **Arthur M. Hopkin.** *AIEE Transactions*, vol. 70, pt. I, 1950, pp. 631–39.

388. Stability of Servomechanisms with Linearly Varying Elements, **M. J. Kirby.** *AIEE Transactions*, vol. 69, pt. II, 1951, pp. 1662–68.

389. Note on the Maximum Precision of Perfectly Stable Servomechanisms (in French), **G. Lehmann.** *Onde Electrique*, vol. 30, June 1950, pp. 267–70. Discussion of the effect of non-minimum phase shift system on the low frequency precision.

390. Improvements in the Characteristics of A-C Lead Networks for Servomechanisms, **Donald McDonald.** *AIEE Transactions*, vol. 69, pt. I, 1950, pp. 293–300.

391. What Size Motor for Proper Operation of Servomechanism?, **G. C. Newton, Jr.** *Machine Design*, vol. 22, Nov. 1950, pp. 125–30, 200, 202.

392. Phase Lead for A-C Servo Systems with Compensation for Carrier Frequency Changes, **Arthur P. Notthoff, Jr.** *AIEE Transactions*, vol. 69, pt. I, 1950, pp. 285–92.

393. Characteristics of Some Magnetic Fluid Clutch Servomechanisms, **A. J. Parziale, P. D. Tilton.** *AIEE Transactions*, vol. 69, pt. I, 1950, pp. 150–57.

394. Design of Viscously Damped Servosystems for Step Function Input (in Czech), **J. Petr.** *Elektrotechnicky Obzor*, vol. 39, March, 1950, pp. 110–16.

395. Magnetic Powder Clutch Servo, **S. Wald.** *Radio-Electronic Engineering*, vol. 15, Sept. 1950, pp. 12A–13A.

396. Effects of Carrier Shifts on Derivative Networks for A-C Servomechanisms, **George M. Attura.** *AIEE Transactions*, vol. 70, pt. I, 1951, pp. 612–18.

397. Network Synthesis by Graphical Methods for A-C Servomechanisms, **George A. Bjornson.** *AIEE Transactions*, vol. 70, pt. I, 1951, pp. 619–25.

398. Optimum Gear Train Ratios for Instrument Servomechanisms, **L. N. Canick.** *Product Engineering*, vol. 22, July 1951, pp. 108–09.

399. Servo Power Calculations, **O. E. Carlson.** *Electronics*, vol. 24, March 1951, p. 134.

400. Remote Control of Positioning Motors, **G. M. Chute.** *Electronics*, vol. 24, July 1951, pp. 92–93.

401. Inverted Servo System for Sensitive Inputs, **H. F. Colvin.** *Product Engineering*, vol. 22, Aug. 1951, pp. 147–51.

402. Servo Guider for Solar Telescopes, **F. E. Fowler, D. S. Johnson.** *Electronics*, vol. 24, May 1951, pp. 118–22.

403. Servomechanism Transient Performance from Decibel-Log Frequency Plots, **H. Harris, Jr., M. J. Kirby, E. F. Von Arx.** *AIEE Transactions*, vol. 70, pt. II, 1951, pp. 1452–59.

404. Stability of Varying-Element Servomechanisms with Polynomial Coefficients, **M. J. Kirby, R. M. Giulianelli.** *AIEE Transactions*, vol. 70, pt. II, 1951, pp. 1447–51.

405. Design of Damper-Stabilized Instrument Servomechanisms, **J. F. Koenig.** *Proceedings*, National Electronics Conference, vol. 7, 1951, pp. 24–27.

406. Pneumatic Servomechanisms in the Iron and Steel Industry, **A. A. Markson.** *Instruments*, vol. 24, June 1951, pp. 647–49.

407. The Effect of Friction on the Behavior of Servomechanisms at Creep Speeds, **J. G. L. Michel, A. Porter.** *Proceedings*, Institution of Electrical Engineers, vol. 98, pt. 2, June 1951, pp. 297–310.

408. Contribution to the Statistical Calculation of Servomechanisms (in French), **M. Pelegrin.** *Comptes Rendus*, l'Academie des Sciences, vol. 232, Feb. 1951, pp. 473–75.

409. Stabilization of Variable Carrier Frequency Servomechanisms, **K. Schurr.** *Proceedings*, National Electronics Conference, vol. 7, 1951, pp. 14–23.

410. Proportionalizing Dither Increases Sensitivity of Hydraulic Servo, **P. B. Sebring.** *Machine Design*, vol. 23, Aug. 1951, pp. 125–28.

411. A Servo System for Heterodyne Oscillators, **T. Slonczewski.** *AIEE Transactions*, vol. 70, pt. I, 1951, pp. 1070–72.

412. A Transient Approach to the Solution of a Linear Servomechanism by an Equivalent Network, **S. P. Tung.** *Proceedings*, National Electronics Conference, vol. 7, 1951, pp. 7–13.

413. Analysis of Friction Damper for Clutch-Type Servomechanisms, **H. K. Weiss.** *Journal of the Aeronautical Sciences*, vol. 18, Oct. 1951, pp. 676–82.

414. Servo Mechanisms, **A. L. Whiteley.** *Proceedings*, Institution of Electrical Engineers, vol. 98, pt. 1, Sept. 1951, pp. 289–97. Review of progress.

415. Hydraulic Servocontrols in the Steel Industry, **H. Ziebolz.** *Instruments*, vol. 24, June 1951, pp. 650–51.

Relay-Type Servomechanisms and Feedback Controllers

416. Automatic Voltage Regulators, Application to Power Transmission Systems, **C. A. Nickle, R. M. Carothers.** *AIEE Transactions (Electrical Engineering)*, vol. 47, 1928, pp. 957–74.

417. The Theory of Deviation Dependent Step Regulator (in German), **M. Lang.** *Zeitschrift fur technische Physik*, vol. 18, 1937, pp. 318–22.

418. Regulating Drive (Without Relay) with "Saddle" Characteristic for Step by Step Switching (in German), **W. Kramer.** *Elektrotechnische Zeitschrift*, vol. 59, March 3, 1938, pp. 215–17.

419. Characteristics of the Tirrill Regulator for High-Speed Regulation (in German), **A. Lang.** *Archiv fur Elektrotechnik*, vol. 32, Oct. 14, 1938, pp. 675–83.

420 Analysis of Relay Servomechanisms, **H. K. Weiss.** *Journal of the Aeronautical Sciences*, vol. 13, July 1946, pp. 364–76.

421. Regulators with Vibrating Contacts (in French), **J. Bardin.** *Revue de l'Electricite et de Mecanique*, no. 71, Oct.-Nov.-Dec. 1947, pp. 10–16.

422. The Behavior of an Oscillator Under the Influence of On-Off Regulation (in German), **I. Flugge-Lotz, H. F. Hodapp, K. Klotter, H. Meissinger, K. Scholtz.** *Zeitschrift fur angewandte Mathematik und Mechanik*, vol. 25/27, July 1947, pp. 97–113.

423. The Discontinuous Regulator-Servo and its Relation to the Continuous Regulator (in German), **F. Galavics.** *Schweizer Archiv fur angewandte Wissenschaft und Technik*, vol. 13, Dec. 1947, pp. 357–70.

424. On the Stability of Motion of a Dynamic System (in Russian), **A. I. Lourye.** *Prikladnaya Matematika i Mekhanika*, vol. 11, July-Aug. 1947, pp. 445–48. Study of a discontinuously controlled system.

425. On a Problem of Automatic Regulation with Non-Linear Characteristics (in Russian), **B. V. Bulgakov, M. Z. Litvin-Sedoi.** *Avtomatika i Telemekhanika*, vol. 10, 1949, pp. 329–41. Analysis of servomotor, amplifier combination having practically relay characteristics.

426. The Simplest Relay Systems of Automatic Regulation (in Russian), **A. A. Feldbaum.** *Avtomatika i Telemekhanika*, vol. 10, 1949, pp. 249–66.

427. An Analysis of Relay Servomechanisms, **David A. Kahn.** *AIEE Transactions*, vol. 68, pt. II, 1949, pp. 1079–88.

428. An Analysis of the Working of Discontinuous Physical Systems and its Application to Servomechanisms. I–III (in French), **F. H. Raymond.** *Annales de Telecommunication*, vol. 4, 1949; July, pp. 250–56, Aug.-Sept., pp. 307–14, Oct., pp. 347–57.

429. Theory of Intermittent Regulation. I. (in Russian), **Ya Z. Tsipkin.** *Avtomatika i Telemekhanika*, vol. 10, no. 3, 1949, pp. 189–224.

430. The Theory of Relay Servomechanisms (in French), **J. R. Dutilh.** *Onde Electrique*, vol. 30, Oct. 1950, pp. 438–45.

431. A Frequency Response Method for Analyzing and Synthesizing Contactor Servomechanisms, **Ralph J. Kochenburger.** *AIEE Transactions*, vol. 69, pt. I, 1950, pp. 270–84.

432. Carrier Controlled Relay Servos, **J. C. Lozier.** *Electrical Engineering*, vol. 69, Dec. 1950, pp. 1052–56.

433. A New Approach to the Design of Pulse-Monitored Servo Systems, **A. Porter, F. W. Stoneman, D. F. Lawden.** *Proceedings*, Institution of Electrical Engineers, vol. 97, pt. 2, Oct. 1950, pp. 597–610.

434. Relay Servomechanisms. The Shunt Motor Servo with Inertia Load, **T. A. Rogers, W. C. Hurty.** *Transactions*, American Society of Mechanical Engineers, vol. 72, Nov. 1950, pp. 1163–72.

435. Analysis of a Sampling Servomechanism, **K. S. Miller, R. J. Schwarz.** *Journal of Applied Physics*, vol. 21, April 1950, pp. 290–94.

436. Parameter Determination for Established Self-Oscillations of Certain Systems (in Russian), **B. A. Ryabov.** *Doklady Akademii Nauk, SSSR*, vol. 71, no. 4, 1950, pp. 663–66. Analysis of a relay type of servomechanism by means of two systems of differential equations; one for each position of the relay element.

437. A General Theory of Sampling Servo Systems, **D. F. Lawden.** *Proceedings*, Institution of Electrical Engineers, vol. 98, pt. 4, Oct. 1951, pp. 31–36.

Industrial Process Control

438. Study of Industrial Processes as a Basis for Regulator Design for Ring Spinning Machines (in German), **F. Oertel.** *Wissenschaftliche Veroeffentlichungen aus dem Siemens-Konzern*, vol. 9, 1930, pp. 266–89.

439. New Applications for Automatic Regulators in the Production and Utilization of Gas (in French), **J. Charles.** *Journal des Usines a Gas*, vol. 56, 1932; Jan. 5, pp. 2–9; Jan. 20, pp. 28–39; Feb. 5, pp. 58–66.

440. Science of Automatic Control in Refining, **C. E. Mason.** *World Petroleum*, vol. 4, 1933; June, pp. 187–90; July, pp. 218–21; vol. 5, 1933; Aug., pp. 252–55; Sept., pp. 281–84.

441. The Control of Chemical Processes, **J. J. Grebe, R. H. Boundy, R. W. Cermak.** *Transactions*, American Institute of Chemical Engineers vol. 29, 1933, pp. 211–56.

442. The Influence of the Characteristics of a Plant on the Performance of an Automatic Regulator, **A. Ivanoff.** *Proceedings*, Chemical Engineering Group, vol. 18, 1936, pp. 138–51.

443. The Application of Automatic Control to a Typical Problem in Chemical Industry, **A. Callender, A. B. Stevenson.** *Proceedings*, Chemical Engineering Group, Society of the Chemical Industry, vol. 18, 1936, pp. 108–16.

444. Automatic Control of Chemical Processes, **W. J. Clark.** *Proceedings*, Chemical Engineering Group, Society of Chemical Industry, vol. 18, 1936, pp. 125–37.

445. Problems in the Regulation of Industrial Processes (in German), **G. Wunsch.** *Zeitschrift des Vereines deutscher Ingenieure*, vol. 81, Sept. 11, 1937, pp. 1057–64.

446. Continuous Control Systems with Variable Characteristics, **H. M. Schmitt.** *Industrial and Engineering Chemistry*, vol. 29, 1937, pp. 1229–31.

447. Elements of Automatic Control, **J. J. Grebe.** *Industrial and Engineering Chemistry*, vol. 29, 1937, pp. 1225–28.

448. Automatic Control and the Chemical Industries, **L. DeFlorez.** *Industrial and Engineering Chemistry*, vol. 29, 1937, pp. 1210–13.

449. Automatic Control of Distillation and Rectification Columns (in French), **G. Grimand.** *Bulletin*, Association des Chemistes, vol. 54, June 1937, pp. 506–16.

450. Contribution to the Study of Butterfly Valves (in French), **D. Gaden.** *Schweizerische Bauzeitung*, vol. 111, 1938, pp. 262–68, 275–77, 291–95.

451. Application of Automatic Controllers to Solvent Refining and Solvent Dewaxing Lube Oil Plants, **J. F. Thornton, T. T. Whipple.** *Refiner*, vol. 18, June 1939, pp. 238–44.

452. Selecting Automatic Control Equipment for Continuous Processes, **H. H. Gorrie.** *Instruments*, vol. 13, 1940, pp. 100–02.

453. Getting the Most from Automatic Control, **J. C. Peters.** *Industrial and Engineering Chemistry*, vol. 33, Sept. 1941, pp. 1095–103.

454. Optimum Settings for Automatic Controllers, **J. G. Ziegler, N. B. Nichols.** *Transactions*, American Society of Mechanical Engineers, vol. 64, Nov. 1942, pp. 759–68.

455. A Study of Damper Characteristics, **P. S. Dickey, H. L. Coplon.** *Transactions*, American Society of Mechanical Engineers, vol. 64, 1942, pp. 137–54.

456. Time Lag in Automatic Control, **H. Seymour.** *Electrician*, vol. 129, July 17, 1942 pp. 63–66.

457. Automatic Process Controls for Self-Supervising Products, **P. A. Borden.** *Electrical Manufacturing*, vol. 31, April 1943, pp. 80–83, 150, 151, 154, 156, 158, 160.

458. New Processes Require More Powerful Automatic Control Equipment, **J. B. McMahon.** *Oil and Gas Journal*, vol. 41, March 25, 1943, pp. 90, 93–94, 96.

459. Industrial Control Instrument Settings, **L. H. Allen, Jr.** *Industrial and Engineering Chemistry*, vol. 35, Dec. 1943, pp. 1223–29.

460. Considering Controllability in Plant Design, **E. D. Haigler.** *Chemical and Metallurgical Engineering*, vol. 50, May 1943, pp. 129–32.

461. Fundamental Principles of Automatic Control, **J. C. Peters, T. R. Olive.** *Chemical and Metallurgical Engineering*, vol. 50, May 1943, pp. 98–107.

462. Process Lags in Automatic Control Circuits, **J. G. Ziegler, N. B. Nichols.** *Transactions*, American Society of Mechanical Engineers, vol. 65, July 1943, pp. 433–44.

463. "On-the-Job" Adjustments of Air-Operated Recorder-Controllers, **J. G. Ziegler.** *Instruments*, vol. 16, 1943, July, pp. 394–97; Oct., pp. 594–96, 634.

464. Instruments for Measuring and Controlling Process Variables, **Editorial Staff Review.** *Chemical and Metallurgical Engineering*, vol. 50, May 1943, pp. 108–25. A review over the whole field of process variables of industrial importance.

465. Automatic-Control Instrument Adjustment. Application of Process Reaction Curves **L. H. Allen, Jr.** *Industrial and Engineering Chemistry*, vol. 36, Aug. 1944, pp. 687–93.

466. Some Fundamental Characteristics of Control Systems, **K. A. Hayes.** *Proceedings*, Chemical Engineering Group, Society of the Chemical Industry, vol. 27, 1945, pp. 173–79.

467. Automatic Control in the Oil Industry, **D. J. Pull.** *Proceedings*, Chemical Engineering Group, Society of the Chemical Industry, vol. 27, 1945, pp. 154–63.

468. Simple Adjustment Procedures for Automatic Controllers of the Proportional Class, **E. D. Haigler.** *Instruments*, vol. 18, March 1945, pp. 151–53.

469. Interconnected Control Instruments, **J. A. Pellettere.** *Instruments*, vol. 18, April 1945, pp. 221–24.

470. Valve Characteristics in Automatic Control, **S. D. Ross,** *Industrial and Engineering Chemistry*, vol. 38, Sept. 1946, pp. 878–84.

471. Some Considerations in the Control of Continuous Processes, **H. C. Frost.** *Instruments*, vol. 19, Oct. 1946, pp. 589–95.

472. Automatic Controlling Mechanisms for Valve Operation. *Product Engineering*, vol. 17, 1946, June, pp. 482–83; July, pp. 128–29.

473. The Effect of Measurement Dead Time in the Control of Certain Processes, **D. P. Eckman.** *Transactions*, American Society of Mechanical Engineers, vol. 68, 1946, pp. 707–11.

474. Theoretical Foundations of Process Control, **G. H. Farrington.** *Journal*, Institution of Electrical Engineers, vol. 94, pt. 2A, 1947, pp. 23–38.

475. Some Recent Developments in Process Control Equipment, **L. S. Yoxall.** *Instrument Practice*, vol. 1, Jan. 1947, pp. 95–100, 110.

476. Cascaded and Multiple Automatic Control Systems, **A. A. Markson, M. J. Boho.** *Instrument Practice*, vol. 1, April 1947, pp. 207–16.

477. Industrial Process Control, **J. G. Ziegler, N. B. Nichols.** *Chemical Engineering Progress*, vol. 43, June 1947, pp. 309–14.

478. Automatic Control in the Chemical Industry, **J. W. Broadhurst, T. C. Broderick, A. W. Foster, G. E. Wheeldon.** *Journal*, Institution of Electrical Engineers, vol. 94, pt. 2A, 1947, pp. 79–99.

479. Sea Water Bromine Process Chemical Control Systems, **P. Hart.** *Instruments*, vol. 20, Oct. 1947, pp. 956–58.

480. Controls for the Chain-Reacting Pile, **E. C. Creutz.** *Instruments*, vol. 20, Feb. 1947, pp. 139–40.

481. Control of Reactors for Synthetic Rubber, **E. E. Rowland**. *Instruments*, vol. 20, Feb. 1947, pp. 136–38.

482. Analyzing the Instrumentation of a Continuous Chemical Process, **A. L. Chaplin**. *Instruments*, vol. 21, June 1948, pp. 532–40; July, pp. 617–19.

483. Basic Design and Field Performance of the Control and Measurement Instrumentation of an Alkylation Unit, **H. F. Moore, G. W. Gross**. *Instruments*, vol. 21, April 1948, pp. 368–74.

484. Some Application Factors Affecting the Regulation of pH in Industry, **A. L. Chaplin**. *Instruments* (serial); vol. 22, 1949, July, pp. 579–87, 608–14; Aug., pp. 680–81, 734–48; Sept., pp. 804–06, 838–54; Oct., pp. 910–11, 950–54; Nov., pp. 1010–11, 1040–46; Dec., pp. 1107, 1138–42; vol. 23, 1950, Jan., pp. 38, 86–94; Feb., pp. 152, 194–202.

485. The Use of Pneumatically-Set Instrument Combinations, **K. E. Coulter, R. W. Cermak**. *Instruments*, vol. 22, April 1949, pp. 312–13.

486. An Application of Feedback Electronic Control to Automatic Continuous Titration, **R. R. Austin, G. K. Turner, L. E. Percy**. *Instruments*, vol. 22, July 1949, pp. 588–89.

487. The ABC's of Multi-Element Control, **C. H. Barnard**. *Instruments*, vol. 22, Feb. 1949, pp. 179–81.

488. Measurement and Control at Trona, **C. H. Gest**. *Instruments*, vol. 22, Dec. 1949, pp. 1155–60.

489. Planning for Automatic Process Control. *Electronics*, vol. 22, Oct. 1949, pp. 72–79.

490. Automatic Control of Moisture, **R. V. Coles**. *Electronics*, vol. 22, Nov. 1949, pp. 82–86. Speed of fabric or paper through drying oven is controlled to keep moisture content constant.

491. Valve Characteristics and Process Control, **J. G. Ziegler, N. B. Nichols**. *Instruments*, vol. 22, Jan., 1949, pp. 75–81.

492. Control Valve Body Design, **D. P. Eckman, R. B. Werey**. *Instruments*, vol. 22, March 1949, pp. 269–73.

493. Pneumatic Transmission Lag, **M. Bradner**. *Instruments*, vol. 22, July 1949, pp. 618–25. Extensive experimental data on the lag in pneumatic transmission lines.

494. The Inverse Derivative. A New Mode of Automatic Control, **C. B. Moore**. *Instruments*, vol. 22, March 1949, pp. 216–19.

495. Measurement and Control Problems in Typical Fixed-Bed Catalytic Processes, **A. W. Hoge, G. F. Hornaday, C. O. Walls, Jr**. *Instruments*, vol. 23, Feb. 1950, pp. 132–35, 174–78.

496. A New Concept of Automatic Control, **R. E. Clarridge**. *Instruments*, vol. 23, Dec. 1950, pp. 1248–51, 1290–92. Rearrangement of proportional, derivative, and reset controls to reduce overshoot during start-up.

497. Process Control, **R. W. Porter, D. M. Considine**. Chemical Engineers Handbook, edited by J. H. Perry, McGraw-Hill Book Comypany, Inc., New York, N. Y., section 19, 1950.

498. Characteristic Functions of Controllers and Technological Processes (in Dutch), **F. C. L. van Vugt**. *Koninklijk Instituut van Ingenieurs-Voordrachten*, vol. 2, Jan. 1950, pp. 44–64.

499. Application of Computing Mechanisms to Industrial Instruments, **M. J. Boho**. *Instruments*, vol. 23, June 1950, pp. 614–16.

500. Design of a Chemical Process for Instrumentation, **C. W. Hills**. *Instruments*, vol. 23, Feb. 1950, pp. 140–42.

501. Theoretical Considerations on the Optimum Adjustment of Regulators, **P. Hazebroek, B. L. van der Waerden**. *Transactions*, American Society of Mechanical Engineers, vol. 72, April 1950, pp. 309–15.

502. An Indirect Method of Process Control, **R. G. Durnal**. *Proceedings*, National Electronics Conference, vol. 6, 1950, pp. 493–98.

503. The Optimum Adjustment of Regulators, **P. Hazebroek, B. L. van der Waerden**. *Transactions*, American Society of Mechanical Engineers, vol. 72, April 1950, pp. 317–22.

504. Unbalanced Force Reactions in Control Valve Plugs and Their Influence on Diaphragm-Motor Design and Operation, **R. A. Rockwell**. *Instruments*, vol. 23, Dec. 1950, pp. 1252–61, 1288.

505. The Effect of Control Point Location Upon Column Control, **K. D. Uitti**. *Instruments*, vol. 23, July 1950, pp. 719–21.

506. Performance Analysis of Butterfly Valves, **S. D. Cohn**. *Instruments*, vol. 24, Aug. 1951, pp. 880–84.

507. The Control Valve in Operation, **W. H. Kidd, G. A. Philbrick**. *Instruments*, vol. 24, Dec. 1951, pp. 1494–502.

508. One Knob Production Control, **C. F. Adeszko**. *Instruments*, vol. 24, Feb. 1951, pp. 215–21.

509. An Electronic Process Controller, **J. R. Boundy, S. A. Bergen**, *Proceedings*, Institution of Electrical Engineers, vol. 98, pt. 2, Oct. 1951, pp. 609–18.

510. Application of Dielectric Measurement to Continuous Processes, **W. H. Howe**. *Instruments*, vol. 24, Dec. 1951, pp. 1434–38, 1484–90.

511. Instrumentation of an Ammonia Plant, **P. Hart, R. C. King**. *Instruments*, vol. 24, Feb. 1951, pp. 158, 176, 177.

512. Process Instrumentation for Crystal Growing Equipment, **S. A. Hluchhan**. *Instruments*, vol. 24, May 1951, pp. 585–90.

513. Some Developments in Electronic Instrumentation Including Process Control, **W. T. Marchment**. *Instruments*, vol. 24, Jan. 1951, pp. 42–44, 50–54.

514. An Improved Pneumatic Control System, **R. E. Clarridge**. *Transactions*, American Society of Mechanical Engineers, vol. 73, April 1951, pp. 297–305.

515. Controller Settings for Optimum Control, **W. A. Wolfe**. *Transactions*, American Society of Mechanical Engineers, vol. 73, May 1951, pp. 413–18.

516. Electronic Control System for Industrial Control Applications, **E. T. Davis**. *Instruments*, vol. 24, June 1951, pp. 642–46. Electronic controller with proportional, reset, and derivative actions.

517. Rule of Thumb Relations for Design and Adjustment of Regulated Processes (in German), **W. Oppelt**. *Chemie-Ingenieur Technik*, no. 8, 1951, pp. 190–93.

Temperature and Pressure Control

518. On a Constant Temperature Oven (in French), **M. Gouy**. *Journal de Physique*, vol. 6, series 3, 1897, pp. 479–83.

519. Thermometric Lag, **D. R. Harper**. *Bulletin*, National Bureau of Standards, vol. 8, 1912, pp. 659–714.

520. A Furnace Temperature Regulator, **W. P. White, L. H. Adams**. *Physical Review*, vol. 14, 1919, pp. 44–48.

521. On a New Automatic Temperature Regulator for Ovens (in German), **E. Haagn**. *Elektrotechnische Zeitschrift*, vol. 40, 1919, pp. 670–72.

522. Some Characteristics of the Gouy Thermoregulator, **T. S. Sligh, Jr**. *Journal*, American Chemical Society, vol. 42, 1920, pp. 60–68.

523. A High Temperature Regulator for Use with Alternating Current, **H. S. Roberts**. *Journal*, Optical Society of America, vol. 6, 1922, pp. 965–77.

524. A Cryostat for Precision Measurements at Temperatures Extending to −180°. **J. E. Walters, A. G. Loomis**. *Journal*, American Chemical Society, vol. 47, Sept. 1925, pp. 2302–06.

525. Mechanical Thermostats, **J. R. Roebuck**. *Journal*, Optical Society of America, vol. 10, 1925, pp. 679–90.

526. A Geophysical Laboratory Furnace Thermostat, **H. S. Roberts**. *Journal*, Optical Society of America, vol. 11, 1925, pp. 171–86.

527. An Automatic Low Temperature Thermostat, **O. Maass, W. H. Barnes**. *Journal*, American Chemical Society, vol. 49, Feb. 1927, pp. 360–63.

528. A Thermostat Constant to One-Thousandth of a Degree Centigrade, **F. R. Winton**. *Journal of Scientific Instruments*, vol. 6, July, 1929, pp. 214–17.

529. The Automatic Regulation of Temperatures up to 600°C by Means of a Platinum Resistance Regulator, **E. A. Cooke, J. C. Swallow**. *Journal of Scientific Instruments*, vol. 6, Sept. 1929, pp. 287–93.

530. The Heat Capacities of Organic Compounds at Low Temperatures. II, A Low Temperature Thermostat, **J. C. Southard, D. H. Andrews**. *Journal*, Franklin Institute, vol. 207, 1929, pp. 324–39.

531. An Automatic Thermoregulator, **J. A. Beattie, D. D. Jacobus**. *Journal of Physical Chemistry*, vol. 34, 1930, pp. 1254–59.

532. A Precision Thermostat for Temperatures from −25°C to 500°C, **J. A. Beattie**. *Review of Scientific Instruments*, vol. 2, Aug. 1931, pp. 458–65.

533. Temperature Regulator for Electrical Resistance Furnaces, **R. F. Proctor, R. W. Douglas**. *Journal of Scientific Instruments*, vol. 9, June 1932, pp. 192–95.

534. Design of Temperature Control Apparatus for Piezo-Electric Oscillators, **V. J. Andrew**. *Review of Scientific Instruments*, vol. 3, July 1932, pp. 341–51.

535. A Sensitive Flexible Thermostat, **J. R. Roebuck**. *Review of Scientific Instruments*, vol. 3, 1932, pp. 93–100.

536. Automatic Temperature Regulation with Resistance Thermometer and Galvanometer Relay (in German), H. **Moser**. *Zeitschrift fur technisches Physik*, vol. 13, 1932, pp. 383–85.

537. Temperature Measurement and Control. *Engineering*, vol. 135, Jan. 20, 1933, pp. 67–69.

538. Temperature Control, **H. H. Darby, C. B. Bridges**. *Journal*, Franklin Institute, vol. 215, June 1933, pp. 723–29.

539. Temperature Control of Furnaces (in German), **M. Lang**. *Elektrotechnische Zeitschrift*, vol. 54, Aug. 17, 1933, pp. 789–91.

540. Expansion Rod Thermostatic Regulators (in German), **L. Nolte**. *Elektrotechnische Zeitschrift*, vol. 54, Aug. 17, 1933, pp. 798–99

541. Oven Temperature Control by Mercury-Arc Rectifiers (in German), **Buchting, H. Klemperer**. *Siemens-Zeitschrift*, vol. 13, Oct. 1933, pp. 300–03.

542. Temperature Control, **W. E. Hoare**. *Electrician*, vol. 111, Dec. 8, 1933, pp. 715–17.

543. Effect of Service Temperature Conditions on the Electromotive Force of Unsaturated Portable Standard Cells, **J. H. Park**. *Journal of Research*, Bureau of Standards, vol. 10, 1933, pp. 89–98.

544. Temperature Measurement and Regulating Devices (in German), **A. Grunwald**. *Siemens-Zeitschrift*, vol. 13, 1933, pp. 141–46.

545. Outline of a Theory of Temperature Regulation (in German), **M. Lang**. *Zeitschrift fur technische Physik*, vol. 14, 1933, pp. 98–105.

546. The Use of the Thyratron for Temperature Control, **R. M. Zabel, R. R. Hancox**. *Review of Scientific Instruments*, vol. 5, Jan. 1934, pp. 28–29.

547. Theoretical Foundations of the Automatic Regulation of Temperature, **A. Ivanoff**. *Journal*, Institute of Fuel, vol. 7, Feb. 1934, pp. 117–38.

548. Temperature Control Box for Saturated Standard Cells, **E. F. Mueller, H. F. Stimson**. *Journal of Research*, Bureau of Standards, vol. 13, Nov. 1934, pp. 699–704.

549. Automatic Pressure and Temperature Control (in German), **H. Lohmann**. *Archiv fur Warmwirtschaft*, vol. 15, Dec. 1934, pp. 311–13.

550. A New Photoelectric Temperature Regulator (in German), **B. Lange, E. Voos**. *Zeitschrift fur technisches Physik*, vol. 15, 1934, pp. 323–26.

551. A Simple Photoelectric Thermoregulator, **W. L. Walsh, N. A. Milas**. *Industrial and Engineering Chemistry* (Analytical Edition), vol. 7, March 1935, pp. 122–23.

552. Back-Pressure Regulators, **N. D. Gove**. *Power*, vol. 80, Jan. 1936, pp. 20–21.

553. Regulation of Superheat Temperature, **A. Konejung.** *Zeitschrift des Vereines deutscher Ingenieure*, vol. 80, April 25, 1936, pp. 501–05.

554. Thyratron Temperature Regulators (in German), **C. R. Himmler.** *Archiv fur technisches Messen*, vol. 5, May 30, 1936, T66–67.

555. Precision Thermostat for Temperature Regulation of a Room, **T. Deighton.** *Journal of Scientific Instruments*, vol. 13, Sept. 1936, pp. 298–300.

556. Automatic Furnace Temperature Regulator, **H. Smethurst, W. L. Lothian.** *Metropolitan-Vickers Gazette*, vol. 16, Sept., 1936, pp. 216–17.

557. Electrical Measurement and Control of Temperature (in German), **H. O. Meyer.** *Elektrotechnische Zeitschrift*, vol. 57, Dec. 3, 1936, pp. 1417–20.

558. Temperature Regulation in Electric Furnaces (in German), **M. Melzer.** *Archiv fur Elektrotechnik*, vol. 30, 1936, pp. 398–409.

559. Self-Oscillation in a Retroacting Thermal Conductor, **L. B. Turner.** *Proceedings*, Cambridge Philosophical Society, vol. 32, 1936, pp. 663–75.

560. Regulation of Automatically Controlled Thermal Systems (in German), **M. Lang.** *Warme*, vol. 60, 1937, Jan. 2, pp. 8–13; Jan. 9, pp. 23–26.

561. Pressure-Difference Regulation in Boiler Feed-Lines, **K. Prantner.** *Warme*, vol. 60, June 26, 1937, pp. 398–400.

562. Use of an Alternating Current Bridge in Laboratory Temperature Control, **M. Benedict.** *Review of Scientific Instruments*, vol. 8, July 1937, pp. 252–54.

563. Note on the Throttling of Electric Heat, **C. O. Fairchild.** *Instruments*, vol. 10, Dec. 1937, pp. 305, 317.

564. A Thyratron Controlled Thermostat, **J. M. Sturtevant.** *Review of Scientific Instruments*, vol. 9, Sept. 1938, pp. 276–79.

565. Application of Temperature Controllers, **E. D. Haigler.** *Transactions*, American Society of Mechanical Engineers, vol. 60, 1938, pp. 633–40.

566. Temperature Control and Switchgear for Electric Furnaces, **K. A. Lohausen, G. Schumann.** *AEG Mitteilungen*, no. 9, Sept. 1939, pp. 415–19.

567. Temperature Regulation, **S. L. Barron.** *Electrical Review*, vol. 125, Oct. 13, 1939, pp. 487–89.

568. Electrical Regulation of Temperature by Means of "Tipping Lever" Apparatus (in German), **A. Kuntze, K. Branditz.** *Elektrotechnische Zeitschrift*, vol. 61, Jan. 25, 1940, pp. 76–77.

569. Automatic Electric Regulators for Temperature and Steam Pressure (in German), **A. Stoff.** *Archiv fur Warmewirtschaft und Dampfkesselwesen*, vol. 21, Feb. 1940, pp. 43–46.

570. A Sensitive Automatic Pressure Control Device, **R. A. Smith.** *Review of Scientific Instruments*, vol. 11, April 1940, pp. 120–22.

571. Pyrometric Regulation of Resistance Furnaces (in French), **A. Clergeot.** *Revue Generale de l'Electricite*, vol. 47, April 13–20, 1940, pp. 277–84.

572. Constant Temperature Control Apparatus, Utilizing Special Type of Voltage Regulator, **J. S. Blair.** *Journal of Scientific Instruments*, vol. 17, Aug. 1940, pp. 203–08.

573. Elementary Theory of Automatic Temperature Control, **C. O. Fairchild.** *Instruments*, vol. 13, Nov. 1940, pp. 334–39.

574. Some ABC's of Automatic Temperature Control, **M. F. Behar.** *Instruments*, vol. 13, Dec. 1940, pp. 397–402.

575. Compensation Temperature Control Apparatus (in German), *Archiv fur technisches Messen*, no. 116, Feb. 1941, J063–4.

576. Wheatstone Bridge Circuits for Automatic Temperature Regulators, **F. W. Jones.** *Journal of Scientific Instruments*, vol. 18, March 1941, pp. 48–49.

577. Steam Pressure Regulation by Automatic Control, **E. S. Bristol.** *Power*, vol. 85, April 1941, pp. 242–44.

578. A Thyratron—Controlled Annealing Furnace, **L. Tarnopol.** *Review of Scientific Instruments*, vol. 12, July 1941, pp. 367–68.

579. A Highly Simplified Thermionic Control of Temperature, **R. H. Wallace, R. J. Bushnell.** *Plant Physiology*, vol. 16, July 1941, pp. 647–50.

580. Electronic Pyrometer Control, **F. B. MacLaren.** *Electronics*, vol. 14, Nov. 1941, pp. 50, 78.

581. Compensation Devices in Temperature Measurement and Regulation (in German), **W. Hunsinger.** *Elektrotechnische Zeitschrift*, vol. 62, 1941, pp. 481–86.

582. Thermometric Time Lag, **R. Beck.** *Transactions*, American Society of Mechanical Engineers, vol. 63, 1941, pp. 531–43.

583. Investigation of Temperature Regulators Having Time Delays in the Regulating Circuit (in German), **C. E. Mason, G. A. Philbrick, F. V. A. Engel.** *Zeitschrift des Vereines deutscher Ingenieure*, vol. 85, 1941, pp. 287–89.

583A. Two-Bridge-Controlled Thyratron Thermostats, **D. Bancroft.** *Review of Scientific Instruments*, vol. 13, Jan. 1942, pp. 24–27, 114.

584. Thermostats Employing External Surface Control, **V. D. Hopper, T. H. Laby.** *Proceedings*, Physical Society, vol. 54, Jan. 1942, pp. 55–62.

585. Simple Pressure Regulators; Principal Types and Their Characteristics, **H. C. McRae.** *Instruments*, vol. 15, Feb. 1942, pp. 44, 45, 59.

586. Governing Turbine Pressures, **R. Sheppard.** *Power*, vol. 86, Feb. 1942, pp. 82–84; March 1942, pp. 155–57.

587. Temperature Control for Oscillators of Stable Frequency, **C. F. Booth, F. J. M. Laver.** *The Post Office Electrical Engineers' Journal*, vol. 35, April 1942, pp. 8–14.

588. Steam-Temperature Control. *Electrical Review*, vol. 130, May 15, 1942, pp. 615–18.

589. A Modulating Electronic Temperature Control, **W. R. Elliot.** *Heating, Piping, and Air Conditioning*, vol. 14, Oct., 1942, p. 631.

590. A Thyratron Thermal Relay, **D. Rittenburg, I. Sucher.** *Review of Scientific Instruments*, vol. 14, Feb. 1943, p. 51.

591. Temperature Regulation with the Same Accuracy as the Chopper-Bar Response Sensitivity (in German), **H. R. Eggers.** *Elektrotechnische Zeitschrift*, vol. 64, Feb. 1943, pp. 98–102.

592. Experimental Details for a Precision High Temperature Control Utilizing the Hull Circuit, **C. E. Waring, G. Robison.** *Review of Scientific Instruments*, vol. 14, May 1943, pp. 143–46.

593. A Simple Temperature Control for Laboratory Electric Furnaces, **W. Hirst, C. G. Cannon.** *Journal of Scientific Instruments*, vol. 20, Aug. 1943, pp. 129–32.

594. Improved Pressure-Regulating Devices, **B. R. Warner.** *Industrial and Engineering Chemistry*, (Analytical Edition), vol. 15, Oct. 1943, pp. 637–38.

595. Automatic Temperature-Recording Control System, **M. E. Moore.** *Transactions*, American Society of Mechanical Engineers, vol. 65, Nov. 1943, pp. 809–15.

596. Temperature Measurement and Control with Solid Photo-Electric Cells, **M. E. Fogle.** *Transactions*, Electrochemical Society, vol. 83, 1943, pp. 77–86.

597. A Wide Range Sensitive Thermoregulator, **G. E. Coates,** *Journal of Scientific Instruments*, vol. 21, May 1944, pp. 86–87.

598. Automatic Pressure Regulation in Vacuum Distillation, **E. A. Coulson, R. J. Warne.** *Journal of Scientific Instruments*, vol. 21, July 1944, pp. 122–23.

599. Industrial Temperature Instruments Employing Electronic Methods and Devices, **C. O. Fairchild.** *Instruments*, vol. 17, Aug. 1944, pp. 468–72, 496.

600. Notes on the Design of Temperature-Control Units, **J. K. Clapp.** *General Radio Experimenter*, vol. 19, Aug. 1944, pp. 1–7.

601. Electronics Control for Resistance Furnaces, **H. J. Hague.** *Steel*, vol. 115, Aug. 14, 1944, pp. 106, 108, 162, 164, 166, 168, 170.

602. Automatic Control of Stills, **R. E. Shrader, E. J. Wood.** *Electronics*, vol. 17, Sept. 1944, pp. 98–99, 242, 246, 250.

603. Multiple-Diaphragm Pressure Regulators and Their Applications, **H. C. McRae.** *Instruments*, vol. 17, Sept. 1944, pp. 529–31.

604. Laboratory Oven Temperature Control, **W. B. R. Agnew.** *Electronics*, vol. 17, Oct. 1944, pp. 108–09.

605. Aircraft-Engine Temperature Control, **W. A. Ray.** *Transactions*, American Society of Mechanical Engineers, vol. 66, Oct. 1944, pp. 595–97.

606. Thermostatic Control, **T. T. Baker.** *Electrical Review*, vol. 135, Dec. 8, 1944, pp. 811–13.

607. Fine Temperature Control, **M. L. Tounson, R. B. Brock.** *Industrial Chemist*, vol. 21, Jan. 1945, pp. 31–35.

608. Automatic Temperature Control I–II; *Engineering and Boiler House Review*, vol. 59, Jan. 1945, pp. 7–11; Feb. 1945, pp. 34–39.

609. Temperature Control in the H.T.S.T. Pasteurization Process, **J. A. Hall.** *Journal of Dairy Research*, vol. 14, March 1945, pp. 1–20.

610. Device for Electronic Control of Reduced Pressure, **G. D. Oliver, W. G. Bickford.** *Review of Scientific Instruments*, vol. 16, May 1945, pp. 130–31.

611. Attachment to Minimize the Effects of Thermal Lag in Furnace Control, **K. Hoselitz.** *Journal of Scientific Instruments*, vol. 22, May 1945, pp. 96–97.

612. Electronic Temperature Control, **D. Fidelman.** *Radio-Electronic Engineering*, vol. 5, July 1945, pp. 8–11, 39–41.

613. An Anticipatory Method for Improving Automatic Temperature Control, **M. J. Manjoine.** *Instruments*, vol. 18, July 1945, pp. 454–55.

614. An Improved Thermal Control Circuit, **R. L. Ives.** *Review of Scientific Instruments*, vol. 16, Oct. 1945, pp. 294–96.

615. Automatic Temperature Control for Aircraft, **R. A. Gund.** *AIEE Transactions (Electrical Engineering)*, vol. 64, Oct. 1945, pp. 730–34.

616. Adjustable Voltage Thermostat System, **W. C. Griffin.** *Industrial and Engineering Chemistry* (Analytical Edition), vol. 17, Oct. 1945, pp. 671–72.

617. Some Aspects of Temperatures Control in Milk Pasteurization, **R. A. Hill.** *Proceedings*, Chemical Engineering Group, Society of the Chemical Industry, vol. 27, 1945, pp. 165–72.

618. Analysis of Operation of a Thermostat with Contact Thermo-Regulator, **Z. Jelonek.** *Proceedings*, Cambridge Philosophical Society, vol. 42, Jan. 1946, pp. 62–72.

619. A Reliable High Vacuum Gauge and Control System, **R. G. Picard, P. C. Smith, S. M. Zollers.** *Review of Scientific Instruments*, vol. 17, April 1946, pp. 125–29.

620. Measuring and Controlling Temperature and Pressure, **E. W. Feller.** *Power*, vol. 90, April 1946, pp. 216–46.

621. A Simple Automatic Furnace Temperature Control, **E. L. Yates.** *Journal of Scientific Instruments*, vol. 23, Oct. 1946, pp. 229–31.

622. Automatic Temperature Control of Industrial Processes, **E. B. Estabrook.** *Transactions*, Instruments and Measurements Conference, 1947, pp. 139–45.

623. Process Reactions Encountered in Automatic Temperature Control Installation and Some Means of Maintaining the Desired Balance or Condition Within the Process with Reduced Lag, **E. Ferner.** *Transactions*, Instruments and Measurements Conference, 1947, pp. 146–49.

624. The Design of Fast Thermopiles and the Ultimate Sensitivity of Thermal Detectors, **D. F. Hornig, B. J. O'Keefe.** *Review of Scientific Instruments*, vol. 18, July 1947, pp. 474–82.

625. A Two Position Proportional Controller, **W. F. Abbott.** *Journal of Scientific Instruments*, vol. 24, July 1947, pp. 179–81.

626. Proportioning Temperature Controller, **D. Lazarus, A. W. Lawson.** *Review of Scientific Instruments*, vol. 18, Oct. 1947, pp. 730–33.

627. Continuous Control Thermoregulator, **P. Wright.** *Journal of Scientific Instruments*, vol. 24, Oct. 1947, pp. 258–61.

628. Precision Pressure Regulation of Various Gases, **J. K. Hamilton.** *Welding Journal*, vol. 26, Nov. 1947, pp. 977–83.

629. Automatic Temperature Control of Jacketed Pans, **G. H. Farrington.** *Transactions*, Society of Instrument Technology, vol. 1, 1947, pp. 2–21.

630. Compensated Feedback Thermostat (in Polish), **J. Keller.** *Kwartalnik Telekomunikacyjny*, vol. 10, 1947, pp. 52–59.

631. The Determination of Thermal Lagging Times, **J. C. Evans.** *Proceedings*, Physical Society, vol. 59, 1947, pp. 242–56.

632. Automatic Temperature Control for Transport Airplanes, **R. E. Hedges.** *AIEE Transactions*, vol. 66, 1947, pp. 1197–202.

633. A Precision Temperature Regulator with Application to an Adiabatic Calorimeter (in French), **L. Weil.** *Comptes Rendus*, l'Academie des Sciences, vol. 224, 1947, pp. 210–12.

634. Use of the Wheatstone Bridge for the Measurement and Regulation of Temperatures: Application to Heating of Buildings (in French), **J. J. Rives.** *Revue Generale de l'Electricite*, vol. 57, May 1948, pp. 181–89.

635. Vacuum Furnace Control, **F. F. Davis.** *Electronics*, vol. 21, May 1948, p. 81.

636. Compensation for the Lag of a Thermostat (in Dutch), **J. Slooves.** *Electro-techniek*, vol. 26, May 6, 1948, pp. 168–69.

637. A Temperature Control Device Employing Thermistors and a Saturable Reactor, **R. L. Burwell, Jr., A. H. Peterson, G. B. Rathmann.** *Review of Scientific Instruments*, vol. 19, Sept. 1948, pp. 608–09.

638. A Simple Temperature Controller, **J. C. Mouzon.** *Review of Scientific Instruments*, vol. 19, Oct. 1948, pp. 659–62.

639. Gas Thermometer for Automatic Control of Low Temperatures, **D. D. Tunnicliff.** *Analytical Chemistry*, vol. 20, Oct. 1948, pp. 962–64.

640. Revisions for a Precision High Temperature Control Unit, **S. Steingiser, G. J. Rosenblit, C. E. Waring.** *Review of Scientific Instruments*, vol. 19, Nov. 1948, pp. 815–16.

641. An Automatic Temperature Control for a Liquid Helium Cryostat, **E. R. Andrew.** *Journal of Scientific Instruments*, vol. 25, Dec. 1948, pp. 416–17.

642. Electronic Controls for Regulating Temperature, **H. B. Clay.** *Electrical Manufacturing*, vol. 42, Dec. 1948, pp. 78–82.

643. Steam Pressure Regulators System Orgres for De-Aerators (in Russian), **P. M. Brik.** *Elektricheskie Stantsii*, no. 7, 1948, pp. 20–22.

644. The Electronic Measurement and Control of Heat, **J. H. Jupe.** *Electronic Engineering*, vol. 21, Jan. 1949, pp. 13–16; Feb. 1949, pp. 48–51; March 1949, pp. 94–97.

645. Photoelectric Control of High-Temperature Furnaces, **F. C. Todd.** *Electronics*, vol. 22, Feb. 1949, pp. 80–83.

646. "Heat Inertia" in Problems of Automatic Control of Temperature, **V. Broida.** *Instruments*, vol. 22, 1949 (serial), Feb., pp. 136–38, 160–66; March, pp. 222–24, 254–64; April, pp. 324–25, 362–66; May, pp. 406, 450–58.

647. The Regulation of Temperature in the Application of High Frequency Induction Heating to Thermodynamic Measurements, **R. Speiser, G. W. Ziegler, Jr., H. L. Johnston.** *Review of Scientific Instruments*, vol. 20, June 1949, pp. 385–88.

648. Experimental Application of Combustion Controls to a Process Heater, **W. E. Boyle, P. R. Hoyt.** *Instruments*, vol. 22, June 1949, pp. 529–32.

649. Dynamic Accuracy in Temperature Measurement, **J. G. Ziegler, N. B. Nichols.** *Instruments*, vol. 23, Jan. 1950, pp. 66–69.

650. Automatic Control of Industrial Furnaces, **L. Walter.** *Engineer*, vol. 189, March 3, 1950, pp. 260–62; March 10, 1950, pp. 292–94; March 17, 1950, pp. 324–25; March 24, 1950, pp. 351–52.

651. A Proportional Reset Furnace Controller for Temperatures up to 1600 Deg. C, **R. W. Nurse, J. H. Welch.** *Journal of Scientific Instruments*, vol. 27, April 1950, pp. 97–99.

652. A Temperature Regulator for Continuous Action Using a Thyratron (in French), **R. Aumont.** *Revue Generale d'Electricite*, vol. 59, April 1950, pp. 175–78.

653. Automatic Control of High-Vacuum Systems, **J. W. Clark, G. H. Witts.** *Electronics*, vol. 23, June 1950, pp. 108–10.

654. Electronic Control of Home Heating, **J. M. Wilson.** *Electronics*, vol. 23, Dec. 1950, pp. 84–87.

655. Design and Operational Characteristics of Cartesian Manostats, **R. Gilmont.** *Analytical Chemistry*, vol. 23, Jan. 1951, pp. 157–62.

656. Electric Controllers for Laboratory Furnaces, **M. H. Roberts.** *Electronic Engineering*, vol. 23, Feb. 1951, pp. 51–54.

657. A Photoelectric Temperature Controller for Multipoint Operation, **G. Mayer, D. R. Thorneycroft, A. G. Haynes.** *Sheet Metal Industries*, vol. 28, Feb. 1951, pp. 155–57, 166.

658. The Dynamic Behavior of the Control Stage in Pressure Control (in German), **P. Profos.** *Schweizer Archiv fur angewandte Wissenschaft und Technik*, vol. 17, April 1951, pp. 114–19. Frequency response diagrams for pressure regulating systems.

659. The Control of Electric Element Furnaces to Fine Limits at High Temperatures for Research Purposes, **T. W. Lomas, M. D. Jepson, J. R. Rait.** *Journal*, Iron and Steel Institute, vol. 168, June 1951, pp. 126–34.

660. Influence of the Transfer of Heat on the Stability of Temperature Controllers (in French), **P.-L. Dubois-Violette.** *Comptes Rendus*, l'Academie des Sciences, vol. 233, July 2, 1951, pp. 26–28; July 16, 1951, pp. 232–34.

661. Radiation Pyrometers Control New High-Gradient Heating Process, **H. W. Cox.** *Instruments*, vol. 24, Aug. 1951, pp. 878–79.

662. An Inexpensive Thyratron Controlled Thermostat Relay, **Charles M. Procter.** *Review of Scientific Instruments*, vol. 22, Dec. 1951, pp. 1023–24.

663. Temperature Regulation in Induction Heating, **Homer E. Henschen, James W. Edwards, Herrick L. Johnston.** *Review of Scientific Instruments*, vol. 22, Dec. 1951, pp. 987–88.

664. Precise Temperature Control, **C. F. Rains, R. C. McMaster.** *Electrical Manufacturing*, vol. 48, Dec. 1951, pp. 110–13.

Flow and Liquid Level Control

665. Feed Water Regulation with Electric and Turbine-Driven Pumps (in German), **H. Kissinger.** *Zeitschrift des Vereines deutscher Ingenieure*, vol. 75, Feb. 14, 1931, pp. 191–94.

666. Automatic Mixing and Proportioning of Gases and Liquids, **H. J. Velten.** *Industrial and Engineering Chemistry*, vol. 29, 1937, pp. 1214–18.

667. Control of Liquid Level in Vessels Under Pressure, **J. B. McMahan.** *Industrial and Engineering Chemistry*, vol. 29, 1937, pp. 1219–24.

668. Electrical Water-Level Control and Recording Equipment for Model of Cape Cod Canal, **H. L. Hazen.** *AIEE Transactions*, (*Electrical Engineering*), vol. 56, Feb. 1937, pp. 237–44.

669. Regulation of Feed-Water Level in Boilers, **V. V. Veenschoten.** *Combustion*, vol. 8, March 1937, pp. 34–36.

670. Decade of Progress in Industrial Fluid Metering and Automatic Control, **R. J. S. Pigott.** *Instruments*, vol. 11, Jan. 1938, pp. 19–25.

671. Automatic Level Controllers, **M. F. Behar.** *Instruments*, vol. 14, Nov. 1941, pp. 326–80.

672. A Study of Damper Characteristics, **P. S. Dickey, H. L. Coplen.** *Transactions*, American Society of Mechanical Engineers, vol. 64, 1942, pp. 137–54.

673. Liquid Level Control, **H. Seymour.** *Electrician*, vol. 129, Sept. 25, 1942, pp. 331–34.

674. Flow and Level Controls. *Electrical Manufacturing*, vol. 32, July 1943, pp. 120, 122, 124, 126, 178, 180, 182, 184, 186.

675. Constant Pressure and Flow Ratio Regulator for Continuously Mixing Two Gases, **N. L. Heikes.** *Industrial and Engineering Chemistry* (Analytical Edition), vol. 15, Feb. 1943, pp. 133–34.

676. A New Energy-Saving Regulating System for Gas Distribution and Collecting Installations, **A. Leyer.** *Brown Boveri Review*, vol. 30, Nov.-Dec., 1943, pp. 337–39.

677. Floatless Electrical Liquid-Level Controller. *Engineering*, vol. 155, Jan. 1, 1943, p. 17.

678. Gas Flow Control Systems, **W. J. Roberts.** *Power and Works Engineer*, vol. 39, Aug. 1944, pp. 180–82.

679. Phototube Control of Fluid Flow, **R. C. McNickle.** *Electronics*, vol. 17, Sept. 1944, pp. 110–13.

680. Photo-electric Automatic Liquid-Level Control, **N. H. Ceaglske, S. A. Kesslinger.** *Industrial and Engineering Chemistry* (Analytical Edition), vol. 16, June 1944, pp. 393–94.

681. Ratio and Multiple-Fuel Controls in the Steel Industry, **H. Ziebolz.** *Transactions*, American Society of Mechanical Engineers, vol. 66, Nov. 1944, pp. 705–12.

682. Measuring and Controlling Liquid Level, **E. W. Feller.** *Power*, vol. 89, April 1945, pp. 220–42.

683. Automatic Liquid Level Controls, **T. A. Cohen.** *Electronics*, vol. 18, April 1945, pp. 120–28.

684. An Electro-Magnetic Liquid Flow Control Valve, **G. G. Blake.** *Chemistry and Industry*, no. 5, Feb. 2, 1946, p. 46.

685. Averaging Liquid Level Control, **J. G. Ziegler.** *Industrial and Engineering Chemistry*, vol. 38, April 1946, pp. 360–64.

686. Fundamentals of Automatic Control of Liquid Level, **L. Walter.** *Water and Water Engineering*, vol. 52, Nov. 1949, pp. 556–66.

687. The Control of Quantity and Mixtures of Gases and Liquids by an Integrating Regulator (in German), **H. Garthe.** *Frequens*, vol. 3, Dec. 1949, pp. 353–63.

688. Instrumentation by and with Controlled Volume Pumps, **R. T. Sheen.** *Instruments*, vol. 22, May 1949, pp. 442–47.

689. History of Bellows-Actuated Flow Meters, **C. B. Nolte.** *Instruments*, vol. 23, Jan. 1950, pp. 79–84.

690. Ball Float Type Liquid Level Controllers, **E. W. Horvick.** *Paper Trade Journal*, vol. 131, Nov. 9, 1950, pp. 33, 34, 36.

691. Automatic Control of Flow in the Process Industries, **A. E. Krogh.** *Instruments*, vol. 24, May 1951, pp. 590–93.

692. Factors in Precise Control of Liquid Flow, **A. R. Catheron.** *Instruments*, vol. 24, June 1951, pp. 705–10.

Generator Voltage Regulation

693. Voltage Regulation of Generators, **H. A. Laycock.** *AIEE Transactions*, vol. 30, 1911, pp. 555–73.

694. Voltage Regulation and Parallel Operation of Generators (in German), **N. Landesberg.** *Elektrotechnische Zeitschrift*, vol. 48, July 14, 1927, pp. 998–1000.

695. Quick Response Excitation for Alternating Current Synchronous Machinery, **C. A. Powell.** *Electric Journal*, vol. 24, April 1927, pp. 157–62.

696. Simultaneous Regulation of Prime Movers and Generators (in German), **H. Korn.** *Elektrotechnik und Maschinenbau*, vol. 46, Jan. 22, 1928, pp. 81–86.

697. Voltage Control of Large Alternators, **H. W. Taylor.** *Journal*, Institution of Electrical Engineers, vol. 68, 1930, pp. 317–38.

698. Problem of Regulation of Electric Generating Units in Parallel Connection During Disturbances (in French), **L. Barbillion.** *Revue Generale de l'Electricite*, vol. 27, 1930, April 12, pp. 575–84; April 19, pp. 623–32.

699. Quick Response Excitation for A-C Machines, **C. Lynn.** *Power*, vol. 74, Oct. 6, 1931, pp. 498–501.

700. Effect of Voltage Regulators on Stability of Parallel Power Stations (in German), **A. V. Timascheff.** *Elektrotechnik und Maschinenbau*, vol. 50, Nov. 20, 1932, pp. 641–50.

701. Effect of Voltage Regulators on the Stability of Alternators (in French), **G. Belfils.** *Congres International de l'Electricite*, Sect. 3, no. 31, 1932, pp. 429–48.

702. Automatic Regulation of Small Alternators (in French), **W. Marolf.** *Bulletin*, Association Suisse des Electriciens, vol. 24, May 12, 1933, pp. 217–20.

703. Variable Speed Constant Voltage D-C Generators, **Fred B. Hornby.** *AIEE Transactions*, vol. 52, 1933, pp. 727–30.

704. Studies on Automatic Voltage Regulators for Measurement Purposes (in German), **W. Hohle.** *Elektrizitaetwirtschaft*, vol. 32, March 15, 1933, pp. 93–98.

705. Selection of Generator Voltage Regulators, **A. G. Gower.** *Electric Journal*, vol. 31, 1934, pp. 145–47.

706. Instantaneous Voltage Regulation of D-C Generators, **T. M. Linville.** *General Electric Review*, vol. 37, 1934, pp. 318–23.

707. Quick Response Excitation, **W. A. Lewis.** *Electric Journal*, vol. 31, Aug. 1934, pp. 308–12.

708. Development and Use of Generator Voltage Regulators, **J. W. Dodge, L. W. Thompson.** *General Electric Review*, vol. 38, Feb. 1935, pp. 77–83.

709. Constant Voltage, Variable-Speed, D-C Generator-Exciter Set, **R.S. Tener, E. S. Dibble.** *General Electric Review*, vol. 38, June 1935, pp. 263–67.

710. Automatic Control of Voltage and Current, **P. A. Borden, M. F. Behar.** *Instruments*, vol. 9, 1936, July, pp. 201–10; Aug., pp. 235–38; Sept., pp. 259–62; Oct., pp. 289–92.

711. Parallel Operation of A-C Generators with Individual Voltage Regulator Control, **J. W. Dodge, L. W. Thompson.** *General Electric Review*, vol. 39, March 1936, pp. 131–38.

712. Compounding a Voltage Regulator (in German), **E. Maurer.** *Bulletin*, Association Suisse des Electriciens, vol. 28, June 11, 1937, pp. 257–61.

713. Automatic Voltage Regulation of D-C Generators for Use with Ungoverned Waterwheels, **R. S. Tener, E. S. Dibble.** *General Electric Review*, vol. 41, April 1938, pp. 191–93.

714. Voltage Regulators. *Engineer*, vol. 165, 1938, May 13, pp. 526–27; May 20, pp. 556–57; May 27, pp. 584–85; June 3, pp. 610–11; June 10, pp. 638–40; June 17, pp. 666–67; June 24, pp. 696–98. Survey of a large number of commercial regulators.

715. Automatic Voltage Regulation in Power Stations (in Italian), **E. Pautrie.** *Elettrotecnica*, vol. 26, Sept. 25, 1939, pp. 622–31.

716. Recent Developments in Generator Voltage Regulation, **C. R. Hanna, K. A. Oplinger, C. E. Valentine.** *AIEE Transactions*, vol. 58, 1939, pp. 838–45.

717. Stabilizing Arrangements with Automatic Voltage Regulators (in German), **A. Lang.** *Archiv fur Elektrotechnik*, vol. 33, Nov. 10, 1939, pp. 687–97.

718. The Importance and Computation of the Effective Exciter Time Constant with Automatic Voltage Regulation of Three-Phase Alternators (in German), **A. Lang.** *Archiv fur Elektrotechnik*, vol. 33, May 12, 1939, pp. 306–25.

719. Modern Voltage Regulators: Time Adjustment and Rapid Action (in Italian), **E. Maggi.** *Elettrotecnica*, vol. 26, Oct. 10, 1939, pp. 642–49.

720. Parallel Operation of Synchronous Generators with Prime Mover Regulators Having a Constant Delay Time (in German), **F. Reinhardt.** *Wissenschaftliche Veroffentlichungen aus den Siemens-Werken*, vol. 18, 1939, pp. 24–44.

721. The Mode of Operation of the High-Speed Voltage Regulator During Parallel Operation of Generators (in German), **H. Happoldt.** *Brown Boveri Company Nachrichten*, vol. 28, Jan.-March 1941, pp. 28–32.

722. Automatic Voltage Regulators Improve Kilowatt Quality, **A. M. Shong.** *Power*, vol. 86, April 1942, pp. 63–64, 132.

723. Voltage Control of D-C Generators by Flux Diversion, **E. C. Davies, W. G. Crawford.** *GEC Journal*, vol. 12, Feb. 1942, pp. 27–37.

724. Power Regulation of Groups of Electric Generators (in French), **G. Nasse.** *Revue Generale de l'Electricite*, vol. 53, April 1944, pp. 59–65.

725. Regulation of A-C Generators with Suddenly Applied Loads, **E. L. Harder, R. C. Cheek.** *AIEE Transactions* (*Electrical Engineering*), vol. 63, June 1944, pp. 310–18.

726. A-C Generator for Constant Voltage Without Regulator (in German), **K. Tardel.** *Elektrotechnische Zeitschrift*, vol. 65, April 20, 1944, pp. 139–42.

727. Steady-State Stability of Synchronous Machines as Affected by Voltage-Regulator Characteristics, **C. Concordia.** *AIEE Transactions* (*Electrical Engineering*), vol. 63, 1944, pp. 215–20.

728. Automatic Regulation of Turbine Generators to Relieve Power-Supply Systems of Steel-Mill Load Swings, **W. W. Eberhardt, C. W. Harrison, E. J. Kohn, A. G. Darling.** *AIEE Transactions* (*Electrical Engineering*), vol. 64, 1945, pp. 751–58.

729. Controlled Excitation, **W. K. Boice.** *General Electric Review*, vol. 48, March 1945, pp. 42–47.

730. Voltage Variation of Suddenly Loaded Generators, **H. C. Anderson Jr.** *General Electric Review*, vol. 48, Aug. 1945, pp. 25–33.

731. Rapid Response Voltage Regulators. Examples of Application at Bissorte and Pradierres Power Stations (in French), **M. Ducrot.** *Revue Generale de l'Electricite*, vol. 54, Sept. 1945, pp. 259–70.

732. Notes on Voltage and Reactive Power Control of Alternators Running in Parallel (in Czech) **S. Matena.** *Elektrotechnicky Obzor*, vol. 35, May-June 1946, pp. 147–55.

733. Alternator Exciter Systems, **R. David.** *Report No. 101*, International Conference on Large Electric, High-Tension Systems, 1946.

734. Stabilization of Synchronous Generators by High-Speed Regulation of the Excitation in Connection with Power Transmission over Long Distances, **W. Frey and C. Lavanchy.** *Brown Boveri Review*, vol. 33, Nov. 1946, pp. 335–54.

735. The Development of Modern Excitation Systems for Synchronous Condensers and Generators, **F. M. Porter, J. H. Kinghorn.** *AIEE Transactions*, vol. 65, 1946, pp. 1020–28.

736. Modern Excitation Systems for Large Synchronous Machines, **J. B. McClure, S. I. Whittlessey, M. E. Hartman.** *AIEE Transactions*, vol. 65, 1946, pp. 939–45.

737. Solution of the General Voltage Regulator Problem by Electrical Analogy, **E. L. Harder.** *AIEE Transactions*, vol. 66, 1947, pp. 815–25.

738. Automatic Voltage Control of Generators, **C. Stewart.** *Journal*, Institution of Electrical Engineers, vol. 94, pt. 2A, 1947, pp. 39–48.

739. Parallel Operation and Over-Compounding with Compensated Voltage Regulators, **W. Blendinger.** *Brown Boveri Review*, vol. 34, June-July 1947, pp. 122–28.

740. Excitation Problems in Hydroelectric Generators Supplying Long Transmission Lines, **C. L. Killgore.** *AIEE Transactions*, vol. 66, 1947, pp. 1277–84.

741. Automatic Voltage Regulators (in French), **J. Debois.** *Charleroi-Jeumont Revue*, no. 3–4, July-Dec. 1947, pp. 104–27.

742. Voltage Regulator—What to Expect of it, **G. A. Hanlon, R. E. Lloyd.** *Power Generation*, vol. 52, March 1948, pp. 68–70.

743. Control of Alternators. *Mechanical World*, vol. 121, April 18, 1948, pp. 367–70.

744. A Semiempirical Approach to Voltage Dip—with Suddenly Applied Loads on A-C Generators, **L. T. Rosenberg.** *AIEE Transactions*, vol. 68, pt. I, 1949, pp. 160–67.

745. Compounding of Powerful Synchronous Generators with Electromagnetic Voltage Corrector (in Russian), **V. L. Inosov, L. V. Tsukernik.** *Elektrichestvo*, no. 9, Sept. 1949, pp. 15–22. Exciter field current is supplied by 3-phase voltage and current transformers from generator output, with regulator action supplied by magnetic amplifiers.

746. Effect of Buck-Boost Voltage Regulator on Steady-State Power Limit, **C. Concordia.** *AIEE Transactions*, vol. 69, pt. I, 1950, pp. 380–85.

747. Notes on the Automatic Regulation of Voltage and Reactive Power of Alternators (in French), **L. Gatesoupe.** *Revue de l'Electricite et de Mecanique*, no. 82, July-Aug.-Sept. 1950, pp. 32–42.

748. Dynamic Stability of a Synchronous Generator with an Excitation Regulator (in Russian), **V. K. Gorushkin.** *Izvestiya Akademii Nauk, SSSR.* Otdelenie Tekhnicheskikh Nauk, no. 1, Jan. 1950, pp. 79–88.

749. Automatic Regulation of Generators, **A. Ernst, P. Biveroni.** *Bulletin Oerlikon*, no. 282, Mar. 1950, pp. 1991–2008. (Also *Engineers' Digest*, vol. 12, Feb. 1951, pp. 44–47.)

750. Automatic Regulation of Unattended Central Stations and Small Power Houses, **H. Bolleter, A. Abegglen.** *Bulletin Oerlikon*, no. 286, Dec. 1950, pp. 2113–25.

751. Introduction to Voltage and Frequency Regulation Problems in Electrical Networks on Aircraft (in French), **J. Duc.** *Bulletin*, Societé Francaise des Electriciens, vol. 10, series 6, 1950, pp. 95–98.

752. Regulation of A-C Generators with Suddenly Applied Loads—Part II, **E. L. Harder, R. C. Cheek, J. M. Clayton.** *AIEE Transactions*, vol. 69, pt. I, 1950, pp. 395–406.

753. Transient Response of Direct-Current Dynamos, **H. E. Koenig.** *AIEE Transactions*, vol. 69, pt. I, 1950, pp. 139–45.

754. Excitation System Performance with Motor-Driven Exciters, **A. G. Mellor, M. Temoshok.** *AIEE Transactions*, vol. 69, pt. I, 1950, pp. 321–27.

755. Excitation Improvement — Electronic Excitation and Regulation of Electric Generators as Compared to Conventional Methods, **A. H. Phillips, W. H. Lambert, D. R. Pattison.** *AIEE Transactions*, vol. 69, 1950, pp. 338–41.

756. Stability of Regulation of Generator Excitation under Rising Characteristics (in Russian), **K. A. Smirnov.** *Elektrichestvo*, no. 1, 1950, pp. 34–39.

757. Measurement of D-C Machine Parameters, **Robert M. Saunders.** *AIEE Transactions*, vol. 70, pt. I, 1951, pp. 700–06.

Generator Voltage Regulators, Rheostatic and Vibrating Types

758. Automatic Voltage Regulators, **C. A. Boddie.** *Electric Journal*, vol. 14, 1917, pp. 75–84. Tirrill regulator.

759. Brown Boveri Quick Acting Regulator, **H. C. Kloninger.** *Brown Boveri Review*, vol. 10, 1923, pp. 199–207. Rocking contact regulator.

760. On the Theory of Tirrill Regulators, **J. Okochi.** *Journal*, Institute of Electrical Engineers, Japan, no. 439, Feb. 1925, pp. 182–204.

761. The Extended Broad-Range Voltage Regulator, **J. H. Ashbaugh.** *Electric Journal*, vol. 22, 1925, pp. 559–61. Tirrill vibrating relay type.

762. A Vibrating Contact Type D-C Automatic Voltage Regulator Sensitized by Means of Thermionic Tubes, **M. Hoshiai.** *Journal*, Institute of Electrical Engineers of Japan, no. 445, Aug. 1925, pp. 679–708.

763. A New Electric Regulator (in German). *Elektrotechnische Zeitschrift*, vol. 46 pt. 2, 1925, pp. 1695–96. Vibrating relay regulator whose frequency is established independently.

764. Direct Acting Automatic Voltage Reg-

ulator, **O. K. Marti.** *Electrical World*, vol. 88, 1926, pp. 1015–17.

765. Operation of Voltage Regulators for Alternating Current Generators, **W. H. Turner.** *Power*, vol. 64, July 27, 1926, pp. 124–25.

766. Care and Adjustment of Voltage Regulators, **W. H. Turner.** *Power*, vol. 66, Aug. 9, 1927, pp. 201–03.

767. Principles of Automatic Voltage Regulators, **J. H. Ashbaugh.** *Power Plant Engineering*, vol. 31, 1927, pp. 732–37. Vibrating relay.

768. Some Applications of the Tirrill Regulator (in French), **M. Mises.** *Revue de l'Electricite et de Mecanique*, no. 3, Jan.-Feb. 1929, pp. 24–38.

769. Quick-Response Generator Voltage Regulator Field Tests Made with Oscillograph, **E. J. Burnham, J. R. North, I. R. Dohr.** *AIEE Journal*, vol. 48, 1929, pp. 465–68.

770. Voltage Regulation by Means of Carbon Resistances (in German), **H. Grob.** *Elektrotechnische Zeitschrift*, vol. 51, Dec. 11, 1930, pp. 1717–20.

771. Carbon Pile Voltage Regulators, **E. H. Wolff.** *Electric Journal*, vol. 27, 1930, pp. 101–03.

772. Automatic Regulator. *Engineer*, vol. 152, Aug. 21, 1931, pp. 203–05. Hydraulic servo for regulator applications.

773. Exciter Rheostatic Regulators, **J. H. Ashbaugh.** *Electric Journal*, vol. 28, May 1931, pp. 294–98.

774. Dynamics of Automatic Rheostatic Type Voltage Regulators (in Russian), **D. A. Vikker.** *Elektrichestvo*, no. 9, 1934, pp. 26–30.

775. The Exciter Rheostatic Regulator, **A. C. Gower, Jr.** *Electric Journal*, vol. 32, 1935, pp. 73–75.

776. The Generator Rheostatic Regulator, **A. G. Gower.** *Electric Journal*, vol. 32, 1935, pp. 143–44.

777. Carbon-Pressure Automatic Voltage Regulators (in German), **H. Grob.** *Zeitschrift fur Fernmeldetechnik*, vol. 17, Aug. 1936, pp. 117–22.

778. Applications of AEG Rapid Regulators of the Tirrill-Type (in German), **M. Herklotz, C. Pelz.** *AEG Mitteilungen*, no. 11, Nov. 1937, pp. 416–21.

779. The Small Size Brown Boveri Quick Acting Voltage Regulator, Type JB-1, for AC and DC, **W. Marolf.** *Brown Boveri Review*, vol. 25, 1938, pp. 241–43.

780. The Fast Acting Properties of Tirrill Regulators (in German), **A. Lang.** *Elektrotechnische Zeitschrift*, vol. 32, 1938, pp. 675–83.

781. Ultra-Rapid Regulation of Synchronous Machines (in German), **A. Gantenbein.** *Bulletin*, Association Suisse des Electriciens, vol. 29, Dec. 23, 1938, pp. 750–56.

782. Carbon Pile Voltage Regulators. *Engineer*, vol. 166, Aug. 26, 1938, pp. 233–34.

783. Ultra-Rapid Regulation of Synchronous Machines, **G. Gantenbein.** *Bulletin Oerlikon*, no. 211–12, Jan. 1940, pp. 1303–08.

784. The Direct-Acting Generator Voltage Regulator, **W. K. Boice, S. B. Crary, Gabriel Kron, L. W. Thompson.** *AIEE Transactions* (*Electrical Engineering*), vol. 59, March 1940, pp. 149–57.

785. A New Mercury Rheostatic Element for Regulation and Control, **K. A. Oplinger.** *AIEE Transactions* (*Electrical Engineering*), vol. 60, Aug. 1941, pp. 846–49.

786. The Application of Voltage Regulators to Aircraft Generators, **L. W. Thompson, F. E. Crever.** *AIEE Transactions*, vol. 61, June 1942, pp. 363–65.

787. Aircraft Voltage Regulator and Cut-out, **R. C. Jones, D. W. Exner, Sherwin H. Wright.** *AIEE Transactions* (*Electrical Engineering*), vol. 61, June, 1942, pp. 334–39.

788. The Application of Voltage Regulators to Aircraft Generators, **L. W. Thompson, F. E. Crever.** *AIEE Transactions*, vol. 61, 1942, pp. 363–65.

789. The Metadyne as Exciter. Excitation of Large Machines (in Italian), **P. Maralli.** *Elettrotecnica*, vol. 29, May 10, 1942, pp. 190–95.

790. Carbon-Pile Voltage Regulators for Aircraft, **W. G. Neild.** *AIEE Transactions* (*Electrical Engineering*), vol. 63, 1944, pp. 839–43.

791. The Plunger Coil Voltage Regulator, **A. Meyerhans.** *Brown Boveri Review*, vol. 32, June 1945, pp. 207–10.

792. Analysis and Redesign of a Carbon Pile Voltage Regulator for Aircraft Generators, **W. B. Kouwenhoven, G. J. Thaler.** *AIEE Transactions*, vol. 67, pt. II, 1948, pp. 1197–203.

793. Operation and Maintenance of Mechanical Voltage Regulators, **W. H. Turner.** *Power Generation*, vol. 53, Nov. 1949, pp. 60–64.

794. Stabilizing System for Electric Machines. *Engineer*, vol. 187, Feb. 11, 1949, pp. 168–69.

795. A New High-Speed Regulator for 3-Phase Generators (in German), **A. Leonard.** *Elektrotechnische Zeitschrift*, vol. 70, Sept. 1, 1949, pp. 329–32. Relay type.

796. Aircraft Carbon-Pile Voltage Regulators, Fundamentals, and Design Improvements, **B. O. Austin, H. H. C. Richards.** *AIEE Transactions*, vol. 68, pt. II, 1949, pp. 983–87.

797. Quick Acting Voltage Regulators Designed According to Generator Size, **A. Ernst, P. Biveroni.** *Bulletin Oerlikon*, no. 282, Jan.-Feb.-March 1950, pp. 1991–2008.

798. Dynamic Characteristics of Carbon Pile Voltage Regulators, **Robert L. Mills.** *AIEE Transactions*, vol. 69, pt. II, 1950, pp. 1347–53.

799. Transient Analysis of a Voltage–Regulated Aircraft D-C System, **Donald G. Scorgie.** *AIEE Transactions*, vol. 69, pt. II, 1950, pp. 1318–23.

800. Steady-State Characteristics of Carbon-Pile Voltage Regulators, **D. G. Scorgie, D. H. Schaefer.** *AIEE Transactions*, vol. 70, pt. II, 1951, pp. 1572–77. An electronic control circuit employing feedback is used to measure the steady-state characteristics.

Generator Voltage Regulators, Electronic Types

801. Application of Electronics to Heavy Current Machines (in German), **F. W. Meyer.** *Elektrotechnische Zeitschrift*, vol. 42, 1921, pp. 689–93, 725–28.

802. Voltage Regulation of D-C Generators with Hot Cathode Tubes (in German), **W. Taeger.** *Elektrotechnische Zeitschrift*, vol. 51, 1924, pp. 1407–09.

803. A Thermionic Valve Type Close Voltage Regulator, **F. C. Turner.** *Engineering*, vol. 124, 1927, pp. 537, 538.

804. On the Practical Application of Certain Methods for Voltage Regulation of Generators by Means of High-Vacuum Tubes (in German), **N. A. J. Voorhoeve.** *Archiv fur Elektrotechnik*, vol. 21, 1928, pp. 228–43.

805. A Vacuum Tube Voltage Regulator for Large Power Units, **L. C. Verman, H. J. Reich.** *Journal*, Optical Society of America, vol. 19, Oct. 1929, pp. 243–49.

806. Valve Voltage Regulators for Alternators, **L. C. Verman, L. A. Richards.** *Review of Scientific Instruments*, vol. 1, Oct. 1930, pp. 581–91.

807. Grid-Glow Tube Rheostatic Regulator, **J. H. Ashbaugh, F. H. Gulliksen.** *Electric Journal*, vol. 28, April 1931, pp. 207–08.

808. Valve Voltage Regulators (in German), **R. G. Berthold.** *VDE Fachberichte*, 1931, pp. 33–35.

809. Thermionic Voltage Regulator for Prevention of Hunting, **F. H. Gulliksen.** *Electrical World*, vol. 98, July 25, 1931, pp. 162–63.

810. Philips Triode Regulator (in German), **N. A. J. Voorhoeve, F. H. de Jong.** *Elektrotechnische Zeitschrift*, vol. 53, June 2, 1932, pp. 530–32.

811. Diode Regulators - Simple Method of Voltage Control. *Electrical Review*, vol. 111, Dec. 16, 1932, p. 886.

812. Thyratron Voltage Regulator for an Alternator, **C. E. Weinland.** *Review of Scientific Instruments*, vol. 3, Jan. 1932, pp. 9–19.

813. Thermionic Regulation of the Voltage of Alternators (in French), **W. Druey.** *Bulletin*, Association Suisse des Electriciens, vol. 24, Dec. 8, 1933, pp. 647–50.

814. Precision Voltage Regulation of Machines by Electron Tubes (in German), **R. G. Berthold.** *Archiv fur technisches Messen*, vol. 3, Sept. 1933, T122–3.

815. Voltage Regulation for A-C Generators (in German), **W. Druey.** *Helvetica Physica Acta*, vol. 67, 1933, pp. 488–90.

816. Electronic Regulator for A-C Generators, **F. H. Gulliksen.** *Electrical Engineering*, vol. 53, 1934, pp. 877–81.

817. New Developments in Precise Electronic Regulators, and Their Applications (in German), **R. G. Berthold, A. V. Engel.** *Siemens Zeitschrift*, vol. 14, June 1934, pp. 214–22.

818. Regulation and Balancing of 3-Phase 3-Wire and 4-Wire Networks by Valve-Controlled Generators (in German), **R. Reese.** *Elektrotechnische Zeitschrift*, vol. 56, 1935, Sept. 26, pp. 1069–72; Oct. 3, pp. 1095–99.

819. A New Continuous Electric Regulator (in German), **C. Himmler.** *Archiv fur Elektrotechnik*, vol. 29, Sept. 10, 1935, pp. 577–99. Survey of the application of electron tubes to the regulation of temperature, pressure, and voltage.

820. Rapid-Response Excitation of Synchronous Machines by Means of Rectifiers (in German), **H. Harz.** *Elektrotechnische Zeitschrift*, vol. 56, July 25, 1935, pp. 833–37.

821. Automatic Voltage Regulator Using Grid-Controlled Mercury Arc Rectifier, **M. Takahashi.** *Journal*, Institute of Electrical Engineers, Japan, vol. 55, Feb. 1935, pp. 73–81.

822. An Electronic Regulator for an Alternator, **Clyde C. Whipple, William E. Jacobsen.** *Electrical Engineering*, vol. 54, June 1935, pp. 663–67.

823. A Thyratron Voltage Control, **C. J. Burbank.** *Review of Scientific Instruments*, vol. 7, 1936, pp. 427–29.

824. Electronic Voltage Regulator for Lamp Testing, **R. R. Brady, C. P. Bernhardt.** *Electronics*, vol. 9, Sept. 1936, pp. 36, 38, 40.

825. An Electronic Voltage Regulator for D-C Generators, **F. H. Gulliksen.** *Electrical Engineering*, vol. 55, Aug. 1936, pp. 873–75.

826. Regulator Systems for Electromagnets. **H. L. Anderson. J. R. Dunning, D. P. Mitchell.** *Review of Scientific Instruments*, vol. 8, 1937, pp. 497–501.

827. An Alternator Voltage Regulator Utilizing a Nonlinear Circuit, **Harry W. Mayne.** *Electrical Engineering*, vol. 56, 1937, pp. 462–64, 476.

828. D-C Voltage Regulator (in German), **K. Sauermann.** *Elektrotechnische Zeitschrift*, vol. 58, Sept. 16, 1937, pp. 1003–07.

829. Vacuum Tube Regulators for A-C Generators on Impulse Loading (in German), **C. Frohmer.** *VDE Fachberichte*, vol. 9, 1937, pp. 153–55.

830. Effect of Ripple Voltages on Automatic Voltage Control of a D-C Generator by Vacuum Tubes, **K. Awaya, M. Emi, S. Hasegawa.** *Electrotechnical Journal*, vol. 2, Jan. 1938, pp. 6–10.

831. Fine Field Regulation of Electrical Machines by Thermionic Valves (in German), **C. H. Sturm.** *Zeitschrift fur Fernmeldetechnik*, vol. 19, 1938, pp. 106, 107.

832. New Vacuum Tube Type Automatic Voltage Regulator, **S. Aoki, Y. Matusita.** *Electrotechnical Journal*, vol. 2, March 1938, pp. 56–60.

833. Voltage Regulation of Direct Current Generators by Means of Triodes, **N. A. J. Voorhoeve, F. H. de Jong.** *Philips Technical Review*, vol. 3, April 1938, pp. 97–103.

834. Concerning Thermionic Regulation of D-C Generators, **W. E. Danforth.** *Review of Scientific Instruments*, vol. 10, 1939, pp. 211–17.

835. Simple Valve Impulse Regulator for A-C Generator with Heavily Fluctuating Load (in German), **C. Frohmer, G. Seulen.** *AEG Mitteilungen*, no. 2, Feb. 1939, pp. 95–99.

836. Vibration Regulator with Valves Instead of Intermediate Relays to Obtain a Larger Regulating Speed and Range (in German), **A. Leonard, A. Lang.** *Elektrotechnik und Maschinenbau*, vol. 57, July 21, 1939, pp. 380–84. Vibrating relay type using electron tubes.

837. Electronic Voltage and Speed Control of Alternators, **J. H. Piddington.** *Journal*, Institution of Engineers, Australia, vol. 11, Nov. 1939, pp. 375–79.

838. Valve-Controlled Voltage Regulators (in German), **F. Kelbe.** *Elektrotechnische Zeitschrift*, vol. 61, Feb. 29, 1940, pp. 209–10.

839. Thermionic Voltage Regulator (in Italian), **S. Ruberti.** *Elettrotecnica*, vol. 27, May 25, 1940, pp. 239–42.

840. Motor-Generator Electronic Control (in Italian), **A. Pinciroli, G. Francini.** *Alta Frequenza*, vol. 10, Oct. 1941, pp. 581–88. Voltage and frequency regulation of an alternator which is driven by a d-c motor.

841. Standard Electronic Valve Regulator with Final Grid-Controlled Rectifier Stage (in German), **N. Burisch, E. H. Ludwig.** *Siemens-Zeitschrift*, vol. 22, July-Sept. 1942, pp. 85–90.

842. A Voltage Stabilizer for a Direct-Current Generator, **W. M. Schwarz.** *Review of Scientific Instruments*, vol. 13, May 1942, pp. 213–14.

843. Electronic Exciter for A-C Generators, **A. Benson, R. Heidbrak.** *Electronics*, vol. 16, Aug. 1943, pp. 112–14, 261.

844. Electronic Regulators for A-C Generators, **A. Benson.** *Electronics*, vol. 16, April 1943, pp. 104–07.

845. Electronic Voltage Regulators Installed at the Measurements Section of the Compania Argentina de Electricidad, **R. M. Diaz.** *Revista Electrotecnica*, vol. 30, Dec. 1944, pp. 559–65.

846. Voltage Stabilizer, **G. N. Patchett.** *Electrical Review*, vol. 134, April 28, 1944, pp. 602–04.

847. Electronic A-C Voltage Regulator, **L. D. Harris.** *Electronics*, vol. 19, Jan. 1946, pp. 150–51.

848. Exciter-Regulator for Aircraft Alternators, **P. T. Hadley, A. W. Forsberg, O. Krauer.** *Electronics*, vol. 19, July 1946, pp. 120–22.

849. Diode-Controlled Voltage Regulators, **L. Helterline.** *Electronics*, vol. 20, June 1947, pp. 96–97. Temperature limited diode acts as reference quantity in conjunction with electronic or magnetic amplifier.

850. Regulator for 400-Cycle Inverter, **C. A. Helber.** *Electronics*, vol. 21, Nov. 1948, pp. 90–91.

851. The Brookhirst-Pearson Voltage-Regulating System. *Engineering*, vol. 167, March 4, 1949, pp. 215–16.

852. Cathode Heater Compensation as Applied to Degenerative Voltage-Stabilized Direct-Current Power Supplies, **R. C. Ellenwood, H. E. Sorrows.** *Journal of Research*, Bureau of Standards, vol. 43, Sept. 1949, pp. 251–55.

853. Electronic Voltage Regulator for Control of Generators, **W. J. R. Farmer.** *Electrical Times*, vol. 115, June 16, 1949, pp. 803–06.

854. Conversion of a Motor Generator into a Low Noise Power Amplifier, **H. S. Sommers, Jr., P. R. Weiss, W. Halpern.** *Review of Scientific Instruments*, vol. 20, 1949, pp. 244–51.

855. Control for Stabilized Testing Power, **L. R. Runaldue, H. F. Parker.** *General Electric Review*, vol. 53, Nov. 1950, pp. 34–38.

856. Equipment for Power Supplying at Constant Voltage and Frequency, **S. E. Lindberg.** *Ericsson Review*, no. 4, 1950, pp. 128–34.

857. An Electronic Current Regulator, **N. F. Verster.** *Applied Scientific Research*, B1, no. 5, 1950, pp. 358–62.

858. Wide Range, Continuously Variable High Current Generator Control, **J. R. Wolff, M. S. Freeman.** *Review of Scientific Instruments*, vol. 22, Oct. 1951, pp. 736–42.

Generator Voltage Regulators, Dynamoelectric and Magnetic Types

859. Operation of Counter-EMF Type Voltage Regulator, **F. A. Byles.** *Power*, vol. 63, Feb. 2, 1926, pp. 171–74.

860. High-Speed Regulator (in German), **J. Kroll.** *VDE Fachberichte*, 1931, pp. 55–57.

861. ASEA High-Speed Voltage Regulator for A-C Generators, **A. Ytterberg.** *ASEA Journal*, vol. 9, Dec. 1932, pp. 174–89.

862. Voltage Regulators (in Italian), **M. de Querquis.** *Elettrotecnica*, vol. 19, Oct. 25, 1932, pp. 745–55.

863. Generator Voltage Regulator Without Moving Parts, **C. P. West, I. D. Applegate.** *Electric Journal*, vol. 33, April 1936, pp. 181–83.

864. Simple Circuit for Generator Voltage Stabilization, **P. Kirkpatrick, K. Harworth.** *Review of Scientific Instruments*, vol. 8, Nov. 1937, pp. 430–31. Direct-connected exciter and bucking battery supply the excitation.

865. An Alternator Voltage Regulator Utilizing a Non-Linear Circuit, **H. W. Mayne.** *Electrical Engineering*, vol. 56, April 1937, pp. 462–64, 476.

866. Direct-Acting Regulators on Large Georgia Generators, **J. T. Logan.** *Electrical World*, vol. 117, May 2, 1942, pp. 42–44.

867. Static Voltage Regulator for Rototrol Exciter, **E. L. Harder, C. E. Valentine.** *AIEE Transactions*, vol. 64, 1945, pp. 601–06.

868. Alternator Field Excitation by Means of Compound Exciters (in Italian), **E. Santuari.** *Elettrotecnica*, vol. 33, 1946, Oct., pp. 234–44; Nov., pp. 281–92. Study of multifield machines.

869. M.-V. Voltage Regulators for Large Turbo-Generators, **B. J. Prigmore.** *Metropolitan-Vickers Gazette*, vol. 21, April 1946, pp. 197–204.

870. Rapid Excitation of Synchronous Machines (in Italian), **A. Carrer.** *Elettrotecnica*, vol. 34, Dec. 10–25, 1947, pp. 480–93. Compares the speed of response with an ordinary exciter and with an amplidyne.

871. Amplidyne Gives Quick Response on Synchronous Condenser Fields, **J. H. Vivian, F. V. Gillum.** *Electrical World*, vol. 128, Dec. 20, 1947, pp. 68–71.

872. Transductor-Type Voltage Regulators for Small A-C Generators, **U. Krabbe.** *ASEA Journal*, vol. 20, Feb.-March 1947, pp. 39–44.

873. Rototrol Excitation Systems, **J. E. Barkle, C. E. Valentine.** *AIEE Transactions*, vol. 67, pt. I, 1948, pp. 529–34.

874. Main Exciter Rototrol Excitation for Turbine Generators, **C. Lynn, C. E. Valentine.** *AIEE Transactions*, vol. 67, pt. I, 1948, pp. 535–39.

875. Excitation of Electrical Machines in Automatic Electromechanical Systems (in Russian), **D. P. Morozov.** *Elektrichestvo*, no. 9, Sept. 1948, pp. 8–12. Transient conditions in a 2-field d-c generator.

876. A Rapid Acting Current Regulator Without Contactors (in Russian), **I. L. Kaganov.** *Elektrichestvo*, no. 5, 1948, pp. 33–39.

877. Generator Regulation by Saturable Reactors, **T. A. Benham.** *Electronics*, vol. 22, July 1949, pp. 150, 152, 154.

878. Voltage Regulation in D-C Generators Using Magnetic Boosters (in Russian), **V. G. Komar.** *Elektrichestvo*, no. 4, April 1949, pp. 24–28.

879. The Transient Behavior of the Two-Stage Rototrol Main Exciter Voltage Regulating System as Determined by Electrical Analogy, **James T. Carleton.** *AIEE Transactions*, vol. 68, pt. I, 1949, pp. 59–63.

880. The Application of Magnetic Amplifiers to Problems of Voltage Regulation (in French), **G. H. Dion.** *Bulletin*, Societe Francaise des Electriciens, vol. 10, Feb. 1950, pp. 115–17.

881. Use of Transductor Regulators with Booster Exciters, **S. E. Hedstrom.** *ASEA Journal*, vol. 23, Feb. 1950, pp. 23–31.

882. Voltage Control of D-C Generators by Magnetic Amplifiers (in German), **A. Leonard.** *Elektrotechnische Zeitschrift*, vol. 71, June 15, 1950, pp. 307–08, Aug. 1, 1950, pp. 387–88.

883. An Amplistat Regulator Applied to a 5-KVA 400-Cycle Aircraft Inverter, **R. E. Morgan, J. A. Walley.** *AIEE Transactions*, vol. 69, pt. II, 1950, pp. 1243–48.

884. "Magnicon" Self-Regulating Alternators. *Engineer*, vol. 190, Nov. 24, 1950, p. 507. "Cross-field" exciter to provide generator with constant voltage characteristics.

885. Maintenance of Static Magnetic Regulators, **W. A. Hunter.** *Power Generation*, vol. 54, Mar. 1950, pp. 76–79.

886. Exciter Series Winding in Conjunction with High-Speed Regulator, **S. E. Hedstrom, K. E. Johansson.** *ASEA Journal*, vol. 23, Nov. 1950, pp. 157–58.

887. Static Magnetic Regulators in Power Generation Field, **W. A. Hunter.** *Power Engineering*, vol. 54, Dec. 1950, pp. 66–71.

888. Regulation of the Output of Electric Generators by Means of a Special Autoregulating Exciter (Dinarele) (in Italian), **G. Silvatici, M. Martinelli.** *Industria Italiana Elettrotecnica*, vol. 4, May 1951, pp. 7–12.

889. Rapid Regulation of Alternator Voltage (in French), **P. Satche, L. Gatesoupe.** *Revue de l' Electricite et de Mecanique*, no. 84, Jan.-Feb.-March 1951, pp. 50–55.

890. Static Magnetic Exciter for Synchronous Alternators, **H. F. Storm.** *AIEE Transactions*, vol. 70, 1951, pt. I, pp. 1014–17.

Line Voltage Regulator, Electromechanical

891. The Use of Induction Regulators in Feeder Circuits, **L. H. A. Carr.** *Journal*, Institution of Electrical Engineers, vol. 63, Sept. 1925, pp. 864–76.

892. Compensating for Voltage Drop with Automatic Voltage Regulators, **J. H. Ashbaugh.** *Electric Journal*, vol. 23, May 1926, pp. 243–46.

893. Automatic Voltage Regulators—Application to Power Transmission Systems, **C. A. Nickle, R. M. Carothers.** *AIEE Journal*, vol. 47, July 1928, pp. 525–28.

894. The Step Induction Regulator for Transformer Voltage Control, **R. M. Field.** *Electric Journal*, vol. 25, July 1928, pp. 351–54.

895. The Development of the Feeder Voltage Regulator, **E. R. Wolfert.** *Electric Journal*, vol. 25, Sept. 1928, pp. 441–46, historical.

896. Application of Induction Regulators to Distribution Networks, **E. R. Wolfert, T. J. Brosnan.** *AIEE Journal*, vol. 48, Sept. 1929, pp. 669–72. Parallel operation of single- and 3-phase units.

897. Application of Induction Voltage Regulators, **W. E. M. Ayres.** *Journal*, Institution of Electrical Engineers, vol. 69, Oct. 1931, pp. 1208–31.

898. Characteristics of the Moving-Coil Voltage Regulator, **E. T. Norris.** *Electrical Review*, vol. 112, March 3, 1933, pp. 301–02.

899. Voltage Control, **E. T. Norris.** *Electrical Review*, vol. 111, Dec. 9, 1932, pp. 846–47.

900. Moving-Coil Voltage Regulator, **E. T. Norris.** *Electrical Times*, vol. 83, May 18, 1933, pp. 641–42.

901. A-C Voltage Regulators. *Engineer*, vol. 156, 1933, Nov. 24, pp. 512–14; Dec. 1, pp. 540–42; Dec. 8, pp. 564–66; Dec. 15, pp. 600–03; Dec. 22, pp. 612–14; Dec. 28, pp. 636–41.

902. Regulation Chart for Automatic Voltage Regulators, **C. Heyel, W. R. Weise.** *Electric Journal*, vol. 30, June 1933, pp. 250–52.

903. Improved Voltage Regulation, **E. T. Norris.** *Electrical Review*, vol. 114, June 8, 1934, pp. 823–24.

904. Induction Regulator. *Electrician*, vol. 113, Nov. 30, 1934, pp. 701–04.

905. Automatic Tap-Changing Voltage Regulator for Distribution Networks (in German), **P. Sporn.** *Elektrotechnik und Maschinenbau*, vol. 52, April 15, 1934, pp. 175–77.

906. Parallel Operation of Automatic Induction Voltage Regulators, **F. B. Haugaard.** *Journal*, Institution of Engineers, Australia, vol. 6, Sept. 1934, pp. 304–09.

907. Voltage Regulator for Low Power (in German), **F. von Ratkovszky.** *Elektrotechnik und Maschinenbau*, vol. 53, Aug. 4, 1935, pp. 361–65.

908. Moving-Coil Voltage Regulator, **E. T. Norris.** *Electrical Times*, vol. 88, Aug. 15, 1935, pp. 197–98.

909. Step-Type Feeder Voltage Regulators, **L. H. Hill.** *Electrical Engineering*, vol. 54, Feb. 1935, pp. 154–58.

910. Automatic Voltage Regulation Dependent on Overload Current, **G. Rydbeck.** *ASEA Journal*, vol. 13, March 1936, pp. 39–42.

911. Automatic Control of Voltage Regulators. *Engineer*, vol. 161, June 5, 1936, p. 604.

912. Voltage Control with Power Regulating Transformers (in German), **W. Thiessen.** *Elektrotechnische Zeitschrift*, vol. 57, Jan. 30, 1936, pp. 113–15.

913. New Automatic Control for Regulating Transformers (in German), **W. Kramer.** *VDE Fachberichte*, 1936, pp. 128–30.

914. Regulator for Correcting Regenerative Voltage, **R. H. Wilsey.** *Electrical World*, vol. 108, Sept. 25, 1937, pp. 53, 106–08.

915. Voltage Regulators on A-C Systems, **D. W. McJannet.** *Electrical Times*, vol. 91, May 13, 1937, pp. 659–61.

916. Regulation of Voltage on Urban Networks (in French), **P. Rivot.** *Revue Generale de l'Electricite*, vol. 44, Nov. 16, 1938, pp. 655–63.

917. Moving Coil Voltage Regulator, **E. T. Norris.** *Journal*, Institution of Electrical Engineers, vol. 83, July 1938, pp. 1–35.

918. Voltage Regulating Equipment Characteristics as a Guide to Application, **P. E. Benner G. S. Lunge.** *General Electric Review*, vol. 41, June 1938, pp. 273–79.

919. Hydraulic Turbine Drive for Regulators (in French), **M. Wenger.** *Bulletin*, Association Suisse des Electriciens, vol. 31, Mar. 8, 1940, pp. 120–22.

920. Voltage Regulation, **L. P. Canaby, J. L· Hegly.** *Electrician*, vol. 124, 1940, June 7, pp. 407–08; June 14, pp. 420–21.

921. Connections for Voltage Regulators Operating in Parallel, **B. Wood.** *Engineer*, vol. 173, Feb. 27, 1942, p. 187.

922. Control of Voltage Regulators. *Electrician*, vol. 128, May 29, 1942, pp. 537–39.

923. The Control of Voltage Regulators. *Engineer*, vol. 173, June 12, 1942, pp. 491–92.

924. A New Voltage-Regulating Relay Plus Line-Drop Compensators, **H. J. Carlin.** *AIEE Transactions (Electrical Engineering)*, vol. 61, Feb. 1942, pp. 63–66.

925. Voltage Regulation in Low Voltage Networks (in German), **M. Schwaiger.** *Siemens Zeitschrift*, vol. 22, July-September 1942, pp. 92–97.

926. A Photo-Electric Voltage Control Gear, **K. A. R. Sampson.** *Electronic Engineering*, vol. 15, May 1943, pp. 516–18.

927. Localized Automatic Control, **E. T. Norris.** *Electrician*, vol. 130, 1943, pp. 161–63.

928. A New Automatic Drive for Regulators for Maintaining Constant Current in a System (in German), **W. Blankenburg.** *Elektrotechnik und Maschinenbau*, vol. 61, April 2, 1943, pp. 143–47.

929. Voltage Regulation and Load Division of Supply Systems by Regulating Transformers and Capacitors (in German), **E. Bornitz.** *Elektrotechnik und Maschinenbau*, vol. 61, Oct. 29, 1943, pp. 525–37.

930. Accuracy of Control Devices for Feeder Voltage Regulators. *Electrical Engineering*, vol. 63, July 1944, pp. 250–54.

931. Power Supply for Microwave Equipment, **O. Hoag.** *Electronics*, vol. 20, Feb. 1947, pp. 110–13. Servo-controlled autotransformer.

932. Two Voltage-Regulating Equipments for Distribution Networks (in French), **Pichon.** *Bulletin*, Societe Francaise des Electriciens (Ser. 6), vol. 7, June 1947, pp. 380–84.

933. Magnetic Voltage Stabilizer, **P. Frehner.** *Brown Boveri Review*, vol. 35, March-April 1948, p. 126.

934. The Problem of Voltage-Regulator Standardization (in Russian), **B. E. Kubuishin.** *Vestnik Elektroprommishlennosti*, no. 2, 1948, pp. 17–22.

935. The Moving Coil-Regulated Transformer, **E. T. Norris.** *Beama Journal*, vol. 55, Sept. 1948, pp. 306–08.

936. Feeder Voltage Regulator Accuracy Standards, **W. E. Birchard.** *AIEE Transactions*, vol. 67, pt. I, 1948, pp. 747–51.

937. An Electro-Mechanically Stabilized Mains Supply Unit, **A. E. Maine.** *Electronic Engineering*, vol. 21, Sept. 1949, pp. 319–21. A motor-operated variable-ratio transformer is controlled by thyratrons and a nonlinear bridge network.

938. New Fully-Automatic Voltage-Regulating Equipment, **M. Wiederkehr.** *Engineers' Digest*, vol. 11, June 1950, pp. 211–12.

939. Automatic Voltage Regulator for Wide Range (in German), **H. Goldstein.** *Elektrotechnische Zeitschrift*, vol. 71, April 20, 1950, pp. 191–92. Moving coil regulator.

940. Modified Moving Coil Voltage Regulator of High Sensitivity, **N. W. W. Ellis.** *Journal of Scientific Instruments*, vol. 27, Sept. 1950, pp. 248–49.

941. An Electromechanical A-C Line Voltage Stabilizer, **D. M. Murray, N. L. Kusters.** *AIEE Transactions*, vol. 70, pt. II, 1951, pp. 1741–48. A series type of induction regulator operated by special motor with thyratron control.

942. Feeder Voltage Regulators with Ninety-Nine Percent Accuracy, **M. T. Reese.** *General Electric Review*, vol. 54, Sept. 1951, pp. 48–50.

Line Voltage and Current Regulator, Electronic

943. An Automatic Voltage Regulator, **F. G. H. Lewis.** *Proceedings*, Physical Society, vol. 34, 1921–22, pp. 17–21. Non-linear bridge.

944. New Automatic Voltage Regulator (in French), **P. Toulon.** *Revue Generale de l'Electricite*, vol. 26, Aug. 3, 1929, pp. 189–91. Neon tube voltage stabilizing circuit.

945. The Use of a Thermionic Tetrode for Voltage Control, **J. C. Street, T. H. Johnson.** *Journal*, Franklin Institute, vol. 214, 1932, pp. 155–62.

946. The Use of Triode Vacuum Tube Rectifiers to Supply Constant Voltage, **L. A. Richards.** *Review of Scientific Instruments*, vol. 4, 1933, pp. 479–82.

947. Voltage Stabilizer Controlled by Thermionic Pentode, **Robley D. Evans.** *Review of Scientific Instruments*, vol. 5, Oct. 1934, pp. 371–75.

948. Automatically-Regulated Precision High Voltage Source, **O. H. A. Schmitt.** *Review of Scientific Instruments*, vol. 5, Dec. 1934, pp. 435–37.

949. Electronic Voltage Regulator for Lamp Testing, **R. R. Brady, C. P. Bernhardt.** *Electronics*, vol. 9, Sept. 1936, pp. 36, 38, 40.

950. Thyratron Voltage Control, **C. J. Burbank.** *Review of Scientific Instruments*, vol. 7, Nov. 1936, pp. 427–29.

951. Automatic Current and Voltage Regulator (in German), **W. Geyger.** *Archiv fur technisches Messen*, no. 68, Feb. 1937, T24, J062–5.

952. Electronic Voltage Regulator with Supplementary Circuit to Supply Low Voltages, **E. B. Working.** *Industrial and Engineering Chemistry* (Analytical Edition), vol. 10, 1938, pp. 434, 435.

953. Neon-Controlled Stabilizer—A Constant-Voltage Rectifier Unit, **H. J. N. Riddle, F. A. Downes.** *Wireless World*, vol. 43, Oct. 13, 1938, pp. 333–35.

954. Compensation Arrangement for Accurate Maintenance of Potentials by Means of Stabilizing Tubes (in German), **A. Aulmann.** *Zeitschrift fur technische Physik*, vol. 19, no. 10, 1938, pp. 320–22.

955. Improving Regulator Performance, **A. G. Bousquet.** *Electronics*, vol. 11, July 1938, pp. 26–27.

956. On Electronic Voltage Stabilizers, **F. V. Hunt, R. W. Hickman.** *Review of Scientific Instruments*, vol. 10, 1939, pp. 6–21. Theory.

957. Two Voltage Regulators, **H. V. Neher, W. H. Picking.** *Review of Scientific Instruments*, vol. 10, Feb. 1939, pp. 53–56.

958. A 5-Ampere Electronic D-C Regulator, **J. N. Coombs, P. T. Nims.** *Electronics*, vol. 13, Jan. 1940, pp. 40, 44, 46

959. High-Voltage Stabilizer, **H. Alfven, S. Eklund.** *Arkiv for Matematik, Astronomi och Fysik*, 27B, vol. 6, 1940.

960. Discharge-Tube Type Voltage Regulator for Therapeutic X-Ray Generators, **S. Suzuki.** *Electrotechnical Journal*, vol. 4, Aug. 1940, pp. 186–87.

961. A Direct Current Supply Apparatus with Stabilized Voltage, **H. J. Lindenhovius, H. Rinia.** *Philips Technical Review*, vol. 6, 1941, pp. 54–61.

962. Stable Power Supplies for Electron Microscopes, **A. W. Vance.** *RCA Review*, vol. 5, 1941, pp. 293–300.

963. Aspects of Stabilizing Power Supplies, **G. Bocking.** *Journal*, British Institute of Radio Engineers, vol. 2, 1941, p. 41.

964. Calculations of Battery Charging Rectifiers with Automatic Control of the Charging Current (in German), **K. Thiel.** *Elektrotechnische Zeitschrift*, vol. 62, Sept. 25, 1941, pp. 791–95.

965. Valve Regulator for D-C Voltages (in German), **W. Holzmuller.** *Physikalische Zeitschrift*, vol. 42, Aug. 1941, pp. 218–19.

966. Emission-Regulating Circuits for an Ionization Gauge, **R. B. Nelson, A. K. Wing, Jr.** *Review of Scientific Instruments*, vol. 13, May 1942, pp. 215–17.

967. Electronic Voltage Stabilizer for 1 to 50 KV and 20 to 500 MA., **L. G. Parratt, J. W. Trischka.** *Review of Scientific Instruments*, vol. 13, Jan. 1942, pp. 17–23.

968. Regulated Rectifiers in Telephone Offices, **D. E. Trucksess.** *AIEE Transactions (Electrical Engineering)*, vol. 61, Aug. 1942, pp. 613–17.

969. On Voltage Stabilizer Circuits, **B. Banerjee.** *Indian Journal of Physics*, vol. 16, April 1942, pp. 87–110.

970. A Voltage Regulator, **W. F. Berg.** *Journal of Scientific Instruments*, vol. 19, July 1942, pp. 108–09.

971. Constant-Voltage Supply, **T. A. Ledward.** *Wireless World*, vol. 48, Feb. 1942, pp. 33–35.

972. Electronic Voltage Regulators, **F. L. Hogg.** *Wireless World*, vol. 49, 1943, Nov., pp. 327–31; Dec., pp. 371–73.

973. Voltage Stabilizer for Electron Diffraction Power Supply, **S. H. Bauer, J. M. Hastings, D. P. MacMillan.** *Review of Scientific Instruments*, vol. 14, Feb. 1943, pp. 30–32.

974. Voltage-Stabilized Bias Supply for Power Tubes, **G. E. Pihl.** *Electronics*, vol. 16, Sept. 1943, pp. 160, 162, 165.

975. A Combined Voltage Regulating and Quenching Circuit for the Geiger-Muller Counter, **W. F. Bale, J. F. Bonner, Jr.** *Review of Scientific Instruments*, vol. 14, 1943, pp. 222, 223.

976. Electronic Voltage Regulator for Precise Densitometric Measurements, **H. W. Dietert, M. F. Hasler.** *Journal*, Optical Society of America, vol. 33, Jan. 1943, pp. 45–49.

977. An Automatic Stabilizer with Small Time Constant, for A-C Mains Voltages (in French), **Lecolazet.** *Comptes Rendus*, l'Academie des Sciences, vol. 216, 1943, pp. 527–29.

978. A Differential Electronic Stabilizer for Alternating Voltages, and Some Applications, **A. Glynne.** *Journal*, Institution of Electrical Engineers, vol. 90, pt. 2, April 1943, pp. 101–15.

979. Voltage-Regulated Power Supplies. Design and Construction Considerations, **A. B. Bereskin.** *Proceedings*, Institute of Radio Engineers, vol. 31, Feb. 1943, pp. 47–52.

980. Voltage-Measuring and -Control Equipment for Electrostatic Generators, **A. O. Hanson.** *Review of Scientific Instruments*, vol. 15, March 1944, pp. 57–63.

981. Current Stabilizers, **J. N. Van Scoyoc, E. H. Schulz.** *Proceedings*, Institute of Radio Engineers, vol. 32, July 1944, pp. 415–18.

982. A New Electronic Stabilizer and Regulator for D-C Voltages, **A. Glynne.** *Journal*, Institution of Electrical Engineers, vol. 91, pt. 2, June 1944, pp. 174–77.

983. Additional Stabilization for the Beam Current in the RCA Type B Electron Microscope, **H. R. Crane.** *Review of Scientific Instruments*, vol. 16, March 1945, p. 58.

984. Electronic Voltage Regulators, **A. R. Keskinen, B. Warriner.** *Bendix Radio Engineer*, vol. 1, Jan. 1945, pp. 11–14.

985. Analysis of Voltage Regulator Operation, **W. R. Hill, Jr.** *Proceedings*, Institute of Radio Engineers, vol. 33, Jan. 1945, pp. 38–45.

986. Analysis of Current Stabilizer Circuits, **W. R. Hill, Jr.** *Proceedings*, Institute of Radio Engineers, vol. 33, Nov. 1945, pp. 785–92.

987. Electronic Voltage Regulator Circuits, **J. F. Sodaro.** *Radio-Electronic Engineering*, vol. 4, Aug. 1945, pp. 9–11, 35–36.

988. Voltage Regulated Power Supplies, **G. E. Hamilton, T. Maiman.** *Communications*, vol. 25, Nov. 1945, pp. 44, 45, 78–81, Dec. 1945, pp. 70–71.

989. Electronic Alternating Current Power Regulator, **L. B. Cherry, R. F. Wild.** *Proceedings*, Institute of Radio Engineers, vol. 33, April 1945, pp. 262–67.

990. Stabilized D-C High-Voltage Supply, **A. M. Gurewitsch, P. C. Noble.** *General Electric Review*, vol. 48, Dec. 1945, pp. 46–52.

991. Basic Theory and Design of Electronically Regulated Power Supplies, **A. Abate.** *Proceedings*, Institute of Radio Engineers, vol. 33, July 1945, pp. 478–82.

992. Multi-Voltage Regulated Power Supplies, **J. R. Mentzer.** *Electronics*, vol. 19, Sept. 1946, pp. 132–33.

993. Electronic Voltage Regulator, **L. D. Harris.** *Electronics*, vol. 19, Jan. 1946, pp. 150–51.

994. Voltage Stabilization, **W. Easton.** *Electrical Review*, vol. 138, 1946, pp. 1013–15. Electronic regulator for wattmeter testing.

995. The Stabilization of X-Ray Tube Current and Voltage, **A. F. LeMieux, W. W. Beeman.** *Review of Scientific Instruments*, vol. 17, April 1946, pp. 130–32.

996. Voltage Regulators in High-Frequency Heating Generators, **E. Mittelmann.** *Radio-Electronic Engineering*, vol. 7, Oct. 1946, pp. 8–10, 25. The output voltage is regulated by means of thyratrons.

997. Principles and Operation of a New Electronic Voltage Stabilizer, **G. Papp.** *Publications*, University of Technical Sciences, no. 2, 1947, pp. 165–70.

998. Voltage Regulation with Electron Tubes (in German), **H. Sobotka.** *Elektro-und Radiotechnik*, vol. 2, April 15, 1947, pp. 52–54.

999. Historic Firsts—Electronic Voltage Regulator. *Bell Laboratories Record*, vol. 25, Dec. 1947, pp. 452–53.

1000. Diode-Controlled Voltage Regulators, **L. Helterline.** *Electronics*, vol. 20, June 1947, pp. 96–97.

1001. Voltage-Regulated Power Supplies, **P. Koontz, E. Dilatush.** *Electronics*, vol. 20, July 1947, pp. 119–23.

1002. Stabilizing Direct-Voltage Supplies, **J. W. Hughes.** *Wireless Engineer*, vol. 24, Aug. 1947, pp. 224–30, discussion, p. 309.

1003. Regulator of Effective Alternating Voltage (in French), **L. LeBlan.** *Comptes Rendus*, l'Academie des Sciences, vol. 224, 1947, pp. 643–45.

1004. Constant Direct Voltages (in German), **V. Kusse.** *Electrotechnik*, vol. 1, Sept. 1947, pp. 95–96. (Also *Engineers' Digest*, vol. 4, Dec. 1947, p. 587.)

1005. An Electronic Voltage Stabilizer, **J. Wesolowski.** *Acta Physica Polonica*, vol. 9, no. 1, 1947, pp. 61–62.

1006. Voltage-Regulated Power Supplies, **L. Mautner.** *Electrical Engineering*, vol. 66, Sept. 1947, pp. 894–900.

1007. Electron Stabilizers for Television Apparatus (in Russian), **S. P. Pivovarov.** *Zhurnal Tekhnicheskoi Physiki*, vol. 17, 1947, pp. 737–42. (Also *Wireless Engineer*, vol. 25, 1948, A139.)

1008. Shunt Voltage Stabilizer, **J. McG. Sowerby.** *Wireless World*, vol. 54, June 1948, pp. 200–03.

1009. Voltage Regulators of the Shunt Type, **W. G. Hoyle.** *Review of Scientific Instruments*, vol. 19, April 1948, pp. 244–46.

1010. A 500–50,000 Volt Regulated Power Supply, **R. E. Anderson.** *Proceedings*, National Electronics Conference, vol. 4, 1948, pp. 315–29.

1011. A Voltage Stabilizer for Photometer Lamps, **R. J. Hercock.** *Journal of Scientific Instruments*, vol. 25, 1948, pp. 320, 321.

1012. A Negative-Current Voltage-Stabilization Circuit, **P. Luo.** *Proceedings*, Institute of Radio Engineers, vol. 36, May 1948, p. 583.

1013. D-C Stabilized Power Supply of Low Impedance, **V. H. Attree.** *Journal of Scientific Instruments*, vol. 25, Aug. 1948, pp. 263–68.

1014. A Note on Stabilizing Power Supplies, **E. J. Harris.** *Electronic Engineering*, vol. 20, March 1948, pp. 96–7.

1015. Notes on an Inductively Coupled High Voltage Stabilizer, **G. Schwarz, E. H. Byerly.** *Review of Scientific Instruments*, vol. 19, April 1948, p. 273.

1016. Stabilized Power Supplies, **M. G. Scroggie.** *Wireless World*, vol. 54, 1948, Oct., pp. 373–78; Nov., pp. 415–18; Dec., pp. 453–56.

1017. A Proton-Controlled Magnetic Field Regulator, **M. Packard.** *Review of Scientific Instruments*, vol. 19, July 1948, pp. 435–39.

1018. Stabilization of the Accelerating Voltage in an Electron Microscope, **A. C. van Dorsten.** *Philips Technical Review*, vol. 10, Nov. 1948, pp. 135–40.

1019. Voltage Stabilization in Industrial Automatic Photoelectric Apparatus (in Russian), **B. I. Filipovich.** *Elektrichestvo*, no. 3, 1948, pp. 15–23.

1020. Electronic A-C Voltage Stabilizer, **B. V. Hamon, F. A. Edwards.** *Electrical Engineer and Merchandiser*, vol. 25, April 15, 1948, pp. 13–19.

1021. An Inductively Coupled Series Tube D-C High Voltage Regulator, **R. Pepinsky, P. Jarmotz.** *Review of Scientific Instruments*, vol. 19, April 1948, pp. 247–54.

1022. A D-C Voltage Regulator for Moderately High Currents, **J. M. McCrea, D. J. LeRoy.** *Review of Scientific Instruments*, vol. 19, Oct. 1948, pp. 692–97.

1023. Automatic Voltage Regulators of the V.E.I. Type (in Russian), **G. R. Gerstenberg.** *Vestnik Elektroprommishlennosti*, no. 8, Aug. 1949, pp. 11–17. Electronic voltage regulators of a new type.

1024. Voltage Stabilizers, **F. A. Benson.** *Electronic Engineering*, vol. 21, 1949, May, pp. 155–58; June, pp. 200–03; July, pp. 243–47; Aug., pp. 300–02. A survey.

1025. Novel Regulator Circuit, **Y. P. Yu.** *Electronics*, vol. 22, May 1949, pp. 170, 172, 174, 177.

1026. 30-KV D-C Regulated Power Supply, **W. Spellman.** *Radio-Electronic Engineering*, vol. 12, May 1949, pp. 16, 17, 30.

1027. Design of a Voltage-Stabilizing Circuit with the Regulating Valve Connected in Parallel (in Russian), **K. B. Mazel.** *Radiotekhnika*, vol. 4, 1949, pp. 74–79. Cathode follower type of stabilizer.

1028. Note on Constant Current Regulators, **E. E. Minett, D. A. MacRae, J. Townsend.** *Review of Scientific Instruments*, vol. 20, Feb. 1949, p. 136.

1029. Valve Circuits as Voltage and Current Stabilizers (in Spanish), **L. Miranda.** *Anales de Mecanica y Electricidad*, vol. 25, July-Aug. 1949, pp. 220–28.

1030. Operation of Voltage-Stabilizing Elements with Current Stabilized Supplies, **J. J. Gilvarry, D. F. Rutland.** *Review of Scientific Instruments*, vol. 20, Sept. 1949, pp. 633–37. Theory.

1031. Stabilized High Voltage Power Supply for Electrostatic Analyzer, **R. L. Henkel, B. Petree.** *Review of Scientific Instruments*, vol. 20, Oct. 1949, pp. 729–32. Steady-state stability of 0.01 per cent secured with phototube-galvanometer type of amplifier.

1032. Phototube Input Impedance for a Voltage Stabilizer, **E. N. Strait, W. W. Buechner.** *Review of Scientific Instruments*, vol. 20, Nov. 1949, pp. 783–85.

1033. Economic Voltage Regulator Design, **B. M. Hadfield.** *Radio-Electronic Engineering*, vol. 12, Jan. 1949, pp. 13–15, 30.

1034. Precision A-C Voltage Stabilizers, **G. N. Patchett.** *Electronic Engineering*, vol. 22, 1950, Sept., pp. 371–77; Oct., pp. 424–28; Nov., pp. 470–73; Dec., pp. 499–503. Survey.

1035. A New Precision A-C Voltage Stabilizer, **G. N. Patchett.** *Proceedings*, Institution of Electrical Engineers, vol. 97, pt. II, Aug. 1950, pp. 529–40.

1036. A Source of Constant Voltage for Measurements (in German), **H. Helke.** *Elektrotechnische Zeitschrift*, vol. 71, April 1, 1950, pp. 171–72.

1037. D-C Voltage Stabilization (in German), **W. Taeger.** *Funk und Ton*, vol. 4, Aug. 1950, pp. 403–11.

1038. Regulating A-C with a Buck-Boost Amplifier, **C. W. Clapp.** *Electronics*, vol. 23, Aug. 1950, pp. 99–101.

1039. A Circuit for the Automatic Stabilization of X-Ray Tube Current, **C. S. Lees, M. D. Armitage.** *Journal of Scientific Instruments*, vol. 27, Nov. 1950, pp. 300–01.

1040. The Regulation of Voltage of Van de Graff Electrostatic Generators (in French), **J. Taieb.** *Onde Electrique*, vol. 30, Nov. 1950, pp. 462–68.

1041. Automatic Regulation of Thermionic Emission, **W. Steckelmacher, S. Van der Meer.** *Journal of Scientific Instruments*, vol. 27, July 1950, pp. 189–91.

1042. A Magnetic Field Stabilization Circuit, **L. Katz, P. A. Forsyth, L. F. Cudney, G. W. Williams, H. E. Johns, R. N. H. Haslam.** *Canadian Journal of Research*, Sec. A, vol. 28, Jan. 1950, pp. 67–72.

1043. A Mains Power Supply for Magnetizing Currents of High Constancy for Electron Lenses (in German), **E. Kinder, F. Schleich.** *Zeitschrift fur Angewandte Physik*, vol. 2, 1950, pp. 332–34.

1044. Wide-Range Voltage Regulator, **C. E. Green.** *Electronics*, vol. 23, March 1950, pp. 192, 194, 196.

1045. Variable Resistance Lamp Regulator Adjusted Automatically by Pilot Relay (in French), **J. M. Jollois.** *Bulletin*, Societe Francaise des Electriciens, vol. 10, March 1950, pp. 110–14.

1046. Voltage Stabilizer for 200 KV Acceleration, **J. T. Dewan.** *Review of Scientific Instruments*, vol. 21, Aug. 1950, pp. 771, 772.

1047. Variable High-Voltage Power Source, **W. S. Ramsey.** *Electronics*, vol. 23, Feb. 1950, pp. 98–101.

1048. The Cathode Follower as a Voltage Regulator, **A. P. Willmore.** *Electronic Engineering*, vol. 22, Sept. 1950, pp. 399–400.

1049. Regulated Low Voltage Supply for Electrolysis and Other Uses, **M. L. Greenough, W. E. Williams, Jr., J. K. Taylor.** *Review of Scientific Instruments*, vol. 22, July 1951, pp. 484–88.

1050. General Theory of Voltage Stabilizers, **J. J. Gilvarry, D. F. Rutland.** *Review of Scientific Instruments*, vol. 22, July 1951, pp. 464–68.

1051. Stabilization of Direct Voltages (in German), **H. Gunther.** *Funk und Ton*, vol. 5, March 1951, pp. 124–32.

1052. Superregulated Power Supplies, **A. W. Vance, C. C. Shumard.** *Electronics*, vol. 24, Dec. 1951, pp. 109–13.

1053. Wide Range Voltage Regulators, **J. Houle.** *Electronics*, vol. 24, Aug. 1951, pp. 202, 204, 206, 208, 210.

1054. Zero-Impedance Power Supply Termination, **J. J. Baruch.** *Electronics*, vol. 24, Aug. 1951, pp. 240, 242, 244.

1055. Voltage Stabilization: Demands and Methods, **A. J. Maddock.** *Journal of Scientific Instruments*, vol. 28, Oct. 1951, pp. 325–33. Survey.

1056. A High Resolution Two-Directional Focusing Beta-Ray Spectrometer, **A. A. Bartlett, K. T. Bainbridge.** *Review of Scientific Instruments*, vol. 22, July 1951, pp. 517–23.

1057. Photoelectric Control Circuits for the Ion Source of a Pressure Type Electrostatic Generator, **L. O. Herwig.** *Review of Scientific Instruments*, vol. 22, Sept. 1951, pp. 668–72.

1058. Magnet Current Regulator, **J. C. Nygard.** *Electronics*, vol. 24, Dec. 1951, pp. 122–24.

1059. Magnet Current Stabilizer, **H. S. Sommers, Jr., P. R. Weiss, W. Halpern.** *Review of Scientific Instruments*, vol. 22, Aug. 1951, pp. 612–18.

Line Voltage and Current Regulator, Magnetic

1060. A Precision Regulator for Alternating Voltage, **H. M. Stoller, J. R. Power.** *AIEE Transactions*, vol. 48, 1929, pp. 808–11. Electronically controlled series transformer.

1061. A Magnetically Operated A-C Voltage Control Device, **J. A. Sola.** *Radio-Engineering*, vol. 11, 1931, p. 24.

1062. Voltage-Regulating Autotransformer, **F. Bedell, J. Kuhn.** *Review of Scientific Instruments*, vol. 3, 1932, pp. 20–23. Compounded transformer.

1063. Static Voltage Regulator (in French), **H. Andre.** *Revue Generale de l'Electricite*, vol. 31, April 2, 1932, pp. 466–67.

1064. Automatic Voltage Regulation, **K. Howe.** *Electronics*, vol. 4, 1932, pp. 164–65.

1065. Automatic Current and Potential Regulators (in German), **W. Geyger.** *Archiv fur technisches Messen*, J062–7, Nov. 1934; J062–8, Dec. 1934.

1066. Voltage Control by Means of D-C Excited Transformers (in German), **W. Scheuring.** *Elektrotechnik und Maschinenbau*, vol. 52, July 15, 1934, pp. 326–28.

1067. A Static Voltage Regulator (in German), **E. Friedlander.** *Siemens Zeitschrift*, vol. 15, 1935, pp. 177–81.

1068. An Electronic Voltage Regulator, **Palmer H. Craig, Frank E. Sanford.** *Electrical Engineering*, vol. 54, Feb. 1935, pp. 166–70. Electronically controlled series-connected transformer.

1069. Electromagnetic Voltage Regulator for Measurements (in German), **W. Geyger.** *Siemens Zeitschrift*, vol. 15, Sept. 1935, pp. 464–67.

1070. A D-C Controlled Voltage Regulator, **Paul H. Odessey.** *Electrical Engineering*, vol. 55, Sept. 1936, pp. 956–60.

1071. Theories and Experiments on Constant-Voltage Devices, **S. Ohtaka.** *Electrotechnical Journal*, vol. 1, Dec. 1937, pp. 198–202. Transformer with capacitor.

1072. Equivalent Networks with Highly Saturated Iron Cores with Special Reference to Their Use in the Design of Stabilizers, **H. A. W. Klinkhamer.** *Philips Technical Review*, vol. 2, Sept. 1937, pp. 276–81.

1073. Inductive Regulation of A-C (in German), **A. Metal, I. Rosenzweig.** *Elektrotechnik und Maschinenbau*, vol. 55, Aug. 22, 1937, pp. 410–13.

1074. Voltage Regulators Using Magnetic Saturation, **K. J. Way.** *Electronics*, vol. 10, July 1937, pp. 14–16.

1075. On the Action and Characteristics of Magnetic Network Voltage Regulators (in German), **R. Miehlich.** *Fachberichte des Verbandes Deutscher Elektrotechniker*, vol. 10, 1938, pp. 154–56.

1076. Static Constant-Current Circuit, **C. M. Summers.** *AIEE Transactions (Electrical Engineering)*, vol. 57, Nov. 1938, pp. 636–39. Parallel resonant circuit.

1077. An Automatic Voltage Regulator Without Moving Parts Employing Ferroresonance, **Palmer H. Craig.** *AIEE Transactions*, vol. 58, 1939, pp. 830–38.

1078. Resonant-Type Constant-Current Regulators, **Roland R. Miner.** *AIEE Transactions*, vol. 58, 1939, pp. 822–29.

1079. Automatic Constant Voltage Transformer (in German), **H. Beck.** *Zeitschrift fur technische Physik*, vol. 20, 1939, pp. 180–85. Primary voltage changes air gap and secondary flux linkages.

1080. Constant Current Sources, **L. C. Green, J. B. H. Kuper.** *Review of Scientific Instruments*, vol. 11, Aug. 1940, pp. 250–56. Resonant circuit.

1081. An Electromagnetic Voltage Regulator Independent of Frequency Variations (in Russian), **Nikiforov.** *Izvestiya Elektropromnishlennosti Slabova Toka* 1940, no. 4–5, pp. 72–78; no. 6, pp. 61–62. (See abstract in *Wireless Engineer*, vol. 20, 1943, p. 514.)

1082. Mains Voltage Stabilizer, **P. Denco.** *Electrician*, vol. 127, 1941, pp. 106, 107. A survey of recent practice.

1083. An Electromagnetic Voltage Stabilizer (in Russian), **R. M. Shewtzuk.** *Elektrosvyaz*, no. 3, March 1941, pp. 7–14.

1084. Widening the Regulating Range of Magnetic Voltage Stabilizers (in German), **E. Beck.** *Elektrotechnische Zeitschrift*, vol. 63, Feb. 12, 1942, pp. 57–60.

1085. Voltage Stabilizing Connections with Iron-Cored Chokes (in German), **W. Taeger.** *Archiv fur Elektrotechnik*, vol. 36, May 31, 1942, pp. 310–21.

1086. Voltage-Regulating Transformers, **R. O. Lambert.** *Electronic Engineering*, vol. 15, Feb. 1943, pp. 384–87.

1087. A-C Voltage Stabilizer, **T. A. Ledward.** *Wireless World*, vol. 49, June 1943, pp. 166–67. D-c saturated choke.

1088. A Static Voltage Regulator Insensitive to Load Power Factor, **C. M. Summers, T. T. Short.** *AIEE Transactions (Electrical Engineering)*, vol. 61, Feb. 1942, pp. 67–70.

1089. Magnetic Voltage Stabilizer for Alternating Current, **A. T. Berthelsen.** *Engineers' Digest*, vol. 2, Dec. 1945, pp. 595–96.

1090. Voltage Stabilizers, **J. A. Uttal.** *Electronic Industries*, vol. 4, Aug. 1945, pp. 90–94, 150, 154, 158. Various magnetic types.

1091. Resonant-Circuit Constant-Current Regulators, **G. M. Kevern.** *AIEE Transactions (Electrical Engineering)*, vol. 64, Dec. 1945, pp. 807–10.

1092. A Magnetic Regulator for Voltage Variations in A-C Supply Systems (in Norwegian), **R. Ursin.** *Elektroteknisk Tiddskrift*, vol. 59, June 5, 1946, pp. 213–16.

1093. Saturated-Iron Voltage Stabilizers (in Italian), **G. Sacerdote, D. Pollara.** *Elettrotecnica*, vol. 34, June 1947, pp. 229–39. (also *Engineers' Digest*, vol. 4, Dec. 1947, pp. 547–51.)

1094. Basis for the Design of Magnetic Voltage Stabilizer with Corrected Waveform (in Norwegian), **A. Rambol.** *Elektroteknisk Tidsskrift*, vol. 60, Oct. 15, 1947, pp. 337–44.

1095. The Influence of Frequency Variation on the Performance of Magnetic-Resonance Voltage Stabilizers (in Russian), **B. V. Belayev.** *Avtomatika i Telemekhanika*, vol. 9, Jan. 1948, pp. 59–73.

1096. Voltage Stabilizers Assure Top Performance. *Electrical Manufacturing*, vol. 42, Sept. 1948, pp. 108–13, 188, 190, 192. Survey of magnetic and electronic types.

1097. A-C Magnetic Voltage Stabilizers, **R. Quimby.** *Electronic Industries*, vol. 2, April 1948, pp. 14, 30.

1098. Transductor Type Supply Voltage Regulator, **S. E. Hedstrom.** *ASEA Journal*, vol. 21, June-Aug. 1948, pp. 78–81.

1099. Magnetic Stabilizer for Direct Current Arcs in Spectroscopy, **G. C. B. Cave.** *Analytical Chemistry*, vol. 20, Sept. 1948, pp. 817–21.

1100. Electromagnetic Voltage Stabilizers for Electronic Valve Circuits (in German), **W. Geyger.** *Funk und Ton*, no. 6, June 1948, pp. 308–14.

1101. Electromagnetic Voltage Stabilizers with Two Inductors in Series (in Russian), **G. K. Evdokimov.** *Vestnik Elektroprommishlennosti*, no. 10, 1948, pp. 11–17.

1102. Theory of the Ferro-Resonance Type of Voltage Stabilizer (in Russian), **S. P. Pivovarov.** *Avtomatika i Telemekhanika*, vol. 10, 1949, pp. 238–46.

1103. Predetermination of Magnetic Constant-Voltage Regulators (in German), **W. Taeger.** *Funk und Ton*, vol. 3, Aug. 1949, pp. 429–37.

1104. Approximate Calculation of the Basic Relationships in Ferro-Resonant Voltage Stabilizers (in Russian), **A. G. Lure.** *Elektrichestvo*, no. 10, Oct. 1950, pp. 67–71.

1105. Reactors for Constant Voltage Regulation, (in Italian), **G. B. Madella.** *Telecomunicazioni*, vol. 3, Dec. 1950, pp. 477–80.

1106. Use of Transductor Regulators with Booster Exciters—A New and Effective Method of High Speed Voltage Control for Synchronous Machines, **S. E. Hedstrom.** *ASEA Journal*, vol. 23, Feb. 1950, pp. 23–31.

1107. Saturable Reactors Regulate X-Ray Tube Output, **W. N. Lundahl.** *Electrical Manufacturing*, vol. 45, June 1950, pp. 92–95, 204.

1108. An Electronic A-C Voltage Stabilizer (in Italian), **G. Tagliaferri, L. Terra.** *Nuovo Cimento*, vol. 7, July 1950, pp. 690–94.

1109. Method of Calculating Saturable Regulating Reactors for Voltage Stabilization of Rectifiers (in Russian), **M. N. Gubanov.** *Elektrichestvo*, no. 3, March 1951, pp. 48–53.

Constant Voltage and Current Devices

1110. The Sensitivity of Barretters (in German), **B. Gati.** *Physikalische Zeitschrift*, vol. 10, 1909, pp. 897–99.

1111. Neon Lamp as Stabilizer, **S. O. Pearson.** *Wireless World and Radio Review*, vol. 25, Aug. 28, 1929, pp. 200–02, Sept. 4, 1929, pp. 229–30.

1112. Corona Tube Voltage Regulator, **H. W. Dodge, C. H. Willis.** *AIEE Transactions*, vol. 50, Dec. 1931, pp. 1466–68.

1113. Glow Type of Potential Divider as Stabilized Current Source (in German), **L. Koros, R. Seidelbach.** *Archiv fur Elektrotechnik*, vol. 26, Aug. 3, 1932, pp. 539–52.

1114. Maintenance of a Constant Potential of About 1000 Volts by Means of a Positive Corona Discharge Portable Apparatus for the Operation of Tube and Point Counters (in German), **G. Medicus.** *Zeitschrift fur technische Physik*, vol. 14, Aug. 1933, pp. 304–06.

1115. D-C Voltage Stabilization, **H. W. Kohler.** *Electronics*, vol. 7, Dec. 1934, pp. 388–89.

1116. Automatic Stabilization of Measurement Voltages with Incandescent Lamps (in German), **W. Geyger.** *Archiv fur Elektrotechnik*, vol. 28, 1934, pp. 270–73. Nonlinear bridge.

1117. Starting of Glow-Tube Voltage Stabilizers (in German), **K. Lammchen.** *Hochfrequenztechnik und Elektroakustik*, vol. 44, Nov. 1934, pp. 160–63.

1118. The Time Constants of Glow Tube Voltage Stabilizers (in German), **K. Lammchen.** *Hochfrequenztechnik und Elektroakustik*, vol. 44, Dec. 1934, pp. 193–95.

1119. Compensation for Supply Voltage Variations in Thermionic Valve Circuits, **B. M. Hadfield.** *The Post Office Electrical Engineers' Journal*, vol. 29, Oct. 1936, pp. 235–36. Nonlinear resistor used for grid bias.

1120. The Performance of Physical Voltage Regulating Devices, **P. J. Higgs.** *Journal of Scientific Instruments*, vol. 13, April 1936, pp. 114–17. Nonlinear bridge.

1121. Efficiency of Glow Discharge Tubes as Voltage Stabilizers (in German), **A. Hinzpeter.** *Hochfrequenztechnik und Elektroakustik*, vol. 48, Aug. 1936, pp. 56–57.

1122. A Voltage Stabilizer Circuit, **J. A. Ashworth, J. C. Mouzon.** *Review of Scientific Instruments*, vol. 8, 1937, pp. 127–29. Pentode with positive control grid.

1123. Performance of Voltage Stabilizers in Continuous Operation (in German), **H. Gockel.** *Physikalische Zeitschrift*, vol. 38, Jan. 15, 1937, pp. 65–67.

1124. A Simple A-C Voltage Regulator, **G. F. Lampkin.** *Electronics*, vol. 10, Aug. 1937, pp. 30, 31, 36, 39, 40. Neon tubes used to stabilize a rectifier power supply.

1125. The Application of the Gaseous Discharge Tube to Problems of Voltage Regulation, **C. Morton.** *Journal of Scientific Instruments*, vol. 14, May 1937, pp. 161–64.

1126. Barretters, **J. G. W. Mulder.** *Philips Technical Review*, vol. 3, March 1938, pp. 74–79.

1127. Cold-Cathode Gas-Filled Tubes as Circuit Elements, **S. B. Ingram.** *AIEE Transactions* (*Electrical Engineering*), vol. 58, 1939, pp. 342–47.

1128. A Fluorescent Lamp Voltage Stabilizer, **M. H. Sweet.** *Electronics*, vol. 13, Aug. 1940, pp. 60, 62.

1129. Voltage Stabilization Equipment (in Spanish), **E. R. Sabato.** *Publicaciones de la Facultad de Ciencias Fisico-Matematicas*, Universidad Nacional de la Plata, no. 139, 1939–1940, pp. 425–32. Neon tube stabilizer.

1130. Voltage Control with a Non-Linear Wheatstone Bridge, **W. Richter.** *Electronics*, vol. 13, June 1940, pp. 20–21, 108.

1131. Current Rating and Life of Cold-Cathode Tubes, **G. H. Rockwood.** *AIEE Transactions* (*Electrical Engineering*), vol. 60, 1941, pp. 901–03.

1132. A Fluorescent Lamp as a Voltage Stabilizer, **L. A. Parratt, R. G. Stephenson.** *Review of Scientific Instruments*, vol. 13, 1942, pp. 233, 234.

1133. Sensitive Valve Voltmeter Relay, **S. S. Orlov, A. A. Piragov.** *Wireless Engineer*, vol. 19, Aug. 1942, pp. 347–50. Two rectifiers having different characteristics used as voltage sensing elements.

1134. Ballast Tubes as Automatic Voltage Regulators, **S. G. Taylor.** *Electronics*, vol. 15, Jan. 1942, pp. 26–30.

1135. Improvement in Voltage Stabilizers (in French), **J. Benoit.** *Comptes Rendus*, l'Academiedes Sciences, vol. 217, Dec. 13, 1943, pp. 597–99. Nonlinear bridge.

1136. A Note on a Simple Barretter, **M. A. El-Sherbini, Y. L. Yousef.** *Proceedings*, Physical Society, vol. 55, Sept. 1943, pp. 428–29.

1137. Bridge Voltage Regulators, **C. Morton.** *Journal of Scientific Instruments*, vol. 21, Jan. 1944, pp. 15–17.

1138. The "Stabilistor," **A. H. B. Walker.** *Wireless World*, vol. 50, Nov. 1944, pp. 339–42.

1139. Utilizing the VR-Series Tube, **W. H. Anderson.** *QST*, vol. 29, Dec. 1945, pp. 36, 37.

1140. The Theory of the Non-Linear Bridge Circuit as Applied to Voltage Stabilizers, **G. N. Patchett.** *Journal*, Institution of Electrical Engineers, vol. 93, pt. 3, Jan. 1946, pp. 16–22.

1141. Characteristics of the Pre-Corona Discharge and Its Use as a Reference Potential in Voltage Stabilizers, **S. C. Brown.** *Review of Scientific Instruments*, vol. 17, Dec. 1946, pp. 543–49.

1142. The Characteristics of Lamps as Applied to the Non-Linear Bridge, Used as the Indicator in Voltage Stabilizers, **G. N. Patchett.** *Journal*, Institution of Electrical Engineers, vol. 93, pt. 3, Sept. 1946, pp. 305–22.

1143. A Voltage Stabilizing Tube for Very Constant Voltage, **T. Jurriaanse.** *Philips Technical Review*, vol. 8, Sept. 1946, pp. 272–77.

1144. Production of a Constant Current Source (in French), **A. Godefroy.** *Comptes Rendus*, l'Academie des Sciences, vol. 224, June 16, 1947, pp. 1703–05. Nonlinear bridge.

1145. The Use of Non-Linear Resistors for Voltage Correction, **G. T. Baker.** *Strowger Journal*, vol. 6, May 1947, pp. 73–78.

1146. The Voltage Stabilization Properties of the Continuous Corona Discharge, **I. H. Blifford, H. Friedman.** *Physical Review*, vol. 72, 1947, p. 185.

1147. Optimum Parameter for Gas Tube Voltage Regulators, **W. R. Berg.** *Electronics*, vol. 20, Oct. 1947, pp. 136, 138.

1148. Characteristics of Certain Voltage-Regulator Tubes, **G. M. Kirkpatrick.** *Proceedings*, Institute of Radio Engineers, vol. 35, May 1947, pp. 485–89.

1149. Barretters (in Russian), **D. Y. Ashkenazi.** *Elektrichestvo*, no. 3, 1948, pp. 58–60.

1150. Circuit Design for Gas-Discharge Regulator Tubes, **W. G. Hoyle.** *Tele-Tech*, vol. 7, Feb. 1948, pp. 46–47, 69–70.

1151. High Stability Diode for Regulation and Automatic Control Purposes (in Russian), **G. R. Herzenberg.** *Vestnik Elektroprommishlennosti*, no. 5, 1948, pp. 17–24.

1152. Voltage Stabilization by Means of Barium Titanate Capacitors (in Russian), **G. I. Skanavi, M. D. Neuman.** *Elektrichestvo*, no. 7, July 1949, pp. 43–46. (Also *Engineers' Digest*, vol. 10, Dec. 1949, pp. 427–29.)

1153. Dry Battery Characteristics and Applications, **N. M. Potter.** *Journal*, British Institution of Radio Engineers, vol. 9, 1949, pp. 61–72.

1154. Variations in the Characteristics of Some Glow-Discharge Voltage Regulator Tubes, **F. A. Benson, W. E. Cain, B. D. Clucas.** *Journal of Scientific Instruments*, vol. 26, 1949, pp. 399–401.

1155. Use of Barium Compounds in Glow Discharge Regulator Tubes, **H. Jacobs, A. P. LaRocque, A. A. Mazzei.** *Sylvania Technologist*, vol. 2, Jan. 1949, pp. 12–14.

1156. Corona-Tube Regulators for High Voltages, **I. H. Blifford, R. G. Arnold, H. Friedman.** *Electronics*, vol. 22, Dec. 1949, pp. 110–11.

1157. Some Characteristics of Glow-Discharge Voltage Regulator Tubes, **E. W. Titterton.** *Journal of Scientific Instruments*, vol. 26, Feb. 1949, pp. 33–36.

1158. A Simple Form of Voltage Stabilizer, **N. K. Saha, B. S. Chandersekhara, M. K. Sundaresen.** *Proceedings*, National Institute of Sciences of India, vol. 16, March-April 1950, pp. 127–33.

1159. Initial Drifts in Running Voltage of Glow Discharge Regulator Tubes, **F. A. Benson.** *Journal of Scientific Instruments*, vol. 27, March 1950, pp. 71–72.

1160. Variations in Extinction Voltages of Glow-Discharge Voltage-Regulator Tubes, **F. A. Benson.** *Journal of Scientific Instruments*, vol. 28, June 1951, p. 186.

1161. Characteristics of Some Miniature High Stability Glow-Discharge Voltage-Regulator Tubes, **F. A. Benson.** *Journal of Scientific Instruments*, vol. 28, 1951, pp. 339–41.

1162. Comments Upon the Behavior of Neon Tubes in Voltage Stabilizing Circuits (in German), **B. Schumacher.** *Frequenz*, vol. 5, May 1951, pp. 121–24.

1163. High Voltage Stabilization by Means of the Corona Discharge Between Coaxial Cylinders, **S. W. Lichtman.** *Proceedings*, Institute of Radio Engineers, vol. 39, April 1951, pp. 419–24.

1164. A Low-Power Alternating Voltage Stabilizer, **D. J. R. Martin, A. J. Maddock.** *Journal of Scientific Instruments*, vol. 28, Jan. 1951, pp. 1–3. Nonlinear circuit.

Motor Speed Regulation

1165. Automatic Speed Regulation, **J. H. Ashbaugh.** *Electrical Engineering*, vol. 50, May 1931, pp. 363–64.

1166. Speed Regulation of Signalling Machines, **W. Dornig.** *Elektrotechnisch Zeitschrift*, vol. 52, Aug. 6, 1931, pp. 1031–33.

1167. A Sensitive Speed Regulator for Electric Motors (in German), **E. Giebe.** *Fordertechnik und Frachtverkehr*, vol. 25, July 1, 1932, pp. 345–48.

1168. Synchronization of D-C Machines with a Metronome of Small Power (in German), **H. Schuchmann.** *Wissenschaftliche Veroeffentlichungen aus dem Siemens-Konzern*, vol. 12, pt. 2, 1933, pp. 24–33.

1169. Paper Machine Modernized by Electronic Speed Regulator, **D. F. Cronin, C. W. Drake.** *Electrical World*, vol. 102, Oct. 21, 1933, pp. 538–40.

1170. A Constant Speed D-C Motor Control, **J. A. Beardon, C. H. Shaw.** *Review of Scientific Instruments*, vol. 5, 1934, pp. 292–95.

1171. Regulation of D-C Motors with Grid-Controlled Rectifiers, **W. Schilling.** *Archiv fur Elektrotechnik*, vol. 29, Sept. 10, 1935, pp. 622–31.

1172. Precise Speed Control for D-C Machines, **R. H. Frazier, J. Eisler, W. F. Frantz.** *Electrical Engineering*, vol. 54, March 1935, pp. 307–12.

1173. Where Constant Motor Speeds are of First Importance, **R. Lee.** *Electrical Manufacturing*, vol. 15, Jan. 1935, pp. 25–27.

1174. Vapor Tube Type Speed Regulator for D-C Motor, **Aoki-Satara, Matusita-Yozio.** *Shibaura Review*, May-June 1935, pp. 181–86.

1175. New Thermionic Motor Speed Regulator, **C. B. Norris.** *Power and Works Engineer*, vol. 30, Aug. 1935, p. 244.

1176. Astatic Speed Regulation of D-C Motors with Electron Tubes (in German), **J. Ratzke.** *Archiv fur Elektrotechnik*, vol. 29, April 5, 1935, pp. 223–41.

1177. Accurate Speed Control for Machine Tools (in German), **H. Bauer.** *Fachberichte des Verbandes Deutscher Elektrotechniker*, 1936, pp. 65–67.

1178. Electronic Speed Governor, **B. G. Ballard.** *Canadian Journal of Research*, vol. 14 (Section A), July 1936, pp. 134–38.

1179. New Speed Governor Compensated by a Stabilizing Centrifugal Governor, **P. Doignon.** *Revue Generale de l'Electricite*, vol. 39, June 6, 1936, pp. 819–21. Clutch type of speed regulator.

1180. Governor-Controlled Fractional Horsepower Motors, **R. W. Groot.** *Product Engineering*, vol. 7, June 1936, pp. 216–18.

1181. Speed Regulation of Ring-Spinning Machines, **A. Johansson.** *ASEA Journal*, vol. 14, Sept. 1937, pp. 127–32. Speed regulation of 3-phase commutator motor.

1182. Speed Regulator for High Requirements (in German), **J. Huber, E. Meisterknecht.** *Siemens Zeitschrift*, vol. 18, Sept. 1938, pp. 430–32. Tirrill regulator applied to adjustable voltage drive.

1183. Speed-Controlled Motors, **F. M. Yarline.** *Product Engineering*, vol. 9, March 1938, pp. 106–09.

1184. Constant Speed Control Theory, **H. K. Weiss.** *Journal of the Aeronautical Sciences*, vol. 6, Feb. 1939, pp. 147–52.

1185. Recent Developments in Speed Regulation, **C. R. Hanna, K. A. Oplinger, S. J. Mikina.** *AIEE Transactions*, vol. 59, 1940, pp. 692–700.

1186. Speed Regulation of D-C Motors by Current Pulses (in German), **K. Balufuss.** *Archiv fur Elektrotechnik*, vol. 34, Oct. 15, 1940, pp. 581–90.

1187. Governing Small Motors, **S. F. Philpott.** *Electrical Review*, vol. 128, Apr. 11, 1941, pp. 539–40.

1188. A Method for the Exact Regulation of Fixed Rotational Speeds of an Axle (in German), **F. Kirchstein.** *Zeitschrift fur Technische Physik*, vol. 23, 1942, pp. 234–40.

1189. Generators and Motors Controlled by Tuning Forks (in German), **K. Schmidt.** *Elektrotechnische Zeitschrift*, vol. 63, July 16, 1942, pp. 327–30.

1190. A Clock Controlled Governor for Close Speed Regulation, **J. C. Prescott, M. N. Karaosman.** *Journal*, Institution of Electrical Engineers, vol. 89, pt. 2, June 1942, pp. 210–16.

1191. Precision Speed Control for World's Largest Induction Motor, **Robert R. Longwell, M. E. Reagan.** *AIEE Transactions* (*Electrical Engineering*), vol. 61, Sept. 1942, pp. 634–38.

1192. Acceleration-Sensitive Governors. *Product Engineering*, vol. 13, March 1942, pp. 150–53.

1193. Governor-Controlled Motors Hold Closely to Preset Speeds, **C. G. Brennecke.** *Electrical Manufacturing*, vol. 32, Sept. 1943, pp. 100–02, 186, 188, 190.

1194. Comparison Between the Different Methods of Regulation of Electrically Driven Turbo-Blowers for Steelworks, **M. Haller.** *Brown Boveri Review*, vol. 30, Nov.-Dec. 1943, pp. 328–36.

1195. Control of D-C Motors by Means of

Vibrating Relays (in German), **C. Moerder.** *Archiv fur Elektrotechnik*, vol. 37, 1943, pp. 571–87.

1196. Centrifugal Control Governor for Universal Motors (in German), **M. Voege.** *Elektrotechnischer Anzeiger*, vol. 59, May 13, 1942, pp. 218–20. (Also *Engineers' Digest*, vol. 4, March 1943, pp. 91–92.)

1197. The Character of Signals From Lighthouses and Beacons (in French), **G. Dupouy.** *Revue Generale de l'Electricite*, vol. 53, Jan. 1944, pp. 3–12.

1198. Electric Aircraft Speed Regulators with Gravity Action (in German), **K. Emden.** *Schweizerische Bauzeitung*, vol. 124, Sept. 2, 1944, pp. 115–19. Motor speed regulator consisting of centrifugal contacts mounted on a horizontal shaft.

1199. Constant Speed Impulse Motors, **H. T. Mitchell, T. Pilling.** *The Post Office Electrical Engineers' Journal*, vol. 37, Jan. 1945, pp. 109–12. Governor controlled motor is compared with one whose speed is matched with an escapement mechanism through a differential gear.

1200. Thyratron Motor Control, **E. W. Forster.** *BTH Activities*, vol. 19, Jan. 1946, pp. 32–35.

1201. Simplified Thyratron Motor Control, **H. H. Leigh.** *General Electric Review*, vol. 49, Sept. 1946, pp. 18–27.

1202. The Velodyne, **F. C. Williams, A. M. Uttley.** *Journal*, Institution of Electrical Engineers, vol. 93, pt. 3A, 1946, pp. 1256–74.

1203. An Electronic Frequency Meter and Speed Regulator, **Ellis Levin.** *AIEE Transactions (Electrical Engineering)*, vol. 65, Dec. 1946, pp. 779–86.

1204. A Carbon-Pile Speed Governor, **C. T. Button.** *AIEE Transactions (Electrical Engineering)*, vol. 65, Jan. 1946, pp. 4–7.

1205. Centrifugal Governor Speed Control for Small Motors, **W. M. Yogerst.** *Product Engineering*, vol. 18, Aug. 1947, pp. 138, 139.

1206. Speed Stability for Continuous Mills, **F. E. Crever, T. M. Linville.** *Iron and Steel Engineer*, vol. 24, June 1947, pp. 50–60.

1207. Constant-Current Systems for Electronic Control of D-C Motors, **O. W. Livingston.** *General Electric Review*, vol. 50, May 1947, pp. 38–44.

1208. Automatic Speed Regulation of Ring Spinning Machines, **A. Janso.** *ASEA Journal*, vol. 30, Feb.-March 1947, pp. 19–38.

1209. General Analysis of Speed Regulators Under Impact Loads, **G. D. McCann, W. O. Osbon, H. S. Kirschbaum.** *AIEE Transactions*, vol. 66, 1947, pp. 1243–52.

1210. Regulation of the Speed of Rotation of D-C Motors by the Use of Saturated Choking Coils (in Russian), **M. I. Kraitsberg.** *Elektrichestvo*, no. 6, 1948, pp. 48–50.

1211. Regulation of the Speed of a 3 Phase Asynchronous Motor with the Aid of Thyratrons and Series Transformers (in Russian), **A. G. Ivakhnenko.** *Elektrichestvo*, no. 9, Sept. 1948, pp. 57–59.

1212. Electronic Speed Regulators for Sectional Paper Machine Drive, **V. B. Baker, J. F. Kovalsky.** *AIEE Transactions*, vol. 67, pt. II, 1948, pp. 1636–42.

1213. Speed Control Systems for High-Speed Squirrel Cage Motors, **G. W. Heumann.** *General Electric Review*, vol. 51, Feb. 1948, pp. 28–34.

1214. Some Considerations on the Theory of Speed Regulation (in German), **I. Obradovic.** *Schweizer Archiv fur angewandte Wissenschaft und Technik*, vol. 14, Aug. 1948, pp. 234–42.

1215. Theory of an Automatic Regulator for Winding Paper Band or Cotton under Tension (in Russian), **F. M. Kurovski.** *Vestnik Elektroprommishlennosti*, no. 9, 1948, pp. 19–23.

1216. Regulation of D-C Motors Supplied Through Thyratrons (in Italian), **C. Calosi.** *Elettrotecnica*, vol. 35, Dec. 1948, pp. 469–88.

1217. How to Obtain Constant Speed Motion Below 10 RPM, **W. Hotine.** *Product Engineering*, vol. 20, Dec. 1949, pp. 118–21.

1218. Precision Speed Control, **A. L. Holcomb.** *Journal*, Society of Motion Picture Engineers, vol. 52, May 1949, pp. 561–70. Electronic regulation of d-c motor.

1219. Speed Control Servo System, **J. C. West.** *Electrical Review*, vol. 144, June 3, 1949, pp. 937–41. Speed regulating systems for small 2-phase motors and similar machines.

1220. Starting Speed Regulator with Free Anchor Movement (in Russian), **Z. M. Akselrod.** *Avtomatika i Telemekhanika*, vol. 10, 1949, pp. 99–112.

1221. D-C Electric Drive with a Wide Range of Motor Speeds (in Russian), **V. P. Bychkov.** *Izvestiya Akademii Nauk, SSSR.* Otdelenie Tekhnicheskikh Nauk, no. 2, Feb. 1950, pp. 167–75.

1222. Electronic Synchronous Speed Regulator, **W. J. M. Moore.** *Electrical Engineering*, vol. 69, June 1950, pp. 532–37. Speed of d-c driving motor is controlled by thyratron rectifier in field circuit. Sensing circuit detects phase angle change between generator frequency and reference.

1223. Servo Control of the Speed of Automatic Machines (in French), **C. V. Dunski.** *Bulletin*, Association des Ingenieurs Electriciens Sortis de l'Institut Electrotechnique Montefiore, vol. 63, June, 1950, pp. 279–94.

1224. An Electronic Speed Control for the Towing Carriage of a Ship-Model Testing Tank, **R. H. Tizard, B. G. V. Harrington.** *Proceedings*, Institution of Electrical Engineers, vol. 97, pt. 2, 1950, pp. 651–62.

1225. Electronic Regulation of Motors (in German), **A. Grun.** *Zeitschrift des Vereines deutscher Ingenieure*, vol. 92, Nov. 1950, pp. 861–66.

1226. Mechanical Systems for Controlling Speed and Tension, **J. H. Gepfert.** *Product Engineering*, vol. 21, Dec. 1950, pp. 85–89.

1227. An Electromechanical Device for Speed Regulation (in Italian), **S. B. Toniolo.** *Elettrotecnica*, vol. 37, May 10–25, 1950, pp. 229–32.

1228. Control of Large D-C Motors Supplied from Ignitron Rectifiers, **O. W. Livingston.** *AIEE Transactions*, vol. 69, pt. I, 1950, pp. 205–10.

1229. The Position Synchronization of a Rotating Drum, **F. C. Williams, J. C. West.** *Proceedings*, Institution of Electrical Engineers, vol. 98, pt. II, Feb. 1951, pp. 29–34.

1230. Broadcast Tape Speed Control, **D. R. Andrews.** *Electronics*, vol. 24, July 1951, pp. 120–23.

1231. Solenoid Motor Control, **G. M. Chute.** *Electronics*, vol. 24, Jan. 1951, p. 105.

1232. Precise Frequency and Voltage Control of Sine-Wave Alternator Set, **B. V. Hamon.** *Australian Journal of Applied Science*, vol. 2, March 1951, pp. 1–25.

Prime Mover Speed Regulation

1233. Speed Regulation in Hydroelectric Plants, **W. F. Uhl.** *Transactions*, American Society of Mechanical Engineers, vol. 34, 1912, pp. 379–434.

1234. Speed Changes of Hydraulic Turbines for Sudden Changes of Load, **E. B. Strowger, S. L. Kerr.** *Transactions*, American Society of Mechanical Engineers, vol. 48, 1926, pp. 209–62.

1235. The Charmilles Acceleration-Tachometric Regulator (in French), **M. E. Volet.** *Bulletin*, Technique de la Suisse Romande, vol. 25, July 31, 1926, pp. 190–96.

1236. Changing Requirements in Hydraulic Turbine Speed Regulation, **F. Nagler.** *Transactions*, American Society of Mechanical Engineers, vol. 52, 1930, pp. HYD 13–24.

1237. Governing of Steam Turbines Working in Parallel, **W. Guilhauman.** *AEG Mitteilungen*, no. 10, Oct. 1931, pp. 572–76.

1238. Regulation of the Power of Hydraulic Turbines Working Under a Variable Head (in French), **O. Yadoff.** *Comptes Rendus*, l'Academie des Sciences, vol. 198, June 11, 1934, pp. 2067–69.

1239. Electric Drive of Governor Pendulums of Hydraulic Turbines, **G. Fisler.** *Brown Boveri Review*, vol. 22, Apr. 1935, pp. 93–96.

1240. Oscillograph Analyzes Governor Performance, **J. E. Allen.** *Power*, vol. 78, Nov. 1934, pp. 610–12.

1241. Valve Regulator for Prime Mover Control (in German), **F. Fritz.** *Elektrotechnik und Maschinenbau*, vol. 53, Nov. 24, 1935, pp. 555–58.

1242. Electromagnetic Control of High Rotational Speed, **T. Davis.** *Review of Scientific Instruments*, vol. 7, Feb. 1936, pp. 96–98.

1243. Superposed-Turbine Regulation Problem, **A. F. Schwendner, A. A. Luoma.** *Transactions*, American Society of Mechanical Engineers, vol. 58, Nov. 1936, pp. 615–20.

1244. Direct Regulation of Frequency with Speed Regulators (in French), **F. Cahen.** *Bulletin*, Societe Francaise des Electriciens, vol. 6, ser. 5, July 1936, pp. 697–720.

1245. Utilization of the Governors of Prime Movers in the Control of Interconnected Networks (in French), **D. Gaden, E. Volet.** *Bulletin*, Association Suisse des Electriciens, vol. 28, Oct. 28, 1937, pp. 559–74.

1246. Some Comments on Frequency and Power Regulation, **F. Werthmann.** *Brown Boveri Review*, vol. 24, 1937, pp. 141–45, 161–66.

1247. A Review of the Quest for Constant Speed, **E. W. Kellogg.** *RCA Review*, vol. 2, 1937, pp. 220–39. Mechanical methods applicable to phonographs and film projectors.

1248. Influence of Steam Space upon Turbine Speed Regulation (in German), **F. Weiss.** *Archiv fur Warmewirtschaft und Dampfkesselwesen*, vol. 18, March 1937, pp. 86–87.

1249. Precise Frequency Control with Reverse Flow Governor, **O. N. Bryant.** *Power*, vol. 82, Feb. 1938, pp. 74, 75.

1250. The Stability of the Speed Regulators of Piston Type Engines Coupled to Parallel Running Synchronous Generators (in German), **R. Meyer.** *Elektrotechnik und Maschinenbau*, vol. 57, June 9, 1939, pp. 305–10.

1251. New Speed Regulator (in German), **R. Keller.** *Bulletin*, Association Suisse des Electriciens, vol. 30, Jan. 6, 1939, pp. 20–23.

1252. Combined Frequency-Output Regulation, **F. Werthmann.** *Brown Boveri Review*, vol. 26, Sept. 1939, pp. 207–14.

1253. A New Electric Governor for Prime Movers, **R. Keller.** *Brown Boveri Review*, vol. 26, June 1939, pp. 141–48.

1254. Steam-Turbine Governors, **R. J. Caughey.** *Transactions*, American Society of Mechanical Engineers, vol. 62, April 1940, pp. 191–98.

1255. Improvements on the Electrical Control of Regulators (in French), **M. Wenger.** *Bulletin*, Association Suisse des Electriciens, vol. 31, March 8, 1940, pp. 120–22. Electric control of hydraulic turbines.

1256. A Supersensitive Governor for Hydraulic Turbines, **W. M. White.** *Transactions*, American Society of Mechanical Engineers, vol. 62, April 1940, pp. 167–70.

1257. Constant System Speed and the Steam Turbine Governor, **A. F. Schwendner.** *Transactions*, American Society of Mechanical Engineers, vol. 62, April 1940, pp. 199–206.

1258. The Field of System Governing, **A. Davis.** *Transactions*, American Society of Mechanical Engineers, vol. 62, April 1940, pp. 207–19.

1259. Experiences in System Speed Regulation, **O. Holden.** *Transactions*, American Society of Mechanical Engineers, vol. 62, April 1940, pp. 237–40.

1260. A New Oerlikon-Escher Wyss Electrical Governor (in French), **M. Hirt, A. Gantenbein.** *Bulletin*, Association Suisse des Electriciens, vol. 32, July 18, 1941, pp. 316–24.

1261. Some Problems Connected with Steam Turbine Governing, **G. W. Higgs-Walker.** *Proceedings*, Institution of Mechanical Engineers, vol. 146, 1941, pp. 117–25; vol. 148, 1942, pp. 26–32.

1262. Some Considerations on Speed Governors for Water Turbines (in Italian), **A. Cita.** *Elettrotecnica*, vol. 28, Sept. 25, 1941, pp. 461–69.

1263. Power System Governing—the Problem, **J. J. Dougherty, A. P. Hayward, A. C. Monteith, S. B. Griscom.** *AIEE Transactions*, vol. 60, 1941, pp. 547–58; discussion, 731–33.

1264. Turbo-Alternator Speed Control, **A. Abbott.** *Electrical Review*, vol. 128, June 6, 1941, pp. 713–14.

1265. A Power System Governor Sensitive to Frequency and Load, **Thomas E. Curtis.** *AIEE*

Transactions (*Electrical Engineering*), vol. 60, March 1941, pp. 89–92.

1266. Effect of Prime-Mover Speed Governor Characteristics on Power-System Frequency Variations and Tie-Line Power Swings, **C. Concordia, S. B. Crary, E. E. Parker.** *AIEE Transactions*, vol. 60, 1941, pp. 559–67; discussion, 733–35.

1267. The Fundamentals of Steam-Turbine Governing, **H. G. Yates.** *English Electric Journal*, vol. 10, June 1941, pp. 76–84.

1268. Electric Speed Regulator for Hydraulic Turbines (in German), **H. Happoldt.** *Elektrotechnische Zeitschrift*, vol. 62, 1941, pp. 191–93.

1269. Experience with Electrical Governors for Prime Movers in the Aarau Power Station, 1937–1941 (in German), **H. Muller.** *Bulletin*, Association Suisse des Electriciens, vol. 32, Dec. 19, 1942, pp. 723–25.

1270. Automatic Speed Control for the Air-Driven Centrifuge, **A. Rothen.** *Review of Scientific Instruments*, vol. 12, 1941, pp. 355–57.

1271. An Electrical Governor, **Frank I. Morgan.** *AIEE Transactions* (*Electrical Engineering*), vol. 60, Feb. 1941, pp. 80–84.

1272. A Turbine-Governor Performance Analyzer, **W. O. Osbon.** *AIEE Transactions* (*Electrical Engineering*), vol. 60, Nov. 1941, pp. 963–67; discussion, vol. 61, 1942, p. 393.

1273. Prime-Mover Speed Governors for Interconnected Systems, **R. J. Caughey, J. B. McClure.** *AIEE Transactions* (*Electrical Engineering*), vol. 60, 1941, pp. 147–51.

1274. Speed Regulation of Kaplan Turbines, **J. D. Scoville.** *Transactions*, American Society of Mechanical Engineers, vol. 63, July 1941, pp. 385–94.

1275. Analyzing Governor-System Performance, **A. F. Schwendner.** *Transactions*, American Society of Mechanical Engineers, vol. 64, Jan. 1942, pp. 43–47.

1276. Which Governor Suits Your Turbine Load? **F. K. Fischer, O. N. Bryant.** *Power*, vol. 86, April 1942, pp. 65–67.

1277. The Brown Boveri Electric Primary Governor in Hydro-Electric Stations, **R. Wild.** *Brown Boveri Review*, vol. 29, Aug. 1942, pp. 198–201.

1278. Supplementary Control of Prime-Mover Speed Governors, **S. B. Crary, J. B. McClure.** *AIEE Transactions* (*Electrical Engineering*), vol. 61, 1942, pp. 209–14.

1279. Governors for Diesel Engines. *Diesel Power*, vol. 21, Oct. 1943, pp. 927–32.

1280. Automatic Load Regulation in Hydroelectric Power Plants (in German), **V. Cavalotti.** *Elektrotechnische Zeitschrift*, vol. 64, Dec. 2, 1943, pp. 635–36.

1281. Regulating Forces in Waterturbines (in German), **H. Gerber.** *Zeitschrift Verein deutscher Ingenieure*, vol. 87, June 1943, pp. 372–73.

1282. Electrical Regulation of Hydraulic Turbines, **A. Garde.** *Teknisk Tidskrift*, vol. 73, Dec. 4, 1943, pp. 179–87.

1283. A Recording and Controlling System for Air-Driven Ultracentrifuges, **T. J. Dietz.** *Journal*, Franklin Institute, vol. 236, Nov. 1943, pp. 451–59.

1284. Water Turbine Regulation (in German), **H. Kieser.** *Elektrotechnik und Maschinenbau*, vol. 62, April 14, 1944, pp. 180–94.

1285. Governing Requirements for Extraction Turbines, **O. N. Bryant.** *Power Plant Engineering*, vol. 48, March 1944, pp. 76–77.

1286. Principles of Synchronous Governing, **J. C. Prescott.** *Journal*, Institution of Electrical Engineers, vol. 91, pt. I, Feb. 1944, pp. 77–80.

1287. Basic Factors in Applying Speed Governors, **G. F. Drake.** *Machine Design*, vol. 16, April 1944, pp. 111–14. Application to internal combustion engines.

1288. Governor Requirements for Aircraft Alternator Drives, **W. K. Boice, L. G. Levoy, Jr.** *AIEE Transactions* (*Electrical Engineering*), vol. 64, July 1945, pp. 534–40.

1289. The Variable-Speed Hydraulic Governor, **J. Z. Bujak.** *Proceedings*, Institution of Mechanical Engineers, vol. 153 (War Emerg. Issue No. 7), 1945, pp. 193–205.

1290. Thyratron Rectifier Controls Steam Turbine Governor, **J. H. Schroeder.** *Electrical World*, vol. 124, July 21, 1945, pp. 68–69.

1291. Influence of the Water Inertia on the Stability of a Hydroelectric Group (in French), **P. Almeras.** *Houille Blanche*, Nov. 1945, pp. 81–90; March 1946, pp. 131–39; May 1946, pp. 189–98.

1292. Control of Load, Frequency, and Time of Interconnected Systems, **C. K. Duff.** *AIEE Transactions* (*Electrical Engineering*), vol. 64, 1945, pp. 778–86.

1293. Constant-Speed Drives for Aircraft Alternators, **C. J. Breitwieser.** *AIEE Transactions* (*Electrical Engineering*), vol. 64, Nov. 1945, pp. 763–68.

1294. Automatic Regulation of Turbine Generators to Relieve Power-Supply Systems of Steel-Mill Load Swings, **W. W. Eberhardt, C. W. Harrison, E. J. Kohn, A. G. Darling.** *AIEE Transactions* (*Electrical Engineering*), vol. 64, 1945, pp. 751–58.

1295. Electrohydraulic Control of Diesel-Electric Drives, **C. B. Lewis, M. A. Edwards.** *Mechanical Engineering*, vol. 68, 1946, pp. 953–55.

1296. Speed Regulation and Automatic Operation of Winding Engines (in French), **E. Carton.** *Charleroi-Jeumont Review*, no. 1–2, Jan.-July 1946, pp. 43–52.

1297. On the Stability of Regulation in Hydro-Electric Plants (in Italian), **G. Evangelisti.** *Energia Elettrica*, vol. 23, Sept.-Oct. 1946, pp. 234–39.

1298. Governor for Variable-Ratio Transmission Used in Developmental 400-Cycle Electric System for Large Aircraft, **P. F. Desch, D. E. Garr, J. G. Hutton.** *AIEE Transactions*, vol. 65, April 1946, pp. 194–98.

1299. The New Brown Boveri System of Multiple Regulation of Steam Turbines, **A. Leyer.** *Brown Boveri Review*, vol. 33, Sept. 1946, pp. 234–39.

1300. La Regolazione Delle Turbine Idrauliche, **G. Evangelisti** (book). Nicola Zanichelli, Bologna, Italy, 1947.

1301. Speed Regulation of Water Turbines (in German), **T. Stein.** *Schweizerische Bauzeitung*, vol. 65, 1947, Sept. 27, pp. 531–35; Oct. 4, pp. 543–47; Oct. 11, pp. 564–68; vol. 66, Feb. 14, 1948, pp. 89–90. *Engineers' Digest*, vol. 5, May-June 1948, pp. 187–92.

1302. Speed Control for Air-Driven Centrifuge, **J. W. Beams, F. W. Linke, P. Sommer.** *Review of Scientific Instruments*, vol. 18, Jan. 1947, pp. 57–60.

1303. Characteristics of the Control Systems (in French), **M. Almeras.** *Houille Blanche*, vol. 2, Nov.-Dec. 1947, pp. 457–67. Comparison of the acceleration-velocity governor with the dashpot type.

1304. Stability of Governors with Time Lag (in German), **L. Collatz.** *Zeitschrift fur angewandte Mathematik und Mechanik*, vol. 27, May 1947, pp. 60–63.

1305. Testing Governor Performance on Electric Power Systems with Improved Instruments, **J. E. Allen, W. B. Hess.** *AIEE Transactions*, vol. 66, 1947, pp. 329–42.

1306. Power System Governing, **T. E. Curtis.** *Electrical Engineering*, vol. 66, Dec. 1947, pp. 1197–200.

1307. Centrifugal Governors with Flyweights of Distributed Mass, **B. W. Millington.** *Engineering*, vol. 163, March 28, 1947, p. 232. Study of error due to considering mass as concentrated at a point.

1308. Magnetic Governor Release for Stand-by Operation, **B. H. Mudgett.** *Electrical World*, vol. 127, May 10, 1947, pp. 100–01.

1309. Rate-Detecting Gyro, **V. J. Canziani.** *Machine Design*, vol. 19, Aug. 1947, pp. 142–44.

1310. Stable Speed Control of Turbo-Alternators Supplying a Load Independent of the Frequency, **R. Keller.** *Brown Boveri Review*, vol. 34, June-July 1947, pp. 99–104.

1311. Effect of Self-Regulation and Damping Time on WR^2 of Hydro-Electric Generators (in French), **T. Stein.** *Bulletin*, Societe Francaise des Electriciens (Ser. 6), vol. 8, Feb. 1948, pp. 93–103.

1312. Automatic Speed Regulation of Hydraulic Turbines (in French), **D. Gaden, P. Nesser.** *Houille Blanche*, vol. 3, May-June 1948, pp. 256–71.

1313. Speed Governing Design Considerations for Multivalve Condensing Steam Turbine-Generators, **J. W. Barnett.** *AIEE Transactions*, vol. 67, pt. II, 1948, pp. 1557–61.

1314. Turbine Regulation Systems with Two Stages of Amplification, **A. V. Tcheglaev.** *Engineers' Digest* (Brit. Ed.) vol. 9, Dec. 1948, pp. 401–04.

1315. Speed Control for the Air Driven Ultracentrifuge, **S. D. Majumdar, G. N. Sarkar.** *Review of Scientific Instruments*, vol. 19, Sept. 1948, pp. 541–44.

1316. Mechanical Computer Would Refine Governing, **T. E. Curtis.** *Electrical World*, vol. 129, Feb. 28, 1948, pp. 78, 79.

1317. Accelerating the Speed Control of Hydraulic Turbines (in French), **Jean Daniel.** *Houille Blanche*, vol. 3, Jan.-Feb. 1948, pp. 7–33; March-April 1948, pp. 147–82. Comprehensive analysis of the stability and performance of turbine governors.

1318. On the Theory of the Isodrome Governor (in Russian), **A. M. Letov.** *Prikladnaya Matematika i Mekhanika*, vol. 12, July-Aug. 1948, pp. 363–68.

1319. Instrumentation as Applied to Speed Control, **J. G. Wilson, H. M. Karr, M. V. Long.** *Petroleum Refiner*, vol. 27, Mar. 1948, pp. 150–59.

1320. Precise Turbine Governor, **Henry E. Warren.** *AIEE Transactions*, vol. 67, pt. I, 1948, pp. 571–76.

1321. Considerations on the Regulators for a Group of Hydraulic Generators of Low Head (in French), **A. Dejou.** *Revue Generale de l'Electricite*, vol. 57, Aug. 1948, pp. 315–22. Analysis of stabilization by means of a signal proportional to the second derivative of speed.

1322. Processes for Improvement of Regulation of Hydroelectric Units (in French), **P. Almeras.** *Houille Blanche*, vol. 4, Jan.-Feb. 1949, pp. 38–43.

1323. Performance Characteristics of Speed Governors, **L. B. Wales.** *Electrical Engineering*, vol. 68, 1949, p. 198.

1324. Hydraulic Steam-Turbine Governor, **A. F. Schwendner, J. R. Carlson.** *Westinghouse Engineer*, vol. 9, March 1949, pp. 42–46.

1325. Governor for Locomotive Oil Engines. *Gas and Oil Power*, vol. 44, Oct. 1949, pp. 259–64.

1326. Governors and AIEE-ASME Governor Performance Specification, **A. F. Schwendner, Wayne C. Astley.** *AIEE Transactions*, vol. 68, pt. II, 1949, pp. 1330–32.

1327. Modern Control Dynamics and Stability Criteria as Applied to Gyroscopic Speed Detectors with Hydraulic Drive, **R. Feiss.** *Transactions*, American Society of Mechanical Engineers, vol. 71, Nov. 1949, pp. 979–88.

1328. On the Automatic Governing of Hydraulic Turbines: Influence of Certain Intervening Characteristics on Stability Conditions (in French), **D. Gaden.** *Houille Blanche*, vol. 4, no. B, 1949, pp. 671–72, 717–23.

1329. Determining Incremental Regulation and Dead Band of Governors on Steam Turbine Generators Under System Load Conditions, **E. L. Tornquist, I. L. Wade.** *AIEE Transactions*, vol. 68, pt. II, 1949, pp. 1343–47.

1330. Constant Speed Transmission for Alternator Drive (in French), **J. Faisandier.** *Bulletin*, Societe Francaise des Electriciens, vol. 10, series 6, Feb. 1950, pp. 99–106. Constant alternator speed secured with a 3 to 1 variation in prime mover speed.

1331. Speed Control of Motors Supplied on a Constant Current System, **H. D. Wheeler.** *L.S.E. Engineering Bulletin*, vol. 1, April 1950, pp. 1–14.

1332. Governor Speed-Droop and Its Elimination (in French), **J. Daniel.** *Houille Blanche*, vol. 5, Jan.-Feb. 1950, pp. 15–31.

1333. Considerations on the Stability of Speed Regulation of Low-Head Hydro-Generator Unit, **D. Gaden, A. Dejou.** *Paper 133*, International Conference on Large Electric High-Tension Systems, 1950.

1334. Electrohydraulic Regulation of

Water-Turbines, **E. Brodersen, S. E. Hedstrom, B. Lof, K. Almstrom, A. Garde.** *Paper 315*, International Conference on Large Electric High-Tension Systems, 1950.

1335. An Electric Speed Governor (in French), **M. Cuenod.** *Houille Blanche*, vol. 5, March-April 1950, pp. 125–30. Frequency dependent governor for water turbines.

1336. Investigation of a System of Frequency Regulation for an A-C Calculating Table (in Russian), **P. I. Zubkov.** *Izvestiya Akademii Nauk, SSSR.* Otdelenie Tekhnicheskikh Nauk, no. 5, May 1950, pp. 646–67.

1337. Recommended Specification for Speed-Governing of Hydraulic Turbines Intended to Drive Electric Generators. AIEE Standard No. *605*, Sept. 1950.

1338. Governors and Controls for Industrial Steam Turbine, **I. A. MacTavish.** *Modern Power and Engineering*, vol. 44, April 1950, pp. 43–46.

1339. Methods for Improving the Stability of Hydroelectric Units (in French), **M. Nechleba.** *Houille Blanche*, vol. 5, Nov.-Dec. 1950, pp. 808–11.

1340. Electronic Synchronous Speed Regulator, **W. J. M. Moore.** *Electrical Engineering*, vol. 69, June 1950, pp. 532–37.

1341. Study of the Stability of Speed Control of a Hydroelectric Generator (in French), **G. Nasse.** *Bulletin*, Society Francaise des Electriciens, Series 7, vol. 1, Jan. 1951, pp. 9–37.

1342. Pneumatic Governor Design for High Rotational Speeds, **P. M. Mueller.** *Product Engineering*, vol. 22, Oct. 1951, pp. 170–75. For high speed air turbines.

1343. Praga Speed Governor for Winding Machines Driven by a Three-Phase Motor (in Czech.), **J. Hrusa.** *Elektrotechnicky Obsor*, vol. 40, no. 4, 1951, pp. 63–70.

1344. The Optimum in the Regulation of Hydraulic Turbines (in Italian), **T. Stein.** *Energia Elettrica*, vol. 28, April 1951, pp. 199–210.

1345. Modern Regulation of Turbines (in Swedish), **G. Enskog.** *Teknisk Tidskrift*, vol. 81, April 7, 1941, pp. 269–76.

Power System Regulation

1346. Hydraulic Turbine Governors and Frequency Control. *Report 13*, National Electric Light Association Dec. 1930. Bibliography.

1347. Operating Characteristics of Turbine Governors, **T. E. Purcell, A. P. Hayward.** *AIEE Transactions*, vol. 49, 1930 pp. 715–22.

1348. Mechanics for Hydraulic Turbine Pressure Regulation, **Arnold Pfau.** *Transactions*, American Society of Mechanical Engineers, vol. 52, 1930, pp. HYD 29–53.

1349. Governor Performance During System Disturbances, **R. C. Buell, R. J. Caughey, E. M. Hunter, V. M. Marquis.** *AIEE Transactions*, vol. 50, 1931, pp. 354–69.

1350. Automatic Power Regulation in Electric Networks (in German), **G. Boll.** *Elektrotechnische Zeitschrift*, vol. 52, March 5, 1931, pp. 305–11.

1351. Frequency and Tie Line Load Control, **P. Sporn, V. M. Marquis.** *Electrical World*, vol. 99, 1932, pp. 618–24.

1352. Stability of Combined Velocity and Pressure Regulation for Steam Turbines (in Italian), **P. Cicala.** *Atti dell' Accademia delle Scienze di Torino*, vol. 68, 1933, pp. 326–36.

1353. Stabilization of Network Frequency (in French), **A. Guillet.** *Comptes Rendus*, l'Academie des Sciences, vol. 197, Nov. 27, 1933, pp. 1307–09.

1354. Centrifugal Power-Absorption Generators, **E. C. Wadlow.** *Engineer*, vol. 157, Feb. 9, 1934, pp. 142–43.

1355. Frequency Regulation of Interconnected Systems, **K. N. Reardon.** *Electric Journal*, vol. 31, Dec. 1934, pp. 465–67, 470.

1356. Remote Control of Load and Frequency in High Voltage Systems (in French), **R. Nierenberger.** *Bulletin*, Societe Francaise des Electriciens, vol. 4, Oct. 1934, pp. 999–1040.

1357. Regulation of Back-Pressure Turbines (in German), **H. Ernst.** *Archiv fur Waermewirtschaft*, vol. 16, Oct. 1935, pp. 269–72.

1358. Automatic Voltage and Current Regulation of Mercury Arc Rectifiers by Grid Control, **U. Lamm.** *ASEA Journal*, vol. 12, Nov. 1935, pp. 142–50.

1359. Precision Frequency Control, **J. C. Orkney.** *Electrical Review*, vol. 117, Nov. 15, 1935, pp. 669–70.

1360. Regulation of Power Plant Variables (in German), **J. Kronert.** *Archiv fur technisches Messen*, Aug. 1935, JO60–1.

1361. Automatic Regulation of Frequency and Output (in French), **J. Fallou.** *Bulletin*, Societe Francaise des Electriciens, vol. 6, May 1936, pp. 461–86.

1362. Power Oscillations in the Regulation of Interconnected Systems (in French), **J. Labouret.** *Bulletin*, Societe Francaise des Electriciens, vol. 6, May 1936, pp. 487–500.

1363. Frequency and Power Regulation of Interconnected Systems (in French), **G. Darrieus.** *Bulletin*, Societe Francaise des Electriciens, vol. 6, May 1936, pp. 501–12.

1364. Automatic Control of Power and Frequency, **Y. Hedin.** *ASEA Journal*, vol. 13, March 1936, pp. 43–47.

1365. Frequency Regulation of A-C Networks by Master Clock (in German), **G. August.** *Elektrotechnische Zeitschrift*, vol. 58, Dec. 30, 1937, pp. 1395–98.

1366. Effect of System Regulation on Hydroelectric Installations (in German), **R. Dubs.** *Bulletin*, Association Suisse des Electriciens, vol. 28, Oct. 29, 1937, pp. 532–36, Discussion, pp. 569–74.

1367. Hydroelectric Problems (in German), **F. Hug.** *Bulletin*, Association Suisse des Electriciens, vol. 28, Oct. 29, 1937, pp. 537–45; discussion, pp. 569–74.

1368. Frequency and Load Regulation on Large Systems (in German), **R. Keller.** *Bulletin*, Association Suisse des Electriciens, vol. 28, Oct. 29, 1937, pp. 545–52; discussion, pp. 569–74.

1369. Load Regulators on Interconnected Systems (in German), **H. Wierer.** *Bulletin*, Association Suisse des Electriciens, vol. 28, Oct. 29, 1937, pp. 552–58; discussion, pp. 569–74.

1370. Frequency and Power Control in Interconnected Systems, **G. Darrieus.** *Bulletin*, Association Suisse des Electriciens, vol. 28, Oct. 29, 1937, pp. 525–32; discussion, pp. 569–74.

1371. Automatic Frequency Regulation (in French), **M. Bouffart.** *Paper No. 106*, International Conference on Large Electric High-Tension Systems, 1937.

1372. Mixed Frequency-Power Regulation of Interconnected Systems (in French), **P. Ailleret.** *Paper No. 143*, International Conference on Large Electric High-Tension Systems, 1937.

1373. Combined Regulation of Power and Frequency (in French), **A. Koechlin.** *Revue Generale de l'Electricite*, vol. 43, Feb. 5, 1938, pp. 163–66.

1374. Methods of Regulation and Control for Interconnected Electric Power Systems (in German), **H. Graner.** *Elektrotechnische Zeitschrift*, vol. 60, Nov. 9, 1939, pp. 1269–76.

1375. Progress in Power and Frequency Regulation of Interconnected Systems (in French), **W. Stablein.** *Paper No. 307*, International Conference on Large Electric High-Tension Systems, 1939.

1376. Frequency and Power Regulation in the Paris Region Network. Present State: Centralized Frequency and Power Regulation (in French), **J. Fallou, G. Nasse.** *Paper No. 315*, International Conference on Large Electric High-Tension Systems, 1939.

1377. Voltage Control of Mercury-Arc Rectifiers, **G. R. McDonald.** *AIEE Transactions* (*Electrical Engineering*), vol. 58, Nov. 1939, pp. 563–68.

1378. Regulation of Power as Function of Frequency in Interconnected Networks (in French), **Schimpf.** *Paper No. 336*, International Conference on Large Electric High-Tension Systems, 1939.

1379. Automatic Regulation of Rectifiers (in German), **F. Holters.** *Elektrotechnische Zeitschrift*, vol. 61, June 6, 1940, pp. 519–24.

1380. Experiences in System Speed Regulation, **O. Holden.** *Transactions*, American Society of Mechanical Engineers, vol. 62, April 1940, pp. 237–40.

1381. Compensating Tanks and Regulation Stability of Hydraulic Turbines (in Italian), **M. Mainardis.** *Energia Elettrica*, vol. 17, Feb. 1940, pp. 78–83.

1382. A Method of Measuring and Recording the Frequency Error of Alternating Current Power Supplies, **F. O. Morrell, G. R. Oman.** *Journal*, Institution of Electrical Engineers, vol. 87, Nov. 1940, pp. 507–20.

1383. Regulation of System Load and Frequency, **H. Estrada, H. A. Dryar.** *Transactions*, American Society of Mechanical Engineers, vol. 62, 1940, pp. 221–35.

1384. Load Regulation with Interconnected Power Stations (in French), **J. Mosebach.** *Revue Generale de l'Electricite*, vol. 49, May 1941, pp. 297–312.

1385. An Experiment in the Struggle for Stable Working of the Azenergo System (in Russian), **I. A. Siromiatnikow.** *Elektrischeskie Stantsii*, no. 1, Jan. 1941, pp. 17–20.

1386. Remote Regulation in Large Grid Systems (in German), **R. Keller.** *Bulletin*, Association Suisse des Electriciens, vol. 32, Dec. 31, 1941, pp. 791–96; discussion, pp. 801–08.

1387. Regulation Problems in Large Power Networks (in German), **R. Mokesch.** *Elektrotechnik und Maschinenbau*, vol. 60, 1942, pp. 308–21. Survey of large number of regulators.

1388. Investigation of Dynamic Power Regulation Problems with Synchronous Systems (in German), **K. Boyateff.** *Elektrotechnik und Maschinenbau*, vol. 60, 1942, pp. 547–55.

1389. Control of Tie-Line Power Swings, **C. Concordia, H. S. Shott, C. N. Weygandt.** *AIEE Transactions* (*Electrical Engineering*), vol. 61, June 1942, pp. 306–14.

1390. The Stability of Regulating Reservoirs and of Systems of These (in German), **C. Jaeger.** *Schweizerische Bauzeitung*, vol. 122, 1943, Nov. 20, pp. 255–57; Dec. 11, pp. 297–300; Dec. 18, pp. 314–17; Dec. 25, pp. 323–25.

1391. Regulation of Interconnected Power Stations (in German), **V. Aigner.** *Elektrotechnik und Maschinenbau*, vol. 61, Sept. 17, 1943, pp. 437–49.

1392. Automatic Regulator for Regulating Rectifier-Fed D-C Loads (in German), **O. Kaufman, W. Blankenburg.** *Elektrotechnische Zeitschrift*, vol. 65, Oct. 12, 1944, pp. 323–28.

1393. Time and Frequency Standards on Interconnected Systems, **R. J. Donaldson.** *Electrical World*, vol. 121, March 18, 1944, pp. 78–81.

1394. The Governing of Generating Sets and the Distribution of the Load in Interconnected Systems, **G. Broggi.** *Brown Boveri Review*, vol. 31, Aug. 1944, pp. 243–51.

1395. Frequency-Power Regulation of Power Transfer (in German), **D. Gaden, R. Keller.** *Bulletin*, Association Suisse des Electriciens, vol. 35, June 28, 1944, pp. 333–49.

1396. System Application of Phase and Voltage Regulators, **A. A. Johnson.** *Electrical World*, vol. 124, July 7, 1945, pp. 104–07.

1397. Automatic Load Control for Turbine Generators, **F. E. Crever, R. L. Jackson.** *AIEE Transactions* (*Electrical Engineering*), vol. 64, Sept. 1945, pp. 656–60.

1398. Automatic Load and Frequency Control in Northwest Power Pool, **S. B. Smith, M. L. Blair.** *Electrical World*, vol. 124, Dec. 22, 1945, pp. 56–60.

1399. Speed and Load Control on Interconnected Systems, **E. E. George.** *Electrical World*, vol. 123, March 17, 1945, pp. 84, 85.

1400. Control of Load, Frequency, and Time of Interconnected Systems, **C. K. Duff.** *AIEE Transactions* (*Electrical Engineering*), vol. 64, Nov. 1945, pp. 778–86.

1401. Power-Frequency Regulation Recording Apparatus (in French), **E. Soloveicik.** *Bulletin*, Association Suisse des Electriciens, vol. 36, Jan. 10, 1945, pp. 11–15.

1402. Simplified Primary Power Regulation (in German), **T. Stein.** *Bulletin*, Association Suisse des Electriciens, vol. 37, Feb. 9, 1946, pp. 76–81.

1403. Stability of Interconnected Hydro-Electric Groups Allowing for Inertia of Water in the Pressure Pipes (in French), **P. Almeras.** *Annales de l'Universite de Grenoble*, vol. 22, 1946, pp. 105–13.

1404. Power System Frequency Control: The Application of Automatic Supplementary Control of Prime Movers, **H. C. Alger.** *Journal*, Institution of Engineers, Australia, vol. 18, Oct.-Nov. 1946, pp. 214–24.

1405. Frequency-Output Regulation for Tie-Line Control Applied to an Important Network (in French), **D. Gaden.** *Report No. 319*, International Conference on Large Electric High-Tension Systems, 1946.

1406. Interconnected Power System Automatic Load and Frequency Control, **R. E. Pierce.** *Report No. 324*, International Conference on Large Electric High-Tension Systems, 1946.

1407. Improvements in Methods of Regulation and Distribution of Loads, **B. Nasse.** *Report No. 329*, International Conference on Large Electric High-Tension Systems, 1946.

1408. Experimental Investigations of the Stability of Governing of Hydroelectric Groups with Pressure Drop and Surge Tank (in Italian), **Augusto Ghetti.** *Energia Elettrica*, vol. 28, Nov. 1951, pp. 619–39, vol. 24, Nov.-Dec. 1947, pp. 542–51.

1409. The Stability of Adducing-Generating Systems of Hydro-Electric Plants Studied by the Leonhard Criterion (in Italian), **Filippo Arredi.** *Energia Elettrica*, vol. 24, Nov.-Dec. 1947, pp. 559–66.

1410. On the Stability of Oscillations in Hydroelectric Plants Provided with a Combined System of Conduit and of Surge Tank (in Italian), **Augusto Ghetti.** *Energia Elettrica*, vol. 24, Nov.-Dec. 1947, pp. 567–78.

1411. Theoretical Approach to Speed and Tie Line Control, **Robert Brandt.** *AIEE Transactions*, vol. 66, 1947, pp. 24–30.

1412. Hydraulic-Turbine Regulators and Frequency Regulation (in Swedish), **C. E. Soderbaum.** *Teknisk Tidskrift*, vol. 77, Feb. 1, 1947, pp. 113–18.

1413. The Stability of Interconnected Waterwheel Alternators Taking into Account the Inertia of the Water (in French), **P. Almeras.** *Revue Generale de l'Electricite*, vol. 56, Jan. 1947, pp. 47–50.

1414. The Escher-Wyss Power Regulator (in German), **M. Hirt, F. Seeberger.** *Bulletin*, Association Suisse des Electriciens, vol. 39, Oct. 30, 1948, pp. 731–38.

1415. Preliminary Considerations of System-Wide Load Division by Means of Accurate Time Control, **T. E. Curtis, W. M. Pickslay.** *AIEE Transactions*, vol. 67, pt. II, 1948, pp. 1562–70.

1416. Simultaneous Frequency and Voltage Regulation on Generator Groups. Effect on Regulation of Power Station Turbine Demands on the Water Course, **R. Keller.** *Report No. 324*, International Conference on Large Electric High-Tension Systems, 1948.

1417. Continuous Load-Frequency Control for Interconnected Power Systems, **H. M. Dimond, G. S. Lunge.** *AIEE Transactions*, vol. 67, 1948, pp. 1483–90.

1418. Steady-State Stability of Synchronous Machines as Affected by Angle-Regulator Characteristics, **C. Concordia.** *AIEE Transactions*, vol. 67, pt. I, 1948, pp. 687–90.

1419. The Stability of Frequency of A-C Systems Connected by a D-C Transmission Line, **F. Busemann.** *Reports*, British Electrical and Allied Industries Research Association, Ref. Z/-T75, 1948.

1420. Modern Methods of Control of the Frequency and Exchange Power Flow in Supply Systems (in Russian), **I. M. Markovich, V. I. Gorushkin.** *Isvestiya Akademii Nauk, SSSR.* Otdelenie Tekhnicheskikh Nauk, no. 2, Feb. 1949, pp. 211–21.

1421. A New Automatic Load Control for Turbine Generators, **H. B. Ruud, S. B. Farnham.** *AIEE Transactions*, vol. 68, pt. II, 1949, pp. 1337–42.

1422. Dynamic Behavior of Rectifier-Inverter Control in D-C Transmission (in German), **A. Leonard.** *Archiv fur Elektrotechnik*, vol. 39, 1950, pp. 561–71.

1423. Considerations on the Problem of Frequency-Power Regulation in Interconnected Networks (in Italian), **A. Giacomoni.** *Energia Elettrica*, vol. 27, July 1950, pp. 424–30.

1424. Stabilization of the Oscillations in Surge Tanks by Means of Temporary Adjustment of Electric Power (in Italian), **A. Gallico.** *Energia Elettrica*, vol. 27, Nov.-Dec. 1950, pp. 725–29.

1425. Automatic Control of Time and Load Division Among Generating Stations in Interconnected Systems, **I. Obradovic.** *Paper No. 334*, International Conference on Large Electric High-Tension Systems, 1950.

1426. Control of Power Flow on Interconnected Systems, **N. Cohn.** *Proceedings*, Midwest Power Conference, vol. 12, 1950, pp. 159–75.

1427. Frequency Regulation of the Swedish Interconnected Power Network (in Swedish), **B. Lof, E. Brodersen.** *Teknisk Tidskrift*, vol. 80, Aug. 5, 1950, pp. 647–57.

1428. Determination of the Moment of Inertia of a Hydro-Electric Set (in French), **M. Cuenod.** *Houille Blanche*, vol. 6, March-April 1951, pp. 132–46.

1429. The Regulation of Electrical Networks. Assistance in Maintenance of Frequency and Voltage Rendered by the Measurement of Interchanged Energy (in French), **M. Cuenod.** *Bulletin*, Association Suisse des Electriciens, vol. 42, Feb. 10, 1951, pp. 86–90.

1430. Stability of a Combined System of Interconnected Hydroelectric Power Stations (in French), **F. Burlando.** *Revue Generale de l'Electricite*, vol. 60, June 1951, pp. 235–43.

1431. Regulation of D-C Transmission (in Russian), **S. R. Buachidze.** *Elektrichestvo*, no. 5, May 1951, pp. 3–8.

1432. Some Hydraulic Stability Problems in Hydroelectric Stations (in Italian), **G. Evangelisti.** *Elettrotecnica*, vol. 38, July 1951, pp. 298–305.

1433. Stabilization of Frequency in the Austrian Interconnected Network (in German), **F. Karlic.** *Oesterreichische Zeitschrift fur Elektrisitaetswirtschaft*, vol. 4, May 1951, pp. 141–48.

Boiler and Combustion Control

1434. Automatic Regulation of Boiler Furnaces (in German), **H. Treitel.** *Archiv fur Warmewirtschaft*, vol. 9, Aug. 1928, pp. 249–55.

1435. Automatic Combustion Control for Boiler furnaces. *Power Engineer*, vol. 23, 1928; April, pp. 126–29; May, pp. 167–71; July, pp. 263–68; Aug., pp. 315–21; Sept., pp. 356–61; Oct., pp. 393–98; Dec., pp. 459–63.

1436. Automatic Boiler Regulators in Power Plants (in German), **J. Hak.** *Elektrotechnische Zeitschrift*, vol. 49, Jan. 26, 1928, pp. 129–33.

1437. Automatic Combustion Control for Boiler Furnaces. *Power Engineer*, vol. 24, Feb. 1929, pp. 68–71.

1438. Automatic Control of Boiler Operation (in German), **H. Balcke.** *Brennstoff und Warmewirtschaft*, vol. 11, 1929, March-April, pp. 81–86, 100-05, 113–17.

1439. Electric Boiler Regulators (in German), **F. Engel, A. G. S. Sandison.** *Waerme*, vol. 52, July 13, 1929, pp. 533–37.

1440. Installation and Operating Results of Siemen's Boiler Control (in German), **M. Moeller.** *Siemens Zeitschrift*, vol. 9, Aug. 1929, pp. 457–63.

1441. Electrical Equipment for Automatic Boiler Regulation (in German), **M. Moeller.** *Siemens Zeitschrift*, vol. 9, 1929, pp. 408–15.

1442. Automatic Combustion Control for Boiler Furnaces, **G. R. Bamber.** *Proceedings*, Institution of Mechanical Engineers, vol. 117, 1929, pt. II, pp. 1099–113.

1443. Automatic Boiler Control, **A. G. S. Sandison.** *Electrical Times*, vol. 79, June 18, 1931, pp. 1097–101. A survey.

1444. Automatic Combustion Control for Boilers, **S. J. Clifton.** *Journal*, Junior Institution of Engineers, vol. 42, Dec. 1931, pp. 127–68.

1445. Simplified Automatic Combustion Control at Powerton Station. *Power*, vol. 75, Sept. 1, 1931, pp. 314–17.

1446. Boiler House Drives from the Standpoint of Automatic Boiler Control (in German), **P. Kaufmann.** *Warme*, vol. 54, Jan. 3, 1931, pp. 1–6.

1447. Automatic Combustion Control, **C. H. Sanderson, E. B. Ricketts.** *AIEE Transactions*, vol. 50, 1931, pp. 1378–87.

1448. The Kent System of Automatic Boiler Control. *Engineering*, vol. 134, Aug. 5, 1932, pp. 148–51.

1449. Steam Generation Control. *Electrical Review*, vol. 111, Dec. 2, 1932, p. 815.

1450. Automatic Combustion Control. *Power*, vol. 77, April 1933, pp. 202–04.

1451. Automatic Regulation of Combustion in Gas Generating Ovens (in German), **G. Alliata.** *Gas- und Wasserfach*, vol. 76, Sept. 30, 1933, pp. 722–25.

1452. Theory of Heating System Regulators (in German), **M. Lang.** *Gesundheits-Ingenieur*, vol. 55, 1933, Nov. 11, pp. 529–32; Nov. 18, pp. 542–45.

1453. Automatic Operation of Electric Boilers, **M. Eaton.** *Engineering Journal*, vol. 16, May 1933, pp. 201–09.

1454. Automatic Electrical Regulation of Steam Boilers (in German), **C. Himmler.** *Wissenschaftliche Veroeffentlichungen aus dem Siemens-Konsern*, vol. 12, no. 2, 1933, pp. 110–26.

1455. Investigation of the Stability of Regulators for Steam Heating Boilers (in German), **M. Lang.** *Gesundheits-Ingenieur*, vol. 57, May 12, 1934, pp. 233–37.

1456. Condensation of Super-Heated Steam as an Oscillatory Problem (in German), **M. Lang.** *Forschung auf dem Gebiete des Ingenieurwesens*, Ausgabe B, vol. 5, Sept.-Oct. 1934, pp. 212–17.

1457. Control and Regulation of Boilers (in French), **J. Vivie.** *Chaleur et Industrie*, vol. 15, April 1934, pp. 819–55.

1458. Fuel Fired Furnace Temperature and Atmosphere Control, **G. H. Barker.** *Metallurgia*, vol. 11, Dec. 1934, pp. 29–32.

1459. Development of Automatic Combustion Control Systems for Industrial and Power Station Boilers, **J. L. Hodgson, L. L. Robinson.** *Proceedings*, Institution of Mechanical Engineers, vol. 126, 1934, pp. 59–169.

1460. Control of Forced-Circulation Steam Generators (in German), **M. Lang.** *Archiv fur Waermewirtschaft*, vol. 16, Nov. 1935, pp. 295–97.

1461. Combustion Control. *Power Plant Engineering*, vol. 39, 1935; Feb., pp. 93–96; March, pp. 162–64, 167; April, pp. 217–18; May, pp. 277–79; June, pp. 328–30; July, pp. 388–89; Aug., pp. 448–49; Sept., pp. 518–20; Oct., pp. 574–76; Nov., pp. 617–20; Dec., pp. 668–71, 680.

1462. Automatic Control in Open Hearth Steel Melting Furnaces, **A. J. Boynton, H. A. Brassert.** *Iron and Steel Engineer*, vol. 13, Jan. 1936, pp. 25–26.

1463. Industrial Boiler and Steam Control, **J. W. Fidoe.** *Engineer and Boiler House Review*, vol. 50, 1936; July, pp. 46, 48, 50; Sept., pp. 184, 186, 188; Nov., p. 330.

1464. Feed-Water Regulation, **V. Walker.** *Electrical Review*, vol. 118, March 20, 1936, p. 421.

1465. Principles of Regulation for Forced-Flow Boilers (in German), **M. Lang.** *Archiv fur Waermewirtschaft und Dampfkesselwesen*, vol. 17, July 1937, pp. 191–94.

1466. Automatic Regulator for Steam Boilers Designed by All-Union Electrotechnical Institute (in Russian), **L. S. Goldfarb.** *Avtomatika i Telemkhanika*, no. 2, 1938, pp. 69–86.

1467. Automatic Control for Modern Boiler Plant. *Engineering and Boiler House Review*, vol. 51, 1938, Jan., pp. 440–42; Feb., pp. 522–25, March, pp. 594–97; April, pp. 665–67; May, pp. 741–44; June, pp. 807–09; vol. 52, 1938, July, pp. 34, 36, 38, 40; Aug., pp. 79–83; Sept., pp. 141–45; Nov., pp. 289–91.

1468. Power Plant Control, **S. J. Clifton.** *Journal*, Junior Institution of Engineers, vol. 50, Sept. 1940, pp. 323–51.

1469. Automatic Control for Land and Marine Boilers, **J. E. O'Breen.** *Transactions*, Institution of Engineers and Shipbuilders in Scotland, vol. 84, pt. 2, 1940, pp. 80–112.

1470. Electroflo System of Automatic Boiler Control. *Power and Works Engineer*, vol. 35, Feb. 1940, pp. 40–45; Mar., pp. 66–69.

1471. Combustion Control for Multi-Fuel Furnaces. *Blast Furnace and Steel Plant*, vol. 29, Feb. 1941, pp. 189–92.

1472. Control of Flue Gas Flow, **F. Alton.** *Engineering and Boiler House Review*, vol. 56, Nov. 1942, pp. 198–203.

1473. Electric Control for Steam Boilers on Diesel-Electric and Straight Electric Locomotives, **E. H. Burgess.** *AIEE Transactions* (*Electrical Engineering*), vol. 61, Aug. 1942, pp. 604–06.

1474. Automatic Boiler Regulation (in French), **L. Bernard.** *Revue Generale de l'Electricite*, vol. 51, May 1942, pp. 269–75. Review of current practice.

1475. Scientific Control of Combustion, **J. W. Young.** *Mining Electrical and Mechanical Engineer*, vol. 24, Dec. 1943, pp. 213–22.

1476. Electronic Circuits Actuate Automatic Combustion Control, **K. D. Knoblock.** *Electrical World*, vol. 120, Oct. 2, 1943, pp. 60–62.

1477. Boiler-House Measurement and Control for Efficient Fuel Utilization, **G. H. Barker, A. L. Hancock.** *Journal*, Institution of Electrical Engineers, vol. 90, pt. 2, 1943, pp. 217–32.

1478. Boiler Feed-Water Regulation, **H. Hillier.** *Transactions*, Institute of Marine Engineers, vol. 56, June 1944, pp. 59–82.

1479. Hard-Working Boilers Demand Responsive Feedwater Control. *Power*, vol. 88, May 1944, pp. 306–09, 349b, c, 350a, b.

1480. Unified Boiler Control System, **W. Szwander.** *Metropolitan-Vickers Gazette*, vol. 21, Jan. 1945, pp. 23–32.

1481. Automatic Boiler Control, **E. Howlett.** *Mechanical World*, vol. 119, Feb. 22, 1945, pp. 199–201.

1482. Automatic Boiler Control System, **S. G. Gerasimov.** *Engineers' Digest*, vol. 3, Aug. 1946, pp. 385–88.

1483. Unified Boiler Control, **W. Szwander.** *Electrical Review*, vol. 138, 1946, Feb. 8, pp. 217–21; Feb. 15, pp. 253–57.

1484. Boiler Control, **P. S. Dickey.** *Instruments*, vol. 19, June 1946, pp. 334–38.

1485. Automatic Control Applied to Modern High-Pressure Boilers, **L. Young.** *Journal*, Institution of Electrical Engineers, vol. 94, pt. 2A, 1947, pp. 66–78.

1486. Automatic Operation of Electric Boilers, **M. Eaton.** *AIEE Transactions*, vol. 66, 1947, pp. 1061–69.

1487. Regulation Theory for Thermal Power Plants Employing a Closed Gas Cycle, **F. Salzmann.** *Transactions*, American Society of Mechanical Engineers, vol. 69, May 1947, pp. 329–35.

1488. Application of Conventional Industrial Instruments to Power Plant Control, **W. H. Fortney.** *Instruments*, Vol. 20, Dec. 1947, pp. 1149–54.

1489. Combustion Control, **B. G. A. Skrotzki.** *Power*, vol. 93, Dec. 1949, pp. 71–106.

1490. Experimental Application of Combustion Controls to a Process Heater, **W. E. Boyle, P. R. Hoyt.** *Instruments*, vol. 22, June 1949, pp. 529–32.

1491. Electronic Loading for Boiler Control, **C. H. Smoot, Jr.** *Proceedings*, Midwest Power Conference, vol. 12, 1950, pp. 251–57.

1492. Measurement and Control in the Utilization of Mixed Fuels and Oxygen in Open Hearth Furnaces, **M. J. Conway, E. H. Cauger.** *Instruments*, vol. 24, Sept. 1951, pp. 1028–34.

1493. The Technique of Electrical Boiler Control (in German), **G. Schroeder.** *Siemens Zeitschrift*, vol. 25, Sept. 1951, pp. 192–98.

1494. Power Plant Controls, **B. F. Heye.** *Instruments*, vol. 24, Jan. 1951, pp. 38–41. A survey.

Industrial Drives

1495. Automatic Electrode Regulation for 3-Phase Arc Furnaces, **K. E. Kjolseth.** *General Electric Review*, vol. 37, June 1934, pp. 301–03.

1496. Electrical Control of Paper Making Machinery, **W. J. Mason.** *GEC Journal*, vol. 8, Nov. 1937, pp. 302–08.

1497. Photoelectric Weft-Straightener Control, **C. W. LaPierre, A. P. Mansfield.** *AIEE Transactions* (*Electrical Engineering*), vol. 57, Sept. 1938, pp. 513–19.

1498. Unit Sectional Drive of a Large Paper Machine, **W. J. Mason.** *GEC Journal*, vol. 9, May 1938, pp. 96–105.

1499. The Adoption of Regulating Drives in Industry (in German), **W. Schlotmann.** *Elektrotechnik und Maschinenbau*, vol. 57, Nov. 24, 1939, pp. 557–67.

1500. Electric Feeler Contact Control of Milling Machines (in German), **P. Volk.** *Werkstattstechnik und Werksleiter*, vol. 33, July 15, 1939, pp. 353–57.

1501. Feeler Controlled Copying Milling Machine (in German), **H. Doring.** *Elektrotechnik und Maschinenbau*, vol. 58, June 21, 1940, pp. 269–74.

1502. Automatic Regulation of Electric Arc Furnaces (in French), **A. Clergeot.** *Revue Generale de l'Electricite*, vol. 47, Feb. 17–24, 1940, pp. 115–22.

1503. Feeler-Controlled Machine Tools (in German), **W. Wolfram.** *Verein deutscher Ingenieure Zeitschrift*, vol. 84, Aug. 31, 1940, pp. 639–42.

1504. A Method for the Control of Electric Arc Furnaces, **T. B. Montgomery.** *Blast Furnace and Steel Plant*, vol. 30, Aug. 1942, pp. 861–68.

1505. Control Method for Electric Arc Furnaces, **T. B. Montgomery.** *Steel*, vol. 111, Sept. 14, 1942, pp. 145–50, 174.

1506. Arc Furnace Control by Regulex Exciters, **T. B. Montgomery, T. H. Bloodworth.** *AIEE Transactions* (*Electrical Engineering*), vol. 62, Oct. 1943, pp. 650–54.

1507. Rotating Regulator for Arc Furnaces, **R. A. Geiselman, C. C. Levy, W. R. Harris.** *AIEE Transactions* (*Electrical Engineering*), vol. 62, Nov. 1943, pp. 671–74.

1508. What the Amplidyne has Contributed to Reversing-Mill Drives, **C. B. Huston,** *Blast Furnace and Steel Plant*, vol. 31, June 1943, pp. 654–58.

1509. Amplidyne Control for Adjustable-Voltage Drives, **C. B. Huston.** *Iron and Steel Engineer*, vol. 20, July 1943, pp. 44–8.

1510. Evaluation of Electric Arc Melting Furnaces, **W. H. Payne.** *Steel*, vol. 113, Dec. 6, 1943, pp. 124–26; Dec. 13, 1943, pp. 139, 140, 148, 150.

1511. Regulation in Automatically Changed Steps. New Regulator for Coilers with Large Speed Range (in German), **B. Drescher.** *Elektrotechnik und Maschinenbau*, vol. 61, June 25, 1943, pp. 292–98. "Fine" and "course" tension control by means of a dancer roll.

1512. On Electric Controls of Large Rolling Mills (in Italian), **V. Serrato.** *Elettrotecnica*, vol. 30, April 10, 1943, pp. 137–44.

1513. Special Systems of Regulation for Continuous Mills in Steel Works, **M. Rosset.** *Brown Boveri Review*, vol. 30, Nov.-Dec. 1943, pp. 324–27.

1514. Templet-Guided Machine Tools, Their Action and Practical Application (in German), **H. Doring.** *Elektrotechnik und Maschinenbau*, vol. 62, June 23, 1944, pp. 293–308.

1515. The Application of Electronic Devices in the Mechanical Field-Control and Regulation of Motor Drives. *Machinery*, Sept. 9, 1944, pp. 292–98.

1516. Electronic Regulator for Arc Furnaces, **J. E. Reilly, C. E. Valentine.** *AIEE Transactions* (*Electrical Engineering*), vol. 63, Aug. 1944, pp. 601–04.

1517. Oerlikon Control with Load-Balance Regulation for Printing Machine Drives, **A. Ochsner.** *Bulletin Oerlikon*, vol. 24 no. 248, 1944, pp. 1589–95.

1518. The Electric Centre-Driven Winder in the Paper Industry, **R. Schnitzer,** *Brown Boveri Review*, vol. 31, March 1944, pp. 113–18.

1519. The Application of "Robots" to Steel-Making Processes, **F. Mohler.** *Iron and Steel Engineer*, vol. 21, Feb. 1944, pp. 47–57.

1520. Electronic Drives on Winding Reels for Metal Strip, **J. H. Hopper.** *Steel*, vol. 116, May 28, 1945, pp. 132, 135.

1521. Control of Electric-Arc Furnaces, **H. G. Frostick.** *Westinghouse Engineer*, vol. 5, Nov. 1945, pp. 188–91. Describes the balanced beam, rotating, and electronic regulators for electrode control.

1522. Electronics Assures Accurate Loop Control, **L. U. C. Kelling.** *Machine Design*, vol. 17, April 1945, pp. 143–46, 172, 174.

1523. Rolling Mill Tension. *Electrical Review*, vol. 137, Nov. 16, 1945, p. 725.

1524. Arc Furnace Regulators, **R. A. Geiselman, J. E. Reilly.** *Steel*, vol. 116, March 19, 1945, pp. 136, 139, 170, 172.

1525. Continuous Control of Automatic Electric Drives (in Russian), **V. Popov.** *Elektrichestvo*, no. 8, Aug. 1945, pp. 25–7. Contrasts the continuous type of regulation with the two-position or relay type.

1526. Machine-Tool Contour Controller, **J. M. Morgan.** *Electronics*, vol. 19, Oct. 1946, pp. 92–6.

1527. Simultaneous Operation of Automatic Regulators for 3-Phase Electric Furnaces for Steel Melting (in Russian), **I. E. Efroimovich.** *Elektrichestvo*, no. 5, 1946, pp. 62–5.

1528. Automatic Regulation of Three-Phase Electric Arc Furnace (in Russian), **C. I. Telnui** *Elektrichestvo*, no. 5, 1946, pp. 53–61.

1529. Photo-Electric Control for Color Printing, **J. Robins, L. E. Varden.** *Electronics*, vol. 19, June 1946, pp. 110–15.

1530. An Electronic Drive for Windup Reels, **K. P. Puchlowski.** *AIEE Transactions* (*Electrical Engineering*), vol. 65, Aug.-Sept. 1946, pp. 585–91.

1531. Electronic Control of Cloth-Drying Machinery, **N. H. Chamberlain.** *Journal*, Textile Institute, vol. 37, July 1946, pp. 249–62.

1532. Control Developments for Modern Arc Furnace, **W. N. Gittings.** *Steel*, vol. 118, March 4, 1946, pp. 146–48, 186, 188, 190, 192, 194.

1533. Electronic Control of Cloth Guiders on Tentering Machines. *Textile Recorder*, vol. 63, April 1946, pp. 36–7.

1534. Variable Voltage Drives for Blooming Mill Tables and Feed Rolls, **Z. W. Whitehouse, A. F. Kenyon.** *Steel*, vol. 119, Dec. 30, 1946, pp. 82–4, 96.

1535. Structure and Characteristics of Modern Automatic D-C Drive Installations (in Russian), **A. A. Bulgakov.** *Elektrichestvo*, no. 4, 1947, pp. 14–21. A survey.

1536. Generalized Dynamic Theory of an Automatic Electric Drive (in Russian), **V. K. Popov.** *Elektrichestvo*, no. 4, 1947, pp. 55–62.

1537. A New Grinding Circuit Feed Regulator, **J. N. Jones.** *AIEE Transactions*, vol. 66, 1947, pp. 1240–42.

1538. Sectional Paper Machine Output Increased with Electronic Regulator, **Y. B. Baker.** *Paper Industry and Paper World*, vol. 29, Oct. 1947, pp. 987–91, 994.

1539. Electronic Speed Control of A-C Commutator Motors, **E. W. Forster, L. C. Ludbrook.** *Engineer*, vol. 184, July 18, 1947, pp. 61–2.

1540. Paper Machine Drives, **H. W. Rogers.** *Electrical Engineering*, vol. 66, Nov. 1947, pp. 1082–88.

1541. An Automatic Arc-Current Regulator, **E. V. Potter, A. Scott.** *Review of Scientific Instruments*, vol. 18, Oct. 1947, pp. 722–26.

1542. The Brown Boveri Automatic Electrohydraulic Electrode Regulation for Electric Furnaces, **P. Schlemker.** *Brown Boveri Review*, vol. 34, April-May 1947, pp. 75–80.

1543. Electric Positioning Systems of High Accuracy for Industrial Use, **D. E. Garr.** *General Electric Review*, vol. 50, July 1947, pp. 17–24.

1544. Electric Sectional Drive. *Engineer*, vol. 183, May 23, 1947, pp. 448–49.

1545. Electric Apparatus for Three-Phase Arc-Furnaces, **N. R. Stansel, A. R. Oltrogge.** *Transactions*, Electrochemical Society, vol. 91, 1947, pp. 363–74.

1546. Constant Tension Reel Drives, **E. S. Murrah.** *Blast Furnace and Steel Plant*, vol. 35, Feb. 1947, pp. 205–14.

1547. Electric Drives for Textile Finishing Ranges, **R. B. Moore, H. C. Uhl.** *AIEE Transactions*, vol. 66, 1947, pp. 684–94.

1548. Problem of Pressure Adjustment on Large Reversing Rolling Mills. An Application of the Amplidyne (in French), **H. Mathiot.** *Revue Alsthom*, April-May-June, 1947, pp. 16–31.

1549. Electrical Control of Tension in the Paper Industry, **G. E. Shaad.** *Paper Industry and Paper World*, vol. 29, Nov. 1947, pp. 1138–47.

1550. Theory of Non-Stationary Processes in Electric Installations with an Elastic Drive (in Russian), **D. P. Morozov.** *Electrichestvo*, no. 4, 1947, pp. 37–47. Drive for cold rolling mill.

1551. Field Weakening with Simultaneous Generator Voltage Increase in the Ward Leonard System (in Russian), **V. P. Nikitin, N. P. Kunitski.** *Doklady Akademii Nauk, SSSR*, vol. 60, 1948, pp. 1339–41.

1552. Calculation of the Reversal Process in Ward-Leonard Drives, Using Three-Field Exciters (in Russian), **M. I. Knigin.** *Elektrichestvo*, no. 9, Sept. 1948, pp. 36–40.

1553. On the Problem of the Static Calculation of Regulating Systems for Electric Drive of Winding Rollers of Cold Rolling Mills (in Russian), **M. E. Goldental.** *Vestnik Elektropromyishlennosti*, no. 12, Dec. 1948, pp. 1–7. Analysis of the constant current control of reel motor with an amplidyne.

1554. Electronic and Servo Electronic Controls and Their Application to the Iron and Steel Industry, **W. G. Thompson.** *Journal*, Iron and Steel Institute, vol. 158, April 1948, pp. 497–509.

1555. Modern Electric Equipment for Cold-Strip Reduction Mills, **W. E. Miller.** *General Electric Review*, vol. 51, March 1948, pp. 22–9.

1556. Servo-Control of a Testing Machine, **H. C. Roberts, H. W. Katz.** *Radio-Electronic Engineering*, vol. 10, May 1948, pp. 6–9, 29.

1557. Transition Processes in Electric Drives of Leonard Type with Amplidyne (in Russian), **K. S. Bobov.** *Electrichestvo*, no. 4, 1948, pp. 48–54.

1558. Paper Rewinding Machines with Regenerative Braking, **R. Cardell.** *ASEA Journal*, vol. 21, Sept. 1948, pp. 99–102.

1559. New High-Speed Rod Mill Utilizes Electronic Speed Regulation, **G. M. Harvey, D. M. Allison.** *Steel*, vol. 123, Dec. 6, 1948, pp. 134, 136, 138.

1560. Drives for Automatic Speed and Tension Control in Wire Processing Equipment, **N. J. Ranney.** *Wire and Wire Products*, vol. 23, Aug. 1948, pp. 676–79, 700–02; Sept. 1948, pp. 763–68, 802, 803.

1561. Maximum Current Peak of a Shunt Motor on Weakening of its Field (in Russian), **V. P. Nikitin, N. P. Kunitskii.** *Elektrichestvo*, no. 11, Nov. 1948, pp. 53–5.

1562. Fundamental Principles of Automatic Control of an Electromechanical D-C System (in Russian), **B. P. Petrov.** *Elektrichestvo*, no. 5, May 1949, pp. 3–8.

1563. Electric Equipment for Wire Winders, **J. A. Roby, H. R. Lloyd.** *Wire and Wire Products*, vol. 24, March 1949, pp. 231–34; April 1949, pp. 320–27, 363.

1564. Automatic Control of Tension, Speed and Position in Handling Metal Strip, **J. H. Hopper.** *Blast Furnace and Steel Plant*, vol. 37, March 1949, pp. 317–22, 386.

1565. Automatic Electrode Regulation by Means of Direct-Current Chokes (in German), **W. Blankenburg.** *Elektrotechnik*, vol. 3, Jan. 1949, pp. 11–15.

1566. High - Speed Electro - Hydraulic Arc Furnace Control, **A. Garde.** *ASEA Journal*, vol. 22, Jan.-Feb. 1949, pp. 3–9.

1567. Investigation into a System of Regulation and Control of a Reversible Rolling Mill Motor Using Metadynes (in Russian), **M. V. Meerov.** *Elektrichestvo*, no. 7, July 1949, pp. 16–24.

1568. Electric Drive of Cold-Strip Mills, **F. Landau.** *ASEA Journal*, vol. 22, May-June 1949, pp. 69–97.

1569. Theory of the Transient Processes in an Electric Drive Elastically Coupled with a Variable Radius of Tension (in Russian), **D. P. Morozov, N. N. Druzhinin.** *Elektrichestvo*, no. 11, Nov. 1949, pp. 20–25.

1570. Metadyne Generator in Service of Industry, **A. A. L. Bentall.** *Metropolitan-Vickers Gazette*, vol. 23, April-May 1949, pp. 54–68.

1571. Electrical Equipment used in Cold Rolling of Thin Steel Sheets (in French), **M. J. Delastre.** *Bulletin*, Societe Francaise des Electriciens, vol. 9, March 1949, pp. 138–47.

1572. Problems in Speeding-Up Strip Mills, **F. Mohler.** *Iron and Steel Engineer*, vol. 26, Dec. 1949, pp. 92–98.

1573. On the Possibility of Compounding the Driven Motor in a Reversible Ward-Leonard System (in Russian), **S. Z. Barskii.** *Vestnik Elektropromyishlennosti*, vol. 20, July 1949, pp. 6–11.

1574. Calculation of Shunt Rheostats for D-C Motors by Taking Into Account the Dynamics of the (regulation) Process (in Russian), **N. P. Kunitskii.** *Isvestiya Academii Nauk, SSSR*, Otdelenie Technicheskikh Nauk, no. 3, 1949, pp. 396–406.

1575. The Servo Electronic Control of a Large Planer, **S. H. Dale.** *GEC Journal*, vol. 16, Jan. 1949, pp. 52–60.

1576. Transient Processes in Some Electrical Transmissions with Elastic Couplings (in Russian), **A. Ya. Lerner.** *Isvestiya Academii Nauk, SSSR.* Otdelenie Tekhnicheskikh Nauk, no. 2, 1950, pp. 187–98.

1577. Automatic Control, by Amplidyne, of a Hoist at the La Mouriere Mines (in French), **R. Castel, M. Jeannin.** *Revue de l'Electricite et de Mecanique*, no. 81, April-May-June 1950, pp. 15–30.

1578. Mechanical Characteristics of the Motor of a Generator-Motor Unit with Feedback (in Russian), **V. G. Sozonov.** *Elektrichestvo*, no. 12, Dec. 1950, pp. 21–24.

1579. Amplidyne Electrode Control for Arc Furnaces, **F. D. Gunton, W. Spence.** *BTH Activities*, vol. 21, May-June 1950, pp. 88–94.

1580. Electrode Control and Associated Operating Mechanisms, **E. A. Hanff.** *AIEE Transactions*, vol. 69, pt. 1, 1950, pp. 567–70.

1581. Amplidyne Regulators for Steel Melting Furnaces of the Arc Type (in Russian), **A. M. Vainberg.** *Elektrichestvo*, no. 3, March 1950, pp. 65–69.

1582. Automatic Regulation of the Electric Arc (in Russian), **M. E. Belyaev.** *Elektrichestvo*, no. 12, Dec. 1950, pp. 37–41.

1583. Amplidyne-Controlled Log Carriage Drive, **W. D. Vincent.** *AIEE Transactions*, vol. 69, pt. II, 1950, pp. 1124–29.

1584. Analysis of Electric Drives with a Falling Characteristic (in Russian), **S. Z. Barskii.** *Elektrichestvo*, no. 5, May 1950, pp. 35–43. Analysis of adjustable voltage drives which incorporate devices to limit current, voltage, speed, acceleration, or power.

1585. Electric Equipment for High Speed 2-Stand Temper Pass Mills, **R. E. Marrs.** *Iron and Steel Engineer*, vol. 27, June 1950, pp. 95–99.

1586. Electric Equipment for Rolling Cold Strip at 70 Mph, **W. E. Miller.** *Iron and Steel Engineer*, vol. 27, Jan. 1950, pp. 119–28.

1587. Electrical Drive for 56-in. Five Stand Tandem Cold Reduction Mill. **R. A. Harvie.** *Iron and Steel Engineer*, vol. 27, Aug. 1950, pp. 43–50.

1588. Theory and Method of Calculation of a Motor-Generator System with Booster Regulation (in Russian), **V. P. Bychkov.** *Elektrichestvo*, no. 2, Feb. 1950, pp. 33–39. Adjustable voltage speed regulating systems with speed ranges of 100 to 1.

1589. Transient Processes of a Separately Excited Motor When Flux and Voltage Vary (in Russian), **V. P. Bychkov.** *Elektrichestvo*, no. 3, March 1950, pp. 44–46.

1590. The Energy Conditions of the Transient Processes of D-C Motors (in Russian), **D. P. Morozov.** *Elektrichestvo*, no. 7, July 1950, pp. 38–44.

1591. Rotary-Electronic Power Regulator for Defibering Equipment (in Russian), **V. D. Baryshnikov, G. M. Levin.** *Promyshlennaya Energetika*, no. 5, May 1950, pp. 7–9.

1592. Current Control of an Electric Drive Having a Variable Voltage Motor and a Transverse Field Machine Amplifier (Metadyne Exciter), (in Russian), **V. P. Nikitin, N. P. Kunitskii.** *Isvestiya Akademii Nauk, SSSR.* Otdelenie Tekhnicheskikh Nauk, no. 1, Jan. 1950, pp. 64–78.

1593. Transient Processes in a Generator-Motor System with a Limiting Mechanical Characteristic of the Motor (in Russian), **V. P. Bychkov.** *Elektrichestvo*, no. 6, June 1951, pp. 29–37. An adjustable voltage drive with 3-field generator treated as a feedback control system.

1594. Ward-Leonard Mine Winder with Closed-Loop Amplidyne Control, **T. H. Petch.** *BTH Activities*, vol. 22, July-Aug. 1951, pp. 106–11.

1595. Acceleration Characteristics of Tandem Cold Reduction Mills, **W. R. Harris, R. W. Moore.** *Iron and Steel Engineer*, vol. 28, July 1951, pp. 63–73.

1596. Electronic Control of Reeling, Including Constant Tension Applications, **J. A. Stokes.** *BTH Activities*, vol. 22, March-April 1951, pp. 60–63.

1597. Electric Equipment for High Speed Strip Rolling Mills at Rogerstone Works of the Northern Aluminum Co., Ltd., **A. S. Wallis.** *BTH Activities*, vol. 22, July-Aug. 1951, pp. 99–105.

1598. Electric Drives for Reversing Hot Mills, **P. E. Peck,** *Journal*, Iron and Steel Institute, vol. 167, March 1951, pp. 309–23.

Transportation

1599. Directional Stability of Automatically Steered Bodies, **N. Minorsky.** *Journal*, American Society of Naval Engineers, vol. 34, 1922, pp. 280–309.

1600. Automatic Stabilization of Ships (book), **T. W. Chalmers.** Chapman and Hall, Ltd., London, England, 1931.

1601. Controlling a Gyro Stabilizer, **E. Frisch.** *Electric Journal*, vol. 28, July 1931, pp. 408–10.

1602. The Automatic Control of the Steering of Ships and Suggestions for its Improvement, **J. B. Henderson.** *Transactions*, Institution of Naval Architects, vol. 76, 1934, pp. 20–34.

1603. Regulating Processes for Diesel Electric Vehicles (in German), **D. P. Max.** *Siemens Zeitschrift*, vol. 14, May 1934, pp. 168–72.

1604. Automatic Control of Aircraft (in German), **A. Thauss, B. V. Kaull.** *Siemens Zeitschrift*, vol. 14, Nov. 1934, pp. 369–72.

1605. Aeroplane Stability and the Automatic Pilot, **F. W. Meredith, P. A. Cooke.** *Journal*, Royal Aeronautical Society, vol. 41, 1937, pp. 415–36.

1606. The Brown Boveri Servo Field-Regulator for Diesel Electric Vehicles, **A. E. Muller.** *Brown Boveri Review*, vol. 25, April 1938, pp. 63–66.

1607. The Effect of Regulation on the Size and Performance of D-C Generators for Diesel-Electric Vehicles (in German). *Brown Boveri Company Nachrichten*, vol. 27, Oct.-Dec., 1940, pp. 77–85.

1608. Course Steering of Aircraft (in German), **G. Wunsch.** *Verein deutscher Ingenieure Zeitschrift*, vol. 85, Jan. 25, 1941, pp. 89–93.

1609. Brake Regulators for Vehicles (in German), **F. Ostwald.** *Verein Deutscher Ingenieure Zeitschrift*, vol. 85, June 14, 1941, pp. 542–43.

1610. Control of Parallel Running of D-C Machines in Vehicles (in German), **K. Hoyer.** *Elektrotechnische Zeitschrift*, vol. 64, Nov. 18, 1943, pp. 607–10.

1611. Remote and Automatic Electric Controls for Aircraft, **W. P. Lear.** *Journal*, Franklin Institute, vol. 238, July 1944, pp. 9–35.

1612. Electric Automatic Pilots for Aircraft, **P. Halpert, O. E. Esval.** *AIEE Transactions (Electrical Engineering)*, vol. 63, Nov. 1944, pp. 861–66.

1613. Electrical Control in Automatic Pilots **C. M. Young, E. E. Lynch, E. R. Boynton.** *AIEE Transactions (Electrical Engineering)*, vol. 63, Dec. 1944, pp. 939–43.

1614. Application of Electronics to Aircraft Flight Control, **W. H. Gille, R. J. Kutzler.** *AIEE Transactions (Electrical Engineering)*, vol. 63, Nov. 1944, pp. 849–53.

1615. Electronic Turbo Regulator for Multi-Engine Airplanes, **W. H. Gille, H. T. Sparrow.** *Electronics*, vol. 17, May 1944, pp. 108–12.

1616. Constant-Speed Drives for Aircraft Alternators, **C. J. Breitwieser.** *AIEE Transactions (Electrical Engineering)*, vol. 64, Nov. 1945, pp. 763–68.

1617. Progress in Dynamic Stability and Control Research, **W. F. Milliken, Jr.** *Journal of the Aeronautical Sciences*, vol. 14, Sept. 1947, pp. 493–519.

1618. Experiments with Activated Tanks, **N. Minorsky.** *Transactions*, American Society of Mechanical Engineers, vol. 69, Oct. 1947, pp. 735–47.

1619. The Use of High Permeability Materials in Magnetometers. The Application of a Saturated Core Type Magnetometer to an Automatic Steering Control, **L. D. Armstrong.** *Canadian Journal of Research*, Section A, vol. 25, May 1947, pp. 124–33.

1620. Developments in Diesel-Electric Traction-Generator Excitation Control Systems, **C. A. Brancke, G. M. Adams.** *AIEE Transactions*, vol. 66, 1947, pp. 223–28.

1621. Electrical Steering of Ships, **Robin Beach.** *Electrical Engineering*, vol. 66, March 1947, pp. 244–48.

1622. A Power Plant Regulating System for Diesel-Electric Locomotives, **C. B. Lewis.** *AIEE Transactions*, vol. 66, 1947, pp. 242–46.

1623. Some Problems of Stability and Control of Large Aircraft, **D. J. Lyons.** *Journal*, Royal Aeronautical Society, vol. 52, Nov. 1948, pp. 723–34.

1624. Application of the Performance Operator to Aircraft Automatic Control, **R. C. Seamans, Jr., B. G. Bromberg, L. E. Payne.** *Journal of the Aeronautical Sciences*, vol. 15, Sept. 1948, pp. 535–55.

1625. Automatic Pilots, **J. C. Owen.** *Electrical Engineering*, vol. 67, June 1948, pp. 551–61.

1626. Application of Servo Systems to Aircraft, **J. R. Moore.** *Aeronautical Engineering Review*, vol. 8, Jan. 1949, pp. 32–43, 71.

1627. The Flutter of Servo-Controlled Aircraft, **J. Winston.** *Journal of the Aeronautical Sciences*, vol. 16, July 1949, pp. 397–404.

1628. Equations for Approximate Solution of Dynamic Problems for Stable Linear Systems, **K. H. Hohenemser.** *Journal of the Aeronautical Sciences*, vol. 16, Dec. 1949, pp. 723–28.

1629. Stability of Automatic Regulation of Diesel-Electric Passenger Transport (in Russian), **A. D. Stepanov.** *Elektrichestvo*, no. 6, June 1949, pp. 24–28.

1630. Application of Frequency-Response Analysis to Aircraft-Autopilot Stability, **C. L. Seacord, Jr.** *Journal of the Aeronautical Sciences*, vol. 17, 1950, pp. 481–98. Extensive bibliography.

1631. Longitudinal Stability of Autopilot-Controlled Aircraft, **A. Vazsonyi.** *Journal of the Aeronautical Sciences*, vol. 17, July 1950, pp. 399–416.

1632. Determination of Frequency Characteristics from Response to Arbitrary Input, **E. R. Walters, J. B. Rea.** *Journal of the Aeronautical Sciences*, vol. 17, July 1950, pp. 446–52.

1633. Dynamometer Control Simulates Road-Testing of Engines, **R. C. Bowers.** *Electronics*, vol. 23, June 1950, pp. 96–99.

1634. The Pulse Method for the Determination of Aircraft Dynamic Performance, **R. C. Seamans, Jr., B. P. Blasingame, G. C. Clementson.** *Journal of the Aeronautical Sciences*, vol. 17, Jan. 1950, pp. 22–38.

1635. A Design Method for Automatic Longitudinal Control Systems, **F. Stevens, K. M. Stevenson.** *Aeronautical Engineering Review*, vol. 10, Jan. 1951, pp. 18–23.

1636. Aerodynamic Stability and Automatic Control, **W. Bollay.** *Journal of the Aeronautical Sciences*, vol. 18, Sept. 1951, pp. 569–617.

1637. Analysis of Systems for Automatic Control of Aircraft, **J. B. Rea.** *Aeronautical Engineering Review*, vol. 10, Nov. 1951, pp. 39–47, 60.

1638. Control Surface Position Feedback in Flight-Control Systems, **L. Becker.** *Aeronautical Engineering Review*, vol. 10, Sept. 1951, pp. 17–19, 33.

Electronic Regulators

1639. Automatic Volume Control for Radio Receiving Sets, **H. A. Wheeler.** *Proceedings*, Institute of Radio Engineers, vol. 16, Jan. 1928, pp 30–39.

1640. Automatic Frequency Control, **T. F. Robertson.** *Electrical World*, vol. 94, Aug. 10, 1929, pp. 267–70.

1641. Regulator for Grid-Controlled Rectifier (in German), **G. Meiners.** *Elektrotechnik und Maschinenbau*, vol. 51, Sept. 17, 1933, pp. 502–04; Sept. 24, 1933, pp. 511–14.

1642. Supervisory and Control Equipment for Audio-Frequency Amplifiers, **H. Sohon.** *Proceedings*, Institute of Radio Engineers, vol. 21, Feb. 1933, pp. 228–37.

1643. Automatic Frequency Control, **C. Travis.** *Proceedings*, Institute of Radio Engineers, vol. 23, 1935, pp. 1125–41.

1644. Automatic Gain Control (in German), **H. Bartels, G. Ulbricht.** *Elektrische Nachrichten-Technik*, vol. 12, Nov. 1935, pp. 368–79.

1645. Frequency Control Equipments, **C. Jacobaeus.** *Ericsson Review*, no. 3, 1936, pp. 100–03.

1646. Automatic Gain Control, **E. C. Jordan.** *Canadian Journal of Research*, vol. 15, Section A, June 1937, pp. 79–84.

1647. Theory of the Discriminator Circuit for Automatic Frequency Control, **H. Roder.** *Proceedings*, Institute of Radio Engineers, vol. 26, May 1938, pp. 590–611.

1648. Time Constants for A.V.C. Filter Circuits, **K. R. Sturley.** *Wireless Engineer*, vol. 15, 1938, pp. 480–94.

1649. Feedback Band Pass Filters (in German), **J. Steinmetz.** *Hochfrequenztechnik und Elektroakustik*, vol. 51, March 1938, pp. 112–15.

1650. Cascade Type Duplex Feedback Systems, **Y. Watanabe, S. Okamura.** *Nippon Electrical Communication Engineering*, no. 14, Dec. 1938, pp. 484–92.

1651. Regulating Functions of Automatic Regulators of Sound Intensity (in Russian), **B. S. Galperin.** *Journal of Technical Physics, USSR*, vol. 9, no. 4, 1939, pp. 315–20.

1652. The Application of Negative Feedback to Frequency-Modulation Systems, **J. G. Chaffee.** *Proceedings*, Institute of Radio Engineers, vol. 27, May 1939, pp. 317–31.

1653. Some Applications of Negative Feedback with Particular Reference to Laboratory Equipment, **F. E. Terman, R. R. Buss, W. R. Hewlett, F. C. Cahill.** *Proceedings*, Institute of Radio Engineers, vol. 27, Oct. 1939, pp. 649–55.

1654. Non-Linear Differential Feedback Oscillator, **G. Hakata, M. Abe.** *Nippon Electrical Communication Engineering*, no. 15, Feb. 1939, pp. 526–36.

1655. D-C Amplified Automatic Volume Control Circuit Time Constants, **K. R. Sturley, F. Duerden.** *Wireless Engineer*, vol. 18, Sept. 1941, pp. 353–60.

1656. Automatic Frequency Control for a Cyclotron, **R. B. Jacques.** *Review of Scientific Instruments*, vol. 12, Sept. 1941, pp. 442–44.

1657. The Zero-Beat Method of Frequency Discrimination, **C. F. Sheaffer.** *Proceedings*, Institute of Radio Engineers, vol. 30, Aug. 1942, pp. 365–67.

1658. Automatic Tuning System for Preheating Plastics, **R. W. Gilbert.** *Electronics*, vol. 17, Dec. 1944, pp. 115–17.

1659. Electrometer Input Circuits, **H. A. Thomas.** *Electronics*, vol. 19, Dec. 1946, pp. 130–31.

1660. U. H. F. and Microwave A. F. C., **A. B. Rosenstein.** *Radio-Electronic Engineering*, vol. 7, Nov. 1946, pp. 8–10, 20.

1661. A.F.C. for R-F Heating, **S. I. Rambo.** *Electronics*, vol. 19, April 1946, pp. 120–22.

1662. Some Automatic Control Circuits for Radar Receivers, **L. A. Moxon, J. Croney, W. G. Johnston, C. A. Laws.** *Journal*, Institution of Electrical Engineers, vol. 93, pt. IIIA, March-May 1946, pp. 1143–58.

1663. A Circuit for the Control of Ionizing Current by a Saturable Core Transformer, **B. M. Banerjee, A. Mukerjee.** *Indian Journal of Physics*, vol. 21, June 1947, pp. 90–100.

1664. Improvement of the Characteristics of Photo-Voltaic and Photo-Conductive Cells by Feedback Circuits, **E. S. Rittner.** *Review of Scientific Instruments*, vol. 18, Jan. 1947, pp. 36–38.

1665. Automatic Frequency Control of Microwave Oscillators, **V. C. Rideout.** *Proceedings*, Institute of Radio Engineers, vol. 35, Aug. 1947, pp. 767–71.

1666. Frequency Stabilization of Microwave Oscillators, **R. V. Pound.** *Proceedings*, Institute of Radio Engineers, vol. 35, Dec. 1947, pp. 1405–15.

1667. An Equipment for Automatic Resonance Control, **G. Lindstrom.** *Arkiv for Matematik, Astronomi och Fysik*, vol. 35A (Paper 5), 1947.

1668. Adjustment Speed of Automatic-Volume-Control Systems, **A. W. Nolle.** *Proceedings*, Institute of Radio Engineers, vol. 36, July 1948, pp. 911–16.

1669. Recent Developments in Frequency Stabilization of Microwave Oscillators, **W. G. Tuller, W. C. Galloway, F. P. Zaffarano.** *Proceedings*, Institute of Radio Engineers, vol. 36, June 1948, pp. 794–800.

1670. Frequency Stabilization of Microwave Oscillators by Spectrum Lines, **W. V. Smith, Garcia de Quevedo.** *Journal of Applied Physics*, vol. 18, Dec. 1947, pp. 1112–15; vol. 19, Sept. 1948, pp. 831–36.

1671. Automatic Volume Control as a Feedback Problem, **B. M. Oliver.** *Proceedings*, Institute of Radio Engineers, vol. 36, April 1948, pp. 466–73.

1672. The Convotrol: A New Battery Charger, **O. D. Grandstaff.** *Automatic Electric Technical Journal*, vol. 1, July 1948, pp. 70–75. Constant battery voltage secured by saturating reactor in the primary circuit of the rectifier transformer. Comparator consists of another saturating inductor with polarizing winding.

1673. A Negative Feedback Dosage-Rate Meter, **R. J. Herbert.** *British Journal of Radiology*, vol. 21, Aug. 1948, pp. 420–24.

1674. Frequency Stabilization of Diathermy Units, **C. K. Gieringer.** *Electronics*, vol. 21, Dec. 1948, pp. 78–80.

1675. Stability of Tandem Regulators in the L-1 Carrier System, **J. P. Kinzer.** *AIEE Transactions*, vol. 68, pt. II, 1949, pp. 1179–86.

1676. Industrial Oscillator Frequency Control, **J. W. Lower.** *Electronics*, vol. 22, Dec. 1949, pp. 84–86.

1677. Error-Actuated Power Filters, **G. Newstead, D. L. H. Gibbings.** *Proceedings*, Institute of Radio Engineers, vol. 37, Oct. 1949, pp. 1115–19.

1678. Application of Negative Feedback to Frequency Modulation Systems, **P. F. Panter, W. Dite.** *Electrical Communication*, vol. 26, June 1949, pp. 173–78.

1679. Carrier Frequency Control: Automatic System for Unattended Transmitting Stations, **J. C. Gallagher.** *B. B. C. Quarterly*, vol. 4, no. 4, 1949–50, pp. 15–22.

1680. Feedback in Very-High-Frequency and Ultra-High-Frequency Oscillators, **F. J. Kamphoefner.** *Proceedings*, Institute of Radio Engineers, vol. 38, June 1950, pp. 630–32.

1681. Automatic Regulation of the Power in High Frequency Heating Installations (in Russian), **A. V. Donskoi.** *Elektrichestvo*, no. 10, Oct. 1950, pp. 46–49.

1682. Automatic Frequency Control for Single-Side Band Receivers, **J. L. Arends.** *Communication News*, vol. 11, Dec. 1950, pp. 101–19.

1683. Intermediate-Frequency Gain Stabilization with Inverse Feedback, **G. F. Montgomery.** *Proceedings*, Institute of Radio Engineers, vol. 38, June 1950, pp. 662–67.

1684. Servo Theory Applied to Frequency Stabilization with Spectral Lines, **W. D. Hershberger, L. E. Norton.** *Journal*, Franklin Institute, vol. 249, May 1950, pp. 359–66.

1685. RC Amplifier Filters, **C. H. Miller.** *Wireless Engineer*, vol. 27, Jan. 1950, pp. 26–29.

1686. Frequency Stabilization of Oscillators (in French), **J. Zakheim.** *La Radio Francaise*, no. 11, Nov. 1950, pp. 1–4.

1687. The "Komptron", A New Electronic Regulator (in German), **H. Skoczdopole.** *Siemens Zeitschrift*, vol. 2, Sept. 1950, pp. 41–46.

1688. Microwave Power Stabilizer, **I. K. Munson.** *Review of Scientific Instruments*, vol. 21, July 1950, pp. 622–24.

1689. A Magnetic Amplifier Frequency Control, **L. J. Johnson, H. G. Schafer.** *AIEE Transactions*, vol. 69, pt. I, 1950, pp. 613–15.

1690. Stepless Automatic Frequency Regulator (in Russian), **V. E. Kazanskii, L. D. Sterninson.** *Elektrichestvo*, no. 4, April 1951, pp. 16–19.

1691. Frequency Regulator with Filters and Magnetic Amplifiers (in Russian), **A. G. Moskalev, I. I. Solovev.** *Elektrichestvo*, no. 7, July 1951, pp. 11–17.

1692. Frequency Stabilization by Microwave Absorption, **H. R. L. Lamont.** *Physica*, vol. 17, March-April 1951, pp. 446–52.

1693. A Regulator for Sound Field Strength (in French), **P. Riety.** *Annales de Telecommunication*, vol. 6, Feb. 1951, pp. 43–48.

1694. Automatic Frequency Control: A Circuit for Controlling the Clock Pulse Frequency in Digital Calculators, **J. M. M. Pinkerton.** *Electronic Engineering*, vol. 23, April 1951, pp. 142–43.

1695. An Automatic Ionosphere Recorder for the Frequency Range 0.55 to 17 Megacycles, **R. Naismith.** *Proceedings*, Institution of Electrical Engineers, vol. 98, pt. 3, 1951, pp. 11–18.

1696. Alternate Ways in the Analysis of a Feedback Oscillator and its Application, **E. J. Post, H. F. Pit.** *Proceedings*, Institute of Radio Engineers, vol. 39, Feb. 1951, pp. 169–74.

1697. Amplified Automatic Gain Control, **S. W. Amos, G. G. Johnstone.** *Wireless World*, vol. 57, Oct. 1951, pp. 415–18.

Servo-Operated Instruments

1698. A Recording Photoelectric Color Analyzer, **A. C. Hardy.** *Journal*, Optical Society of America, vol. 18, Feb. 1929, pp. 96–117.

1699. Distribution of Particles in Disperse Systems, **T. Svedberg, H. Rinde.** *Journal*, American Chemical Society, vol. 45, 1923, pp. 943–54. Self-balancing chemical balance.

1700. A New Electronic Recorder, **H. L. Bernarde, L. J. Lunas.** *Electrical Engineering*, vol. 52, March 1933, pp. 168–70.

1701. A High-Speed Level Recorder for Acoustic Measurements, **E. H. Bedell.** *Bell Laboratories Record*, vol. 13, 1934, pp. 75–79.

1702. Recording Electrical Instruments, **P. A. Borden, M. F. Behar.** *Instruments*, vol. 8, 1935, pp. 7–14, 34–44.

1703. An Automatic Curve Follower, **H. L. Hazen, J. J. Jaeger, G. S. Brown.** *Review of Scientific Instruments*, vol. 7, Sept. 1936, pp. 353–57.

1704. Photo-Electrically Balanced Recording Potentiometer, **C. O. Fairchild, V. L. Parsegian.** *Review of Scientific Instruments*, vol. 9, Dec. 1938, pp. 422–25.

1705. An Electronic Recording Analytical Balance, **R. H. Muller, R. L. Garman.** *Industrial and Engineering Chemistry*, Analytical Edition, vol. 10, 1938, pp. 436–40.

1706. Combined Thyratron and Tachometer Speed Control of Small Motors, **A. J. Williams, Jr.** *AIEE Transactions (Electrical Engineering)*, vol. 57, Oct. 1938, pp. 565–68.

1707. The "Speedomax" Power-Level Recorder, **William Russell Clark.** *AIEE Transactions*, vol. 59, 1940, pp. 957–64.

1708. An Electro-Pneumatic Regulator with Photoelectric Compensation (in German), **E. Weiss.** *Elektrotechnische Zeitschrift*, vol. 62, Dec. 18, 1941, pp. 975–79.

1709. Direct Pen Recording of Galvanometer Deflections, **D. J. Pompeo, C. J. Penther.** *Review of Scientific Instruments*, vol. 13, 1942, pp. 218–22.

1710. High-Speed Photoelectric Recorder, **H. L. Clark.** *General Electric Review*, vol. 45, July 1942, pp. 384–86.

1711. Electronic Curve Tracer, **P. Padva.** *Electronics*, vol. 16, Feb. 1943, pp. 87–90, 202.

1712. Photoelectric Potentiometer Recorder **D. F. Hang.** *General Electric Review*, vol. 46, 1943, pp. 623–25.

1713. High Speed Multiple-Point Potentiometer Recorder for Measuring Thermocouple Temperatures During Test Plane Flights, **I. M. Stein, A. J. Williams, Jr., W. R. Clark.** *Transactions*, American Society of Mechanical Engineers, vol. 66, 1944, pp. 271–75.

1714. Potentiometer Recorder-Controller. *Journal of Scientific Instruments*, vol. 21, April 1944, pp. 70–71.

1715. A Resistance-Coupled Thyratron Recording Circuit, **J. B. Wilkie.** *Review of Scientific Instruments*, vol. 16, 1945, p. 97.

1716. Solution of Instrumentation Problems by Pneumatic Null Balance Methods, **C. B. Moore.** *Instruments*, vol. 18, Sept. 1945, pp. 598–603.

1717. An Electronic Potentiometer Pyrometer, **J. J. Fraser.** *Electronic Engineering*, vol. 17, Jan. 1945, pp. 340–44.

1718. Electric Measuring Instruments, **D. M. Nielsen.** *Electrical Engineering*, vol. 65, Feb. 1946, pp. 66–74.

1719. New Power Operated Sensitive Recorder, **P. G. Weiller.** *Electronics Industries*, vol. 5, Jan. 1946, pp. 88, 89, 136, 138, 140.

1720. Recorder-Controller for Temperature and Humidity, **V. D. Hauck, R. E. Sturm, R. B. Colt.** *Electronics*, vol. 19, Sept. 1946, pp. 96–99.

1721. Electronically Balanced Recorder for Flight Testing and Spectroscopy, **A. J. Williams, Jr., W. R. Clark, R. E. Tarpley.** *AIEE Transactions (Electrical Engineering)*, vol. 65, April 1946, pp. 205–08.

1722. A Photo-Electric Curve Follower, **M. J. Tucker, G. Collins.** *Electronic Engineering*, vol. 19, Dec. 1947, pp. 398–400, 403.

1723. A Continuously Balanced Thermoelectric Potentiometer Pyrometer, **H. M. Schmitt.** *Transactions*, Instruments and Measurements Conference, 1947, pp. 160–62.

1724. Linear Recording Meter, **I. Cogan.** *Radio-Electronic Engineering*, vol. 12, May 1949, pp. 8, 9, 28.

1725. Damper Stabilized Instrument Servomechanisms, **Albert C. Hall.** *AIEE Transactions*, vol. 68, pt. I, 1949, pp. 299–306.

1726. Self-Balancing Instruments for Continuous Industrial Processes, **J. E. M. Coombes, F. B. Hinderwell.** *Metropolitan-Vickers Gazette*, vol. 23, Nov.-Dec. 1950, pp. 255–60. (Also *Engineering*, vol. 170, Oct. 1950, pp. 297–300).

1727. An Electronic Recording Analytical Balance, **I. W. Lohmann.** *Review of Scientific Instruments*, vol. 21, Dec. 1950, pp. 999–1002.

1728. Automatic, Recording Potentiometer with High Sensitivity (in Swedish), **S. Ekelof, B. Nisson.** *Tidskrift for Teknisk-Vetenskaplig Forskning*, vol. 21, 1950, pp. 153–62.

1729. A Photoelectrically Controlled Chopper-Bar Recorder (in German), **L. Jager.** *Acta Physica Austriaca*, vol. 4, 1950, pp. 213–17.

1730. The New AEG Chopper-Bar Regulator and its Practical Applications (in German), **H. Lindorf.** *AEG Mitteilungen*, vol. 41, March-April 1951, pp. 60–64.

1731. A Self-Balancing Microwave Power Measuring Bridge, **L. A. Rosenthal, J. L. Potter.** *Proceedings*, Institute of Radio Engineers, vol. 39, Aug. 1951, pp. 927–31.

1732. Self-Balancing Strain Gauge Equipment, **A. B. Kaufman.** *Radio-Electronic Engineering*, vol. 16, Aug. 1951, pp. 12–14.

1733. Self-Balancing Instruments and Their Application to Nucleonic Measurement, **R. S. Medlock, W. A. Kealy.** *Journal*, British Institution of Radio Engineers, vol. 11, 1951, pp. 393–405.

Feedback Amplifiers

1734. Reaction Amplifiers (in German), **Y. Watanabe.** *Zeitschrift fur Hochfrequenztechnik*, vol. 32, Sept. 1928, pp. 77–83.

1735. A Note on the Stability of a Valve Amplifier, **E. B. Moullin.** *Proceedings*, Cambridge Philosophical Society, vol. 25, 1929, pp. 508–13.

1736. Double-Valued Characteristic of a Direct Current Feedback Amplifier, **P. B. Carwile, F. A. Scott.** *Philosophical Magazine*, vol. 8 (Series 7), 1929, pp. 680–84.

1737. Regeneration Theory, **H. Nyquist.** *Bell System Technical Journal*, vol. 11, Jan. 1932, pp. 126–47.

1738. Self-Oscillation of Amplifiers by Coupling of the Anode Circuits (in German), **W. O. Schumann.** *Archiv fur Elektrotechnik*, vol. 26, Aug. 3, 1932, pp. 580–86.

1739. Reaction Arrangement Independent of Frequency (in French), **L. Brillouin, M. Levy.** *Comptes Rendus*, l'Academic des Sciences, vol. 194, April 4, 1932, pp. 1151–53.

1740. Simple Reaction Arrangement Having Properties Independent of Frequency (in French), **M. Levy.** *Revue d'Acoustique*, vol. 2, Nov. 1933, pp. 471–83.

1741. Feedback in Amplifiers (in German), **R. Schienemann.** *Telegraphen-Fernsprech-Funk-und Fernsehtechnik*, vol. 22, May 1933, pp. 115–17.

1742. Theory of Reaction (in French), **M. Rousseau.** *Bulletin*, Association des Ingenieurs Electriciens, vol. 11, Nov. 1933, pp. 335–51.

1743. Graphical Calculation of Linear and Non-Linear Feedback (in German), **H. Bartels.** *Elektrische Nachrichten-Technik*, vol. 11, 1934, pp. 319–29.

1744. Regeneration Theory and Experiment **E. Peterson, J. G. Kreer, L. A. Ware.** *Bell System Technical Journal*, vol. 13, Oct. 1934, pp. 680–700.

1745. Stabilized Feedback Amplifiers, **H. S. Black.** *Electrical Engineering*, vol. 53, Jan. 1934, pp. 114–20. (Also *Bell System Technical Journal*, vol. 13, 1934, pp. 1–18.)

1746. Amplification of a Galvanometer Deflection by Retroaction with a Photocell, **W. L. Watton.** *Journal of Scientific Instruments*, vol. 12, 1935, pp. 115–18.

1747. L-F Amplifier with Reaction (in French), **M. Marinesco.** *Comptes Rendus*, l'Academie des Sciences, vol. 201, July 16, 1935, pp. 193–95.

1748. Theoretical Considerations on the Effects of Reaction in Amplifiers (in French), **M. Rousseau.** *Onde Electrique*, vol. 14, 1935, pp. 228–42.

1749. Non-Linear Distortion of Amplitude Regulators and Regulating Requirements (in German), **E. Holzler.** *Elektrische Nachrichten-Technik*, vol. 13, Feb. 1936, pp. 29–36.

1750. Dynamically Controlled Amplifier and Pure Tone Regulation (in German), **W. Burck, P. Kotowski, H. Lichte.** *Elektrische Nachrichten-Technik*, vol. 13, Feb. 1936, pp. 47–73.

1751. Feedback Amplifier Systems, **Z. Kamayachi.** *Nippon Electrical Communication Engineering*, no. 2, Feb. 1936, pp. 150–54.

1752. Input Admittance of Feedback Network, **E. Takagisi.** *Nippon Electrical Communication Engineering*, no. 3, May 1936, pp. 192–96.

1753. Negative Feedback Amplifiers, **W. T. Cocking.** *Wireless World*, vol. 39, Nov. 6, 1936, pp. 475–78.

1754. Negative Feedback Amplification, **W. T. Cocking.** *Wireless World*, vol. 39, Dec. 25, 1936, pp. 669–70.

1755. Negative Reaction (in French), **M. Marinesco.** *Onde Electrique*, vol. 15, July 1936, pp. 469–75.

1756. Retroaction in Audio Amplifiers, **M.**

Marinesco. *Wireless Engineer*, vol. 13, March 1936, pp. 131–34.

1757. A Negative Feedback Amplifier, **A. C. Timmis.** *Post Office Electrical Engineers' Journal*, vol. 29, April 1936, pp. 71–72.

1758. Retroaction in Phase-Opposition (in Italian), **F. Marietti.** *Alta Frequenza*, vol. 6, Sept. 1937, pp. 588–617.

1759. Amplifiers with Contra-Retroaction (in French), **M. Belus.** *Annales des Postes, Telegraphes et Telephones*, vol. 26, Sept. 1937, pp. 804–12.

1760. Negative Feed-back, **P. K. Turner.** *Wireless World*, vol. 41, Oct. 15, 1937, pp. 386–87.

1761. Regeneration in Linear Amplifiers, **G. S. Brayshaw.** *Wireless Engineer*, vol. 14, Nov. 1937, pp. 597–605.

1762. Inverse Feedback, **B. D. H. Tellegen, V. C. Henriquez.** *Wireless Engineer*, vol. 14, Aug. 1937, pp. 409–13.

1763. Back-Coupled Amplifiers (in German), **R. Feldtkeller, E. Thon.** *Telegraphen-Fernsprech-Funk-und-Fernsehtechnik*, vol. 26, Jan. 1937, pp. 1–7.

1764. Feedback Amplifier Design, **F. E. Terman.** *Electronics*, vol. 10, Jan. 1937, pp. 12–15.

1765. Practical Feedback Amplifiers, **J. R. Day, J. B. Russell.** *Electronics*, vol. 10, April 1937, pp. 16–19.

1766. Distortion in Negative Feedback Amplifiers, **M. Marinesco.** *Wireless Engineer*, vol. 15, 1938, p. 22.

1767. Negative Resistances and High Selectivity by Simultaneous Application of Direct and Inverse Feedback (in Italian), **F. Vecchiacchi.** *Alta Frequenza*, vol. 6, June 1937, pp. 351–64; July 1937, pp. 435–47.

1768. An Analysis of Admittance Neutralization by Means of Negative Transconductance Tubes, **E. W. Herold.** *Proceedings*, Institute of Radio Engineers, vol. 25, Nov. 1937, pp. 1399–413.

1769. Inverse Feedback, **B. D. H. Tellegen.** *Philips Technical Review*, vol. 2, Oct. 1937, pp. 289–94.

1770. Some Properties of Negative Feedback Amplifiers, **L. I. Farren.** *Wireless Engineer*, vol. 15, Jan. 1938, pp. 23–25.

1771. Study of the Principles of Reaction (in French) **F. Bedeau, J. de Mare.** *Onde Electrique*, vol. 17, April 1938, pp. 153–73; May 1938, pp. 248–65.

1772. Use of Negative Feedback in Radio Telephony Receivers (in French), **R. Aschenbrenner.** *Onde Electrique*, vol. 17, Nov. 1938, pp. 510–20.

1773. A Study on Characteristics of the Fundamental Wave in a Feedback Amplifier, **K. Kobayasi, Y. Degawa.** *Nippon Electrical Communication Engineering*, no. 9, Feb. 1938, pp. 79–82.

1774. Input and Output Impedances of Feedback Amplifier, **K. Kobayasi.** *Nippon Electrical Communication Engineering*, no. 9, Feb. 1938, pp. 40–43.

1775. Non-Linear Characteristics of Simplex Feedback Amplifier, **K. Kobayasi, Y. Degawa.** *Nippon Electrical Communication Engineering*, no. 11, June 1938, pp. 266–74.

1776. Frequency Discrimination by Inverse Feedback, **G. H. Fritzinger.** *Proceedings*, Institute of Radio Engineers, vol. 23, Feb. 1938, pp. 207–25.

1777. Balanced Feedback Amplifiers, **E. L. Ginzton.** *Proceedings*, Institute of Radio Engineers, vol. 26, Nov. 1938, pp. 1367–79.

1778. Use of Feedback to Compensate for Vacuum-Tube Input-Capacitance Variations with Grid Bias, **R. L. Freeman.** *Proceedings*, Institute of Radio Engineers, vol. 26, Nov. 1938, pp. 1360–66.

1779. A Study of Feedback Amplifiers by Their Equivalent Circuits, **Y. Watanabe, S. Okamura.** *Nippon Electrical Communication Engineering*, no. 17, July 1939, pp. 10–17.

1780. Feedback Amplifier with Frequency Response of Constant Inclination (Feed-Back Equalizer), **K. Kobayashi, T. Kurokawa.** *Nippon Electrical Communication Engineering*, no. 18, Oct. 1939, p. 122.

1781. Frequency Response Characteristics of Amplifiers Employing Negative Feedback, **F. E. Terman, W. Y. Pan,** *Communications*, vol. 19, 1939, pp. 5–7, 42, 44, 45.

1782. The Input Resistance of Back-Coupled Amplifiers (in German), **H. Bartels.** *Elektrische Nachrichten-Technik*, vol. 16, June 1939, pp. 155–61.

1783. Transient Phenomena of Simplex Feedback Amplifiers, **Y. Watanabe, S. Okamura.** *Nippon Electrical Communication Engineering*, no. 18, Oct. 1939, pp. 3–10.

1784. Reflexed Amplifiers, **S. J. Watson.** *AWA Technical Review*, vol. 4, Jan. 1939, pp. 35–50.

1785. Impedance Matching at the Output Terminals and the Maximum Overhead Output of Feed-Back Amplifier, **K. Kobayashi.** *Nippon Electrical Communication Engineering*, no. 18, Oct. 1939, pp. 121–22.

1786. Control of the Effective Internal Impedance of Amplifiers by Means of Feedback, **H. F. Mayer.** *Proceedings*, Institute of Radio Engineers, vol. 27, March 1939, pp. 213–17.

1787. The Application of Feedback to Wide-band Output Amplifiers, **F. A. Everest, H. R. Johnston.** *Proceedings*, Institute of Radio Engineers, vol. 28, Feb. 1940, pp. 71–6.

1788. High-Gain Duplex Feedback Amplifier, **Y. Watanabe, S. Okamura.** *Nippon Electrical Communication Engineering*, no. 21, July 1940, pp. 46–51.

1789. Feedback Circuit of Multi-Stage Amplifier and the Constant-Current 4-Pole Network, **K. Yamamoto.** *Nippon Electrical Communication Engineering*, no. 21, July 1940, p. 62.

1790. Transient Phenomena of Feedback Amplifiers, **Y. Watanabe, S. Okamura, H. Totiya.** *Nippon Electrical Communication Engineering*, no. 19, Jan. 1940, pp. 158–64.

1791. Relations Between Attenuation and Phase in Feedback Amplifier Design, **H. W. Bode.** *Bell System Technical Journal*, vol. 19, July 1940, pp. 421–54.

1792. Stabilization for Self-Oscillation in Feedback Amplifiers, **K. Kobayashi, T. Kurokawa.** *Nippon Electrical Communication Engineering*, no. 21, July 1940, pp. 9–15.

1793. Compression with Feed-Back, **H. H. Stewart, H. S. Pollock.** *Electronics*, vol. 13, Feb. 1940, pp. 19–21.

1794. Feedback, **E. K. Sandeman.** *Wireless Engineer*, vol. 17, Aug. 1940, pp. 342–53.

1795. Equivalent Circuits of the Feedback Amplifier, **A. Fairweather.** *Wireless Engineer*, vol. 18, 1941, pp. 151–53.

1796. Novel D-C Amplifiers (in German), **R. Eberhardt, G. Nusslein, H. Rupp.** *Elektrotechnische Zeitschrift*, vol. 62, May 29, 1941, pp. 493–97.

1797. Equivalent Characteristics of Vacuum Tubes Operating in Feedback Circuits, **J. H. Pratt.** *RCA Review*, vol. 6, July 1941, pp. 102–13.

1798. A Direct-Current Amplifier and its Application to Industrial Measurements and Control, **D. C. Gall.** *Journal*, Institution of Electrical Engineers, vol. 89, pt. 2, Oct. 1942, pp. 434–46. Galvanometer-phototube input which controls a single thyratron.

1799. Comparison of Voltage—and Current-Feedback Amplifiers, **E. H. Schulz.** *Proceedings*, Institute of Radio Engineers, vol. 31, Jan. 1943, pp. 25–8.

1800. Effect of Feedback on Impedance, **R. B. Blackman.** *Bell System Technical Journal*, vol. 22, Oct. 1943, pp. 269–77.

1801. Influence of Feedback on Source Impedance, **R. W. Crane.** *Electronics*, vol. 17, Sept. 1944, pp. 122–23.

1802. Feedback and the Loudspeaker, **S. W. Amos.** *Wireless World*, vol. 50, Dec. 1944, pp. 354–57.

1803. Feedback Amplifier for C-R Oscilloscopes, **G. R. Mezger.** *Electronics*, vol. 17, April 1944, pp. 126–31, 254.

1804. Negative Feedback in Hearing Aid Amplifiers, **F. E. Planer, E. A. Marland.** *Electronic Engineering*, vol. 17, April 1945, pp. 450–53, 455.

1805. Methods of Applying Negative Feedback—A Reference Chart. *Electronic Engineering*, vol. 17, Nov. 1945, pp. 770–71.

1806. Valve Equivalent Circuit Conventions and Negative Feedback, **G. W. O. Howe.** *Wireless Engineer*, vol. 22, Sept. 1945, pp. 417–19.

1807. A Variation on the Gain Formula for Feedback Amplifiers for a Certain Driving-Impedance Configuration, **T. W. Winternitz.** *Proceedings*, Institute of Radio Engineers, vol. 34, Sept. 1946, pp. 639–41.

1808. Termination Effects in Feedback Amplifier Chains, **A. J. Ferguson.** *Canadian Journal of Research*, vol. 24A. July 1946, pp. 56–78.

1809. A Simple Galvanometer Amplifier with Negative Feedback, **J. S. Preston.** *Journal of Scientific Instruments*, vol. 23, Aug. 1946, pp. 173–76.

1810. A Feedback Amplifier for Ionization Currents, **F. T. Farmer.** *British Journal of Radiology*, vol. 19, Jan. 1946, pp. 27–30.

1811. The Effect of Negative Voltage Feedback on Power Supply Hum in Audio-Frequency Amplifiers, **G. Builder.** *Proceedings*, Institute of Radio Engineers, vol. 34, March 1946, pp. W140–44.

1812. Three Feedback Amplifier Charts, **J. S. Wells.** *Proceedings*, Institution of Radio Engineers, vol. 7, Nov. 1946, pp. 4–7. The gain, phase shift, and improvement in gain stability with feedback are shown as functions of gain magnitude and phase angle.

1813. Note on "A Simple Galvanometer with Negative Feedback", **D. K. C. MacDonald.** *Journal of Scientific Instruments*, vol. 24, Sept. 1947, pp. 232–33

1814. On Feedback Amplifiers (in Swedish), **A. Hautanen.** *Kraft och Ljus*, nos. 5–6, May-June 1947, pp. 99–110.

1815. Impedances in the Feedback Amplifier (in French), **P. M. Prache.** *Bulletin*, Societe Francaise des Electriciens, vol. 7 (series 6), Sept. 1947, pp. 515–28.

1816. Two-Stage Amplifiers with Inverse Feedback, **H. Mayr, T. H. Wien.** *Microtecnic*, vol. 11, April 1948, pp. 86–89.

1817. Electromechanical Feedback, **J. De Boer, G. Schenkel.** *Journal*, Acoustical Society of America, vol. 20, Sept. 1948, pp. 641–47.

1818. Linear Electrical Transmission Systems (in German), **G. Kraus.** *Oesterreichisches Ingenieur Archiv.*, vol. 2, 1948, pp. 286–98.

1819. D-C Amplifier Stabilized for Zero and Gain, **A. J. Williams, Jr., R. E. Tarpley, W. R. Clark.** *AIEE Transactions*, vol. 67 pt. I, 1948, pp. 47–57.

1820. Correction Circuits in the Negative-Feedback Amplifier (in French), **H. Chireix.** *Bulletin*, Societe Francaise des Electriciens, vol. 8, Nov. 1948, pp. 86, 523–35.

1821. Improvements in Negative-Feedback Amplifiers (in French), **J. Polonsky.** *Annales de Radioelectricite*, vol. 3, July 1948, pp. 240–51.

1822. General Formulae for Feedback Amplifiers (in French), **F. Job.** *Annales de Telecommunication*, vol. 3, Dec. 1948, pp. 436–44.

1823. The Group Transmission Time in a Feedback Amplifier (in German), **G. Schaffstein.** *Frequenz*, vol. 2, Nov. 1948, pp. 291–95.

1824. Impedances in Negative Feedback Amplifiers (in French), **P. M. Prache.** *Cables et Transmission*, vol. 2, Jan. 1948, pp. 15–29.

1825. The Stability Question with Feedback Amplifiers (in German), **J. Lehmann.** *Zeitschrift fur angewandte Mathematik und Mechanik*, vol. 28, Jan. 1948, pp. 23–29; Feb. 1948, pp. 59–64.

1826. Selective Amplification at Low Frequency (in French), **L. de Queiroz Orsini.** *Onde Electrique*, vol. 29, Nov. 1949, pp. 408–13.

1827. Study of a High-quality Voltage Amplifier (in French), **J. Mey.** *Annales de Telecommunication*, vol. 4, Nov. 1949, pp. 383–84.

1828. On the Power Gain and the Bandwidth of Feedback Amplifier Stages, **A. van der Ziel, K. S. Knol.** *Philips Research Reports*, vol. 4, June 1949, pp. 167–78.

1829. Feedback Amplifier Design, Conditions for Flat Response, **H. Mayr.** *Wireless Engineer*, vol. 26, Sept. 1949, pp. 297–305.

1830. Negative-Feedback Amplifiers: Conditions for Maximal Flatness, **C. F. Brockelsby.** *Wireless Engineer*, vol. 26, Feb. 1949, pp. 43–49. Staggering of time constants to produce an essentially flat frequency characteristic.

1831. Feedback Improves Response of D-C Amplifiers, **J. F. Lash.** *Electronics*, vol. 22, Feb. 1949, pp. 109–11.

1832. A Galvanometer Amplifier, **B. Frankenhaeuser, D. K. C. MacDonald.** *Journal of Scientific Instruments*, vol. 26, May 1949, pp. 145–47.

1833. Wide-Band D-C Amplifier Stabilized for Gain and for Zero, **A. J. Williams, Jr., W. G. Amey, Will McAdam.** *AIEE Transactions*, vol. 68, pt. II, 1949, pp. 811–15.

1834. Calculator and Chart for Feedback Problems, **J. H. Felker.** *Proceedings*, Institute of Radio Engineers, vol. 37, Oct. 1949, pp. 1204–06.

1835. Investigation of the Conditional Stability of Feedback Amplifiers (in German), **K. H. R. Weber.** *Frequenz*, vol. 3, Sept. 1949, pp. 253–59.

1836. Negative Feedback Amplifiers (in French), **E. Chamagne, G. Guyot.** *Annales de Telecommunication*, vol. 4, April 1949, pp. 119–22.

1837. Combined Current and Voltage Feedback, **K. R. Sturley.** *Electronic Engineering*, vol. 21, May 1949, pp. 159–61. A strict analysis of both types of feedback acting simultaneously, with regard to their interaction.

1838. Single-Stage Negative Feedback Amplifier for A-C (in German), **W. Geyger.** *Funk und Ton*, vol. 3, May 1949, pp. 278–85. Reviews the theory of triode amplifiers with current, voltage, and mixed feedbacks.

1839. R-C Amplifier Filters, **C. H. Miller.** *Wireless Engineer*, vol. 27, Jan. 1950, pp. 26–29.

1840. Stabilization of Wide-Band Direct-Current Amplifiers for Zero and Gain, **E. A. Goldberg.** *RCA Review*, vol. 11, June 1950, pp. 296–300.

1841. Feedback D-C Amplifier (in German), **W. Geyger.** *Archiv fur technisches Messen*, no. 169, T22–24, Feb. 1950.

1842. Negative Feedback D-C Amplifier (in German), **W. Geyger.** *Archiv fur technisches Messen*, no. 172, T57, May 1950.

1843. Control, Positive and Negative Feedback, and Negative Resistance, Coordinated (in German), **W. Reichardt.** *Elektrotechnik*, vol. 4, Feb. 1950, pp. 47–53; March 1950, pp. 73–80.

1844. Amplifiers with Selective Negative Feedback (in German), **H. Boucke, O. Schmidt.** *Fernmeldetechnische Zeitschrift*, vol. 3, Nov. 1950, pp. 417–20.

1845. Automatic Stabilization of Amplifier Gain, **A. W. Keen.** *Journal*, British Institution of Radio Engineers, vol. 10, June 1950, pp. 198–207.

1846. Selective Amplification by Means of RC Feedback Networks (in Italian), **M. Picchi.** *Alta Frequenza*, vol. 19, April 1950, pp. 59–85.

1847. An Improved Video-Frequency Amplifier Circuit with Negative Feedback (in Russian), **O. B. Lure.** *Journal of Technical Physics, USSR*, vol. 20, May 1950, pp. 602–06.

1848. A Note on the Maximum Feedback Obtainable in an Amplifier of the Cathode Feedback Type, **J. te Winkel.** *Philips Research Reports*, vol. 5, Feb. 1950, pp. 1–5.

1849. Galvanometers with Photoelectric Feedback, **P. Selenyi.** *Hungarica Acta Physica*, vol. 1, no. 6, 1950, pp. 1–8.

1850. Negative-Feedback Amplifiers, Conditions for Critical Damping, **J. E. Flood.** *Wireless Engineer*, vol. 27, July 1950, pp. 201–09.

1851. Intermediate-Frequency Gain Stabilization with Inverse Feedback, **G. F. Montgomery.** *Proceedings*, Institute of Radio Engineers, vol. 38, June 1950, pp. 662–67.

1852. Combining Positive and Negative Feedback, **J. M. Miller, Jr.** *Electronics*, vol. 23, March 1950, pp. 106–09.

1853. Some Considerations in the Design of Negative-Feedback Amplifiers, **W. T. Duerdoth.** *Proceedings*, Institution of Electrical Engineers, vol. 97, pt. 3, May 1950, pp. 138–58.

1854. A Note on Negative Feedback Amplifiers (in German), **E. Kirschner.** *Frequenz*, vol. 5, Aug. 1951, pp. 223–30.

1855. Distortion and Power Output of Class A Output Valves with Negative Feedback (in German), **R. Siegert.** *Telefunken Zeitung*, vol. 24, June 1951, pp. 100–17.

1856. Amplifiers Having Small Gain Variations (in Dutch), **J. J. Zaalberg van Zelst.** *Tijdschrift van het Nederlandsch Radiogenootschap*, vol. 16, May 1951, pp. 117–36.

1857. On Parallel Voltage Feedback (in German), **K. R. H. Weber.** *Elektrotechnik*, vol. 5, April 1951, pp. 180–83.

1858. Vision Amplifier with Negative Feedback for Reduction of Microphony and Input Noise (in German), **W. Dillenburger.** *Funk und Ton*, vol. 5, March 1951, pp. 113–23.

1859. Shunt-Regulated Amplifiers, **V. J. Cooper.** *Wireless Engineer*, vol. 28, May 1951, pp. 132–45.

1860. Negative-Feedback Circuits, **W. T. Cocking.** *Wireless Engineer*, vol. 28, June 1951, pp. 165–67.

1861. D-C Amplifier with Reduced Zero-Offset, **W. McAdam, R. E. Tarpley, A. J. Williams, Jr.** *Electronics*, vol. 24, Aug. 1951, pp. 128–32.

1862. The Automatic Compensation of Zero-Drift in Direct-Coupled Feedback Systems, **F. A. Summerlin.** *Proceedings*, Institution of Electrical Engineers, vol. 98, pt. 2, Feb. 1951, pp. 59–66.

Regulating Devices

1863. Automatic Regulators. *Engineer*, vol. 139, March 27, 1925, pp. 351–52.

1864. Automatic Electric Regulators with Hydraulic Servomotors (in German), **M. Bogen.** *Elektrotechnische Zeitschrift*, vol. 47, 1926, pp. 1350–52.

1865. A Direct-Acting Automatic Regulator, **O. K. Marti.** *Electrical World*, vol. 88, Nov. 13, 1926, pp. 1015–17. Rocking contact type.

1866. Principles of Selsyn Equipment and Their Operation, **L. F. Holder.** *General Electric Review*, vol. 33, Sept. 1930, pp. 500–04.

1867. New Electric Measurement and Control Devices (in German), **A. Grunwald.** *Waerme*, vol. 57, Jan. 27, 1934, pp. 51–56.

1868. New Developments in Electron Tube Regulators and Their Application (in German), **R. G. Berthold, A. V. Engel.** *Siemens Zeitschrift*, vol. 14, June 1934, pp. 214–22.

1869. Selsyn Instruments for Position Systems, **T. M. Linville, J. S. Woodward.** *AIEE Transactions (Electrical Engineering)*, vol. 53, 1934, pp. 953–60.

1870. Electrically Operated Automatic Regulator (in German), **W. Pomtow.** *Zeitschrift des Vereines deutscher Ingenieure*, vol. 78, July 14, 1934, pp. 848–50.

1871. Continuous Electrical Regulator (in German), **C. Himmler.** *Archiv fur Electrotechnik*, vol. 29, 1935, pp. 577–99.

1872. Quick-Acting Regulators. *Bulletin Oerlikon*, no. 175–76, 1936, pp. 945–50.

1873. New Moving Element for Regulators and Relays (in German), **A. Gantenbein.** *Bulletin*, Association Suisse des Electriciens, vol. 27, Oct. 30, 1936, pp. 636–37.

1874. The Astatic Voltage Relay, **E. T. Norris.** *Electrician*, vol. 116, April 3, 1936, pp. 442–43.

1875. High-Speed Regulator in Industrial Installations (in German), **H. Happoldt.** *Elektrotechnische Zeitschrift*, vol. 58, March 4, 1937, pp. 233–35.

1876. Progress in the Construction and Application of High Speed Regulators (in German), **H. Happoldt.** *VDE Fachberichte*, vol. 9, 1937, pp. 162–64.

1877. Modern Valve Regulators (in German), **W. Jacobi.** *Zeitschrift fur technische Physik*, vol. 18, 1937, pp. 421–26.

1878. Carbon Resistance Regulators (in German), **A. Staininger.** *AEG Mitteilungen*, no. 11, Nov. 1937, pp. 414–16.

1879. The Small Size Brown Boveri Quick Acting Voltage Regulator, Type JB-1, for Alternating and Direct Currents, **W. Marolf.** *Brown Boveri Review*, vol. 25, Nov. 1938, pp. 241–43.

1880. Selsyns for Remote Transmission of Angular Displacement (in Russian), **G. L. Shturman.** *Vestnik Elektroprommishlennosti*, no. 7, 1938, pp. 18–27.

1881. Recent Developments in Automatic Regulation. *Engineer*, vol. 166, July 1, 1938, pp. 18–20.

1882. A Method of Reducing Sparking at Voltage Regulator Contacts, **F. G. Spreadbury.** *Electrician*, vol. 120, Jan. 7, 1938, pp. 3–4.

1883. Friction Wheel Drives for Control, Measurement, and Computation Mechanisms (in German), **A. Kuhlenkamp.** *Zeitschrift des Vereines deutscher Ingenieure*, vol. 83, 1939, pp. 677–83.

1884. The Elements of Pendulum Dampers, **R. W. Zdanowich, T. S. Wilson.** *Proceedings*, Institution of Mechanical Engineers, vol. 143, 1940, pp. 182–210.

1885. Regulating Devices, **C. R. Hanna, R. H. Wright.** *Iron and Steel Engineer*, vol. 18, July 1941, pp. 29–38.

1886. Technique of Regulating-Gear Construction (in German), **W. Oppelt.** *Zeitschrift des Vereines deutscher Ingenieure*, vol. 85, Feb. 22, 1941, pp. 191–94.

1887. An Electro-Pneumatic Regulator with Photoelectric Compensation (in German), **E. Weis.** *Elektrotechnische Zeitschrift*, vol. 62, Dec. 18, 1941, pp. 975–79.

1888. Voltage-Regulating Inverse Time Relay, **H. J. Carlin.** *Electrical World*, vol. 118, Oct. 17, 1942, pp. 102, 104–05.

1889. Electric Measuring Devices for Regulating Systems (in German), **E. Dahnken.** *Elektrotechnische Zeitschrift*, vol. 64, 1943, pp. 319–23, 344–46.

1890. Pneumatic Vs. Electrical Automatic Control, **E. L. Stilson.** *Chemical and Metallurgical Engineering*, vol. 50, May 1943, pp. 137–39.

1891. Automatic Control, **E. T. Norris.** *Electrician*, vol. 132, June 30, 1944, pp. 555–58. Astatic relay.

1892. Position Control, **L. R. Fink.** *General Electric Review*, vol. 47, Dec. 1944, pp. 40–44. Selsyn applications.

1893. Electronic Regulation of Industrial Processes, **S. L. Burgwin.** *Instruments*, vol. 17, June 1944, pp. 328–30, 369.

1894. Electronic Tools for Process Control Applications, **H. D. Middel.** *Electrical World*, vol. 123, April 14, 1945, pp. 103–05.

1895. Electronic Control for Magnetic Clutches, **R. L. Jaeschke.** *Electronics*, vol. 18, Aug. 1945, pp. 102–06.

1896. The Solution of Instrumentation Problems by the Pneumatic Null Balance Method, **C. B. Moore.** *Instruments*, vol. 18, Sept. 1945 p 598–603.

1897. Analysis and Design of a D-C Selsyn System, **Joseph Manildi.** *AIEE Transactions (Electrical Engineering)*, vol. 64, July 1945, pp. 512–16.

1898. A Time Basis Proportioning Controller, **A. A. Orning.** *Review of Scientific Instruments*, vol. 16, May 1945, pp. 129–30.

1899. Electronic Mechanisms for Measurement and Control in Plant and Laboratory, **T. A. Cohen.** *Instruments*, vol. 18, April 1945, pp. 228–33, 248, 250.

1900. Comparisons of Force-Balance and Position-Balance Control Mechanisms, **W. B. Heinz.** *Instruments*, vol. 18, July 1945, pp. 456–60.

1901. Selsyn Design and Application, **T. C. Johnson.** *AIEE Transactions (Electrical Engineering)*, vol. 64, Oct. 1945, pp. 703–08.

1902. Small Two-Phase Motor. *Electrician*, vol. 135, Nov. 30, 1945, pp. 599–600.

1903. Valve Characteristics in Automatic Control, **S. D. Ross.** *Industrial and Engineering Chemistry*, Industrial Edition, vol. 38, Sept. 1946, pp. 878–84.

1904. Precision Autosyns for Servo-Systems, **J. P. Glass, P. F. Bechberger.** *Aeronautical Engineering Review*, vol. 5, June 1946, pp. 5–10.

1905. Electrical Accuracy of Selsyn Generator-Control Transformer System, **Harold**

Chestnut. *AIEE Transactions (Electrical Engineering)*, vol. 65, Aug.-Sept. 1946, pp. 570–76.

1906. Prime Relays for Automatic-Control Systems, **M. F. Behar.** *Instruments*, vol. 19, Aug. 1946, pp. 446–49.

1907. Variable Speed Metadyne (in Italian), **A. Carrer.** *Energia Elettrica*, vol. 24, Oct. 1947, pp. 465–70.

1908. Vane-Actuated Controller, **W. H. Wannamaker, Jr.** *Electronics*, vol. 20, June 1947, pp. 117–19.

1909. A Two Position Proportional Controller, **W. F. Abbott.** *Journal of Scientific Instruments*, vol. 24, July 1947, pp. 179–81.

1910. An Air Operated Automatic Controller. *Engineer*, vol. 184, Aug. 22, 1947, pp. 171–73.

1911. Data-Transmission Systems, **J. Bell.** *Journal*, Institution of Electrical Engineers, vol. 94, pt. IIA, no. 2, 1947, pp. 222–35.

1912. Modern Synchros, **J. L. Everett.** *Machine Design*, vol. 19, April 1947, pp. 135–40.

1913. Electronic Circuits for Control of Clutch Type Servomechanisms, **F. E. Edwards, Jr.** *Proceedings*, National Electronics Conference, vol. 4, 1948, pp. 54–58.

1914. Automatic Regulators, System VTI (in Russian), **V. D. Mironov.** *Elektricheskie Stantsii*, no. 7, 1948, pp. 8–13.

1915. The Derivative Controller, **V. V. Tivy.** *Petroleum Processing*, vol. 3, July 1948, pp. 679–88.

1916. Air-Operated Automatic Controllers; Principles Used in the Principal Types, **W. G. Holzbock.** *Instruments*, vol. 21, Aug. 1948, pp. 710–14.

1917. The Derivative Controller, **V. V. St. L. Tivy.** *Instruments*, vol. 21, Dec. 1948, pp. 1096–99, 1130.

1918. A Packaged Servomechanism, **W. C. Robinette.** *Electronics*, vol. 21, Jan. 1948, pp. 100–06.

1919. A Comparison of Small and Medium Power Electric Servomotors, **R. S. Edwards.** *Instruments*, vol. 21, Dec. 1948, pp. 1137–41.

1920. The Primary Element Response, **M. F. Behar.** *Instruments*, vol. 21, Aug. 1948, pp. 691–98.

1921. D-C Operated Servo Amplifier, **S. Wald.** *Radio-Electronic Engineering*, vol. 11, Aug. 1948, pp. 14–15, 28.

1922. An Hydraulic Torque Amplifier (in German), **H. Wilcke.** *Zeitschrift des Vereines deutscher Ingenieure*, vol. 91, 1949, p. 115.

1923. Operating Characteristics of 2-Phase Servomotors, **R. J. W. Koopman.** *AIEE Transactions*, vol. 68, pt. I, 1949, pp. 319–29.

1924. Process Control Valves, **N. B. Nichols, J. G. Ziegler.** *Machine Design*, vol. 21, Jan. 1949, pp. 129–32, 178, 180.

1925. The Problem of the Inertia of Separately Excited D-C Servomotors (in Russian), **I. Ya. Lekhtman.** *Elektrichestvo*, no. 10, Oct. 1949, pp. 49–54.

1926. Selecting Electronic Servomotors, **R. S. Edwards.** *Machine Design*, vol. 21, Jan. 1949, pp. 104–09.

1927. Unorthodox Pneumatic Circuits Make Simple Standard Devices Perform Extraordinary Jobs, **R. D. Webb.** *Instruments*, vol. 22, Aug. 1949, pp. 675–78.

1928. Simplified Instrumentation, **J. S. Leslie.** *Instruments*, vol. 22, Aug. 1949, pp. 670–74. Self-regulating valves.

1929. The Design of D-C Motors for Use in Automatic Control Systems, **Paul Lebenbaum, Jr.** *AIEE Transactions*, vol. 68, pt. II, 1949, pp. 1089–94.

1930. Electronic D-C to A-C Converter for Use in Servo Systems, **E. E. St. John.** *Proceedings*, Institute of Radio Engineers, vol. 37, Dec. 1949, pp. 1474–78.

1931. Comparison of Hydraulic and Electric Servo Motors, **G. C. Newton, Jr.** *Proceedings*, National Conference on Industrial Hydraulics, vol. 3, March 1950, pp. 64–85.

1932. The Oscillations of Pneumatic Amplifiers and its Effect on the Mode of Action (in German), **S. Wintergest.** *Technik*, vol. 5, Feb. 1950, pp. 82–83.

1933. Designing an Eddy Current Clutch Servo, **A. S. Gutman.** *Machine Design*, vol. 22, 1950, pp. 109–15, 154.

1934. Static Accuracy Performance of the Selsyn Generator Control-Transformer System, **G. Kronacher.** *AIEE Transactions*, vol. 69, pt. I, 1950, pp. 645–54.

1935. Designing Amplifiers for Servomechanisms, **R. Herst.** *Electrical Manufacturing*, vol. 46, July 1950, pp. 88–93, 188, 190, 192, 194.

1936. Anti-Hunt Servo Amplifier, **J. F. Engelberger.** *Electrical Manufacturing*, vol. 45, Feb. 1950, pp. 111–16.

1937. "Balanced" and "Variable-Linked" Automatic Reset, **C. H. Gest.** *Instruments*, vol. 24, Nov. 1951, 1292–94.

1938. Synchro Data Switching Circuit, **J. Corwin, S. Adler.** *Electronics*, vol. 24, Jan. 1951, pp. 112–13.

1939. Investigation of a Vibration-Type Acceleration Regulator (in Russian), **B. P. Petrov.** *Elektrichestvo*, no. 6, June 1951, pp. 47–51.

1940. Electro-Hydraulic Control and Regulating Mechanisms (in German), **O. Grebe.** *AEG Mitteilungen*, vol. 41, May-June 1951, pp. 101–03.

1941. The Control Valve in Operation, **W. H. Kidd, G. A. Philbrick.** *Instruments*, vol. 24, 1951, pp. 1494–502.

1942. Transient Response of Small 2-Phase Induction Motors, **A. M. Hopkin.** *AIEE Transactions*, vol. 70, pt. I, 1951, pp. 881–86.

1943. Transfer Function for a 2-Phase Induction Servo Motor, **Lloyd O. Brown, Jr.** *AIEE Transactions*, vol. 70, pt. II, 1951, pp. 1890–93.

1944. 2-Phase A-C Servo Motor Operation for Varying Phase Angle of the Control Winding Applied Voltage, **Mark A. Steinhacker, Wilbur E. Meserve.** *AIEE Transactions*, vol. 70, pt. II, 1951, pp. 1987–93.

1945. Analysis of the Drag-Cup A-C Tachometer by Means of 2-Phase Symmetrical Components, **R. H. Frazier.** *AIEE Transactions*, vol. 70, pt. II, 1951, pp. 1894–906.

1946. Pneumatic Operators for Throttling Control, **D. P. Eckman.** *Instruments*, vol. 24, Dec. 1951, pp. 1430–33, 1490.

1947. Elimination of Brush Ripple in D-C Tachometer-Generators Used in Servomechanisms, **J. C. West, T. W. Hey.** *Journal of Scientific Instruments*, vol. 28, Jan. 1951, pp. 18–20.

1948. A Phase Sensitive Detector Circuit Having High Balance Stability, **N. A. Schuster.** *Review of Scientific Instruments*, vol. 22, April 1951, pp. 254–55.

1949. Performance Analysis of Butterfly Valves, **S. D. Cohn.** *Instruments*, vol. 24, 1951, pp. 880–84.

Dynamo Amplifiers

1950. Elementary Theory of the Static Operation of the Metadyne (in French), **J. M. Pestarini.** *Revue Generale de l'Electricite*, vol. 27, 1930, pp. 355–65, 395–406.

1951. Theory of the Dynamic Operation of the Metadyne (in French), **J. M. Pestarini.** *Revue Generale de l'Electricite*, vol. 28, 1930, pp. 227–37, 260–69.

1952. Metadynes and Their Derivatives (in French), **J. M. Pestarini.** *Revue Generale de l'Electricite*, vol. 28, 1930, pp. 813–20, 851–63, 900–07.

1953. Dynamoelectric Amplifier for Power Control, **E. F. W. Alexanderson, M. A. Edwards, K. K. Bowman.** *AIEE Transactions*, vol. 59, 1940, pp. 937–39, 1136.

1954. The Design Characteristics of Amplidyne Generators, **Alec Fisher.** *AIEE Transactions*, vol. 59, 1940, pp. 939–44, 1135.

1955. Industrial Applications of Amplidyne Generators, **D. R. Shoults, M. A. Edwards, F. E. Crever.** *AIEE Transactions*, vol. 59, 1940, pp. 944–49, 1136–37.

1956. Application of the Metadyne to the Electric Control of Rolling Mills (in Italian), **J. Borriello.** *Elettrotecnica*, vol. 28, Jan. 25, 1941, pp. 22–37.

1957. Development of the D-C Cross-Field Machine (in German), **L. Monath.** *Elektrotechnische Zeitschrift*, vol. 63, Jan. 15, 1942, pp. 23–30.

1958. Rototrol—A Versatile Electrical Regulator, **W. H. Formhals.** *Westinghouse Engineer*, vol. 2, May 1942, pp. 51–4.

1959. Steady-State Theory of the Amplidyne Generator, **Troy D. Graybeal.** *AIEE Transactions (Electrical Engineering)*, vol. 61, Oct. 1942, pp. 750–56.

1960. Fundamental Principles of Amplidyne Applications, **F. E. Crever.** *AIEE Transactions (Electrical Engineering)*, vol. 62, Sept. 1943, pp. 603–06.

1961. The Amplidyne System of Control, **E. F. W. Alexanderson, M. A. Edwards, K. K. Bowman.** *Proceedings*, Institute of Radio Engineers, vol. 32, Sept. 1944, pp. 513–20.

1962. Improvements in the Connections of the "Figure-Eight" Metadyne (in Italian), **A. Carrer.** *Elettrotecnica*, vol. 31, Jan. 10, 1944, p. 12.

1963. Contribution to the Theory of the Amplidyne (in German), **H. Sequenz.** *Elektrotechnik und Maschinenbau*, vol. 62, April 14, 1944, pp. 173–79. Considers the general, cross-field, d-c machine.

1964. Fundamentals of the Amplidyne Generator, **J. L. Bower.** *AIEE Transactions (Electrical Engineering)*, vol. 64, 1945, pp. 873–81.

1965. Rototrol Regulating Systems, **A. W. Kimball.** *Iron and Steel Engineer*, vol. 22, Nov. 1945, pp. 80–86.

1966. Industrial Application of Rototrol Regulators, **W. R. Harris.** *AIEE Transactions (Electrical Engineering)*, vol. 65, March 1946, pp. 118–23.

1967. The Amplidyne, **E. C. Barwick.** *BTH Activities*, vol. 19, April 1946, pp. 48–51.

1968. The Amplidyne Electrical Control System. *Engineering*, vol. 162, Aug. 2, 1946, pp. 103–05.

1969. Electric Drive for Reversible Rolling Mill with Amplidyne Control (in Russian), **M. V. Meerov, E. L. Ettinger.** *Vestnik Elektropromishlennosti*, vol. 17, no. 4, 1946, pp. 5–10.

1970. Excitation Period of a "Regulex" (in Russian), **F. A. Goryainov.** *Electrichestvo*, no. 12, 1946, pp. 59–61. Analysis of a 2-field exciter.

1971. Electromechanical Amplifiers of the All-Russian Electrical Institute (in Russian), **Y. S. Epshtein.** *Elektrichestvo*, no. 11, 1946, pp. 59–62. A survey of Russian designed amplidynes.

1972. Exciter with Brush-Shifting for Continuous Regulation of Ward-Leonard Drives (in German), **F. Fiedler.** *Elektrotechnik und Maschinenbau*, vol. 63, Nov.-Dec. 1946, pp. 251–54.

1973. Two-Stage Rototrol for Low-Energy Regulating Systems, **A. W. Kimball.** *AIEE Transactions*, vol. 66, 1947, pp. 1507–11.

1974. Rotating Stability Regulators for Synchronous Motor Drives, **W. Schaelchlin.** *AIEE Transactions*, vol. 66, 1947, pp. 884–87.

1975. The Multistage Rototrol, **M. M. Liwschitz.** *AIEE Transactions*, vol. 66, 1947, pp. 564–68.

1976. Amplidyne Regulating Systems, **B. Adkins.** *Journal*, Institution of Electrical Engineers, vol. 94, pt. 2A, 1947, pp. 49–60.

1977. Rototrol and its Applications, **E. Frisch.** *Westinghouse Engineer*, vol. 7, July 1947, pp. 121–27.

1978. Leonard System with Amplidyne Exciter for a Limited Torque of the Motor when at Rest (in Russian), **V. P. Nikitin, N. P. Kunitskii.** *Elektrichestvo*, no. 7, July 1947, pp. 47–51.

1979. Amplifying Dynamos. The Amplidyne (in French), **A. Valentin.** *Bulletin*, Societe Francaise des Electriciens, vol. 8 (series 6), June 1948, pp. 304–28.

1980. Calculation of the Magnetic Circuit in Electromechanical Amplifiers (in Russian), **F. A. Goryainov, G. K. Salgus.** *Elektrichestvo*, no. 9, Sept. 1948, pp. 27–30.

1981. Electromechanical Amplifiers as an Element in Control Systems (in Russian), **N. M. Yakimenko.** *Electrichestvo*, no. 9, Sept. 1948, pp. 20–26. Analysis of several amplidyne regulating systems.

1982. The Rototrol (in French), **J. Helot.** *Bulletin*, Societe Francaise des Electriciens, vol. 9, July 1949, pp. 328–42.

1983. Electrical Analogue of a 2-Stage Rototrol, **James T. Carleton.** *Electrical Engineering*, vol. 68, May 1949, p. 410.

1984. The Dynamoelectric Amplifier—Class A Operation, **Robert M. Saunders.** *AIEE Transactions*, vol. 68, pt. II, 1949, pp. 1368–73.

1985. An Analysis of Rotating Amplifiers, **Bernard Litman.** *AIEE Transactions*, vol. 68, pt. II, 1949, pp. 1111–17.

1986. Asynchronous Short-Circuited Regulating Machine of Low Power (in Russian), **G. M. Kasprzhak.** *Elektrichestvo*, no. 2, Feb. 1949, pp. 63–67. Operating characteristics of a 2-phase servomotor.

1987. The Amplidyne Generator—Its Performance and Design, **M. S. Hoffenberg.** *Transactions*, South African Institute of Electrical Engineers, vol. 40, Aug. 1949, pp. 175–91.

1988. Motor Regulator with Critical Self-Excitation (in Russian), **S. R. Pyasetskii.** *Elektrichestvo*, no. 8, Aug. 1949, pp. 10–15. D-c generator with critical self-excitation having additional field windings for regulation purposes.

1989. Amplidyne Control of Tension in the Metal Industries, **W. Spence.** *BTH Activities*, vol. 20, Nov.-Dec. 1949, pp. 185–89.

1990. The Magnavolt Exciter—A Rotating Amplifier, **E. A. Binney.** *English Electric Journal*, vol. 11, March 1950, pp. 71–76.

1991. The Application of Magnavolt (Rotating Amplifier), **A. Asbury,** *English Electric Journal*, vol. 11, March 1950, pp. 76–82.

1992. Static States of an Electric Machine Regulator with Longitudinal Field (in Russian), **F. A. Goryainov.** *Isvestiya Akademii Nauk, SSSR.* Otdelenie Tekhnicheskikh Nauk, no. 2, Feb. 1950, pp. 176–86.

1993. Electric Machine Regulators with Critical Self-Excitation (in Russian), **E. V. Nitusov.** *Isvestiya Akademii Nauk, SSSR.* Otdelenie Tekhnicheskikh Nauk, no. 2, Feb. 1950, pp. 161–66.

1994. The Amplidyne. Modern Cross-Field Machines and Their Application for Industrial Drives (in German), **H. Renker.** *VDE Fachberichte*, vol. 14, 1950, pp. 33–38.

1995. The Amplidyne in the Motoring State (in Russian), **V. A. Borisov.** *Elektrichestvo*, no. 8, Aug. 1950, pp. 21–27.

1996. Exciter Series Winding in Conjunction with High-Speed Regulator, **S. E. Hedstrom, K. E. Johansson.** *ASEA Journal*, vol. 23, Nov. 1950, pp. 157–58.

1997. Dynamoelectric Amplifiers, **R. M. Saunders.** *Electrical Engineering*, vol. 69, Aug. 1950, pp. 711–16.

1998. D-C Generator Amplifier, **J. C. West.** *Electrical Review*, vol. 147, Nov. 24, 1950, pp. 819–22.

1999. Working Results of the New Winding Motor with Amplidyne Control (in French), **R. Jung.** *Bulletin*, Societe Belge des Electriciens, vol. 67, April-June 1951, pp. 65–78.

2000. The Magnicon, **J. Griffin.** *Electrical Times*, vol. 119, 1951, April 12, pp. 596–99, April 19, pp. 646–48.

2001. Use of Controlled D-C Generators in Excavators (in Russian), **M. I. Kraitsberg.** *Elektrichestvo*, no. 4, April 1951, pp. 37–43.

2002. Constant-Current, Amplifying, and Regulating Machines for D-C (Metadyne, Amplidyne and Rototrol) (in German), **E. Kubler.** *Elektrotechnische Zeitschrift*, vol. 72, Nov. 1, 1951, pp. 623–28.

2003. The Rototrol. A New D-C Electrical Machine (in German), **F. Tschappu.** *Bulletin*, Association Suisse des Electriciens, vol. 42, Oct. 6, 1951, pp. 796–805.

Experimental Studies

2004. An Experimental Study of Regulation **N. A. Tenot.** *Mesures*, no. 28, May 1938. (Translation in *Technical Memoranda on Automatic Control*, Industrial Instrument Division, Scientific Apparatus Makers of America, Chicago, Ill., 1938).

2005. Experimental Studies of Automatic Control, **J. C. Peters.** *Transactions*, American Society of Mechanical Engineers, vol. 64, April 1942, pp. 247–55.

2006. An Apparatus for Investigating the Behavior of Regulating Devices, **J. von Freudenreich.** *Brown Boveri Review*, vol. 31, July 1944, pp. 228–32.

2007. Electrical-Analogy Method for Fundamental Investigations in Automatic Control, **D. P. Eckman, W. H. Wannamaker.** *Transactions*, American Society of Mechanical Engineers, vol. 67, Feb. 1945, pp. 81–86.

2008. Analysis of Problems in Dynamics by Electronic Circuits, **J. R. Ragazzini, R. H. Randall, F. A. Russell.** *Proceedings*, Institute of Radio Engineers, vol. 35, 1947, pp. 442–52.

2009. Laboratory Aids for Electromechanical System Development, **George C. Newton, Jr., W. T. White.** *AIEE Transactions*, vol. 66, 1947, pp. 315–21.

2010. An Instrument to Measure Servomechanism Performance, **H. I. Tarpley.** *Review of Scientific Instruments*, vol. 18, Jan. 1947, pp. 39–43.

2011. Methods of Testing Small Servomechanisms and Data-Transmission Systems, **E. W. Marchant, A. C. Robb.** *Journal*, Institution of Electrical Engineers, vol. 94, pt. IIA, May 1947, pp. 292–97.

2012. Electronic Servo Simulators, **F. C. Williams, F. J. U. Ritson.** *Journal*, Institution of Electrical Engineers, vol. 94, pt. IIA, May 1947, pp. 112–24.

2013. Designing Industrial Controllers by Analogs, **G. A. Philbrick.** *Electronics*, vol. 21, June 1948, pp. 108–11.

2014. Frequency Response Characteristics of Recording Instruments, **T. D. Graybeal.** *AIEE Transactions*, vol. 67, pt. I, 1948, pp. 755–66.

2015. Signal Generators for Servo System Measurement, **C. F. White.** *Proceedings*, National Electronics Conference, vol. 4, 1948, pp. 59–71.

2016. Evaluating Servomechanisms Performance, **G. M. Attura.** *Proceedings*, National Electronics Conference, vol. 4, 1948, pp. 72–90.

2017. Investigation of Non-Linear Systems of Automatic Regulation by Method of Combination of Tested Objects with an Electrointegrator (in Russian), **G. L. Polisar.** *Isvestiya Akademii Nauk, SSSR.* Otdelenie Tekhnicheskikh Nauk, no. 3, March 1949, pp. 384–95.

2018. Application of the California Institute of Technology Electric Analog Computer to Nonlinear Mechanics and Servomechanisms, **G. D. McCann, C. H. Wilts, B. N. Locanthi.** *AIEE Transactions*, vol. 68, pt. I, 1949, pp. 652–60.

2019. Summary of Transformations Useful in Constructing Analogs of Linear Vibration Problems, **James P. Corbett.** *AIEE Transactions*, vol. 68, pt. I, 1949, pp. 661–64.

2020. The Servograph—A New Electrical Graph Recorder. *Electronic Engineering*, vol. 22, May 1950, pp. 181–82.

2021. Phase Calibrated Variable-Frequency Supply for Testing of Servomechanisms, **D. Morris.** *Proceedings*, Institution of Electrical Engineers, vol. 97, pt. 2, Feb. 1950, pp. 37–45, 483–84.

2022. Analogue Computers for Servo Problems, **D. McDonald.** *Review of Scientific Instruments*, vol. 21, Feb. 1950, pp. 154–57.

2023. Standardized Parts Speed Servomechanism Development, **J. G. Cunningham.** *Product Engineering*, vol. 21, Feb. 1950, pp. 122–23.

2024. Experimental Frequency Analysis of Servo Elements, **A. Garde, E. Persson.** *ASEA Journal*, vol. 23, Dec. 1950, pp. 163–66.

2025. Modern Servomechanism Testers, **G. A. Korn, T. M. Korn.** *Electrical Engineering*, vol. 69, Sept. 1950, pp. 814–16.

2026. A Theory of Models for Regulator Circuits (in German), **H. Hochrainer.** *Oesterreichisches Ingenieur-Archiv*, vol. 4, Nov. 1950, pp. 376–87.

2027. Electronic Phasemeter for Stability Tests, **R. Renchon.** *Paper 304*, International Conference on Large Electric High-Tension Systems, 1950.

2028. Frequency Response of Instruments, **R. J. W. Koopman.** *Instruments*, vol. 23, May 1950, pp. 506–08.

2029. Indicating Instruments at the Servomechanism Frequencies, **Wilson S. Pritchett, Robert M. Saunders.** *AIEE Transactions*, vol. 69, pt. II, 1950, pp. 980–85.

2030. Vector Measuring Detector Instruments and Their Calculation (in Russian), **S. P. Inozemtsev.** *Elektrichestvo*, no. 10, Oct. 1950, pp. 61–6.

2031. Electrical Representation of the Inert Behavior of Large Machine Systems (in German), **A. Ganglbauer.** *Elektrotechnik und Maschinenbau*, vol. 68, Feb. 15, 1951, pp. 73–82.

2032. The Electro-Analogue, An Apparatus for Studying Regulating Systems. **J. M. L. Janssen, L. Ensing.** *Philips Technical Review*, vol. 12, March 1951, pp. 257–71; May 1951, pp. 319–35.

2033. Design and Analysis of a Conservative Dynamic Load Simulator, **E. H. Gamble, B. W. Hatten.** *Journal of Applied Physics*, vol. 22, Oct. 1951, pp. 1250–57.

2034. A Model Electrical Control Circuit of Very Long Time of Operation (in German), **O. Schafer.** *Elektrotechnische Zeitschrift*, vol. 72, June 15, 1951, pp. 379–81.

Miscellaneous Regulators

2035. Mechanically-Controlled Bolometer (in German), **H. Sell.** *Zeitschrift fur technische Physik*, vol. 15, 1934, pp. 112–17, 129–35.

2036. Photoelectric Guiding of Astronomical Telescopes, **A. E. Whitford, G. E. Kron.** *Review of Scientific Instruments*, vol. 8, 1937, pp. 78–82.

2037. Regulating Apparatus for Automatic Control of Central Heating and Air Conditioning (in French), **A. Antoni.** *Genie Civil*, vol. 115, 1939, Sept. 23, pp. 251–54; Sept. 30, 1939, pp. 269–71; Oct. 7, 1939, pp. 277–80.

2038. A Light Regulator, **B. Chance.** *Electronics*, vol. 13, Feb. 1940, pp. 24–25.

2039. Regulation of Blood Circulation (in German), **K. Kramer.** *Zeitschrift des Vereines deutscher Ingenieure*, vol. 85, no. 4, 1941, pp. 97–99.

2040. Voltage Regulator for a Densitometer Lamp, **S. L. Parsons,** *Journal*, Optical Society of America, vol. 32, March, 1942, pp. 153–55.

2041. Automatic Capacity Control, **W. L. McGrath.** *Refrigerating Engineering*, vol. 43, March 1942, pp. 1–5 April 1942, pp. 1–6.

2042. Method of Stabilizing High Voltages (in Italian), **G. Occhialini.** *Ricerca Scientifica Ricostrusione*, vol. 13, June-July 1942, pp. 319–21.

2043. Regulated Rectifiers in Telephone Offices, **D. E. Trucksess.** *AIEE Transactions* (*Electrical Engineering*), vol. 61, 1942, pp. 613–17.

2044. A Load-Regulating System for Synchronous Converters, **L. H. Fietemeyer.** *Transactions*, Electrochemical Society, vol. 83, 1943, pp. 101–11.

2045. Some Experiments on the Automatic Correction of Power Factor to a Predetermined Value, **H. T. Aspinall.** *Transactions*, South African Institute of Electrical Engineers, vol. 34, Sept. 1943, pp. 113–42.

2046. Characteristics of Electric Apparatus Used on Electrotinning Lines, **G. E. Stoltz, W. G. Cook.** *Transactions*, Electrochemical Society, vol. 84, 1943, pp. 259–77.

2047. Electronics Applied to Heat Transfer Tests, **R. V. Brown.** *Electronics*, vol. 16, July 1943, pp. 113–15.

2048. Select Right Instruments in Setting up Automatically Controlled Plating Processes, **D. M. Nielsen.** *Steel*, vol. 113, Nov. 15, 1943, pp. 118, 120, 160, 162.

2049. Apparatus for Automatic Control of Electrodeposition with Graded Cathode Potential, **C. W. Caldwell, R. C. Parker, H. Diehl.** *Industrial and Engineering Chemistry*, (Analytical Edition) vol. 16, Aug. 1944, pp. 532–35.

2050. Connections for Compensating Large Electromagnetic Time Constants (in German), **A. Leonhard.** *Elektrotechnische Zeitschrift*, vol. 65, June 29, 1944, pp. 253–57.

2051. Electrically Controlled Dry-Disc Rectifier, **Allen Rosenstein, H. N. Barnett.** *AIEE Transactions (Electrical Engineering)*, vol. 63, Jan. 1944, pp. 21–23.

2052. Better Welds Through Regulated Welding Current, **B. Cooper.** *Welding Journal*, vol. 23, Jan. 1944, pp. 5–10.

2053. Automatic Digester Control for Alkaline Pulp Cooking, **H. O. Ehrisman.** *Paper Trade Journal*, vol. 119 (TAPPI Section) Nov. 16, 1944, pp. 195–98.

2054. Selection and Application of Automatic Control for Capacitors, **T. W. Schroeder, W. C. Bloomquist.** *General Electric Review*, vol. 48, Oct. 1945, pp. 7–11; Dec. 1945, pp. 22–31; vol. 49, March 1946, pp. 37–41.

2055. New Developments in Combination Controls, **J. W. Kelly.** *Transactions*, American Society of Mechanical Engineers, vol. 68, 1946, pp. 701–06.

2056. Electronic Control of Frequency Converter Sets for Testing Aircraft Models, **G. W. Heumann, W. F. Strong.** *AIEE Transactions*, vol. 65, (Supplement), Dec. 1946, pp. 931–39.

2057. Some Characteristics of a Human Operator, **J. A. V. Bates,** *Journal*, Institution of Electrical Engineers, vol. 94, pt. 2A, 1947, pp. 298–304.

2058. The Nature of the Operator's Response in Manual Control, **A. Tustin.** *Journal*, Institution of Electrical Engineers, vol. 94, pt. 2A, 1947, pp. 190–202.

2059. Automatically Controlled Copper-Oxide Rectifiers for Electroplating and Anodizing Applications, **Joseph J. Buckley.** *AIEE Transactions*, vol. 66, 1947, pp. 181–84.

2060. Avostat Controlled Dry Plate Rectifiers with Battery Reserve, **J. Lamm.** *ASEA Journal*, vol. 20, Jan. 1947, pp. 3–9.

2061. Influence of Reactive Feedback Networks on the Response of Galvanometers, **P. Savic.** *Nature*, vol. 162, Oct. 9, 1948, pp. 569–70.

2062. An Electronic Intensity Regulator for a Hydrogen Discharge Tube, **W. L. Pondrom, W. W. Robertson.** *Review of Scientific Instruments*, vol. 19, Sept. 1948, pp. 561–64.

2063. Automatic Control of the Feeders of a District Heating System (in Russian), **A. P. Safonov.** *Elektricheskie Stantsii*, no. 11, Nov. 1949, pp. 22–4.

2064. Circuit and Constructional Details of the Precision Electronic pH Control System, **J. E. Breeze.** *Publication no.* 1889, National Research Council of Canada, Feb. 1949.

2065. Servo-Controlled Tensile Strength Tester, **G. S. Burr.** *Electronics*, vol. 22, May 1949, pp. 101–05.

2066. Lateral Feedback Disc Recorder, **G. R. Yenzer.** *Audio Engineering*, vol. 33, Sept. 1949, pp. 22–26, 44, 45.

2067. The Automatic Control of Lead-Acid-Battery Charging Equipment, **R. A. Harvey.** *Proceedings*, Institution of Electrical Engineers, vol. 96, pt. 2, Aug. 1949, pp. 607–23.

2068. The Application of Negative Feedback to Electro-Acoustic Systems (in French), **P. Chavasse, P. Poincelot.** *Comptes Rendus*, l'Academie des Sciences, vol. 230, Feb. 6, 1950, pp. 529–30.

2069. The Application of Feedback to an Electromechanical Transducer for Seismograph Testing, **P. M. Honnell.** *Bulletin*, Seismological Society of America, vol. 40, July 1950, pp. 217–31.

2070. Negative Feedback Valve-Voltmeters for D-C (in German), **W. Geyger.** *Archiv fur technisches Messen*, no. 170, March 1950, pp. T31–33, Ref. J8335–5.

2071. Automatic Control of Inaccessible Terminal Voltages, **R. L. Cosgriff, E. H. Gamble.** *Proceedings*, National Electronics Conference, vol. 6, 1950, pp. 434–40. Equivalent circuit used to regulate air-gap flux in 2-phase motor.

2072. Electronic Equipment for Regulating the Intensity of Fluorescent Lighting Installations (in German), **W. Gruber.** *Bulletin*, Association Suisse des Electriciens, vol. 41, Dec. 23, 1950, pp. 955–57.

2073. Synchronized Air-Borne Camera System, **V. J. White, S. J. Horwitz.** *Electrical Engineering*, vol. 69, April 1950, pp. 324–27.

2074. Modern Electric Automatic Control Systems (in Italian), **C. Costadoni.** *Elettrotecnica*, vol. 37, March 10–25, 1950, pp. 82–95; April 12, 1950, pp. 126–48.

2075. Automatic Exposure Control, **G. Bruck, J. Higgins, J. Ward.** *Electronics*, vol. 23, May 1950, pp. 74–78.

2076. Electronic Control of Anesthesia, **R. G. Bickford.** *Electronics*, vol. 23, Sept. 1950, pp. 107–09.

2077. Feedback Controlled Calibrater for Phonograph Pickups, **J. G. Woodward.** *RCA Review*, vol. 11, 1950, pp. 301–09.

2078. Automatic Regulation of Power in High Frequency Heating Installations (in Russian), **A. V. Donskoi.** *Elektrichestvo*, no. 10, 1950, pp. 46–49.

2079. The Cascaded Binary Counter with Feedback, **G. F. Montgomery.** *Journal of Applied Physics*, vol. 22, June 1951, pp. 780–82.

2080. A Method of Keeping the Luminance of a Lamp Constant Without the Use of an Electric Meter, **R. W. G. Hunt.** *Journal of Scientific Instruments*, vol. 28, June 1951, pp. 180–81.

2081. A Note on Automatic Control for Maintaining Constant Intensity of a Light Source, **K. C. Wight.** *Journal of Scientific Instruments*, vol. 28, Sept. 1951, pp. 276–77.

2082. Some Engineering Aspects of the Mechanism of Body Control, **Robert Mayne.** *Electrical Engineering*, vol. 70, March 1951, pp. 207–12.

2083. Block Diagram Network Transformation, **T. D. Graybeal.** *Electrical Engineering* vol 70, Nov. 1951, pp. 985–90.

List of Periodicals

Acta Physica Austriaca, Vienna, Austria
Acta Physica Polonica, Cracow, Poland
AEG Mitteilungen, Berlin, Germany
Aeronautical Engineering Review, New York, N. Y.
AIEE Journal, New York, N. Y.
AIEE Transactions, New York, N. Y.
Alta Frequenza, Milan, Italy
American Journal of Physics, New York, N. Y.
Anales de Mecanica y Electricidad, Madrid, Spain
Annales de Radioelectricite, Paris, France
Annales de Telecommunication, Paris, France
Annales des Postes, Telegraphes et Telephones, Paris, France
Annales de l'Universite de Grenoble, Grenoble, France
Analytical Chemistry, Easton, Pa.
Applied Scientific Research, The Hague, Holland
Archiv der electrischen Uebertragung, Wiesbaden, Germany
Archiv fur das Eisenhuettenwesen, Dusseldorf, Germany
Archiv fur Elektrotechnik, Berlin, Germany
Archiv fur technisches Messen, Munich, Germany
Archiv fur Waermewirtschaft und Dampfkesselwesen, Berlin, Germany
Arkiv for Matemaik, Astronomi och Fysik, Stockholm, Sweden
ASEA Journal, London, England
Atti dell' Accademia delle Scienze di Torino, Turin, Italy
Audio Engineering, New York, N. Y.
Australian Journal of Applied Science, Melbourne, Australia
Automatic Electric Technical Journal, Chicago, Ill.
Avtomatika i Telemkhanika, Moscow, U.S.S.R.
AWA Technical Review, Sydney, Australia
B.B.C. Quarterly, London, England
Beama Journal, London, England
Bell Laboratories Record, New York, N. Y.
Bell System Technical Journal, New York, N. Y.
Bendix Radio Engineer, Baltimore, Md.
Blast Furnace and Steel Plant, Pittsburgh, Pa.
Brennstoff und Waermewirtschaft, Halle, Germany
Brennstoff-Waerme-Kraft, Dusseldorf, Germany
British Electrical and Allied Industries Research Association, London, England
British Journal of Radiology, London, England
Brown Boveri Company Nachrichten, Mannheim, Germany
Brown Boveri Review, London, England
BTH Activities, Rugby, England
Bulletin, Association des Ingenieurs Electriciens sortis de l'Institut Electrotechnique Montefiore, Liege, Belgium
Bulletin, Association des Chemistes, Paris, France
Bulletin, Association Suisse des Electriciens, Zurich, Switzerland
Bulletin, l'Academie des Sciences, Moscow, U. S. S. R.
Bulletin, National Bureau of Standards, Washington, D. C.
Bulletin Oerlikon, London, England
Bulletin, Seismological Society of America, Berkeley, California
Bulletin, Societe Belge des Electriciens, Marcinelle, Belgium
Bulletin, Societe Francaise des Electriciens, Paris, France
Bulletin, Technique de la Suisse Romande, Lausanne, Switzerland
Cables et Transmission, Paris, France
Canadian Journal of Research, Ottawa, Canada
Chaleur et Industrie, Paris, France
Charleroi-Jeumont Revue, Charleroi, Belgium
Chemical and Metallurgical Engineering, New York, N. Y.
Chemical Engineering Progress, New York, N. Y.
Chemie-Ingenieur Technik, Weinheim, Germany
Chemistry and Industry, London, England
Combustion, New York, N. Y.
Communication News, London, England
Communications, New York, N. Y.
Comptes Rendus Hebdomadaires des Seances de l'Academie des Sciences, Paris, France
Comptes Rendus de l'Academie des Sciences de l'URSS, Moscow, U.S.S.R.
Congres International de l'Electricite, Paris, France
Der Civilingenieur, Leipzig, Germany
Diesel Power, New York, N. Y.
Die Technik, Berlin, Germany
Doklady Akademii Nauk, SSSR, Moscow, U.S.S.R.
Electrical Communication, New York, N. Y.
Electrical Engineer and Merchandiser, Melbourne, Australia
Electrical Engineering, New York, N. Y.
Electrical Manufacturing, New York, N. Y.

Electrical Review, London, England
Electrical Times, London, England
Electrical World, New York, N. Y.
Electrichestvo, Moscow, U.S.S.R.
Electrician, London, England
Electric Journal, East Pittsburgh, Pa.
Electronic Engineering, London, England
Electronic Industries, New York, N. Y.
Electronics, New York, N. Y.
Electrotechnical Journal, Tokyo, Japan
Electro-techniek, The Hague, Holland
Elektrichestvo, Moscow, U.S.S.R.
Elektricheskie Stantsii, Moscow, U.S.S.R.
Elektrische Nachrichten-Technik, Berlin, Germany
Elektrizitaetswirtschaft, Berlin, Germany
Elektrosvyaz, Leningrad, U.S.S.R.
Elektrotechnicky Obzor, Prague, Czechoslovakia
Elektrotechnik, Berlin, Germany
Elektrotechnik und Maschinenbau, Vienna, Austria
Elektrotechnischer Anseiger, Berlin, Germany
Elektrotechnishe Zeitschrift, Berlin, Germany
Elektroteknisk Tidsskrift, Oslo, Norway
Elektro-und Radiotechnik, Vienna, Austria
Elettrotecnica, Milan, Italy
Energia Elettrica, Milan, Italy
Engineer, London, England
Engineering, London, England
Engineering and Boiler House Review, London, England
Engineering Journal, Montreal, Canada
Engineers' Digest, New York, N. Y.
English Electric Journal, Stafford, England
Ericsson Review, Stockholm, Sweden
Fachberichte des Verbandes deutscher Elektrotechniker, Berlin, Germany
Fernmeldetechnische Zeitschrift, Brunswick, Germany
Feinmechanik und Praezision, Berlin, Germany
Fordertechnik und Frachtverkehr, Halle, Germany
Forschung auf dem Gebiete des Ingenieurwesens, Berlin, Germany
Frequenz, Berlin, Germany
Funk und Ton, Berlin, Germany
Gas and Oil Power, London, England
Gas- und Wasserfach, Munich, Germany
GEC Journal, London, England
General Electric Review, Schenectady, N. Y.
General Radio Experimenter, Cambridge, Mass.
Genie Civil, Paris, France
Gesundheits-Ingenieur, Munich, Germany
Heating, Piping, and Air Conditioning, Chicago, Ill.
Helvetica Physica Acta, Basle, Switzerland
H. F. Electricite, Courants Faibles, Electronique, Brussels, Belgium
Hochfrequenztechnik und Elektroakustik, Leipzig, Germany
Houille Blanche, Grenoble, France
Hungarica Acta Physica, Budapest, Hungary
Indian Journal of Physics, Calcutta, India
Industria Italiana Elettrotecnica, Milan, Italy
Industrial and Engineering Chemistry, Easton, Pa.
Industrial Chemist, London, England
Ingenieur, The Hague, Holland
Ingenieur-Archiv, Berlin, Germany
Ingenioren, Copenhagen, Denmark
Instrument Practice, London, England
Instruments, Pittsburgh, Pa.
International Conference on Large Electric High-Tension Systems, Paris, France
Inzhenernii Sbornik Akademii Nauk, SSSR, Leningrad, U.S.S.R.
Iron and Steel Engineer, Pittsburgh, Pa.
Izvestiya Akademii Nauk, SSSR. Otdelenie Tekhnicheskikh Nauk, Moscow, U.S.S.R.
Izvestiya Elektropromnishlennosti Slabova Toka, Leningrad, U.S.S.R.
Journal, Acoustical Society of America, New York, N. Y.
Journal, American Chemical Society, Easton, Pa.
Journal, American Society of Navel Engineers, Washington, D. C.
Journal, British Institution of Radio Engineers, London, England
Journal de Physique et le Radium, Paris, France
Journal des Usines a Gaz, Paris, France
Journal, Franklin Institute, Philadelphia, Pa.
Journal, Institution of Electrical Engineers of Japan, Tokyo, Japan
Journal, Institute of Fuel, London, England
Journal, Institution of Electrical Engineers, London, England
Journal, Institution of Engineers, Sydney, Australia
Journal, Institution of Mechanical Engineers, London, England
Journal, Iron and Steel Institute, London, England
Journal, Junior Institution of Engineers, London, England
Journal of Applied Mechanics, New York, N. Y.
Journal of Applied Physics, New York, N. Y.
Journal of Dairy Research, London, England
Journal of Physical Chemistry, Baltimore, Md.
Journal of Research, Bureau of Standards, Washington, D. C.
Journal of Scientific Instruments, London, England
Journal of Technical Physics, Leningrad, U.S.S.R.
Journal of the Aeronautical Sciences, New York, N. Y.
Journal, Optical Society of AmericaNew York, N. Y.
Journal, Royal Aeronautical Society, London, England
Journal, Society of Motion Picture Engineers, New York, N. Y.
Journal, Textile Institute, Manchester, England
Koninklijk Institut van Ingenieurs, The Hague, Holland
Kraft och Ljus, Helsinki, Finland
Kwartalnik Telekomunikacyjny, Warsaw, Poland
L.S.E. Engineering Bulletin, London, England
Luftfahrtforshung, Munich, Germany
Machine Design, Cleveland, Ohio
Machinery, London, England
Mathematische Annalen, Leipzig, Germany
Mechanical Engineering, New York, N. Y.
Mechanical World, Manchester, England
Mesures, Paris, France
Metallurgia, Manchester, England
Metropolitan-Vickers Gazette, Manchester, England
Microtecnic, Lausanne, Switzerland
Mining Electrical and Mechanical Engineer, Manchester, England
Modern Power and Engineering, Toronto, Canada
National Advisory Committee for Aeronautics, Washington, D. C.
National Electric Light Association, New York, N. Y.
Nature, London, England
Nippon Electrical Communication Engineering, Tokyo, Japan
Nuovo Cimento, Bologna, Italy
Oil and Gas Journal, Tulsa, Okla.
Oesterreichisches Ingenieur Archiv, Vienna, Austria
Oesterreichische Zeitschrift fur Elektrizitaetswirtschaft, Vienna, Austria
Onde Electrique, Paris, France
Paper Industry and Paper World, Chicago, Ill.
Paper Trade Journal, New York, N. Y.
Petroleum Processing, New York, N. Y.
Petroleum Refiner, Houston, Texas
Philips Research Reports, Eindhoven, Holland
Philips Technical Review, Eindhoven, Holland
Philosophical Magazine, London, England
Philosophical Transactions, The Royal Society, London, England
Physica, The Hague, Holland
Physical Review, New York, N. Y.
Physikalische Zeitschrift, Leipzig, Germany
Physikalische Zeitschrift der Sowjetunion, Kharkov, U.S.S.R.
The Post Office Electrical Engineers' Journal, London, England
Plant Physiology, Lancaster, Pa.
Power, New York, N. Y.
Power and Works Engineering, London, England
Power Engineering, Chicago, Illinois
Power Generation, New York, N. Y.
Power Plant Engineering, Chicago, Ill.
Prikladnaya Matematika i Mekhanika, Moscow, U. S. S. R.
Proceedings, Cambridge Philosophical Society, London, England
Proceedings, Chemical Engineering Group, Society of the Chemical Industry, London, England
Proceedings, Institute of Radio Engineers, New York, N. Y.
Proceedings, Institution of Electrical Engineers, London, England
Proceedings, Institution of Mechanical Engineers, London, England
Proceedings, Institution of Radio Engineers, Sydney, Australia
Proceedings, Midwest Power Conference, Chicago, Ill.
Proceedings, National Conference on Industrial Hydraulics, Chicago, Ill.
Proceedings, National Institute of Sciences of India, Delhi, India
Proceedings, National Electronics Conference, Chicago, Ill.
Proceedings, Physical Society, London, England
Proceedings, The Royal Society, London, England
Proceedings, Third International Congress for Applied Mechanics,

Stockholm, Sweden
Product Engineering, New York, N. Y.
Promyshlennaya Energetika, Moscow, U.S.S.R.
Publicaciones de la Facultad de Ciencias Fisico-Matematicas, Universidad Nacional de la Plata, La Plata, Argentina
Publications, University of Technical Sciences, Budapest, Hungary
Quarterly of Applied Mathematics, Providence, R. I.
QST, West Hartford, Conn.
Radio-Electronic Engineering, Chicago, Ill.
Radio Engineering, New York, N. Y.
La Radio Francaise, Paris, France
Radiotekhnika, Moscow, U.S.S.R.
RCA Review, Princeton, N. J.
Refiner, Houston, Texas
Refrigerating Engineering, New York, N. Y.
Review of Scientific Instruments, New York, N. Y.
Revista Electrotecnica, Buenos Aires, Argentina
Revue Alsthom, Paris, France
Revue d'Acoustique, Paris, France
Revue de l'Electricite et de Mecanique, Paris, France
Revue Generale de l'Electricite, Paris, France
Ricerca Scientifica Ricostruzione, Rome, Italy
Ricerche di Ingegneria, Rome, Italy
Schweizer Archiv fur angewandte Wissenschaft und Technik, Solothurn, Switzerland
Schweizerische Bauzeitung, Zurich, Switzerland
Sheet Metal Industries, London, England
Shibaura Review, Tokyo, Japan
Siemens Zeitschrift, Erlangen, Germany
Steel, Cleveland, Ohio
Strowger Journal, Liverpool, England
Sylvania Technologist, Kew Gardens, N. Y.
Technik, Berlin, Germany
Teknisk Tidskrift, Stockholm, Sweden
Telecomunicazioni, Rome, Italy
Telefunken Zeitung, Berlin, Germany
Telegraphen-Fernsprech-Funk-und Fernsehtechnik, Berlin, Germany
Tele-Tech, New York, N. Y.
Textile Recorder, Manchester, England
Tijdschrift van het Nederlandsch Radiogenootschap, Baarn, Holland
Transactions, American Institute of Chemical Engineers, New York, N. Y.
Transactions, American Society of Mechanical Engineers, New York, N. Y.
Transactions, Electrochemical Society, New York, N. Y.
Transactions, Institute of Marine Engineers, London, England
Transactions, Institution of Engineers and Shipbuilders in Scotland, Glasgow, Scotland
Transactions, Institution of Naval Architects, London, England
Transactions, Instruments and Measurements Conference, Stockholm, Sweden
Transactions, Society of Instrument Technology, London, England
Transactions, South African Institute of Electrical Engineers, Johannesburg, South Africa
VDE Fachberichte, Wuppertal, Germany
Verein deutscher Ingenieure Zeitschrift, Berlin, Germany
Vestnik Elektropromyishlennosti, Moscow, U.S.S.R.
Waerme, Berlin, Germany
Water and Water Engineering, London, England
Welding Journal, New York, N. Y.
Werkstattstechnik und Werksleiter, Berlin, Germany
Westinghouse Engineer, Pittsburgh, Pa.
Wire and Wire Products, New York, N. Y.
Wireless Engineer, London, England
Wireless World, London, England
Wireless World and Radio Review, London, England
Wissenschaftliche Veroeffentlichungen aus den Siemens-Werken, Berlin, Germany
World Petroleum, Hoboken, N. J.
Zeitschrift des Vereines deutcher Ingenieure, Berlin, Germany
Zeitschrift fur angewandte Mathematik und Mechanik, Berlin, Germany
Zeitschrift fur angewandte Physik, Berlin, Germany
Zeitschrift fur Fernmeldetechnik, Berlin, Germany
Zeitschrift fur Hochfrequenztechnik, Berlin, Germany
Zeitschrift fur technische Physik, Leipzig, Germany
Zhurnal Tekhnicheskoi Physiki, Leningrad, U.S.S.R.

No Discussion

Backlash in a Velocity Lag Servomechanism

NATHANIEL B. NICHOLS
MEMBER AIEE

THE frequency response method of analysis of servomechanisms has been extensively applied in the analysis and synthesis of linear systems, and several studies have shown that useful results can be obtained in certain nonlinear cases. The application of the sinusoidal frequency response method to nonlinear systems has been based on the assumption that the input to the nonlinear element is sinusoidal and that the behavior of the complete system can be satisfactorily represented by considering only its fundamental Fourier series component. Tustin and Goldfarb applied this method to the analysis of servomechanisms having backlash and nonviscous friction.[1,2] Kochenburger has found good experimental agreement with the theoretical results of this method in several contactor servomechanisms.[3] He has shown that this method serves as a useful guide in designing appropriate linear equalizing networks to improve their performance. These networks allow the system to remain stable for smaller dead zones and also give a higher range of frequency over which the contactor servomechanism's output reproduces its input with small error. He used this method to compute the over-all frequency response for various amplitudes of the sinusoidal input to the system and showed that it was possible to obtain well damped performance as evidenced by a low resonance peak. Johnson has shown how the gain phase angle transfer locus may be used to indicate the presence of sustained constant amplitude oscillation in a nonlinear system and has shown that nonlinear equalizing networks may be used to eliminate sustained oscillations and improve system performance.[4] In this paper the amplitude and period of sustained oscillations computed by this method for a velocity lag servomechanism incorporating only one time constant (which will be referred to as the motor time constant) will be compared with an exact treatment of this problem given by Oldenbourg and Sartorius.[5]

The Nonlinear System

Fig. 1 shows a block diagram of this system where θ_r is the reference input, and θ_c is the control variable, which in this case is also the primary feedback and has been commonly called the output. θ_e is the actuating signal (commonly called

---

Paper 53-394, recommended by the AIEE Feedback Control Systems Committee and approved by the AIEE Committee on Technical Operations for presentation at the AIEE Fall General Meeting, Kansas City, Mo., November 2–6, 1953. Manuscript submitted July 6, 1953; made available for printing August 25, 1953.

NATHANIEL B. NICHOLS is with the Raytheon Manufacturing Company, Waltham, Mass.

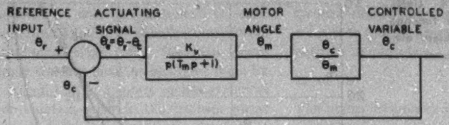

Fig. 1 (above). Velocity lag servomechanism with backlash

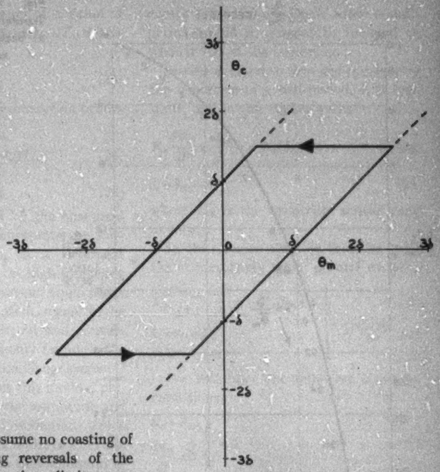

Fig. 2 (right). Backlash characteristic

the actuating error or merely error) and θ_m is the motor position or angle. The quantities θ_r, θ_c, θ_e, and θ_m will be considered as angles to aid in visualizing the application of this method to an angle control and to provide a better example for examining the reasonableness of the results. Quite obviously, the results are equally applicable to any other system which can be described by the block diagram of Fig. 1. The servomotor and amplifier are contained within the element between θ_e and θ_m. This element is considered to be linear and is described by the following differential equation

$$T_m\frac{d^2\theta_m}{dt^2}+\frac{d\theta_m}{dt}=K_v\theta_e \tag{1}$$

where T_m is the motor time constant and K_v is the velocity error constant of the linear system which is approached as the backlash in the other element is reduced to zero. In other words, we have assumed that the transfer function of the nonlinear element approaches unity as the backlash is reduced to zero, and any gear reductions in the system are included in the linear portion.

The transfer function of the linear element may then be written

$$\frac{\theta_m}{\theta_e}=\frac{K_v}{p(T_m p+1)}=\frac{K_v}{j\omega(j\omega T_m+1)} \tag{2}$$

where the $j\omega$ form is the customary complex notation with ω equal to the radian frequency and $j=\sqrt{-1}$. The nonlinear element may be defined by the backlash characteristic of Fig. 2 where 2δ is the free play in the element; θ_m is the input angular displacement to it and θ_c is the resulting output. This characteristic may also be defined

$$\theta_c=\theta_m-\delta\frac{\dot\theta_c}{|\dot\theta_c|};\ 0<\left|\frac{d\theta_c}{dt}\right|=|\dot\theta_c| \tag{3}$$

$$\dot\theta_c=0;\qquad |\theta_c-\theta_m|<\delta \tag{4}$$

The output of the backlash element θ_c lags behind its input θ_m by an amount δ except at reversals where the output stands still until the motor position θ_m takes up the backlash, whereupon the output again lags behind the motor by an amount δ. It is seen that the free play 2δ is the maximum amount by which the motor can be turned without moving the output θ_c. We will neglect any loading effects at θ_c on the motor and as shown in Fig. 2, we will also assume no coasting of the output θ_c during reversals of the motor. These assumptions limit us to small inertia loading at θ_c compared to the motor inertia, and require the presence of sufficient friction on θ_c to prevent any overcoasting.

Fundamental Component Transfer Functions

The fundamental component transfer function or describing function as used by Johnson is obtained by considering θ_m as a sinusoidal input, computing the output θ_c by means of the backlash characteristic, and determining the amplitude and phase shift of the fundamental Fourier series component of θ_c. The transfer gain will be the ratio of the amplitude of the fundamental component of θ_c to the amplitude of θ_m. The transfer phase shift will be the phase angle difference between the input sinusoid θ_m and the fundamental component of the output θ_c. The time behavior of these two quantities will be as given in Fig. 3, where $\bar\theta_m$ is the sinusoidal amplitude of θ_m, and t_1 is the time during which θ_c stands still while the motor is taking up the backlash at reversal. Carrying this out analytically

$$\theta_m=\bar\theta_m\cos\omega t \tag{5}$$

$$\theta_c=\bar\theta_m-\delta\qquad 0<t<t_1 \tag{6}$$

$$\theta_c=\bar\theta_m\cos(\omega t)+\delta,\quad t_1<t<\pi/\omega \tag{7}$$

$$\omega t_1=\cos^{-1}(1-2\delta/\bar\theta_m)=\cos^{-1}(1-2n) \tag{8}$$

where θ_c is defined for one half-period. Further half-periods may be written from the symmetry conditions if needed. The fundamental component θ_{c1} of θ_c may be written

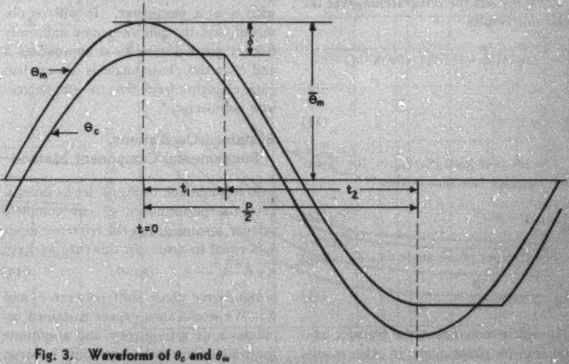

Fig. 3. Waveforms of θ_c and θ_m

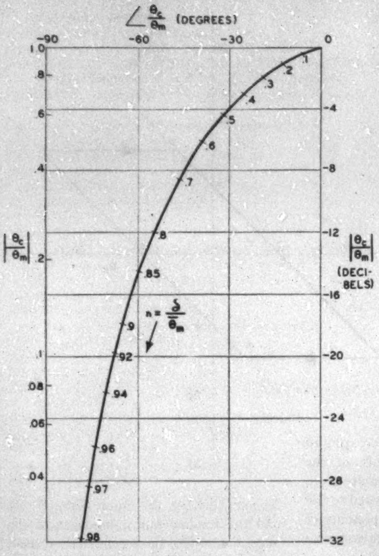

Fig. 4 (left). Transfer function of backlash element

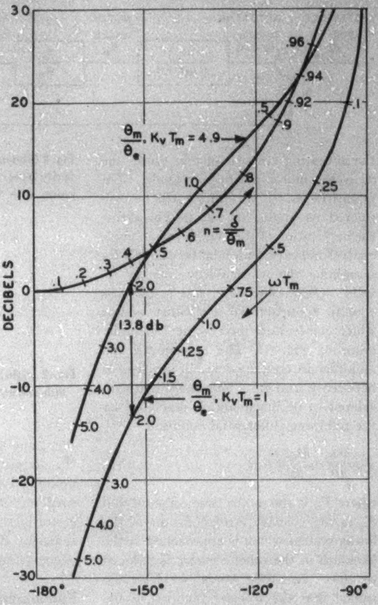

Fig. 5 (right). Graphical solution for sustained oscillations

$$\frac{\theta_{c1}}{\theta_m} = A\cos\omega t + B\sin\omega t = (A^2+B^2)^{1/2}\times \cos\left(\omega t - \tan^{-1}\frac{B}{A}\right) \quad (9)$$

where

$$A = \frac{2}{\pi}\int_0^{\omega t_1}(1-n)\cos\omega t\, d\omega t + \frac{2}{\pi}\int_{\omega t_1}^{\pi}(n+\cos\omega t)\cos\omega t\, d\omega t \quad (10)$$

$$B = \frac{2}{\pi}\int_0^{\omega t_1}(1-n)\sin\omega t\, d\omega t + \frac{2}{\pi}\int_{\omega t_1}^{\pi}(n+\cos\omega t)\sin\omega t\, d\omega t \quad (11)$$

Carrying out the integrations gives the following results

$$A = \frac{1}{\pi}[\cos^{-1}(2n-1)+2(1-2n)\sqrt{n(1-n)}] \quad (12)$$

$$B = \frac{4}{\pi}n(1-n) \quad (13)$$

The transfer gain $|\theta_{c1}/\theta_m|$ of the backlash transfer function is then

$$\left|\frac{\theta_{c1}}{\theta_m}\right| = (A^2+B^2)^{1/2} \quad (14)$$

The transfer phase angle $\angle\theta_{c1}/\theta_m$ is then

$$\angle\frac{\theta_{c1}}{\theta_m} = -\tan^{-1}\frac{B}{A} \quad (15)$$

It will be noted that the transfer gain and transfer phase angle, in other words, the backlash transfer function, is a function of the dimensionless parameter $n = \delta/\theta_m$. Physical reasoning will convince one that the gain approaches unity as the nonlinearity parameter n approaches zero, which corresponds to the motor amplitude becoming large compared to the backlash. Also, as n approaches zero, the phase angle will approach zero. As n approaches 1, the gain obviously approaches zero, and inspection of Fig. 3 shows that the phase angle approaches −90 degrees. Fig. 4 gives a plot of the gain in decibels (db) versus phase angle with n as a parameter. It will be observed that the gain decreases uniformly from 1 toward zero as n approaches 1 and that the phase angle is always lagging, changing from zero to −90 degrees as n approaches 1.

Sustained Oscillations, Fundamental Component Method

Referring back to Fig. 1, let us investigate the performance of our complete system, assuming that the reference input θ_r is equal to zero. In this case we have

$$\theta_e = \theta_r - \theta_c = -\theta_c \quad (\theta_r \equiv 0) \quad (16)$$

a 180-degree phase shift between θ_c and θ_e. We would then expect sustained oscillations at a frequency and amplitude for which the total phase shift between θ_e and θ_c is 180 degrees, and for which the total gain between θ_e and θ_c is exactly unity. This means that the product of the two transfer functions is equal to −1. Writing out these conditions for sustained oscillations we have

$$\left|\frac{\theta_m}{\theta_e}\right|\left|\frac{\theta_c}{\theta_m}\right| = 1 \quad (17)$$

$$\angle\frac{\theta_m}{\theta_e} + \angle\frac{\theta_c}{\theta_m} = -\pi = -180 \text{ degrees} \quad (18)$$

where

$$\left|\frac{\theta_m}{\theta_e}\right| = \frac{K_v T_m}{\omega T_m[(\omega T_m)^2+1]^{1/2}} \quad (19)$$

$$\angle\frac{\theta_m}{\theta_e} = -\frac{\pi}{2} - \tan^{-1}\omega T_m \quad (20)$$

$$\left|\frac{\theta_c}{\theta_m}\right| = \frac{1}{\pi}\{[\cos^{-1}(2n-1)+(1-2n)\times \sqrt{n(1-n)}]^2 + 16n^2(n-1)^2\}^{1/2} \quad (21)$$

$$\angle\frac{\theta_c}{\theta_m} = \tan^{-1}\times \left[\frac{4n(n-1)}{\cos^{-1}(2n-1)+2(1-2n)\sqrt{n(1-n)}}\right] \quad (22)$$

Equations 21 and 22 are obtained from equations 12 through 15. Our basic problem may now be stated. Given values of K_v, T_m, and δ, will sustained oscillations be present, and if they are present, what will be their amplitude and period? It will be convenient to solve equations 17 and 18 simultaneously by a graphic method using the gain phase angle transfer locus as has been done by Johnson.[3] Fig. 5 shows such a graphical construction wherein the transfer phase $\angle\theta_m/\theta_e$ has been plotted as a function of the transfer gain $|\theta_m/\theta_e|$ (in db) of the linear element. Two curves are shown corresponding to two different values of the velocity error constant K_v. The dimensionless frequency ωT_m is shown as a parameter. The other curve is a plot of the reciprocal of the transfer gain $|\theta_c/\theta_m|$ versus the transfer phase angle of the nonlinear element with the nonlinearity parameter n indicated. This corresponds to graphical solutions of equations 17 and 18, written as follows

$$\left|\frac{\theta_m}{\theta_e}\right|=\frac{1}{\left|\frac{\theta_c}{\theta_m}\right|} \qquad \textbf{(17A)}$$

$$\angle\frac{\theta_m}{\theta_e}=-\pi-\angle\frac{\theta_c}{\theta_m} \qquad \textbf{(18A)}$$

Inspection of Fig. 5 shows no intersection for $K_vT_m=1$. Furthermore, careful consideration of the analytical form of equations 17 and 18 shows that the two curves would not even intersect as ωT_m approaches zero and n approaches one. Sustained oscillations will then not be present when $K_vT_m=1$. The second curve corresponding to K_vT_m equals 4.9 (13.8 db) is seen to intersect the backlash transfer function at two points. The low-frequency intersection occurs at a value of n equal to 0.94 at a frequency $\omega T_m=0.34$ with an amplitude

$$\bar{\theta}_m=1.10\delta \qquad \textbf{(23)}$$

The higher frequency intersection occurs at

$$\omega T_m=1.6, \qquad P=\frac{2\pi}{\omega}=4.0T_m \qquad \textbf{(24)}$$

$$\delta/\bar{\theta}_m=0.5, \qquad \bar{\theta}_m=2.0\delta \qquad \textbf{(25)}$$

where P is the period of the sustained oscillation. Johnson interprets the low-frequency intersection as a divergent equilibrium point, and the high-frequency intersection as a convergent equilibrium point. This interpretation seems to be equivalent to the divergent and convergent limit cycles commonly found in the phase plane analysis of nonlinear systems.[6]

It is readily seen that this method permits determination of the amplitude and period of the sustained oscillations which are present when K_vT_m is above a certain critical value as well as this minimum or critical value for which sustained oscillations are present. Smaller values of K_vT_m would then, according to this approximate method, yield stable servo performance. Comparison with an exact treatment will be made in a later section.

Transient Behavior, Exact Analysis

We would expect that the transient behavior, at least after the first half-cycle of transient, would be similar to Fig. 3, except that the amplitude after a half-period would in general be unequal to what it was at the beginning.

Setting θ_r equal to zero and considering the t_1 portion of a half-period, θ_c is constant, and in this region we have

$$T_m\frac{d^2\theta_m}{dt^2}+\frac{d\theta_m}{dt}=-K_v(\bar{\theta}_{m0}-\delta) \qquad \textbf{(26)}$$

$$\theta_c=\bar{\theta}_{m0}-\delta \qquad \textbf{(27)}$$

where $\bar{\theta}_{m0}$ is the maximum motor angle at $t=0$.

In the t_2 region we note that the backash is completely taken up and we have

$$\left.\begin{aligned} &T_m\frac{d^2\theta_m}{dt^2}+\frac{d\theta_m}{dt}=-K_v(\theta_m+\delta) && \textbf{(28)}\\ &\theta_c=\theta_m+\delta && \textbf{(29)}\\ &P/2=t_1+t_2 && \textbf{(30)}\end{aligned}\right\} t_1<t<t_1+t_2$$

We will have the following boundary conditions

$$\left.\begin{aligned}&\theta_m=\bar{\theta}_{m0}\\ &\frac{d\theta_m}{dt}=0\end{aligned}\right\}t=0 \qquad \textbf{(31)}$$

$$\left.\begin{aligned}&\theta_m=\bar{\theta}_{m0}-2\delta\\ &\frac{d\theta_m}{dt}=\text{continuous}\end{aligned}\right\}t=t_1 \qquad \textbf{(32)}$$

$$\left.\begin{aligned}&\theta_m=-\bar{\theta}_{m2}\\ &\frac{d\theta_m}{dt}=0\end{aligned}\right\}t=t_1+t_2 \qquad \textbf{(33)}$$

Introducing the parameters

$$\alpha=(4K_vT_m-1)^{-1/2} \qquad \textbf{(34)}$$

$$\tau=\frac{t}{2T_m}(4K_vT_m-1)^{1/2}=\frac{t}{2\alpha T_m} \qquad \textbf{(35)}$$

$$\varphi=\frac{\theta_m}{\delta}, \qquad \varphi_0=\frac{\bar{\theta}_{m0}}{\delta}, \qquad \varphi_2=\frac{\bar{\theta}_{m2}}{\delta} \qquad \textbf{(36)}$$

will simplify this writing of the piecewise linear solution.

For $0<\tau<\tau_1$

$$\varphi=\varphi_0-\frac{\alpha^2+1}{4\alpha^2}(\varphi_0-1)(2\alpha\tau-1+e^{-2\alpha\tau}) \qquad \textbf{(37)}$$

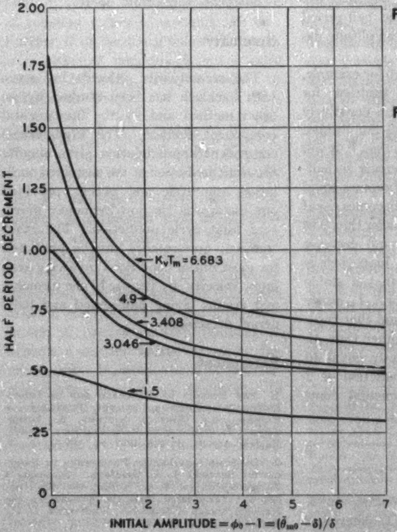

Fig. 6 (left). Half-period decrement versus amplitude

Fig. 7 (below). Half-period versus amplitude

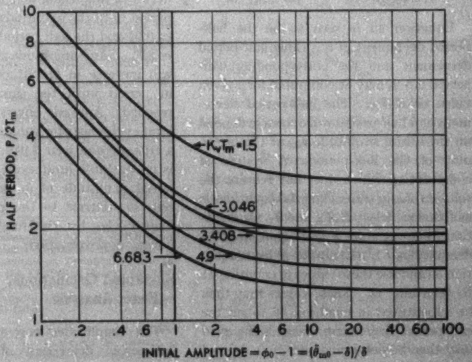

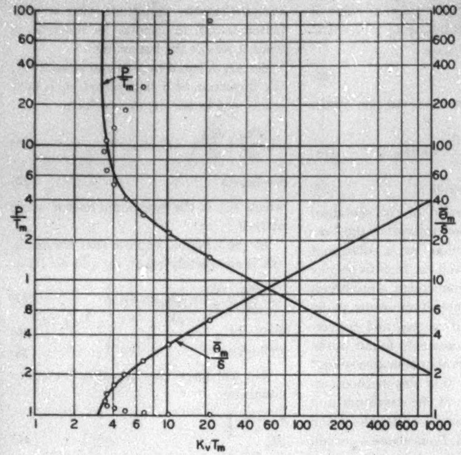

Fig. 8. Sustained oscillation parameters

For $\tau_1<\tau<\tau_1+\tau_2$

$$\varphi=-1+(\varphi_0-1)e^{-\alpha(\tau-\tau_1)}\cos(\tau-\tau_1)+(\varphi_0-1)\left[\alpha-\frac{\alpha^2+1}{2\alpha}D\right]e^{-\alpha(\tau-\tau_1)}\times\sin(\tau-\tau_1)\qquad(38)$$

where

$$D=1-e^{-2\alpha\tau_1}\qquad(39)$$

$$2\alpha\tau_1-1+e^{-2\alpha\tau_1}=\frac{8\alpha^2}{\alpha^2+1}\cdot\frac{1}{\varphi_0-1}\qquad(40)$$

At $\tau=\tau_1+\tau_2$ we have the slope going to zero which yields

$$\tan(\pi-\tau_2)=\frac{D/\alpha}{2-D}\qquad(41)$$

$$\frac{-\varphi_2-1}{\varphi_0-1}=\frac{\bar{\theta}_{m2}-\delta}{\bar{\theta}_{m0}-\delta}=\frac{1-D+\frac{\alpha^2+1}{4\alpha^2}D^2}{1-1/2D}e^{-\alpha\tau_2}\cos(\pi-\tau_2)\qquad(42)$$

Equation 42 is seen to be the half-period decrement of θ_c. This half-period decrement and the corresponding half-period $\tau_1+\tau_2$ may be computed for a given value of K_vT_m. The half-period decrement and half-period will of course depend on the initial amplitude $\bar{\theta}_{m0}$ at the beginning of the half-period. A system of computation which does not require the solution of any transcendental equations is as follows: Select K_vT_m and τ_1, use equation 34 to compute α and equation 40 to compute φ_0-1. Compute D from equation 39 and use these values in equation 41 to determine τ_2. These values may then be substituted in equation 42 to get the half-period decrement. The half-period may then be determined as

$$\frac{P/2}{T_m}=2\alpha(\tau_1+\tau_2)\qquad(43)$$

Fig. 6 gives results for several values of K_vT_m where the half-period decrement is plotted versus the initial amplitude of the controlled variable θ_c. Fig. 7 plots the results for the half-period against the same parameter.

Examination of Fig. 6 shows that the half-period decrement is less than 1 for all initial amplitudes when K_vT_m is less than 3.046, indicating that any transient will decay to zero although the half-period approaches infinity as the amplitude decreases.

Larger values of K_vT_m, 4.9 for example, give a positively damped transient for large initial amplitudes and a negatively damped transient for small amplitudes. Thus, any amplitude larger than 0.9δ will decay in amplitude and increase in half-period until the amplitude becomes equal to 0.9δ and the half period becomes equal to $2T_m$. Any amplitude smaller than 0.9δ will increase in amplitude and decrease in period until the same limit cycle is reached. Analysis shows that a stable limit cycle exists for values of K_vT_m above a critical value near 3.046, and that there is no unstable limit cycle other than an initial amplitude of θ_c exactly equal to zero in contrast to the prediction of 2 limit cycles by the fundamental component approximation.

Sustained Oscillations, Exact Analysis

The amplitudes corresponding to a half-period decrement of 1 determine limit cycle amplitudes which could be compared with the fundamental component method, although a slight extension of the previous analysis will enable determination of the complete limit cycle behavior. Sustained constant amplitude oscillations occur for equation 42 set equal to 1. Solving equation 41 for D and substituting in equation 42 gives

$$e^{-\alpha\tau_2}=\alpha\sin(\pi-\tau_2)+\cos(\pi-\tau_2)\qquad(44)$$

which enables us to calculate τ_2 as a function of α(or K_vT_m). We may then use equations 41 and 39 to solve for τ_1

$$\tau_1=\frac{1}{2\alpha}\ln\left[\frac{1+\alpha\tan(\pi-\tau_2)}{1-\alpha\tan(\pi-\tau_2)}\right]\qquad(45)$$

This value of τ_1 may then be substituted in equation 37, remembering that $\theta_m=\bar{\theta}_{m0}-2\delta$ when $\tau=\tau_1$

$$\varphi_0=\frac{\bar{\theta}_m}{\delta}=1+\frac{8\alpha^2/(\alpha^2+1)}{2\alpha\tau_1-(1-e^{-2\alpha\tau_1})}\qquad(46)$$

The period may also be determined from these values of τ_1 and τ_2

$$P/T_m=4\alpha(\tau_1+\tau_2)\qquad(47)$$

Equations 44 to 47 are substantially those given by Oldenbourg and Sartorius.[4]

The sustained amplitudes and periods calculated by this method are given in Fig. 8. Approximate results obtained by the fundamental component method are given by the circles.

The fundamental component method is seen to give quite close agreement with the exact treatment if one uses the so-called convergent equilibrium point.

Summary

The second-order velocity lag servo with backlash has been studied by an exact method and by the fundamental component method. The fundamental component approximation gives a quite accurate prediction of the sustained oscillation amplitude and period, provided one disregards the low-frequency divergent limit cycle prediction. The exact transient performance can be predicted for most initial conditions involving zero input velocity, by the use of the formulas and graphs giving half-period and half-period decrement.

References

1. THE EFFECTS OF BACKLASH AND OF SPEED-DEPENDENT FRICTION ON THE STABILITY OF CLOSED-CYCLE CONTROL SYSTEMS, **A. Tustin.** *Journal, Institution of Electrical Engineers*, London, England, vol. 94, pt. IIA, 1947, pp. 143–51.

2. ON SOME NON-LINEAR PHENOMENA IN REGULATORY SYSTEMS, **L. C. Goldfarb.** *Avtomatika i Telemechanika*, vol. 8, no. 5, Sept.-Oct. 1947, pp. 349–83. (Translated from the Russian by the National Bureau of Standards, Washington, D. C., *Report 1691*, May 29, 1952.)

3. A Frequency Response Method for Analyzing and Synthesizing Contactor Servomechanisms, Ralph J. Kochenburger. *AIEE Transactions*, vol. 69, 1950, pp. 270–84.

4. Sinusoidal Analysis of Feedback-Control Systems Containing Nonlinear Elements, E. C. Johnson. *AIEE Transactions*, vol. 71, July 1952, pt. II, pp. 169–81.

5. Dynamics of Automatic Control (book), R. C. Oldenbourg, H. Sartorius. American Society of Mechanical Engineers, New York, N. Y., 1948, pp. 168–73.

6. Theory of Oscillations (book), A. A. Andronow, C. E. Chaikin. Princeton University Press, Princeton, N. J., 1949.

◆

No Discussion

Determination of the Maximum Modulus, or of the Specified Gain, of a Servomechanism by Complex-Variable Differentiation

THOMAS J. HIGGINS
MEMBER AIEE

CLIFFORD M. SIEGEL
ASSOCIATE MEMBER AIEE

A PROBLEM of frequent occurrence in servomechanism analysis and design is that of determining the maximum modulus M_m, and the angular frequency at which it occurs, of the over-all frequency-transfer function $M(j\omega)=C(j\omega)/R(j\omega)$. Those textbooks[1–4] which present a comprehensive, integrated account of basic servomechanism theory advance, in considerable detail, two procedures for determining the maximum modulus M_m of $M(j\omega)$ for a unity feedback system, namely, by plot of the transfer function $G(j\omega)$ on a chart of circles of constant values of modulus $|M(j\omega)|$, or on a Nichol's chart of circles of constant values of modulus $|M(j\omega)|$. Further, if the feedback transfer function $H(s)$ although nonunity is yet a pure numeric $H(s)=K_h$, then, according to well-known theory

$$\frac{C(j\omega)}{R(j\omega)}=M(j\omega)=\frac{1}{K_h}\frac{G(j\omega)K_h}{1+G(j\omega)K_h}=\frac{1}{K_h}\times M_1(j\omega) \quad (1)$$

and M_m can yet be determined by obtaining M_{1m} through plot of $G_1(j\omega)=G(j\omega)K_h$ as just mentioned and thence calculating M_m from $M_m=M_{1m}/K_h$.

If, however, the $H(s)$ is a frequency-dependent function—and this case often arises in practice, as in the use of tachonometric or passive network feedback to achieve a certain desired operating improvement—M_m cannot be directly determined from plots as just discussed. In such case M_m must be obtained by other means: say, from a plot of $|M(j\omega)|$ as a function of ω. Usually, however, effectance of this plot requires rather lengthy and tedious computation; especially if, as is often the case, the plot of $|M(j\omega)|$ is broadly peaked, whence then $|M(j\omega)|$ changes slowly with ω in the vicinity of the maximum and thus ω_m is not sharply limited; or if the plot of $|M(j\omega)|$ contains two or more rather widely separated maxima. Again, even when charts can be used directly, considerable computatation is commonly required to obtain thereon a plot of $G(j\omega)$ or $G_1=[G(j\omega)K_h]$ that yields accurate determination of both M_m and ω_m.

Now in virtue of the just discussed undesirable aspects which accrue to these plotting procedures, it is natural to inquire if less computational labor attends determination of ω_m and M_m through the usual procedures for determining maxima and minima by the calculus: namely, by differentiating $|M(j\omega)|$ with respect to the real variable ω; setting the resulting derivative equal to zero; solving the equation so obtained for the values of ω_m; calculating the corresponding values of $|M(j\omega_m)|=M_m$; and when necessary, testing these latter as to maxima or minima by calculating $[d^2|M(j\omega)|/d\omega^2]_{\omega=\omega_m}$, whereof a positive value indicates the corresponding value $|M(j\omega_m)|$ to be a minimum, and a negative value indicates a maximum. In turn, however, such attempt reveals that a computational difficulty accrues to this procedure in that $M(j\omega)$ is usually of rather complicated form, either being the ratio of two polynomials of which at least one is of fair-sized order or involving transcendental terms (when distributed parameters occur in the network); whence determination of $d|M(j\omega)|/d\omega$ proves to be a lengthy and often involved process. If, however, instead of direct differentiation of $|M(j\omega)|$ as a real variable, the desired equation $d|M(j\omega)|/d\omega=0$ is effected by an appropriate differentiation of $M(j\omega)$ as a function of a complex variable, a relatively simple analysis results. Obviously, knowledge of this latter procedure is most desirable to the servo analyst; yet, it is advanced in none of the servomechanism textbooks referred to. Accordingly, the prime purpose of this paper is to advance the desired procedure.

Basic Theory

Let $M(j\omega)$ be expressed in polar form. Thus

$$M(j\omega)=|M(j\omega)|\epsilon^{j\phi(\omega)}=M(\omega)\epsilon^{j\phi(\omega)} \quad (2)$$

where, as indicated, $M(\omega)$ and $\phi(\omega)$ designate the modulus and phase of $M(j\omega)$ and are functions of ω. The derivative of $M(j\omega)$ with respect to ω is

$$\frac{dM(j\omega)}{d\omega}=\frac{dM(\omega)}{d\omega}\epsilon^{j\phi(\omega)}+jM(\omega)\epsilon^{j\phi}\frac{d\phi}{d\omega} \quad (3)$$

Dividing each member of equation 3 by $M(j\omega)=M(\omega)\epsilon^{j\phi(\omega)}$ yields

$$\frac{1}{M(j\omega)}\frac{dM(j\omega)}{d\omega}=\frac{1}{M(\omega)}\frac{dM(\omega)}{d\omega}+j\frac{d\phi(\omega)}{d\omega} \quad (4)$$

From equation 4 we thus obtain

$$Re\left[\frac{1}{M(j\omega)}\frac{dM(j\omega)}{d\omega}\right]=\frac{1}{M(\omega)}\frac{dM(\omega)}{d\omega} \quad (5)$$

and

$$Im\left[\frac{1}{M(j\omega)}\frac{dM(j\omega)}{d\omega}\right]=\frac{d\phi(\omega)}{d\omega} \quad (6)$$

From equation 5 it follows that if the left-hand member vanishes for a particular value of $\omega=\omega_m$, then so must also the right-hand member and thus, unless $M(\omega_m)=\infty$ or $-\infty$, which possibility is easily checked, $[dM(\omega)/d\omega]_{\omega=\omega_m}=0$. Accordingly, those values ω_m which render $|M(j\omega)|$ a maximum or a minimum are usually those which satisfy the equation

$$Re\left[\frac{1}{M(j\omega)}\frac{dM(j\omega)}{d\omega}\right]=0 \quad (7)$$

In similar fashion it follows from equation 6 that those values $\omega=\omega_p$ which

---

Paper 53-392, recommended by the AIEE Feedback Control Systems Committee and approved by the AIEE Committee on Technical Operations for presentation at the AIEE Fall General Meeting, Kansas City, Mo., November 2–6, 1953. Manuscript submitted June 29, 1953; made available for printing August 27, 1953.

Thomas J. Higgins is with the University of Wisconsin, Madison, Wis.; Clifford M. Siegel is with the University of Virginia, Charlottesville, Va.

render $\phi(\omega)$ an extremum are those which satisfy the equation

$$Im\left[\frac{1}{M(j\omega)}\frac{dM(j\omega)}{d\omega}\right]=0 \qquad (8)$$

Now the frequency-transfer function $M(j\omega)$ is commonly obtained by substitution of $s=j\omega$ in the operational transfer function $M(s)$. Accordingly, equivalent equations, somewhat more convenient to calculation are, per equations 7 and 8 respectively

$$Re\left[j\frac{1}{M(s)}\frac{dM(s)}{ds}\right]_{s=j\omega}=0 \qquad (9)$$

and

$$Im\left[j\frac{1}{M(s)}\frac{dM(s)}{ds}\right]_{s=j\omega}=0 \qquad (10)$$

In a system without distributed parameters $M(s)$ results as the ratio of two polynomials, say $M(s)=A(s)/B(s)$. In such case

$$\frac{dM(s)}{ds}=\frac{1}{B(s)}\frac{dA(s)}{ds}-\frac{A(s)}{B^2(s)}\frac{dB(s)}{ds} \qquad (11)$$

Substituting from equation 11 in equations 9 and 10 yields

$$Re\left\{j\left[\frac{1}{A(s)}\frac{dA(s)}{ds}-\frac{1}{B(s)}\frac{dB(s)}{ds}\right]\right\}_{s=j\omega}=0 \qquad (12)$$

and

$$Im\left\{j\left[\frac{1}{A(s)}\frac{dA(s)}{ds}-\frac{1}{B(s)}\frac{dB(s)}{ds}\right]\right\}_{s=j\omega}=0 \qquad (13)$$

Equations 12 and 13 are especially convenient to calculation inasmuch as, for a particular servo system, $A(s)$ and $B(s)$ are directly ascertainable from the block diagram of the system. In illustration of this, and of the general course of application of these equations, we turn to a solution of the following typical problem.

Illustrative Examples

In the unity-feedback system of the illustrative example on page 230 of Chestnut and Mayer,[3] the given transfer function $G(s)$ is

$$G(s)=3/s(1+0.2s)(1+0.05s)=3/(s+0.25s^2+0.01s^3) \qquad (14)$$

Accordingly, by well-known theory

$$M(s)=\frac{G(s)}{1+G(s)}=\frac{3}{3+s+0.25s^2+0.01s^3} \qquad (15)$$

Thus, $dA(s)/ds=0$, $dB(s)/ds=1+0.5s+0.03s^2$. Substituting in equation 12 yields

$$3\times10^{-4}\omega^4+0.085\omega^2-0.5=0 \qquad (16)$$

Solution of this quadratic equation in ω^2 and selection of the positive root yields $\omega_m{}^2=5.76$; whence selection, in turn, of the positive square root yields the desired value $\omega_m=2.4$. Therewith, we easily obtain from equation 15 that $|M(j\omega_m)|=1.09$. Corroboratively, the value of $M_m=1.09$ is identical with the text value; the value of $\omega_m=2.4$ is somewhat more accurate than the interpolated text value of $\omega_m\cong2.5$. Further, comparison of the just presented calculation of these desired resonance values with the extended numerical calculation required to effect the $|M(j\omega)|$ versus ω plot of the text evidences the considerably less numerical labor required in the former calculation, using the procedure given in this paper.

Conclusion

In conclusion, it may be remarked that the analysis of the basic theory is directly applicable to solution of yet another problem often encountered in servo work: namely, that of determining both the value of the gain parameter K such that M_m takes on a certain maximum value $M_m{}'$ and the corresponding frequency ω_m, at which the maximum occurs. Obviously, this can be done by obtaining ω_m in terms of K; substituting the resulting expression for $\omega_m=f(K)$ in $M(\omega,K)$; imposing the stated restriction $M(\omega_m,K)=M[f(K),K]=M_m{}'$; solving this equation for K; and finally determining ω_m from $\omega_m=f(K)$. Alternatively—and not seldom this approach requires less numerical labor than the first—the equation in ω_m and K can be solved for K rather than ω_m; the resulting expression $K=g(\omega_m)$ substituted in $M(\omega,K)$; the stated restriction $M(\omega_m,K)=M[\omega_m,g(\omega_m)]=M_m{}'$ imposed; this equation solved for ω_m; and finally K then determined from $K=g(\omega_m)$.

In closing, it may be noted that such calculation of K and ω_m is more straightforward and also enables K and ω_m to be determined with greater accuracy than the usually used graphical procedures which are advanced in the literature.[1-4]

References

1. PRINCIPLES OF SERVOMECHANISMS (book), **G. S. Brown, D. P. Campbell.** John Wiley and Sons, New York, N. Y., 1948, pp. 176–94, 253–62.
2. AUTOMATIC FEEDBACK CONTROL (book), **W. R. Ahrendt, J. F. Taplin.** McGraw-Hill Book Company, Inc., New York, N. Y., 1951, pp. 134–6.
3. SERVOMECHANISMS AND REGULATING SYSTEM DESIGN (book), **H. Chestnut, R. W. Mayer.** John Wiley and Sons, New York, N. Y., 1951, pp. 229–44, 318–26.
4. SERVOMECHANISM ANALYSIS (book), **G. J. Thaler, R. G. Brown.** McGraw-Hill Book Company, Inc., New York, N. Y., 1953, pp. 182–91, 266–70.

◆

Discussion

Jack Sklansky (Electronics Research Laboratories, Columbia University, New York, N. Y.): For handling this problem there exists an alternative procedure which has the advantage of the neatness of approach obtained in eliminating use of ω as a variable. In both methods, one must find the roots of essentially the same equation.

In the alternate procedure one finds the negative real roots in s^2 of

$$\frac{d}{d(s^2)}[M(s)M(-s)]=0 \qquad (17)$$

(The proof follows from the fact that $M(j\omega)M(-j\omega)=|M(j\omega)|^2$.)

$M(s)M(-s)$ should be expressed in terms of s^2. If given in the factored form $M(s)=K(a_1+s)\ldots/(b_1+s)\ldots$, one immediately obtains

$$M(s)M(-s)=K\frac{(a_1-s^2)\ldots}{(b_1-s^2)\ldots} \qquad (18)$$

If given in the polynomial form, one should write $M(s)=[A_1(s)+sA_2(s)]/[B_1(s)+sB_2(s)]$, where the $A_1(s)$ and $B_1(s)$ are even, from which one obtains

$$M(s)M(-s)=\frac{A_1^2(s)-s^2A_2^2(s)}{B_1^2(s)-s^2B_2^2(s)} \qquad (19)$$

Applying the method to the example of the paper, we have

$$\frac{d}{d(s^2)}[(3+0.25s^2)^2-s^2(1+0.01s^2)^2]=0 \qquad (20)$$

This gives

$$3\times10^{-4}5^4-0.085s^2-0.5=0 \qquad (21)$$

which is equation 16 of the paper with ω^2 replaced by $-s^2$. The negative real root in s^2 is $s_m{}^2=-(2.58).^2$ Substituting this in equation 19 gives $M_m{}^2=(1.09)^2$.

The general concept from which the method springs is of value. Whenever one is interested in the absolute value of a transfer function $M(s)$ along the imaginary axis it is often mathematically convenient to deal with its square. The reason is simply that $|M(j\omega)|^2$ can be analytically continued to the entire complex plane by the function $M(s)M(-s)$, which permits the application of function theory to its analysis. On the other hand, since for dissipative physical systems $M(s)$ cannot be even, $|M(j\omega)|$ has discontinuous derivatives and hence cannot be continued analytically. Thus, the function $M(s)M(-s)$ should often prove useful when dealing with $|M(j\omega)|$.

Thomas J. Higgins and **Clifford M. Siegel**: The procedure suggested by Mr. Sklansky is effectively a procedure for direct evaluation of $d|M(j\omega)|/d\omega$ and possesses precisely the disadvantages mentioned in the third paragraph of our paper. To evidence this fact, we note that

$$\frac{d|M(j\omega)|^2}{d(j\omega)^2}=\frac{d|M(j\omega)|^2}{dj\omega}\frac{dj\omega}{d(j\omega)^2}=\frac{1}{2}\frac{d|M(j\omega)|^2}{dj\omega}$$

$$=|M(j\omega)|\frac{d|M(j\omega)|}{dj\omega}$$

$$=-j|M(j\omega)|\frac{d|M(j\omega)|}{d\omega} \quad (22)$$

and inasmuch as

$$\frac{d|M(j\omega)|^2}{d(j\omega)^2}=\frac{dM(j\omega)M(-j\omega)}{d(j\omega)^2}$$

$$=\left[\frac{dM(s)M(-s)}{ds^2}\right]_{s=\pm j\omega} \quad (23)$$

it follows from comparison of the right-hand members of equations 22 and 23 that

$$\left[\frac{dM(s)M(-s)}{ds^2}\right]_{\substack{s^2=\omega^2\\ s^2=\pm j\omega}}$$

$$=-j|M(j\omega)|\frac{d|M(j\omega)|}{d\omega} \quad (24)$$

Accordingly, if $s_i^2=-\omega_i^2$ is a zero of the left-hand member, then $s_{i1}=j\omega_i$ and $s_{i2}=-j\omega_i$ are zeros of the right-hand member; and thus also of $d|M(j\omega)|/d\omega$, providing this factor, and not $|M(j\omega)|$ only, vanishes for $s_i^2=-\omega_i^2$ (a point not mentioned by Mr. Sklansky).

But to obtain $M(s)M(-s)$ for differentiation thereof requires the polynomial multiplication and collection of corresponding powers of s indicated in $A(s)A(-s)=A_1^2(s)-s^2A_2^2(s)$ and $B(s)B(-s)=B_1^2(s)-s^2B_2^2(s)$; and this is a laborious task when $B(s)$, and also not unoften $A(s)$, are high-order polynomials such as occur in the analysis of industrial servomechanism systems. Next, it is then necessary to differentiate the ratio of two polynomials $[A(s)A(-s)/B(s)B(-s)]=M(s)M(-s)$; which is another tedious task, encompassing precisely the disadvantage mentioned in the third paragraph of our paper.

Contrariwise, in the procedure set out in our paper, equations 12 and 13 evidence that it is necessary: first, to deal only with $A(s)$ and $B(s)$ as given; and second, only to differentiate the polynomials $A(s)$ and $B(s)$, a simple task—even for high-order polynomials—compared with differentiation of the ratio $A(s)A(-s)/B(s)B(-s)$, except perhaps in a rather simple case $A(s)=$constant as in our illustrative example, which was deliberately selected with view to keeping the algebraic manipulation to a minimum, while yet exemplifying the general course of analytic procedure.

Accordingly, the authors hold that whereas Mr. Sklansky's suggested procedure is a feasible alternative (also one much used in filter, and other network, analysis), it commonly requires more tedious computation than does the complex variable differentiation procedure set out in our paper; particularly when $B(s)$, and not unoften also $A(s)$, are high-order polynomials (or transcendental functions) such as are commonly encountered in industrial servomechanism analysis.

A Discussion of the Detroit Committee on Electrolysis

R. L. RAYNER
MEMBER AIEE

THE Detroit Committee on Electrolysis is a voluntary organization of companies and municipal departments constituted for finding the best engineering solution to the electrolysis and corrosion problems confronting its members. There are over 25 cities and areas in the United States and Canada which have active electrolysis committees including New York, Chicago, Philadelphia, Detroit, Southern Ontario, Cleveland, Milwaukee, Omaha, Des Moines, Louisville, Miami, and, of course, many others. The Detroit Committee has been chosen as the subject of this paper not only because it is typical of such committees, but also because it has had a long and outstanding history.

In 1921, the representatives of the companies owning underground structures in Detroit called a meeting where the ground work was laid for the organization of the Detroit Committee which was effected the following year. The constitution of the Detroit Committee on Electrolysis was drawn up and formally adopted July 6, 1922. It has been revised on three occasions at later dates. This committee has functioned without interruption from that date to the present time.

The objective of the Detroit Committee on Electrolysis, as defined in its constitution, is to promote co-operation, to interchange information and to make definite recommendations for the solution of corrosion problems among the interests concerned, and to extend every effort to have such recommendations put into effect. In Detroit and surrounding communities, there is a very large investment in pipes and cables installed underground, which are owned by municipal and private interests. The size of this investment warrants finding and applying the best technical solutions to the corrosion problems which are encountered.

Co-operative effort is essential in electrolysis and corrosion problems, because independent action is likely to result in the application of measures which would protect the property of one company and at the same time create a hazard to the property of another. A common result of nonco-operation is competitive drainage, which is an undesirable practice under this condition, where each party attempts to drain as much current as possible instead of as little current as is necessary for protection. It is conceivable that nonco-operation might not only result in unnecessary damage to structures, but also unnecessary arguments between companies and the cost of such arguments in wasted time might easily exceed the cost of correct co-operative mitigative measures which would have prevented the damage.

Membership in the Detroit Committee on Electrolysis may be maintained by any company or municipal department which has property in Detroit or adjacent communities and is involved in creating conditions which may cause electrolysis or possesses property which may be damaged thereby. At the present time there are 30 member organizations. These are listed in Appendix I. The member companies and municipal departments appoint representatives to attend the meetings of the committee. Representation for the purpose of voting is arranged so that each member organization has one vote.

The Detroit Committee on Electrolysis is divided into three departments which are: The General Committee, The Executive Committee, and The Technical Committee.

The General Committee is composed of one official representative and one alternate from each member organization. Additional representatives without voting power may also attend committee meetings. The representatives to the

---

Paper 53-413, recommended by the AIEE Chemical, Electrochemical, and Electrothermal Applications Committee and approved by the AIEE Committee on Technical Operations for presentation at the AIEE Fall General Meeting, Kansas City, Mo., November 2–6, 1953. Manuscript submitted February 29, 1953; made available for printing August 24, 1953.

R. L. RAYNER is with the Michigan Bell Telephone Company, Detroit, Mich.

General Committee are usually officials, executives, engineers, or supervisors of the companies which they represent. Since these people hold positions of influence on questions concerning electrolysis and corrosion in their respective companies, they expedite the approval of recommendations made by the committee and they also expedite the approval of necessary testing work and remedial measures.

The constitution provides that the General Committee shall meet at least three times per year. These meetings have been noon luncheon meetings. It invariably happens that ideas are exchanged prior to or during the luncheon period which assist in the solution of problems when these are brought up for formal discussion.

The routine work of the General Committee consists primarily of reviewing the work of the Technical Committee over which it has general supervision. It is often required to make recommendations or decisions on controversial subjects. The scope of the committee's activities is limited to problems which affect its member organizations. Problems concerning unsatisfactory conditions which affect other organizations or individuals are not undertaken as a committee function.

It has been the practice for over 10 years to supplement the business session of General Committee meetings with papers presented by outstanding speakers. The subjects of those papers not only cover corrosion and electrolysis but also subjects broadly relating to the interests of the committee. In Appendix II there is a list showing a sample of the subjects of papers and the speakers who presented them.

In addition to its routine work, the General Committee has entered into several additional activities. Some of these are discussed as follows:

1. *Educational Lecture Series:* In 1946, the committee sponsored a lecture series on methods of detecting electrolysis hazards and methods of preventing damage from stray current and local cell action. The series consisted of nine weekly meetings held in the Lawrence Institute of Technology. There were 95 men enrolled in the course and there was a high percentage attendance at the meetings.

2. *Electrolysis Records:* The Detroit Committee on Electrolysis maintains very extensive records of structures and equipment used by member organizations in the prevention of electrolysis damage. These records contain information on electrical drains and bonds, cathodic protection using Galvanic anodes, and cathodic protection using rectifiers. They consist of detailed data in tabular form supplemented by sketches. The records are indexed by geographical location and also by company ownership.

3. *Safety Recommendation:* The storage tanks associated with gasoline filling stations, when not properly installed, are subject to corrosion followed by leakage. Part of the lost gasoline often finds its way into manholes and cases have occurred where manholes have been found to contain over 100 gallons of gasoline. This situation is a fire hazard to the utilities using the manholes and the surrounding neighborhood. The Detroit Committee on Electrolysis drafted specifications for the installation of underground gasoline storage tanks which would greatly retard corrosion and probably prevent subsequent leakage. These specifications were transmitted to the Department of Buildings and Safety Engineering of the City of Detroit.

4. *Record of Pipe and Cable Failures:* For several years the Detroit Committee on Electrolysis maintained a record of pipe and cable failures together with the cost of associated repairs and it was extended to show other related data. This report has been temporarily discontinued because it was quite difficult for some companies to furnish the desired information (especially the pipe owning companies).

The officers of the General Committee are a Chairman and Vice Chairman who are elected and a Secretary-Treasurer who is appointed by the Chairman. The work of the Secretary-Treasurer includes making arrangements and distributing announcements for noon luncheons. It also includes the preparation and distribution of minutes of meetings. From the time the committee was organized, it has been the practice to furnish all members with copies of the minutes of all meetings.

The expenses associated with the work of the Secretary-Treasurer and other officers of the General Committee are absorbed by the companies which they represent. For this reason, it has been the practice to rotate the appointment of the Secretary-Treasurer among the major companies represented on the committee. The constitution provides that an assessment may be levied on the member companies to cover expenses. However, no such assessment has ever been made.

In addition to the General Committee, there are two standing committees, as referred to above, which are known as the Executive Committee and the Technical Committee.

The Executive Committee consists of the officers of the General Committee, the Chairman of the Technical Committee, plus two members selected at large from the General Committee. The Executive Committee plans and controls the general order of business of the Detroit Committee on Electrolysis. It also makes decisions from time to time on controversial questions which could not be handled conveniently in a large group.

At the present time, the Technical Committee has in the neighborhood of 20 member organizations represented. They usually are field people engaged in the detection, measurement and mitigation of corrosion problems, and it is not necessary that they be members of the General Committee.

The officers of the Technical Committee consist of a Chairman and a Secretary. The Secretary sends out notice of meetings and also prepares and distributes minutes of meetings to all members. In addition, the Secretary records data of joint testing sessions and distributes copies of these to all members on the Technical Committee mailing list. The Technical Committee meets at least four times per year, and more often when necessary, with monthly meetings being about average in recent years.

The Technical Committee reviews reports of unsatisfactory electrolysis conditions, devises tests methods, calls upon member organizations for the assistance of men and the use of testing equipment to carry out joint testing sessions, analyzes the data obtained from the tests, recommends remedial measures and reports to the General Committee on technical details regarding the cases handled. At the present time (1953) there are 14 active cases. During 1952 seven cases were opened and three cases were closed. The Technical Committee has handled 80 cases since 1937 when the present case-numbering system was started.

The following notes cover a few cases handled by the Technical Committee which illustrates the types of troubles with which it is confronted.

1. Woodward Terminal of the Department of Street Railways (DSR) (Case 53-47): Although this case involves stray current from street railways, it is outstanding because it could not be solved by conventional drainage wire methods. At this terminal, the negative bus was connected to a big rail network through a very-low-resistance cable using a large amount of copper. This made the rail substantially of the same potential as the negative bus, and made cables and pipes near the rail network positive to rail and positive to ground regardless of the size of drainage wire used. The problem was solved when the DSR moved the connection from bus bar to rail to a more remote location.

2. Detroit-Windsor Vehicular Tunnel (Case 13-43): This case was unusual because it involved two sources of stray current, one from the DSR and the other from electrically operated trains in the New York Central Tunnel. The stray currents created a hazard to telephone and power cables as well as signaling cables owned by the tunnel

company. The hazard could not be corrected by connecting the cables to a DSR negative bus at the Detroit end because it made cables highly negative to other structures at the Detroit end, while the cables were still highly positive in the tunnel. A partial correction of the situation was obtained by connecting an insulated drainage wire from the DSR negative bus at the Detroit end to the cables at the midpoint of the tunnel. The situation was finally solved by connecting a rectifier between the DSR negative bus and the insulated drainage wire, the positive side of the rectifier being connected to the DSR negative bus.

3. Montrose Substation (Case 58-48): This case is significant because it originated from the replacement of streetcars with trolley coaches. When trolley-coach service was established, a negative feeder with defective insulation was left connected to the negative bus at the Montrose substation, although it was disconnected from the rail. The feeder, without a load, assumed the potential of the negative bus and the Detroit Edison Company cables were found to be highly positive to it as well as to ground in the vicinity of the feeder. The case was cleared by disconnecting the abandoned feeder from the negative bus.

4. Detroit-Southern Pipe Line (Case 63-48): This case involves a right angle crossing between a bare steel pipe and an underground telephone cable in tile conduit. It is of interest because both the cable and the pipe use cathodic protection.

When rectifiers were placed on the cable they were spaced and located so that the cable was neutral to ground at the point of pipe crossing.

At a later date, cathodic protection was applied to the pipe, which made the telephone cable highly positive to ground at the crossing. Arrangements were made with the pipe line company for a bond between the cable and the pipe. The bond had a resistance which limited the current to a predetermined amount. This removed the hazard created by the cathodic protection system on the pipe line.

In conclusion, it may be stated that the Detroit Committee on Electrolysis has handled electrolysis and corrosion problems in Detroit and surrounding communities to the mutual satisfaction of all of its members for well over a quarter of a century. Through its General Committee, it has held the interest of executives and supervisory people and it has used them to control policies and expedite approval of recommended measures. Through its Technical Committee, it has handled detailed problems and arranged for joint testing programs. These were followed by the application of remedial measures, which have resulted in enormous savings.

When the committee was organized, practically all problems related to stray current from street railway systems. In recent years, many street railway lines have been discontinued, but with the addition of pipe lines with cathodic protection and with the extension of other underground structures, electrolysis and corrosion problems have increased both in number and complexity. Therefore, the work of the Detroit Committee on Electrolysis is fully as important now as at any time in its history.

Appendix I. Member Organizations of the Detroit Committee on Electrolysis

Telephone and Telegraph Companies

Michigan Bell Telephone Company
American Telephone and Telegraph Company
The Bell Telephone Company of Canada
Western Union Telegraph Company

Power Companies

The Detroit Edison Company
The Consumers Power Company
The Public Lighting Commission (A Detroit Municipal Department)

Michigan Consolidated Gas Company

Municipal Departments of the City of Detroit

The Department of Street Railways
The Department of Water Supply
The Fire Department
The Police Department
Department of Buildings and Safety Engineering

Municipal Department of Adjacent Communities, Representing Water, Police, and Fire Signal Service

City of Dearborn
City of Highland Park
City of Royal Oak

Pipe Line Companies

Aurora Gasoline Company
Detroit Southern Pipe Line Company
Pan Handle Western Pipe Line Company
Sinclair Pipe Line Company
Socony Vacuum Oil Company, Inc.
Sun Pipe Line Company
Transit and Storage Company
Union Gas Company of Canada, Ltd.

Tunnel and Bridge Companies

New York Central Railroad Company
Detroit International Bridge
Detroit and Canada Tunnel Corporation

Appendix II. Sample of the Papers Presented at General Committee Meetings of the Detroit Committee on Electrolysis

Dr. John Piper, Chemical Supervisor, The Detroit Edison Company: "Corrosion Control on Galvanized Steel Towers"

J. P. Oliver, Union Carbide and Carbon Corporation: "Various Applications of Graphite Anodes in Cathodic Protection"

T. J. Maitland, American Telephone and Telegraph Company, Long Lines Department: "Instruments Used for Electrolysis Measurements"

Leroy R. Wagner, Department of Street Railways: "A Discussion of The Department of Street Railways"

Mayor Eugene I. VanAntwerp, City of Detroit: "Early History of Detroit"

F. J. McElhatton, Panhandle Eastern Pipe Lines: "Cathodic Protection of Pipe Lines"

Clark Varnum, The Detroit-Windsor Tunnel Company: "The Detroit-Windsor Tunnel"

A. G. Andrews, Michigan Bell Telephone Company: "Salt as a Medium of Corrosion"

◆

No Discussion